United States
Department of
Agriculture

Agricultural
Research
Service

December 2012

Southeast Poultry Research Laboratory

Research Publications 2011

ARS Mission

The Agricultural Research Service conducts research to develop and transfer solutions to agricultural problems of high national priority and provides information access and dissemination to ensure high-quality, safe food and other agricultural products; to assess the nutritional needs of Americans; to sustain a competitive agricultural economy; to enhance the natural resource base and the environment; and to provide economic opportunities for rural citizens, communities, and society as a whole.

The U.S. Department of Agriculture (USDA) prohibits discrimination in all its programs and activities on the basis of race, color, national origin, age, disability, and where applicable, sex, marital status, familial status, parental status, religion, sexual orientation, genetic information, political beliefs, reprisal, or because all or part of an individual's income is derived from any public assistance program. (Not all prohibited bases apply to all programs.) Persons with disabilities who require alternative means for communication of program information (Braille, large print, audiotape, etc.) should contact USDA's TARGET Center at (202) 720-2600 (voice and TDD). To file a complaint of discrimination, write to USDA, Director, Office of Civil Rights, 1400 Independence Avenue, S.W., Washington, D.C. 20250-9410, or call (800) 795-3272 (voice) or (202) 720-6382 (TDD). USDA is an equal opportunity provider and employer.

Photo caption and credit: Baby chicks. Photo courtesy of Agricultural Research Service.

David Swayne
Laboratory Director
Southeast Poultry Research Laboratory
ARS-USDA
934 College Station Road
Athens, GA 30605
Phone: 706-546-3434, Fax: 706-546-3161

David L. Suarez
Research Leader
Exotic and Emerging Avian Viral Diseases
Southeast Poultry Research Laboratory
ARS-USDA
934 College Station Road
Athens, GA 30605
Phone: 706-546-3479, fax: 706-546-3161

Laszlo Zsak
Research Leader
Endemic Poultry Viral Diseases Unit
Southeast Poultry Research Laboratory
ARS-USDA
934 College Station Road
Athens, GA 30605
Phone: 706-546-3654, fax: 706-546-3161

Southeast Poultry Research Laboratory

The Agricultural Research Service's Southeast Poultry Research Laboratory (SEPRL) brings together scientific expertise in an integrated research approach that includes virology, molecular biology, pathology, and immunology. This expertise is key to developing prevention, management, and control and eradication strategies to protect the $25-billion-a-year U.S poultry industry, which contributes $2.5 billion in U.S exports annually. SEPRL is a major international resource to control highly pathogenic Avian Influenza and virulent Newcastle Ddisease, which pose a major threat to the U.S poultry industry as well as a severe risk to public health.

Research at the laboratory has been expanded in the last five years to address priority domestic viral diseases that also impact the U.S poultry industries. SEPRL, which was established in 1960, has two research units: the Exotic and Emerging Avian Viral Diseases Research Unit and the Endemic Poultry Viral Diseases Research Unit.

This research provides government regulatory agencies and the poultry industries with improved intervention strategies against poultry viral diseases. SEPRL will require new laboratory and animal housing facilities if it is to continue providing rapid responses to new and emerging disease threats and effectively respond to the research needs of the United States.

Mission

Provide scientific solutions to national and international exotic, emerging, and endemic poultry viral diseases through a comprehensive research program emphasizing basic and applied research in diagnostics, prevention, and control strategies, prediction of disease outbreaks, molecular epidemiology, and understanding disease pathogenesis.

Program Objectives

SEPRL's objectives are to produce new research knowledge and technology to--

- prevent, reduce, or eliminate losses from impaired performance and increased deaths and condemnations;
- develop more sensitive, specific, and faster diagnostic tests;
- Improve vaccines and vaccine delivery methods;
- improve our understanding of the ecology and epidemiology of viruses at the wild bird-domestic poultry interface; and
- improve our understanding of the genetic and pathobiological basis of virulence.

Priority Diseases

High-pathogenicity Avian Influenza virus – Select Agent
Virulent Newcastle Disease virus – Select Agent
Low-pathogenicity Avian Influenza virus – Nonselect Agent
Low-virulence Newcastle Disease virus – Nonselect agent
Marek's Disease herpesvirus - Nonselect Agent
Enteric viruses of poultry - Nonselect Agent

Stakeholder groups

National Turkey Federation
National Chicken Council
United Egg Producers
State poultry associations
State Departments of Agriculture, Animal Bureaus, and Animal Commissions
Animal and Plant Inspection Service
Food Safety and Inspection Service
U.S. Food and Drug Administration
Centers for Disease Control and Prevention
University diagnostic laboratories
U.S. veterinary colleges

Research Facilities

- 32 acres, 29 buildings (25 completed in 1963, 1 BSL-3AG completed 1976, 2 SPF flock houses completed in 1983, replacement sewage decontamination facility 2001)
- Laboratory spaces and decontamination procedures
- BSL-2/3E, ABSL-2/3E, and animal holding spaces
- BSL-3Ag loose animal rooms
- Administrative, storage, support, and utility spaces
- Breeding (SPF) and production spaces

Personnel

Scientists: 11
Technicians: 19
Administration and support staff: 13
Total: 43

Accomplishments

- Developed and used rapid, real-time reverse transcriptase-polymerase chain reaction (RRT-PCR) diagnostic tests that were used in live bird markets in Virginia in 2001-2002.
- Collaborated with corporate partners in research that resulted in the licensing and commercialization of two avian influenza vaccines: fowlpox recombinant-avian influenza H5 gene insert and inactivated H5 avian influenza.
- Collaborated with corporate partners in research that resulted in two licensed ELISA test kits for avian influenza diagnostics.
- Used molecular epidemiology to track sources and links in the Mexican H5 outbreak (1994-95), H7N2 outbreak in LBM of northeastern USA (1994-2002), Hong Kong H5N1 outbreaks (1997-2001), and Chilean H7N3 outbreak (2002).
- Provided scientific data to USDA to support negotiations on trade in poultry and poultry products including validating pasteurization as a way to inactivate LPAI virus in egg products and determining that there was a low risk of LPAI virus being transmitted in broiler meat.
- Demonstrated the susceptibility of turkeys to 2010 pandemic H1N1 and modified RT-PCR diagnostic tests for biosurveillance in poultry.
- Used molecular epidemiology to track sources of the virulent Newcastle Disease (NDV) in the Mexican outbreak (2000) and the California and Texas outbreaks (2002-2003).
- Demonstrated that recent NDV isolates, isolates recovered during disease outbreaks since the 1970s, and new clades of virus emerging in Asia are phylogenetically distinct from current vaccine viruses and standard challenge strains.
- Completed a genetic characterization of the first U.S. avian pneumovirus isolate, which resulted in it being classified as type C, different from European types A and B.
- Demonstrated that waterfowl outside of Minnesota can carry and potentially disseminate avian metapneumoviruses.
- Isolated the first astrovirus and demonstrated its involvement in poultry enteritis mortality syndrome (PEMS).
- Developed and transferred to diagnostic laboratories a multiplex PCR test for simultaneous demonstration of astrovirus, reovirus, and coronavirus.
- Demonstrated that astrovirus is resistant to inactivation by common disinfectants and that Virkon S is the only effective disinfectant.
- Demonstrated that inoculation of turkeys with West Nile Virus (WNV) did not produce disease and that WNV replicates poorly in turkeys, so there is minimal potential to infect mosquitoes and contribute to WNV ecology.
- Demonstrated that WNV can cause severe neurological disease and death in young domestic geese.

Table of Contents

Description

1. Characterization of H5N1 highly pathogenic avian influenza viruses isolated from poultry in Pakistan 2006–2008
2. Development of DIVA (differentiation of infected from vaccinated animals vaccines utilizing heterologous NA and NS1 protein strategies for the control of triple reassortant H3N2 influenza in turkeys
3. Effect of age on the pathogenesis and innate immune responses in Pekin ducks infected with different H5N1 highly pathogenic avian influenza viruses
4. Experimental Infection with Low and High Pathogenicity H7N3 Chilean Avian Influenza Viruses in Chiloe Wigeon (Anas sibilatrix) and Cinnamon Teal (Anas cyanoptera)
5. In vivo transcriptional cytokine responses and association with clinical and pathological outcomes in chickens infected with different Newcastle disease virus isolates using formalin-fixed paraffin-embedded samples
6. Low Pathogenicity Avian Influenza Viruses Infect Chicken Layers by Different Routes of Inoculation
7. Molecular Signatures Associated with Mx1-Mediated Resistance to Highly Pathogenic Influenza Virus Infection: Mechanisms of Survival
8. Pekin and Muscovy ducks respond differently to vaccination with a H5N1 highly pathogenic avian influenza (HPAI) commercial inactivated vaccine
9. Association of Mx1 Asn631 variant alleles with reductions in morbidity, early mortality, viral shedding, and cytokine responses in chickens infected with a highly pathogenic avian influenza virus
10. Avian Influenza In Ovo Vaccination with Replication Defective Recombinant Adenovirus in Chickens: Vaccine Potency, Antibody Persistence, and Maternal Antibody Transfer
11. Avian Influenza Mucosal Vaccination in Chickens with Replication-Defective Recombinant Adenovirus Vaccine
12. Virulent Newcastle disease virus elicits a strong innate immune response in chickens
13. Comparison of Pooling 11 or 5 Oropharyngeal Swabbings for Detecting Avian Influenza Virus by Real-Time Reverse Transcription–PCR in Broiler Chickens
14. H7 avian influenza virus vaccines protect chickens against challenge with antigenically diverse isolates
15. Viral diagnostics: will new technology save the day?
16. Comparative full genome analysis of four infectious laryngotracheitis virus (Gallid herpesvirus-1) virulent isolates from the United States
17. Deletion of the M2-2 gene from avian metapneumovirus subgroup C impairs virus replication and immunogenicity in Turkeys
18. Generation and evaluation of a recombinant Newcastle disease virus expressing the glycoprotein (G) of avian metapneumovirus subgroup C as a bivalent vaccine in turkeys
19. Molecular characterization of avian astroviruses
20. The complete genome sequence and genetic analysis of ΦCA82 a novel uncultured microphage from the turkey gastrointestinal system
21. Thermal Inactivation of Avian Viral and Bacterial Pathogens in an Effluent Treatment System Within a Biosafety Level 2 and 3 Enhanced Facility
22. Comparative genomic sequence analysis of the Marek's disease vaccine strain SB-1
23. Genotypic characterization of two bacterial artificial chromosome clones derived from a single DNA source of the very virulent gallid herpesvirus-2 strain C12/130
24. Chicken interferon alpha pretreatment reduces virus replication of pandemic H1N1 and H5N9 avian influenza viruses in lung cell cultures from different avian species
25. Cross reactive cellular immune responses in chickens previously exposed to low pathogenic avian influenza
26. Pandemic H1N1 Influenza Virus in Chilean Commercial Turkeys with Genetic and Serologic Comparisons to U.S. H1N1 Avian Influenza Vaccine Isolates

27. Analysis of the Genome of the Sexually Transmitted Insect Virus Helicoverpa zea Nudivius 2
28. Characterization of Live LaSota Vaccine Strain–Induced Protection in Chickens upon Early Challenge with a Virulent Newcastle Disease Virus of Heterologous Genotype
29. Characterization of Newcastle Disease Viruses Isolated from Cormorant and Gull Species in the United States in 2010
30. Complete Genome and Clinicopathological Characterization of a Virulent Newcastle Disease Virus Isolate from South America
31. Disease of Swine
32. Early Occurrence of Apoptosis in Lymphoid Tissues from Chickens Infected with Strains of Newcastle Disease Virus of Varying Virulence
33. A single amino acid substitution in the haemagglutinin–neuraminidase protein of Newcastle disease virus results in increased fusion promotion and decreased neuraminidase activities without changes in virus pathotype
34. The cellular endosomal sorting complex required for transport pathway is not involved in avian metapneumovirus budding in a virus-like-particle expression system
35. Topology and cellular localization of the small hydrophobic protein of avian metapneumovirus
36. Clinicopathological Characterization in Poultry of Three Strains of Newcastle Disease Virus Isolated From recent Outbreaks
37. Neurological lesions in chickens experimentally infected with virulent Newcastle disease virus isolates
38. Newcastle Disease Virus
39. A Reassortment-Incompetent Live Attenuated Influenza Virus Vaccine for Protection against Pandemic Virus Strains
40. Assessment of national strategies for control of high-pathogenicity avian influenza and lowpathogenicity notifiable avian influenza in poultry, with emphasis on vaccines and vaccination
41. Avian Influenza: Public Health and Food Safety Concerns
42. Avian Influenza Viruses and Avian Paramyxoviruses in Wintering and Breeding Waterfowl Populations in North Carolina, USA
43. Homo- and Heterosubtypic Low Pathogenic Avian Influenza Exposure on H5N1 Highly Pathogenic Avian Inflenzua Virus Infection in Wood Ducks (Aix sponsa)
44. Influenza-A Viruses in Ducks in Northwestern Minnesota: Fine Scale Spatial and Temporal Variation in Pre Subtype Diversity
45. The influence of economic indicators, poultry density and the performance of Veterinary Services on the control of high-pathogenicity avian influenza in poultry
46. Thermal Inactivation of Avian Influenza Virus and Newcastle Disease Virus in a Fat-Free Egg Product

Virus Genes (2012) 44:247–252
DOI 10.1007/s11262-011-0689-2

Characterization of H5N1 highly pathogenic avian influenza viruses isolated from poultry in Pakistan 2006–2008

Jamie L. Wasilenko · Mary Pantin-Jackwood · Taseer Ahmed Khan · Ayaz Ahmed · Shafqat F. Rehmani · Nazir Ahmed Lone · David E. Swayne · Erica Spackman

Received: 22 August 2011 / Accepted: 31 October 2011 / Published online: 15 November 2011
© Springer Science+Business Media, LLC (Outside the USA) 2011

Abstract Nine avian influenza viruses (AIV), H5N1 subtype, were isolated from dead poultry in the Karachi region of Pakistan from 2006 to 2008. The intravenous pathogenicity indices and HA protein cleavage sites of all nine viruses were consistent with highly pathogenic AIV. Based on phylogenetic analysis of the HA genes, these isolates belong to clade 2.2 and both the HA and NA are closely related to each other (nucleotide identities above 99.0%) and to other Middle Eastern H5N1 AIV isolates (nucleotide identities above 98.0%). The phylogenetic data suggest that the virus in both epornitics of H5N1 HPAIV in commercial poultry in the Karachi region of Pakistan between 2006 and 2008 were from a very closely related source, however, there is inadequate epidemiological data to determine what the reservoir was for the virus between the 2006 and 2007 outbreaks other than that there was a single introduction into the region.

J. L. Wasilenko · M. Pantin-Jackwood · D. E. Swayne · E. Spackman (✉)
Southeast Poultry Research Laboratory, USDA-Agricultural Research Service, 934 College Station Rd., Athens, GA 30605, USA
e-mail: Erica.Spackman@ars.usda.gov

T. A. Khan · A. Ahmed · S. F. Rehmani · N. A. Lone
Sindh Poultry Vaccine Center, Animal Science Complex, Korangi, Karachi, Pakistan

T. A. Khan
Department of Physiology, University of Karachi, Karachi 75270, Pakistan

Keywords Avian influenza · High pathogenicity · H5N1 · Pakistan · Hemagglutinin · Neuraminidase

Introduction

Avian influenza virus (AIV) was first reported in Pakistan in 1995 when an H7N3 high pathogenicity avian influenza virus (HPAIV) infected commercial poultry [1, 2]. Since then there have been sporadic outbreaks of H7N3 HPAIV and low pathogenicity (LP) AIV and H9N2 LPAIV resulting in the loss of large numbers of poultry [2–4]. The H7N3 and H9N2 outbreaks have been controlled primarily by vaccination and biosecurity. In February 2006, the first H5N1 HPAIV outbreaks occurred in the northwest Frontier region of Pakistan in commercial poultry farms and later in 2006 extended to the capital region of Islamabad [5]. In early 2007, the H5N1 HPAIV was detected in wild birds [5], and later that same year the first human cases of H5N1 HPAIV infection in Pakistan were reported [6]. Cases of H5N1 were not reported in commercial poultry in the southern region of Pakistan (Karachi/Sindh region) until March of 2007, although a 2006 AIV isolate (A/chicken/Pakistan/NARC-228/2006) was later identified to be an H5N1 HPAIV. Similar to the other outbreaks in Pakistan, localized vaccination and stamping out procedures were employed to try to contain the virus and were temporarily successful until additional outbreaks were reported in the Karachi region in January of 2008 [5]. Pakistan declared itself free of H5N1 HPAI in September of 2008 with no further H5N1 outbreaks reported to date. In this brief report, we characterize several H5N1 isolates from Pakistan and discuss the epidemiological implications of these isolates.

Table 1 Percent nucleotide identity (HA top, NA bottom), intravenous pathogenicity index, and GenBank accession numbers for the H5N1 HPAIVs from Pakistan included in this study

Isolate name	NARC-228/06	SPVC-5/07	SPVC-8/07	SPVC-7/07	SPVC-1/08	SPVC-7/08	SPVC-8/08	SPVC-15/08	SPVC-20/08	IVPI	GenBank accession number	
											HA	NA
A/chicken/Pakistan/NARC-228/06	100	99.2	99.6	99.4	99.8	99.8	99.6	99.6	99.4	2.8	CY068896	CY068897
A/chicken/Pakistan/SPVC-5/07	99.3	100	99.4	98.9	99.4	99.4	99.1	99.2	99.6	2.5	CY068904	CY068905
A/chicken/Pakistan/SPVC-7/07	99.7	99.6	100	99.4	99.8	99.8	99.6	99.6	99.5	2.7	CY068906	CY068907
A/chicken/Pakistan/SPVC-8/07	99.4	99.0	99.4	100	99.5	99.5	99.3	99.3	99.1	2.6	CY068910	CY068911
A/chicken/Pakistan/SPVC-1/08	99.5	99.1	99.5	99.8	100	99.9	99.7	99.7	99.5	2.9	CY068900	CY068901
A/chicken/Pakistan/SPVC-7/08	99.6	99.5	99.9	99.3	99.3	100	99.7	99.7	99.5	2.7	CY068908	CY068909
A/chicken/Pakistan/SPVC-8/08	99.7	99.6	100	99.4	99.5	99.9	100	99.8	99.2	2.9	CY068912	CY068913
A/chicken/Pakistan/SPVC-15/08	99.7	99.6	100	99.4	99.5	99.9	100	100	99.3	2.8	CY068898	CY068899
A/chicken/Pakistan/SPVC-20/08	99.3	100	99.6	99.0	99.1	99.5	99.6	99.6	100	2.5	CY068902	CY068903

IVPI Intravenous pathogenicity index

Materials and methods

Viruses

Nine H5N1 HPAIV isolates (Table 1) were selected for genetic (full HA and NA gene sequencing) and pathogenicity testing to add to epidemiological and biological information about the H5N1 AIVs in Pakistan. All nine isolates were obtained from oral swabs or tracheal tissue from dead chickens suspected to be infected with AIV at commercial poultry operations in the Karachi region of Pakistan. Virus was isolated and propagated in embryonating chicken eggs as per standard methods [7].

Fig. 1 Phylogenetic analysis of the coding region of the **a** HA and **b** NA genes from Pakistani H5N1 HPAIV viruses. The tree was constructed with MEGA 4.0 using the neighbor-joining method with 1,000 bootstrap replicates. Evolutionary distances were computed using the Kimura 2-parameter method and are listed as units of the number of base substitutions per site. The trees were rooted to the A/goose/Guangdong/1/96 sequence and the nine Pakistani virus isolates referred to in this study are indicated in *bold* and other viruses from Pakistan are labeled with an *asterisk* (*)

Fig. 1 continued

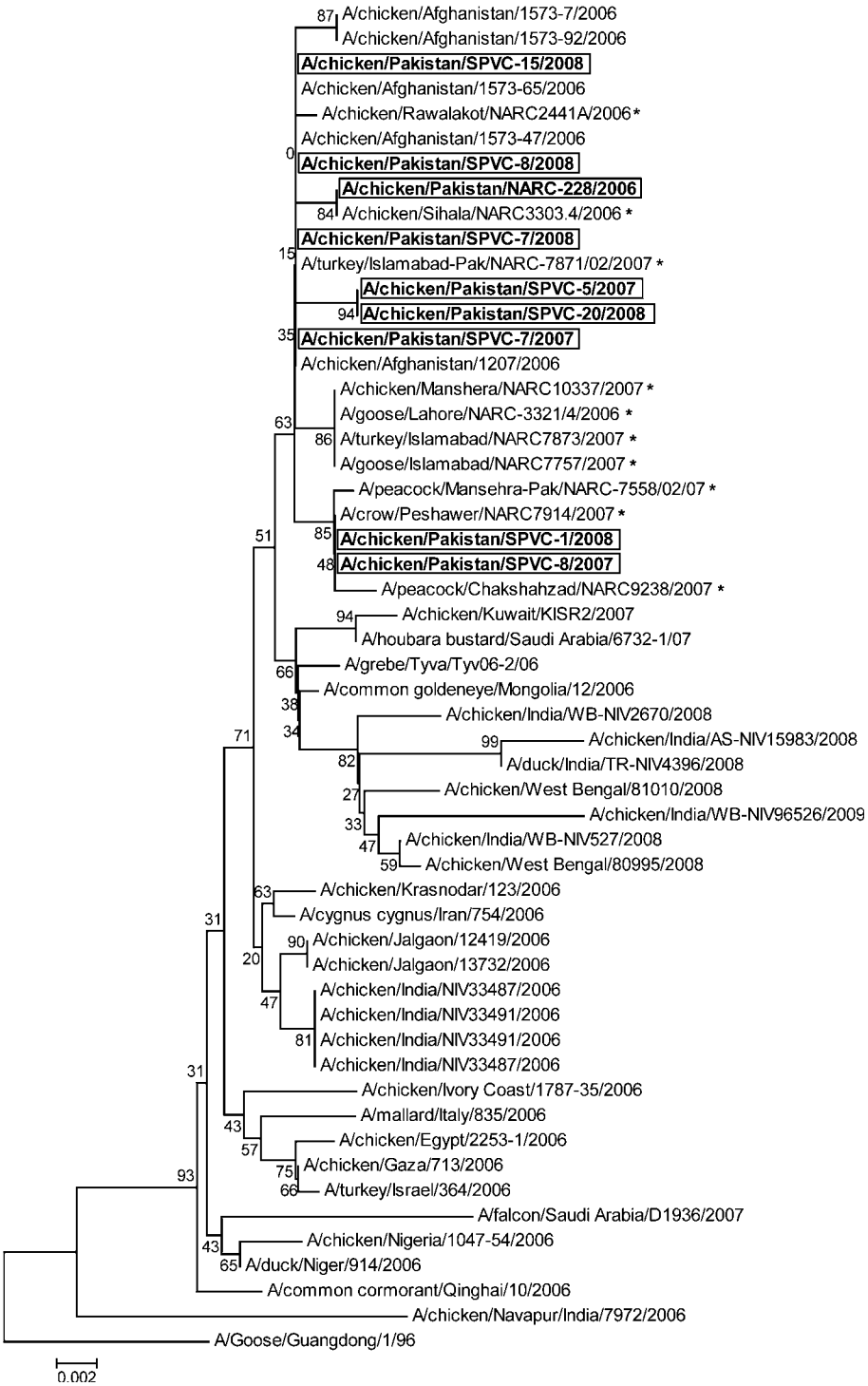

Pathogenicity testing

Pathogenicity tests for the intravenous pathogenicity index (IVPI) was conducted in accordance with the procedures of the World Organization for Animal Health (OIE) [5] at the Sindh Poultry Vaccine Center, Karachi, Pakistan. In brief, eight specific pathogen-free chickens were inoculated intravenously with each AIV isolate which had been propagated in embryonated chickens eggs. The chickens were observed for 10 days for morbidity and mortality which was used to calculate the IVPI.

Sequencing

The full HA and NA genes were sequenced directly at Southeast Poultry Research Laboratory in Athens, GA, USA, as described previously [8].

Sequence analysis

Phylogenetic analysis was conducted by aligning the sequences with the CLUSTAL W algorithm and trees were constructed with Molecular Evolutionary Genetics Analysis (MEGA) software version 4.0 [9] using the neighbor-joining method with 1,000 bootstrap replicates and evolutionary distances were computed using the Kimura 2-parameter method [10] and are listed as units of the number of base substitutions per site. Additional H5 and N1 genes were selected to include in the trees to best demonstrate the most closely related isolated and the relationship of the nine Pakistani viruses to other H5 and N1 genes within their clade and more globally, respectively. The trees were rooted to the A/goose/Guangdong/1/1996 sequence (Fig. 1).

Results

Pathogenesis studies

The IVPI for the nine isolates ranged from 2.5 to 2.9 (Table 1), which is consistent with HPAIV according to the OIE standards where isolates with a score of >1.2 are classified as HPAIV based on the OIE standard test [5].

HA and NA sequences

All nine virus isolates had the same HA proteolytic cleavage site: RRRKKR*G, which is consistent with H5 HPAIV [5, 11] and the in vivo studies. The HA gene sequences of all nine isolates assorted into clade 2.2. Among the HA genes of the nine viruses, there was 99.0–99.8% nucleotide (nt) and 98.8–99.6% amino acid (aa) identity. The NA genes of these nine viruses had 99.0–100% nt and 98.9–100% aa identity and all had a stalk deletion from residues 49 to 68. Both the HA and NA of all nine viruses were most closely related to H5N1 HPAIVs from Pakistan and Afghanistan collected during the same time frame (2006–2008) with nt identities above 98.0%.

Discussion

Characterization of the H5N1 HPAIVs from the Karachi region of Pakistan is crucial for understanding the epidemiology and biology of this virus lineage in the region and globally. Since AIV is a rapidly mutating virus and the animal health labs in Pakistan largely rely on conventional RT-PCR for the detection and identification of AIV, maintaining an up-to-date database of AIV sequence information is critical to assuring that diagnostic tests are reliable. Also, although the results of the pathogenicity tests are expected, it demonstrates that the H5N1 HPAIV has maintained its high virulence for chickens.

Isolates from the Middle East and Russia were closely related to these isolates indicating that all these clade 2.2 isolates were introduced into these regions by likely a common mechanism during 2006 when the H5N1 HPAIV spread from Southeast Asia. Consistent with this is that the NA gene from these isolates had the same NA stalk deletion reported with the viruses from the outbreak at Qinghai lake in 2005 and 2006 [12]. These outbreaks were notable as a benchmark for the spread of the H5N1 virus out of Asia in 2006 because of the infection of migratory wild birds at Qinghai Lake [13]. One epidemiological question for the virus in Pakistan is how it was maintained for 6 months while there were no reported detections in commercial poultry. One possibility is wild birds or non-commercial domestic birds harbored the virus. Successful control of H5N1 HPAIV in Pakistan was primarily accomplished by a combination of vaccination and good biosecurity in commercial poultry. Although surveillance for HPAIV in poultry in Pakistan continues and new isolates will be characterized as they are collected, presently H5N1 HPAIV appears to have been eradicated from the country and has not been isolated since 2008.

Acknowledgments The authors gratefully acknowledge Joan Beck, Joyce Bennett and Melissa Scott at Southeast Poultry Research Laboratory for technical assistance. Funding was provided by the United States Department of State Biosecurity Engagement Program through a Memorandum of Agreement with the United States Department of Agriculture, Agricultural Research Service.

References

1. K. Naeem, The Avian Influenza H7N3 Outbreak in South Central Asia. 4th international symposium on avian influenza, Athens, GA, 1997, pp. 31–35
2. K. Naeem, M. Hussain, Vet. Rec. **137**, 439 (1995)
3. K. Naeem, N. Siddique, M. Ayaz, M.A. Jalalee, Avian Dis. **51**, 189–193 (2007)
4. K. Naeem, A. Ullah, R.J. Manvell, D.J. Alexander, Vet. Rec. **145**, 560 (1999)
5. OIE, Avian influenza: home page. World Organization for Animal Health, 2008
6. WHO, Human cases of avian influenza A (H5N1) in north-west frontier province, Pakistan, October–November 2007. Wkly Epidemiol Rec, Geneva, 2008, pp. 359–364
7. D.E. Swayne, D. Senne, D.L. Suarez, in *Isolation and Identification of Avian Pathogens*, ed. by L. Dufour-Zavala, D.E. Swayne, J. Glisson, J. Pearson, W. Reed, M. Jackwood, P.

Woolcock (American Association of Avian Pathologists, Jacksonville, 2008), pp. 128–134
8. D.L. Suarez, M. Garcia, J. Latimer, D. Senne, M. Perdue, J. Virol. **73**, 3567–3573 (1999)
9. K. Tamura, J. Dudley, M. Nei, S. Kumar, Mol. Biol. Evol. **24**, 1596–1599 (2007)
10. M. Kimura, J. Mol. Evol. **16**, 111–120 (1980)
11. D.A. Senne, B. Panigrahy, Y. Kawaoka, J.E. Pearson, J. Suss, M. Lipkind, H. Kida, R.G. Webster, Avian Dis. **40**, 425–437 (1996)
12. H. Chen, Y. Li, Z. Li, J. Shi, K. Shinya, G. Deng, Q. Qi, G. Tian, S. Fan, H. Zhao, Y. Sun, Y. Kawaoka, J. Virol. **80**, 5976–5983 (2006)
13. G. Wang, D. Zhan, L. Li, F. Lei, B. Liu, D. Liu, H. Xiao, Y. Feng, J. Li, B. Yang, Z. Yin, X. Song, X. Zhu, Y. Cong, J. Pu, J. Wang, J. Liu, G.F. Gao, Q. Zhu, J. Gen. Virol. **89**, 697–702 (2008)

Vaccine 29 (2011) 7966–7974

Contents lists available at SciVerse ScienceDirect

Vaccine

journal homepage: www.elsevier.com/locate/vaccine

Development of DIVA (differentiation of infected from vaccinated animals) vaccines utilizing heterologous NA and NS1 protein strategies for the control of triple reassortant H3N2 influenza in turkeys

Leyi Wang[a,b,1], Zhuoming Qin[a,c], Mary Pantin-Jackwood[d], Olivia Faulkner[d], David L. Suarez[d], Maricarmen Garcia[e], Blanca Lupiani[f], Sanjay M. Reddy[f], Yehia M. Saif[a,b], Chang-Won Lee[a,b,*]

[a] Food Animal Health Research Program, Ohio Agricultural Research and Development Center, The Ohio State University, Wooster, OH 44691, USA
[b] Department of Veterinary Preventive Medicine, College of Veterinary Medicine, The Ohio State University, Columbus, OH 43210, USA
[c] Institute of Poultry Science, Shandong Academy of Agricultural Sciences, Jinan 250023, Peoples Republic of China
[d] Southeast Poultry Research Laboratory, USDA-ARS, Athens, GA 30605, USA
[e] Department of Avian Medicine, College of Veterinary Medicine, University of Georgia, Athens, GA 30602, USA
[f] Department of Veterinary Pathobiology, College of Veterinary Medicine & Biomedical Sciences, Texas A&M University, College Station, TX 77843, USA

ARTICLE INFO

Article history:
Received 5 April 2011
Received in revised form 1 August 2011
Accepted 14 August 2011
Available online 9 September 2011

Keywords:
Avian influenza
Triple reassortant
H3N2
DIVA
Vaccine
Turkey

ABSTRACT

Since 2003, triple reassortant (TR) swine H3N2 influenza viruses containing gene segments from human, avian, and swine origins have been detected in the U.S. turkey populations. The initial outbreak that occurred involved birds that were vaccinated with the currently available H3 swine- and avian-origin influenza vaccines. Antigenically, all turkey swine-lineage TR H3N2 isolates are closely related to each other but show little or no antigenic cross-reactivity with the avian origin or swine origin influenza vaccine strains that are currently being used in turkey operations. These results call for re-evaluation of currently available influenza vaccines being used in turkey flocks and development of more effective DIVA (differentiation of infected from vaccinated animals) vaccines. In this study, we selected one TR H3N2 strain, A/turkey/OH/313053/04 (H3N2) that showed broad cross reactivity with other recent TR turkey H3N2 isolates, and created NA- and NS-based DIVA vaccines using traditional reassortment as well as reverse genetics methods. Protective efficacy of those vaccines was determined in 2-week-old and 80-week-old breeder turkeys. The reassortant DIVA vaccines significantly reduced the presence of challenge virus in the oviduct of breeder turkeys as well as trachea and cloaca shedding of both young and old breeder turkeys, suggesting that proper vaccination could effectively prevent egg production drop and potential viral contamination of eggs in infected turkeys. Our results demonstrate that the heterologous NA and NS1 DIVA vaccines together with their corresponding serological tests could be useful for the control of TR H3N2 influenza in turkeys.

© 2011 Elsevier Ltd. All rights reserved.

1. Introduction

Influenza A viruses are segmented, single stranded, negative sense RNA viruses which belong to the *Orthomyxoviridae* family. Due to the segmented nature of the viral genome, it is possible for genetic reassortment to occur in cells infected with two or more influenza viruses resulting in drastic change in virus genotype (genetic shift) [1]. In 1998, triple reassortant (TR) H3N2 viruses with gene segments from human (polymerase basic 1 (PB1), hemagglutinin (HA), and neuraminidase (NA)), swine (nucleoprotein (NP), matrix (M), and nonstructural (NS)), and avian (polymerase basic 2 (PB2) and polymerase acid (PA)) influenza viruses were first isolated from swine populations [2], supporting the hypothesis that pigs can serve as a mixing vessel for the generation of strains with interspecies transmission potential. In 2003, Choi et al. [3] reported the first isolation of TR H3N2 from turkeys in two geographically distant farms in the U.S. Further antigenic and genetic analysis led to speculation [3] and subsequent confirmation [4] that not only interspecies transmission from swine to turkeys but also intraspecies transmission among turkeys occur. Since 2003, TR H3N2 virus infection in turkeys has been reported in several farms in the U.S. and Canada [5,6], raising concerns about control of this new virus lineage.

It is well known that biosecurity is the first line of defense to protect birds from any pathogen. However, biosecurity alone

* Corresponding author at: 1680 Madison Avenue, Wooster, OH 44691, USA. Tel.: +1 330 2633750; fax: +1 330 2633677.
E-mail address: lee.2854@osu.edu (C.-W. Lee).
[1] Present address: Division of Infectious Diseases, Cincinnati Children's Hospital Medical Center, Cincinnati, OH 45229, USA.

0264-410X/$ – see front matter © 2011 Elsevier Ltd. All rights reserved.
doi:10.1016/j.vaccine.2011.08.067

sometimes is not enough to stop the spread of influenza virus [7]. To complement the prevention and control effort against influenza, vaccines have sporadically been used in the U.S. to control low pathogenic avian influenza outbreaks [8]. Vaccination can increase resistance of poultry to virus infection, protect poultry against morbidity and mortality, and reduce virus shedding and egg-production losses. The use of inactivated vaccines allowing differentiation of infected from vaccinated animals (DIVA), together with strict biosecurity and serological surveillance, have been successfully used to control H7N1 and H7N3 outbreaks in Italy [9]. For the control of turkey TR H3N2 avian influenza, a commercial inactivated monovalent DIVA vaccine made with the A/duck/Minnesota/79 (H3N4) strain is available, however, this vaccine strain shows poor antigenic cross reactivity against currently circulating field strains and could not provide turkey breeder hens effective protection against recent TR H3N2 isolate challenge [10]. Thus, there is an urgent need to update vaccine seed strains and development of more efficacious vaccines.

Several strategies have been used to develop inactivated vaccines to comply with a DIVA program. The heterologous NA strategy is based on the rationale that the same HA in both vaccine strain and field viruses will provide protection to immunized birds, while a different NA in vaccine strain and field virus could be used to differentiate infected from vaccinated birds [9,11]. However, this strategy cannot be used in certain countries or regions where many subtypes of influenza virus are circulating in the field at the same time. To overcome this problem, vaccine strains with a rare NA have been generated by classical reassortment or reverse genetics methods [12–14]. On the other hand, a DIVA program based on antibody response against non-structural protein (NS1) has been tested in horses and poultry [15–17]. Since NS1 protein is a non-structural protein, theoretically anti-NS1 antibodies can be detected only in the serum samples of infected animals and not in vaccinated animals by serological tests [15,18,19]. Experimentally, this approach failed with commercial inactivated vaccines in chickens [16]. It was speculated that commercial inactivated vaccines are contaminated with small amounts of residual NS1 protein due to partial purification of vaccine virus after amplification in eggs, and thus vaccinated chickens will have antibodies against NS1 protein. By diluting serum before serological test, this strategy could differentiate infected from vaccinated birds experimentally [16]. However, field evidence on the efficacy of the NS1 DIVA strategy is still lacking. Recently, immunodominant 5B19 epitope of the S2 glycoprotein of murine hepatitis virus inserted into NA, or tetanus toxoid as exogenous markers were used in vaccines for serological differentiation between vaccinated and infected chickens [20,21]. The main drawback of both new marker vaccines is the inability to differentiate vaccinated and subsequently infected birds from vaccinated birds.

In the present study, we selected a turkey TR H3N2 isolate which shows broad cross reactivity with other recent turkey TR H3N2 subtype viruses, and utilized heterologous NA and NS1 protein strategies to generate DIVA vaccines. Vaccine efficacy was evaluated in both 2-week-old and 80-week-old breeder turkeys and N2- and NS1-enzyme-linked immunosorbent assay (ELISA), modified Neuraminidase inhibition (NI) assay, and NS1-fluorescence microsphere immunoassay (FMIA) were evaluated as DIVA serological tests.

2. Materials and methods

2.1. Viruses, cells and birds

The virus strains used in this study, A/turkey/OH/313053/04 (H3N2), A/duck/LA/B174/86 (H8N4), and A/turkey/OR/71-Ddel-pc4 (H7N3) [22] were obtained from the repository of the Food Animal Health Research Program (OSU, Wooster, OH) and were passaged once in 10-day-old specific pathogen free (SPF) embryonated chicken eggs (ECEs) (SPAFAS, Inc., Norwich, CT) to propagate viruses for the study from the stock strains. MDCK (Madin Darby canine kidney) and 293-T (human kidney cells, kindly provided by Dr. Yoshihiro Kawaoka at the University of Wisconsin) cells were grown and maintained in Dulbecco's modified Eagle's medium (DMEM) supplemented with 10% fetal bovine serum and 1% gentamicin. Cells were incubated in a 37 °C incubator with 5% CO_2. Experimental turkeys were obtained from turkey flocks maintained at the Ohio Agricultural Research and Development Center, Wooster, OH.

2.2. Generation of reassortant viruses by traditional reassortment method

The parental viruses, A/turkey/OH/313053/04 (H3N2) and either A/duck/LA/B174/86 (H8N4) or A/turkey/OR/71-Ddel-pc4 (H7N3), were mixed in a proportion of 1:1 and inoculated into the allantoic cavity of 10-day-old SPF ECE [26]. Three days post inoculation, allantoic fluid was harvested and used for plaque assay to purify reassortant viruses as previously described [23]. In brief, confluent monolayers of MDCK cells in 6 well plates were infected with 10-fold serial dilutions of allantoic fluid. After adsorbing the virus at 37 °C for 1 h, infected cells were overlaid with 1% agar in serum free media supplemented with 0.75 μg/ml of trypsin (Sigma–Aldrich, St. Louis, MO). Three days after infection, a second agar overlay was done with an addition of neutral red (Sigma). Individual plaques were picked and resuspended into 0.5 ml sterile phosphate buffered saline (PBS) followed by inoculation into ECEs for amplification. Viral RNA was extracted with the RNeasy Mini kit (Qiagen, Valencia, CA) from allantoic fluids as previously described [24]. Standard RT-PCR was first carried out with the Qiagen one-step RT-PCR kit (Qiagen) using H3 and N4 or NS specific primers followed by direct sequencing of the PCR product. Additional sequencing was performed on the remainder genes to confirm the genetic makeup of the reassortant viruses. Sequencing was done in an ABI PRISM 377 DNA sequencer at the Molecular and Cellular Imaging Center (Ohio Agricultural Research and Development Center, Wooster, OH).

2.3. Generation of reassortant viruses by reverse genetics

RNA from A/turkey/OH/313053/04 (H3N2) was extracted with the RNeasy mini kit (Qiagen, Valencia, CA) from infected allantoic fluid. All eight gene segments of A/turkey/OH/313053/04 (H3N2) were amplified by RT-PCR and cloned into pHH21 transcriptional vector between the promoter and terminator sequences of RNA polymerase I. The transcription plasmids that contain the NS genes of A/turkey/OR/71-Ddel-pc3 (H7N3) was previously described [22]. Four expression plasmids (pCAGGS-WSN-NP, pcDNA774-PB1, pcDNA762-PB2, and pcDNA787-PA) were kindly provided by Dr. Yoshihiro Kawaoka [25]. Recombinant viruses (rTK/OH/04-Ddel-pc3 (H3N2) and rTK/OH/04-Ddel-pc4 (H3N2)) containing the NS gene segment from either A/turkey/OR/71-Ddel-pc3 (H7N3) or A/turkey/OR/71-Ddel-pc4 (H7N3) and remaining gene segments from A/turkey/OH/313053/04 (H3N2) were generated in 293-T cells by reverse genetics as described previously [25]. The rescued viruses were propagated in 10-day-old ECE to make working stocks. The authenticity of the recovered reassortant viruses was verified by sequencing.

2.4. Immunization with inactivated vaccines and challenge studies in young and breeder turkeys

Vaccination studies were undertaken in four groups of 2-week-old turkeys (six birds per group), including three vaccine groups and one non-vaccination control group. Infectious allantoic fluids containing wild type A/turkey/OH/313053/04 (H3N2) (TK/OH/04 wt), and reassortant DIVA vaccine strains, rH3N4 and rH3N3-NS-Ddel-pc4 (rH3N3-NSdel), were inactivated with 0.1% β-propiolactone. Montanide™ ISA-70 VG adjuvant (Seppic, France) was mixed with inactivated viruses in a proportion of 2.3:1 and administered into turkeys subcutaneously in the nape of the neck (0.5 ml/turkey). Two weeks post vaccination, sera were collected to test for HA and NA specific antibody responses by the hemagglutination inhibition (HI) [26] and neuraminidase inhibition (NI) tests, respectively, followed by challenge with 10^6 EID_{50}/0.2 ml of wild type A/turkey/OH/313053/04 (H3N2) by intranasal inoculation. At 2 and 5 days post challenge (DPC), tracheal and cloacal swabs from all four groups were collected. Individual swabs were placed into 1.5 ml of PBS containing 1% gentamicin. RNA was extracted from the tracheal and cloacal swabs suspensions using the Viral RNA kit (Qiagen). Virus load was quantified by real-time RT-PCR as described previously [12,24]. Birds were observed for 14 days for clinical signs of disease and serum samples were collected on the last day to check antibody response to HA and NA by HI and NI assays, respectively.

Similar vaccination and challenge study was also done in four groups of 80-week-old breeder turkeys (n = 8 per group). Vaccination and challenge protocols were the same as described above. At 2 and 4 DPC, tracheal and cloacal swabs were collected for virus isolation. At 7 DPC, 2 birds from each group were bled to collect sera and euthanized. Tissues (trachea, lung, kidney, spleen, portions of small and large intestine, and four different parts of the oviduct) were collected and preserved in 10% neutral buffered formalin for histopathology. Infundibulum, magnum, isthmus, and uterus (1 g each) of the oviduct were also collected separately to determine viral load. At 14 DPC, sera were collected from remaining birds to check HA and NA specific antibody responses by HI and NI tests, respectively.

Tissues fixed in 10% neutral buffered formalin were embedded in paraffin and 5 μm sections were prepared and stained with hematoxylin and eosin (HE) as previously described [27]. Based on the extent of histopathological lesions, tissues with no lesion were scored as "−", mild lesions as "+", moderate lesions as "++", and severe lesions as "+++".

2.5. Immunization with live vaccines and challenge studies in young turkeys

Two vaccine groups were inoculated with 10^6 EID_{50}/0.2 ml of live vaccine candidates (rTK/OH/04-Ddel-pc3 (H3N2) and rTK/OH/04-Ddel-pc4 (H3N2)) by the intranasal route. Immunizations with live and inactivated vaccines in young turkeys were done at the same time and the same non-vaccinated challenge control group described above was used in both experiments. Two weeks post vaccination sera were collected to test specific influenza virus antibody responses by HI test. Virus challenge was done as described above for inactivated vaccines. At 2 and 5 DPC, tracheal and cloacal swabs from vaccinated and non-vaccinated challenged groups were collected for virus isolation. Birds were observed for 14 days for clinical signs and serum samples were collected at the end of the experiment to check HA antibody responses by HI test.

2.6. N2 and NS1 protein-based serological tests

ELISA and FMIA were used to detect anti-NS1 antibody as described [28]. For FMIA assay, purified recombinant NP and NS1 proteins were bound to carboxyl-functionalized fluorescent polystyrene microspheres (Luminex Inc., Austin, TX) using the Bio-Plex Amine Coupling Kit (BioRad Laboratories, Hercules, CA) as per the manufacturer's instructions. Unused sites in the coated microsphere were blocked with 1% BSA in PBS. Coupled microspheres were incubated with 100 μl serum diluted 1:100 in PBS (1% BSA) for 30 min at room temperature in the dark. Following two washes with 200 μl of assay buffer, plates were incubated with 50 μl of 0.5 μg/ml biotinylated donkey anti-chicken IgY (Jackson ImmunoResearch Laboratories Inc., West Grove, PA) for 30 min at room temperature (RT). Plates were further washed twice with assay buffer and incubated with 50 μl of 10 μg/ml streptavidin–phycoerythrin conjugates for 30 min at RT. Following two additional washes, beads were resuspended in 125 μl assay buffer per well, analyzed with a Luminex100 instrument, data collected with the IS2.3 software (Luminex Inc., Austin, TX) and results were expressed as mean fluorescence intensity (MFI). The cut-off of NS1- and NP-FMIA was set as 1500 and 5000, respectively, as previously described [28].

N2-ELISA was performed as previously described [29] using a baculovirus expressed N2 protein from A/turkey/OH/313053/04 (H3N2) virus. The expression of N2 protein was optimized, and purified protein was utilized for ELISA. The antigen and sera concentrations used in the ELISA were optimized using a homologous N2 turkey polyclonal antisera.

N2 antibody titers were also determined using an NI assay. The substrate 2′-(4-methylumbelliferyl)-α-D-*N*-acetylneuraminic acid sodium salt hydrate (MUN; Sigma Chemical Co., St. Louis, MO) reacts with *N*-acetylneuraminic acid yielding fluorescent 4-methylumbelliferone [30]. Neuraminidase activity was determined by adding 7.6 μM MUN to a 2-fold dilution of BPL-inactivated A/turkey/OH/313053/04 (H3N2) in calcium saline (CaS; 20 mM sodium borate, 7 mM calcium chloride, 154 mM sodium chloride, and 12.5 mM sodium acetate; at pH 7.2). Relative 4-methylumbellifrone fluorescence versus the inverse virus dilution ($1/x$, where $x = \log_2$ dilution factor) was determined to find the fluorescence linear limit of the assay for this N2 protein. A 96-well plate was blocked with BSA (50 mM Tris–HCl, 0.14 M NaCl, 1% BSA at pH 8.0) for 30 min, and washed with wash buffer (50 mM Tris–HCl, 0.14 M NaCl, 0.05% Tween 20 at pH 8.0). Turkey sera were pretreated in 0.5% milk in PBS for 30 min. A black flat-bottom 96-well plate was blocked with BSA for 30 min and washed. Serum samples were diluted 4-fold in BPL-inactivated A/turkey/OH/313053/04 (H3N2) that was diluted 1:8 in PBS. BPL-inactivated A/turkey/OH/313053/04 (H3N2) was diluted 2-fold in PBS to determine the fluorescence signal. Serum samples were incubated with the virus at room temperature for 15 min. After incubation, 7.6 μM MUN CaS (1:1 with the virus dilution) was added to each well. Normal turkey serum was added to BPL-inactivated A/turkey/OH/313053/04 (H3N2) that was diluted 1:8 in CaS to account for non-specific antibody binding to the NA that would block the fluorescent signal. The kinetic production of 4-methylumbelliferone was measured every 3 min for 15 min at 360 nm excitation wavelength and at 460 nm emission wavelength using a Synergy HT Multi-Detection microplate reader that was warmed to 37 °C (Bio-Tek, Winooski, VT). Fluorescence readings lower than the normal sera were considered as neuraminidase inhibitory. Sera that were neuraminidase inhibitory above $3 \log_2$ were considered N2-positive. Selected samples were also tested with A/turkey/MO/24093/99 (H1N2), which has a related neuraminidase gene but a heterologous hemagglutinin gene using the same procedure as described above.

2.7. Statistical analyses

To determine the significant differences of virus shedding in the trachea and cloaca of turkeys between vaccinated and

Table 1
Protection of 2-week-old turkeys vaccinated with inactivated DIVA vaccines after challenge with 10^6 EID_{50}/0.2 ml of A/turkey/OH/313053/04 (H3N2) virus.

Vaccine group	Viral load[a]					Average HI titer[c]	
		2 DPC[b]		5 DPC		14 DPV[d]	14 DPC
TK/OH/04 wt	Tracheal	3/6[e]	0.9 + 0.7[f,*]	2/6	0.6 + 0.3[*]	7.5 + 0.6	8.8 + 0.4
	Cloacal	2/6	1.5 + 0.1	5/6	1.3 + 0.3		
rH3N4	Tracheal	5/6	1.3 + 0.4[*]	6/6	1.6 + 0.6	6.5 + 0.6	9.2 + 0.4
	Cloacal	6/6	1.5 + 0.5	3/6	1.3 + 0.7		
rH3N3-NSdel	Tracheal	5/6	1.2 + 0.7[*]	5/6	0.8 + 0.5[*]	7.5 + 0.8	10.2 + 0.8
	Cloacal	4/6	1.6 + 0.3	3/6	0.8 + 0.2[*]		
Non-vaccinated control	Tracheal	6/6	2.2 + 0.8	6/6	2.2 + 1.0	<2	10.2 + 1.7
	Cloacal	5/6	1.1 + 0.4	5/6	2.3 + 1.0		

[a] Virus titers were obtained by extrapolation from real-time RT-PCR assay.
[b] Days post-challenge.
[c] The HI titer is expressed as the $\log_2$ reciprocal of the endpoint in a twofold dilution of sera.
[d] Days post-vaccination.
[e] Number of birds positive/number tested.
[f] Average virus titer is expressed as $\log_{10}$ EID_{50}/ml + standard deviation.
[*] Indicates $P < 0.05$ compared to virus titer from unvaccinated-challenge control group.

non-vaccinated control groups, non-parametric Mann–Whitney test was performed. *P*-values were set at 0.05 ($P < 0.05$).

3. Results

3.1. Screening and selection of reassortant viruses for seed vaccine

Infectious allantoic fluid from eggs co-inoculated with A/turkey/OH/313053/04 (H3N2) and either A/duck/LA/B174/86 (H8N4) or A/turkey/OR/71-Ddel-pc4 (H7N3) were extensively screened by plaque purification followed by gene segment specific RT-PCR. All eight gene segments of several plaque purified viruses that had HA gene from A/turkey/OH/313053/04 (H3N2) and NA or NS gene from other two viruses were sequenced and two DIVA vaccine strains, rH3N4 and rH3N3-NSdel, were selected. After desired reassortant viruses, NA-based DIVA strain rH3N4 and NS1-based DIVA strain rH3N3-NSdel, were identified, the composition of internal genes were also determined by sequencing. Reassortant rH3N4 virus has HA, NP, and M genes from A/turkey/OH/313053/04 (H3N2), and remaining genes from A/duck/LA/B174/86 (H8N4). Reassortant rH3N3-NSdel virus has HA and PB2 genes from A/turkey/OH/313053/04 (H3N2), and remaining genes from A/turkey/OR/71-Ddel-pc4 (H7N3). Both rH3N4 and rH3N3-NSdel viruses replicated well in ECE and the titers of stock viruses ($10^{7.3}$ and $10^{8.3}$ EID_{50}/ml, respectively) were comparable to that of wild type A/turkey/OH/313053/04 (H3N2) ($10^{7.7}$ EID_{50}/ml) virus. Two recombinant viruses (rTK/OH/04-Ddel-pc3 (H3N2) and rTK/OH/04-Ddel-pc4 (H3N2)) containing the NS gene segment from either A/turkey/OR/71-Ddel-pc3 (H7N3) or A/turkey/OR/71-Ddel-pc4 (H7N3) and remaining gene segments from A/turkey/OH/313053/04 (H3N2), generated by reverse genetics showed titers of $10^{6.8}$ and $10^{6.0}$ EID_{50}/ml, respectively.

3.2. Efficacy of inactivated vaccines in 2-week-old turkeys

Two weeks after a single vaccination, both rH3N4 and rH3N3-NSdel inactivated vaccines elicited similar antibody immune responses against HA protein as the vaccine made with wild type strain (Table 1). Compared to the non-vaccinated control group, vaccination with rH3N4 significantly reduced virus shedding in the trachea at 2DPC, and vaccination with rH3N3-NSdel significantly prevented virus shedding in trachea at 2 and 5 DPC and in cloaca at 5 DPC. In birds vaccinated with wild type vaccine, the level of virus shedding in trachea and cloaca at 2 and 5 DPC was similar to birds vaccinated with recombinant vaccines; however less number of birds was positive for virus shedding in trachea at 2 and 5 DPC and cloaca at 2 DPC. On the contrary, less number of birds vaccinated with recombinant vaccines shed viruses in cloaca at 5 DPC (Table 1).

3.3. Efficacy of inactivated vaccines in 80-week-old breeder turkeys

Both reassortant DIVA vaccines induced similar HA antibody immune responses to the wild type vaccine after a single immunization in breeder turkeys (Table 2). Vaccination with rH3N4 and rH3N3-NSdel significantly reduced virus shedding in cloaca at 4 DPC compared to the non-vaccinated control group. In addition, compared to non-vaccinated challenge control group, immunization with TK/OH/04 wt (H3N2) and DIVA vaccines significantly reduced challenge virus shedding in all four sections of the oviduct, as no virus or very low levels of virus ($10^{1.1}$ EID_{50}/ml) were detected in vaccinated birds compared to higher virus levels ($10^{2.5}$–$10^{3.9}$ EID_{50}/ml) in non-vaccinated control birds (Table 2). In the non-vaccinated control group, the higher levels of virus present in the oviduct explain the effect of virus infection in breeder turkeys observed in the field in which decreased in egg production is characteristic.

Histopathologic examination of trachea, lung, spleen, and kidney collected at 7 DPC showed no difference in these organs among vaccinated and non-vaccinated groups (data not shown). Lesions consisted of mild to moderate hyperplasia of tracheal epithelium with mild infiltration of lymphocytes and heterophils; mild congestion and peribronchial lymphohistiocytic infiltration in lungs; mild lymphoid depletion in spleen; and mild to severe tubule necrosis and associated lymphocytic interstitial nephritis. However, lesions in the large intestine and especially in the oviduct were more severe in the non-vaccinated group compared to the vaccinated groups, and included moderate lymphocytic infiltration in large intestines, and mild to moderate degeneration of the oviduct epithelium and generalized glandular atrophy as well as cysts present in the glands especially in the uterus.

3.4. Efficacy of live vaccine candidate in 2-week-old turkeys

At 2 weeks post vaccination, immune response induced by the live vaccines (Table 3) were about 3 $\log_2$ lower than that induced by inactivated wild type vaccine (Table 1). Compared to non-vaccinated challenge control group, rTK/OH/04-Ddel-pc3 (H3N2)

Table 2
Protection of 80-week-old turkeys vaccinated with inactivated DIVA vaccines after challenge with 10^6 EID_{50}/0.2 ml of A/turkey/OH/313053/04 (H3N2) virus.

Vaccine group	Viral load[a]							Average HI titer[c]	
		2 DPC[b]		4 DPC		7 DPC		14 DPV[d]	14 DPC
TK/OH/04 wt	Tracheal	6/8[e]	1.6 + 0.2[f]	7/8	1.9 + 0.4			6.3 + 1.3	8.0 + 1.1
	Cloacal	6/8	2.0 + 0.5	8/8	1.7 + 0.3				
	Infundibulum					0/2	0		
	Magnum					0/2	0		
	Isthmus					1/2	1.1		
	Uterus					0/2	0		
rH3N4	Tracheal	7/8	1.7 + 0.4	6/8	1.5 + 0.2			6.4 + 2.1	7.8 + 2.1
	Cloacal	7/8	1.8 + 0.2	2/8	1.8 + 0.5*				
	Infundibulum					0/2	0		
	Magnum					0/2	0		
	Isthmus					0/2	0		
	Uterus					0/2	0		
rH3N3-NSdel	Tracheal	4/8	1.6 + 0.8	7/8	1.6 + 0.4			7.3 + 1.3	7.6 + 2.1
	Cloacal	6/8	1.2 + 0.2	7/8	1.4 + 0.4*				
	Infundibulum					0/2	0		
	Magnum					0/2	0		
	Isthmus					0/2	0		
	Uterus					0/2	0		
Non-vaccinated control	Tracheal	7/8	1.8 + 0.5	5/8	1.7 + 0.4			<2.0	8.4 + 2.6
	Cloacal	7/8	1.6 + 0.5	8/8	2.5 + 1.2				
	Infundibulum					1/2	3.8		
	Magnum					2/2	2.5 + 0.2		
	Isthmus					1/2	3.9		
	Uterus					2/2	2.6 + 1.9		

[a] Virus titers were obtained by extrapolation from real-time RT-PCR assay.
[b] Days post-challenge.
[c] The HI titer is expressed as the $\log_2$ reciprocal of the endpoint in a twofold dilution of sera.
[d] Days post-vaccination.
[e] Number of birds positive/number tested.
[f] Average virus titer is expressed as $\log_{10}$ EID_{50}/ml + standard deviation.
* Indicates $P < 0.05$ compared to virus titer from unvaccinated-challenge control group.

and rTK/OH/04-Ddel-pc4 (H3N2) vaccination significantly reduced both the number of birds shedding and amount of virus shedding in trachea (Table 3). Although the antibody immune response induced by live vaccination was lower than by inactivated vaccines, live vaccines provided comparable protection to inactivated vaccines (Tables 1 and 3).

3.5. N2 and NS1 serological tests to differentiate infected from vaccinated birds

To evaluate the usefulness of N2-ELISA and NI assays in differentiation of infected and vaccinated birds, serum samples collected from young turkeys and breeder turkeys at 2 weeks post vaccination (wpv) by inactivated vaccines and at 2 weeks post challenge (wpc) were tested (Table 4). In the young turkey experiment, serum samples from all non-vaccinated and vaccinated groups were anti-N2 antibody negative at 2 wpv according to the N2-ELISA; however, 3 out of 6 TK/OH/04 wt (H3N2), rH3N4, or rH3N3-NS1del vaccinated young turkeys were N2-positive 2 wpv by NI assay. At 2 wpc, all 6 birds in the non-vaccinated and wild type vaccinated groups, 3 out of 6 birds in the rH3N4 group and none in the rH3N3-NSdel group were positive for N2 antibodies by ELISA. Based on NI assay result, the rH3N3-NS1del vaccinated young turkeys had a four-fold increase in N2 antibody titers and the non-vaccinated young turkeys increased by 5.0 $\log_2 \pm 0.6$. Selected samples from the young turkeys were also tested with the

Table 3
Protection of 2-week-old turkeys vaccinated with live DIVA vaccines after challenge with 10^6 EID_{50}/0.2 ml of A/turkey/OH/313053/04 (H3N2) virus.

Vaccine group	Viral load[a]					Average HI titer[c]	
		2 DPC[b]		5 DPC		14 DPV[d]	14 DPC
rTK/OH/04-Ddel-pc3 (H3N2)	Tracheal	3/6[e]	1.2 + 0.4[f,*]	3/6	1.3 + 0.6*	4.7 + 0.8	7.5 + 1.1
	Cloacal	5/6	1.4 + 0.3	3/6	0.8 + 0.6		
rTK/OH/04-Ddel-pc4 (H3N2)	Tracheal	2/6	0.9 + 0.7*	3/6	1.6 + 0.8	3.8 + 2.2	8.3 + 1.8
	Cloacal	5/6	2.2 + 1.1	4/6	1.0 + 0.3		
Non-vaccinated control	Tracheal	6/6	2.2 + 0.8	6/6	2.2 + 1.0	<2	10.2 + 1.7
	Cloacal	5/6	1.1 + 0.4	5/6	2.3 + 1.0		

[a] Virus titers were obtained by extrapolation from real-time RT-PCR assay.
[b] Days post-challenge.
[c] The HI titer is expressed as the $\log_2$ reciprocal of the endpoint in a twofold dilution of sera.
[d] Days post-vaccination.
[e] Number of birds positive/number tested.
[f] Average virus titer is expressed as $\log_{10}$ EID_{50}/ml + standard deviation.
* Indicates $P < 0.05$ compared to virus titer from unvaccinated-challenge control group.

Table 4
Antibody response to N2 protein in turkeys vaccinated with inactivated wild type and DIVA vaccines and challenged with A/turkey/OH/313053/04 (H3N2) virus as determined by an indirect N2-ELISA and neuraminidase inhibition (NI) assay.

Vaccine group	N2-ELISA				NI Assay			
	Young Turkeys		Breeder Turkeys		Young Turkeys		Breeder Turkeys	
	2 wpv[a]	2 wpc[b]	2 wpv	2 wpc	2 wpv	2 wpc	2 wpv	2 wpc
TK/OH/04 H3N2 wt	0/6[c]	6/6	2/5	5/5	3/6 (6.7 ± 0.3)[d]	3/6 (6.0 ± 0.6)	5/6 (4.6 ± 0.4)	3/6 (5.0 ± 1.0)
rH3N4	0/6	3/6	4/8	4/8	3/6 (6.3 ± 0.3)	2/6 (6.0 ± 1.0)	3/8 (5.0 ± 0.6)	3/8 (4.7 ± 0.3)
rH3N3-NS1del	0/6	0/6	4/8	4/8	3/6 (4.7 ± 0.3)	6/6 (6.8 ± 0.9)*	6/8 (4.2 ± 0.2)	2/8 (7.5 ± 3.5)
Non-vaccinated control	0/6	6/6	0/8	4/8	0/6 (0)	4/6 (5.0 ± 0.6)*	0/8 (0)	5/8 (5.0 ± 0.3)*

[a] Week post vaccination.
[b] Week post challenge.
[c] Number of birds positive/number tested.
[d] Mean ± SEM N2-positive antibody titer.
* Indicates $P < 0.05$ difference between 2 wpv and 2 wpc within turkey age and vaccine group.

A/turkey/MO/24093/99 (H1N2) antigen because of concerns about steric hindrance from the HA protein giving false positive results. All the samples tested after vaccination, but before challenge were seronegative with this antigen. Several of the birds after challenge seroconverted, but at lower titers than when using the H3N2 antigen (data not shown). In the case of 80-week-old breeder turkeys, in contrast to the results in young turkey experiment, some of the birds in the vaccinated group were N2 positive at 2 wpv. As in young turkey experiment, all birds in wild type vaccinated group were anti-N2 sero-positive after challenge but not all serum samples from rH3N4 and rH3N3-NSdel vaccinated groups and unvaccinated control group turned to anti-N2 sero-positive after challenge. Previous avian influenza virus infection history of the breeder turkeys was unknown.

NS1-ELISA and FMIA were used to evaluate NS1 as a marker to differentiate infected from vaccinated birds. In the young turkey experiment with killed vaccines, serum samples from the non-vaccinated group and vaccine groups of wild type virus and rH3N3-NSdel were anti-NS1 antibody negative tested by either NS1-ELISA or FMIA at 2 wpv (Table 5). Only one bird from the rH3N4 vaccinated group tested had anti-NS1 antibodies by both assays at 2 wpv. In contrast, some birds from all vaccinated groups, two from wild type vaccinated group, three from rH3N4 group, and five from rH3N3-NSdel group, had anti-NP antibodies by NP-FMIA at 2 wpv. At 2 wpc, 4 out of 6 birds in the non-vaccinated group, 2 out of 6 birds in the rH3N4 group, 1 out of 6 in the wild type virus vaccinated group, and none in the rH3N3-NSdel group were positive for NS1 antibodies tested by NS1-ELISA, while five from the non-vaccinated group, one from either wild type virus or rH3N4 vaccine groups, and none in the rH3N3-NSdel group were positive for NS1 antibodies tested by NS1-FMIA. All serum samples from non-vaccinated and vaccinated groups were positive for NP antibody by NP FMIA. In the case of breeder turkeys, all inactivated vaccine groups and the non-vaccinated control group showed 100% positivity for anti-NS1 antibody at 2 wpv (data not shown), suggesting that these breeder turkeys may have previous influenza virus infection.

The two live vaccine strains with NS deletion genes, rTK/OH/04-Ddel-pc3 (H3N2) and rTK/OH/04-Ddel-pc4 (H3N2), were also used to vaccinate 2-week-old turkeys. The NS1-ELISA and FMIA serological results are shown in Table 6. Similar to results of birds with killed vaccines, all birds from the two live vaccinated groups were negative for anti-NS1 antibodies by both NS1-ELISA and FMIA at 2 wpv. There was only one bird in live rTK/OH/04-Ddel-pc3 (H3N2) vaccine group positive for NP antibodies at 2 wpv. At 2 wpc, only one bird from rTK/OH/04-Ddel-pc4 (H3N2) group was positive for anti-NS1 antibodies by both NS1-ELISA and FMIA. In contrast, with the NP-FMIA serological test, all birds from both live vaccinated groups and nonvaccinated control group were positive for NP antibody.

4. Discussion

Since 1998, TR H3N2 virus has been successfully established in swine population. Since influenza interspecies transmission between swine and turkeys had previously occurred, turkey producers started immunizing turkey breeders with autogenous killed swine TR H3N2 virus vaccines or the A/duck/Minnesota/79 (H3N4) vaccine commercially available that could potentially be used as a DIVA vaccine [10]. However, since 2003, several TR H3N2 outbreaks have been reported not only from unvaccinated but also from vaccinated turkey flocks. Subsequent genetic and antigenic studies demonstrated that despite a high percentage of genetic similarity between them, turkey H3N2 viruses were antigenically poorly related to the swine-origin TR vaccine virus. In addition, both poor antigenic reactivity and low genetic similarity were observed between the turkey isolates and the commercial H3N4 duck-origin vaccine strain, which was further confirmed by a recent protection-challenge study [10]. Taken together, field and

Table 5
Antibody response to NS1 protein in 2-week-old turkeys immunized with killed vaccines as detected by an indirect NS1-ELISA and fluorescence microsphere immunoassays (FMIA).

Vaccine group	NS1-ELISA		NS1-FMIA		NP-FMIA	
	2 wpv[a]	2 wpc[b]	2 wpv	2 wpc	2 wpv	2 wpc
TK/OH/04 wt	0/6[c] (0)[d]	1/6 (0.09)	0/6 (0)[e]	1/6 (3772)	2/6 (7941 + 1590)	6/6 (17,563 + 5835)
rH3N4	1/6 (0.42)	2/6 (0.19 + 0.09)	1/6 (7018)	1/6 (3411)	3/6 (12,781 + 3661)	6/6 (19,069 + 6532)
rH3N3-NSdel	0/6 (0)	0/6 (0)	0/6 (0)	0/6 (0)	5/6 (15,740 + 7957)	6/6 (23,126 + 323)
Unvaccinated control	0/6 (0)	4/6 (0.132 + 0.04)	0/6 (0)	5/6 (3033 + 1151)	0/6 (0)	6/6 (20,604 + 2147)

[a] Week post vaccination.
[b] Week post challenge.
[c] Number of birds positive/number tested.
[d] Mean OD value + standard deviation.
[e] Mean fluorescent intensity + standard deviation.

Table 6
Antibody response to NS1 protein in 2-week-old turkeys immunized with live vaccines as detected by an indirect NS1-ELISA and fluorescence microsphere immunoassays (FMIA).

Group	NS1-ELISA		FMIA		NP-FMIA	
	2 wpv[a]	2 wpc[b]	2 wpv	2 wpc	2 wpv	2 wpc
rTK/OH/04-Ddel-pc3 (H3N2)	0/6[c] (0)[d]	0/6 (0)	0/6 (0)[e]	0/6 (0)	1/6 (6578)	6/6 (16943 + 3576)
rTK/OH/04-Ddel-pc4 (H3N2)	0/6 (0)	1/6 (0.384)	0/6 (0)	1/6 (6523)	0/6 (0)	6/6 (17530 + 6864)
Unvaccinated Control	0/6 (0)	4/6 (0.132 + 0.04)	0/6 (0)	5/6 (3033 + 1151)	0/6 (0)	6/6 (20604 + 2147)

[a] Week post vaccination.
[b] Week post challenge.
[c] Number of birds positive/number tested.
[d] Mean OD value + standard deviation.
[e] Mean fluorescent intensity + standard deviation.

experimental evidence of currently available vaccines indicates an urgent need for update of vaccine strain and development of effective DIVA vaccines to control turkey TR H3N2. In the present study, we chose the A/turkey/OH/313053/04 (H3N2) strain characterized by its broad cross reactivity with other recent TR H3N2 turkey isolates and developed NA-based and NS1-based DIVA vaccines.

To reduce the possibility of the same NA of field viruses with heterologous NA-based DIVA vaccine strain, we chose a rare N4 and created NA-based vaccine strain, rH3N4, which has not been previously identified in commercial poultry in the U.S. The NS1-based DIVA vaccine strains, rH3N3-NSdel, rTK/OH/04-Ddel-pc3 (H3N2) and rTK/OH/04-Ddel-pc4 (H3N2) encode a truncated NS1 protein [22]. Our previous study demonstrated that the amount of NS1 proteins in cells infected with A/turkey/OR/71-Ddel-pc3 (H7N3) or A/turkey/OR/71-Ddel-pc4 (H7N3) was below detection limits or much less than that of wild type virus, respectively [22]. Therefore, incorporation of NS1 truncation into NS1-based DIVA vaccine strains would drastically decrease possibility of NS1 protein contamination in the vaccine strains, and thus reduce or avoid the anti-NS1 immune response after vaccination, even if small residual quantities of NS1 protein contamination occurs due to insufficient purification of the vaccine strain [16]. It should be noted that vaccine strains used in our study were all prepared from allantoic fluid of ECEs. One turkey from killed rH3N4 vaccine group was positive for anti-NS1 antibodies by either NS1-ELISA or -FMIA, which is most likely due to the contamination of NS1 protein in the vaccine strain, as previously described [16]. In contrast, our NS1 serological data demonstrated that all turkeys immunized with either killed or live vaccine strains containing NS1 truncation were negative for anti-NS1 antibodies at 2 wpv (Tables 5 and 6). Thus, the vaccine candidates developed in our study are less likely to interfere with DIVA vaccine strategy.

In vivo evaluation of DIVA vaccine efficacy was carried out in 2-week-old and 80-week-old breeder turkeys. At 2 weeks post vaccination, a single immunization of inactivated vaccine induced good HI antibody titers in turkeys (Tables 1 and 2). Overall, immunization with rH3N4 and rH3N3-NSdel induced similar protection as A/turkey/OH/313053/04 (H3N2) wild type vaccine regardless of ages, indicating that the heterologous NA did not affect vaccine efficacy.

Although HI antibody titers induced by live vaccination were 3 $\log_2$ lower than those of killed vaccines, protection induced by rTK/OH/04-Ddel-pc3 (H3N2) and rTK/OH/04-Ddel-pc4 (H3N2) was comparable to that of killed vaccines, as they significantly reduced virus shedding in trachea (Table 3). In breeder turkeys, rH3N4 and rH3N3-NSdel killed vaccines significantly reduced virus shedding in cloaca at 4 DPC (Table 2). Although both killed and live vaccines reduced virus shedding in trachea and cloaca, most of vaccinated birds regardless of ages still shed challenge virus in trachea and cloaca at both time points tested. One possible explanation could be the high challenge dose (10^6 EID_{50}/0.2 ml) used in our study. Capua et al. demonstrated that challenge dose is important when determining vaccine protection rates [31]. In the aforementioned study, three challenge doses (10^2 EID_{50}, 10^4 EID_{50}, and 10^6 EID_{50}) were tested, and only 10^4 EID_{50} challenge dose was able to evaluate the efficacy of inactivated vaccine. However, even with a high challenge dose (10^6 EID_{50}), TR H3N2 viruses replicated to relatively low titers in trachea and cloaca of non-vaccinated control groups in both ages of turkeys (Tables 1 and 2), demonstrating that trachea and cloaca swabs may not adequately determine vaccine efficacy against TR H3N2 viruses in turkeys. In contrast, in our protection-challenge study with breeder turkeys, vaccination with reassortant inactivated vaccines significantly prevented virus replication in the oviduct, while lesions and virus replication was present in the oviduct of most birds in the non-vaccinated challenge control group (Table 2), which emphasizes the effect of virus infection on egg production.

Histopathology results also supported the capability of inactivated vaccine to reduce virus damage in the oviduct, as less severe lesions were observed in the oviduct of vaccinated birds compared to non-vaccinated birds. Thus, our study provides additional support to the idea that testing of vaccine efficacy in turkey against H3N2 influenza should be done using laying hens and an important sampling target should include the oviduct as well as the trachea and cloaca to obtain a clear evaluation of the effects of vaccination on challenge virus replication, as suggested in our previous study [27]. We were not able to assess egg production as a measure of vaccine protection since we used 80-week-old breeder turkeys for the study, and these older breeder turkeys were almost at the end of their egg production. However, difference in viral amount and histopathology observed in the oviduct between vaccinated and non-vaccinated groups suggests that immunization with both NA-based and NS1-based DIVA vaccines could reduce the drop in egg production.

A practical DIVA strategy should have an accompanying serological test that is capable of high-throughput serological monitoring. Indirect immunofluorescent antibody test (iFAT) [11], ELISA [14], and micro NA inhibition (micro-NI) assays [32] have been used for NA-based DIVA program, and recently ELISA [15–17] and FMIA [28] were developed for NS1-based DIVA approach. These assays are limited to be used in each laboratory and there is no commercial DIVA serological test available. In our study, N2-ELISA was used to monitor N2 antibodies for differentiation between vaccinated and infected birds. N2-ELISA has the ability to differentiate between non-infected and infected young turkeys and between infected and vaccinated young turkeys (Table 4). In the case of monitoring vaccinated groups, none of the A/turkey/OH/313053/04 (H3N2) wild type vaccinated birds were positive for N2 antibodies at 2 wpv, although 100% of birds in this group tested to be positive by N2-ELISA after challenge. A similar result was obtained by N2-ELISA in a previous study with wild type H9N2 vaccinated birds [14]. Possible explanations could be that the structure of NA protein is affected during the chemical inactivation process or that the immune response to NA is significantly suppressed due

to HA-dominated antigenic competition [33]. At 2 wpc of young turkeys with killed vaccine, 50% and 0% were N2 antibody positive in reassortant rH3N4 and rH3N3-NSdel virus vaccinated groups by N2-ELISA. In similar studies in chickens, the NI titers continue to increase until 4 weeks post-challenge [34], suggesting further investigations with a higher number of samples taken at different time-points should be undertaken to validate the sensitivity of N2-ELISA. It appears that the NI assay in our study produced false-positive reactions in young turkeys maybe due to steric hindrance by homologous H3 HA-specific antibodies [35,36]. The use of an antigen with a heterologous HA subtype (H1N2) eliminated the false positive results, but also had lower sensitivity compared to the N2 ELISA test. Based on the result from this study, it is reasonable to conclude that currently available ELISA-based DIVA tests will be useful for flock monitoring but not for diagnosis of individual birds.

In our study, both ELISA and FMIA serological tests were used to monitor immune response to NS1 in turkeys vaccinated with inactivated as well as live vaccines. Both NS1-ELISA and -FMIA assays detected anti-NS1 antibodies in turkeys experimentally infected with TR H3N2 virus but not in the majority of turkeys vaccinated with either killed or live vaccines in line with previous studies [15–17,37]. However, when monitoring infection in both killed and live vaccine groups, the results of both NS1-ELISA and -FMIA showed that only low percentage of birds seroconverted in killed vaccine groups of wild type and rH3N4 as well as live rTK/OH/04-Ddel-pc4 (H3N2) vaccine group after homologous A/turkey/OH/313053/04 (H3N2) virus challenge, although all turkeys from each group were positive for NP antibodies by NP-FMIA. There are couple explanations for this result. First, unlike highly pathogenic avian influenza (HPAI) virus, low pathogenic avian influenza (LPAI) virus normally replicates in a limited area and does not cause systemic spread in naïve birds. In the case of vaccinated birds, the replication of a LPAI virus could be much lower than in unvaccinated controls; therefore, LPAI infection in vaccinated birds may produce a very weak or undetectable immune response against NS1 protein as previously reported [38]. Second, the duration of the anti-NS1 immune response is variable among different subtypes of avian influenza virus and different species [28,39]. It remains to be determined duration for detectable anti-NS1 antibodies in both naïve and vaccinated turkeys with TR H3N2 infection. Previous studies in chickens have shown that the NS1 response continues to rise until 3 weeks post-challenge, and more birds may have seroconverted in this experiment if samples were taken later [38].

Several DIVA strategies including heterologous NA and NS1 have been proposed to differentiate naturally infected from vaccinated birds [40]. To our knowledge, our study is the first to simultaneously evaluate two different DIVA vaccine strategies, heterologous NA and NS1. Regarding NS1 as a DIVA marker, several previous studies have proven this concept by only showing its ability to differentiate infection from vaccination [15–17,37]. Two studies have recently determined whether NS1 could be used to define infection in both naïve and previously vaccinated chickens [38,41]. Compared with those earlier studies, unexpectedly, it was found that none or low percentage of naïve chickens infected with different subtypes of LPAI viruses have anti-NS1 antibody. Furthermore, antibody against NS1 was detected only in extremely low percentage of vaccinated chickens after challenge with LPAI viruses [38]. In the present study, it was demonstrated that NS1 could be used as a marker to distinguish infection between infected and vaccinated turkeys. Although the result of identifying infection in vaccinated turkeys is similar to that in chickens [38], our study is first to determine whether NS1 could be used to define TR H3N2 infection in vaccinated turkey species, and also adds evidence to that NS1 could have limited ability as a DIVA vaccine marker to identify LPAI virus infection in immunized poultry. On the other hand, the data from our study and previous field evidence [40] support that heterologous NA-based DIVA vaccine could be more practical than NS1-based DIVA vaccine used to control avian influenza in poultry.

In conclusion, we developed heterologous NA-based and truncated NS1-based DIVA influenza vaccines to protect against turkey TR H3N2 and demonstrated that the vaccines could effectively reduce virus in the oviduct of breeder turkeys and as well as trachea and cloaca. Thus, proper vaccination can effectively prevent drop in egg production and potential viral contamination of eggs in infected turkeys in the fields. With further optimization and validation, N2-ELISA and NS1-FMIA could be used as useful diagnostic assays to distinguish between infected and vaccinated birds to control TR H3N2 influenza in turkeys.

Acknowledgements

We would like to thank Megan Strother, Keumsuk Hong and Regina Hokanson for technical assistance with this work. The study was partly funded by U.S. Poultry & Egg Association Harold E. Ford Foundation awarded to C.W.L.; USDA/AFRI/NIFA/AICAP grant 2005-3560515388 (Z507201) and DHS National Center for Foreign Animal and Zoonotic Disease grant No. DHS BAA N00014-04-1-0-0660 awarded to B.L. and S.M.R.

References

[1] Shaw ML, Palese P. Orthomyxoviridae: the viruses and their replication. In: Knipe DM, Howley PM, editors. Fields virology. Philadelpha, PA: Lippincott Williams & Wilkins; 2007. p. 1647–89.
[2] Zhou NN, Senne DA, Landgraf JS, Swenson SL, Erickson G, Rossow K, et al. Genetic reassortment of avian, swine, and human influenza A viruses in American pigs. J Virol 1999;73(October (10)):8851–6.
[3] Choi YK, Lee JH, Erickson G, Goyal SM, Joo HS, Webster RG, et al. H3N2 influenza virus transmission from swine to turkeys, United States. Emerg Infect Dis 2004;10(December (12)):2156–60.
[4] Yassine HM, Al-Natour MQ, Lee CW, Saif YM. Interspecies and intraspecies transmission of triple reassortant H3N2 influenza A viruses. Virol J 2007;4:129.
[5] Olsen CW, Karasin AI, Carman S, Li Y, Bastien N, Ojkic D, et al. Triple reassortant H3N2 influenza A viruses, Canada, 2005. Emerg Infect Dis 2006;12(July (7)):1132–5.
[6] Tang Y, Lee CW, Zhang Y, Senne DA, Dearth R, Byrum B, et al. Isolation and characterization of H3N2 influenza A virus from turkeys. Avian Dis 2005;49(June (2)):207–13.
[7] Halvorson DA. The control of H5 or H7 mildly pathogenic avian influenza: a role for inactivated vaccine. Avian Pathol 2002;31(February (1)):5–12.
[8] Halvorson DA, Karunakaran D, Abraham AS, Newman JA, Sivanandan V, Poss PE. Efficacy of vaccine in the control of avian influenza. In: Beard CW, Easterday BC, editors. Proceedings of the second international symposium on avian influenza. Richmond, VA: U.S. Animal Health Association; 1987. p. 264–70.
[9] Capua I, Marangon S. The use of vaccination to combat multiple introductions of notifiable avian influenza viruses of the H5 and H7 subtypes between 2000 and 2006 in Italy. Vaccine 2007;25(June (27)):4987–95.
[10] Kapczynski DR, Gonder E, Liljebjelke K, Lippert R, Petkov D, Tilley B. Vaccine-induced protection from egg production losses in commercial turkey breeder hens following experimental challenge with a triple-reassortant H3N2 avian influenza virus. Avian Dis 2009;53(March (1)):7–15.
[11] Capua I, Terregino C, Cattoli G, Mutinelli F, Rodriguez JF. Development of a DIVA (differentiating infected from vaccinated animals) strategy using a vaccine containing a heterologous neuraminidase for the control of avian influenza. Avian Pathol 2003;32(February (1)):47–55.
[12] Lee CW, Senne DA, Suarez DL. Generation of reassortant influenza vaccines by reverse genetics that allows utilization of a DIVA (differentiating infected from vaccinated animals) strategy for the control of avian influenza. Vaccine 2004;22(August (23–24)):3175–81.
[13] Beato MS, Rigoni M, Milani A, Capua I. Generation of avian influenza reassortant viruses of the H7N5 subtype as potential vaccine candidates to be used in the framework of a "DIVA" vaccination strategy. Avian Dis 2007;51(March (1 Suppl.)):479–80.
[14] Kwon JS, Kim MC, Jeong OM, Kang HM, Song CS, Kwon JH, et al. Novel use of a N2-specific enzyme-linked immunosorbent assay for differentiation of infected from vaccinated animals (DIVA)-based identification of avian influenza. Vaccine 2009;27(May (24)):3189–94.
[15] Ozaki H, Sugiura T, Sugita S, Imagawa H, Kida H. Detection of antibodies to the nonstructural protein (NS1) of influenza A virus allows distinction between vaccinated and infected horses. Vet Microbiol 2001;82(September (2)):111–9.
[16] Tumpey TM, Alvarez R, Swayne DE, Suarez DL. Diagnostic approach for differentiating infected from vaccinated poultry on the basis of antibodies to NS1, the

nonstructural protein of influenza A virus. J Clin Microbiol 2005;43(February (2)):676–83.
[17] Zhao S, Jin M, Li H, Tan Y, Wang G, Zhang R, et al. Detection of antibodies to the nonstructural protein (NS1) of avian influenza viruses allows distinction between vaccinated and infected chickens. Avian Dis 2005;49(December (4)):488–93.
[18] Krug RM, Etkind PR. Cytoplasmic and nuclear virus-specific proteins in influenza virus-infected MDCK cells. Virology 1973;56(November (1)):334–48.
[19] Birch-Machin I, Rowan A, Pick J, Mumford J, Binns M. Expression of the nonstructural protein NS1 of equine influenza A virus: detection of anti-NS1 antibody in post infection equine sera. J Virol Methods 1997;65(May (2)):255–63.
[20] James CM, Foong YY, Mansfield JP, Fenwick SG, Ellis TM. Use of tetanus toxoid as a differentiating infected from vaccinated animals (DIVA) strategy for sero-surveillance of avian influenza virus vaccination in poultry. Vaccine 2007;25(August (31)):5892–901.
[21] Li C, Ping J, Jing B, Deng G, Jiang Y, Li Y, et al. H5N1 influenza marker vaccine for serological differentiation between vaccinated and infected chickens. Biochem Biophys Res Commun 2008;372(July (2)):293–7.
[22] Wang L, Suarez DL, Pantin-Jackwood M, Mibayashi M, Garcia-Sastre A, Saif YM, et al. Characterization of influenza virus variants with different sizes of the nonstructural (NS) genes and their potential as a live influenza vaccine in poultry. Vaccine 2008;26(July (29–30)):3580–6.
[23] Lee CW, Jung K, Jadhao SJ, Suarez DL. Evaluation of chicken-origin (DF-1) and quail-origin (QT-6) fibroblast cell lines for replication of avian influenza viruses. J Virol Methods 2008;153(October (1)):22–8.
[24] Spackman E, Senne DA, Myers TJ, Bulaga LL, Garber LP, Perdue ML, et al. Development of a real-time reverse transcriptase PCR assay for type A influenza virus and the avian H5 and H7 hemagglutinin subtypes. J Clin Microbiol 2002;40(September (9)):3256–60.
[25] Neumann G, Watanabe T, Ito H, Watanabe S, Goto H, Gao P, et al. Generation of influenza A viruses entirely from cloned cDNAs. Proc Natl Acad Sci U S A 1999;96(August (16)):9345–50.
[26] Swayne DE, Senne DA, Beard CW. Avian influenza. In: Swayne DE, editor. A laboratory manual for the isolation and identification of avian pathogens. Kennett Square, PA: American Association of Avian Pathologists; 1998. p. 150–5.
[27] Pillai SP, Pantin-Jackwood M, Jadhao SJ, Suarez DL, Wang L, Yassine HM, et al. Pathobiology of triple reassortant H3N2 influenza viruses in breeder turkeys and its potential implication for vaccine studies in turkeys. Vaccine 2009;27(February (6)):819–24.
[28] Watson DS, Reddy SM, Brahmakshatriya V, Lupiani B. A multiplexed immunoassay for detection of antibodies against avian influenza virus. J Immunol Methods 2009;340(January (2)):123–31.
[29] Liu Y, Mundt E, Mundt A, Sylte M, Suarez DL, Swayne DE, et al. Development and evaluation of an avian influenza, neuraminidase subtype 1, indirect enzyme-linked immunosorbent assay for poultry using the differentiation of infected from vaccinated animals control strategy. Avian Dis 2010;54(March (1 Suppl.)):613–21.
[30] Myers RW, Lee RT, Lee YC, Thomas GH, Reynolds LW, Uchida Y. The synthesis of 4-methylumbelliferyl alpha-ketoside of N-acetylneuraminic acid and its use in a fluorometric assay for neuraminidase. Anal Biochem 1980;101(January (1)):166–74.
[31] Capua I, Terregino C, Cattoli G, Toffan A. Increased resistance of vaccinated turkeys to experimental infection with an H7N3 low-pathogenicity avian influenza virus. Avian Pathol 2004;33(April (2)):158–63.
[32] Sylte MJ, Hubby B, Suarez DL. Influenza neuraminidase antibodies provide partial protection for chickens against high pathogenic avian influenza infection. Vaccine 2007;25(May (19)):3763–72.
[33] Johansson BE, Kilbourne ED. Dissociation of influenza virus hemagglutinin and neuraminidase eliminates their intravirionic antigenic competition. J Virol 1993;67(October (10)):5721–3.
[34] Avellaneda G, Sylte MJ, Lee CW, Suarez DL. A heterologous neuraminidase subtype strategy for the differentiation of infected and vaccinated animals (DIVA) for avian influenza virus using an alternative neuraminidase inhibition test. Avian Dis 2010;54(March (1 Suppl.)):272–7.
[35] Aymard M, Ferraris O, Gerentes L, Jolly J, Kessler N. Neuraminidase assays. Dev Biol (Basel) 2003;115:75–83.
[36] Kilbourne ED, Johansson BE, Grajower B. Independent and disparate evolution in nature of influenza A virus hemagglutinin and neuraminidase glycoproteins. Proc Natl Acad Sci U S A 1990;87(January (2)):786–90.
[37] Brahmakshatriya VR, Lupiani B, Reddy SM. Characterization and evaluation of avian influenza NS1 mutant virus as a potential live and killed DIVA (differentiating between infected and vaccinated animals) vaccine for chickens. Vaccine 2010;28(March 12):2388–96.
[38] Avellaneda G, Mundt E, Lee CW, Jadhao S, Suarez DL. Differentiation of infected and vaccinated animals (DIVA) using the NS1 protein of avian influenza virus. Avian Dis 2010;54(March (1 Suppl)):278–86.
[39] Dundon WG, Maniero S, Toffan A, Capua I, Cattoli G. Appearance of serum antibodies against the avian influenza nonstructural 1 protein in experimentally infected chickens and turkeys. Avian Dis 2007;51(March (1 Suppl.)):209–12.
[40] Suarez DL. Overview of avian influenza DIVA test strategies. Biologicals 2005;33(December (4)):221–6.
[41] Takeyama N, Minari K, Kajihara M, Isoda N, Sakamoto R, Sasaki T, et al. Detection of highly pathogenic avian influenza virus infection in vaccinated chicken flocks by monitoring antibodies against non-structural protein 1 (NS1). Vet Microbiol 2011;147(January 3–4):283–91.

Virus Research 167 (2012) 196–206

Contents lists available at SciVerse ScienceDirect

Virus Research

journal homepage: www.elsevier.com/locate/virusres

Effect of age on the pathogenesis and innate immune responses in Pekin ducks infected with different H5N1 highly pathogenic avian influenza viruses

Mary J. Pantin-Jackwood*, Diane M. Smith, Jamie L. Wasilenko, Caran Cagle, Eric Shepherd, Luciana Sarmento, Darrell R. Kapczynski, Claudio L. Afonso

Exotic and Emerging Avian Viral Diseases Research Unit, Southeast Poultry Research Laboratory, Agricultural Research Service, U.S. Department of Agriculture, 934 College Station Road, Athens, GA 30605, USA

ARTICLE INFO

Article history:
Received 16 December 2011
Received in revised form 11 April 2012
Accepted 27 April 2012
Available online 15 May 2012

Keywords:
Ducks
Highly pathogenic avian influenza
H5N1
Pathogenesis
Innate immune response
Host gene expression

ABSTRACT

The pathogenicity of H5N1 highly pathogenic avian influenza (HPAI) viruses in domestic ducks varies between different viruses and is affected by the age of the ducks, with younger ducks presenting a more severe disease. In order to better understand the pathobiology of H5N1 HPAI in ducks including the role of host responses, 2 and 5-week-old Pekin ducks were infected with three different H5N1 HPAI viruses. Virus-induced pathology ranged from no clinical signs to severe disease and mortality, with the 2-week-old ducks being more severely affected by the more virulent viruses. However, these more virulent viruses induced higher body temperatures in the 5-week-old ducks than in the 2-week-old ducks indicating possible differences in innate immune responses. To analyze the ducks host responses to H5N1 HPAI virus infection, expression of innate immune-related genes was measured in the spleens and lungs of infected ducks at the peak of virus infection. IFN-α, RIG-I, and IL-6 RNA levels were increased in spleens regardless of the virus given and the age of the ducks, however differences were observed in the levels of up-regulation of IFN-α and RIG-I between the 2 and the 5-week-old ducks with the more virulent virus. Differences in IL-2 gene expression were also observed. In the lungs, the levels of expression of innate immune-related genes were lower than in the spleen, with mostly up-regulation of RIG-I and IL-6 and down-regulation of IFN-α and IL-2; no significant difference in expression was found between the 2 and the 5-week-old ducks. The differences observed in the innate immune responses to infection with H5N1 HPAI viruses could explain in part the differences in pathogenicity found between the 2 and 5-week-old ducks, however earlier time points after infection and additional innate immune-related genes should be examined.

Published by Elsevier B.V.

1. Introduction

The H5N1 highly pathogenic avian influenza (HPAI) viruses continue circulating in poultry in Asia and have also spread to countries in the Middle East, Europe and Africa, causing great losses to the poultry industry. H5N1 HPAI virus infections are constantly monitored worldwide not only because of the high mortality they produce in poultry but also because of the spread to humans and fear of a pandemic. Both wild and domestic ducks have been implicated in the dissemination of H5N1 HPAI viruses (Chen et al., 2004; Gilbert et al., 2006; Hulse-Post et al., 2005; Li et al., 2004; Songserm et al., 2006; Sturm-Ramirez et al., 2005). Domestic ducks not only can be affected by H5N1 HPAI, but also serve as key intermediates in the transmission of the virus and therefore are included in control programs including vaccination (Li et al., 2004; Swayne, 2006).

Normally avian influenza (AI) viruses, including the highly pathogenic H5 and H7 strains, do not cause disease or death in ducks (Swayne and Halvorson, 2008). Mortality among ducks naturally infected with AI viruses was first reported in 2001 during an outbreak of H7N1 HPAI virus in Italy, and then in 2002, with Asian-origin H5N1 HPAI viruses causing mortality in wild birds and waterfowl (Capua and and Mutinelli, 2001; Ellis et al., 2004). Since then, a number of H5N1 HPAI viruses have been found to cause disease in ducks (reviewed in Pantin-Jackwood and Swayne, 2009). This pathogenicity is not consistently observed with all H5N1 HPAI viruses, and the age and species of the ducks appears to influence the outcome of the infection (Cagle et al., 2011; Londt et al., 2010; Pantin-Jackwood et al., 2007; Phuong et al., 2011; Wasilenko et al., 2011). Vaccination has proven effective in protecting ducks against H5N1 HPAI and is being used in several Asian countries to control the disease (Sims, 2007); however, virus circulation may still occur in clinically healthy vaccinated populations, which may contribute to endemic situations (Capua and Alexander, 2008).

* Corresponding author at: Southeast Poultry Research Laboratory, Agricultural Research Service, U.S. Department of Agriculture, 934 College Station Road, Athens, GA 30605, USA. Tel.: +1 706 5463419; fax: +1 706 5463161.
E-mail address: mary.pantin-jackwood@ars.usda.gov (M.J. Pantin-Jackwood).

0168-1702/$ – see front matter. Published by Elsevier B.V.
http://dx.doi.org/10.1016/j.virusres.2012.04.015

In order to curtail the spreading of H5N1 HPAI, it's necessary to control AI in ducks, and this will be facilitated by a better understanding of viral pathogenesis including host–pathogen interactions and host immune responses to virus infection. Control of influenza virus infections in naive hosts is based on innate immunity and subsequent adaptive cytotoxic T cell and B cell immunity. Cytokine production appears to play an important role in the pathogenesis of H5N1 HPAI viruses in mammals (Basler and Aguilar, 2008; Cameron et al., 2008; de Jong et al., 2006; Hayden et al., 1998; Peiris et al., 2004; Szretter et al., 2007). High virulence in mammals has been associated with induction of high levels of pro-inflammatory cytokines, commonly referred to as "cytokine storms", and in humans, clinical features associated with H5N1 HPAI infections have been linked with cytokine dysregulation (Chan et al., 2005; To et al., 2001). The role of cytokines in the pathogenesis of H5N1 HPAI viruses in avian species is less well understood. Several studies have addressed individual innate immune gene expression in chickens, and chicken or duck-origin cells, infected with AI viruses (Adams et al., 2009; Burggraaf et al., 2011; Degen et al., 2006; Liang et al., 2011; Rebel et al., 2011; Reemers et al., 2009, 2010; Sarmento et al., 2008a,b; Suzuki et al., 2009; Wasilenko et al., 2008, 2009; Watanabe et al., 2011; Xing et al., 2009), but studies exploring gene expression *in vivo* in ducks infected with AI viruses are less common (Barber et al., 2010; Burggraaf et al., 2011; Cagle et al., 2011; Sarmento et al., 2010). Viral replication has been associated with increased pro-inflammatory responses in chickens and ducks infected with H5N1 HPAI viruses (Burggraaf et al., 2011; Cagle et al., 2011; Suzuki et al., 2009). Expression of iNOS in organs was also associated with a higher severity of H5N1 HPAI virus infection, with higher levels of expression in chickens compared to ducks (Burggraaf et al., 2011). It is still unclear whether infection with different AI virus strains results in host gene expression patterns that are specific to each virus or are representative of a common response to infection with HPAI viruses. In addition, the role of host factors, including species, physiologic status and age of the bird, needs to be elucidated.

Previous studies have shown differences in response to H5N1 HPAI virus infection between domestic ducks of different ages, with younger ducks presenting a more severe disease and higher mortality (Kishida et al., 2005; Londt et al., 2010; Pantin-Jackwood et al., 2007). A difference in age susceptibility was also reported in natural outbreaks of H5N1 HPAI in commercial ducks (Kwon et al., 2005). As for wild ducks, the age of mallard ducks infected with a low pathogenicity avian influenza (LPAI) virus did not affect susceptibility to infection but did affect the extent of virus shedding (Costa et al., 2010). Results of a study examining age-related susceptibility to H9N2 influenza infection in Japanese quail, indicated that adult birds had consistently stronger immune responses than young and aged birds, however, clinical signs and duration of viral infection was similar in the different age groups (Lavoie et al., 2007). In another study, differences between 1 and 4-week-old chickens infected with H9N2 virus were related to strength and timing of host responses, which could be a key factor in age-dependent susceptibility to infection (Reemers et al., 2009). Differences in the outcome of hepatitis B virus infection in ducks of different ages has been attributed to both increasing maturation of the immune system with age, and a link between host cell maturation and the capacity to support viral replication (Jilbert et al., 1998). Also, baby ducks were more vulnerable to persistence of hepatitis B virus infection than older ducks with evidence that the innate immune response is less effective in the young ducks (Tohidi-Esfahani et al., 2010).

The objective of this study was to investigate the effect of age on the pathogenesis of H5N1 HPAI viruses in domestic ducks and to examine the innate immune responses to infection. For this, three H5N1 HPAI viruses of different virulence in ducks were used to infect 2 and 5-week-old domestic Pekin ducks. Innate immune-related gene expression associated with virus infection was compared by conducting quantitative real-time RT-PCR for selected genes in spleens and lungs. The information generated provides insights into HPAI virus pathogenesis and host responses that can be used to develop improved strategies to control AI in avian species.

2. Materials and methods

2.1. Viruses

The following H5N1 HPAI viruses were used in this study: Chicken/Hong Kong/220/97 (Ck/97) (Perkins and Swayne, 2001), A/Egret/HK/757.2/02 (Egret/02) (Pantin-Jackwood et al., 2007), and Duck/Vietnam/218/05 (Dk/05) (Pfeiffer et al., 2009). Virus stocks were propagated in embryonating chicken eggs (ECE) as previously described (Pantin-Jackwood and Swayne, 2007). Serial titrations were performed in ECE and 50% egg infectious dose (EID_{50}) titers were determined by testing hemagglutination activity (Swayne et al., 1998). A sham inoculum was made using sterile allantoic fluid diluted 1:300 in brain heart infusion (BHI) medium. All experiments using H5N1 HPAI viruses, including work with animals, were performed in biosecurity level-3 enhanced (BSL-3E) facilities at Southeast Poultry Research Laboratory (SEPRL), Agricultural Research Service, United States Department of Agriculture (USDA), and all personnel were required to wear a powered air protection respirator with high efficiency particulate air (HEPA)-filtered air supply (3M^{TM}, St. Paul, MN).

2.2. Pathogenicity studies in Pekin ducks

Two identical experiments were conducted using domestic Pekin ducks (*Anas platyrhynchos*, var. *domestica*) obtained from a commercial hatchery. In the first experiment the ducks were two weeks of age and in the second experiment they were five weeks of age. The two experiments were run separately because of space limitations, however all possible measures were taken to minimize differences in experimental conditions. Serum samples were collected from fifteen ducks in each experiment prior to inoculation to ensure that the birds were serologically negative for AI virus as determined by an ELISA test using IDEXX FlockChek AI MultiS-Screen (Idexx Laboratories, ME). Ducks were housed in self-contained isolation units that were ventilated under negative pressure with HEPA-filtered air, and maintained under continuous lighting. Feed and water were provided with *ad libitum* access. General care was provided as required by the SEPRL Institutional Animal Care and Use Committee. The experimental design has been previously described (Pantin-Jackwood and Swayne, 2007). Briefly, ducks were separated into a control group and three virus-inoculated groups. All groups contained 14 ducks. Control birds were intranasally (IN) inoculated through the choanal slit with 0.1 ml of the sham inoculum. The three virus-inoculated groups were inoculated IN with 0.1 ml of inoculum containing 10^5 EID_{50} of the viruses. The virus dose used is above the median infectious dose (ID50) for H5N1 HPAI in ducks (Aldous et al., 2010). At 2 days post-inoculation (dpi) six ducks per group were bled for serum. In addition, four ducks from each group were euthanized and necropsied. Tissues from three of these ducks per group were collected in 10% neutral buffered formalin solution to determine microscopic lesions and the extent of virus replication in tissues as previously described (Pantin-Jackwood and Swayne, 2007). Portions of brain, lung, skeletal muscle, heart and spleen were also collected from three ducks per group in BHI with antibiotics for virus titration. In addition, portions of the spleen and lung from

all four euthanized ducks were collected for RNA isolation. Tissue samples were ground through 100 μm cell strainers (BD Falcon, Franklin Lakes, NJ) into 2 ml of Dulbecco's Modified Eagle Medium (DMEM). The cell suspension was then added to 6 ml of TRIzol reagent (Invitrogen, Carlsbad, CA) and stored at −70 °C.

The remaining ducks (ten per group) were observed for signs of illness over a 9 day period during which time the clinical signs were recorded daily. Body temperatures were taken with a rectal digital thermometer from all ducks at 2 and 3 dpi. Body weights were taken from all ducks at the day of inoculation and at 3 dpi. Oropharyngeal and cloacal swabs from three ducks per group were also taken at 3 dpi to determine virus shedding. Sample birds, moribund birds (recumbent ducks that would not eat or drink, or had severe neurological signs), and all birds remaining at the end of the nine day period were euthanized by the intravenous (IV) administration of sodium pentobarbital (100 mg/kg body weight).

Tissues and swabs collected in BHI were stored frozen at −70 °C and titers of infectious virus were subsequently determined as previously described (Swayne et al., 1998). Briefly, tissues were normalized by weight and homogenized in BHI medium and clarified homogenates were titrated for virus infectivity in embryonating chicken eggs. The minimal detectable titer was $10^{0.9}$ EID_{50}/ml from swabs and $10^{1.97}$ EID_{50}/g from tissue.

One-way ANOVA with Tukey's post-test was used to analyze body temperature, body weight, and virus titers in swabs using Prism v.5.01 software (GraphPad Software Inc.). Statistical significance was set at $P < 0.05$. The survival rate data was analyzed using the Mantel–Cox Log-rank test.

2.3. RNA extraction

Spleen and lung cell suspensions stored in TRIzol were thawed at room temperature and 1.6 ml of chloroform was added. Samples were incubated for 10 min on ice and then spun at 2400 × *g* for 15 min. The aqueous phase was removed and an equal volume of 70% ethanol was added. The RNA was then extracted using the Qiagen RNeasy midi prep kit (Qiagen, Valencia, CA). RNA integrity (RIN) of the samples was measured with the Agilent 2100 Bioanalyzer (Agilent Technologies, Santa Clara, CA) and confirmed to have values above 7. RNA concentrations from the four individual birds per group were determined using a Nanodrop ND-1000 Spectrophotometer (Nanodrop Technologies, Wilmington, DE). To eliminate possible contamination with genomic DNA, 100 micrograms of RNA from each sample was treated with on column DNase digestion (RNase-Free DNase Set, Qiagen, Valencia, CA) in the Qiagen RNeasy mini prep kit (Qiagen, Valencia, CA) for 15 min at room temperature.

2.4. Quantitative real-time RT-PCR

The relative quantitation of IFN-α, RIG-I, and IL-6 gene expression following infection was performed using primers previously reported (Cagle et al., 2011). Primers for IL-2 gene were designed based on published GenBank sequences (AY821656) (forward primer: ctggcaaactctgcaatgttact; reverse primer: tgggggaattaggtccataagtt). Amplification and detection of specific products was performed using the Applied Biosystems 7500 Fast Real-Time PCR System (Applied Biosystems, CA). Total RNA extracted from spleen and lung homogenates from four individual ducks from the infected groups and from four ducks from the non-infected controls was used in the reactions. Reactions were done in triplicate using the Power SYBR® Green RNA-to-C_T™ 1-Step Kit (Applied Biosystems, CA) and 50 ng of total RNA per reaction. Quantitative real-time RT-PCR (qRRT-PCR) conditions and cycling parameters were the same for all primer pairs used and were as follows: one cycle at 50 °C for 30 min, one cycle at 95 °C for 15 min, 40 cycles of 95 °C for 15 s and 58 °C for 32 s followed by dissociation curve determination of the products with one cycle at 95 °C for 15 s, 55 °C for 20 s, 99 °C for 15 s and 60 °C for 15 s. Expression fold change was determined by the $2^{-\Delta\Delta Ct}$ method using β-actin as the endogenous reference gene to normalize the level of target gene expression (Cagle et al., 2011). The Mann–Whitney test was used to determine the statistical significance between fold change values of the two age ducks, and one-way ANOVA with Tukey's post-test was used to determine the statistical difference between the fold change values obtained with the three viruses using Prism v.5.01 software (GraphPad Software Inc.). Statistical significance was set at $P < 0.05$.

An estimate of the virus titers in spleen and lung was also determined for infected ducks by real-time RT-PCR. This was done to examine if differences in virus replication could affect the cytokine gene expression results. RNA (50 ng/ul) from all duck samples previously used in the qRRT-PCR assay were run with a test targeting the influenza A matrix gene (Spackman et al., 2002). All reactions were run in triplicate with ABI PRISM 7500 using Power SYBR Green RNA-to-C_T 1-Step Kit (Applied Biosystems, CA) for 1 cycle at 95 °C for 10 min, 45 cycles of 95 °C for 15 s and 57 °C for 30 s.

Table 1
Morbidity, mortality, and mean death times resulting from intranasal inoculation of 2 and 5-week-old ducks with 10^5 EID_{50} of the H5N1 HPAI viruses.

Groups	Sick/dead/total (MDT)[a]	
	2-Week-old ducks	5-Week-old ducks
Controls	0/0/10	0/0/10
Ck/97	0/0/10	0/0/10
Egret/02	10/10/10 (5.5)	10/6/10 (6.5)
Dk/05	10/10/10 (3.9)	10/10/10 (4.4)

[a] MDT = mean death time (days).

2.5. Nitric oxide assay

Total nitrate and nitrite content produced by nitric oxide synthase (NOS) was measured in serum samples collected at 2 dpi from six ducks from each virus-infected group and four ducks from the non-infected controls. Sera were passed through a 10 kDa ultrafilter (Millipore Corp., Billerica, MA) prior to analysis. The total protein in the filtered sera was measured using a DC Protein Assay (Bio-Rad, Hercules, CA). A Nitric Oxide Synthase Assay kit (Calbiochem, Gibbstown, NJ) was used according to the manufacturer's specifications on 40 μL of filtered serum. Values were normalized to the total protein in the filtered sera. One-way ANOVA with Tukey's post-test was used the results using Prism v.5.01 software (GraphPad Software Inc.). Statistical significance was set at $P < 0.05$.

3. Results

3.1. Pathogenicity of H5N1 HPAI virus infections in ducks

Differences in pathogenicity between three H5N1 HPAI viruses were determined in 2 and 5-week-old Pekin ducks. These ages were chosen based on results of our previous study indicating differences in response to H5N1 HPAI virus infection in Pekin ducks of different ages (Pantin-Jackwood and Swayne, 2007). Serum samples collected from ducks prior to inoculation showed that the ducks were serologically negative for AIV.

3.1.1. Clinical signs and gross lesions

The morbidity and mortality induced by infection with the viruses in 2 and 5-week-old ducks is summarized in Table 1, and survival curves are shown in Fig. 1. Survival rates were significantly different ($P < 0.05$) upon infection with the three viruses in each age group. Survival of the 2 and 5-week-old ducks infected with

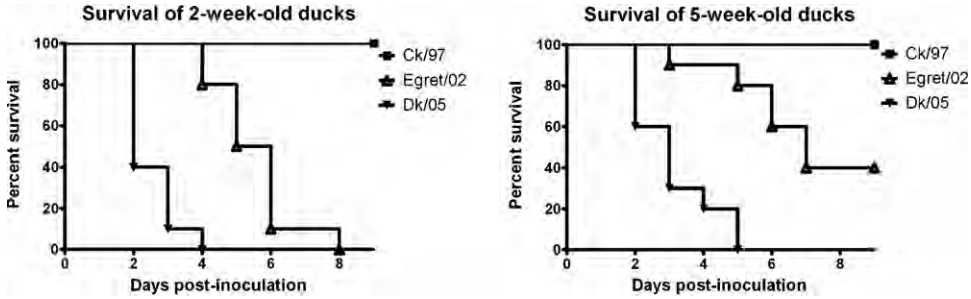

Fig. 1. Survival rate of ducks after inoculation with the H5N1 HPAI viruses. Two and 5-week-old ducks were inoculated with 10^5 EID_{50} of the viruses and mortality was monitored for 9 days. Survival rates were statistically different between the three virus-inoculated groups within each age, as determined by the log rank test ($P < 0.05$). Significant difference in survival rate was also observed between the 2 and 5-week-old ducks infected with Egret/02.

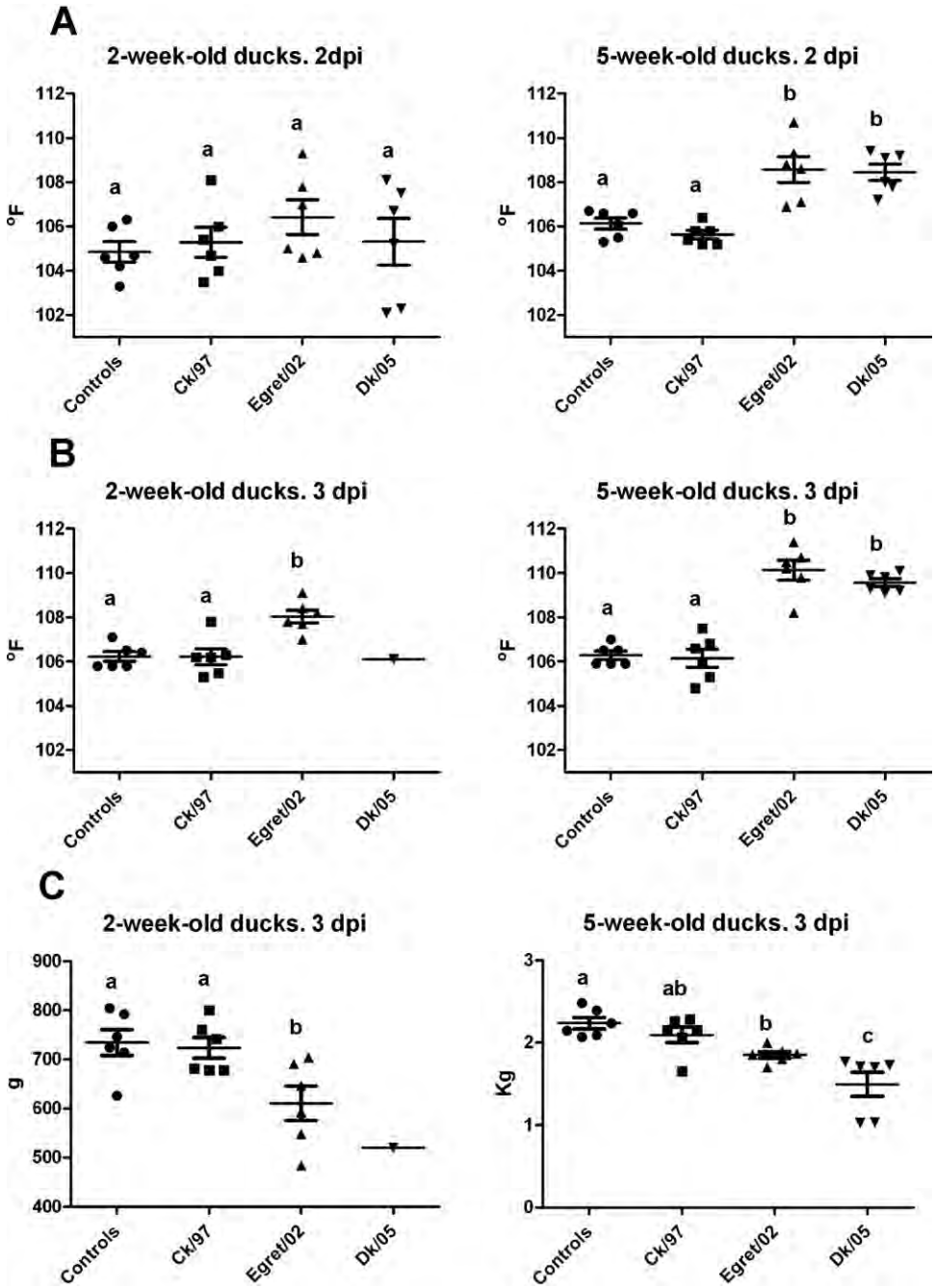

Fig. 2. Body temperatures of 2 and 5-week-old ducks infected with H5N1 HPAI viruses and compared to controls, 2 days post inoculation (dpi) (A) and 3 dpi (B). Body weights of 2 and 5-week-old ducks infected with H5N1 HPAI viruses and compared to controls, 3 dpi (C). Bars indicate the average ± SEM for each group. Groups with different lowercase letters within the respective age group are significantly different ($P < 0.05$).

Egret/02, but not with Dk/05, was also statistically different when compared to each other. No clinical signs or mortality was observed in the sham-inoculated control ducks or in the ducks inoculated with the Ck/97 virus in either of the two experiments. Ducks inoculated with the Egret/02 or Dk/05 viruses had clinical signs ranging from moderate to severe. Two-week-old ducks inoculated with the Egret/02 or Dk/05 viruses presented 100% mortality with lower mean death times when compared to the 5-week-old ducks. All ducks inoculated with Egret/02 and Dk/05 showed moderate to severe depression and anorexia as early as 2 dpi. Body temperatures taken at 2 and 3 dpi demonstrated that these ducks had fever, with higher temperatures observed in the 5 week-old ducks (Fig. 2). Significantly higher body temperatures were observed in the 5-week-old ducks inoculated with Egret/02 or Dk/05 when compared to the control ducks or the ducks inoculated with Ck/97, at 2 and 3 dpi. No significant difference in body temperature was observed between the 2-week-old ducks at 2 dpi, but ducks inoculated with Egret/02 had significantly higher body temperatures at 3 dpi. The body temperatures of two of the 2-week-old ducks inoculated with Dk/05 and examined at 2 dpi were very low indicating these ducks were probably in a moribund state. At the moment of infection there was no weight difference among the different experimental groups (data not shown). A clear effect on weight after infection was observed at 3 dpi (Fig. 2). In addition, all ducks infected with Egret/02 and Dk/05 displayed mild to severe neurological signs beginning at 2 dpi and characterized by tremors, lack of coordination, tilted head, seizures, and paralysis. Five-week-old ducks that survived from the Egret/02-inoculated group continued to have mild neurological signs until the end of the experiment.

At necropsy, control ducks and ducks inoculated with Ck/97 lacked lesions. Gross lesions were observed and were similar between the ducks inoculated with Egret/02 and Dk/05, and dehydration, empty intestines, splenomegaly, and thymus atrophy was present in most. Also commonly observed were nasal discharge, cyanotic bill and toes, dilated and flaccid heart with increased pericardial fluid, renomegaly and/or renal pallor and accentuated lobular surface architecture, congested, malacic brain, impacted proventriculus and gizzard with intense bile staining of the mucosa, and yellowish pancreas with petechia.

3.1.2. Microscopic lesions and viral antigen distribution

The distribution and severity of histologic lesions and avian influenza antigen staining in tissues collected from the 2 and 5-week-old ducks at 2 dpi are summarized in Table 2. The two week-old ducks had slightly more severe lesions and more widespread viral staining in tissues than the 5 week-old ducks. In ducks inoculated with Ck/97, mild to moderate tracheitis and bronchitis was observed, as well as mild focal degeneration of pancreatic acinar cells and splenic macrophages, mild lymphocyte depletion in the thymus and bursa, and mild lymphocyte infiltration in liver and kidneys. Mild to severe lesions in several organs were found in ducks inoculated with Egret/02 and Dk/05, however lesions were more severe and more organs were affected in ducks infected with Dk/05. The trachea presented mild to moderate degenerative changes of the overlying epithelium and mild lymphocytic infiltration in the submucosa. The lesions present in the lung were mild to severe consisting of congestion and interstitial inflammation with mixed mononuclear cells. Mild to moderate necrotizing bronchitis with lumen cellular debris, and mild airsacculitis was also observed. In the brain, randomly scattered foci of malacia with gliosis, mild lymphoplasmacytic perivascular cuffs, and mild perivascular edema were observed. In the heart, random multifocal to confluent myocardial degeneration to necrosis and minimal to mild mononuclear cell inflammation was observed. Mild to severe multifocal cellular swelling and necrosis of the pancreatic acinar epithelium occurred in all of the sampled ducks. The corticotrophic cells, and less consistently the chromaffin cells, of the adrenal gland had mild to moderate multifocal to confluent areas of vacuolar degeneration to necrosis. Skeletal muscle sampled from the thigh presented degeneration to necrosis of individual myofibers. The intestinal epithelium was only minimally to mildly affected, with mild inflammatory changes in the lamina propria. In all groups, the proventriculus and gizzard occasionally contained small foci of superficial heterophilic infiltration that was accompanied by mild epithelial necrosis. Mild to moderate necrosis of hepatocytes with sinusoidal histiocytosis was observed in the liver. The spleen, thymus, bursa, and mucosa-associated lymphoid tissue had moderate to severe lymphoid depletion ranging from apoptosis to necrosis in remaining lymphocytes. Both cortical and medullary regions of bursa and thymus were affected. Renal changes indicative of dehydration, such as mild dilatation of the distal segments of nephrons, were observed in some of the ducks.

In ducks inoculated with Ck/97, viral antigen staining was less common than the observed with the other two viruses (Table 2). In the Egret/02 and Dk/05 virus-inoculated ducks, viral antigen staining was present in multiple organs and was more widespread in tissues from ducks infected with Dk/05. In lymphoid organs, viral antigen was only identified in resident and infiltrating phagocytes and not in apoptotic lymphocytes. Vascular endothelium was consistently negative for the presence of viral antigen. Viral antigen was detected in the epithelium of the trachea, phagocytes and alveolar epithelium of the lung, air sac epithelium, the neurons and glial cells of the brain, cardiac and skeletal myocytes, adrenal corticotrophic cells, bursal phagocytes, medullary epithelium and tingible body macrophages of the thymus, phagocytes of the spleen, and pancreatic acinar epithelium. Viral antigen staining was rare or infrequent in renal tubular epithelium and in the epithelium and autonomic ganglia of the enteric tract. In ducks infected with Dk/05, viral staining was also found in hepatocytes and Kupfer cells in the liver, and smooth muscle of the gizzard and epithelial cells of the proventriculus.

3.2. Replication of H5N1 HPAI viruses in ducks

Virus was recovered from the oropharyngeal route at 3 dpi in all three of the 2 week-old ducks and in two of the 5-week-old ducks infected with Ck/97 (Table 3). However virus was only detected in the cloacal swabs of two of the 2-week-old ducks inoculated with this virus. Infectious virus could be recovered from all the oropharyngeal and cloacal swabs collected from 2 and 5-week-old ducks inoculated with Egret/02 and Dk/05. Oropharyngeal virus titers were higher in the 2 week-old ducks than in the 5 week-old ducks infected with Egret/02 and Dk/05 viruses, but were not statistically significant. Cloacal shedding of these two viruses was statistically higher than for Ck/97 in both 2 and 5-week-old ducks.

Virus replication was also examined at 2 dpi in brain, lung, spleen, heart, and muscle tissue following infection with the HPAI H5N1 viruses (Fig. 3). Differences in virus titers were found between tissues of ducks infected with Ck/97, Egret/02 or Dk/05 when comparing within the age groups. Most of the tissues from ducks infected with Egret/02 or Dk/05 had significantly higher virus titers than tissues from ducks infected with Ck/97 (data not shown). Infection of 2-week-old ducks with the Ck/97 virus resulted in no detectable viral titers in heart and muscle, and low titers in brain, lung and spleen. In the 5-week-old ducks inoculated with Ck/97, virus was only detected in the lung and spleen in low titers. Infection of 2 and 5-week-old ducks with Egret/02 and Dk/05 resulted in detectable virus in all organs examined. A significant difference in tissue titers between the different age ducks was only found between brains of ducks infected with Ck/97.

Table 2
Histological lesions and distribution of viral antigen in tissues from 2 and 5-week-old ducks inoculated with H5N1 HPAI viruses. Tissues were taken from three ducks at 2 days post infection and were immunohistochemically stained with antibodies to avian influenza virus nucleoprotein to visualize the viral antigen (histological lesions/viral antigen staining).[a]

Tissue	2 Week-old ducks			5 Week-old ducks		
	Ck/97	Egret/02	Dk/05	Ck/97	Egret/02	Dk/05
Trachea	++/++	++/++	+++/++	++/+	+/+	++/++
Lung	++/++	+++/++	+++/+++	+/+	++/++	+++/+++
Heart	−/−	+/++	+++/+++	−/−	++/++	++/+++
Brain	−/−	++/++	+++/+++	−/−	++/++	++/+++
Adrenal	−/−	+/+	+++/+++	−/−	−/−	+/++
Enteric tract	−/−	+/−	++/+	−/−	−/−	+/++
Pancreas	+/+	++/+	+++/+++	+/+	+/+	++/++
Liver	+/+	++/−	++/++	+/+	++/+	+/+
Kidney	−/−	−/−	+/+	+/−	−/−	+/+
Spleen	++/++	+/+	++/+++	++/++	+/++	+++/+++
Bursa	+/−	+/++	++/++	+/−	++/+	++/++
Thymus	+/+	+/++	+++/+++	+/+	++/++	++/+++
Muscle	−/−	+/+	++/++	−/−	−/+	+/++
Gizzard	−/−	−/−	+/+	−/−	−/−	+/+
Proventriculus	+/−	−/−	+++/+++	+/−	−/−	+/++

[a] Lesions were scored as follows: − = no lesions; + = mild; ++ = moderate; +++ = severe. The intensity of viral antigen staining in each section was scored as follows: − = no antigen staining; + = infrequent; ++ = common; +++ = widespread.

Table 3
Oropharyngeal and cloacal viral titers in ducks infected with H5N1 HPAI viruses, 3 days post inoculation. Virus titers were determined in eggs and are expressed as the $\log_{10}$ EID_{50}/ml. Data are presented as means ± standard deviation of titers of positive samples. The threshold of detection is 0.9 $\log_{10}$ EID_{50}/ml. The number of birds that shed virus is indicated in parentheses (number shedding/number tested).

H5N1 virus	Virus titer			
	2 Week-old ducks		5 Week-old ducks	
	Oropharyngeal	Cloacal	Oropharyngeal	Cloacal
Ck/97	2.2 ± 0.4 (3/3)[a]	0.6 ± 1.1 (2/3)[a]	1.5 ± 1.3 (2/3)[a]	(0/3)[a]
Egret/02	3.6 ± 0.6 (3/3)[a]	2.5 ± 0.5 (3/3)[b]	3.2 ± 1.3 (3/3)[a]	2.3 ± 0.3 (3/3)[b]
Dk/05	3.4 ± 0.9 (3/3)[a]	2.5 ± 0.3 (3/3)[b]	3.4 ± 0.6 (3/3)[a]	2.3 ± 0.3 (3/3)[b]

Different lowercase superscripts denote significance between treatment groups (within columns) ($P < 0.05$).

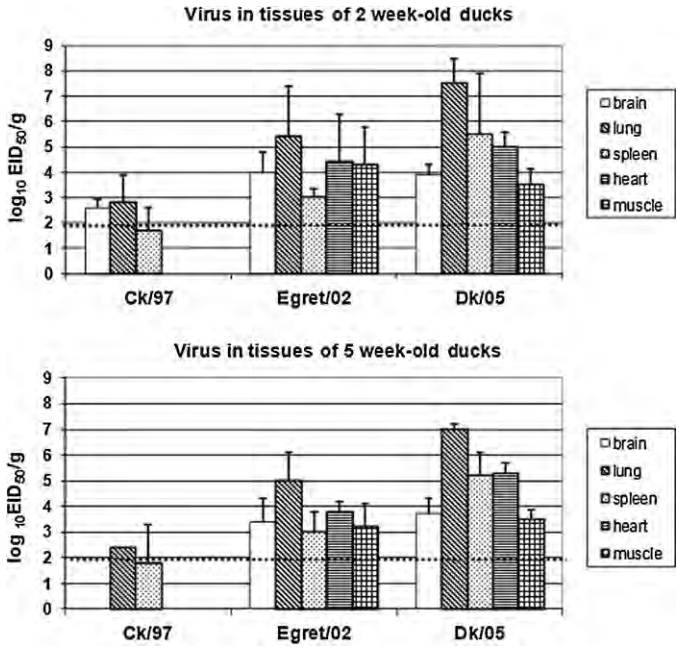

Fig. 3. Virus titers in the brain, lung, spleen, heart, and skeletal muscle of 2 and 5-week-old ducks after infection with H5N1 HPAI viruses. Tissues were collected at 2 dpi. Virus titers were determined in eggs and are expressed as the $\log_{10}$ EID_{50}/g. Values are the mean + standard error ($n = 3$). The threshold of detection is 1.97 $\log_{10}$ EID_{50}/gram of tissue. Titers from some tissues from ducks infected with Ck/97 were under the threshold of detection.

3.3. Immune-related genes expression following H5N1 HPAI virus infection

Relative quantitative real-time RT-PCR (qRRT-PCR) assays were conducted using RNA extracted from the spleens and lungs of the 2 and 5-week-old ducks infected with Ck/97, Egret/02 and Dk/05 and from sham-inoculated ducks. Gene expression of a type I interferon (IFN-α), a pro-inflammatory cytokine (IL-6), a RNA sensor present in duck cells (RIG-I), and a T cell proliferative interleukin (IL-2) was examined. Baseline levels of expression of these innate immune genes in the spleens and lungs of the non-infected ducks were present and similar when comparing expression between the two age groups. However, there was a difference in the baseline values of the tested genes when comparing organs, with similar levels of IFN-α and RIG-I but lower baseline levels of IL-6 and IL-2 in the lungs compared to the spleens. qRRT-PCR revealed increased levels of IFN-α, RIG-I, IL-6, and IL-2 RNA in most of the spleens from virus-infected 2 and 5-week-old ducks when compared to controls (Fig. 4). Significant higher levels of IFN-α, RIG-I and IL-2 gene expression were found in the 5-week-old ducks when compared to the 2-week-old ducks infected with the more virulent virus, Dk/05. All three viruses induced similar up-regulation of IFN-α, RIG-I and IL-6, but differences in expression of IL-2 were observed between the viruses.

The levels of expression of the innate immune-related genes in the lung of the virus-infected ducks were lower compared to the levels of expression for the same genes in the spleens, in some cases even down-regulated when compared to controls. No significant differences were observed in expression of any

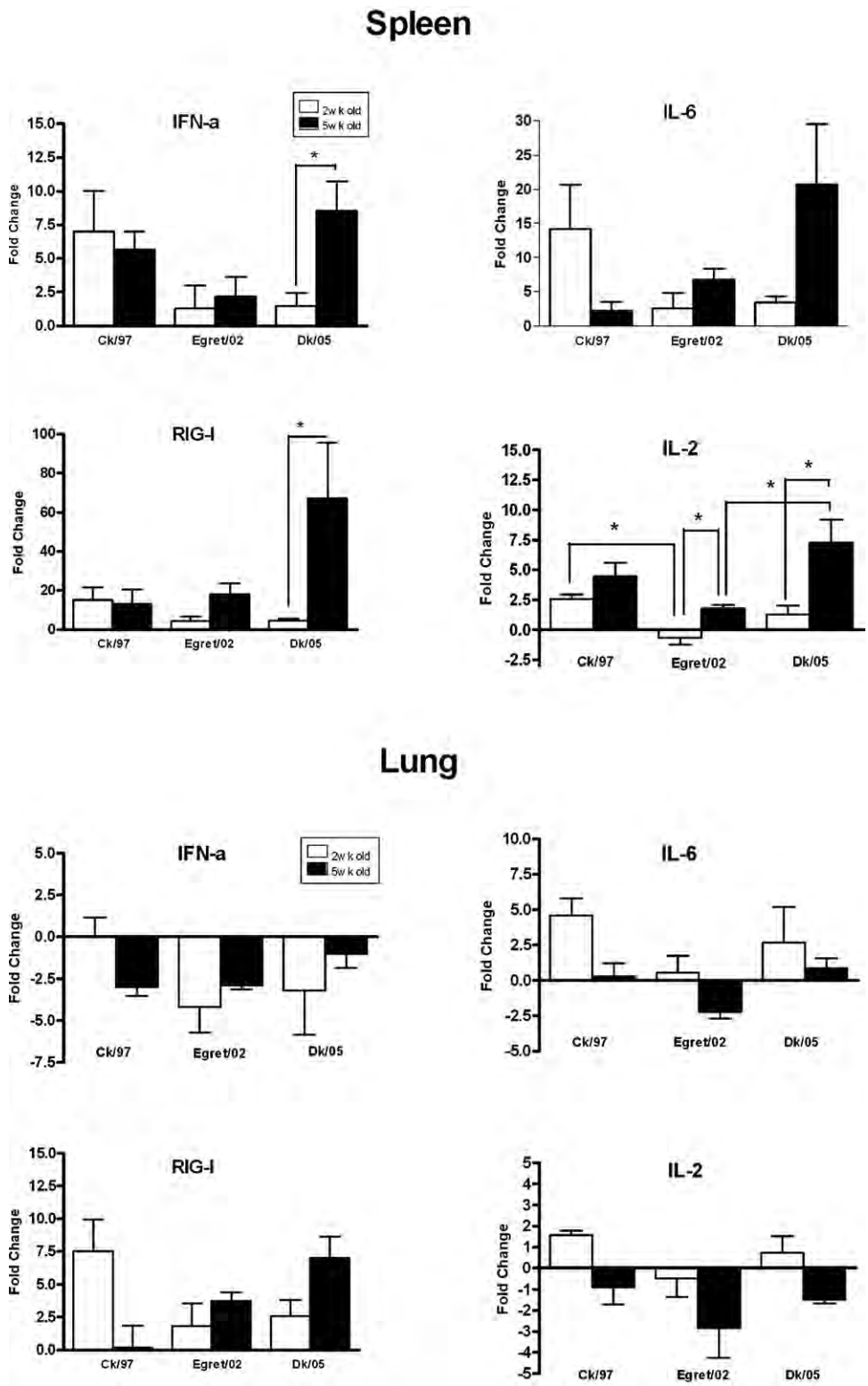

Fig. 4. Fold change expression of immune-related genes in spleens and lungs of 2 and 5-week-old ducks infected with Ck/97, Egret/02 and Dk/05 H5N1 HPAI viruses and compared to controls, 2 days post inoculation. Changes were quantified by qRRT-PCR and expressed as fold change in the birds infected ($n = 4$) compared with non-infected birds ($n = 4$). Bars represent standard error of the mean. Presence of the asterisk indicates significant difference in cytokine expression between groups ($P < 0.05$).

of the genes examined, when comparing the 2 and 5-week-old ducks or the viruses. RIG-I and IL-6 genes expression were mostly up-regulated, with the exception of IL-6 in the 5-week-old ducks. Levels of IFN-α RNA were decreased in the lungs of all ducks except in the lungs of the 2-week-old ducks that received Ck/97. IL-6 gene expression was up-regulated in the lungs of all ducks except in the 5-week-old ducks infected with Egret/02. Expression of IL-2 was variable, and in most cases down-regulated.

The relative amounts of viral RNA in spleen and lung were also determined by real-time RT-PCR using RNA from the same samples

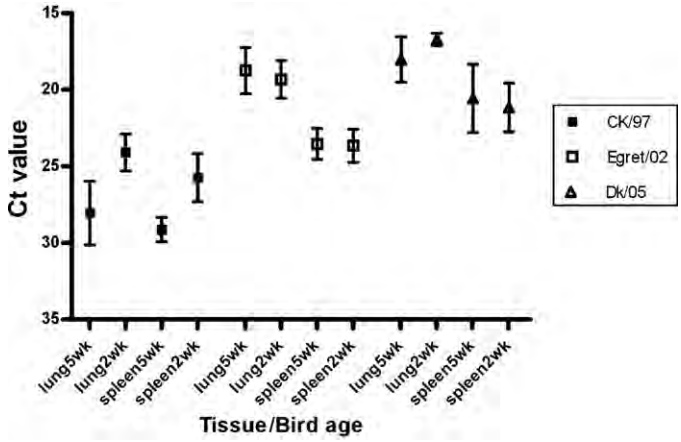

Fig. 5. Cycle threshold values representing titers of H5N1 HPAI viruses in spleen and lungs of infected ducks.

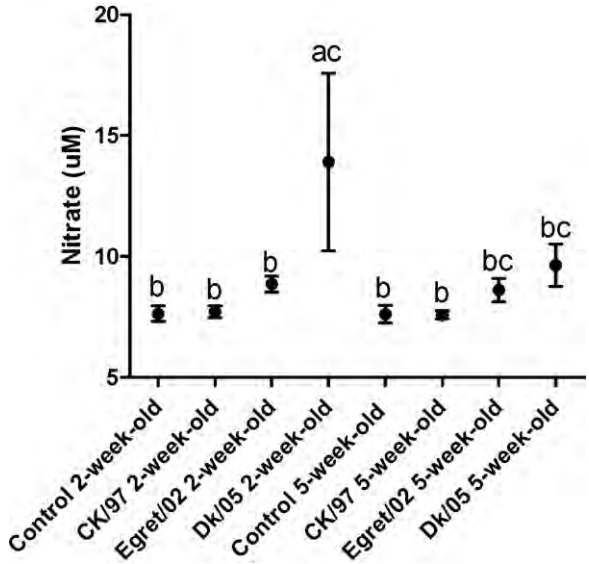

Fig. 6. Total nitrate and nitrite content produced by NO in serum samples taken at 2 dpi from H5N1 HPAI virus-infected ducks and non-infected controls and normalized to the total protein in the filtered sera. Values are the mean ± standard error ($n = 6$). Different lowercase letters indicate significant differences of the means ($P < 0.05$).

(Fig. 5). Similar levels of viral RNA were present in the lungs and spleens of the 2 and 5-week old ducks infected with Egret/02 and Dk/05, with higher titers present in lung. The 2-week-old ducks inoculated with Ck/97 had higher titers in lung and spleen the 5-week-old ducks.

3.4. Nitric oxide levels in serum

Total nitrate and nitrite content produced by NOS measured in serum samples from infected ducks when compared to non-infected controls showed a significant increase in ducks infected with Dk/05 when compared to the control ducks and ducks infected with Ck/97 (Fig. 6). A mild increase was also observed in ducks infected with Egret/02.

4. Discussion

In the present study we examined the pathobiology and host gene expression responses in 2 and 5-week-old ducks infected with H5N1 HPAI viruses. Clear differences in pathogenicity were observed between the three viruses studied and also between the younger and older ducks, similar to what we have previously described (Pantin-Jackwood and Swayne, 2007; Pantin-Jackwood et al., 2007; Pfeiffer et al., 2009). The loss of body weight correlated with the severity of the disease produced by the viruses, and interestingly, body temperatures measured after infection were higher in the 5-week-old ducks inoculated with the more virulent viruses, Egret/02 and Dk/05, than in the 2-week-old ducks inoculated with these same viruses, indicating possible differences in the innate immune responses.

Previous studies have demonstrated that the pathogenicity of H5N1 HPAI viruses in ducks directly correlates with levels of virus replication in tissues, with the more pathogenic viruses replicating to higher titers and in more tissues (Pantin-Jackwood and Swayne, 2007; Pfeiffer et al., 2009; Wasilenko et al., 2011). Ducks that died after infection with these pathogenic viruses presented neurological signs and heart damage, either lesions being possible contributors to death. In the present study, and as previously observed, viral titers in tissues were also elevated in ducks infected with the two more virulent viruses, Egret/02 and Dk/05, and antigen staining in tissues from these ducks indicated replication of the viruses in several organs and in association with the histological lesions observed. However, clear differences in viral titer in tissues between the 2-week-old and 5-week-old infected ducks was only observed in the ducks infected with the less pathogenic Ck/97 virus, with higher or detectable titers found in the younger ducks. This was also seen with the RT-PCR results when examining for presence of viral RNA in lungs and spleens. Nevertheless, the higher titers of Ck/97 in the younger ducks were not reflected in increased clinical signs or the outcome of infection. Contrary to this, in a similar study, 2 and 5-week-old ducks infected with two different H5N1 HPAI viruses showed that one virus grew to similar high titers in tissues in both age groups, and the other virus grew to higher titers in the younger ducks (Pantin-Jackwood et al., 2007); but higher mortality was observed in the younger ducks infected with either virus. Although showing similar patterns, minor incongruence was observed between the immunohistochemistry (IHC) results and the virus titers in tissues and swabs (Tables 2 and 3 and Fig. 3). Virus staining in tissues can help determine in which cells the virus is replicating in and how widespread is this replication; however, IHC is not a very sensitive assay and not the most adequate method to quantify virus replication in tissues. This is in part because of the high virus titers needed for virus visualization and the possible loss of infected cells during the IHC procedure. In addition, and compared to virus isolation, during microscopic examination only a small portion of the tissue is examined. Similar viral titers and viral distribution in tissues at 2 dpi in 2 and 5-week-old ducks infected with Egret/02 and Dk/05 viruses, suggests that other factors might be contributing to the differences observed in clinical presentation and survival. Since little difference in viral RNA expression in lungs and spleens was found between the 2 and 5-week-old ducks infected with these two viruses, the differences observed in innate immune-related gene expression are probably caused by differences in host responses between age groups.

Influenza virus infection triggers a cascade of host defenses that are responsible for virus control and clearance, but also for many of the symptoms associated with clinical disease. In mammals, high virulence is also linked with substantial levels of viral replication *in vivo* (Basler and Aguilar, 2008); but the manner with which viral replication contributes to virulence remains to be determined. High virulence in mammals has also been associated with potent, perhaps excessive, inflammatory responses, and it is possible that these responses may prove to be the direct cause of the damage seen in severe disease (Basler and Aguilar, 2008; de Jong et al., 2006; Kash et al., 2004). Clinical features that are prominent in human H5N1 infections, such as acute respiratory

distress syndrome (ARDS) and multiple organ dysfunctions have been associated with cytokine dysregulation (Chan et al., 2005; Peiris et al., 2004; To et al., 2001). Studies to define which aspects of the pro-inflammatory immune response are beneficial and which are detrimental have only begun, sometimes giving contradictory results (Basler and Aguilar, 2008). Not much is known on the role of the innate immune responses to AI infection in avian species and how much of the clinical signs observed after infection are consequence of these responses.

Upon viral infection, production of type-I interferon (IFN) and IFN-induced genes is a typical innate defense response resulting in an antiviral state of non-infected neighboring target cells. Type I IFN is also known to act as an important immune inducer and immunoregulatory factor. In this study, type I (IFN-α) interferon gene expression was induced in the spleens of ducks following H5N1 HPAI virus infection and varied depending on the virus and the age of the ducks with significant differences in expression only observed with the Dk/05 virus. Up-regulation of IFN-α was also observed in spleens of Pekin and Muscovy ducks infected with another virulent H5N1 HPAI virus (Cagle et al., 2011). In both cases, levels of viral RNA in the spleen did not always correlate with IFN-α gene expression, suggesting differences between viruses in the induction of innate responses but also, like in the case of the Dk/05 virus, an effect of age on host responses to infection. Future studies will need to address the fluctuation of gene expression at different times after viral infection. This fluctuation could in part explain the down-regulation of IFN-α observed in the lungs of most virus-infected ducks in our study. However, differences in types of cells found in spleens and lungs likely play a role in the differences observed in the innate immune responses to virus infection between spleens and lung. The results obtained are the average gene expression of cells in the entire tissue including infected and uninfected cells.

Viral replication efficiencies and host immune responses against H5N1 HPAI virus infection has been shown to vary among established chicken cell lines (Watanabe et al., 2011). In the host, macrophages constitute a major component of the innate immune response against virus infections. At the local sites of infection, activated macrophages induce pro-inflammatory responses aimed at the elimination of invading pathogens and infected cells. Our immunohistochemistry data on tissues from the infected ducks showed the presence of the virus in resident and infiltrating macrophages in several tissues. It is not clear to what degree the virus replicates in macrophages *in vivo*, but the role of these cells in clearing virus and releasing immune mediators likely has a very important effect on AI pathogenicity. The presence of circulating or resident macrophages in tissues would surely affect the magnitude of the innate immune responses.

Increase of pro-inflammatory cytokine IL-6 gene expression in spleens was previously reported in Pekin and Muscovy ducks infected with a H5N1 HPAI virus (Cagle et al., 2011). Up-regulation of IL-6 was also found in tissues of ducks infected with the three H5N1 HPAI viruses used in this study. However no significant differences in gene expression were observed between the 2 and 5 week-old ducks. Differences in IL-2 gene expression were observed in the spleens and lungs of the infected ducks, indicating that modulation of the T-helper cytokine response might be differently induced by these viruses or affected by the age of the ducks.

Up-regulation of RIG-I in ducks after infection with H5N1 HPAI viruses has been reported previously (Barber et al., 2010; Cagle et al., 2011). RIG-I is present in ducks and plays a critical role in the innate immune response to influenza (Barber et al., 2010). RIG-I initiates interferon pathways which initiate antiviral defenses (Magor, 2011). In this study, the higher levels of expression of RIG-I in the spleens of the 5-week-old ducks infected with Dk/05when compared to the 2-week-old ducks, could indicate a more efficient innate immune response to infection in the older ducks.

To date there is little information available about fever in birds, although there is evidence that suggests that functional characteristics of avian fever are similar to those found in mammals (Gray et al., 2005). Very little is known about the mediators and modulators of the febrile response in avian species. There is some evidence that suggests that prostaglandins (PGs), as in mammalian fevers, play a role in the generation of fever in birds (Baert et al., 2005; Gray et al., 2005; Macari et al., 1993). A role for cytokines, including IL-1 β and IL-6 has been suggested in the signaling pathways that lead to prostaglandin synthesis (Macari et al., 1993). Elevated levels of IL-6 gene expression were found in the spleens of the 5-week-old ducks infected with the most virulent virus. These ducks also had high fever, but the levels of IL-6 did not seem to correlate with the differences observed in body temperature. Nitric oxide (NO) has also been postulated to play a role in fever genesis (De Paula et al., 2000). Currently, little is known about the role of NO in avian fever. Studies in Pekin ducks suggested that lipopolysaccharide (LPS)-induced fever is mediated by prostaglandins and nitric oxide and is modulated by adrenocorticoid hormones (Gray et al., 2005). Levels of NO in serum were elevated in the ducks infected with the two more virulent viruses when compared to the non-infected ducks, but the highest levels were observed in the 2-week-old ducks infected with Dk/05 and did not correlate with increased body temperature.

The inflammatory response observed after infection with H5N1 HPAI virus infection is compounded by significant necrosis and increased oxidative stress in tissues. The activation of these pathology-associated pathways in AI virus infection results in the development of severe disease and consequently death. In mature ducks these responses could have curtailed and eventually controlled virus infection as seen after infection with Egret/02 in the 5-week-old ducks. However, with the more pathogenic Dk/05 virus, the host responses were not sufficient to control the virus and all infected ducks died.

The data presented indicates that differences in the severity of HPAI virus infections in ducks were associated with differences in viral replication and, to certain extent, host gene expression. The more virulent viruses replicated to high titers in tissues of both the 2 and 5-week-old ducks, however, some of the older ducks survived infection, and the ones that died lived longer than the younger ducks. The inability to fight off infection observed in younger ducks could be explained in part by a less efficient innate immune response. The weaker expression of some immune-related genes in the younger ducks suggests that the immune system in younger ducks is still not completely developed and consequently is not as efficient in fighting infection as in more mature ducks. More studies examining innate immune responses at earlier time points after virus infection would help to elucidate this.

Acknowledgements

The authors appreciate the assistance provided by Tracy Smith-Faulkner, Ronald Graham and Roger Brock in conducting these studies. The authors also thank the FSIS histopathology laboratory at Russell Research Center-USDA for technical assistance. This research was supported by USDA/ARS CRIS project #6612-32000-048. Mention of trade names or commercial products in this presentation is solely for the purpose of providing specific information and does not imply recommendation or endorsement by the U.S. Department of Agriculture. USDA is an equal opportunity provider and employer.

References

Aldous, E.W., Seekings, J.M., McNally, A., Nili, H., Fuller, C.M., Irvine, R.M., Alexander, D.J., Brown, I.H., 2010. Infection dynamics of highly pathogenic avian influenza and virulent avian paramyxovirus type 1 viruses in chickens, turkeys and ducks. Avian Pathology 39 (4), 265–273.

Adams, S.C., Xing, Z., Li, J., Cardona, C.J., 2009. Immune-related gene expression in response to H11N9 low pathogenic avian influenza virus infection in chicken and Pekin duck peripheral blood mononuclear cells. Molecular Immunology 46 (8–9), 1744–1749.

Baert, K., Duchateau, L., De Boever, S., Cherlet, M., De Backer, P., 2005. Antipyretic effect of oral sodium salicylate after an intravenous *E. coli* LPS injection in broiler chickens. British Poultry Science 46 (2), 137–143.

Barber, M.R., Aldridge Jr., J.R., Webster, R.G., Magor, K.E., 2010. Association of RIG-I with innate immunity of ducks to influenza. Proceedings of the National Academy of Sciences of the United States of America 107 (13), 5913–5918.

Basler, C.F., Aguilar, P.V., 2008. Progress in identifying virulence determinants of the 1918 H1N1 and the Southeast Asian H5N1 influenza A viruses. Antiviral Research 79 (3), 166–178.

Burggraaf, S., Bingham, J., Payne, J., Kimpton, W.G., Lowenthal, J.W., Bean, A.G., 2011. Increased inducible nitric oxide synthase expression in organs is associated with a higher severity of H5N1 influenza virus infection. PLoS One 6 (1), e14561.

Cagle, C., To, T.L., Nguyen, T., Wasilenko, J., Adams, S.C., Cardona, C.J., Spackman, E., Suarez, D.L., Pantin-Jackwood, M.J., 2011. Pekin and Muscovy ducks respond differently to vaccination with a H5N1 highly pathogenic avian influenza (HPAI) commercial inactivated vaccine. Vaccine 29, 6549–6557.

Cameron, C.M., Cameron, M.J., Bermejo-Martin, J.F., Ran, L., Xu, L., Turner, P.V., Ran, R., Danesh, A., Fang, Y., Chan, P.K., Mytle, N., Sullivan, T.J., Collins, T.L., Johnson, M.G., Medina, J.C., Rowe, T., Kelvin, D.J., 2008. Gene expression analysis of host innate immune responses during Lethal H5N1 infection in ferrets. Journal of Virology 82 (22), 11308–11317.

Capua, I., Mutinelli, F., 2001. Mortality in Muscovy ducks (*Cairina moschata*) and domestic geese (*Anser anser* var. *domestica*) associated with natural infection with a highly pathogenic avian influenza virus of H7N1 subtype. Avian Pathology 30, 179–183.

Capua, I., Alexander, D.J., 2008. Avian influenza vaccines and vaccination in birds. Vaccine 26 (Suppl. 4), D70–D73.

Chan, M.C., Cheung, C.Y., Chui, W.H., Tsao, S.W., Nicholls, J.M., Chan, Y.O., Chan, R.W., Long, H.T., Poon, L.L., Guan, Y., Peiris, J.S., 2005. Proinflammatory cytokine responses induced by influenza A (H5N1) viruses in primary human alveolar and bronchial epithelial cells. Respiratory Research 6, 135.

Chen, H., Deng, G., Li, Z., Tian, G., Li, Y., Jiao, P., Zhang, L., Liu, Z., Webster, R.G., Yu, K., 2004. The evolution of H5N1 influenza viruses in ducks in southern China. Proceedings of the National Academy of Sciences of the United States of America 101 (28), 10452–10457.

Costa, T.P., Brown, J.D., Howerth, E.W., Stallknecht, D.E., 2010. The effect of age on avian influenza viral shedding in mallards (*Anas platyrhynchos*). Avian Diseases 54 (Suppl. 1), 581–585.

de Jong, M.D., Simmons, C.P., Thanh, T.T., Hien, V.M., Smith, G.J., Chau, T.N., Hoang, D.M., Chau, N.V., Khanh, T.H., Dong, V.C., Qui, P.T., Cam, B.V., Ha do, Q., Guan, Y., Peiris, J.S., Chinh, N.T., Hien, T.T., Farrar, J., 2006. Fatal outcome of human influenza A (H5N1) is associated with high viral load and hypercytokinemia. Nature Medicine 12 (10), 1203–1207.

De Paula, D., Steiner, A.A., Branco, L.G., 2000. The nitric oxide pathway is an important modulator of stress-induced fever in rats. Physiology and Behavior 70 (5), 505–511.

Degen, W.G., Smith, J., Simmelink, B., Glass, E.J., Burt, D.W., Schijns, V.E., 2006. Molecular immunophenotyping of lungs and spleens in naive and vaccinated chickens early after pulmonary avian influenza A (H9N2) virus infection. Vaccine 24 (35–36), 6096–6109.

Ellis, T.M., Bousfield, R.B., Bissett, L.A., Dyrting, K.C., Luk, G.S., Tsim, S.T., Sturm-Ramirez, K., Webster, R.G., Guan, Y., Malik Peiris, J.S., 2004. Investigation of outbreaks of highly pathogenic H5N1 avian influenza in waterfowl and wild birds in Hong Kong in late 2002. Avian Pathology 33 (5), 492–505.

Gilbert, M., Chaitaweesub, P., Parakamawongsa, T., Premashthira, S., Tiensin, T., Kalpravidh, W., Wagner, H., Slingenbergh, J., 2006. Free-grazing ducks and highly pathogenic avian influenza, Thailand. Emerging Infectious Diseases 12 (2), 227–234.

Gray, D.A., Maloney, S.K., Kamerman, P.R., 2005. Lipopolysaccharide-induced fever in Pekin ducks is mediated by prostaglandins and nitric oxide and modulated by adrenocortical hormones. American Journal of Physiology: Regulatory Integrative and Comparative Physiology 289 (5), R1258–R1264.

Hayden, F.G., Fritz, R., Lobo, M.C., Alvord, W., Strober, W., Straus, S.E., 1998. Local and systemic cytokine responses during experimental human influenza A virus infection. Relation to symptom formation and host defense. Journal of Clinical Investigation 101 (3), 643–649.

Hulse-Post, D.J., Sturm-Ramirez, K.M., Humberd, J., Seiler, P., Govorkova, E.A., Krauss, S., Scholtissek, C., Puthavathana, P., Buranathai, C., Nguyen, T.D., Long, H.T., Naipospos, T.S., Chen, H., Ellis, T.M., Guan, Y., Peiris, J.S., Webster, R.G., 2005. Role of domestic ducks in the propagation and biological evolution of highly pathogenic H5N1 influenza viruses in Asia. Proceedings of the National Academy of Sciences of the United States of America 102 (30), 10682–10687.

Jilbert, A.R., Botten, J.A., Miller, D.S., Bertram, E.M., Hall, P.M., Kotlarski, J., Burrell, C.J., 1998. Characterization of age- and dose-related outcomes of duck hepatitis B virus infection. Virology 244 (2), 273–282.

Kash, J.C., Basler, C.F., Garcia-Sastre, A., Carter, V., Billharz, R., Swayne, D.E., Przygodzki, R.M., Taubenberger, J.K., Katze, M.G., Tumpey, T.M., 2004. Global host immune response: pathogenesis and transcriptional profiling of type A influenza viruses expressing the hemagglutinin and neuraminidase genes from the 1918 pandemic virus. Journal of Virology 78 (17), 9499–9511.

Kishida, N., Sakoda, Y., Isoda, N., Matsuda, K., Eto, M., Sunaga, Y., Umemura, T., Kida, H., 2005. Pathogenicity of H5 influenza viruses for ducks. Archives of Virology 150 (7), 1383–1392.

Kwon, Y.-K., Joh, S.-J., Kim, M.-C., Sung, H.-W., Lee, Y.-J., Choi, J.-G., Lee, E.-K., Kim, J.-H., 2005. Highly pathogenic avian influenza (H5N1) in the commercial domestic ducks of South Korea. Avian Pathology 34, 367–370.

Lavoie, E.T., Sorrell, E.M., Perez, D.R., Ottinger, M.A., 2007. Immunosenescence and age-related susceptibility to influenza virus in Japanese quail. Developmental and Comparative Immunology 31 (4), 407–414.

Li, K.S., Guan, Y., Wang, J., Smith, G.J., Xu, K.M., Duan, L., Rahardjo, A.P., Puthavathana, P., Buranathai, C., Nguyen, T.D., Estoepangestie, A.T., Chaisingh, A., Auewarakul, P., Long, H.T., Hanh, N.T., Webby, R.J., Poon, L.L., Chen, H., Shortridge, K.F., Yuen, K.Y., Webster, R.G., Peiris, J.S., 2004. Genesis of a highly pathogenic and potentially pandemic H5N1 influenza virus in eastern Asia. Nature 430 (6996), 209–213.

Liang, Q.L., Luo, J., Zhou, K., Dong, J.X., He, H.X., 2011. Immune-related gene expression in response to H5N1 avian influenza virus infection in chicken and duck embryonic fibroblasts. Molecular Immunology 48 (6–7), 924–930.

Londt, B.Z., Nunez, A., Banks, J., Alexander, D.J., Russell, C., Richard-Londt, A.C., Brown, I.H., 2010. The effect of age on the pathogenesis of a highly pathogenic avian influenza (HPAI) H5N1 virus in Pekin ducks (*Anas platyrhynchos*) infected experimentally. Influenza and Other Respiratory Viruses 4 (1), 17–25.

Macari, M., Furlan, R.L., Gregorut, F.P., Secato, E.R., Guerreiro, J.R., 1993. Effects of endotoxin, interleukin-1 beta and prostaglandin injections on fever response in broilers. British Poultry Science 34 (5), 1035–1042.

Magor, K.E., 2011. Immunoglobulin genetics and antibody responses to influenza in ducks. Developmental and Comparative Immunology 35 (9), 1008–1016.

Pantin-Jackwood, M.J., Swayne, D.E., 2007. Pathobiology of Asian Highly Pathogenic Avian Influenza H5N1 virus infections in ducks. Avian Diseases 51, 250–259.

Pantin-Jackwood, M.J., Suarez, D.L., Spackman, E., Swayne, D.E., 2007. Age at infection affects the pathogenicity of Asian highly pathogenic avian influenza H5N1 viruses in ducks. Virus Research 130 (1–2), 151–161.

Pantin-Jackwood, M.J., Swayne, D.E., 2009. Pathogenesis and pathobiology of avian influenza virus infection in birds. Revue Scientifique et Technique 28 (1), 113–136.

Peiris, J.S., Yu, W.C., Leung, C.W., Cheung, C.Y., Ng, W.F., Nicholls, J.M., Ng, T.K., Chan, K.H., Lai, S.T., Lim, W.L., Yuen, K.Y., Guan, Y., 2004. Re-emergence of fatal human influenza A subtype H5N1 disease. Lancet 363 (9409), 617–619.

Perkins, L.E., Swayne, D.E., 2001. Pathobiology of A/chicken/Hong Kong/220/97 (H5N1) avian influenza virus in seven gallinaceous species. Veterinary Pathology 38 (2), 149–164.

Pfeiffer, J., Pantin-Jackwood, M., To, T.L., Nguyen, T., Suarez, D.L., 2009. Phylogenetic and biological characterization of highly pathogenic H5N1 avian influenza viruses (Vietnam 2005) in chickens and ducks. Virus Research 142 (1–2), 108–120.

Phuong, D.Q., Dung, N.T., Jorgensen, P.H., Handberg, K.J., Vinh, N.T., Christensen, J.P., 2011. Susceptibility of Muscovy (*Cairina moschata*) and mallard ducks (*Anas platyrhynchos*) to experimental infections by different genotypes of H5N1 avian influenza viruses. Veterinary Microbiology 148 (2–4), 168–174.

Rebel, J.M., Peeters, B., Fijten, H., Post, J., Cornelissen, J., Vervelde, L., 2011. Highly pathogenic or low pathogenic avian influenza virus subtype H7N1 infection in chicken lungs: small differences in general acute responses. Veterinary Research 42 (1), 10.

Reemers, S.S., Groot Koerkamp, M.J., Holstege, F.C., van Eden, W., Vervelde, L., 2009. Cellular host transcriptional responses to influenza A virus in chicken tracheal organ cultures differ from responses in in vivo infected trachea. Veterinary Immunology and Immunopathology 132 (2–4), 91–100.

Reemers, S.S., van Leenen, D., Koerkamp, M.J., van Haarlem, D., van de Haar, P., van Eden, W., Vervelde, L., 2010. Early host responses to avian influenza A virus are prolonged and enhanced at transcriptional level depending on maturation of the immune system. Molecular Immunology 47 (9), 1675–1685.

Sarmento, L., Afonso, C.L., Estevez, C., Wasilenko, J., Pantin-Jackwood, M., 2008a. Differential host gene expression in cells infected with highly pathogenic H5N1 avian influenza viruses. Veterinary Immunology and Immunopathology 125 (3–4), 291–302.

Sarmento, L., Pantin-Jackwood, M., Kapczynski, D.R., Swayne, D.E., Afonso, C.L., 2008b. Immediate early responses of avian tracheal epithelial cells to infection with highly pathogenic avian influenza virus. Developmental Biology (Basel) 132, 175–183.

Sarmento, L., Wasilenko, J., Pantin-Jackwood, M., 2010. The effects of NS gene exchange on the pathogenicity of H5N1 HPAI viruses in ducks. Avian Diseases 54 (Suppl. 1), 532–537.

Sims, L.D., 2007. Experience in control of avian influenza in Asia. Developmental Biology (Basel) 130, 39–43.

Songserm, T., Jam-on, R., Sae-Heng, N., Meemak, N., Hulse-Post, D.J., Sturm-Ramirez, K.M., Webster, R.G., 2006. Domestic ducks and H5N1 Influenza Epidemic, Thailand. Emerging Infectious Diseases 12 (4), 575–581.

Spackman, E., Senne, D.A., Myers, T.J., Bulaga, L.L., Garber, L.P., Perdue, M.L., Lohman, K., Daum, L.T., Suarez, D.L., 2002. Development of a real-time reverse

transcriptase PCR assay for type A influenza virus and the avian H5 and H7 hemagglutinin subtypes. Journal of Clinical Microbiology 40 (9), 3256–3260.

Sturm-Ramirez, K.M., Hulse-Post, D.J., Govorkova, E.A., Humberd, J., Seiler, P., Puthavathana, P., Buranathai, C., Nguyen, T.D., Chaisingh, A., Long, H.T., Naipospos, T.S., Chen, H., Ellis, T.M., Guan, Y., Peiris, J.S., Webster, R.G., 2005. Are ducks contributing to the endemicity of highly pathogenic H5N1 influenza virus in Asia? Journal of Virology 79 (17), 11269–11279.

Suzuki, K., Okada, H., Itoh, T., Tada, T., Mase, M., Nakamura, K., Kubo, M., Tsukamoto, K., 2009. Association of increased pathogenicity of Asian H5N1 highly pathogenic avian influenza viruses in chickens with highly efficient viral replication accompanied by early destruction of innate immune responses. Journal of Virology 83 (15), 7475–7486.

Swayne, D.E., 2006. Principles for vaccine protection in chickens and domestic waterfowl against avian influenza: emphasis on Asian H5N1 high pathogenicity avian influenza. Annals of the New York Academy of Sciences 1081, 174–181.

Swayne, D.E., Halvorson, D.A., 2008. Influenza. In: Glisson, J.R., Saif, Y.M., Fadly, A.M., McDougald, L.R., Nolan, L. (Eds.), Diseases of Poultry. , 12th ed. Blackwell, Ames, IA.

Swayne, D.E., Senna, D.A., Beard, C.W., 1998. Avian influenza. In: Swayne, J.R.G.D.E., Jackwood, M.W., Pearson, J.E., Reed, W.M. (Eds.), A Laboratory Manual for the Isolation and Identification of Avian Pathogens. , 4th ed. American Association of Avian Pathologists, Kennett Square, PA, pp. 150–155.

Szretter, K.J., Gangappa, S., Lu, X., Smith, C., Shieh, W.J., Zaki, S.R., Sambhara, S., Tumpey, T.M., Katz, J.M., 2007. Role of host cytokine responses in the pathogenesis of avian H5N1 influenza viruses in mice. Journal of Virology 81 (6), 2736–2744.

To, K.F., Chan, P.K., Chan, K.F., Lee, W.K., Lam, W.Y., Wong, K.F., Tang, N.L., Tsang, D.N., Sung, R.Y., Buckley, T.A., Tam, J.S., Cheng, A.F., 2001. Pathology of fatal human infection associated with avian influenza A H5N1 virus. Journal of Medical Virology 63 (3), 242–246.

Tohidi-Esfahani, R., Vickery, K., Cossart, Y., 2010. The early host innate immune response to duck hepatitis B virus infection. Journal of General Virology 91 (Pt 2), 509–520.

Wasilenko, J.L., Arafa, A.M., Selim, A.A., Hassan, M.K., Aly, M.M., Ali, A., Nassif, S., Elebiary, E., Balish, A., Klimov, A., Suarez, D.L., Swayne, D.E., Pantin-Jackwood, M.J., 2011. Pathogenicity of two Egyptian H5N1 highly pathogenic avian influenza viruses in domestic ducks. Archives of Virology 156 (1), 37–51.

Wasilenko, J.L., Lee, C.W., Sarmento, L., Spackman, E., Kapczynski, D.R., Suarez, D.L., Pantin-Jackwood, M.J., 2008. NP, PB1, and PB2 viral genes contribute to altered replication of H5N1 avian influenza viruses in chickens. Journal of Virology 82 (9), 4544–4553.

Wasilenko, J.L., Sarmento, L., Pantin-Jackwood, M.J., 2009. A single substitution in amino acid 184 of the NP protein alters the replication and pathogenicity of H5N1 avian influenza viruses in chickens. Archives of Virology 154 (6), 969–979.

Watanabe, C., Uchida, Y., Ito, H., Ito, T., Saito, T., 2011. Host immune-related gene responses against highly pathogenic avian influenza virus infection in vitro differ among chicken cell lines established from different organs. Veterinary Immunology and Immunopathology 144 (3–4), 187–199.

Xing, Z., Cardona, C.J., Adams, S., Yang, Z., Li, J., Perez, D., Woolcock, P.R., 2009. Differential regulation of antiviral and proinflammatory cytokines and suppression of Fas-mediated apoptosis by NS1 of H9N2 avian influenza virus in chicken macrophages. Journal of General Virology 90 (Pt 5), 1109–1118.

AVIAN DISEASES 55:459–461, 2011

Research Note—

Experimental Infection with Low and High Pathogenicity H7N3 Chilean Avian Influenza Viruses in Chiloe Wigeon (*Anas sibilatrix*) and Cinnamon Teal (*Anas cyanoptera*)

Mariana Sá e Silva,[A] Christian Mathieu-Benson,[AB] Yong-kuk Kwon,[AC] Mary Pantin-Jackwood,[A] and David E. Swayne[AD]

[A]United States Department of Agriculture, Agriculture Research Service, Southeast Poultry Research Laboratory, 934 College Station Road, Athens, GA 30605

Received 21 January 2011; Accepted and published ahead of print 1 April 2011

SUMMARY. Two different wild duck species common in Chile and neighboring countries, Chiloe wigeon (*Anas sibilatrix*) and cinnamon teal (*Anas cyanoptera*), were intranasally inoculated with 10^6 mean embryo infective dose (EID_{50}) of the H7N3 low pathogenicity (LP) avian influenza virus (AIV) (A/chicken/Chile/176822/02) or high pathogenicity (HP) AIV (A/chicken/Chile/184240-1/02), in order to study the infectivity and pathobiology of these viruses. None of the virus-inoculated ducks had clinical signs or died, but most seroconverted by 14 days postinoculation (DPI), indicating a productive virus infection. Both LPAIV and HPAIV were isolated from oral swabs from two of six Chiloe wigeons and from oral and/or cloacal swabs from all five of the cinnamon teal at 2 DPI. Both LPAIV and HPAIV were efficiently transmitted to cinnamon teal contacts but not to Chiloe wigeon contacts. This study demonstrates that the cinnamon teal and Chiloe wigeons were susceptible to infection with both Chilean H7N3 LPAIV and HPAIV, but only the cinnamon teal showed contact transmission of the virus between birds, suggesting that the cinnamon teal has the potential to be a reservoir for these viruses, especially the LPAIV, as was demonstrated in 2001 with isolation of a genetically related H7N3 LPAIV strain in a cinnamon teal in Bolivia. However, the definitive source of the H7N3 Chilean LPAIV still remains unknown.

RESUMEN. *Nota de Investigación*—Infección experimental con virus de influenza aviar de baja y de alta patogenicidad subtipo H7N3 originarios de Chile en patos reales (*Anas sibilatrix*) y en patos colorados (*Anas cyanoptera*).

Dos especies diferentes de patos silvestres comunes en Chile y en los países vecinos, el pato real o (*Anas sibilatrix*) y el pato colorado (*Anas cyanoptera*), fueron inoculados por vía intranasal con 10^6 dosis infectantes para embrión de pollo (EID50) de virus de la influenza aviar de baja patogenicidad subtipo (A/pollo/Chile/176822/02) o del virus de influenza aviar de alta patogenicidad (A/pollo/Chile/184240-1/02), con el fin de estudiar la infectividad y la patobiología de estos virus. Ninguno de los patos inoculados mostró signos clínicos o mortalidad, pero la mayoría de las aves mostraron seroconversión por el día 14 después de la inoculación, lo que indica una infección viral productiva. Ambos virus de influenza aviar, de baja y de alta patogenicidad fueron aislados a partir de hisopos orales de dos patos reales de un total de seis, mientras que fue aislado a partir de hisopos orales y/o cloacales de los cinco patos colorados, a los dos días después de la inoculación. Ambos virus de baja y alta patogenicidad fueron transmitidos de manera eficiente a los patos colorados que se utilizaron como aves contacto, pero esto no sucedió con los patos reales. Este estudio demuestra que el pato colorado y el pato real fueron susceptibles a la infección con ambos virus de influenza aviar originarios de Chile subtipo H7N3 de baja y de alta patogenicidad, pero sólo se observó transmisión por contacto en el pato colorado, lo que sugiere que el pato colorado tiene el potencial de servir como un reservorio para estos virus, especialmente para el virus de la influenza aviar de baja patogenicidad, como quedó demostrado en año 2001, con el aislamiento de un virus de baja patogenicidad subtipo H7N3 genéticamente relacionado con patos colorados de Bolivia. Sin embargo, el origen definitivo del virus de influenza aviar de baja patogenicidad subtipo H7N3 de Chile permanece desconocido.

Key words: avian influenza, Chiloe wigeon, cinnamon teal, H7N3, wild ducks

Abbreviations: AI = avian influenza; AIV = avian influenza virus; DPI = days postinoculation; EID_{50} = mean embryo infective dose; H7N3/HP = A/chicken/Chile/184240-1/02; H7N3/LP = A/chicken/Chile/176822/02; HP = high pathogenicity; IN = intranasal; LP = low pathogenicity; SEPRL = Southeast Poultry Research Laboratory

Avian influenza virus (AIV) is a segmented, single-stranded, negative-sense RNA virus belonging to the *Orthomyxoviridae* family, genus *Influenzavirus A* (13). Shorebirds and waterfowl species are commonly infected by low pathogenicity (LP) AIV in nature, and two groups of wild aquatic birds, the Charadriiformes and the Anseriformes, are known as reservoirs of the virus (2,6,12,15). The subtypes identified in wild aquatic birds may vary, and most of the viruses isolated from ducks are H3, H4, and H6 (12). The prevalence of H5 and H7 LPAIV is low, and infection with high pathogenicity (HP) AIV in wild species is rare (8,12). So far, the only HPAIVs associated with high mortality in wild birds have been H5N1 HPAIV in Asia, Europe, and Africa from the early 2000s, and H5N3 in common terns (*Sterna hirundo*) from South Africa during 1961 (8,15).

The first outbreak of avian influenza (AI) in South America was reported in Chile in 2002 (10), and it was caused by a H7N3 LPAIV. After a month, the mortality rate increased, and an emergent

[B]Present address: Servicio Agrícola y Ganadero, Departamento de Laboratorios y Estaciones Cuarentenarias Agrícola y Pecuaria, Km 22, Ruta 68, Lo Aguirre, Pudahuel, Chile.

[C]Present address: National Veterinary Research and Quarantine Service, Anyang, Gyeonggi 480-757, South Korea.

[D]Corresponding author: E-mail: David.Swayne@ars.usda.gov

HPAIV was isolated from the same company farm (10). Even though the source of the LPAIV in that outbreak remains unknown, the virus could have been introduced by migratory birds (5,11). Previously, in 2001, an H7N3 LPAIV was isolated from a cinnamon teal in Bolivia, and it was genetically and biologically similar to the Chilean LPAIV isolated from the 2002 outbreak (11).

The aim of this study was to determine the infectivity, pathogenicity, and transmissibility of H7N3 LPAIV and HPAIV isolated from the Chilean outbreak in two common wild waterfowl species, Chiloe wigeons (*Anas sibilatrix*) and cinnamon teal (*Anas cyanoptera*). These two bird species are commonly present in South America, including Chile, and knowledge of whether or not AIV can infect these ducks and/or cause clinical disease is important for a better understanding of the ecology and epidemiology of AI.

MATERIALS AND METHODS

The viruses A/chicken/Chile/176822/02 (H7N3/LP) and A/chicken/Chile/184240-1/02 (H7N3/HP) were obtained from the Agriculture and Livestock Service in Chile and processed at the National Veterinary Services Laboratory (NVSL) in Ames, IA, and Southeast Poultry Research Laboratory (SEPRL), Athens, GA. Previously, the H7N3/LP virus was shown to be LP and H7N3/HP was shown to be HP based on an intravenous pathogenicity index test in chickens (5,14), which is the international standard test for determining AIV pathogenicity (7). All the procedures for virus propagation, virus isolation from swabs and tissues, and virus titration were performed in embryonating chicken eggs using standard procedures (7).

Ten 4-mo-old Chiloe wigeons (*Anas sibilatrix*) and nine 4-mo-old cinnamon teal (*Anas cyanoptera*) (Chenoa Waterfowl, Martin, TN) were placed into six groups, three groups per species: 1) shams ($n = 2$) inoculated with allantoic fluid diluted 1:300 in brain-heart infusion medium (BD Bioscience, Sparks, MD), 2) LPAIV inoculates ($n = 3$ for Chiloe wigeons; $n = 2$ for cinnamon teal) that received 10^6 mean embryo infective doses (EID_{50}) in 0.1 ml of H7N3/LP, and 3) HPAIV inoculates ($n = 3$) that received 10^6 EID_{50} in 0.1 ml of H7N3/HP. Additionally, one contact duck, matching the species, was placed in each of the two LPAIV and two HPAIV groups, 24 h after intranasal (IN) inoculation of ducks with AIV.

All the ducks were weighed, and blood samples were taken at 0 (prechallenge) and 14 days postinoculation (DPI). A blocking ELISA (FlockCheck AI MultiS-Screen Antibody Test Kit; IDEXX Laboratories, Westbrook, ME) was performed on the serum according to Brown *et al.* (1). Oral and cloacal swabs were taken at 2 DPI. All ducks were euthanatized and submitted to necropsy at 14 DPI. Lung, kidney, heart, brain, and muscle samples were collected for virus isolation. Samples from brain, spleen, liver, heart, lung, cloacal bursa, thymus, kidney, gonad, adrenal gland, duodenum, pancreas, jejunum, cecum, trachea, and skeletal muscle were also collected for histopathology and viral antigen detection by immunohistochemistry as previously described (5).

All the experiments, including inoculation, sampling, necropsy, and laboratory techniques, were performed at SEPRL facilities with approval by the Institutional Animal Care and Use, and Institutional Biosafety Committees.

RESULTS AND DISCUSSION

None of the sham ducks developed clinical signs, seroconverted, or had pathologic changes (Table 1). Moreover, virus was not detected in oral or cloacal swabs at 2 DPI, and it was not isolated from any of the sampled tissues at 14 DPI, indicating the sham ducks lacked AIV infection.

At 2 DPI, a low quantity of virus was isolated from oral swabs of two IN-inoculated Chiloe wigeons (H7N3/LP, $n = 1$; H7N3/HP, $n = 1$), but five IN-inoculated Chiloe wigeons developed antibodies (H7N3/LP, $n = 3$; H7N3/HP, $n = 2$). Virus was not isolated from the two Chiloe wigeon contacts and one of the H7N3/HP IN-inoculates, and these ducks did not seroconvert by 14 DPI. In contrast, all five H7N3/LP and H7N3/HP IN-inoculated and both contact cinnamon teal seroconverted, and virus was detected in either oral or cloacal swabs, or both at 2 DPI (Table 1). At 14 DPI, no virus was isolated from tissues of any of the IN-inoculated or contact Chiloe wigeons or cinnamon teal. The higher rate of virus shedding from oropharyngeal and cloacal swabs of cinnamon teal (5 of 5) versus Chiloe wigeons (2 of 6), especially cloacal swabs, could have been responsible for the contact transmission and infection in the cinnamon teal, since the main route of infection for ducks has been proposed to be fecal-oral (3). In addition, cinnamon teal may be more susceptible than the Chiloe wigeon to infection by either AIV.

Table 1. Antibody response and virus shed titers for Chiloe wigeons and cinnamon teal inoculated intranasally with H7N3/LP and H7N3/HP viruses.

	ELISA[A]		Virus isolation (log_{10} EID_{50}/ml)[B]	
	0 DPI	14 DPI	Oral	Cloacal
Chiloe wigeon				
81 – Sham	–	–	–	–
82 – Sham	–	–	–	–
83 – Contact LPAIV	–	–	–	–
84 – Contact HPAIV	–	–	–	–
85 – LPAIV	–	+	0.97	–
86 – LPAIV	–	+	–	–
87 – LPAIV	–	+	–	–
88 – HPAIV	–	–	–	–
89 – HPAIV	–	+	1.7	–
90 – HPAIV	–	+	–	–
Cinnamon teal				
91 – Sham	–	–	–	–
92 – Sham	–	–	–	–
93 – Contact LPAIV	–	+	1.5	–
94 – Contact HPAIV	–	+	1.23	1.5
95 – LPAIV	–	+	1.9	1.23
96 – LPAIV	–	+	–	0.97
97 – HPAIV	–	+	–	1.5
98 – HPAIV	–	+	1.5	0.97
99 – HPAIV	–	+	–	1.5

[A]ELISA = enzyme-linked immunosorbent assay.
[B]Virus isolation from oral and/or cloacal swabs at 2 DPI.

The H7N3 LPAIV and HPAIV infections did not produce clinical signs, gross lesions, or weight loss in either duck species, and at 14 DPI, histologic lesions were absent in most tissues except the respiratory tract. Most IN-inoculated ducks had mild chronic lymphoplasmacytic rhinitis with glandular hyperplasia, mild lymphocytic tracheitis, and mild interstitial pneumonia. These lesions were most consistent in the ducks infected with the HPAIV. The mild interstitial pneumonia was more frequent in the cinnamon teals infected with the HPAIV, and the lesions in the Chiloe wigeons were mostly found in the upper respiratory tissues, i.e., nasal cavity and trachea. Influenza A virus specific antigen was not demonstrated in any of the tissues at 14 DPI. The lack of disease in the IN-inoculated and contact ducks agrees with previous reports that experimental LPAIV and HPAIV infection in wild waterfowl does not usually produce clinical signs, except for the recent H5N1 HPAIVs (8,15,16). The histologic lesions at 14 DPI, especially with H7N3/HP, suggested earlier AIV replication in the respiratory tract, as was confirmed by virus recovery from oropharyngeal swabs at 2 DPI and/or seroconversion at 14 DPI. Although LPAIVs typically show low virulence or are

avirulent in all bird species, the virulence of HPAIV infection is variable in different domestic and wild bird species (9). The same virus strain can produce experimental infection without disease in wild aquatic birds but still retain HP for chickens (8). The H7N3/HP virus used in this current study had low virulence for Chiloe wigeons and cinnamon teal, but in previous studies, inoculation of chickens caused severe clinical disease and high death rate, i.e., typical of a highly virulent HPAIV (5).

The initial AIVs from the 2002 Chilean outbreak were LPAIV, but within a month, HPAIV was isolated from the same region in Chile (5). The HPAIV virus was shown to have a 10 amino acids inserted at the HA0 cleavage site as the result of recombination by insertion of a portion of the nucleoprotein into the hemagglutinin proteolytic cleavage site (14). This ability to mutate from LP to HP has been reported for other H5 and H7 LPAIVs (17). However, the increase in virulence for chickens by this insertion in the hemagglutinin proteolytic cleavage site of H7N3/LP (5) did not translate to an increase virulence of the recombinant AIV, i.e., the H7N3/HP, for Chiloe wigeon and cinnamon teal of the current study.

In nature, H3N8 and H4N5 LPAIVs have been isolated from fecal samples of cinnamon teal in surveillance studies in Peru (4). Furthermore, the H7N3 LPAIV isolated from a wild cinnamon teal in 2001 in Bolivia has been shown to be genetically closely related to the 2002 Chilean H7N3 tested in this study (11). Serologic evidence of infection by AIV in a Chiloe wigeon has also been reported in a surveillance study in Argentina (1). These field surveillance data plus the infectivity and contact transmissibility of H7N3/LP viruses in current studies reinforce the ecologic role of cinnamon teal in LPAIV maintenance and spread within South America, including potential involvement in introduction of the Chilean H7N3 outbreak of LPAIV. However, the definitive source of the H7N3 Chilean LPAIV still remains unknown.

REFERENCES

1. Brown, J. D., M. P. Luttrell, M. M. Uhart, H. V. Ferreyra, M. M. Romano, M. V. Rago, and D. E. Stallknecht. Antibodies to Type A influenza virus in wild water birds from Argentina. J. Wildl. Dis. 46:1040–1045. 2010.

2. Feare, C. J. The role of wild birds in the spread of HPAI H5N1. Avian Dis. 51:440–447. 2007.

3. Fouchier, R. A. M., and V. J. Munster. Epidemiology of low pathogenic avian influenza viruses in wild birds. Rev. Sci. Tech. 28:49–58. 2009.

4. Ghersi, B. M., D. L. Blazes, E. Icochea, R. I. Gonzalez, T. Kochel, Y. Tinoco, M. y M. Sovero, S. Lindstrom, B. Shu, A. Klimov, A. E. Gonzalez, and J. M. Montgomery. Avian influenza in wild birds, central coast of Peru. Emerg. Infec. Dis. 15. Available from: http://www.cdc.gov/EID/content/15/6/935.htm. 2009.

5. Jones, Y. L., and D. E. Swayne. Comparative pathobiology of low and high pathogenicity H7N3 Chilean avian influenza viruses in chickens. Avian Dis. 48:119–128. 2004.

6. Latorre-Margalef, N., G. Gunnarsson, V. J. Munster, R. A. M. Fouchier, A. D. M. E. Osterhaus, J. Elmberg, B. Olsen, A. Wallensten, P. D. Haemig, T. Fransson, L. Brudin, and J. Waldenstrom. Effects of influenza A virus infection on migrating mallard ducks. Proc. R. Soc. B. 276: 1029–1036. 2009.

7. OIE (World Organisation for Animal Health). Chapter 2.3.4. Avian influenza. In: Manual of diagnostic tests and vaccines for terrestrial animals [Internet]. [cited 2010 Oct 10]. Available from: http://www.oie.int/fr/normes/mmanual/2008/pdf/2.03.04_AI.pdf. 2009.

8. Olsen, B., V. J. Munster, A. Wallensten, J. Waldenstrom, A. D. M. E. Osterhaus, and R. A. M. Fouchier. Global patterns of influenza A virus in wild birds. Science 312:384–388. 2006.

9. Perkins, L. E. L., and D. E. Swayne. Pathobiology of A/Chicken/Hong Kong/220/97 (H5N1) avian influenza virus in seven gallinaceous species. Vet. Pathol. 38:149–164. 2001.

10. Rojas, H., R. Moreira, P. Avalos, I. Capua, and S. Marangon. Avian influenza in poultry in Chile. Vet. Rec. 151:188. 2002.

11. Spackman, E., K. G. McCracken, K. Winker, and D. E. Swayne. H7N3 avian influenza virus found in a South American wild duck is related to the Chilean 2002 poultry outbreak, contains genes from equine and North American wild bird lineages, and is adapted to domestic turkeys. J. Virol. 80:7760–7764. 2006.

12. Stalknecht, D. E., and J. D. Brown. Chapter 3: Ecology of avian influenza in wild birds. In: Avian influenza. D. E. Swayne, ed. Blackwell Publishing, Ames, IA. pp. 43–58. 2008.

13. Suarez, D. L. Influenza A virus. In: Avian influenza. D. E. Swayne, ed. Blackwell Publishing, Ames, IA. pp. 3–22. 2008.

14. Suarez, D. L., D. A. Senne, J. Banks, I. H. Brown, S. C. Essen, C. W. Lee, R. J. Manvell, C. Mathieu-Benson, V. Moreno, J. C. Pedersen, B. Panigrahy, H. Rojas, E. Spackman, and D. J. Alexander. Recombination resulting in virulence shift in avian influenza outbreak, Chile. Emerg. Infec. Dis. 10. Available from: http://www.cdc.gov/ncidod/EID/vol10no4/03-0396.htm. 2004.

15. Swayne, D. E. Understanding the complex pathobiology of high pathogenicity avian influenza viruses in birds. Avian Dis. 51:242–249. 2007.

16. Tang, U., P. Wu, D. Peng, X. Wang, H. Wan, P. Zhang, J. Long, W. Zhang, Y. Li, W. Wang, X. Zhang, and X. Liu. Characterization of duck H5N1 influenza viruses with differing pathogenicity in mallard (*Anas platyrhynchos*) ducks. Avian Pathol. 38:457–467. 2009.

17. Toshihiro, I., H. Goto, E. Yamamoto, H. Tanaka, M. Takeuchi, M. Kuwayama, Y. Kawaoka, and K. Otsuki. Generation of a highly pathogenic avian influenza A virus from an avirulent field isolate by passaging in chickens. J. Virol. 75:4439–4443. 2001.

ACKNOWLEDGMENTS

We thank Joan Beck, Kira Moresco, and James Doster for the technical assistance.

Veterinary Immunology and Immunopathology 141 (2011) 221–229

Contents lists available at ScienceDirect

Veterinary Immunology and Immunopathology

journal homepage: www.elsevier.com/locate/vetimm

Research paper

In vivo transcriptional cytokine responses and association with clinical and pathological outcomes in chickens infected with different Newcastle disease virus isolates using formalin-fixed paraffin-embedded samples

Roselene Ecco[a,*], Corrie Brown[a], Leonardo Susta[a], Caran Cagle[b], Ingrid Cornax[b], Mary Pantin-Jackwood[b], Patti J. Miller[b], Claudio L. Afonso[b]

[a] Department of Veterinary Pathology, College of Veterinary Medicine, University of Georgia, Athens, GA 30602-7388, United States
[b] Southeast Poultry Research Laboratory, USDA-ARS, 934 College Station Rd., Athens, GA 30605, United States

ARTICLE INFO

Article history:
Received 26 August 2010
Received in revised form 13 January 2011
Accepted 3 March 2011

Keywords:
Newcastle disease virus
Chicken
Pathotype
Gene expression
Cytokines

ABSTRACT

Little is known about the host response of chickens infected with Newcastle disease virus (NDV) and the relationship between the innate immune response and the severity of clinical disease. Measurement of cytokine responses during infection *in vivo* can help to elucidate the mechanisms of virus pathogenesis. The transcriptional response of several cytokines from paraffin-embedded, formalin-fixed spleen of chicken naturally infected by NDV velogenic viscerotropic viruses was compared to the responses of atypical velogenic, velogenic neurotropic, and mesogenic strains during the first five days after infection. The RNA expression for IFN-γ and IL-6 was enhanced at day two in the highly virulent velogenic viscerotropic viruses (California and rZJ1 strains) and corresponded with the presence of the virus in tissues. However, in one atypical velogenic viscerotropic virus (Australia strain), two velogenic neurotropic viruses (Turkey ND and Texas GB) and, a mesogenic virus (Anhinga strain) the cytokine responses to infection were delayed or reduced. Increased levels of IFN-β RNA expression were only detected in the velogenic viscerotropic virus infected chickens (California and rZJ1 strains) at 3 days post-infection and one mesogenic strain (Anhinga) early in infection. The RNA expression levels of IL-2 did not increase upon infection with any of the viruses. A pronounced increase of RNA expression levels of IL-6 and IFN-γ was detected simultaneously with infiltration of macrophages and/or lymphoid necrosis in the histopathological analysis of the spleen and cecal tonsils. The differences in the RNA expression levels may help explain possible underlying mechanisms of clinical disease and/or immune responses in birds infected with strains of APMV-1 that cause distinct pathologic changes.

© 2011 Elsevier B.V. All rights reserved.

1. Introduction

Newcastle disease (ND) is a highly contagious problem of recurring concern to poultry industries internationally because of its worldwide distribution, extensive flock losses and/or trade restrictions. In the United States, outbreaks caused by virulent strains of Newcastle disease virus (NDV) are referred to as exotic Newcastle disease (END) (USDA, 2006). NDV, also known as avian paramyxovirus 1 (APMV-1) is a non-segmented, single-stranded, negative-sense RNA virus, belonging to the *Paramyxoviridae* family, and a member of the genus *Avulavirus* (Alexander and Senne, 2008). The RNA genome contains six genes encoding the six structural proteins: nucleo-

* Corresponding author. Tel.: +55 31 3409 2261; fax: +55 31 3409 2230.
E-mail addresses: eccoro72@gmail.com, ecco@vet.ufmg.br (R. Ecco).

0165-2427/$ – see front matter © 2011 Elsevier B.V. All rights reserved.
doi:10.1016/j.vetimm.2011.03.002

protein (NP), phosphoprotein (P), matrix (M), fusion (F), hemagglutinin-neuraminidase (HN) and large protein (L) (Chambers et al., 1986; Alexander and Senne, 2008).

The World Organization for Animal Health defines ND as "notifiable" if the virus has an intracerebral pathogenicity index (ICPI) equal to or greater than 0.7 and/or possesses multiple basic amino acids at the C-terminus of the fusion protein cleavage site (OIE, 2009). Virus strains are classified into three pathotypes depending on the severity of disease (velogen, mesogen and lentogen) (Brown et al., 1999). Velogens are further divided into viscerotropic and neurotropic based on their behavior subsequent to inoculation into adult birds (Alexander and Senne, 2008). Although both types of velogens cause severe clinical disease, the viscerotropic and neurotropic strains determine distinct disease syndromes. Clinically, infection of chickens with velogenic viscerotropic NDV (VVND) causes grave systemic illness, with marked depression and death within 5 days of infection (Brown et al., 1999; Kommers et al., 2001). In contrast, velogenic neurotropic strains (VNND) result in a longer disease course characterized predominantly by paresis and paralysis (Brown et al., 1999). Chickens infected with mesogenic strains can show clinical signs (respiratory and neurological signs) (Bhaiyat et al., 1995) or may not show any overt clinical signs (Brown et al., 1999). Lentogenic NDV isolates do not usually cause evident clinical signs in adult birds (Brown et al., 1999).

Pathologically, the responses in tissues also vary. The VVND viruses appear to preferentially target the lymphoid tissues, with greatest infection in and damage to macrophages, and extensive and early necrosis (Brown et al., 1999; Kommers et al., 2001). In contrast, the VNND strains generally focus on infection of neurons in CNS, although some virus-induced damage may be evident in lympoid/macrophage areas, as well (Brown et al., 1999). With respect to mesogenic isolates (for example, Roakin), there are splenic lymphoid hyperplasia and moderate myocarditis (Brown et al., 1999) with some strains later causing encephalomyelitis (Susta et al., 2010a). In birds infected with lentogenic isolates (B1 and QV4) the only pathologic change noted is splenic lymphoid hyperplasia (Brown et al., 1999).

Despite extensive research characterizing the pathogenesis of different isolates and pathotypes, little is known about host response to NDV infection and its relationship to the severity of clinical disease, lesions and death. Quantitative measuring of cytokine levels in ND would increase the understanding of the mechanisms of both pathogenesis and immunity (Sharma, 2008). Classically, innate responses are considered important in the earliest phases of microbial invasion, limiting the spread of the pathogen. When the pathogens cannot be controlled by the innate immune system, the host initiates a specific immune response (adaptive immunity). A protective avian immune response to NDV apparently depends on two principal antigens, the F and HN surface glycoproteins (Seal et al., 2000). Cytokines are important mediators and regulators of both types (innate and specific) of host response. It is unknown if chickens infected with different isolates of NDV can induce expression of antiviral interferon (IFN)-β or interleukin (IL)-2 and other pro-inflammatory cytokines such as IL-6. Krishnamurthy et al. (2006) using normal human skin fibroblast cells showed that these cells secreted IFN-β controlling the spread of NDV. However, *in vitro* response to NDV infection is insufficient to understand the nature of the host response to NDV *in vivo*.

This study was designed to investigate the early *in vivo* host response to NDV infection using strains of different virulence. The RNA expression of four cytokines was compared. Association between RNA expression of cytokines, histologic lesions, clinical disease and death was done in an attempt to understand the early pathogenesis in chickens infected with different pathotypes of NDV. Four cytokines were chosen for this study: IFN-γ, produced by Th-1 cells, which is a potent activator of macrophages, enhancing destruction of cell-associated pathogens (Lowenthal et al., 1995; Degen et al., 2005); IFN-β, produced mainly by macrophages, helps to protect neighboring cells from viral infection (Abbas et al., 2010); IL-6 which comes from activated macrophages, fibroblasts, and endothelial cells and serves to enhance vascular permeability and stimulates recruitment of inflammatory cells to the affected site (Lynagh et al., 2000; Kaiser et al., 2000); IL-2, also produced by T cells, and critical for the proliferation of a number of immune cells, including Th-1, Th-2, NK and B lymphocytes (Abbas et al., 2010).

2. Materials and methods

2.1. Tissue samples

Tissues used in this study included archived formalin-fixed, paraffin-embedded (FFPE) spleens from 4-week-old White Leghorn chickens. All the tissues were harvested in identical manners from different pathogenesis experiments (Brown et al., 1999; Susta et al., 2010a,b) using immunohistochemistry (IHC) and in situ hybridization (ISH). All birds were infected with 100 μl of approximately 10^5 EID_{50} (dose required to infect 50% of inoculated chicken embryos at 7–10 days of embryonation) of virus via eye-drop instillation. Birds were euthanized by intravenous injection of pentobarbital and tissues collected into 10% neutral buffered formalin immediately postmortem. After 52 h in formalin, tissues were processed for histology. Archived paraffin blocks were stored at room temperature. All chickens were from the same source flock kept at the Southeast Poultry Research Laboratory (SEPRL). Chickens were infected with Newcastle disease viruses (NDV) including the viscerotropic velogens California 2002, also known as CA02, (CA/S0212676/2002), rZJ1 (recombinant derived of wild ZJ1 virus from China), and Australia viruses (AUS/9809-19-1107/1998); the neurotropic velogens Turkey ND virus (Turkey ND/43084/92) and Texas GB/48 strains; the mesogen Anhinga virus (Anhinga/U.S. (Fla.)/44083/93). Birds infected with California, and rZJ1 were sampled at 2 and 3 days post infection (dpi); birds infected with Australia were sampled at 2, 3 and 5 dpi. Birds infected with Turkey ND and Texas GB strains were sampled at 2 and 5 dpi. Birds infected with Anhinga were sampled at 1, 2 and 3 dpi. Either phosphate buffered saline (PBS) or brain heart infusion (BHI) broth was used to inoculate non-infected control birds. For CA02 strain, 5 birds

Table 1
Primers sequences used in real time RT-PCR.

RNA target	Location	Primers sequence	Product size (bp)
β-actin	Forward:1F2180-2203	agaggctcccctgaaccccaaagc	94
	Reverse:1R2774-2797	ctggatggctacatacatggctgg	
IFN-γ	Forward	gtgaagaaggtgaaagatatcatgga	71
	Reverse	gctttgcgctggattctca	
IL-6	Forward	gctcgccggcttcga	71
	Reverse	ggtaggtctgaaaggcgaacag	
IL-2	Forward	ttggaaaatatcaagaacaagattcatc	93
	Reverse	tcccaggtaacactgcagagttt	
IFN-β	Forward	gcccacacactccaaaacactg	150
	Reverse	ttgatgctgaggtgagcgttg	
Virus matrix (M) gene	Forward	agtgatgtgctcggaccttc	121
	Reverse	cctgaggaggcatttgcta	

were used at 2 dpi and 2 birds at 3 dpi. For Anhinga, 5 birds were used at 1 and 2 dpi and 2 birds were used at 3 dpi. For all other strains, 2 or 3 infected birds were used. Spleens from a total of 5 non-infected control birds and 40 infected birds were used in this study.

2.2. RNA extraction from FFPE tissues

RNA extraction was performed using the Pure Link™ FFPE Total RNA Isolation kit (Invitrogen, Carlsbad, CA) according to manufacturer's instructions on FFPE chicken spleen samples that were cut to 5 μm of thickness (8–10 sections), and placed in RNase-free, 2 ml Eppendorf tubes. Resulting RNA yield ranged between 150 and 1440 ng/μl of total RNA in a total volume of 60 μl. RNA integrity values (Bioanalyzer RNA 6000 Nanokit Agilent Technology, Santa Clara, CA) obtained from FFPE tissues were low (2.3–2.45) due to RNA cross-linking (Invitrogen Pure Link™ protocol), however the OD260/280 ratios (NanoDrop® ND-1000 Spectrophotometer, Thermo Fisher Scientific, Wilmington, DE) were consistently high (1.9–2.0), and quantitative RT-PCR results were reproducible.

2.3. Prevention of genomic DNA contamination

Total RNA was treated to remove contaminating DNA using Deoxyribonuclease I, Amplification Grade (Invitrogen, Carlsbad, CA), according to the manufacturer's instructions. Conventional PCR to check residual genomic DNA contamination was done using reagents from Promega (Promega, Madison, WI) for β-actin DNA. Samples with residual genomic DNA were re-subjected to DNase I treatment, and assayed again for DNA contamination.

2.4. Primers

The β-actin primers were manually selected according to the available nucleotide sequences in GenBank (X00182) and properties verified using the Oligonucleotide Properties Calculator (www.basic.northwestern.edu/biotools/oligocalc.html). The primers were designed to span introns in the genomic DNA, thereby minimizing signal from contaminating genomic DNA. Primers from previously published sequence included IFN-γ, IL-6, IL-2 (Kaiser et al., 2003) and IFN-β (Degen et al., 2005). The presence of viral RNA in tissues was examined using the USDA-validated the Matrix-gene primer (Wise et al., 2004). All primers were synthesized by Integrated DNA Technologies (IDT, San Diego, CA). Sequences are provided in Table 1.

Single product formation was confirmed for all selected primers with reverse transcription PCR (RT-PCR) using RNA from fresh spleen. Briefly, 60 ng of total RNA was added in a 25 μl reaction in the presence of 10 μmol each primer, dNTP mix (10 μmol of each), 5× buffer (12.5 mM $MgCl_2$), enzyme mix and nuclease free water (OneStep RT-PCR Kit, QIAGEN, Valencia, CA). RT-PCR was performed with initial 50 °C for 30 min, 95 °C for 30 min, followed for 35 cycles of denaturation (94 °C, 30 s), annealing (58 °C, 30 s), extension (72 °C, 1 min) and a final cycle of extension for 5 min at 72 °C. To evaluate virus presence in the samples, RT-PCR was performed for NDV virus using the M-gene. Each reaction included 60 ng of total RNA added in a 25 μl reaction and the reaction was performed using SuperScript III One-Step RT-PCR System with Platinum Taq DNA Polymerase (Invitrogen).

2.5. Quantitative RT-PCR

Relative changes in RNA expression of IFN-γ, IL-6, IL-2, IFN-β, virus matrix gene (M-gene) and β-actin for samples from mock-infected control birds and for samples from infected chickens were measured as changes in SYBR green fluorescence after amplification with specific primer sets. Reactions were done in triplicate on 20 μl reaction mixtures containing 60 ng of total RNA, 500 nM of each primer, 10 μl of 2× master mix SYBR, 0.16 μl of enzyme mix (125×) (Power SYBR® Green RNA-to-CT™ 1-Step Kit, Applied Biosystems, CA, USA). Amplification and detection of specific products were performed using the Applied Biosystems 7500 Fast Real-Time PCR System with the following cycle profile: one cycle at 48 °C for 30 min, one cycle at 95 °C for 15 min, 40 cycles at 95 °C for 15 s and at 58 °C at 32 s. One cycle for dissociation curve for all reactions was added and melting curve analyzed.

2.6. Quantification of cytokine RNA relative expression

Relative changes in gene expression were calculated according to the Pflaffl method (Pflaffl, 2001) using Lin-

RegPCR version 12 (Ramakers et al., 2003) to calculate individual specific primer efficiency by linear regression. All cycle threshold fluorescence (Ct) values were corrected to the average Ct of mock-infected control for each gene of interest and the endogenous control (β-actin).

2.7. Validation assay

Changes in relative gene expression for IFNγ, IL-6, IFNβ, matrix gene and stability of the endogenous control seen in FFPE tissues were confirmed using fresh-frozen spleens from the same five mock-infected and five Anhinga-infected birds (1 dpi) that yielded the FFPE tissue. A section of fresh spleen was aseptically collected and passed through a 70 μM pore size mesh cup, immediately into Trizol (Invitrogen, Carlsbad, CA) and stored at −80 °C after collection of all samples for that day. Samples were later thawed at room temperature and chloroform was added according to the manufacturer's protocol. Samples were incubated for 10 min on ice. Following centrifugation at 2400 × *g* for 15 min, the aqueous phase was removed, mixed with an equal volume of 70% ethanol, and applied to Qiagen RNeasy midi prep columns (Qiagen, Valencia, CA). RNA quantity was assessed using a Nanodrop spectrophotometer on the RNA-40 setting and quality was assessed using a nanochip on a Bioanalyzer (Agilent Technologies, Santa Clara, CA). All RNA samples had a RNA integrity value greater than 8.6 with an average of 9.7. Quantitative RT-PCR was conducted as described above on 60 ng samples of RNA.

2.8. Data analysis

When three or more samples were available (Anhinga: 1 and 2 dpi, CA02: 2 dpi and Texas GB 5 dpi) statistical significance of mean changes in relative gene expression versus mock-infected control was determined by student *t* test (JMP 8.0 SAS Institute, Raleigh, NC). Relative gene expression in fresh and FFPE spleens was also compared using student *t* test. *p*-values less than or equal to 0.05 were considered significant changes in gene expression.

3. Results

3.1. Measuring gene expression in FFPE tissues

In order to validate qRT PCR results for gene expression in FFPE tissues, a trial comparing relative gene expression in FFPE tissue and fresh-frozen tissue from five mock and five Anhinga-infected birds was performed at 1 dpi (Fig. 1). Overall, formalin fixation led to greater variability in relative gene expression; however, the direction of change for all genes tested was similar between samples that were fresh-frozen and formalin-fixed. There were no statistically significant differences in splenic gene expression 1 dpi in mock-infected birds (lowest *p*-value 0.499 for IFN-β). Among the birds infected with Anhinga there was a significant increase in IFNγ RNA expression ($p = 0.013$) and a nearly significant increase in IL-6 RNA levels in FFPE spleen compared to fresh-frozen ($p = 0.055$). There were no significant differences between FFPE and fresh-frozen spleens among Anhinga infected birds in β-actin, matrix and IFN-β RNA expression ($p = 0.253$, $p = 0.114$ and $p = 0.253$, respectively).

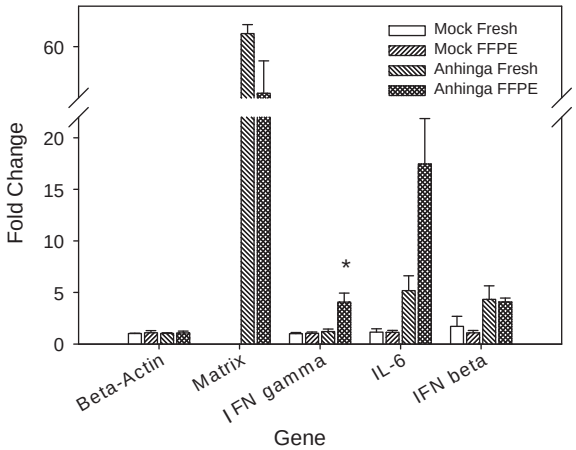

Fig. 1. Relative gene expression in FFPE and fresh-frozen spleens from birds infected with Anhinga (5 birds) and mock-infected control birds (5 birds) at 1 dpi. Asterisk indicates significant difference in gene expression between fresh-frozen and FFPE tissue sample. Bars represent standard error of the mean.

3.2. Cytokine gene expression for velogenic viscerotropic strains

Relative changes in cytokine expression are presented graphically for the two traditional VVND viruses (CA02 and rZJ-1) and for the atypical VVND Australia virus versus mock-infected control (Fig. 2A and B, respectively). There was marked upregulation of IFN-γ and especially IL-6 relative expression for both traditional VVND viruses. At 2 dpi, birds infected with CA02 strain showed a statistically significant 4.9-fold increase in IFN-γ RNA amounts ($p < 0.001$) and birds infected with rZJ1 strain showed a 14.3-fold increase. At 3 dpi, the fold change for IFN-γ RNA expression was higher, especially for rZJ1 (74.5-fold increase). Birds infected with CA02 strain showed lesser increase (18.8-fold) in IFN-γ expression. IL-6 upregulation appeared to greater than IFN-γ upregulation. At 2 dpi, a 5.4-fold increase of IL-6 expression was detected in birds infected with CA02 strain ($p < 0.001$) and 33.7-fold increase for the rZJ1 strain. Increases at 3 dpi appeared to be even greater, with the CA02 strain showing a 67.5-fold increase and rZJ1 showing a 48.0-fold increase in relative IL-6 levels. Relative IL-2 RNA expression did not appear to change for either virus at either 2 or 3 dpi. IFN-β RNA expression also did not show any marked changes at 2 dpi, however at 3 dpi IFN-β amounts were increased 21.1-fold and 14.9-fold in the CA02 and rZJ1 strains, respectively.

In comparison with the other two VVND viruses (CA02 and rZJ1), the RNA expression levels for Australia strain were less remarkable. At 2, 3 and 5 dpi, IFN-γ was increased (19.3, 7.1 and 7.3-fold, respectively). IL-6 expression had a stepwise pattern of upregulation 2,

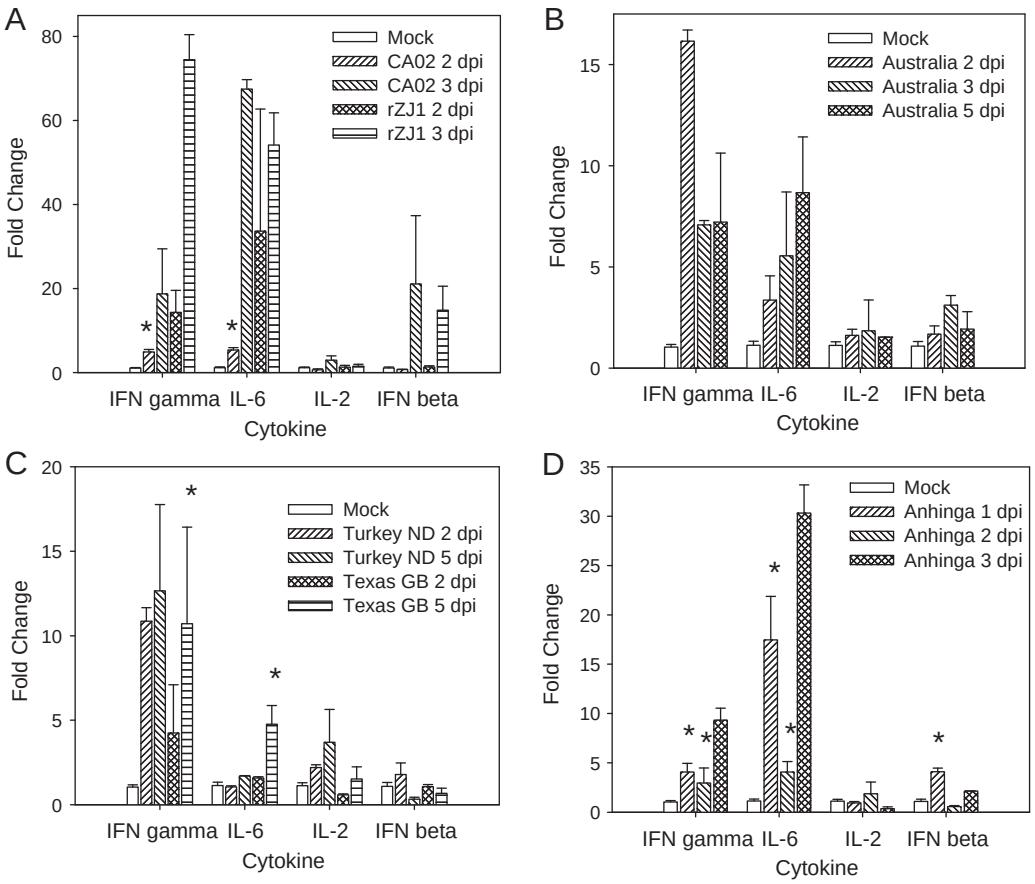

Fig. 2. Relative changes in IFN-γ, IL-6, IL-2 and IFNβ expression in birds infected with traditional velogenic, visterotropic NDV (panel A); atypical velogenicviscerotropic NDV (panel B); velogenic neurotropic NDV (panel C); mesogenic NDV (panel D). When more than 2 samples were available (CA02 2 dpi, Texas GB 5 dpi and Anhinga 1 and 2 dpi) changes in gene expression were compared to control by student t test. Asterisks indicate significant differences compared to control ($p \leq 0.05$) and bars represent standard error of the mean.

3 and 5 dpi that was not as marked as IFN-γ upregulation (3.4, 5.6 and 8.7-fold, respectively). IL-2 and IFN-β showed no notable changes at any of the time points examined.

3.3. Cytokine gene expression for velogenic neurotropic strains

Relative changes in gene expression for the two velogenic neurotropic strains versus mock-infected control are presented graphically (Fig. 2C). Relative changes in cytokine RNA expression were not as marked in VNND virus strains those seen in the VVND strains (CA02 and rZJ1). At 2 and 5 dpi, IFN-γ RNA amounts were upregulated in both VNND virus strains (10.7 and 12.7-fold for Turkey ND; 4.2 and 10.7 for Texas GB, respectively). IL-6 RNA expression remained relatively unchanged for both strains, with the exception of a statistically significant 4.8-fold increase in IL-6 RNA expression seen at 5 dpi for Texas GB ($p = 0.030$). Turkey ND showed slight increases in IL-2 expression at 2 and 5 dpi (2.2 and 3.7-fold, respectively), but IL-2 RNA levels remained unchanged in Texas GB. There were no significant changes in IFN-β RNA levels for either virus at either time point.

3.4. Cytokine gene expression for a mesogenic strain

Relative changes in cytokine expression at 1, 2 and 3 dpi for the mesogenic Anhinga strain of NDV are represented graphically (Fig. 2D).

3.5. Quantification of virus RNA relative expression

Relative changes in viral matrix gene expression in the spleen versus an arbitrary calibrator Ct (35 cycles, equivalent to number of cycles necessary for initiation of nonspecific amplification seen in mock-infected control birds) was corrected for β-actin expression for each virus over time (Fig. 3). Overall, relative matrix expression increased from 2 dpi through 5 dpi. The VVND strains (CA02 and rZJ1) showed exceptionally high relative matrix expression (ranging from 19.8 for CA02 on 2 dpi to 45137.2 for rZJ1 on 3 dpi). Matrix expression for the Australia strain was intermediate between the traditional VVND strains and the other VNND and mesogenic strains (ranging from 9.5 on 2 dpi to a high of 195.7 on 5 dpi). Matrix RNA expression for the VNND strain and Anhinga ranged from 4.8 (Anhinga 2 dpi) to 30.7 (Texas GB 5 dpi).

Table 2
Clinical signs, pathologic features and presence of virus as detected by immunohistochemistry (IHC) in spleens of birds infected with NDV strains of varying virulence.

Strain	2 dpi			3 dpi			5 dpi		
	Clinical	Histologic lesions	IHC	Clinical	Histologic lesions	IHC	Clinical	Histologic lesions	IHC
California (VVND)	Depressed	Mild necrosis	+	Dying	Marked necrosis	+++		NA	
rZJ1 (VVND)	Depressed	Mild necrosis	+	Dying	Marked necrosis	+++		NA	
Australia (VVND)	Normal	Normal	+	Depressed	Normal	+	Mild CNS signs	Mild lymphoid hyperplasia	+
Texas GB (VNND)	Normal	Normal	–		ND		Paralysis	Mild lymphoid depletion	–
Turkey ND (VNND)	Normal	Normal	–		ND		Normal	Mild lymphoid depletion	+
Anhinga (mesogen)	Normal	Mild lymphoid hyperplasia	–	Normal	Mild lymphoid depletion	–		ND	

IHC, immunohistochemistry; NA, not applicable because birds died prior to 5 dpi; ND, not done, birds not sampled at this time.

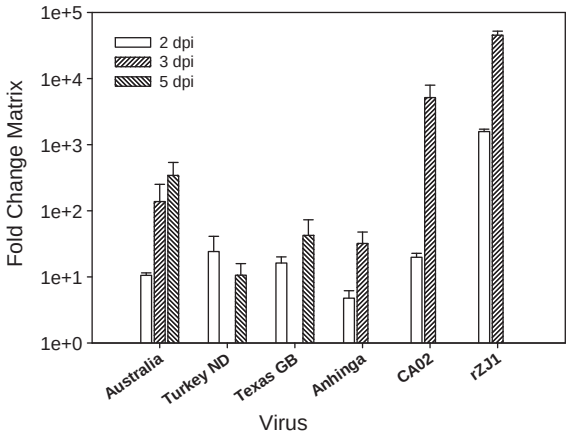

Fig. 3. Changes in viral matrix RNA expression in the spleen of infected birds over time. Bars represent standard error of the mean.

3.6. Clinical disease and pathology

Several of the clinical and pathological data have been previously published (Brown et al., 1999; Susta et al., 2010a). However, to better understand the relationship between cytokine RNA expression and pathology and clinical disease, some of this information is again included in this study. Pertinent clinical and pathologic information from infected birds at the relevant time points is presented in Table 2. Briefly, birds inoculated with either of two velogenic viscerotropic viruses, CA02 and rZJ1, at 2 dpi had evident clinical disease (depression, open-mouthed breathing and reluctance to move) which became progressively more severe until death at 3 or 4 dpi. Histologically, the spleen had evidence of early necrosis in lymphoid areas beginning at 2 dpi and becoming progressively more severe with time. There was abundant viral nucleoprotein signal (as detected by immunohistochemistry) in macrophages in spleen, with increasing signal over time (Brown et al., 1999; Susta et al., 2010b). In birds inoculated with Australia strain, an atypical viscerotropic velogen (Susta et al., 2010b), depression and open-mouthed breathing were observed on days 3–5. Also, mild neurological signs, such as head tremors and twitching were observed at 4 and 9 dpi, but birds returned to clinically normal by 10 dpi (Susta et al., 2010a). Histologically, the only abnormalities noted in spleen were mild lymphoid hyperplasia at 5 dpi. Viral nucleoprotein was present in small quantities in the spleen at each time interval. With the Texas GB strain (neurotropic velogen), birds were bright and alert at 2 dpi but were in lateral recumbency and unable to right themselves by 5 dpi. One bird died at this time point and the other two birds were euthanized. Chickens inoculated with Turkey ND, another neurotropic velogen, were clinically normal at 5 dpi but at 10 dpi were depressed, with unilateral leg paresis (Brown et al., 1999). Spleen had mild lymphoid depletion at 5 dpi. Birds inoculated with the mesogenic strain (Anhinga) were euthanized at 2 or 3 dpi and clinical signs were not observed (data not shown). Histologically there was mild follicular hyperplasia in the spleen at 2 dpi with some lymphoid

depletion noted at 3 dpi. Immunohistochemistry demonstrated none or only minimal amounts of virus signal in spleen with these 3 strains.

4. Discussion

The host immune response to pathogens in the earliest stages of infection can be a critical determinant of disease course. Much of this early response is dictated by cytokines (Swaggerty et al., 2008). The role of cytokines in the pathogenesis of Newcastle disease *in vivo* still is poorly understood. It has been shown in multiple studies that macrophages and also lymphocytes contain NDV antigens and viral RNA during the early stages of infection, especially in animals infected with the velogenic strains (Brown et al., 1999; Kommers et al., 2002). These cells are also the main source of numerous cytokines (Lowenthal et al., 1995). In this study, we investigated cytokine transcriptional responses in the spleen, a macrophage-lymphocyte-rich organ, from chickens infected with different pathotypes of NDV and demonstrated increased transcriptional levels of key pro-inflammatory cytokines associated with increased viral gene expression, and with marked lesions.

Increased IFN-γ RNA expression was detected in spleens from chickens infected with the two typical velogenic viscerotropic strains, CA02 and rZJ1. The highest levels corresponded with the marked clinical signs and the beginning of necrotizing inflammation in the lymphoid tissue. Th1 type cells typically produce IFN-γ, crucially driven by early IL-12 and IL-18. Th1 cells are associated with inflammatory cytolytic responses, generally necessary for destroying cells infected with intracellular agents (Degen et al., 2005). IFN-γ is a known inducer of macrophage activation, and when macrophages are strongly activated, they can injure normal host tissues by release of lysosomal enzymes, reactive oxygen species and nitric oxide (Abbas et al., 2010). These antimicrobial compounds (reactive peroxynitrite radicals) do not distinguish between self and invading antigens. As a result, if these products enter the extracellular environment, they are capable of causing tissue injury (Abbas et al., 2010). Nitric oxide also leads to the inhibition of virus replication (Djeraba et al., 2002; Parvizi et al., 2009). Macrophages affected by IFN-γ also act to upregulate the expression of MHC-II molecules, which enhances specific immunity (Cao et al., 1989). In all birds in this study, the increase in the relative amount of viral RNA coincided with the relative increases on IFN-γ expression. For example, in birds infected with rZJ1 strain, at 3 dpi, an almost 75-fold increase for IFN-γ was detected, when relative amount of viral RNA was markedly increased (>45,000-fold increase). For Australia strain, IFN-γ RNA was upregulated at all time points when virus matrix RNA was present.

In this study, IL-6 RNA levels were notably increased, in almost all the strains, but most especially in the CA02 and rZJ1 strains. IL-6 is produced by activated macrophages and lymphocytes, as well as endothelial cells (Van Snick, 1990; Hamal et al., 2010; Suzuki et al., 2009). It is particularly important in the early phase of the innate immune response, recruiting and activating leukocytes and setting the stage for appropriate action in response to infection (Abbas et al., 2010). IL-6 stimulates vascular endothelial cells to synthesize prostaglandin E_2 which binds to the EP3 receptor in neural cells in the hypothalamus generating fever (Suzuki et al., 2009). Also, IL-6 is considered as a multifunctional pro-inflammatory cytokine, which is involved in differentiation and activation of B and T lymphocytes, development of macrophages and hematopoiesis in chickens (Kaiser et al., 2000; Wigley and Kaiser, 2003). In our study, in general, IL-6 RNA levels were associated with the amount of viral RNA expression and the extent of clinical illness.

Notable differences in clinical signs between the classic velogenic viscerotropic and velogenic neurotropic strains were observed. Birds infected with velogenic viscerotropic strains CA02 and rZJ1 became severely ill with marked depression. In contrast, for the most part, birds infected with velogenic neurotropic strains manifested less severe clinical signs and they became paralyzed over time, but were bright and alert. Marked clinical signs with severe depression in birds infected with velogenic viscerotropic could be related to the high levels of cytokines, especially IFN-γ and IL-6. This may indicate that IFN-γ and IL-6 RNA expression are also important in NDV pathogenesis, a possibility that warrants further study.

Type I IFN (α and β subtypes), is an innate defense system of the host against viral infection (Samuel, 2001). Stimulated by the presence of double-stranded RNA, type I interferon is exported from the cell and causes neighboring cells to transcribe products (interferon stimulated genes-ISGs) that create an antiviral state that blocks viral replication (Krishnamurthy et al., 2006). Because NDV is an RNA virus, it would be expected that type I interferons would be strongly expressed early in infection. In this study, increase IFN-β RNA levels were detected only in birds infected with CA02 and rZJ1 at 3 dpi and birds infected with Anhinga at 1 dpi. Some studies have demonstrated that NDV has a capacity to block type I IFN production. NDV uses an auxiliary protein derived from the P protein and designated V protein, to counteract the host immune response. The V protein induces degradation of the signal transducers and activators of transcription (STAT-1) protein, leading to transcriptional inactivation of ISGs and down regulation of type I IFN (Huang et al., 2003; Munir et al., 2005). *In vitro* studies using human skin fibroblasts demonstrated that NDV replication is completely inhibited upon endogenous IFN-β production (Krishnamurthy et al., 2006). The high relative quantity of viral RNA for California and rZJ1 strains, suggesting rapid and efficient viral replication in spleen, (possibly in macrophages and lymphocytes), was not associated with a marked type I IFN (IFN-β) RNA increase level in the spleen (similarly for Australia and Turkey ND strains), suggesting that the V protein is effectively blocking expression of this host gene. Another possibility is that IFN-β is upregulated at earlier time points in the host response to NDV infection. Birds infected with Anhinga showed significant increases in IFN-β RNA expression at 1 dpi. Future studies should aim to determine the relative levels of IFN-β at earlier time points for multiple strains of NDV to determine the influence of the V protein over time.

Chickens infected with all pathotypes in this study, showed non-induction or minimal induction of IL-2 RNA expression in the spleen. This result could be the consequence of the virus directly infecting macrophages and lymphocytes and therefore possible impairment of some of the functions of these cells.

In summary, the results from this work provide the following hypothesis regarding cytokine production subsequent to NDV infection. Macrophages infected with NDV, especially with CA02 and rZJ1, the typical VVND strains, become activated, resulting in a great increase in IFN-γ production, and overall stimulation of adaptive immune response. However, activated macrophages are also producing reactive intermediates which damage the tissue locally (Abbas et al., 2010). IL-6, also from activated macrophages, is produced in large quantities, causing hyperthermia and severe clinical illness. Because there is negligible type I interferon production, presumably because of the NDV inhibitory capacity, the virus continues to replicate in macrophages and lymphocytes, causing more tissue damage. In contrast, the other strains (VNND and mesogens) may not invade macrophages and/or lymphocytes to the same extent, so that even though there is still inhibition of the type I interferon, the innate response is not so damaging that the animal survives longer and viruses can move on to other organs, notably brain, to cause the clinical disease seen.

The advances in RNA expression analysis from FFPE tissues allows for the recovery of valuable information from archived materials (Godfrey et al., 2000). In this study, archived blocks from various earlier pathogenesis experiments were used to obtain data without the need for new animal experiments. Despite the improved RNA isolation methods attempted, the RNA obtainable from fixed tissues is still of fairly small size (less than 200 bp) and, smaller amplicon sizes are needed to provide optimal sensitivity. Gloghini et al. (2004) recommended using primers with product sizes in a range of 60–120-bp. McKinney et al. (2009) described that product sizes in a range of 70–150-bp as ideal. Godfrey et al. (2000) found that the absolute Ct values on fixed tissues were an average of approximately 5 cycles higher than on matched fresh tissues. Our data indicated similar differences in the Ct values when fresh RNA was compared with FFPE RNA, especially for the oldest blocks. Nevertheless, our experimental data was highly reproducible and corresponded with previous pathological data (especially viral RNA levels) indicating confidence results when we evaluated the Ct values comparing non-infected birds, mesogen and velogenic strains.

In conclusion, in the present study we demonstrated differences in the cytokine RNA expression in birds infected with velogenic viscerotropic, velogenic neurotropic, and mesogenic NDV strains. The data here demonstrate that IFN-γ and IL-6 RNA expression levels are increased during the very early phases of infection in velogenic viscerotropic viruses in comparison with mesogenic and velogenic neurotropic viruses. Higher levels of these cytokines were detected at the same time periods when the birds showed severe clinical signs, which is also the onset of necrosis in the lymphoid tissues as seen by histopathologic analysis of the spleen. These differences might explain the underlying mechanisms of clinical disease and/or immune responses in birds infected with different strains of APMV-1.

Acknowledgements

R. E. was supported by the Brazilian government sponsoring agency "Conselho Nacional de Desenvolvimento Cientıfico e Tecnologico" (CNPq) and Universidade Federal de Minas Gerais (UFMG).

We would like to thank Dawn Williams-Coplin and Diane Smith for their technical assistance.

This work was funded by USDA CRIS project number 6612-32000-049-00D. Mention of trade names or commercial products in this manuscript is solely for the purpose of providing specific information and does not imply recommendation or endorsement by the U.S. Department of Agriculture.

References

Abbas, K.A., Lichtman, A.H., Pillai, S., 2010. Cellular and Molecular Immunology. Elsevier, p. 566.

Alexander, D.J., Senne, D.A., 2008. Newcastle Disease, other avian Paramyxoviruses, and Pneumovirus infection. Diseases of Poultry. Blackwell Publishing, Iowa, pp. 75–115.

Bhaiyat, M.I., Kobayashi, Y., Itakura, C., Islam, M.A., Kida, H., 1995. Brain lesions in chickens experimentally infected with a neuroadapted strain of mesogenic Newcastle disease virus. J. Vet. Med. Sci. 57, 237–244.

Brown, C., King, D.J., Seal, B.S., 1999. Pathogenesis of Newcastle disease in chickens experimentally infected with viruses of different virulence. Vet. Pathol. 36, 125–132.

Cao, H., Wolff, R.G., Meltzer, M.S., Crawford, R.M., 1989. Differential regulation of class II MHC determinants on macrophages by IFN-gamma and IL-4. J. Immunol. 143, 3524–3531.

Chambers, P., Millar, N.S., Emmerson, P.T., 1986. Nucleotide sequence of the gene encoding the fusion glycoprotein of Newcastle disease virus. J. Gen. Virol. 67, 2685–2694.

Degen, W.G., Daal, N., Rothwell, L., Kaiser, P., Schijns, V.E., 2005. Th1/Th2 polarization by viral and helminth infection in birds. Vet. Microbiol. 105, 163–167.

Djeraba, A., Musset, E., Bernardet, N., Le Vern, Y., Quéré, P., 2002. Similar pattern of iNOS expression, NO production and cytokine response in genetic and vaccination-acquired resistance to Marek's disease. Vet. Immunol. Immunopathol. 85, 63–75.

Gloghini, A., Canal, B., Klein, U., Dal Maso, L., Perin, T., Dalla-Favera, R., Carbone, A., 2004. RT-PCR analysis of RNA extracted from Bouin-fixed and paraffin-embedded lymphoid tissues. J. Mol. Diagn. 6, 290–296.

Godfrey, T.E., Kim, S.H., Chavira, M., Ruff, D.W., Warren, R.S., Gray, J.W., Jensen, R.H., 2000. Quantitative mRNA expression analysis from formalin-fixed, paraffin-embedded tissues using 5′ nuclease quantitative reverse transcription-polymerase chain reaction. J. Mol. Diagn. 2, 84–91.

Hamal, K.R., Wideman, R.F., Anthony, N.B., Erf, G.F., 2010. Differential gene expression of proinflammatory chemokines and cytokines in lungs of ascites-resistant and -susceptible broiler chickens following intravenous cellulose microparticle injection. Vet. Immunol. Immunopathol. 133, 250–255.

Huang, Z., Krishnamurthy, S., Panda, A., Samal, S.K., 2003. Newcastle disease virus V protein is associated with viral pathogenesis and functions as an alpha interferon antagonist. J. Virol. 77, 8676–8685.

Kaiser, P., Rothwell, L., Galyov, E.E., Barrow, P.A., Burnside, J., Wigley, P., 2000. Differential cytokine expression in avian cells in response to invasion by *Salmonella typhimurium*, *Salmonella enteritidis* and *Salmonella gallinarum*. Microbiology 12, 3217–3226.

Kaiser, A., Bercovici, N., Abastado, J.P., Nardin, A., 2003. Naive CD^{8+} T cell recruitment and proliferation are dependent on stage of dendritic cell maturation. Eur. J. Immunol. 33, 162–171.

Kommers, G.D., King, D.J., Seal, B.S., Brown, C.C., 2001. Virulence of pigeon-origin Newcastle disease virus isolates for domestic chickens. Avian Dis. 45, 906–921.

Kommers, G.D., King, D.J., Seal, B.S., Carmichael, K.P., Brown, C.C., 2002. Pathogenesis of six pigeon-origin isolates of Newcastle disease virus for domestic chickens. Vet. Pathol. 39, 353–362.

Krishnamurthy, S., Takimoto, T., Scroggs, R.A., Portner, A., 2006. Differentially regulated interferon response determines the outcome of Newcastle disease virus infection in normal and tumor cell lines. J. Virol. 80, 5145–5155.

Lynagh, G.R., Bailey, M., Kaiser, P., 2000. Interleukin-6 is produced during both murine and avian *Eimeria* infections. Vet. Immunol. Immunopathol. 76, 89–102.

Lowenthal, J.W., Digby, M.R., York, J.J., 1995. Production of interferon-gamma by chicken T cells. J. Interferon Cytokine Res. 11, 933–938.

McKinney, M.D., Moon, S.J., Kulesh, D.A., Larsen, T., Schoepp, R.J., 2009. Detection of viral RNA from paraffin-embedded tissues after prolonged formalin fixation. J. Clin. Virol. 44, 39–42.

Munir, S., Sharma, J.M., Kapur, V., 2005. Transcriptional response of avian cells to infection with Newcastle disease virus. Virus Res. 107, 103–108.

OIE, 2009. Manual of diagnostic tests and vaccines for terrestrial animals: mammals, birds and bees. In: Biological Standards Commission. World Organization for Animal Health, Paris, pp. 576–589.

Parvizi, P., Read, L.R., Abdul-Careem, M.F., Sarson, A.J., Lusty, C., Lambourne, M., Thanthrige-Don, N., Burgess, S.C., Sharif, S., 2009. Cytokine gene expression in splenic CD^{4+} and CD^{8+} T cell subsets of genetically resistant and susceptible chickens infected with Marek's disease virus. Vet. Immunol. Immunopathol. 132, 209–217.

Pflaffl, M., 2001. A new mathematical model for relative quantification in real-time PCR. Nucleic Acids Res. 29, 2002–2007.

Ramakers, C., Ruijter, J.M., Deprez, R.H.L., Moorman, A.F.M., 2003. Assumption-free analysis of quantitative real-time polymerase chain reaction (PCR) data. Neurosci. Lett. 339, 62–66.

Samuel, C.E., 2001. Antiviral actions of interferons. Rev. Clin. Microbiol. Rev. 14, 778–809.

Seal, B.S., King, D.J., Sellers, H.S., 2000. The avian response to Newcastle disease virus. Dev. Comp. Immunol. 24, 257–268.

Sharma, J.M., 2008. Host factors for disease resistance. In: Diseases of Poultry. Blackwell Publishing, Iowa, pp. 47–72.

Swaggerty, C.L., Pevzner, I.Y., Kaiser, P., Kogut, M.H., 2008. Profiling pro-inflammatory cytokine and chemokine mRNA expression levels as a novel method for selection of increased innate immune responsiveness. Vet. Immunol. Immunopathol. 126, 35–42.

Susta, L., Miller, P.J., Afonso, C.L., Brown, C.C., 2010a. Clinicopathological characterization in poultry of three strains of Newcastle disease virus isolated from recent outbreaks. Vet. Path. 48, 349–360.

Susta L, Miller PJ, Hu S, Liu X, Rue CA, Afonso CL, Brown CC., 2010b. Clinicopathological Characterization of Two Recombinant Newcastle Disease Viruses Derived From a Virulent Chinese Strain. Annual Meeting of the American Association of Avian Pathologists, Atlanta, July 2010.

Suzuki, K., Okada, H., Itoh, T., Tada, T., Mase, M., Nakamura, K., Kubo, M., Tsukamoto, K., 2009. Association of increased pathogenicity of Asian H5N1 highly pathogenic avian influenza viruses in chickens with highly efficient viral replication accompanied by early destruction of innate immune responses. J. Virol. 83, 7475–7486.

USDA, 2006. The office of the Federal Register national Archives and Records Administration Code of Federal Regulations. Title 9. Animals and Animal Products: Chapter I APHIS, Department of Agriculture; Part 94, page 490, p. 534.

Wigley, P., Kaiser, P., 2003. Avian cytokines in health and disease. Rev. Bras. Cienc. Avic. 5, 1–14.

Wise, M.G., Sellers, H.S., Alvarez, R., Seal, B.S., 2004. RNA-dependent RNA polymerase gene analysis of worldwide Newcastle disease virus isolates representing different virulence types and their phylogenetic relationship with other members of the paramyxoviridae. Virus Res. 104, 71–80.

Van Snick, J., 1990. Interleukin-6: an overview. Annu. Rev. Immunol. 8, 253–278.

AVIAN DISEASES 56:276–281, 2012

Low Pathogenicity Avian Influenza Viruses Infect Chicken Layers by Different Routes of Inoculation

Mary J. Pantin-Jackwood,[A] Diane M. Smith, Jamie L. Wasilenko, and Erica Spackman

Exotic and Emerging Avian Viral Diseases Research Unit, Southeast Poultry Research Laboratory, Agricultural Research Service, United States Department of Agriculture, 934 College Station Road, Athens, GA 30605

Received 27 September 2011; Accepted 28 November 2011; Published ahead of print 29 November 2011

SUMMARY. In order to develop better control measures against avian influenza, it is necessary to understand how the virus transmits in poultry. In a previous study in which the infectivity and transmissibility of the pandemic H1N1 influenza virus was examined in different poultry species, we found that no or minimal infection occurred in chicken and turkeys intranasally (IN) inoculated with the virus. However, we demonstrated that the virus can infect laying turkey hens by the intracloacal (IC) and intraoviduct (IO) routes, possibly explaining the drops in egg production observed in turkey breeder farms affected by the virus. Such novel routes of exposure have not been previously examined in chickens and could also explain outbreaks of low pathogenicity avian influenza (LPAI) that cause a decrease in egg production in chicken layers and breeders. In the present study, 46-wk-old specific-pathogen-free chicken layers were infected by the IN, IC, or IO routes with one of two LPAI viruses: a poultry origin virus, A/chicken/CA/1255/02 (H6N2), and a live bird market isolate, A/chicken/NJ/12220/97 (H9N2). Only hens IN inoculated with the H6N2 virus presented mild clinical signs consisting of depression and anorexia. However, a decrease in number of eggs laid was observed in all virus-inoculated groups when compared to control hens. Evidence of infection was found in all chickens inoculated with the H6N2 virus by any of the three routes and the virus transmitted to contact hens. On the other hand, only one or two hens from each of the groups inoculated with the H9N2 virus shed detectable levels of virus, or seroconverted and did not transmit the virus to contacts, regardless of the route of inoculation. In conclusion, LPAI viruses can also infect chickens through other routes besides the IN route, which is considered the natural route of exposure. However, as seen with the H9N2 virus, the infectivity of the virus did not increase when given by these alternate routes.

RESUMEN. Los virus de la influenza aviar de baja patogenicidad infectan a gallinas de postura por diferentes vías de inoculación.

Con el fin de desarrollar mejores medidas de control contra la influenza aviar, es necesario entender cómo se transmite el virus dentro de la avicultura comercial. En un estudio previo en el que se examinó la infectividad y la transmisibilidad del virus de la influenza pandémico H1N1 entre diferentes especies de aves, se encontró que la infección es nula o mínima en pollos y pavos inoculados con este virus por vía intranasal. Sin embargo, se ha demostrado que el virus puede infectar pavas reproductoras en producción por las rutas intracloacal e intraoviductal, lo que puede explicar las bajas en la producción de huevos observadas en las granjas de pavos reproductoras afectadas por el virus. Estas nuevas rutas de exposición no habían sido previamente examinadas en los pollos y también podrían explicar los brotes de influenza aviar de baja patogenicidad, que causan una disminución en la producción de huevos en las gallinas de postura y en las aves reproductoras. En el presente estudio, se infectaron aves de postura de 46 semanas de edad libres de patógenos específicos por las rutas intranasal, intracloacal, o intraoviductal con uno de dos virus de la influenza aviar de baja patogenicidad: un virus de origen aviar, el aislamiento denominado A/pollo/CA/1255/02 (H6N2), y un aislamiento obtenido de un mercado de aves vivas, A/pollo/NJ/12220/97 (H9N2). Solamente las gallinas inoculadas por vía intranasal con el virus H6N2 presentaron leves signos clínicos consistentes en depresión y anorexia. Sin embargo, se observó disminución en el número de huevos producidos en todos los grupos inoculados con los virus cuando se compararon con las gallinas del grupo control. Se encontró evidencia de infección en todos los pollos inoculados con el virus H6N2 por cualquiera de las tres rutas y el virus se transmitió a gallinas expuestas por contacto. Por otro lado, sólo una ó dos gallinas procedentes de cada uno de los grupos inoculados con el virus H9N2 eliminaron virus con niveles detectables o seroconvirtieron y no transmitieron el virus a las aves expuestas por contacto, independientemente de la vía de inoculación. En conclusión, los virus de influenza aviar baja patogenicidad pueden infectar a los pollos a través de otras vías, además de la vía intranasal, que se considera la vía natural de exposición. Sin embargo, como se observó con el virus H9N2, la infectividad del virus no aumentó cuando se administró por estas rutas alternas.

Key words: low pathogenic avian influenza, H6N2 type, H9N2 type, routes of inoculation, chickens

Abbreviations: AI = avian influenza; BHI = brain heart infusion; C = cloacal; dpi = days postinoculation; EID_{50} = 50% egg infectious dose; HI = hemagglutination inhibition; HPAI = highly pathogenic avian influenza; IC = intracloacal; IHC = immunohistochemistry; IN = intranasal; IO = intraoviduct; LPAI = low pathogenicity avian influenza; OP = oropharyngeal; pH1N1 = pandemic H1N1; qRRT-PCR = quantitative real-time reverse transcriptase-polymerase chain reaction; SEPRL = Southeast Poultry Research Laboratory; SPF = specific-pathogen-free

Avian influenza (AI) continues to be a threat to commercial poultry. AI viruses occasionally transmit from their natural reservoirs, wild aquatic birds, to domestic birds producing subclinical infections and sometimes respiratory disease and drops in egg production. These viruses are typically termed low pathogenicity AI (LPAI) viruses and can be a combination of most 16 hemagglutinin and nine neuraminidase subtypes. Some H5 and H7 LPAI viruses, after circulating in domestic poultry, mutate into highly pathogenic AI (HPAI) viruses and cause high mortality (34). Most LPAI viruses produce subclinical infections in experimental

[A]Corresponding author. E-mail: Mary.Pantin-Jackwood@ARS.USDA.gov

studies but, under commercial rearing conditions and probably complicated by secondary pathogens, environmental stress, and immunosuppression, these viruses can also produce mild to moderate disease. Secondary bacterial, fungal, or viral infections are usually necessary to produce sufficiently severe respiratory damage to result in illness or death; however, some LPAI virus strains, such as certain Asian H9N2 lineages adapted to efficient replication in poultry, can cause more-prominent signs and also significant mortality (1,15,24).

Typically, LPAI viruses have limited local replication in the respiratory and alimentary tracts (33). Rarely, LPAI viruses have spread outside the respiratory or alimentary tract causing infection and damage in epithelial-containing tissues of visceral organs such as kidney, pancreas, and oviduct. Clinical signs will differ with the virus strain, host species, and age of the host and pathophysiologic changes can be found in the respiratory, digestive, urinary, and reproductive systems (18,33).

The intranasal (IN) route of exposure is routinely used to emulate the natural route of infection for AI viruses in experimental settings (31). However, in studies done to evaluate the pathogenicity of the 2009 pandemic H1N1 (pH1N1) virus in breeder turkeys, infection was not produced easily by IN inoculation. Therefore, intracloacal (IC) and intraoviduct (IO) inoculation were tested in an attempt to explain infection of breeder turkeys with the virus and were successful in infecting the turkeys (19,35). In another study, more than 50% of 8-to-10-wk-old turkeys inoculated by the cloacal (C) route with the pH1N1 virus became infected and virus replication was demonstrated in the cecal tonsil and bursa (2). Cloacal exposure has been shown to be important to the transmission of other pathogens in poultry. For example, cloacal contact with feces that have been contaminated with *Histomonas meleagridis* is thought to be one way in which blackhead is transmitted from bird to bird (14), and IC inoculation or vaccination has been used experimentally with Newcastle disease virus and infectious laryngotracheitis virus (4,5,26). Infection following alimentary tract exposure has also been demonstrated in chickens and ducks infected with an H5N1 HPAI virus (11). The initiation of H5N1 HPAI virus infection in birds is still favored by a respiratory route of exposure, but alimentary initiated infection is possible if birds consume high doses of virus, such as by cannibalizing infected carcasses (11). Little is known about the ability of LPAI viruses to infect chickens by alternate routes of exposure.

LPAI viruses are known to affect lay of eggs and replicate in the reproductive tract of turkeys and, as with turkeys infected with the pH1N1 virus, drops in egg production are commonly reported with LPAI virus outbreaks in turkey breeders (8,13,15,22,29,32,37). Decreases in egg production have also been observed in chicken breeders and layers infected with LPAI viruses (3,12,15,24,40). In 2000, an outbreak of H6N2 LPAI occurred in California and 12 separate incidences were reported primarily involving layer-type birds, but the virus was also isolated from backyard chickens and a primary broiler breeder (7,39). Drops in egg production and increased mortality were among the clinical signs reported in the layer flocks. Yolk peritonitis was a feature also described (39).

The IO route of exposure provided an explanation of how turkey breeders became infected with the pH1N1 virus through the practice of artificial insemination and highlighted the importance of exploring alternate routes of infection for AI viruses in poultry (19). In 1970, Samadieh and Bankowski showed that egg production was severely affected in laying turkey hens inseminated with semen contaminated with a turkey influenza virus (25), but no other studies have been published exploring the transmission of AI virus by semen. The presence of virus antigen has been found in testicles of birds infected with HPAI viruses (6; Pantin-Jackwood, pers. obs.) but has not been reported for LPAI viruses.

To evaluate whether LPAI viruses could infect chickens through the cloacal route and reproductive tract, we inoculated chicken layers with two different LPAI viruses given by three different routes, IN, IC, and IO, and examined them for the presence of clinical signs, gross and microscopic lesions, virus in tissues, virus shedding, seroconversion, and transmission to contacts.

MATERIALS AND METHODS

Viruses. Two LPAI viruses from the Southeast Poultry Research Laboratory (SEPRL) repository were used in this study: A/chicken/CA/1255/02 (H6N2) and A/chicken/NJ/12220/97 (H9N2). The H6N2 virus was isolated from 118-week-old layers (39) and the H9N2 virus was a chicken isolate from a live bird market. The H6N2 virus was chosen because of its history of producing drops in egg production in layer flocks and its known ability to infect chickens experimentally (10,39). The H9N2 isolate had not been previously examined in chickens and was chosen to see if the route of inoculation would have an effect on infectivity in hens. The viruses were propagated in 9-day-old specific-pathogen-free (SPF) embryonating chicken eggs and titrated as described (27,38). Allantoic fluid was harvested from the eggs 48 hr postinoculation and diluted in brain heart infusion (BHI) medium (BD Bioscience, Sparks, MD) in order to obtain 10^6 50% egg infectious dose (EID_{50}) per 0.1 ml/bird. A sham inoculum was made using allantoic fluid from noninfected eggs diluted 1:300 in BHI. All experiments were performed in biosecurity level-2 enhanced facilities at SEPRL.

Experimental design. Seventy 46-wk-old, SPF white leghorn chickens (*Gallus domesticus*) in lay, from SEPRL's in-house flock, were used in this study. The hens were housed in self-contained isolation units that were ventilated under negative pressure with inlet and exhaust HEPA-filtered air and maintained under continuous lighting. Feed and water were provided with *ad libitum* access. Hens were cared for in accordance to SEPRL's Institutional Animal Care and Use Committee-approved animal use protocol. Hens were acclimated to the isolators for 3 days before the beginning of the study to ensure that they were all laying eggs.

Hens were divided into 7 groups of 10 birds each. Hens from groups 1–3 were inoculated with 0.1 ml of inoculum containing 10^6 EID_{50} of the H6N2 virus IN via the choanal slit ($n = 10$), IC by applying the inoculum to the cloacal lips ($n = 10$), and IO by depositing the virus inside the vagina ($n = 10$). Hens from groups 4–6 were similarly inoculated: IN ($n = 10$), IC ($n = 10$), and IO ($n = 10$) with 0.1 ml of inoculum containing 10^6 EID_{50} of the H9N2 virus. Hens from group 7 were IN inoculated with sham inoculum ($n = 10$; Table 1).

Hens were observed daily for clinical signs of disease and laid eggs were counted. Eggs were collected at 4 days postinoculation (dpi) for virus detection. Oropharyngeal (OP) and C swabs were collected at 2, 4, 7, and 14 dpi from all birds to determine viral shedding by quantitative real-time RT-PCR (qRRT-PCR). Swab samples were suspended in 2 ml sterile BHI broth containing an antibiotic-antimycotic mixture and frozen at −70 C until processing. Two hens from each group were euthanatized at 3 dpi with 0.2 ml sodium pentobarbital (5 g/ml) per bird, gross lesions recorded, and the following tissues: lung, spleen, heart, kidney, and oviduct, were collected separately in BHI for virus isolation and stored frozen at −70 C. Trachea, lungs, bursa, kidneys, adrenal gland, thymus, brain, liver, heart, ventriculus, pancreas, intestine, spleen, ovary, oviduct, beak, and thigh tissue were also collected at necropsy. Tissues were fixed in 10% neutral buffered formalin solution, sectioned, and stained with hematoxylin and eosin. Immunohistochemistry (IHC) was used to stain duplicate sections to determine influenza viral antigen distribution in individual tissues as described previously (17). Two new hens were added to each group at 3 dpi, serving as contacts to study virus transmission. At 14 dpi, all the hens were bled, euthanatized, and necropsied to examine the oviduct.

Table 1. Number of eggs laid by hens inoculated through different routes with 10^6 EID_{50}/0.1 ml of H6N2 or H9N2 viruses or by sham-inoculated controls.

Groups[A]	No. eggs laid 1 to 7 dpi	No. eggs laid 8 to 14 dpi	Total no. of eggs	No. of hens with active oviducts at 14 dpi
1. H6N2 IN	21	6	27	3/10
2. H6N2 IC	26	15	41	4/10
3. H6N2 IO	19	10	29	4/10
4. H9N2 IN	19	11	30	6/10
5. H9N2 IC	21	15	36	6/10
6. H9N2 IO	25	10	35	7/10
7. Controls	33	23	56	8/10

[A]IN = intranasal; IC = intracloacal, IO = intraoviduct.

Serology. Hemagglutination inhibition (HI) assays were performed with serum collected from chickens 14 days after virus challenge to quantify the antibody response. The assay antigens were prepared by inactivating the allantoic fluid from virus-infected chicken eggs with 0.1% beta-propriolactone and adjusting the pH to 7.0 with sodium-bicarbonate. The HI assays were performed in accordance with standard procedures (20). Titers were calculated as the reciprocal of the last HI-positive serum dilution, and samples with HI titers of 4 (2^2) or below were considered negative. A one-way ANOVA with a Tukey's post-test was used to analyze HI titers, after confirming normality, using Prism v.5.01 software (GraphPad Software Inc., La Jolla, CA) and values expressed as the mean ± SD ($P < 0.05$).

Virus detection. RNA was extracted from OP and C swabs using a previously described combination of Trizol LS reagent (Invitrogen Inc., Carlsbad, CA) and the MagMax AI/ND RNA isolation kit (Ambion, Inc., Austin, TX) (9). A qRRT-PCR targeting the influenza M gene (30) was performed using the SmartCycler® 2 (Cepheid Inc., Sunnyvale, CA) and the OneStep RT-PCR kit (Qiagen®, Valencia, CA). A standard curve for virus quantification was established with RNA extracted from dilutions of the same titrated stock of the viruses in duplicate and results reported as EID_{50}/ml equivalents (21). The calculated qRRT-PCR detection limit was 10^2 EID_{50}/ml per reaction.

Tissues (lung, spleen, heart, kidney, and sections of the oviduct) were normalized by weight and homogenized in BHI medium, and titers of infectious virus were subsequently determined in embryonated chicken eggs as previously described (36). Similarly, albumin collected from eggs laid on 4 dpi was also examined for the presence of virus. The minimal detectable titer was $10^{0.9}$ EID_{50}/ml from swabs and $10^{1.97}$ EID_{50}/g from tissues.

RESULTS

Clinical signs and gross lesions. Only hens IN-inoculated with the H6N2 virus presented clinical signs consisting of mild depression and a decrease in feed consumption which lasted until 7 dpi. The hens from all groups were laying at the beginning of the experiment and eggs were collected from all groups until the end of the study. However, a decrease in the number of eggs laid was observed in most groups during the second week of the study (Table 1). A decrease in total eggs laid was observed in all virus-inoculated groups when compared to sham-inoculated controls. Hens inoculated with the H6N2 virus produced, in total, 27%–52% fewer eggs and hens inoculated with the H9N2 virus produced 36%–46% less eggs. Hens inoculated with the H6N2 virus by the IN and IO route had the largest decrease in eggs laid. When oviducts were examined at the end of the experiment, 6–7 out of 10 hens per group inoculated with the H6N2 virus had stopped laying eggs *vs.* 3–4 hens per group from the H9N2-inoculated hens and two from the sham-inoculated hens.

Gross and microscopic lesions and viral antigen staining in tissues. Two hens per group were euthanatized at 3 dpi and necropsied. No gross lesions were observed in sham-inoculated control hens. As for the virus-inoculated hens, the only changes observed consisted of congestion of the oviduct. All hens examined had active oviducts. Tissues collected from the hens were also examined for microscopic lesions and viral antigen staining. No, or minimal, lesions were observed in most hens with the exception of hens IN-inoculated with the H6N2 virus in which the trachea presented mild to moderate degenerative changes of the epithelium and the lungs had mild congestion, mild interstitial inflammation with mixed mononuclear cells, and mild catarrhal bronchitis. Mild to moderate hyperplasia of the intestinal epithelium and mild proliferation of gut-associated lymphoid tissues was also present in many hens. Remaining organs, including the oviduct, lacked significant histopathologic lesions. No viral antigen staining, detected by IHC, was present in tissues of any of the hens examined.

Virus detection and serology. No virus was detected in swabs or tissues from the sham-inoculated control birds. The virus shedding and seroconversion data for the virus-inoculated groups is presented in Table 2. All hens became infected with the H6N2 virus when exposed by any of the three routes; IN, IC, or IO. This was demonstrated by seroconversion, with hens from all three groups showing antibodies to the virus at 14 days after inoculation. No statistical difference in HI titers was found between the groups (data not shown). However, differences in numbers of birds shedding virus were observed between hens inoculated with the H6N2 virus by the three different routes. Six to 8 out of 8–10 hens inoculated shed virus through the oropharyngeal route at 2, 4, and 7 dpi, but only 3 of 8 hens shed virus through the cloaca and only at 4 dpi. In hens IC-inoculated, most viral shedding occurred at 4 dpi, and by

Table 2. Virus detection in OP and C swabs and seroconversion in hens inoculated through different routes with 10^6 EID_{50}/0.1 ml of H6N2 or H9N2 viruses.

	Virus shedding at 2 dpi; no. of positive hens/total hens (log_{10} titer)[B]		Virus shedding at 4 dpi; no. of positive hens/total hens (log_{10} titer)		Virus shedding at 7 dpi; no. of positive hens/total hens (log_{10} titer)		Seroconversion at 14 dpi
Groups[A]	OP	C	OP	C	OP	C	HI positive hens/ total hens (titer[C])
H6N2 IN	8/10 (4.8±.5[D])	0/10	8/8 (5.3 ± 0.5)	3/8 (3.0 ± 0.5)	6/8 (1.2 ± 0.3)	0/8	8/8 (6.6 ± 1.9)
H6N2 IC	1/10 (4.2)	3/10 (4.3 ± 0.8)	5/8 (4.3 ± 1.7)	4/8 (4.4 ± 0.1)	1/8 (2.1)	1/8 (1.8)	8/8 (5.5 ± 1.5)
H6N2 IO	1/10 (4.0)	2/10 (4.7 ± 0.4)	4/8 (4.1 ± 1.6)	6/8 (4.3 ± 1.1)	5/8 (2.9 ± 0.6)	4/8 (1.5 ± 0.6)	8/8 (6.8 ± 1.8)
H9N2 IN	–	–	1/8 (3.2)	0/8	0/8	0/8	1/8 (7)
H9N2 IC	–	–	0/8	0/8	0/8	0/8	2/8 (2)
H9N2 IO	–	–	0/8	0/8	0/8	0/8	2/8 (3.0±.7)

[A]IN = intranasal; IC = intracloacal; IO = intraoviduct.
[B]OP = oropharyngeal; C = cloacal.
[C]Mean log_2 HI titer of the sera ± standard deviation.
[D]Mean virus titer ± standard deviation for positive samples as determined by qRRT-PCR and reported as log_{10} EID_{50}/ml.

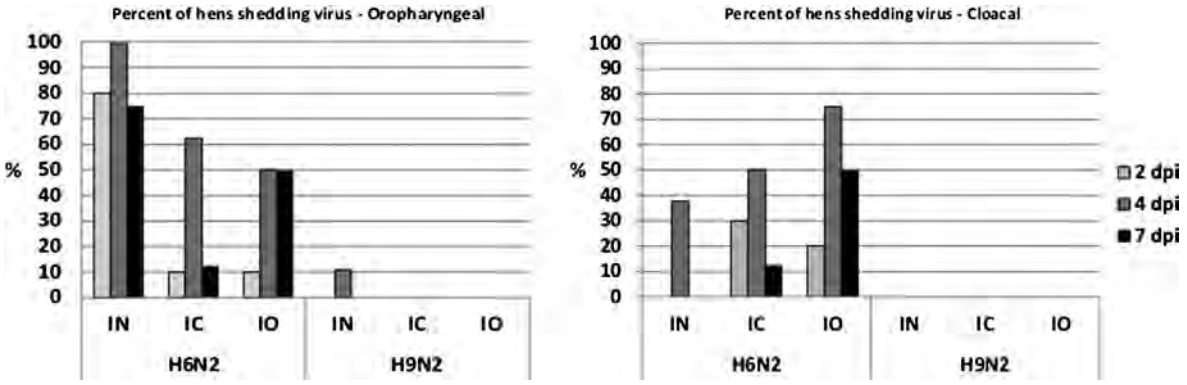

Fig. 1. Percentage of hens shedding virus at 2, 4, and 7 days after being inoculated through different routes with H6N2 or H9N2 viruses.

both the OP and the C route, but at 7 dpi only one hen was shedding virus. In hens IO-inoculated, virus was shed by half or more of the hens at both 4 and 7 dpi and by both routes. The highest virus titers were shed by the OP route from hens IN-inoculated. The percentage of hens shedding viruses at each time point can be better appreciated in Fig. 1. More than 75% of the hens IN-inoculated shed virus through the OP route at all time points, with 37% of hens shedding virus though the cloaca at only 4 dpi. Only 30% of the hens IC-inoculated shed virus initially though the cloaca, but virus was also detected in the oropharynx at 2, 4, and 7 dpi in 10%, 62.5%, and 12.5% of the hens, respectively. In addition, only 10%–20% of hens IO-inoculated shed virus at 2 dpi but more than 50% shed virus through both routes at 4 and 7 dpi. As for hens inoculated with the H9N2 virus, only 1 or 2 hens from each group shed detectable levels of the virus or seroconverted.

The two contact hens from the H6N2 IN- and IC-inoculated groups were positive for virus shedding at 4 days after being introduced into the isolators and seroconverted (Table 3). Only one of the contacts from the IO-inoculated group got infected. None of the contacts from the H9N2 groups showed evidence of infection.

Virus replication was also examined at 2 dpi in tissues collected from hens inoculated with the H6N2 LPAI virus. Virus was only detected in the lung of the two hens IN-inoculated (titers of 1.97 and 2.7 EID_{50}/g), in one hen IC-inoculated (titer of 1.97 EID_{50}/g), in the oviduct of one hen IN-inoculated (titer of 1.97 EID_{50}/g), and in one hen IO-inoculated (titer of 2.7 EID_{50}/g). No virus was detected in albumin samples from all eggs collected at 4 dpi. Tissues and eggs from hens inoculated with the H9N2 virus were not examined because most did not show evidence of infection by virus shedding and seroconversion.

Table 3. Virus detection in OP and C swabs of contact hens, examined at 4 days after introduction into the different groups, and HI titers measured at 12 days.

Groups[A]	Virus shedding; no. of positive hens/total hens (titer)[B]		Seroconversion; no. of positive hens/total hens (titer)
	OP	C	
H6N2 IN	2/2 (3.7, 3.1[C])	0/2	2/2 (7.0, 7.0[D])
H6N2 IC	2/2 (4.5, 3.2)	0/2	2/2 (6.0, 5.0)
H6N2 IO	1/2 (3.7)	0/2	1/2 (10.0)
H9N2 IN	–	–	0/2
H9N2 IC	–	–	0/2
H9N2 IO	–	–	0/2

[A]IN = intranasal; IC = intracloacal; IO = intraoviduct.
[B]OP = oropharyngeal; C = cloacal.
[C]Mean virus titers as determined by qRRT-PCR and reported as $\log_{10}$ EID_{50}/ml.
[D]Mean $\log_2$ HI titer of the sera ± standard deviation.

DISCUSSION

As demonstrated in this study, LPAI viruses can also infect chickens through other routes besides the IN route, which has been traditionally considered the natural route of exposure. The H6N2 virus infected all hens regardless of the route of inoculation and, although most hens didn't show signs of infection when given the H9N2 virus, one or two hens got infected when inoculated by any of the three routes. Hens inoculated IN with the H6N2 virus presented mild clinical signs and shed higher titers of the virus through the OP route at 2 and 4 dpi than did hens inoculated by the IC or IO routes. Interestingly, in hens inoculated with the virus by the IC or IO routes, the respiratory tract eventually got infected, reflected by virus shed by the OP route at 4 dpi. Likewise, hens IN-inoculated shed virus by the cloaca at 4 dpi. This most likely indicates infection by re-exposure to the virus by the different routes, probably by virus present in the isolators after being shed by the hens. The virus infected the hens when given through the cloaca or the oviduct; however, it is not clear in what tissues or cells the virus replicated in, as no virus staining was observed in tissues collected at 3 dpi. Nevertheless, the virus did not initially replicate as well when given by the IC or IO route when compared to the IN route, as more hens inoculated by this route were shedding virus at the earlier time point.

The H6N2 virus was originally isolated from 118-wk-old layers presenting with drops in egg production, increased mortality, and decrease of feed consumption (39). In our study, we saw a decrease in egg production in hens inoculated with this virus but only found evidence of virus replication in the oviduct of two of the hens examined at 3 dpi. However, at the end of the study, half of the hens inoculated with the H6N2 virus had stopped laying eggs compared to eight out of 10 of the sham-inoculated controls. Hens inoculated with the H9N2 virus also laid fewer eggs than did the controls, in spite of the lack of evidence of infection in most of the hens inoculated with this virus. A study examining the pathogenesis of an H4N8 LPAI virus in SPF laying hens indicated that this virus had a tissue tropism for the respiratory and urogenital systems, but lesions were only observed in the oviduct of some of the virus-inoculated hens at 5 and 8 dpi and none at 1.5 and 3 dpi (28). Similar to our study, no virus was isolated from the internal contents of eggs; however, virus was recovered from ovarian and oviduct tissues (28). Those authors concluded that AI virus isolated from the kidney,

magnum, and ovary of hens resulted from a localized infection of the respiratory tract and was not the result of systemic influenza infection but was probably the result of viral infection of the air-sac epithelium associated with the serosal surface of the internal organs. Our study indicates a second alternative: the direct or retrograde infection of the intestine and the oviduct by exposure to the virus by the IC or IO routes. Environmental exposure to the virus by the cloacal route is feasible, and IO exposure is a possibility in chicken breeders if the reproductive organs of the males are infected with the virus or via transmission by semen as reported previously for turkeys (25).

When conducting controlled experiments, it is difficult to reproduce the conditions present in the farms and many factors, including the number of birds used and the presence of secondary infectious agents, could explain the differences observed in the presentation of the disease. For instance, in breeder turkeys, LPAI infections commonly result in decreased egg production, and co-infection with other agents can worsen the clinical presentation and, in some cases, induce complete cessation of egg production (8,13,16,22,29,32,37). Environmental factors such as animal density and housing can also contribute to the differences in infection and transmission observed between the field and experimental situations (2). On the other hand, Pillai *et al.* showed that a triple reassortant H3N2 virus associated with drops in egg production in turkey breeders can, by itself, cause drastic reduction or complete cessation of egg production and pathology of the reproductive tract in IN-inoculated 26-wk-old breeder turkeys (22) and that this virus could be detected from internal egg contents following experimental infection (23). In our study, we did not observe virus staining in the oviduct as seen in studies in turkeys (19,22), and virus isolation from the oviduct or egg albumin was low or under the levels of detection. Therefore, it is not clear why the hens infected with the LPAI viruses produced fewer eggs than did the controls. One explanation could be that the mild disease produced by infection caused distress or affected feed and water consumption enough to affect lay. More studies are needed to better understand the effect of LPAI on the reproductive tract of hens.

In conclusion, LPAI viruses can also infect chickens when given by the IC or IO routes, can locally replicate, and can re-infect by the respiratory route, which is considered the natural route of exposure. This has implications in the transmission and pathogenesis of AI viruses in poultry and can inform future management decisions for control of the virus, among them better cleaning and disinfection of the premises and examination of alternate routes of transmission, including through AI virus-infected males.

REFERENCES

1. Bano, S., K. Naeem, and S. A. Malik. Evaluation of pathogenic potential of avian influenza virus serotype H9N2 in chickens. Avian Dis. 47:817–822. 2003.

2. Berhane, Y., D. Ojkic, J. Neufeld, M. Leith, T. Hisanaga, H. Kehler, A. Ferencz, H. Wojcinski, C. Cottam-Birt, M. Suderman, K. Handel, S. Alexandersen, and J. Pasick. Molecular characterization of pandemic H1N1 influenza viruses isolated from turkeys and pathogenicity of a human pH1N1 isolate in turkeys. Avian Dis. 54:1275–1285. 2010.

3. Bowes, V. A., S. J. Ritchie, S. Byrne, K. Sojonky, J. J. Bidulka, and J. H. Robinson. Virus characterization, clinical presentation, and pathology associated with H7N3 avian influenza in British Columbia broiler breeder chickens in 2004. Avian Dis. 48:928–934. 2004.

4. Brandly, C. A., and L. D. Bushell. A report of some investigations of infectious laryngotracheitis. Poult. Sci. 13:212–217. 1934.

5. Bwala, D. G., S. Clift, N. M. Duncan, S. P. Bisschop, and F. F. Oludayo. Determination of the distribution of lentogenic vaccine and virulent Newcastle disease virus antigen in the oviduct of SPF and commercial hen using immunohistochemistry. Res. Vet. Sci. 2011. (E-pub ahead of print).

6. Capua, I., and F. Mutinelli. A color atlas and text on avian influenza. Papi Editore, Edizioni Tecnico Scientifiche, Bologna, Italy. p. 47. 2001.

7. Cardona, C. J., B. R. Charlton, and P. R. Woolcock. Persistence of immunity in commercial egg-laying hens following vaccination with a killed H6N2 avian influenza vaccine. Avian Dis. 50:374–379. 2006.

8. Choi, Y. K., J. H. Lee, G. Erickson, S. M. Goyal, H. S. Joo, R. G. Webster, and R. J. Webby. H3N2 influenza virus transmission from swine to turkeys, United States. Emerg. Infect. Dis. 10:2156–2160. 2004.

9. Das, A., E. Spackman, M. J. Pantin-Jackwood, and D. L. Suarez. Removal of real-time reverse transcription-polymerase chain reaction (RT-PCR) inhibitors associated with cloacal swab samples and tissues for improved diagnosis of avian influenza virus by RT-PCR. J. Vet. Diagn. Invest. 21:771–778. 2009.

10. Jackwood, M. W., D. L. Suarez, D. Hilt, M. J. Pantin-Jackwood, E. Spackman, P. Woolcock, and C. Cardona. Biologic characterization of chicken-derived H6N2 low pathogenic avian influenza viruses in chickens and ducks. Avian Dis. 54:120–125. 2010.

11. Kwon, Y. K., and D. E. Swayne. Different routes of inoculation impact infectivity and pathogenesis of H5N1 high pathogenicity avian influenza virus infection in chickens and domestic ducks. Avian Dis. 54:1260–1269. 2010.

12. Lu, H., P. A. Dunn, E. A. Wallner-Pendleton, D. J. Henzler, D. C. Kradel, J. Liu, D. P. Shaw, and P. Miller. Investigation of H7N2 avian influenza outbreaks in two broiler breeder flocks in Pennsylvania, 2001–02. Avian Dis. 48:26–33. 2004.

13. Ludwig, S., A. Haustein, E. F. Kaleta, and C. Scholtissek. Recent influenza A (H1N1) infections of pigs and turkeys in northern Europe. Virology 202:281–286. 1994.

14. McDougald, L. R. Blackhead disease (histomoniasis) in poultry: a critical review. Avian Dis. 49:462–476. 2005.

15. Mutinelli, F., I. Capua, C. Terregino, and G. Cattoli. Clinical, gross, and microscopic findings in different avian species naturally infected during the H7N1 low- and high-pathogenicity avian influenza epidemics in Italy during 1999 and 2000. Avian Dis. 47:844–848. 2003.

16. Olsen, C. W., A. I. Karasin, S. Carman, Y. Li, N. Bastien, D. Ojkic, D. Alves, G. Charbonneau, B. M. Henning, D. E. Low, L. Burton, and G. Broukhanski. Triple reassortant H3N2 influenza A viruses, Canada, 2005. Emerg. Infect. Dis. 12:1132–1135. 2006.

17. Pantin-Jackwood, M. J., and D. E. Swayne. Pathobiology of Asian highly pathogenic avian influenza H5N1 virus infections in ducks. Avian Dis. 51:250–259. 2007.

18. Pantin-Jackwood, M. J., and D. E. Swayne. Pathogenesis and pathobiology of avian influenza virus infection in birds. Rev. Sci. Tech. 28:113–136. 2009.

19. Pantin-Jackwood, M., J. L. Wasilenko, E. Spackman, D. L. Suarez, and D. E. Swayne. Susceptibility of turkeys to pandemic-H1N1 virus by reproductive tract insemination. Virol. J. 7:27. 2010.

20. Pedersen, J. C. Hemagglutination-inhibition test for avian influenza virus subtype identification and the detection and quantitation of serum antibodies to the avian influenza virus. Methods Mol. Biol. 436:53–66. 2008.

21. Pfeiffer, J., D. L. Suarez, L. Sarmento, T. L. To, T. Nguyen, and M. J. Pantin-Jackwood. Efficacy of commercial vaccines in protecting chickens and ducks against H5N1 highly pathogenic avian influenza viruses from Vietnam. Avian Dis. 54:262–271. 2010.

22. Pillai, S. P., M. Pantin-Jackwood, S. J. Jadhao, D. L. Suarez, L. Wang, H. M. Yassine, Y. M. Saif, and C. W. Lee. Pathobiology of triple reassortant H3N2 influenza viruses in breeder turkeys and its potential implication for vaccine studies in turkeys. Vaccine 27:819–824. 2009.

23. Pillai, S. P., Y. M. Saif, and C. W. Lee. Detection of influenza A in eggs laid by infected turkeys. Avian Dis. 54:830–833. 2010.

24. Roussan, D. A., G. Y. Khawaldeh, R. H. Al Rifai, W. S. Totanji, and I. A. Shaheen. Avian influenza virus H9 subtype in poultry flocks in Jordan. Prev. Vet. Med. 88:77–81. 2009.

25. Samadieh, B., and R. A. Bankowski. Effect of avian influenza-A viruses upon egg production and fertility of turkeys. Avian Dis. 14:715–722. 1970.

26. Seal, B. S., D. J. King, D. P. Locke, D. A. Senne, and M. W. Jackwood. Phylogenetic relationships among highly virulent Newcastle disease virus isolates obtained from exotic birds and poultry from 1989 to 1996. J. Clin. Microbiol. 36:1141–1151. 1998.

27. Senne, D. Virus propagation in embryonating eggs. In: A laboratory manual for the isolation, identification and characterization of avian pathogens, 5th ed. D. E. Swayne, L. Dofour-Zavala, J. R. Gilsson, J. E. Pearson, M. W. Jackwood, W. M. Reed, and P. R. Woolcock, eds. American Association of Avian Pathologists, Jacksonville, FL. pp. 204–208. 2008.

28. Shalaby, A. A., R. D. Slemons, and D. E. Swayne. Pathological studies of A/chicken/Alabama/7395/75 (H4N8) influenza virus in specific-pathogen-free laying hens. Avian Dis. 38:22–32. 1994.

29. Skeeles, J., J. N. Beasley, P. Blore, and S. Klopp. Severe egg-production drops in turkey breeders in Southcentral Missouri. Avian Dis. 25:764–767. 1981.

30. Spackman, E., D. A. Senne, T. J. Myers, L. L. Bulaga, L. P. Garber, M. L. Perdue, K. Lohman, L. T. Daum, and D. L. Suarez. Development of a real-time reverse transcriptase PCR assay for type A influenza virus and the avian H5 and H7 hemagglutinin subtypes. J. Clin. Microbiol. 40:3256–3260. 2002.

31. Spickler, A. R., D. W. Trampel, and J. A. Roth. The onset of virus shedding and clinical signs in chickens infected with high-pathogenicity and low-pathogenicity avian influenza viruses. Avian Pathol. 37:555–577. 2008.

32. Suarez, D. L., P. R. Woolcock, A. J. Bermudez, and D. A. Senne. Isolation from turkey breeder hens of a reassortant H1N2 influenza virus with swine, human, and avian lineage genes. Avian Dis. 46:111–121. 2002.

33. Swayne, D. E., and D. A. Halvorson. Influenza. In: Diseases of poultry, 12th ed. J. R. Glisson, Y. M. Saif, A. M. Fadly, L. R. McDougald, and L. Nolan, eds. Blackwell Publishing, Ames, Iowa. 2008.

34. Swayne, D. E., and M. Pantin-Jackwood. Pathobiology of avian influenza virus infections in birds and mammals. In: Avian influenza. D. E. Swayne, ed. Blackwell Publishing, Ames, Iowa. pp. 87–122. 2008.

35. Swayne, D. E., M. Pantin-Jackwood, D. Kapczynski, E. Spackman, and D. L. Suarez. Susceptibility of poultry to pandemic (H1N1) 2009 virus [letter]. Emerg. Infect. Dis. 15:2061–2063. 2009.

36. Swayne, D. E., D. A. Senne, and C. W. Beard. Avian influenza. In: A labortatory manual for the isolation and identification of avian pathogens, 4th ed. J. R. Glisson, D. E. Swayne, M. W. Jackwood, J. E. Pearson, and W. M. Reed, eds. American Association of Avian Pathologists, Kennett Square, PA. pp. 150–155. 1998.

37. Tang, Y., C. W. Lee, Y. Zhang, D. A. Senne, R. Dearth, B. Byrum, D. R. Perez, D. L. Suarez, and Y. M. Saif. Isolation and characterization of H3N2 influenza A virus from turkeys. Avian Dis. 49:207–213. 2005.

38. Villegas, P. Titration of virological suspensions. In: A laboratory manual for the isolation, identification and characterization of avian pathogens, 5th ed. D. E. Swayne, L. Doufour-Zavala, J. R. Gilsson, J. E. Pearson, M. W. Jackwood, W. M. Reed, and P. R. Woolcock, eds. American Association of Avian Pathologists Jacksonville, FL. pp. 217–221. 2008.

39. Woolcock, P. R., D. L. Suarez, and D. Kuney. Low-pathogenicity avian influenza virus (H6N2) in chickens in California, 2000–02. Avian Dis. 47:872–881. 2003.

40. Ziegler, A. F., S. Davison, H. Acland, and R. J. Eckroade. Characteristics of H7N2 (nonpathogenic) avian influenza virus infections in commercial layers, in Pennsylvania, 1997–98. Avian Dis. 43:142–149. 1999.

ACKNOWLEDGMENTS

We appreciate the assistance provided by Ronald Graham and Scott Lee in conducting these studies. We also thank the FSIS histopathology laboratory at Russell Research Center–United States Department of Agriculture for technical assistance.

JVI Journals.ASM.org

Molecular Signatures Associated with Mx1-Mediated Resistance to Highly Pathogenic Influenza Virus Infection: Mechanisms of Survival

Cristian Cilloniz,[a] Mary J. Pantin-Jackwood,[b] Chester Ni,[c] Victoria S. Carter,[a] Marcus J. Korth,[a] David E. Swayne,[b] Terrence M. Tumpey,[d] and Michael G. Katze[a,e]

Department of Microbiology, School of Medicine, University of Washington, Seattle, Washington, USA[a]; Southeast Poultry Research Laboratory, Agricultural Research Service, U.S. Department of Agriculture, Athens, Georgia, USA[b]; Benaroya Research Institute, Seattle, Washington, USA[c]; Influenza Division, National Center for Immunization and Respiratory Diseases, Centers for Disease Control and Prevention, Atlanta, Georgia, USA[d]; and Washington National Primate Research Center, University of Washington, Seattle, Washington, USA[e]

Understanding the role of host factors during lethal influenza virus infection is critical to deciphering the events that determine the fate of the host. One such factor is encoded by the Mx1 gene, which confers resistance to influenza virus infection. Here, we compared pathology and global gene expression profiles in lung tissue from BALB/c (Mx1^{-}) and BALB · A2G-Mx1 mice (Mx1$^{+/+}$) infected with the fully reconstructed 1918 pandemic influenza virus. Mx1$^{+/+}$ mice showed less tissue damage than Mx^{-} animals, and pathology and mortality were further reduced by treating the mice with interferon prior to infection. Using global transcriptional profiling, we identified distinct molecular signatures associated with partial protection, complete protection, and the contribution of interferon to the host response. In the absence of interferon treatment, partial protection was characterized by the generation of an acute response with the upregulation of genes associated with apoptosis, reactive oxygen species, and cell migration. Complete protection was characterized by the downregulation of cytokine and chemokine genes previously associated with influenza virus pathogenesis. The contribution of interferon treatment to total protection in virus-infected Mx1$^{+/+}$ mice was characterized by the altered regulation of cell cycle genes. These genes were upregulated in Mx1$^{+/+}$ mice treated with interferon but downregulated in the absence of interferon treatment. Our results suggest that Mx1$^{+/+}$ mice generate a protective antiviral response by controlling the expression of key modulator molecules associated with influenza virus lethality.

The continued emergence of new influenza viruses highlights the need to better understand influenza virus-host interactions and mechanisms of pathogenicity. Such an understanding is necessary to facilitate the development of safe and effective therapeutics and vaccines, critical aspects of preparedness for future pandemics. A clear reminder of the lethal potential of influenza virus infection is the 1918 pandemic, which resulted in over 50 million deaths worldwide (11). In addition, highly pathogenic avian H5N1 influenza viruses continue to circulate in diverse parts of the world (21, 37), and with human infections resulting in a greater than 50% mortality rate, there is considerable concern over the potential for a deadly new pandemic. Here, we sought to compare the host transcriptional responses to the reconstructed 1918 virus in Mx1$^{+/+}$ mice with the goal of gaining insights into the underlying protective mechanisms that make these animals resistant to lethal influenza virus infection. The expression of the Mx1 gene is under tight transcriptional control of type I and III interferon (26) and codes for a nuclear 72-kDa protein with antiviral properties that controls influenza A virus infection in mice (9, 30).

A study comparing the virulence of influenza A virus in a mouse model of infection (6) found that an unusual influenza virus strain was virulent in Mx1$^{+/+}$ mice. Interestingly, this virus was well controlled by Mx1$^{+/+}$ mice treated with interferon before infection, suggesting that rapid virus growth can outcompete the antiviral response. The results from an independent study using mouse infection models suggest that the Mx1 gene protects mice against highly lethal influenza viruses (33). In that study, Mx1 was reported to be a key component of the innate immune system that mediates protection against both zoonotic and human pandemic strains of influenza viruses of high virulence. Another study using a mouse infection model and *in vitro* experiments showed that the origin of the viral NP gene determines Mx sensitivity and that human influenza viruses acquired adaptive mutations to evade MxA restriction (40).

In the present study, we examined the host response to the 1918 virus in wild-type BALB/c and Mx1$^{+/+}$ mice; additional findings were obtained from animals treated with interferon before infection. The Mx1$^{+/+}$ mice were partially protected from lethal 1918 virus infection; however, complete protection was achieved only upon interferon treatment before infection. In contrast, untreated and interferon-treated BALB/c mice succumbed to 1918 virus infection. Global gene expression profiling data revealed distinct molecular signatures associated with partial protection (untreated mice), complete protection (interferon-treated Mx1$^{+/+}$ mice), and the specific contribution of interferon to complete protection of Mx1$^{+/+}$ mice. In summary, these findings suggest that mice exhibiting a fully functional Mx1 phenotype are able to generate a strong antiviral state by downregulating key modulator molecules associated with influenza virus lethality.

Received 26 August 2011 **Accepted** 9 December 2011
Published ahead of print 21 December 2011
Address correspondence to Michael G. Katze, honey@u.washington.edu.
Supplemental material for this article may be found at http://jvi.asm.org/.
Copyright © 2012, American Society for Microbiology. All Rights Reserved.
doi:10.1128/JVI.06156-11

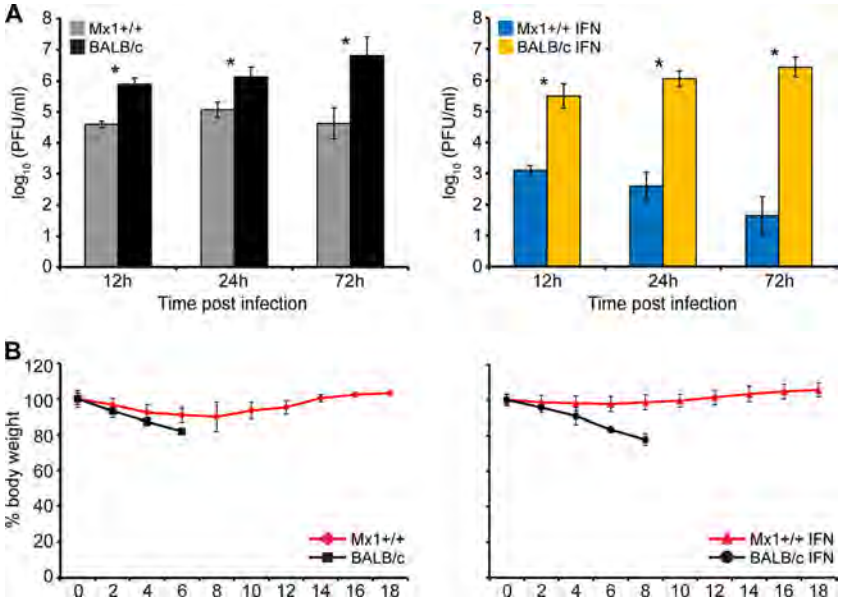

FIG 1 Mx1 competent mice control lethal influenza virus infection. (A) Lung virus titer data from a total of 36 mice (3 animals per time point/treatment/mouse strain). The limit of detection of the assay was $10^{0.95}$ PFU/ml. (B) Morbidity data from a total of 36 mice (9 mice per group). The error bars indicate standard deviations.

MATERIALS AND METHODS

Viruses. The reconstructed 1918 H1N1 virus (32), possessing the A/South Carolina/1/18 hemagglutinin (HA), was previously shown to be highly virulent for both mice and ferrets (15, 31, 32). The 1918 virus was generated utilizing the 12-plasmid reverse-genetics system in a mixture of Madin-Darby canine kidney (MDCK) (ATCC, Manassas, VA) and 293T (ATCC) cells as previously described (31). The titers of virus stocks were determined by plaque assay on MDCK cells, and stocks were maintained in Dulbecco's Modified Eagle's Medium (DMEM) (Gibco, Grand Island, NY) supplemented with 10% fetal calf serum (FCS) (HyClone, Logan, UT) and 1% penicillin/streptomycin (Gibco). The reconstructed 1918 virus was grown as previously described (22). All virus challenge experiments were performed under the guidance of the U.S. National Select Agent Program in negative-pressure HEPA-filtered biosafety level 3 enhanced (BSL-3+) laboratories and with the use of a battery-powered Racal HEPA filter respirator (Racal Health and Safety Inc., Frederick, MD) according to Biomedical Microbiological and Biomedical Laboratory procedures (35).

Mouse experiments. All animal research was conducted according to the guidance of the CDC's Institutional Animal Care and Use Committee and in a facility accredited by the Association for Assessment and Accreditation of Laboratory Animal Care International. BALB/c mice carrying a defective allele of the Mx1 resistance gene (29) or congenic BALB · A2G-Mx1 mice carrying the functional Mx1 allele (28) (kindly provided by Peter Staeheli, University of Freiburg, Freiburg, Germany), were anesthetized by intraperitoneal injection of 0.2 ml of 2,2,2-tribromoethanol in tert-amyl alcohol (Avertin; Sigma-Aldrich, Milwaukee, WI). One hundred times the 50% lethal dose (LD_{50}), 3.2×10^5 PFU of the reconstructed 1918 virus in 50 μl of infectious virus diluted in phosphate-buffered saline (PBS), was inoculated intranasally. LD_{50} titers were calculated by the method of Reed and Muench (25).

The replication of the reconstructed 1918 virus in mice (3 animals/group/time point) was examined by determining the virus titers in the lung (12, 24, and 72 h), brain, and spleen (24 and 72 h) following intranasal inoculation of virus. The clarified homogenates were titrated for virus infectivity in eggs from an initial dilution of 1:10 (lung). Additional inoculated mice (6 animals/group, making a total of 24 animals) were followed for morbidity and mortality. In addition, half of the animals were intranasally treated with 10,000 units of recombinant human alpha interferon (IFN-α) A/D (R&D Systems, Minneapolis, MN) before infection with the reconstructed 1918 virus and euthanized 12, 24, and 72 h post-treatment.

Histopathology. Collected lung sections were fixed by submersion in 10% neutral buffered formalin, routinely processed, and embedded in paraffin. Sections were cut to 5 μm, stained with hematoxylin and eosin (HE), and examined microscopically for histopathological alterations.

RNA preparation and oligonucleotide microarray processing. For RNA isolation, lungs (3 animals/group/time point) were frozen in individual tubes and stored in solution D (4 M guanidinium thiocyanate, 25 mM sodium citrate, 0.5% sarcosyl, 0.1 M β-mercaptoethanol) as previously described (2). RNA was extracted from mouse lungs using a Qiagen RNeasy Minikit with RNA Later solution (Qiagen, Valencia, CA) according to the manufacturer's instructions. The RNA was further purified using RNeasy columns (Qiagen, Valencia, CA). RNA samples were spectroscopically verified for purity, and the quality of the intact RNA was assessed using an Agilent 2100 Bioanalyzer. For each set of treatment conditions, three of the five RNA samples exhibiting the highest RNA integrity number (RIN) determined using the Bioanalyzer were used for microarray analysis. cRNA probes were generated from each sample by the use of an Agilent one-color LowInput Quick Amp Labeling Kit (Agilent Technologies, Santa Clara, CA). Individual cRNA samples were hybridized to Agilent mouse whole-genome oligonucleotide 4 by 44 microarrays (approximately 39,000 unique mouse genes) according to the manufacturer's instructions. Samples from individual animals were not pooled to enable examination of animal-to-animal variation as part of the data analysis: they included three animals per time point for each virus (60 animals in total). Select samples were hybridized a second time ($n = 2$ technical replicates) to verify the quality of the process.

Slides were scanned with an Agilent DNA microarray scanner, and the resulting images were analyzed using Agilent Feature Extractor version 8.1.1.1. This software was used to perform image analysis, including the significance of signal and spatial detrending and to apply a universal error model. For these hybridizations, the most conservative error model was applied. Quality control (QC) reports generated from Agilent Feature Extraction software were used to assess data quality for each microarray

and to identify outliers. The raw data were then loaded into a custom-designed laboratory information management system.

Microarray analysis and bioinformatics. Global gene expression in infected lungs was analyzed using GeneData Expressionist, Analyst Module (version 2.2.1); Spotfire DecisionSite for Functional Genomics version 9; and Ingenuity Pathways Analysis (IPA) (Ingenuity Systems, Inc., Redwood City, CA). Raw intensity data from all microarrays were normalized by applying the central tendency algorithm with the standard reference set at the 75th percentile of each microarray. One- or two-way analysis of variance (ANOVA) was carried out for various groups of samples stratified by mouse strains and/or time points (see Results for more grouping details). Fixed-effect models were built to identify gene signatures associated with protection phenotypes against 1918 virus infection (see Fig. 3, 5, and 7). The Benjamini-Hochberg algorithm was used to control the false discovery rate (FDR) of multiple testing (1). Primary data are available (http://viromics.washington.edu) in accordance with proposed Minimum Information about a Microarray Experiment (MIAME) standards. Functional and network analysis of statistically significant gene expression changes was performed using IPA. The Benjamini-Hochberg algorithm was applied to correct for multiple testing in determining the probability that each biological function assigned to the genes within each statistical analysis result was due to chance alone.

RESULTS

Mx1$^{+/+}$ mice partially control 1918 virus infection. Previous studies by our group and others (6, 27, 33) have shown that knock-in mice carrying a fully functional Mx1 gene are resistant to lethal influenza virus infection; however, those studies did not investigate the host response elicited under such experimental conditions. In the present study, our main goal was to understand the contribution of the elicited host response to survival. To achieve this goal, we performed global gene expression analyses on lung tissue from mice infected with the fully reconstructed 1918 virus.

Our initial experiments showed that Mx1$^{+/+}$ mice were able to reduce the growth of the 1918 virus by 1 log unit at 12 and 24 h postinfection (p.i.) with a reduction of 2 log units by 72 h p.i. compared to the virus growth observed in Mx1^{-} mice (Fig. 1A, left). Administration of interferon to the animals prior to infection resulted in an even greater decrease of 1918 virus growth in Mx1$^{+/+}$ mice, with 2.5-, 3.5-, and 5-log-unit reductions at 12, 24, and 72 h p.i., respectively. However, there was no significant change in virus growth in BALB/c (Mx1^{-}) mice (Fig. 1A, right); these observations were in agreement with previous studies (33). Although there was a large amount of virus detected in the lungs of infected animals, especially in BALB/c mice, we did not detect viral dissemination to the brain or spleen (data not shown). However, morbidity data showed dramatic differences between the two mouse strains. While BALB/c mice were highly susceptible to 1918 virus infection, as shown by the rapid and steady decrease in body weight, interferon-treated Mx1$^{+/+}$ mice were insensitive to 1918 infection (as measured by weight loss) throughout the experiment. In the absence of interferon treatment, an initial slight decline followed by a recovery in body weight in Mx1$^{+/+}$ mice may be observed as a characteristic of interferon treatment (Fig. 1B).

1918 virus infection generates less tissue damage in Mx1$^{+/+}$ mice. In the absence of interferon treatment, infection with the 1918 virus resulted in lung and airway lesions typical of influenza A virus infection in both Mx1$^{+/+}$ and BALB/c mice. The lesions varied depending on the individual animals and the area of the lung examined, but in general, the lesions in BALB/c mice were more severe than the lesions observed in the Mx1$^{+/+}$ mice (Fig. 2).

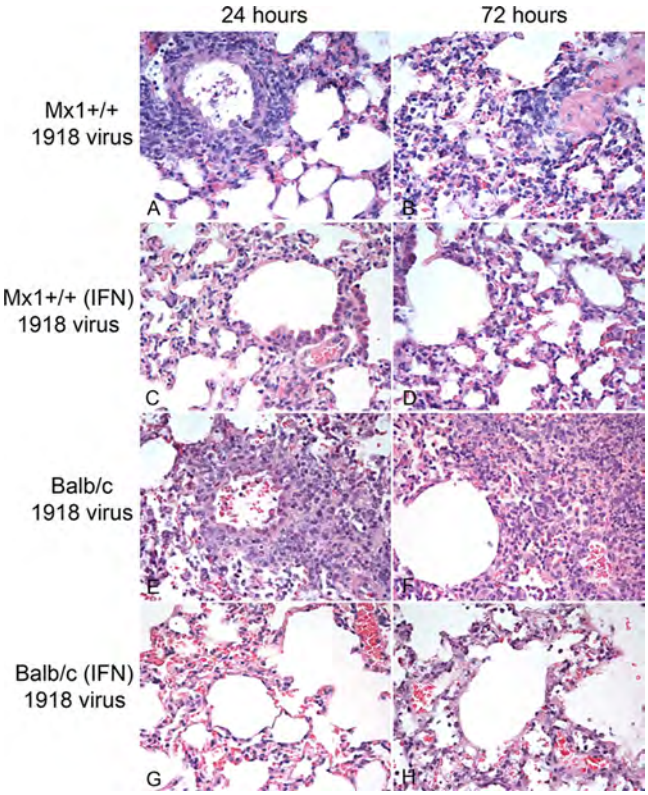

FIG 2 Histopathological changes in tissues from 1918 virus-infected mice. Shown are photomicrographs of lung tissue sections stained with hematoxylin and eosin. (A) Severe necrotizing bronchiolitis and associated peribronchiolar lymphocytic inflammation and congestion in a 1918 virus-infected Mx1$^{+/+}$ mouse at 24 h p.i. (B) Severe histiocytic-to-lymphocytic alveolitis with some neutrophils, congestion, and edema in a 1918 virus-infected Mx1$^{+/+}$ mouse at 72 h p.i. (C) Loss of bronchiolar epithelium with minimal peribronchiolar inflammation and moderate histiocytic alveolitis in an interferon-treated Mx1$^{+/+}$ mouse at 24 h p.i. (D) Moderate histiocytic alveolitis with congestion of the alveolar epithelium in an interferon-treated Mx1$^{+/+}$ mouse at 72 h p.i. (E) Severe necrotizing bronchiolitis and associated peribronchiolar histiocytic inflammation and congestion in a 1918 virus-infected BALB/c mouse at 24 h p.i. (F) Severe diffuse histiocytic alveolitis with presence of lymphocytes, neutrophils, and plasma cells in a 1918 virus-infected BALB/c mouse 72 h p.i. (G) Moderate histiocytic alveolitis with loss of the bronchial epithelium and congestion in an interferon-treated 1918 virus-infected BALB/c mouse 24 h p.i. (H) Alveolar and bronchial epithelial necrosis with edema and congestion in an interferon-treated 1918 virus-infected BALB/c mouse 72 h p.i.

At 24 h p.i., BALB/c mice exhibited moderate to severe necrotizing bronchiolitis and bronchitis. The bronchiolar walls showed vacuolation and loss of epithelium and were thickened by the presence of edema fluid, fibrin, neutrophils, eosinophils, and mononuclear cells. There was perivascular and peribronchiolar infiltration of macrophages, lymphocytes, and plasma cells. At this time point, Mx1$^{+/+}$ mice exhibited only mild diffuse histiocytic alveolitis with congestion and edema, whereas BALB/c mice had moderate interstitial pneumonia. At 72 h p.i., loss of the bronchial and bronchiolar epithelium was evident, accompanied by severe perivascular and peribronchiolar inflammation, mostly composed of macrophages, but also lymphocytes, plasma cells, and neutrophils. Mild to severe diffuse interstitial pneumonia was present, with thickening of the alveolar walls; presence of inflammatory cells; congestion; and areas of alveolar necrosis, atelectasia, hemorrhage, or consolidation.

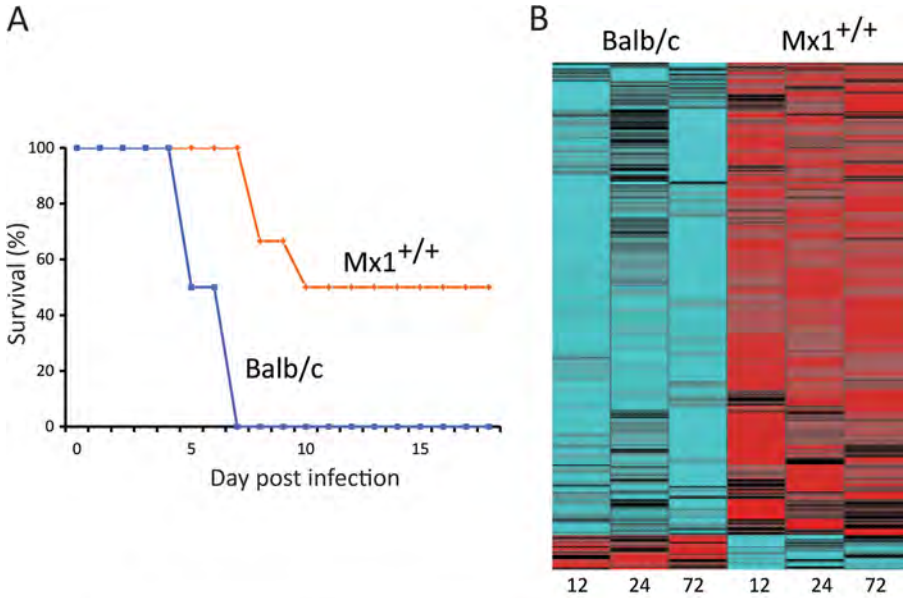

C

Biological function	P-value
Cellular movement	7.89E-02 – 2.2E-01
Cellular growth and proliferation	7.89E-02 – 2.2E-01
Cellular development	7.89E-02 – 2.33E-01
Cell cycle	2.2E-02 – 2.2E-01
Cell death	2.2E-02 – 2.34E-01
Cell morphology	2.2E-02 – 2.33E-01
Amino acid metabolism	2.2E-01 – 2.2E-01
Cellular assembly and organization	2.2E-01 – 2.2E-01
DNA replication, recombination and repair	2.2E-01 – 2.2E-01
Small molecule biochemistry	2.2E-01 – 2.2E01

FIG 3 Mx1$^{+/+}$ mice are partially protected against 1918 virus infection. (A) Survival plot of a total of 18 mice (9 animals/mouse strain). (B) Heat map illustrating 547 differentially transcribed genes associated with 50% protection of animals compared to the wild-type animals in the absence of interferon treatment; cutoff values were ≥2-fold change and a *P* value of ≤0.01 (ANOVA), FDR corrected. Blue indicates downregulation. Red indicates upregulation in the activation of genes. (C) Top 10 biological functions assigned to the 547 differentially regulated genes determined by IPA. The *P* values of the functional categories are shown on the right.

The character of the lesions varied in both the virus-infected Mx1$^{+/+}$ mice and BALB/c mice treated with interferon compared to the mice not treated with interferon. At 24 h p.i., lesions to the bronchiolar and bronchial epithelium were moderate in all mice with, in some cases, loss of the respiratory epithelium, but with minimal or no peribronchial or peribronchiolar inflammation. Alveolar lesions were moderate to severe at this time point, with diffuse alveolar necrosis, hemorrhage, and edema. At 72 h p.i., Mx1$^{+/+}$ mice had mild to moderate diffuse interstitial pneumonia with alveolar necrosis, and the inflammatory cells were mostly macrophages. In contrast, the BALB/c mice exhibited more severe pathology, with mild to severe necrotizing bronchiolitis and moderate to severe alveolitis with alveolar necrosis, congestion, and edema.

Mx1$^{+/+}$ mice exhibit increased survival of 1918 virus infection. Our results indicated that when infected with the 1918 virus, Mx1$^{+/+}$ mice had lower viral titers and less severe lung lesions than BALB/c mice. In addition, whereas the 1918 virus was uniformly lethal in BALB/c mice, 50% of the Mx1$^{+/+}$ mice survived infection (Fig. 3A). In order to assess the effects of both genetic background (MX1$^{+/+}$ and BALB/c) and time points (12, 24, and 72 h) on gene expression, two-way ANOVA was performed using genetic backgrounds and time points as two independent variables. We identified 547 genes that were differentially expressed (Fig. 3B). A large proportion of these genes were downregulated in the BALB/c animals, whereas the same genes were strongly upregulated in the Mx1$^{+/+}$ mice. The top 10 biological categories in which these genes are involved are shown in Fig. 3C.

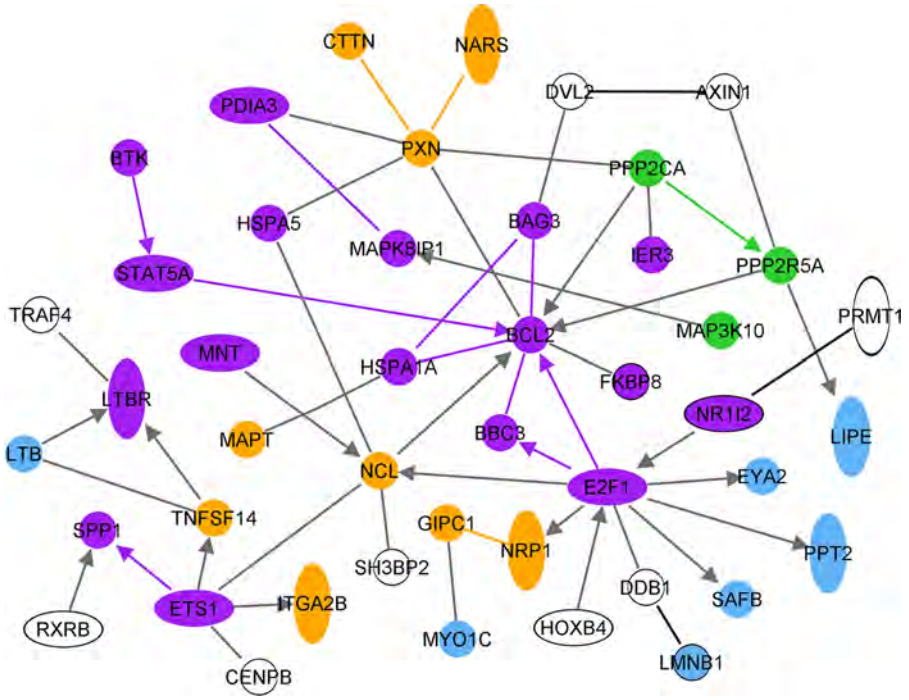

FIG 4 Molecular signature associated with partial protection of Mx1$^{+/+}$ mice. The biological network shows the direct functional relationship of genes associated with partial protection determined by IPA identified from the 547 differentially regulated genes. This network highlights upregulated and downregulated (SPP1 and PPP2R5A only) genes in Mx1$^{+/+}$ mice in the absence of interferon treatment. Purple, apoptosis; orange, cell migration; light blue, connective tissue disorder; white, production of reactive oxygen species.

We used IPA to generate a network of genes functionally associated with survival. As annotated in IPA, the resulting network included genes associated with apoptosis, cell migration, connective tissue disorders, and the production of reactive oxygen species (Fig. 4). All of these genes, with the exception of spp1 and Ppp2r5a, were upregulated in the Mx1$^{+/+}$ mice but were downregulated in BALB/c mice. These results suggest that increased survival of Mx1$^{+/+}$ mice is associated with the upregulation of these pathways.

Interferon-dependent host response associated with complete protection. Previous studies by our group and others (6, 33) showed that pretreatment of Mx1$^{+/+}$ mice with interferon results in increased resistance to influenza virus infection. In the present study, we observed similar results, with all Mx1$^{+/+}$ mice pretreated with interferon surviving a challenge with a high dose of 1918 virus (Fig. 5A). In this context, we wanted to gain insights into the specific host response required for complete protection. Using a two-way ANOVA approach, we identified 2,071 differentially expressed genes between the Mx1$^{+/+}$ and BALB/c interferon-treated mice (Fig. 5B). There was a clear anticorrelation in gene expression between the two mouse strains; however, the Mx1$^{+/+}$ mice showed a strong upregulation of these genes by 12 h p.i. that continued, although to a lesser extent, at later time points. Functional analysis of these genes using IPA showed that the majority of the genes were associated with host physiological functions, such as cell-to-cell signaling and interaction or cellular movement (Fig. 5C). Network analysis of these genes allowed us to identify a set of physically interacting genes that might be responsible for survival (Fig. 6). The most striking feature of this molecular signature was that the Mx1$^{+/+}$ mice were able to downregulate the expression of inflammatory cytokine and chemokine genes, as well as acute-phase genes. These results suggest that complete survival of mice is linked to the downregulation of key modulator molecules. We also note that these changes in gene expression were not due to differences in the response to interferon, since in the absence of infection, the gene expression signatures of interferon-treated Mx1$^{+/+}$ and BALB/c mice were similar (see Table S1 in the supplemental material for a complete list of differentially expressed genes).

Specific contribution of interferon to survival. Because treatment of Mx1$^{+/+}$ mice with interferon prior to 1918 virus infection increased survival from 50% to 100% (Fig. 7A), we next investigated the contribution of interferon to differences in the host transcriptional response to infection. Using two-way ANOVA, we identified 234 differentially expressed genes between these two experimental conditions (Fig. 7B), and the top 10 functional categories assigned to these genes are indicated in Fig. 7C.

Network analysis identified functionally related genes associated with survival. All of the genes depicted in this specific network were related to cell cycle regulation, including cyclins (CCNA1, CCNA2, CCNB1, and CCNB2), cell cycle DNA damage check point regulation (BRCA1, CDK1, CKS2, TOP2A), and cell division cycle-associated genes (CDCA5, CDCA8) (Fig. 8). A large proportion of these genes were upregulated in the interferon-treated animals but were downregulated in the absence of interferon, suggesting that tight control of this specific set of genes involved in cell cycle regulation is important to elicit a response capable of providing complete protection. Although during our previous studies we found that the expression of some cell cycle-related genes was differentially regulated upon influenza virus infection, the extent and functional network of cell cycle genes as-

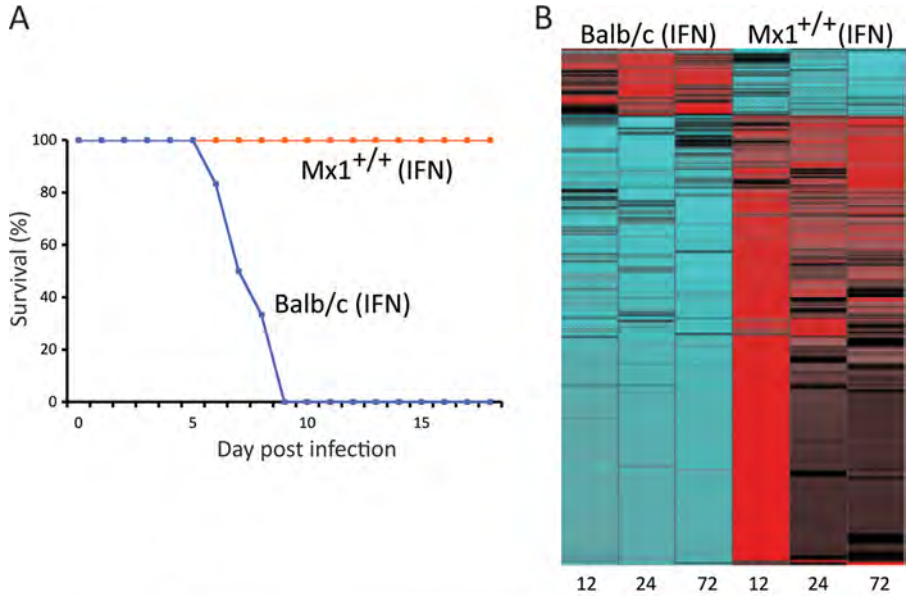

C

Biological function	P-value
Cell-to-cell signaling and interaction	1.91E-06 – 7.17E-02
Cellular movement	1.17E-05 – 7.17E-02
Antigen presentation	3.5E-04 – 7.09E-02
Cellular growth and proliferation	2.90E-03 – 7.17E-02
Cellular development	5.56E-03 – 7.06E-02
Cell signaling	5.79E-03 – 6.09E-02
Molecular transport	5.79E-03 - 6.67E-02
Vitamin and mineral metabolism	5.79E-03 - 6.52E-02
Amino acid metabolism	1.05E-02 – 3.42E-02
Gene expression	1.05E-02 – 6.52E-02

FIG 5 Interferon-treated Mx1$^{+/+}$ mice are resistant to lethal 1918 virus infection. (A) Survival plot of a total of 18 mice (9 animals/mouse strain). (B) Heat map illustrating 2,071 differentially transcribed genes associated with complete protection of Mx1$^{+/+}$ animals compared to the wild-type animals during interferon treatment; cutoff values were ≥2-fold change and a *P* value of ≤0.01 (ANOVA), FDR corrected. Blue indicates downregulation. Red indecates upregulation in the activation of genes. (C) Top 10 biological functions assigned to the 2,071 differentially regulated genes determined by IPA. The *P* values of the functional categories are shown on the right.

sociated with IFN pretreatment of Mx1$^{+/+}$ mice challenged with the 1918 virus is a novel finding.

DISCUSSION

In this study, we observed that Mx1$^{+/+}$ mice were able to partially control 1918 virus growth and that this control was highly enhanced by pretreatment of the animals with interferon. In contrast, BALB/c mice were not able to control virus growth in the presence or absence of interferon treatment. We were not able to detect viral dissemination to brain or spleen in either mouse strain. Histopathological analysis indicated that Mx1$^{+/+}$ animals had less severe lung damage than was present in BALB/c mice, and pathology was further reduced by interferon pretreatment. These results indicate that the ability of Mx1$^{+/+}$ mice to control virus growth is linked to reduced disease severity and lethality. This is consistent with earlier studies using a highly pathogenic mouse-adapted virus (6) or the 1918 pandemic strain (33). Nevertheless, because pretreatment of Mx1$^{+/+}$ mice with interferon was required for full protection, additional elements of the host response are required. We therefore used gene expression profiling to obtain a picture of the global host transcriptional response to infection under each experimental condition.

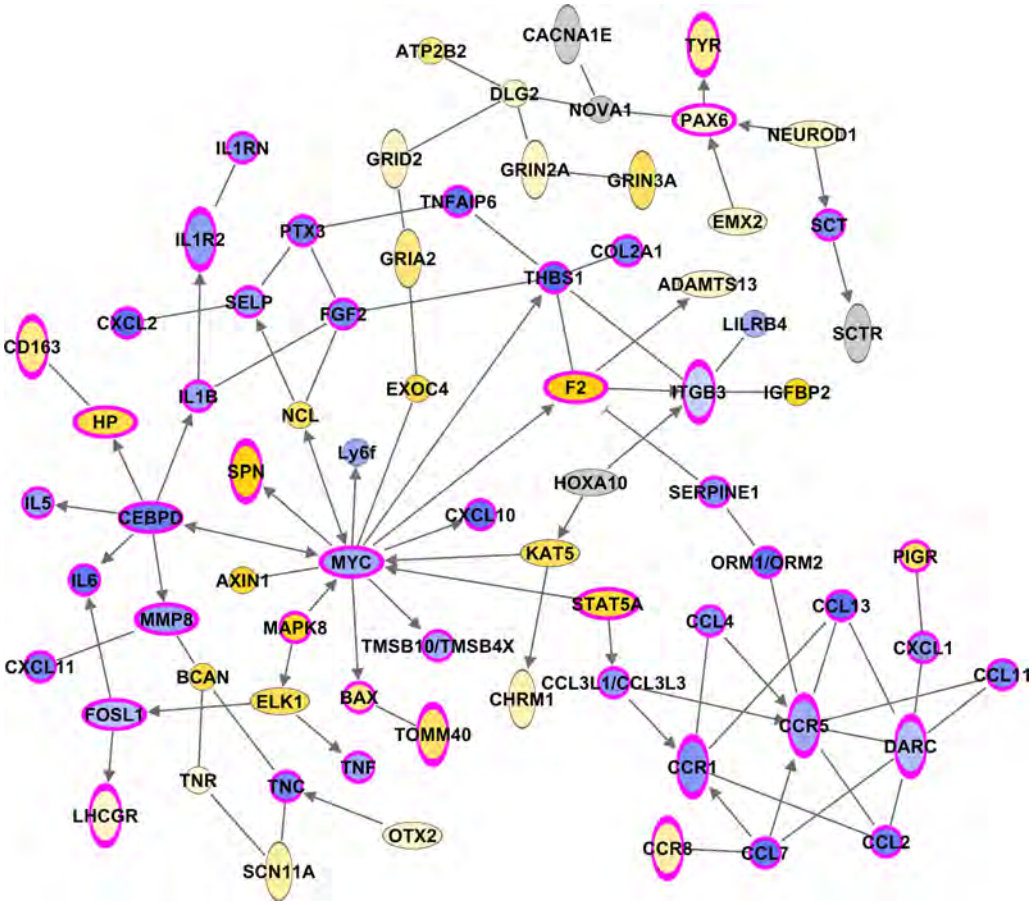

FIG 6 Molecular signature associated with complete protection of Mx1$^{+/+}$ mice. The biological network shows the direct functional relationship of genes associated with complete protection determined by IPA identified from the 2,071 differentially regulated genes. This network highlights the upregulation (yellow) and downregulation (blue) of genes in Mx1$^{+/+}$ interferon-treated mice. Genes associated with the inflammatory response are outlined in pink.

Elicited host response in untreated mice. Comparison of the transcriptional responses of Mx1$^{+/+}$ and BALB/c mice showed a striking anticorrelation in the response to 1918 virus infection. Our results suggest that under these experimental conditions, the normal interferon response is not enough to fully potentiate the protective nature of the Mx1 protein. One of the initial consequences during influenza virus infection is the rapid virus-mediated antagonism of the host innate response to avoid the generation of a strong antiviral state (8). This is accomplished by several tactics, such as inhibition of the RIG-I signaling pathway (7, 17, 19), dysregulation of gene expression (18, 23), downregulation of type I and II interferon receptor signaling (20, 24, 34), inhibition of PKR (12, 14) and OAS (14), and modulation of apoptosis (5, 13, 16, 36, 38, 39). Consequently, on one hand, the 1918 virus antagonizes the innate response, but on the other hand, Mx1 competent animals are able to partially control virus growth. This decrease in virus growth, however, was not enough to fully protect all Mx1$^{+/+}$ animals.

Our functional genomics analysis performed on lungs from 1918 virus-infected Mx1$^{+/+}$ mice allowed us to identify a specific molecular signature associated with partial protection of mice. The novelty of this finding is the altered regulation of specific acute-response components, such as genes associated with apoptosis (BCL2, BAG3, BBC3, HSPA1A, SPP1, ETS1, BTK, STAT5A, LTBR, PDIA3, HSPA5, IER3, MAPK8IP1, MNT, FKBP8, and NR1I2) and cell migration (TNFSF14, ITGA2B, MAPT, NCL, GIPC1, NRP1, PXN, CTTN, and NARS). We also observed the upregulation and direct functional relationship of genes associated with connective tissue disorders (LTB, MYO1C, SAFB, EYA2, PPT2, LIPE, and LMNB1) and genes involved in the production of reactive oxygen species in macrophages (PPP2CA, PPP2R5A, and MAP3K10). This functional signature illustrates a striking dichotomy in the gene expression profiles during the course of the experimental infection, where Mx1$^{+/+}$ mice elicited a steady upregulation of an acute-response environment that likely generated an antiviral state that partially protected the 1918 virus-infected animals.

Interferon-dependent host response is associated with complete protection. Analysis of the global transcriptional responses of interferon-treated Mx1$^{+/+}$and BALB/c mice challenged with the 1918 virus revealed a striking difference in the expression of 2,071 genes. We found that the majority of these genes were downregulated in BALB/c mice but upregulated in the Mx1$^{+/+}$ animals. Using a functional analysis approach, we identified a molecular signature associated with complete protection of Mx1$^{+/+}$ mice. The most relevant feature of this signature was the downregulation of genes involved in hypercytokinemia and hyperchemokinemia, including interleukin 6 (IL-6), IL-1β, tumor necrosis factor (TNF), CCL4, CCL12, CCR1, CCR5, CXCL10, and IL-1RN genes. These results are particularly interesting in the context of our pre-

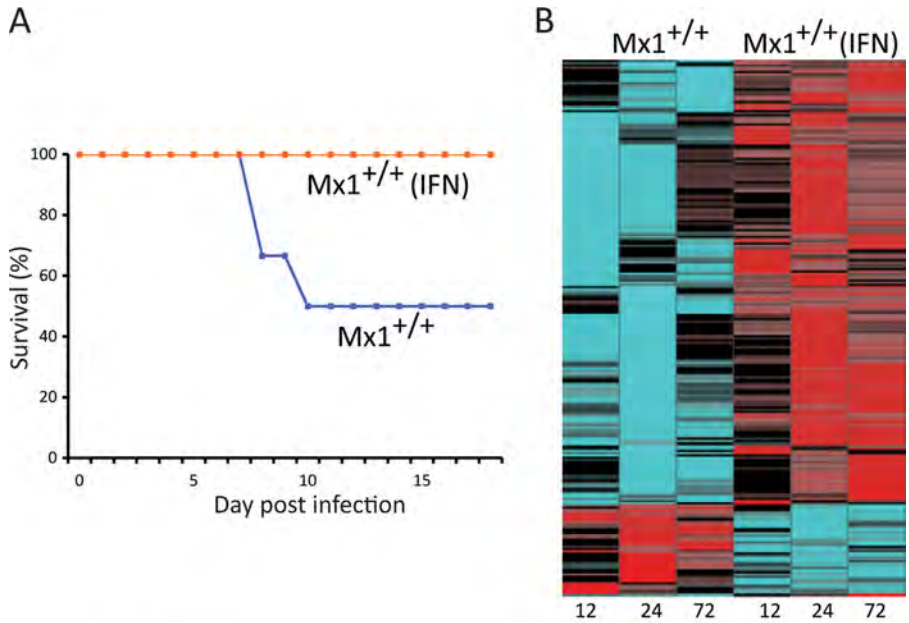

C

Biological function	P-value
Cell cycle	2.45E-14 – 6.46E-02
Cellular assembly and organization	3.29E-10 - 5.81E-02
DNA replication, recombination and repair	3.29E-10 - 5.81E-02
Cellular movement	1.15E-07 – 5.81E-02
Cellular growth and proliferation	8.43E-04 – 6.35E-02
Cellular function and maintenance	1.58E-03 - 5.81E-02
Cellular compromise	3.48E-03 - 5.81E-02
Cellular development	8.30E-03 – 6.35E-02
Cell death	1.17E-02 – 6.29E-02
Gene expression	2.44E-02 – 5.81E-02

FIG 7 Contribution of interferon to complete protection. (A) Survival plot of a total of 18 mice (9 animals/treatment). (B) Heat map illustrating 234 differentially transcribed genes that may contribute to the additional 50% difference to achieve complete protection of $Mx1^{+/+}$ treated versus $Mx1^{+/+}$ untreated animals; cutoff values were ≥2-fold change and a *P* value of ≤0.01 (ANOVA), FDR corrected. Blue indicates downregulation. Red indicates upregulation in the activation of genes. (C) Top 10 biological functions assigned to the 234 differentially regulated genes determined by IPA. The *P* values of the functional categories are shown on the right.

vious studies, where we have shown that lethal influenza virus infection of mice is associated with strong upregulation of the inflammatory response, which includes multiple cytokines and chemokines (3). These results suggest that Mx1 exerts its strongest role against influenza virus infection by targeting and downregulating an excessive cytokine response, which in mice lacking a functional Mx1 is highly upregulated to the detriment of the host.

Specific contribution of interferon treatment to survival. Our experimental approach allowed us to identify the genes responsible for complete protection that were not activated in the absence of interferon pretreatment of $Mx1^{+/+}$ mice. Functional analysis of the 234 differentially regulated genes between the treated and untreated $Mx1^{+/+}$ animals allowed us to identify a molecular signature associated with complete protection upon interferon treatment. At first glance, this functional network illustrates the upregulation of a large proportion of genes related to cell cycle regulation (CCNA1, CCNA2, CCNB1, CDK1, CKAP2, CKS2, CDC20, CDCA8, CDCA5, BIRC5, PBK, AURKB, SPAG5, MKI67, TK1, UBE2C, MYB, and BRCA1). These results suggest that complete protection of mice required the activation of a specific set of cell cycle-related genes that were downregulated in the untreated $Mx1^{+/+}$ animals, which elicited only partial protection. Our previous studies of nonhuman primates and

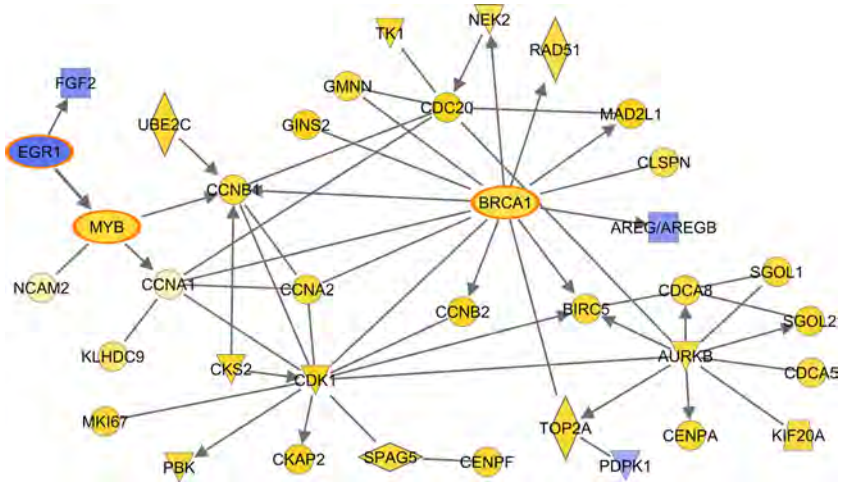

FIG 8 Molecular signature of the contribution of interferon to complete protection. The biological network shows the direct functional relationship of cell cycle regulation genes associated with the specific contribution of interferon to survival determined by PA identified from the 234 differentially regulated genes. This network highlights the upregulation (yellow) and downregulation (blue) of genes in the Mx1$^{+/+}$ interferon-treated mice.

mice infected with highly pathogenic viruses have also shown the differential regulation of cell cycle-related genes (3, 4), suggesting that this is an important mechanism for host survival during lethal influenza virus infection. This is interesting, because it has been shown that influenza virus infection induces cell cycle arrest, which promotes a favorable environment for influenza virus protein expression (10). Consequently, the activation of cell cycle regulatory genes counters this mechanism by promoting host cell proliferation. Our results depict a scenario where complete protection of the Mx1$^{+/+}$ animals was achieved only when there was sustained upregulation of genes related to apoptosis, reactive oxygen species, migration of cells, cytokines, chemokines, and the cell cycle, suggesting that modulation of

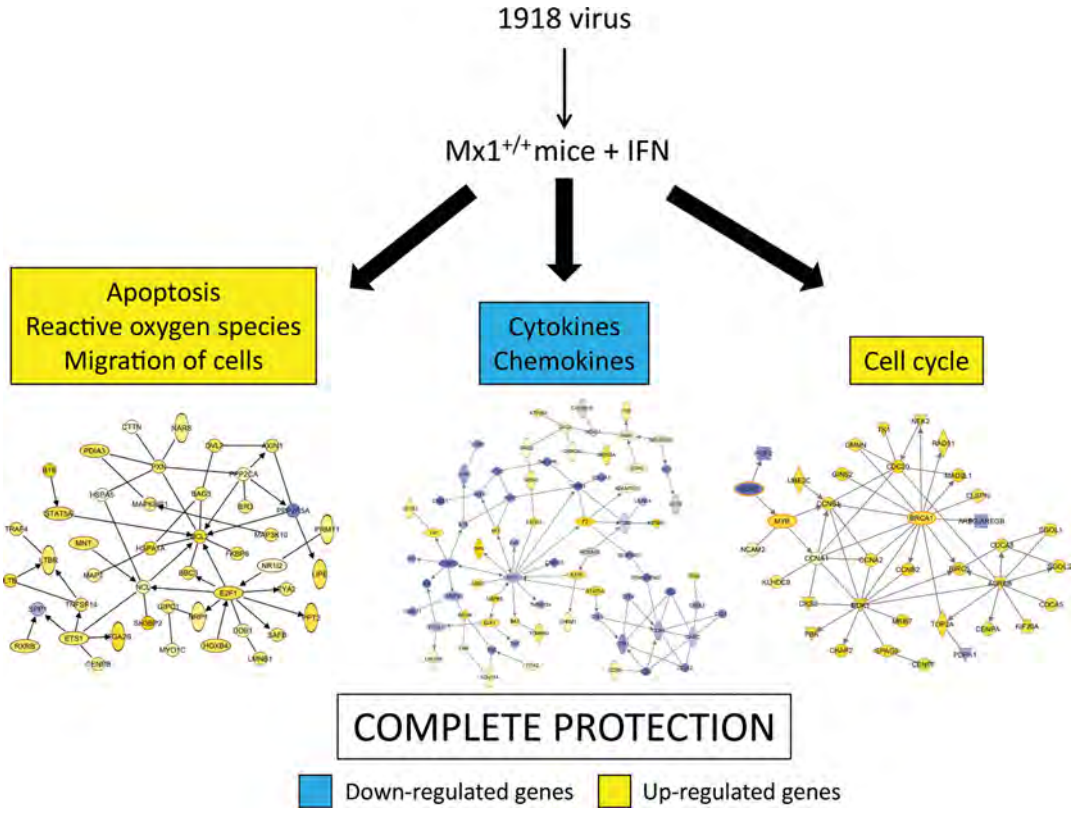

FIG 9 Model illustrating our understanding of the host response necessary for complete protection against 1918 virus infection in Mx1 competent mice pretreated with interferon. The graph depicts the events leading to complete protection of Mx1$^{+/+}$ animals under the described experimental conditions. Yellow indicates the upregulation of genes. Blue indicates the downregulation of genes.

the activities of these genes is essential for the generation of a strong antiviral state that protects all interferon-treated $Mx1^{+/+}$ mice from 1918 virus infection (Fig. 9).

In summary, our results suggest that a functional Mx1 is not sufficient to protect all mice from challenge with the fully reconstructed 1918 virus. We identified molecular signatures associated with partial protection ($Mx1^{+/+}$ mice), complete protection ($Mx1^{+/+}$ mice pretreated with interferon), and the specific contribution of interferon treatment to the host response. Partial protection of untreated mice was characterized by the generation of an acute-response environment, whereas complete protection was characterized by the downregulation of inflammatory cytokines and chemokines. The contribution of interferon to total protection in the 1918 virus-infected $Mx1^{+/+}$ mice was characterized by the differential upregulation of cell cycle-related genes in the $Mx1^{+/+}$ treated mice, which were downregulated in the absence of interferon treatment. Thus, novel therapies aimed at regulating the cytokine and chemokine environment may be of particular benefit in treating highly pathogenic influenza virus infection.

ACKNOWLEDGMENTS

This study was funded in part by Public Health Service grant P01AI058113 from the National Institute of Allergy and Infectious Diseases.

We thank Pavel Sova (Department of Microbiology, University of Washington) for helpful discussions and reviewing the manuscript.

The findings and conclusions in this report are those of the authors and do not necessarily represent the views of the funding agency.

REFERENCES

1. **Benjamini Y, Hochberg Yosef.** 1995. Controlling the false discovery rate—a practical and powerful approach to multiple testing. J. R. Stat. Soc. **57**:289–300.
2. **Chomczynski P, Sacchi N.** 1987. Single-step method of RNA isolation by acid guanidinium thiocyanate-phenol-chloroform extraction. Anal. Biochem. **162**:156–159.
3. **Cilloniz C, et al.** 2010. Lethal dissemination of H5N1 influenza virus is associated with dysregulation of inflammation and lipoxin signaling in a mouse model of infection. J. Virol. **84**:7613–7624.
4. **Cilloniz C, et al.** 2009. Lethal influenza virus infection in macaques is associated with early dysregulation of inflammatory related genes. PLoS Pathog. **5**:e1000604.
5. **Ehrhardt C, et al.** 2007. Influenza A virus NS1 protein activates the PI3K/Akt pathway to mediate antiapoptotic signaling responses. J. Virol. **81**:3058–3067.
6. **Grimm D, et al.** 2007. Replication fitness determines high virulence of influenza A virus in mice carrying functional Mx1 resistance gene. Proc. Natl. Acad. Sci. U. S. A. **104**:6806–6811.
7. **Guo Z, et al.** 2007. NS1 protein of influenza A virus inhibits the function of intracytoplasmic pathogen sensor, RIG-I. Am. J. Respir. Cell Mol. Biol. **36**:263–269.
8. **Hale BG, Albrecht RA, Garcia-Sastre A.** 2010. Innate immune evasion strategies of influenza viruses. Future Microbiol. **5**:23–41.
9. **Haller O, Frese M, Kochs G.** 1998. Mx proteins: mediators of innate resistance to RNA viruses. Rev. Sci. Tech. **17**:220–230.
10. **He Y, et al.** 2010. Influenza A virus replication induces cell cycle arrest in G0/G1 phase. J. Virol. **84**:12832–12840.
11. **Johnson NP, Mueller J.** 2002. Updating the accounts: global mortality of the 1918–1920 "Spanish" influenza pandemic. Bull. Hist. Med. **76**:105–115.
12. **Katze MG, et al.** 1988. Influenza virus regulates protein synthesis during infection by repressing autophosphorylation and activity of the cellular 68,000-Mr protein kinase. J. Virol. **62**:3710–3717.
13. **Kurokawa M, Koyama AH, Yasuoka S, Adachi A.** 1999. Influenza virus overcomes apoptosis by rapid multiplication. Int. J. Mol. Med. **3**:527–530.
14. **Li S, Min JY, Krug RM, Sen GC.** 2006. Binding of the influenza A virus NS1 protein to PKR mediates the inhibition of its activation by either PACT or double-stranded RNA. Virology **349**:13–21.
15. **Maines TR, et al.** 2005. Avian influenza (H5N1) viruses isolated from humans in Asia in 2004 exhibit increased virulence in mammals. J. Virol. **79**:11788–11800.
16. **Mao H, et al.** 2009. Influenza virus directly infects human natural killer cells and induces cell apoptosis. J. Virol. **83**:9215–9222.
17. **Mibayashi M, et al.** 2007. Inhibition of retinoic acid-inducible gene I-mediated induction of beta interferon by the NS1 protein of influenza A virus. J. Virol. **81**:514–524.
18. **Nemeroff ME, Barabino SM, Li Y, Keller W, Krug RM.** 1998. Influenza virus NS1 protein interacts with the cellular 30 kDa subunit of CPSF and inhibits 3′ end formation of cellular pre-mRNAs. Mol. Cell **1**:991–1000.
19. **Opitz B, et al.** 2007. IFNbeta induction by influenza A virus is mediated by RIG-I which is regulated by the viral NS1 protein. Cell. Microbiol. **9**:930–938.
20. **Pauli EK, et al.** 2008. Influenza A virus inhibits type I IFN signaling via NF-kappaB-dependent induction of SOCS-3 expression. PLoS Pathog. **4**:e1000196.
21. **Peiris JS, et al.** 2004. Re-emergence of fatal human influenza A subtype H5N1 disease. Lancet **363**:617–619.
22. **Perrone LA, et al.** 2009. Intranasal vaccination with 1918 influenza virus-like particles protects mice and ferrets from lethal 1918 and H5N1 influenza virus challenge. J. Virol. **83**:5726–5734.
23. **Plotch SJ, Bouloy M, Ulmanen I, Krug RM.** 1981. A unique cap(m7GpppXm)-dependent influenza virion endonuclease cleaves capped RNAs to generate the primers that initiate viral RNA transcription. Cell **23**:847–858.
24. **Pothlichet J, Chignard M, Si-Tahar M.** 2008. Cutting edge: innate immune response triggered by influenza A virus is negatively regulated by SOCS1 and SOCS3 through a RIG-I/IFNAR1-dependent pathway. J. Immunol. **180**:2034–2038.
25. **Reed LJ, Muench H.** 1938. A simple method of estimating fifty percent endpoints. Am. J. Hyg. **27**:493–497.
26. **Sadler AJ, Williams BR.** 2008. Interferon-inducible antiviral effectors. Nat. Rev. Immunol. **8**:559–568.
27. **Salomon R, et al.** 2007. Mx1 gene protects mice against the highly lethal human H5N1 influenza virus. Cell Cycle **6**:2417–2421.
28. **Staeheli P, Dreiding P, Haller O, Lindenmann J.** 1985. Polyclonal and monoclonal antibodies to the interferon-inducible protein Mx of influenza virus-resistant mice. J. Biol. Chem. **260**:1821–1825.
29. **Staeheli P, Grob R, Meier E, Sutcliffe JG, Haller O.** 1988. Influenza virus-susceptible mice carry Mx genes with a large deletion or a nonsense mutation. Mol. Cell. Biol. **8**:4518–4523.
30. **Staeheli P, Haller O, Boll W, Lindenmann J, Weissmann C.** 1986. Mx protein: constitutive expression in 3T3 cells transformed with cloned Mx cDNA confers selective resistance to influenza virus. Cell **44**:147–158.
31. **Tumpey TM, et al.** 2005. Characterization of the reconstructed 1918 Spanish influenza pandemic virus. Science **310**:77–80.
32. **Tumpey TM, et al.** 2007. A two-amino acid change in the hemagglutinin of the 1918 influenza virus abolishes transmission. Science **315**:655–659.
33. **Tumpey TM, et al.** 2007. The Mx1 gene protects mice against the pandemic 1918 and highly lethal human H5N1 influenza viruses. J. Virol. **81**:10818–10821.
34. **Uetani K, et al.** 2008. Influenza A virus abrogates IFN-gamma response in respiratory epithelial cells by disruption of the Jak/Stat pathway. Eur. J. Immunol. **38**:1559–1573.
35. **Wilson DE, Chosewood LC.** 2009. Laboratory biosafety level criteria, p 30–59. *In* Wilson DE, Chosewood LC (ed), Biosafety in microbiological and biomedical laboratories, 5th ed. Centers for Disease Control and Prevention, Atlanta, GA.
36. **Xing Z, et al.** 2009. Differential regulation of antiviral and proinflammatory cytokines and suppression of Fas-mediated apoptosis by NS1 of H9N2 avian influenza virus in chicken macrophages. J. Gen. Virol. **90**:1109–1118.
37. **Yuen KY, et al.** 1998. Clinical features and rapid viral diagnosis of human disease associated with avian influenza A H5N1 virus. Lancet **351**:467–471.
38. **Zhirnov OP, Klenk HD.** 2007. Control of apoptosis in influenza virus-infected cells by up-regulation of Akt and p53 signaling. Apoptosis **12**:1419–1432.
39. **Zhirnov OP, Konakova TE, Wolff T, Klenk HD.** 2002. NS1 protein of influenza A virus down-regulates apoptosis. J. Virol. **76**:1617–1625.
40. **Zimmermann P, Manz B, Haller O, Schwemmle M, Kochs G.** 2011. The viral nucleoprotein determines Mx sensitivity of influenza A viruses. J. Virol. **85**:8133–8140.

Vaccine 29 (2011) 6549–6557

Contents lists available at ScienceDirect

Vaccine

journal homepage: www.elsevier.com/locate/vaccine

Pekin and Muscovy ducks respond differently to vaccination with a H5N1 highly pathogenic avian influenza (HPAI) commercial inactivated vaccine

Caran Cagle[a], Thanh Long To[b], Tung Nguyen[b,c], Jamie Wasilenko[a], Sean C. Adams[d], Carol J. Cardona[d,e,1], Erica Spackman[a], David L. Suarez[a], Mary J. Pantin-Jackwood[a,*]

[a] Southeast Poultry Research Laboratory, Exotic and Emerging Avian Viral Diseases Unit, Agricultural Research Service, U.S. Department of Agriculture, 934 College Station Road, Athens, GA 30605, USA
[b] National Centre for Veterinary Diagnosis, Department of Animal Health, Hanoi, Viet Nam
[c] Graduate School, Hanoi University of Agriculture, Hanoi, Viet Nam
[d] Department of Population Health and Reproduction, University of California, Davis, CA 95616, USA
[e] Veterinary Medicine Extension, University of California, Davis, CA 95616, USA

ARTICLE INFO

Article history:
Received 24 October 2010
Received in revised form 27 June 2011
Accepted 4 July 2011
Available online 21 July 2011

Keywords:
H5N1
Avian influenza
Vaccination
Ducks
Innate immunity

ABSTRACT

Domestic ducks are key intermediates in the transmission of H5N1 highly pathogenic avian influenza (HPAI) viruses, and therefore are included in vaccination programs to control H5N1 HPAI. Although vaccination has proven effective in protecting ducks against disease, different species of domestic ducks appear to respond differently to vaccination, and shedding of the virus may still occur in clinically healthy vaccinated populations. In this study we compared the response to vaccination between two common domestic duck species, Pekin (*Anas platyrhynchos domesticus*) and Muscovy (*Cairina moschata*), which were vaccinated with a commercial inactivated vaccine using one of three different schedules in order to elicit protection to H5N1 HPAI before one month of age. Clear differences in responses to vaccination were observed; the Muscovy ducks developed lower viral antibody titers induced by the same vaccination as Pekin ducks and presented with higher morbidity and mortality after challenge with an H5N1 HPAI virus. When comparing the response to infection in non-vaccinated ducks, differences were also observed, with infected Muscovy ducks presenting a lower mean death time and more severe neurological signs than Pekin ducks. However Pekin ducks had significantly higher body temperatures and higher levels of nitric oxide in the blood at 2 days post challenge than Muscovy ducks, indicating possible differences in innate immune responses. Comparison of the expression of innate immune related genes in spleens of the non-vaccinated infected ducks showed differences including significantly higher levels of expression of RIG-I in Pekin ducks and of IL-6 in Muscovy ducks. Both duck species showed an up-regulation of IFNα and MHC-I expression, and a down-regulation of MHC-II. In conclusion, differences in response to infection and vaccination were observed between the two domestic duck species. This information should be taken into account when developing effective vaccination programs for controlling H5N1 HPAI in different species of ducks.

Published by Elsevier Ltd.

1. Introduction

Highly pathogenic avian influenza (HPAI) subtype H5N1 virus infections are constantly monitored worldwide not only because of their negative effects on poultry, but also because of spread to humans and fear of a pandemic. The H5N1 HPAI viruses are widespread in poultry in Asia and have also spread to countries in the Middle East, Europe and Africa, causing great losses to commercial poultry production resulting from high mortality in affected flocks, loss of markets, as well as costs to prevent, manage, or eradicate the viruses and disease. Ducks have been implicated in the dissemination and evolution of H5N1 HPAI viruses [1–8]. In addition to their own economic importance, domestic ducks that are in contact with wild waterfowl and poultry function as key intermediates in the transmission of avian influenza and therefore are included in vaccination programs [9].

Since 2002, a number of H5N1 HPAI viruses have been found to cause disease and death in ducks [5,6,10–14], although the level of observed pathogenicity is not consistent among different H5N1 HPAI viruses [5,11], and the age and species of the ducks appear to influence the outcome of the infection [15–18]. Host immune responses most likely play a role in the differences observed in

* Corresponding author. Tel.: +1 706 5463419; fax: +1 706 5463161.
E-mail address: mary.pantin-jackwood@ars.usda.gov (M.J. Pantin-Jackwood).
[1] Present address: Veterinary and Biomedical Sciences, University of Minnesota, Saint Paul, MN 55108, USA.

0264-410X/$ – see front matter. Published by Elsevier Ltd.
doi:10.1016/j.vaccine.2011.07.004

pathogenicity; however little is known about the immune response of ducks to AI virus infection. Vaccination has proven effective in protecting ducks against H5N1 HPAI and is being used in several countries to control the disease [19]; but virus infection may still occur in clinically healthy vaccinated populations, which may result in an endemic situation and in the emergence of antigenic variants [20]. Because of their proposed role in spreading H5N1 HPAI virus, it is of vital importance to control AI in domestic ducks. But improvement of AI control methods, including vaccination, depends on a better understanding of viral pathogenesis including host–pathogen interactions and host immune responses to infection.

Several studies have been conducted to evaluate vaccine efficacy in ducks against a HPAI virus lethal challenge [10,21–28]. Vaccine protection from infection and virus shedding varied depending on single or double-dose vaccination [26], and the challenge virus strain [21]. The majority of the published vaccine studies in ducks have been done in either Pekin (*Anas platyrhynchos domesticus*) [10,22–25] or mallard (*A. platyrhynchos*) ducks [29–31], and less research has been done using Muscovy ducks (*Cairina moschata*) [32,33], even though Muscovy ducks are economically significant as they are not only produced in Asia, but also represent 90% of the ducks hatched in France, the primary producer in Europe [33]. Vaccine efficacy studies in ducks conducted by Steensels et al. [25,32] using fowlpox-vectored AI vaccination (TROVAC AIV H5, rFP-AIV-H5) revealed oropharyngeal virus shedding in Muscovy ducks as late as 19 days post infection (dpi) while no shedding was detectable in Pekin ducks at any point after infection with the same HPAI H5N1virus. However, no research has been done comparing the responses of Pekin and Muscovy ducks to vaccination in the same study and under the same conditions.

In addition to response to vaccination, differences in virus pathogenicity among duck species have been reported. A comparison of three separate studies using either Pekin, Muscovy, or Mallard ducks all involving infection with viruses from the same H5N1 HPAI virus HA clade (2.2.1), dose, and mode of inoculation revealed differences in initial appearance of clinical signs and elapsed time to reach 100% mortality [33–35]. However, because the studies were done by different groups, multiple experiment variables could explain the differences. In a recent study, mallard and Muscovy ducks infected with different H5N1 HPAI viruses (HA clades 1, 2.3.2, and 2.3.4) showed clear differences in response to infection, with the Muscovy ducks presenting high mortality regardless of the virus given, contrary to the mortality in mallards which ranged from 0 to 100%, suggesting that Muscovy ducks are more susceptible to H5N1 HPAI virus infection [18]. Still, distinctions are not necessarily based on domestic versus wild ducks species differences. A single study comparing morbidity, mortality and viral shedding in five species of wild North American ducks with two different H5N1 HPAI viruses found only one of the five duck species became sick or died with either virus [15]. The two studies by Steensels et al. previously mentioned also showed differences in pathogenicity between Pekin and Muscovy ducks infected with the same clade 1 H5N1 HPAI virus, with only 20% of Pekin ducks presenting clinical signs compared to 100% of the Muscovy ducks [25,32].

Control of influenza virus infections in naive hosts is based on innate immunity and subsequent adaptive cytotoxic T and B cell immunity. The role of host immune elements in the control of AI virus infection in avian species is poorly understood. In addition, the potential contribution of host immune responses to the pathology observed in birds is largely undefined. Some studies have addressed individual innate immune genes expression in duck-origin cells infected with AI viruses by the use of RT-PCR assays [36,37], but studies exploring host gene expression in ducks infected with AI viruses have been very limited [38].

The purpose of this study was to compare the protection induced by vaccination against H5N1 HPAI in two types of domestic ducks, Pekin and Muscovy, using a commercially available inactivated vaccine. Three vaccine schedules were compared in order to determine which would confer the best protection before ducks were one month of age. The differences in pathogenesis and host's innate immune responses after infection with H5N1 HPAI virus were also examined. We expect to be able to explain the differences observed in the field in regards to vaccination and presentation of disease in these species of ducks.

2. Materials and methods

2.1. Virus and vaccine

The H5N1 HPAI virus A/Dk/Nam Dinh(VietNam)/NCVD-88/2007 (A/Dk/VN/88/07) (HA clade 2.3.4) was obtained from the National Center for Veterinary Diagnosis, Hanoi, Vietnam. The virus was inoculated into the allantoic cavity of 9 day-old embryonating chicken eggs and grown for 30 h at 37 °C. The allantoic fluid was harvested and frozen at −70 °C until further use. The commercially available inactivated reassortant avian influenza virus vaccine (H5N1 subtype, Re-1 Strain), produced by Harbin Veterinary Research Institute (Chinese Academy of Agricultural Sciences, Harbin, People's Republic of China) was used to vaccinate the ducks. This vaccine was produced by reverse genetics and derived it's HA and NA genes from A/Goose/Guangdong/96. This virus was attenuated by removing the multiple basic amino acids at the HA cleavage site. The six internal genes of this recombinant virus were derived from the high-growth A/Puerto Rico/8/34 (PR8) virus [39].

2.2. Duck vaccination experiment

One-day-old domestic white Pekin ducks and Muscovy ducks obtained from commercial farms were divided into groups as indicated in Table 1. Serum samples were collected from fifteen ducks of each species prior to vaccination to ensure that the birds were serologically negative for AI virus as determined by an ELISA test using IDEXX FlockChek AI MultiS-Screen (Idexx Laboratories, ME). Ducks were cared for and housed in accordance to an Institutional Animal Care and Use Committee approved animal use protocol at the Southeast Poultry Research Laboratory (SEPRL), Agricultural Research Service (ARS), United States Department of Agriculture (USDA), Athens, GA, USA. Experiments were performed in USDA-certified Biosafety Level 3-enhanced [40] facilities. Ducks had *ad libitum* access to feed and water.

Groups of ten ducks each were vaccinated subcutaneously in the nape of the neck with the recommended dose of Re-1 vaccine (0.2 ml of vaccine for the 1 day and 7 days-old ducks, and 0.5 ml for the 14 and 21 days-old ducks) following one of three different schedules (Table 1). Ten ducks were vaccinated at one day of age and at 14 days of age; ten only at 14 days of age, and ten at 7 and 21 days of age. Ten Pekin ducks and ten Muscovy ducks served as non-vaccinated infected controls and four Pekin and four Muscovy ducks served as non-vaccinated non-infected (sham inoculated) controls. At thirty days of age, blood samples were collected from all ducks for serology. At this same time, ducks from all vaccine schedules, including non-vaccinated controls were challenged intranasally via the choanal slit with $10^{5.0}$ EID_{50} of A/Dk/VN/88/07 H5N1 HPAI virus in 0.1 ml. Ducks were observed daily for clinical signs of disease. Oropharyngeal and cloacal swabs were collected at 3, 5, 7, 9, and 12 days post challenge (dpch) to quantify viral shedding. At 2 dpch body temperatures were taken from all ducks using a rectal thermometer. One-way ANOVA with Tukey's post-test was used to analyze body temperatures using Prism v.5.01

Table 1
Morbidity and mortality. Pekin and Muscovy ducks were vaccinated with an inactivated AI vaccine following three different schedules. Ducks were intranasally challenged at 30 days of age with 10^5 EID_{50} of A/Dk/VN/88/07 H5N1 HPAI (clade 2.3.4) virus.

Groups	Number of ducks with neurological signs/total ducks	Number of dead ducks/total ducks	Mean death time (days)
Pekin vaccinated at 1 and 14 days of age	2/8	1/8	6.0
Pekin vaccinated at 14 days of age	2/8	1/8	6.0
Pekin vaccinated at 7 and 21 days of age	0/8	0/8	–
Pekin not vaccinated, not challenged	0/4	0/4	–
Pekin not vaccinated, challenged	6/6	6/6	3.6
Muscovy vaccinated at 1 and 14 days of age	5/8	3/8	5.0
Muscovy vaccinated at 14 days of age	4/8	2/8	7.0
Muscovy vaccinated at 7 and 21 days of age	0/8	0/8	–
Muscovy not vaccinated, not challenged	0/4	0/4	–
Muscovy not vaccinated, challenged	6/6	6/6	3.1

software (GraphPad Software Inc.). Statistical significance was set at $P < 0.05$.

Blood samples were collected at 2 dpch from all four of the non-vaccinated non-infected groups and from four ducks from the non-vaccinated infected groups. The same ducks were then euthanized with 0.5 ml sodium pentobarbital (5 g/ml) per bird, and spleens collected and frozen immediately at −70 °C for subsequent use in cytokine detection by quantitative real-time RT-PCR. Moribund ducks, in pain, or that were unable to reach food or water during the experiment, were also euthanized. Blood samples were collected at 12 dpch from all surviving ducks and the experiment was terminated at this time when the remaining ducks were euthanized.

2.3. Serology

Hemagglutination inhibition (HI) assays were performed as previously described [41] to quantify antibody responses to vaccination, with serum collected from vaccinated ducks immediately before virus challenge and 12 days after challenge. Beta-propiolactone-inactivated antigen (Ag) made from either a virus with a similar HA to the recombinant vaccine virus (Goose/Hong Kong/437-6/99) or the challenge virus (A/Dk/VN/88/07) was used in the test. HI titers were reported as $\log_2$ titers, with 3 $\log_2$ titers being the minimum positive titer. A one-way ANOVA with Tukey's post-test was used to analyze HI titers using Prism v.5.01 software (GraphPad Software Inc.). Statistical significance was set at $P < 0.05$.

2.4. Determination of virus shedding

Oropharyngeal and cloacal swab samples collected from the ducks were suspended in 2 ml sterile brain heart infusion (BHI) broth containing an antibiotic/antimycotic mixture, and frozen at −70 °C until RNA extraction. RNA was extracted using a previously described combination of Trizol LS reagent (Invitrogen Inc., Carlsbad, CA) and the MagMax AI/ND RNA isolation kit (Ambion, Inc., Austin, TX)[42]. Quantitative real-time RT-PCR (qRRT-PCR) targeting the influenza M gene [43] was performed using the SmartCycler® 2 (Cepheid Inc., Sunnyvale, CA) and the OneStep RT-PCR kit (Qiagen, Valencia, CA) in accordance with the U.S. National Veterinary Services Laboratories protocol AVSOP1521.01. A standard curve for virus quantification was established with RNA extracted from dilutions of the same titrated stock of the challenge virus, and results reported as EID_{50}/ml equivalents [21]. The calculated qRRT-PCR detection limit was 10^2 EID_{50}/ml per reaction.

2.5. RNA extraction from spleens

Approximately 100 g of the collected spleens was normalized by weight and homogenized in BHI medium. Total RNA was extracted from spleen homogenates using the Qiagen RNeasy midi prep kit (Qiagen, Valencia, CA) according to the manufacturers' instructions. RNA integrity (RIN) numbers were measured with the Bioanalyzer 2100 (Agilent Technologies, Santa Clara, CA) and were between 7.5 and 10. RNA concentrations from the four individual birds per group were determined using a Nanodrop ND-1000 Spectrophotometer (Nanodrop Technologies, Wilmington, DE). To eliminate possible contamination with genomic DNA, 100 μg of RNA from each sample was treated with on column DNase digestion (RNase-Free DNase Set; Qiagen, Valencia, CA) in the Qiagen RNeasy mini prep kit (Qiagen, Valencia, CA) for 15 min at room temperature.

2.6. Quantitative real-time RT-PCR

The relative quantitation in gene expression following infection was performed using primers designed by Lasergene 7.0 primer select software (DNAstar, Madison, WI). Interferon alpha (IFN-α), major histocompatibility complex class I (MHC-I) and class II (MHC-II) primer design was based on published GenBank sequences (Table 2). Primers for interleukin 6 (IL-6), retinoic acid inducible gene (RIG-I) and β-actin were reported previously. Primer pair specificity among duck species for each pair was determined by dissociation curves, and primer validation for all primer sets was done according to Applied Biosystems recommendations (Applied Biosystems, CA) and MIQE guidelines [44]. In addition, PCR products were cloned into pCR-TOPO2.1 sub-cloning vectors (Invitrogen, Carlsbad, CA) and sequenced in order to confirm correct target amplification. Sequence identity between species of the products amplified was >95% for the cytokines examined. β-Actin and glyceraldehyde 3 phosphate dehydrogenase (GAPDH) were investigated as possible endogenous controls, but sequence differences among these duck species in the GAPDH prevented its use. However, β-actin sequences had >99% identity between the two duck species and invariant expression in both controls (non-vaccinated non-infected ducks) and experimental groups.

Amplification and detection of specific products was performed using the Applied Biosystems 7500 Fast Real-Time PCR System (Applied Biosystems, CA). Total RNA extracted from spleen homogenates from four individual ducks from the non-vaccinated infected groups and from four ducks from the non-vaccinated non-infected groups was used in the reactions. Reactions were done in triplicate using the Power SYBR® Green RNA-to-C_T™ 1-Step Kit (Applied Biosystems, CA) and 50 ng of total RNA per reaction. qRRT-PCR conditions and cycling parameters were the same for all primer pairs used and were as follows: one cycle at 50 °C for 30 min, one cycle at 95 °C for 15 min, 40 cycles of 95 °C for 15 s and 58 °C for 32 s followed by dissociation curve determination of the products with one cycle at 95 °C for 15 s, 55 °C for 20 s, 99 °C for 15 s and 60 °C for 15 s. Expression fold change was determined by the $2^{-\Delta\Delta Ct}$ method using β-actin as the endogenous reference gene to normalize the level of target gene expression. The Student's *t*-test

Table 2
Primers sequences used in quantitative RRT-PCR.

Target	Forward primer	Reverse primer	Source
IFN-α	gggccccgcaacctt	ctgtaggtgtggttctggaggaa	DQ861429
IL6	ttcgacgaggagaaatgctt	ccttatcgtcgttgccagat	[36]
RIG-1	gtgtatggaggaaaaccctatttctt	ggagggtcatacctgttgtttgat	[50]
MHC-I	cccactccctgcgctatttctaca	cctccccatccacataccccacac	AB115246
MHC-II	tggatgaagaacgggcaggag	ggatgaagggcaggtaggagaact	AY905539
β-Actin	cccccgtgctgtgttcccatctatcg	gggtgctcctcaggggctactctcac	[38]

(GraphPad Prism) was used to determine the statistical significance between fold change values of the two duck species. Statistical significance was set at $P < 0.05$.

An estimate of virus titers in spleen was also determined for infected Pekin and Muscovy ducks by real-time RT-PCR. This was done to examine if differences in virus replication in the spleen could affect the cytokine gene expression results. RNA (50 ng/μl) from all duck samples previously used in the qRRT-PCR assay was run with a test targeting the influenza A matrix gene [43]. All reactions were run in triplicate with ABI PRISM 7500 using Power SYBR Green RNA-to-C_T 1-Step Kit (Applied Biosystems, CA) for 1 cycle at 95 °C for 10 min, 45 cycles of 95 °C for 1 s and 57 °C for 30 s. Viral titers among Pekin and Muscovy ducks were determined by comparing input RNA:*C*t ratio.

2.7. Nitric oxide assay

Total nitrate and nitrite content produced by nitric oxide synthase (NOS) were measured in serum samples collected at 2 dpch from four ducks from the non-vaccinated, infected groups and four ducks from the non-vaccinated, non-infected groups. Sera were passed through a 10 kDa ultrafilter (Millipore Corp., Billerica, MA) prior to analysis. Total protein in the filtered sera was measured using a DC Protein Assay (Bio-Rad, Hercules, CA). A Nitric Oxide Synthase Assay kit (Calbiochem, Gibbstown, NJ) was used according to the manufacturer's specifications on 40 μL of filtered serum. Values were normalized to the total protein in the filtered sera.

3. Results

3.1. Morbidity, mortality and clinical signs

All non-vaccinated ducks infected with the H5N1 HPAI virus died in less than 4 days (Table 1). Similar high mortality in ducks has been previously reported with HA clade 2.3.4 H5N1 HPAI viruses from Vietnam [13,21]. Muscovy ducks presented with more severe neurological signs and had a lower mean death times than the Pekin ducks. Most vaccinated ducks survived the virus challenge; however almost all presented with mild clinical signs consisting of conjunctivitis, anorexia, and mild lethargy. Nine of the vaccinated infected Muscovy ducks and four of the vaccinated infected Pekin ducks had mild to severe neurological signs. Of these, five of the Muscovy ducks and two of the Pekin ducks had such severe neurological signs that the ducks died or had to be euthanized. By 12 dpch most surviving ducks had recovered, with the exception of two Muscovy ducks and one Pekin duck which still presented mild neurological signs. Based on the morbidity and mortality results for both duck species, the best vaccination schedule was a prime at 7 days old followed by a boost at 21 days of age. Ducks vaccinated on this schedule did not present neurological signs or mortality. Vaccinating the ducks twice, at day of age and at 14 days of age, did not confer better protection than vaccinating only at 14 days of age.

3.2. Body temperatures

Body temperatures of non-vaccinated infected Pekin ducks were significantly higher ($P < 0.05$) than the non-vaccinated infected Muscovy ducks at 2 dpch (Fig. 1). Body temperatures were significantly lower in vaccinated infected ducks compared to non-vaccinated infected ducks regardless of the duck species, with the exception of the Muscovy ducks vaccinated at 7 and 21 days of age, where temperatures were not statistically different than infected Muscovy ducks.

3.3. Hemagglutination inhibition titers

Testing for H5 antibodies was conducted using HI assays on serum. Mean HI titers ($\log_2$) are shown in Fig. 2. The highest pre-challenge HI titers, when using the vaccine-like virus in the test (homologous virus), in both Pekin and Muscovy ducks, were found in the group of ducks vaccinated at 7 and 21 days of age; however the titers were not in all cases significantly different from the other groups. When the test was run using the challenge virus (heterologous virus) no positive HI titers were detected ($\geq 3 \log_2$ titers considered positive). Interestingly, Pekin ducks had higher antibody titers than Muscovy ducks regardless of the vaccination schedule used. High post-challenge HI titers (mean $>9 \log_2$) were observed in all groups of vaccinated ducks when using the vaccine virus in the test. HI titers were lower when using the challenge virus in the test ($>6 \log_2$) and were similar in all groups except for the Pekin ducks vaccinated at 7 and 21 days of age which had lower titers than all. Differences in HI titers when using a heterologous virus to run the HI test have been previously reported [21]. However in previous studies as in ours, ducks were still protected in spite of the low HI titers observed when using the challenge virus as antigen in the HI test, indicating cross protection between the vaccine virus and the challenge virus.

3.4. Virus shedding

Differences were observed between Pekin and Muscovy ducks relative to the number of ducks shedding and duration of virus shedding (Table 3). Virus shedding was detected from both the oropharyngeal and cloacal routes from all non-vaccinated infected Pekin and Muscovy ducks at 3 dpch. All but one vaccinated infected Muscovy duck shed virus through both routes at 3 dpch, in contrast to the vaccinated Pekin ducks of which only one to four ducks per group were shedding virus through the oropharynx and none shed cloacally. At 5 dpch, two to five Muscovy ducks per group were shedding virus, especially through the oropharyngeal route, compared to none to two Pekin ducks per group. Virus was detected in swabs from two Muscovy ducks at 7 and 12 dpch, and from two Pekin ducks at 7 dpch. Minimal difference in the total of ducks shedding was observed when comparing the different vaccination schedules in each duck species. Titers of the virus were highest in the oropharyngeal swabs at 3 and 5 dpch in Muscovy ducks, and at 3 dpch in Pekin ducks.

3.5. Innate immune-related host genes expression

Quantitative real-time RT-PCR (qRRT-PCR) results showed similar trends of up- or down-regulation of innate immune related genes in spleens collected from non-vaccinated, infected Pekin and

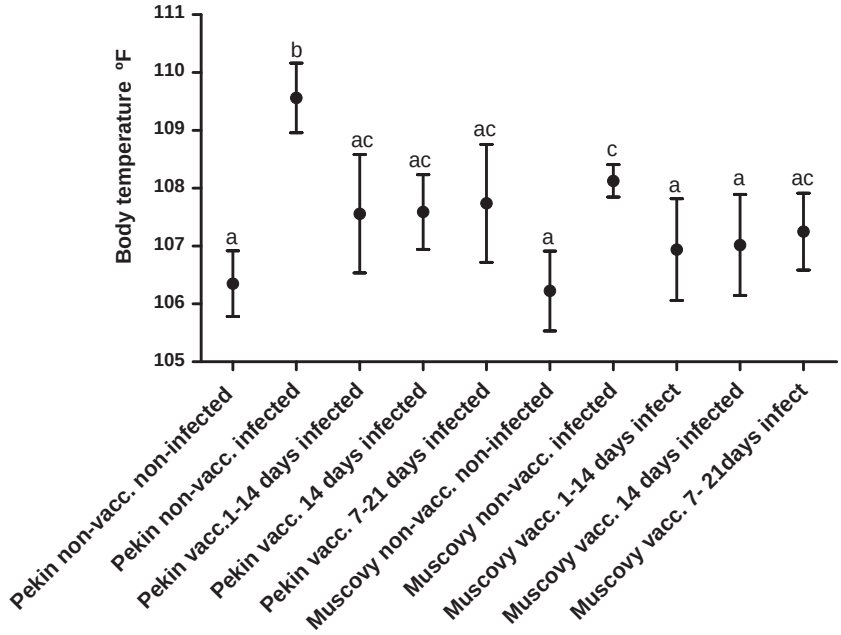

Fig. 1. Body temperatures of Pekin and Muscovy ducks after infection with a H5N1 HPAI virus compared to non-infected ducks; 2 days after challenge. The bars represent the mean and standard deviation. Groups with different lowercase letters are significantly different ($P < 0.05$).

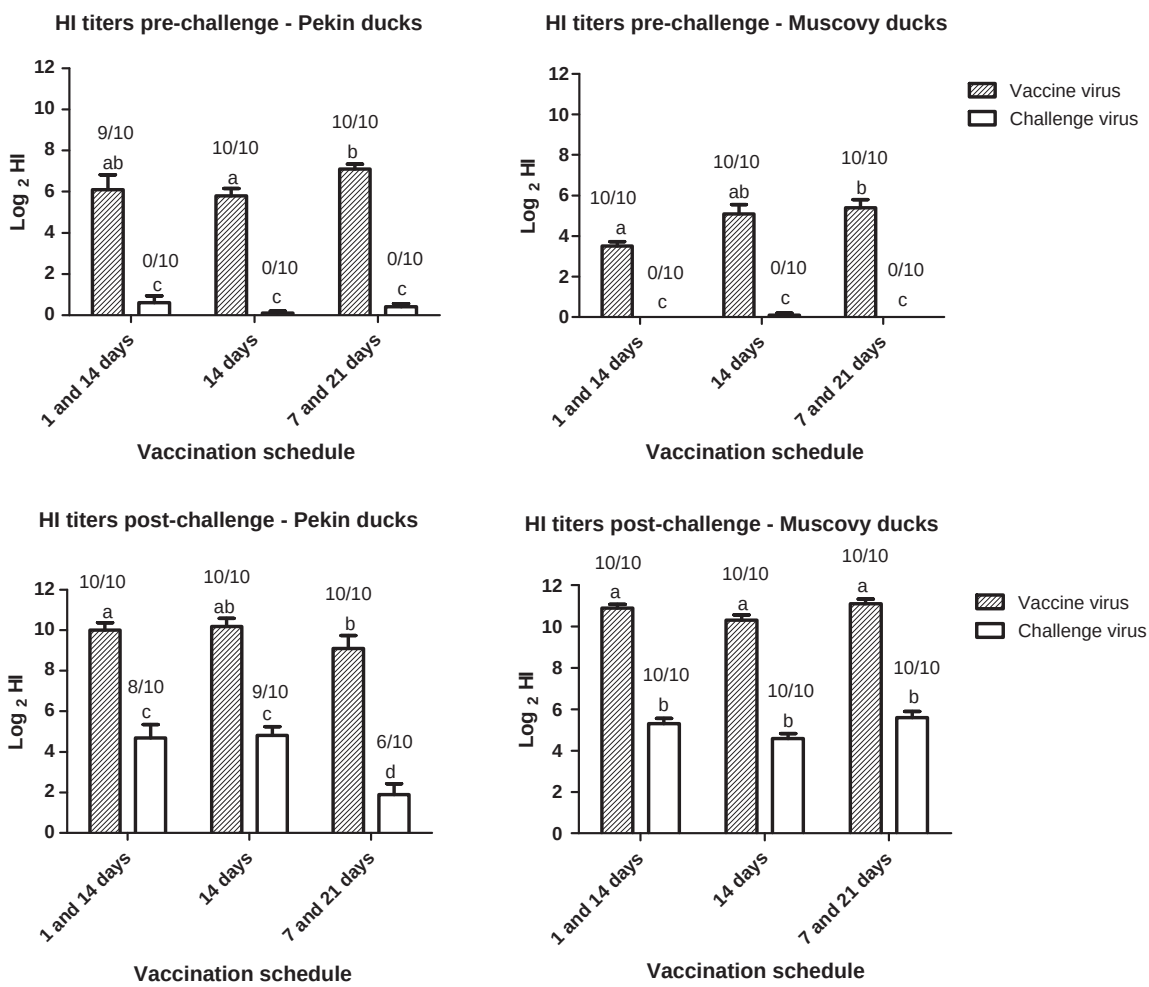

Fig. 2. Mean HI titers ($\log_2$) in vaccinated Pekin and Muscovy ducks. Ducks were vaccinated with an inactivated commercial vaccine following one of three different schedules: ten ducks were vaccinated at one day of age and at 14 days of age, ten at 14 days of age, and ten at 7 and 21 days of age. Serum samples were taken at 30 days of age, when ducks were challenged with A/Dk/VN/88/07 H5N1 HPAI virus, and at 12 days post-challenge. HI titers were obtained using a virus similar to the vaccine or the challenge virus as antigen in the test. The number of ducks with positive HI titers is shown ($\geq$ threshold of positivity/total number of sera tested). Different lowercase letters indicate significant differences in HI titers ($P < 0.05$) between the vaccination schedules when using either antigen. Bars represent standard error of the mean.

Table 3
Virus shedding. Pekin and Muscovy ducks were vaccinated with an inactivated AI vaccine and intranasally challenged at 30 days of age with 10^5 EID_{50} of A/Dk/VN/88/07 H5N1 HPAI virus.

Groups	Virus titers from swabs collected at different days after challenge No. of positive ducks/total ducks[a] (EID_{50} equivalents)[b]									
	Day 3		Day 5		Day 7		Day 9		Day 12	
	Oral	Cloacal	Oral	Cloacal	Oral	Cloacal	Oral	Cloacal	Oral	Cloacal
Pekin vaccinated at 1 and 14 days	4/10 (5.0)	0/10	2/8 (2.7)	0/8	0/7	0/7	0/7	0/7	0/7	0/7
Pekin vaccinated at 14 days	3/10 (5.0)	0/10	0/8	0/8	2/8 (<2.0)	0/7	0/7	0/7	0/7	0/7
Pekin vaccinated at 7 and 21 days	1/10 (3.7)	0/10	2/8 (3.7)	2/8 (2.7)	0/8	0/8	0/8	0/8	0/8	0/8
Pekin non-vaccinated	4/4 (5.9)	4/4 (2.7)	–	–	–	–	–	–	–	–
Muscovy vaccinated at 1 and 14 days	10/10 (5.5)	10/10 (4.5)	2/8 (5.7)	1/8 (5.0)	0/5	0/5	0/5	0/5	0/5	0/5
Muscovy vaccinated at 14 days	10/10 (6.6)	10/10 (5.0)	5/8 (4.7)	2/8 (2.7)	1/8 (4.0)	1/8 (2.7)	0/6	0/6	1/6 (<2.0)	0/6
Muscovy vaccinated at 7 and 21 days	10/10 (5.25)	9/10 (4.1)	3/8 (4.0)	1/8 (2.7)	0/8	1/8 (<2.0)	0/8	0/8	0/8	1/8 (<2.0)
Muscovy non-vaccinated	3/3 (7.0)	3/3 (5.5)	–	–	–	–	–	–	–	–

–, not applicable.
[a] Swab samples were taken from all birds remaining at each time point post challenge.
[b] Log EID_{50}-equivalents were determined using real-time RT-PCR specific for type A avian influenza matrix gene [43]. Numbers in parentheses are averages of viral titers shed from birds in each group.

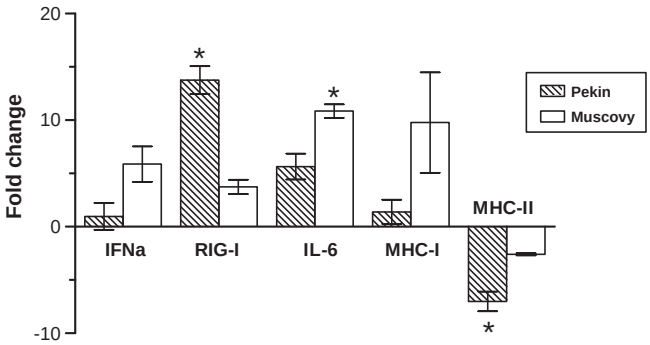

Fig. 3. Changes in expression of IFNα, RIG-I, IL-6, MHC-I and MHC-II genes in spleens of Pekin and Muscovy ducks infected with A/Dk/VN/88/07 H5N1 HPAI virus at 2 dpi. Changes were quantified by qRRT-PCR and expressed as fold change in the birds infected ($n = 4$) compared with non-infected birds ($n = 4$). Bars represent standard error of the mean. Asterisk indicates significant difference in gene expression ($P < 0.05$) between Pekin and Muscovy ducks.

Muscovy ducks when compared to non-vaccinated non-infected controls. INFα, RIG-I, IL-6, and MHC-I were all up-regulated, while MHC-II was down-regulated in both challenged Pekin and Muscovy ducks. Statistical differences were detected between Pekin and Muscovy ducks for RIG-I, IL-6, and MHC-II. RIG-I was up-regulated 13-fold in Pekin ducks, but only 3-fold in Muscovy ducks, but IL-6 expression was more up-regulated in Muscovy ducks, 10-fold compared to 5-fold in Pekin ducks. MHC-II gene expression was significantly more down-regulated in Pekin ducks compared to the Muscovy ducks (Fig. 3).

RRT-PCR for virus detection was also done on spleens from infected ducks. Ratio comparison (input RNA:CT) between Pekin and Muscovy ducks using RNA extracted from spleens from infected ducks indicated a similar level of virus presence in the spleen of the Muscovy ducks (2.30) when compared to the Pekin ducks (2.16), and the small difference was not found to be statistically significant (data not shown).

3.6. Nitric oxide levels in serum

Total nitrate and nitrite content produced by NOS measured in serum samples from non-vaccinated infected ducks when compared to non-vaccinated non-infected controls showed a significant increase in infected Pekin ducks, while infected Muscovy ducks had a marginal, non-significant increase (Fig. 4). No statistical difference was observed between infected Pekin and Muscovy ducks.

4. Discussion

In a previous study, 7-day-old Pekin ducks were vaccinated against H5N1 HPAI virus to determine if vaccination at this age would induce good protection [21]. Interference of maternally-derived antibodies with protection elicited by avian influenza inactivated vaccines has been reported in poultry [45–47], and with increased vaccination of domestic ducks, day-old ducks would likely have maternal antibodies that, although providing some protection could also interfere with vaccine efficacy. Vaccination at 7 days of age would help minimize the maternal antibody interference so the ducks would still be able to acquire early immunity. Vaccination at this age, although conferring good protection against disease, did not stop virus shedding, and in certain cases, the ducks shed viruses for more than five days [21]. In order to explore other alternatives for the efficient vaccination of ducks, in the present study we used three different vaccination schedules to immunize domestic ducks against H5N1 HPAI virus, two of which involved two doses of a commercial inactivated vaccine, given at 1 and 14 days of age or 7 and 21 days of age, and a third schedule using one dose given at 14 days of age. Based on the morbidity and mortality

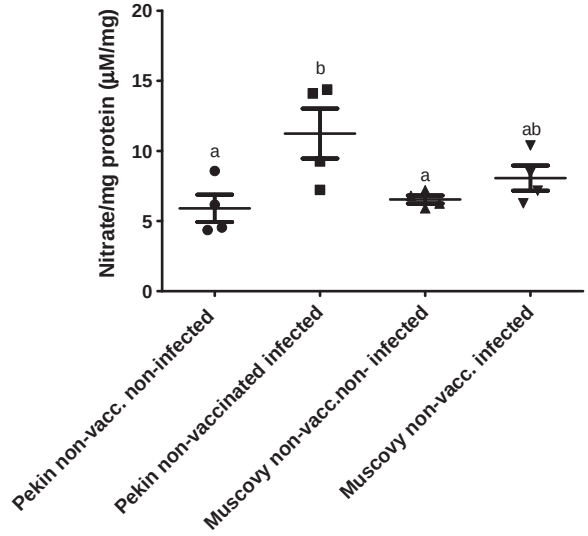

Fig. 4. Total nitrate and nitrite content produced by NOS, measured in serum samples from 4 ducks from infected and non-infected groups at 2 days post challenge and normalized to the total protein in the filtered sera. The lines represent the mean and standard error of the mean. Different lowercase letters indicate significant differences of means ($P < 0.05$).

results, the option that conferred the best protection for both the Pekin and the Muscovy ducks was to vaccinate at 7 days followed by a boost at 21 days of age. Vaccinating ducks at one day of age followed by a boost at 14 days of age did not protect the ducks any better than vaccinating only at 14 days of age. The rationale for vaccinating at day of age would be to induce early protection in ducklings that for some reason had acquired low levels of maternal antibodies. In this study, since the ducks were free of maternal antibodies, better protection was expected by vaccinating at 1 and 14 days of age than only vaccinating at 14 days of age, which was not seen. A reason for this could be the immaturity of the immune system of the ducks at day of age that would have prevented an adequate immune response [48]. The pre-challenge HI titers of the ducks vaccinated at 7 and 21 days of age compared to the other two vaccination schedules was not in all cases significantly higher, which does not correlate with the better protection that this schedule conferred. However, protection in vaccinated ducks may also be due to a priming of duck secretory or mucosal immunoglobulins, or cell mediated immunity [48,49], which were not examined in this study and could explain these results.

It has been reported that in field conditions Muscovy ducks do not respond the same to vaccination as other domestic ducks do (personal communication, Dr. Tung Nguyen). The results of this study confirm that Muscovy ducks indeed do not respond as well as Pekin ducks to vaccination, showing lower pre-challenge antibody titers, and higher morbidity and mortality and virus shedding after virus challenge. Consequently a different vaccination program must be considered when vaccinating Muscovy ducks and perhaps different vaccine formulations need to be used.

Previous studies have shown that the pathogenicity of H5N1 HPAI viruses in ducks directly correlates with the extent of virus replication in tissues, with the more pathogenic viruses replicating in more tissues and to higher titers [11,13,18]. The H5N1 HPAI virus used in this study was very virulent for both Pekin and Muscovy ducks; however Muscovy ducks presented with more severe neurological signs, had a lower MDT and shed more virus than the Pekin ducks, indicating that Muscovy ducks are more susceptible to infection with H5N1 HPAI viruses. This confirms results from previous studies and observations from field situations [18,25,32]. In addition, body temperatures of non-vaccinated infected ducks measured two days after virus infection were higher in Pekin ducks than in Muscovy ducks, suggesting possible differences in pro-inflammatory responses between these duck species. Gene expression results of RIG-I, IL-6, MHC-I, MHC-II, and INFα obtained by quantitative RRT-PCR on splenic tissues of infected ducks compared to non-infected controls support this idea. RIG-I, a cytoplasmic 5′ppp RNA sensor found in ducks but not chickens, initiates expression of other antiviral genes [50–52]. RIG-I expression in 6-week-old mallard ducks after infection with H5N1 was greatly induced, but expression levels varied depending on the time after infection [50]. Up-regulation of RIG-I was also observed in both duck species tested here, but was significantly higher in Pekin ducks when compared to Muscovy ducks which may partly contribute to a more efficient viral recognition after infection, and consequently a stronger innate immune response.

Traditionally, antiviral activity and the innate immune response are associated with increased levels of type I interferon (IFNα) and the involvement of macrophages through the induction of pro-inflammatory cytokines like IL-6 at the site of infection, and MHC molecules presenting processed antigen and consequently increased specific immunity by activation of B and T cells. Previous studies confirmed IFNα and IL-6 induction after infection with LPAI virus in duck peripheral blood mononuclear cells (PBMC) [36] and in chickens infected with a H5N1 HPAI virus [53,54]. Our results also show IFNα and IL-6 up-regulation in both duck species, with IL-6 levels significantly higher in the Muscovy ducks. Induction of high levels of proinflammatory cytokines in mammals infected with H5N1 viruses has been hypothesized to contribute to the severity of pathological changes and death [55]. The role of cytokines in the pathogenesis of H5N1HPAI viruses in avian species is less well understood. A quick and intensive production of proinflammatory cytokines, including IL-6, was observed in chickens infected with H5N1 HPAI viruses [54]. The higher levels of IL-6 expression observed in the Muscovy ducks could be related to the more severe clinical signs observed in these ducks when compared to the Pekin ducks. Furthermore, we noted the inverse expression of MHC molecules in both duck species where MHC I expression increased, while MHC II expression decreased. Again, this result mirrors a similar gene expression pattern with MHC molecules observed in a previous study [36]. All immune related genes tested here showed similar trends in up- or down-regulation in both Pekin and Muscovy ducks; however, the extent of each fold change was species dependent. Future studies will need to address this distinction at multiple time points after infection in order to determine if differences exist throughout the duration of the viral infection.

The higher body temperatures observed in the infected Pekin ducks in this study not only suggest differences in innate immune response between duck species, but also offers insight into the febrile response in birds. Prior studies in Pekin ducks indicated lipopolysaccharide (LPS)-induced fever is in part mediated by NO [56]. Levels of NO were elevated in Pekin ducks infected with a H5N1 HPAI virus when compared to uninfected ducks [57]. Enzymes of the nitric oxide synthase (NOS) family such as the inducible form of NOS (iNOS) generate NO, which serves as a potent anti-viral molecule to combat infection in combination with acute phase proteins and cytokines [57]. Numerous cytokines also stimulate NO expression (either directly or indirectly) and the effective component and/or component combination is cell and species dependent [58]. Results of the NO assay presented in this study show a higher increase of NO levels in serum in infected Pekin ducks than in Muscovy ducks, which correlates also with the increase in body temperatures observed. This could explain in part the higher susceptibility to infection in Muscovy ducks and further supports the possibility that immune response differences may be attributed to a difference in innate immunity between different duck species.

In conclusion, the best protection was conferred by vaccination at 7 and 21 days of age for both Pekin and Muscovy ducks. Higher pre-challenge antibody titers, no mortality and no neurological signs were observed in these groups; however some ducks still presented mild clinical signs and virus shedding was still observed, especially in the Muscovy ducks. Furthermore, differences in body temperature, immune-related host gene and nitric oxide expression in non-vaccinated infected ducks indicate differences in the host innate immune response which consequently affects the adaptive immune responses. When assessing vaccine efficacy in field settings, strategies that account for differences between duck species will need to be implemented. Based on these results, even if ducks have been vaccinated and received a follow-up boost, mild disease and shedding of infectious virus may still occur. Better matching of vaccines with circulating viruses, and optimized vaccines and vaccination programs should improve the results of influenza immunization in ducks.

Acknowledgments

The authors would like to thank Diane Smith and Scott Lee for excellent technical support and also Ronald Graham and Roger Brock for providing care to the animals. This study was supported by a Specific Cooperative Agreement with the Foreign Agriculture Service of the USDA, and the Agriculture Research Service CRIS Project 6612-32000-048. Mention of trade names or commercial products

in this publication is solely for the purpose of providing specific information and does not imply recommendation or endorsement by the U.S. Department of Agriculture. USDA is an equal opportunity provider and employer.

References

[1] Songserm T, Jam-on R, Sae-Heng N, Meemak N, Hulse-Post DJ, Sturm-Ramirez KM, et al. Domestic ducks and H5N1 influenza epidemic, Thailand. Emerg Infect Dis 2006;12(4):575–81.

[2] Henning J, Henning KA, Morton JM, Long NT, Ha NT, Vu LT, et al. Highly pathogenic avian influenza (H5N1) in ducks and in-contact chickens in backyard and smallholder commercial duck farms in Viet Nam. Prev Vet Med 2010 [June 29].

[3] Henning J, Wibawa H, Morton J, Usman TB, Junaidi A, Meers J. Scavenging ducks and transmission of highly pathogenic avian influenza, Java, Indonesia. Emerg Infect Dis 2010;16(August (8)):1244–50.

[4] Chen H, Deng G, Li Z, Tian G, Li Y, Jiao P, et al. The evolution of H5N1 influenza viruses in ducks in southern China. Proc Natl Acad Sci USA 2004;101(July (28)):10452–7.

[5] Hulse-Post DJ, Sturm-Ramirez KM, Humberd J, Seiler P, Govorkova EA, Krauss S, et al. Role of domestic ducks in the propagation and biological evolution of highly pathogenic H5N1 influenza viruses in Asia. Proc Natl Acad Sci USA 2005;102(July (30)):10682–7.

[6] Sturm-Ramirez KM, Hulse-Post DJ, Govorkova EA, Humberd J, Seiler P, Puthavathana P, et al. Are ducks contributing to the endemicity of highly pathogenic H5N1 influenza virus in Asia? J Virol 2005;79(September (17)):11269–79.

[7] Ellis TM, Bousfield RB, Bissett LA, Dyrting KC, Luk GS, Tsim ST, et al. Investigation of outbreaks of highly pathogenic H5N1 avian influenza in waterfowl and wild birds in Hong Kong in late 2002. Avian Pathol 2004;33(October (5)):492–505.

[8] Kim JK, Negovetich NJ, Forrest HL, Webster RG. Ducks: the "Trojan horses" of H5N1 influenza. Influenza Other Respi Viruses 2009;3(July (4)):121–8.

[9] Swayne DE. Principles for vaccine protection in chickens and domestic waterfowl against avian influenza: emphasis on Asian H5N1 high pathogenicity avian influenza. Ann NY Acad Sci 2006;1081:174–81 [October].

[10] Kim JK, Seiler P, Forrest HL, Khalenkov AM, Franks J, Kumar M, et al. Pathogenicity and vaccine efficacy of different clades of Asian H5N1 avian influenza A viruses in domestic ducks. J Virol 2008;82(November (22)):11374–82.

[11] Pantin-Jackwood MJ, Swayne DE. Pathobiology of Asian highly pathogenic avian influenza H5N1 virus infections in ducks. Avian Dis 2007;51(March (Suppl. 1)):250–9.

[12] Swayne DE. Understanding the complex pathobiology of high pathogenicity avian influenza viruses in birds. Avian Dis 2007;51(March (Suppl. 1)):242–9.

[13] Pfeiffer J, Pantin-Jackwood M, To TL, Nguyen T, Suarez DL. Phylogenetic and biological characterization of highly pathogenic H5N1 avian influenza viruses (Vietnam 2005) in chickens and ducks. Virus Res 2009;142(June (1–2)):108–20.

[14] Wasilenko JL, Arafa AM, Selim AA, Hassan MK, Aly MM, Ali A, et al. Pathogenicity of two Egyptian H5N1 highly pathogenic avian influenza viruses in domestic ducks. Arch Virol 2011;156(1):37–51.

[15] Brown JD, Stallknecht DE, Beck JR, Suarez DL, Swayne DE. Susceptibility of North American ducks and gulls to H5N1 highly pathogenic avian influenza viruses. Emerg Infect Dis 2006;12(November (11)):1663–70.

[16] Pantin-Jackwood MJ, Suarez DL, Spackman E, Swayne DE. Age at infection affects the pathogenicity of Asian highly pathogenic avian influenza H5N1 viruses in ducks. Virus Res 2007;130(December (1–2)):151–61.

[17] Londt BZ, Nunez A, Banks J, Alexander DJ, Russell C, Richard-Londt AC, et al. The effect of age on the pathogenesis of a highly pathogenic avian influenza (HPAI) H5N1 virus in Pekin ducks (*Anas platyrhynchos*) infected experimentally. Influenza Other Respi Viruses 2010;4(January (1)):17–25.

[18] Phuong DQ, Dung NT, Jorgensen PH, Handberg KJ, Vinh NT, Christensen JP. Susceptibility of Muscovy (*Cairina Moschata*) and mallard ducks (*Anas Platyrhynchos*) to experimental infections by different genotypes of H5N1 avian influenza viruses. Vet Microbiol 2010;148(2–4):168–74.

[19] Sims LD. Experience in control of avian influenza in Asia. Dev Biol (Basel) 2007;130:39–43.

[20] Capua I, Alexander DJ. Avian influenza vaccines and vaccination in birds. Vaccine 2008;26(September (Suppl. 4)):D70–3.

[21] Pfeiffer J, Suarez DL, Sarmento L, To TL, Nguyen T, Pantin-Jackwood MJ. Efficacy of commercial vaccines in protecting chickens and ducks against H5N1 highly pathogenic avian influenza viruses from Vietnam. Avian Dis 2010;54(March (Suppl. 1)):262–71.

[22] van der Goot JA, van Boven M, Stegeman A, van de Water SG, de Jong MC, Koch G. Transmission of highly pathogenic avian influenza H5N1 virus in Pekin ducks is significantly reduced by a genetically distant H5N2 vaccine. Virology 2008;382(December (1)):91–7.

[23] Beato MS, Toffan A, De Nardi R, Cristalli A, Terregino C, Cattoli G, et al. A conventional, inactivated oil emulsion vaccine suppresses shedding and prevents viral meat colonisation in commercial (Pekin) ducks challenged with HPAI H5N1. Vaccine 2007;25(May (20)):4064–72.

[24] Middleton D, Bingham J, Selleck P, Lowther S, Gleeson L, Lehrbach P, et al. Efficacy of inactivated vaccines against H5N1 avian influenza infection in ducks. Virology 2007;359(March (1)):66–71.

[25] Steensels M, Bublot M, Van Borm S, De Vriese J, Lambrecht B, Richard-Mazet A, et al. Prime-boost vaccination with a fowlpox vector and an inactivated avian influenza vaccine is highly immunogenic in Pekin ducks challenged with Asian H5N1 HPAI. Vaccine 2009;27(January (5)):646–54.

[26] Boltz DA, Douangngeun B, Sinthasak S, Phommachanh P, Midouangchanh P, Walker D, et al. Field assessment of an H5N1 inactivated vaccine in chickens and ducks in Lao PDR. Arch Virol 2009;154(6):939–44.

[27] Webster RG, Webby RJ, Hoffmann E, Rodenberg J, Kumar M, Chu HJ, et al. The immunogenicity and efficacy against H5N1 challenge of reverse genetics-derived H5N3 influenza vaccine in ducks and chickens. Virology 2006;351(August (2)):303–11.

[28] Chua TC, Leung CYH, Fang HE, Chow C-K, Ma S-K, Sia S-F, et al. Evaluation of a subunit H5 vaccine and an inactivated H5N2 avian influenza marker vaccine in ducks challenged with Vietnamese H5N1 highly pathogenic avian influenza virus. Influenza Research Treatment 2010;2010(2010) (Article ID 489213, 10 pp).

[29] Fereidouni SR, Starick E, Beer M, Wilking H, Kalthoff D, Grund C, et al. Highly pathogenic avian influenza virus infection of mallards with homo- and heterosubtypic immunity induced by low pathogenic avian influenza viruses. PLoS One 2009;4(8):e6706.

[30] Marjuki H, Scholtissek C, Franks J, Negovetich NJ, Aldridge JR, Salomon R, et al. Three amino acid changes in PB1-F2 of highly pathogenic H5N1 avian influenza virus affect pathogenicity in mallard ducks. Arch Virol 2010;155(June (6)):925–34.

[31] Jourdain E, Gunnarsson G, Wahlgren J, Latorre-Margalef N, Brojer C, Sahlin S, et al. Influenza virus in a natural host, the mallard: experimental infection data. PLoS One 2010;5(1):e8935.

[32] Steensels M, Van Borm S, Lambrecht B, De Vriese J, Le Gros FX, Bublot M, et al. Efficacy of an inactivated and a fowlpox-vectored vaccine in Muscovy ducks against an Asian H5N1 highly pathogenic avian influenza viral challenge. Avian Dis 2007;51(March (Suppl. 1)):325–31.

[33] Guionie O, Guillou-Cloarec C, Courtois D, Bougeard BS, Amelot M, Jestin V. Experimental infection of Muscovy ducks with highly pathogenic avian influenza virus (H5N1) belonging to clade 2.2. Avian Dis 2010;54(March (Suppl. 1)):538–47.

[34] Londt BZ, Nunez A, Banks J, Nili H, Johnson LK, Alexander DJ. Pathogenesis of highly pathogenic avian influenza A/turkey/Turkey/1/2005 H5N1 in Pekin ducks (*Anas platyrhynchos*) infected experimentally. Avian Pathol 2008;37(December (6)):619–27.

[35] Keawcharoen J, van Riel D, van Amerongen G, Bestebroer T, Beyer WE, van Lavieren R, et al. Wild ducks as long-distance vectors of highly pathogenic avian influenza virus (H5N1). Emerg Infect Dis 2008;14(April (4)): 600–7.

[36] Adams SC, Xing Z, Li J, Cardona CJ. Immune-related gene expression in response to H11N9 low pathogenic avian influenza virus infection in chicken and Pekin duck peripheral blood mononuclear cells. Mol Immunol 2009;46(May (8–9)):1744–9.

[37] Soubies SM, Volmer C, Guerin JL, Volmer R. Truncation of the NS1 protein converts a low pathogenic avian influenza virus into a strong interferon inducer in duck cells. Avian Dis Mar 2010;54(Suppl. 1):527–31.

[38] Sarmento L, Wasilenko J, Pantin-Jackwood M. The effects of NS gene exchange on the pathogenicity of H5N1 HPAI viruses in ducks. Avian Dis 2010;54(March (Suppl. 1)):532–7.

[39] Tian G, Zhang S, Li Y, Bu Z, Liu P, Zhou J, et al. Protective efficacy in chickens, geese and ducks of an H5N1-inactivated vaccine developed by reverse genetics. Virology 2005;341(October (1)):153–62.

[40] Barbeito MS, Abraham G, Best M, Cairns P, Langevin P, Sterritt WG, et al. Recommended biocontainment features for research and diagnostic facilities where animal pathogens are used. First International Veterinary Biosafety Workshop. Rev Sci Tech 1995 Sep;14(3):873–87.

[41] Swayne DE, Senne DA, Beard CW. Avian Influenza. In: Swayne DE, Glisson JR, Jackwood MJ, Pearson JE, Reed WM, editors. A labortatory manual for the isolation and identification of avian pathogens. 4th ed. Kennet Square, PA: American Association of Avian Pathologists; 1998. p. 150–5.

[42] Das A, Spackman E, Pantin-Jackwood MJ, Suarez DL. Removal of real-time reverse transcription polymerase chain reaction (RT-PCR) inhibitors associated with cloacal swab samples and tissues for improved diagnosis of Avian influenza virus by RT-PCR. J Vet Diagn Invest 2009;21(November (6)):771–8.

[43] Spackman E, Senne DA, Myers TJ, Bulaga LL, Garber LP, Perdue ML, et al. Development of a real-time reverse transcriptase PCR assay for type A influenza virus and the avian H5 and H7 hemagglutinin subtypes. J Clin Microbiol 2002;40(September (9)):3256–60.

[44] Bustin SA, Benes V, Garson JA, Hellemans J, Huggett J, Kubista M, et al. The MIQE guidelines: minimum information for publication of quantitative real-time PCR experiments. Clin Chem 2009;55(April (4)):611–22.

[45] De Vriese J, Steensels M, Palya V, Gardin Y, Dorsey KM, Lambrecht B, et al. Passive protection afforded by maternally-derived antibodies in chickens and the antibodies' interference with the protection elicited by avian influenza-inactivated vaccines in progeny. Avian Dis 2010;54(March (Suppl. 1)):246–52.

[46] Sarfati-Mizrahi D, Lozano-Dubernard B, Soto-Priante E, Castro-Peralta F, Flores-Castro R, Loza-Rubio E, et al. Protective dose of a recombinant Newcastle disease LaSota-avian influenza virus H5 vaccine against H5N2 highly pathogenic avian influenza virus and velogenic viscerotropic Newcastle disease virus in broilers with high maternal antibody levels. Avian Dis 2010;54(March (Suppl. 1)):239–41.

[47] Kim JK, Kayali G, Walker D, Forrest HL, Ellebedy AH, Griffin YS, et al. Puzzling inefficiency of H5N1 influenza vaccines in Egyptian poultry. Proc Natl Acad Sci USA 2010;107(June (24)):11044–9.

[48] Magor KE. Immunoglobulin genetics and antibody responses to influenza in ducks. Dev Comp Immunol 2011;35:1008–16 [March 4].
[49] Suarez DL, Schultz-Cherry S. Immunology of avian influenza virus: a review. Dev Comp Immunol 2000;24(Mar/Apr (2–3)):269–83.
[50] Barber MR, Aldridge Jr JR, Webster RG, Magor KE. Association of RIG-I with innate immunity of ducks to influenza. Proc Natl Acad Sci USA 2010;107(March (13)):5913–8.
[51] Yoneyama M, Kikuchi M, Natsukawa T, Shinobu N, Imaizumi T, Miyagishi M, et al. The RNA helicase RIG-I has an essential function in double-stranded RNA-induced innate antiviral responses. Nat Immunol 2004;5(July (7)): 730–7.
[52] Loo YM, Fornek J, Crochet N, Bajwa G, Perwitasari O, Martinez-Sobrido L, et al. Distinct RIG-I and MDA5 signaling by RNA viruses in innate immunity. J Virol 2008;82(January (1)):335–45.
[53] Daviet S, Van Borm S, Habyarimana A, Ahanda ML, Morin V, Oudin A, et al. Induction of Mx and PKR failed to protect chickens from H5N1 infection. Viral Immunol 2009;22(December (6)):467–72.
[54] Suzuki K, Okada H, Itoh T, Tada T, Mase M, Nakamura K, et al. Association of increased pathogenicity of Asian H5N1 highly pathogenic avian influenza viruses in chickens with highly efficient viral replication accompanied by early destruction of innate immune responses. J Virol 2009;83(August (15)):7475–86.
[55] Chan MC, Cheung CY, Chui WH, Tsao SW, Nicholls JM, Chan YO, et al. Proinflammatory cytokine responses induced by influenza A (H5N1) viruses in primary human alveolar and bronchial epithelial cells. Respir Res 2005;6:135.
[56] Gray DA, Maloney SK, Kamerman PR. Lipopolysaccharide-induced fever in Pekin ducks is mediated by prostaglandins and nitric oxide and modulated by adrenocortical hormones. Am J Physiol Regul Integr Comp Physiol 2005;289(November (5)):R1258–64.
[57] Burggraaf S, Bingham J, Payne J, Kimpton WG, Lowenthal JW, Bean AG. Increased inducible nitric oxide synthase expression in organs is associated with a higher severity of H5N1 influenza virus infection. PLoS One 2011;6(1):e14561.
[58] MacMicking J, Xie QW, Nathan C. Nitric oxide and macrophage function. Annu Rev Immunol 1997;15:323–50.

Immunogenetics
DOI 10.1007/s00251-010-0509-1

ORIGINAL PAPER

Association of Mx1 Asn631 variant alleles with reductions in morbidity, early mortality, viral shedding, and cytokine responses in chickens infected with a highly pathogenic avian influenza virus

Sandra J. Ewald · Darrell R. Kapczynski · Emily J. Livant · David L. Suarez · John Ralph · Scott McLeod · Carolyn Miller

Received: 28 October 2010 / Accepted: 27 December 2010
© Springer-Verlag 2011

Abstract Myxovirus-resistance (Mx) proteins are produced by host cells in response to type I interferons, and some members of the *Mx* gene family in mammals have been shown to limit replication of influenza and other viruses. According to an early report, chicken Mx1 variants encoding Asn at position 631 have antiviral activity, whereas variants with Ser at 631 lack activity in experiments evaluating Mx1 complementary DNA (cDNA) expressed ectopically in a cell line. We evaluated whether the Mx1 631 dimorphism influenced pathogenesis of highly pathogenic avian influenza virus (HPAIV) infection in chickens of two commercial broiler lines, each segregating for Asn631 and Ser631 variants. Following intranasal infection with HPAIV strain A/Chicken/Queretaro/14588-19/1995 H5N2, chickens homozygous for Asn631 allele were significantly more resistant to disease based on early mortality, morbidity, or virus shedding than Ser631 homozygotes. Higher amounts of splenic cytokine transcripts were observed in the Ser631 birds after infection, consistent with higher viral loads seen in this group and perhaps contributing to their higher morbidity. Nucleotide sequence determination of *Mx1* cDNAs demonstrated that the Asn631 variants in the two chicken lines differed at several amino acid positions outside 631. In vitro experiments with a different influenza strain (low pathogenicity) failed to demonstrate an effect of Mx1 Asn631 on viral replication suggesting that in vivo responses may differ markedly from in vitro, or that choice of virus strain may be critical in demonstrating effects of chicken Mx1. Overall, these studies provide the first evidence that Mx1 has antiviral effects in chickens infected with influenza virus.

Keywords Chicken · Mx1 · Influenza · Genetic resistance · Cytokines

S. J. Ewald (✉)
Department of Pathobiology, Auburn University,
166 Greene Hall,
Auburn, AL 36849-5519, USA
e-mail: ewaldsj@auburn.edu

S. J. Ewald · E. J. Livant
Department of Poultry Science, Auburn University,
Auburn, AL, USA

D. R. Kapczynski · D. L. Suarez
Southeast Poultry Research Laboratory, ARS-USDA,
Athens, GA, USA

J. Ralph · S. McLeod · C. Miller
Aviagen,
Crossville, TN, USA

Introduction

Type I interferons (IFNs) (alpha and beta) are powerful inducers of an antiviral state; mice that are unable to respond to type I IFN due to receptor knockout are extremely susceptible to infection by numerous viruses (Muller et al. 1994). Type I IFNs mediate their protective effect by inducing expression of other genes, called interferon-stimulated genes or ISGs. The best known antiviral proteins encoded by ISGs are Myxovirus resistance (Mx), 2′,5′-oligoadenylate synthetase (OAS), and protein kinase R (PKR). Mx proteins are large GTPases that interact directly with viral constituents (reviewed in

Published online: 01 February 2011

Haller et al. 2007). In mice, the *Mx1* gene is a critical and decisive determinant of resistance to influenza virus (Grimm et al. 2007; Haller 1981; Tumpey et al. 2007). Humans have a related gene, *MxA*, encoding a protein that is also effective in restricting replication of influenza virus in vivo (Pavlovic et al. 1995) and in vitro (Pavlovic et al. 1990).

Chickens have a single *Mx* gene (*Mx1*) that is induced by type I IFN (Schumacher et al. 1994). The original evaluation of chicken Mx1 indicated the encoded protein lacked antiviral activity (Bernasconi et al. 1995). Ko et al. (2002), however, reported that the chicken *Mx1* gene is highly polymorphic, and complementary DNAs (cDNAs) of some but not all *Mx1* alleles transfected into mouse 3T3 cells conferred protection against vesicular stomatitis virus (VSV) in vitro. Among numerous single nucleotide polymorphisms (SNPs) distributed throughout the cDNA sequences, only the SNP in a codon for amino acid 631 (c.1892G>A in exon 14) in the mature protein determined antiviral activity: Ser (G) at this position resulted in an Mx1 protein lacking antiviral activity, whereas Asn (A) conferred antiviral activity (Ko et al. 2002, 2004). In a comparison of one Asn631 variant allele and one Ser631 allele for activity against H5N1 highly pathogenic avian influenza virus (HPAIV) strain, expression of the Asn631 variant reduced virus replication, but the Ser631 variant had no effect (Ko et al. 2002). Subsequent experiments by another group, however, have failed to support the anti-influenza activity of chicken Mx Asn631 in a variety of in vitro systems (Benfield et al. 2008). Additionally, the evidence for antiviral activity of Asn631 alleles against other viruses (such as VSV, Newcastle disease virus, and Thogoto virus) is controversial, with one group finding no antiviral activity (Benfield et al. 2010) and a second reporting positive antiviral activity of the Asn631 Mx allele (Yin et al. 2010).

The ultimate question is whether (by accepted measures of disease or viral infection in vivo) chickens positive for an Mx1 Asn631 variant resist influenza more effectively than genetically similar chickens with a Ser 631 variant or differ significantly in innate immune responses following infection. Here, we report results of experiments that were designed to test the hypothesis that the single SNP determining amino acid Asn631Ser substitution in the chicken Mx1 protein may increase resistance to intranasal infection with a highly pathogenic avian influenza strain in chickens.

Materials and methods

Chickens

Two chicken lines from different commercial broiler companies were used to address the question. Meat-type chickens and their ancestors have low frequency of the Asn631 variant (Balkissoon et al. 2007; Livant et al. 2007; Ewald and Livant, unpublished data). The two genetic lines selected for the present studies have Asn631 variant alleles present in a somewhat low frequency (0.09 and 0.1), which is nevertheless higher than most commercial broiler lines (many of which are fixed for Ser631 and none with a higher frequency than 0.16 for the Asn631 allele). Breeder flocks segregating for Mx1 Asn631 or Ser631 variants at equal frequency within a chicken genetic line were established. At about 6-month intervals, chickens from one of two different genetic lines (line 1 or 2), owned by two different commercial meat-type breeder companies, were screened by PCR restriction fragment length polymorphism (RFLP) for the Mx1 631 SNP (below). Females and males that were heterozygous (Mx1 Asn631/Ser631) were selected and subsequently mated to produce chicks for virus infection studies. Progeny chicks were typed by the same Mx1 PCR-RFLP method as parents. Only Mx1 Asn631/Asn631 and Mx1 Ser631/Ser631 homozygous chicks were selected to undergo infection with HPAIV at the Southeast Poultry Research Laboratory. Chickens were 19–23 days old at time of challenge, except the 10^4 and 10^6 virus doses in chicks from line 1, in which case chicks were 11 days old. (Scheduling difficulties for BSL3 facilities dictated that this latter hatch must be typed and transported for infection earlier than originally planned. Space limitations in the BSL3 facility also precluded evaluation of heterozygotes in this experiment, in the interest of evaluating large numbers of homozygotes. For that reason, heterozygotes were not included in later experiments.) Numbers of progeny chicks included in experiments varied between doses and lines because of requirements for advance scheduling of limited BSL3 space, coupled with unpredictable start of lay and overall fertility of hens, as well as unpredictable distribution of homozygotes of each type within any given hatch. In each experiment, we matched numbers of Asn631 and Ser631 groups closely, with the group having the smallest number of available chicks being the limiting factor for maximum numbers in challenge groups. Numbers of chicks assessed for mortality/morbidity in each experiment are provided in Fig. 1 and Table 1. Embryos from the same breeder flocks were used to establish chick embryo kidney (CEK) and fibroblast (CEF) cultures for infection with a low pathogenic avian influenza virus (LPAIV) strain and nucleotide sequence determination of Mx1 cDNA, respectively (below).

Parents and progeny were maintained under strict biosecurity. Parents were vaccinated against Marek's disease with HVT and SB1 vaccines. Progeny were not vaccinated. Serological tests of serum samples from progeny chicks 4–5 weeks after hatch were negative for chicken infectious anemia virus, avian encephalomyelitis

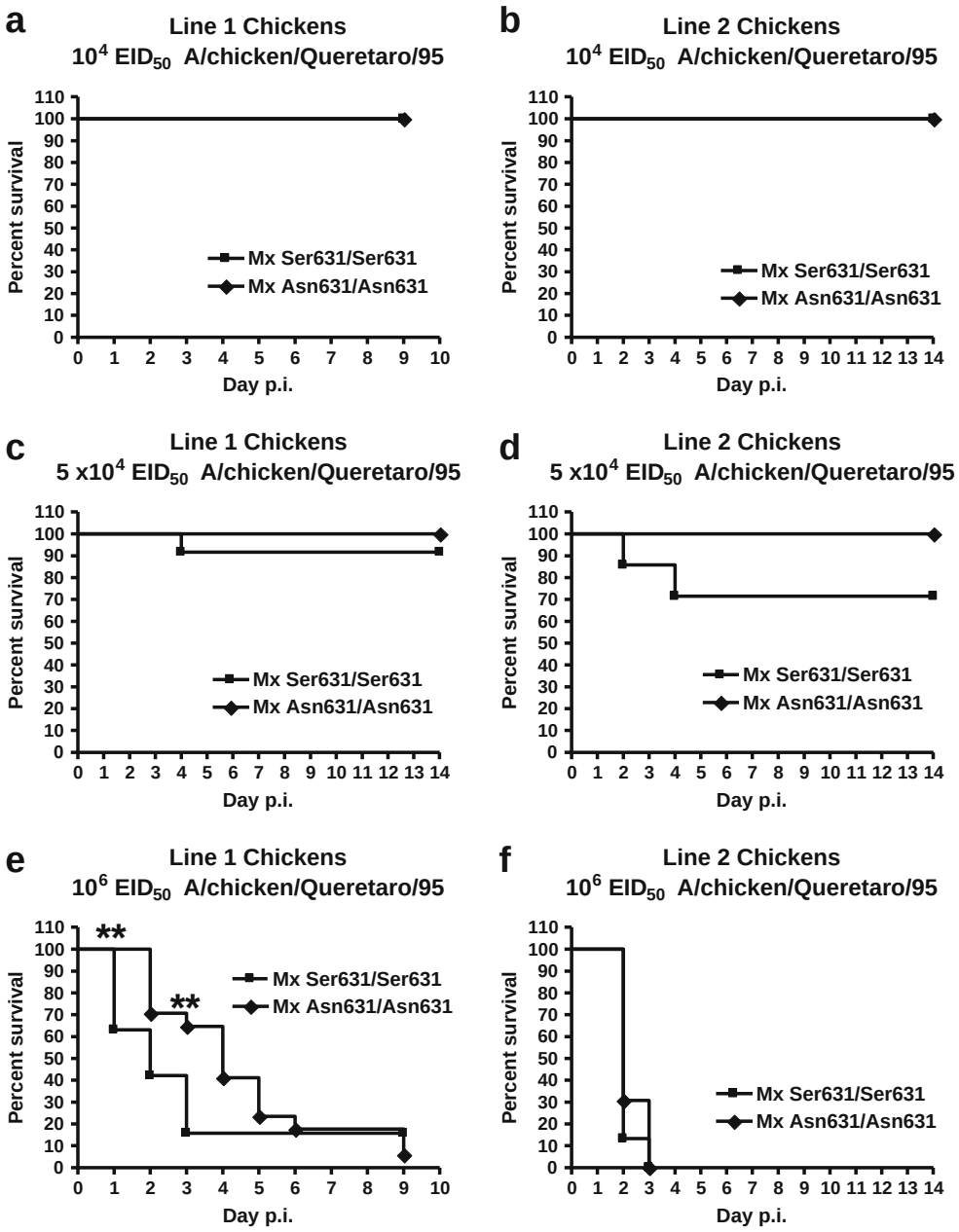

Fig. 1 Mortality in chickens from line 1 (**a**, **c**, **e**) and line 2 (**b**, **d**, **f**) after intranasal inoculation with varying doses of A/chicken/Queretaro/95 HPAIV. Numbers of chicks in line 1 experiments were as follows: 10^4 virus dose, n=13 Ser631/Ser631 and 14 Asn631/Asn631; 5×10^4 virus dose, n=12 Ser631/Ser631, and 9 Asn631/Asn631 chickens; 10^6 virus dose, n=19 Ser631/Ser631 and 17 Asn631/Asn631. Numbers of chicks in line 2 experiments are as follows: 10^4 virus dose, n=8 Ser631/Ser631 and 8 Asn631/Asn631; 5×10^4 virus dose, n=7 Ser631/Ser631 and 7 Asn631/Asn631 chickens; 10^6 virus dose, n=15 Ser631/Ser631 and 13 Asn631/Asn631. **P<0.01 by Fisher's exact test comparing cumulative mortality in Asn631 versus Ser631 groups at 1 and 3 days post-infection

virus, infectious bursal disease virus, infectious bronchitis virus, Newcastle disease virus, reovirus, *Mycoplasma gallisepticum* and *Mycoplasma synoviae*, and influenza antibodies (Thompson Bishop Sparks Diagnostic Laboratory, Auburn, AL, USA). All experiments involving chickens complied with federal guidelines and institutional policies for animal care and use.

Mx1 631 SNP typing

Methods for Mx1 SNP typing were simultaneously and independently developed in the Auburn University and the industry partner's laboratories. Each group validated its protocol for allelic variant detection in its laboratory. Initial experiments were conducted using chicks from a flock established by one of the breeder companies on a commercial site. DNA was isolated by standard methods from blood obtained from potential parents and from progeny. PCR primers were as follows: 5′-GCACTGT CACCTCTTAATAGAGTACC-3′ (upstream) and 5′-AGGAATCTGATTGCTCAGGCGTTAA-3′ (downstream). The penultimate "A" in the downstream primer (underlined) was a mismatch introduced to create a *Hin*cII restriction digest site if the SNP top strand was "G" (in the codon for Ser631). The 25 µl reaction mixture consisted of 2.5 µl 10× PCR buffer, 0.625 U Taq polymerase (Invitrogen), 1.5 mM $MgCl_2$, 0.5 µM each primer, 0.2 mM of each dNTP, and 100–500 ng DNA. The PCR

Table 1 Reduced morbidity in line 2 Asn631 Mx chickens infected with 5×10^4 EID_{50} A/chicken/Queretaro/95 HPAIV

Morbidity (by day)	Asn631/Asn631 (affected/total)	Ser631/Ser631 (affected/total)	Clinical signs in Ser631 chicks[a]
D1	0/7	1/7	1 @ +2
			6 @ 0
D2	0/7	2/7	1 @ +3
			1 @ +2
			5 @ 0
D3	0/7	2/6	1 @ +2
			1 @ +1
			4 @ 0
D4	0/7	4/6*	1 @ +3
			3 @ +1
			2 @ 0
D5	0/7	2/5	2 @ +1
			3@ 0
D6	0/7	1/5	1 @ +1
			4 @ 0
D7	0/7	0/5	5 @ 0
D8 through D14	0/7	0/5	5 @ 0

*p=0.021 by Fisher's exact test

[a] Clinical signs: 0=normal, 1=sick (including depression and ruffled feathers), 2=severely sick (including cyanosis of limbs or comb and immobility), 3=dead

mixtures were overlaid with 25 μl mineral oil, and amplification was performed in a thermocycler without a heated lid. The reaction conditions were an initial hold at 94°C for 2 min, 40 cycles of 94°C for 30 s, 53°C for 30 s, 72°C for 30 s, and a final hold at 72°C for 2 min. The resulting PCR product was 124 bp. After restriction digestion with *Hin*cII, the variant with "G" produced two bands of 101 and 23 bp, whereas a variant with "A" at the SNP encoding position 631 was not cut.

In subsequent experiments, chicks to be reared for the parent flock were imported to Auburn University from a commercial farm or hatchery. At about 3 weeks of age, potential parents were screened for Mx1 631 SNP to identify heterozygotes to establish the breeder flock. Mx1 631 SNP typing methods for parents and progeny were the same. DNA was isolated from 5 μl of blood or packed red cells using GenElute Blood Genomic DNA Kit (Sigma-Aldrich, Inc., St. Louis, MO, USA) according to manufacturer's instructions. Mx1 exon 14 (previously identified as exon 13 according to Ensembl Mx gene annotation at the time; Livant et al. 2007) was amplified with an upstream primer, 5′-GAATAGCAACTCCA TACCGTG-3′, designed from *Mx1* intron 13–14 (Ensembl Chicken Genome coordinates 102640550 to 102640570). The downstream primer used in early experiments, 5′-GTAT TAAAGGTTGCTGCTAATG-3′, was derived from the 3′ untranslated region (Ensembl Chicken Genome Coordinates 102640978 to 102640999). A downstream primer, 5′-GTCTACCAGGTATTGGTAGGCTTTG-3′, derived from the 3′ end of Mx1 Exon 14 (Ensembl Chicken Genome coordinates 102640866 to 102640890) was used in experiments with genetic line 2 to avoid an insertion/deletion encountered in the 3′ untranslated region in that line. The 25 μl reaction mix consisted of 2.5 μl 10× PCR buffer II, 1.2 U Amplitaq Gold (Applied Biosystems, Foster City, CA, USA), 2 mM $MgCl_2$, 1 μM each primer, 0.2 mM of each dNTP, and 100–300 ng DNA. The reaction conditions were an initial hold at 94°C for 11 min, 40 cycles of 94°C for 1 min, 50°C for 30 s, 72°C for 1 min, and a final hold at 72°C for 10 min.

The restriction enzyme *Hpy*8I (Fermentas, Inc., Glen Burnie, MD, USA) was used to digest the PCR product following the manufacturer's instructions. The products were run on 2.5% agarose gel containing Sybr Green (Invitrogen Carlsbad, CA, USA) at 120 V for 30 min or on 2% or 4% agarose ethidium bromide E-gels (Invitrogen Carlsbad, CA, USA) following the manufacturer's instructions. *Hpy*8I recognizes a site in the 1892G (Ser631) variant, but the 1892A site (Asn631) variant is not cut by the enzyme. An additional enzyme site exists in the 5′ end of the amplicon from both Mx1 631 variants (with some exceptions, see below), serving as a positive indicator of enzymatic activity. Restriction of products amplified using the downstream primer from exon 14 yielded two fragments for Asn 631 [307 base pairs (bp), 31 bp) and three fragments for Ser 631 (206, 101, and 31 bp) variants (using the downstream primer located in the 3′ untranslated region yields an additional 112 bp fragment for both variants). Primers were placed to avoid indels (insertions and deletions) in intron 13–14 and the 3′-UTR that were encountered in lines 1 and 2 during the course of evaluating *Mx1* exon 14 amplicons by nucleotide sequence analyses. Despite locating primers in intron 13–14 close to the 5′ end of exon 14 (upstream primer) and the 3′ end of exon 14 (downstream primer), a restriction fragment length polymorphism within a portion of intron 13–14 in the amplicon was observed in the Ser631 variants in line 2, but it did not interfere with typing.

Virus infections of chickens

For in vivo experiments, chicks were arranged by Mx1 631 genotype and placed in separate cages in a BSL3Ag facility under IACUC approved protocols. Birds were infected intranasally with HPAIV A/chicken/Queretaro/14588-19/1995 H5N2 (A/chicken/Queretaro/95) in doses of 10^4 EID_{50}, 5×10^4 EID_{50}, or 10^6 EID_{50}. In some experiments, three chickens were removed from each Mx1 genotype and virus dose group at day 2 post-infection, to evaluate cytokine expression in spleen tissue by quantitative real-time RT-PCR (RRT-PCR). The remaining birds were

monitored daily for mortality and, in some experiments, for morbidity. Separate hatches were used for different virus doses, except the 10^4 and 10^6 doses in line 1 chickens that came from the same hatch.

Assessment of morbidity

Following AI infection, birds were monitored daily for morbidity and mortality for 14 days. Birds were scored between 0 and 3 daily for clinical signs of disease [0=normal, 1=sick (including depression and ruffled feathers), 2=severely sick (including cyanosis of limbs or comb and immobility), and 3=dead]. Birds displaying severe clinical signs of disease were euthanized by overdose of sodium pentobarbital.

Analysis of cytokine expression by RRT-PCR

Relative cytokine expression in spleens of infected and non-infected Mx1 631 genotype birds was examined by RRT-PCR. Interleukin (IL)-1β, IFN-α, and IFN-γ expression was determined day 2 post-infection as previously described (Kapczynski and Kogut 2008). Briefly, quantitative PCR was performed for each sample in triplicate in a total volume of 25 μl, consisting of 12.5 μl iQ Sybrgreen supermix (Bio-Rad Laboratories, Los Angeles, CA, USA) with 1 μl of each primer at concentration of 10 pmol/μl, 5.5 μl RNase/DNase-free water, and 5 μl diluted RNA. PCR conditions were the same for each targeted gene and are as follows: 1 min at 50°C, 95°C for 5 min, followed by 45 cycles of 95°C for 10 s and 56°C for 30 s. For each reaction, melting curves were analyzed to determine the specificity of each gene. Primer pairs were used as follows (forward and reverse primers, respectively): IL-1β, (ACATGTCGTGTGTGATGAG, CAGCCGGTAGAA GATGAAGC); IFN-α, (GACAGCCAACGCCAAAGC, GTCGCTGCTGTCCAAGCATT); IFN-γ, (TGTACTTG GAAATGCTTGAAAAC, ACCTTCTTCACGCCAT CAG); and 28S (GGCGAAGCCAGAGGAAACT, GAC GACCGATTTGCACGTC). RNA from individual spleen samples was normalized using the 28S house-keeping gene. For each gene, amplification was verified using four 10-fold serial dilutions of standard spleen cell RNA in the same PCR run. Expression was determined by the standard curve method (Morrison et al. 1998). Data are expressed as fold change in cytokine messenger RNA (mRNA) levels in infected groups compared with those from uninfected groups.

Detection of AIV by RRT-PCR to evaluate virus shedding

Oropharyngeal samples were obtained at day 2 post-infection from all chickens in line 1 (10^4 and 10^6 virus doses) to detect the presence of viral genome in respiratory tissue. RRT-PCR for detection of the matrix gene of AIV was performed as previously described (Spackman et al. 2002).

Serology

The hemagglutination inhibition (HI) test was performed on sera recovered from surviving birds at day 14 post-infection using homologous H5N2 HPAIV as previously described (Swayne et al. 1998).

In vitro infection with low pathogenicity avian influenza virus

CEK cultures were produced from individual 17–18-day embryos from the breeder flock segregating for Mx1 631 SNP. Each embryo culture was typed for the Mx1 SNP as described above. CEK were cultured initially in MEM (Invitrogen Corporation, Carlsbad, CA, USA) containing 10% tryptose phosphate broth and 80 μg/ml tylosin (both from Sigma-Aldrich, St. Louis, MO, USA), 100 μg/ml gentamycin, and 2% fetal bovine serum (FBS) (the last two reagents from Invitrogen). The next day, the medium was replaced with medium containing 0.2% FBS and graded doses of recombinant IFN-α (4-fold dilutions to produce IFN concentrations from 10,000 U/ml to 0.6 U/ml). [rIFN-α comprised supernatant fluid from COS cells transfected with an expression construct for chicken interferon-α. The determination of IFN titer in the supernatant fluid was performed on CEF cultures infected with vesicular stomatitis virus, Indiana strain, with antiviral activity assessed by cytopathic effect inhibition assay using standard methods.] The expression construct was the kind gift of Dr. Peter Staeheli, University of Freiburg, Freiburg, Germany. CEK cultures were incubated with rIFN-α for 16 h. Cultures were infected with 100 $TCID_{50}$ A/Turkey/Wisconsin/68 (H5N9) LPAIV for 1 h, after which rIFN-α was added back at the initial concentration in medium containing 2% FBS for the duration of the culture. All cultures were inspected microscopically for cytopathic effect (CPE). No effect of IFN-α treatment on CPE in either Mx631 group was observed until a minimal concentration of 156 U/ml. Supernatant fluid was collected from infected cultures that were untreated, and those treated with IFN-α (at concentrations higher than 156 U/ml) 48 h p.i. for determination of virus yield by $TCID_{50}$ determination on CEK cultures (Hy-Vac SPF).

Nucleotide sequence determination of cDNA from Mx1 Asn631 and Ser631 variants

Mx1 cDNA was synthesized from RNA from chick embryo fibroblasts (CEF) and from peripheral blood mononuclear cells (PBMC). CEF cultures were prepared from individual

10-day-old embryos from lines 1 and 2 that were typed for Mx1 631 genotype by PCR-RFLP to select homozygotes of each variant. Second passage CEF were cultured in MEM medium containing 10% tryptose phosphate broth, 2% FBS, 80 μg/ml tylosin, and 100 μg/ml gentamycin. PBMC were prepared from three progeny chicks from line 2 homozygous for Mx1 Asn631 and three for Mx1 Ser631. Mononuclear cells were isolated by centrifugation of heparinized wing vein blood over Histopaque 1077. PBMC were cultured at a density of 2×10^6 cells/ml in six-well plates in RPMI 1640 medium containing 5% FBS, 80 μg/ml tylosin, and 100 μg/ml gentamycin in 5% CO_2 at 38°C. *Mx1* expression was induced by incubation with recombinant chicken IFN-α (1,000 U/ml) for 11–12 h (CEF) or 14–17 h (PBMC) before RNA extraction.

RNA was extracted from CEFs either by trypsinization with Triple E (Invitrogen Corporation, Carlsbad, CA, USA) and extraction of total RNA using High Pure RNA Isolation Kit (Roche Applied Science, Indianapolis, IN, USA) or by lysis in Trizol directly in the cell culture dish and extraction of total RNA using Trizol Plus RNA Purification Kit System (Invitrogen Corporation, Carlsbad, CA, USA). RNA was extracted from PBMCs using Trizol Plus RNA Purification Kit System. Immediately following RNA extraction, cDNA was synthesized using Thermoscript RT-PCR kit (Invitrogen Corporation, Carlsbad, CA, USA) following manufacturer's instructions.

The complete sequence of the protein-encoding region of *Mx1* cDNA was amplified using forward primer designed from exon 2, Mx56F (CAAGAGTGGTCGGYGTCRA TAA) in combination with reverse primer from the 3′-untranslated region, Mx2432R (GCTTTGACAAGGG TAGGCATMTCA), or the combination Mx52F (CTGTCAAGAGTGGTCGGYGTCRAT), with Mx2435R (GCAGCTTTGACAAGGGTAGGCAT). The latter pair was designed by moving the targeted sequence for primers a few base pairs to improve amount of amplicon. The 50-μl PCR reaction consisted of 200 nM of each primer, 1 mM $MgSO_4$, 200 μM of each dNTP, 5 μl of RT-PCR reaction, 1 U of Platinum Taq High Fidelity DNA polymerase, and 5 μl of 10× High Fidelity PCR Buffer (Invitrogen Corporation, Carlsbad, CA, USA). The PCR conditions were an initial hold at 94°C followed by 38 cycles of 94°C for 30 s, 57°C for 30 s, 68°C of 2.5 min, and a final 10 min extension at 68°C. *Mx1* was amplified from cDNAs from individual birds or embryos except that cDNA from three Ser631 PBMC cultures and three Asn631 CEF cultures from line 2 were each pooled for use in Mx1 PCR.

The RT-PCR amplicons were ligated into pT7Blue-3 plasmid and cloned into Nova Blue Singles competent cells using Novagen pT7Blue-3 Perfectly Blunt® Cloning Kit (EMD Chemicals, Inc., Gibbstown, NJ, USA) in accordance with the manufacturer's instructions.

Nucleotide sequences of cloned inserts were determined by automated sequence analysis (Genomics and Sequencing Laboratory, Auburn University, Auburn, AL, USA). For each sequence reported, five to nine full-length clones were sequenced initially in one direction to determine if more than one allelic sequence was present, and at least three clones of each Mx allele (except for line 2 Ser631 allele 2, for which only two clones were obtained) were sequenced completely in both directions.

Statistical analysis

Mortality results were analyzed by Kaplan–Meier, one-tailed test using Prism 5 (GraphPad Co., San Diego, CA, USA) software. Mortality results from line 1 (10^6 virus dose) were also analyzed on individual days (day 1, 2, and 3 p.i.) by Fisher's exact test (Prism 5), comparing the cumulative number dead and number of survivors on that day in each group. Fisher's exact test was also used to analyze comparisons of Mx1 Asn631 and Ser631 variant chickens for morbidity, viral shedding, and cytokine expression. *P* values reported for Fisher's exact test are two-tailed.

Results

Mortality in chicks differing in Mx1 631 variant after challenge with highly pathogenic AIV

No deaths were noted in either line 1 (Fig. 1a) or line 2 (Fig. 1b) chickens challenged with 10^4 EID_{50} A/chicken/Queretaro/95 HPAIV in either Mx1 631 variant group. HI titers for these birds were all ≤1:4 2 weeks post-challenge, indicating they likely were not infected by this challenge dose (data not shown). However, 5×10^4 EID_{50} killed a small fraction of Ser631chickens in both lines 1 and 2 but none of the Asn631 birds in either line1 or 2 (Fig. 1c, d). At this dose, Kaplan–Meier analysis indicated that the curves comparing Asn631 and Ser631 groups were not significantly different ($p=0.208$ for line 1 and 0.071 for line 2). The highest dose (10^6 EID_{50}) killed most all the birds in both Mx1 631 groups (Fig. 1e, f). In line 1, median survival was 4 days in the Asn631 and 2 days in the Ser631 groups. Kaplan–Meier analysis of mortality data (Fig. 1e) indicated that the survival curves of the Asn631 and Ser631 groups did not differ significantly ($p=0.105$). However, most of the Ser631 birds (84%) were dead by day 3 post-challenge (16 dead/19 total), whereas a minority of the Asn631 birds (35%) were dead at this time (6 dead/17 total). This difference in survival past 3 days was significantly different ($p=0.0054$ by Fisher's exact test). On day 1 post-challenge, more than one-third of the Ser631 birds (7/19, 37%) were

dead, whereas none of the Asn631 birds (0/17, 0%) had died (p=0.0084 by Fisher's exact test). Line 2 chickens infected with 10^6 EID_{50} (Fig. 1f) were all dead by day 3 p.i. However, these chicks were smaller than previous hatches from the same line, and the difference from line 1 response to the same virus dose may be a hatch effect. Kaplan–Meier comparison of survival curves in the Ser631 chicks from lines 1 and 2 challenged with 5×10^4 virus (Fig. 1c, d) indicated no statistical difference. Additionally, the fact that all Asn631 chicks in both lines survived this virus dose suggests that there are minimal differences in susceptibility to the A/chicken/Queretaro/95 HPAIV between chicken lines 1 and 2.

Morbidity following intermediate dose of HPAIV in chickens differing in Mx1 631 SNP

Although only two of seven chicks died in the Ser631 group of line 2 birds infected with 5×10^4 HPAIV (Fig. 1d), high morbidity in this group was observed. The majority of clinical signs associated with surviving birds were ruffled feathers and mild depression. Each day from day 1 to 6 p.i., at least one Ser631 chicken was positive for morbidity, whereas no Asn631 chicks showed signs of morbidity at any time point (Table 1). At day 4 p.i., four of the six remaining Ser631 chicks were morbid (including one death on that day). This fraction differed significantly from Asn631 chicks (p=0.021 by Fisher's exact test). Testing of sera from the five remaining birds indicated two had HI titers of 1:16 and three had titers of 1:8 (data not shown). Similarly, birds in Asn631 group displayed HI titers of 1:8 (6 birds) and 1:16 (1 bird) 2 weeks post-infection.

Virus shedding in HPAIV-infected chicks differing in Mx1 631 SNP

Viral shedding by the oropharyngeal route was evaluated by RRT-PCR analysis of swab samples 2 days post-challenge. In line 1 chickens infected with a sublethal dose of HPAIV (10^4 EID_{50}, Fig. 1a), none of the chicks of either Mx1 genotype shed detectable virus, indicating these birds likely were not infected by this dose. Among the line 1 birds challenged with a high dose of HPAIV (10^6 EID_{50}, Fig. 1e), which caused high mortality in both Mx1 631 groups, some but not all birds were positive for viral genomes in oropharyngeal swabs. In birds challenged with the high dose of HPAIV, 9/19 Ser631and 12/17 Asn631 birds were still alive at the time of sampling. Of these, 56% of the Ser631 birds were positive for virus, whereas only 8% of the Asn631 birds were positive (Table 2). The Mx1 631 genotype groups differed significantly in fraction of chickens that were positive for viral shedding 2 days after challenge (p=0.046 by Fisher's exact test). Every bird that was positive for viral shedding at day 2 p.i. was dead by the following day.

Table 2 Reduced viral shedding in line 1 Asn631 chickens on day 2 p.i. with 10^6 EID_{50} A/chicken/Queretaro/95 HPAIV

Mx1 631 variant	Fraction positive for AIV by RRT-PCR (% positive)	Fraction of AIV positive birds dead within 1 day
Ser631	5/9 (56%)	5/5
Asn631	1/12 (8%)[a]	1/1

Virus shedding was determined by RRT-PCR of oropharyngeal samples obtained 2 days post-challenge with 10^6 EID_{50} A/Queretaro/95 HPAIV

[a] Mx1 genotype groups differ significantly in fraction of positive birds by Fisher's exact test (p=0.045)

Cytokine expression in chicks differing in Mx1 631 SNP after challenge with highly pathogenic AIV

RRT-PCR of RNA isolated from spleen samples 2 days post-infection of line 1 birds was performed to evaluate expression of cytokines IL-1β, IFN-α, and IFN-γ. Following low-dose challenge (10^4 per bird) with HPAIV (A/chicken/Queretaro/95), IL-1β, IFN-α, and IFN-γ were all upregulated compared to non-challenged controls (Fig. 2a). There were no statistically significant differences between Mx 631 variants in expression for any of the three cytokines at this dose.

At the higher dose (10^6 EID_{50} per bird) of infection, line 1 Asn631 birds expressed IL-1β, IFN-α, and IFN-γ significantly lower than Ser631 birds (Fig. 2b), which correlated with increased survival (Fig. 1e). Expression of these cytokines in the Asn631 group was between 1.5 and 4.5 times lower than the Ser631 birds. The higher levels of cytokine expression exhibited by the Ser631 birds may have contributed to the increased mortality, or they may simply be due to higher viral loads in this group (Table 2).

In line 2 birds, significantly higher levels of IL-1β were observed in the Mx1 Ser631 group compared to the Asn631 group in the spleen at 2 days post-infection with a low-dose challenge (Fig. 3a). No differences in interferon expression were observed between the two allele groups.

As seen with the line 1 birds, following a higher dose (5×10^4 EID_{50}) challenge, birds in line 2 containing the Asn631 allele expressed significantly lower levels of IL-1β, IFN-α, and IFN-γ compared to the Ser631 group (Fig. 3b). Expression levels of IL-1β, IFN-α, and IFN-γ were approximately four, 15, and six times higher, respectively, in the Ser631 group than the Asn631 group.

Sequence of Asn631 and Ser631 variants in lines 1 and 2

Benfield et al. (2008) were not able to demonstrate an antiviral effect of an Asn631 variant in experiments conducted in vitro. One possibility raised by these experiments is that position 631 in the Mx1 protein may not be

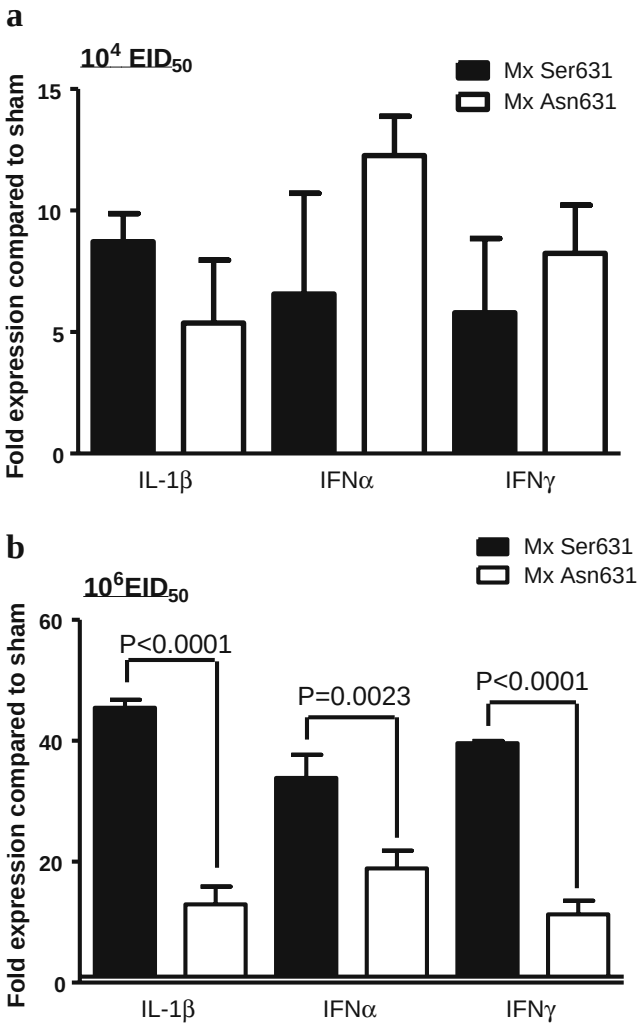

Fig. 2 Differential expression of selected genes in line 1-Mx Ser631 and Asn631/chickens using real-time RT-PCR (RRT-PCR). Chickens received either 10^4 EID$_{50}$ (**a**) or 10^6 EID$_{50}$ (**b**) doses of A/chicken/Queretaro/95 H5N2 HPAIV via intranasal route. Total RNA was prepared from spleen tissue in H5N2-infected chickens at 48 h post-infection. The expression of three immune-related genes, IL-1β, interferon-alpha (IFN-α), and interferon-gamma (IFN-γ) was compared with control chickens with different Mx631 alleles using the 28S housekeeping gene for endogenous RNA standardization. Fold change was determined using $2^{-\Delta\Delta Ct}$ format with statistical analysis performed using Fisher's exact test ($P<0.05$)

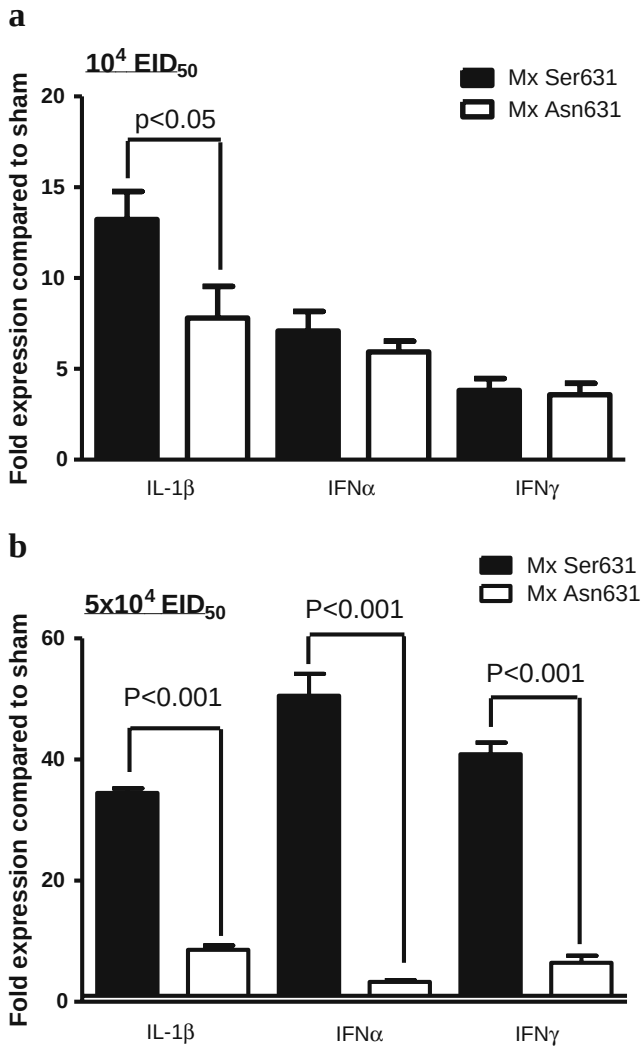

Fig. 3 Differential expression of selected genes in line 2-Mx Ser631 and Asn631 chickens using real-time RT-PCR (RRT-PCR). Chickens received either 10^4 EID$_{50}$ (**a**) or 5×10^4 EID$_{50}$ (**b**) doses of A/chicken/Queretaro/95 H5N2 HPAI via intranasal route. Total RNA prepared from spleen tissue in H5N2-infected chickens at 48 h post-infection. The expression of three immune-related genes, IL-1β, interferon-alpha (IFN-α), and interferon-gamma (IFN-γ) was compared with control chickens with different Mx631 alleles using the 28S housekeeping gene for endogenous RNA standardization. Fold change was determined using $2^{-\Delta\Delta Ct}$ format with statistical analysis performed using Fisher's exact test ($P<0.05$)

the only requirement for antiviral activity and that other polymorphisms in addition to Asn631 may be required for an inhibitory effect on influenza virus.

To determine the nucleotide sequences of the Mx1 alleles in lines 1 and 2, cDNA from Mx1 Asn631 and Ser631 cultures (CEF or PBMC treated with recombinant IFN-α) from both lines was cloned and sequenced. In line 1, one Mx1 Asn631 variant allele and one Ser631 variant allele were demonstrated. Line 2 had one Mx1 Asn631 allele and two Ser631 variant alleles. *Mx1* nucleotide sequences are deposited in GenBank under accession numbers HM775376 and HQ014737 to HHQ014740.

As seen in Table 3, Asn631 variants from lines 1 and 2 differ from each other at several polymorphic positions (21, 308, 339, and 548). Although both line 1 Asn631 and line 2 Asn631 variants provided a measure of protection against HPAIV in vivo (Fig. 1 and Tables 1 and 2), both alleles differ from the SHK Asn631 variant allele previously shown to have anti-influenza activity in cells expressing Mx1 ectopically (Ko et al. 2002). The line 1 Asn631 variant allele is not identical to any Mx sequence in GenBank. It differs from each of its three closest relatives [TB (gb_EF575608), WL (gb_EF575624), and RIR

Table 3 Polymorphism in the Mx1 proteins of lines 1 and 2

Line	631 variant	Amino acid in Mx1protein at position														
		5	21	41	42	85	94	185	199	202	232	308	339	548	583	631
1	Asn	*R*	*Q*	P	L	*L*	*R*	*K*	G	S	*G*	I	A	*V*	*T*	*N*
2	Asn	*R*	R	P	L	*L*	*R*	*K*	G	S	*G*	*V*	*T*	A	*T*	*N*
1	Ser	*R*	*Q*	P	L	*L*	*R*	*K*	G	*T*	*G*	I	A	A	*T*	S
2	Ser 1	*R*	*Q*	P	L	*L*	*R*	*K*	G	*T*	*G*	I	A	A	*T*	S
2	Ser2	*R*	*Q*	*R*	*S*	*L*	*R*	*K*	G	S	*G*	*V*	*T*	A	*T*	S
Ref Seq	Ser	W	*Q*	*R*	*S*	*L*	Q	*K*	G	S	*G*	I	A	A	A	S
SHK	Asn	*R*	*Q*	*R*	*S*	*L*	*R*	*K*	*S*	*T*	*G*	*V*	*T*	*V*	*T*	*N*

Polymorphisms at the 15 reported polymorphic positions in Mx1 proteins are shown for line 1 and 2 chickens used in this study, with the reference sequence (Ref Seq) from a White Leghorn chicken (from Staeheli; GenBank number NM204609) and from Shamo (SHK) chicken line shown for comparison. The SHK Mx1 allele is the only allele for which anti-influenza activity has been reported in transfection experiments (Ko et al. 2002); amino acids at polymorphic positions in this allele are in italics, and also in line 1 and 2 alleles that match SHK

(gb_EF575618),] at three amino acid positions. The line 2 Asn631 variant is identical in protein sequence to the Mx1 allele in the B1 CEF line of Benfield et al. (2008); the B1 CEF line (with an Asn631 variant) reportedly did not inhibit influenza virus replication by comparison with CEF lines with an Mx1 Ser631 variant.

In comparing all the line 1 and 2 alleles with the SHK allele, Asn at 631 is uniquely present in all the alleles that have been associated with anti-influenza activity and absent in the alleles that lacked anti-influenza activity [in our studies and those of Ko et al.(2002)]. These results suggest that Asn631 in fact determines the ability of the chicken Mx1 protein to limit influenza virus replication.

Effect of Mx1 631 SNP on in vitro replication of LPAIV

It would be useful to develop an in vitro system to study chicken Mx1 effects on viral replication, especially one that that did not require BSL3 facilities. To that end, we evaluated replication of a low pathogenic avian influenza virus (LPAIV) in CEK cells differing in Mx1 631 genotype. In addition to respiratory and intestinal epithelium, chick embryo kidney cells were recently shown to support multicycle replication of LPAIV (Cauthen et al. 2007). CEK were prepared from individual embryos that were then typed for Mx1 631 SNP. The LPAIV strain A/Tk/WI/68 (H5N9) was used to infect CEK.

Compared with aged chicken embryo cell cultures, CEK secrete very small amounts of IFN-α upon infection (Cauthen et al. 2007). Chicken embryo kidney cell cultures of Asn631 and Ser631 homozygous embryos were pretreated with two different doses of IFN-α to induce an antiviral state, then infected with A/Turkey/WI/68 H5N9 virus. IFN-α induced a strong, dose-related antiviral state in CEK of both genotypes. Virus yields determined from 48 h supernatants, however, did not differ significantly between Mx1 genotypes (Fig. 4).

Discussion

The present study evaluated the in vivo effect of naturally occurring variants of the *Mx1* gene in non-inbred chicken lines, as opposed to mouse studies that target the *Mx1* gene more precisely using transgenic, knockout or congenic mouse lines. For that reason, the *Mx1* gene can only be implicated as the effector of differential influenza resistance by demonstrating a statistically significant association of a specific polymorphism with differences in mortality, morbidity, virus shedding, and cytokine responses. In theory, this association of genetic resistance with Mx1 Asn631 variants in chickens could potentially be mediated not by the *Mx1* gene itself, but by another polymorphic gene in strong linkage disequilibrium with the Mx1 position 631 polymorphism [another possibility would be differences in

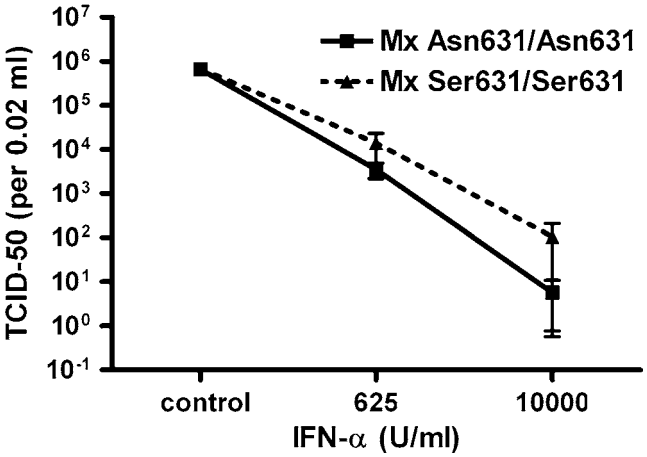

Fig. 4 Virus yields from Mx1 Asn631/Asn631 (n=3) and Mx1 Ser631/Ser631 (n=3) individual CEK cultures from line 1 flock, treated with rIFN-α at the indicated concentrations for 16–20 h before infection with 100 $TCID_{50}$ A/Turkey/WI/68 LPAIV. Supernatants were collected 48 h p.i. and evaluated for virus yield. No significant differences were seen between Mx1 genotypes at any IFN concentration

amount of transcripts from the Mx1 631 variants; however, the Asn631 and Ser631 variant alleles are expressed in equivalent amounts at the mRNA level, by quantitative RT-PCR analysis of Mx1 transcripts in cells treated with IFN-α (Livant and Ewald, manuscript in preparation)].

In light of the fact that commercial broiler breeder lines retain a high degree of genetic variation, it is especially interesting that significant differences in response to HPAIV were seen in association with Mx1 631 variants. Polymorphisms of other antiviral genes like *PKR* and *OAS*, as well as pathogen recognition receptors (like toll-like receptors), cytokines/chemokines or their receptors, or intracellular signaling molecules, may exist in these lines. Functionally different variants of any genes critical to the anti-influenza response would be expected to obscure effects of the Mx1 631 variant because they would probably segregate independently of the Mx1 gene and thus randomize among chicks of both Mx1 631 genotypes [indeed, we have identified a variant of the *OAS* gene, resulting in a truncated protein (Tatsumi et al. 2000), in both lines 1 and 2 used in these experiments (unpublished results)].

The chicken Mx1 Asn631 variants evaluated in these experiments did not provide as strong protection against A/Ck/Queretaro/95 H5N2 HPAIV strain as *Mx1* gene in mice typically provides [depending on the virus strain, up to 10,000-fold difference in LD_{50} compared with *Mx1* deficient mice (reviewed in Haller 1981)]. In mice, the presence of an intact *Mx1* gene is of paramount importance even in resisting death from highly pathogenic influenza 1918 and H5N1 strains, with complete or near complete survival of *Mx1*+ mice at virus doses that kill all *Mx1*− mice (Haller et al. 2007; Tumpey et al. 2007). However, an influenza strain that has unusually high replication fitness in mice kills all *Mx1*+ and *Mx1*− mice within a few days. Pretreatment of the mice with IFN-α protects all the *Mx1*+ mice, but the *Mx1*− mice all die regardless of IFN-α treatment (Grimm et al. 2007). These results indicate the importance of IFN-α in protection against a rapidly fatal influenza virus, but as well demonstrate that a functional Mx1 protein is crucial for the IFN-α to induce an effective antiviral state. HPAIV strains in chickens, including the Queretaro strain used here, are similar in aggressiveness to the strain with high replication fitness in mice, in that infected chickens die within 1–3 days after infection with a lethal dose of virus. It would be interesting to determine if administration of exogenous IFN-α before and during Queretaro infection would improve resistance of Mx1 Asn631 variant birds relative to those with Ser631.

There are several examples of single genes that do not prevent lethality from influenza, but rather extend the time to death or protect a fraction of animals from death. Mice (from a strain with defective endogenous *Mx1* gene) that are transgenic for human *MxA* gene have enhanced resistance to influenza, indicated by about a 2-day lag until death compared with nontransfected mice after infection with a virus that is ultimately lethal for all (Pavlovic et al. 1995). In the absence of a functional *Mx1* gene, mice with a functional (wild-type) *PKR* gene have a partial protection from influenza compared with *PKR* knockout mice (Balachandran et al. 2000). Similarly, the *ISG15* (Lenschow et al. 2007) and *IFN-beta* genes (Koerner et al. 2007) have been implicated as critical in protection against influenza, on the basis of a 2-day difference in mean survival between knock-out and wild-type mice.

Although Asn631 variant did not confer full resistance to mortality from Queretaro strain, selective breeding for this polymorphism might be of value. Genetic resistance to avian diseases such as Marek's disease (Bacon et al. 2001) and salmonellosis (Calenge et al. 2010) are typically complex traits, with multiple genes (quantitative trait loci, or QTL) each contributing a fraction toward resistance. Thus, identification of additional QTL independently contributing to AIV resistance in commercial chicken lines would be necessary to achieve strong genetic resistance by selection. However, it would be necessary first to demonstrate an in vivo antiviral effect of chicken Mx Asn631 alleles against additional influenza strains (either HPAIV or LPAIV) or other important viral pathogens of chickens.

Our results showing an effect of Mx1 Asn631 polymorphism on influenza pathogenesis are in contrast to results of an in vitro study indicating no effect on viral replication (Benfield et al. 2008) but in agreement with earlier studies by Ko et al. (2002). The reason for the discrepancy may relate to the differences in virus strain evaluated in the various studies. Ko et al. evaluated an H5N1 HPAIV strain, whereas Benfield and co-workers used several different strains of either human origin (A/WI/33; A/PR/8/34) or of low pathogenicity in chickens [A/Duck/England/62 (H4N6) and A/Duck/Singapore/97 (H5N3)]. Thus, the question of antiviral effect of Asn631 alleles against influenza remains unsettled; however, our results indicate that at least one influenza strain is partially susceptible to chicken MxAsn631 alleles.

Importantly, Dittmann et al. (2008) demonstrated that influenza A virus strains differ in sensitivity to the antiviral activity of human MxA and mouse Mx1 proteins. Interestingly, all the human influenza isolates that were evaluated, including the 1918 flu strain, were relatively insensitive to the human MxA protein (but sensitive to mouse Mx1). The authors hypothesized that widespread and long-term circulation of these virus strains in the human population had led to selection for viruses that could better resist MxA. A similar picture may emerge for avian influenza strains and chicken Mx Asn631 alleles, with the strains that we evaluated (A/chicken/Queretaro/95) in vivo and the Ko

group evaluated in vitro (A/Hong Kong/483/97) retaining some susceptibility to Mx Asn631 proteins, whereas the viral strains evaluated by others who obtained negative results had lost their Mx susceptibility.

Finally, the complexity of the in vivo infection may not be easily replicated by in vitro experiments. The only in vivo experiments thus far to evaluate Mx1 Asn631Ser polymorphism were conducted by Sironi et al. (2008). These authors found no difference in survival that correlated with Mx1 631 polymorphism when they infected chickens of different genetic lines (differing in Mx 631 alleles) with an H7N1 influenza virus strain. They did, however, find large differences in resistance among the genetic lines. Discrepancy between their results and ours may have several possible explanations. In addition to virus strain differences, a major difference is that our experiments were designed to evaluate the Mx1 631 variant alleles within a single "pure" line (line 1) or a commercially available cross of two pure lines (line 2). Although the pure lines are not highly inbred, by comparing progeny within a family, the "background" genes are randomized. Furthermore, the genetic variation within a genetic line is more restricted than between lines. In the Sironi experiments, three of the lines were fixed for either Asn631 or Ser631 alleles. Only two of the five lines evaluated were segregating for the Mx631 polymorphism, with the Asn631 alleles in such low frequency that only one or two Asn631 homozygotes were present in the infected group in each line.

Typically, infection of immunologically naive chickens with HPAIV results in >90% mortality. In our studies, infection with a H5N2 HPAIV strain was evaluated at multiple doses to more thoroughly evaluate the role of the Mx1 631 allele. Swayne and Slemons (2008) recently demonstrated that the mean bird infectious dose (BID_{50}) and mean bird lethal dose (BLD_{50}) for HPAI viruses are not necessarily the same. In three of 11 HPAIV isolates tested, increased doses of virus were necessary to go from a BID_{50} to BLD_{50}. Although the A/chicken/Queretaro/95 virus was not one identified, differences in the type of chickens used may explain those differences, as lower doses were necessary to infect and kill the specific pathogen-free White Leghorn birds than the commercial birds tested here. Furthermore, the apparent increase in HI antibody titers of surviving birds challenged at 5×10^4 EID_{50} here suggests they produced antibodies against the HPAIV, either through infection or immunological processing of challenge virus particles, and many were able to overcome the infection. Thus, a BID_{50} plateau was achieved, which allowed for testing the innate influence of Mx1 631 alleles, without reaching a BLD_{50}. Nonetheless, the difference between BID_{50} and BLD_{50} is typically small for the HPAIV strains, and the viruses are so virulent that they quickly overwhelm the defenses of chickens at a lethal dose. We interpret the reduced early mortality (from 1 to 3 days p.i.) and viral shedding in the Asn631 group of line 1 infected with 10^6 EID_{50} (Fig. 1e) as a "delaying action" mounted by the Mx Asn631 protein, which was ultimately overtaken by viral replication. The birds dying from day 4 to 9 p.i. in the Asn631 group may not have been infected by the initial experimental virus exposure, but instead by transmission from initially infected cage mates shedding large amounts of virus. The middle dose of virus (5×10^4 EID_{50}) in line 2 chickens happened to fall in the range between BID_{50} and BLD_{50}, allowing the Mx Asn631 protein to control virus sufficiently to prevent signs of morbidity but demonstrating the failure of the Ser631 allele (Table 1).

The observation of differential regulation of cytokines between Asn631 and Ser631 chickens following challenge with HPAIV is intriguing. IL-1β is a pro-inflammatory cytokine that is highly secreted by monocytes, macrophages, dendritic cells, and epithelial cells at mucosal surfaces. Transgenic mice that are deficient in IL-1 receptor do not differ from wild-type mice infected with a strain of H5N1 virus that causes high lethality in mice; however, the deficient mice are more susceptible to morbidity and mortality following infection with a strain exhibiting lower mortality in mice, coupled with a higher viral load late in infection. These results indicate an important (though strain-dependent) role of IL-1 in viral clearance (Szretter et al. 2007). In experiments evaluating type I IFN receptor knockout mice, IFN-α and IFN-β were implicated as playing an important role in early control of H5N1 virus replication in mice (Szretter et al. 2009). IFN-γ has diverse effects on the mouse immune response to influenza virus, including induction of nitric oxide synthase-2, which is immunosuppressive (Karupiah et al. 1998).

Uncontrolled expression of pro-inflammatory cytokines (the so-called "cytokine storm") is a feature of infection with highly pathogenic H5N1 strains in humans and several animal models (Baskin et al. 2009; Boon et al. 2009; Peiris et al. 2009; Schmolke et al. 2009). There is evidence that elevated IL-1 contributes to the severity of influenza in mice. Perrone et al. (2010) recently reported that mice deficient in receptors for TNF and IL-1 exhibit reduced morbidity, delay in mortality, and reduced lung inflammation compared with wild-type mice after infection with a highly pathogenic H5N1 virus. Our results in chickens infected with HPAIV demonstrate a correlation between increased disease severity and heightened IL-1β levels (in Mx Ser631 birds), consistent with the hypothesis that dysregulated expression of pro-inflammatory cytokines results in greater disease severity following HPAI infection. Elevated IFN-γ in the Ser631 birds could also contribute to immunopathology by inducing nitric oxide synthase-2 (Karupiah et al. 1998) or through other mechanisms. Levels of expression of IFN-α in Asn631 birds may be less

elevated (controlled) due to lower viral load, yet sufficient to induce Mx1 expression at a time when it can exert an antiviral effect. Further testing is needed to better understand the role and expression of cytokines in innate resistance to avian influenza.

Our observation that Asn631 CEK did not differ from Ser631 CEK in supporting viral replication of a second (low pathogenicity) influenza virus strain, with or without IFN-α pretreatment, is in contrast with our in vivo results indicating the Mx1 631 variant influences influenza pathogenesis. Several possible explanations may account for the disparity: (1) different virus strains were used in vivo and in vitro, and the strains may differ in susceptibility to inhibitory effects of Mx1 Asn631; (2) tissue differences in Mx1 expression or activity may exist [CEK express *Mx1* transcripts less well than chick embryo fibroblasts and blood mononuclear cells in response to recombinant IFN-α; Livant et al., manuscript in preparation]; (3) immune responses in vivo following influenza infection may be too complex to be modeled by an in vitro response, at any rate in a cell type like CEK (cells of the immune system and respiratory and intestinal epithelial cells are more relevant to pathogenesis of naturally acquired disease). A similar disparity has been noted between in vivo defects in *ISG15* knockout mice infected with influenza virus, coupled with a lack of differences in viral replication in mouse embryo fibroblasts derived from wild-type and knockout mice (Lenschow et al. 2007).

Much remains to be learned about the chicken Mx1 protein, its potential antiviral activity against various avian viruses, and its mechanism of action. Chicken and duck *Mx1* genes encode a large region at the N-terminal end of the protein that is unique to birds. This avian-specific region appears to be under positive diversifying selection (Berlin et al. 2008), suggesting a role of pathogen pressure in its evolution.

Acknowledgments This project was supported by the National Research Initiative Competitive Grant no. 2006-35205-16676 from the USDA National Institute of Food and Agriculture, and USDA Agricultural Research Service CRIS project no. 6612-32000-053. We thank Clayton Floyd and Roger Brock for animal care. We also thank Dr. Igal Pevzner and Mr. Randy Shumate of Cobb-Vantress, Inc., for the chickens, and Dr. Peter Staeheli (University of Freiburg, Freiburg, Germany) for the expression construct for recombinant chicken IFN-α. We gratefully acknowledge the technical expertise of Ms. Milla Kaltenboeck, Ms. Tracy Faulkner, Mr. Cam Greene, and Ms. Aniko Zsak.

Conflict of interest The authors declare that they have no conflict of interest.

References

Bacon LD, Hunt HD, Cheng HH (2001) Genetic resistance to Marek's disease. Curr Top Microbiol Immunol 255:121–141

Balachandran S, Roberts PC, Brown LE, Truong H, Pattnaik AK, Archer DR, Barber GN (2000) Essential role for the dsRNA-dependent protein kinase PKR in innate immunity to viral infection. Immunity 13:129–141

Balkissoon D, Staines K, McCauley J, Wood J, Young J, Kaufman J, Butter C (2007) Low frequency of the Mx allele for viral resistance predates recent intensive selection in domestic chickens. Immunogenetics 59:687–691

Baskin CR, Bielefeldt-Ohmann H, Tumpey TM, Sabourin PJ, Long JP, García-Sastre A, Tolnay AE, Albrecht R, Pyles JA, Olson PH, Aicher LD, Rosenzweig ER, Murali-Krishna K, Clark EA, Kotur MS, Fornek JL, Proll S, Palermo RE, Sabourin CL, Katze MG (2009) Early and sustained innate immune response defines pathology and death in nonhuman primates infected by highly pathogenic influenza virus. Proc Natl Acad Sci USA 106:3455–3460

Benfield CT, Lyall JW, Kochs G, Tiley LS (2008) Asparagine 631 variants of the chicken Mx protein do not inhibit influenza replication in primary chicken embryo fibroblast cells or in vitro surrogate assays. J Virol 82:7533–7539

Benfield CTO, Lyall JW, Tiley LS (2010) The cytoplasmic location of chicken Mx is not the determining factor for its lack of antiviral activity. PLoS ONE 5:e12151

Berlin S, Qu L, Li X, Yang N, Ellegren H (2008) Positive diversifying selection in avian Mx genes. Immunogenetics 60:689–697

Bernasconi D, Schultz U, Staeheli P (1995) The interferon-induced Mx protein of chickens lacks antiviral activity. J Interferon Cytokine Res 15:47–53

Boon AC, deBeauchamp J, Hollmann A, Luke J, Kotb M, Rowe S, Finkelstein D, Neale G, Lu L, Williams RW, Webby RJ (2009) Host genetic variation affects resistance to infection with a highly pathogenic H5N1 influenza A virus in mice. J Virol 83:10417–10426

Calenge F, Kaiser P, Vignal A, Beaumont C (2010) Genetic control of resistance to salmonellosis and to Salmonella carrier-state in fowl: a review. Genet Sel Evol 42:11

Cauthen A, Swayne DE, Sekellick MJ, Marcus PI, Suarez DL (2007) Amelioration of influenza virus pathogenesis in chickens attributed to the enhanced interferon-inducing capacity of a virus with a truncated NS1 gene. J Virol 81:1838–1847

Dittmann J, Stertz S, Grimm D, Steel J, García-Sastre A, Haller O, Kochs G (2008) Influenza A virus strains differ in sensitivity to the antiviral action of Mx-GTPase. J Virol 82:3624–3631

Grimm D, Staeheli P, Hufbauer M, Koerner I, Martínez-Sobrido L, Solórzano A, García-Sastre A, Haller O, Kochs G (2007) Replication fitness determines high virulence of influenza A virus in mice carrying functional Mx1 resistance gene. Proc Natl Acad Sci USA 104:6806–6811

Haller O (1981) Inborn resistance of mice to orthomyxoviruses. Curr Top Microbiol Immunol 92:25–52

Haller O, Kochs G, Weber F (2007) Interferon, Mx, and viral countermeasures. Cytokine Growth Factor Rev 18:425–433

Kapczynski DR, Kogut MH (2008) Measurement of avian cytokines with real time RT-PCR following infection with the avian influenza virus. Meth Mol Biol 436:127–134

Karupiah G, Chen JH, Mahalingam S, Nathan CF, MacMicking JD (1998) Rapid interferon gamma-dependent clearance of influenza A virus and protection from consolidating pneumonitis in nitric oxide synthase 2-deficient mice. J Exp Med 188:1541–1546

Ko J-H, Jin H-K, Asano A, Takada A, Ninomiya A, Kida H, Hokiyama H, Ohara M, Tsuzuki M, Nishibori M, Mizutani M, Watanabe T (2002) Polymorphisms and the differential antiviral activity of the chicken Mx gene. Genome Res 12:595–601

Ko JH, Takada A, Mitsuhashi T, Agui T, Watanabe T (2004) Native antiviral specificity of chicken Mx protein depends on amino acid variation at position 631. Gen 35:119–122

Koerner I, Kochs G, Kalinke U, Weiss S, Staeheli P (2007) Protective role of beta interferon in host defense against influenza A virus. J Virol 81:2025–2030

Lenschow DJ, Lai C, Frias-Staheli N, Giannakopoulos NV, Lutz A, Wolff T, Osiak A, Levine B, Schmidt RE, García-Sastre A, Leib DA, Pekosz A, Knobeloch KP, Horak I, Virgin HW 4th (2007) IFN-stimulated gene 15 functions as a critical antiviral molecule against influenza, herpes, and Sindbis viruses. Proc Natl Acad Sci USA 104:1371–1376

Livant EJ, Avendano S, McLeod S, Ye X, Lamont SJ, Dekkers JD, Ewald SJ (2007) MX1 exon 13 polymorphisms in broiler breeder chickens and associations with commercial traits. Genet 38:177–179

Morrison TB, Weis JJ, Wittwer CT (1998) Quantification of low-copy transcripts by continuous SYBR Green I monitoring during amplification. Biotechniques 24:954–962

Muller U, Steinhoff U, Reis LFL, Hemmi S, Pavlovic J, Zinkernagel RM, Aguet M (1994) Functional role of type I and type II interferons in antiviral defense. Science 264:1918–1921

Pavlovic J, Zurcher T, Haller O, Staeheli P (1990) Resistance to influenza virus and vesicular stomatitis virus conferred by expression of human MxA protein. J Virol 64:3370–3375

Pavlovic J, Arzet HA, Hefti HP, Frese M, Rost D, Ernst B, Kolb E, Staeheli P, Haller O (1995) Enhanced virus resistance of transgenic mice expressing the human MxA protein. J Virol 69:4506–4510

Peiris JS, Cheung CY, Leung CY, Nicholls JM (2009) Innate immune responses to influenza A H5N1: friend or foe? Trends Immunol 30:574–584

Perrone LA, Szretter KJ, Katz JM, Mizgerd JP, Tumpey TM (2010) Mice lacking both TNF and IL-1 receptors exhibit reduced lung inflammation and delay in onset of death following infection with a highly virulent H5N1 virus. J Infect Dis 202:1161–1170

Schmolke M, Viemann D, Roth J, Ludwig S (2009) Essential impact of NF-kappaB signaling on the H5N1 influenza A virus-induced transcriptome. J Immunol 183:5180–5189

Schumacher B, Bernasconi D, Schultz U, Staeheli P (1994) The chicken Mx promoter contains an ISRE motif and confers interferon inducibility to a reporter gene in chick and monkey cells. Virology 203:144–148

Sironi L, Williams JL, Moreno-Martin AM, Ramelli P, Stella A, Jianlin H, Weigend S, Lombardi G, Cordioli P, Mariani P (2008) Susceptibility of different chicken lines to H7N1 highly pathogenic avian influenza virus and the role of Mx gene polymorphism coding amino acid position 631. Virology 380:152–156

Spackman E, Senne DA, Myers TJ, Bulaga LL, Garber LP, Perdue ML, Lohman K, Daum LT, Suarez DL (2002) Development of a real-time reverse transcriptase PCR assay for type A influenza virus and the avian H5 and H7 hemagglutinin subtypes. J Clin Micro 40:3256–3260

Swayne DE, Slemons RD (2008) Using mean infectious dose of high- and low-pathogenicity avian influenza viruses originating from wild duck and poultry as one measure of infectivity and adaptation to poultry. Avian Dis 52:455–460

Swayne DE, Senne DA, Beard CW (1998) Avian influenza. In: Swayne DE (ed) A laboratory manual for the isolation and identification of avian pathogens, 4th edn. American Association of Avian Pathologists, Kennett Square, pp 150–155

Szretter KJ, Gangappa S, Lu X, Smith C, Shieh WJ, Zaki SR, Sambhara S, Tumpey TM, Katz JM (2007) Role of host cytokine responses in the pathogenesis of avian H5N1 influenza viruses in mice. J Virol 81:2736–2744

Szretter KJ, Gangappa S, Belser JA, Zeng H, Chen H, Matsuoka Y, Sambhara S, Swayne DE, Tumpey TM, Katz JM (2009) Early control of H5N1 influenza virus replication by the type I interferon response in mice. J Virol 83:5825–5834

Tatsumi R, Hamada K, Sekiya S, Wakamatsu M, Namikawa T, Mizutani M, Sokawa Y (2000) 2′, 5′-oligoadenylate synthetase gene in chicken: gene structure, distribution of alleles and their expression. Biochim Biophys Acta 1494:263–268

Tumpey TM, Szretter KJ, Van Hoeven N, Katz JM, Kochs G, Haller O, García-Sastre A, Staeheli P (2007) The Mx1 gene protects mice against the pandemic 1918 and highly lethal human H5N1 influenza viruses. J Virol 81:10818–10821

Yin CG, Zhang CS, Zhang AM, Qin HW, Wang XQ, Du LX, Zhao GP (2010) Expression analyses and antiviral properties of the Beijing-You and White Leghorn myxovirus resistance gene with different amino acids at position 631. Poult Sci 89:2259–2264

AVIAN DISEASES 55:285–292, 2011

Avian Influenza *In Ovo* Vaccination with Replication Defective Recombinant Adenovirus in Chickens: Vaccine Potency, Antibody Persistence, and Maternal Antibody Transfer

Alexander Mesonero,[A] David L. Suarez,[B] Edzard van Santen,[C] De-chu C. Tang,[D] and Haroldo Toro[AE]

[A]College of Veterinary Medicine, Auburn University, Auburn, AL 36849-5519
[B]Southeast Poultry Research Laboratory, United States Department of Agriculture, Athens, GA 30605
[C]Department of Agronomy and Soils, Auburn University, Auburn, AL 36849-5412
[D]Vaxin Inc., 1500 1st Avenue North, Birmingham, AL 35203

Received 23 November 2010; Accepted and published ahead of print 26 February 2011

SUMMARY. Protective immunity against avian influenza (AI) can be elicited in chickens in a single-dose regimen by *in ovo* vaccination with a replication-competent adenovirus (RCA)-free human adenovirus serotype 5 (Ad)-vector encoding the AI virus (AIV) hemagglutinin (HA). We evaluated vaccine potency, antibody persistence, transfer of maternal antibodies (MtAb), and interference between MtAb and active *in ovo* or mucosal immunization with RCA-free recombinant Ad expressing a codon-optimized AIV H5 HA gene from A/turkey/WI/68 (AdTW68.H5$_{ck}$). Vaccine coverage and intrapotency test repeatability were based on anti-H5 hemagglutination inhibition (HI) antibody levels detected in *in ovo* vaccinated chickens. Even though egg inoculation of each replicate was performed by individuals with varying expertise and with different vaccine batches, the average vaccine coverage of three replicates was 85%. The intrapotency test repeatability, which considers both positive as well as negative values, varied between 0.69 and 0.71, indicating effective vaccination. Highly pathogenic (HP) AIV challenge of chicken groups vaccinated with increasing vaccine doses showed ~90% protection in chickens receiving $\geq 10^8$ ifu (infectious units)/bird. The protective dose 50% (PD$_{50}$) was determined to be $10^{6.5}$ ifu. Even vaccinated chickens that did not develop detectable antibody levels were effectively protected against HP AIV challenge. This result is consistent with previous findings of Ad-vector eliciting T lymphocyte responses. Higher vaccine doses significantly reduced viral shedding as determined by AIV RNA concentration in oropharyngeal swabs. Assessment of antibody persistence showed that antibody levels of *in ovo* immunized chickens continued to increase until 12 wk and started to decline after 18 wk of age. Intramuscular (IM) booster vaccination with the same vaccine at 16 wk of age significantly increased the antibody responses in breeder hens, and these responses were maintained at high levels throughout the experimental period (34 wk of age). AdTW68.H5$_{ch}$-immunized breeder hens effectively transferred MtAb to progeny chickens. The level of MtAb in the progenies was consistent with the levels detected in the breeders, i.e., intramuscularly boosted breeders transferred higher concentrations of antibodies to the offspring. Maternal antibodies declined with time in the progenies and achieved marginal levels by 34 days of age. Chickens with high maternal antibody levels that were vaccinated either *in ovo* or via mucosal routes (ocular or spray) did not seroconvert. In contrast, chickens without MtAb successfully developed specific antibody levels after either *in ovo* or mucosal vaccination. These results indicate that high levels of MtAb interfered with active Ad-vectored vaccination.

RESUMEN. Vacunación *in ovo* para influenza aviar en pollos utilizando un adenovirus recombinante de replicación defectiva: potencia de la vacuna, persistencia de anticuerpos, y transferencia de anticuerpos maternos.

La inmunidad protectora contra la influenza aviar puede ser estimulada en pollos bajo un régimen con una dosis única mediante vacunación *in ovo* con un adenovirus humano serotipo 5 libre de adenovirus competentes para la replicación como un vector que codifica a la hemaglutinina del virus de la influenza aviar. Se evaluó la potencia como vacuna, la persistencia de anticuerpos, la transferencia de anticuerpos maternos y la interferencia entre los anticuerpos maternos con la inmunización activa *in ovo* o por mucosas con este adenovirus recombinante libre de partículas virales competentes para la replicación que expresaba el gene de la hemaglutinina H5 con codones optimizados del virus de la influenza aviar A/Pavo/WI/68 (AdTW68.H5$_{ck}$). La cobertura vacunal y la repetibilidad de la prueba para determinar la potencia interna se basaron en los niveles de anticuerpos inhibidores de la hemaglutinación contra H5, detectados en los pollos vacunados *in ovo*. A pesar de que la inoculación de los huevos de cada repetición fue realizada por personas con diferentes grados de experiencia y con lotes diferentes de vacunas, la cobertura promedio de la vacuna de las tres repeticiones fue de 85%. La repetibilidad de la prueba para la potencia interna que considera tanto valores positivos como negativos, varió entre 0.69 y 0.71, lo que indica una vacunación efectiva. El desafío con un virus de la influenza aviar de alta patogenicidad en grupos de pollos vacunados con dosis vacunales incrementadas, mostraron una protección de aproximadamente un 90% en los pollos que recibieron $\geq 10^8$ unidades infecciosas (ifu) por pollo. La dosis protectora 50% (DP$_{50}$) se determinó que era $10^{6.5}$ unidades infecciosas. Incluso los pollos vacunados que no desarrollaron niveles detectables de anticuerpos estaban protegidos eficazmente contra el desafío con el virus de influenza aviar alta patogenicidad. Este resultado es consistente con los hallazgos anteriores sobre las respuestas de linfocitos T estimuladas por este vector de adenovirus. Dosis vacunales más altas redujeron significativamente la eliminación del virus según lo determinado por la concentración de ARN del virus de influenza aviar en hisopos orofaríngeos. La evaluación de la persistencia de anticuerpos mostró que los niveles de anticuerpos en aves inmunizadas *in ovo* siguió aumentando hasta las 12 semanas y comenzó a declinar después de las 18 semanas de edad. La vacunación de refuerzo intramuscular con la misma vacuna a las 16 semanas de edad aumentó de manera significativa la respuesta de anticuerpos en gallinas reproductoras y estas respuestas se mantuvieron con niveles altos durante todo el periodo experimental (34 semanas de edad). Las gallinas reproductoras inmunizadas con el vector AdTW68.H5$_{ch}$ transfirieron de manera efectiva anticuerpos maternales a la progenie. El nivel de anticuerpos maternales en la progenie fue consistente con los niveles detectados en los reproductores, es decir, los reproductores que recibieron un refuerzo intramuscular transmitieron mayores concentraciones de anticuerpos a la

[E]Corresponding author. E-mail: torohar@auburn.edu

descendencia. Los anticuerpos maternos se redujeron después de un tiempo en las progenies y alcanzó niveles marginales a los 34 días de edad. Los pollos con niveles altos de anticuerpos maternos que fueron vacunados ya sea *in ovo* o por vías mucosas (ocular o por aspersión) no mostraron seroconversión. Por el contrario, los pollos sin anticuerpos maternales desarrollaron con éxito niveles de anticuerpos específicos después de la vacunación ya sea *in ovo* o por mucosas. Estos resultados indican que los altos niveles de anticuerpos maternos interfieren con la vacunación activa con este vector de adenovirus.

Key words: avian influenza virus, recombinant vaccine, adenovirus, chickens

Abbreviations: Ad = adenovirus serotype 5; AI = avian influenza; AIV = avian influenza virus; BSL = biosafety level; EID = embryo infective dose; HA = hemagglutinin; HI = hemagglutination inhibition; HP = highly pathogenic; ifu = infectious units; IM = intramuscular; MtAb = maternal antibodies; PD_{50} = protective dose 50%; qRT-PCR = quantitative reverse transcriptase-PCR; RCA = replication-competent adenovirus; SEM = standard error of the mean; SEPRL = Southeast Poultry Research Laboratory; SPF = specific-pathogen-free; USDA = United States Department of Agriculture; VACC = vaccine accordance

Highly pathogenic (HP) avian influenza (AI) viruses (AIV) belonging to the H5 or H7 subtypes threaten the world poultry industry and are zoonotic agents with pandemic potential for humans (17). We previously reported that protective immunity against AI can be elicited in chickens in a single-dose regimen by *in ovo* vaccination with a replication-competent adenovirus (RCA)-free human adenovirus serotype 5 (Ad5)-vector encoding either the AI virus H5 (AdTW68.H5) or H7 (AdCN94.H7) hemagglutinins (HA). Vaccinated chickens were protected against HP AI homologous virus challenges (15,16). We have shown that chickens vaccinated *in ovo* with AdTW68.H5 and subsequently vaccinated intramuscularly with AdCN94.H7 after hatch develop antibodies against both the H5 and H7 HA proteins. This result suggests that preexisting Ad5 immunity in chickens does not significantly interfere with the potency of Ad5-vectored vaccines. Similarly, simultaneous *in ovo* vaccination with AdTW68.H5 and AdCN94.H7 also elicits robust hemagglutination inhibition (HI) antibody levels to both H5 and H7 AI strains (13), allowing the adoption of an immunization strategy with a broad antigen repertoire. Others evaluated a replication defective Ad-vector encoding the M2eX-HA-hCD40L or M1-M2 fusion from a human HP AI (H5N2) isolate administered via the intramuscular (IM) and intranasal route in mice (4). Their vaccine delivery regimen resulted in both potent mucosal immunity as well as strong systemic humoral and T-cell responses. A natural follow up of these studies was to evaluate vaccine potency, antibody persistence, and transfer of maternal antibodies (MtAb) to progeny chickens. Evaluation of vaccine potency includes determination of the 50% protective dose (PD_{50}) as well as demonstration of repeatability. In this study PD_{50} was determined by HP AI challenge. Because serum HI antibody titers in poultry are strongly correlated with protection against HP AI (9), repeatability of *in ovo* immunization was determined from antibody levels achieved by the vaccinated chickens as described (2). Initial studies on antibody persistence showed that *in ovo* immunization with AdTW68.H5 induced anti-H5 antibody titers lasting at least until 52 days of age (16). Thus, in the current study we extended the time span for antibody monitoring in chickens vaccinated via the *in ovo* route to 34 wk of age. Passively transferred MtAb are relevant in disease prevention in the poultry industry. However, maternally derived antibodies have been shown to interfere with active vaccination (reviewed in (6) and references therein). In the current study, we evaluated transfer of MtAb from breeder hens, which were either singly immunized *in ovo* with $AdTW68.H5_{ch}$ or in addition received an IM booster vaccination at 16 wk of age. We also evaluated active *in ovo* or mucosal (ocular, spray) vaccination in progenies originating from $AdTW68.H5_{ch}$-vaccinated breeders; that is, with maternal immunity.

MATERIALS AND METHODS

Chickens. Specific-pathogen-free (SPF; Sunrise Farms, Catskill, NY) white leghorn chickens or their progenies were used in the experiments described below. Experimental procedures and animal care were performed in compliance with all applicable federal and institutional animal use guidelines both at Auburn University College of Veterinary Medicine and at the United States Department of Agriculture (USDA) Southeast Poultry Research Laboratory (SEPRL).

1) To determine PD_{50} and repeatability, SPF chickens were hatched and maintained in Horsfall-type isolators in biosafety level (BSL) 2 facilities. Challenge with HP AI was performed in BSL 3+ facilities at SEPRL. Feed and water were provided *ad libitum*.
2) To determine antibody persistence, effect of booster vaccination, and transfer of maternal immunity, a vaccinated and an unvaccinated breeder flock were established. The vaccinated flock consisted of 70 females and eight males. This flock was divided into two flocks (with or without booster vaccination) of 35 females and four males at 16 wk of age (see experimental design below). The unvaccinated flock consisted of the same number of birds. Each breeder flock was maintained in environmentally controlled BSL 2 floor pen facilities. Feed, temperature, and light were adjusted to meet the breeder's physiological requirements during the rearing and egg production periods.

RCA-free recombinant adenovirus vector expressing codon-optimized H5 HA gene. The RCA-free Ad-vectored AI vaccine encoding the AI H5 HA was developed essentially as previously described using a synthetic AI H5 HA gene from the A/tk/WI/68 (H5N9) strain with the codon optimized to match the tRNA pool found in chicken cells (15,16). Modifications included the use of AdHigh technology (12), which allows the homologous recombination between the Ad-backbone and a shuttle vector to occur in *E. coli* (12). In brief, the fragment containing the full-length synthetic H5 HA gene was inserted into the *Hin*dIII-*Bam*HI site of the newly developed shuttle plasmid pAdHigh (12) to generate the plasmid pAdHigh-TW68.H5 with the H5 HA gene under transcriptional control of the human cytomegalovirus immediate-early promoter. An RCA-free, E1/E3-defective Ad vector encoding the codon-optimized A/tk/WI/68 HA gene ($AdTW68.H5_{ck}$) was subsequently generated in PER.C6 cells, using the AdHigh system as described (12). The $AdTW68.H5_{ck}$ recombinant virus was validated by DNA sequencing. Titer (infectious units [ifu]/ml) was determined by the Adeno-X rapid titer kit (BD Clontech, Mountain View, CA).

Determination of repeatability. Determination of repeatability was performed by *in ovo* injection with 0.2 ml of vaccine suspension containing an escalating dose (10^5, 10^6, 10^7, 10^8, 10^9 ifu) of $AdTW68.H5_{ck}$. Each virus dose was applied to three replicates; each replicate consisted of 20 eggs. In order to stress the model, each replicate was inoculated with a different freshly thawed Ad batch and by a different person. Among the three persons, one was an expert (had performed *in ovo* vaccination for several years), another was a Ph.D.

student with moderate experience, and the third person was a new graduate student without prior experience (this person was trained *in ovo* injection just prior to performing an independent experiment). Total number of hatched chickens for each vaccine dose was as follows: 10^5 ifu, $n = 54$; 10^6 ifu, $n = 52$; 10^7 ifu, $n = 57$; 10^8 ifu, $n = 55$; 10^9 ifu, $n = 56$. Each group was subsequently divided into three subgroups (17–19/group) and placed in different Horsfall-type isolators. Thus, a total of 15 groups were established. An additional group without vaccination was included as the unvaccinated control ($n = 19$). Blood samples were obtained from all chicken groups by wing vein puncture on days 7, 18, 25, 32, and 39 after hatch. Individual serum samples were inactivated in a water bath at 56 C for 30 min, treated with receptor-destroying enzyme (3), and thus prediluted 1:4 before testing by HI as described (11) for antibodies against the A/turkey/WI/68 (H5N9) AI strain. Vaccine coverage was determined, and it was based on the number of antibody-positive chickens in each group. The vaccine accordance (VACC) or intrapotency test repeatability was assessed based on antibody titers due to the congruence of HI antibody titer and disease protection (9). Repeatability analysis within vaccine dose (VACC) utilizes the frequency of animals testing antibody positive (p^2), the frequency of animals testing negative (q^2), as well as the total number of replicates per vaccine dose group (N) according to the formula described by Goris *et al.* (2). According to Goris *et al.* (2), it is clear from the formula that high repeatability is achieved when the vaccination is either highly effective or ineffective because VACC is lowest (0.50) at $p = q = 0.5$.

Determination of PD_{50}. Fertile chicken eggs were injected *in ovo* with an increasing dose (10^5, 10^6, 10^7, 10^8, 10^9 ifu) of AdTW68.$H5_{ck}$ as described above. Each dose was injected into 20 fertile eggs (0.2 ml/egg) on day 18 of embryonation. Hatched chickens were placed in separate Horsfall-type isolation units. The total number of hatched chickens in each group was as follows: 10^5 ifu, $n = 15$; 10^6 ifu, $n = 17$; 10^7 ifu, $n = 14$; 10^8 ifu, $n = 18$; 10^9 ifu, $n = 15$. An additional group without vaccination was included as the unvaccinated control ($n = 17$). Challenge was performed at 42 days of age mainly as previously described (15) in a BSL 3+ facility by oropharyngeal instillation of $10^{6.5}$ embryo infective doses (EID_{50})/bird of the HP AI virus strain A/chicken/Queretaro/14588-19/95 (H5N2 (1)). The H5 HA of this challenge strain has 94% deduced amino acid sequence similarity with the H5 HA of the A/tk/WI/68 (H5N9) strain expressed from the Ad5 vector (GenBank accession nos. U79448 and U79456). Challenged birds were observed daily for mortality throughout 8 days. Mortality data were analyzed by logistic regression using SAS® PROC NLMIXED (Cary, NC). Degrees of freedom for the calculation of confidence intervals were adjusted to number of treatment groups minus number of fitted parameters as suggested by Schabenberger and Pierce (5).

Oropharyngeal swabs from individual birds were obtained for quantitation of AI RNA by quantitative reverse transcriptase-PCR (qRT-PCR) on days 3 and 5 after challenge, suspended in 1 ml of brain-heart infusion medium (Difco, Kansas City, MO), and stored at −70 C. RNA was extracted using the RNeasy mini kit (Qiagen Inc., Valencia, CA). qRT-PCR was performed with primers specific for type A influenza virus matrix RNA as described (8). Copy number of viral RNA was interpolated from the cycle thresholds using standard curves generated from known amounts of control A/chicken/Queretaro/95 RNA ($10^{1.0}$ to $10^{6.0}$ EID_{50}/ml).

Antibody persistence, effect of booster vaccination, and transfer of MtAb. Breeders of the vaccinated flocks were vaccinated *in ovo* at 18 days of embryonation with 300 µl of AdTW68.$H5_{ck}$ containing 1.5×10^9 ifu as previously reported (15,16). The vaccinated breeder flock was further divided into two flocks at 16 wk of age. One group received a booster vaccination (10^8 ifu/300 µl) intramuscularly at 16 wk of age, and the second group was not given the booster application. An unvaccinated control breeder flock was the control. Blood samples were collected from all breeders, starting at 55 days of age and at monthly intervals until 34 wk of age. Sera were tested for AI antibodies as described above. Fertile eggs were collected from all breeder flocks at 28 wk of age and incubated and hatched. Progeny chickens ($n = 15$) from breeders vaccinated *in ovo* only, from breeders vaccinated *in ovo* + IM boost ($n = 18$), as well as progenies ($n = 12$) from unvaccinated breeders were maintained in BSL 2 facilities, and blood samples were obtained at 3, 11, 20, 28, and 34 days of age. Sera were tested for anti-H5 HA (maternally derived) antibodies by HI as described above. HI titers detected in the groups were compared by ANOVA followed by a multiple comparisons posttest.

***In ovo* vaccination in progeny chickens with maternal immunity.** To assess possible interference between maternal immunity and active *in ovo* vaccination, chicken groups (30/group) were vaccinated *in ovo* with 4.33×10^{11} ifu/300 µl of AdTW68.$H5_{ck}$. Chicken groups were the progeny of breeders at 41 wk of age that had been either vaccinated *in ovo*, vaccinated *in ovo* + IM boost, or maintained as unvaccinated controls (described above). Blood was collected from the progeny chickens at 11, 20, 28, 34 days of age, and sera was tested by HI for the presence of anti-H5 antibodies. HI titers detected in the chicken groups were compared by ANOVA followed by a multiple comparisons posttest.

Mucosal vaccination in progeny chickens with maternal immunity. To assess possible interference between maternal immunity and active mucosal vaccination, chickens (18/group) were vaccinated either ocularly or by spray at 3 days old and boosted at 18 days old. These chickens originated either from unvaccinated breeders or from breeders that had been vaccinated *in ovo* and boosted intramuscularly with the Ad-vectored AI vaccine (described above). Ocular vaccination was performed with 100 µl AdTW68.$H5_{ck}$ per eye of vaccine suspension containing 1.3×10^{10} ifu. Spray vaccination was performed in a Spra-Vac® vaccination cabinet (Merial Select, Inc., Gainesville, GA) with a vaccine volume of 60 ml at the same concentration as used in the ocular vaccination. Additional chickens from each breeder group were maintained as untreated controls. Blood was collected from the progeny chickens at 17, 32, 42, and 59 days of age, and sera was tested by HI for the presence of anti-H5 antibodies. HI titers detected in the groups were compared by ANOVA followed by a multiple comparisons posttest.

RESULTS

Vaccine coverage. HI antibodies were detected in chickens vaccinated with 10^8 and 10^9 ifu on days 25, 32, and 39 of age. Only a few chickens inoculated with 10^7 (5/54) showed detectable antibodies on day 39 of age. Vaccine dosages $<10^7$ ifu did not elicit detectable antibody responses throughout the experimental period. Unvaccinated control birds maintained an antibody negative status. A dose-response kinetic was observed with highest antibody levels achieved by chickens inoculated with the highest vaccine dose (10^9 ifu). Vaccine coverage (number of antibody-positive birds) did not vary significantly ($P > 0.05$) between days 25, 32, and 39 of age. For example, groups vaccinated with 10^9 ifu showed percentages of antibody-positive birds on day 25 of age (three replicates) of 69% (11/16), 87% (13/15), and 100% (16/16) with an average of 85%. The variation in coverage between the groups is likely associated with the level of expertise of each of the individuals participating in the vaccination process (described above).

Intrapotency test repeatability. The values for VACC or intrapotency test repeatability are shown in Table 1. As seen in this table, highest VACC were obtained in the dose group 10^9 ifu with values varying between 0.69 and 0.71, indicating effective vaccination. Values for 10^8 ifu varied between 0.51 and 0.64. Values of 1, as seen at lower vaccine dosages, are based on the fact that the negative results (absence of a response) also had a high repeatability.

Protective dose 50%. Antibody titers detected in 29-day-old SPF chickens vaccinated *in ovo* with increasing doses 10^5, 10^6, 10^7, 10^8, 10^9 ifu of AdTW68.$H5_{ck}$ are shown in Fig. 1. The values obtained showed the same tendency as the results shown above; i.e., highest vaccine dosages (10^8 and 10^9 ifu) elicited the highest antibody levels and frequency of antibody-positive birds. However, the percentage of AI antibody-positive birds was lower: 61% (11/18) in the 10^8 and 50% (8/16) in the 10^9 groups.

The survival rate of chickens vaccinated with increasing vaccine dosage is shown in Fig. 2. Unvaccinated chickens showed 0% survival; all birds (17/17) had died by day 5 after challenge. In contrast, all vaccinated groups, even with the lowest vaccine dosage (10^5 ifu) showed some level of protection against HP AI challenge. Highest protection was observed in the groups receiving 10^8 or 10^9 ifu with 90% (16/18) and 88% (13/15) survival, respectively. Dose 10^7 ifu resulted in 74% (10/16) of birds surviving the challenge, followed by 41% (7/17) survival of dose 10^6, and 7% (1/15) survival of dose 10^5. The PD_{50} was calculated by logistic regression based on mortality, which declined with increasing vaccine dose. The PD_{50} (Fig. 3) was estimated to be $10^{6.55}$. The 95% confidence interval ranged from $10^{5.83}$ to $10^{7.27}$.

AI viral RNA of HP AI A/chicken/Queretaro/19/95 (H5N2) in challenged chickens determined by qRT-PCR in oropharyngeal swabs collected 3 and 5 days after challenge are shown in Fig. 4. AIV genomes were detected in all bird groups at 3 and 5 days after challenge without significant differences between days within each group. Birds vaccinated with 10^7 and 10^8 ifu showed significantly lower ($P < 0.05$) AI RNA concentrations in oropharyngeal swabs than birds vaccinated with lower vaccine doses or unvaccinated controls on day 3 after challenge (Fig. 4A). On day 5 after challenge, there was a tendency that showed higher vaccine dosage may reduce viral shedding (Fig. 4B). However, the differences did not reach statistical significance, which can be attributed to the reduced number of survivors, both in unvaccinated controls and in chickens vaccinated with the lowest vaccine dose.

Antibody persistence in AdTW68.H5$_{ck}$ *in ovo* vaccinated breeder hens. Anti-H5 antibody titers in breeders peaked at 12 wk of age (mean 4.6 $\log_2$), the plateau was maintained through 18 wk and slowly declined overtime, averaging 2.8 $\log_2$ at 34 wk of age (Fig. 5A). Chickens vaccinated *in ovo* + IM boost at 16 wk of age showed a significant increase ($P < 0.05$) of anti-H5 antibody titers at 21 wk of age (mean 8.4 $\log_2$) compared with *in ovo* only or unvaccinated controls. High antibody titers in *in ovo* + IM boost chickens were maintained through 34 wk of age (Fig. 5B). Unvaccinated breeder hens maintained an AI antibody negative status throughout the experimental period (not shown).

Anti-H5 MtAb in progeny chickens. Anti-H5 antibodies were detected in progeny chickens from AdTW68.H5$_{ck}$-vaccinated breeders (Fig. 6). Highest anti-H5 maternally derived antibodies (mean 7.2 $\log_2$) were detected in progenies from breeders that received an *in ovo* + IM boost vaccination. Mean antibody titers declined with time and achieved marginal levels at 34 days of age. Thirty-three percent (5/15) of chickens from breeders vaccinated *in ovo*-only showed antibody levels varying between 2 and 4 $\log_2$ at 3 days of age, while the rest remained antibody negative. With the exception of one bird, no antibodies were detected in this group (Fig. 6) on or after day 11 after hatch. Progeny chickens from unvaccinated controls maintained an AI antibody negative status throughout the experimental period (not shown).

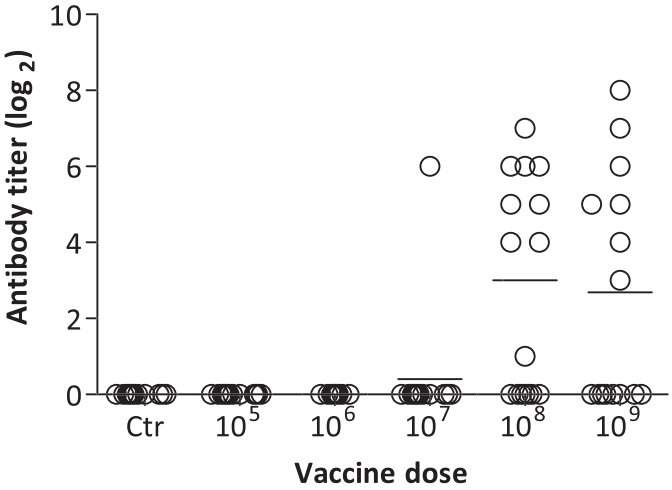

Fig. 1. Individual HI anti-H5 antibody titers ($\log_2$) detected in 29-day-old SPF chickens (14–18/group) vaccinated *in ovo* with increasing doses (10^5, 10^6, 10^7, 10^8, 10^9 ifu) of AdTW68.H5$_{ck}$ prior to HP AIV challenge.

Anti-H5 antibody in progeny chickens actively immunized *in ovo*. Progeny chickens from breeders vaccinated with AdTW68.H5$_{ck}$ *in ovo* + IM boost showed homogeneous anti-H5 antibody levels averaging 6.4 $\log_2$ on day 11 after hatch. As seen in Fig. 7, these antibody levels steadily declined through day 34 of age. In contrast progenies from both breeders vaccinated *in ovo* only and unvaccinated controls increased their antibody levels significantly ($P < 0.05$) after day 20 of age. Thus, high levels of MtAb seemed to interfere with AdTW68.H5$_{ck}$ *in ovo* vaccination.

Anti-H5 antibody in progeny chickens actively immunized by mucosal routes. As seen in Fig. 8A both ocularly and spray-vaccinated chickens originating from unvaccinated breeders develop antibodies against AI (levels increased significantly [$P < 0.05$] compared with unvaccinated controls). In ocularly and spray-vaccinated groups as well as unvaccinated chickens, the MtAb declined steadily and similarly (without significant differences between groups) throughout the experimental period and never increased antibody levels (Fig. 8B). Thus, high levels of MtAb seemed to interfere with AdTW68.H5$_{ck}$ mucosal vaccination.

DISCUSSION

Serum HI antibody titers in poultry have been reported to be strongly correlated with protection against HP AI (9). Thus, in the

Table 1. Repeatability analysis within vaccine dose (VACC) using the frequency of animals testing antibody positive as well as the frequency of animals testing negative.[A]

	Day 0		Day 25		Day 32		Day 39	
$\log_{10}$	Frequency (+)	VACC	Frequency (+)	VACC	Frequency (+)	VACC	Frequency (+)	VACC
5	0.00	1.00	0.00	1.00	0.00	1.00	0.00	1.00
6	0.00	1.00	0.00	1.00	0.00	1.00	0.00	1.00
7	0.00	1.00	0.00	1.00	0.00	1.00	0.25	0.84
8	0.00	1.00	0.69	0.64	0.44	0.54	0.44	0.51
9	0.00	1.00	0.69	0.69	0.63	0.71	0.75	0.69

[A]VACC calculated from three replicates (cages; each $n = 15$) per dose × day combination using the formula by Goris *et al.* (2). Any antibody level ($\log_2$) >0 was considered a positive reaction.

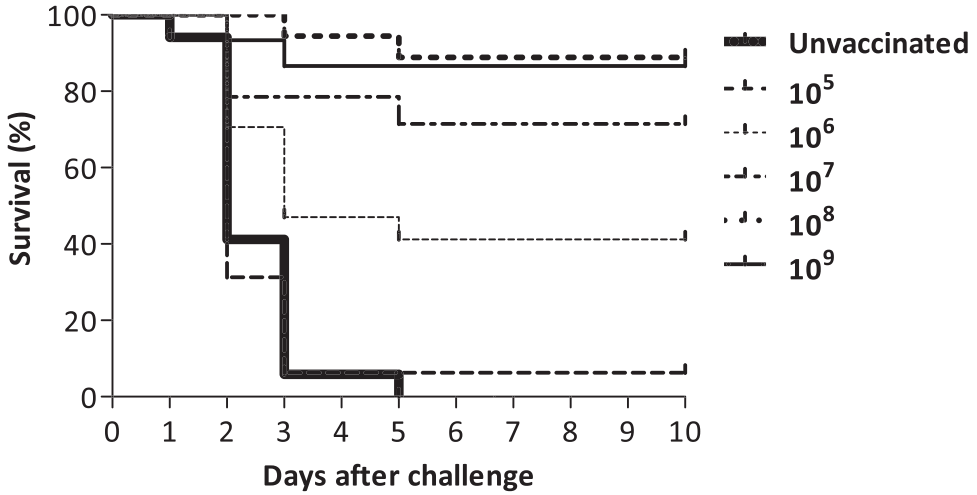

Fig. 2. Survival rate of SPF chickens (14–18/group) vaccinated *in ovo* with increasing dose of AdTW68.H5$_{ck}$ and challenged with $10^{6.5}$ EID$_{50}$/bird of HP AIV A/chicken/Queretaro/14588-19/95 (H5N2) at 42 days of age. Highest protection was observed in the groups receiving 10^8 or 10^9 ifu with 90% (16/18) and 88% (13/15) survival, respectively.

current study vaccine coverage and intrapotency test repeatability were based on anti-H5 HI antibody levels detected in the chickens. We observed variation between replicates in vaccine coverage that was consistent with the expertise of the individuals inoculating the eggs. Still the average in vaccine coverage of three replicates was 85%. Such variation would likely be reduced by using automated *in ovo* injectors as routinely used by the industry. The intrapotency test repeatability or VACC, which considers both positive as well as negative values, varied between 0.69 and 0.71. Even though these values indicate effective vaccination, they were rather low, which may also be explained by the differences in the expertise of the vaccinators.

The challenge study aimed at determining the PD$_{50}$ was performed using $10^{6.5}$ EID$_{50}$ of HP AI A/chicken/Queretaro/19/95 (H5N2) per bird. This dose was rather high as the lethal dose 50% of this strain has been determined to be 10^3 EID$_{50}$. Indeed all unvaccinated birds had died by day 5 after inoculation. Based on dose and mortality, the PD$_{50}$ was determined to be $10^{6.6}$ ifu. This dosage seems rather high when compared to replicating live vaccines

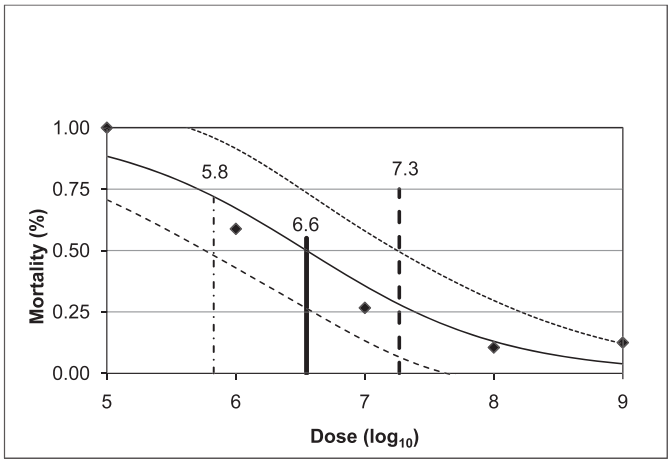

Fig. 3. (PD$_{50}$) based on mortality *vs.* dose. Logistic regression adjusted to *n* of treatment groups minus *n* of fitted parameters as suggested by Schabenberger and Pierce (2003). CL = confidence limit. The PD$_{50}$ was estimated to be $10^{6.55}$. The 95% confidence interval ranged from $10^{5.83}$ to $10^{7.27}$.

used routinely by the poultry industry against other viral pathogens. However, Ad-vector vaccine production in the PER C6 cell line can potentially produce 5×10^{15}ifu (several million doses over the PD$_{50}$) in a few days (12), and the safety of a nonreplicating virus provides remarkable advantages over replicating viruses.

The results of the challenge study aimed at determining the PD$_{50}$ clearly indicate that the antibody response induced by the recombinant vaccine is not exclusively responsible for protection against AI. Recent results have shown that RCA-free Ad-vectored vaccines encoding the AI HA gene elicit effector, memory, and effector memory CD8+ T lymphocyte responses in chickens (7). In the current study several chickens that did not develop detectable antibody levels (Fig. 1) were effectively protected against HP AI challenge (Fig. 2). These results emphasize the importance of T-cell responses after Ad-mediated vaccination (7) as the protection achieved by these antibody negative animals was likely associated with T lymphocyte responses. At the same time, they indicate that measurement of the potency of Ad-vectored vaccines should not only be based on antibody responses.

In the present study only higher doses (10^7, 10^8, 10^9 ifu) of the Ad-vectored vaccine reduced but not eliminated viral shedding as determined by AI RNA concentration in oropharyngeal swabs. This finding was rather disappointing because the risk of virus spread within or between flocks would not be completely eliminated using these vaccine dosages. In a previous study we vaccinated chickens intramuscularly with 1.1×10^{11} ifu at day 28 of age with an Ad vector expressing the H7 HA gene of the AI strain A/chicken/NY/13142-5/94. AI RNA of the challenge AI strain (A/chicken/Chile/4957/02 [H7N3]) was detectable in oropharyngeal swabs of only 1 of 11 immunized chickens but in almost all (8/11) nonimmunized control chickens at 2 days after challenge (16). Therefore, a dosage higher than 10^9 ifu would be necessary to considerably reduce or even eliminate viral shedding.

In initial studies we followed antibody persistence in chickens immunized *in ovo* with AdTW68.H5 through 40 days of age (16). The current results indicate that antibody levels continue to increase achieving a plateau at 12 wk of age. Antibodies declined after 18 wk of age, but antibody persisted in some birds through 34 wk of age. This long-lasting antibody persistence is an excellent result that we cannot explain at this time point. We know that the vaccine virus is replication deficient and that naïve birds do not seroconvert when

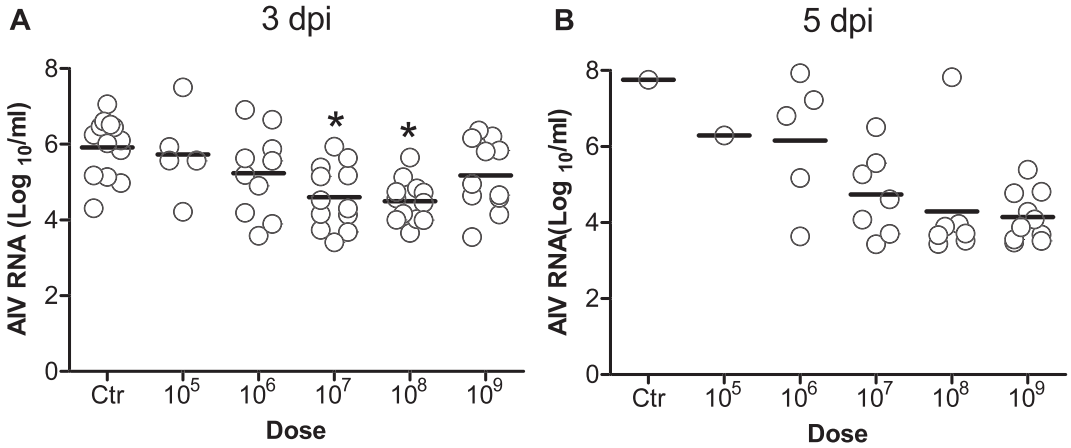

Fig. 4. Viral shedding determined in SPF chickens (16/group), which were vaccinated *in ovo* with 10^5, 10^6, 10^7, 10^8, or 10^9 ifu of AdTW68.H5$_{ck}$ and challenged with $10^{6.5}$ EID$_{50}$/bird of HP AIV A/chicken/Queretaro/14588-19/95 (H5N2) at 42 days of age. Viral shedding determined by qRT-PCR in oropharyngeal swabs at (A) 3 or (B) 5 days postinoculation (dpi). (*) indicates significant difference ($P < 0.05$) *vs.* unvaccinated control (Ctr; Kruskal-Wallis and Dunn's tests). No significant differences were achieved at 5 days after challenge due to the reduced number of unvaccinated survivals on this day.

raised in the same cage with vaccinated birds. Thus, the virus is not spreading between birds and does not assist in explaining the long-lasting antibody responses. We have recently attempted to detect the Ad-vector DNA by qPCR in newly hatched chickens vaccinated *in ovo*. We were able to detect the virus at 2 days after hatch, but all birds were negative by 9 days after hatch (14). Thus the virus seems to be cleared from the host rather quickly. The enduring antibody response may be attributed to a robust activation of the immune system, which carries on after the vaccine disappears.

It is very interesting that IM booster vaccination with the same vaccine construct increases the antibody responses significantly. We had previously shown that successive vaccination with Ad-vectors expressing the H5 and the H7 genes successfully induces strong antibody responses against both AI proteins (16). Thus, in contrast to fowlpox-vectored vaccines (10), preexisting immunity to the vector does not seem to affect booster vaccination with Ad-vectored vaccines. In the current study IM boost elicited a significant increase of specific antibody levels that were maintained throughout the experimental period (34 wk of age). From an applied perspective, these results indicate that IM boosting of hens (layers or breeders), which have been primed by the *in ovo* route with Ad-vectored vaccines, would provide protection throughout most of the production period.

Maternally derived antibodies represent an integral part in disease prevention in young chickens. In the current study, we evaluated the transfer of MtAb from breeder hens that were either singly immunized *in ovo* with AdTW68.H5$_{ck}$ or received an IM booster vaccination at 16 wk of age. As expected, specific H5 antibodies were effectively transferred to progeny chickens of Ad-vectored vaccinated breeders. The level of MtAb in the progenies was consistent with the levels detected in the breeders; i.e., breeders that had been boosted transferred higher concentrations of antibodies to their offspring. MtAb declined with time and achieved marginal levels by 34 days of age, similar to MtAb resulting from other vaccines routinely used in the poultry industry. Chickens with maternal immunity were not challenged in the current study, but because specific antibodies are associated with protection (9), we would anticipate that they should be protected against homologous challenge at least during the first 20 days of life.

Maternally derived antibodies have been shown to interfere with active vaccination (reviewed by (6)). The current results showed that progeny chickens with high maternal immunity (originating from breeders primed and boosted with AdTW68.H5$_{ck}$) never increased their antibody levels after *in ovo* or mucosal (ocular or spray) vaccination. Instead, they steadily declined at the same pace as progeny chickens that were not immunized (described above). In

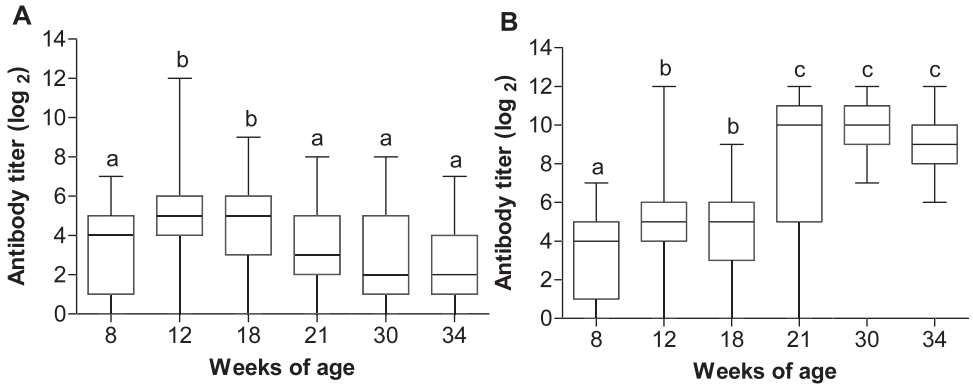

Fig. 5. Anti-H5 antibody titers detected in SPF white leghorn hens vaccinated either (A) *in ovo* only ($n = 35$) or (B) *in ovo* + IM boost ($n = 35$) at 16 wk of age with 10^8 ifu/300 µl of AdTW68.H5$_{ck}$. Boxes: 25th percentile, median, 75th percentile; Whiskers: Minimum & Maximum. Control hens ($n = 10$) maintained a negative AI antibody status (not shown). Different letters indicate significant differences ($P < 0.05$).

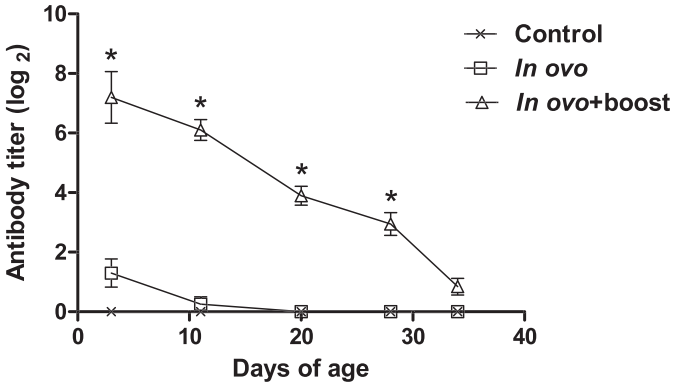

Fig. 6. Anti-H5 antibodies in progeny chickens from breeders vaccinated with AdTW68.H5$_{ck}$ *in ovo* (n = 15), vaccinated *in ovo* + IM boost (n = 15), or unvaccinated controls (n =10). Sera collected at 3, 11, 20, 28, 34 days of age, and anti-H5 antibodies measured by HI test. Bars: SEM = standard error of the mean. (*) Significant difference ($P <$ 0.001) *vs.* controls (two-way ANOVA followed by Bonferroni posttest).

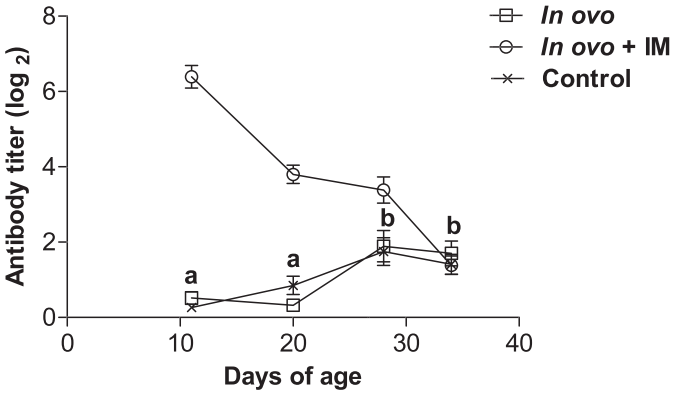

Fig. 7. Anti-H5 antibodies in progeny chickens from breeders vaccinated with AdTW68.H5$_{ck}$ *in ovo, in ovo* + boost, or unvaccinated breeders. Progeny chickens were vaccinated *in ovo* with 4.3×10^{11} ifu/ 300 µl of AdTW68.H5$_{ck}$. Bars: SEM = standard error of the mean. A significant increase ($P < 0.05$) in anti-H5 antibodies was detected in chickens originating both from breeders vaccinated *in ovo* only (different letters) and unvaccinated controls (not indicated). In contrast, no increase in antibody levels was detected in progeny chickens from breeders receiving a booster vaccination, i.e., their levels steadily declined throughout the experimental period.

contrast, both negative control progeny chickens (from naïve breeders) as well as the offspring from breeders that were vaccinated only once (*in ovo*) increased their antibody levels significantly following *in ovo* vaccination. A similar result was obtained when vaccinating maternal antibody-positive chickens via mucosal routes. These results indicate that high levels of maternally derived antibodies actively interfered with Ad vaccination.

It is interesting to notice that *in ovo* vaccinated breeders responded to the IM booster vaccination in spite of the presence of specific antibodies. In contrast, progenies with high levels of specific antibodies did not respond to *in ovo* vaccination. These apparently contradictory results may be explained by the different antibody levels (~8 log $_2$ in the progenies *vs.* ~4 log $_2$ in the hens at the time of booster vaccination), by the route of vaccination (IM used to booster adult hens *vs. in ovo* or ocular used in progeny chickens), and by the maturity of the immune system (adult *vs.* 18-day-old embryo or 3-day-old chicken).

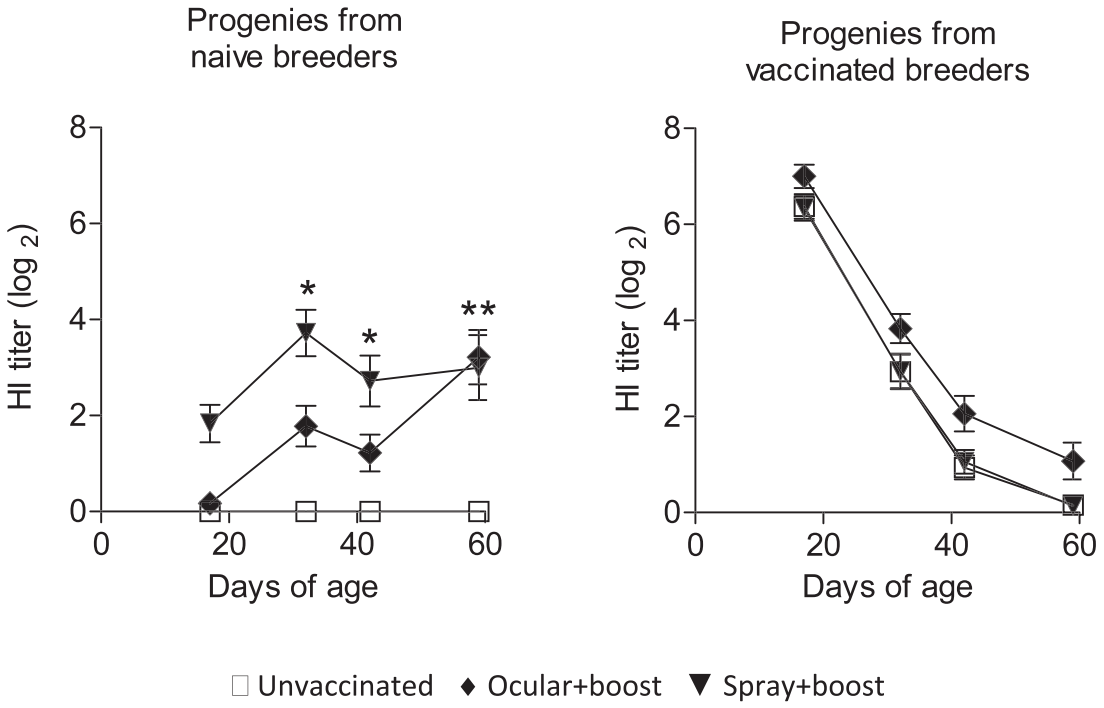

Fig. 8. HI antibodies detected in chickens (18/group) vaccinated with AdTW68.H5$_{ck}$ at 3 days old and boosted at 18 days old either ocularly or by spray. These chickens originated either from (A) unvaccinated breeders or from (B) breeders subjected to *in ovo* and IM boost with AdTW68.H5$_{ck}$. (A) Both ocularly and spray-vaccinated progeny chickens from unvaccinated breeders develop antibodies against AI (levels increased significantly [$P < 0.05$] compared with unvaccinated controls). (*) indicates significant difference compared with control (two-way ANOVA followed by Bonferroni posttest).(B) Active antibody responses were neither detected in vaccinated nor in unvaccinated progenies from vaccinated breeders; instead MtAb declined steadily in all groups throughout the experimental period without significant differences between the groups.

REFERENCES

1. Garcia, A., H. Johnson, D. K. Srivastava, D. A. Jayawardene, D. R. Wehr, and R. G. Webster. Efficacy of inactivated H5N2 influenza vaccines against lethal A/chicken/Queretaro/19/95 infection. Avian Dis. 42:248–256. 1998.

2. Goris, N., P. Merkelbach-Peters, V. I. Diev, D. Verloo, V. M. Zakharov, H.-P. Kraft, and K. D. Clercq. European Pharmacopoeia foot-and-mouth disease vaccine potency testing in cattle: between test variability and its consequences. Vaccine 25:3373–3379. 2007.

3. Palmer, D. F., M. T. Coleman, W. D. Dowdle, and G. C. Schild. Advanced laboratory techniques for influenza diagnosis. Immunology series no. 6. United States Department of Health, Education, and Welfare, Public Health Service, Centers of Disease Control, Atlanta, GA. pp. 51–52. 1975.

4. Park, K. S., J. Lee, S. S. Ahn, Y. H. Byun, B. L. Seong, Y. H. Baek, M. S. Song, Y. K. Choi, Y. J. Na, I. Hwang, Y. C. Sung, and C. G. Lee. Mucosal immunity induced by adenovirus-based H5N1 HPAI vaccine confers protection against a lethal H5N2 avian influenza virus challenge. Virology 395:182–189. 2009.

5. Schabenberger, O., and F. J. Pierce, eds. Contemporary statistical models for the plant and soil sciences. CRC Press, Boca Raton, FL. 2003.

6. Schijns, V. E. J. C., J. Sharma, and I. Tarpey. Practical aspects of poultry vaccination. In: Avian immunology. F. Davison, B. Kaspers, and K. A. Schat, eds. Elsevier Ltd., London. pp. 373–393. 2008.

7. Singh, S., H. Toro, D. Tang, W. E. Briles, L. M. Yates, R. T. Kopulos, and E. W. Collisson. Non-replicating adenovirus vectors expressing avian influenza virus hemagglutinin and nucleocapsid proteins induce chicken specific effector, memory and effector memory CD8+ T lymphocytes. Virology 405:62–69. 2010.

8. Spackman, E., D. A. Senne, T. J. Myers, L. L. Bulaga, L. P. Garber, M. L. Perdue, K. Lohman, L. T. Daum, and D. L. Suarez. Development of a real-time reverse transcriptase PCR assay for type A influenza virus and the avian H5 and H7 hemagglutinin subtypes. J. Clin. Microbiol. 40:3256–3260. 2002.

9. Suarez, D. L., and S. Schultz-Cherry. Immunology of avian influenza virus: a review. Dev. Comp. Immunol. 24:269–283. 2000.

10. Swayne, D. E., J. R. Beck, and N. Kinney. Failure of a recombinant fowl poxvirus vaccine containing an avian influenza hemagglutinin gene to provide consistent protection against influenza in chickens pre-immunized with a fowl pox vaccine. Avian Dis. 44:132–137. 2000.

11. Swayne, D. E., D. A. Senne, and D. L. Suarez. Avian influenza. In: A laboratory manual for the isolation, identification and characterization of avian pathogens, 5th ed. L. Dufour-Zavala, ed. American Association of Avian Pathologists, Athens, GA. pp. 128–134. 2008.

12. Tang, D. C., J. Zhang, H. Toro, Z. Shi, and K. R. v. Kampen. Adenovirus as a carrier for the development of influenza virus-free avian influenza vaccines. Expert Rev. Vaccines 8:469–481. 2009.

13. Toro, H., F. van Ginkel, D. C. Tang, B. Schemera, S. Rodning, and J. Newton. Avian influenza vaccination in chickens and pigs with RCA-free human recombinant adenovirus 5. Avian Dis. 54(Suppl. 1):224–231. 2010.

14. Toro, H., K. Minc, C. Bowman, S. Gulley, D. C. Tang, and J. Hathcock. Avian influenza vaccination with non-replicating adenovirus vector: target tissues in chicken embryo (poster session). In: Annual Meeting American Association of Avian Pathologists. Atlanta, GA. August 1–4, 2010.

15. Toro, H., D. C. Tang, D. L. Suarez, M. J. Sylte, J. Pfeiffer, and K. R. Van Kampen. Protective avian influenza in ovo vaccination with non-replicating human adenovirus vector. Vaccine 25:2886–2891. 2007.

16. Toro, H., D. C. Tang, D. L. Suarez, J. Zhang, and Z. Shi. Protection of chickens against avian influenza with non-replicating adenovirus-vectored vaccine. Vaccine 26:2640–2646. 2008.

17. Ungchusak, K., P. Auewarakul, S. F. Dowell, R. Kitphati, W. Auwanit, P. Puthavathana, M. Uiprasertkul, K. Boonnak, C. Pittayawonganon, N. J. Cox, S. R. Zaki, P. Thawatsupha, M. Chittaganpitch, R. Khontong, J. M. Simmerman, and S. Chunsutthiwat. Probable person-to-person transmission of avian influenza A (H5N1). N. Engl. J. Med. 352:333–340. 2005.

ACKNOWLEDGMENTS

The authors wish to thank Cassandra Breedlove, Frederik van Ginkel, Lisa Parsons, and Rodrigo Gallardo at Auburn University, Suzanne DeBlois at SEPRL, Jianfeng Zhang, Tsungwei Feng, and Zhongkai Shi at Vaxin Inc. for technical assistance during this work. This work was funded by USDA Avian Influenza Coordinated Agricultural Project and the Small Business Research Funding Opportunities, National Institutes of Health.

AVIAN DISEASES 55:43–47, 2011

Avian Influenza Mucosal Vaccination in Chickens with Replication-Defective Recombinant Adenovirus Vaccine

Haroldo Toro,[AD] David L. Suarez,[B] De-chu C. Tang,[C] Frederik W. van Ginkel,[A] and Cassandra Breedlove[A]

[A]Department of Pathobiology, Auburn University College of Veterinary Medicine, 264 Greene Hall, Auburn, AL 36830
[B]United States Department of Agriculture, Southeast Poultry Research Laboratory, 934 College Station Road, Athens, GA 30605
[C]Vaxin Inc., 1500 1st Avenue North, Birmingham, AL 35203

Received 8 September 2010; Accepted and published ahead of print 15 November 2010

SUMMARY. We evaluated protection conferred by mucosal vaccination with replication-competent adenovirus-free recombinant adenovirus expressing a codon-optimized avian influenza (AI) H5 gene from A/turkey/WI/68 (AdTW68.H5$_{ck}$). Commercial, layer-type chicken groups were either singly vaccinated ocularly at 5 days of age, singly vaccinated via spray at 5 days of age, or ocularly primed at 5 days and ocularly boosted at 15 days of age. Only chickens primed and boosted via the ocular route developed AI systemic antibodies with maximum hemagglutination inhibition mean titers of 3.9 $\log_2$ at 32 days of age. In contrast, single vaccination via the ocular or spray routes maintained an antibody status similar to unvaccinated controls. All chickens (16/16) subjected to ocular priming and boosting with AdTW68.H5$_{ck}$ survived challenge with highly pathogenic AI virus A/chicken/Queretaro/14588-19/95 (H5N2). Single ocular vaccination resulted in 63% (10/16) of birds surviving the challenge followed by a 44% (7/16) survival of single-sprayed vaccinated birds. Birds vaccinated twice via the ocular route also showed significantly lower ($P < 0.05$) AI virus RNA concentrations in oropharyngeal swabs compared to unvaccinated–challenged controls.

RESUMEN. Vacunación en las mucosas contra la influenza aviar en pollos con una vacuna elaborada con un adenovirus recombinante con replicación defectuosa.

Se evaluó la protección conferida por la vacunación en las mucosas con un adenovirus recombinante libre de adenovirus competentes para la replicación que expresaba el gene H5 optimizado en sus codones, del virus de la influenza aviar A/pavo/WI/68 (AdTW68.H5ck). Grupos de aves tipo ponedoras comerciales fueron vacunadas a) ocularmente con una dosis simple a los 5 días de edad, b) vacunadas por aerosol con una dosis a los 5 días de edad, c) vacunadas por vía ocular a los 5 días y con una vacunación ocular de refuerzo a los 15 días de edad. Solamente los pollos vacunados y revacunados por vía oftálmica desarrollaron anticuerpos sistémicos contra la influenza aviar mostrando los mayores títulos medios por inhibición de la hemaglutinación de 3.9 $\log_2$ a los 32 días de edad. En contraste, con la vacunación con una sola aplicación a través de la ruta ocular o por aerosol se mantuvieron niveles de anticuerpos similares a los controles no vacunados. Todos los pollos (16/16) sometidos a la primo vacunación y refuerzo por vía ocular con el virus AdTW68.H5ck sobrevivieron al desafío con el virus de influenza aviar altamente patógeno A/pollo/Querétaro/14588-19/95 (H5N2). La vacunación ocular con una aplicación resultó en que el 63% (10/16) de las aves sobrevivientes al desafío seguido de un 44% (7/16) de supervivencia de las aves vacunadas con una sola aplicación por aspersión. Las aves vacunadas dos veces por vía oftálmica también mostraron concentraciones menores de ARN del virus de la influenza aviar en los hisopos orofaríngeos que fueron significativamente menores ($P < 0.05$) en comparación con los controles no vacunados y desafiados.

Key words: adenovirus, avian influenza virus, chickens, recombinant vaccine

Abbreviations: Ad = adenovirus serotype 5; AI = avian influenza; BSL = biosafety level; EID_{50} = embryo infective doses; HA = hemagglutinin; HG = Harderian gland; HI = hemagglutination inhibition; HP = highly pathogenic; IgA = immunoglobulin A; IgG = immunoglobulin G; IL-6 = interleukin-6; qRT-PCR = quantitative reverse transcriptase–polymerase chain reaction; RCA = replication competent adenovirus; rNDV = recombinant Newcastle disease virus; RT = reverse transcriptase; SEPRL = Southeast Poultry Research Laboratory; vp = viral particles; VSV = vesicular stomatitis virus

Highly pathogenic (HP) avian influenza (AI) viruses belonging to the H5 or H7 subtypes threaten the world poultry industry and are potentially zoonotic agents with a pandemic threat for humans (23). We previously reported that protective immunity against AI can be elicited in chickens in a single-dose regimen by *in ovo* vaccination with a replication-competent adenovirus (RCA)-free human adenovirus serotype 5 (Ad) vector encoding either the AI virus H5 (AdTW68.H5) or H7 (AdCN94.H7) hemagglutinins (HA). Vaccinated chickens were protected against HPAI homologous virus challenges (21,22). Successful results have also been reported with Ad-vectored AI vaccines in mice (11). The use of a synthetic AI H5 gene with codons optimized to match the chicken tRNA pool is more immunogenic than is its cognate counterpart without codon optimization (22). Thus, propagation of influenza virus during recombinant Ad-vector vaccine production is not required. We have shown that chickens vaccinated *in ovo* with AdTW68.H5, and subsequently vaccinated intramuscularly with AdCN94.H7 after hatch, develop antibodies against both the H5 and H7 HA proteins. This result suggests that pre-existing Ad immunity in chickens does not significantly interfere with the potency of Ad-vectored vaccines. Similarly, simultaneous *in ovo* vaccination with AdTW68.H5 and AdCN94.H7 also elicits robust hemagglutination inhibition (HI) antibody levels to both H5 and H7 AI strains (20), allowing the adoption of an immunization strategy with a broad antigen repertoire. In addition to *in ovo* injection, ocular administration of Ad expressing the H5 gene of AI elicits specific serum antibodies, specific immunoglobulin A (IgA) responses in lachrymal fluids, and increased interleukin-6 (IL-6) expression in Harderian gland-derived lymphocytes (24). Similar results were obtained more recently in chickens vaccinated via spray with the Ad construct vectoring the H7 gene. Spray-vaccinated chicken groups showed higher specific IgA levels in tear fluids on day 10 of age (9 days postvaccination). IgA levels declined with time in singly vaccinated chickens. Chickens

[D]Corresponding author. E-mail: torohar@auburn.edu

receiving a booster spray vaccination on day 16 of age showed an increase of specific IgA on day 30 of age. Spray-vaccinated chickens also displayed increased IL-6 in paraocular lymphocytes. However, these chickens did not show detectable antibody levels in the sera (20). A natural follow-up of these studies was to evaluate protection against HPAI challenge conferred by mucosal vaccination with RCA-free Ad expressing a codon-optimized H5 gene.

MATERIALS AND METHODS

Chickens. One-day-old commercial layer chickens (Hy-line, Mansfield, GA) were used for mucosal immunization experiments. Chickens were maintained in Horsfall-type isolators in biosafety level (BSL) 2 facilities until 40 days of age and moved to BSL 3+ facilities at the United States Department of Agriculture, Agriculture Research Service, Southeast Poultry Research Laboratory (SEPRL) for challenge. Feed and water were provided *ad libitum*. Experimental procedures and animal care were performed in compliance with all applicable federal and institutional animal use guidelines at both Auburn University College of Veterinary Medicine and at SEPRL.

RCA–free recombinant adenovirus vector expressing codon-optimized H5 gene. The Ad-vectored AI vaccine encoding the AI H5 glycoprotein of A/turkey/WI/68 (H5N9) was developed, essentially, as previously described (21,22). Modifications include the use of Ad_{high} technology (19). In brief, RCA-free Ad encoding the AI H5 protein was developed using a codon-optimized H5 gene. The fragment containing the full-length H5 gene was inserted into the *Hind*III-*Bam*HI site of the newly developed shuttle plasmid pAd_{high} (19) to generate the plasmid pAd_{high}-H5 with the H5 gene under transcriptional control of the human cytomegalovirus immediate-early promoter. RCA-free, E1/E3-defective Ad-vector with the codon-optimized AI gene ($AdTW68.H5_{ck}$) was subsequently constructed in *Escherichia coli* by recombination following cotransfection of pAd_{high}-H5 with the Ad backbone plasmid pJM17, as described (19). The RCA-free Ad-vector encoding the H5 protein was subsequently packaged in human PER.C6 cells. The $AdTW68.H5_{ck}$ recombinant virus was validated by DNA sequencing. Ad viral particles (vp) were determined by quantitative PCR (qPCR), as described, except a subfragment of the Ad fiber gene was amplified using the Taqman technology (8).

Protection induced by mucosal delivery. Chickens were divided into four groups ($n = 16$/group) and vaccinated with $AdTW68.H5_{ck}$ as follows. Group 1 was vaccinated by eye-drop on day 5 of age with 200 μl (100 μl in each eye) containing 2×10^8 vp; group 2 was vaccinated ocularly at 5 days and revaccinated via the same route on day 15 of age using the same vaccine dose as in group 1; and group 3 was vaccinated via spray at 5 days old. In previous experiments, we have used a commercial spray cabinet (20) that provides a droplet size of 120–150 μm. In the current study, we used a fog electric atomizer sprayer (Farm Tek, Dyersville, AL) that provides ultra low volume mist, 10–46 μm droplet size, with an average droplet of 20 μm. We suspended 10 ml of $AdTW68.H5_{ck}$ vaccine (containing 1×10^8 vp/ml) in 20 ml of Dulbecco's phosphate-buffered saline (Gibco/Invitrogen, Grand Island, NY) and sprayed the complete volume (30 ml) onto 16 chickens that had been placed in an open plastic box (length: 47 cm × width: 43 cm × depth: 20 cm). The spraying procedure lasted approximately 10 sec and ended with the chickens being visibly damp. In previous studies, we have used an empty Ad-vector or an Ad-vector encoding an irrelevant protein in negative control chickens, and we demonstrated that neither specific antibody nor T cell responses are generated (14,21). Thus, in this study, an unvaccinated group of chickens (group 4) was used as the negative control.

Blood samples were obtained from all chicken groups by wing vein puncture on days 9, 20, 32, and 40 after the first vaccination (5 days of age). Individual serum samples were inactivated in a water bath at 56 C for 30 min, treated with receptor destroying enzyme (9) and thus prediluted 1:4, and tested by HI as described (18) for antibodies against the homologous A/turkey/WI/68 (H5N9) AI strain. HI titers between groups were compared by one-way analysis of variance followed by the Tukey multiple comparison test.

Challenge was performed at 42 days of age, mainly as previously described (21), in a BSL 3+ facility by oropharyngeal instillation of $10^{6.5}$ embryo infective doses (EID_{50})/bird of HPAI virus strain A/chicken/Queretaro/14588-19/95 (H5N2) (2). This challenge dose is equivalent to 1000 lethal $dose_{50}$, and the H5 of this challenge strain has 94% deduced amino acid sequence similarity with the HA of the A/turkey/Wisconsin/68 (H5N9) strain expressed from the Ad vector (GenBank accessions U79448 and U79456). Challenged birds were observed daily for morbidity and mortality throughout an experimental period of 10 days. Oropharyngeal swabs from individual birds were obtained for quantitation of AI genomes by quantitative RT-PCR at days 3 and 5 after challenge, suspended in 1 ml of brain heart infusion medium (Difco, Kansas City, MO), and stored at −70 C. RNA was extracted by using the MagMax AI/ND Viral RNA Isolation kit (Ambion Inc., Valencia, CA). qRT-PCR was performed with primers specific for type A influenza virus matrix RNA as described (15). The copy number of viral RNA was interpolated from the cycle thresholds by using standard curves generated from known amounts of control A/chicken/Queretaro/14588-19/95 RNA ($10^{1.0}$–$10^{6.0}$ EID_{50}/ml).

RESULTS

Chickens primed on day 5, and boosted on day 15 of age via the ocular route, developed HI serum antibody responses against the H5 encoded by the Ad-vectored vaccine (Fig. 1). Serum antibody levels achieved a maximal mean titer of 3.9 $\log_2$ at 32 days of age. These antibody titers were significantly higher ($P < 0.05$) than the antibody levels elicited in chickens vaccinated once, either ocularly or by spray, as well as in unvaccinated controls. As seen in Fig. 1, single vaccination via the ocular or spray routes did not increase antibody levels significantly ($P > 0.05$) as compared to unvaccinated controls.

The survival rate of vaccinated and unvaccinated chickens is shown in Fig. 2. Nineteen percent (3/16) of unvaccinated–challenged chickens had survived by day 6 after challenge. One-hundred percent of chickens (16/16) subjected to ocular priming and subsequent ocular boosting with $AdTW68.H5_{ck}$ survived the challenge. Single ocular vaccination resulted in 63% (10/16) of birds surviving the challenge followed by a 44% (7/16) survival of single-sprayed vaccinated birds.

AI viral RNA of HPAI A/chicken/Queretaro/14588-19/95 (H5N2) in challenged chickens, quantitatively determined by real time RT-PCR in oropharyngeal swabs collected 3 and 5 days after challenge, are shown in Fig. 3. AI virus genomes were detected in all bird groups at 3 days and 5 days after challenge without significant differences between days within each group. Birds vaccinated twice via the ocular route showed significantly lower ($P < 0.05$) AI RNA concentrations in oropharyngeal swabs compared to the unvaccinated–challenged controls. Chickens vaccinated once ocularly also showed significantly lower AI RNA concentrations compared to the unvaccinated controls on day 3, but no statistical significance was achieved on day 5 after challenge. Finally, single-spray vaccinated chickens showed AI RNA concentrations similar to the unvaccinated–challenged controls.

DISCUSSION

We previously demonstrated that protective immunity against AI can be elicited in chickens in a single-dose regimen by *in ovo* vaccination with a RCA-free Ad-vector encoding either the AI virus H5 or H7 hemagglutinins. Vaccinated chickens were protected

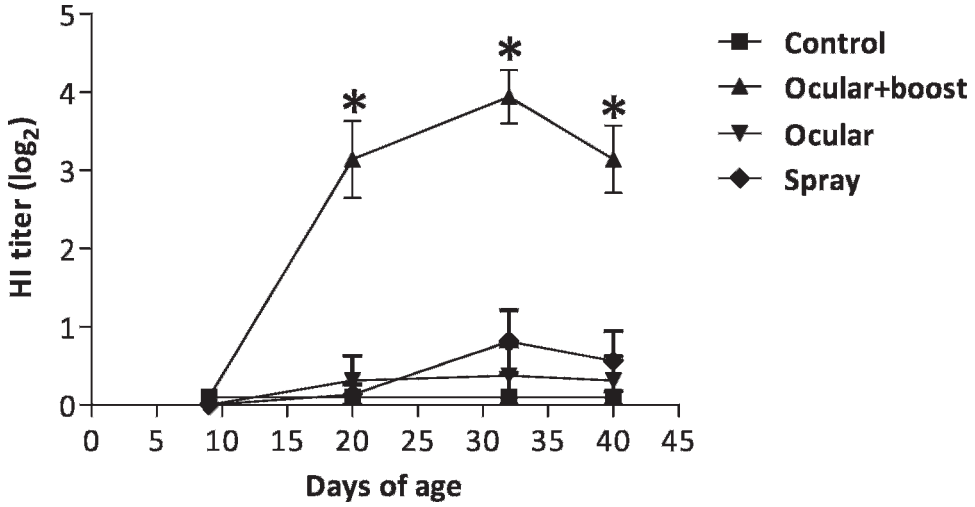

Fig. 1. HI antibody titers detected in layer-type chickens ($n = 16$/group) of commercial origin vaccinated by mucosal routes with RCA-free Ad expressing codon-optimized H5 from low pathogenic AI strain A/turkey/WI/68 (H5N9) (AdTW68.H5$_{ch}$). Vaccine groups: 1) single ocular at 5 days of age; 2) single spray at 5 days of age; 3) ocular at 5 days and 15 days of age; and 4) unvaccinated control. Ocular priming followed by ocular boost with AdTW68.H5 significantly (*) increased serum HI titers on days 20, 34, and 40 of age, compared to chickens vaccinated once either ocularly or by spray, as well as to unvaccinated controls ($P < 0.05$). All groups were challenged with HPAI on day 45 of age (see Fig. 2).

against HPAI homologous virus challenges (21,22). We have previously shown expression of the H5 glycoprotein in the Harderian gland (HG) of ocularly vaccinated chickens by immunohistochemistry. H5 expression induced IgA and immunoglobulin G (IgG) antibody-secreting cells in the HGs specific for both H5 and Ad as measured by enzyme-linked immunospot assay. The IgA and IgG spot-forming cells peaked on day 9 for Ad and on day 11 for the H5 protein. In addition to B cell responses in the HG, ocular immunization also induced Ad- and H5-specific antibodies in the systemic compartment that differed in IgA antibody composition in tears based on western blot and immunoprecipitation analyses (24). We have also shown that chickens vaccinated with this type of vaccine delivered via mucosal routes developed mucosal interferon-γ and IL-6 responses (20). Others evaluated a replication-defective Ad-vector encoding the M2eX-HA-hCD40L or M1-M2 fusion from a human HPAI (H5N2) isolate administered via the intramuscular and intranasal route in mice (11). The Park *et al.* vaccine delivery regimen resulted in both potent mucosal immunity and in strong systemic humoral and T cell responses. The current results confirm that the immune responses induced by Ad-vectored vaccination via the ocular route confer protection against HPAI challenge in chickens.

Currently licensed and available vaccines for avian influenza virus require parenteral injection for killed adjuvant vaccines or for subcutaneous or dermal scarification for fowlpox recombinant vaccines. However, all of these techniques are manpower intensive and are difficult to perform during an outbreak. Newcastle disease virus recombinant (rNDV) vaccines are delivered via the ocular route and likely induce adequate immunity if applied by spray. However, because NDV is known to affect a wide spectrum of avian and mammalian species (1), rNDV vaccines may also replicate in nontarget species. More-recently developed experimental recombinant vaccines using vesicular stomatitis virus (VSV) vectors are

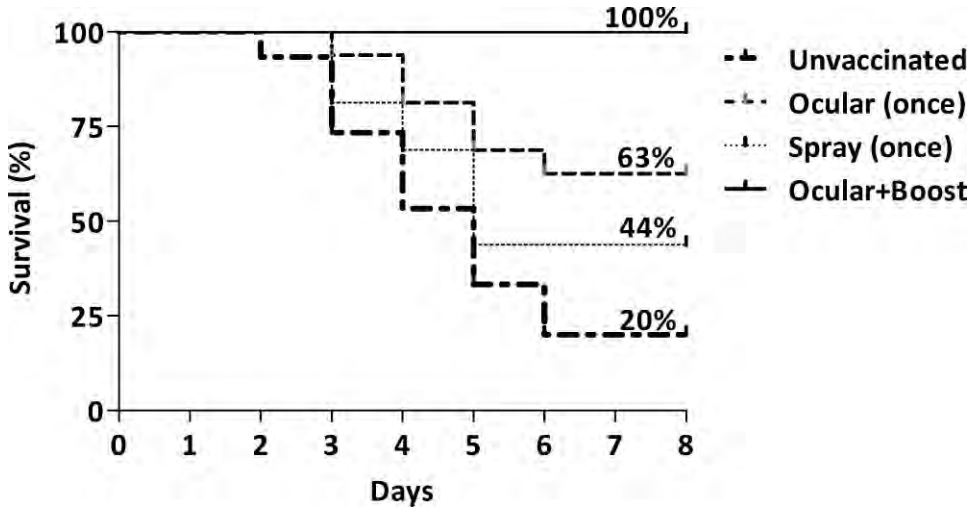

Fig. 2. Survival rates of chickens ($n = 16$/group) vaccinated as described in Fig. 1 and challenged on day 45 of age with $10^{6.0}$ EID$_{50}$/bird of HPAI A/Chicken/Queretaro/14588-19/95 (H5N2). H5 of this challenge strain has a 94% deduced amino acid sequence similarity with the H5 expressed from the Ad vector. Ocular priming, followed by ocular boost with AdTW68.H5$_{ck}$, significantly ($P < 0.05$) protected chickens against lethal challenge as compared to the unvaccinated controls.

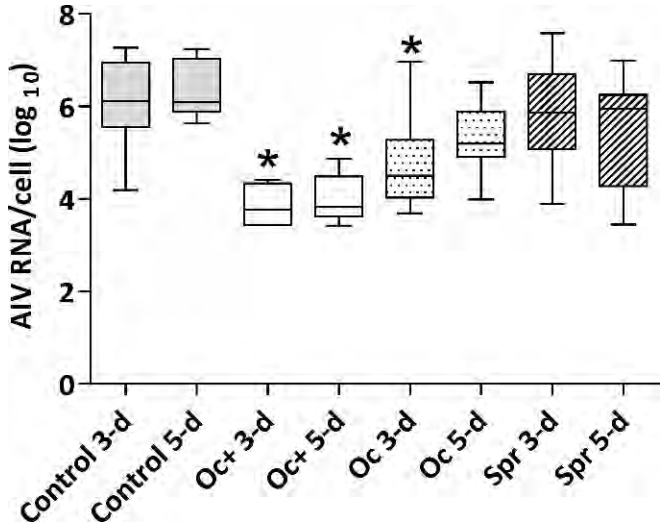

Fig. 3. AI viral RNA, determined by qRT-PCR in oropharyngeal swabs collected 3 and 5 days (d) after challenge with HPAI described in Fig. 2. Ocular priming followed by ocular boost with AdTW68.H5 significantly ($P < 0.05$) reduced (*) viral shedding as compared to the unvaccinated controls. A significant reduction was also detected on day 3 in chickens vaccinated once ocularly as compared to controls. Single-spray vaccinated chickens showed AI RNA concentrations similar to the unvaccinated–challenged controls.

promising, as they are unlikely to spread to nontarget species (5). No information is available on the possibility of applying VSV recombinant vaccines in chickens via mucosal routes. A mass vaccination approach for avian influenza is greatly desired to allow vaccination of large numbers of birds in a cost-effective manner. This study was designed to evaluate two mucosal vaccination methods, the ocular and aerosol routes of exposure. Both delivery methods, when used without boost, induced an immune response in at least some of the birds based on challenge protection. However, the aerosol route of exposure provided a relatively poor overall response; this suggests that the Ad-vectored vaccine, being a nonreplicating vaccine, provides insufficient viral particles to infect an adequate number of immune-related cells in a manner that generates an acceptable immune response. The ocular route seemed to provide a better response, likely because a high concentration of vaccine virus is able to reach the HG and the conjunctiva-associated lymphoid tissue, which contain a high concentration of immune effector cells. This explanation is confirmed by the fact that the antibody responses, survival rate, and virus shedding achieved by our different mucosal vaccination attempts were extremely consistent with the virus concentration expected to reach the cells by each of these methods; i.e., highest by the ocular and lowest by the aerosol route. It is conceivable that aerosol vaccination, followed by aerosol booster, is required to achieve acceptable protection in chicken populations.

The high level of protection conferred by ocular priming and booster vaccinations with AdTW68.H5$_{ck}$ is promising, as it provides a vaccination alternative for breeder and layer hens in response to an emerging AI epizootic. Interestingly, even though ocularly primed and boosted birds had serum antibody levels 3 to 4 log $_2$ lower than those obtained by *in ovo* or intramuscular vaccination (21,22), chickens were fully protected against challenge. This result suggests that the mucosal immune responses (e.g., IgA), previously detected in the upper respiratory tract of ocularly vaccinated chickens (24), likely play an important role in protection against challenge. The results from this challenge corroborate this assumption by the fact that Ad spray-vaccinated chickens, which were negative to systemic AI antibodies, still showed some level of protection against challenge. We previously found that single Ad spray vaccination elicits specific IgA in tears but elicits no serum-specific antibodies (20). This lack of a detectable serum antibody response makes it difficult to predict protection or to monitor for the percentage of birds that responded to the vaccine. Samples can be taken to measure for specific antibodies, but the amount of antibodies is lower on the mucosal surface and standard methods are inadequate for quantitation. The finding that ocular vaccination reduced, but did not eliminate, viral shedding was rather disappointing because the risk of virus spread within or between flocks would not be completely eliminated.

In this study, we used chickens of commercial origin rather than specific-pathogen-free chickens. Chickens were transported directly from the commercial hatchery to our experimental facilities and were, therefore, not exposed to high concentrations of other avian pathogens usually found in poultry operations. No interference of either actively induced or maternally derived antibodies to AI was anticipated to occur in these chickens because commercial chickens in the United States are free of antibodies to H5- (and H7)-type AI viruses. The fact that the vaccine was able to induce protection against AI in these chickens indicates that other passively transferred antibodies (routinely found in commercial chicken populations) did not interfere with active Ad-vectored immunization.

RCA-free Ad-vectored AI vaccines can be produced in large scale in the well-characterized PER.C6 cell line in serum-free suspension bioreactors (7). This Ad-vectored AI vaccine is in compliance with a strategy that differentiates between infected and vaccinated animals because the vector only encodes the viral HA. Thus, the routinely used serologic tests detecting conserved AI viral proteins allows easy discrimination between AI naturally infected and Ad-vectored vaccinated chickens.

Numerous experimental recombinant and genetically modified live vaccines have been developed in recent years, some of which have been reported to efficiently protect chickens against HPAI challenge (e.g., 3,6,12,17). However, live bioengineered viruses have the risk of generating revertants and allow the spread of genetically modified organisms in both target and nontarget species in the environment (13). Moreover, pre-existing immunity against avian virus vectors may preclude the development of an efficacious immune response against the antigen, as has been shown for the fowl pox vector (10,16). In contrast to live virus vaccines that may generate undesirable new reassortants with concurrently circulating wild influenza viruses (4), it is not possible for the DNA genome of Ad to undergo reassortment with the segmented RNA genome of an influenza virus. The Ad-vector system overcomes these issues, and the RCA-free Ad vector will not propagate, even in human cells, in the absence of expression of the Ad E1 gene.

REFERENCES

1. Alexander, D. J., and D. A. Senne. Newcastle disease. In: Diseases of poultry, 12th ed. Y. M. Saif, A. M. Fadly, J. R. Glisson, L. R. McDougald, L. K. Nolan, and D. E. Swayne, eds. Blackwell Publishing, Ames, IA. pp. 75–115. 2008.

2. Garcia, A., H. Johnson, D. K. Srivastava, D. A. Jayawardene, D. R. Wehr, and R. G. Webster. Efficacy of inactivated H5N2 influenza vaccines against lethal A/Chicken/Queretaro/19/95 infection. Avian Dis. 42:248–256. 1998.

3. Ge, J., G. Deng, Z. Wen, G. Tian, Y. Wang, J. Shi, X. Wang, Y. Li, S. Hu, Y. Jiang, C. Yang, K. Yu, Z. Bu, and H. Chen. Newcastle disease virus-based live attenuated vaccine completely protects chickens and mice from lethal challenge of homologous and heterologous H5N1 avian influenza viruses. J. Virol. 81:150–158. 2007.

4. Hilleman, M. R. Realities and enigmas of human viral influenza: pathogenesis, epidemiology and control. Vaccine 20:3068–3087. 2002.

5. Kalhoro, N. H., J. Veits, S. Rautenschlein, and G. Zimmer. A recombinant vesicular stomatitis virus replicon vaccine protects chickens from highly pathogenic avian influenza virus (H7N1). Vaccine 27:1174–1183. 2009.

6. Lee, C. W., D. A. Senne, and D. L. Suarez. Generation of reassortant influenza vaccines by reverse genetics that allows utilization of a DIVA (differentiating infected from vaccinated animals) strategy for the control of avian influenza. Vaccine 22:3175–3181. 2004.

7. Lewis, J. A., E. L. Brown, and P. A. Duncan. Approaches to the release of a master cell bank of PER.C6 cells; a novel cell substrate for the manufacture of human vaccines. Devel. Biol. (Basel) 123:165–176. 2006.

8. Ma, L., H. A. Bluyssen, M. De Raeymaeker, V. Laurysens, N. van der Beek, H. Pavliska, A. J. van Zonneveld, P. Tomme, and H. H. van Es. Rapid determination of adenoviral vector titers by quantitative real-time PCR. J. Virol. Methods 93:181–188. 2001.

9. Meijer, A., A. Bosman, E. E. van de Kamp, B. Wilbrink, H. van Beest Holle, R. Mdu, and M. Koopmans. Measurement of antibodies to avian influenza virus A (H7N7) in humans by hemagglutination inhibition test. J. Virol. Methods 132:113–120. 2006.

10. Paoletti, E. Applications of pox virus vectors to vaccination: an update. Proc. Natl. Acad. Sci. U. S. A. 93:11349–11353. 1996.

11. Park, K. S., J. Lee, S. S. Ahn, Y. H. Byun, B. L. Seong, Y. H. Baek, M. S. Song, Y. K. Choi, Y. J. Na, I. Hwang, Y. C. Sung, and C. G. Lee. Mucosal immunity induced by adenovirus-based H5N1 HPAI vaccine confers protection against a lethal H5N2 avian influenza virus challenge. Virology 395:182–189. 2009.

12. Park, M. S., J. Steel, A. Garcia-Sastre, D. Swayne, and P. Palese. Engineered viral vaccine constructs with dual specificity: Avian influenza and Newcastle disease. Proc. Natl. Acad. Sci. U. S. A. 103:8203–8208. 2006.

13. Poulet, H., J. Minke, M. C. Pardo, V. Juillard, B. Nordgren, and J. C. Audonnet. Development and registration of recombinant veterinary vaccines. The example of the canarypox vector platform. Vaccine 25:5606–5612. 2007.

14. Singh, S., H. Toro, D. Tang, W. E. Briles, L. M. Yates, R. T. Kopulos, and E. W. Collisson. Non-replicating adenovirus vectors expressing avian influenza virus hemagglutinin and nucleocapsid proteins induce chicken specific effector, memory and effector memory CD8+ T lymphocytes. Virology 405:62–69. 2010.

15. Spackman, E., D. A. Senne, T. J. Myers, L. L. Bulaga, L. P. Garber, M. L. Perdue, K. Lohman, L. T. Daum, and D. L. Suarez. Development of a real-time reverse transcriptase PCR assay for type A influenza virus and the avian H5 and H7 hemagglutinin subtypes. J. Clin. Microbiol. 40:3256–3260. 2002.

16. Swayne, D. E., J. R. Beck, and N. Kinney. Failure of a recombinant fowl poxvirus vaccine containing an avian influenza hemagglutinin gene to provide consistent protection against influenza in chickens preimmunized with a fowl pox vaccine. Avian Dis. 44:132–137. 2000.

17. Swayne, D. E., M. Garcia, J. R. Beck, N. Kinney, and D. L. Suarez. Protection against diverse highly pathogenic H5 avian influenza viruses in chickens immunized with a recombinant fowlpox vaccine containing an H5 avian influenza hemagglutinin gene insert. Vaccine 18:1088–1095. 2000.

18. Swayne, D. E., D. A. Senne, and D. L. Suarez. Avian influenza. In: A laboratory manual for the isolation, identification and characterization of avian pathogens, 5th ed. L. Dufour-Zavala, ed. American Association of Avian Pathologists, Athens, GA. pp. 128–134. 2008.

19. Tang, D. C., J. Zhang, H. Toro, Z. Shi, and K. R. Van Kampen. Adenovirus as a carrier for the development of influenza virus-free avian influenza vaccines. Expert Review of Vaccines 8:469–481. 2009.

20. Toro, H., F. van Ginkel, D. C. Tang, B. Schemera, S. Rodning, and J. Newton. Avian influenza vaccination in chickens and pigs with RCA-free human recombinant adenovirus 5. Avian Dis. (Suppl)54:224–231. 2010.

21. Toro, H., D. C. Tang, D. L. Suarez, M. J. Sylte, J. Pfeiffer, and K. R. Van Kampen. Protective avian influenza in ovo vaccination with non-replicating human adenovirus vector. Vaccine 25:2886–2891. 2007.

22. Toro, H., D. C. Tang, D. L. Suarez, J. Zhang, and Z. Shi. Protection of chickens against avian influenza with non-replicating adenovirus-vectored vaccine. Vaccine 26:2640–2646. 2008.

23. Ungchusak, K., P. Auewarakul, S. F. Dowell, R. Kitphati, W. Auwanit, P. Puthavathana, M. Uiprasertkul, K. Boonnak, C. Pittayawonganon, N. J. Cox, S. R. Zaki, P. Thawatsupha, M. Chittaganpitch, R. Khontong, J. M. Simmerman, and S. Chunsutthiwat. Probable person-to-person transmission of avian influenza A (H5N1). New England J. Med. 352:333–340. 2005.

24. van Ginkel, F. W., D. C. Tang, S. L. Gulley, and H. Toro. Induction of mucosal immunity in the avian Harderian gland with a replication-deficient Ad5 vector expressing avian influenza H5 hemagglutinin. Devel. Comp. Immunol. 33:28–34. 2009.

ACKNOWLEDGMENTS

The authors thank Stephen Gulley and Rodrigo Gallardo for technical assistance during this work and Stuart Price for editorial suggestions. This work was funded by the United States Department of Agriculture, Avian Influenza Coordinated Agricultural Project.

Journal of General Virology (2011), **92**, 931–939 DOI 10.1099/vir.0.025486-0

Virulent Newcastle disease virus elicits a strong innate immune response in chickens

Cary A. Rue,[1] Leonardo Susta,[2] Ingrid Cornax,[1] Corrie C. Brown,[2] Darrell R. Kapczynski,[1] David L. Suarez,[1] Daniel J. King,[1] Patti J. Miller[1] and Claudio L. Afonso[1]

Correspondence
Claudio L. Afonso
Claudio.Afonso@ars.usda.gov

[1]Southeast Poultry Research Laboratory, Agricultural Research Service, United States Department of Agriculture, Athens, GA 30605, USA

[2]Department of Veterinary Pathology, College of Veterinary Medicine, University of Georgia, Athens, GA 30602, USA

Received 4 August 2010
Accepted 21 December 2010

Newcastle disease virus (NDV) is an avian paramyxovirus that causes significant economic losses to the poultry industry worldwide. There is limited knowledge about the avian immune response to infection with virulent NDVs, and how this response may contribute to disease. In this study, pathogenesis and the transcriptional host response of chickens to a virulent NDV strain that rapidly causes 100 % mortality was characterized. Using microarrays, a strong transcriptional host response was observed in spleens at early times after infection with the induction of groups of genes involved in innate antiviral and pro-inflammatory responses. There were multiple genes induced at 48 h post-infection including: type I and II interferons (IFNs), several cytokines and chemokines, IFN effectors and inducible nitric oxide synthase (iNOS). The increased transcription of nitric oxide synthase was confirmed by immunohistochemistry for iNOS in spleens and measured levels of nitric oxide in serum. *In vitro* experiments showed strong induction of the key host response genes, alpha IFN, beta interferon, and interleukin 1β and interleukin 6, in splenic leukocytes at 6 h post-infection in comparison to a non-virulent NDV. The robust host response to virulent NDV, in conjunction with severe pathological damage observed, is somewhat surprising considering that all NDV encode a gene, V, which functions as a suppressor of class I IFNs. Taken together, these results suggest that the host response itself may contribute to the pathogenesis of this highly virulent strain in chickens.

INTRODUCTION

Newcastle disease virus (NDV) is an avian paramyxovirus that causes significant economic damage to the poultry industry. NDV is a negative-stranded RNA virus with a 15 kb genome that contains six genes: nucleoprotein (NP), phosphoprotein (P) (RNA editing of the P gene can also result in expression of V and W), matrix (M), fusion (F), haemagglutinin-neuraminidase (HN) and polymerase (L). Over 200 avian species are naturally or experimentally susceptible to NDV. Isolates are of a single serotype, but have a wide range of naturally occurring pathogenicities from avirulent (lentogen), to mildly virulent (mesogen) and highly virulent (velogen) (Alexander & Senne, 2008).

While the highly virulent strains of NDV are not normally found in poultry in the USA, an outbreak of Newcastle disease (ND) in the South-western USA in 2002 required extensive culling and surveillance for control and resulted in a loss of millions of dollars (Yu *et al.*, 2001). This outbreak was caused by a highly virulent isolate that typically causes 100 % mortality in susceptible poultry 3–6 days post-infection (p.i.) (Wakamatsu *et al.*, 2006a). Virulent NDV is endemic in a large number of countries around the world, and there are reports of disease occurring in vaccinated birds (Yu *et al.*, 2001). In addition, some NDV strains are now becoming particularly virulent in avian species, e.g. geese, which had generally been resistant to clinical disease with virulent NDV infections (Liu *et al.*, 2003).

The host innate immune response to virus infection is an immediate reaction designed to retard virus growth and aid the host in developing specific protection from the adaptive immune responses. Research has shown that, in chicken cells, NDV can induce nitric oxide (NO) *in vitro* in heterophils (Sick *et al.*, 2000) and peripheral blood mononuclear cells (Ahmed *et al.*, 2007), alpha (IFN-α) and beta (IFN-β) interferon mRNA in macrophages (Sick *et al.*, 1998) and gamma interferon (IFN-γ) mRNA in peripheral blood mononuclear cells (Ahmed *et al.*, 2007). Yet this existing knowledge of the *in vitro* response to NDV

Supplementary material is available with the online version of this paper.

is insufficient to understand the nature of the host response to virulent NDV *in vivo* or to understand the underlying mechanisms of pathogenesis. Despite decades of research characterizing pathogenesis of different isolates, little is known about the underlying molecular mechanisms of disease caused by NDV. Here, we report a global analysis of the host response to infection *in vivo* with a virulent NDV strain from the 2002 outbreak in California (NDV-CA02), and characterize the early host response of splenocytes.

RESULTS

NDV-CA02 induces a robust host response in spleens *in vivo*

To measure the early host response to NDV *in vivo*, microarray experiments using complete chicken genome array slides were performed on spleens from specific-pathogen-free (SPF) chickens inoculated bilaterally intranasal and into the conjunctiva with an embryo infectious doses (EID_{50}) per 0.1 ml dose of $10^{5.3}$ NDV-CA02 or 0.1 ml of PBS control. The host gene expression profiles in the spleens of birds inoculated with PBS were compared with NDV-CA02 at both 1 and 2 days p.i. (five birds per treatment per time point). Spleens were chosen for analysis because these organs are known to be infected early and are lymphoid in nature. At 1 day p.i., the microarray analysis identified 125 genes that were induced by NDV-CA02 at least twofold, and 65 genes that were repressed at least twofold out of 6772 genes with significant data ($P<0.05$). By 2 days p.i., out of 6317 genes with significant data ($P<0.05$), 704 were induced at least twofold and 405 were repressed at least twofold (complete results presented in Supplementary Table S1, available in JGV Online). For certain genes, the microarray analysis generated no data. This occurs when appropriate probes representing genes are not present on the array or when the raw hybridization of the fluorescently labelled cDNA to the probe is too weak to produce a reliable signal. Of the significantly induced or repressed genes detected, genes specifically involved in the host inflammatory response, the innate antiviral response and well-characterized cytokines were chosen for further discussion in this study.

Many genes associated with an early innate host response were induced by NDV-CA02 at 1 day p.i., including the pro-inflammatory cytokine interleukin 6 (IL-6), chemokine macrophage inflammatory protein-3 alpha (MIP-3α), myxovirus resistance (Mx), lysozyme, interferon-induced protein with tetratricopeptide repeats 5 (IFIT-5), interferon-stimulated gene (ISG)12-2, and melanoma differentiation associated protein-5 (MDA-5) and IFN-γ precursor (Table 1). Changes in mRNA expression at 1 day p.i. of four early innate response genes were confirmed by quantitative RT-PCR on spleens from infected chickens (Supplementary Fig. S1, available in JGV Online). By 2 days p.i., each of these genes were further upregulated. In addition, several other markers of the innate immune response that were not induced at 1 day p.i. were upregulated at 2 days p.i., such as, iNOS, the pro-inflammatory cytokines IL-1β, IL-18, IL-8 and IFN-γ. The fact that expression of a subset of genes associated with an early host response increased from 1–2 days p.i. concomitant with an increase in virus titres in the spleen is evidence that these times are early in the infection. Further changes after 2 days p.i. were not measured in this study because they could be complicated by the host's transition from an innate to an adaptive immune response.

In addition to upregulating Mx, NDV-CA02 induced expression of the antiviral IFN effector genes protein kinase R (PKR) and 2′-5′-oligoadenylate synthetase (OAS) (Table 1). Also induced were numerous cytokines: K203, ah221, CXCL13/BCA-1, CCL21, MIP-3α and MIP-1β. Several of these cytokines are chemokines, most notably MIP-3α and MIP-1β that function to set up later cell-mediated responses by recruiting effector leukocytes like neutrophils. Finally, many genes that were significantly induced by NDV-CA02 infection are part of the innate response signalling processes: regulator of G-protein signalling 1 (ADORA), suppressor of cytokine signalling (SOCS)-1 and -3, N-myc and STAT interactor (signal transducer and activator of transcription), STAT4 and IFN regulatory factors (IRF) 1, 7 and 10 (Table 1).

NDV-CA02 infection *in vivo* induces a strong iNOS response

With evidence from microarrays that NDV-CA02 was inducing iNOS expression in spleens, immunohistochemistry (IHC) for iNOS was done. Fig. 1(a), left panel shows that intense immunoreactivity for iNOS was seen in spleens of NDV-CA02-infected birds at 3 days p.i. The immunostaining is most intense in areas where lymphocytic depletion is most severe and, not surprisingly, the accumulated fixed macrophages are positive for iNOS antigen. Spleen tissue sections from PBS-inoculated birds demonstrated no positive signal (Fig. 1a, right panel). Also, an assay to measure the product of active iNOS, NO, was done (Fig. 1b). Serum from NDV-CA02-infected birds were assayed for nitrites (the assay converts NO and nitrates to stable nitrites) at 1, 2 and 3 days p.i. and compared with PBS-inoculated bird serum. NDV-CA02 induced NO production in serum as early as 2 days p.i. with greater than a twofold induction that increased to over fourfold by day 3.

Characterization of early pathogenesis of NDV-CA02 *in vivo*

Virulent NDV from the 2002 outbreak in California virus was administered to 15 naïve, SPF chickens bilaterally intranasal and into the conjunctiva with a $10^{5.3}$ EID_{50} per 0.1 ml dose. Eyelids, caecal tonsils and spleens harvested from five birds at 1, 2 and 3 days p.i. were used to characterize early infection and pathogenesis. These organs

Table 1. Selected genes significantly upregulated in the spleen during infection with NDV-CA02

GenBank best hit	24 h*		48 h		Gene description
	Fold increase	Probability	Fold increase	Probability	
BU138064	21.75	0.00132	37.9	2.76e−05	IFIT-5
X05343	11.35	0.00747	29.03	0.000223	Mature avidin
AB088533	18.6	0.00814	25.84	7.87e−06	Mx protein
BX275358	12.24	2.48E-05	17.22	0.000277	Putative ISG12-2 protein
CO765511	13.77	0.00832	14.41	0.000934	Lysozyme
AJ309540	5.584	0.014	12.45	0.000489	IL-6 (IFN-β2)
BX933162	9.837	0.00177	12.21	0.00104	Chemokine ah221
BX929857	8.891	0.000164	11.39	4.68e−05	Chemokine (C-C motif) ligand 19 (MIP-3β)
Y18692	3.364	0.0247	8.97	0.00243	Chemokine K203
TC218839	6.602	0.0201	8.886	1.67e−05	MDA-5
TC190629	3.377	0.000447	8.65	0.000635	Chemokine ah221
CR389044	2.291	0.037	7.412	0.00345	Chemokine (C-C motif) ligand 4
CR522995	0.854	0.019	6.992	0.000635	Small inducible cytokine A21 isoform 1
Y14971	1.609	0.00391	6.691	0.00344	IL-8
BX933215	4.462	0.00296	6.029	3.04e−05	SOCS-1
AF424806	2.578	0.0106	4.936	0.00118	SOCS-3
AB002586	2.472	0.0219	4.833	5.45e−05	OAS
BX950337	4.138	0.000152	4.656	1.97e−05	N-myc and STAT interactor
AB125660	2.794	0.0145	4.591	3.04e−05	PKR
AY775780	1.713	0.0635	4.269	0.00229	IL-18
NM_205372	2.433	0.00434	4.258	0.0011	IRF7
BX264625	0.969	0.71	4.217	0.0115	Chemokine CXCL13/BCA-1
NM_205415	1.572	0.000654	3.397	0.00011	IRF1
U46504	0.769	0.017	3.233	0.00174	iNOS
BX935231	0.789	0.699	3.088	0.00266	MHC class I antigen
AB101005	0.948	0.544	2.862	0.00185	Chemokine (C-C motif) ligand 20 (MIP-3α)
BX932486	1.811	0.0276	2.815	2.96e−05	Phorbol-12-myristate-13-acetate-induced protein 1
BX933123	†		2.658	0.00997	STAT4
AY705909	1.861	0.0315	2.611	0.00614	IFN-γ precursor
Y15006	1.515	0.04	2.238	0.00617	IL-1β
CF255763	1.556	0.111	2.166	0.0012	ADORA
AF380350	1.364	0.0709	2.143	0.000904	IRF10

*24 h data for all genes in the 48 h list are included regardless of fold-change or *P*-value.
†Raw signal of fluorescent cDNA hybridized to probe was insignificant.

have been shown previously to be sites of early replication for NDV, and all have abundant lymphoid cells (Alexander & Senne, 2008; Wakamatsu *et al.*, 2006b). Results of histopathological evaluation and IHC for virus are presented in Table 2. Overall, there were minimal pathological changes seen histologically at 1 day p.i. The spleen and eyelids both had very mild lymphocyte depletion, while the caecal tonsils did not show lesions. The IHC for NDV at 1 and 2 days p.i. were weakly positive in the spleen of each bird. A mean NDV-CA02 titre of $10^{4.2}$ EID_{50} per 1 mg tissue (with a range of $10^{2.9}$–$10^{4.3}$) was detected in the spleen by 1 day p.i. and titres increased by 2 days p.i. to $10^{6.8}$ EID_{50} per 1 mg tissue (with a range of $10^{5.9}$–$10^{7.1}$). By day 2 the disease progressed, and moderate to severe lymphocyte depletion was observed by haematoxylin and eosin (H&E) in the spleens of three birds, and lesions were found mostly in the periarteriolar lymphoid sheaths (Fig. 2a, b). The splenic lesions progressed to severe multifocal to coalescing splenic necrosis and severe lymphocytic depletion by 3 days p.i. (data not shown). The lymphocyte depletion was associated with accumulation of macrophages and scattered heterophils, and the necrosis was characterized by areas of homogeneous amorphous cellular debris especially in the periarteriolar lymphoid sheaths. IHC of the spleens was weakly positive for NDV-CA02-infected birds at 2 days p.i., and nucleoprotein was detected mainly in the macrophages near the periarteriolar lymphoid sheaths. By 3 days p.i., NDV antigen was no longer confined to the periarteriolar region, consistent with dissemination of the virus to the spleen. Virus titres in the spleen remained high with a mean EID_{50} mg^{-1} of tissue of $10^{7.2}$ (with a range of $10^{5.7}$–$10^{7.7}$).

In the caecal tonsils, the pathological changes were similar but occurred slightly later than those in the spleen.

Table 2. Histological analysis of spleens of NDV-CA02-infected chickens

ND, Not determined.

		Day 1		Day 2		Day 3	
	Bird #	H&E*	IHC†	H&E	IHC	H&E	IHC
Spleen	1	−	−	+	ND	+++	ND
	2	+	ND	+	+	+++	ND
	3	−	ND	++	ND	+++	ND
	4	+/−	ND	++	ND	++	+++
	5	−	−	++	+/−	++	+++
Caecal tonsil	1	−	−	+	ND	++	ND
	2	−	ND	+	++	++	ND
	3	−	ND	+	++	+++	ND
	4	ND	ND	++	ND	+++	ND
	5	ND	−	++	ND	+++	+++
Eyelid	1	−	ND	+	+	+++	+++
	2	+/−	+	+	+	+++	ND
	3	+/−	ND	+	ND	+++	ND
	4	−	ND	+	ND	+++	+++
	5	−	−	+	ND	++	+++

*−, Normal; +/−, minimal lymphocytic depletion; +, mild to moderate lymphocytic depletion and increase in histiocytes; ++, moderate to severe lymphocyte depletion, necrosis, histiocytosis ; +++, severe lymphocytic depletion, severe necrosis, haemorrhages, histiocytosis and heterophilic infiltration.
†−, Negative; +, scattered-positive cells in the tissue for NDV nucleoprotein (N); ++, moderate amount of viral N detected; +++, large amount of NDV nucleoprotein detected (N).

Pathological changes in these tissues were also characterized by severe lymphocytic depletion, marked macrophage accumulation and moderate to severe heterophil infiltration by 3 days p.i. (Fig. 2d). IHC revealed moderate staining in the macrophages by day 2, in greater amounts than what was detected at the same time in the spleen. By 3 days p.i., the caecal tonsils were strongly immunopositive for NDV. The areas with severe lymphocyte depletion were those that had

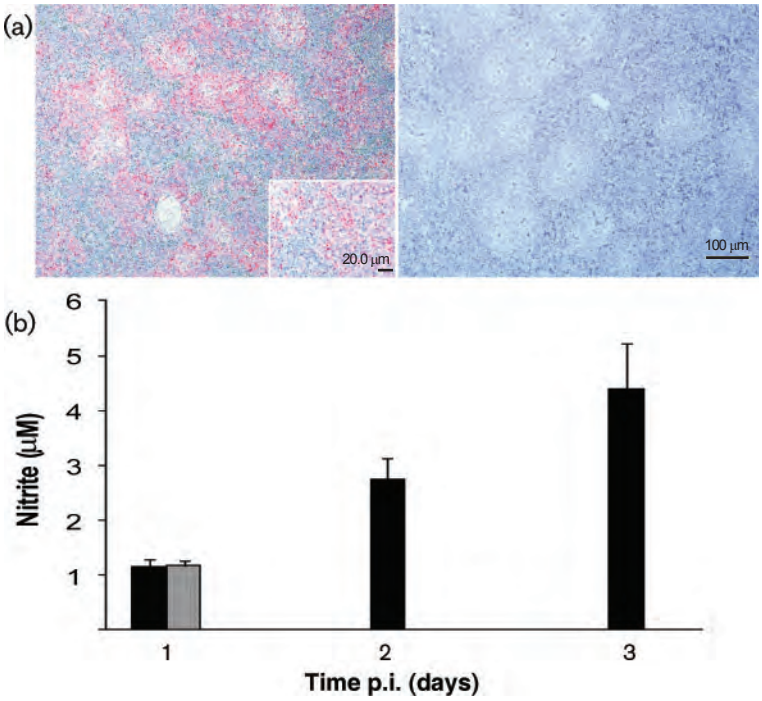

Fig. 1. iNOS response to NDV-CA02 infection in chicken spleen and serum. (a) IHC using anti-iNOS antibody on spleen tissue sections 3 days p.i. Image of spleen section from NDV-CA02-inoculated birds on the left (CA02) and PBS-inoculated birds on the right (PBS). Fast Red chromogen and haematoxylin counterstain. CA02 image includes ×5 magnified insert. (b) NO levels in the serum of NDV-CA02-infected birds. Serum from each of five NDV-CA02 (CA02)-inoculated birds at each time point was assayed for nitrites by a colorimetric assay and compared with values from serum of PBS-inoculated birds. Hatched bar represents PBS control and solid bar represents NDV-CA02.

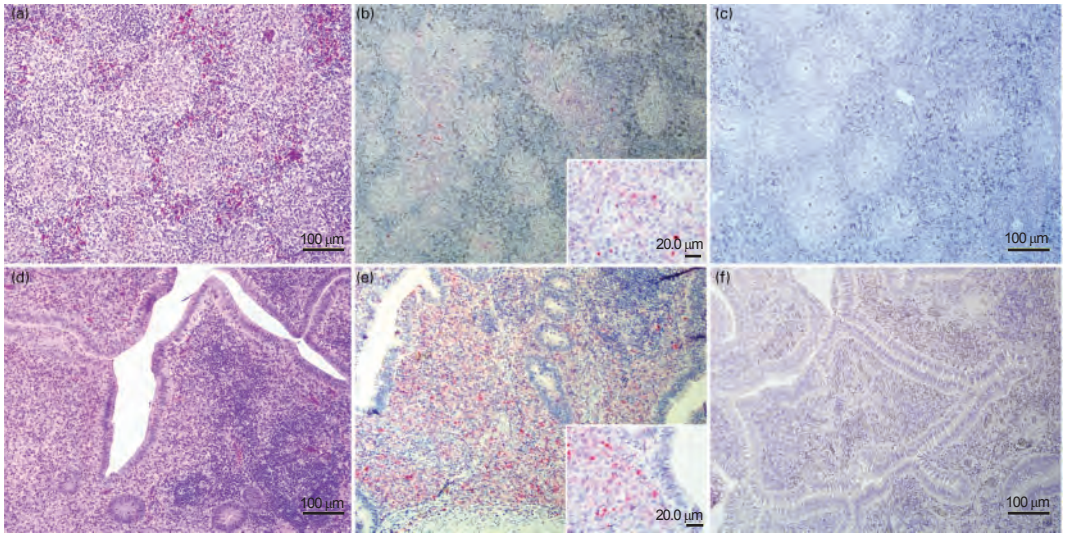

Fig. 2. Histological analysis of NDV-CA02-infected birds. Two days p.i. spleen (a–c) and 3 days p.i. caecal tonsil (d–f) sections were stained with H&E alone (a, d) or anti-NDV IHC with Fast Red substrate and haematoxylin counterstain (b, c, e and f). Control PBS-inoculated sections (c and f) are also shown. (b and e) Include ×5 magnified inserts. At 2 days p.i., there is extensive depletion of lymphocytes. At this same time period, using IHC, there is abundant viral antigen.

the greatest numbers of cells positive for NDV antigen (Fig. 2e) in comparison to the uninfected control (Fig. 2f).

Pathological changes in the eyelids followed a similar pattern of disease progression. At 3 days p.i., lymphocyte depletion, macrophage accumulation, necrosis and heterophil infiltration were predominant. IHC for NDV was mildly positive by 2 days p.i., while at 3 days p.i. the immunoreactivity was intense. The nucleoprotein appeared mainly confined to the macrophage population and some of the muscular cells of the eyelid.

Overall, the lesions observed in all the three organs are consistent with a necrotizing pattern of inflammation, and for all the tissue, the detection of the antigen by IHC was greatest at 3 days p.i. Both the anatomical lesions and the IHC results follow an increasing severity pattern from 1 to 3 days p.i.

NDV-CA02 infection of chicken splenocytes *in vitro* induces strong early cytokine response

To confirm that the most relevant early response genes were induced at early times post-infection, real-time RT-PCR was performed with RNA samples from chicken splenocytes following infection with NDV-CA02 *in vitro*. Splenocytes were infected with purified NDV-CA02 or LaSota (vaccine strain) at an m.o.i. of 1 and RNA was collected at 6 h p.i. Real-time RT-PCR was done with primers against IFN-α, IFN-γ, IL-1β and IL-6 (Fig. 3). Both type I and type II interferons, IFN-α and IFN-γ, were induced significantly by NDV-CA02, six- and sevenfold, respectively, while LaSota did not induce them over twofold relative to mock (Fig. 3). The pro-inflammatory cytokines, IL-1β and IL-6 were induced to a much greater degree by NDV-CA02, 18- and 35-fold, respectively. LaSota did not induce IL-1β over twofold and IL-6 was only modestly induced sixfold. These results corroborate the microarray and RT-PCR data from spleens *in vivo*, and show that NDV-CA02 induces a strong cytokine response in chickens.

DISCUSSION

The use of a whole chicken genome array (42 000 probes) to analyse the host response to infection *in vivo* allowed the identification of a large number of genes (704) that are part of the host early innate response to NDV. This included groups of functionally related genes, such as ISGs and pro-inflammatory chemokines, thus providing an additional level of confidence to the results. At 1 and 2 days p.i. *in vivo*, both type I and type II IFN responses were detected using microarrays. The induction of IRF1 and 7 are consistent with a type I IFN response since these proteins are upstream signals in the Toll-like receptor response to viruses that initiate IFN-α and IFN-β production (Au *et al.*, 1998; Parrington *et al.*, 1993). In addition, MDA-5, an RNA helicase that recognizes viral dsRNA and initiates a type I IFN response to many viruses [although reportedly not NDV (Loo *et al.*, 2008)], is induced by NDV-CA02. Downstream effectors of IFN action include several IFN-stimulated-response genes (ISRGs) including, Mx, OAS and PKR that were upregulated following NDV-CA02 infection.

In vitro experiments suggest that a pronounced and rapid innate immune response may be induced by virulent

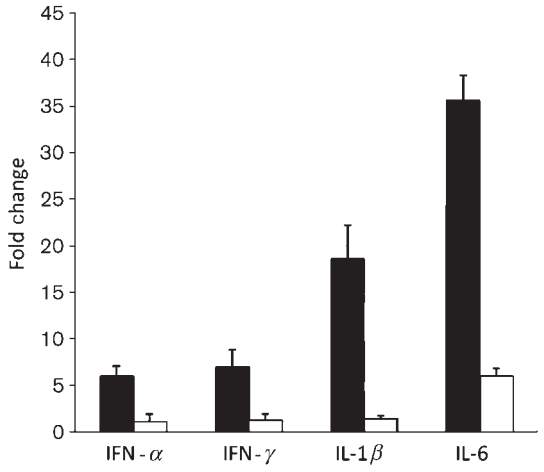

Fig. 3. Real-time RT-PCR of NDV-CA02 and LaSota vaccine strain-infected chicken splenocytes *in vitro*. Total RNA isolated from chicken splenocytes infected with NDV-CA02 and LaSota for 6 h was used for real-time RT-PCR using SYBR Green for IFN-α, IFN-γ, IL-1β and IL-6. Results were normalized against 28S rRNA and fold-changes relative to mock-infected samples are shown. Open bar represents LaSota and solid bar represents NDV-CA02 (CA02).

viruses in splenocytes. Using real-time RT-PCR of RNA isolated from NDV-infected splenocytes, we have demonstrated that the virulent CA-NDV, but not the lentogenic LaSota virus, is capable of rapidly and strongly inducing IFN-γ, IFN-α, IL-6 and IL-1β at 6 h p.i., genes integral to a pro-inflammatory response. Unfortunately, since LaSota does not reach the spleen but only replicates at the site of inoculation (Wakamatsu *et al.*, 2006b, c), parallel *in vivo* experiments to compare the relative host response to velogenic and lentogenic viruses were not possible. Our results confirm and extend *in vitro* analysis of gene expression patterns from chicken embryo cells in response to virulent NDV reported previously (Munir *et al.*, 2005). There, the effect of a low m.o.i. (0.01) was analysed throughout a 36 h period, and a significant but late induction of 22 genes was noted (probably as a result of the low m.o.i. used). Upregulated genes included some similar functions to the IFN and pro-inflammatory response that was observed here, including some ISGs, IL-8 and STAT1.

NDV encodes the V protein that blocks various components of IFN pathways. Specifically, the NDV V protein targets STAT1 for degradation and recombinant NDVs that do not express V have drastically lower virulence *in vivo* (Huang *et al.*, 2003; Wakamatsu *et al.*, 2006a, b, c). STAT1 is a particularly important signalling molecule for ISRG regulation because unlike STAT2, which is targeted by the V proteins of other paramyxoviruses (Parisien *et al.*, 2001), STAT1 is a transactivator for both IFN types I and II pathways (Darnell, 1997). Our data would indicate that at least at the mRNA level, a block of IFN pathways is not occurring with this particular NDV isolate. Here, we show that transcription of the types I and II IFNs and many ISGs are being induced by NDV-CA02, therefore further studies are necessary to determine the expression level and effectiveness of NDV-CA02 V protein during infection in both lymphoid and epithelial cells. In addition to detecting upregulation of IFN and pro-inflammatory genes, we also measured increased iNOS expression in tissues and increased levels of NO in serum. These results are in agreement with the observed upregulation of IFN-γ in microarray since IFN-γ induces iNOS expression (Kapczynski & Kogut, 2008; Koide *et al.*, 1993). Assaying NO levels was particularly valuable because it allowed for confirmation of the microarray data at a functional level, while using a validated commercially available assay. Constitutive low-level expression of NO in the vascular endothelium plays a beneficial role in maintaining blood vessel homeostasis (Palmer *et al.*, 1987), but high levels of NO produced by macrophages in response to pathogens can have toxic effects on the host. NO can indiscriminately modify many chemical groups and result in well-characterized decrease of protein function and cellular processes (Pacher *et al.*, 2007). The nitrite (μM) concentrations measured in NDV-CA02-infected chicken serum are well within its range required for detrimental effect (Shiva *et al.*, 2001). The significant upregulation of iNOS in spleens and NO in serum is a potentially destructive innate response of chickens to NDV infection, but in light of the robust replication and rapid mortality of this virus, it seems quite possible that NO is contributing to mortality not recovery.

Our data are consistent with a strong innate immune response that is unable to protect birds from disease and death, as we observed a clear innate IFN and cytokine response to NDV-CA02 *in vivo*. In spleens, there was a strong correlation between virus titres, pathological changes, and host innate immune response at 1 and 2 days p.i. The spleens and caecal tonsils of infected birds showed significant lymphoid depletion and infiltration of fixed macrophages by 2 days p.i. that progressed to necrotic lesions. This histopathology provides a good visual correlation to the microarray and PCR assays of cytokine expression levels. The histology and IHC of the spleens demonstrate that the cytokine increases are associated with tissue destruction and increasing quantities of virus.

The spleen was chosen for analysis of the early innate host response because it is a lymphoid organ that the virus reaches early in disease (Brown *et al.*, 1999b). However, analysis of the response to infection in the spleen may not be sufficient to completely understand NDV mechanisms of disease or death. The global analysis of the innate response to NDV *in vivo* and analysis of select innate genes *in vitro* provide a good overview of the host response; however, the roles of individual cell types in this response cannot be effectively measured in this way. Several major cell types present in spleens (macrophages, heterophils, B-cells and T-cells) appear to be permissive to NDV (Brown *et al.*,

1999a; Dalgaard *et al.*, 2010; Lam, 1996; Lam *et al.*, 1996; von Bulow & Klasen, 1983). Our data highlight the important role that splenocytes have in the host response to NDV. IL-6 and IL-1β were greatly induced in spleens by NDV-CA02 and are two well-characterized early innate response genes of macrophages to viruses through Toll-like receptor activation (Alexopoulou *et al.*, 2001). Additionally, the iNOS induction measured at the transcript and functional (NO) levels is mainly produced by macrophages. Given the proclivity of macrophages to be present at the sites of infection, often harbouring virus (Fig. 1 and Brown *et al.*, 1999b), future analysis of the role of individual leukocyte cell populations in the innate response to NDV are warranted.

The existence of new virulent NDV genotypes throughout the world and the susceptibility of wild avian species are cause for concern over the continued effectiveness of the currently used 50-year-old vaccine. The development of better vaccines and control strategies will require a greater understanding of the mechanisms of pathogenesis. Our report of the first global analysis of the natural host's response to an avian paramyxovirus *in vivo* provides basic information needed to extend our understanding of the nature of the virus–host interactions.

METHODS

Viruses. NDV from chicken isolate California/S0212676/2002 (NDV-CA02) was originally isolated from the field during the 2002–2003 California exotic ND outbreak (Pedersen *et al.*, 2004). This isolate was plaque-purified three times on chicken embryo fibroblasts and amplified by inoculation of SPF 9–11-day-old embryonating chicken eggs (ECE). The pathotype of the plaque-purified isolate was confirmed as a virulent by having a mean death time of 54 h in ECE (<60 being virulent) and intracerebral pathogenicity index of 1.85 (>1.5 being virulent) using standard procedures (Alexander, 1998). The low virulence NDV vaccine virus, LaSota, was received from Lohmann Animal Health International (Gainesville, Ga). For *in vitro* splenocyte infections, viruses were first purified by ultracentrifugation for 1 h (35 000 ***g***) at 4 °C through a 10 % sucrose cushion. Pellets were resuspended in PBS with 1 % BSA, and mock infections were done with PBS with 1 % BSA. Virus inoculated into birds was harvested from infected allantoic fluid, titrated in ECE and diluted in PBS.

Birds and eggs. The source of SPF chickens and ECE was the Southeast Poultry Research Laboratory's SPF White Leghorn chicken flock.

Cells. Splenocytes used for *in vitro* infections and real-time RT-PCR assays were isolated from 2-week-old SPF White Leghorn chickens. Spleens were collected aseptically and placed in sterile 4 °C PBS. Single-cell suspensions were prepared by gently pushing the splenic pulp through a sterile nylon mesh with a pore size of 70 μM (Fisher Scientific). Cells were washed and resuspended in 3 ml cold PBS and then layered over 3 ml Histopaque 1077 (Sigma). The preparations were enriched for leukocytes by centrifugation (450 ***g***) for 30 min at 18 °C. Cells were recovered from the interface, resuspended in cold PBS, and washed twice in 3 ml cold PBS.

Animal experiment and tissue collection. Each of 15 chickens was inoculated with a total dose of $10^{5.3}$ 50 % EID_{50} in 0.1 ml of virus divided into the right nares (50 %) and both eyes (25 % each). PBS was used as inocula for non-infected controls. Five infected birds were sampled each day. The five non-infected control birds were sampled only on 1 day p.i. Birds were anaesthetized and blood samples were drawn from the heart. Birds were then euthanized with an intravenous injection of pentobarbital (Sigma-Aldrich). Immediately post-mortem, eyelid, spleen and caecal tonsils were harvested aseptically for histology, IHC and RNA extraction. Spleens harvested for analysis were cut into three pieces, with one piece of each used for histology, RNA isolation and virus titration. Virus titres of spleens were determined after homogenization in 10 % (w/v) PBS. Confirmation that sampled birds were infected with virus was based on virus recovery from oral or cloacal swabs collected before or on the day tissue samples were collected. Oral and cloacal swabs from all birds were positive by haemagglutination assay for NDV-CA02 by 2 and 3 days p.i., respectively.

RNA isolation, reverse transcription, labelling and microarray hybridization. Spleen cell suspensions were generated by pushing freshly isolated tissue through a 70 μM pore-size mesh cup, immediately into Trizol (Invitrogen) and stored at −80 °C after collection of all samples for that day. Samples were later thawed at room temperature and chloroform was added according to the manufacturer's protocol. Samples were incubated for 10 min on ice. Following centrifugation at 2400 ***g*** for 15 min, the aqueous phase was removed, mixed with an equal volume of 70 % ethanol, and applied to Qiagen RNeasy midi prep columns. RNA quantity was assessed using a Nanodrop spectrophotometer on the RNA-40 setting and quality was assessed using a nanochip on a Bioanalyser (Agilent Technologies). All RNA samples had an RNA integrity number greater than 8.6 with a mean of 9.7. Total RNA (50–500 ng) was reverse transcribed to cDNA, amplified, and labelled with Cy3 or Cy5 using the Two-colour Linear Amplification kit (Agilent Technologies). Complete chicken genome microarray slides (42 000 probes) were purchased from Agilent and labelled cRNAs were hybridized for 17 h at 65 °C with Gene Expression Hybridization Solution (Agilent Technologies). Slides were disassembled from their hybridization chambers in Gene Expression Wash Buffer 1 then washed for 1 min in Gene Expression Wash Buffer 1, 1 min in Gene Expression Wash Buffer 2, 1 min in acetonitrile, and 30 s in Stabilization and Drying Solution (Agilent Technologies) following manufacturer's specifications. RNA from individual NDV-CA02-inoculated animals (n=4) were considered as separate experiments and compared with pooled RNA from the PBS-inoculated animals (n=4 and n=3 for 24 and 48 h experiments, respectively).

Microarray data collection and analysis. Differential expression measurements based on simultaneous two-colour hybridizations were performed with a GenePix 4200A scanner using a 5 μm resolution and the GenePix Pro 6.1 data acquisition and analysis software (Axon Instruments; Molecular Devices). GeneSpring GX computer software (Agilent Technologies) was used for all normalization and statistical analysis of the GenePix output. RNA from PBS-inoculated birds was pooled and compared with RNA from individual NDV-CA02-infected birds for a total of four arrays. The intensity ratio of expression for each gene was calculated by dividing the measured infected bird values (test channel) by the intensity of the mock-infected bird values (control channel). All outputs with control channel values of less than 300.0 were not considered. Intensity-dependent normalization was used to reduce the ratios to the residual of the Lowess fit of the intensity-versus-ratio curve. Per-chip normalization was done by creating an artificial-positive control for each sample with the 50th percentile of all measurements across the entire chip. Chips were scanned with high laser strength and low laser strength independently to generate non-saturated data for the maximum number of spots. Individual sample t tests were calculated as the mean of replicate normalized values for a single gene – 1/standard error. This analysis produces low P-values when the mean of replicate normalized values (fold-changes) is significantly different from one and the standard error is small.

Quantitative RT-PCR. *In vitro* determination of cytokine induction of chicken splenoytes following NDV-CA02 infection was performed as previously described (Kapczynski & Kogut, 2008). Briefly, isolation of total RNA from infected splenocytes was performed using the Qiagen RNeasy Mini kit following the manufacturer's recommendations. Standard cycling conditions were used with iScript one-step RT-PCR kit with SYBR Green (Bio-Rad) with annealing temperatures optimized for each primer pair. Each RT-PCR experiment was run in triplicate with a no-template control, test samples and a $\log_{10}$ dilution series of standard RNA. Regression analysis of the mean values of three replicate RT-PCRs for the $\log_{10}$ diluted RNA was used to generate standard curves. Primer pairs used were (forward, reverse): IFN-α (5′-GACAGCCAACGCCAAAGC-3′, 5′-AATGCTTGAGCAGCAGCGAC-3′); IFN-γ (5′-GCCAGACTTACAACTTGTTTG-3′, 5′-AGAACTGGACAGAGAGAGAAATGAG-3′); IL-1β (5′-ACATGTCGTGTGTGATGA-3′, 5′-GCTTCATCTTCTACCGCCTG-3′); IL-6 (5′-GCGAGAACAGCATGGAGATG-3′, 5′-CTGTTCGCCTTTCAGACCTAC-3′); 28S (5′-GGCGAAGCCAGAGGAAACT-3′, 5′-GACGACCGATTTGCACGTC-3′).

NO assay. Blood was drawn into S-monovette Z Serum V 4.5 ml syringes containing the clotting stimulant kaolin (Sarstedt) and centrifuged at 1000 ***g*** for 15 min to separate the serum. Serum samples (250 µl each) were applied to pre-rinsed 10 kDa molecular mass cut-off microfuge filters (Millipore) and centrifuged at 5000 ***g*** for 40 min. The flow-through was used in the nitric oxide synthase assay kit (Calbiochem) according to the manufacturer's instructions. Serum from each of five birds for each condition were read and averaged. NO levels were calculated using a standard curve.

Histopathology and IHC. Sample tissues were immediately fixed in 10 % neutral buffered formalin for approximately 52 h. All sampled tissues were routinely processed into paraffin blocks, and 3 µm sections were cut onto positively charged slides (Probe On Plus; Fisher Scientific) both for H&E staining and IHC. All tissues were examined histologically, with recording of severity of lesions. For IHC, two infected birds from each sampling day were assayed for the presence of NDV nucleoprotein. For this procedure, after deparaffinization, tissue sections were subjected to antigen retrieval by microwaving in citrate buffer solution (Antigen Unmasking Solution; Vector Laboratories) for 10 min at full power. Blocking was performed with a universal blocking reagent (Biogenex) as recommended by the manufacturer. The primary antibodies, polyclonal rabbit anti-NDV nucleoprotein (peptide) (Kapczynski & Kogut, 2008; Kommers *et al.*, 2001) and polyclonal rabbit anti-iNOS (Thermo Scientific Anatomical Pathology) were diluted in 10 % normal sheep serum, and incubated at 37 °C for 1 h. The dilutions used were 1 : 8000 for rabbit anti-nucleoprotein, and 1 : 75 for rabbit anti-iNOS. After washes, the slides were incubated with an alkaline phosphatase-based polymer system specific for the Fc portion of rabbit IgG (Ultra Vision One; Thermo Scientific Anatomical Pathology). The reaction was revealed with a naphthol-based chromogen, Fast Red (Biogenex). Sections were counterstained lightly with haematoxylin and coverslipped with Permount for a permanent record.

Quantitative RT-PCR confirmation of mRNA expression changes seen on microarray. RNA was isolated from spleens 24 h p.i. as described above. Changes in mRNA gene expression of IL-6, IFN-γ, iNOS and IFN-β were monitored as changes in SYBR Green fluorescence after amplification with specific primer sets. Primers for amplifying IFN-γ, IL-6, iNOS and IFN-β were derived from previously published sequences (Degen *et al.*, 2005; Kaiser *et al.*, 2003). β-Actin primers were manually selected according to the available nucleotide sequences available in GenBank (accession no. X00182) and properties were verified using the Oligonucleotide Properties Calculator (www.basic.northwestern.edu/biotools/oligocalc.html). The primers were designed to span introns in the genomic DNA to prevent DNA contamination. All primers were synthesized by Integrated DNA Technologies. Sequences are as follows: β-actin (5′-AGAGGCTCCCCTGAACCCCAAAGC-3′, 5′-CTGGATGGCTACATACATGGCTGG-3′); IFN-γ (as above); IL-6, (as above); IFN-β (5′-GGTAGGTCTGAAAGGCGAACAG-3′, 5′-TTGATGCTGAGGTGAGCGTTG-3′); and iNOS (5′-TTGGAAACCAAAGTGTGTAATATCTTG-3′, 5′-CCCTGGCCATGCGTACAT-3′).

One-step quantitative RT-PCR amplification and detection were performed using a 7500 FAST real-time PCR System (Applied Biosystems) with SYBR Green fluorescence detection of PCR product on 20 µl reaction mixtures containing: 10 µl Power SYBR Green RNA-to-C *1*-Step kit (Applied Biosystems), 500 nmol l^{-1} each of forward and reverse specific primer and 60 ng RNA. Thermocycler conditions were as follows: one cycle at 48 °C for 30 min, one cycle at 95 °C for 15 min, 40 cycles at 95 °C for 15 s and at 58 °C at 32 s. One cycle for dissociation curve for all reactions was added and the melting curve analysed.

Relative changes in gene expression were calculated according to the Pflaffl method (Pflaffl, 2001) using LinRegPCR version 12 (Ramakers *et al.*, 2003) to calculate individual specific primer efficiency by linear regression. All cycle threshold fluorescence (C_t) values were corrected to the mean C_t of PBS, mock-infected control for each gene of interest and β-actin was used as the endogenous control.

ACKNOWLEDGEMENTS

We gratefully acknowledge Tim Olivier, Aniko Zsak, Tracy Smith-Faulkner and Dawn Williams-Coplin for technical assistance. This work was funded by USDA CRIS project numbers 6612-32000-049-00D and 6612-32000-053-00D. Mention of trade names or commercial products in this paper is solely for the purpose of providing specific information and does not imply recommendation or endorsement by the US Department of Agriculture.

REFERENCES

Ahmed, K. A., Saxena, V. K., Ara, A., Singh, K. B., Sundaresan, N. R., Saxena, M. & Rasool, T. J. (2007). Immune response to Newcastle disease virus in chicken lines divergently selected for cutaneous hypersensitivity. *Int J Immunogenet* **34**, 445–455.

Alexander, D. J. (1998). Newcastle disease virus and other avian paramyxoviruses. In *A Laboratory Manual for the Isolation and Identification of Avian Pathogens*, 4th edn, pp. 156–163. Kennett Square, PA: American Association of Avian Pathologists.

Alexander, D. J. & Senne, D. A. (2008). Newcastle disease, other avian paramyxoviruses, and pneumovirus infections. In *Diseases of Poultry*, 12th edn, pp. 75–115. Edited by Y. M. Saif. Ames, IA: Blackwell.

Alexopoulou, L., Holt, A. C., Medzhitov, R. & Flavell, R. A. (2001). Recognition of double-stranded RNA and activation of NF-κB by Toll-like receptor 3. *Nature* **413**, 732–738.

Au, W. C., Moore, P. A., LaFleur, D. W., Tombal, B. & Pitha, P. M. (1998). Characterization of the interferon regulatory factor-7 and its potential role in the transcription activation of interferon A genes. *J Biol Chem* **273**, 29210–29217.

Brown, C., King, D. J. & Seal, B. S. (1999a). Pathogenesis of Newcastle disease in chickens experimentally infected with viruses of different virulence. *Vet Pathol* **36**, 125–132.

Brown, C. C., King, D. J. & Seal, B. S. (1999b). Comparison of pathology-based techniques for detection of viscerotropic velogenic Newcastle disease virus in chickens. *J Comp Pathol* **120**, 383–389.

Dalgaard, T. S., Norup, L. R., Rubbenstroth, D., Wattrang, E. & Juul-Madsen, H. R. (2010). Flow cytometric assessment of antigen-specific

proliferation in peripheral chicken T cells by CFSE dilution. *Vet Immunol Immunopathol* **138**, 85–94.

Darnell, J. E., Jr (1997). STATs and gene regulation. *Science* **277**, 1630–1635.

Degen, W. G., Daal, N., Rothwell, L., Kaiser, P. & Schijns, V. E. (2005). Th1/Th2 polarization by viral and helminth infection in birds. *Vet Microbiol* **105**, 163–167.

Huang, Z., Krishnamurthy, S., Panda, A. & Samal, S. K. (2003). Newcastle disease virus V protein is associated with viral pathogenesis and functions as an alpha interferon antagonist. *J Virol* **77**, 8676–8685.

Kaiser, A., Bercovici, N., Abastado, J. P. & Nardin, A. (2003). Naive $CD8^+$ T cell recruitment and proliferation are dependent on stage of dendritic cell maturation. *Eur J Immunol* **33**, 162–171.

Kapczynski, D. & Kogut, M. (2008). Measurement of avian cytokines with real-time RT-PCR following infection with the avian influenza virus. In *Avian Influenza Virus*, pp. 127–134. Edited by E. Spackman. Totowa, NJ: Humana Press.

Koide, M., Kawahara, Y., Tsuda, T. & Yokoyama, M. (1993). Cytokine-induced expression of an inducible type of nitric oxide synthase gene in cultured vascular smooth muscle cells. *FEBS Lett* **318**, 213–217.

Kommers, G. D., King, D. J., Seal, B. S. & Brown, C. C. (2001). Virulence of pigeon-origin Newcastle disease virus isolates for domestic chickens. *Avian Dis* **45**, 906–921.

Lam, K. M. (1996). Newcastle disease virus-induced apoptosis in the peripheral blood mononuclear cells of chickens. *J Comp Pathol* **114**, 63–71.

Lam, K. M., Kabbur, M. B. & Eiserich, J. P. (1996). Newcastle disease virus-induced functional impairments and biochemical changes in chicken heterophils. *Vet Immunol Immunopathol* **53**, 313–327.

Liu, X. F., Wan, H. Q., Ni, X. X., Wu, Y. T. & Liu, W. B. (2003). Pathotypical and genotypical characterization of strains of Newcastle disease virus isolated from outbreaks in chicken and goose flocks in some regions of China during 1985–2001. *Arch Virol* **148**, 1387–1403.

Loo, Y. M., Fornek, J., Crochet, N., Bajwa, G., Perwitasari, O., Martinez-Sobrido, L., Akira, S., Gill, M. A., García-Sastre, A. & other authors (2008). Distinct RIG-I and MDA5 signaling by RNA viruses in innate immunity. *J Virol* **82**, 335–345.

Munir, S., Sharma, J. M. & Kapur, V. (2005). Transcriptional response of avian cells to infection with Newcastle disease virus. *Virus Res* **107**, 103–108.

Pacher, P., Beckman, J. S. & Liaudet, L. (2007). Nitric oxide and peroxynitrite in health and disease. *Physiol Rev* **87**, 315–424.

Palmer, R. M., Ferrige, A. G. & Moncada, S. (1987). Nitric oxide release accounts for the biological activity of endothelium-derived relaxing factor. *Nature* **327**, 524–526.

Parisien, J. P., Lau, J. F., Rodriguez, J. J., Sullivan, B. M., Moscona, A., Parks, G. D., Lamb, R. A. & Horvath, C. M. (2001). The V protein of human parainfluenza virus 2 antagonizes type I interferon responses by destabilizing signal transducer and activator of transcription 2. *Virology* **283**, 230–239.

Parrington, J., Rogers, N. C., Gewert, D. R., Pine, R., Veals, S. A., Levy, D. E., Stark, G. R. & Kerr, I. M. (1993). The interferon-stimulable response elements of two human genes detect overlapping sets of transcription factors. *Eur J Biochem* **214**, 617–626.

Pedersen, J. C., Senne, D. A., Woolcock, P. R., Kinde, H., King, D. J., Wise, M. G., Panigrahy, B. & Seal, B. S. (2004). Phylogenetic relationships among virulent Newcastle disease virus isolates from the 2002–2003 outbreak in California and other recent outbreaks in North America. *J Clin Microbiol* **42**, 2329–2334.

Pflaffl, M. (2001). A new mathematical model for relative quantification in real-time PCR. *Nucleic Acids Res* **29**, 2002–2007.

Ramakers, C., Ruijter, J. M., Deprez, R. H. L. & Moorman, A. F. M. (2003). Assumption-free analysis of quantitative real-time polymerase chain reaction (PCR) data. *Neurosci Lett* **339**, 62–66.

Shiva, S., Brookes, P. S., Patel, R. P., Anderson, P. G. & Darley-Usmar, V. M. (2001). Nitric oxide partitioning into mitochondrial membranes and the control of respiration at cytochrome c oxidase. *Proc Natl Acad Sci U S A* **98**, 7212–7217.

Sick, C., Schultz, U., Münster, U., Meier, J., Kaspers, B. & Staeheli, P. (1998). Promoter structures and differential responses to viral and nonviral inducers of chicken type I interferon genes. *J Biol Chem* **273**, 9749–9754.

Sick, C., Schneider, K., Staeheli, P. & Weining, K. C. (2000). Novel chicken CXC and CC chemokines. *Cytokine* **12**, 181–186.

von Bülow, V. & Klasen, A. (1983). Effects of avian viruses on cultured chicken bone-marrow-derived macrophages. *Avian Pathol* **12**, 179–198.

Wakamatsu, N., King, D. J., Kapczynski, D. R., Seal, B. S. & Brown, C. C. (2006a). Experimental pathogenesis for chickens, turkeys, and pigeons of exotic Newcastle disease virus from an outbreak in California during 2002-2003. *Vet Pathol* **43**, 925–933.

Wakamatsu, N., King, D. J., Seal, B. S., Peeters, B. P. & Brown, C. C. (2006b). The effect on pathogenesis of Newcastle disease virus LaSota strain from a mutation of the fusion cleavage site to a virulent sequence. *Avian Dis* **50**, 483–488.

Wakamatsu, N., King, D. J., Seal, B. S., Samal, S. K. & Brown, C. C. (2006c). The pathogenesis of Newcastle disease: a comparison of selected Newcastle disease virus wild-type strains and their infectious clones. *Virology* **353**, 333–343.

Yu, L., Wang, Z., Jiang, Y., Chang, L. & Kwang, J. (2001). Characterization of newly emerging Newcastle disease virus isolates from the People's Republic of China and Taiwan. *J Clin Microbiol* **39**, 3512–3519.

AVIAN DISEASES 56:227–229, 2012

Research Note—

Comparison of Pooling 11 or 5 Oropharyngeal Swabbings for Detecting Avian Influenza Virus by Real-Time Reverse Transcription–PCR in Broiler Chickens

Brian S. Ladman,[AC] Erica Spackman,[B] and Jack Gelb Jr.[A]

[A]Avian Biosciences Center, University of Delaware, Newark, DE 19716-2150
[B]Southeast Poultry Research Laboratory, USDA-ARS, Athens, GA 30605

Received 21 June 2011; Accepted and published ahead of print 21 August 2011

SUMMARY. The effect of pooling 11 or 5 oropharyngeal (O/P) swabbings on detecting avian influenza virus (AIV) by real-time reverse transcription (RRT)–PCR was evaluated. The model used for the evaluation was designed to minimize viral load and, thus, assess the effect of the pooling on detection. Two-week-old broiler chickens were inoculated via the intranasal route with the low pathogenicity chicken/Maryland/Minh Ma/04 H7N2 strain or remained uninoculated. On days 2, 3, 4, 5, 7, 9, 11, and 14 postinoculation (PI), O/P swabbings were collected from individual infected birds and pooled with either 10 or 4 O/P swabs from uninfected broilers to produce 10 replicate pools of 11 or 5 swabbings, respectively. AIV was readily detected (80%–100%) by RRT-PCR in the pools of 11 and pools of 5 swabbings from days 2 through 5 PI. Detection in pools of both types decreased to similar levels on day 7 (40% for the pools of 11 and 50% for the pools of 5). AIV was not detected on day 9, 11, and 14 PI in pools of either size. On a given sample day PI, mean cycle threshold (Ct) values were consistently higher (lower genome levels) in the pools of 11 compared to the pools of 5. These differences were statistically significant on days 3 and 5 PI, yet Ct values associated with both types of pools were clearly interpretable as AIV positive.

RESUMEN. *Nota de Investigación*—Comparación de muestras agrupadas con 11 ó 5 hisopados orofaríngeos para la detección de virus de la influenza aviar en pollos de engorde mediante transcripción inversa y reacción en cadena de la polimerasa en tiempo real.

Se evaluó el efecto de agrupar 5 o 11 hisopos orofaríngeos (O/P) en la detección del virus de la influenza aviar por transcripción inversa y reacción en cadena en tiempo real (RRT)-PCR. El modelo utilizado para la evaluación fue diseñado para reducir al mínimo la carga viral y por tanto, evaluar el efecto de la agrupación de muestras en la detección. Pollos de engorde de dos semanas de edad, fueron inoculados por vía intranasal con una cepa del virus de la influenza aviar de baja patogenicidad Pollo/Maryland/Minh Ma/04 H7N2, o se mantuvieron como controles no inoculados. En los días 2, 3, 4, 5, 7, 9, 11, y 14 después de la inoculación, se recolectaron hisopos orofaríngeos de las aves infectadas individualmente y se combinaron con cuatro o 10 hisopos de pollos de engorda no infectados para producir 10 replicas de 5 y 11 hisopos, respectivamente. El virus de la influenza aviar fue detectado con facilidad (en un 80% a un 100%) mediante RRT-PCR en las muestra agrupadas con cinco y once hisopos desde los dos a los cinco días después de la inoculación. La detección en las muestras agrupadas de ambos tipos se redujo a niveles similares en el día 7 (40% para muestras agrupadas con 11 y 50% de la muestras agrupadas con 5). El virus de la influenza aviar no se detectó a los 9, 11 o 14 días después de la inoculación. En un día de muestreo determinado los valores promedio de ciclos umbrales (Ct) fueron consistentemente mayores (niveles de genoma mas bajos) en las muestras de 5 hisopos en comparación con las muestras con 11 hisopos. Estas diferencias fueron estadísticamente significativas en los días 3 y 5 después de la inoculación, sin embargo, los valores de Ct asociados con ambos tipos de muestras agrupadas eran claramente interpretables como positivos al virus de la influenza aviar.

Key words: notifiable avian influenza, avian influenza virus, Delmarva Peninsula, chicken, detection, surveillance, real-time reverse transcription–PCR, oropharyngeal swabbing pool, low pathogenicity

Abbreviations: ACIA = antigen capture immunoassay; AI = avian influenza; AIV = avian influenza virus; APHIS = Animal and Plant Health Inspection Service; Ct = cycle threshold; HP = high pathogenicity; ISRCP = Initial State Response and Containment Plan; LP = low pathogenicity; NAI = notifiable avian influenza; O/P = oropharyngeal; PI = postinoculation; RRT-PCR = real-time reverse transcription–polymerase chain reaction; USDA = United States Department of Agriculture; VS = Veterinary Services

Since 2006, all flocks of commercial broiler chickens in the United States have undergone surveillance testing for notifiable avian influenza (NAI) (2). States, in cooperation with the poultry industry, have implemented surveillance programs consisting of active surveillance of healthy flocks prior to slaughter and passive surveillance of sick flocks. Antigen–genome or antibody-based tests (or both) may be used in NAI surveillance programs. For antigen–genome surveillance, 11 swabbings from individual broilers is the statistically determined number of samples needed from a commercial-sized flock (10,000 birds or more) to detect 25% infection with 95% confidence (11). In the states of Delaware and Maryland, the National Poultry Improvement Plan-approved Initial State Response and Containment Plan (ISRCP) and the United States Department of Agriculture (USDA) Animal and Plant Health Inspection Service (APHIS) Veterinary Services (VS)-approved State Cooperative Agreements for NAI Prevention and Control Program are used in conjunction to address regional NAI programs. These documents specify that active preslaughter surveillance of broilers be performed by testing two pools of oropharyngeal (O/P) swabbings prepared from five and six individual birds from each farm. The pools may be tested by real-time reverse transcription (RRT)–PCR or by antigen

[C]Corresponding author. E-mail: bladman@udel.edu

Table 1. Experimental design for detecting LP H7N2 AIV in pools of 11 or 5 O/P swabbings from broiler chickens using RRT-PCR.

Number of individual broiler swabbings			Swabbings collected on sample day post-inoculation	Number of replicate pools evaluated per sample day
Total in pool	From AIV-infected broilers[A]	From uninfected broilers[B]		
11	1	10	2,3,4,5,7,9,11,14	10
5	1	4	2,3,4,5,7,9,11,14	10

[A]AIV-infected broilers were identified and used to create either the pools of 11 or 5 swabbings for the purpose of minimizing the variability in AIV genome levels between the two types of pools.
[B]Uninfected broilers were randomly selected to create the pools of 11 or 5 swabbings.

capture immunoassay (ACIA). While both ACIA and RRT-PCR testing are used to carry out active (preslaughter) surveillance programs, RRT-PCR is considered to be essential because it is more sensitive than ACIA for detecting avian influenza virus (AIV) infection (3,4,5). The cost of RRT-PCR, which is approximately 2 to 3-fold greater than ACIA, has had the effect of limiting the number of RRT-PCR tests performed in surveillance programs. Moreover, support from USDA/APHIS/VS for NAI surveillance programs has been steadily diminishing and further cuts are predicted in the future. Increasing the number of individual swabbings in pools has been proposed as a way to reduce RRT-PCR costs while still maximizing the level of surveillance. The purpose of this study was to examine the feasibility of using pools of 11 swabbings to perform one RRT-PCR reaction instead of the current program of testing two pools per farm.

MATERIALS AND METHODS

One-hundred and sixty, 1-day-old broiler chickens were obtained from a commercial hatchery. The chicks received standard Marek's disease vaccine (herpesvirus of turkeys and SB1) *in ovo* but did not receive vaccinations for infectious bronchitis virus or Newcastle disease virus. Twenty broilers were randomly assigned to the AIV-infected treatment group. The remaining 140 birds were assigned to the uninfected control group (Table 1). Broilers were maintained under BSL-3 containment in negative-pressure glove-port isolation units with disinfectant dip tanks at the Charles C. Allen Laboratory, University of Delaware, Newark, Delaware. Birds were provided a commercial diet and drinking water *ad libitum*. At 2 wk of age, broilers in the AIV-infected treatment group were inoculated with 10^5 50% embryo infectious dose per bird with the H7N2 low pathogenicity (LP) AIV strain, chicken/Maryland/Minh Ma/04, via the intranasal route. On days 2, 3, 4, 5, 7, 9, 11, and 14 postinoculation (PI), O/P swabbings were collected from individual AIV-infected and uninfected control broilers. A goal of the research was to simulate situations of low viral loads in the pools, thus making detection more difficult. Therefore, only one swab from an AIV-infected broiler from each sample day was pooled with either 10 or 4 individual swabbings from uninfected broilers to create the pools of 11 or 5 swabbings, respectively. The same AIV-infected broilers were used to prepare either the pools of 11 or pools of 5 to minimize variability in AIV genome levels between the two types of pools. Uninfected control broilers were randomly selected for swabbing to create the final pools. A total of 10 replicate pools of 11 or 5 swabbings were prepared on each sample collection day. Swabbings were collected with a plastic shaft Dacron swab (Fisher Scientific, Fairlawn, NJ) and placed into a tube containing 3 ml brain heart infusion broth (Fisher Scientific). To simulate laboratory procedures performed during routine NAI surveillance testing of commercial broilers at National Animal Health Laboratory Network facilities, each swab was agitated 4–5 times and pushed against the side of the tube, expressing the liquid out of the swab as it was drawn out of the tube. Swab pools were frozen at −80 C. After thawing at room temperature, viral RNA was extracted from an aliquot of each O/P swab pool and screened by RRT-PCR for the presence of the AIV matrix gene (8).

Mean AIV RRT-PCR cycle threshold (Ct) values were analyzed between pools of 11 and pools of 5 for a given sample day by *t*-test ($P < 0.05$). The number of AIV-positive pools for a given sample day was analyzed by chi-square analysis ($P < 0.05$). Pools with Ct values >35 were considered negative (10). Pools yielding undetectable Ct values were assigned a Ct value of 46 for the purpose of data analysis. All calculations were made using Excel (Microsoft, Redmond, WA).

RESULTS AND DISCUSSION

Our findings demonstrate that H7N2 LP AIV was readily detected by RRT-PCR in pools of 11 O/P swabbings consisting of one swabbing from AIV-infected broiler chickens and the remaining 10 from uninfected broilers (Table 2). On sample days 2, 3, 4, and 5 PI, 80%–100% of both types of pools were found to be avian

Table 2. Comparison of pooling 11 (one positive and 10 negative swabbings) or 5 (one positive and 4 negative swabbings) on detection of LP H7N2 AIV in broiler chickens using RRT-PCR.

	Pool of 11 oropharyngeal swabbings		Pool of 5 oropharyngeal swabbings	
Sample day postinoculation	Mean AIV RRT-PCR Ct values[A]	Number of AIV-positive pools/total replicates[B]	Mean AIV RRT-PCR Ct values[A]	Number of AIV-positive pools/total replicates[B]
2	31.75	9/10	29.51	10/10
3	30.47*	10/10	27.03*	10/10
4	33.36	10/10	30.19	10/10
5	33.34*	8/10	30.04*	10/10
7	35.37	4/10	35.59	5/10
9	44.51	0/10	42.54	0/10
11	45.14	0/10	Undetectable	0/10
14	Undetectable	0/10	Undetectable	0/10

[A]Asterisks (*) within a row indicate that mean AIV RRT-PCR Ct values, analyzed between pools of 11 or 5 for a given sample day, are statistically different (*t*-test, $P < 0.05$).
[B]Number of AIV-positive pools of 11 or 5 swabbings for a given sample day were analyzed (chi-square analysis, $P < 0.05$). Swab pools with Ct values >35 were considered AI negative. Samples yielding undetectable Ct values were assigned a Ct value of 46 for the purpose of data analysis. No statistical differences were found.

influenza (AI) positive. Mean RRT-PCR Ct values of the pools of 11 swabbings were statistically higher ($P < 0.05$) on day 3 and day 5 PI compared to the pools of 5. Although statistically significant (days 3 and 5 PI) and numerical differences (days 2 and 4 PI) were observed when comparing mean Ct values of the pools of 11 or 5, Ct values for both types of pools were still readily interpretable as AIV positive (Ct < 35). By day 7 PI, mean Ct values increased and the number of AIV-positive pools decreased to similar levels in both the pools of 11 or 5, reflecting lower AIV genome levels. The genome levels observed are consistent with previous findings (6,7).

The LP strain used in the study was readily detected in the swab pools of 11 in spite of the reduction in AIV genome levels observed from days 3–7 PI. Compared to high pathogenicity (HP) AIV infections, LP infections may be more difficult to detect. Levels of genome in swabbings are lower than are typically found in HP infections (9). Therefore, it is likely that swab pools of 11 will be sufficient to detect HPAIV as well.

Based on the findings of the current study, the practice of pooling 11 swabbings for active preslaughter surveillance should receive serious consideration. Moreover, in an actual LPAIV field infection, it is likely that more than a single broiler selected for pooled testing in a flock would be positive for AIV. In addition, the ISRCP stipulates that on-farm NAI surveillance consist of sampling mortalities within the prior 24 hr. ''Barrel surveillance'' swabbing of broilers biases the sampling towards detecting AIV (1).

Cost considerations will continue to drive policy decisions regarding NAI surveillance. There is little doubt that the development of RRT-PCR technology and its application to AIV has been a scientific and, more importantly, a practical success for detecting a disease agent that still threatens a major food animal industry. Further research comparing pooling of 11 or 5 swabbings using other AIV strains and pathotypes is warranted to verify and possibly extend these findings. Policy makers could consider provisional use of pooling 11 swabbings for active preslaughter surveillance testing of healthy flocks until additional data are available.

REFERENCES

1. Akey, B. L. Low-pathogenicity H7N2 avian influenza outbreak in Virginia during 2002. Avian Dis. 47:1099–1103. 2003.

2. Anonymous. Avian influenza info. Washington, D.C., January 12, 2006. Industry to maintain ''full confidence'' in product safety [Internet]. [cited 2011 June 6]. Available from: http://www.avianinfluenzainfo.com/news/1_12_06.html.

3. Das, A. M., E. Spackman, C. Thomas, D. E. Swayne, and D. L. Suarez. Detection of H5N1 high-pathogenicity avian influenza virus in meat and tracheal samples from experimentally infected chickens. Avian Dis. 52:40–48. 2008.

4. Dormitorio, T. V., J. J. Giambrone, K. Guo, and G. R. Hepp. Evaluation of field and laboratory protocols used to detect avian influenza viruses in wild aquatic birds. Poult. Sci. 88:1825–1831. 2009.

5. Elvinger, F., B. L. Akey, D. A. Senne, F. W. Pierson, B. A. Porter-Spalding, E. Spackman, and D. L. Suarez. Characteristics of diagnostic tests used in the 2002 low-pathogenicity avian influenza H7N2 outbreak in Virginia. J. Vet. Diagn. Invest. 19:341–348. 2007.

6. Ladman, B. S., S. C. Rosenberger, J. K. Rosenberger, C. R. Pope, and J. Gelb Jr. Virulence of low pathogenicity H7N2 avian influenza viruses from the Delmarva Peninsula for broiler and leghorn chickens and turkeys. Avian Dis. 52:623–631. 2008.

7. Spackman, E., J. Gelb, L. A. Preskenis, B. S. Ladman, C. R. Pope, M. J. Pantin-Jackwood, and E. T. Mckinley. The pathogenesis of low pathogenicity H7 avian influenza viruses in chickens, ducks and turkeys. Virol. J. 7:331. 2010.

8. Spackman, E., D. A. Senne, T. J. Myers, L. L. Bulaga, L. P. Garber, M. L. Perdue, K. Lohman, L. T. Daum, and D. L. Suarez. Development of a real-time reverse transcriptase PCR assay for type A influenza virus and the avian H5 and H7 hemagglutinin subtypes. J. Clin. Microbiol. 40:3256–3260. 2002.

9. Swayne, D. E., and J. R. Beck. Experimental study to determine if low-pathogenicity and high-pathogenicity avian influenza viruses can be present in chicken breast and thigh meat following intranasal virus inoculation. Avian Dis. 49:81–85. 2005.

10. Takekawa, J. Y., N. J. Hill, A. K. Schultz, S. A. Iverson, C. J. Cardona, W. M. Boyce, and J. P. Dudley. Rapid diagnosis of avian influenza virus in wild birds: use of a portable RRT-PCR and freeze-dried reagents in the field. Immunology and infection. [Internet]. [cited 2011 Nov 7]. Field J. Vis. Exp. 54:e2829. Available from: http://www.JOVE.com/video/2829

11. U.S. Department of Agriculture Animal and Plant Health Inspection Service, June 29, 2007. National Avian Influenza Surveillance Plan [Internet]. [cited 2011 Aug 11]. Available from: http://www.aphis.usda.gov/vs/nahss/poultry/ai/avian_influenza_surveillance_plan_062907.pdf

ACKNOWLEDGMENTS

This research was supported by USDA Multistate Regional Research Project NC-1180. Funding was also provided by the State of Delaware via state lines, ''Poultry Disease Research'' and ''Poultry Diagnostic Laboratory.'' We thank David Shapiro, Don Ritter, and Heather Hirst for reviewing the manuscript.

Vaccine 29 (2011) 7424–7429

Contents lists available at ScienceDirect

Vaccine

journal homepage: www.elsevier.com/locate/vaccine

H7 avian influenza virus vaccines protect chickens against challenge with antigenically diverse isolates

Muhammad Athar Abbas[a,d], Erica Spackman[b,*], Ron Fouchier[c], Derek Smith[c,e,f], Zaheer Ahmed[a], Naila Siddique[a], Luciana Sarmento[b], Khalid Naeem[a], Enid T. McKinley[b], Abdul Hameed[d], Shafqat Rehmani[g,h], David E. Swayne[b]

[a] National Reference Laboratory for Poultry Diseases, NARC, Islamabad 45500, Pakistan
[b] Southeast Poultry Research Laboratory, USDA-ARS, 934 College Station Rd., Athens, GA 30605, USA
[c] Department of Virology, Erasmus Medical Center, Rotterdam, Netherlands
[d] Department of Microbiology and Biotechnology, Quaid-i-Azam University, Islamabad 45320, Pakistan
[e] University of Cambridge, Department of Zoology, Downing Street, Cambridge, CB2 3EJ, UK
[f] Fogarty International Center, National Institutes of Health, Bethesda, MD 20892, USA
[g] Sindh Poultry Vaccine Center, Karachi, Pakistan
[h] University of Veterinary and Animal Sciences Lahore, Pakistan

ARTICLE INFO

Article history:
Available online 29 July 2011

Keywords:
Antigenic cartography
Avian influenza virus
H7
Poultry
Vaccination

ABSTRACT

Vaccination has been a critical tool in the control of some avian influenza viruses (AIV) and has been used routinely in Pakistan to help control sporadic outbreaks of highly pathogenic (HP) H7 AIV since 1995. During that time, several AIV isolates were utilized as inactivated vaccines with varying degrees of success. In order to evaluate which H7 AIV strains may serve as optimal vaccines for diverse H7 AIVs from Pakistan we conducted vaccination-challenge studies with five H7 vaccines against challenge with two HPAIVs: A/chicken/Murree/NARC-1/1995 H7N3 and A/chicken/Karachi/SPVC-4/2004 H7N3. To further characterize the isolates antigenic cartography was used to visually demonstrate the antigenic relationships among the isolates. All vaccines provided similar protection against mortality, morbidity and shedding of challenge virus from the respiratory tract. However, some minor (not statistically significant) differences were observed and correlated with antibody levels induced by the vaccine prior to challenge.

Published by Elsevier Ltd.

1. Introduction

Avian influenza virus (AIV) is among the most important pathogens of poultry world-wide and H7 highly pathogenic (HP) AIV, which is rapidly fatal for chickens has caused outbreaks in commercial poultry in Australia, Canada, Chile, England, The Netherlands, Italy and Pakistan during the past two decades [1–4]. Most frequently, HPAIV is controlled by traditional stamping-out programs. However, in some countries that do not have adequate financial and manpower resources for traditional stamping-out programs, vaccination has been used to reduce virus spread. In Pakistan H7 AIV vaccination has become routine, even when an active outbreak is not underway [5].

Since 1995 there have been several outbreaks of H7 HPAIV and H7 low pathogenic AIV in commercial poultry in Pakistan [2,6,7]. Vaccination was a key component to controlling the virus and is still practiced routinely by some producers. Since 1995 several H7 AIV isolates have been utilized as vaccine seed strains for inactivated oil emulsified poultry vaccines. These seed strains were changed as the viruses in the field evolved and as some strains appeared to provide decreased protection to poultry in the field; sometimes field protection was achieved after administration of multiple vaccinations, at times as many as 3 vaccinations.

To investigate the protection to challenge with viruses which had been used as vaccines in Pakistan against the most recent and the oldest H7 viruses from Pakistan we conducted vaccination-challenge studies using 2 challenge viruses and 5 vaccine seed strains. Two additional viruses were included as vaccines (1 from South America and 1 from Europe) to evaluate whether relatively unrelated viruses were protective against the H7 AIVs from Pakistan. Antigenic cartography was used to further characterize

Abbreviations: AIV, avian influenza virus; AU, antigenic unit; EID, egg infectious doses; HA, hemagglutination; HI, hemagglutination inhibition; HP, highly pathogenic; LP, low pathogenic; NARC, National Agriculture Research Center; OP, oro-pharyngeal; SEPRL, Southeast Poultry Research Laboratory; SPF, specific pathogen free; SPVC, Sindh Poultry Vaccine Center.

* Corresponding author. Tel.: +1 706 546 3617; fax: +1 706 546 3161.
E-mail address: Erica.spackman@ars.usda.gov (E. Spackman).

0264-410X/$ – see front matter. Published by Elsevier Ltd.
doi:10.1016/j.vaccine.2011.07.064

the isolates from Pakistan by visualizing the antigenic relatedness among them and between the vaccines and challenge viruses.

2. Materials and methods

2.1. Viruses

A total of 13 AIV isolates from Pakistan were selected for analyses, including six isolates from the repository of National Reference Laboratory for Poultry Diseases at the National Agricultural Research Center (NARC), Islamabad, Pakistan and seven isolates from 2004 from the Sindh Poultry Vaccine Center (SPVC), Karachi, Pakistan. Since at the time of initial virus selection, neither complete sequence data nor antigenic data for the Pakistani isolates was available isolates for vaccines and challenge were selected to represent different times of isolation, different sectors of poultry production, and different geographical origins to approximate isolate diversity (sequence data supported the initial selection). All isolates were propagated in specific pathogen free embryonating chicken eggs by standard procedures [8]. Allantoic fluid containing infectious virus was used as an antigen source for vaccines and reference antigen.

2.2. Antigenic cartography

To explore the antigenic relationships among the viruses, the 13 H7 AIVs from Pakistan and an additional 6 H7 viruses from the Americas and Europe (A/mallard/Netherlands/12/00 H7N3, A/mallard/Netherlands/9/05 H7N7, A/turkey/Italy/4580/99 H7N1, A/chicken/BritishColumbia/314514-2/04 H7N3, A/mallard/OH/421/87 H7N8 and A/chicken/Chile/176822/02 H7N3) were characterized by hemagglutination inhibition (HI) assay and antigenic cartography as described [9,10]. The HI assay was performed by standard procedures [11] using isolate specific polyclonal chicken sera produced for each of the 19 isolates. Reference sera were produced with an oil emulsion vaccine prepared in-house with Montanide ISA50V adjuvant (SEPPIC, Inc., Paris, France) using infectious allantoic fluid that was inactivated with 0.1% beta-propriolactone. Three week-old specific pathogenic free white leghorn chickens from Southeast Poultry Research Laboratory (SEPRL) in-house flocks were inoculated with 0.5 ml of vaccine by the subcutaneous route and serum was collected 3 weeks post vaccination. Sera were treated with 5% chicken red blood cells for 30 min at ambient temperature to adsorb non-specific agglutinins. Antigenic map construction was performed using the HI assay data. Briefly, antigenic cartography is a method to facilitate the quantitative interpretation and visualization of HI data. In an antigenic map, the distance between antiserum point S and antigen point A corresponds to the difference between the $\log_2$ of the maximum titer observed for antiserum S against any antigen and the $\log_2$ of the titer for antiserum S against antigen A. Thus, each titer in an HI table can be thought of as specifying a target distance for the points in an antigenic map. Modified multidimensional scaling methods are then used to arrange the antigen and antiserum points in an antigenic map to best satisfy the target distances specified by the HI data. The result is a map in which the distance between the points represents antigenic distance as measured by the HI assay in which the distances between antigens and antisera are inversely related to the $\log_2$ HI titer. Because antisera are tested against multiple antigens, and antigens tested against multiple antisera, many measurements can be used to determine the position of the antigen and antiserum in an antigenic map, thus improving the resolution of HI data [9,10].

2.3. Hemagglutination inhibition assay

Sera were tested by the hemagglutination inhibition (HI) assay both to produce the data for antigenic cartography and to evaluate antibody levels in vaccinated birds both pre- and post-challenge. The assay antigens were prepared by inactivating the allantoic fluid from infected chicken eggs with 0.1% beta-propriolactone and adjusting the pH to 7.0 with sodium-bicarbonate. The HI assays were performed in accordance with standard procedures [11]. Titers were calculated as the reciprocal of the last HI positive serum dilution and samples with HI titers of 8 (2^3) or below were considered negative.

2.4. Phylogenetic tree

Protein sequence data for the HA of all isolates has been previously reported [12] and is available from GenBank. Phylogenetic analysis was performed by producing a multiple alignment with ClustalV (Lasergene 7.1, DNASTAR, Madison, WI). The tree was constructed with BEAST v. 1.4.8 [13] using BLOSUM62, gamma + invariant sites, relaxed lognormal clock, Yule Process tree prior with default operators with UPGMA starting tree and MCMC length of 10^6.

2.5. Vaccines

Three H7N3 viruses from Pakistan: A/chicken/Murree/NARC-01/1995 (NARC-1/95), A/Chicken/Karachi/NARC-23/2003 (NARC-23/03), and A/Chicken/Chakwal/NARC-148/2004 (NARC-148/04) were selected for use as vaccine antigens based on chronological and geographic diversity among the H7 isolates from Pakistan. For additional diversity, two other H7 viruses were selected: A/Chicken/Chile/176288/2002 H7N3 (Chile/02) and A/Mallard/Netherlands/9/2005 H7N7 (ML/9/05). Oil emulsion, adjuvanted vaccines were prepared as described by Stone et al. [14]. The hemagglutination (HA) titers of the allantoic fluid used to produce the vaccines after BPL inactivation ranged between 64 and 2048 and the 50% egg infectious doses (EID_{50}) range from $10^{9.3}$ to $10^{10.3}$ per ml (EID_{50} titers were not determined for ML/9/05 or Chile/02) (Table 1). Sham vaccine was prepared with allantoic fluid from uninfected chicken's eggs and prepared with the same oil adjuvant system.

2.6. Vaccination-challenge studies in chickens

One-hundred twenty 3 week-old specific pathogen free (SPF) white leghorn chickens from SEPRL in-house flocks were divided into 12 treatment groups of 10 chickens each (Table 1) and were tagged for individual identification. Ten randomly selected chickens were bled for serum to confirm that the birds were free of AIV antibody. Each vaccine was administered by the subcutaneous route (0.5 ml per bird). Three weeks post-vaccination serum was collected to evaluate antibody responses and the birds were challenged by the intranasal route with 10^6 EID_{50} per bird of the appropriate isolate, NARC-1/95 or A/Chicken/Pakistan/SPVC-4/2004 (SPVC-4/04). Oro-pharyngeal swabs were collected 2 days post challenge (DPC) from all birds challenged with SPVC-4/04 and 3 DPC from birds challenged with NARC-1/95 to evaluate virus shed titers. Swabs were collected on different days because the sham vaccinated birds exposed to SPVC-4/04 were exhibiting clinical signs 2 DPC (but not the NARC-1/95 challenged chickens), therefore there was concern that they may die by 3 DPC. Fourteen DPC sera were collected from surviving birds to evaluate antibody and the birds were humanely euthanized.

Table 1
Morbidity, mortality, mean death times and oral virus shed titers 2 DPC (SPVC-4/04) and 3 DPC (NARC-1//95). Uppercase superscripts indicate statistical groups.

Challenge virus	Vaccine virus	Vaccine antigen		Morbidity (# pos./total)	Mortality (# pos./total)	Mean death time (DPC)	Oropharyngeal swabs	
		EID_{50}/ml (log_{10})	HA titer				# pos./total	Mean titer (log_{10})
Chicken/Murree/NARC-1/95	Chicken/Murree/NARC-1/95	9.3	64	3/10	3/10	3.0	$10/10^{C}$	4.2^{BC}
	Chicken/Karachi/NARC-23/03	9.7	2048	0/10	0/10	NA[a]	$5/10^{AB}$	$\leq 3.1^{AB}$
	Chicken/Chakwal/NARC-148/04	10.3	1024	0/10	0/10	NA	$2/10^{A}$	$\leq 3.1^{A}$
	Mallard/Netherlands/9/05	ND[b]	128	0/10	0/10	NA	$7/10^{ABC}$	$\leq 3.1^{AB}$
	Chicken/Chile/176822/02	ND	256	0/9	0/9	NA	$7/9^{BC}$	$\leq 3.7^{BC}$
	Sham	NA	NA	9/10	9/10	4.2	$10/10^{C}$	4.8^{C}
Chicken/Karachi/SPVC-4/04	Chicken/Murree/NARC-1/95	9.3	64	2/10	2/10	3.0	$9/10^{A}$	$\leq 4.1^{C}$
	Chicken/Karachi/NARC-23/03	9.7	2048	0/10	0/10	NA	$6/10^{A}$	$\leq 3.6^{BC}$
	Chicken/Chakwal/NARC-148/04	10.3	1024	0/10	0/10	NA	$7/10^{A}$	$\leq 3.4^{AB}$
	Mallard/Netherlands/9/05	ND	128	0/10	0/10	NA	$10/10^{A}$	3.9^{BC}
	Chicken/Chile/176822/02	ND	256	1/10	1/10	NA	$9/10^{A}$	$\leq 3.9^{BC}$
	Sham	NA	NA	10/10	10/10	3.4	$7/10^{A}$	$\leq 3.6^{BC}$

[a] NA = not applicable.
[b] ND = not done

2.7. Quantitative real-time RT-PCR

Oro-pharyngeal swabs collected at 2 and 3 days PI from chickens exposed to SPVC-4/04 and NARC-1/95, respectively, were processed for quantitative real-time RT-PCR to determine virus titers. RNA was extracted as described by Das et al. [15] using a combination of Trizol LS (Invitrogen, Inc., Carlsbad, CA) and the MagMAX 96 AI/ND Viral RNA isolation kit (Ambion, Inc. Austin, TX) with the KingFisher magnetic particle processor (Thermo Scientific, Waltham, MA). Quantitative rRT-PCR which targets the influenza M gene [16] was performed using the 7500 FAST Real-time PCR System (Applied Biosystems, Foster City, CA), and the AgPath-ID OneStep RT-PCR kit (Ambion, Inc.) in accordance with the U.S. National Veterinary Services Laboratories protocol AVSOP1521.01. The standard curve for virus quantification was established with RNA extracted from dilutions of the same titrated stock of each virus used to challenge the chickens and was run in duplicate. The limit of detection was determined to be $10^{3.0}$ 50% egg infectious doses per ml, therefore rRT-PCR negative samples were statistically treated as $<10^{3.0}$/ml.

2.8. Statistical methods

The number of birds in each group shedding virus and the titers shed were tested for statistical significance with one-way ANOVA, all pair-wise with the Tukey test. If normality failed then Kruskal–Wallis one-way ANOVA on ranks, Dunn's method was used (SigmaStat 3.1, Systat Software, Richmond, CA). Student's *T*-test was used to compare homologous antibody levels produced to each vaccine (pair-wise). A *p*-value of <0.05 was considered to be significant.

3. Results

3.1. Antigenic cartography

A detailed analysis of the sequences of the viruses in this study and their genetic relationship has been reported previously [12]. Here, the phylogenetic grouping of viruses was compared with the placement of viruses and antisera in an antigenic map. The H7 reference viruses from Europe and North America grouped together at the top of the antigenic map (Fig. 1, in blue). Most of the 2003 and 2004 isolates from Pakistan grouped together at the lower right of the map (Fig. 1, in red) and were within 2 antigenic units (AU) of one-another. One antigenic unit equals a 2-fold dilution in the HI assay, and is represented in the map by one square of the grid. Four H7 viruses from Pakistan did not cluster together. NARC-1/95, SPVC-6/04 and NARC-46/03 were located on the left hand side of the map, approximately 3 AU away from the main Pakistan cluster. The placement of these three strains in the antigenic map did not correspond to particular phylogenetic grouping (Fig. 2). NARC-35/01 clustered with the group of the North American and European viruses, in agreement with the genetic data (Fig. 2). The two challenge viruses selected for the present study, NARC-1/95 and SPVC-4/04 were about 3.5 AU apart, corresponding to a ~12-fold dilution difference of antisera in the HI assay.

The serum positions for the antisera raised against the viruses from Pakistan clustered together at the bottom of the map, with the exception of antisera raised against NARC-35/01 and NARC-1/95, which were positioned at the top of the map, close to positions of antisera raised against the North American and European isolates (Fig. 1). The antisera raised against the vaccine strains selected for this study were well distributed throughout the map. Most sera were within 2 AU from the NARC-1/95 challenge virus and between 2 and 4.5 AU from the SPVC-4/04 challenge virus.

3.2. Serology

Post-vaccination antibody titers to both the vaccine and challenge viruses were evaluated immediately prior to challenge (3 weeks post vaccination). Antibody levels to each vaccine were determined by HI assay and showed that NARC-1/95 and Chile/02 induced significantly ($p < 0.05$) lower antibody titers than NARC-23/03, NARC-148/04 and ML/9/05 (Fig. 3). Pre-challenge seroconversion to the vaccine viruses varied among the groups (Fig. 3) and ranged from 60 to 100% with geometric mean titers ranging among the treatment groups from 28 to 194. Pre-challenge titer against the challenge viruses ranged from 5 to 274 among the vaccine groups (Fig. 3). No antibody was detected in sham-vaccinated birds prior to challenge.

3.3. Vaccination-challenge studies

Pre-challenge antibody titers to the challenge virus correlated inversely with virus titers upon challenge; both challenge group birds with pre-challenge antibody titers above 32 (SPVC-4/04 challenge) or above 64 (NARC-1/95) were shedding approximately 2 log_{10} less virus than birds with lower antibody titers (Fig. 3). There was some correlation with antibody levels against the vaccine virus, however higher antibody titers did not correlate with decreased virus shedding consistently for birds challenged with SPVC-4/04.

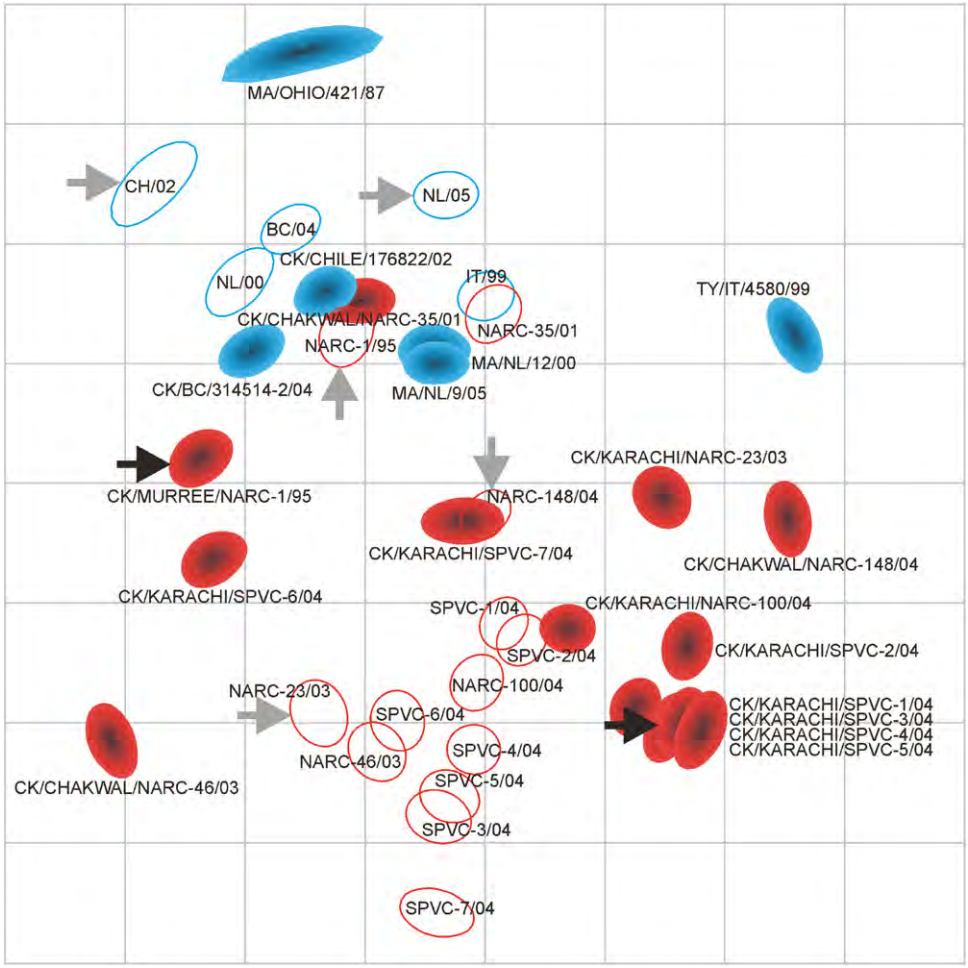

Fig. 1. Antigenic map of H7 avian influenza viruses produced with chicken antisera. The relative positions of viruses (colored shapes) and antisera (open shapes) were adjusted such that the distances between viruses and antisera in the map represent the corresponding HI measurements with the least error. The periphery of each shape denotes a 0.5-unit increase in the total error; thus size and shape represent a confidence area in the placement of viruses and antisera. Red and blue fill color refers to H7 viruses from Pakistan and elsewhere respectively, and red and blue outline color refers to antisera raised against these strains. The vertical and horizontal axes both represent antigenic distance, and because only the relative positions of antigens and antisera can be determined, the orientation of the map within these axes is free. The spacing between grid lines is 1 unit of antigenic distance, corresponding to a 2-fold dilution of antiserum in the HI assay. Black arrows mark the challenge viruses used in the present study and grey arrows mark antisera against the vaccine strains. (For interpretation of the references to color in this figure legend, the reader is referred to the web version of this article.)

There was 90% mortality and morbidity in the group which received sham vaccine that was exposed to NARC-1/95 and virus was detected in oropharyngeal (OP) swabs from 100% of the sham vaccinated chickens with a mean titer of $10^{4.8}$ EID_{50}/ml. This vaccination-challenge study included one homologous challenge: NARC-1/95, this group had 20% morbidity and mortality (Table 1) and shed virus orally at titers similar to those of the sham inoculates. There was no morbidity or mortality in chickens challenged with NARC-1/95 and vaccinated with NARC-23/03, NARC-148/04, ML/9/05 or Chile/02 (Table 1) and mean shed titers were reduced significantly ($p < 0.05$) compared to sham vaccinates in groups vaccinated with NARC-23/03, NARC-148/04, or ML/9/05 (Fig. 3).

There was 100% mortality and morbidity in the sham vaccinated group exposed to SPVC-4/04 and 70% of the birds had detectable titers of virus in OP swabs with a mean titer of $10^{3.6}$ EID_{50}/ml (Table 1). In the group challenged with SPVC-4/04 and vaccinated with NARC-1/95 there was 20% morbidity and mortality (Table 1). Although there was no morbidity or mortality in chickens vaccinated with NARC-23/03, NARC-148/04, ML/9/05 or Chile/02 and challenged with SPVC-4/04, neither the number of birds shedding virus nor the titers shed were significantly different from the sham vaccinates.

Statistically all vaccines protected equally against morbidity and mortality for both challenge viruses and virus shedding was statistically decreased in only one group (NARC-148/04 vaccine with NARC-1/95 challenge) as compared to sham vaccinates and groups vaccinated with NARC-1/95 and Chile/02. All other vaccine groups in the SPVC-4/04 challenge group shed statistically equal levels of virus among all birds challenged (including the sham vaccinates). Among the groups challenged with NARC-1/95, sham vaccinates did shed more than NARC-23/03, NARC-148, Chile/02 or ML/9/05 vaccinated groups.

There was no significant correlation between mortality and morbidity with regard to antigenic distance between the antisera and challenge virus. One non-statistically significant trend was observed with the groups challenged with SPVC-4/04. These groups shed higher virus titers and had lower antibody titers to the challenge virus prior to challenge, which appeared to be associated with antigenic distance between each vaccine and the SPVC-4/04 challenge virus (Fig. 2).

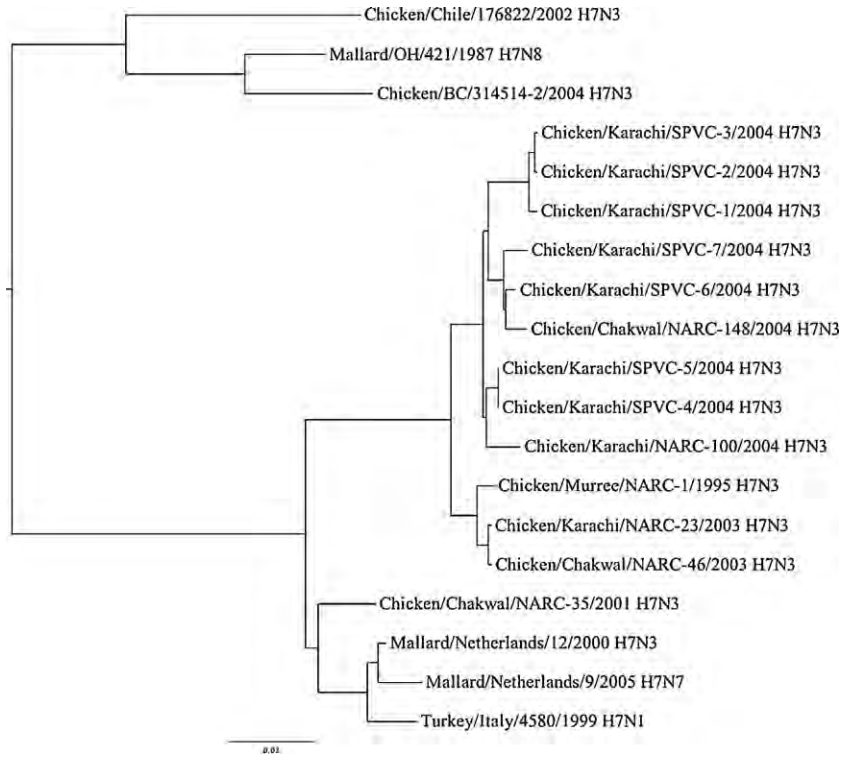

Fig. 2. Phylogenetic tree of the H7 HA protein of all isolates included in this study built with BEAST v. 1.4.8.

4. Discussion

Vaccination for AIV is critical for controlling the virus in poultry in regions where it has become endemic and during sporadic outbreaks in order to minimize economic losses, prevent further spread and assure food security and livelihoods of rural populations. The H7 subtype is one of the most common in poultry worldwide and has been controlled by vaccination programs in Pakistan since 1995 [2,5] although outbreaks have been sporadic, rather than continuous [2,5,6]. During this time several isolates have been used as vaccine seed strains and phylogenetic studies have shown that there were likely two introductions of H7 viruses into poultry in Pakistan [12]. What is not known is the antigenic relatedness among the isolates, nor is it known which isolates could serve as optimal vaccines to the most recent H7 viruses. In this study we evaluated 5 H7 viruses for their ability to protect against challenge with 2 H7 HPAI viruses from Pakistan.

In this study all 5 vaccines protected chickens from mortality and morbidity equally well against challenge with each of the challenge viruses (no statistically significant differences). Unexpectedly the group with the highest mortality was the homologous challenge group with NARC-1/95, which interestingly provided poor protection when used as a vaccine in the field [5,7]. This vaccine groups also had the highest mortality with the SPVC-4/04 challenge. Furthermore, vaccines prepared with NARC-1/95 induced the lowest levels of antibody based on homologous HI prior to challenge. This suggests that the HA from this virus may not be very immunogenic.

Antigenic load in the vaccine may also be a factor in protection and antibody induction. For example poor protection to a virus with a good antigenic match could occur due to a low titer, or a higher antigenic load could make-up for the poorer antigenic match. Here there were differences among the vaccines in the titers (HA and EID_{50}) of virus used to produce them (typically the highest titer which can be achieved is used to produce a vaccine to optimize protection). The NARC-1/95 vaccine, which provided the poorest protection, had the lowest HA titer (64), although was only 1 $\log_2$ from the ML/9/05 virus (titer of 128) which protected similarly to the viruses from Pakistan which had much higher HA titers. The EID_{50} titer of NARC-1/95 was also the lowest of those tested (although $10^{9.3}$ EID_{50}/ml is considered a high titer for AIV). Therefore the antigenic load may have been below some threshold for immunological stimulation, especially if this is a poorly immunogenic virus.

In this study antigenic cartography was used to further characterize the viruses from Pakistan in relation to themselves and some H7 viruses selected as references. There was no clear temporal or geographic pattern of the Pakistani viruses, although most of the Karachi 2004 viruses did cluster together. Some of the differences may be attributed to antigenic drift, which may be affected by vaccination for H7 AIV which was routine in Pakistan during the time these viruses were circulating, however a the virus was eradicated before a dominant lineage could emerge, likely because these minor antigenic differences were not sufficient for the virus to escape vaccine induced immune protection as evidenced by this study.

These findings indicate that any of these AIV isolates (or related isolates) used as vaccines could provide protection against challenge with H7 viruses in Pakistan, with the exception of the NARC-1/95 isolate. One reason for the breadth of protection from most isolates, excluding NARC-1/95, is that the use of the oil adjuvant may have broadened the immune response so that antigenic match is less important. Since nearly all AIV poultry vaccines are inactivated oil adjuvanted vaccines, this effect is relevant for the field. However, it also needs to be taken into account that protection in a laboratory setting, with SPF chickens that have relatively few stresses compared to chickens in commercial conditions will always be superior [17].

With further work we aim to investigate the factors in vaccine efficacy for AIV in chickens and how they relate to antigenic relatedness more specifically and also to investigate the role of specific amino acids in antigenic grouping.

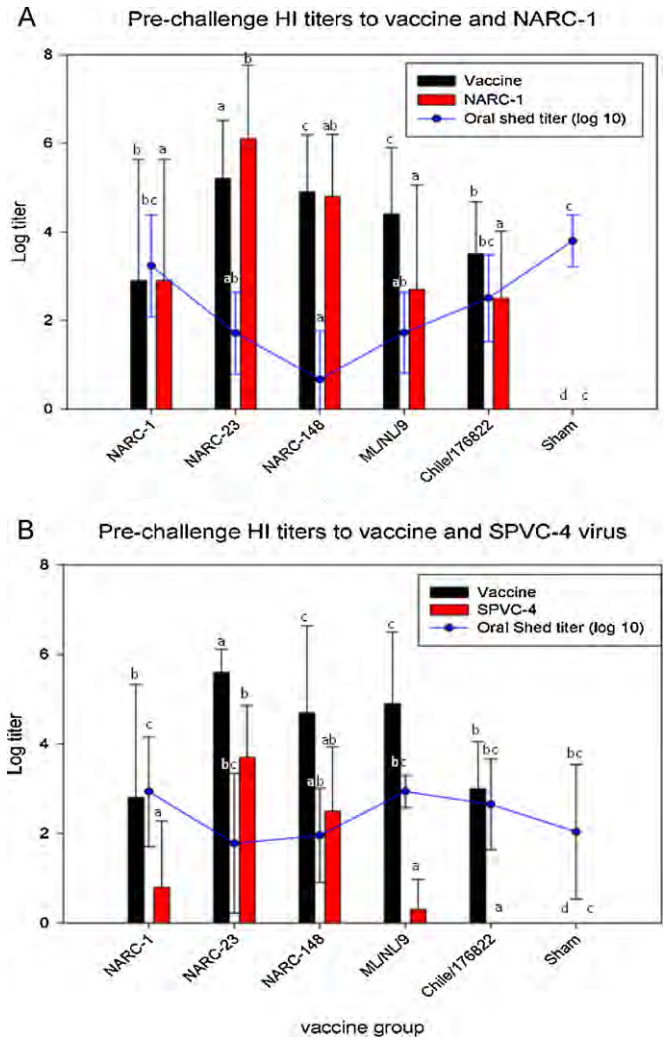

Fig. 3. Pre-challenge HI titers to the vaccine virus and challenge virus versus oral shed titers (a) NARC-1/95 challenge; (b) SPVC-4/04 challenge. Letters over error bars denote statistical groups for virus shed, pre-challenge antibody to the vaccine, and pre-challenge antibody titers to the challenge virus.

Acknowledgements

The authors gratefully acknowledge Joan Beck, Scott Lee, Kira Moresco and James Doster for technical assistance with this work. Funding was partly provided by the United States Department of State Biosecurity Engagement Program through a Memorandum of Agreement with the United States Department of Agriculture, Agricultural Research Service and by the FAO grant OSRO/RAS/703. DJS was supported by an NIH Director's Pioneer Award DP1-OD000490-01, RF by NIAID/NIH contract HHSN266200700010C and both DJS and RF by FP7 grant 223498 EMPERIE from the European Union.

Mention of trade names or commercial products in this publication is solely for the purpose of providing specific information and does not imply recommendation or endorsement by the U.S. Department of Agriculture.

References

[1] Alexander DJ. Summary of avian influenza activity in Europe, Asia, Africa, and Australia, 2002–2006. Avian Dis 2007;51:161–6.
[2] Naeem K, Siddique N, Ayaz M, Jalalee MA. Avian influenza in Pakistan: outbreaks of low- and high-pathogenicity avian influenza in Pakistan during 2003–2006. Avian Dis 2007;51:189–93.
[3] Pasick J, Handel K, Robinson J, Copps J, Ridd D, Hills K, et al. Intersegmental recombination between the haemagglutinin and matrix genes was responsible for the emergence of a highly pathogenic H7N3 avian influenza virus in British Columbia. J Gen Virol 2005;86:727–31.
[4] Rojas H, Moreira R, Avalos P, Capua I, Marangon S. Avian influenza in poultry in Chile. Vet Rec 2002;151:188.
[5] Naeem K, Siddique N. Use of strategic vaccination for the control of avian influenza in Pakistan. Dev Biol (Basel) 2006;124:145–50.
[6] Naeem K. The avian influenza H7N3 outbreak in South Central Asia. In: 4th International Symposium on Avian Influenza. 1997. p. 15–31.
[7] Naeem K, Hussain M. An outbreak of avian influenza in poultry in Pakistan. Vet Rec 1995;137:439.
[8] Senne DA. Virus propagation in embryonating eggs. In: Swayne DE, Gilsson JR, Jackwood MW, Pearson JE, Reed WM, editors. A laboratory manual for the isolation and identification of avian pathogens. 4th ed. Kennett Square, PA: American Association of Avian Pathologists; 1998. p. 235–40.
[9] Fouchier RA, Smith DJ. Use of antigenic cartography in vaccine seed strain selection. Avian Dis 2010;54:220–3.
[10] Smith DJ, Lapedes AS, de Jong JC, Bestebroer TM, Rimmelzwaan GF, Osterhaus ADME, et al. Mapping the antigenic and genetic evolution of influenza virus. Science 2004:1097211.
[11] Pedersen JC. Hemagglutination-inhibition test for avian influenza virus subtype identification and the detection and quantitation of serum antibodies to the avian influenza virus. Methods Mol Biol 2008;436:53–66.
[12] Abbas M, Spackman E, Swayne D, Ahmed Z, Sarmento L, Siddique N, et al. Sequence and phylogenetic analysis of H7N3 avian influenza viruses isolated from poultry in Pakistan 1995–2004. Virol J 2010;7:137.
[13] Drummond AJ, Rambaut A. BEAST: Bayesian evolutionary analysis by sampling trees. BMC Evol Biol 2007;7:214.
[14] Stone HD, Brugh M, Hopkins SR, Yoder HW, Beard CW. Preparation of inactivated oil-emulsion vaccines with avian viral or Mycoplasma antigens. Avian Dis 1978;22:666–74.
[15] Das A, Spackman E, Pantin-Jackwood MJ, Suarez DL. Removal of real-time reverse transcription polymerase chain reaction (RT-PCR) inhibitors associated with cloacal swab samples and tissues for improved diagnosis of Avian influenza virus by RT-PCR. J Vet Diagn Invest 2009;21:771–8.
[16] Spackman E, Senne DA, Myers TJ, Bulaga LL, Garber LP, Perdue ML, et al. Development of a real-time reverse transcriptase PCR assay for type A influenza virus and the avian H5 and H7 hemagglutinin subtypes. J Clin Microbiol 2002;40:3256–60.
[17] Swayne DE, Suarez DL. Highly pathogenic avian influenza. Rev Sci Tech 2000;19:463–82.

Avian Pathology (June 2012) **41(3),** 251–258

Taylor & Francis
Taylor & Francis Group

REVIEW

Viral diagnostics: will new technology save the day?

Erica Spackman*

Southeast Poultry Research Laboratory, USDA-ARS, 934 College Station Road, Athens, GA 30605, USA

Technology for infectious agent detection continues to evolve, particularly molecular methods that first emerged in the mid-1970s. The goals of new technology in diagnostics, whether in humans or in animals, including poultry, are to achieve the highest sensitivity and specificity possible to accurately identify the infection status of an individual or flock in the shortest time possible. Ease of use, low cost and increased information from a single test (e.g. multiplexing) are also critical areas frequently targeted for improvement. New tests and modifications of current tests are reported often, and diagnostic tests are now commonly developed by commercial companies. As one would expect, most advances in diagnostic technology are applied first to human health, and then may be adapted to animal health if practical. In the present review the trends and novel innovative technologies in primarily viral diagnostics are reviewed and the practicality of these methods and application for poultry health are discussed briefly. Also, influenza will seem to be over-represented in viral diagnostics since it is frequently used as a proof-of-concept target for novel technology due to its importance for animal and public health. Finally, the review is intended to be a brief survey of some of the innovative diagnostic technologies reported in recent years. It is not entirely comprehensive of all technology and the author makes no claims or endorsements of any of the technology or products mentioned.

Downloaded by [National Agricultural Library] at 06:02 14 September 2012

A Brief History of Diagnostics

The classical age. It is noteworthy how rapidly technology for viral diagnostics has evolved over the past century. However, some of the oldest classical or molecular methods are still in use, although with some modifications.

Viruses were first identified as filterable agents in 1898, when foot and mouth disease was discovered by Loeffler & Frosch (1898). The ability to propagate viruses outside an animal host was an enormous advance for virology and was first reported in embryonated chicken eggs with Rous sarcoma virus in 1911 (Rous & Murphy, 1911); however, it was not until the 1930s, after it was reported that fowlpoxvirus could be propagated in embryonated chicken eggs (Woodruff & Goodpasture, 1931), that the method began to be used more widely. By the mid-1930s methods to propagate Variola virus, mumps and herpesviruses were reported (Goodpasture *et al.*, 1931; Lazarus *et al.*, 1937; Nelson, 1939). It was not until 1948 that cell culture was first reported when Weller and Enders developed cell culture for mumps and influenza (Weller & Enders, 1948).

Antibody-based assays constituted the first era in viral diagnostics. Complement fixation was described in 1929 for several viruses (Bedson & Bland, 1929) and a fluorescent antibody test for influenza was reported in 1956 (Liu, 1956). Electron microscopy using negative staining was first described for virus detection in 1959 (Brenner & Horne, 1959), and then a vast improvement in electron microscopy came about in 1967 when Best *et al.* described the use of specific antibody, in what is now known as immune electron microscopy, for rubella virus detection (Best *et al.*, 1967). Monoclonal antibodies, first reported in 1975 (Kohler & Milstein, 1975), were the next great technological leap and led the way for improved antibody-based tests for virus detection.

Protein separation by electrophoresis was developed in the mid-1960s (Davis, 1964; Ornstein, 1964) and allowed for virus proteins to be identified by weight and, more specifically, by antibody once the western blot was established (Towbin *et al.*, 1979). The original protein assays were primarily used in research settings, but western blotting has been used to diagnose virus infection by antibody detection for viruses that establish chronic infections such as human immunodeficiency virus (Burke *et al.*, 1987) and even feline immunodeficiency virus (Egberink *et al.*, 1991). Western blot and enzyme-linked immunosorbent assay technology evolved into lateral-flow antigen-detection immunoassays in the mid-1980s by utilizing the antibody in the solid phase and the antigen in the liquid phase (Gary *et al.*, 1985; Rivera *et al.*, 1986). Antigen-detection immunoassays were soon optimized to be substantially cheaper and easier to run. Faster, point-of-care commercial kits were marketed and validation studies began to be reported (Dascal *et al.*, 1989) and are now among the most common commercial diagnostic test formats in human and veterinary medicine. For example, in North America at least five companies manufacture kits for seasonal influenza and six companies manufacture kits for respiratory syncytial virus.

This review was presented as the Houghton Lecture at the 17th Congress of the World Veterinary Poultry Association in Cancun, Mexico, 2011
*To whom correspondence should be addressed. Tel: +1 706 546 3617. Fax: +1 706 546 3161. E-mail: Erica.spackman@ars.usda.gov
Received 14 November 2011
ISSN 0307-9457 (print)/ISSN 1465-3338 (online)/12/030251-08 © 2012 Houghton Trust Ltd
http://dx.doi.org/10.1080/03079457.2012.675051

Downloaded by [National Agricultural Library] at 06:02 14 September 2012

The molecular era. The development of molecular biological methods represented a substantial change in microbiological research and diagnostics by making the genetic material of an organism accessible and identifiable. The initial advantage of molecular diagnostic tests was that they could achieve a level of specificity well beyond that of classical methods. As the technology has been refined, molecular tests are now able to exceed classical tests in sensitivity and most can provide additional specific relevant information about the target, such as type, subtype, lineage, drug resistance, serotype, and so forth.

During the mid-1970s, molecular methods began to emerge when Southern blotting was described. Material could now be probed with radio-labelled nucleic acids for specific DNA sequences (Southern, 1975). Related methods such as northern blotting (Alwine *et al.*, 1977), restriction fragment-length polymorphism analysis (Mears *et al.*, 1978) and refinements of the original methods soon followed. Although there were some reports of the application of this technology for the detection of infectious agents, Southern and northern blotting were never widely adopted by clinical diagnostic laboratories because they are slow, expensive and at that time were further complicated by necessity of using radionuclides to visualize the results. The potential advantages of molecular methods over classical methods thus did not offset the disadvantages.

The method of polymerase chain reaction (PCR) was first reported in 1985 (Saiki *et al.*, 1985) for primer-mediated enzymatic amplification of specific target sequences in genomic DNA. The technique was revolutionary in that it enabled the rapid and accurate detection of specific DNA sequences in pathogenic organisms. At that time, PCR reactions had to be carried out by hand; tubes were manually moved between water baths at different temperatures to complete each cycle and fresh polymerase enzyme needed to be added after each cycle because thermostable polymerases had not yet been utilized. The method was greatly enhanced when thermostable polymerases were introduced in 1988 (Saiki *et al.*, 1988), which also improved the specificity of PCR because higher cycling temperatures were possible. Another problem was resolved when reverse transcription (RT)-PCR was developed in 1988, making it possible to produce DNA copies of target RNA viruses (Rappolee *et al.*, 1988). Soon after its development, PCR was applied to the detection of human papillomavirus (Shibata *et al.*, 1988) and RT-PCR was applied to human immunodeficiency virus type 1 detection (Hart *et al.*, 1988). A multiplex test for influenza A and influenza B followed a few years later (Fan *et al.*, 1998). Real-time PCR, which visualizes the results as the reaction is running, was introduced in 1996 (Heid *et al.*, 1996) and was first applied to viral diagnostics in 1999 when tests for SV40 and hepatitis B were first reported (Abe *et al.*, 1999; Shi *et al.*, 1999). However, as with earlier molecular tests, PCR-based methods were not picked up quickly by clinical diagnostic laboratories.

Not surprisingly, as molecular technologies have expanded, commercial companies producing tests have multiplied; in 2011 there were approximately 350 companies that manufacture *in vitro* molecular medical tests (Carlson, 2011). However, commercial molecular tests are primarily found only in the developed world, with 79% of the market being in the US and Europe (Carlson, 2011).

Molecular diagnostics for poultry diseases. The early 1990s was also the time when PCR methods were first introduced for the detection of poultry viruses with tests for chicken infectious anaemia virus, infectious bronchitis virus, infectious bursal disease virus, Marek's disease virus, infectious laryngotracheitis virus and avian leucosis viruses (Tham & Stanislawek, 1992; Todd *et al.*, 1992; van Woensel *et al.*, 1992; Williams *et al.*, 1992; Kwon *et al.*, 1993; Stauber *et al.*, 1995; Jackwood *et al.*, 1996). The first RT-PCR for avian influenza virus (AIV) was reported in 1995 (Horimoto & Kawaoka, 1995), but as a method to amplify the haemagglutinin for sequencing to evaluate pathotype rather than for initial virus detection. In addition to identifying infected flocks, some of the earlier applications of PCR methods in poultry health were aimed at detecting vaccine contaminants (Bruckner *et al.*, 1996; Reimann & Werner, 1996). As with human medicine, research laboratories adopted the technology much earlier than diagnostic laboratories.

Current Capabilities

Current achievable detection limits are a single molecule: virion, protein, RNA or DNA. However, few tests with that level of sensitivity and specificity are available clinically. In general the adoption of new technology lags behind its development, so the state of the art does not necessarily correlate with routine practice. One reason is that there are numerous barriers to adoption that must be overcome for any new technology to be adopted by diagnosticians. These include: cost of new equipment; fit into workflow; new skills/training needed for personnel; and validation and regulatory approval.

Finally, because of wide variation in resources and needs among veterinary (and public health) laboratories worldwide, it is difficult to identify a "standard" method or technology. However, it is apparent that in both veterinary medicine and human health two of the most widely used methods for virus detection are PCR-based methods and virus culture, depending on the target.

It is also interesting to point out a difference between veterinary and human health laboratories, where the veterinary laboratories have the advantage in adopting new technology. Although veterinary diagnostic programmes, particularly for food animals, generally do not have the same resources as public health, less strict regulations can promote more rapid adoption of new technologies (and frequently there are grey areas as regulations often lag behind the emergent technology). In public health, *in vitro* diagnostic tests are typically commercial kits, which frequently require some form of licensing (e.g. approval by the Food and Drug Administration in the US and the CE-IVD mark in Europe). In veterinary medicine, in-house tests are used much more commonly as there are fewer commercial kits available, due to the smaller market (but note that commercial veterinary kits often do require licensing as well). However, this extra freedom has also meant that harmonization has been difficult to achieve. Some harmonization has been established since the World Organisation for Animal Health (OIE) has been able to recommend specific methods for agents that are listed diseases (OIE, 2011). An additional difference between human and animal diagnostic tests is that tests for animal diseases can be tested and validated using

Downloaded by [National Agricultural Library] at 06:02 14 September 2012

experimentally-generated specimens from the target host. This allows for better information on test performance, an easier paradigm for refining tests and better validation data.

In poultry health laboratories, in-house tests (i.e. any test that is not available as a commercial kit, including peer-reviewed published assays and unpublished assays) are not uncommon. Commercially produced test kits have become increasingly available for important animal diseases, including tests for poultry (Table 1). By far the most targeted agent by commercial kits is AIV due to its zoonotic potential and because it is an OIE-listed disease. In some cases the same kit for AIV (type A influenza) marketed for poultry has been validated and is available for humans, swine, horses, and so forth, and *vice versa*. An interesting illustration of this is shown in Figure 1, which compares graphically the number of publications in the PubMed database for AIV PCR tests, Newcastle disease virus (NDV) PCR tests and Marek's disease virus PCR tests by year. Although not all papers are necessarily for diagnostic tests, this demonstrates the focus on AIV versus NDV and Marek's disease virus, both of which are historically more important for poultry production but are not zoonotic concerns; market potential has thus driven discovery to some degree. Commercialization of new kits for poultry diseases will probably be slow due to limited markets compared with public health. However, bacterial agents that are important for food safety (e.g. *Salmonella enteriditis*, *Campylobacter jejuni*) have also been targeted widely for commercial kits.

Among the in-house tests, real-time PCR-based methods are probably the assay of choice. In veterinary diagnostics, real-time PCR is the preferred test for numerous OIE-listed diseases (Hoffmann *et al.*, 2009). Currently real-time RT-PCR is probably the most common test for AIV and NDV, where it is used as a screening test with virus isolation in embryonated chicken eggs being used as a confirmatory test. PCR-based tests (real-time or conventional) have been reported for detecting almost all poultry viral and bacterial diseases of poultry, and a few have been developed to further characterize isolates such as (not a comprehensive list): tests that differentiate NDV lineages (Wise *et al.*, 2004; Farkas *et al.*, 2009), AIV subtypes (Spackman *et al.*, 2002; Das & Suarez, 2007) and infectious bursal disease virus pathotypes (Ghorashi *et al.*, 2011; Hernandez *et al.*, 2011) and that identify infectious bronchitis virus serotypes/genotypes (Jackwood *et al.*, 1997; Keeler *et al.*, 1998; Moscoso *et al.*, 2005; Wang & Khan, 1999; Jones *et al.*, 2011). Although PCR-based methods, including conventional and real time, are used widely, kits for few poultry agents have been commercialized.

Novel Technologies

In diagnostics there are limited numbers of targets to choose for agent detection: proteins from the target agent, the nucleic acid of the target agent, or the host's specific immune response to the target agent. Detection assays can either amplify the target or the signal to improve sensitivity, and refinements to these can substantially improve sensitivity and specificity of the established tests. We now have the technology to detect a single molecule of RNA, DNA or protein, including a single virion. Thus we have hit what is probably the limit for sensitivity and specificity, and now the trend in technology is to improve convenience (time, cost, ease of use, multiplexing, reusable or disposable), or to specialize for a specific situation ("personalized" medicine) in order to provide in-depth information.

PCR-based assays are the most common tests that target agent nucleic acids, and most protein detection assays utilize antibody for specific target detection. Of course improvements and modifications continue to be developed for each target type, which increase sensitivity, specificity, and information, and which can reduce cost and time to result. Overall trends in diagnostic assay

Table 1. *Commercial test kits available for poultry diagnostics (availability varies regionally).*

Format	Target	Agents	
Enzyme-linked immunosorbent assay	Antibody	Avian encephalomyelitis virus	*Bordetella avium*
		Avian influenza virus	*Mycoplasma gallisepticum*
		Avian leucosis virus	*Mycoplasma synoviae*
		Avian pneumovirus	*Mycoplasma meleagridis*
		Avian reovirus	*Ornithobacterium rhinotracheale*
		Chicken anaemia virus	*Pasteurella multocida*
		Infectious bronchitis virus	*Salmonella enteriditis*
		Infectious bursal disease	
		Infectious laryngotracheitis virus	
		Haemorrhagic enteritis virus	
		Newcastle disease virus	
		Reticuloendotheliosis virus	
Serum plate agglutination	Antibody	*Mycoplasma gallisepticum, Mycoplasma synoviae, Mycoplasma meleagridis, Salmonella pullorum*	
Agar gel immunodiffusion assay	Antibody or antigen	Avian influenza virus	
Lateral flow immunoassay	Antigen	Avian influenza virus	
PCR (including real-time PCR)	Nucleic acid	Avian influenza virus, Newcastle disease virus, *Salmonella* spp.	
Nucleic acid sequence-based amplification	Nucleic acid	Avian influenza virus, Newcastle disease virus	

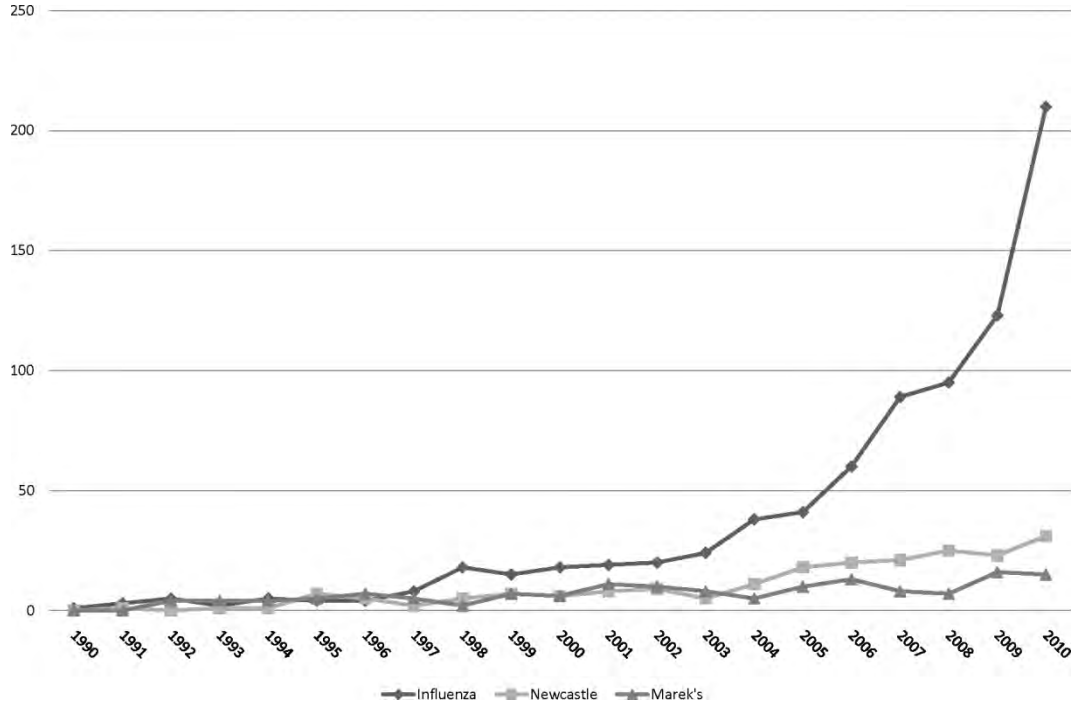

Figure 1. *Number of publications in the PubMed database by year with "PCR" and "avian influenza", "Newcastle disease" or "Marek's disease".*

Downloaded by [National Agricultural Library] at 06:02 14 September 2012

improvements are presented in Table 2. To be viable, and also successful, technologies must involve improvements in numerous areas compared with any current tests. Instrumentation is a major area of development, and new assays frequently rely on test-kit-specific instruments (which is also due to commercialization).

Nucleic acid detection. There are numerous nucleic acid detection technologies available: PCR based, isothermic amplification, and microarray—but PCR-based assays are probably the most widely used. Assays to further characterize nucleic acids include sequencing, microarray and restriction fragment-length polymorphism, and are usually only utilized by reference laboratories. A full examination of nucleic acid detection technology is beyond the scope of this review, so the focus is on some of those that have had the most impact.

Isothermic amplification methods such as loop-mediated isothermal amplification and nucleic acid sequence-based amplification have been used for years, and have the advantage that thermo-cyclers are not necessary and the reactions can be incubated in a simple water bath. They have similar sensitivity and specificity to PCR, but can be more expensive to run due to the cost of the reagents.

Microarrays have been proposed as a diagnostic tool that can provide a high level of information, so not only can one identify the target agent but also crucial information such as strain, lineage, pathotype, and so forth, can be gained. Microarrays are similar to Southern blots as they both rely on DNA hybridization, but microarrays use a glass slide that has hundreds of DNA probes attached to it instead of a single probe in the liquid phase. The microarray slide is incubated with nucleic acid from a specimen, and if the nucleic acid in the sample matches (a complementary match) a probe sequence on the microarray slide it will bind, which produces a fluorescent signal. The signal can be detected and differentiated from that of all the other sequences on the slide, so the specific sequence that is bound can be identified from among the hundreds on the slide, thus providing specific sequence information on the target. If multiple sequences from the specimens bind they can be read separately, which can provide additional information by multiplexing. Unfortunately, however, microarrays have relatively poor sensitivity and require prior enrichment of the target; they also take more time to run than PCR tests, and cost substantially more per sample. If some of these problems can be resolved, microarrays would be a useful tool for reference laboratories to investigate new disease outbreaks (such as an index case), or even new variants of infectious agents. However, gene sequencing has become so fast and cheap that in-depth analysis of PCR products is common and can provide much of the same information that a microarray can, and more efficiently. Currently, microarrays have the most diagnostic utility for genetic conditions such as cancer, rather than for infectious disease.

Numerous modifications have been reported to improve PCR-based methods and many involve improving the sensitivity and specificity of the reaction. Real-time PCR probes can be constructed in many ways (hairpins, two probe systems, different dyes), all of which have different advantages and disadvantages for cost, sensitivity and specificity that can be optimized for a given test or instrument. The simplest modifications are those that optimize the temperature cycling parameters to exploit the characteristics of the enzyme and template. Some examples are linear-after-the-exponential PCR and touch-down PCR. Other modifications involve using molecularly altered primers (and sometimes probes with real-time PCR). An example is minor groove binding protein (Kutyavin *et al.*, 2000), which enhances binding allowing for shorter probes by raising the melting temperature. Probes with minor groove binding protein have been applied to the detection of several viral

Table 2. *Trends in improving diagnostic tests and some common approaches.*

Description	Goal	Approach
Specificity	Improved accuracy	Modifications to proteins and nucleic acids Cycling parameters
Sensitivity	Improved accuracy	Detection of analyte Cycling parameters Probe design
Stability	Lower cost Increased utility	Isothermic reactions Stable enzymes Stable dyes
Smaller volumes	Lower cost per test Higher capacity Faster results	Instrumentation
Automation	Reduce operator error and cost Reduce errors with interpretation of results Remote analysis possible	Instrumentation
Multiplexing	Cheaper More information per test	Instrumentation Reporter molecules (dyes, nanoparticles, quantum dots, etc.)
Point of care	Convenience Provides immediately actionable information	Instrumentation Stable reagents

diseases of poultry including AIV, infectious laryngotracheitis virus and NDV (Di Trani *et al.*, 2006; Lu *et al.*, 2008; Farkas, *et al.*, 2009; McMenamy *et al.*, 2011). This approach works well for highly variable targets where conserved regions are too short for a conventional probe.

Ultra-small particles such as nanoparticles, quantum dots and microspheres have also been utilized to modify PCR-based assays and have also been employed widely for antibody-based assays. Each of these has different features and needs to be used with specific instrumentation, but can be uniquely labelled and used to specifically identify a PCR amplification product. One of the most practical features of nanoparticles, microspheres and quantum dots is that there are many unique labels that can be used so, in theory, reactions can be highly multiplexed, even into hundreds. Of course there are other technical issues with interference and competition when PCR is highly multiplexed and the instrumentation is expensive, but as the technology improves it will become more practical.

Owing to advances in microfluidics in recent years, improved PCR instrumentation and reaction automation has been developed. One innovation is all-in-one/self-contained cartridges that extract the DNA or RNA and run the reaction. The cartridges are run in vendor-specific, dedicated instruments that analyse the results; for example, Gene Xpert (Cephied Inc., Sunnyvale, CA, USA) and Film Array (Idaho Technologies Inc., Salt Lake City, UT, USA). Microfluidics have also allowed sample volumes to decrease, which increases the sample capacity, decreases the cost per reaction and reduces the time needed to run the reaction; one example is the Integrated Cycler (3M, Focus and Simplexa, Focus Diagnostics, Inc. Cypress, CA, USA), which runs 96 samples in a small single-use carousel and heats with infrared radiation. Digital PCR (Applied Biosystems, Life Technologies Corp., Carlsbad, CA, USA) uses microfluidics to partition a PCR reaction into volumes so low that only a single molecule of analyte should be present, thus allowing absolute quantitation.

Biosensors. Biosensors are instruments that use everything from chemical reactions to electrical resistance to detect a wide range of analytes as diverse as chemicals, viruses and bacteria. Currently most commercially available biosensors are for chemicals, such as drugs and explosives, but perhaps the most common biosensors are blood glucose monitors. Biosensors have been reported for several viruses using DNA and viral proteins as targets (Wang *et al.*, 1996; Inoue *et al.*, 1999; Baeumner *et al.*, 2002; Zhou *et al.*, 2002; Xu *et al.*, 2007), but none have been adopted clinically. If the technology can be validated for viruses, portable biosensors would provide an advantage over other technologies, as samples frequently require minimal processing, making them appropriate for point-of-care testing. Most are reusable or have minimal consumables; the costs of individual tests should therefore be low.

Reporter cell lines. Reporter cell lines are cell lines that have been modified to produce a measurable signal when they are infected by a target virus. For example, the enzyme-linked virus inducible system cell line (Proffitt & Schindler, 1995), which is now commercially available, is engineered to produce β-galactosidase when infected with herpes simplex virus. The β-galactosidase gene was inserted into the cell line and linked to a promoter that is controlled by viral proteins, so β-galactosidase is only produced when replicating herpes simplex virus is present. In some cases, cell lines that would not be naturally susceptible to infection with a virus can be engineered to be susceptible by inserting the appropriate receptor.

Although reporter cell lines are specific and sensitive, they take a relatively long time to yield results and require a high degree of technical skill and resources. Also, there is some limitation for the agents these cell lines can target because a high degree of detail of the virus replication cycle has to be known, and the disease in question needs to be important enough to merit the skill and resources required to make the tests practical and cost-effective.

Detection of a specific immune response. One novel approach is to detect the host-specific anamnestic immune response to a pathogen, instead of the pathogen itself. A commercially available kit using this technology is the "Quantiferon" kit (Cellestis Ltd., Melbourne, Australia), a tuberculosis test. A cytomegalovirus test is also available and is marketed for pre-organ transplant testing. Some of the details of the test are proprietary, but essentially blood from the patient is exposed to antigen from the target pathogen, and the test then evaluates the level of interferon induced from immune cells in the blood. The advantage of this format is that both active and latent infection can be detected in individuals while tests for the agent itself (including culture) or the agent's nucleic acid would be negative in a latent infection. In some ways Quantiferon is similar to the tube or plate agglutination tests used for avian

Downloaded by [National Agricultural Library] at 06:02 14 September 2012

mycoplasma, except that it detects active or latent infection instead of antibody. This format would probably not work well for acute infections and so far has not been applied to poultry infections.

Sample collection, transport and processing. One critical area, which has been largely ignored by diagnostic test developers, is sample collection and processing. Sampling methods for viruses (i.e. media, swab types, sample transport and storage) were originally based on bacterial methods and there are relatively few reports in veterinary or human medicine of validation studies of sample collection and transport. Similarly there are few reports of improvements in sample collection technology. Two relatively recent notable technologies are the use of flocked swabs and FTA cards (Whatman Inc. Whatman Plc, Maidstone, Kent UK). Flocked swabs are composed of a nylon material that is claimed to have superior capture and release characteristics compared with conventional swabs, thus improving sensitivity by increasing the amount of analyte in the sample (Daley *et al.*, 2006; Dalmaso *et al.*, 2008; Scansen *et al.*, 2010). FTA cards have probably had the greatest impact on sample collection and transport of any technology in past decade. They can be used to collect any fluid that can be spotted on the card. Chemicals in the cards inactivate most pathogens and stabilize the nucleic acid, which can then be safely shipped at ambient temperatures and without International Air Transport Association classification as a live pathogen, which saves money. Nucleic acids are extracted from discs punched from the card at the destination laboratory and can be processed for any nucleic acid detection assay. The use of FTA cards has been reported for specimen collection, shipping and subsequent detection of AIV, infectious bronchitis virus, infectious bursal disease virus and NDV (Moscoso *et al.*, 2005, 2006; Perozo *et al.*, 2006; Purvis *et al.*, 2006; Abdelwhab *et al.*, 2011; Kraus *et al.*, 2011).

Some sample processing and collection innovations are too new to have been widely adopted or are still in commercial development. A novel method for nucleic acid purification is syncronous coefficient of drag alternatives (Marziali *et al.*, 2005), which uses the unique electro-chemical properties of DNA and RNA to purify them from cells and contaminants that could be inhibitory for PCR and other assays. This method has been described by its inventor, Andre Marziali, as "focusing DNA in a spot in a gel while all other molecules are excluded" due to their unique behaviour in an electric field (Roberts, 2011). Another approach to sample collection that is still in development is a mask to collect respiratory agents from coughs, which concentrates them in a buffered solution (Deton Corp., Pasadena, CA, USA) (Roberts, 2011). The latter will probably never be practical for poultry, but is a good example of emergent sample collection technology.

What Does the New Technology Mean for Poultry Health?

Regardless of technological capabilities the market will always determine what tests are implemented. Many of the above technologies were developed with human health in mind, where an individual is the target. In contrast, the approach to poultry and food animal health differs somewhat when the target is a population. Also, just because we can do something does not mean it is necessary or practical; for example, sensitivity to the point of single-molecule detection. Would detection of a single AIV virion or *Mycoplasma gallisepticum* cell really improve control or would it complicate control? Is detection of a single molecule clinically relevant? Is such detection necessary and can the cost be justified? The answers to these questions vary by agent and situation, and the utility and success of a test is heavily reliant on whether it is fit-for-purpose: the best test is the one that fulfils the needs of the situation. The needs vary among different compartments and regions, whether testing is for flock health versus food safety and trade, the importance of the test target, and so forth. For example, a test that works well for the broiler industry in Mexico may not be as practical for layers in the US. This leads to perhaps one of the most important questions when implementing a test, and one that should be considered during development: *how will the results be used?*

Looking at how new technology has been implemented in the past shows an interesting trend; molecular methods have not completely supplanted classical methods, such as culture. AIV and NDV are good examples where molecular tests have improved detection in the field, so that immediate action can be taken in the case of a positive flock, but culture is still required to obtain a live agent for regulatory action, to characterize the virus present, and for development of vaccines. This paradigm, where molecular tests and point-of-care tests are used as screening tests and then additional confirmatory tests (often culture) must be conducted, is utilized for numerous veterinary and human diseases. The new technology has added to our arsenal, but in many cases has not truly replaced the original test. This is likely to be true with the newest innovations; the molecular methods could be modified or replaced, but the classical methods, specifically culture, will not be abandoned.

In general, many novel technologies will not be easily adopted due to cost or an impractical format. But if one was to select one of the technologies outlined above as having the most promise for poultry diagnostics, the biosensor would probably be the best because it could make pen-side testing possible. However, biosensors are among those that are furthest from adoption (development is still nascent for virus and bacteria detection with biosensors). Microfluidics could also be useful for the diagnostic laboratory to increase capacity and decrease costs if the equipment is affordable. As some of the new technologies become cheaper the improvements may be able to justify the cost of adoption. At the very least there will definitely be improvements for poultry diagnostics from some of the simple modifications becoming available for nucleic acid detection assays even if substantial changes in format are unlikely in the near future.

Acknowledgements

This review was presented as the Houghton Lecture at the 17th Congress of the World Veterinary Poultry Association in Cancun, Mexico, 2011.

Mention of trade names or commercial products in this publication is solely for the purpose of providing specific information and does not imply recommendation or endorsement by the US Department of Agriculture.

Downloaded by [National Agricultural Library] at 06:02 14 September 2012

Downloaded by [National Agricultural Library] at 06:02 14 September 2012

References

Abdelwhab, E. M., Lüschow, D., Harder, T.C. & Hafez, H.M. (2011). The use of FTA(R) filter papers for diagnosis of avian influenza virus. *Journal of Virololgical Methods*, 174, 120–122.

Abe, A., Inoue, K., Tanaka, T., Kato, J., Kajiyama, N., Kawaguchi, R. & Kohara, M. (1999). Quantitation of hepatitis B virus genomic DNA by real-time detection PCR. *Journal of Clinical Microbiology*, 37, 2899–2903.

Alwine, J.C., Kemp, D.J. & Stark, G.R. (1977). Method for detection of specific RNAs in agarose gels by transfer to diazobenzyloxymethyl-paper and hybridization with DNA probes. *Proceedings of the National Academy of Sciences USA*, 74, 5350–5354.

Baeumner, A J., Schlesinger, N.A., Slutzki, N.S., Romano, J., Lee, E.M. & Montagna, R.A. (2002). Biosensor for dengue virus detection: sensitive, rapid, and serotype specific. *Analytical Chemistry*, 74, 1442–1448.

Bedson, S. & Bland, J. (1929). Complement-fixation with filterable viruses and their antisera. *British Journal of Experimental Pathology*, 10, 393–404.

Best, J., Banatvala, J.E., Almeida, J. & Waterson, A.P. (1967). Morphological characteristics of rubella virus. *The Lancet*, 290, 237–239.

Brenner, S. & Horne, R.W. (1959). A negative staining method for high resolution electron microscopy of viruses. *Biochimica et Biophysica Acta*, 34, 103–110.

Bruckner, L., Stauber, N., Brechtbuhl, K. & Hofmann, M. A. (1996). Detection of extraneous agents in vaccines using the polymerase chain reaction of Newcastle disease virus in poultry biologicals. *Developments in Biololgical Standards*, 86, 175–182.

Burke, D.S., Brandt, B.L., Redfield, R.R., Lee, T.H., Thorn, R.M., Beltz, G.A. & Hung, C.H. (1987). Diagnosis of human immunodeficiency virus infection by immunoassay using a molecularly cloned and expressed virus envelope polypeptide. Comparison to Western blot on 2707 consecutive serum samples. *Annals of Internal Medicine*, 106, 671–676.

Carlson, B. (2011). Molecular diagnostics: potential and reality. *Genetic Engineering and Biotechnology News*, 31, 18–19.

Daley, P., Castriciano, S., Chernesky, M. & Smieja, M. (2006). Comparison of flocked and rayon swabs for collection of respiratory epithelial cells from uninfected volunteers and symptomatic patients. *Journal of Clinical Microbiology*, 44, 2265–2267.

Dalmaso, G., Bini, M., Paroni, R. & Ferrari, M. (2008). Qualification of high-recovery, flocked swabs as compared to traditional rayon swabs for microbiological environmental monitoring of surfaces. *PDA Journal of Pharmaceutical Science and Technology*, 62, 191–199.

Das, A. & Suarez, D.L. (2007). Development and bench validation of real-time reverse transcription polymerase chain reaction protocols for rapid detection of the subtypes H6, H9, and H11 of avian influenza viruses in experimental samples. *Journal of Veterinary Diagnostic Investigation*, 19, 625–634.

Dascal, A., Chan-Thim, J., Morahan, M., Portnoy, J. & Mendelson, J. (1989). Diagnosis of herpes simplex virus infection in a clinical setting by a direct antigen detection enzyme immunoassay kit. *Journal of Clinical Microbiology*, 27, 700–704.

Davis, B.J. (1964). Disc electrophoresis-II. Method and application to human serum proteins. *Annals of the New York Academy of Sciences*, 121, 404–427.

Di Trani, L., Bedini, B., Donatelli, I., Campitelli, L., Chiappini, B., De Marco, M. A., Delogu, M., Buonavoglia, C. & Vaccari, G. (2006). A sensitive one-step real-time PCR for detection of avian influenza viruses using a MGB probe and an internal positive control. *BMC Infectious Diseases*, 6, 87.

Egberink, H.F., Lutz, H. & Horzinek, M.C. (1991). Use of western blot and radioimmunoprecipitation for diagnosis of feline leukemia and feline immunodeficiency virus infections. *Journal of the American Veterinary Medical Association*, 199, 1339–1342.

Fan, J., Henrickson, K.J. & Savatski, L.L. (1998). Rapid simultaneous diagnosis of infections with respiratory syncytial viruses A and B, influenza viruses A and B, and human parainfluenza virus types 1, 2, and 3 by multiplex quantitative reverse transcription-polymerase chain reaction-enzyme hybridization assay (Hexaplex). *Clinical Infectious Diseases*, 26, 1397–1402.

Farkas, T., Szekely, E., Belak, S. & Kiss, I. (2009). Real-time PCR-based pathotyping of Newcastle disease virus by use of TaqMan minor groove binder probes. *Journal of Clinical Microbiology*, 47, 2114–2123.

Gary, G.W., Jr., Kaplan, J.E., Stine, S.E. & Anderson, L.J. (1985). Detection of Norwalk virus antibodies and antigen with a biotin-avidin immunoassay. *Journal of Clinical Microbiology*, 22, 274–278.

Ghorashi, S.A., O'Rourke, D., Ignjatovic, J. & Noormohammadi, A.H. (2011). Differentiation of infectious bursal disease virus strains using real-time RT-PCR and high resolution melt curve analysis. *Journal of Virololgical Methods*, 171, 264–271.

Goodpasture, E.W., Woodruff, A.M. & Buddingh, G.J. (1931). The cultivation of vaccine and other viruses in the chorioallantoic membrane of chick embryos. *Science*, 74, 371–372.

Hart, C., Schochetman, G., Spira, T., Lifson, A., Moore, J., Galphin, J., Sninsky, J. & Ou, C. Y. (1988). Direct detection of HIV RNA expression in seropositive subjects. *Lancet*, 332, 596–599.

Heid, C.A., Stevens, J., Livak, K.J. & Williams, P.M. (1996). Real time quantitative PCR. *Genome Research*, 6, 986–994.

Hernandez, M., Tomas, G., Hernandez, D., Villegas, P., Banda, A., Maya, L., Panzera, Y. & Perez, R. (2011). Novel multiplex RT-PCR/RFLP diagnostic test to differentiate low- from high-pathogenic strains and to detect reassortant infectious bursal disease virus. *Avian Diseases*, 55, 368–374.

Hoffmann, B., Beer, M., Reid, S.M., Mertens, P., Oura, C.A., van Rijn, P.A., Slomka, M J., Banks, J., Brown, I.H., Alexander, D.J. & King, D.P. (2009). A review of RT-PCR technologies used in veterinary virology and disease control: sensitive and specific diagnosis of five livestock diseases notifiable to the World Organisation for Animal Health. *Veterinary Microbiology*, 139, 1–23.

Horimoto, T. & Kawaoka, Y. (1995). Direct reverse transcriptase PCR to determine virulence potential of influenza A viruses in birds. *Journal of Clinical Microbiology*, 33, 748–751.

Inoue, K., Arai, T. & Aoyagi, M. (1999). Sensitivity of real time viral detection by an optical biosensor system using a crude home-made antiserum against measles virus as a ligand. *Biological and Pharmaceutical Bulletin*, 22, 210–213.

Jackwood, D.J., Hanes, G. & Miller, S. H. (1996). Infectious bursal disease viral RNA amplification using RT/PCR from bursa tissue following phenol:chloroform inactivation of the virus. *Avian Diseases*, 40, 457–460.

Jackwood, M.W., Yousef, N.M. & Hilt, D.A. (1997). Further development and use of a molecular serotype identification test for infectious bronchitis virus. *Avian Diseases*, 41, 105–110.

Jones, R.M., Ellis, R.J., Cox, W.J., Errington, J., Fuller, C., Irvine, R.M. & Wakeley, P.R. (2011). Development and validation of RT-PCR tests for the detection and S1 genotyping of infectious bronchitis virus and other closely related gammacoronaviruses within clinical samples. *Transboundary and Emerging Diseases*, 58, 411–420.

Keeler, C.L., Jr., Reed, K.L., Nix, W.A. & Gelb, J. Jr. (1998). Serotype identification of avian infectious bronchitis virus by RT-PCR of the peplomer (S-1) gene. *Avian Diseases*, 42, 275–284.

Kohler, G. & Milstein, C. (1975). Continuous cultures of fused cells secreting antibody of predefined specificity. *Nature*, 256, 495–497.

Kraus, R.H., van Hooft, P., Waldenstrom, J., Latorre-Margalef, N., Ydenberg, R.C. & Prins, H.H. (2011). Avian influenza surveillance with FTA cards: field methods, biosafety, and transportation issues solved. *Journal of Visualized Experiments*, 54, e2832.

Kutyavin, I.V., Afonina, I.A., Mills, A., Gorn, V.V., Lukhtanov, E.A., Belousov, E.S., Singer, M.J., Walburger, D.K., Lokhov, S.G., Gall, A.A., Dempcy, R., Reed, M.W., Meyer, R.B. & Hedgpeth, J. (2000). 3'-minor groove binder-DNA probes increase sequence specificity at PCR extension temperatures. *Nucleic Acids Research*, 28, 655–661.

Kwon, H.M., Jackwood, M.W. & Gelb, J. Jr. (1993). Differentiation of infectious bronchitis virus serotypes using polymerase chain reaction and restriction fragment length polymorphism analysis. *Avian Diseases*, 37, 194–202.

Lazarus, A S., Eddie, B. & Meyer, K.F. (1937). Propagation of variola virus in the developing egg. *Proceedings of the Society of Experimental Biology and Medicine*, 36, 7–8.

Liu, C. (1956). Rapid diagnosis of human influenza infection from nasal smears by means of fluorescein-labeled antibody. *Proceedings of the Society of Experimental Biology and Medicine*, 92, 883–887.

Loeffler, F. & Frosch, P. (1898). Berichte der Kommission zur Erforschung der Maul und Klauenseuche bei dem Institut für Infektionskrankheiten in Berlin. *Zentralblatt für Bakteriologie, Parasitenkunde und Infektionskrankheiten*, 23, 371–391.

Lu, Y.Y., Yan, J.Y., Feng, Y., Xu, C.P., Shi, W. & Mao, H.Y. (2008). Rapid detection of H5 avian influenza virus by TaqMan-MGB real-time RT-PCR. *Letters in Applied Microbiology*, 46, 20–25.

Marziali, A., Pel, J., Bizzotto, D. & Whitehead, L.A. (2005). Novel electrophoresis mechanism based on synchronous alternating drag perturbation. *Electrophoresis*, 26, 82–90.

McMenamy, M.J., McKillen, J., Hjertner, B., Kiss, I., Yacoub, A., Leijon, M., Duffy, C., Belak, S., Welsh, M. & Allan, G. (2011). Development and comparison of a Primer-Probe Energy Transfer based assay and a 5' conjugated Minor Groove Binder assay for sensitive real-time PCR detection of infectious laryngotracheitis virus. *Journal of Virological Methods*, 175, 149–155.

Mears, J.G., Ramirez, F., Leibowitz, D., Nakamura, F., Bloom, A., Konotey-Ahulu, F. & Bank, A. (1978). Changes in restricted human cellular DNA fragments containing globin gene sequences in thalassemias and related disorders. *Proceedings of the National Academy of Sciences USA*, 75, 1222–1226.

Moscoso, H., Alvarado, I. & Hofacre, C.L. (2006). Molecular analysis of infectious bursal disease virus from bursal tissues collected on FTA filter paper. *Avian Diseases*, 50, 391–396.

Moscoso, H., Raybon, E.O., Thayer, S.G. & Hofacre, C.L. (2005). Molecular detection and serotyping of infectious bronchitis virus from FTA filter paper. *Avian Diseases*, 49, 24–29.

Nelson, J. B. (1939). The behavior of pox viruses in the respiratory tract. II. The response of mice to the nasal instillation of variola virus. *Journal of Experimental Medicine*, 70, 107–116.

OIE. (2011). Manual of Diagnostic Tests and Vaccines for Terrestrial Animals 2011 Retrieved November 14, 2011, from http://www.oie.int/index.php?id = 170

Ornstein, L. (1964). Disc Electrophoresis. I. Background and Theory. *Annals of the New York Academy of Sciences*, 121, 321–349.

Perozo, F., Villegas, P., Estevez, C., Alvarado, I. & Purvis, L. B. (2006). Use of FTA filter paper for the molecular detection of Newcastle disease virus. *Avian Pathology*, 35, 93–98.

Proffitt, M.R. & Schindler, S. A. (1995). Rapid detection of HSV with an enzyme-linked virus inducible system (ELVIS) employing a genetically modified cell line. *Clinical and Diagnostic Virology*, 4, 175–182.

Purvis, L.B., Villegas, P. & Perozo, F. (2006). Evaluation of FTA paper and phenol for storage, extraction and molecular characterization of infectious bursal disease virus. *Journal of Virololgical Methods*, 138, 66–69.

Rappolee, D.A., Mark, D., Banda, M.J. & Werb, Z. (1988). Wound macrophages express TGF-alpha and other growth factors in vivo: analysis by mRNA phenotyping. *Science*, 241, 708–712.

Reimann, I. & Werner, O. (1996). Use of the polymerase chain reaction for the detection of reticuloendotheliosis virus in Marek's disease vaccines and chicken tissues. *Zentralblatt für Veterinarmedizin B*, 43, 75–84.

Rivera, E., Sjoland, L. & Karlsson, K.A. (1986). A solid phase fluorescent immunoassay for the rapid detection of virus antigen or antibodies in fetuses infected with porcine parvovirus. *Archives of Virology*, 88, 19–26.

Roberts, J. (2011). Streamlining nucleic acid sample prep: advances in long-read technology, target enrichment, and collection reshape operations. *Genetic Engineering and Biotechnology News*, 31, 26–28.

Rous, P. & Murphy, J. (1911). Tumor implantations in the developing embryo. *Journal of the American Medical Association*, 56, 741–742.

Saiki, R.K., Gelfand, D.H., Stoffel, S., Scharf, S.J., Higuchi, R., Horn, G.T., Mullis, K.B. & Erlich, H. A. (1988). Primer-directed enzymatic amplification of DNA with a thermostable DNA polymerase. *Science*, 239, 487–491.

Saiki, R.K., Scharf, S., Faloona, F., Mullis, K.B., Horn, G.T., Erlich, H.A. & Arnheim, N. (1985). Enzymatic amplification of beta-globin genomic sequences and restriction site analysis for diagnosis of sickle cell anemia. *Science*, 230, 1350–1354.

Scansen, K.A., Bonsu, B.K., Stoner, E., Mack, K., Salamon, D., Leber, A. & Marcon, M.J. (2010). Comparison of polyurethane foam to nylon flocked swabs for collection of secretions from the anterior nares in performance of a rapid influenza virus antigen test in a pediatric emergency department. *Journal of Clinical Microbiology*, 48, 852–856.

Shi, L., Ho, J., Norling, L. A., Roy, M. & Xu, Y. (1999). A real time quantitative PCR-based method for the detection and quantification of simian virus 40. *Biologicals*, 27, 241–252.

Shibata, D.K., Arnheim, N. & Martin, W. J. (1988). Detection of human papilloma virus in paraffin-embedded tissue using the polymerase chain reaction. *Journal of Experimental Medicine*, 167, 225–230.

Southern, E.M. (1975). Detection of specific sequences among DNA fragments separated by gel electrophoresis. *Journal of Molecular Biology*, 98, 503–517.

Spackman, E., Senne, D.A., Myers, T.J., Bulaga, L.L., Garber, L.P., Perdue, M.L., Lohman, K., Daum, L.T. & Suarez, D.L. (2002). Development of a real-time reverse transcriptase PCR assay for type A influenza virus and the avian H5 and H7 hemagglutinin subtypes. *Journal of Clinical Microbiology*, 40, 3256–3260.

Stauber, N., Brechtbuhl, K., Bruckner, L. & Hofmann, M.A. (1995). Detection of Newcastle disease virus in poultry vaccines using the polymerase chain reaction and direct sequencing of amplified cDNA. *Vaccine*, 13, 360–364.

Tham, K.M. & Stanislawek, W.L. (1992). Detection of chicken anaemia agent DNA sequences by the polymerase chain reaction. *Archives of Virology*, 127, 245–255.

Todd, D., Mawhinney, K.A. & McNulty, M.S. (1992). Detection and differentiation of chicken anemia virus isolates by using the polymerase chain reaction. *Journal of Clinical Microbiology*, 30, 1661–1666.

Towbin, H., Staehelin, T. & Gordon, J. (1979). Electrophoretic transfer of proteins from polyacrylamide gels to nitrocellulose sheets: procedure and some applications. *Proceedings of the National Academy of Sciences USA*, 76, 4350–4354.

van Woensel, P.A., van Blaaderen, A., Moorman, R.J. & de Boer, G.F. (1992). Detection of proviral DNA and viral RNA in various tissues early after avian leukosis virus infection. *Leukemia*, 6(Suppl 3), 135S–137S.

Wang, J., Cai, X., Rivas, G., Shiraishi, H., Farias, P.A. & Dontha, N. (1996). DNA electrochemical biosensor for the detection of short DNA sequences related to the human immunodeficiency virus. *Analytical Chemistry*, 68, 2629–2634.

Wang, X. & Khan, M.I. (1999). A multiplex PCR for Massachusetts and Arkansas serotypes of infectious bronchitis virus. *Molecular and Cellular Probes*, 13, 1–7.

Weller, T.H. & Enders, J.F. (1948). Production of hemagglutinin by mumps and influenza A viruses in suspended cell tissue cultures. *Proceedings of the Society of Experimental Biology and Medicine*, 69, 124–128.

Williams, R.A., Bennett, M., Bradbury, J.M., Gaskell, R.M., Jones, R.C. & Jordan, F.T.W. (1992). Demonstration of sites of latency of infectious laryngotracheitis virus using the polymerase chain reaction. *Journal of General Virology*, 73, 2415–2420.

Wise, M.G., Suarez, D.L., Seal, B.S., Pedersen, J.C., Senne, D.A., King, D.J., Kapczynski, D.R. & Spackman, E. (2004). Development of a real-time reverse-transcription PCR for detection of Newcastle disease virus RNA in clinical samples. *Journal of Clinical Microbiology*, 42, 329–338.

Woodruff, A.M. & Goodpasture, E.W. (1931). The susceptibility of the chorio-allantoic membrane of chick embryos to infection with the fowl-pox virus. *American Journal of Pathology*, 7, 209–222.

Xu, J., Suarez, D. & Gottfried, D.S. (2007). Detection of avian influenza virus using an interferometric biosensor. *Analytical and Bioanalyical Chemistry*, 389, 1193–1199.

Zhou, X., Liu, L., Hu, M., Wang, L. & Hu, J. (2002). Detection of hepatitis B virus by piezoelectric biosensor. *Journal of Pharmaceutical and Biomedical Analysis*, 27, 341–345.

Downloaded by [National Agricultural Library] at 06:02 14 September 2012

Virus Genes
DOI 10.1007/s11262-011-0696-3

Comparative full genome analysis of four infectious laryngotracheitis virus (*Gallid herpesvirus-1*) virulent isolates from the United States

S. J. Spatz · J. D. Volkening · C. L. Keeler · G. F. Kutish · S. M. Riblet · C. M. Boettger · K. F. Clark · L. Zsak · C. L. Afonso · E. S. Mundt · D. L. Rock · M. Garcia

Received: 1 October 2011 / Accepted: 28 November 2011
© Springer Science+Business Media, LLC (Outside the USA) 2011

Abstract *Gallid herpesvirus-1* (GaHV-1), commonly named infectious laryngotracheitis (ILT) virus, causes the respiratory disease in chickens known as ILT. The molecular determinants associated with differences in pathogenicity of GaHV-1 strains are not completely understood, and a comparison of genomic sequences of isolates that belong to different genotypes could help identify genes involved in virulence. Dideoxy sequencing, 454 pyrosequencing and Illumina sequencing-by-synthesis were used to determine the nucleotide sequences of four genotypes of virulent strains from GaHV-1 groups I–VI. Three hundred and twenty-five open reading frames (ORFs) were compared with those of the recently sequenced genome of the Serva vaccine strain. Only four ORFs, ORF C, U_L37, ICP4 and U_S2 differed in amino acid (aa) lengths among the newly sequenced genomes. Genome sequence alignments were used to identify two regions (5′ terminus and the unique short/repeat short junction) that contained deletions. Seventy-eight synonymous and 118 non-synonymous amino acid substitutions were identified with the examined ORFs. Exclusive to the genome of the Serva vaccine strain, seven non-synonymous mutations were identified in the predicted translation products of the genes encoding glycoproteins gB, gE, gL and gM and three non-structural proteins U_L28 (DNA packaging protein), U_L5 (helicase-primase) and the immediate early protein ICP4. Furthermore, our comparative sequence analysis of published and newly sequenced GaHV-1 isolates has provided evidence placing the cleavage/packaging site (*a*-like sequence) within the inverted repeats instead of its placement at the 3′ end of the U_L region as annotated in the GenBank's entries NC006623 and HQ630064.

Keywords Infectious laryngotracheitis · *Gallid herpesvirus-1* · DNA sequence · Virulence · Attenuation

Electronic supplementary material The online version of this article (doi:10.1007/s11262-011-0696-3) contains supplementary material, which is available to authorized users.

S. J. Spatz (✉) · L. Zsak · C. L. Afonso
United States Department of Agriculture, Southeast Poultry Research Laboratory, Agricultural Research Service, Athens, GA 30605, USA
e-mail: Stephen.Spatz@ars.usda.gov

J. D. Volkening
BASE2BIO, Madison, WI 53714, USA

C. L. Keeler · C. M. Boettger · K. F. Clark
Department of Animal and Food Sciences, University of Delaware, Newark, DE 19716-2150, USA

G. F. Kutish
Department of Pathobiology and Veterinary Science and Center of Excellence for Vaccine Research, University of Connecticut, Storrs, CT 06269, USA

S. M. Riblet · E. S. Mundt · M. Garcia
Poultry Diagnostic and Research Center, College of Veterinary Medicine, University of Georgia, 953 College Station Road, Athens, GA, USA

D. L. Rock
Department of Pathobiology, College of Veterinary Medicine, University of Illinois, Urbana, IL 61802, USA

Introduction

Infectious laryngotracheitis (ILT) is a respiratory disease of chickens occurring worldwide and is caused by *Gallid herpesvirus-1* (GaHV-1) [18]. This virus of the genus *Iltovirus* in the *Alphaherpesvirinae* subfamily of *Herpesviridae* [5] is responsible for the highly contagious disease characterized by acute respiratory symptoms that include gasping, coughing,

Published online: 16 December 2011

sneezing, depression, nasal discharge and conjunctivitis [17]. The disease is largely controlled through mass vaccination via aerosol or drinking water, with live attenuated strains that have been attenuated by multiple passages in either embryonated eggs [chicken embryo origin (CEO)] or tissue culture [tissue culture origin (TCO)] [11, 46]. To date, differentiating vaccine strains from virulent field isolates has involved (i) restriction fragment length polymorphisms of PCR products (multilocus PCR–RFLP analyses) [4, 31, 40, 43] and (ii) limited nucleotide sequence analysis [19, 40]. Overall, U.S. strains can be grouped into nine genotypes (I–IX) according to Oldoni et al. [43]. In a recent study in the U.S., 63% of field isolates from commercial farms were shown to be closely related to the CEO vaccine strains (groups IV and V) [18]. Because of this, it is believed that vaccine strains in North America have reverted to virulence and that these revertants have become established in the poultry population, capable of re-emerging as non-attenuated CEO-related viral isolates [42]. Moreover, in Europe, a study of strains collected over 35 years showed that 94% (98/104) of EU strains were also related to ILT vaccines [40].

The molecular biology of GaHV-1 has recently been reviewed [9, 27]. The GaHV-1 genome was initially characterized using restriction endonuclease analysis [22, 29, 38] and was shown to contain a type D arrangement with two unique regions (U_L and U_S) with the U_S region flanked by inverted repeat sequences. In the late 1980s, Sanger-based DNA sequencing data of GaHV-1 became publicly available [13–16]. However, it was not until 2006 that the first complete genomic sequence of GaHV-1 was assembled by Thureen and Keeler [48] from overlapping genomic contigs of different strains analyzed in six different laboratories [6–8, 10, 13–16, 23–26, 30, 33–36, 44, 53–55]. Recently, Lee et al. [37] have determined the complete *non-composite* nucleotide sequence of the European CEO Serva vaccine strain of GaHV-1 and reported significant differences in the lengths of 12 ORFs in comparison with those published for the composite sequence. To expand on this and investigate the potential genetic basis for GaHV-1 pathogenicity, full genome sequences of four virulent U.S. isolates, including the USDA standard challenge strain (group I genotype), broiler breeder isolate 81658 (group III genotype), broiler isolate 63140 (group V genotype) and broiler isolate 1874C5 (group VI genotype), were obtained, and a comparative sequence analysis of these with the genome of the Serva vaccine strain was performed.

Materials and methods

Virus and cells

The GaHV-1 strain used in this study (USDA reference strain, obtained from the National Veterinary Services Laboratory, Ames, IA, USA) was propagated on confluent monolayers of primary chicken embryo fibroblast cells (CEF). Fibroblasts were isolated from 11-day-old chicken embryos by the warm trypsinization methods [48] and plated in Dulbecco's modified essential medium supplemented with penicillin (50 μg/ml), streptomycin (50 μg/ml) and 8% fetal bovine serum. Group III strain 81658 previously genotyped as closely related to tissue culture origin (TCO) vaccine was obtained from a 60-week-old non-vaccinated broiler breeder flock with severe signs of the disease, where males vaccinated with the TCO vaccine (Schering-Plough Animal Health, Omaha, NE, USA) were introduced 51 weeks prior to the outbreak. GaHV-1 isolate 63140 (group V), previously genotypes as closely related to the CEO vaccine, was obtained in 2006 from an unvaccinated broiler flock in Georgia with signs of severe upper respiratory disease and high mortality. GaHV-1 group VI strain 1874C5 was obtained in 2005 from an unvaccinated broiler flock in Delaware—as with previous isolates the flock showed severe respiratory disease and high mortality. All isolates were propagated in chicken kidney (CK) cells as described previously by Tripathy and Garcia [49]. Virus DNA from cells infected with strains USDA reference and 63140 was purified using the modified Hirt's supernatant protocol [20]. The micrococcal nuclease/polyethylene glycol procedure [50] was used to isolate nucleocapsid DNA from strains 81658, 63140 and 1874C5.

Determination of the TR_S/U_L junction in GaHV-1 genomic concatamers

Standard PCR was used to amplify the TR_S/U_L junction sequence using the forward primer GATTCTGTGATC GCGCTTCGAGG (isolate 63140 nucleotide coordinates 153217–153239) and reverse primer TGCTTGCCTGCA TATACCGGATGC (isolate 63140 nucleotide coordinates 273–296) and Hirt's supernatant DNA of strain 63140 as the template. High-fidelity platinum Taq polymerase (Invitrogen, Carlsbad CA) was used in standard amplification reactions containing 2 mM Magnesium, 1× PCR buffer and 62°C annealing temperatures. PCR products were separated on a 1.5% agarose gel and stained with ethidium bromide. The nucleotide sequence of the PCR product was determined using standard Sanger-based sequencing.

High-throughput DNA sequencing

Sequencing of the viral genomes was accomplished using three DNA sequencing technologies: Sanger dideoxy, 454 pyrosequencing and Illumina sequence-by-synthesis. The USDA reference strain was sequenced using dideoxy chain terminator sequencing chemistry from pUC19 libraries of

cloned random DNA fragments (>1.0 Kb) generated by incomplete enzymatic digestions with either *Taq*I or *Aci*I restriction endonucleases (New England BioLabs, Beverly, MA). Plasmid DNA was purified by alkaline lysis according to the manufacturer's instructions (Eppendorf 5 Prime, Boulder CO) and sequenced from both ends with M13 forward and reverse primers using dideoxy chain termination and the ABI PRISM 3730xl automated DNA sequencer (Applied Biosystems, Foster City, CA).

Strain 63140 was initially sequenced commercially on a pyrosequencing platform, the Genome Sequencer 20 (GS20) system (454 Life Sciences). This involved the construction of random libraries from 5.0 micrograms of nucleocapsid-purified DNA using the methodology described by Margulies et al. [39]. Subsequently, strain 1874C5 and strain 81658 were sequenced using the Illumina HISeq 2000 sequencing platform (Illumina Inc., San Diego, CA) at two different facilities. Isolate 1874C5 was sequenced at the University of Delaware Sequencing and Genotyping Center in Newark, DE, and isolate 81658 was sequenced at the Genome Services Lab at Hudson Alpha Institute for Biotechnology (Huntsville, Alabama). Sequencing of both isolates was carried out on a HiSeq2000, running HiSeq Control Software (HCS) v1.4.8. Single-read genomic (1874C5) DNA libraries were prepared from 5 μg of partially purified genomic DNA that was sheared by nebulization (1874C5) or sonication (81658) to an average length of 200 bp. The samples were processed according to Illumina Library Creation kit's instructions and sequenced on one lane of a HiSeq Flowcell v1.5. Libraries were clustered on a cBot v1.4.36.0 using Illumina's Truseq PE Cluster Kit v2.0 and sequenced using a 200 cycle TruSeq SBS HS v2 kit. The clustered flow-cell was sequenced for 206 cycles and broken down into 3 separate reads. The first read was 100 cycles in length, followed by a six-cycle index read. Following the index read, paired end re-synthesis was performed also using Truseq PE Cluster Kit v2.0, which was then followed by another 100 cycles. Image analysis and base calling were performed using the standard Illumina Pipeline consisting of Real time Analysis (RTA) version v1.12.4.2 and Casava v1.8 with default settings.

GaHV-1 DNA sequence analysis

The genome of the USDA reference strain was assembled with the Phrap and CAP3 software programs (http://www.phrap.org) [21], and sequence gap closure was achieved by primer walking of gap-spanning clones and sequencing of PCR products. PCR products were generated using a battery of oligonucleotides and Platinum Taq polymerase (Life Technologies, Carlsbad, CA).

The 63140 genome was assembled from 28,100 reads using GS De Novo Assembler (Roche, Indianapolis, IN), Sequencher (Gene Codes, Ann Arbor, MI) and the Mira Assembler [2]. Ambiguities in the sequencing data and problematic regions containing mononucleotide reiterations which mapped to the existing 5,454 scaffolds using Mira were resolved through resequencing using Illumina technology. The complete genomic sequence of 63140 therefore represents hybrid assembly from two sequencing technologies. The sequence of strain 81658 was assembled from the Illumina dataset using Mira in de novo assembly mode, and the sequence of 1874C5 was determined by read alignment to the published ILTV reference sequence using Genome Studio (Illumina) and CLC Genomics Workbench (CLC bio, Cambridge, MA).

All genomic sequences were maintained and analyzed using Lasergene (DNASTAR, Madison, WI), NCBI Entrez and other web-based tools. Homology searches were conducted using the NCBI program blastP with default settings. Multiple alignments of proteins and nucleotide sequences were generated using MAFFT [28], Multalin [3] and SCAN2 (Softberry.com).

Results and discussion

Sequencing, coverage and assembly

Genomic sequencing using classical Sanger dideoxy chemistry of individual clones enabled the generation of a consensus sequence of 137,997 bp after de novo assembly of the GaHV-1 USDA reference strain. This included the genomic subregions U_L, TR_L U_S and 800 bp of the U_S/TR_S junction. The TR_S subregion was generated by reverse complementing the TR_L sequencing data. Final DNA consensus sequence represented, on average, 10-fold redundancy at each base position, with a Consed estimated error rate of less than 0.01 error per 10 kbp [12]. Using 454 pyrosequencing, 58,924 reads were generated from strain 63140 with a mean length of 249 bp, of which 44,398 reads aligned to the ILTV genome. The assembled sequence represented approximately 77-fold coverage at each base pair, but sequence coverage was uneven with a number of gaps. Illumina sequencing was used to fill these gaps as well as resolve homopolymer stretches ambiguous in the 454 data. 7,817,890 100 mer Illumina reads aligned to the 63140 genome for an average fold coverage of 5,363. A similar average fold coverage of 5,759 was obtained from the assembly of 8,370,909 reads for the 81658 genome. With an average read length of 41.5 nucleotides (147,530 reads), the 6,122,687 nucleotides of 1874C5 sequence generated by Illumina technology represented a 41-fold coverage of the genome. The comparatively low 1874C5 coverage corresponded to the concentration of the viral DNA in the initial preparation. Eighty-five percent of the

Illumina reads represented chicken chromosomal DNA sequence. The GenBank accession numbers for the GaHV-1 genomes are as follows: 1874C5 (JN542533), USDA reference strain (JN542534), 81658 (JN542535) and 63140 (JN542536).

Genomic organization

The genomes of the USDA reference strain (group I), 81658 (group III), 63140 (group V) and 1874C5 (group VI) were determined to be 151769, 150335, 153633 and 150691 nucleotides in length. These sizes were comparable to the lengths of the composite genome (148,687 bp) and the genome of the Serva vaccine strain (152,630 bp). To further characterize these differences in genomic lengths, the sizes of the genomic subregions unique long [U_L], internal repeat short [IR_S], unique short [U_S] and terminal repeat short [TR_S]) were defined (Table 1). The unique long (U_L) sequences were 109,580 (USDA reference strain), 109,575 (81658), 112,915 (63140) and 113,030 (1874C5) bp in length and contained two 102-bp inverted repeats separated by a 726-bp sequence (Fig. 1) encoding microRNA miR-l1-5p and miR-l1-3P [45]. Flanking the unique long were two inverted repeat sequences (ATTCGAAACCCCTCGCG and CGCGAGGGGTTTCGAAT) of 17 nucleotides in length. Although this would qualify the GaHV-1 genome as a class E genome, only two isomers of the genome have been reported [22, 38].

The unique short (U_S) and flanking inverted regions (IR), respectively, were 13,095 and 14,547 (USDA reference strain), 13,094 and 13,833 (81658), 13,094 and 13,812 (63140) and 13,094 and 12,283/12,284 (1874C5) nucleotides in length. The Serva genome is annotated to contain the largest unique long region (113,930 bp) with relatively short inverted repeats (12,803 bp) and a standard length U_S region (13,094 bp) (Table 1). The average length of the GaHV-1 genomes sequenced in this report is 151,607 bp in length with the lengths of the U_S genomic subregions to be the most conserved among all GaHV-1 genomes.

Interestingly, the genome of the Serva strain, sequenced using the SOLiD^{TM} system and assembled based on the composite sequence, contains a truncated terminal repeat short (TR_S) region. A 1,015-bp sequence annotated to be at the 3′ end of the unique long of the Serva genome, when reverse-complemented, mapped to the end (TR_S) of the linear genomes of all four virulent viruses. Alignment of the reads using 454 pyrosequencing clearly defines the ends of the linear GaHV-1 genome since all the data are flush with the 3′ end. Furthermore, the sequencing data of the ICP4 genes of the GaHV-1 strains SA-2 and CSW-1 (accession numbers U27243 and U27244) are in full agreement with our definition of the GaHV-1 genomic termini [24]. Therefore, these data suggest that the genomic subregion (U_L) of the Serva may not be 113,930 bp but rather 112,915 nucleotides in length, and the inverted repeats may not be 12,803 bp but rather 13,818 bp for a genomic unit length of 153,645 bp rather than 152,630 bp as previously indicated [37] (Table 1).

To experimentally define the 3′ terminus of the GaHV-1 genome, forward and reverse oligonucleotides were used in an amplification reaction with DNA isolated from infected CK cells using the Hirt's supernatant protocol. The forward primer was specific for sequences in the disputed 1,015-bp sequence, while the reverse primer was specific for the 5′ terminus of the unique long. Since a PCR product of approximately 700 bp (Fig. 2c) was amplified, this clearly demonstrated that the 1,015-bp sequence is present at the 3′ end of the TR_S region and not at the 3′ end of the U_L region as annotated in the Serva genome. Sequencing of the PCR product (Fig. 2d) revealed that an extra thymidine residue is present between the sequences at the 3′ terminus (TR_S) and the 5′ terminus of the U_L in concatameric GaHV-1 (63140) genomes. A comparison of the termini sequences of GaHV-1, including cleavage and packaging sites, relative to sequences found at the ends of other herpesvirus genomes is presented in Fig. 3.

Open reading frames within the genomes of virulent GaHV-1 strains

The genomes of the newly sequenced virulent strains of GaHV-1 contain over 300 ORFs that are at least 60 amino acids in length. Each predicted translation products of these 325 ORFs were analyzed using NCBI BLAST program to determine the percentage similarity to other proteins found in the GenBank data base. Of these, only 80 ORFs showed

Table 1 Comparison of the lengths of the genomes and genomic subregions of the *Gallid herpesvirus-1* strains USDA (group I), 80658 (group III), 63140 (group V), 1874C5 (group VI) and the Serva vaccine strain

Genome	UL	IRS	US	TRS	Total
USDA	109,580	14,547	13,095	14,547	151,769
81658	109,575	13,833	13,094	13,833	150,335
63140	112,915	13,812	13,094	13,812	153,633
1874C5	113,030	12,283	13,094	12,284	150,691
Averages	111,275	13,619	13,094	13,619	151,607
Serva	113,930	12,803	13,094	12,803	152,630

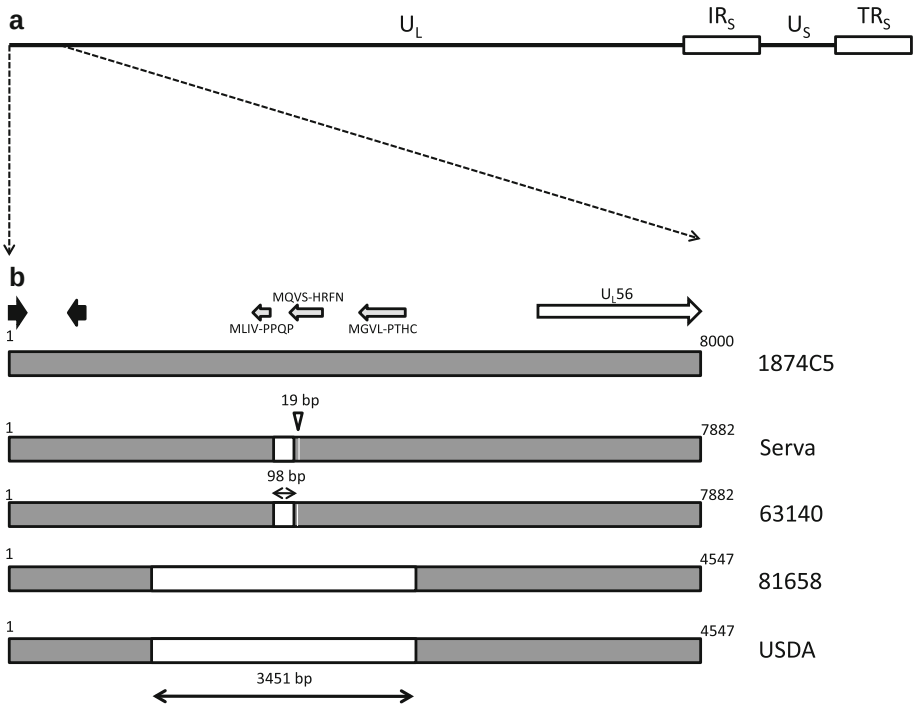

Fig. 1 Schematic alignments of the 5′ terminus of five Gallid herpesvirus 1 genomes. **a** The D-type organization of the GaHV-1 genome as described previously. **b** The locations of the two 102-bp inverted repeats (*black arrows*) and the U_L56 ORF (*open arrow*). Three short ORFs MLIV-PPQP, MQVS-HRFN and MGVL-PTHC are shown in *open gray arrows*. The ORFs are named according to their first and last four amino acids. The positions of the 98-bp deletions in the Serva (after nucleotide 3,265) and 63140 (after nucleotide 3,264) genomes and the larger 3,451-bp deletions within the genomes of 81658 and USDA after nucleotide positions 2,153 and 2,155, respectively, are shown as *open white boxes*. The smaller 19-bp downstream deletions (CCCTTTTTAACAAAAACAG) after nucleotide positions 3,459 and 3,458 of the Serva and 63,140 genomes, respectively, are shown as *white lines*

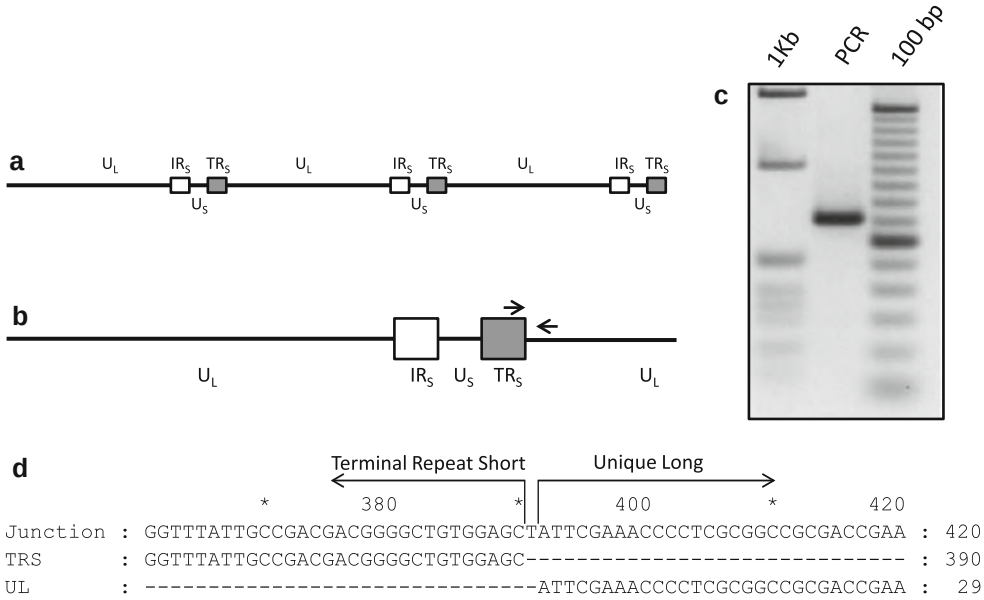

Fig. 2 Amplification scheme used to define the 3′ terminus of the GaHV-1 genome. **a** Cartoon of the concatameric GaHV-1 genomes. **b** The location of the forward and reverse oligonucleotides used in the amplification reaction (PCR) with templates prepared from Hirt's supernatants. **c** Visualization of the PCR product in an ethidium bromide–stained 1.5% agarose gel. **d** The nucleotide sequence at the junction between the terminal repeat short (TR_S) and the unique long (U_L)

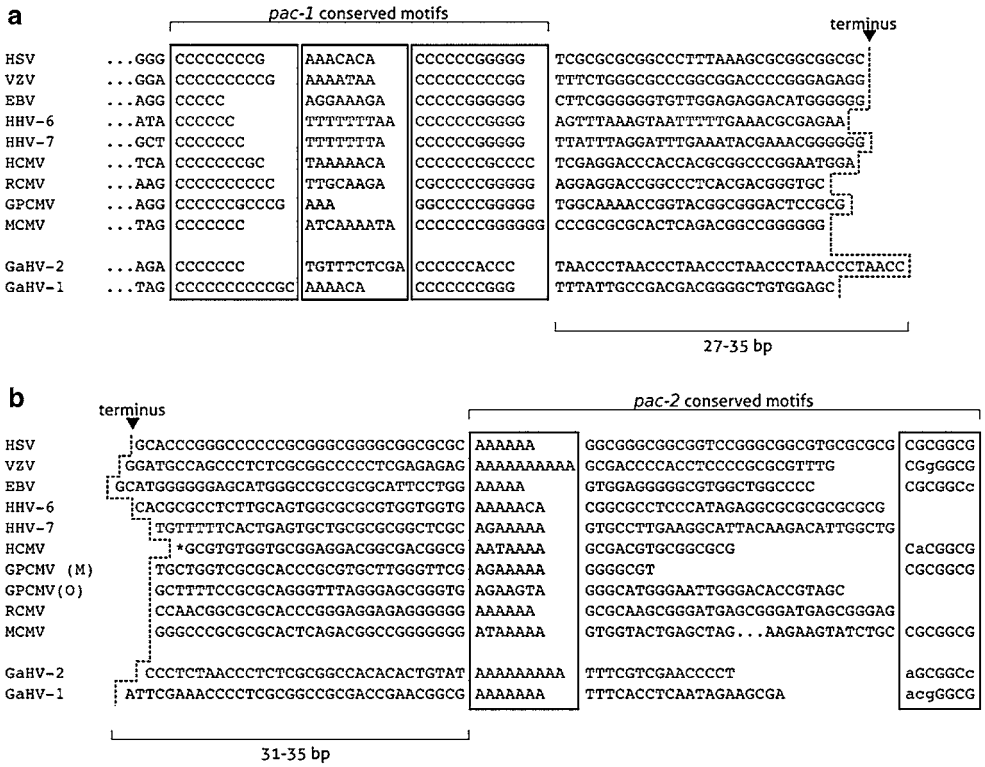

Fig. 3 The proposed cleavage/packaging sequence of GaHV-1 aligned with *a*-like sequences of other alpha-, gamma- and beta-herpesviruses. Domains conserved among members of the family *Herpesviridae* are *boxed*. **a** Alignments of *pac-1* sites at the 3′ terminus of *Herpesviridae* genomes. **b** Alignments of the *pac-2* sites at the 5′ terminus of *Herpesviridae* genomes. HSV (Herpes simplex virus-1 or *Human herpesvirus-1*), VZV (Varicella-zoster virus or *Human herpesvirus-3*), EBV (Epstein-Barr virus or *Human herpesvirus-4*), HHV-6 (*Human herpesvirus-6*), HHV-7 (*Human herpesvirus-7*), HCMV (Human cytomegalovirus or *Human herpesvirus-5*), RCMV (Rhesus cytomegalovirus or *Macacine herpesvirus-3*) GPCMV (Guinea pig cytomegalovirus or *Caviid herpesvirus-2*), MCMV (Mouse cytomegalovirus or *Murid herpesvirus-1),* GaHV-2 (*Gallid herpesvirus-2* or Marek's disease virus-1) and GaHV-1 (*Gallid herpesvirus-1 or* Infectious laryngotracheitis virus)

significant sequence similarity to protein sequence found in GenBank. No novel ORFs with significant similarity to protein sequences within GenBank were discovered other than those already described by Thureen and Keeler [48]. Although the number of genes within the GaHV-1 genome has been established since 2006, discrepancies in the lengths of some ORF have been reported by Spatz et al. in 2010 [47] and confirmed by Lee [37]. Differences in the size of predicted translation products of 18 genes were identified between the composite genome and the genomes of the four virulent strains (Table 2). The lengths of groups I, II, V and VI ORFs are all in agreement with their orthologues found within the Serva genome, except for the reported sequence length heterogeneity of the ICP4 ORF [1, 24, 52].

In the analysis of the GaHV-1 ORFs within the four sequenced genomes, only four ORFs (ORF C, U_L37, U_S2 protein kinase and ICP4) differed among the U.S. virulent isolates and Serva vaccine strain (Table 2). A truncated variant of ORF C (303 aa) is encoded within the genome of group III (81658). This variant is missing the last 31 amino acids due to a cytosine to thymidine mutation at nucleotide position 913 resulting in the introduction of an ocher stop codon. Also, within the group III genome, three nucleotides CTA are missing for the UL37 gene after nucleotide position 1,383. This in-frame deletion of the codon for leucine occurs in a region containing four CTA codons. Within the U_S2 gene of the USDA reference strain, an extra thymidine base after nucleotide position 638 is predicted to cause a reading frame shift resulting in a truncated U_S2 protein of 217 amino acids, while all other U_S2 genes of GaHV-1 are predicted to encode a 229-amino-acid protein. The lengths of ORFs 66 and 80 encoding ICP4 vary among virulent U.S. isolates and the Serva vaccine strain: 1,482 bp (Serva and 93140), 1,486 bp (USDA and 81658) and 1,492 bp (1874C5) (Table 2, Fig. 4).

Insertions and deletions (INDELS)

To investigate the presence of INDELS within the genomes of virulent GaHV-1 strains, a multiple sequence alignment was generated using the web-based alignment program MAFFT [28]. Sequence heterogeneity was localized within two genomic subregions (U_L and IR): specifically the

Table 2 Summary of ORFs that differ in lengths between the published composite sequence (GenBank # NC006623) and the sequences of genomes of the *Gallid herpesvirus-1* strains Serva, USDA, 81658, 63140 and 1874C5

Gene	Region	Homolog	Composite	USDA	81658	1874C5	63140	Serva
ORF1	U_L	U_L56	**284**	274	274	274	274	274
ORF2	U_L	ORF F	**752**	746	746	746	746	746
ORF3	U_L	U_L54	**420**	544	544	544	544	544
ORF4	U_L	U_L53	**337**	339	339	339	339	339
ORF15	U_L	ORFC	334	334	**303**	334	334	334
ORF21	U_L	U_L25	**572**	592	592	592	592	592
ORF26	U_L	U_L29	**999**	1,176	1,176	1,176	1,176	1,176
ORF27	U_L	U_L30	**1,008**	1,092	1,092	1,092	1,092	1,092
ORF28	U_L	U_L31	**339**	314	314	314	314	314
ORF33	U_L	U_L36	**2,556**	2,784	2,784	2,784	2,784	2,784
ORF34	U_L	U_L37	**890**	1,022	**1,021**	1,022	1,022	1,022
ORF35	U_L	U_L38	**412**	482	482	482	482	482
ORF36	U_L	U_L39	**785**	786	786	786	786	786
ORF38	U_L	U_L41	**398**	399	399	399	399	399
ORF39	U_L	U_L42	**432**	436	436	436	436	436
ORF40	U_L	U_L43	**395**	394	394	394	394	394
ORF 66	IRs	RS1	**1,463**	**1,486**	**1,486**	**1,492**	**1,482**	**1,482**
ORF69	Us	US2	229	**217**	229	229	229	229
ORF80	TRs	RS1	**1,463**	**1,486**	**1,486**	**1,492**	**1,482**	**1,482**

Bold denotes amino acid lengths that differ among the majority of the open reading frames

diploid ICP4 loci near the IR/U_S junctions and the 5′ end of the unique long region. As shown in Fig. 4, INDELS map throughout the inverted repeats. Heterogeneity within the ORFs encoding ICP4 of the four GaHV-1 strains has been previously described [1, 52]. The ICP4 ORF of the composite genome, which was based on the sequencing data of Johnson et al. [24], is 1,463 aa in length. The size of the ICP4 ORF within the Serva vaccine genomes is 1,482 aa [37]. We now report two additional lengths of 1,486 (USDA and 81658) and 1,492 (1874C5) aa. These size differences can be attributed to three in-frame indels. The sequence AAGAACCGCAACAACCGC is only present at the 3′ end of the ICP4 gene within the 1874C5 genome and is deleted after nucleotide positions 149,368, 146,076, 149,371 and 147,501 within the genomes of 63140, 81658, Serva and USDA, respectively, while an additional sequence (GCGGCCCAAGAC) is missing from the genomes of 63140 and Serva. The deletion of the second sequence occurs after nucleotide position 147,069 within the Serva genome and after nucleotide position 147,066 in the 63140 isolate's genome. The sequence AGATT is present after nucleotide position 4,380 in the ICP4 gene of the Australian vaccine strain SA-2 as sequenced by Johnson et al. [24] and results in a premature termination yielding a truncated form of ICP4. In the analysis of 28 full-length GenBank sequences of ICP4 genes from various GaHV-1 strains, the most common length was 1,482 aa, occurring in 42.8% of the sequences examined, while 1,492, 1,486 and 1,463 length variants comprised 28.6, 25 and 3.6% of the total sequences examined, respectively. The variant encoding the 1,463 ICP4 appears to be unique to the SA-2 strain and was used in the composite genome sequence [48]. Since neither the SA-2 genome nor its ICP4 gene has been resequenced, it is not known whether this is true variation or a sequencing artifact.

In addition to the small in-frame deletions within the ICP4 genes, two large deletions were identified between the promoters of the ICP4 and U_S10 genes (Fig. 4, white boxes). The largest deletion of 1,582 bp was identified upstream of the U_S10 promoter in the 1874C5 genome starting after nucleotide position 141,322. Within the genome of the USDA reference strain, a small deletion of 143 bp (after nucleotide position 141,578) was identified which overlaps the 3′ region of the 1,582-bp deletion mapped within the 1874C5 genome. Surprisingly, these deletions are within the 280-bp hairpin structure comprising the origin of DNA replication (OriS) as first identified by Walter Fuchs (GenBank number AM238250). Although PCR products of approximately 556 bp could be amplified and cloned using flanking primers (GGTTGCTCATGTGAGAAGACAATG ACC and AATACGCTCTTGCGACAGACCGTGG) with USDA and 1874C5 DNA (data not shown), numerous attempts to sequence these clones using Sanger-based sequencing failed to resolve the 280-bp palindrome. This region was also absent in the composite sequence as reported by Thureen and Keeler [48]. However, since PCR products could be generated and cloned, this region is likely present in the USDA and 1874C5 genomes, but difficult to sequence due to its thermostability (dG values of −190.87, −190.03, −190.67 and −185.45 kcal/mol for AM238250, Serva,

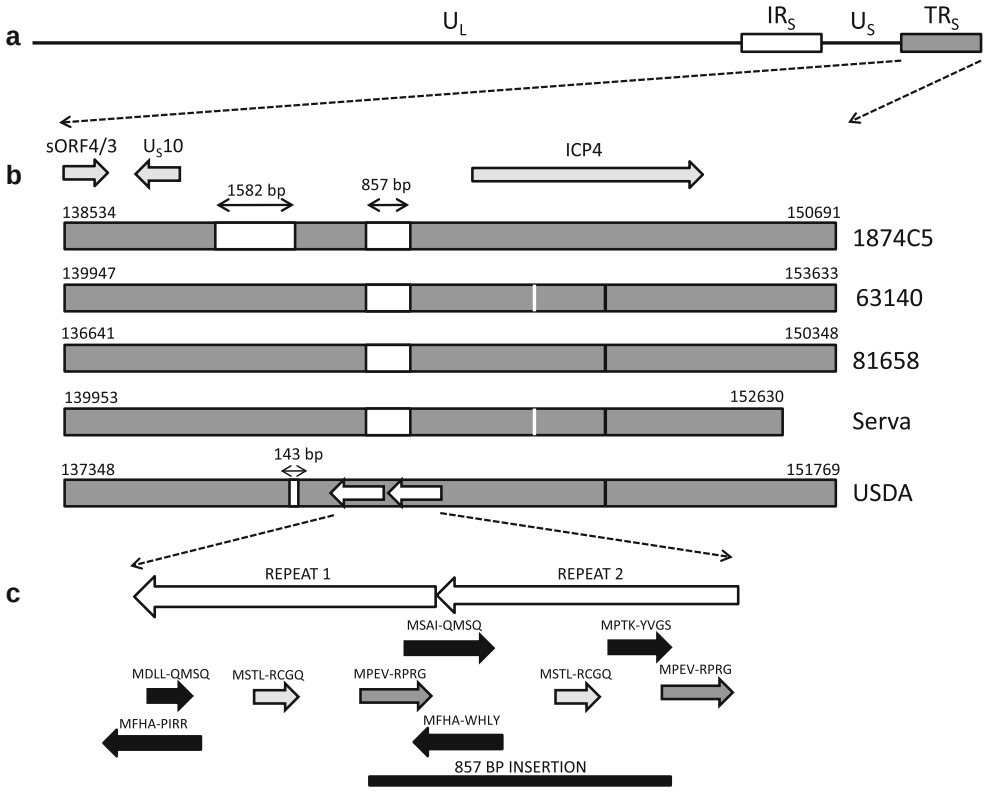

Fig. 4 Schematic alignments of the 3′ terminus of five Gallid herpesvirus 1 genomes. **a** The D-type organization of the GaHV-1 genome showing the unique long (U_L) region and the internal repeat short, (IR_S) and terminal repeat short (TR_S) regions bracketing the unique short (U_S) region. **b** The location of three genes encoding sORF4/3, U_S10 and ICP4 (*open gray arrows*). The positions of the 1,582-, 857- and 143-bp deletions are denoted by *open white boxes*. Two near-perfect direct repeats of 855 and 857 bp within the USDA genome are denoted by *open white arrows*. The location of small in-frame deletions within the ICP4 genes of 63140, 81658, Serva and USDA is marked by *vertical black* (AAGAACCGCAACAACCGC) or *white* (GCGGCCCAAGAC) *lines*. **c** ORFs within the repeat regions. The ORFs are named according to their first and last four amino acids. ORFs that are duplicated are *shaded* identically

81658 and 63140). A multiple sequence alignment of the OriS within the inverted repeat regions is shown in Fig. 5. Within the stem regions of the hairpin structures, base pair substitutions occur only when matched with complementary nucleotides on the reverse strand. Only the loop region contains mismatched nucleotides.

A smaller 857-bp deletion upstream of the ICP4 promoter region was identified in the genomes of 1874C5, 63140, 81658 and Serva after nucleotide positions 143,133, 146,109, 142,801 and 146,112, respectively (Fig. 4b). This deletion mapped to a region in the USDA genome containing two near-perfect direct repeats of 855 and 857 bp. Four single nucleotide polymorphisms and a 2-bp insertion in the larger 857-bp repeat differentiate the two repeats. Several small novel ORFs map within these repeats. The MPTK-YVGS novel ORF is solely present in the 857-bp repeat due to a 2-bp deletion in the 855-bp repeat immediately downstream of the start codon (Fig. 4c). These repeats have been found in varying copy numbers in other sequenced GaHV-1 strains [9, 53] and represent an expansion region similar to the 132-bp repeat region found in the GaHV-2 genome [41].

The largest deletions identified in this study mapped to the 5′ terminus of two GaHV-1 genomes in a region devoid of large open reading frames (ORFs) and microRNAs (Fig. 1). These 3,451-bp deletions within the genomes of 81658 and USDA initiate after nucleotide positions 2,153 and 2,155, respectively. Similarly, a large deletion of 3,575 bp relative to the Australian vaccine strain SA-2 has been reported in the genome of the virulent GaHV-1 strain A489 by Johnson and others [25]. Three short ORFs (MLIV-PPQP, MQVS-HRFN and MGVL-PTHC of 83, 143 and 199 aa, respectively), which are absent in the 81658 and USDA genomes, map to this region within the 1874C5 genome. BLAST analysis of these ORFs however failed to reveal any meaningful similarity to known proteins. Lastly, two smaller deletions of 98 and 19 bp also mapped to this general region within the genomes of the Serva and 63140 strains of GaHV-1.

Single nucleotide polymorphisms

In order to identify amino acid changes associated with attenuation and/or virulence, the nucleotide sequence of the

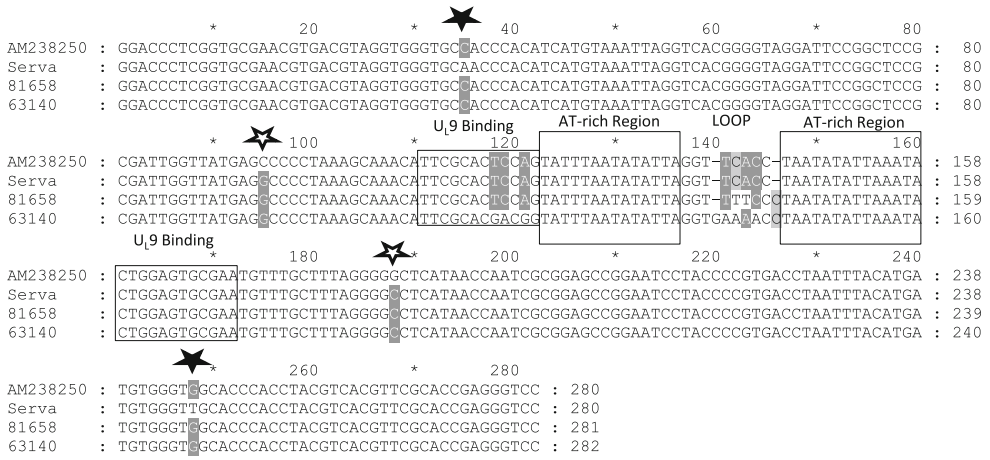

Fig. 5 Alignment of the sequences comprising the near-perfect hairpin structure at the origin of DNA replication (OriS) within the inverted repeat regions of AM238250, Serva, 81658 and 63140. The AT-rich regions are boxed as well as domains likely to be involved in the binding of the U_L9 protein. Base pair substitutions with matched complementary nucleotides are indicated by *open* and *closed stars*

vaccine strain Serva was aligned to nucleotide sequences of the four sequenced virulent strains (USDA, 81658, 1874C5 and 63140) using the web-based programs, Multalin and MAFFT. Over 190 single nucleotide polymorphisms (SNPs) were identified in the predicted translation products. Of these, 76 occurred within coding regions without amino acid substitutions (synonymous). Relative to codon used in the Serva genes, 39, 49, 13, and 27 synonymous substitutions were identified in the corresponding genes within the USDA, 1874C5, 63140 and 81685 genomes, respectively (Sup. 1). A list of the 118 non-synonymous mutations is presented in Table 3. Non-synonymous substitutions exclusively found in the Serva genome were identified in the genes U_L27-, U_L1-, U_L10-, U_S8-encoded glycoproteins B, L, M and E, respectively, and the non-structural proteins were involved in DNA packaging (U_L28), DNA replication (U_L5 helicase-primase) and the immediate early protein ICP4. The most significant substitutions that are likely to affect structure and/or function are $Thr^{42} \rightarrow Ala^{42}$ (U_L10 encoding gM), $Lys^{343} \rightarrow Glu^{343}$ (U_L5 encoding the helicase-primase protein) and $Gln^{141} \rightarrow Pro^{141}$ (U_L1 encoding gL).

Conclusions

Sequence analysis of the genomes of four virulent GaHV-1 isolates and their comparison within the composite and Serva vaccine strain genomes generated an ORF consensus for 80 genes (out of 325 examined) that showed homology to well-characterized alphaherpesvirus genes and unique GaHV-1 genes previously described [9]. Sixty ORFs had amino acid lengths identical to those found in the composite sequence, while 18 differed. Excluding the composite sequence, only four ORFs were predicted to encode proteins that differed in amino acid lengths among the newly sequenced genomes. This study has identified differences in the lengths of the ORFs encoding the transcriptional activator ICP4 (1,482, 1,486 and 1,492 aa), ORF C (303 and 334 aa), U_L37 (1021 and 1022 aa) and U_S2 protein kinase (217 and 229 aa). Relative to the group VI genome (1874C5), 3,451-bp deletions at the 5′ terminus were identified in genotype groups I USDA and III 81658 genomes, while smaller deletions of 98 bp were identified in the same region of the Serva vaccine and virulent genotype group V 63140. Relative to the group I genome (USDA), 857 bp were missing from the genomes of Serva and groups III, V and VI isolates. Within the genomes of the groups I and VI, deletions within the inverted repeats mapped to the origin of replication. These deletions are likely due to the inability to resolve highly structured regions containing inverted repeats using Sanger sequencing. The lack of the 5′ proximal deletions in the Serva and the virulent groups V 63140 genomes, and the 857-bp deletions of both the vaccine strain and virulent isolates suggest that neither changes in these areas of the genome are related to virulence.

In a comparison with the predicted translation products of >80 ORF within the genomes of groups I, III, V, VI and the Serva vaccine strain, 78 synonymous and 118 non-synonymous amino acid substitutions were identified. A total of seven non-synonymous amino acid substitutions in U_L27, U_L1, U_L10 and U_S8 genes encoding glycoproteins gB, gL, gM and gE, respectively, and three non-structural proteins (U_L28, U_L5 and ICP4) genes were identified that could differentiate the Serva vaccine strain from all four GaHV-1 virulent isolates collectively. In particular, the surface glycoprotein changes may reflect the different geographical origin of the Serva strain (Europe) and the

Table 3 Single nucleotide polymorphisms resulting in non-synonymous amino acid substitutions in ORFs within the genomes of the GaHV-1 strains Serva, USDA, 81658, 63140 and 1874C5

	Non-synonymous				
	Serva	USDA	1874C5	63140	81685
ORF U_L56					
Trp190 Pro190	tgg	*cca*	tgg	tgg	*cca*
ORF F					
Ser78 Thr78	tca	tca	tca	*aca*	tca
Cys271 Tyr271	tgt	*tat*	tgt	tgt	*tat*
ORF U_L54					
Tyr50 Cys50	tat	*tgt*	tat	tat	*tgt*
ORF U_L52					
Ala167 Glu167	gcg	*gag*	gcg	gcg	*gag*
Thr263 Ala263	aca	*gca*	aca	aca	*gca*
Tyr527 Ser527	tat	*tct*	tat	tat	*tct*
ORF U_L50					
Phe320 Leu320	ttc	ttc	*ctc*	ttc	ttc
ORF U_L46					
Tyr327 Asp327	tac	tac	tac	tac	*gac*
ORF A					
Pro126 Ser126	ccc	ccc	*tcc*	ccc	ccc
ORF B					
Tyr2 His2	tat	*cat*	tat	tat	*cat*
Cys83 Arg83	tgc	tgc	*cgc*	tgc	tgc
Glu129 Asp129	gag	gag	*gat*	gag	gag
ORF E					
Gly133 Ala133	ggc	ggc	ggc	*gcc*	ggc
Gln245 Arg245	caa	caa	*cga*	caa	caa
Leu405 Arg405	ctg	*cgg*	ctg	ctg	*cgg*
ORF U_L22					
Leu568 Ser568	tta	tta	*tca*	tta	tta
ORF U_L23					
Arg97 Trp97	cgg	cgg	cgg	*tgg*	cgg
Asp212 Asn212	gac	gac	*aac*	gac	gac
ORF U_L26					
Gln179 Arg179	cag	cag	cag	*cgg*	cag
Ile210 Met210	att	att	*atg*	att	att
ORF U_L27					
Val116 Ala116	**gtc**	*gcc*	*gcc*	*gcc*	*gcc*
Met348 Thr348	atg	atg	atg	atg	*acg*
Arg496 His496	cgc	cgc	cgc	*cac*	cgc
Ile644 Thr644	ata	*aca*	*aca*	*aca*	ata
Pro799 Ser799	ccc	ccc	*tcc*	ccc	ccc
Lys805 Arg805	aag	aag	*aga*	aag	aag
Glu809	gag	gag	gag	*N/A*	gag
ORF U_L28					
Glu363 Gly363	gaa	*gga*	gaa	gaa	gaa
Gln374 Arg374	caa	caa	caa	caa	*cga*
Ile509 Thr509	att	*act*	*act*	att	att

Table 3 continued

	Non-synonymous				
	Serva	USDA	1874C5	63140	81685
Val638 Ala638	**gtc**	*gcc*	*gcc*	*gcc*	*gcc*
Asp735 Gly735	gac	gac	gac	*ggc*	gac
ORF U_L29					
Gly905 Asp905	ggc	ggc	ggc	ggc	*gac*
ORF U_L30					
Arg91 Gly91	aga	*gga*	*gga*	aga	*gga*
Ala312 Val312	gcc	*gtc*	*gtc*	gcc	*gtc*
Ala578 Val578	gcg	gcg	*gtg*	gcg	gcg
Glu1010 Lys1010	gaa	gaa	*aaa*	gaa	gaa
Thr1011 Leu1011	act	act	*ctt*	act	act
Ser1012 Leu1012	tct	tct	*ctt*	tct	tct
Leu1013 Met1013	ttg	ttg	*atg*	ttg	ttg
ORF U_L36					
Asp84 Ala84	gac	gac	*gcc*	gac	gac
Ser359 Gly359	agc	agc	agc	*ggc*	agc
ORF U_L10					
Thr42 Ala42	**acc**	*gcc*	*gcc*	*gcc*	*gcc*
Pro248 Ser248	cct	cct	*tct*	cct	cct
ORF U_L9					
Val10 Ala10	gtc	gtc	*gcc*	gtc	gtc
ORF U_L6					
Ala258 Thr258	gcc	gcc	*acc*	gcc	gcc
Glu693 Lys693	gaa	gaa	*aaa*	gaa	gaa
ORF U_L5					
Lys343 Glu343	**aaa**	*gaa*	*gaa*	*gaa*	*gaa*
Ala391 Thr391	gca	gca	gca	gca	*aca*
ORF U_L1					
Pro8 Gln8	ccg	*cag*	ccg	ccg	*cag*
Gln141 Pro141	**cag**	*ccg*	*ccg*	*ccg*	ccg
ORF U_L0					
Thr18 Ala18	acg	*gcg*	acg	acg	*gcg*
Val117 Ala117	gtt	*gct*	gtt	gtt	*gct*
Pro153 Ser153	cca	*tca*	cca	cca	cca
Ser273 Phe273	tcc	tcc	*ttc*	tcc	tcc
Leu341 Pro341	cta	cta	*cca*	cta	cta
Thr378 Ala378	aca	*gca*	aca	aca	aca
ORF ilt240					
Gly2 Asp2	ggt	*gat*	*gat*	ggt	*gat*
Asn11 Ile11	aac	*atc*	*atc*	aac	*atc*
Arg18 Cys18	cgc	*tgc*	*tgc*	cgc	*tgc*
Leu24 Pro24	ctt	*cct*	*cct*	ctt	*cct*
Asn40 Lys40	aat	*aaa*	*aaa*	aat	*aaa*
Lys41 Gln41	aag	*cag*	*cag*	aag	*cag*
ORF ilt239					
Phe6 Ile6	ttt	*att*	*att*	ttt	*att*
Stop10 Cys10	tga	*tgc*	*tgc*	tga	*tgc*

Table 3 continued

	Non-synonymous				
	Serva	USDA	1874C5	63140	81685
ORF ilt244					
His21 Tyr21	cac	*tac*	cac	cac	cac
Asp40 Val40	gat	*gtt*	gat	gat	gtt
ORF ilt246					
Ala37 Val37	gcg	gcg	*gtg*	gcg	gcg
ORF ilt247					
Gly3 Trp3	ggg	*tgg*	ggg	ggg	*tgg*
ORF ilt248					
His6 Pro6	cat	cat	*cct*	cat	cat
Gln16 Arg16	cag	cag	*cgg*	cag	cag
ORF ilt249					
Leu26 Trp26	ttg	ttg	*N/A*	ttg	*tgg*
ORF U_S10					
Met136 Ile136	atg	atg	atg	atg	*ata*
ORF U_S3					
Ala99 Thr99	gct	*act*	gct	gct	*act*
Lys291 Thr291	aag	aag	*acg*	aag	aag
ORF sORF1					
Gly279 Asp279	ggc	ggc	ggc	ggc	*gac*
ORF U_S4					
His98 Asn98	cac	cac	*aac*	cac	cac
Val115 Gly115	gtg	gtg	*ggg*	gtg	gtg
Gly220 Leu220	ggt	ggt	*ctt*	ggt	ggt
ORF U_S5					
Arg162 Trp162	cgg	*tgg*	cgg	cgg	*tgg*
Val293 Ala293	gtg	*gcg*	gtg	gtg	*gcg*
Ala340 Thr340	gcc	gcc	gcc	*acc*	gcc
Ala684 Thr684	gcc	gcc	*acc*	gcc	gcc
ORF U_S7					
Ala178 Asp178	gct	gct	*gat*	gct	gct
ORF U_S8					
Lys210 Arg210	**aaa**	*aga*	*aga*	*aga*	*aga*
Thr386 Ala386	acc	*gcc*	acc	acc	*gcc*
ORF U_S9 (8A?)					
Thr91 Ile91	aca	aca	*ata*	aca	aca
Gly115 Asp115	ggc	ggc	*gac*	ggc	ggc
ORF ICP4					
Ala267 Thr267	gcc	gcc	*acc*	gcc	gcc
Gln414 His414	cag	cag	*cat*	cag	cag
Arg618 Pro618	cgc	cgc	*ccg*	cgc	cgc
Ser716 Thr716	agc	agc	*acg*	agc	agc
Asp743 Asn743	aac	*gac*	*gac*	aac	aac
Arg781 His781	**cac**	*cgc*	*cgc*	*cgc*	*cgc*
Gln860 Arg860	caa	caa	*caa/cga*	caa	caa
Ser876 Tyr876	tct	tct	*tct/tat*	tct	tct
Ala1131 Val1131	gtg	*gcg*	*gcg*	gtg	*gcg*
Pro1292 Leu1292	ctg	*ccg*	*ccg*	ctg	*ccg*
Gly1328 Arg1328	agg	*ggg*	agg	agg	*ggg*
Gly1329 Asp1329	gac	*ggc*	gac	gac	gac
Pro1423 Leu1423	ccc	ccc	*ctc*	ccc	ccc
Thr1437 Ser1437	tcc	*acc*	tcc	tcc	*acc*

All Serva ORFs encoding amino acid of lengths >60 were examined for non-synonymous amino acids substitutions in comparison with homologous ORFs found within the genomes of the four virulent strains. The list includes 80 ORFs as defined by Lee et al. within the Serva genome as well as seven additional short ORFs (ilt239, ilt240, ilt244, iltv246, ilt247, ilt248 and ilt249, located between the ICP4 and U_S10 genes) that contained non-synonymous substitutions. Codons in bold are exclusive for Serva genes and not used in the corresponding genes in the genomes of the virulent isolates. Codons that differ relative to the Serva codons are italicized

U.S. virulent isolates, while difference in the U_L28, U_L5 and ICP4 genes may be related to the attenuation of the Serva strain or virulence of the genotypes I, III, V and VI U.S. isolates. Interestingly, no mutations were found in regions that encode microRNAs [32, 45, 51]. The identification of both intragenic and intergenic deletions and single nucleotide polymorphism mutations that differentiate the Serva vaccine genome from the genomes of four virulent isolates will further advance our understanding of genes involved in virulence.

Acknowledgments We thank Robert Mullis for his contributions in the bioinformatic analysis of the sequencing data. This research was funded by the United States Department of Agriculture CRIS program (project number 6612-32000-052) and the US Poultry and Egg Association (Project F032).

References

1. P.C. Chang, Y.L. Lee, J.H. Shien, H.K. Shieh, Rapid differentiation of vaccine strains and field isolates of infectious laryngotracheitis virus by restriction fragment length polymorphism of PCR products. J. Virol. Methods **66**, 179–186 (1997)
2. B. Chevreux, T. Wetter, S. Suhai, Genome sequence assembly using trace signal and additional sequence information. Comput. Sci. Biol. GCB **1**, 45–56 (1999)
3. F. Corpet, Multiple sequence alignment with hierarchical clustering. Nucleic Acids Res. **16**, 10881–10890 (1988)
4. J.L. Creelan, V.M. Calvert, D.A. Graham, S.J. McCullough, Rapid detection and characterization from field cases of infectious laryngotracheitis virus by real-time polymerase chain reaction and restriction fragment length polymorphism. Avian Pathol. **35**, 173–179 (2006)
5. A.J. Davison, R. Eberle, G.S. Hayward, D.J. McGeoch, A.C. Minson, P.E. Pellet, B. Roizman, M.J. Studdert, E. Thiry, Family Herpesviridae, in *Virus Taxonomy: Eight Report of the International Committee on Taxonony of Viruses*, ed. by C.M. Fauquet,

M.A. Mayo, J. Maniloff, U. Desselberger, L.A. Ball (Academic Press, San Diego, 2005), pp. 193–212
6. W. Fuchs, T.C. Mettenleiter, DNA sequence and transcriptional analysis of the UL1 to UL5 gene cluster of infectious laryngotracheitis virus. J. Gen. Virol. **77**(Pt 9), 2221–2229 (1996)
7. W. Fuchs, T.C. Mettenleiter, DNA sequence of the UL6 to UL20 genes of infectious laryngotracheitis virus and characterization of the UL10 gene product as a nonglycosylated and nonessential virion protein. J. Gen. Virol. **80**(Pt 8), 2173–2182 (1999)
8. W. Fuchs, T.C. Mettenleiter, The nonessential UL49.5 gene of infectious laryngotracheitis virus encodes an *O*-glycosylated protein which forms a complex with the non-glycosylated UL10 gene product. Virus Res. **112**, 108–114 (2005)
9. W. Fuchs, J. Veits, D. Helferich, H. Granzow, J.P. Teifke, T.C. Mettenleiter, Molecular biology of avian infectious laryngotracheitis virus. Vet. Res. **38**, 261–279 (2007)
10. W. Fuchs, K. Ziemann, J.P. Teifke, O. Werner, T.C. Mettenleiter, The non-essential UL50 gene of avian infectious laryngotracheitis virus encodes a functional dUTPase which is not a virulence factor. J. Gen. Virol. **81**, 627–638 (2000)
11. E. Gelenczei, E. Marty, Strain stability and immunologic characteristics of tissue-culture modified infectious laryngotracheitis virus. Avian Dis. **9**, 44–56 (1962)
12. D. Gordon, C. Abajian, P. Green, Consed: a graphical tool for sequence finishing. Genome Res. **8**, 195–202 (1998)
13. A.M. Griffin, The complete sequence of the capsid p40 gene from infectious laryngotracheitis virus. Nucleic Acids Res. **18**, 3664 (1990)
14. A.M. Griffin, Identification of 21 genes of infectious laryngotracheitis virus using random sequencing of genomic DNA. J. Gen. Virol. **70**(Pt 11), 3085–3089 (1989)
15. A.M. Griffin, The nucleotide sequence of the glycoprotein gB gene of infectious laryngotracheitis virus: analysis and evolutionary relationship to the homologous gene from other herpesviruses. J. Gen. Virol. **72**(Pt 2), 393–398 (1991)
16. A.M. Griffin, M.E. Boursnell, Analysis of the nucleotide sequence of DNA from the region of the thymidine kinase gene of infectious laryngotracheitis virus; potential evolutionary relationships between the herpesvirus subfamilies. J. Gen. Virol. **71**(Pt 4), 841–850 (1990)
17. J.S. Guy, T.J. Bagust, Laryngotracheitis, in *Disease of Poultry*, 11th edn., ed. by Y.M. Saif, H.J. Barnes, J.R. Glisson, A.M. Fadly, L.R. McDougald, D.E. Swayne (Iowa State Press, Ames, 2003), pp. 121–134
18. J.S. Guy, M. Garcia, *Infectious Laryngotracheitis Virus*, 12th edn. (Wiley-Blackwell, Hoboken, 2008)
19. M.G. Han, S.J. Kim, Analysis of Korean strains of infectious laryngotracheitis virus by nucleotide sequences and restriction fragment length polymorphism. Vet. Microbiol. **83**, 321–331 (2001)
20. B. Hirt, Selective extraction of polyoma DNA from infected mouse cell cultures. J. Mol. Biol. **26**, 365–369 (1967)
21. X. Huang, A. Madan, CAP3: a DNA sequence assembly program. Genome Res. **9**, 868–877 (1999)
22. M.A. Johnson, C.T. Prideaux, K. Kongsuwan, M. Sheppard, K.J. Fahey, Gallid herpesvirus 1 (infectious laryngotracheitis virus): cloning and physical maps of the SA-2 strain. Arch. Virol. **119**, 181–198 (1991)
23. M.A. Johnson, C.T. Prideaux, K. Kongsuwan, S.G. Tyack, M. Sheppard, ICP27 immediate early gene, glycoprotein K (gK) and DNA helicase homologues of infectious laryngotracheitis virus (gallid herpesvirus 1) SA-2 strain. Arch. Virol. **140**, 623–634 (1995)
24. M.A. Johnson, S.G. Tyack, C. Prideaux, K. Kongsuwan, M. Sheppard, Nucleotide sequence of infectious laryngotracheitis virus (gallid herpesvirus 1) ICP4 gene. Virus Res. **35**, 193–204 (1995)
25. M.A. Johnson, S.G. Tyack, C.T. Prideaux, K. Kongsuwan, M. Sheppard, Nucleotide sequence of the left-terminus of infectious laryngotracheitis virus (Gallid herpesvirus 1) SA-2 strain. Arch. Virol. **142**, 1903–1910 (1997)
26. M.A. Johnson, S.G. Tyack, C.T. Prideaux, K. Kongsuwan, M. Sheppard, Sequence characteristics of a gene in infectious laryngotracheitis virus homologous to glycoprotein D of herpes simplex virus. DNA Seq. **5**, 191–194 (1995)
27. R.C. Jone, Viral respiratory diseases (ILT, aMPV infections, IB): are they ever under control? Br. Poult. Sci. **51**, 1–11 (2010)
28. K. Katoh, K. Kuma, H. Toh, T. Miyata, MAFFT version 5: improvement in accuracy of multiple sequence alignment. Nucleic Acids Res. **33**, 511–518 (2005)
29. C.L. Keeler Jr., J.W. Hazel, J.E. Hastings, J.K. Rosenberger, Restriction endonuclease analysis of Delmarva field isolates of infectious laryngotracheitis virus. Avian Dis. **37**, 418–426 (1993)
30. D.H. Kingsley, J.W. Hazel, C.L. Keeler Jr, Identification and characterization of the infectious laryngotracheitis virus glycoprotein C gene. Virology **203**, 336–343 (1994)
31. N.C. Kirkpatrick, A. Mahmoudian, D. O'Rourke, A.H. Noormohammadia, Differentiation of infectious laryngotracheitis virus isolates by restriction fragment length polymorphic analysis of polymerase chain reaction products amplified from multiple genes. Avian Dis. **50**, 28–34 (2006)
32. B.W. Kong, Identification of virus encoding microRNAs using 454 FLX sequencing platform. Methods Mol. Biol. **733**, 81–91 (2011)
33. K. Kongsuwan, M.A. Johnson, C.T. Prideaux, M. Sheppard, Identification of an infectious laryngotracheitis virus gene encoding an immunogenic protein with a predicted M(r) of 32 kilodaltons. Virus Res. **29**, 125–140 (1993)
34. K. Kongsuwan, M.A. Johnson, C.T. Prideaux, M. Sheppard, Use of lambda gt11 and monoclonal antibodies to map the gene for the 60, 000 dalton glycoprotein of infectious laryngotracheitis virus. Virus Genes **7**, 297–303 (1993)
35. K. Kongsuwan, C.T. Prideaux, M.A. Johnson, M. Sheppard, K.J. Fahey, Nucleotide sequence of the gene encoding infectious laryngotracheitis virus glycoprotein B. Virology **184**, 404–410 (1991)
36. K. Kongsuwan, C.T. Prideaux, M.A. Johnson, M. Sheppard, S. Rhodes, Nucleotide sequence analysis of an infectious laryngotracheitis virus gene corresponding to the US3 of HSV-1 and a unique gene encoding a 67 kDa protein. Arch. Virol. **140**, 27–39 (1995)
37. S.W. Lee, P.F. Markham, J.F. Markham, I. Petermann, A.H. Noormohammadi, G.F. Browning, N.P. Ficorilli, C.A. Hartley, J.M. Devlin, First complete genome sequence of infectious laryngotracheitis virus. BMC Genomics **12**, 197 (2011)
38. D.A. Leib, J.M. Bradbury, C.A. Hart, K. McCarthy, Genome isomerism in two alphaherpesviruses: Herpesvirus saimiri-1 (Herpesvirus tamarinus) and avian infectious laryngotracheitis virus. Brief Report. Arch. Virol. **93**, 287–294 (1987)
39. M. Margulies, M. Egholm, W.E. Altman, S. Attiya, J.S. Bader, L.A. Bemben, J. Berka, M.S. Braverman, Y.J. Chen, Z. Chen, S.B. Dewell, L. Du, J.M. Fierro, X.V. Gomes, B.C. Godwin, W. He, S. Helgesen, C.H. Ho, G.P. Irzyk, S.C. Jando, M.L. Alenquer, T.P. Jarvie, K.B. Jirage, J.B. Kim, J.R. Knight, J.R. Lanza, J.H. Leamon, S.M. Lefkowitz, M. Lei, J. Li, K.L. Lohman, H. Lu, V.B. Makhijani, K.E. McDade, M.P. McKenna, E.W. Myers, E. Nickerson, J.R. Nobile, R. Plant, B.P. Puc, M.T. Ronan, G.T. Roth, G.J. Sarkis, J.F. Simons, J.W. Simpson, M. Srinivasan, K.R. Tartaro, A. Tomasz, K.A. Vogt, G.A. Volkmer, S.H. Wang, Y. Wang, M.P. Weiner, P. Yu, R.F. Begley, J.M. Rothberg, Genome sequencing in microfabricated high-density picolitre reactors. Nature **437**, 376–380 (2005)
40. C.J. Neff, C. Sudler, R.K. Hoop, Characterisation of western European field isolates of avian infectious laryngotracheitis virus by restriction fragment length polymorphisms and sequencing. Avian Dis. **52**, 278–283 (2008)

41. M. Niikura, J.B. Dodgson, H.H. Cheng, Stability of Marek's disease virus 132-bp repeats during serial in vitro passages. Arch. Virol. **151**, 1431–1438 (2006)
42. D. Ojkic, J. Swinton, M. Vallieres, E. Martin, J. Shapiro, B. Sanei, B. Binnington, Characterization of field isolates of infectious laryngotracheitis virus from Ontario. Avian Pathol. **35**, 286–292 (2006)
43. I. Oldoni, A. Rodriguez-Avila, S. Riblet, M. Garcia, Characterization of infectious laryngotracheitis virus (ILTV) isolates from commercial poultry by polymerase chain reaction and restriction fragment length polymorphisms (PCR-RFLP). Avian Dis. **52**, 59–63 (2008)
44. D.J. Poulsen, C.R. Burton, J.J. O'Brian, S.J. Rabin, C.L. Keeler Jr, Identification of the infectious laryngotracheitis virus glycoprotein gB gene by the polymerase chain reaction. Virus Genes **5**, 335–347 (1991)
45. R. Rachamadugu, J.Y. Lee, A. Wooming, B.W. Kong, Identification and expression analysis of infectious laryngotracheitis virus encoding microRNAs. Virus Genes **39**, 301–308 (2009)
46. Y. Samberg, I. Aronovici, The development of a vaccine against avian infectious laryngotracheitis I. Modification of a laryngotracheitis virus. Refug. Vet. **26**, 54–59 (1969)
47. S.J. Spatz, M. Garcia, C.L. Keeler Jr., C.L. Afonso, E. Mundt, S. Riblet, L. Zsak, D.L. Rock, in Presented at the 5th international workshop on the molecular pathogenesis of Marek's disease virus and 1st symposium on avian herpesviruses, Athens, GA, USA.
48. D.R. Thureen, C.L. Keeler Jr, Psittacid herpesvirus 1 and infectious laryngotracheitis virus: comparative genome sequence analysis of two avian alphaherpesviruses. J. Virol. **80**, 7863–7872 (2006)
49. D.N. Tripathy, M. García, Laryngotracheitis, in *Isolation and Identification of Avian Pathogens*, 5th edn., ed. by D.E. Swayne, J.R. Glisson, M.W. Jackwood, W.M. Reed (American Association of Avian Pathologist, University of Pennsylvania, New Bolton Center, 2008), pp. 94–98
50. J.D. Volkening, S.J. Spatz, Purification of DNA from the cell-associated herpesvirus Marek's disease virus for 454 pyrosequencing using micrococcal nuclease digestion and polyethylene glycol precipitation. J. Virol. Methods **157**, 55–61 (2009)
51. L.A. Waidner, J. Burnside, A.S. Anderson, E.L. Bernberg, M.A. German, B.C. Meyers, P.J. Green, R.W. Morgan, A microRNA of infectious laryngotracheitis virus can downregulate and direct cleavage of ICP4 mRNA. Virology **411**, 25–31 (2011)
52. W. Wanasawaeng, N. Chansiripornchai, Molecular classification of infectious laryngotracheitis virus from chick embryo origin vaccine, tissue culture origin vaccine and field isolates. Thai J. Vet. Med. **40**, 393–398 (2010)
53. M.A. Wild, S. Cook, M. Cochran, A genomic map of infectious laryngotracheitis virus and the sequence and organization of genes present in the unique short and flanking regions. Virus Genes **12**, 107–116 (1996)
54. K. Ziemann, T.C. Mettenleiter, W. Fuchs, Gene arrangement within the unique long genome region of infectious laryngotracheitis virus is distinct from that of other alphaherpesviruses. J. Virol. **72**, 847–852 (1998)
55. K. Ziemann, T.C. Mettenleiter, W. Fuchs, Infectious laryngotracheitis herpesvirus expresses a related pair of unique nuclear proteins which are encoded by split genes located at the right end of the UL genome region. J. Virol. **72**, 6867–6874 (1998)

Virus Genes (2011) 42:339–346
DOI 10.1007/s11262-011-0577-9

Deletion of the M2-2 gene from avian metapneumovirus subgroup C impairs virus replication and immunogenicity in Turkeys

Qingzhong Yu · Carlos N. Estevez · Jason P. Roth · Haixia Hu · Laszlo Zsak

Received: 11 November 2010 / Accepted: 17 January 2011 / Published online: 2 February 2011
© Springer Science+Business Media, LLC (Outside the USA) 2011

Abstract The second matrix (M2) gene of avian metapneumovirus subgroup C (aMPV-C) contains two overlapping open reading frames (ORFs), encoding two putative proteins, M2-1 and M2-2. Both proteins are believed to be involved in viral RNA transcription or replication. To further characterize the function of the M2-2 protein in virus replication, the non-overlapping region of the M2-2 ORF was deleted from an infectious cDNA clone of the aMPV-C strain, and a viable virus was rescued by using reverse genetics technology. The recombinant virus, raMPV-C ΔM2-2, was characterized in vitro and in vivo. In Vero cells, raMPV-C ΔM2-2 replicated slightly less efficiently than the parental virus, 10-fold reduction at 48-h post-infection. The raMPV-C ΔM2-2 virus induced typical cytopathic effects (CPE) that were indistinguishable from those seen with the parental virus infection. In specific-pathogen-free (SPF) turkeys, raMPV-C ΔM2-2 was attenuated and caused no clinical signs of disease. Less than 20% of the inoculated birds shed detectable virus in tracheal tissue during the first 5 days post-infection, and no virus shedding was detected afterward. Forty percent of infected birds produced a weak antibody response at 14 days post-infection. Upon challenge with a virulent aMPV-C strain, more than 80% of the raMPV-C ΔM2-2-inoculated birds showed typical disease signs and virus shedding in tracheal tissue. These results suggest that the M2-2 protein of aMPV-C virus is not essential for virus replication in vitro, but is required for sufficient virus replication to maintain pathogenicity and immunogenicity in the natural host.

Keywords aMPV-C · Reverse genetics · M2-2 gene deletion · Virus replication · Pathogenicity · Immunogenicity

Q. Yu (✉) · C. N. Estevez · J. P. Roth · H. Hu · L. Zsak
United States Department of Agriculture, Southeast Poultry Research Laboratory, Agricultural Research Service, 934 College Station Road, Athens, GA 30605, USA
e-mail: qingzhong.yu@ars.usda.gov

Present Address:
C. N. Estevez
Texas Veterinary Medical Diagnostic Lab, 1 Sippel Road, TAMUS 4471, College Station, TX 77843, USA

Introduction

Avian metapneumovirus (aMPV) causes turkey rhinotracheitis (TRT), an acute upper respiratory tract infection of turkeys, and is associated with swollen head syndrome (SHS) in chickens [1, 2]. Isolates of aMPV are members of the genus *Metapneumovirus* within the subfamily *Pneumovirinae* of the family *Paramyxoviridae* [3]. Based on the level of genetic variations and antigenic differences, aMPV isolates have been classified into four subgroups: A, B, C, and D [4–7]. Interestingly, the aMPV subgroup C virus is phylogenetically related more closely to the human metapneumovirus (hMPV) than its avian counterparts [8]. While the aMPV subgroups A and B are present in Europe and most countries in the world, excluding USA, only aMPV-C is present in the USA and to a limited degree in France and Korea [9, 10]. The aMPV-D subgroup has only been reported in France [5].

The genome of aMPV is a non-segmented, single-stranded, negative-sense RNA of 13 kb that contains eight genes, in the order 3′-nucleocapsid (N)-phosphoprotein (P)-matrix (M)-fusion (F)-second matrix (M2)-small hydrophobic (SH)-glycoprotein (G)-large polymerase (L)-5′, flanked by an untranslated 3′ leader and 5′ trailer [11–14].

Among these eight genes, the M2 gene is unique and contains two overlapping open reading frames (ORFs). The first ORF encodes the M2-1 protein of 184 amino acids (aa) for subgroup C or 186 aa for subgroups A and B. The second ORF encodes the M2-2 polypeptide of 71 aa of subgroup C or 73 aa of subgroups A and B [11–15]. The expression of the protein products of the two ORFs is believed to be regulated by a coupled translation termination/initiation process, which depends on sequences and structures presented in the mRNA molecule [16, 17]. Studies with human respiratory syncytial virus (RSV) and hMPV have shown that the M2-1 protein is an mRNA elongation and anti-termination factor [18–21], whereas the M2-2 protein is a regulatory factor involved in the balance between RNA replication and transcription [18, 22–24]. Deletion of the M2-2 gene from the RSV or hMPV genome using reverse genetics attenuated virus replication both in vitro and in vivo, but did not significantly impair virus immunogenicity, which provided protection against wild-type virus challenge in animal models [24–26].

The deletion of specific genes by reverse genetics has been used to explore the function of aMPV proteins during in vitro and in vivo infections [27–29]. When the M2-2 ORF was deleted from aMPV-A, virus replication was impaired more severely in turkeys than in cell culture, and only some birds showed evidence of antibody production [30]. Since no challenge experiment was conducted in this particular study, it is not clear if the immune response induced by the aMPV-A M2-2 deletion virus in turkeys was protective against the virus. In this study, we sought to investigate the function of the M2-2 protein of aMPV-C in virus replication, pathogenicity, and immunogenicity in specific-pathogen-free (SPF) turkeys. We deleted the second ORF of the M2 gene from an aMPV-C infectious clone [29] and rescued a viable aMPV-C M2-2 deletion virus using a reverse genetics approach. The biological properties of the M2-2 deletion virus, raMPV-C ΔM2-2, were assessed in vitro and in vivo.

Materials and methods

Viruses and cell cultures

The aMPV-C Colorado strain (aMPV-CO) was obtained from the aMPV repository bank at the Southeast Poultry Research Laboratory (USDA–ARS, Athens, GA, USA). The construction and rescue of the recombinant aMPV-C virus (raMPV-C sG) in HEp-2 cells (ATCC, CCL-23) were described previously [29]. The raMPV-C sG and the aMPV-CO strains were propagated in Vero cells (ATCC, Manassas, VA, and CCL-81) and maintained at passage level five as a stock. The virulent aMPV-C virus stock (aMPV-CO Tr) was prepared from the tracheal tissues of aMPV-C Colorado strain-infected SPF turkeys and titrated in SPF turkeys for 50% infective dose (ID_{50}) as described previously [29].

Generation of aMPV-C ΔM2-2 deletion virus

The previously generated aMPV-C infectious clone, paMPV-C sG, was used as a template to construct the M2-2 ORF deletion clone [29]. A M2-2 gene-specific reverse primer, dM2-2 up (5′-gcaacgtctctTTAATCAGAGTTTG CACTATCTTGCATGGCA-3′) and a M2-2 gene-specific forward primer, dM2-2 down (5′-gcaacgtctcaTTAAGT TAATAAAAAATTGGGACAAGTCAACATGGAGC-3′), were designed to anneal to the nucleotide (nt) positions 5212–5242 (dM2-2 up) and 5407–5444 (dM2-2 down) of the aMPV-CO genome [12]. The lower case letters in the primer sequences represent the engineered *Bsm*BI sites. The paMPV-C sG cDNA clone was amplified, which excluded the non-overlapping region of the M2-2 ORF, by PCR using the dM2-2 up and dM2-2 down primers and the *pfu*Ultra™ II Fusion HS DNA polymerase (Stratagene, La Jolla, CA) according to the manufacturer's instructions. The amplified PCR product was digested with *Bsm*BI (NEB, Ipswich, MA), gel purified, self-ligated using T4 DNA ligase (NEB), and subsequently transformed into the STBL2 cells (Invitrogen, Carlsbad, CA), according to the manufacturer's instructions. The positive clones were selected by sequencing the M2 gene and flanking regions. Finally, an M2-2 ORF deleted full-length cDNA clone, designated as paMPV-C ΔM2-2, was amplified in STBL2 cells at 30°C for 24 h and purified using a QIAprep Spin Miniprep kit (Qiagen, Valencia, CA).

Rescue of the M2-2 ORF-deleted aMPV-C virus was performed by transfecting paMPV-C ΔM2-2 into HEp-2 cells using the reverse genetics system described previously [29]. In brief, a mixture of 1 μg of paMPV-C ΔM2-2, 1 μg of pN, 0.5 μg of pP, 0.1 μg of pL, and pM2-1 supporting plasmids was transfected into MVA/T7-infected HEp-2 cells using Lipofectamine™ 2000 (Invitrogen) reagent, according to the manufacturer's protocol. At 6-h post-transfection, the cells were washed 1× with phosphate buffered saline (PBS) and maintained in Dulbecco's Modified Eagle Medium (D-MEM) supplemented with 2% fetal bovine serum (FBS) and antibiotics (100 U/ml Penicillin, 100 μg/ml Streptomycin, and 0.25 μg/ml Amphotericin B, Thermo Scientific). At 72-h post-transfection, the transfected HEp-2 cells were scraped and co-cultured on an existing 50% monolayer of Vero cells. The co-cultured cells were incubated at 37°C in 5% CO_2 for 5 days. The rescued M2-2 deletion virus, designated as raMPV-C ΔM2-2, was propagated in Vero cells and maintained at passage level five as a stock.

Nucleotide sequencing

All RT-PCR products and purified plasmids were sequenced directly with M13 universal primers or gene-specific primers using the Applied Biosystems-PRISM fluorescent big dye sequencing kit and the ABI 3730 DNA sequencer (ABI, Foster City, CA). Nucleotide sequence editing, assembling, and comparison analysis were done with the DNASTAR program (Madison, WI).

Virus titrations and growth curves

The titers of the raMPV-C ΔM2-2 virus, its parental virus, and the aMPV-CO wild-type virus stocks were determined by infecting Vero cell monolayers with 100 µl of serial 10-fold dilutions of the viruses as described previously [31]. Titers were calculated by the Reed and Muench method [32] and expressed as 50% tissue culture infective dose ($TCID_{50}$). Growth kinetics of the M2-2 deletion virus, its parental virus, and the aMPV-CO virus were examined using Vero cells in two independent experiments. In brief, Vero cell monolayers were infected with aMPV-CO, raMPV-C sG, or raMPV-C ΔM2-2 at 0.1 multiplicity of infection (MOI). Every 24-h post-infection, the monolayers were harvested. The mean virus titers of duplicate samples at each time point from the two independent experiments were determined and expressed as $\log_{10}$ $TCID_{50}$/ml.

Animal experimental design

The animal experiment to assess the pathogenicity and immunogenicity of the raMPV-C ΔM2-2 mutant was carried out in the same experiment to characterize the aMPV-C G gene variants, which was previously reported [29]. Figure 1 illustrates the design of the animal experiment where turkeys were infected with various aMPV viruses and samples were taken periodically. In brief, 40 one-week-old SPF turkey poults were randomly divided into four groups of 10 birds. Birds in group 1 received 100 µl of PBS via intranasal (IN) and intraocular (IO) routes per bird as a control. Birds in groups 2 and 3 were inoculated with 100 µl of raMPV-C sG (3.16×10^6 $TCID_{50}$/ml) or raMPV-C ΔM2-2 (5.65×10^6 $TCID_{50}$/ml) per bird, respectively, via IN and IO routes. Each bird in group 4 was infected with 100 µl of aMPV-CO Tr (4.2×10^4 ID_{50}/ml), the challenge virus stock, via IN and IO routes as a positive control. Daily after inoculation, birds were observed for clinical signs of aMPV disease and recorded. Intra-tracheal swabs were collected at 3, 5, and 7 days post-inoculation (DPI) from each bird for detection of virus replication or viral RNA shedding in the respiratory tract. Each of the swabs was stored in 1 ml of Brain Heart Infusion (BHI) medium containing antibiotics (100 U/ml Penicillin, 100 µg/ml Streptomycin, and 0.25 µg/ml Amphotericin B, Thermo Scientific) at −70°C. At 14 DPI, serum was taken from each bird for detection of an antibody response and measured by ELISA. Immediately after serum collection, birds in all the groups were challenged with 100 µl (per bird) of aMPV-CO Tr (4.2×10^4 ID_{50}/ml) via the IN/IO routes. The challenged birds were monitored daily for clinical signs. Tracheal swabs were collected from each of the challenged birds at 3, 5, and 7 days post-challenge (DPC) for detection of virus shedding.

Detection of viral RNA shedding and antibody response

Virus replication or viral RNA shedding in the turkey tracheal tissues was detected by RT-PCR with a pair of aMPV-C N gene-specific primers described previously [29]. Anti-aMPV-C antibody response in turkeys after infection was determined by an ELISA test described previously [29]. A standard negative serum pool, collected from turkeys inoculated with PBS, was included in each plate of the ELISA test as a negative control. The positive anti-aMPV-C serum pool, collected from turkeys following infection with the virulent challenge virus, was diluted two-fold from 1:100 to 1:3200 and used to establish a standard curve for determining antibody titers of the test sera. Sera were deemed positive when the mean chemiluminescence relative light unit (RLU) value was greater than the mean RLU plus 2× standard deviation of the three dilutions (1:100–1:400) of the negative turkey serum pool.

Statistical analysis

The numbers of birds with clinical signs, serum conversion, and the presence of viral RNA in the animal experiment were analyzed for significant differences between each treatment group by Fisher's exact test (SigmaStat 2.0.3, SPSS Inc, Chicago, IL). Significant differences between each viral growth curve were analyzed using pairwise multiple comparisons with Kruskal–Wallis One Way method (SigmaStat 2.0.3). All the tests were performed with a 5% level of significance.

Results

Generation of recombinant aMPV-C ΔM2-2 virus

In order to generate an aMPV-C ΔM2-2 deletion virus, we constructed a recombinant full-length clone by PCR amplification of paMPV-C sG, which excluded the

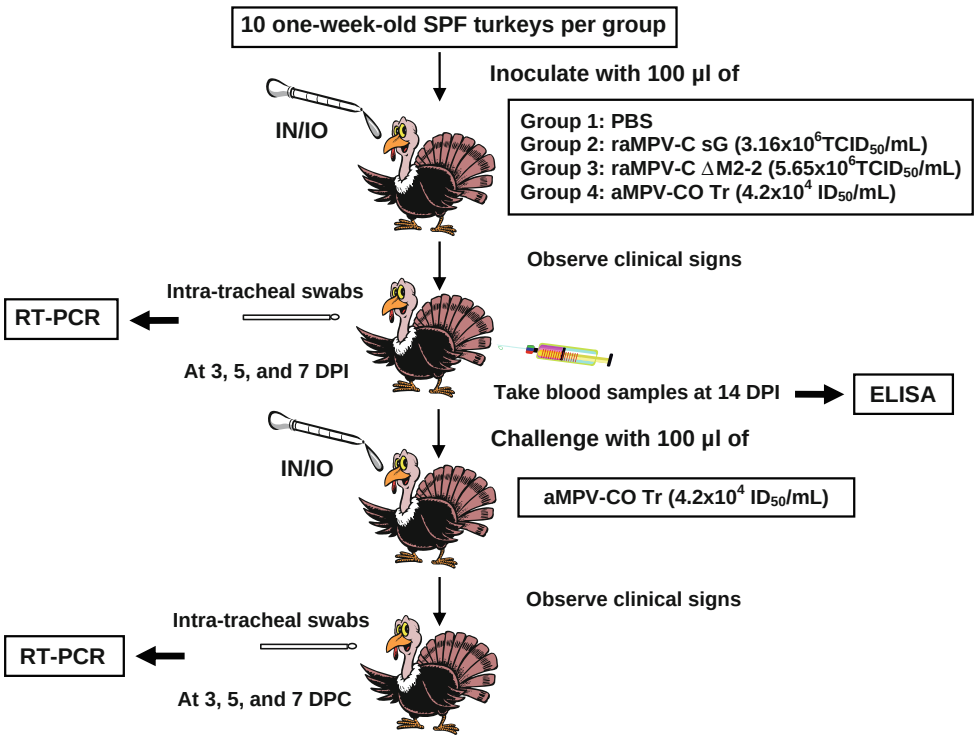

Fig. 1 Experimental design of challenge experiments in vaccinated turkeys. *DPI* days post-inoculation, *DPC* days post-challenge, *IN/IO* intranasal and intraocular routes of administration

non-overlapping region of the M2-2 ORF. The deleted region is composed of 168 nucleotides, which encodes 56 aa and represents approximately 79% of the M2-2 ORF. This M2-2 ORF deletion does not alter the M2-1 ORF coding capacity. After co-transfection of the paMPV-C ΔM2-2 clone and the supporting plasmids in HEp-2 cells and subsequent amplification in Vero cells, a viable aMPV-C ΔM2-2 deletion virus was rescued and propagated. The fidelity of the rescued M2-2 deletion mutant was confirmed by sequence analysis of RT-PCR products of the viral genome (data not shown).

Biological characterization of the raMPV-C ΔM2-2 deletion virus in cell culture

To determine if the M2-2 deletion affects virus replication and growth characteristics in vitro, raMPV-C ΔM2-2, its parental virus raMPV-C sG, and the aMPV-CO wild-type virus were examined in Vero cells for growth kinetics and cytopathic effects (CPE). The M2-2 deletion mutant replicated slightly less efficiently than both the parental recombinant and the CO wild-type viruses (Fig. 2). The titer of raMPV-C ΔM2-2 was approximately 10-fold lower than that of raMPV-C sG and the CO wild-type viruses at 48-h post-infection, but statistically it is not significantly different from that of its parental virus. The raMPV-C ΔM2-2 virus induced typical CPE that were indistinguishable from those seen with the parental virus or the aMPV-CO strain in infected cell cultures (Fig. 3).

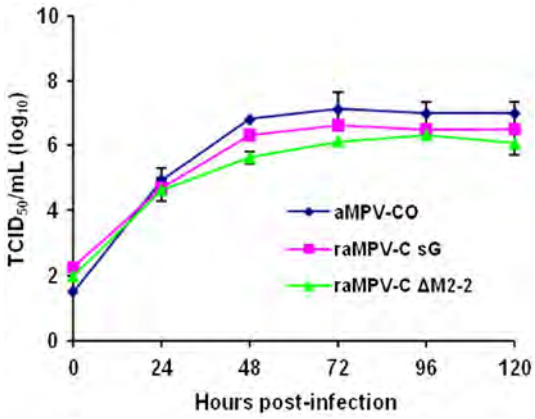

Fig. 2 Growth curves of raMPV-C ΔM2-2, raMPV-C sG, and aMPV-CO in Vero cells. Vero cell monolayers were infected with raMPV-C ΔM2-2, raMPV-C sG, or aMPV-CO at 0.1 MOI $TCID_{50}$/cell. Every 24-h post-infection, cellular monolayers were harvested. Viral titers were determined by $TCID_{50}$ titration in Vero cells for each time point in duplicate from two independent experiments, and log_{10} values of each mean were charted with *error bars*

Pathogenicity of the raMPV-C ΔM2-2 deletion virus in turkeys

Experimental infection of 1-week-old SPF turkeys was carried out to evaluate the effects of the M2-2 deletion on virus replication and pathogenicity in vivo. From 3 DPI, the turkey poults infected with the virulent aMPV-CO Tr exhibited typical clinical signs of the disease, showing nasal exudates when squeezed, nasal discharge, and/or

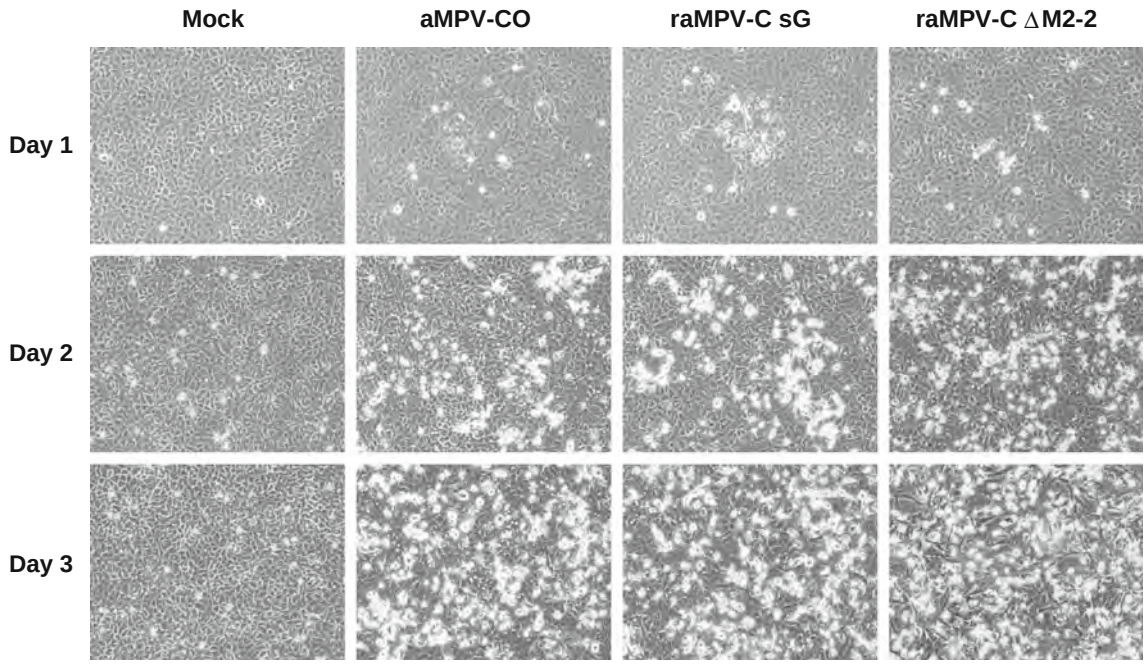

Fig. 3 Cytopathic effects induced by aMPV-C infection. Vero cell monolayers were infected with raMPV-C ΔM2-2, raMPV-C sG, or aMPV-CO at 0.1MOI $TCID_{50}$/cell, or mock infected with D-MEM. At days 1, 2, and 3 post-infection, the monolayers were digitally photographed using an inverted microscope at ×100 magnifications (Olympus America, Melville, NY)

Table 1 Clinical signs of disease observed in turkeys at different days post-inoculation (DPI)

Inoculums	Number of birds showing clinical signs/number in group on given day									
	1	2	3	4	5	6	7	8	9	10
PBS	0/10	0/10	0/10	0/10	0/10	0/10	0/10	0/10	0/10	0/10
aMPV-CO Tr	0/10	0/10	7/10[a]	7/10[a]	9/10[a]	10/10[a]	8/10[a]	4/10	2/10	0/10
raMPV-C sG	0/9	0/9	0/9	0/9	0/9	0/9	0/9	0/9	0/9	0/9
raMPV-C ΔM2-2	0/10	0/10	0/10	0/10	0/10	0/10	0/10	0/10	0/10	0/10

[a] Significant difference ($P < 0.05$) between groups within a column

frothy eyes. These clinical signs gradually disappeared after 9 DPI. However, neither raMPV-C ΔM2-2- nor raMPV-C sG-infected birds showed any clinical signs of the disease (Table 1). Viral RNA was detected in tracheal tissues in 100% of aMPV-CO Tr-infected birds at 3 and 5 DPI and 60% of those birds were still shedding virus at 7 DPI (Table 2). However, only 10–22% of raMPV-C sG and raMPV-C ΔM2-2 inoculated turkeys were positive for viral RNA, indicating low virus replication and shedding at 3 and 5 DPI. At 7 DPI, the number of positive birds that shed viral RNA from the raMPV-sG-infected group increased to 63%, whereas no viral RNA was detected in tracheal tissue from the raMPV-C ΔM2-2-infected birds, which is significantly different from the viral RNA shedding rate in raMPV-C sG-infected birds (Table 2).

Table 2 Virus shed in turkey trachea at different days post-inoculation (DPI)

Viruses	No. and % of birds in which viral RNA was detected/number in group		
	3 DPI	5 DPI	7 DPI
aMPV-CO Tr	10/10 (100%)	10/10 (100%)	6/10 (60%)
raMPV-C sG	2/9 (22%)[a]	2/9 (22%)[a]	5/8 (63%)
raMPV-C ΔM2-2	1/10 (10%)[a]	2/10 (20%)[a]	0/10 (0%)[a]

[a] Significant difference ($P < 0.05$) between groups within a column

Immunogenicity of the raMPV-C ΔM2-2 deletion virus in turkeys

To detect and empirically measure the immune response in inoculated turkeys, antibody levels were quantified. All

Table 3 Serum antibody response in turkeys 14 days post-inoculation

Inoculums	No. and % of Ab positive sera in group	Number of sera with ELISA titer (log_2)					Mean ± SD (log_2)
		≤5.6	6.6	7.6	8.6	9.6	
PBS	0/10 (0%)[a]	10					
aMPV-CO Tr	9/9 (100%)[b]		1	4	4		7.9 ± 0.7
raMPV-C sG	6/8 (75%)[b,c]	2	6				6.4 ± 0.4
raMPV-C ΔM2-2	4/10 (40%)[a,c]	6	4				6.0 ± 0.6

[a,b,c] Each superscript letter denotes a significantly different ($P < 0.05$) group compared to other inoculums

birds inoculated with the challenge virus had positive serum conversion with a mean titer of 7.9 log_2, whereas all sera collected from PBS inoculated birds, unvaccinated, were negative after14 DPI (Table 3). Six of eight, 75%, turkeys inoculated with the raMPV-C sG virus had a positive antibody response with a mean titer of 6.4 log_2. However, only four of ten, 40%, birds inoculated with the raMPV-C ΔM2-2 deletion virus had a positive antibody response with a mean titer of 6.0 log_2.

Protection of the raMPV-C ΔM2-2 deletion virus-vaccinated turkeys against challenge

To examine if the immune response in turkeys induced by raMPV-C ΔM2-2 was protective against aMPV-C disease, the vaccinated birds were challenged with aMPV-CO Tr. Seven of nine, 78%, birds vaccinated with the raMPV-C ΔM2-2 deletion mutant were not protected against the challenge, and developed typical clinical signs of the disease (Table 4). In contrast, seven of eight, 87%, birds vaccinated with the parental raMPV-C sG virus were protected against the challenge. The birds inoculated with aMPV-CO Tr were fully protected against challenge with the same virus (Table 4). All unvaccinated birds, PBS control, showed typical clinical signs of the disease. Furthermore, detection of the challenge virus replication in tracheal tissue revealed that 89% of the raMPV-C ΔM2-2 vaccinated birds and 63% of the raMPV-C sG vaccinated birds had detectable levels of virus RNA shedding at 3 DPC (Table 5). After 5 DPC, the shedding of challenge virus RNA was dramatically decreased below detectable levels for the raMPV-C sG vaccinated birds. In contrast, the raMPV-C ΔM2-2 vaccinated turkeys still shed the challenge virus at 5 DPC, 44%, and 7 DPC, 11%. All unvaccinated birds shed challenge virus at 3 and 5 DPC, whereas no shedding of the challenge virus was detected from turkeys vaccinated with the same aMPV-CO Tr virus.

Table 5 Virus shed in turkey trachea at different days post-challenge (DPC)

Vaccines	No. and % of birds in which viral RNA was detected/number in group		
	3 DPC	5 DPC	7 DPC
PBS	10/10 (100%)	10/10 (100%)	0/10 (0%)
aMPV-CO Tr	0/9 (0%)[a]	0/9 (0%)[a]	0/9 (0%)
raMPV-C sG	5/8 (63%)	0/8 (0%)[a]	0/8 (0%)
raMPV-C ΔM2-2	8/9 (89%)	4/9 (44%)[a]	1/9 (11%)

[a] Significant difference ($P < 0.05$) between groups within a column

Discussion

In the present study, we successfully rescued a recombinant aMPV-C virus in which the non-overlapping region of the M2-2 ORF was deleted. The viability of raMPV-C ΔM2-2 in Vero cells confirmed that the M2-2 ORF of aMPV-C virus is an accessory gene and dispensable for growth in vitro, as found in other pneumoviruses [18, 22, 30].

Table 4 Clinical signs of disease observed in turkeys at different days post-challenge

Vaccines	Number of birds showing clinical signs/number in group on given day									
	1	2	3	4	5	6	7	8	9	10
PBS	0/10	0/10	9/10	10/10	9/10	6/10	2/10	0/10	0/10	0/10
aMPV-CO Tr	0/9	0/9	0/9[a]	0/9[a]	0/9[a]	0/9[a]	0/9	0/9	0/9	0/9
raMPV-C sG	0/8	0/8	1/8[a]	1/8[a]	1/8[a]	1/8[a]	0/8	0/8	0/8	0/8
raMPV-C ΔM2-2	0/9	0/9	4/9	7/9	6/9	4/9	3/9	0/9	0/9	0/9

[a] Significant difference ($P < 0.05$) between groups within a column

However, the effects of the M2-2 deletion on virus growth kinetics in cells appeared to be different between the avian metapneumoviruses and the mammalian pneumoviruses. This aMPV-C M2-2 knockout virus replicated in Vero cells slightly less efficiently than the parental recombinant virus and the wild-type CO strain during the initial stages of infection, with approximately 10-fold virus titer reduction. But during later stages of infection the M2-2 deletion virus displayed similar levels of growth kinetics as the parental virus. In contrast, replication of the RSV M2-2 knockout virus in cell culture was severely impaired, and the titers were reduced 1,000-fold during the initial 2–5 days and 10-fold by 7–8 days post-infection [22]. The exact reason for the different impact on virus growth dynamics is unknown, but it may be related to the differing levels of the M2-2 protein expression needed for efficient virus replication in cells. In wild-type RSV-infected cells, the M2-2 protein was readily detected as a minor constituent by sera raised against a fusion protein containing the RSV M2-2 sequence [33] or by antibody against the bacterially expressed M2-2 protein [26]. However, sera raised against a fusion protein containing the aMPV-A M2-2 protein failed to detect the M2-2 protein in aMPV-A-infected cells [33]. In vitro transcription and translation of the M2 gene cloned from an aMPV-A virus also failed to express the M2-2 protein at detectable levels [34]. Recently, using a minigenome system, the expression of a reporter gene from the second ORF of the aMPV-A M2 gene was detected, but at levels approximately 67-fold lower than its counterpart in RSV [17]. This suggests that aMPV may require lower levels of M2-2 gene expression or maybe less dependent on the M2-2 protein than RSV to facilitate efficient virus replication in infected cells. Thus, the M2-2 deletion from the aMPV-C genome would have less of an impact on virus replication compared to the similar deletion in RSV. Interestingly, raMPV-C ΔM2-2 induced CPE that were indistinguishable from those seen with the parental virus infection, whereas the RSV M2-2 gene deleted recombinant virus exhibited altered growth characteristics and produced different sizes of plaques in cells [35]. The different effect of the M2-2 deletion on CPE between RSV and aMPV-C may have resulted from the differing dependency on the M2-2 protein to maintain wild-type virus replication in cells.

The clinical signs observed in the animal experiment have shown that raMPV-C ΔM2-2 exhibited a non-pathogenic phenotype and caused no clinical disease. This is somewhat expected because its parental virus, raMPV-C sG, was less virulent than the wild-type CO strain. While deletion of the M2-2 gene from a less virulent aMPV strain may have resulted in complete attenuation, the effect of additional cell culture passages on virulence during construction of the recombinant can not be ruled out completely [29, 36]. Importantly, the effect of the M2-2 deletion on virus pathogenicity could be evaluated by detection of virus replication efficiency in the tracheal tissues of the infected turkeys. Data presented here show that, during the initial 3–5 days post-infection, both raMPV-C ΔM2-2 and its parental virus replicated at low levels in the tracheal tissue. Subsequently, the parental virus replicated more efficiently in the trachea by 7 DPI, whereas the raMPV-C ΔM2-2 virus was completely cleared from the trachea by 7 DPI. These results indicate that the M2-2 deletion impaired virus replication and attenuated the virus more in vivo than in vitro. Interestingly, a similar situation has been reported for the aMPV-A virus, where the deletion of aMPV-A M2-2 gene impaired virus replication in turkeys more severely than in vitro [30]. On the other hand, the M2-2 deletion from RSV and hMPV had an opposite effect where the gene deletion impaired virus replication more severely in vitro than in vivo [24–26]. Nevertheless, all evidence reported so far supports the idea that in the absence of the M2-2 gene in pneumoviruses viral replication is attenuated both in vitro and in vivo with differing efficiencies of impairment.

A number of recombinant RSV and hMPV viruses with deletions of specific genes or a combination of genes generated by the reverse genetics have been evaluated as vaccine candidates in animal models with different degrees of success [37, 38]. Among these recombinants, rA2ΔM2-2 and rhMPVΔM2-2 were very promising vaccine candidates. Despite the virus attenuation, they were highly immunogenic and protective against challenge in African green monkeys (AGM) [25, 35]. In contrast, the data presented in this study shows that less than half of the raMPV-C ΔM2-2 virus-inoculated turkeys produced a positive antibody response at all and most of the birds were not protected against the challenge virus. The reason for the different impact of the M2-2 deletion on immunogenicity between the avian metapneumovirus and mammalian pneumoviruses is unknown, but is most likely due to different levels of viral attenuation in vivo. Our data show that the deletion of the M2-2 protein severely impaired virus replication in turkeys. Such a low level of virus replication may not produce a sufficient amount of viral antigens to induce protective immune responses in vivo. However, in rhMPVΔM2-2-infected AGM, virus replication was moderately restricted during the first 12 days post-infection, showing a mean virus titer of 1.7 or 2.1 $\log_{10}$PFU/ml from the upper or lower respiratory tract samples, respectively [25]. Apparently, this level of virus replication produced a sufficient amount of viral antigens for inducing an immune response against the challenge virus in vivo.

In summary, we successfully rescued a viable recombinant aMPV-C virus lacking the majority of the M2-2

ORF, and characterized this M2-2 deletion virus in vitro and in vivo. Our results show that the deletion of the M2-2 gene slightly decreased virus replication in cell culture but severely impaired virus replication and immunogenicity in turkeys. Inoculation of turkeys with raMPV-C ΔM2-2 failed to produce clinical disease and a protective immune response. These results suggest that the M2-2 protein of aMPV-C is not essential for virus viability in vitro, but it is required for sufficient virus replication to maintain pathogenicity and immunogenicity in vivo. Taking into account the similar results found in aMPV-A studies and conflicting results with RSV and hMPV, the M2-2 protein in avian metapneumoviruses may be involved in both major viral pathways; a minor role in virus replication, and perhaps a larger role in counteracting the host cell's immune response.

Acknowledgments The authors wish to thank Xiuqin Xia and Fenglan Li for excellent technical assistance and Melissa Scott and Joyce Bennett for performing the automated nucleotide sequencing, Darrell Kapczynski for assistant in statistical analysis, and Patti Miller for critical reading of the manuscript. This research was supported by USDA, ARS CRIS project 6612-32000-056-00D.

References

1. J.K. Cook, Vet. J. **160**, 118–125 (2000)
2. R.E. Gough, R.C. Jones, in *Diseases of Poultry*, ed. by Y.M. Saif, A.M. Fadly, J.R. Glisson, L.R. McDougald, L.K. Nolan, D.E. Swayne (Blackwell Publishing, Ames, 2008), pp. 100–110
3. C.R. Pringle, Arch. Virol. **143**, 1449–1459 (1998)
4. C. Banet-Noach, L. Simanov, S. Perk, Avian Pathol. **34**, 220–226 (2005)
5. M.H. Bayon-Auboyer, C. Arnauld, D. Toquin, N. Eterradossi, J. Gen. Virol. **81**, 2723–2733 (2000)
6. K. Juhasz, A.J. Easton, J. Gen. Virol. **75**, 2873–2880 (1994)
7. B.S. Seal, Anim. Health. Res. Rev. **1**, 67–72 (2000)
8. B.G. van den Hoogen, T.M. Bestebroer, A.D. Osterhaus, R.A. Fouchier, Virology **295**, 119–132 (2002)
9. E. Lee, M.S. Song, J.Y. Shin, Y.M. Lee, C.J. Kim, Y.S. Lee, H. Kim, Y.K. Choi, Virus Res. **128**, 18–25 (2007)
10. D. Toquin, O. Guionie, V. Jestin, F. Zwingelstein, C. Allee, N. Eterradossi, Virus Genes **32**, 97–103 (2006)
11. R. Ling, A.J. Easton, C.R. Pringle, J. Gen. Virol. **73**(Pt 7), 1709–1715 (1992)
12. H.C. Lwamba, R. Alvarez, M.G. Wise, Q. Yu, D. Halvorson, M.K. Njenga, B.S. Seal, Virus Res. **107**, 83–92 (2005)
13. M. Sugiyama, H. Ito, Y. Hata, E. Ono, T. Ito, Virus Genes. **41**, 389–395 (2010)
14. Q. Yu, P.J. Davis, J. Li, D. Cavanagh, Virology **186**, 426–434 (1992)
15. A.M. Dar, S. Munir, S.M. Goyal, V. Kapur, J. Clin. Microbiol. **41**, 2748–2751 (2003)
16. O. Dibben, L.C. Thorpe, A.J. Easton, Virus Res. **131**, 47–53 (2008)
17. P.S. Gould, A.J. Easton, J. Virol. **81**, 8488–8496 (2007)
18. U.J. Buchholz, S. Biacchesi, Q.N. Pham, K.C. Tran, L. Yang, C.L. Luongo, M.H. Skiadopoulos, B.R. Murphy, P.L. Collins, J. Virol. **79**, 6588–6597 (2005)
19. R. Fearns, P.L. Collins, J. Virol. **73**, 5852–5864 (1999)
20. R.W. Hardy, G.W. Wertz, J. Virol. **72**, 520–526 (1998)
21. M.N. Teng, P.L. Collins, J. Virol. **72**, 5707–5716 (1998)
22. A. Bermingham, P.L. Collins, Proc. Natl. Acad. Sci. USA **96**, 11259–11264 (1999)
23. P.L. Collins, M.G. Hill, J. Cristina, H. Grosfeld, Proc. Natl. Acad. Sci. USA **93**, 81–85 (1996)
24. J.H. Schickli, J. Kaur, M. Macphail, J.M. Guzzetta, R.R. Spaete, R.S. Tang, Virol. J. **5**, 69 (2008)
25. S. Biacchesi, Q.N. Pham, M.H. Skiadopoulos, B.R. Murphy, P.L. Collins, U.J. Buchholz, J. Virol. **79**, 12608–12613 (2005)
26. H. Jin, H. Zhou, X. Cheng, R. Tang, M. Munoz, N. Nguyen, Virology **273**, 210–218 (2000)
27. D. Govindarajan, S.H. Kim, S.K. Samal, Avian Dis. **54**, 59–66 (2010)
28. C.J. Naylor, C. Lupini, P.A. Brown, Vaccine **28**, 6800–6807 (2010)
29. Q. Yu, C. Estevez, M. Song, D. Kapczynski, L. Zsak, Virus Res. **147**, 182–188 (2010)
30. R. Ling, S. Sinkovic, D. Toquin, O. Guionie, N. Eterradossi, A.J. Easton, J. Gen. Virol. **89**, 525–533 (2008)
31. D.R. Kapczynski, H.S. Sellers, Avian Dis. **47**, 1376–1383 (2003)
32. L.J. Reed, H. Muench, Am. J. Hyg. **27**, 493–497 (1938)
33. G. Ahmadian, P. Chambers, A.J. Easton, J. Gen. Virol. **80**(Pt 8), 2011–2016 (1999)
34. Q. Yu, P.J. Davis, T.D. Brown, D. Cavanagh, J. Gen. Virol. **73**, 1355–1363 (1992)
35. H. Jin, X. Cheng, H.Z. Zhou, S. Li, A. Seddiqui, J. Virol. **74**, 74–82 (2000)
36. D.P. Patnayak, B.R. Gulati, A.M. Sheikh, S.M. Goyal, Vaccine **21**, 1371–1374 (2003)
37. U.J. Buchholz, K. Nagashima, B.R. Murphy, P.L. Collins, Expert Rev. Vaccines **5**, 695–706 (2006)
38. P.L. Collins, S.S. Whitehead, A. Bukreyev, R. Fearns, M.N. Teng, K. Juhasz, R.M. Chanock, B.R. Murphy, Adv. Virus Res. **54**, 423–451 (1999)

Vaccine 29 (2011) 8624–8633

Contents lists available at SciVerse ScienceDirect

Vaccine

journal homepage: www.elsevier.com/locate/vaccine

Generation and evaluation of a recombinant Newcastle disease virus expressing the glycoprotein (G) of avian metapneumovirus subgroup C as a bivalent vaccine in turkeys

Haixia Hu[a,b], Jason P. Roth[a], Carlos N. Estevez[a,1], Laszlo Zsak[a], Bo Liu[b], Qingzhong Yu[a,*]

[a] Southeast Poultry Research Laboratory, Agricultural Research Services, United States Department of Agriculture, 934 College Station Road, Athens, GA 30605, USA
[b] College of Animal Science and Veterinary Medicine, Jilin University, 5333 Xi An Road, Changchun 130062, Jinlin, China

ARTICLE INFO

Article history:
Received 27 July 2011
Received in revised form 19 August 2011
Accepted 2 September 2011
Available online 14 September 2011

Keywords:
NDV
aMPV-C
Reverse genetics
Glycoprotein
Recombinant vector
Bivalent vaccine

ABSTRACT

Virulent strains of Newcastle disease virus (NDV) and avian metapneumovirus (aMPV) can cause serious respiratory diseases in poultry. Vaccination combined with strict biosecurity practices has been the recommendation for controlling both NDV and aMPV diseases in the field. In the present study, an NDV based, LaSota strain recombinant vaccine virus expressing the glycoprotein (G) of aMPV subgroup C (aMPV-C) was generated as a bivalent vaccine using a reverse genetics approach. The recombinant virus, rLS/aMPV-C G was slightly attenuated *in vivo*, yet maintained similar growth dynamics, cytopathic effects, and virus titers *in vitro* when compared to the parental LaSota virus. Expression of the aMPV G protein in rLS/aMPV-C G-infected cells was detected by immunofluorescence assay. Vaccination of turkeys with one dose of rLS/aMPV-C G induced moderate aMPV-C-specific immune responses and comparable NDV-specific serum antibody responses to a LaSota vaccination control. Partial protection against pathogenic aMPV-C challenge and complete protection against velogenic NDV challenge was conferred. These results suggest that the LaSota recombinant virus is a safe and effective vaccine vector and that expression of the aMPV-C G protein alone is not sufficient to provide full protection against an aMPV-C infection. Expression of other immunogenic protein(s) of the aMPV-C virus alone or in conjunction with the G protein may be needed to induce a stronger protective immunity against the aMPV-C disease.

Published by Elsevier Ltd.

1. Introduction

Avian metapneumovirus (aMPV) is an economically important pathogen of turkeys with a worldwide distribution [1]. It causes turkey rhinotracheitis (TRT) and is also associated with "swollen head syndrome (SHS)" in chickens [2]. Typical clinical signs of the disease in turkey poults include coughing, sneezing, nasal discharge, tracheal rales, foamy conjunctivitis, and swollen infraorbital sinuses. The virus also affects egg quality and causes a rapid drop in egg production in breeding and layer turkeys [3,4]. The disease is usually accompanied by secondary bacterial infection that can increase morbidity and mortality, resulting in significant economic losses to the poultry industry [1,5]. Isolates of aMPV have been classified into four subgroups, A, B, C, and D, based on the level of genetic variations and antigenic differences [1]. While the aMPV subgroups A and B are present in Europe and most countries in the world, excluding the USA, aMPV-C is mainly present in the USA and to a limited degree in France and Korea [6,7]. Currently, the aMPV subgroup D has only been reported in France [8].

Control efforts against aMPV have included flock management, biosecurity, controlled exposure, and vaccination with live, attenuated or killed vaccines. In European and South American countries, cell culture-attenuated or inactivated vaccines are currently used to control the disease caused by subgroups A and B [9–11]. Although these live, attenuated subtype A and B vaccines have been approved and appear to be effective in most countries where the disease is prevalent, several reports suggest that the stability and safety of these live vaccines are a concern [12–14]. It has been reported that outbreaks of respiratory disease in turkeys, which has been diagnosed as TRT, has occurred following aMPV vaccination. This phenomenon has been attributed to the fact that the vaccine virus is becoming more virulent due to reversion during virus replication in unvaccinated birds [12,13,15]. Recently in Brazil [16] and Italy [14], field evidence has suggested that the existing vaccines do not fully protect against the field strains of the virus circulating in these countries. In the US, a Vero cell-attenuated aMPV-C vaccine has been used to control the disease in the endemic areas [17]. This live, attenuated vaccine appears to be effective against aMPV-C disease

* Corresponding author. Tel.: +1 706 546 3628; fax: +1 706 546 3161.
E-mail address: qingzhong.yu@ars.usda.gov (Q. Yu).
[1] Present <fn0005>address: Boehringer-Ingelheim Vetmedica, 2621 North Belt Highway, St. Joseph, MO 64506, USA.

0264-410X/$ – see front matter. Published by Elsevier Ltd.
doi:10.1016/j.vaccine.2011.09.007

under experimental and field conditions, however, vaccinated birds shed live virus that may revert back to virulent form after further passages in *vivo*, which has been observed with the aMPV-A vaccine in Europe [12,15]. To overcome the problems associated with vaccine safety and stability, efforts have been made to develop inactivated, subunit, virosomal, vectored or genetically engineered vaccines [18–25]. In contrast to live attenuated vaccine, inactivated vaccines are safe, but their protective efficacy remains controversial [18,21]. Virosomal and DNA vaccines with the N, F, or M gene of aMPV-C or the recombinant fowlpox virus expressing the aMPV-A F protein achieved differing degrees of protective immunoresponses [19,20,22,25]. However, the administration of these vaccines is not practical to large commercial poultry operations.

Newcastle disease virus (NDV) is the causative agent of Newcastle disease and has been classified into one serotype and three different pathotypes: velogenic (highly virulent), mesogenic (moderately virulent) or lentogenic (low virulence) viruses [26]. Velogenic strains can cause severe disease, characterized by extensive lesions and high mortality in both the laboratory and field, and such outbreaks require reporting to the World Organization for Animal Health (OIE) by member nations [26,27]. Vaccination combined with strict biosecurity practices has been the recommendation for controlling NDV outbreaks for over 60 years [28]. Naturally occurring lentogenic NDV strains, such as B1, VG/GA, and LaSota strains, are routinely used as live vaccines throughout the world to prevent Newcastle disease [26,28]. These live vaccines induce strong local immune responses, in addition to strong systemic responses, and can be readily administered through the drinking water supply or spraying the birds directly.

During the past decade, NDV has been developed as a vector to express foreign antigens, such as avian influenza hemagglutinin (HA) protein and infectious bursal disease virus VP2 protein, serving as a bivalent vaccine to protect chickens against NDV and the targeted avian pathogen [29–33]. In this study, we generated an NDV-based, LaSota strain, recombinant vaccine virus expressing the major surface attachment glycoprotein (G) of aMPV-C using reverse genetics techniques. We evaluated this recombinant virus *in vitro* and *in vivo* for its safety, stability, and expression of the G protein for its potential use as a bivalent vaccine against NDV and aMPV-C diseases.

2. Materials and methods

2.1. Cells, viruses and RNA preparation

HEp-2 (CCL-81; ATCC) and DF-1 (CRL-12203; ATCC) cell lines were grown in Dulbecco's Modified Eagle Medium (DMEM, Invitrogen, Carlsbad, CA) supplemented with 10% fetal bovine serum (FBS, Invitrogen) and antibiotics (100 U/ml penicillin, 100 μg/ml streptomycin, 0.25 μg/ml amphotericin B, Thermo Scientific). The DF-1 cells were maintained at 37 °C and 5% CO_2 in DMEM supplemented with 10% allantoic fluid (AF) from 10-day-old specific-pathogen-free (SPF) chicken embryos for all subsequent infections unless otherwise indicated. The NDV LaSota strain was obtained from ATCC and propagated in 9-day-old SPF chicken embryos. The velogenic strain of NDV, California 2002 (NDV/CA02; game chicken/US(CA)/S0212676/02), and the aMPV-C Colorado strain (aMPV-CO) were obtained from the pathogen repository bank at the Southeast Poultry Research Laboratory (SEPRL, USDA-ARS, Athens, GA, USA). The virulent aMPV-C virus stock (aMPV-CO Tr) was prepared from the tracheal tissues of aMPV-CO strain-infected SPF turkeys and titrated in SPF turkeys for 50% infective dose (ID_{50}) as described previously [34]. The modified vaccinia Ankara/T7 recombinant virus (MVA/T7) was used during virus rescue to provide the bacteriophage T7 RNA polymerase [35]. Viral RNA from the NDV-infected chicken embryo AF or DF-1 cells was extracted using the TRIzol-LS reagent according to the manufacturer's instructions (Invitrogen). Total cellular RNA from tracheal tissues was extracted using a MagMAX™ AI/ND Viral RNA Isolation kit (ABI, Austin, TX) following the manufacturer's procedures.

2.2. Construction of a full-length cDNA clone of the LaSota virus

Three cDNA fragments of approximately 5 kbp each, coding for the complete sequence of the LaSota virus genomic RNA, were generated by reverse transcription and polymerase chain reaction (RT-PCR) of the viral RNA. These fragments were sequentially cloned into the modified pBluescript vector [36] using an In-Fusion® PCR cloning kit, a restriction endonuclease (RE) site independent cloning system (Clontech, Mountain View, CA). Primers sets used to amplify the cDNA fragments and the linearized vector backbone for each ligation reaction were designed to contain a 15-nucleotide (nt) overlapping region of homology at their 5′ end (Table 1), as required for the In-Fusion® PCR cloning kit. A Superscript™ III one step RT-PCR system with platinum *Taq* Hi-Fi kit (Invitrogen) and the *pfu*Ultra™ II Fusion HS DNA polymerase (Stratagene, La Jolla, CA) were used for the RT-PCR or PCR amplification of the cDNAs or vectors, according to the manufacturer's instructions, throughout the cloning process unless otherwise indicated. Briefly, three cDNA fragments, together spanning the entire viral genome of the LaSota strain, were generated by RT-PCR with three pairs of specific primers (LS-F1 F and LS-F1 R, LS-F2 F and LS-F2 R, or LS-F3 F and LS-F3 R, Table 1). The plasmid vector was linearized before each round of RE independent ligation reactions by PCR with a pair of specific primers (pVec up and pVec down, pVec F1 up and pVec down, or pVec F2 up and pVec down, Table 1). The individual subgenomic cDNA fragments and corresponding linearized vectors were ligated using the In-Fusion® PCR cloning kit (Clontech) and subsequently transformed into Stbl2 competent cells (Invitrogen) following the manufacturer's instructions. These procedures were repeated until the complete genome of the LaSota virus was cloned (Fig. 1A). The final plasmid contained the full-length LaSota strain genome, designated as pFLC-LaSota, was amplified in Stbl2 cells at 30 °C for 24 h and purified using a QIAprep Spin Miniprep kit (Qiagen, Valencia, CA).

2.3. Construction of a recombinant LaSota cDNA clone containing the G gene of aMPV-C

The full-length LaSota cDNA clone, pFLC-LaSota, was used as a backbone to construct a recombinant cDNA clone containing the aMPV-C G gene between the fusion (F) and hemagglutinin-neuraminidase (HN) genes in the LaSota genome as an additional transcription unit (Fig. 1A). To facilitate the foreign gene insertion, a subclone containing the LaSota M and F gene junction region was constructed using an In-Fusion® PCR cloning kit (Clontech) with a pair of specific primers (M–F F and M–F R, Table 1) and a TOPO TA Cloning® vector (Invitrogen). The LaSota F coding sequences in the resulting subclone, pT-LS MF, was replaced with the open reading frame (ORF) of the aMPV-C G gene by using the In-Fusion® PCR cloning kit (Clontech) with paired specific primers (pM–F up and pM–F down for linearizing the vector, and aMPV-C NI G F and aMPV-C NI G R for amplifying the G ORF from the aMPV-C gG infectious clone [34], Table 1), forming a LaSota/aMPV-C G recombinant subclone. Finally, a cDNA fragment containing the LaSota M non-coding sequences, gene end (GE) and gene start (GS) signals, and the ORF of the aMPV-C G was amplified by PCR from the recombinant subclone with paired specific primers (LS F–M F and LS aMPV-C G RE, Table 1) and cloned into the LaSota F gene behind the translation stop codon in the full-length clone vector that was linearized by PCR with a pair of specific primers (LS vec F–M up and LS vec

Table 1
Primer sequences used in the study.

Primer	Primer sequence[d]	Primer name
1[a]	5′-cgactcactatagggACCAAACAGAGAATCCGTGAG-3′	LS-F1 F
2[a]	5′-gggaccatgccggccAAATCCCCTGGTTGTGCTTAC-3′	LS-F1 R
3[a]	5′-acaaccaggggatttGCCTCGGCA-3′	LS-F2 F
4[a]	5′-gggaccatgccggccGGCTAGGATCCCTTCCGCCAT-3′	LS-F2 R
5[a]	5′-gaagggatcctagccGATCAGATTGCACCTTTCT-3′	LS-F3 F
6[a]	5′-gggaccatgccggccACCAAACAAAGATTTGGTGAA-3′	LS-F3 R
7[b]	5′-GGCCGGCATGGTCCCAGCC-3′	pVec down
8[b]	5′-CCCTATAGTGAGTCGTATTAGCGGCCGCTTCC-3′	pVec up
9[b]	5′-AAATCCCCTGGTTGTGCTTAC-3′	pVec F1 up
10[b]	5′-GGCTAGGATCCCTTCCGCCAT-3′	pVec F2 up
11[b]	5′-CATCTTGCACCTGGAGGGCGCCAAC-3′	pM–F up
12[b]	5′-AAGGGCGAATTCCAGCACACTGGC-3′	pM–F down
13[b]	5′-TCACATTTTTGTAGTGGCTCTCATC-3′	LS vec F–M up
14[b]	5′-ACACAGATGAGGAACGAAGGTTTCCCTAATAG-3′	LS vec F down
15[c]	5′-CAATCCTTTTAAGAAATAAGC-3′	M–F F
16[c]	5′-TCACATTTTTGTAGTGGCTCTC-3′	M–F R
17[c]	5′-tccaggtgcaagatgGAGGTCAAGGTAGAGAATG-3′	aMPV-C NI G F
18[c]	5′-ctggaattcgcccttCTAACTCCAGTTGTACGAGTTG-3′	aMPV-C NI G R
19[c]	5′-actacaaaaatgtgaGCTGCGTCTCTGAGATTGCG-3′	LS F–M F
20[c]	5′-gttcctcatctgtgtACGCTAACTCCAGTTGTACGAGTTGC-3′	LS-aMPV-C G RE

[a] Primers 1–6 were used to RT-PCR amplify the genome of the NDV LaSota strain.
[b] Primers 7–14 were used to amplify or linearize the pFLC or subclone vectors.
[c] Primers 15–20 were used to amplify the aMPV-C G gene or cDNA fragments from subclones.
[d] Nucleotides shown in lower case letters represent homology sequences with a vector backbone, which were used to facilitate the RE independent cloning using the In-Fusion® PCR cloning kit (Clontech).

F down, Table 1) using the In-Fusion® PCR cloning kit (Clontech). The resulting recombinant clone, designated as pLS/aMPV-C G, was amplified in Stbl2 cells at 30 °C for 24 h and purified using a QIAprep Spin Miniprep kit (Qiagen).

2.4. Virus rescue and propagation

Rescue of the recombinant LaSota/aMPV-C G virus was performed by transfecting the full-length cDNA clone and supporting plasmids into HEp-2 cells as described previously [36]. Briefly, the HEp-2 cells were seeded on a six-well plate at 1×10^6 cells/well and infected with MVA/T7 to provide the T7 polymerase at a multiplicity of infection (MOI) of 3. A mixture of 2 μg of pLS/aMPV-C G, 1 μg of pTM-NP, 0.5 μg of pTM-P, and 0.1 μg of pTM-L was transfected into the MVA-T7 infected HEp-2 cells using Lipofectamine™ 2000 (Invitrogen) according to manufacturer's instruction. At 6 h post-transfection, the cells were washed once with phosphate buffered saline (PBS) and maintained in DMEM medium containing 2% FBS and antibiotics. At 72 h post-infection, the rescued virus, rLS/aMPV-C G, was harvested by freeze-thawing the infected cells three times. The rescued virus was amplified by inoculating 100 μl of the cell lysate into the allantoic cavity of 9-day-old SPF chicken embryos and incubating the embryos at 37 °C. After 4 days of incubation, the AF was harvested and used for detection of rescued virus by the hemagglutination (HA) test [37] and an immunofluorescence assay (IFA, see below). The AF was terminally diluted during subsequent passages to remove any possible MVA contamination. The rescued virus that had been positively confirmed by the HI or IFA test was amplified in SPF chicken embryos three times and the AF was harvested, aliquoted and stored at −80 °C as a stock.

2.5. Nucleotide sequencing

All plasmids and purified RT-PCR products generated during the FLC construction or from the rescued recombinant virus were sequenced directly with M13 universal primers or gene-specific primers using the Applied Biosystems-PRISM fluorescent big dye sequencing kit and the ABI 3730 DNA sequencer (ABI, Foster City, CA). Nucleotide sequence editing, assembling, and comparison analysis were carried out using the DNASTAR program (Madison, WI).

2.6. Virus titration, pathogenicity, and growth dynamics assays

Analyses of the virus stock titers were performed by conducting the standard HA test in a 96-well microplate, the 50% tissue infectious dose ($TCID_{50}$) assay on DF-1 cells, and the 50% egg infective dose (EID_{50}) assay in 9-day-old SPF chicken embryos [37]. Virus titers in cell cultures and eggs were calculated by the Reed and Muench method [38]. Pathogenicity of the recombinant virus was assessed by performing the standard mean death time (MDT) and intracerebral pathogenicity index (ICPI) tests [37]. The MDT for each virus was statistically analyzed using the unpaired, two-tailed Student's *t*-test with a 1% level of significance (Microsoft Excel, Redmond, WA). Cytopathic effects (CPE) induced by virus infection were examined by infecting confluent monolayers of DF-1 cells in 12-well plates with rLS/aMPV-C G or its parental LaSota strain at 0.01 MOI. At days 1, 2, and 3 post-infection, the monolayers were digitally photographed using an inverted microscope at 100× magnifications (Nikon, Eclipse T*i*, Melville, NY). Growth dynamics of the recombinant virus was examined on DF-1 cells in 12-well plates and compared with its parental virus. Monolayers of DF-1 cells were infected with rLS/aMPV-C G or LaSota strain at 0.01 MOI, and incubated at 37 °C in 5% CO_2. Every 12 h post-infection, cellular monolayers were harvested by freeze-thawing three times. Viral titers were determined by a $TCID_{50}$ titration on DF-1 cells in 96-well plates for each time point in triplicates from two independent experiments, and $\log_{10}$ values of each mean were charted with error bars. The growth curves for each virus were statistically analyzed using two-factor ANOVA with a 1% level of significance (Microsoft Excel).

2.7. Immunofluorescence assay (IFA)

To examine expression of the aMPV-C G protein by the recombinant virus, DF-1 cells were grown in a 12-well plate and infected with rLS/aMPV-C G or the parental LaSota strain at 0.01 MOI, or aMPV-CO at 0.1 MOI. At 24 h post-infection, the infected cells were washed three times with PBS and fixed with 10% zinc formalin

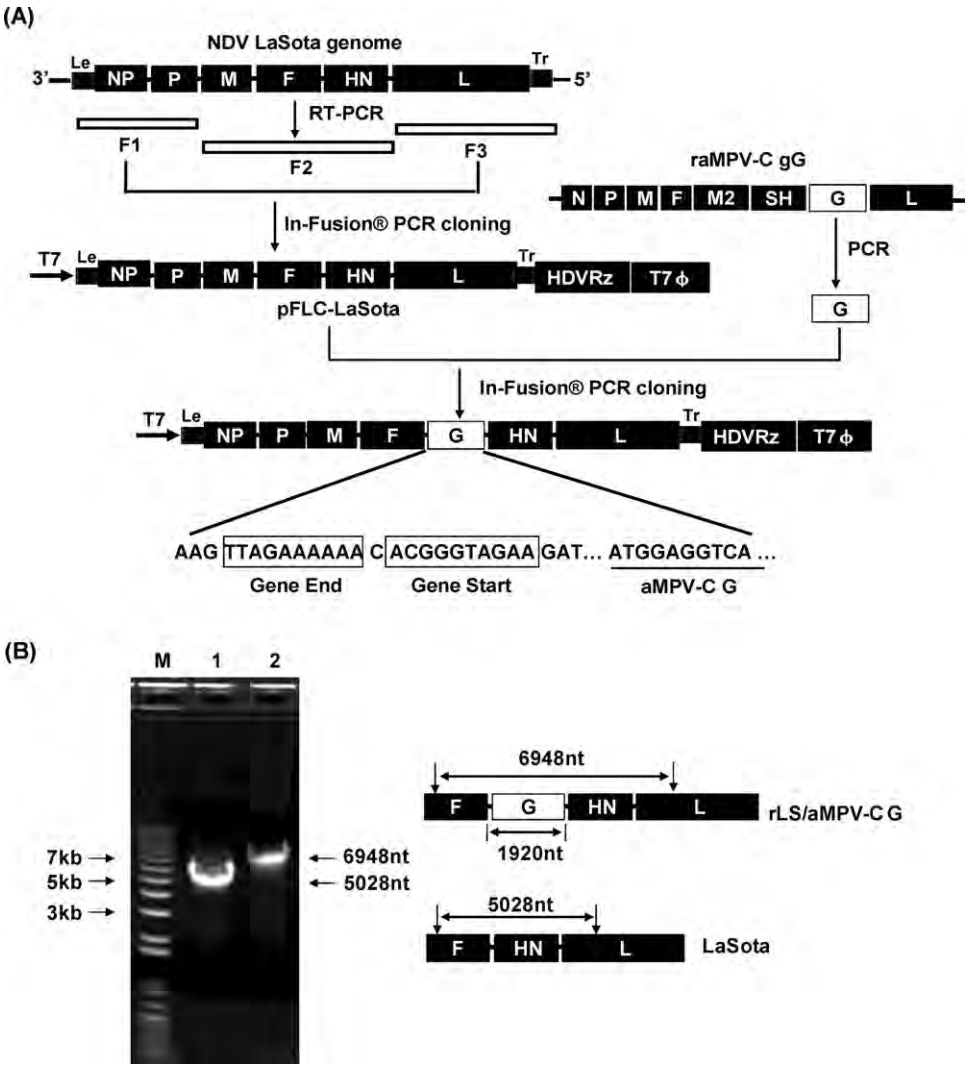

Fig. 1. Schematic representation of recombinant LaSota/aMPV-C G cDNA clone construction and detection of the rescued rLS/aMPV-C G virus. (A) Three cDNA fragments, marked by F1, F2, and F3, were generated by RT-PCR from NDV LaSota genomic RNA. These cDNA fragments were sequentially cloned and assembled into a modified pBluescript vector using In-Fusion® PCR cloning kit (Invitrogen). The open reading frame of the aMPV-C G gene, amplified from the raMPV-C gG infectious clone, was cloned into the intergenic region between the F and HN genes in the LaSota full-length clone as an additional transcription unit. The NDV Gene Start and Gene End signal sequences and the aMPV-C G sequences are boxed or underlined. The direction of the T7 promoter is indicated by a bold black arrow. HDV Rz and T7Φ represent the site of the hepatitis delta virus ribozyme and the T7 terminator sequences, respectively. (B) RT-PCR products that span the foreign gene insertion site were generated from the rescued rLS/aMPV-C G virus or LaSota viral RNA with a pair of primers, LS-F2 F and LS-F2 R, and were analyzed by agarose gel electrophoresis. Lane M: 1 kb DNA marker; lane 1: RT-PCR product from LaSota; lane 2: RT-PCR product from rLS/aMPV-C G.

(Fisher Scientific, Pittsburgh, PA) for 15 min at room temperature, followed by adding 0.5% Triton X-100 (Sigma, St. Louis, MO) to permeabilize the cells at room temperature for 10 min. The permeabilized cells were blocked with 5% goat serum (SouthernBiotech, Birmingham, AL) for 30 min at 37 °C. After blocking, the cells were incubated with chicken anti-aMPV-C serum (a gift of Dr. Lizhong Luo from Canadian Food Inspection Agency, Canada) and/or mouse anti-NDV HN monoclonal antibody (Mab, a gift of Dr. Ron Iorio from University of Massachusetts Medical School, USA), then with Fluorescein (FITC) conjugated goat anti-chicken IgG (H+L) (SouthernBiotech) and/or Alexa Fluor® 568 labeled goat anti-mouse IgG (H+L) (Invitrogen) for 30 min for each incubation at 37 °C. The cells were washed three times with PBS after each treatment. Finally, the cells were mounted with Fluoromount-G (SouthernBiotech). Fluorescence was examined and digitally photographed using an inverted fluorescence microscope at 100× magnifications with a matching wavelength filter for FITC or Alexa Fluor® 568 (Nikon, Eclipse T*i*, Melville, NY).

2.8. Immunization and challenge experiments

Two animal experiments were performed to evaluate rLS/aMPV-C G as a bivalent vaccine in SPF turkeys, which were obtained from the SEPRL facility. Turkeys were housed in Horsfal isolators (Federal Designs, Inc., Comer, GA) with *ad libitum* access to feed and water. In experiment 1, turkeys were vaccinated with one dose of the vaccine candidate and challenged with the virulent aMPV-CO Tr or NDV/CA02 virus. Because the velogenic NDV/CA02 strain is a BSL-3 pathogen, experiment 1 was carried out in a BLS-3E animal facility. In experiment 2, turkeys were vaccinated twice at an interval of 14 days and challenged with the virulent aMPV-CO Tr only, thus it was performed in a BSL-2 animal facility. Typical clinical signs of the aMPV disease, nasal exudates when squeezed (score 1), nasal discharge (score 2), and/or frothy eyes (score 3), were assessed everyday for both experiments using the scoring system of Cook et al. [39]. The clinical sign scores after challenge, between each vaccine treatment for each experiment and between each experiment for rLS/aMPV-C G vaccine treatment, were statistically

analyzed using two-factor ANOVA with a 1% level of significance (Microsoft Excel).

Experiment 1. Sixty one-week-old SPF turkey poults were randomly divided into six groups of 10 birds. Each bird in groups 1 and 2 was inoculated with 100 μl PBS via intranasal (IN) and intraocular (IO) routes as controls. Birds in groups 3 and 4 were vaccinated with 100 μl of rLS/aMPV-C G (1.0×10^7 $TCID_{50}$/ml), and birds in groups 5 and 6 were vaccinated with 100 μl of LaSota strain (1.0×10^7 $TCID_{50}$/ml) per bird via IN/IO routes. At 14 days post-vaccination (DPV), blood sample was collected from each bird for detection of serum antibody responses. Immediately after blood collection, the birds in groups 1, 3, and 5 were challenged with 100 μl of virulent aMPV-CO Tr (4.2×10^4 ID_{50}/ml) via IN/IO routes, and birds in groups 2, 4, and 6 were challenged with the velogenic NDV/CA02 virus in a dose of 10^5 EID_{50}/bird via IN/IO routes as described elsewhere [40]. The aMPV-CO Tr-challenged birds were monitored daily for scoring clinical signs of aMPV disease for 14 days. Tracheal swabs were collected from each of the aMPV-CO Tr-challenged birds at 3, 5, and 7 days post-challenge (DPC) for detection of virus shedding as described below. Mortality of the NDV/CA02-challenged birds was monitored and recorded daily for two weeks.

Experiment 2. Twenty one-day-old SPF turkeys were randomly divided into two groups of 10 birds. Each bird in group 1 was vaccinated with 100 μl of rLS/aMPV-C G (1.0×10^7 $TCID_{50}$/ml), and birds in group 2 were vaccinated with 100 μl of LaSota strain (1.0×10^7 $TCID_{50}$/ml) per bird via IN/IO. At 14 DPV, birds were inoculated with the same dose of the corresponding vaccine via IN/IO routes as a boost of vaccination. At day 14 post-boost (28 days after the first vaccination), the birds were challenged with 100 μl of virulent aMPV-CO Tr (4.2×10^4 ID_{50}/ml) via IN/IO routes. Immediately before boost and challenge, blood sample was taken from each bird for detection of antibody responses. After challenge, the birds were monitored daily for recording clinical scores and tracheal swabs were collected at 3, 5, and 7 DPC for detection of virus shedding as described in experiment 1.

2.9. Serological analysis

The aMPV-C-specific antibody response in turkeys after vaccination or boost was determined by an enzyme-linked immunosorbent assay (ELISA) as described previously [34]. A standard negative serum pool, collected from turkeys inoculated with PBS, was included in each plate of the ELISA test as a negative control. Sera were deemed positive when the mean chemiluminescence relative light unit (RLU) value was greater than the mean RLU plus 2× standard deviation of the three dilutions (1:100–1:400) of the negative turkey serum pool. The NDV-specific serum antibody response following immunization was determined by conducting the standard hemagglutination inhibition (HI) test [37] with the NDV LaSota virus as an antigen. The HI titers were expressed with the mean value of $\log_2$ plus a standard deviation for each of turkey groups.

2.10. Detection of aMPV-C viral RNA shedding after challenge

Virus replication or viral RNA shedding in the turkey tracheal tissues following the challenge with aMPV-C CO Tr was detected by RT-PCR with a pair of aMPV-C N gene-specific primers as described previously [34,41]. Briefly, the tracheal swabs in the brain heart infusion (BHI) medium were treated by one-round of freeze-thawing and vortexing. Fifty microliters of the tracheal swab medium were used for RNA isolation as described above. Ten microliters of serial 10-fold dilutions of the isolated RNA was used to detect the presence of aMPV-C viral RNA by RT-PCR using a Superscript™ one-step RT-PCR kit (Invitrogen) and the N-gene-specific primers. The RT-PCR amplified products were analyzed and visualized by agarose gel electrophoresis.

3. Results

3.1. Generation of the rLS/aMPV-C G virus

A full-length cDNA clone (FLC) encoding the complete antisense genome of the NDV vaccine LaSota strain was constructed through three steps of RT-PCR and In-Fusion PCR cloning (Fig. 1A). The aMPV-C G gene ORF together with the NDV transcriptional signals derived from the M–F gene junction region were inserted into the F gene end non-coding region in the LaSota FLC as an additional transcription unit (Fig. 1A), resulting in a LaSota/aMPV-C G recombinant cDNA clone, named pLS/aMPV-C G. This added transcription-unit cassette consists of 1758 nucleotides (nts) for the aMPV-C G ORF (coding for 585 amino acids) and 162 nts for the NDV GE and GS signals and spacer sequences. The total length of the recombinant LaSota/aMPV-C G clone is 17,106 nts and is divisible by 6, which abides by the "Rule of Six" that is critical for efficient replication of the virus genome [42]. After co-transfection of the pLS/aMPV-C G clone and the supporting plasmids in HEp-2 cells and subsequent amplification in SPF chicken embryonated eggs as described previously [36], a LaSota recombinant virus vectoring the aMPV-C G gene was rescued and propagated. The addition of the foreign gene in the LaSota vector was demonstrated by comparing the sizes of RT-PCR products generated from the recombinant and parental viruses (Fig. 1B). The fidelity of the rescued rLS/aMPV-C G virus was confirmed by sequence analysis of the RT-PCR products from the viral genome (data not shown).

3.2. Biological characterization of the rLS/aMPV-C G virus

To determine if the addition of the aMPV-C G affects the virus pathogenicity and growth dynamics, the rLS/aMPV-C G virus was examined *in vitro* and *in vivo* by conducting the MDT and ICPI tests and several titration assays. As shown in Table 2, the recombinant virus appeared to be slightly attenuated in embryonated eggs and day-old chickens with a significantly longer MDT (>150 h, $p < 0.01$) and a lower ICPI (0.0) than the parental LaSota strain. However, the titers of the recombinant virus grown in embryonated eggs or in DF-1 cells, measured by EID_{50}, $TCID_{50}$ and HA, were reduced by 50% but were comparable to the titers of the parental LaSota strain (Table 2). In addition, cytopathic effects induced by the rLS/aMPV-C G virus infection were indistinguishable from those seen with the parental LaSota virus in infected DF-1 cells (Fig. 2). Finally, no significant difference in the growth kinetics between the rLS/aMPV-C G and the parental LaSota viruses was detected (Fig. 3).

3.3. Expression of the aMPV-C G protein by rLS/aMPV-C G

The expression of the aMPV-C G protein in DF-1 cells infected with the rLS/aMPV-C G virus was examined by IFA using chicken anti-aMPV-C serum and the FITC-labeled goat anti-chicken IgG. To pinpoint the location of the G expression relevant to the recombinant virus infection, the NDV HN protein in the rLS/aMPV-C G-infected DF-1 cells was also detected by IFA using the mouse anti-NDV HN monoclonal antibody (Mab) and Alexa Fluor® 568 conjugated goat anti-mouse IgG. As shown in Fig. 4, aMPV-CO-infected cells (Fig. 4A, 3) but not NDV LaSota-infected cells (Fig. 4A, 1) were positively stained with the chicken anti-aMPV-C serum. Likewise, only LaSota-infected cells (Fig. 4A, 2) but not aMPV-CO-infected cells (Fig. 4A, 4) were stained with anti-NDV HN Mab, demonstrating the specificity of the antibodies and conjugates. When examining the rLS/aMPV-C G infected DF-1 cells by IFA with a mixture of the anti-aMPV-C and anti-NDV HN antibodies and then stained with a mixture of the FITC- and Alexa-conjugates, both green (Fig. 4B, 1) and red (Fig. 4B, 2) fluorescence was observed by fluorescence microscopys. After merging both fluorescent images, green and red fluorescence co-localized to the same cells (Fig. 4B,

Table 2
Biological assessments of the NDV recombinant virus.

Virus	MDT[a]	ICPI[b]	HA[c]	EID_{50}[d]	$TCID_{50}$[e]
LaSota	110 h	0.15	1024	6.8×10^8	3.5×10^7
rLS/aMPV-C G	>150 h	0	512	3.2×10^8	1.8×10^7

[a] Mean death time assay in embryonated eggs.
[b] Intracerebral pathogenicity index assay in day-old chickens.
[c] Hemagglutination assay.
[d] The 50% egg infective dose assay in embryonated eggs.
[e] The 50% tissue infectious dose assay on DF-1 cells.

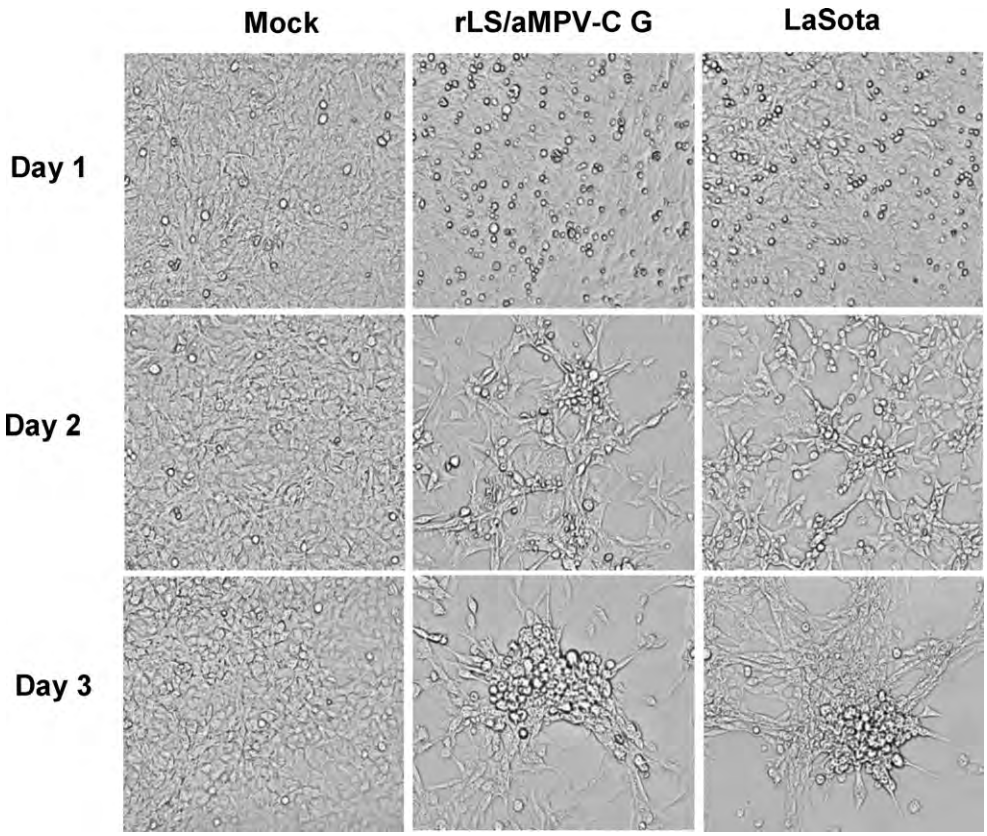

Fig. 2. Cytopathic effects induced by the recombinant virus. Monolayers of DF-1 cells were infected with rLS/aMPV-C G, or LaSota virus at 0.01 MOI. Mock infection was included as a control. At days 1, 2, and 3 post-infection, infected cells were digitally photographed using an inverted microscope at 100× magnifications (Nikon, Eclipse, *Ti*, Melville, NY).

4) and corresponded to viral CPE observed in the same field of the infected cells (Fig. 4B, 3). This result confirms that the aMPV-C G protein is co-expressed with the NDV HN protein of the recombinant virus in the infected cells.

3.4. Immune response and protection against virulent aMPV-C challenge

To examine if the rLS/aMPV-C G virus induced protective immunity in turkeys against virulent aMPV-C challenge, two animal experiments were carried out with either one- or two-dose immunization scheme. After the initial vaccination and the boost with the recombinant virus, the turkey poults appeared healthy without any signs of vaccine side-effects. Turkey sera collected after vaccination or boost were analyzed for aMPV-C-specific antibody by ELISA, as shown in Table 3. Four out of ten rLS/aMPV-C G vaccinated birds seroconverted and developed an antibody response to aMPV-C following the first vaccination and five out of ten birds seroconverted after the booster. No aMPV-C-specific antibodies were detected by

Table 3
Serum antibody response against aMPV-C following vaccination and aMPV-C virus shedding in trachea following challenge.

Experiment	Viruses	Positive Ab sera by ELISA (# of birds)		Viral RNA shedding (# of birds)		
		14 DPV[a]	28 DPV	3 DPC[b]	5 DPC	7 DPC
1	LaSota	0/10	–	10/10	10/10	8/10
	rLS/aMPV-C G	4/10	–	10/10	9/10	7/10
2	LaSota	0/10	0/10	10/10	10/10	10/10
	rLS/aMPV-C G	4/10	5/10	10/10	10/10	8/10

–, not measured.
[a] Days post-vaccination.
[b] Days post-challenge.

Table 4
Clinical signs of disease observed in turkeys at different days post-challenge.

Experiment	Viruses	Number of birds showing clinical sign/number in group on given day									
		1	2	3	4	5	6	7	8	9	10
1	LaSota	0/10	0/10	8/10	8/10	10/10	8/10	7/10	2/10	1/10	0/10
	rLS/aMPV-C G	0/10	0/10	1/10	6/10	7/10	6/10	6/10	1/10	0/10	0/10
2	LaSota	0/10	0/10	8/10	10/10	10/10	8/10	7/10	3/10	0/10	0/10
	rLS/aMPV-C G	0/10	0/10	0/10	5/10	5/10	6/10	1/10	1/10	0/10	0/10

Table 5
Serum antibody response against NDV following vaccination and survival of turkeys after challenge with a lethal dose of NDV/CA02.

Experiment 1	Antibody response		Survivors
	Seropositive birds	HI titer[a]	
PBS	0/10	0	0/10
LaSota	10/10	3.5 ± 0.8	10/10
rLS/aMPV-C G	10/10	3.2 ± 1.7	10/10

[a] Hemagglutination inhibition (HI) titer was expressed in $\log_2$ of the mean ± standard deviation.

the ELISA from turkeys in the LaSota vaccine control group after either initial or boost vaccination.

After challenge with the virulent aMPV-CO Tr virus, the turkeys were examined daily in two experiments and clinical signs were scored. From 3 DPC, most, if not all, turkey poults in the LaSota vaccine control group exhibited typical clinical signs of the disease, showing nasal exudates when squeezed (score 1), nasal discharge (score 2), and/or frothy eyes (score 3) (Fig. 5 and Table 4). The infected birds showed peak clinical signs between 6 and 7 DPC and gradually decreased in severity thereafter. Turkeys vaccinated with the rLS/aMPV-C G virus in both experiments resulted in significantly less severe clinical signs than those in the LaSota vaccine group (Fig. 5, $p < 0.01$). While 50–70% of the rLS/aMPV-C G vaccinated birds had nasal exudates when squeezed, this mild clinical sign of the disease appeared only between 4 and 7 DPC (Table 4). In addition, no significant difference was seen between the one-dose (E1) or two-dose (E2) rLS/aMPV-C G vaccination (Fig. 5).

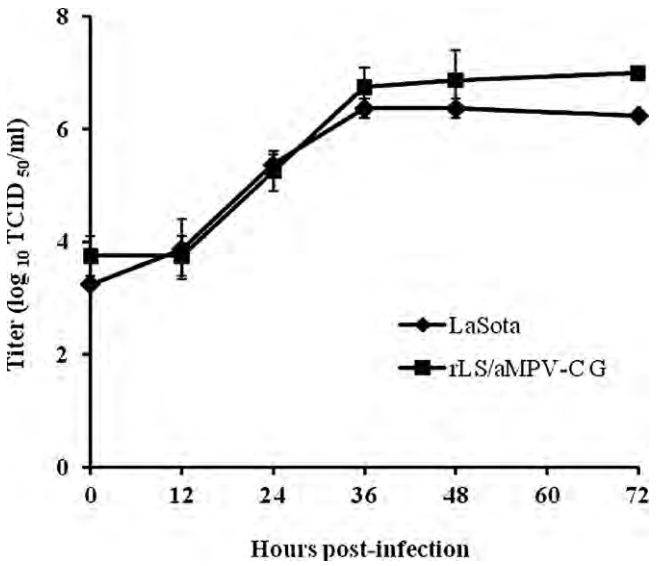

Fig. 3. Growth dynamics of the recombinant virus. DF-1 cells were infected with rLS/aMPV-C G or LaSota strain at 0.01 MOI. Every 12 h post-infection, the cells were harvested. Virus titers at each time point, in duplicate, were determined by $TCID_{50}$ titration in DF-1 cells. The mean titer of the two tests at each time point is expressed in $\log_{10}$ $TCID_{50}$/ml with error bars. No significant difference was seen between each virus.

Viral RNA shedding, or the presence of the challenge virus in the tracheal lumen, was detected in 100% of LaSota vaccinated birds in both experiments at 3, 5, and 7 DPC, with the exception of two birds at 7 DPC in experiment 1 (Table 3). Viral shedding of the challenge virus was somewhat less in the rLS/aMPV-C G vaccinated turkeys, specifically at 7 DPC when 30% and 20% of the birds were negative for viral RNA in experiments 1 and 2, respectively (Table 3).

3.5. *Immune response and protection against velogenic NDV challenge*

To evaluate protective efficacy conferred by rLS/aMPV-C G against Newcastle disease, groups of turkeys in experiment 1 were inoculated by IN/IO routes with the rLS/aMPV-C G virus, the LaSota vaccine, or PBS and challenged with a lethal dose of the NDV/CA02 virus at 14 DPV. All of the turkeys that had been immunized with the LaSota vaccine or rLS/aMPV-C G were completely protected against NDV challenge without showing any sign of disease (Table 5). In contrast, all of the birds in the unvaccinated control group (inoculated with PBS) displayed disease signs with conjunctivitis and severe depression from 2 to 4 DPC and 100% mortality at 5 DPC. The serum samples collected immediately before the challenge were analyzed for NDV-specific antibody response by HI assay. As shown in Table 5, immunization of turkeys with either the recombinant virus or the parental LaSota vaccine induced NDV-specific serum antibody responses.

4. Discussion

In the present study, we have successfully developed an NDV-based, LaSota strain, live vector expressing the aMPV-C G protein as a bivalent vaccine candidate. The recombinant virus, rLS/aMPV-C G, was evaluated *in vitro* and *in vivo* for the safety, stability, and protective efficacy against virulent aMPV-C and NDV challenges. The recombinant virus was slightly attenuated in embryonated chicken eggs and young chickens compared to the parental LaSota strain (Table 2). This recombinant virus was stable and did not show any apparent biological changes in MDT and virus titers after 10 passages in SPF chicken embryos (data not shown). Vaccination of day-old turkeys with rLS/aMPV-C G via IN/IO routes at a higher dose than the recommended dose for the commercial LaSota vaccine did not cause any vaccine reactions (mild signs of respiratory disease), which may occur in young chickens when the commercial LaSota vaccine is administered [26,28]. These results demonstrated the safety, stability, and possibility of application of this recombinant vaccine candidate in young turkeys, which is the most vulnerable population for NDV and aMPV diseases [1,26,43].

Attenuation in recombinant NDV replication associated with the addition of a foreign gene seems common, and it has been reported by several researchers [31,44,45]. Based on the well-accepted paramyxovirus replication mechanism [46], attenuation of the rLS/aMPV-C G virus can be attributed to the combination of the increase in genome length (1920 nts, approximately 13% of the genome) and the addition of the aMPV-C G gene transcription

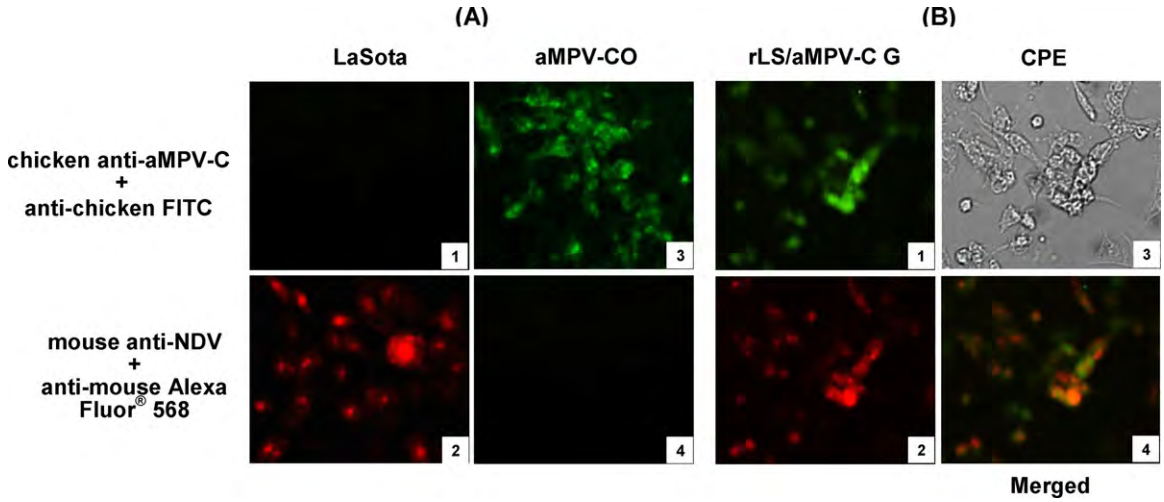

Fig. 4. Detection of aMPV-C G protein expression by IFA. (A) DF-1 cells were infected with LaSota (A, 1 and 2) at 0.01 MOI or aMPV-CO (A, 3 and 4) at 0.1 MOI. At 24 h post-infection, the infected cells were fixed and treated with chicken anti-aMPV-C (A, 1 and 3) or mouse anti-NDV HN Mab (A, 2 and 4), followed by staining with anti-chicken IgG FITC (A, 1 and 3) or anti-mouse IgG Alexa Fluor® 568 conjugates (A, 2 and 4). The fluorescence of the infected cells was examined and digitally photographed using an inverted fluorescence microscope at 100× magnifications under UV light with a matching wavelength filter for FITC or Alexa Fluor® 568 (Nikon, Eclipse, *Ti*, Melville, NY). (B) DF-1 cells were infected with rLS/aMPV-C G (B, 1–4) at 0.01 MOI. At 24 h post-infection, the infected cells were fixed and treated with a mixture of chicken anti-aMPV-C and mouse anti-NDV Mab followed by staining with a mixture of FITC and Alexa Fluor® 568 conjugated antibodies. The fluorescence of the infected cells was examined and digitally photographed as described above. The green and red fluorescent images (B, 1 and 2) taken from the same field of rLS/aMPV-C G-infected cells were merged (B, 4). Viral CPE induced by rLS/aMPV-C G infection in the same field of the fluorescent images was digitally photographed (B, 3) using the same inverted microscope at 100× magnifications under regular light. (For interpretation of the references to color in this figure legend, the reader is referred to the web version of this article.)

unit, which would attenuate transcription of the down-stream HN and L genes of NDV and consequently decrease virus replication efficiency in the host. Despite the attenuation *in vivo*, the recombinant virus maintained similar growth dynamics and virus titers in cultured cells and embryonated eggs compared to the parental LaSota vaccine. This combined feature of slight attenuation of pathogenicity *in vivo* and little change in growth ability *in vitro* would make this recombinant virus a desirable bivalent vaccine vector.

The G protein of aMPV is thought to be responsible for attachment of the virus particles to the host cell surface receptors to initiate infection. However, recent studies with genetically manipulated aMPV mutants have shown that aMPV lacking the G gene is still able to grow in cell cultures and in turkeys [24,47,48], indicating that the G protein is not the sole viral protein mediating the attachment during infection and an alternate viral protein may play a role of attachment during infection. The G deletion or truncation mutants of aMPV-C were attenuated in SPF turkeys and induced a weaker immune response than the wild-type virus [34,47], implying that the G protein ought to play a role in immunogenicity in the natural host. Thus, we selected the G protein to be expressed by the recombinant NDV LaSota vector to investigate the role of the G protein in inducing protective immunity against aMPV-C challenge as well as the protective efficacy conferred by the NDV vector against NDV challenge in turkeys.

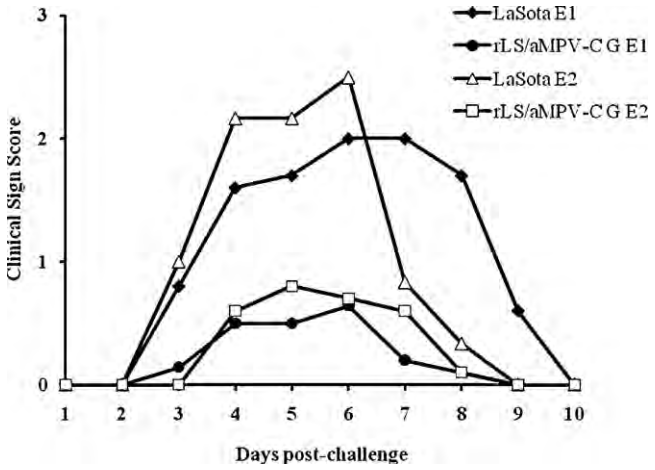

Fig. 5. Mean clinical sign scores of turkeys after challenge with aMPV-CO Tr in two experiments. Turkey poults were vaccinated with rLS/aMPV-C G or LaSota strain once in experiment 1 (E1) or twice in experiment 2 (E2) at an interval of 14 days and then challenged with the virulent aMPV-CO Tr virus. The birds were examined daily for clinical signs and the mean from each group of birds in both experiments were plotted. Significant reductions in clinical signs were seen in the rLS/aMPV-C G virus compared to the LaSota virus in each experiment ($p < 0.01$) however, no significant difference was seen between the one-dose (E1) or two-dose (E2) rLS/aMPV-C G vaccinations.

Our results showed that about 40% of turkeys vaccinated with rLS/aMPV-C G in both animal experiments had a detectable aMPV-C-specific serum antibody response at 14 DPV. After challenge with pathogenic aMPV-C, the recombinant virus-vaccinated turkeys showed milder clinical signs than the birds in the LaSota vaccine control group. In addition, most turkeys vaccinated with either rLS/aMPV-C G or LaSota shed the challenge virus back into the tracheal lumen indicating virus replication, which should not occur following proper vaccination. All turkeys vaccinated with one dose of either rLS/aMPV-C G or LaSota vaccine had comparable levels of NDV-specific HI antibody response and survived the lethal dose NDV challenge without any sign of disease. The booster administration of the recombinant vaccine in experiment 2 did not significantly enhance the aMPV-C antibody response and protective efficacy against challenge. This is somewhat unexpected because the booster immunization in birds with either the recombinant virus or the LaSota vaccine increased the NDV-specific HI titers about 2 $\log_2$ (data not shown).

The moderate percentage of seroconversion, the presence of challenge virus in the trachea, and the partial protection conferred by the recombinant virus suggest that the aMPV-C G protein is either a weak immunogen or insufficiently expressed by the NDV vector during infection. Our immunofluorescence assay data showed that an equivalent amount of the aMPV G and NDV HN proteins was expressed in the recombinant virus-infected DF-1 cells with similar levels of green and red fluorescence and their

co-localization (Fig. 4). We anticipated that a similar level of the G and HN production would occur in turkeys as well, although the possibility of a lower level of G expression in turkeys cannot be ruled out.

Immunogenicity of several major structural proteins of aMPV has been investigated by using different approaches. Immunization of turkeys with the N or M protein subunit vaccine induced an anti-aMPV-C antibody response and partially protected birds against challenge [19]. A DNA vaccine expressing the N gene could not induce neutralization antibody response and, therefore, could not provide protection against challenge [22]. Whereas, DNA vaccination with the F gene was able to prime the induction of the humoral immune response and provided a partial protection against challenge [22,49]. This result is in agreement with the previous finding that the immune response against the F protein expressed by a fowlpox recombinant virus contributed to the protection of vaccinated turkeys against aMPV-A disease [25]. Our data presented here on the G protein, inducing partial protective immunity, together with the findings by others on immunogenicity of individual aMPV structural proteins, demonstrates that a single aMPV protein would unlikely induce immune response that could provide a complete protection against aMPV disease. It is reasonable to speculate that, co-expression of two or more major structural proteins of the virus, i.e. the F, G and/or M proteins, perhaps by the NDV vector may be able to induce an enhanced protective immunity against aMPV infection.

In summary, in the present study we successfully generated an NDV/aMPV-C G recombinant virus and described the role of the aMPV-C G protein in the induction of protective immunity in turkeys for the first time. Biological characterization of the rLS/aMPV-C G virus showed that it was slightly attenuated in chicken embryos and young chickens, but maintained similar growth kinetics and virus titers in cultured cells. Turkeys vaccinated with rLS/aMPV-C G were completely protected against velogenic NDV challenge and partially protected against pathogenic aMPV-C challenge. The results suggest that the LaSota strain-based recombinant virus is a safe and effective vaccine vector. The aMPV-C G protein is a weak antigen and other immunogenic components of the virus, most likely the F protein, may need to be added into the recombinant LaSota vaccine vector in the future to improve the bivalent vaccine protective efficacy against aMPV-C infection. Finally, we are currently assessing the potential application of expressing the aMPV-A or B G gene in bivalent vaccines since the aMPV subgroups vary in distribution, antigenicity, and pathogenesis.

Acknowledgements

The authors wish to thank Xiuqin Xia and Fenglan Li for excellent technical assistance, Melissa Scott and Joyce Bennett for performing the automated nucleotide sequencing, and Lizhong Luo and Ron Iorio for a gift of chicken anti-aMPV-C serum and anti-NDV HN monoclonal antibody, respectively. This research was supported by USDA, ARS CRIS project 6612-32000-056-00D.

References

[1] Gough RE, Jones RC. Avian metapneumovirus. In: Saif YM, Fadly AM, Glisson JR, McDougald LR, Nolan LK, Swayne DE, editors. Diseases of poultry. 12th ed. Ames, IA, USA: Blackwell Publishing; 2008. p. 100–10.
[2] Cook JK. Avian pneumovirus infections of turkeys and chickens. Vet J 2000;160(2):118–25.
[3] Cook JK, Chesher J, Orthel F, Woods MA, Orbell SJ, Baxendale W, et al. Avian pneumovirus infection of laying hens: experimental studies. Avian Pathol 2000;29(6):545–56.
[4] Jones RC, Williams RA, Baxter-Jones C, Savage CE, Wilding GP. Experimental infection of laying turkeys with rhinotracheitis virus: distribution of virus in the tissue and serological response. Avian Pathol 1988;17:841–50.
[5] Cook JK, Ellis MM, Huggins MB. The pathogenesis of turkey rhinotracheitis virus in turkey poults inoculated with the virus alone or together with two strains of bacteria. Avian Pathol 1991;20(1):155–66.
[6] Lee E, Song MS, Shin JY, Lee YM, Kim CJ, Lee YS, et al. Genetic characterization of avian metapneumovirus subtype C isolated from pheasants in a live bird market. Virus Res 2007;128(1–2):18–25.
[7] Toquin D, Guionie O, Jestin V, Zwingelstein F, Allee C, Eterradossi N. European and American subgroup C isolates of avian metapneumovirus belong to different genetic lineages. Virus Genes 2006;32(1):97–103.
[8] Bayon-Auboyer MH, Arnauld C, Toquin D, Eterradossi N. Nucleotide sequences of the F, L and G protein genes of two non-A/non-B avian pneumoviruses (APV) reveal a novel APV subgroup. J Gen Virol 2000;81(Pt 11):2723–33.
[9] Cook JK, Orthel F, Orbell S, Woods MA, Huggins MB. An experimental turkey rhinotracheitis (TRT) infection in breeding turkeys and the prevention of its clinical effects using live-attenuated and inactivated TRT vaccines. Avian Pathol 1996;25(2):231–43.
[10] Ganapathy K, Bufton A, Pearson A, Lemiere S, Jones RC. Vaccination of commercial broiler chicks against avian metapneumovirus infection: a comparison of drinking-water, spray and oculo-oral delivery methods. Vaccine 2010;28(23):3944–8.
[11] Jones RC. Viral respiratory diseases (ILT, aMPV infections, IB): are they ever under control? Br Poult Sci 2010;51(1):1–11.
[12] Catelli E, Cecchinato M, Savage CE, Jones RC, Naylor CJ. Demonstration of loss of attenuation and extended field persistence of a live avian metapneumovirus vaccine. Vaccine 2006;24(42–43):6476–82.
[13] Catelli E, Lupini C, Cecchinato M, Ricchizzi E, Brown PA, Naylor CJ. Field avian metapneumovirus evolution avoiding vaccine induced immunity. Vaccine 2010;28(4):916–21.
[14] Cecchinato M, Catelli E, Lupini C, Ricchizzi E, Clubbe J, Battilani M, et al. Avian metapneumovirus (AMPV) attachment protein involvement in probable virus evolution concurrent with mass live vaccine introduction. Vet Microbiol 2010;146(1–2):24–34.
[15] Brown PA, Lupini C, Catelli E, Clubbe J, Ricchizzi E, Naylor CJ. A single polymerase (L) mutation in avian metapneumovirus increased virulence and partially maintained virus viability at an elevated temperature. J Gen Virol 2011;92(Pt 2):346–54.
[16] Chacon JL, Mizuma M, Vejarano MP, Toquin D, Eterradossi N, Patnayak DP, et al. Avian metapneumovirus subtypes circulating in Brazilian vaccinated and nonvaccinated chicken and turkey farms. Avian Dis 2011;55(1):82–9.
[17] Patnayak DP, Sheikh AM, Gulati BR, Goyal SM. Experimental and field evaluation of a live vaccine against avian pneumovirus. Avian Pathol 2002;31(4):377–82.
[18] Cha RM, Khatri M, Sharma JM. Protection against avian metapneumovirus subtype C in turkeys immunized via the respiratory tract with inactivated virus. Vaccine 2011;29(3):459–65.
[19] Chary P, Njenga MK, Sharma JM. Protection by recombinant viral proteins against a respiratory challenge with virulent avian metapneumovirus. Vet Immunol Immunopathol 2005;108(3–4):427–32.
[20] Kapczynski DR. Development of a virosome vaccine for protection in turkeys against avian metapneumovirus subtype C. Avian Dis 2004;48(3):332–43.
[21] Kapczynski DR, Perkins LL, Sellers HS. Mucosal vaccination with formalin-inactivated avian metapneumovirus subtype C does not protect turkeys following intranasal challenge. Avian Dis 2008;52(1):28–33.
[22] Kapczynski DR, Sellers HS. Immunization of turkeys with a DNA vaccine expressing either the F or N gene of avian metapneumovirus. Avian Dis 2003;47(4):1376–83.
[23] Naylor CJ, Ling R, Edworthy N, Savage CE, Easton AJ. Avian metapneumovirus SH gene end and G protein mutations influence the level of protection of live-vaccine candidates. J Gen Virol 2007;88(Pt 6):1767–75.
[24] Naylor CJ, Lupini C, Brown PA. Charged amino acids in the AMPV fusion protein have more influence on induced protection than deletion of the SH or G genes. Vaccine 2010;28(41):6800–7.
[25] Qingzhong Y, Barrett T, Brown TD, Cook JK, Green P, Skinner MA, et al. Protection against turkey rhinotracheitis pneumovirus (TRTV) induced by a fowlpox virus recombinant expressing the TRTV fusion glycoprotein (F). Vaccine 1994;12(6):569–73.
[26] Alexander DJ, Senne DA. Newcastle disease, other avian paramyxoviruses, and pneumovirus infections. In: Saif YM, Fadly AM, Glisson JR, McDougald LR, Nolan LK, Swayne DE, editors. Diseases of poultry. 12th ed. Ames, IA, USA: Blackwell Publishing; 2008. p. 75–100.
[27] Pedersen JC, Senne DA, Woolcock PR, Kinde H, King DJ, Wise MG, et al. Phylogenetic relationships among virulent Newcastle disease virus isolates from the 2002–2003 outbreak in California and other recent outbreaks in North America. J Clin Microbiol 2004;42(5):2329–34.
[28] Hitchner SB. History of biological control of poultry diseases in the USA. Avian Dis 2004;48(1):1–8.
[29] Ge J, Deng G, Wen Z, Tian G, Wang Y, Shi J, et al. Newcastle disease virus-based live attenuated vaccine completely protects chickens and mice from lethal challenge of homologous and heterologous H5N1 avian influenza viruses. J Virol 2007;81(1):150–8.
[30] Huang Z, Elankumaran S, Yunus AS, Samal SK. A recombinant Newcastle disease virus (NDV) expressing VP2 protein of infectious bursal disease virus (IBDV) protects against NDV and IBDV. J Virol 2004;78(18):10054–63.
[31] Nayak B, Rout SN, Kumar S, Khalil MS, Fouda MM, Ahmed LE, et al. Immunization of chickens with Newcastle disease virus expressing H5 hemagglutinin

protects against highly pathogenic H5N1 avian influenza viruses. PLoS One 2009;4(8):e6509.
[32] Park MS, Steel J, Garcia-Sastre A, Swayne D, Palese P. Engineered viral vaccine constructs with dual specificity: avian influenza and Newcastle disease. Proc Natl Acad Sci USA 2006;103(21):8203–8.
[33] Veits J, Wiesner D, Fuchs W, Hoffmann B, Granzow H, Starick E, et al. Newcastle disease virus expressing H5 hemagglutinin gene protects chickens against Newcastle disease and avian influenza. Proc Natl Acad Sci USA 2006;103(21):8197–202.
[34] Yu Q, Estevez CN, Song M, Kapczynski DR, Zsak L. Generation and biological assessment of recombinant avian metapneumovirus subgroup C (aMPV-C) viruses containing different length of the G gene. Virus Res 2010;147(2):182–8.
[35] Wyatt LS, Moss B, Rozenblatt S. Replication-deficient vaccinia virus encoding bacteriophage T7 RNA polymerase for transient gene expression in mammalian cells. Virology 1995;210(1):202–5.
[36] Estevez CN, King DJ, Seal B, Yu Q. Evaluation of Newcastle disease virus chimeras expressing the hemagglutinin-neuraminidase protein of velogenic strains in the context of a mesogenic recombinant virus backbone. Virus Res 2007;129(2):182–90.
[37] Alexander DJ. Newcastle disease virus and other avian paramyxoviruses. In: Swayne D, Glisson JR, Jackwood MW, Pearson JE, Reed WM, editors. A laboratory manual for the isolation and identification of avian pathogens. 4th ed. Kennett Square, PA: American Association of Avian Pathologists; 1998.
[38] Reed LJ, Muench H. A simple method for estimating fifty percent endpoints. Am J Hyg 1938;27:493–7.
[39] Cook JK, Ellis MM, Dolby CA, Holmes HC, Finney PM, Huggins MB. A live attenuated turkey rhinotracheitis virus vaccine: 1. Stability of the attenuated strain. Avian Pathol 1989;18:511–22.
[40] Kapczynski DR, King DJ. Protection of chickens against overt clinical disease and determination of viral shedding following vaccination with commercially available Newcastle disease virus vaccines upon challenge with highly virulent virus from the California 2002 exotic Newcastle disease outbreak. Vaccine 2005;23(26):3424–33.
[41] Yu Q, Estevez CN, Roth JP, Hu H, Zsak L. Deletion of the M2-2 gene from avian metapneumovirus subgroup C impairs virus replication and immunogenicity in Turkeys. Virus Genes 2011;42(3):339–46.
[42] Kolakofsky D, Roux L, Garcin D, Ruigrok RW. Paramyxovirus mRNA editing, the “rule of six” and error catastrophe: a hypothesis. J Gen Virol 2005;86(Pt 7):1869–77.
[43] Jones RC, Baxter-Jones C, Wilding GP, Kelly DF. Demonstration of a candidate virus for turkey rhinotracheitis in experimentally inoculated turkeys. Veter Rec 1986;119(24):599–600.
[44] Krishnamurthy S, Huang Z, Samal SK. Recovery of a virulent strain of Newcastle disease virus from cloned cDNA: expression of a foreign gene results in growth retardation and attenuation. Virology 2000;278(1):168–82.
[45] Zhao H, Peeters BP. Recombinant Newcastle disease virus as a viral vector: effect of genomic location of foreign gene on gene expression and virus replication. J Gen Virol 2003;84(Pt 4):781–8.
[46] Lamb RA, Parks GD. Paramyxoviridae: the viruses and their replication. In: Knipe DM, Howley PM, Griffin DE, Lamb RA, Martin MA, Roizman B, et al., editors. Fields virology. 5th ed. New York, NY: Lippincott Williams & Wilkins (a Wolters Kluwer Business); 2007. p. 1440–96.
[47] Govindarajan D, Kim SH, Samal SK. Contribution of the attachment G glycoprotein to pathogenicity and immunogenicity of avian metapneumovirus subgroup C. Avian Dis 2010;54(1):59–66.
[48] Ling R, Sinkovic S, Toquin D, Guionie O, Eterradossi N, Easton AJ. Deletion of the SH gene from avian metapneumovirus has a greater impact on virus production and immunogenicity in turkeys than deletion of the G gene or M2-2 open reading frame. J Gen Virol 2008;89(Pt 2):525–33.
[49] Tarpey I, Huggins MB, Davis PJ, Shilleto R, Orbell SJ, Cook JK. Cloning, expression and immunogenicity of the avian pneumovirus (Colorado isolate) F protein. Avian Pathol 2001;30(5):471–4.

Arch Virol (2011) 156:235–244
DOI 10.1007/s00705-010-0849-z

ORIGINAL ARTICLE

Molecular characterization of avian astroviruses

M. J. Pantin-Jackwood · K. O. Strother · E. Mundt · L. Zsak · J. M. Day · E. Spackman

Received: 28 August 2010 / Accepted: 21 October 2010 / Published online: 11 November 2010
© Springer-Verlag (outside the USA) 2010

Abstract Astroviruses are frequently associated with enteric diseases in poultry, being isolated from cases of runting-stunting syndrome (RSS) of broiler chickens, poult enteritis complex (PEC), and poult enteritis mortality syndrome (PEMS) of turkeys. Currently, five types of avian astrovirus have been identified: turkey astroviruses 1 and 2 (TAstV-1, TAstV-2), avian nephritis virus (ANV), chicken astrovirus (CAstV) and duck astrovirus (DAstV). The objective of this study was to molecularly characterize the different types of avian astroviruses circulating in commercial poultry. Sequence analysis of a region of ORF2, which encodes the capsid precursor protein associated with serotype and viral pathogenesis, revealed extensive variation in amino acid sequence within each subtype: TAstV-2 (81.5%-100%), ANV (69.9%-100%), and CAstV (85.3%-97.9%). However, this region was more conserved in TAstV-1's (96.2%-100%). Furthermore, a novel astrovirus was detected in chicken samples and found to be <64% similar to ANV and <30.6% similar to CAstV. The results of this study underline the great genetic variability of avian astroviruses and indicate that there are most likely multiple serotypes of each avian astrovirus circulating in commercial poultry.

M. J. Pantin-Jackwood (✉) · L. Zsak · J. M. Day · E. Spackman
Southeast Poultry Research Laboratory,
Agricultural Research Laboratory,
U.S. Department of Agriculture,
934 College Station Road, Athens, GA 30605, USA
e-mail: Mary.Pantin-Jackwood@ARS.USDA.gov

K. O. Strother
Louisiana Animal Disease Diagnostic Laboratory,
School of Veterinary Medicine, Louisiana State University,
1909 Skip Bertman Drive, Baton Rouge, LA, USA

E. Mundt
Department of Population Health,
College of Veterinary Medicine, University of Georgia,
953 College Station Road, Athens, GA, USA

Introduction

Astroviruses have been associated with enteric disease in humans and young animals such as calves, lambs, pigs, deer, mice, dogs, cats, and minks [28]. In avian hosts, astroviruses have been linked to enteritis and increased mortality in young turkeys, chickens and guinea fowl [4, 5, 15, 18–20, 25, 34, 37, 40, 45, 46, 54, 60], to nephritis in chickens [17, 23], and to fatal hepatitis in ducklings [11, 13].

The family *Astroviridae* is divided into two genera: *Mamastrovirus* (mammal astroviruses) and *Avastrovirus* (avian astroviruses). Within each genus, numerous groups have been described based on serotype and genetic differences [1]. Astroviruses are small, non-enveloped, single-stranded, positive-sense RNA viruses of 28-30 nm diameter and have a star-like morphology [24]. Their genome is 6.4-7.7 kb in length and has three open reading frames (ORFs) and a poly-A tail [11, 28]. ORF1a and ORF1b encode the non-structural proteins, and ORF2 encodes a capsid precursor protein [28]. The greatest sequence variability in the astrovirus genome is found in ORF2; however, a high degree of conservation of the N-terminal 415 amino acids of ORF2 has been shown for HAstVs and other mammalian astroviruses. The avian astroviruses vary considerably from the mamastroviruses, although the basic character of the ORF2 amino terminus is

also conserved [28]. Downstream of the conserved 415 residues, considerable sequence variability is seen among astroviruses isolated from different species and even among different serotypes from the same animal species. Based on structural predictions, the conserved amino-terminal half of the astrovirus capsid protein could play a role in assembly of the capsid core, whereas the hyper-variable carboxy-terminal region could form the spikes of the virion and participate in the early interactions of the virus with the cellular receptors on the host cell [28].

Enteric diseases cause substantial economic losses of commercial turkeys and broilers due to reduced weight gain, increased morbidity and mortality, poor condition of the flock, and increased production costs from poor feed conversions and increased use of therapeutic anti-microbial treatments. Three enteric disease syndromes have been described: runting-stunting syndrome of broilers (RSS), poult enteritis complex (PEC), and poult enteritis mortality syndrome (PEMS). These diseases are considered to be polymicrobial, and numerous viruses have been associated with them; however, no definitive cause has been identified. Astroviruses are among the most common viruses found in cases of PEC and PEMS [2, 3, 19, 21, 35, 36, 38, 39, 60]. Astroviruses have also been isolated from recent cases of RSS in broilers and have been associated previously with poor weight gain, enteric disease and kidney disease in chickens [4, 12, 21, 41–43, 53]. To date, five different astroviruses have been identified in avian species based on the species of origin and viral genome characteristics: two turkey-origin astroviruses (TAstV-1 and TAstV-2); two chicken-origin astroviruses, avian nephritis virus (ANV) and chicken astrovirus (CAstV); and a duck-origin astrovirus (DAstV). ANV has also been detected in commercial turkey poults [30], and TAstV-2 in guinea fowl [5]. Molecular characterization of these viruses has been done mostly by sequencing ORFs 1a and 1b. However, with the exception of TAstV-2 viruses [31, 47], little or no characterization has been done of the ORF2 or capsid gene.

The study of the capsid protein genes is important for understanding the relatedness of these viruses. Antigenic characterization of avian astroviruses has been limited by the difficulty in isolating and growing these viruses. Currently, two serotypes of ANV and two of TAstV-2 have been described [17, 50], but sequence data suggest that there may be many more [47]. There also appears to be more than one serotype of CAstV [31, 55]. No serological characterization of TAstV-1 isolates has been reported.

In this study, we sequenced new astrovirus isolates from chickens and turkeys and analyzed a region of the ORF2 (capsid proteins) of all available astroviruses detected in poultry.

Material and methods

Viruses

The viruses sequenced were obtained from the Southeast Poultry Research Laboratory (SEPRL) repository of intestinal contents collected from commercial turkeys and chickens throughout the United States between 2003 and 2007 [32, 33]. Specimens were from both healthy flocks and poorly performing flocks (Table 1). All samples were stored at -80°C until utilized for RNA extraction.

Viral RNA extraction and RT-PCR

Two-hundred microliters of intestinal contents was diluted in 1.2 ml of PBS, homogenized with sterile glass beads in a FastPrep homogenizer (Thermo-Savant, Inc., Waltham, MA) and centrifuged for 10 min at 800 × g. Total RNA was extracted directly from 250 µl of the supernatant using TRIzol LS reagent (Invitrogen Inc., Carlsbad, CA) according to the manufacturer's instructions. For the initial detection and characterization of the viruses, a segment of the polymerase gene (ORF1b) was amplified by standard RT-PCR using a QIAGEN OneStep RT-PCR Kit (QIAGEN Inc., Valencia, CA). The primers, which amplify all four avian astroviruses, have been reported previously [51]. Sequence data for the capsid gene (ORF2) were obtained by designing primers based on published sequence data from reference isolates of TAstV-1 (Y15936.2), TAstV-2 (AF206663.2), ANV-1(AB046864) and ANV-2(AB033 998.1). All primers were designed using the PrimerSelect program (DNASTAR, Madison, WI). Sequence data from the capsid gene was also obtained by RT-PCR using an oligo dT primer and specific primers directed toward the polymerase gene. The variation found in the capsid sequence among the astroviruses studied was so high that more than 96 sequencing primers had to be developed in order to obtain sequence data. Rarely could one set of primers be used on more than one astrovirus, even if it belonged to the same type. Amplifications were performed in a MJ Research DNA Thermal Cycler (Waltham, MA). The RT-PCR products were separated on an agarose gel by electrophoresis, and amplicons of the appropriate size were excised from the gel and extracted using a QIAquick Gel Extraction Kit (QIAGEN Inc.). Purified RT-PCR products were sequenced directly using a BigDye Terminator Kit (Applied Biosystems, Foster City, CA) run on an ABI 3730 sequencer (Applied Biosystems). Sequences were assembled and edited with LASERGENE 7.2 (DNASTAR) and then aligned to previously published astrovirus ORF2 sequences.

Table 1 Chicken and turkey astroviruses examined in this study

Isolate name	Flock condition	Age in days	Genotype	GenBank accession number
NC-TK-SEP T1-489-05*	Healthy	28	TAstV-1	HQ185551
NC-TK-SEP T1-552-05	Healthy	36	TAstV-1	HQ185552
NC-TK-SEP T1-703-05	Healthy	84	TAstV-1	HQ185553
MO-TK-SEP T1-822-05	Healthy	15	TAstV-1	HQ185554
NC-TK-SEP T1-928-06	Healthy	14	TAstV-1	HQ185555
VA-TK-SEP T2-33-03*	PEC	22	TAstV-2	HQ185556
NC-TK-SEP T2-222-03*	Unknown	57	TAstV-2	HQ185557
TX-TK-SEP T2-311-04*	Unknown	Unknown	TAstV-2	HQ185558
CA-TK-SEP T2-269-05*	Enteric disease	8	TAstV-2	HQ185559
GA-CK-SEP-CA-457-05*	RSS	6	CAstV	HQ185560
DE-CK-SEP CA-651-05*	Poor	7	CAstV	HQ185561
DE-CK-SEP CA-811-05	RSS	10	CAstV	HQ185562
GA-CK-SEP-CA-364-05*	RSS	7	CAstV	HQ185563
MO-CK-SEP-CA-883-06	RSS	15	CAstV	HQ185564
DE-CK-SEP ANV-651-05*	Poor	7	ANV-2	HQ188692
DE-CK-SEP ANV-811-05	RSS	10	ANV-2	HQ188693
GA-CK-SEP ANV-368-05*	RSS	10	ANV-2	HQ188694
NC-TK-SEP ANV-537-05*	Healthy	56	ANV-2	HQ188695
GA-CK-SEP ANV-451-05*	RSS	11	ANV-2	HQ188696
NC-TK-SEP-ANV-670-05*	Healthy	84	ANV-2	HQ188697
GA-CK-SEP- ANV-364-05*	RSS	7	ANV-2	HQ188698
GA-CK-SEP- ANV-458-05	Healthy	11	ANV-2	HQ188699
GA-CK-SEP-ANV-792-05	RSS	Unknown	ANV-like	HQ185565

*Partial ORF1b reported previously [30, 31]

Sequence analysis

An 861-894-nucleotide region of ORF2 was used to evaluate phylogenetic relationships among avian astroviruses. This region corresponded to the following regions of the reference viruses: TAstV-1, nucleotides (nt) 5329-6204; TAstV-2, nt 5474-6340; ANV-1, nt 5054-5945; DAstV, nt 5844-6710. There is no full-genome sequence published for CAstV. The following capsid sequences from avian astrovirus published in GenBank were included in the phylogenetic analysis: TAstV-1 (Y15936.2); TAstV-2 (AF206663.2), AK/98, CA/00, CO/01, MN/01, MO/01, PA/01, MI/01, TX/00, VA/99 (EU143843.1 to EU143851.1), TAstV-1987 (AY769616.1), TAstV-2001 (AY769615.1); ANV-1 (AB046864); ANV-2 (AB033998.1); DAstV (FJ434664.1); HAstV-1 (L123513); HAstV-2 (Q82446.1); HAstV-3 (AAD17224.1); HAstV-4 (BAA93446.1); HAstV-5 (AAA56750.1); HAstV-6 (CAA86616); HAstV-7 (CAA 69922); HAstV-8 (AAF85964); Dog AstV (CAR82569.1); porcine AstV (CAB95000); sea lion TAstV (ACR54274.1); Bat AstV (EU847155); feline AstV (AAC13556.1); ovine AstV (Y15937); bottlenose dolphin AstV (ACR54280.1); mink AstV (AY179509). Also included was the sequence of CAstV-3 (US Patent 209009263) and GA-UGA_Ast1-Oct2006 (CAstV-UGA-2006, Patent WO/2010/059899), a CAstV isolated at the University of Georgia, Athens, GA, from a flock of chickens with RSS (GenBank accession number HQ185566).

The sequence information was compiled using the Seqman progam (Lasergene V. 6.01, DNASTAR, Madison, WI), and multiple alignments of nucleotide and amino acid sequences were constructed with the Megalign application of the same software package using the Clustal W alignment algorithm (Slow/Accurate, Gonnet). Pairwise sequence alignments were also performed with the Megalign program to determine nucleotide and amino acid sequence identity.

In addition, a 2.5-kb region of the ANV-2's corresponding to nt 3710 to 6569 of ANV-1, spanning part of ORF1b and ORF2, was analyzed using SimPlot software version 3.5.1 [22]. The polymerase-capsid region was aligned using Clustal W of the MEGA 4 software [49], and ANV-1 and GA-CK-SEP- ANV-364-05 were used as the query sequences for similarity analysis. Similarity was calculated in each window of 200 bp using the Kimura two-parameter method.

Phylogenetic trees

Sequences were aligned with Clustal W (Lasergene, V. 8.0.2 DNAStar, Madison WI). Nucleotide trees were

constructed with merged duplicate runs of BEAST v. 1.4.8 [9] using HKY substitution, empirical base frequency, gamma heterogeneity, codon 2 partitions, relaxed lognormal clock, Yule process tree prior with default operators with unweighted pair group mean with arithmetic average starting tree, and a Markov chain Monte Carlo length of 10^6. Protein trees were constructed with the same program and parameters, except the Blosum 62 substitution matrix and the gamma + invariant site heterogeneity model were used.

Sequence accession numbers

The assigned GenBank accession numbers for the sequences generated from the capsid region of TAStV-1, TAstV-2, CAstV, and ANV viruses are HQ185551-65, and the ANV sequences encompassing ORF1b and capsid are HQ1888692-99 (Table 1).

Results and discussion

The capsid precursor protein gene is the most variable astrovirus gene, containing sequence differences that certainly reflect variation in antigenicity and possibly also in pathogenicity [45]. In this study, we compared the nucleotide and predicted amino acid sequences of a section of the hypervariable region of the capsid (ORF2) of 19 avian astroviruses from chickens and turkeys, along with capsid gene sequences of 22 other avian astroviruses retrieved from the database. Pairwise comparisons of the nucleotide and amino acid sequences of the ORF2 region of the viruses analyzed in this study showed great variability among all groups of avian astroviruses, with the exception of TAstV-1, which had between 96.2% and 100% amino acid identity (Table 2). TAstV-2 had between 81.5% and 100% amino acid identity, and CAstV had between 85.3% and 97.9% amino acid identity. ANV strains were most closely related to the reference ANV-2 strain, with 85.8%-100% amino acid identity among them, and 69.9% to 74.0% amino acid identity with ANV-1. One astrovirus detected in chickens (GA-CK-SEP ANV-792-05) did not group with any of the known avian astroviruses but was most closely related to ANV-1, with which it had 64% amino acid identity. DAstV was closest to TAstV-2 in amino acid sequence similarity, with 72.8%-75.7% identity. This is interesting, considering that these two viruses differ in their genome organization [11].

The amount of variation observed in most of the avian astroviruses groups studied suggests that there is antigenic variation among them, since for HAstV, Walter *et al.* [56] found that when two strains had less than 95% nucleotide homology, they could be distinguished serologically. TAstV2001 and TAstV1987 have been reported to represent distinct serotypes, sharing only 82.8% amino acid sequence identity for the complete capsid region [52]. This level of sequence conservation is close to that of HAStV capsid genes from different serotypes (<80% nt similarity). These sequence distances suggest that many of the astroviruses studied may represent different serotypes in each group. However, in order to corroborate this, serological cross-reactivity analysis of the viruses still needs to be conducted. Similar remarkably high genetic diversity has also been observed within bat astroviruses [6, 61].

The degree of similarity at the amino acid level to mamastroviruses in the region examined was 20.7%-29.3% for TAstV-2, 21.1%-26.7% for TAstV-1, 20.3-28.9 for CAstV, and 22.4%-27.9% for ANV. The mamastroviruses analyzed were 31.4% to 61.2% similar among themselves,

Table 2 Range of percent amino acid and nucleotide (*italics*) identity among avian astrovirus isolates analyzed in this study. One ANV-1, nine ANV-2, seven CAstV, six TAstV-1, fifteen TAstV-2, one DAstV, and isolate ANV792 viruses were compared

	ANV-1	ANV-2	CAstV	TAstV-1	TAstV-2	DAstV	ANV792
ANV-1	-	69.9-74.0	31.6-33.7	30.4-38.1	28.6-31.7	28.1	64.0
	-	*66.0-67.5*	*42.9-44.8*	*45.6-46.0*	*42.6-45.2*	*42.0*	*65.1*
ANV-2		85.8-100	29.4-33.7	28.6-39.2	29.4-33.7	26.1-29.9	61.5-64.4
		85.4-98.2	*42.7-47.2*	*45.8-48.0*	*42.7-47.2*	*42.8-44.9*	*61.9-63.6*
CAstV			85.3-97.9	38.7-42.9	39.0-42.0	41.3-42.4	29.5-30.6
			74.0-91.8	*49.2-51.0*	*48.2-53.2*	*48.5-50.0*	*40.7-43.5*
TAstV-1				96.2-100	45.0-48.2	45.3-45.9	29.3-37.2
				95.5-100	*52.1-54.6*	*51.2-51.6*	*45.5-46.4*
TAstV-2					81.5-100	72.8-75.7	28.2-45.2
					81.4-100	*65.2-70.1*	*43.7-45.2*
DAstV						-	29.2
						-	*42.5*

with the exception of human and feline astroviruses, which were > 72.6% similar (data not shown).

Phylogenetic analysis based on the partial ORF2 amino acid sequences shows that the avian astrovirus form four groups (Fig. 1): TAstV-1-like, TAstV-2-like, CAstV-like and ANV-1-like viruses, similar to previous reports analyzing ORF1b sequences [30]. The phylogenetic relationships of the nt sequences were similar to those of the aa sequences. The ANV group contained both chicken-origin and turkey-origin isolates. The TAstV-1, TAstV-2 and CAstV groups contained only turkey and chicken-origin viruses, respectively. The TAstV-2 group was distant from TAstV-1 and was closely related in this region to DAstV. A phylogenetic tree based on amino acid sequences of the ORF2 region of the avian and selected mammalian astroviruses shows that the avian astroviruses form distinct groups consistent with the nucleotide tree and are separate from the mammalian isolates (Fig. 2). The mammalian isolates vary widely in their similarity to one another. The HAstV isolates clustered together with the feline astroviruses on a branch that was distant from other astrovirus groups. Several other isolates formed species-specific branches, including the porcine, canine, bottlenose dolphin and sea lion astroviruses. Conversely, some disparate isolates including mink, ovine and bat astroviruses clustered together.

A 2.5-kb nucleotide sequence spanning a region of the polymerase and capsid genes of eight ANV was also analyzed by comparison to the ANV-1 reference strain. The SimPlot computer program [22] was used to analyze the alignment of the eight ANV using a window size of 200 nucleotides that was moved along in 20-nucleotide steps. The percent identity was calculated for each window and plotted in a line chart. Figure 3 shows that the ANV-1 reference strain shared a lower level of sequence identity in the capsid region with the ANV analyzed, whereas, based on the phylogenetic analysis, these viruses were more closely related to ANV-2, a different ANV serotype. Because there are no sequence data available for the ORF1b of the ANV-1 virus, it was not included in the analysis. Alignment of the ORF1b-ORF2 region sequences of eight ANV2 strains showed that they shared high levels of sequence identity in the conserved domain (N-terminal 415 amino acids), whereas the carboxy-terminus of ORF2 showed higher levels of variation (Figure 4). This is consistent with results reported previously for HAstV [14, 27, 57]. Recent work by Strain *et al.* involving the analysis of nine complete turkey astrovirus genomes provided evidence for recombination between astrovirus genomes and

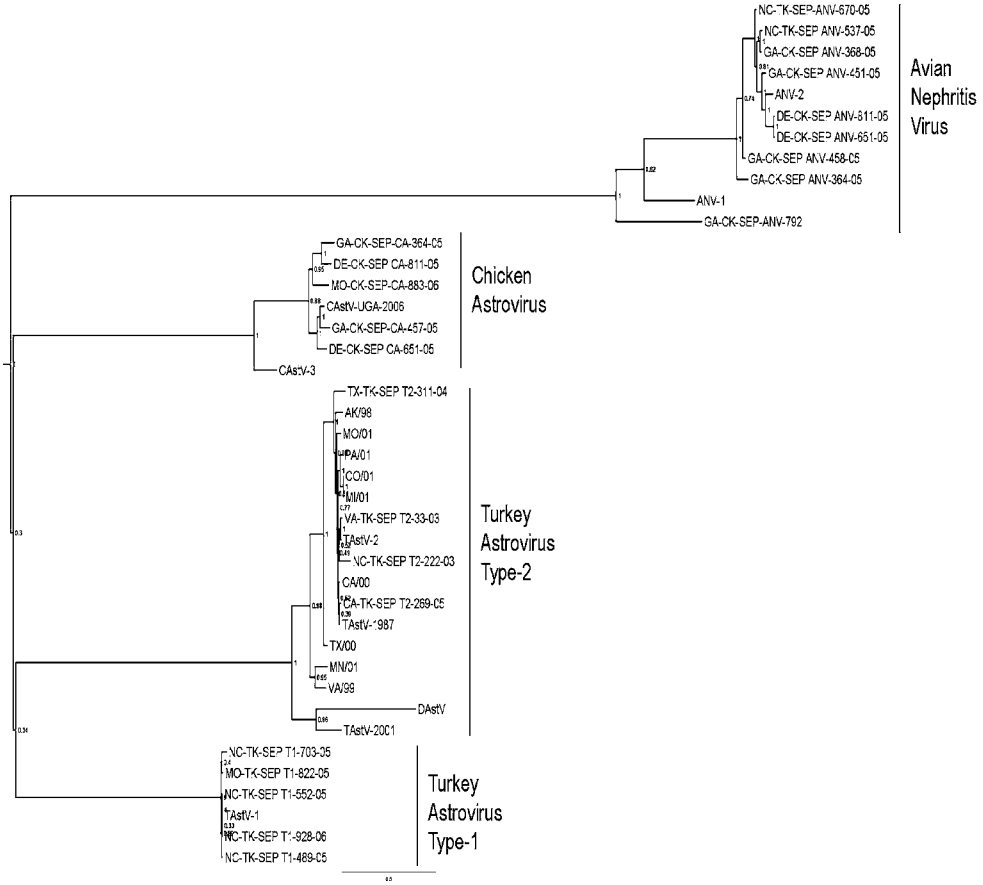

Fig.1 Phylogenetic tree of the nucleotide sequences of avian astrovirus capsid genes. Node posterior values are given

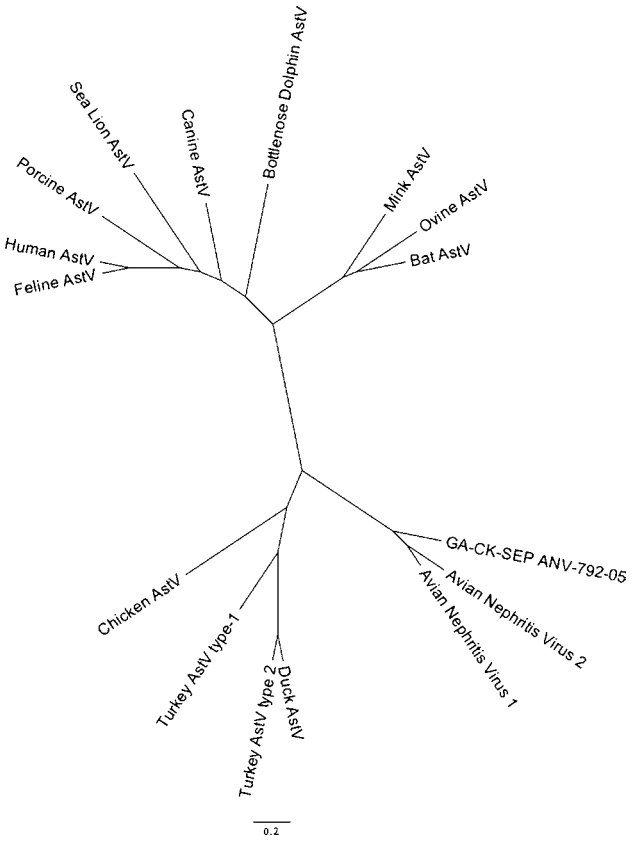

Fig. 2 Unrooted phylogenetic tree of the amino acid sequences of phylogenetically representative isolates from different species groups

supported the view that sequences from different regions of the astrovirus genome should be considered for phylogenetic analysis on which taxonomic subdivisions might be based [47]. With recombination, it is possible that different ANV-1 ORF1b sequences could be contiguous with ANV-1 capsid protein sequences, or conversely, they could have different ORF2 sequences, as was observed with the ANV-2 isolates analyzed. These data suggest that potential recombination could occur within ORF2, resulting in the emergence of new viruses.

Astroviruses appear to be widely disseminated and endemic in poultry in the US, and concomitant infection of flocks with two or more enteric viruses is common [19, 30, 32, 33]. The high incidence of astroviruses in turkeys affected with enteric disease has been documented previously [37]. Astroviruses have also been found in turkeys with poult enteritis mortality syndrome (PEMS), a disease that has caused severe economic losses to the turkey industry [2, 3, 35, 59, 60]. Although TAstV-2 is frequently detected in turkey poults, it is not clear how many serotypes exist. Phylogenetic analysis of TAstV-2 isolates revealed a high level of genetic variation, particularly in the capsid gene, suggesting the possibility of several serotypes [31, 47, 52]. Tang and Saif antigenically characterized two TAstV-2 isolates, TAstV1987 and TAstV2001, showing that they belonged to different serotypes [50], and in our analysis, these viruses are clearly of different genotypes. Until more serology is done to determine how many TAstV-2 serotypes exist, genetic characterization of the virus serves as a useful alternative for type assignment of avian astroviruses and permits the characterization of the astroviruses circulating in poultry. TAstV-1 strains, on the other hand, appear to be more closely related to each other and are less commonly detected on turkey farms. The reason for this is not clear, but it could be due to sample bias or real biological features of the virus.

Avian nephritis virus (ANV), previously classified as a member of the genus *Enterovirus*, family *Picornaviridae*, has been isolated from chickens and was re-classified as an astrovirus following the complete sequencing of the viral genome [17]. This virus was first isolated in 1976 and is associated with growth depression and kidney lesions in young chickens [17]. Avian nephritis virus has been shown to be widely distributed in chicken flocks in Japan [16], some European countries [7, 8, 29], and even in specific-pathogen-free flocks [26]. Under field conditions, clinical signs associated with this virus infection in broiler chickens have varied from subclinical to outbreaks of RSS and baby chick nephropathy [10, 16, 23, 42, 44, 48, 58]. At least two serotypes of ANV and different pathotypes have been reported [43, 54]. Based on sequence comparisons of part of the non-structural protease gene (ORF 1a), ANV could be grouped into three genotypes [23]. ANV has also been reported in turkeys [30], and antibodies to ANV have been detected in turkeys in Northern Ireland and England, but nothing has been reported about clinical signs of infection [7, 29]. The ANVs analyzed in this study, although closely related to ANV-1 in ORF1b, were mostly ANV-2-like based on ORF2, indicating the possibility of recombination. It is not clear if the GA-CK-SEP ANV-792-05 is in fact an ANV. Further genetic analysis of these viruses is required.

A second type of chicken astrovirus was shown to be antigenically and genetically distinct from ANV [4]. Although the sequence of this virus is still not available, we will refer to it as the reference CAstV (it has been patented as CAstV-2). CAstVs sharing high levels of nucleotide sequence identity with this first characterized CAstV have been detected in the United States in broiler chickens affected with RSS [30]. Recently, molecular and antigenic characterization of entero-like viruses (ELVs) demonstrated that they were CAstV, some of them closely related to the reference CAstV, and some of them more distantly related [54]. CAstV was detected by serology in broiler flocks in the United Kingdom, the Netherlands, Spain, Australia, and the United States [4]. Serological evidence also indicated that CAstV infections were common in

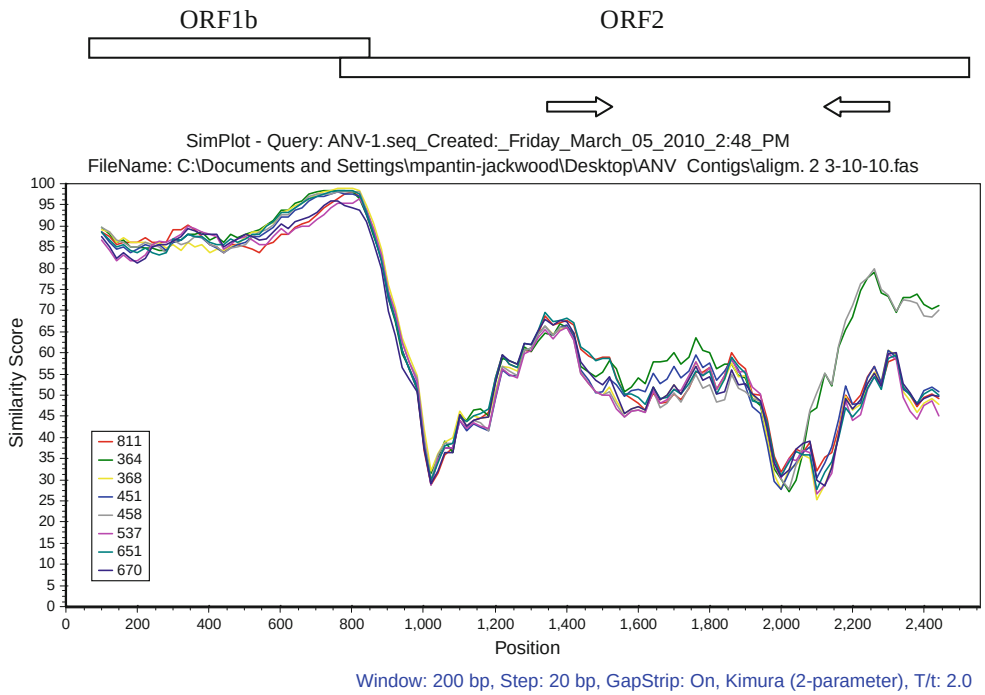

Fig. 3 Similarity analysis of ANV based on partial sequences of ORF1b and ORF2. Nucleotide identity plot of the 2.5 kb region comprising the amplified polymerase and capsid regions of the following ANVs compared with ANV-1: DE-CK-SEP ANV-651-05 (651), DE-CK-SEP ANV-811-05 (811), GA-CK-SEP ANV-368-05 (365), NC-TK-SEP ANV-537-05 (537), GA-CK-SEP ANV-451-05 (451), NC-TK-SEP-ANV-670-05 (670), and GA-CK-SEP-ANV-364-05 (364). The bar above the plot represents the regions corresponding to ORF-1b (polymerase) and ORF-2 (capsid). The arrows indicate the region amplified from the capsid gene and used in the phylogenetic analysis

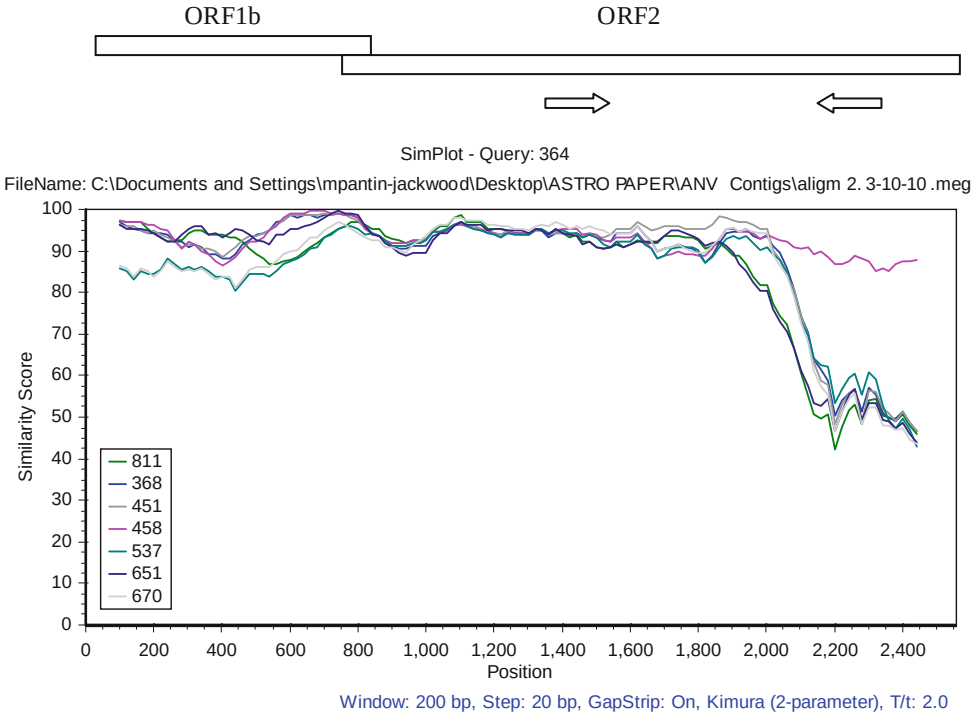

Fig. 4 Similarity analysis of ANV based on partial sequences of ORF1b and ORF2. Nucleotide identity plot of the 2.5-kb region comprising the amplified polymerase and capsid regions of the following ANVs: DE-CK-SEP ANV-651-05 (651), DE-CK-SEP ANV-811-05 (811), GA-CK-SEP ANV-368-05 (365), NC-TK-SEP ANV-537-05 (537), GA-CK-SEP ANV-451-05 (451), NC-TK-SEP-ANV-670-05 (670), and GA-CK-SEP-ANV-364-05 (364). The query isolate used was isolate 364. The bar above the plot represents the region corresponding to ORF-1b (polymerase) and ORF-2 (capsid). The arrows indicate the region amplified from the capsid gene and used in the phylogenetic analysis

broiler parent flocks within the United Kingdom and also appeared to be widespread in European breeder flocks [55]. CAstV was commonly detected by RT-PCR in broiler flocks with growth problems or ones that were affected by RSS [30, 45, 55]. Phylogenetic analysis based on a region of the ORF1b demonstrated the existence of two distinct clades [30, 45]. In this study, the CAstV isolates grouped separately from CAstV-3 and also formed two different groups (Fig.1). The complete genome of CAstV has not been published, so many question related to the genome structure and how they relate to other avian astroviruses remain to be answered.

A virus producing hepatitis in ducks (DHV-2) was identified to have astrovirus morphology and was renamed

duck astrovirus 1 (DAstV-1) [1, 13]. Sequence analysis of the ORF 1b region of this virus showed that it was closely related to CAstV. A second virus, DHV-3, was also identified as an astrovirus, but based on the amino acid identities in the ORF 1b region of this virus with that of DHV-2 (69%) it appears that they might be of different genotypes, and DHV-3 is more closely related to TAstV-2 [54]. The complete sequence of a duck astrovirus (DAstV) associated with an outbreak of fatal hepatitis in ducklings in China was published recently, and phylogenetic analysis revealed that DAstV was most closely related to TAstV-2 [11]. Our results also corroborate this.

A new taxonomy proposal for avian astroviruses has been submitted to the International Committee on Taxonomy of Viruses (ICTV) for approval (http://talk.ictvonline.org/files/proposals/taxonomy_proposals_vertebrate1/m/vert01/2358.aspx). This proposal is the result of the work done in agreement by all members of the *Astroviridae* Study Group during the preparation of the 9th ICTV Report. Based on new data, the *Astroviridae* Study Group states that a classification based on genetic criteria is more appropriate than classifying the viruses into species within the genus *Avastrovirus* based only on the host of origin. A phylogenetic analysis of avastroviruses based on the amino acid sequence of the full-length ORF2 results in three groups (genotype species). Mean amino acid genetic distances (p-dist) range between 0.576-0.742 and 0.204-0.284 between and within groups, respectively. This new classification establishes three new species within the genus: *Avastrovirus* GI.A, including turkey astrovirus 1; *Avastrovirus* GI.B, including avian nephritis virus 1 and 2; and *Avastrovirus* GII.A, including turkey astrovirus 2 and duck astrovirus. Some chicken astroviruses for which only partial sequences are available (chicken astrovirus 2, DQ324850), or no sequences at all, are deposited in GenBank (chicken astrovirus 3) and would be listed as "related viruses that might be members of the genus *Avastrovirus* but have not been assigned to a species".

As more sequence data become available, a clearer picture will emerge with regard to avian astroviruses. This will have to be complemented by serological and biological characterization of these viruses.

In conclusion, comparative analysis of avian astrovirus capsid genes revealed extensive genetic variation and the presence of distinct genotypes of TAstV-2, ANV and CAstV circulating in poultry. Changes in the capsid protein induced by mutations or recombination most likely have an effect on the pathogenicity and antigenicity of the viruses, and consequently, practical implications for virus detection methods, epidemiological studies and development of potential vaccines against astrovirus infections.

Acknowledgments The authors gratefully appreciate the assistance provided by Diane Smith in conducting this study. The authors also thank the SAA sequencing facility at SEPRL and Melissa Scott for technical assistance. This work was supported by USDA CRIS project 6612-32000-054 and by Grant F0008 from the U.S. Poultry and Egg Association.

References

1. (2006) Index of Viruses-Astroviridae. In: Buchen-Osmond C (ed) ICTVdB- The Universal Virus Database, version 4. Columbia University, New York, USA
2. Barnes GL, Guy JS, Vaillancourt JP (2000) Poult enteritis complex. Rev Sci Tech 19:565–588
3. Barnes HJ, Guy JS (2003) Poult Enteritis-Mortality Syndrome. In: Saif YM, Barnes HJ, Glisson JR, Fadly AM, McDougald LR, Swayne DE (eds) Diseases of Poultry, 11th edn. Blackwell, Ames, IA, pp 1171–1180
4. Baxendale W, Mebatsion T (2004) The isolation and characterisation of astroviruses from chickens. Avian Pathol 33:364–370
5. Cattoli G, Toffan A, De Battisti C, Salviato A, Terregino C, Capua I (2005) Astroviruses found in the intestinal contents of guinea fowl suffering from enteritis. Vet Rec 156:220
6. Chu DK, Peiris JS, Chen H, Guan Y, Poon LL (2008) Genomic characterizations of bat coronaviruses (1A, 1B and HKU8) and evidence for co-infections in Miniopterus bats. J Gen Virol 89:1282–1287
7. Connor TJ, McNeilly F, McFerran JB, McNulty MS (1987) A survey of avian sera from Northern Ireland for antibody to avian nephritis virus. Avian Pathol 16:15–20
8. Decaesstecker M, and Meulemans (1991) An ELISA for the detection of antibodies to avian nephritis virus and related entero-like viruses. Avian Pathol 20: 523-530
9. Drummond AJ, Rambaut A (2007) BEAST: Bayesian evolutionary analysis by sampling trees. BMC Evol Biol 7:214
10. Frazier J A HK, Reece R L, Kidd A W, Cavanagh D (1990) Isolation of noncytopathic viruses implicated in the aetiology of nephritis and baby chick nephropathy and serologically related to avian nephritis virus. Avian Pathol 19:139–160
11. Fu Y, Pan M, Wang X, Xu Y, Xie X, Knowles NJ, Yang H, Zhang D (2009) Complete sequence of a duck astrovirus associated with fatal hepatitis in ducklings. J Gen Virol 90:1104–1108
12. Goodwin MA, Davis JF, McNulty MS, Brown J, Player EC (1993) Enteritis (so-called runting stunting syndrome) in Georgia broiler chicks. Avian Dis 37:451–458
13. Gough RE, Collins MS, Borland E, Keymer LF (1984) Astrovirus-like particles associated with hepatitis in ducklings. Vet Rec 114:279
14. Guo L, Gonzalez R, Wang W, Li Y, Paranhos-Baccala G, Vernet G, Wang J (2010) Complete genome sequence of human astrovirus genotype 6. Virol J 7:29
15. Guy JS, Miles AM, Smith L, Fuller FJ, Schultz-Cherry S (2004) Antigenic and genomic characterization of turkey enterovirus-like virus (North Carolina, 1988 isolate): identification of the virus as turkey astrovirus 2. Avian Dis 48:206–211
16. Imada T, Yamaguchi S, Miura N, Kawamura H (1980) Antibody survey against avian nephritis virus among chickens in Japan. Natl Inst Anim Health Q (Tokyo) 20:79–80
17. Imada T, Yamaguchi S, Mase M, Tsukamoto K, Kubo M, Morooka A (2000) Avian nephritis virus (ANV) as a new member of the family Astroviridae and construction of infectious ANV cDNA. J Virol 74:8487–8493
18. Jindal N, Patnayak DP, Ziegler AF, Lago A, Goyal SM (2009) Experimental reproduction of poult enteritis syndrome: clinical

findings, growth response, and microbiology. Poult Sci 88:949–958
19. Jindal N, Patnayak DP, Chander Y, Ziegler AF, Goyal SM (2010) Detection and molecular characterization of enteric viruses from poult enteritis syndrome in turkeys. Poult Sci 89:217–226
20. Koci MD, Seal BS, Schultz-Cherry S (2000) Molecular characterization of an avian astrovirus. J Virol 74:6173–6177
21. Koci MD, Schultz-Cherry S (2002) Avian astroviruses. Avian Pathol 31:213–227
22. Lole KS, Bollinger RC, Paranjape RS, Gadkari D, Kulkarni SS, Novak NG, Ingersoll R, Sheppard HW, Ray SC (1999) Full-length human immunodeficiency virus type 1 genomes from subtype C-infected seroconverters in India, with evidence of intersubtype recombination. J Virol 73:152–160
23. Mandoki M, Bakonyi T, Ivanics E, Nemes C, Dobos-Kovacs M, Rusvai M (2006) Phylogenetic diversity of avian nephritis virus in Hungarian chicken flocks. Avian Pathol 35:224–229
24. Matsui SM, Greenberg HB (2001) Astroviruses. In: Howley DMKaPM (ed) Fields Virology, 4th edn. Lippincott Williams and Wilkins, Baltimore, MD
25. McNulty MS, Curran WL, McFerran JB (1980) Detection of astroviruses in turkey faeces by direct electron microscopy. Vet Rec 106:561
26. McNulty MS, Connor TJ, McNeilly F (1989) A survey of specific pathogen-free chicken flocks for antibodies to chicken anemia agent, avian nephritis virus and group A rotavirus. Avian Pathol 18:215–220
27. Mendez-Toss M, Romero-Guido P, Munguia ME, Mendez E, Arias CF (2000) Molecular analysis of a serotype 8 human astrovirus genome. J Gen Virol 81:2891–2897
28. Mendez E, Arias CF (2007) Astroviruses. In: Knipe DM, Howley PM (eds) Fields Virology. Lippincott Williams and Wilkins, Philadelphia, pp 981–1000
29. Nicholas RAJ, Goddard RD, Luff PR (1988) Prevalence of avian nephritis virus in England. Vet Rec 123:398
30. Pantin-Jackwood MJ, Spackman E, Woolcock PR (2006) Molecular characterization and typing of chicken and turkey astroviruses circulating in the United States: implications for diagnostics. Avian Dis 50:397–404
31. Pantin-Jackwood MJ, Spackman E, Woolcock PR (2006) Phylogenetic analysis of Turkey astroviruses reveals evidence of recombination. Virus Genes 32:187–192
32. Pantin-Jackwood MJ, Spackman E, Day JM, Rives D (2007) Periodic monitoring of commercial turkeys for enteric viruses indicates continuous presence of astrovirus and rotavirus on the farms. Avian Dis 51:674–680
33. Pantin-Jackwood MJ, Day JM, Jackwood MW, Spackman E (2008) Enteric viruses detected by molecular methods in commercial chicken and turkey flocks in the United States between 2005 and 2006. Avian Dis 52:235–244
34. Pantin-Jackwood MJ, Spackman E, Day JM (2008) Pathogenesis of type 2 turkey astroviruses with variant capsid genes in 2-day-old specific pathogen free poults. Avian Pathol 37:193–201
35. Qureshi MA, Yu M, Saif YM (1999) A novel "Small round virus" Inducing Poult Enteritis and Mortality Syndrome and Associated with Immnue Alterations. Avian Dis 44:275–283
36. Reynolds DL, Saif YM (1986) Astrovirus: a cause of an enteric disease in turkey poults. Avian Dis 30:728–735
37. Reynolds DL, Saif YM, Theil KW (1986) A Survey of Enteric Viruses of Turkey Poults. Avian Dis 31:89–98
38. Saif YM, Saif LJ, Hofacre CL, Hayhow C, Swayne DE, Dearth RN (1990) A small round virus associated with enteritis in turkey poults. Avian Dis 34:762–764
39. Schultz-Cherry S, Kapczynski DR, Simmons VM, Koci MD, Brown C, Barnes HJ (2000) Identifying agent(s) associated with poult enteritis and mortality syndrome:importance of the thymus. Avian Dis 44:256–265
40. Sellers H, Linneman E, Icard AH, Mundt E (2010) A purified recombinant baculovirus expressed capsid protein of a new astrovirus provides partial protection to runting-stunting syndrome in chickens. Vaccine 28:1253–1263
41. Shirai J, Nakamura K, Narita M, Furuta K, Kawamura H (1990) Avian nephritis virus infection of chicks: virology, pathology, and serology. Avian Dis 34:558–565
42. Shirai J, Obata H, Nakamura K, Furuta K, Hihara H, Kawamura H (1990) Experimental infection in specific-pathogen-free chicks with avian reovirus and avian nephritis virus isolated from broiler chicks showing runting syndrome. Avian Dis 34:295–303
43. Shirai J, Nakamura K, Shinohara K, Kawamura H (1991) Pathogenicity and antigenicity of avian nephritis isolates. Avian Dis 35:49–54
44. Shirai J, Tanimura N, Uramoto K, Narita M, Nakamura K, Kawamura H (1992) Pathologically and serologically different avian nephritis virus isolates implicated in etiology of baby chick nephropathy. Avian Dis 36:369–377
45. Smyth VJ, Jewhurst HL, Adair BM, Todd D (2009) Detection of chicken astrovirus by reverse transcriptase-polymerase chain reaction. Avian Pathol 38:293–299
46. Spackman E, Day JM, Pantin-Jackwood MJ Astrovirus, reovirus, and rotavirus concomitant infection causes decreased weight gain in broad-breasted white poults. Avian Dis 54: 16-21
47. Strain E, Kelley LA, Schultz-Cherry S, Muse SV, Koci MD (2008) Genomic analysis of closely related astroviruses. J Virol 82:5099–5103
48. Takase K, Shinohara K, Tsuneyoshi M, Yamamoto M, Yamada S (1989) Isolation and characterization of cytopathic avian enteroviruses from broiler chickens. Avian Pathol 18:631–642
49. Tamura K, Dudley J, Nei M, Kumar S (2007) MEGA4: Molecular Evolutionay Genetics Analysis (MEGA) software version 4.0. Mol Biol Evol 24:1596–1599
50. Tang Y, Saif YM (2004) Antigenicity of two turkey astrovirus isolates. Avian Dis 48:896–901
51. Tang Y, Ismail MM, Saif YM (2005) Development of antigen-capture enzyme-linked immunosorbent assay and RT-PCR for detection of turkey astroviruses. Avian Dis 49:182–188
52. Tang Y, Murgia AM, Saif YM (2005) Molecular characterization of the capsid gene of two serotypes of turkey astroviruses. Avian Dis 49:514–519
53. Todd D, Trudgett J, McNeilly F, McBride N, Donnelly B, Smyth VJ, Jewhurst HL, Adair BM Development and application of an RT-PCR test for detecting avian nephritis virus. Avian Pathol 39: 207-213
54. Todd D, Smyth VJ, Ball NW, Donnelly BM, Wylie M, Knowles NJ, Adair BM (2009) Identification of chicken enterovirus-like viruses, duck hepatitis virus type 2 and duck hepatitis virus type 3 as astroviruses. Avian Pathol 38:21–30
55. Todd D, Wilkinson DS, Jewhurst HL, Wylie M, Gordon AW, Adair BM (2009) A seroprevalence investigation of chicken astrovirus infections. Avian Pathol 38:301–309
56. Walter JE, Mitchell DK, Guerrero ML, Berke T, Matson DO, Monroe SS, Pickering LK, Ruiz-Palacios G (2001) Molecular epidemiology of human astrovirus diarrhea among children from a periurban community of Mexico City. J Infect Dis 183:681–686
57. Willcocks MM, Kurtz JB, Lee TW, Carter MJ (1995) Prevalence of human astrovirus serotype 4: capsid protein sequence and comparison with other strains. Epidemiol Infect 114:385–391
58. Yamaguchi S, Imada T, Kawamura H (1979) Characterisation of a picornavirus isolated from broiler chicks. Avian Dis 23:571–581
59. Yu M, Ismail MM, Qureshi MA, Dearth RN, Barnes HJ, Saif YM (2000) Viral agents associated with poult enteritis and mortality

syndrome: the role of a small round virus and a turkey coronavirus. Avian Dis 44:297–304
60. Yu M, Tang Y, Guo M, Zhang Q, Saif YM (2000) Characterization of a small round virus associated with the poult enteritis and mortality syndrome. Avian Dis 44:600–610
61. Zhu HC, Chu DK, Liu W, Dong BQ, Zhang SY, Zhang JX, Li LF, Vijaykrishna D, Smith GJ, Chen HL, Poon LL, Peiris JS, Guan Y (2009) Detection of diverse astroviruses from bats in China. J Gen Virol 90:883–887

Zsak et al. Virology Journal 2011, 8:331
http://www.virologyj.com/content/8/1/331

VIROLOGY JOURNAL

RESEARCH Open Access

The complete genome sequence and genetic analysis of ΦCA82 a novel uncultured microphage from the turkey gastrointestinal system

Laszlo Zsak[1*], J Michael Day[1], Brian B Oakley[2] and Bruce S Seal[2]

Abstract

The genomic DNA sequence of a novel enteric uncultured microphage, ΦCA82 from a turkey gastrointestinal system was determined utilizing metagenomics techniques. The entire circular, single-stranded nucleotide sequence of the genome was 5,514 nucleotides. The ΦCA82 genome is quite different from other microviruses as indicated by comparisons of nucleotide similarity, predicted protein similarity, and functional classifications. Only three genes showed significant similarity to microviral proteins as determined by local alignments using BLAST analysis. ORF1 encoded a predicted phage F capsid protein that was phylogenetically most similar to the *Microviridae* ΦMH2K member's major coat protein. The ΦCA82 genome also encoded a predicted minor capsid protein (ORF2) and putative replication initiation protein (ORF3) most similar to the microviral bacteriophage SpV4. The distant evolutionary relationship of ΦCA82 suggests that the divergence of this novel turkey microvirus from other microviruses may reflect unique evolutionary pressures encountered within the turkey gastrointestinal system.

Keywords: microphage, microviridae, turkey, enteric, metagenomics

Introduction

Metagenomics analyses have lead to the discovery of a variety of microbial nucleotide sequences from environmental samples [1]. These techniques have also allowed for the discovery of uncultured viral nucleotide sequences that are commonly from bacteriophages [2-4] that has also resulted in the discovery of useful enzymes for molecular biology [5]. There has been a resurgent interest in bacteriophage biology and their use or use of phage gene products as antibacterial agents [6-8]. Bacteriophages are thought to be the most abundant life form as a group [9] and the importance of phage to bacterial evolution [10,11], the role of phage or prophage encoded virulence factors that contribute to bacterial infectious diseases [12-14] and their contribution to horizontal gene transfer [15] cannot be over stated. Additionally, the contribution to microbial ecology [16] and to agricultural production [17,18] is also extremely important.

Enteric diseases are an important economic production problem for the poultry industry worldwide. One of the major economically important enteric diseases for the poultry industry are the poult enteritis complex (PEC) and poult enteritis mortality syndrome (PEMS) in turkeys and a runting-stunting syndrome (RSS) in broiler chickens [19]. Consequently, studies have been ongoing to identify novel enteric viruses among poultry species at our laboratory. In a recent study, we utilized the Roche/454 Life Sciences GS-FLX platform to compile an RNA virus metagenome from turkey flocks experiencing enteric disease [20]. This approach yielded numerous sequences homologous to viruses in the BLAST nr protein database, many of which have not been described in turkeys.

Additionally, we have successfully applied a random PCR-based method for detection of unknown microorganisms from enteric samples of turkeys that resulted in identification of genomic sequences and subsequent

* Correspondence: laszlo.zsak@ars.usda.gov
[1]Southeast Poultry Research Laboratory, Agricultural Research Service, United States Department of Agriculture, 934 College Station Road, Athens, GA 30605 USA
Full list of author information is available at the end of the article

BioMed Central
© 2011 Zsak et al; licensee BioMed Central Ltd. This is an Open Access article distributed under the terms of the Creative Commons Attribution License (http://creativecommons.org/licenses/by/2.0), which permits unrestricted use, distribution, and reproduction in any medium, provided the original work is properly cited.

determination of the full-length genome from a previously uncultured parvovirus [21]. During these ongoing investigations to further characterize the turkey gut microbiome and identify novel viral pathogens of poultry, bacteriophage genomic sequences have also been identified. Herein we report the complete genomic sequence of a putative novel member of the *Microviridae* obtained from turkey gastrointestinal DNA samples utilizing metagenomics approaches. The protein sequences of ΦCA82 were most similar to those of *Chlamydia* phages.

Materials and Methods

Assembly of ΦCA82, a novel member of the *Microviridae* family

Forty-two complete intestinal tracts (from duodenum/pancreas to cloaca, including cecal tonsils) from a turkey farm in California, U.S.A. with histories of enteric disease problems were received at the Southeast Poultry Research Laboratory (SEPRL). The intestines were processed and pooled into a single sample, as previously described [22]. A sequence-independent polymerase chain reaction (PCR) protocol was employed to amplify particle-associated nucleic acid (PAN) present in turkey intestinal homogenates, and has been described elsewhere in detail [22]. Using this approach, a total of 576 clones were identified and sequenced with the M13 forward and reverse primers on an AB-3730 automated DNA sequencer. The sequenced clones were used as query sequences to search the GenBank non-redundant nucleotide and protein databases using the blastn and blastx algorithms [23]. In total, the majority of clones with inserts had no hit in the databases using tblastx [24]. However, 46% of the cloned DNA had homology to cellular DNA, bacterial DNA, bacteriophage DNA, and several eukaryotic viral DNA genomes. Twelve DNA clones had sequence similarity to single-stranded DNA microphages, which have also been identified predominantly in microbialites [25]. A contig, CA82 with an average of eightfold coverage and length of 1962 nt was assembled from eight of those clones. This contig had no significant nucleotide similarity to database sequences, but the deduced amino acid sequence revealed significant similarity to the members of the family *Microviridae*. This initial contig was used to design PCR primers in the opposite orientation of the circular ssDNA to assemble into a contiguous ΦCA82 genome. The PCR amplification resulted in a 3.4 kb product that closed the gap between the CA82 contig and the rest of the circular genome. The final sequence was confirmed by sub-cloning and primer walking with primers resulting ~1 kb fragments containing 250 bp overlapping sequences across the genome. The circular DNA genome was assembled from contigs exhibiting 100% nucleotide identity within the overlapping regions.

Sequence analysis

The ΦCA82 genome and ORFs were aligned with selected microvirus sequences using ClustalW [26]. Putative ORFs within the ΦCA82 genome were predicted using the FGENESV Trained Pattern/Markov chain-based viral gene prediction method from the Softberry website [27]. Searches for conserved domains within the ΦCA82 genome were performed with the Conserved Domain Database (CDD) Search Service v2.17 at the National Center for Biotechnology Information (NCBI) website [28].

Comparative genomics of the *Microviridae*

The sequence of phage ΦCA82 was compared to 14 other members of the *Microviridae* (Table 1) obtained

Table 1 Microviridae sequences used for comparative genomic analyses

Taxonoid	Genome Name	NCBI Taxon ID	Gene Count	Genome Size (bp)	Abbreviation
638275790	Chlamydia phage 1	10857	12	4877	Chp1
638275791	Chlamydia phage 2	105154	8	4563	Chp2
638275792	Chlamydia phage 3	225067	8	4554	Chp3
638275793	Chlamydia phage 4	313629	8	4530	Chp4
638275794	Chlamydia pneumoniae phage CPAR39	117575	7	4532	CPAR39
638275834	Coliphage ID18	338139	11	5486	Col-ID18
638275865	Coliphage WA13	338104	10	6068	Col-WA13
638275985	Enterobacteria phage G4	10843	11	5577	EntG4
645044532	Enterobacteria phage St-1	10845	11	6094	Ent-St1
638276022	Enterobacteria phage alpha3	10849	10	6087	Ent-alpha3
638276027	Enterobacteria phage phiX174	10847	11	5386	X174
638276133	Guinea pig Chlamydia phage	90963	9	4529	CPG1
638276608	Phage phiMH2K	145579	11	4594	MH2K
638276842	Spiroplasma phage 4	10855	9	4421	SpV4

Abbreviations are as shown in Figure 4.

from the integrated microbial genomes (IMG) system [29]. To first determine nucleotide level similarities, tetra-nucleotide comparisons between genomes were performed with jspecies [30]. Pairwise genome comparisons were based on regressions of normalized tetra-nucleotide frequency counts and the distributions of the R^2 values from these comparisons were visualized in R [31]. To compare genomes based on similarity of predicted gene sequences, the program CD-HIT [32] was used.

Genomic functional comparisons were based on pfam categories for each predicted gene as classified by the IMG annotation pipeline [29]. A data table of pfam categories and gene counts for each genome was used to construct a similarity matrix and dendrogram in R. To determine which predicted genes were unique to ΦCA82 and those which were shared with other *Microviridae* members, the *Microviridae* pangenome was constructed as the union of all predicted genes from the 14 *Microviridae* genomes and compared to predicted genes for ΦCA82 using both CD-HIT and our data analysis pipeline as described above and blastp run with default parameters except for an e-value cutoff of 0.01.

Nucleotide accession number

The nucleotide sequence of ΦCA82 genome was deposited in GenBank under accession number HQ264138.

Results and Discussion

The ΦCA82 genome

The entire circular, single-stranded nucleotide sequence for the uncultured microvirus ΦCA82 genome was determined to be 5,514 nucleotides. The complete genome sequence had a nucleotide composition of A (38.6%), C (19.6%), G (20.1%), and T (21.6%) with an overall G + C content of 39.7%, which is similar to the chlamydial phages (37-40%). The ΦCA82 genome was organized in a modular arrangement similar to microviruses [33,34] and encoded predicted proteins homologous to those chlamydial bacteriophage types [35] and to the *Bdellovibrio bacteriovorus* ΦMH2K [36]. The coding capacity of the genome is 91% as it encodes ten ORFs, greater than 99 nucleotides similarly to other chlamydial microvirus genomes [35]. The genome size, number of ORFs and total coding % of nucleotides as depicted in Figure 1 is larger than most of the chlamydial phages and is closer in size to the ΦX174 genome [33,34].

Capsid proteins of ΦCA82

The amino acid identities and homologies between ΦCA82 ORF gene products and predicted proteins from selected phages are presented in Table 2. A total of ten genes could be identified of which only three gene products could be assigned with a known function based upon BLAST analysis. The predicted major capsid protein VP1 encoded by ORF1 belongs to the family of single-stranded bacteriophages and is the major structural component of the virion that may contain as many as 60 copies of the protein [37,38]. The closest sequence similarity of the 565 amino acid ΦCA82 VP1 protein was with the *Spiroplasma* phage 4 (SpV4) capsid protein [39] and the chlamydial phage VP1 proteins [35,38,40-42], as well as the *Chlamydia* prophage CPAR39 [43] and *Bdellovibrio* phage ΦMH2K major capsid protein [36]. A putative minor capsid protein of 234 amino acids was encoded by ORF2 that had similarity to the chlamydial bacteriophages [35,40-43] and the *Bdellovibrio* phage ΦMH2K [36] that was originally postulated to be an attachment protein [38].

Recent studies using a comparative metagenomic analysis of viral communities associated with marine and freshwater microbialites indicated that identifiable sequences in these were dominated by single-stranded DNA microphages [25]. Partial sequence analysis of the VP1 gene from these microphages showed that the similarity between metagenomic clones and cultured microphage capsid sequences ranged from 47.5 to 61.2% at the nucleic-acid level and from 37.2 to 69.3% at the protein level, respectively. Interestingly, the VP1 gene of ΦCA82 has a similarly high level of sequence similarity (69.1% at the amino acid level) with the seawater metagenomic phages within the same VP1 region (data not shown). This observation is consistent with an environmental origin of modern poultry phages that have since undergone significant host-specific evolutionary divergence in agricultural settings.

A multiple alignment of major capsid proteins among diverse members shows similarities within the entire

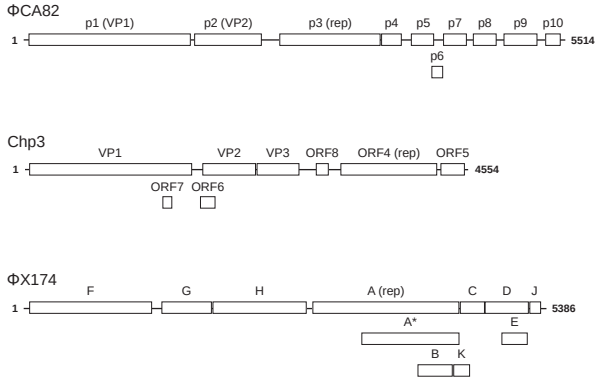

Figure 1 Comparative graphical representations of the genome organizations for ΦCA82, Chp3, and ΦX174 microviruses. Computer-predicted open reading frames and the full length genome in nucleotides are indicated. The numbering of nucleotides commences with the start codon of gene 1.

Table 2 Putative ΦCA82 ORFs and amino acid (aa) homologies with members of *Microviridae*

ΦCA82 ORF	No. of aa	Predicted function	Homologous protein (GenBank accession #)	% amino acid identity (homology)
01	565	major capsid protein	SpV4-VP1 (NC_003438)	30.0 (60.0)
			Chp3-VP1 (NC_008355)	27.0 (63.5)
			CPAR39-VP1 (NC_002180)	28.0 (62.2)
			ΦMH2K-VP1 (NC_002643)	26.0 (58.2)
02	234	minor capsid protein	Chp3-VP2 (NC_008355)	22.0 (45.6)
			ΦMH2K-VP2 (NC_002643)	17.9 (50.8)
03	353	replication initiation	SpV4-rep (NC_003438)	22.6 (54.5)
			ΦMH2K-rep (NC_002643)	17.0 (53.2)
04	71	hypothetical		
05	78	hypothetical		
06	39	hypothetical		
07	80	hypothetical		
08	80	hypothetical		
09	117	hypothetical		
10	52	hypothetical		

[a] Amino acid identity and homology was determined using ClustalW. Homology was calculated by the sum of identical, strongly similar and weakly similar residues and expressed as percentages of the total.

predicted coding region with the exception of the predicted surface-exposed IN5 loop and Ins (Figure 2). Amino acids located within these regions are involved in forming large protrusions at the threefold icosahedral axes of symmetry in the intracellular microvirus phages [36,41,43]. The IN5 loop, forming a globular protrusion on the virus coat and is the most variable region in the VP1 proteins from *Chlamydia* and *Spiroplasma* phages [44] is potentially located from residues 198 through 295 of ΦCA82 VP1, which is the most highly variable portion of the protein by BLAST. The hydrophobic nature of the cavity at the distal surface of the SpV4 protrusions suggests that this region may function as the receptor-recognition site during host infection. The

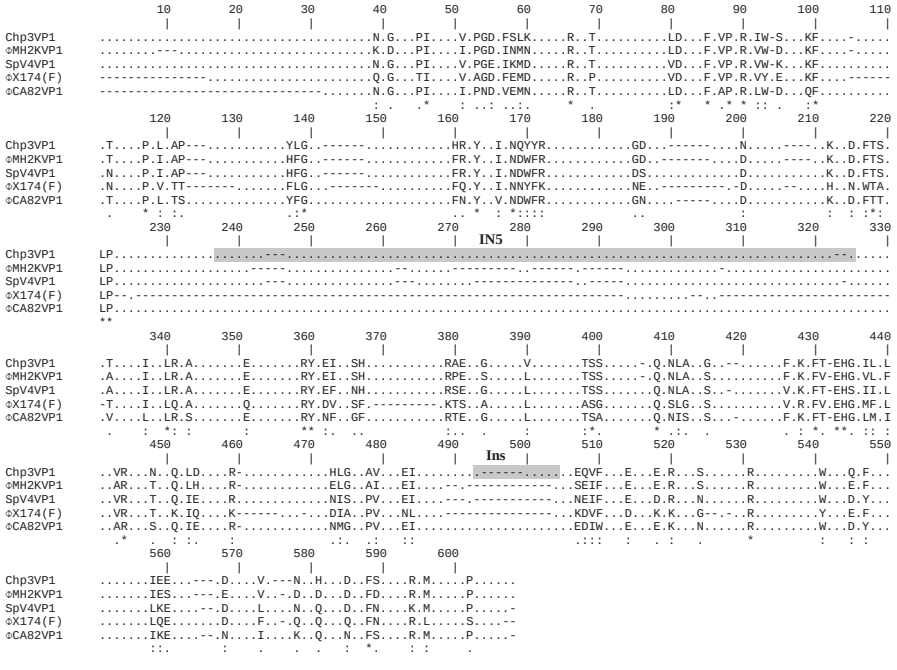

Figure 2 Multiple amino acid alignment of the major structural protein, VP1 of ΦCA82 with VP1 proteins from other *Microviridae* members. Deletions (-), non-homologous amino acids (dots in the sequence), identical amino acids (*), residues with strong similarity (:), and weak similarity (.) are indicated. Variable large IN5 and short Ins regions are shaded gray.

short variable Ins sequences of ΦCA82 are putatively located from residues 459 through 464 of the VP1 protein.

Chipman et al [44] predicted that the IN5 trimer structure in VP1 may function as a substitute for spike proteins of the ΦX174-like viruses, which are not found in SpV4 or the *Chlamydia* phages, and as such may be responsible for receptor recognition. It has also been suggested that the diverse sequence in this region is associated with host range of phages [36,41,43,44]. The presence of a large insertion in ΦCA82 further supports that it is closer to the intracellular phage subfamily and the sequence dissimilarity within this region between the ΦCA82 and various other phages strongly indicates that this domain indeed may function as a host range determinant.

Rep protein of ΦCA82

ORF3 encoded a putative replication initiation protein that was most similar to the SpV4-rep [39] and the *Bdellovibrio* phage ΦMH2K-rep [36] proteins (Table 2). Pairwise alignment of the ΦCA82 VP3 (rep) protein and SpV4 p1 (rep) protein revealed the presence of two conserved domains (Figure 3) from residues 73 through 176 and 195 through 320 of the ΦCA82 protein. Overall, the two rep proteins only had 22.6% identity, but shared many of the same sequences throughout the conserved regions that were recognized by BLAST as putative replication initiation protein regions. Rep protein plays an essential role in viral DNA replication and binds the origin of replication where it cleaves the dsDNA replicative form I (RFI) and becomes covalently bound to it via phosphotyrosine bond (see active sites in Figure 3). The conservation of the functional domains between the ΦCA82 phage rep protein and other microviral replication initiation proteins suggests a similar pathway/mechanism for DNA replication and virion packaging.

Full genome comparisons of ΦCA82 with other members of the *Microviridae*

The ΦCA82 genome is quite different from other members of *Microviridae* as indicated by comparisons of nucleotide similarity, predicted protein similarity, and functional classifications. Comparisons of ΦCA82 to 14 other *Microviridae* genomes showed very low correlations of tetra-nucleotide frequencies as a measure of genome similarity. ΦCA82 was most similar to SpV4, but the correlation of tetra-nucleotide frequencies was poor (R^2 = 0.33; Figure 4A). Only ΦMH2K had lower similarities to other *Microviridae* (Figure 4A). Clustering of predicted proteins showed ΦCA82 was most closely related to a clade comprised of the chlamydial phages, but as in the nucleotide comparisons, the predicted proteins of ΦCA82 are quite distinct from those of the other microviruses (Figure 4B). Function-based clustering of genomes using pfam categories showed that ΦCA82 was most similar to SpV4 (Figure 4C), based on shared membership of the ΦCA82 ORF1 in pfam02305, an F super family capsid protein. These results were confirmed by comparisons of predicted proteins from

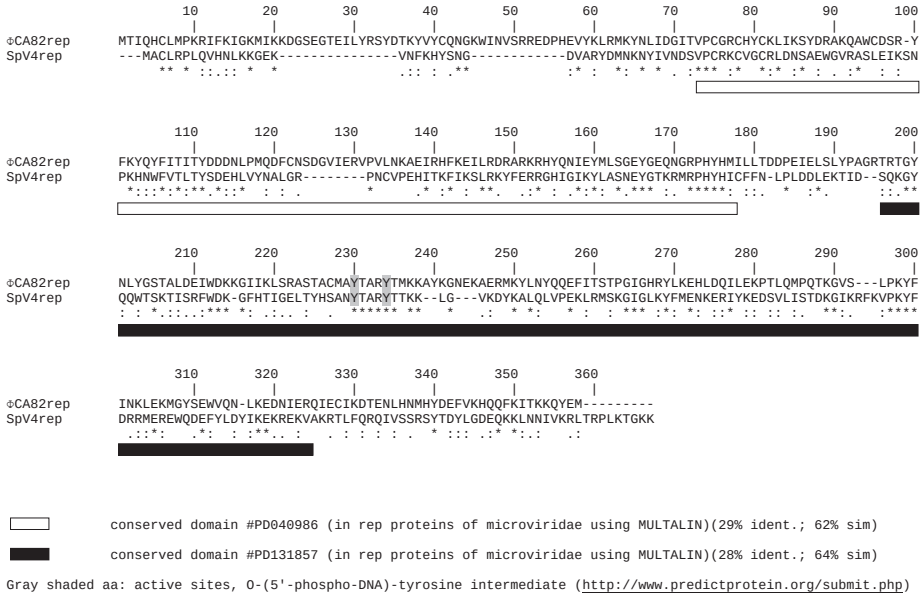

Figure 3 Pairwise amino acid alignment of the replication initiation protein from ΦCA82 (GenBank accession number HQ264138**) and SpV4 (GenBank accession number** NC_003438**) microphages**. Identical amino acids (*), residues with strong similarity (:), and weak similarity (.) are shown. Locations of conserved domains are boxed. The active sites of the rep protein are shaded gray.

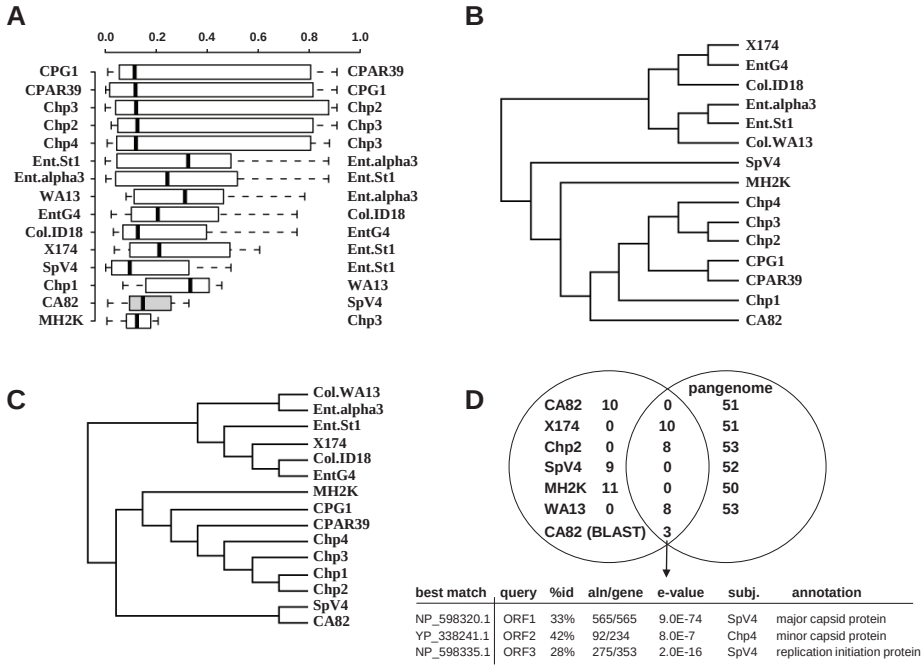

Figure 4 Genome-based comparisons of ΦCA82 and 14 other *Microviridae*. A) Comparisons of tetra-nucleotide frequencies as a measure of genome similarity at the nucleotide level. Boxplot represents the distributions of R^2 values for pairwise comparisons of tetra-nucleotide frequencies for each genome compared to all others. For each genome, the closest match (highest R^2) is shown to the right. B) Genomic sequence similarity as assessed by clustering of predicted amino-acid sequences. Clustering was completed with CD-HIT as described in the text, which accomplishes an all-versus-all comparison of each predicted protein. Sequence clusters were determined with a 40% similarity cutoff (sequences must be >40% similar for membership within the same cluster); tree is based on cluster memberships across all genomes. C) Genomic functional similarity as assessed by gene counts for each genome in pfam categories as classified by IMG. Tree construction methodology is essentially identical to (B), but based on functional cluster membership rather than clustering based on sequence similarity. D) Shared and unique predicted genes between ΦCA82 and all 14 other *Microviridae* members as determined by the CD-HIT clustering used for (B) and BLAST as described in the text.

the ΦCA82 genome to a *Microviridae* pangenome. This analysis showed only three genes with significant similarity as determined by local alignments using blastp with no overlap between ΦCA82 and the *Microviridae* pangenome based on global alignments at a 40% similarity cutoff (Figure 4D). ΦCA82 is only distantly related to other *Microviridae*, but is most similar to SpV4 and the chlamydial phages. In summary, the whole genome comparisons of ΦCA82 to other *Microviridae* members indicate a distant evolutionary relationship, perhaps suggesting that the divergence of ΦCA82 from other microviruses reflects unique evolutionary pressures encountered within the turkey gastrointestinal system.

Acknowledgements
These investigations were supported by ARS-USDA CRIS Project No. 6612-32000-054-00 "Epidemiology, Pathogenesis and Countermeasures to Prevent and Control Enteric Viruses of Poultry" at SEPRL and Project No. 6612-32000-055-00 "Molecular Characterization and Gastrointestinal Tract Ecology of Commensal Human Food-Borne Bacterial Pathogens in the Chicken" at PMSRU. The authors thank to Fenglan Li for excellent technical assistance and to the SEPRL sequencing facility for outstanding support.

Author details
[1]Southeast Poultry Research Laboratory, Agricultural Research Service, United States Department of Agriculture, 934 College Station Road, Athens, GA 30605 USA. [2]Poultry Microbiological Safety Research Unit, Agricultural Research Service, United States Department of Agriculture, 950 College Station Road, Athens, GA 30605 USA.

Authors' contributions
LZ conceived and coordinated the study, performed the PCR and sequencing, and wrote the paper. JMD prepared the samples and performed bioinformatic analyses. BBO coordinated the bioinformatic analyses. BSS provided technical input and intellectually contributed to the study design and writing the paper. All authors read and approved the final manuscript.

Competing interests
The authors declare that they have no competing interests.

Received: 25 March 2011 Accepted: 29 June 2011
Published: 29 June 2011

References
1. Handelsman J: **Metagenomics: application of genomics to uncultured microorganisms.** *Microbiol Mol Biol Rev* 2004, **68**:669-685.
2. Breitbart M, Salamon P, Andresen B, Mahaffy JM, Segall AM, Mead D, Azam F, Rohwer F: **Genomic analysis of uncultured marine viral communities.** *Proc Natl Acad Sci USA* 2002, **99**:14250-14255.

3. Edwards RA, Rohwer F: **Viral metagenomics.** *Nat Rev Microbiol* 2005, **3**:504-510.
4. Kristensen DM, Mushegian AR, Dolja VV, Koonin EV: **New dimensions of the virus world discovered through metagenomics.** *Trends Microbiol* 2010, **18**:11-19.
5. Schoenfeld T, Liles M, Wommack KE, Polson SW, Godiska R, Mead D: **Functional viral metagenomics and the next generation of molecular tools.** *Trends Microbiol* 2010, **18**:20-29.
6. Fischetti VA: **Bacteriophage lysins as effective antibacterials.** *Curr Opin Microbiol* 2008, **11**:393-400.
7. Liu J, Dehbi M, Moeck G, Arhin F, Bauda P, Bergeron D, Callejo M, Ferretti V, Ha N, Kwan T, McCarty J, Srikumar R, Williams D, Wu JJ, Gros P, Pelletier J, DuBow M: **Antimicrobial drug discovery through bacteriophage genomics.** *Nat Biotechnol* 2004, **22**:185-191.
8. Merril CR, Scholl D, Adhya SL: **The prospect for bacteriophage therapy in Western medicine.** *Nat Rev Drug Discov* 2003, **2**:489-497.
9. Suttle CA: **Marine viruses–major players in the global ecosystem.** *Nat Rev Microbiol* 2007, **5**:801-812.
10. Ackermann HW: **Bacteriophage observations and evolution.** *Res Microbiol* 2003, **154**:245-251.
11. Brüssow H, Canchaya C, Hardt WD: **Phages and the evolution of bacterial pathogens: from genomic rearrangements to lysogenic conversion.** *Microbiol Mol Biol Rev* 2004, **68**:560-602.
12. Boyd EF, Brüssow H: **Common themes among bacteriophage-encoded virulence factors and diversity among the bacteriophages involved.** *Trends Microbiol* 2002, **10**:521-529.
13. Chen J, Novick RP: **Phage-mediated intergeneric transfer of toxin genes.** *Science* 2009, **323**:139-141.
14. Wagner PL, Waldor MK: **Bacteriophage control of bacterial virulence.** *Infect Immun* 2002, **70**:3985-3993.
15. Canchaya C, Fournous G, Chibani-Chennoufi S, Dillmann ML, Brüssow H: **Phage as agents of lateral gene transfer.** *Curr Opin Microbiol* 2003, **6**:417-424.
16. Paul JH, Sullivan MB, Segall AM, Rohwer F: **Marine phage genomics.** *Comp Biochem Physiol* 2002, **133**:463-476.
17. Brüssow H, Desiere F: **Comparative phage genomics and the evolution of Siphoviridae: insights from dairy phages.** *Mol Microbiol* 2001, **39**:213-222.
18. Sturino JM, Klaenhammer TR: **Bacteriophage defense systems and strategies for lactic acid bacteria.** *Adv Appl Microbiol* 2004, **56**:331-378.
19. Barnes HJ, Guy JS, Barnes HJ, Glisson JR, Fadly AM, McDougald LR, Swayne DE: **Poult enteritis mortality syndrome.** In *Diseases of Poultry*.. 11 edition. Edited by: Saif Y. Iowa State Press; 2003:1171-1180.
20. Day JM, Ballard LL, Duke MV, Scheffler BE, Zsak L: **Metagenomic analysis of the turkey gut RNA virus community.** *Virol J* 2010, **7**:313.
21. Day JM, Zsak L: **Determination and analysis of the full-length chicken parvovirus genome.** *Virology* 2010, **399**:59-64.
22. Zsak L, Strother KO, Kisary J: **Partial genome sequence analysis of parvoviruses associated with enteric disease in poultry.** *Avian Pathol* 2008, **37**:435-441.
23. Altschul SF, Gish W, Miller W, Myers EW, Lipman DJ: **Basic local alignment search tool.** *J Mol Biol* 1990, **215**:403-410.
24. Altschul SF, Madden TL, Schaffer AA, Zhang J, Zhang Z, Miller W, Lipman DJ: **Gapped BLAST and PSI-BLAST: a new generation of protein database search programs.** *Nucleic Acids Res* 1997, **25**:3389-3402.
25. Desnues C, Rodriguez-Brito B, Rayhawk S, Kelley S, Tran T, Haynes M, Liu H, Furlan M, Wegley L, Chau B, Ruan Y, Hall D, Angly FE, Edwards RA, Li L, Thurber RV, Reid RP, Siefert J, Souza V, Valentine DL, Swan BK, Breitbart M, Rohwer F: **Biodiversity and biogeography of phages in modern stromatolites and thrombolites.** *Nature* 2008, **452**:340-343.
26. Thompson JD, Higgins DG, Gibson TJ: **CLUSTAL W: improving the sensitivity of progressive multiple sequence alignment through sequence weighting, position-specific gap penalties and weight matrix choice.** *Nucleic Acids Res* 1994, **22**:4673-4680.
27. Markov: **Markov chain-based viral gene prediction.**[http://linux1.softberry.com/berry.phtml?topic=virus&group=programs&subgroup=gfindv].
28. Marchler-Bauer A, Anderson JB, Chitsaz F, Derbyshire MK, DeWeese-Scott C, Fong JH, Geer LY, Geer RC, Gonzales NR, Gwadz M, He S, Hurwitz DI, Jackson JD, Ke Z, Lanczycki CJ, Liebert CA, Liu C, Lu F, Lu S, Marchler GH, Mullokandov M, Song JS, Tasneem A, Thanki N, Yamashita RA, Zhang D, Zhang N, Bryant SH: **CDD: specific functional annotation with the Conserved Domain Database.** *Nucleic Acids Res* 2009, **37**:205-210.
29. Markowitz VM, Korzeniewski F, Palaniappan K, Szeto E, Werner G, Padki A, Zhao X, Dubchak I, Hugenholtz P, Anderson I, Lykidis A, Mavromatis K, Ivanova N, Kyrpides NC: **The integrated microbial genomes (IMG) system.** *Nucleic Acids Res* 2006, **34**:344-348.
30. Richter M, Rossello-Mora R: **Shifting the genomic gold standard for the prokaryotic species definition.** *Proc Natl Acad Sci USA* 2009, **106**:19126-19131.
31. Team RDC: **A language and environment for statistical computing. R Foundation for Statistical Computing, Vienna, Austria.** 2008 [http://www.R-project.org], ISBN 3-900051-07-0.
32. Li W, Godzik A: **Cd-hit: a fast program for clustering and comparing large sets of protein or nucleotide sequences.** *Bioinformatics* 2006, **22**:1658-1659.
33. Rokyta DR, Abdo Z, Wichman HA: **The genetics of adaptation for eight microvirid bacteriophages.** *J Mol Evol* 2009, **69**:229-239.
34. Rokyta DR, Burch CL, Caudle SB, Wichman HA: **Horizontal gene transfer and the evolution of microvirid coliphage genomes.** *J Bacteriol* 2006, **188**:1134-1142.
35. Garner SA, Everson JS, Lambden PR, Fane BA, Clarke IN: **Isolation, molecular characterisation and genome sequence of a bacteriophage (Chp3) from Chlamydophila pecorum.** *Virus Genes* 2004, **28**:207-214.
36. Brentlinger KL, Hafenstein S, Novak CR, Fane BA, Borgon R, McKenna R, Agbandje-McKenna M: **Microviridae, a family divided: isolation, characterization, and genome sequence of φMH2K, a bacteriophage of the obligate intracellular parasitic bacterium Bdellovibrio bacteriovorus.** *J Bacteriol* 2002, **184**:1089-1094.
37. McKenna R, Bowman BR, Ilag LL, Rossmann MG, Fane BA: **Atomic structure of the degraded procapsid particle of the bacteriophage G4: induced structural changes in the presence of calcium ions and functional implications.** *J Mol Biol* 1996, **256**:736-750.
38. Storey CC, Lusher M, Richmond SJ: **Analysis of the complete nucleotide sequence of Chp1, a phage which infects avian Chlamydia psittaci.** *J Gen Virol* 1989, **70**:3381-3390.
39. Renaudin J, Pascarel MC, Bove JM: **Spiroplasma virus 4: nucleotide sequence of the viral DNA, regulatory signals, and proposed genome organization.** *J Bacteriol* 1987, **169**:4950-4961.
40. Sait M, Livingstone M, Graham R, Inglis NF, Wheelhouse N, Longbottom D: **Identification, sequencing and molecular analysis of Chp4, a novel chlamydiaphage of Chlamydophila abortus belonging to the family Microviridae.** *J Gen Virol* 2011, **92**:1733-1737.
41. Hsia RC, Ting LM, Bavoil PM: **Microvirus of Chlamydia psittaci strain guinea pig inclusion conjunctivitis: isolation and molecular characterization.** *Microbiology* 2000, **46**:1651-1660.
42. Liu BL, Everson JS, Fane B, Giannikopoulou P, Vretou E, Lambden PR, Clarke IN: **Molecular characterization of a bacteriophage (Chp2) from Chlamydia psittaci.** *J Virol* 2000, **74**:3464-3469.
43. Read TD, Brunham RC, Shen C, Gill SR, Heidelberg JF, White O, Hickey EK, Peterson J, Umayam L, Utterback T, Berry K, Bass S, Linher K, Weidman J, Khouri H, Craven B, Bowman C, Dodson R, Gwinn M, Nelson W, DeBoy R, Kolonay J, McClarty G, Salzberg SL, Eisen J, Fraser CM: **Genome sequences of Chlamydia trachomatis MoPn and Chlamydia pneumoniae AR39.** *Nucleic Acids Res* 2000, **28**:1397-1406.
44. Chipman PR, Agbandje-McKenna M, Renaudin J, Baker TS, McKenna R: **Structural analysis of the Spiroplasma virus, SpV4: implications for evolutionary variation to obtain host diversity among the Microviridae.** *Structure* 1998, **6**:135-145.

doi:10.1186/1743-422X-8-331
Cite this article as: Zsak *et al*.: The complete genome sequence and genetic analysis of ΦCA82 a novel uncultured microphage from the turkey gastrointestinal system. *Virology Journal* 2011 **8**:331.

Thermal Inactivation of Avian Viral and Bacterial Pathogens in an Effluent Treatment System Within a Biosafety Level 2 and 3 Enhanced Facility

Revis Chmielewski, Michael Day, Stephen Spatz, Qingzhong Yu, Richard Gast, Laslo Zsak, and David Swayne*

United States Department of Agriculture, Athens, Georgia

Abstract

Avian influenza (AI) virus, avian paramyxovirus Type 1 (APMV-1 or NDV), reovirus, rotavirus, turkey astrovirus (TAst), avian metapneumovirus (aMPV), Marek's disease virus (MDV-1), avian parvovirus (ChPV), and Salmonella enterica *serovar Enteritidis are significant biosafety level 2 (BSL-2) or biosafety level 3 enhanced (BSL-3E) pathogens of poultry that are studied in veterinary medical research laboratories worldwide. The purpose of this study was to determine the effectiveness of a moderate temperature, effluent decontamination system (EDS) to inactivate avian pathogens. First, the thermal inactivation processes for AI virus, APMV-1, reovirus, and rotaviruses were determined in phosphate-buffered saline (PBS) using* in vitro *assays from which thermal death rates* (D_t) *and changes in heat resistance* (zD) *of the AI virus and APMV-1 were determined at various time/temperature parameters. The PBS validation process demonstrated that 6 log_{10} reduction was achieved following heating at 82.2ºC within 30 seconds for AI virus and APMV-1, 1.8 minutes for astrovirus, while reoviruses and rotaviruses were destroyed within 3 minutes. Second, to determine whether pathogens were adequately inactivated in a moderate temperature EDS system, vials containing avian viruses (5.1-11.1 log_{10} TCID, EID_{50}/ml, or infectious particle/ml) and bacteria (9.1 log_{10} cfu/ml) were placed in the effluent tank and exposed to a standard cycle of 82.2ºC for 6 hours. The EDS process totally inactivated enveloped and non-enveloped viruses with complete inactivation of greater than 5.1-11.1 log_{10} TCID/ml of specific pathogens. The data from the inactivation models and the EDS validation test showed that the 6 log_{10} reduction required for a sanitary assurance level of effluent was achieved with a significant margin of safety.*

Introduction

Liquid effluent waste from Biosafety Level 2 and 3 Enhanced laboratories (BSL-2E and BSL-3E) and animal facilities (ABSL-2E and ABSL-3E) must be decontaminated before discharge into the public sewer system. The Clean Water Act (CWA) of 1972 sections 301(a,b), 304(b), 304(g), 304(m), and 307(b) and the secondary treatment regulation prescribe water quality discharges of pollutant in the wastewater (Anonymous, 1972; Anonymous, 1981). The intent of the effluent guidelines and pretreatment standards is reduction of chemical, physical, and biological contaminants discharged to surface water. One measure to prevent biological contaminants in a water source is pretreatment of wastewater through indirect steam heating prior to discharge into the surface water or public sewer system. Most biohazard inactivation efficacy tests are based on the inactivation of bacterial spores. Microbes and transmissible agents have varying degrees of tolerance to heat; the most thermally resistant are prions, followed by (in decreasing order of thermal resistance) bacterial spores, mycobacteria, non-lipid or naked viruses, fungi, vegetative bacteria, and lipid encapsulated viruses (CDC, 2007). Historically, the validation process for effluent discharge from an effluent decontamination system (EDS) has used a spore test to ensure sterility at an assurance level (SAL) where a 6 log_{10} reduction is achieved by the steam inactivation process for those thermal-resistant microbes (CDC, 2007). Therefore, the focus of the decontamination process is to inactivate not only pathogens used within the specific laboratory, but also to prevent a theoretical most severe case scenario.

Heat inactivation studies have not been reported for enveloped and non-enveloped avian viruses and vegetative bacteria for purposes of effluent decontamination. However, heat inactivation studies at 60ºC-70ºC for enveloped avian influenza and Newcastle disease viruses have shown that the time required to reduce the viruses by 6 logs in homogenized whole eggs and chicken meat was less than 2 minutes and 4 minutes, respectively (Swayne et al., 2004; Thomas et al., 2008).

The purpose of this study was to determine inactivation of enveloped and non-enveloped avian viruses and a vegetative bacterium in an operational indirect steam effluent decontamination system (EDS). We also developed predictive models to validate the inactivation

for low-pathogenicity notifiable avian influenza virus (LPNAIV), high-pathogenicity avian influenza virus (HPAIV), and virulent (*v*NDV) and lentogenic Newcastle disease viruses (*l*NDV), at various time/temperature parameters. Linear or non-linear regression models were used to obtain thermal inactivation rates and changes in thermal resistance (D_t and *zD*) in a phosphate buffer system.

Materials and Methods

Thermal Inactivation Modeling of Pathogens

Avian Influenza and Newcastle Disease Viruses. Viruses were diluted with phosphate-buffered saline to achieve a median embryo infectious dose of 6-8 $\log_{10}$ (EID_{50})/ml (Table 1). Ninety microliter (µl) aliquots of the inoculated PBS were dispensed into 200 µl thin-walled polypropylene tubes. Samples were equilibrated at 25ºC for 2 minutes, then heated to the desired temperature. Upon reaching the desired temperature, samples at the zero time point were removed and the timing commenced. Samples were heated at 53º, 55º, 57º, 58º, 59º, 61º, and/or 63ºC for 0, 1, 2, 3, 4, 6, 8, 12, 15, and 20 minutes in a PCR thermocycler block (GeneAmp® PCR System 9700, Perkin Elmer, Boston, MA), and then were immediately cooled to 4ºC in a cooling block (Diversified Biotech, Dedham, MA). For some sampling times, triplicate samples were pooled. The purpose of the pooling was to obtain sufficient volume (270 µl) to titer the undiluted sample (10^0) and increase the detection limit to 1 $\log_{10}$. For viral assay titration, samples were serially diluted (10^0 to 10^7) in media (MEM with antibiotics) for inoculation into cell cultures. Each experiment was replicated in triplicate.

Reoviruses and Rotaviruses. Ninety microliter aliquots of inoculated samples of reovirus (Reo/TX/98) and rotavirus (Ro/1145/08) (6 $\log_{10}$/ml EID_{50}) were dispensed into 200 µl thin-walled thermocycler polypropylene tubes (Table 1). Samples were equilibrated at 25ºC for 2 minutes then heated to the desired temperature. Samples were exposed to an anisothermic inactivation by linear ramping of temperatures from 30ºC to 82.2ºC within 150 seconds in a PCR thermocycler block. Upon reaching 82.2ºC, samples were removed and immediately cooled to 4ºC in a cooling block.

Tissue Culture Assay. Monolayer chicken embryo

Table 1

The names and strains of enveloped and non-enveloped avian viruses used in the validation process of the effluent decontamination system[1].

Pathogen	Genetic Characteristics	Acronym	Strain
Enveloped Viruses			
Avian metapneumovirus	*RNA, ss-*	aMPV-CO	aMPV/Colorado/96/C
Marek's disease virus	DNA, ds	MDV/CV1988	*Gallid herpesvirus 2* vaccine strain CVI988
Lentogenic Newcastle virus	*RNA, ss-*	*l*NDV/B1/48	Chicken/United States/B1/1948
Virulent Newcastle	*RNA, ss-*	*v*NDV/CA/2002	Chicken/United States (CA)/212676/2002
High pathogenic Avian Influenza virus	*RNA, ss-*	HPAI/PA/83	A/chicken/Pennsylvania/1370/83 (H5N2)
Low pathogenic notifiable avian influenza virus	*RNA, ss-*	LPNAI/NY/94	A/chicken/New York/13142-5/94 (H7N2)
Non-enveloped Viruses			
Reovirus strain	*RNA, ds*	Reo/TX/98	Turkey/Texas/SEP/98
Reovirus strain	*RNA, ds*	Reo/TX/99	Turkey/Texas/SEP/99
Rotavirus strain	*RNA, ds*	Ro/996/07	Turkey/North Carolina/SEP-Ro996/07
Rotavirus strain	*RNA, ds*	Ro/1145/08	Turkey/North Carolina/SEP-Ro1145/08
Avian astrovirus	*RNA, ss+*	TAstV/07	Turkey/California/SEP-A938/07
Avian parvovirus	DNA, ss	CkPV-P1	Chicken parvovirus, ChPV-P1
Vegetative Bacteria			
Salmonella enteritidis	gram -ve		*Salmonella enterica* serovar Enteritidis, phage type 13a, accession # 19299-52-1

[1] 6 hours, 82.2ºC

fibroblast (CEF) cells were used to titer *l*NDV and *v*NDV, and Madin-Darby Canine Kidney (MDCK) cells were used to titer LPNAIV and HPAIV in 96-well microtiter plates. The monolayers were washed three times with PBS, inoculated with viruses, and incubated for 1 hour. Following incubation, media supplement with trypsin was added to the inoculated monolayers and incubated at 37ºC under 5% CO_2 humidified atmosphere for 4 days. The viruses were titered using standard hemagglutination assays. Briefly, 50 µl aliquot of supernatant from the inoculated cells were transferred into a microtiter plate, serially diluted (1:2), then overlaid with 0.5% red blood cells (RBC). After 30 minutes of incubation, the presence or absence of hemagglutination was recorded. Virus titers were determined by calculation of $TCID_{50}$ (Reed et al., 1938).

Statistical Analysis. Inactivation curves were generated by plotting the log value of the infectious dose of the virus ($TCID_{50}$) as a function of the heating times at specific temperatures using Microsoft Excel 2003®. The statistical distribution of the data was examined to determine whether the model was linear or non-linear. Linear, exponential, and polynomial regression was fitted to the curves. The D_t or time (minutes) to inactivate the viral load by 90% was calculated from the inverse value of the slope (1/-slope) of the regression plot. The *zD* value is the temperature required to change the D_t by 1 log or 10-fold and was determined by computing the regression of the mean log D_t versus heating temperatures. *zD* values were the absolute values of the inverse slope.

Effluent Decontamination System Validation

Effluent Decontamination System (EDS) Validation Operation for the Inactivation of Avian Pathogens. The EDS includes four non-pressurized, large, cold steel tanks that thermally treat and cool the liquid waste prior to release into the municipal sewage system (Figure 1). Each tank has a total volume of 15,142 L (4,000 gallons) with a working capacity for each cycle of approximately 12,113 L (3,200 gallons). The tanks were cylindrically shaped with dimensions of 6 meters long, 2 meters high (20' x 6'), and surrounded by 5 centimeters of fiberglass insulation encased in plastic. Each tank contained a 4.5 m (15')-long steam bundle with a 6.4 cm (2.5") diameter used for heating the effluent. The steam bundle ran about three-fourths the length of the tank and was placed so that the bottom of the steam bundle was 25 cm (9.8") from the bottom of the tank. The tank cycle included fill, warm-up, thermal maintenance, and cool off/purge. The EDS tanks contained a low-pressure (5 psi) air supply system within each tank to allow slow mixing of liquid to ensure limited temperature stratification. The EDS was non-pressurized and used a moderate temperature (minimum of 180ºF [82.2ºC]) for a minimum of 6 hours along with the low air pressure mixing system to ensure that the effluents were heated evenly, thus ensuring that all viral and bacterial pathogens used in the facilities would be inactivated.

Inactivation Procedure for BSL-2 Viruses in EDS Tank. Two milliliters (ml) of virus-containing liquid were

Figure 1

Depiction of EDS cook tank as modified in 2002. Actual schematics are *not* available.

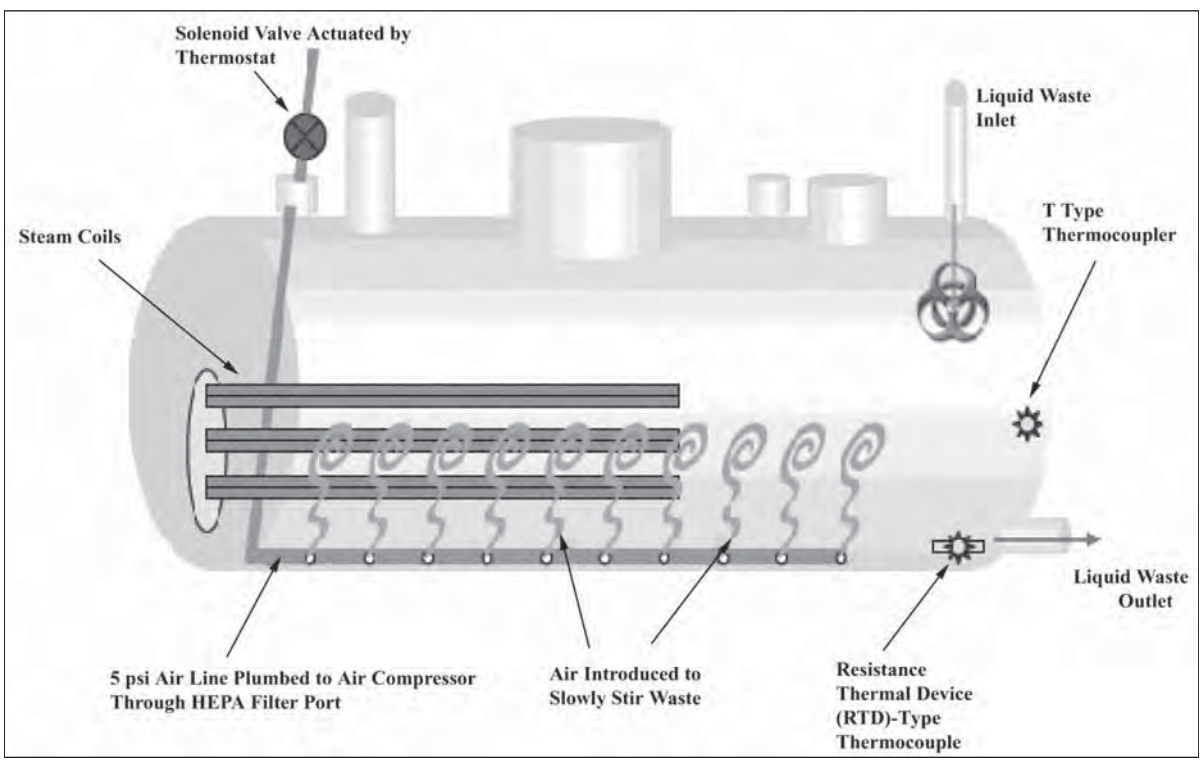

added to each of four 4 ml internally threaded cryogenic vials (Corning #430491, Lowell, MA). All vials were sealed in 5-ply polyethylene plastic pouches using a vacuum packaging system (FoodSaver, Tilia International, Inc., Rye, NY). Each vial was considered as one replication for a total of three replicates for each EDS treatment plus one control per virus. Sealed vials containing titrated cultures of different viruses and bacteria were submerged into an EDS tank to evaluate survivability. Three replicates of each virus type were immersed into the EDS system, while one replicate of each virus was maintained at -70ºC as a positive control. For the bacterial samples, there were four replicates for EDS treatment and four controls.

Inactivation Procedure for BSL-3E Viruses in EDS Tank. Vials containing highly pathogenic viruses currently held in BSL-3E labs were decontaminated by direct immersion into phenolic disinfectant (One Stroke Environ®, Steris Inc., Mentor, OH), placed in a plastic bag, sealed, and directly transferred to the BSL-2E laboratory where they were vacuum-sealed within a biological safety cabinet. The vacuum-sealed vials were directly transported to the EDS room in a sealed plastic bag and were immersed as described below. The entire procedure of removal of the viruses from BSL-3E, vacuum-sealing, and transfer to the EDS tank was conducted without interruption so that the BSL-3E viruses were not stored for any length of time at BSL-2E. All virus transfers between buildings were in compliance with established Southeast Poultry Research Laboratory Guidelines (SEPRL, 2009).

Tank Immersion Procedure. In this EDS validation study, there were two heating cycles. The first cycle was the inactivation of any pathogens in the effluent before opening the tank and adding the vials containing virus into the EDS. The effluent was exposed to one heat decontamination cycle, then allowed to cool to 60ºC. The second cycle was the evaluation of the thermal inactivation of avian viruses within the vials. Individually sealed cryovials containing live viruses or bacteria were inserted into an expandable mesh sleeve (Halar®, Solvay Solexis, Inc., Houston, TX). The sleeve was closed and a weight was added to the bottom of the mesh sleeve to maintain the sample vials vertically at the approximate center of the tank during the thermal inactivation process. A primary barrier was set up around the tank port prior to sampling. Briefly, a plastic (CPVC) frame covering the sample port wrapped with a large 60" x 60" four-ply plastic bag was attached at the base of the sample port with duct tape. Prior to unsealing the sample port, a weighted sleeve containing the sample vials was attached to a new sample port cap with stainless steel chains. The samples along with a spray bottle of disinfectant (5.25% sodium hypochlorite, Garden Scientific, Van Nuys, CA) were placed inside the primary containment barrier (Figure 2). The unsealing of the sample port and the loading and unloading of the samples into the EDS tank were operated from outside the primary barrier. After the samples were added and the port was sealed, the tanks were cycled through a second standard decontamination cycle at 82.2ºC for a minimum of 6 hours at 5 psi in the bubble/mixing system. To remove the samples, the process using the primary barrier was

Figure 2

A. Sealed sample vial; **B.** EDS tank; **C.** Plastic frame, disinfectant bottle, Halar® mesh sleeve and metal cap on top of EDS tank port; and **D.** EDS tank with attached plastic bag barrier.

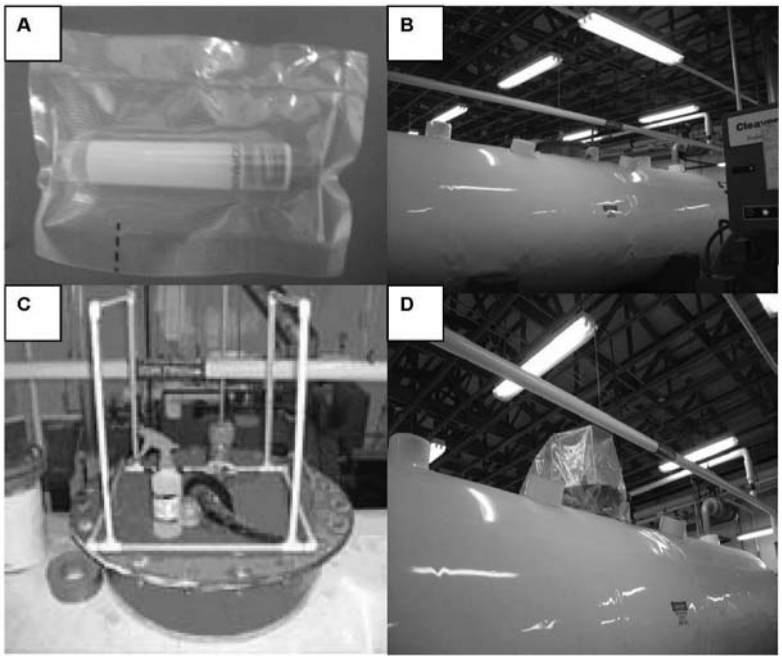

performed in reverse. The sample port cap with sleeve and weight was removed from the tank and the original cap was placed on the sample port. The plastic bag containing samples was removed from the tank. All contents in the primary barrier (the cap, sleeve and weight, sample bag, the disinfectant bottle, and the inside of the plastic bag barrier) were disinfected, sealed in a plastic bag, and taken directly to the BSL-2E laboratory (Figure 2). The vials containing the highly pathogenic viruses were immediately chilled, placed in a secondary container, and taken directly to the BSL-3E laboratory for processing.

Temperature Validation. Thermocouples were used to monitor the temperature of the effluent in the EDS tank. The thermocouples were validated previously (ENV, Inc., New York, NY) and were calibrated to within +/- 0.25ºC. As a secondary temperature monitoring system for validation of the temperature reached within the sleeve, test strips (Thermax®, Burlington, NJ) were placed in the mesh sleeve in the EDS test location. The test strips have a surface temperature indicator range of 65º-93ºC or 149º-199ºF.

Validation for Vial and Outer Pouch Integrity. Vials filled with PBS were vacuum-sealed in the outer pouch, then inserted into weighted sleeves and attached to the cap of the sample port, then suspended into the EDS tank. The vials were exposed to the complete EDS cycle. The EDS cycle consisted of fill, warm up, heat treatment (82.2ºC for 6 hours at 5 psi), and cooling. Next, the vials and the sealed outer plastic pouch barrier were examined for volume change and evidence of leak or evidence of loss of structure integrity.

Preparation of Virus Samples and Re-isolation Procedures After EDS Treatment

Avian Influenza Virus and Avian Paramyxovirus. The enveloped viruses, LPNAI/NY/94, HPAI/PA/83, *l*NDV-B1/48, and *v*NDV/CA/2002 (Table 1), were propagated by inoculation of 10-day-old specific pathogen free (SPF) embryonating white leghorn chicken eggs (ECE) (Southeast Poultry Research Laboratory, Athens, GA). Titration of the virus stock was completed using standard methods (Swayne et al., 1998). Briefly, 10-fold serial dilutions of infected allantoic fluid were inoculated into Brain Heart infusion broth (BHI, Becton Dickinson, Sparks, MD) containing antibiotics (gentamicin 200 µg/ml, penicillin 2000 units/ml, amphotericin B 4 mg/ml, Sigma Chemical Co., St. Louis, MO). One hundred microliter aliquots were then inoculated into five SPF eggs. Virus titer was determined by calculation of the 50% egg infectious dose (EID_{50}) (Reed et al., 1938). In preparation for the EDS treatment, an initial titer of 6 $\log_{10}$ EID_{50} was used for avian influenza viruses (HPAI and LPNAI) and avian paramyxovirus (*v*NDV and *l*NDV). After EDS treatment, AIV and NDV were re-isolated in accordance with established procedures (Alexander, 2005; Senne, 2008). Briefly, samples were inoculated into five 9-to-10-day-old chicken embryos by the chorioallantoic sac (CAS) route. Following the 4 days of incubation, allantoic fluids from each embryo were harvested and tested for hemagglutination of RBC. Pooled allantoic fluids were inoculated into embryos for a second passage and then retested for the presence of virus using the hemagglutination assay. The positive control samples were titrated using the hemagglutination assay.

Avian Metapneumovirus. aMPV subtype C Colorado strain (aMPV-CO) (Table 1) was propagated in Vero cells as described previously (Yu et al., 2010). An initial titer of 7.5 $\log_{10}$ 50% tissue culture infectious dose ($TCID_{50}$) of aMPV-CO was used for EDS treatment. The re-isolation of avian metapneumovirus following EDS treatment was in accordance with established procedures for aMPV detection (Yu et al., 2010). Briefly, each of the three replicates of the virus and control vial was serially diluted in D-MEM cell culture medium and plated in triplicate onto confluent Vero cells in a 96-well format. Cell culture plates were monitored each day for 5 days for typical cytopathic effects (CPE). Viral titers of the EDS treated and untreated aMPV-CO samples were calculated and compared by the $TCID_{50}$ (Reed et al., 1938).

Marek's Disease Virus Type-1. MDV-1/CV1988 (Table 1) was propagated in chicken embryo fibroblast (CEF) cells supplemented with media (DMEM/0.2% FBS) and incubated at 39ºC with 5% CO_2 in a humidified atmosphere for 4-6 days. Following infection (based on visual CPE), infected cells were trypsinized, pelleted for 5 minutes at 300 x g, and resuspended in freezing medium (72.5% DMEM; 20% FBS (Gibco®, Invitrogen Corp., Carlsbad, CA), 7.5% DMSO). The cellular suspension was divided into 4 x 1 ml aliquots and slowly cooled to -80ºC before transfer to liquid nitrogen for storage. Following EDS treatment, treated samples, along with the untreated control, were serially diluted in DMEM containing 5% FBS (10^0-10^{-5}). Each dilution was used to infect one well (24-well) of CEF at ~90% confluency in DMEM with 5% FBS. After approximately 12 hours, the medium was removed and replaced with DMEM/0.2% FBS, and the infected cells were incubated at 39ºC with 5% CO_2 humidified atmosphere for an additional 4 days. Cells were then fixed with a 50:50 mixture of acetone/methanol, and viral foci were enumerated using immunohistochemistry with a monoclonal antibody specific for glycoprotein B of MDV-1. Viral titers of treated and untreated samples were calculated and compared.

Avian Parvovirus. Aliquots of 5 x 1 ml ChPV-P1 (Table 1) stock virus (6 $\log_{10}$ infectious particle per ml) were added to 5 x 4 ml internally threaded cryogenic vials (Corning #430491, Lowell, MA). Sterile PBS was added to four cryovials to serve as negative controls. Three replicates were immersed in the EDS system, while two replicates of each virus were maintained at -80ºC during the process to serve as a positive control. Following EDS inactivation, the test vials were stored at -80ºC prior to testing. Since chicken parvovirus (ChPV) does not grow *in vitro*, the safety test was evaluated

in vivo in chickens. Four hundred microliters of treated virus from each of three vials were pooled for testing. Ten 1-day-old SPF chickens were orally inoculated with 100 µl of pooled treated virus. Positive control birds (n=10) received 100 µl of untreated virus. Cloacal swab samples were taken at 7, 14, and 21 days post inoculation from each test sample and control birds. DNA was extracted from cloacal swab samples (DNA Extraction Kit, Qiagen, Germantown, MD) and processed using a chicken parvovirus-specific PCR assay (Zsak et al., 2009).

Avian Reovirus and Rotavirus. Reo/TX/98 and Ro/996/07 viruses (Table 1) were propagated and prepared for EDS treatment as previously described for avian influenza (Spackman et al., 2005; Theil et al., 1986). Following EDS treatment, each of the three replicates per virus and control vial were serially diluted in culture medium (DMEM with antibiotics) and plated in triplicate onto VERO cells (reovirus) or MA-104 cells (rotavirus) grown to approximately 80% confluency in 96-well plates. Cell culture plates were monitored each day for 5 days for CPE typical of reovirus and rotavirus.

Astrovirus. TAstV/07 (Table 1) was propagated and prepared for EDS treatment as previously described (Schultz-Cherry et al., 2001; Spackman et al., 2005). Following EDS treatment, three replicates were inoculated into ten 20-day-old SPF embryonating turkey eggs via the yolk sack. Eggs were candled daily for 7 days to check for mortality. When the eggs reached 27 days of incubation, intestines were harvested, diluted (1:2), and homogenized. RNA was extracted from the homogenate using a Trizol-MagMax procedure and tested via RT-PCR for the presence of turkey astrovirus RNA (Das et al., 2009; Day et al., 2007). Control virus held at -70ºC served as a positive control and was tested in an identical manner.

***Salmonella Enterica* Serovar Enteritidis**. *Salmonella enterica* serovar Enteritidis was propagated into tryptone soya broth and incubated for 24 hours at 37ºC, centrifuged for 10 minutes at 3,000 x *g*, then washed twice in 0.85% saline. The cell concentration was determined spectrophotometrically at O.D. 600 nm and adjusted to a final cell concentration of 7 $\log_{10}$ cfu/ml. Two milliliters of culture were added to eight vials. Four vials were immersed into the EDS system, while the remaining vials were maintained at -70ºC and served as positive controls. Following EDS treatment, the cell count (cfu/ml) from treated and control vials was determined by serial dilution in saline, then enumeration on brilliant green and trypticase soy agar. Negative control vials containing PBS were processed as above.

Results and Discussion

Enveloped viruses (AI virus, APMV-1, aMPV, and Marek's disease virus type-1) and non-enveloped viruses (ChPV, TAstV, reo- and rotaviruses) and *Salmonella* have had detrimental economic impact in the poultry industry worldwide; therefore, research on avian pathogens is essential to find control measures. These pathogens are handled in the animal health research facility environment including isolation cabinets, open-housing rooms, and necropsy facilities. The pathogens accumulate during room clean up with some quantities amassing in effluent tanks. HPAIV and *v*NDV are Select Agents and as such are handled in a high-containment facility (BSL-3E) and require effluent inactivation. The others are BSL-2 pathogens and are not required to be inactivated in effluent; however, our facility chose to also inactivate these in the effluent prior to release to the municipal waste. Enveloped and non-enveloped viruses have different thermal resistances. Non-enveloped viruses are usually more heat-resistant than enveloped viruses (Blümel et al., 2002). The non-enveloped parvovirus has a single-stranded (ss) DNA and is one of the most thermostable viruses. Studies by Emmoth and others showed that swine parvovirus heated at 70ºC for 60 minutes resulted in 2.6 to 3.2 $\log_{10}$ titer reduction, while Alexander et al. (2004) demonstrated that enveloped ss RNA Newcastle disease virus could be inactivated (1 $\log_{10}$) at 70ºC within 82 seconds (Blümel et al., 2002; Emmoth, 2010). Heating medium influences heat sensitivity for some viruses (Yunoki et al., 2003). For example, enteroviruses in fresh sludge can be inactivated (5 $\log_{10}$ reduction) following heat exposure of 60ºC for 30 minutes, while in digested sludge 4 $\log_{10}$ reduction occurred within 4 minutes (Foliguet et al., 1972; Moce-Llivina et al., 2003).

Thermal Inactivation Modeling

Thermal Inactivation Models for Representative Enveloped and Non-enveloped Viruses. Thermal inactivation curves were developed using AI viruses and NDV as representatives of enveloped RNA viruses. These viruses included the highly virulent forms which are Select Agents that are handled and used under BSL-3E and ABSL-3E conditions. Also, low-virulent forms of these viruses (LPNAI including H5 and H7, and *l*NDV) which are BSL-2 viruses were included in these studies. Thermal inactivation curves were generated for HPAI/PA/83 (H5N2) and resulted in a thermal death rate as presented in Table 2. Heat exposure at 59ºC resulted in 5 $\log_{10}$ reduction within 6 minutes while exposure to heat treatment at 70º-82.2ºC resulted in total inactivation (6.6 log) in less than 30 seconds. The thermal inactivation data (D_t and *zD* values) for LPNAI/NY/94 (H7N2), presented in Table 3, show that as the temperature increased, LPNAI virus survival declined exponentially, inactivating 5 $\log_{10}$ at 59ºC within 5.5 minutes of heat exposure and total inactivation (6.25 $\log_{10}$) at 70ºC-82.2ºC in less than 30 seconds.

Thermal inactivation for *v*NDV/CA (Table 4) at 59ºC required at least 10 minutes and at 70ºC at least 5.5 minutes for a 6 $\log_{10}$ viral reduction, while heat exposure at 82.2ºC resulted in 8.8 $\log_{10}$ reduction in less than 30 seconds. For *l*NDV/B1 (Table 5) exposure at 59ºC

Table 2

D_t values (time required to reduce virus titer by 90% or 10^1 $TCID_{50}$) with standard deviation generated from predictive thermal inactivation equation of HPAI-A/ck/PA/1370/83 (H7N2).

Temperature (ºC)	D_t Value (min)	SD	Equation	R^2
55	12	+/-0.005	y = -0.0837x + 6.3116	0.96
57	4.8	+/-0.01	y = -0.2105x + 5.7903	0.96
58	2.3	+/-0.031	$y = 5.996e^{-0.1034x}$	0.99
59	1.3	+/-0.21	$y = 0.0444x^2 - 0.861x + 5.0173$	0.97
61	1.0	+/-0.09	y = -0.969x + 3.436	0.85
70	ND[4]	—	—	—
82.2	ND[5]	—	—	—
zD Value	5.3ºC	+/-0.03	y = -0.1883x + 11.372	0.93

[1] Infected with an initial titer of 6.4 log ($TCID_{50}$/ml) in PBS.
[2] Experiment was replicated three times.
[3] The correlation coefficient (R^2) indicated the goodness of fit of the predictive equation.
[4] ND—6.4 log_{10} reduction upon reaching 70ºC at time zero.
[5] ND—6.4 log_{10} reduction upon reaching 82.2ºC at time zero.

Table 3

D_t values (time required to reduce virus titer by 90% or 10^1 $TCID_{50}$) with standard deviation generated from predictive thermal inactivation equation of LPNAI A/ck/NY/13142-5/94.

Temperature (ºC)	D_t Value (min)	SD	Equation	R^2
53	21.7	+/-0.58	y = -0.0461x + 5.4767	0.61
55	2.8	+/-0.32	y = -0.3473x + 4.0462	0.87
57	2.2	+/-0.78	y = -0.4457x + 3.22	0.84
58	1.2	+/-0.28	y = -0.8817x + 4.74	0.96
59	1.1	+/-0.30	y = -0.7913x + 3.2837	0.99
61	0.8	+/-0.58	y = -1.1167x + 2.616	1.0
70	ND[4]	—	—	—
82.2	ND[5]	—	—	—
zD Value	5.7ºC	+/-0.04	y = -0.1575x + 9.353	0.80

[1] Infected with an initial titer of 6.25 log_{10} ($TCID_{50}$/ml) in PBS.
[2] Experiment was replicated three times.
[3] The correlation coefficient (R^2) indicated the goodness of fit of the predictive equation.
[4] ND—6.25 log_{10} reduction upon reaching 70ºC at time zero.
[5] ND—6.25log_{10} reduction upon reaching 82.2ºC at time zero.

resulted in the inactivation of 6 log_{10} viral titer within 16 minutes of heating; at 70ºC there was a 6 log_{10} reduction within 5 minutes, and at 82.2ºC, a greater than 6 log_{10} reduction of *l*NDV/B1 occurred within less than 30 seconds. Previous research supports our observation that AI viruses can be inactivated rapidly at temperatures above 59ºC. Thomas and colleagues (2008) observed the rapid inactivation of AI and NDV (7 log_{10} reduction) in chicken meat within 5 seconds of cooking at 73.9ºC. The change in thermal resistance data (*zD*) demonstrated that HPAI/PA/83 and LPNAI/NY/83 (Tables 2 and 3) had the most thermal resistance followed by *v*NDV/CA (Table 3), then *l*NDV/B1 (Table 4). The *zD* values for HPAI/PA/83 and LPNAI/NY/94 suggest that although they differ in being of high- and low-pathogenicity types, respectively, they had similar change in thermal resistance. *v*NDV was more thermally resistant than *l*NDV up to 70ºC, but at 82.2ºC *l*NDV demonstrated slightly more thermal resistance.

Ro/1145/08 and Reo/TX/99 were used to develop

Table 4

D_t values (time required to reduce virus titer by 90% or 10^1 $TCID_{50}$) with standard deviation generated from predictive thermal inactivation equation of *v*NDV Chicken/CA/212676/2002.

Temperature (ºC)	D_t Value (min)	SD	Equation	R^2
55	11.2	+/-0.6	y = -0.0893x + 8.7735	0.97
56	6	+/-0.4	y = -0.1694x + 8.7401	0.99
57	3.1	+/-0.37	$y = 8.6295e^{-0.0435x}$	0.98
58	3.1	+/-0.03	$y = 0.0149x^2 - 0.6161x + 8.8421$	0.992
59	1.5	+/-0.09	$y = 0.0193x^2 - 0.7107x + 8.00$	0.93
70	0.91	+/-0.08	y = -0.74x + 1.5	1
82.2	ND[4]	—	—	—
zD Value	4.9	+/-0.02	y = -0.2033x + 12.186	0.95

[1] Infected with an initial titer of 8.8 log_{10} ($TCID_{50}$/ml) in PBS.
[2] Experiment was replicated three times.
[3] The correlation coefficient (R^2) indicated the goodness of fit of the predictive equation.
[4] ND—8.8 log_{10} reduction within 30 seconds at 82.2ºC.

Table 5

D_t values (time required to reduce virus titer by 90% or 10^1 $TCID_{50}$) with standard deviation generated from predictive thermal inactivation equation of *l*NDV Chicken/U.S./B1/1948.

Temperature (ºC)	D_t Value (min)	SD	Equation	R^2
53	4.4	+/-0.02	$y = 9.0336e^{-0.0352x}$	0.82
55	3.2	+/-0.03	$y = 7.5789e^{-0.0394x}$	0.89
57	2.8	+/-0.05	$y = 8.0925e^{-0.1513x}$	0.97
58	2.9	+/-0.10	$y = 6.0713e^{-0.2132x}$	0.88
59	2.7	+/-0.12	$y = 4.7738e^{-0.1146x}$	0.8
61	1.95	+/-0.1	$y = 6.5755e^{-0.2732x}$	0.96
70	0.82	+/-0.15	$y = 2.84x^2 - 4.46x + 2.95$	1
82.2	ND[4]	—	—	—
zD Value	0.92	+/-0.05	y = 264.35e-0.0792	0.97

[1] Infected with an initial titer of 9.8 log_{10} ($TCID_{50}$/ml) in PBS.
[2] Experiment was replicated three times.
[3] The correlation coefficient (R^2) indicated the goodness of fit of the predictive equation.
[4] ND—9.8 log_{10} after 30 seconds of heat exposure at 82.2ºC.

anisothermic models to represent non-enveloped, double-stranded RNA viruses in the PBS model system. The survival data for Ro/1145/08 and Reo/TX/99 following anisothermic heat treatment at 25ºC to 82.2ºC for 140 seconds indicated that these viruses were more heat-resistant than AI viruses and NDV, requiring exposure of more than 2 minutes at 82.2ºC to inactivate 5 log_{10} $TCID_{50}$/ml of both viral populations. No virus was recovered for Ro/1145/08, Reo/TX/99 (5.3-5.8 log_{10} $TCID_{50}$/ml), and TAstV/07 following heat exposure at 82.2ºC for 140 seconds (2.3 minutes) (Table 6). Previous studies of survival and infectivity of reovirus and rotavirus following heat exposure determined that rotavirus was rapidly inactivated at 50ºC in 30 minutes with only 1% survival while 50% of a $4x10^7$ pfu/ml population of reovirus survived similar heat exposure (Estes et al., 1979).

The heat inactivation method of Reo/TX/99 and Ro/1145/08 used anisothermic heating gradient; therefore, thermal death rate at specific temperatures (D_t) or the change in thermal resistance (*zD*) could not be calculated. Nevertheless, thermal resistance or stability were observed in the anisothermic curve between 25ºC-50ºC

Table 6

Survival of Reovirus TX/99, Rotavirus 1145, and astrovirus following heat exposure from 25ºC to 82.2ºC over a ramping up time of 0 to 140 seconds with no holding time using a thermocycler. Astrovirus heated at 82.2ºC for 30 minutes.

Temperature (ºC)	Time (sec)	Titer (Log EID50/ml) Reovirus TX/99	Titer (Log EID50/ml) Rotavirus 1145	Survival of Astrovirus
25	10	5.33	5.8	9/10
40	35	4.73	5.73	—
50	60	4.73	5.77	—
60	85	4.03	3.67	7/10
70	110	<1.6	2.1	0/9
82.2	140	<1.6	<1.8	0/10
82.2	30 minutes holding time	—	—	0/10
zD (ºC)	—	1.5	1.2	—

[1] Astrovirus was detected in turkey embryo intestinal homogenates via RT-PCR.

followed by an exponential rate of decline between 50ºC and 82.2ºC. This trend could be supported by previous research which showed an initial lag phase between 45ºC-50ºC followed by a rapid exponential decline as temperature increased (Middleton et al., 2002). The thermal inactivation data suggest that Ro/1145/08 is more thermostable than Reo/TX/99 (Table 6). The thermal death rate (D_t) for both AIV and NDV viruses was between 1.1-2.7 minutes at 60ºC, and less than 30 seconds at 82.2ºC. The thermal inactivation for Reo/TX/99 and Ro/1145/08 was greater than a 4 $\log_{10}$ reduction within 2 minutes upon reaching 82.2ºC. Therefore, to obtain the 6 $\log_{10}$ sterility assurance level required, less than 30 seconds of heating at 82.2ºC for AI (HPAI/PA/83, LPNAI/NY/94, and *v*NDV/CA/2002, *l*NDV/B1/48), 1.8 minutes for TAstV/07, and at least 3 minutes for Reo/TX/99and Ro/1145/08 viruses are required.

EDS Validation of Enveloped and Non-enveloped Viruses

Thermal inactivation is an effective means of inactivating pathogens including viruses in liquid or sludge. In many facilities, the effluent is collected in tanks and exposed to indirect steam heating prior to discharge into the public sewerage. The Clean Water Act (CWA) of 1972 regulates water quality and the standard for the disposal of waste sludge set the standard for pathogen level in sludge waste, and for enteric viruses only 1PFU/4g sludge is acceptable (Anonymous, 1972; Anonymous, 1993). The *Biosafety in Microbiological and Biomedical Laboratories* (*BMBL*) manual recommends that thermal inactivation processes for laboratory waste (such as EDS) should ensure a sterility assurance level (SAL) of a 6 log reduction (CDC, 2007). In our validation study, enveloped and non-enveloped viruses were exposed to indirect steam heating at 82.2ºC for 6 hours using static EDS. For our final validation tests, no viable virus was recovered from any of the submerged vials of viruses in the EDS tanks (Table 7).

Enveloped Viruses

Avian metapneumovirus (aMPV) is relatively heat-labile and is routinely inactivated (> 3 $\log_{10}$) in laboratory procedures following 30 minutes of heat exposure at 56ºC or 60ºC for 10 minutes or autoclaving at 121ºC (15 psi) for 20 minutes (Calnek et al., 1971; Cook, 2000; Elhafi et al., 2004). Marek's disease virus is an avidly cell-associated virus and is extremely sensitive to environmental conditions so most research information is limited (Jarosinski et al., 2007; Nazerian et al., 1970). However, research on a related alphaherpes virus, pseudorabies virus (PrV) which is cell-free, shows that it can be inactivated by 7.1 $\log_{10}$ ffu/ml following pasteurization in milk (60ºC for 30 minutes), and by 6.6 $\log_{10}$ ffu/ml in plasma following steam treatment (60ºC for 10 hours plus 80ºC for 1 hour) (Chang et al., 2010; Sofer, 2003). Our EDS process completely inactivated 7.5 $\log_{10}$ aMPV $TCID_{50}$/ml and 9 $\log_{10}$ ffu/ml MDV, so inactivation was greater than the SAL requirement for EDS by at least 1.3-fold.

Avian influenza viruses (LPNAI/NY/94 and HPAI/PA/83) and Newcastle disease viruses (*l*NDV/1948/B1 and *v*NDV/CA/2002) were totally inactivated by the EDS process by greater than the required 6 $\log_{10}$ SAL or more than 1.3 times the SAL requirement (Table 7). The susceptibility of AI viruses and NDV to heat treatment has been demonstrated previously by, showing 7 $\log_{10}$ viral reduction of HPAI Korea/03, *v*NDV/CA and lNDV/Ulster in chicken meat following cooking at 70ºC for 5 seconds.

Table 7

The survival of enveloped and non-enveloped RNA and DNA viruses following the exposure to the effluent decontamination system (EDS) for 6 hours at 82.2ºC.

Virus Name	Initial Titer (log EID_{50}/ml, $TCID_{50}$/ml or infectious particle/ml)	Final Titer (log EID_{50}/ml, $TCID_{50}$/ml or infectious particle/ml)
Enveloped Viruses		
Avian metapneumovirus Colorado strain	7.5	<1
Marek's disease virus strain *Gallid herpesvirus 2* vaccine strain CVI988 (Merial)	9.0	<1
Lentogenic avian paramyxovirus strain Chicken/U.S./B1/1948 (B1)	8.2	<1
Velogenic avian paramyxovirus strain CK/U.S.(CA)/212676/2002 (S0212676)	8.5	<1
Highly pathogenic avian influenza virus strain A/chicken/PA/1370/1983 (H5N2)	6.5	<1
Low pathogenic notifiable avian influenza virus strain A/chicken/NY/13142-5/1994 (H7N2)	7.5	<1
Non-enveloped Viruses		
Reovirus strain Turkey/TX/SEP/98	11.1	<1.1
Rotavirus strain Turkey/NC/SEP-Ro996/07	5.1	<1.1
Astrovirus strain Turkey/CA/SEP-A938/07	8/10	0/10
Avian parvovirus strain chicken parvovirus, ChPV-P1	6.0	<1
Vegetative Bacteria	**CFU/ml**	**CFU/ml**
Salmonella enterica Enteritidis	9.1	<1

Other investigations showed similar log reduction in liquid egg products in less than 2.5 minutes at 63ºC (Swayne et al., 2004; Thomas et al., 2007; Thomas et al., 2008).

Non-enveloped Viruses

Non-enveloped viruses are usually more thermally resistant than enveloped viruses at the temperature range of 54ºC-61ºC (Blümel et al., 2002). Reovirus is more thermostable than rotavirus and both can survive and remain infectious following heat treatment at 50ºC for 30 minutes (Estes et al., 1979). Recent work (Middleton et al., 2002) demonstrated that heating at 62ºC for 30 minutes was required to inactivate 5 log pfu/ml. Astrovirus is highly thermostable and is difficult to titer at low concentration; therefore, for the EDS safety test the enumeration process was based on a fraction negative calculation. The initial inoculum of TAstV/07 was positive in 8/10 of the inoculated eggs. Following the EDS heat processing, all inoculated eggs were negative for astrovirus (Table 7). Astrovirus associated with Poult Enteritis Mortality Syndrome is considered relatively heat-resistant, surviving heat exposure at 60ºC for 10 minutes (Richards, 2001; Schultz-Cherry et al., 2001).

In the EDS validation process (82.2ºC for 6 hours), 6 $\log_{10}$ infectious dose/ml of chicken parvovirus (ChPV-P1) was totally inactivated as determined by *in vivo* tests (Table 7). Parvovirus is very thermostable and animal parvoviruses are more heat-stable than human parvovirus. Animal parvoviruses can resist heat exposure of 60ºC for 30 minutes, and some strains of bovine parvovirus (BPV) can be heat-resistant up to 100ºC dry heat for 30 minutes (Bräuniger et al., 2000; Yunoki et al., 2003). As an example, exposure of bovine parvovirus (BPV) to dry heat between 40ºC and 95ºC for 1 hour resulted in inactivation of less than 0.8 $\log_{10}$ $TCID_{50}$/ml, and for 2-hour incubation only 0.9 $\log_{10}$ $TCID_{50}$/ml was inactivated (Sauerbrei et al., 2009). In some strains of BPV, infectivity can be maintained for 4 days at 56ºC or for 8 hours at 70ºC (Durham et al., 1985). Animal parvovirus can survive the pasteurization process for human serum albumin at 60ºC for 10 hours (Blümel et al., 2002). One of the features of the heat inactivation of parvovirus is that the DNA is released from an intact capsid, thereby losing its ability to infect a host (Sauerbrei et al., 2009).

Salmonella

Following the EDS validation process (82.2ºC for 6 hours), 9.1 $\log_{10}$/ml of *Salmonella enterica* serovar Enteritidis was totally inactivated (Table 7). The EDS process should adequately inactivate *Salmonella* as shown in previous research where thermal death rate (D_t) for *Salmonella* spp. in ground chicken meat ranged from

43.3 minutes at D_{55} to 0.07 minutes at D_{70} with a change in thermal resistance (*zD* values) of 5.3ºC, and in homogenized whole eggs with thermal inactivation rates of 5.7 minutes at D_{54}, and 0.17 minutes at D_{60} with *zD* value of 3.95ºC (Jin et al., 2008; Murphy et al., 2004). The log reduction for *Salmonella* in the EDS process was more than 1.5-fold higher than the SAL requirement.

This validation of a moderate temperature (82.2ºC for 6 hours) EDS process verifies the effectiveness of the inactivation of both enveloped and non-enveloped RNA and DNA viruses, and *Salmonella* in liquid media showing greater than the 6 $\log_{10}$ reduction required by the Clean Water Act for wastewater discharge (Anonymous, 1972). However, fecal pathogens have been shown to survive better in solid waste than in liquid waste, suggesting that waste with a high content of organic matter may require longer thermal treatment times for inactivation of pathogens (Moce-Llivina et al., 2003; Yunoki et al., 2003). In our effluent decontamination system, the effluent had low quantities of organic matter, supporting the validity of our model system and the lack of a need to develop models that included high organic matter content. Our validation process indicates the following to support effective effluent decontamination from an avian pathogen research facility: 1) greater than 6-9 $\log_{10}$ EID_{50} or $TCID_{50}$/ml reduction for enveloped single-stranded RNA viruses (LPNAI/NY/94, HPAI/PA/83, *l*NDV/B1, *v*NDV/CA/2002, and aMPV) and enveloped double-stranded DNA virus (Marek's disease virus CVI988); 2) greater than 9 $\log_{10}$ cfu/ml reduction of a vegetative bacterial pathogen (S*almonella enterica* serovar Enteritidis); 3) greater than 5 $\log_{10}$ and 11 $\log_{10}$ $TCID_{50}$/ml reduction for non-enveloped double-stranded RNA viruses (rotavirus Ro/996/07) and reovirus Reo/TX/98, respectively; 4) no recovery of non-enveloped positive sense RNA virus (astrovirus TAstV/07) using 10 embryonating turkey eggs; and 5) at least 6 $\log_{10}$ reduction in non-enveloped single-stranded DNA virus (chicken parvovirus ChPV-P1). This assures that the effluent released to the municipal wastewater system is free of bacterial and viable viral pathogens (Table 7).

Conclusion

The heat inactivation models predicted that the reduction of 6 $\log_{10}$ $TCID_{50}$/ml of the BSL-3 agents (HPAI/PA/83 (H5N2) and *v*NDV/CA/2002) would occur within 30 seconds at 82.2ºC; therefore, the EDS treatment at 82.2ºC for 6 hours has a margin of safety 720-fold higher than is required. The BSL-2 agents would require at least 3 minutes to inactivate 6 $\log_{10}$ virus $TCID_{50}$/ml, so the EDS treatment would be 120-fold higher than is necessary.

The EDS tank inactivation system demonstrated that the enveloped and non-enveloped RNA and DNA viruses and *Salmonella* would be inactivated within the 6 hours at 82.2ºC, giving a significant margin of safety. The EDS validation process confirms that the 6 log reduction of pathogens required for sanitary assurance level for effluent release to the municipal waste system can be achieved.

Acknowledgments

This study was funded by the U.S. Department of Agriculture, Agriculture Research Service through Cooperative State Information System (CRIS) Project #6612-32000-048-00D. *Correspondence should be addressed to David E. Swayne at david.swayne@ars.usda.gov.

References

Alexander, D. J., & Manvell, R. J. (2004). Heat inactivation of Newcastle disease virus (strain Herts 33/56) in artificially infected chicken meat homogenate. *Avian Pathology, 33*(2), 222-225.

Alexander, D. J. (2005). Avian influenza. *Manual for diagnostic tests and vaccines for terrestrial animals* (p. 2.7.12). Paris: World Organization for Animal Health.

Anonymous. (1972). Clean Water Act, 33 CFR. 301(d), 304(b), 304(g), 304(m) and 307(b). 86. United States of America.

Anonymous. (1981). Secondary Treatment Regulation. 1314(d)(1) U.S.C. 86. United States of America.

Anonymous. (1993). Standards for the Use and Disposal of Sludge. 40 CFR. 503.32 D(a)(3). United States of America.

Blümel, J., Schmidt, I., Willkommen, H., & Löwer, J. (2002). Inactivation of parvovirus B19 during pasteurization of human serum albumin. *Transfusion, 42,* 1011-1018.

Bräuniger, S., Peters, J., Borchers, U., Kao, M., & Borchers, U. (2000). Further studies on thermal resistance of bovine parvovirus against moist and dry heat. *International Journal of Hygiene and Environmental Health, 203,* 71-75.

Calnek, B. W., & Adldinger, H. K. (1971). Some characteristics of cell-free preparations of Marek's disease virus. *Avian Diseases, 15,* 508-517.

Centers for Disease Control and Prevention (CDC). (2007). Viral agents. In *Biosafety in microbiological and biomedical laboratories,* (5th ed.). Washington, DC: U.S. Health and Human Services Publication, Government Printing Office.

Chang, J. T., Chou, Y. C., Lin, M. S., & Wang, S. R. (2010). Inactivation strategy for pseudorabies virus in milk for production of biopharmaceuticals. *Japan Journal of Veterinary Research, 58,* 179-183.

Cook, J. K. A. (2000). Avian pneumovirus infections of turkeys and chickens. *The Veterinary Journal, 160,* 118-125.

Das, A., Spackman, E., Pantin-Jackwood, M. J., & Suarez, D. L. (2009). Removal of real-time reverse transcription polymerase chain reaction (RT-PCR) inhibitors associated with cloacal swab samples and tissues for improved diagnosis of avian influenza virus by RT-PCR. *Journal of Veterinary Diagnostic Investigation, 21,* 771-778.

Day, J. M., Spackman, E., & Pantin-Jackwood, M. (2007). A multiplex RT-PCR test for the differential identification of turkey astrovirus type 1, turkey astrovirus type 2, chicken astrovirus, avian nephritis virus, and avian rotavirus. *Avian Diseases, 51,* 681-684.

Durham, P. J. K., & Johnson, R. H. (1985). Properties of an Australian isolate of bovine parvovirus type 1. *Veterinary Microbiology, 10,* 335-345.

Elhafi, G., Naylor, C. J., Savage, C. E., & Jones, R. C. (2004). Microwave or autoclave treatments destroy the infectivity of infectious bronchitis virus and avian pneumovirus but allow detection by reverse transcriptase-polymerase chain reaction. *Avian Pathology, 33,* 303-306.

Emmoth, E. (2010). *Virus inactivation—Evaluation of processes used in biowaste management.* Thesis. Uppsala, Sweden: Department of Biomedical Sciences and Veterinary Public Health Swedish University of Agricultural Sciences.

Estes, M. K., Graham, D. Y., Smith, E. M., & Gerba, C. P. (1979). Rotavirus stability and inactivation. Available at: http://vir.sgmjournals.org/cgi/content/abstract/43/2/403.

Foliguet, J.-M., & Doncoeur, F. (1972). Inactivation assays of enteroviruses and *Salmonella* in fresh and digested wastewater sludges by pasteurization. *Water Research, 6,* 1399-1407.

Jarosinski, K. W., Margulis, N. G., Kamil, J. P., Spatz, S. J., Nair, V. K., & Osterrieder, N. (2007). Horizontal transmission of Marek's disease virus requires US2, the UL13 protein kinase, and gC. *Journal of Virology, 81,* 10575-10587.

Jin, T., Zhang, H., Boyd, G., & Tang, J. (2008). Thermal resistance of *Salmonella enteritidis* and *Escherichia coli* K12 in liquid egg determined by thermal-death-time disks. *Journal of Food Engineering, 84,* 608-614.

Middleton, J. K., Severson, T. F., Chandran, K., Gillian, A. L., Yin, J., & Nibert, M. L. (2002). Thermostability of reovirus disassembly intermediates (ISVPs) correlates with genetic, biochemical, and thermodynamic properties of major surface protein. *Journal of Virology, 76,* 1051-1061.

Moce-Llivina, L., Muniesa, M., Pimenta-Vale, H., Lucena, F., & Jofre, J. (2003). Survival of bacterial indicator species and bacteriophages after thermal treatment of sludge and sewage. *Applied and Environmental Microbiology, 69,* 1452-1456.

Murphy, R. Y., Osaili, T., Duncan, L. K., & Marcy, J. A. (2004). Thermal inactivation of *Salmonella* and *Listeria monocytogenes* in ground chicken thigh/leg meat and skin. *Poultry Science, 83,* 1218-1225.

Nazerian, K., & Witter, R. L. (1970). Cell-free transmission and *in vivo* replication of Marek's disease virus. *Journal of Virology, 5,* 388-397.

Reed, L. J., & Muench, H. (1938). A simple method of estimating fifty percent endpoints. *The American Journal of Hygiene, 27,* 493-497.

Richards, G. P. (2001). Enteric virus contamination of foods through industrial practices: A primer on intervention strategies. *Journal of Industrial Microbiology and Biotechnology, 27,* 117-125.

Sauerbrei, A., & Wutzler, P. (2009). Testing thermal resistance of viruses. *Archives of Virology, 154,* 115-119.

Schultz-Cherry, S., King, D. J., & Koci, M. D. (2001). Inactivation of an astrovirus associated with Poult Enteritis Mortality Syndrome. *Avian Diseases, 45,* 78-82.

Senne, D. (2008). Virus propagation in embroyonating eggs. In L. Dufour-Zavala (Ed.), *A laboratory manual for the isolation, identification and characterization of avian pathogens.* Jacksonville, FL: American Association of Avian Pathologists.

Sofer, G. (2003). *Part 3a, Plasma and plasma products (heat and solvent/detergent treatment)*. Virus Inactivation Series. Available at: http://biopharminternational.findpharma.com/biopharm/issue/issueDetail.jsp?id=2428.

Southeast Poultry Research Laboratory (SEPRL). (2009). *Biosafety/Biosecurity Guidelines, V* (p. 36). Athens, GA: SEPRL.

Spackman, E., Pantin-Jackwood, M., Day, J. M., & Sellers, H. (2005). The pathogenesis of turkey origin reoviruses in turkeys and chickens. *Avian Pathology, 34,* 291-296.

Swayne, D. E., & Beck, J. R. (2004). Heat inactivation of avian influenza and Newcastle disease viruses in egg products. *Avian Pathology, 33,* 512-518.

Swayne, D. E., Senne, D. A., & Beard, C. W. (1998). Avian influenza. In D. E. Swayne, J. R. Glisson, M. W. Jackwood, J. E. Pearson, & W. M. Reed (Eds.), *A laboratory manual for the isolation and identification of avian pathogens* (pp. 150-155). Tallahassee, FL: American Association of Avian Pathologists.

Theil, K. W., Reynolds, D. L., & Saif, Y. M. (1986). Isolation and serial propagation of turkey rotaviruses in a fetal rhesus monkey kidney (MA104) cell line. *Avian Diseases, 30,* 93-104.

Thomas, C., King, D. J., & Swayne, D. E. (2008). Thermal inactivation of avian influenza and Newcastle disease viruses in chicken meat. *Journal of Food Protection, 71,* 1214-1222.

Thomas, C., & Swayne, D. E. (2007). Thermal inactivation of H5N1 high pathogenicity avian influenza virus in naturally infected chicken meat. *Journal of Food Protection, 70,* 674-680.

Yu, Q., Estevez, C., Song, M., Kapczynski, D., & Zsak, L. (2010). Generation and biological assessment of recombinant avian metapneumovirus subgroup C (aMPV-C) viruses containing different lengths of the G gene. *Virus Research, 147,* 182-188.

Yunoki, M., Tsujikawa, M., Urayama, T., Sasaki, Y., Morita, M., Tanaka, H., et al. (2003). Heat sensitivity of human parvovirus B19. *Vox Sanguinis, 85,* 67-68.

Zsak, L., Strother, K. O., & Day, J. M. (2009). Development of a polymerase chain reaction procedure for detection of chicken and turkey parvoviruses. *Avian Diseases, 53,* 83-88.

Virus Genes (2011) 42:331–338
DOI 10.1007/s11262-011-0573-0

Comparative genomic sequence analysis of the Marek's disease vaccine strain SB-1

Stephen J. Spatz · Karel A. Schat

Received: 9 October 2010 / Accepted: 9 January 2011 / Published online: 20 February 2011
© Springer Science+Business Media, LLC (Outside the USA) 2011

Abstract Marek's disease virus (MDV), an oncogenic alphaherpesvirus, induces a rapid onset T-cell lymphoma and demyelinating disease in chickens. Since the 1970s the disease has been controlled through mass vaccination with herpesvirus of turkeys [meleagrid herpesvirus type 1 (MeHV-1)]. Over time this vaccine's efficacy decreased, and in the 1980s a bivalent vaccine consisting of MeHV-1 and a non-oncogenic gallid herpesvirus type 3 (GaHV-3) strain known as SB-1 was introduced. The complete DNA sequence (165,994 bp) of this GaHV-3 strain was determined using 454 pyrosequencing. A total of 524 open reading frames (ORFs) were examined for homology to protein sequences present in GenBank using BLAST (*E*-values <0.9). Of the 128 ORF hits, 75 ORFs showed homology to well-characterized alphaherpesviral proteins. Phylogenetically, this strain partitions in its own branch along with the GaHV-3 strain HPRS24 and shows more relatedness to MeHV-1 than gallid herpesvirus type 2 (GaHV-2, Marek's disease virus). When comparing the GaHV-3 ORFs to their homologues in MeHV-1 and GaHV-2, a greater percentage of amino acid similarity was found with homologous ORFs in the genome of SB-1 than with those in the HPRS24 genome. Overall, twice as many of the 75 ORFs within the SB-1 genome showed greater sequence identities and similarities to homologous ORFs in the Marek's disease genome than those within the HPRS24 genome. This paper describes the sequence difference between the two GaHV-3 genomes. Overall 19 ORFs differ in the number of predicted amino acids; of these, eight ($U_L3.5$, U_L5, U_L9, U_L28, U_L30, U_L36, U_L37, and U_L50) encode well-characterized alphaherpesviral proteins A sequence within the unique short region of the SB-1 genome exhibited significant sequence homology to long terminal repeat (LTR) sequences of avian retroviruses. This sequence was only found in the SB-1 genome and not the HPRS24 genome.

Keywords Marek's disease · Gallid herpesvirus type 3 · DNA sequence · Vaccine · SB-1

S. J. Spatz (✉)
Southeast Poultry Research Laboratory, Agricultural Research Service, United States Department of Agriculture, Athens, GA 30605, USA
e-mail: Stephen.Spatz@ars.usda.gov

K. A. Schat
Department of Microbiology and Immunology, College of Veterinary Medicine, Cornell University, Ithaca, NY 14853, USA
e-mail: kas24@cornell.edu

Introduction

Marek's disease (MD) is a contagious lymphoproliferative disorder of chickens and has been identified as a major cause of poultry mortality in many countries since its description as polyneuritis by Josef Marek in 1907 [1]. The causative agent of MD is an avidly cell-associated alphaherpesvirus called gallid herpesvirus type 2 (GaHV-2), commonly called Marek's disease virus type 1 (MDV-1) [2]. Based on data obtained by indirect immunofluorescence, agar gel precipitin and neutralization tests, three so-called serotypes of MDV have historically been described [3, 4]. Serotype 1 (MDV-1) is the oncogenic virus that causes MD. Serotype 2 (MDV-2) or gallid herpesvirus 3 (GaHV-3) is the non-oncogenic type which is used along with serotype 3 (MDV-3) in bivalent vaccine formulations. Confusingly, MDV-3 is really a herpesvirus of turkeys

(HVT) and is currently called meleagrid herpesvirus type 1 (MeHV-1) [1].

The first effective vaccines against Marek's disease were developed by Churchill et al. [5] in the late 1960s. These vaccines were live-attenuated serotype 1 viruses that lost their oncogenicity following extensive serial passage in cell culture. However, it was shown that these viruses could revert to their original oncogenic potential through back passage in birds. Within a year of their introduction, a safer vaccine was developed based on the non-oncogenic serotype 3 HVT [6, 7]. Later it was demonstrated by Calnek el al. [8] that inclusion of the serotype 2 strain SB-1 in HVT vaccines provided greater protection against challenge with the newly discovered very virulent (vv) pathotype of MDV.

There are three representative isolates of serotype 2 viruses: SB-1, HPRS24, and HN-1 [9]. Interestingly, not all serotype 2 strains protect equally against MD. It has been reported that SB-1 is superior to HPRS24 in protection against virulent MDV (Schat, K, personal communication). In 2000, Izumiya et al. [9] determined the nucleotide sequence of the HPRS24 strain. Our purpose in determining the nucleotide sequence of SB-1 was to investigate whether a bioinformatic comparison of the sequences would provide insight into why SB-1 is superior in eliciting protective immunity. We now present the complete DNA sequence of the SB-1 strain of serotype 2 and its comparison to HPRS24 and very virulent plus (vv+) serotype 1 strain Md5.

Materials and methods

Virus and cells

Gallid herpesvirus type 3 strain SB-1 at passage 27 was used in this study. Primary or secondary chicken embryo fibroblasts (CEFs) were maintained in Dulbecco's modified essential medium supplemented with 8% fetal bovine serum and used to propagate SB-1. Nucleocapsid DNA was isolated from infected CEFs using the methods described by Volkening and Spatz [10].

DNA sequencing and analysis

Sequencing of 5.0 μg of SB-1 was carried out commercially on a pyrosequencing platform, the Genome Sequencer 20 (GS20) system (454 Life Sciences). This involved the construction of random libraries of SB-1 DNA using the methodology described by Margulies et al. [11] with slight modifications as detailed by 454 Life Sciences. The SB-1 DNA sequence was assembled from 54248 reads using GS De Novo Assembler (454 Life Sciences) and Sequencher (Gene Codes, Ann Arbor, MI). The final sequence represents a 30-fold coverage at each base pair. Ambiguities in the sequencing data and problematic regions containing mono-nucleotide reiterations were re-sequenced from PCR products generated in reactions containing Platinum Taq DNA polymerase (Invitrogen, Carlsbad, CA) and numerous custom primers. The BigDye terminator cycle sequencing protocol was used for Sanger-based DNA sequencing. Reactions were resolved on a model ABI-3730 XL DNA Analyzer (Applied Biosystems, Foster City, CA). DNA sequences were maintained and analyzed using Lasergene (DNASTAR, Madison, WI), NCBI Entrez and other web-based tools. Homology searches were conducted using the NCBI program blastP with default settings. Multiple alignments of proteins and nucleotide sequences were generated using MAFFT [12] and SCAN2 (Softberry.com).

Results and discussion

Phylogenetic relatedness

The nucleotide sequence of the GaHV-3 strain SB-1 has been assigned GenBank accession number HQ840738. Phylogenetically, SB-1 and HPRS24 are more similar to the turkey herpesvirus (MeHV-1) than to the chicken virus (GaHV-2), the causative agent of Marek's disease (Fig. 1). Both GaHV-3 and MeHV-1 are used as vaccines against Marek's disease, so this is somewhat surprising since GaHV-3 and GaHV-2 are chicken viruses. Furthermore, SB-1 was originally added to the MeHV-1 Marek's disease vaccine to increase its protective index. Two other economically important avian herpesviruses—GaHV-1, the causative agent of infectious laryngotracheitis, and DEV (duck enteritis virus), which causes duck plague—are only distantly related to the GaHV-3 strains.

Genomic organization

The SB-1 genome was found to contain 54% G+C base composition with a length of 165,994 base pairs (bp), a size slightly larger than the other sequenced GaHV-3 strain, HPRS24 (164,270 bp). There is 98.4% sequence identity between the two GaHV-3 genomes. Both genomes show approximately 61% sequence identity with the sequence of the GaHV-2 strain Md5. The GaHV-3 genomes, like those of GaHV-2 and MeHV-1, are organized similar to other class E alphaherpesviruses with six genomic regions (see Davison for review) [13, 14]. The unique long (U_L) region of SB-1 is 109,744 bp in length and extends from positions 12,209 to 121,952. The unique short (U_S) region is 12,910 bp in length and extends from positions 143,514 to

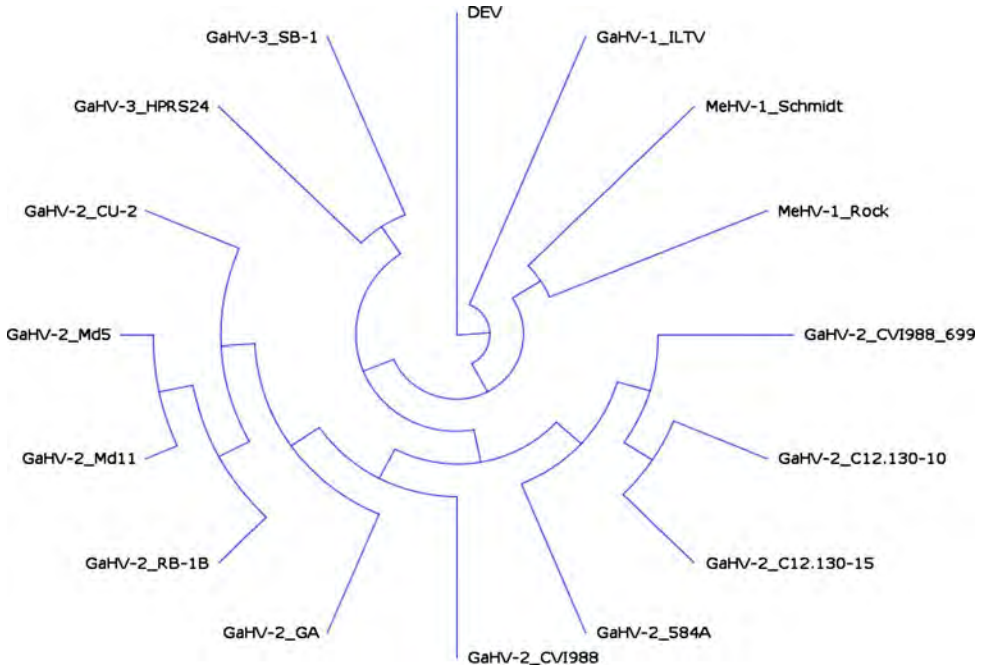

Fig. 1 Dendrogram showing the evolutionary relatedness of the avian herpesvirus strains whose nucleotide sequence has been determined: gallid herpesvirus 1 (GaHV-1), gallid herpesvirus 2 (GaHV-2), gallid herpesvirus 3 (GaHV-3), meleagrid herpesvirus 1 (MeHV-1) and duck enteritis virus (DEV); the GenBank accession numbers are NC_006623, AF243438, AB049735, AF291866 and EU082088, respectively. Alignments and tree drawing were done using the MAFFT program

156,423. The sequencing technology used in this study is incapable of differentiating the repeats due to the lengths of the reads (<500 bp). The U_L region is flanked by the terminal repeat long (TR_L) and internal repeat long regions which differ in length (11,943 bp and 11,989 bp, respectively). An extra 46 bp sequence is present in one of the repeats. The internal repeat short (IR_S) and terminal repeat short (TR_S) regions flanking the U_S region also differ in length (9307 and 9306 bp).

The exact TR_L–U_L, U_L–IR_L, IR_S–U_S, and U_S-TR_S boundaries were determined by multiple alignments of complementary and reverse complimentary DNA sequences surrounding the junctions and extending into unique regions. Table 1 summarizes the differences in the genomics regions of SB-1 and another strain of GaHV-3, HPRS24. There are minor differences in the junctions separating the genomic regions. Visual inspection of a whole genome alignment of SB-1 and HPRS24 has identified a HPRS24-specific 48 bp sequence (GCGGGCGAC GACGCGGGCGACGACCCGGGCGCCGACCCGGGC GACGAC) at the beginning of the unique long region. This sequence is not found in the SB-1 genome. Because of this, the genes spanning the junctions differ in size. These genes (ORF 044) are positional homologues of pp24 in GaHV-2 and differ by 16 amino acids (aa) (175 aa for HPRS24 and 159 aa for SB-1). Likewise, there are slight sequence differences in the U_L/IR_L junctions. A 48 bp sequence (CGCGCTCGGCGCGCCGGAGCAGGCGCGCGTGCGC CTCGTCCGCGTCCG) which is part of the IR_L of SB-1 is at the 3′ end of the U_L of HPRS24. Similar heterogeneity has been reported at the ends of the U_L and U_S regions of the herpes simplex virus type 1 genome Furthermore, there is a SB-1-specific 84 bp sequence (CGTCCGCGCCCGGG TCGTCGCCCGGGTCGTCGCCCGGGTCGGCGCCCGG GTCGTCGCCCGCGCCCGCGCCCGCGTCGTCGCCCG) at the beginning of the internal repeat long that is absent in the HPRS24 genome. Because of these two differences, the lengths of the genes (ORF 369, positional homologues of GaHV-2 pp38) spanning the U_L/IR_L junctions also differ (249 aa for SB-1 and 221 aa for HPRS24. Other differences between these genomes occur at the IR_L/IR_S junction containing the a-like sequence. Within the SB-1 genome there is a 650 base pair sequence downstream of the *pac-2* site which is absent in the HPRS24 genome. Differences also exist within the a-like sequences of the two genomes in terms of the number of telomeric sequences (TAACCC). This is not surprising since sequence variability within a-like sequences and immediately adjacent regions have been reported in GaHV-2 genomes [15].

One notable difference between the sequences of the SB-1 and HPRS24 genomes is the length of the U_S region (Table 1). This region differs by 801 bp in the two strains (Table 1: 12,910 bp in SB-1 vs. 12,109 in HPRS24). Analysis of the SB-1/HPRS24 genomic alignment identified a unique 792 bp sequence within the 3′ end of the U_S region in the SB-1 genome next to the TR_S region. Search

Table 1 A comparison of the lengths of the six subgenomic regions within the genomes of GaHV-3 strains SB-1 and HPRS24

	Start	End	Length		Start	End	Length
SB-1				HPRS24			
a-like	1	265	265	a-like	1	7	7
TRL	266	12208	11943	TRL	8	11825	11818
UL	12209	121952	109744	UL	11826	121757	109932
IRL	121953	133941	11989	IRL	121758	133575	11818
a-like	133942	134206	265	a-like	133576	134052	477
IRS	134207	143513	9307	IRS	134053	142680	8628
US	143514	156423	12910	US	142681	154789	12109
TRS	156424	165729	9306	TRS	154790	163408	8619
a-like	165730	165994	265	a-like	163409	164270	862

The length of the a-like sequences from *pac*1 through *pac*2 is also presented

of the nucleotide sequence collection in GenBank revealed that this sequence is homologous (*E*-value 5e−91) to the long terminal repeat (LTR) of Rous sarcoma virus 0. This sequence of three repeats (Fig. 2) is not found in HPRS24 and largely accounts for the length difference in the U_S region between the two GaHV-3 strains. Interestingly, similar LTR insertions have been identified in the related avian herpesvirus GaHV-2 within this junction region [16–22]. These insertions have been identified in field isolates as well as in the end results of co-cultivation experiments. The significance of this is unknown but it is likely that these insertions will affect the expression of neighboring genes. It is also unknown whether the insertion occurred during passage of SB-1 in cell culture or was present in the original isolate. Since we sequenced the 27th passage, it will be interesting to amplify this region and determined its nucleotide sequence from earlier passages.

Differences in open reading frames between SB-1 and HPRS24

The genome of SB-1 contains 524 open reading frames (ORFs) encoding proteins with at least 50 amino acids (aa). Using the NCBI BLAST program each ORF was investigated for similarity to other proteins found in GenBank (*E*-value cutoff of 0.9). Of these, only 128 translated ORFs showed sequence homology to proteins in the GenBank data set. This was not unexpected since human herpesviruses encode between 71 ORFs (human herpesvirus type 3, 124 Kb genome) and 203 (human herpesvirus type 5, 239 Kb genome) [23]. Only 75 SB-1 ORFs exhibited homology to OFRs annotated in the genome of HPRS24. Most of these ORFs were identical in length to those found in the HPRS24 genome except for the 19 ORFs listed in Table 2. Eight nucleotides (four nucleotides in two regions) differed in the ORF encoding RLORF1 between HPR24 and SB-1. Within the SB-1 genome, 4, 6, 5 and 5 base pairs were absent in ORFs 5, 6, 28 and 37, respectively, relative to HPRS24. The differences in the lengths of ORFs 24, 25, 29, 53, 68, 72, 241, 299 and 331 were due to single nucleotide changes. Open reading frames 43 and 369 differed in length due to heterogeneity at the termini of the U_L region. There is a 108 bp difference in the length of U_L9 (ORF 098) in the two genomes. Because of this the U_L9 of HPRS24 and SB-1 are predicted to encode 875 and 839 aa proteins, respectively. The 841 amino acid size of U_L9 (SB-1) is identical in length to the U_L9 homologue

```
                    *        20         *        40         *        60         *        80
Repeat1     : TGAAGCCTTCTGCTTCATTCAGGTGTTCGCAATCGTTAGGGACTCAACGGTCTGTCCATCTACCCAGGTGCACACCAATGTG :  82
Repeat2     : ---------------------------------CGTTAGGGACTCAACGGTCTGTCCATCTACCCAGGTGCACACCAATGTG :  49
Repeat3     : ---------------------------------CGTTAGGGACTCAACGGTCTGTCCATCTACCCAGGTGCACACCAATGTG :  49
PDRC-3249   : TGAAGCCTTCTGCTTCATTCAGGTGTTCGCAATCGTTAGGGACTCAACGGTCTGTCCATCTACCCAGGTGCACACCAATGTG :  82

                   *       100         *       120         *       140         *       160
Repeat1     : GTGAATGGTAAAATGGCGTTTATTTGATGGTGGCAACAGCTTATATAATCGTGCATAGCTTCGTCTACGCCCATATGTCCTT : 164
Repeat2     : GTGAATGGTAAAATGGCGTTTATTTGATGGTGGCAACAGCTTATATAATCGTGCATAGCTTCGTCTACGCCCATATGTCCTT : 131
Repeat3     : GTGAATGGTAAAATGGCGTTTATTTGATGGTGGCAACAGCTTATATAATCGTGCATAGCTTCGTCTACGCCCATATGTCCTT : 131
PDRC-3249   : GTGAATGGTAAAATGGCGTTTATTTGATGGTGGCAACAGCTTATATAATCGTACATAGCTTCGTCTACGCCCATATGTCCTT : 164

                 *       180         *       200         *       220         *       240
Repeat1     : GCGTCATTCCTTCCTTATCTAGTTGCCACCAATGAGCATATGGAATGTCTTGCTTTTTCCTTATTTGGTCTTTAGACTATTC : 246
Repeat2     : GCGTCATTCCTTCCTTATCTAGTTGCCACCAATGAGCATATGGAATGTCTTGCTTTTTCCTTATTTGGTCTTTAGACTATTC : 213
Repeat3     : GCGTCATTCCTTCCTTATCTAGTTGCCACCAATGAGCATATGGAATGTCTTGCTTTTTCCTTATTTGGTCTTTAGACTATTC : 213
PDRC-3249   : GCGTCATTCCTTCCTTATCTAGTCGCCACCAATGAGCATATGGAATGTCTTGCTTTTTCCTTATTTGGTCTTTAGACTATTC : 246

               *       260         *       280         *       300         *       320
Repeat1     : AAGTTGCCTCTGGCTCTATTTGACTACATTTCCCCCTCCCTAT-------------------------------------- : 289
Repeat2     : AAGTTGCCTCTGGCTCTATTTGACTACATTTCCCCCTCCCTAT-------------------------------------- : 256
Repeat3     : AAGTTGCCTCTGGCTCTATTTGACTACA----------------------------------------------------- : 241
PDRC-3249   : AAGCTACCTCTGGCTCTATTTGACTACATTTCCCCCTCCCTATGCAAAAGCGCAACTACTATATCCTGAGGGGACTCCTAAC : 328
```

Fig. 2 Multiple nucleotide sequence alignment of a 792 bp sequence found at the U_S/TR_S junction within the SB-1 genome. The sequence consisting of three connected repeats (1, 2 and 3) was broken down to demonstrate the sequence identities with LTR of the avian leucosis strain PDRC-3249 (GenBank accession number EU070902)

Table 2 A comparison of 19 ORFs that differ in amino acid lengths between the SB-1 and HPRS24 genomes

Gene #	Common name	SB-1	HPRS24	MDV	HVT	Function
2	R-LORF1	63	176	198		Unknown
5		63	29			Unknown
6		50	52			Unknown
24		54	39			Unknown
25		97	102			Unknown
28		51	96			Unknown
29		62	49			Unknown
37		170	263			Unknown
43	pp24	159	175	155		Unknown
53		363	437			Unknown
68	UL3.5	84	89	58	74	Tegument protein, virus egress
72	UL5	857	858	858	858	DNA helicase–primase associated protein
98	UL9	839	875	841	839	Origin binding protein
199	UL28	787	811	793	787	DNA packaging protein
219	UL30	1211	1190	1220	1205	DNA polymerase
241	UL36	3068	3064	3334	3112	Large tegument protein
261	UL37	1099	1040	1046	1041	Tegument protein
331	UL50	435	395	436	437	dUTPase
369	pp38	249	221	290		Unknown

The sizes of predicted polypeptides from homologous genes in the genomes of GaHV-2 strain Md5 (GenBank accession number AF243438) and MeHV-1 strain (GenBank accession number AF291866) are also included

encoded by MeHV-1. ORF 219, encoding the U_L30 homologue, also differs significantly (63 bp) when comparing the two genomes (1211 aa for SB-1 and 1190 aa for HPRS24). In aligning the U_L37 homologue (ORF 261) of the two strains, gaps were identified in three stretches of nucleotides, totaling 22 bp. It is hard to assess whether these differences in amino acid length are real or the result of sequencing errors. The fold coverage for the HPRS24 genome was not reported by Izumiya. In order to resolve this, these regions of difference would have to be resequenced using HPRS24 DNA. However, the SB-1 ORFs encoding U_L9, U_L28, U_L30, U_L37, and U_L50 are statistically more similar to the average length of homologous ORFs in the genomes of MDV and HVT than those in the HPRS24 genome.

To further investigate differences in the ORFs encoding $U_L3.5$, U_L9, U_L28, U_L30, U_L37, and U_L50, multiple alignments were generated with corresponding homologues found in the genomes of the other sequenced avian herpesviruses: GaHV-2, MeHV-1, GaHV-1, and DEV. These alignments are presented in Fig. 3a, b. The carboxyl terminus of $U_L3.5$ in the SB-1 and HPRS24 genomes differs due to an additional cytosine residue within $U_L3.5$ of HPRS24. An additional 36 aa are present in the predicted translation product of the UL9 gene of HPRS24. This in-frame addition occurred in a stretch of 9 amino acids [RL(L/I)IQ(I/L)ESL] that is highly conserved among avian herpesviruses. Twenty-one amino acids appear to be missing in the U_L30 gene of HPRS24. This also occurred in an area of highly conserved amino acids. A single guanine residue near the 3′ end of the U_L28 gene differentiates SB-1 from HPRS24. Since the carboxyl termini of other gallid herpesviruses U_L28 homologues are conserved, the missing guanine residue in HPRS24 is likely a sequencing error. There are three areas within the U_L37 gene that differs between the GaHV-3 genomes. One region is shown in Fig. 3a, in which a 6 aa stretch appears to be missing in the U_L37 gene of HPRS23. However, it occurred in a region of low sequence conservation so it is hard to draw any conclusions regarding the accuracy of the sequencing data. Lastly, a cytosine residue near the 3′ terminus of U_L50 differentiates the two GaHV-3 genomes. This is predicted to cause a reading frame shift, since in this case there is significant sequence conservation (See GFGSTG in Fig. 3b) at the carboxyl terminus, and suggests a sequencing error with HPRS24. Overall, the sequencing comparison suggests the possibility of errors in the published HPRS24 nucleotide sequence. This is not surprising since this sequence was generated using Sanger-based technologies with radioactive nucleotides, numerous urea gels and manual reads. However, resequencing of the HPRS24 genome or at least selected genomic regions is needed to definitively resolve these problems.

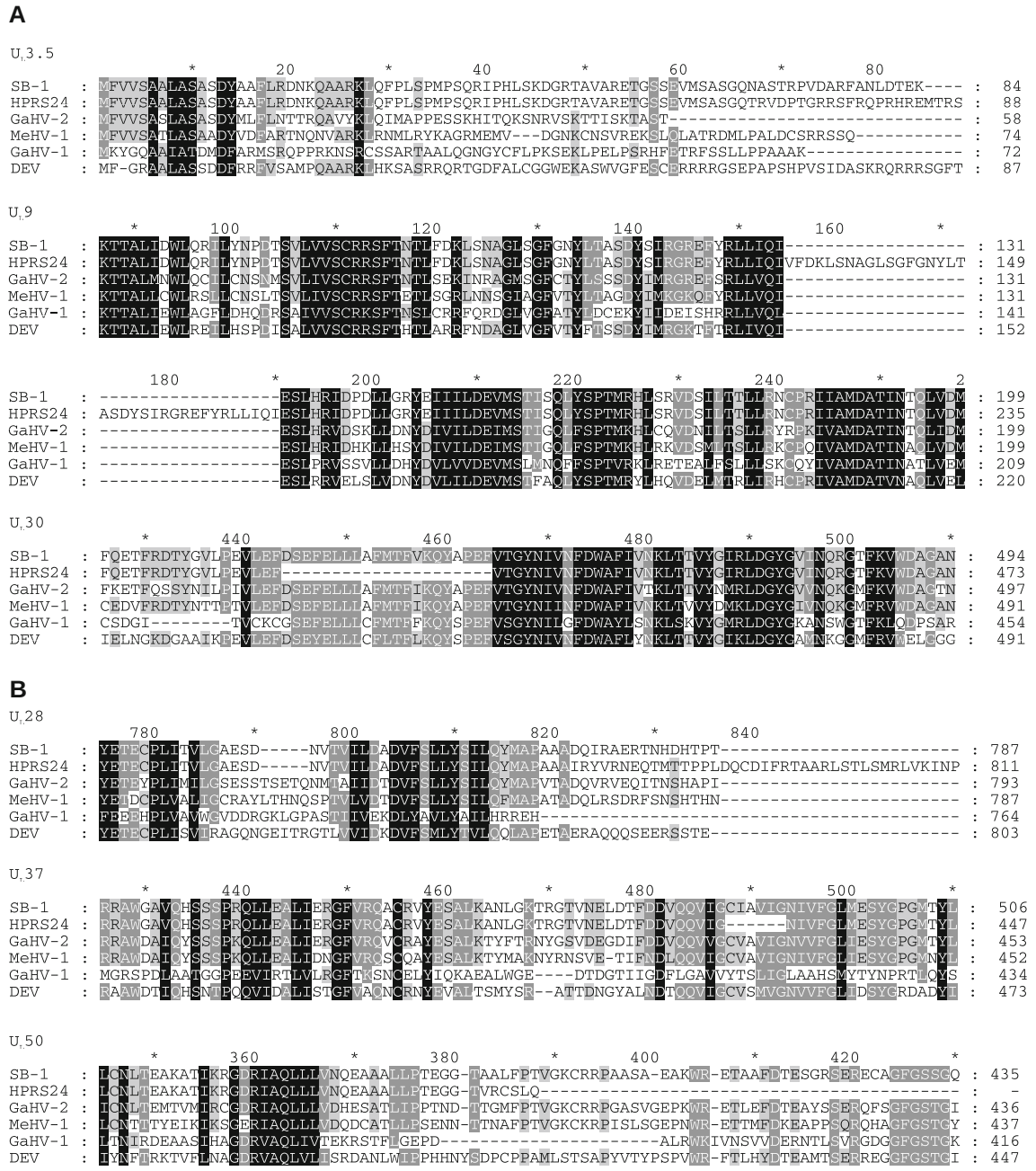

Fig. 3 Multiple alignments of translation products from the genes encoding $U_L3.5$, U_L9, U_L30 (**a**) and U_L28, U_L37 and U_L50 (**b**) of the two GaHV-3 strains (SB-1 and HPRS24) along with homologues found in the GaHV-1, GaHV-2, MeHV-1 and DEV genomes. Only selected regions were included to demonstrate differences in alignments

The last remaining question is why SB-1 protects better against virulent challenge of GaHV-2 than does HPRS24. To investigate this, each translated ORF of interest in HPRS24 and SB-1 was analyzed for percentage identity and percentage similarity. As shown in Table 3A, B, twice as many ORF (25 vs. 12) in the SB-1 genome exhibit greater sequence identity and similarity between homologues in SB-1 and the genome of very virulent plus GaHV-2 strain Md5 than between HPRS24 and Md5 homologues. In comparison, only twelve ORFs have greater identity and similarity between HPRS24 and Md5 homologues than between SB-1 and Md5 homologues. Therefore, protection against challenge may simply reflect the percentage of similar epitopes between the vaccine and the challenge strain.

Conclusions

Sequence comparison between GaHV-3 strains HPRS24 and SB-1 has identified regions of sequence disparity

Table 3 A and B. Percentage amino acid sequence identity and similarity of SB-1 ORFs that differed (<100%) relative to those found in the HPRS24 genome, with homologous ORFs found in the genome of GaHV-2 (Marek's disease virus) very virulent strain Md5

ORF #	Common name	Identity (%)			Similarity (%)		
		Md5 v. SB1	Md5 v. HPRS24	SB1 v. HPRS24	Md5 v. SB1	Md5 v. HPRS24	SB1 v. HPRS24
A							
2	R-LORF1	**21.3**	19.2	23.9	**26.4**	22.2	31.4
22	R-LORF4	6.7	**8.1**	99.4	10.9	10.9	99.4
37	R-LORF9	**2.1**	2.0	64.6	3.2	3.2	67.0
38	R-LORF8	9.5	**10.0**	48.5	14.9	**15.8**	54.0
43	pp24	**28.9**	28.8	89.7	36.1	**37.0**	89.7
53	LORF2	12.3	**45.9**	20.7	18.9	**58.8**	30.3
68	UL3.5	**28.1**	27.8	65.4	**38.2**	37.8	66.3
72	UL5	**79.4**	78.3	98.6	**88.3**	87.5	99.0
98	UL9	**72.1**	69.1	95.9	**83.6**	80.2	95.9
104	UL10	76.3	**77.6**	98.4	86.5	**88.0**	98.4
139	UL19	**86.5**	86.3	99.8	**93.8**	93.6	99.9
181	UL25	**72.4**	72.3	97.8	**83.8**	83.7	97.8
185	UL26	57.5	57.5	99.8	69.6	**69.7**	99.8
199	UL28	**68.8**	68.7	94.9	**78.9**	78.7	95.1
231	UL32	**68.2**	68.1	99.8	**78.6**	78.4	99.8
241	UL36	**50.7**	50.4	99.1	**64.7**	64.1	99.2
242		12.3	**12.4**	90.8	16.9	**17.0**	91.7
261	UL37	**63.1**	62.7	99.2	**77.9**	77.3	99.3
266	UL38	**62.8**	62.4	99.6	**77.8**	77.4	99.6
279	UL40	73.2	**72.9**	99.7	**82.7**	82.4	99.7
281	UL41	64.7	**64.8**	98.6	75.0	**75.1**	98.6
B							
287	UL42	74.0	73.7	99.7	83.2	82.9	99.7
294	UL43	56.2	54.3	97.6	71.6	69.2	97.6
299	UL44	72.0	72.0	99.8	81.7	81.7	99.8
304		17.1	15.2	91.9	20.5	18.6	91.9
305	UL45	72.0	70.6	98.1	83.4	82.0	98.1
317	UL47	48.6	47.1	97.7	61.3	60.0	98.0
322	UL48	56.6	56.6	99.5	65.7	65.5	99.5
331	UL50	59.0	58.4	98.2	72.5	71.9	98.2
335	UL51	53.2	52.8	98.8	64.2	63.4	99.2
343	UL53	64.4	64.1	99.7	76.8	76.6	99.7
352	LORF4	50.2	45.4	91.4	61.6	55.4	91.9
367	UL56	33.8	28.5	72.6	53.8	47.4	79.3
369	pp38	26.4	26.4	88.8	38.7	38.8	88.8
413		1.0	1.1	97.9	1.6	1.7	97.9
417		4.6	12.7	13.8	7.3	21.3	15.1
422		2.3	3.1	24.2	3.3	3.8	24.5
442		3.5	44.6	9.9	4.7	54.9	9.9
452	SORF2	9.0	0.8	64.1	13.7	1.5	68.9
463	SORF4	12.9	51.1	16.0	20.6	66.7	23.4
469	US3	13.2	57.2	13.1	18.5	68.8	22.9
477	US8	44.0	43.1	95.6	59.4	58.7	96.0

Numbers in *bold* illustrate which genome (SB-1 versus HPRS24) contained the higher percentage identity and similarity of an individual ORF with a homologous ORF found in the Md5 genome

within the repeat long regions and at the TR_L/U_L, U_L/IR_L and U_S/TR_S junctions. A sequence exhibiting high nucleotide conservation to the LTR of avian retroviruses was identified at the U_S/TR_S junction region of the SB-1 genome. Nineteen ORFs that varied in amino acid length were also identified in the comparison. In sequence length and amino acid conservation comparisons, these ORFs within the SB-1 genome were more related to homologues found in other avian herpesviruses than were those in the HPRS24 genome. In other homology studies, 25 ORFs within the SB-1 genome had a greater percentage of sequence identity and similarity to homologues in the genome of virulent GaHV-2 than corresponding ORFs within the HPRS24 genome. Only 12 ORFs within the HPRS24 had a greater percentage of sequence identity and similarity to homologues in the genome of GaHV-2 than those ORFs within the SB-1 genome. Therefore, of these 37 ORFs that exhibit differentiating homology with virulent GaHV-2, twice as many SB-1 ORFs are more homology to the challenge virus (Md5) than those of HPRS24. This could be of significance since SB-1 elicits better protection against virulent MDV challenge than does HPRS24. Finally, it can be stated that there are regions in the HPRS24 genome which are highly suspected of containing sequencing errors. Resequencing of the HPRS24 genome or selected regions is needed to investigate this further.

Acknowledgments We would like to thank Jeremy Volkening for his assistance in all stages of this project.

References

1. P.M. Biggs, The history and biology of Marek's disease virus, in *Current Topics in Microbiology and Immunology*, ed. by K. Hirai (Springer-Verlag, Berlin, 2001), pp. 1–24
2. B.W. Calnek, H.K. Adldinger, D.E. Kahn, Feather follicle epithelium: a source of enveloped and infectious cell-free herpesvirus from Marek's disease. Avian Dis. **14**(2), 219–233 (1970)
3. V.V. Bulow, P.M. Biggs, Differentiation between strains of Marek's disease virus and turkey herpesvirus by immunofluorescence assays. Avian Pathol. **4**(2), 133–146 (1975)
4. V.V. Bulow, P.M. Biggs, Precipitating antigens associated with Marek's disease viruses and a herpesvirus of turkeys. Avian Pathol. **4**(2), 147–162 (1975)
5. A.E. Churchill, L.N. Payne, R.C. Chubb, Marek's disease immunization against Marek's disease using a live attenuated virus. Lancet **1**(7595), 610–611 (1969)
6. W. Okazaki, H.G. Purchase, B.R. Burmester, Protection against Marek's disease by vaccination with a herpesvirus of turkeys. Avian Dis. **14**(2), 413–429 (1970)
7. R.L. Witter, K. Nazerian, H.G. Purchase, G.H. Burgoyne, Isolation from turkeys of a cell-associated herpesvirus antigenically related to Marek's disease virus. Biken J. **13**(1), 53–57 (1970)
8. B.W. Calnek et al., Field trials with a bivalent vaccine (HVT and SB-1) against Marek's disease. Avian Dis. **27**(3), 844–849 (1983)
9. Y. Izumiya et al., A complete genomic DNA sequence of Marek's disease virus Type 2, strain HPRS24, in *Current Topics in Microbiology and Immunology*, ed. by K. Hirai (Springer-Verlag, Berlin, 2001), pp. 191–221
10. J.D. Volkening, S.J. Spatz, Purification of DNA from the cell-associated herpesvirus Marek's disease virus for 454 pyrosequencing using micrococcal nuclease digestion and polyethylene glycol precipitation. J. Virol. Methods **157**(1), 55–61 (2009)
11. M. Margulies et al., Genome sequencing in microfabricated high-density picolitre reactors. Nature **437**(7057), 376–380 (2005)
12. K. Katoh et al., MAFFT version 5: improvement in accuracy of multiple sequence alignment. Nucl. Acids Res. **33**(2), 511–518 (2005)
13. A.J. Davison, Herpesvirus systematics. Veterinary Microbiol. **143**(1), 52–69 (2010)
14. D.J. McGeoch, F.J. Rixon, A.J. Davison, Topics in herpesvirus genomics and evolution. Virus Res. **117**(1), 90–104 (2006)
15. S.J. Spatz, R.F. Silva, Polymorphisms in the repeat long regions of oncogenic and attenuated pathotypes of Marek's disease virus 1. Virus Genes **35**(1), 41–53 (2007)
16. Z. Cui et al., Molecular and biological characterization of a Marek's disease virus field strain with reticuloendotheliosis virus LTR insert. Virus Genes **40**(2), 236–243 (2010)
17. I. Davidson et al., Molecular indications for in vivo integration of the avian leukosis virus, subgroup J-long terminal repeat into the Marek's disease virus in experimentally dually-infected chickens. Virus Genes **24**(2), 173–180 (2002)
18. R.J. Isfort et al., Integration of multiple chicken retroviruses into multiple chicken herpesviruses: herpesviral gD as a common target of integration. Virology **203**(1), 125–133 (1994)
19. R. Kost et al., Retrovirus insertion into herpesvirus: characterization of a Marek's disease virus harboring a solo LTR. Virology **192**(1), 161–169 (1993)
20. M. Sakaguchi et al., Insertion of tandem direct repeats consisting of avian leukosis virus LTR sequences into the inverted repeat region of Marek's disease virus type 1 DNA. Virus Genes **14**(2), 157–162 (1997)
21. A.J. Sun et al., Functional evaluation of the role of reticuloendotheliosis virus long terminal repeat (LTR) integrated into the genome of a field strain of Marek's disease virus. Virology **397**(2), 270–276 (2010)
22. Z. Zhang, Z. Cui, Isolation of recombinant field strains of Marek's disease virus integrated with reticuloendotheliosis virus genome fragments. Sci. Chin. C **48**(1), 81–88 (2005)
23. M.M. Alba et al., Genomewide function conservation and phylogeny in the Herpesviridae. Genome Res. **11**(1), 43–54 (2001)

Journal of General Virology (2011), **92**, 1500–1507 DOI 10.1099/vir.0.027706-0

Genotypic characterization of two bacterial artificial chromosome clones derived from a single DNA source of the very virulent gallid herpesvirus-2 strain C12/130

Stephen J. Spatz,[1] Lorraine P. Smith,[2] Susan J. Baigent,[2] Lawrence Petherbridge[2] and Venugopal Nair[2]

[1]Southeast Poultry Research Laboratory, Agricultural Research Service, United States Department of Agriculture, Athens, GA 30605, USA

[2]Institute for Animal Health, Compton, Berkshire RG20 7NN, UK

Correspondence
Stephen J. Spatz
Stephen.Spatz@ars.usda.gov

Received 12 October 2010
Accepted 28 March 2011

The identification of specific genetic changes associated with differences in the pathogenicity of Marek's disease virus strains (GaHV-2) has been a formidable task due to the large number of mutations in mixed-genotype populations within DNA preparations. Very virulent UK isolate C12/130 induces extensive lymphoid atrophy, neurological manifestations and early mortality in young birds. We have recently reported the construction of several independent full-length bacterial artificial chromosome (BAC) clones of C12/130 capable of generating fully infectious viruses with significant differences in their pathogenicity profiles. Two of these clones (vC12/130-10 and vC12/130-15), which showed differences in virulence relative to each other and to the parental strain, had similar replication kinetics both *in vitro* and *in vivo* in spite of the fact that vC12/130-15 was attenuated. To investigate the possible reasons for this, the nucleotide sequences of both clones were determined. Sequence analysis of the two genomes identified mutations within eight genes. A single 494 bp insertion was identified within the genome of the virulent vC12/130-10 clone. Seven non-synonymous substitutions distinguished virulent vC12/130-10 from that of attenuated vC12/130-15. By sequencing regions of parental DNA that differed between the two BAC clones, we confirmed that C12/130 does contain these mutations in varying proportions. Since the individual reconstituted BAC clones were functionally attenuated *in vivo* and derived from a single DNA source of phenotypically very virulent C12/130, this suggests that the C12/130 virus population exists as a collection of mixed genotypes.

INTRODUCTION

Marek's disease (MD) is a highly contagious neoplastic and neuropathic disease of chickens (Calnek, 2001). The causative agent is gallid herpesvirus type 2 (GaHV-2), a member of the genus *Mardivirus* within the subfamily *Alphaherpesvirinae* of the family *Herpesviridae* (Roizman *et al.* 1981; Lee *et al.* 2000). Over the past 40 years the disease has been controlled with vaccines consisting of the related mardivirus herpesvirus of turkey, non-oncogenic serotype 2 strains (also known as gallid herpesvirus type 3), and attenuated derivatives of oncogenic GaHV-2 (Witter 2001a, b). Unfortunately, over this same period field strains have evolved to greater virulence (Witter, 1997). To understand the genetic changes involved in the generation of very virulent or very virulent plus (vv+) strains, the nucleotide sequences of large genomic regions and whole genomes representing the five pathotypes of GaHV-2 have been determined (Lee *et al.* 1971; Tulman *et al.* 2000; Niikura *et al.* 2006; Spatz & Silva, 2007a, 2007b; Spatz & Rue, 2008). This information has shed some light on the mutations needed for attenuation, but it is complicated by the sheer number of mutations identified (Spatz *et al.* 2008; Volkening & Spatz, 2009). To avoid these limitations, scientists have cloned GaHV-2 genomes as bacterial artificial chromosomes (BAC) to get a 'molecular snapshot' of the mutations on a single molecule (Osterrieder & Vautherot, 2004).

We have previously reported that the very virulent strain C12/130 isolated from Europe induces high mortality and atrophy of the lymphoid organs with increased tropism for the central nervous system (Barrow & Venugopal 1999; Barrow *et al.* 2003a, b). To study the molecular basis for these biological characteristics, several BAC clones derived

The GenBank/EMBL/DDBJ accession numbers for the sequences reported in this paper are FJ436096 and FJ436097.

from a single source of C12/130 DNA were constructed and characterized in pathogenicity studies (Smith *et al.* 2011). Surprisingly, viruses reconstituted from these clones and used to infect chickens had distinct pathogenic properties. One of the reconstituted viruses, named vC12/130-10, had mortality rates reaching that of the parental virus. Another reconstituted virus vC12/130-15 exhibited a relatively attenuated phenotype. To characterize further these clones, the *in vitro* replication kinetics in chicken embryo fibroblasts (CEFs), the relative copies numbers in peripheral blood lymphocytes (PBL) and feather follicle epithelial (FFE) cells *in vivo* were determined. As the BAC clones of these viruses represented single genome copies, the complete genomic nucleotide sequence of C12/130-10 and C12/130-15 was determined in the hope of identifying mutations involved in attenuation.

RESULTS

Characterization of reconstituted viruses from pC12/130-10 and pC12/130-15 DNA

Comparison of the *in vitro* replication rates of both vC12/130-10 and vC12/130-15 relative to wild-type virus (Fig. 1) indicated that all viruses grew at nearly the same rate. The *in vitro* growth curves of the three viruses were analysed using a two-way ANOVA analysis and the F values for the viruses (3.038) were lower than the F crit (3.885), thereby indicating no significant differences between the growth of each virus in culture. We also analysed the *in vivo* replication kinetics of the three viruses by measuring the virus load in the DNA samples prepared from PBL and feather tips collected at different times after infection, using the meq-ovotransferrin duplex real-time qPCR test (Baigent *et al.* 2005). GaHV-2 genome copy numbers in the PBL from birds infected with the three viruses were maintained at similar levels (~10^3 per 10^4 PBL) after the initial sampling period of 7 days post-infection (p.i.) (Fig. 2a). Relative to the copy number in the PBL, DNA samples prepared from feather samples showed a significantly higher GaHV-2 genome copy number (10^6 per 10^4 FFE cells) from the second sampling period of 14 days p.i. The replication kinetics of the viruses, as measured by viral DNA content, were fairly comparable between the three viruses at late time points. However, at 4 days p.i., the parental strain replicated to approximately 1.5–2.0 logs higher than the reconstituted viruses (Fig. 2b).

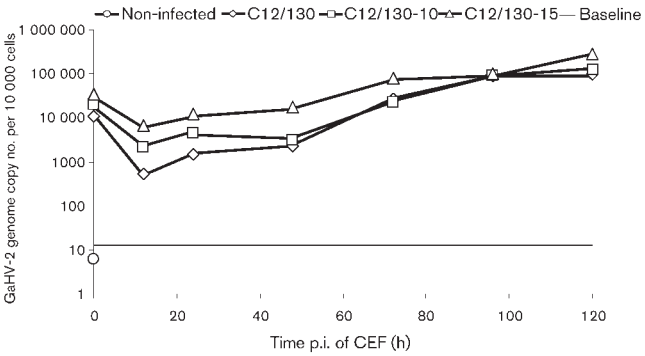

Fig. 1. *In vitro* growth rates of wild-type C12/130, vC12/130-10 and vC12/130-15 on CEFs at different times after inoculation. Virus titres (p.f.u. ml^{-1}) are plotted on a logarithmic scale with 95 % confidence limits.

Deep sequencing of pC12/130-10 and pC12/130-15

The complete nucleotide sequences of BACs pC12/130-10 and pC12/130-15 were determined commercially by using 454 Life Sciences pyrosequencing. DNA sequences of pC12/130-10 and pC12/130-15 were assembled from 54 248 and 16 253 reads representing 30-fold and ninefold coverage at each base pair, respectively. Individual reads were initially assembled into large contigs representing the unique long

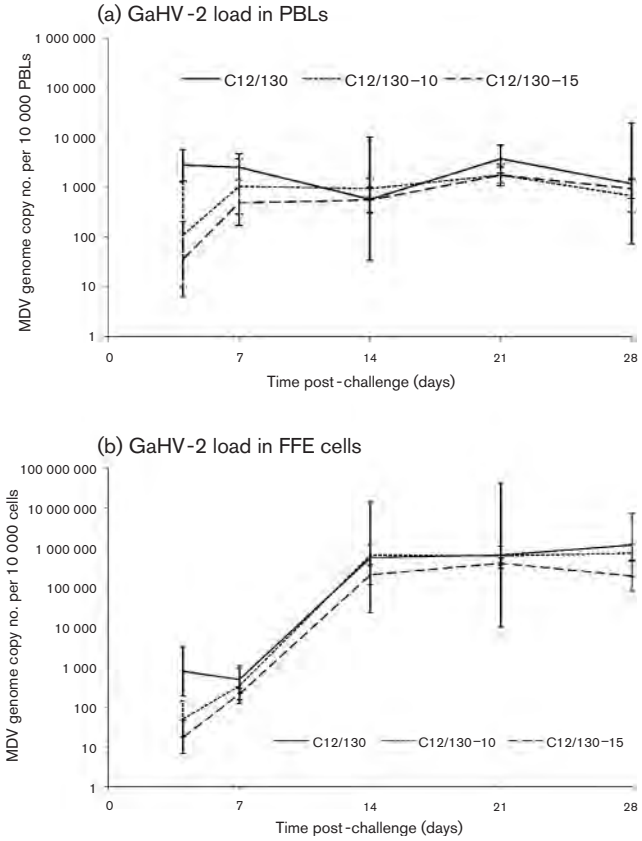

Fig. 2. Comparison of the *in vivo* replication kinetics of the wild-type C12/130, vC12/130-10 and vC12/130-15 viruses as mean genome copies per 10^4 PBLs (a) and FFE cells (b) from groups of five chickens plotted on a logarithmic scale with 95 % confidence limits.

(U_L), unique short (U_S), repeat long (R_L) and repeat short (R_S) genomic segments. Single nucleotide polymorphisms within R_L elements were randomly assigned to either terminal (T) R_L or internal (I) R_L regions. This procedure was repeated for single nucleotide polymorphisms (SNPs) within the IR_S/TR_S regions. Ambiguities in the number of mononucleotide reiterations were resolved by using conventional dideoxy-based sequencing of PCR products. These reiterations occurred in five single copy genes (MDV063, MDV086.2, MDV086.4, MDV086.5 and MDV086.6) and five diploid genes (MDV001/080, MDV03.6/078.2, MDV084.8/099.5, MDV085/099 and MDV085.3/098.9).

Genomic statistics

The complete sequences of pC12/130-10 and pC12/130-15 are 183850 and 184432 nt in length, respectively. If the BAC sequences were removed and the U_S2 gene restored then the lengths would be 177118 and 177694 nt, respectively, similar to other sequenced GaHV-2 genomes. The nucleotide sizes of the various subgenomic regions of C12/130-10 and C12/130-15, respectively, are as follows: TR_L 12851/12852; U_L 114016/113523; IR_L 12830/12831; *a-like* sequence 767/763; IR_S 12379/12912; U_S without BAC sequences and with the U_S2 gene, 11157/11159; TR_S 12375/12912; and *a-like* sequence 743/742. From this analysis it is apparent that there is a gross size difference in two regions: the U_L and the R_S regions. There is a 494 bp insertion within the U_L region of the C12/130-10 genome. The differences in the lengths of the short regions (IR_S and TR_S) can be attributed to differences in the number of 60 bp repeats adjacent to the IR_L/IR_S junction. There are 18 60 bp repeats containing the sequence 5′-TAGAGGGCGCGT-GCGCAGTCGGAGTTTTCCTATTTTCGGCCCCGCGCA-CGCGCGGTCATG-3′ adjacent to the *a-like* sequences in the genome of C12/130-10 and only nine in the genome of C12/130-15. Differences in lengths of other subgenomic regions are due to varying lengths of mononucleotide reiterations.

Mutations that differ among C12/130-10 and C12/130-15

Lists of mutations that differ between C12/130-10 and C12/130-15 are presented in Tables 1–3. The majority of intergenic differences occur in homopolymer stretches of mononucleotide reiterations between small novel genes within the R_L region of the genome (Table 1). Since pyrosequencing is limited in its ability to resolve mononucleotide reiterations greater than nine, these regions had to be resolved by using PCR and Sanger sequencing. Only five mutations mapped outside this region. Two occurred within the U_L region: within the promoter of MDV057 encoding glycoprotein C and between MDV071.4 and MDV071.8. Two occurred within the *a-like* sequence involved in packaging the genome and one mapped to the 3′ UTR of ICP4 and the promoter of RSORF1. Six mutations, resulting in a shift in reading frame (Table 2), were mapped to eight genes (MDV078.2, MDV084.5/MDV099.5, MDV085/MDV099, MDV085.3/MDV098.9, MDV086.5, MDV086.2/MDV097.6, MDV086.4 and MDV086.6). Most of these mutations mapped to mononucleotide reiterations within the R_S/U_S junction. Interestingly, this junction is quite polymorphic among strains (Spatz & Silva 2007a, 2007b) and retrovirus sequences have been found within this region in some attenuated strains (Jones *et al.* 1993; Isfort *et al.* 1994).

Table 3 contains a list of the three synonymous and seven non-synonymous SNP mutations that were identified. Of the seven non-synonymous mutations, three changes (in bold, Table 3) are likely to affect the structure of the encoded proteins. These occur within the tegument protein MDV050 (Pro→Ser), antisense RNA protein MDV083 (Gly→Arg) and SORF3 kinase-like protein MDV090 (Ile→Met) of the virulent C12/130-10 versus attenuated C12/130-15 strains, respectively.

The most noticeable difference between the genomes of C12/130-10 and C12/130-15 is the large 494 bp insertion between MDV071 (LORF10) and MDV072 (LORF11) in the genome of the virulent strain C12/130-10. This insertion occurs in a region containing repetitive sequences (Fig. 3) and probably resulted from gene duplication. In comparison to other GaHV-2 viruses (virulent and attenuated) whose genomic sequence has been determined, this insertion is only found in virulent C12/130-10.

To determine whether the mutations that differ between C12/130-10 and C12/130-15 were present in the DNA preparation used to generate the two BAC constructs, and were not introduced during their construction, parental viral DNA was used as a template in amplification reactions to determine the nucleotide sequences of selected regions. All SNPs were confirmed to be present within the parental DNA in varying proportions. Interestingly, the primer pairs used to amplify the region containing the 494 bp insertion generated three bands that differed by approximately 500 bp (data not shown). Cloning and sequencing of these variants indicated that within the parental DNA three variants do exist. This is not likely to be a PCR artefact since the BAC clones C12/130-10 and C12/130-15 resulted from the cloning of two of the three (if not more) possible genomes present in the parental DNA preparation.

DISCUSSION

Comparison of the complete nucleotide sequences of two BAC constructs derived from DNA isolated from the very virulent C12/130 strain indicates generalized conservation at the nucleotide level. Few mutations were identified that could differentiate C12/130-10 from C12/130-15. Furthermore, phenotypically the *in vitro* and *in vivo* replication rates were very similar for the two reconstituted viruses. However, mortality rates did differ significantly among the two strains, and vC12-130-15 was less virulent

Table 1. Intergenic mutations that differ between C12/130-10 and C12/130-15

Diploid genes are only listed once. Base pair changes are in bold and underlined. The nucleotide sequence surrounding each mutation is listed first for C12/130-10 and then for C12/130-15.

Genomic location	Intragenic	Mutation
U_L	MDV056 and MDV057	GACTGGACTC-TTTTTTTTTG
		GACTGGACTC**T**TTTTTTTTTG
U_L	MDV071.4 and MDV071.8	TAATATGCCA**T**ATCCAAAAAAG
		TAATATGCCA**C**AGCCAAAAAAG
R_L	MDV075.1 and MDV075.2	ATAAGCAAAT**A**AAAAAAAAAAG
		ATAAGCAAAT-AAAAAAAAAAG
R_L	MDV075.1 and MDV075.2	AGAACGGCGA-TTTTTTA
		AGAACGGCGA**T**TTTTTTA
R_L	MDV075.1 and MDV075.2	TAATCCGATA--TTTTTTTTG
		TAATCCGATA**TT**TTTTTTTTTG
R_L	MDV075.1 and MDV075.2	TTAATATTTT--AAAAAAAAT
		TTAATATTTT**AA**AAAAAAAAT
R_L	MDV075.4 and MDV075.7	GGTGTATATG**TT**TTTTTTTTTTTA
		GGTGTATATG--TTTTTTTTTTA
R_L	MDV075.4 and MDV075.7	AGCAGGACTG**A**AAAAAAAAAAAAAC
		AGCAGGACTG-AAAAAAAAAAAAAC
R_L	MDV075.7 and MDV075.9	CTCGAGGCTT-TTTTTTTTTTTG
		CTCGAGGCTT**T**TTTTTTTTTTTG
R_L	MDV075.9 and MDV 075.91	GATCAAGGTT-AAAAAAAG
		GATCAAGGTT**A**AAAAAAAG
R_L	MDV075.91 and MDV075.92	TTATTTTCTT**C**CCCCCCCCCCCCCG
		TTATTTTCTT-CCCCCCCCCCCCCG
R_L	MDV075.92 and MDV076.4	ATACGGAGAC**GG**GGGGGGGGGGGA
		ATACGGAGAC--GGGGGGGGGGGA
R_L	MDV076 and MDV078.1	TGCCTGGCTG-TTTTTTTTTTTTTTTA
		TGCCTGGCTG**T**TTTTTTTTTTTTTTTA
R_L	Intron 2 of MDV078	AGGTTTTCCC**T**TTTGTAGCTTTGCTC
		AGGTTTTCCC-TTTGTAGCTTTGCTC
R_L	MDV078 and M DV078.5	AAGAAGGCAC-TTTTTTTTC
		AAGAAGGCAC**T**TTTTTTTTC
	a-like	GGATGGGGGT**G**GGGGGGGGGT
		GGATGGGGGT-GGGGGGGGGT
	a-like	GTTCGACGAA**TT**TTTTTTTTTA
		GTTCGACGAA--TTTTTTTTTA
R_S	MDVO82 and M DV084	TGAGTGATTC**G**TACTAGTTCGACACTT
		TGAGTGATTC**A**TACTAGTTCGACACTT

than vC12/130-10. Both strains, however, were somewhat attenuated in comparison to the parental strain (Smith *et al.*, 2011). This could be due in part to the presence of the mini F cassette within the US2 genes of C12/130-10 and C12/130-15, as removal of the mini F and restoration of US2 within another GaHV-2 BAC (RB-1B) restored the reconstituted virus to the wild-type phenotype (Zhao *et al.* 2008). Therefore, the major question raised is which mutations between the BAC clones make C12/130-10 more virulent than C12/130-15. The data presented identified a number of mutations that can be grouped into three categories: mononucleotide reiterations, cistronic mutations and insertions.

The majority (72 %) of the differentiating mononucleotide reiterations (Table 1) that occurred between ORFs mapped to the R_L subgenomic region. This region contains the highest proportion of unique mardiviral-specific genes within the GaHV-2 genome. It is possible that these differences may affect the expression of neighbouring genes. Differences in mononucleotide reiterations were also identified in small novel ORFs within the internal R_S/U_S junctions. As reported with other GaHV-2 strains, these junctions contain significant sequence heterogeneity, not only with respect to differences in mononucleotide reiterations but also due to the presence of inserted retroviral sequences (Isfort *et al.* 1994; Spatz & Silva, 2007a, 2007b). Although some attenuated strains contain retroviral insertions within these junctions, a functional correlation between the inserted elements and an attenuated phenotype has not been reported. It is also unknown

Table 2. A list of intragenic mutations between the C12/130-10 and C12/130-15 genomes that result in a reading frame shift

Diploid genes are only listed once. Base pair changes are in bold and underlined. The nucleotide sequence surrounding each mutation is listed first for C12/130-10 and then for C12/130-15.

Genomic location	Frameshift	Mutation
R_L	MDV78.2	GGTTCGTGGG**T**TTTTTTTTTTA GGTTCGTGGG-TTTTTTTTTTA
IR_S/U_S junction	Overlapping MDV084.5 and MDV085	TGTTCTCGAT**CC**CCCCCCCCCCCCCCCCA TGTTCTCGAT--CCCCCCCCCCCCCCCCA
IR_S/U_S junction	MDV085.3	GAACGCGCTC----AAAAAAAAAAAAAAAAAAAAAAAC GAACGCGCTC**AAAA**AAAAAAAAAAAAAAAAAAAAAAAC
IR_S/U_S junction	Overlapping MDV086.2 and MDV086.4	GCAGATGGGT**CCCCCCC**CCCCCCCCCCA GCAGATGGGT-------CCCCCCCCCCA
IR_S/U_S junction	Overlapping MDV086.2 and MDV086.5	CGCAGATGGGTCCCCCCCCCCCC**CA**AAAAAAAAAG CGCAGATGGGTCCCCCCCCCCCC--AAAAAAAAAGG
U_S	MDV086.6	CGAAAAAAAA--GGGGGGGGGAGAATATTC CGAAAAAAAA**GG**GGGGGGGGGAGAATATTC

whether the short ORFs in the internal R_S/U_S junctions are expressed. These mutations will have to be examined using a functional approach.

In the absence of a functional examination of the reiteration mutations reported here, the sequencing data does identify two classes of mutations that could contribute to the differing phenotypes. The non-synonymous substitutions in the genes encoding the U_L37 tegument protein (MDV050), U_L39 ribonucleotide reductase (MDV052), ICP4 (MDV084), antisense RNA protein (MDV083), SORF3 (MDV090) and the insertion within the LORF10 promoter in the C12/130-10 genome are potential candidates for consideration. As shown in Table 3, three substitutions (Ser in MDV050, Ala in MDV052 and Ala in MDV084) within the genome of C12/130-15 are unique and not found within these genes in all other sequenced GaHV-2 strains. Similarly, Tyr in MDV084, Gly in MDV083 and Val in MDV090 within the genome of C12/130-10 are unique and not found in other sequenced GaHV-2 strains. The Ser substitution

Table 3. Synonymous and non-synonymous SNPs between C12/130-10 and C12/130-15

The amino acid position within each gene is indicated along with the amino acid substitution in other GaHV-2 strains. Amino acids in bold are unique to C12/130 and are not found in other sequenced GaHV-2 genomes.

Gene	Amino acid Position	Strains									Function
		C12/130-10	C12/130-1	584Ap80	CU-2	RB-1B-5	CVi988	Md5	Md11	GA	
						Synonymous					
MDV043	60	Ala	Ala	Ala	Ala	Ala	Ala	Ala	Ala	Ala	UL30 DNA polymerase
MDV060	206	Arg	Arg	Arg	Arg	Arg	Arg	Arg	Arg	Arg	UL47 tegument phosphoprotein, VP13/14
MDV071.8	78	Leu	Leu	Leu	Leu	Leu	Leu	Leu	Leu	Leu	Unknown
						Non-synonymous					
MDV050	719	Pro	**Ser***	Pro	Pro	Pro	Pro	Pro	Pro	Pro	UL37 tegument protein
MDV052	756	Val	**Ala**	Val	Val	Val	Val	Val	Val	Val	UL39 ribonucleotide reductase, large subunit
MDV084	578	Val	**Ala**	Val	Val	Val	Val	Val	Val	Val	Immediate-early, ICP4
MDV084	1634	**Tyr**	Ser	Ser	Ser	Ser	Ser	Ser	Ser	Ser	Immediate-early, ICP4
MDV083	58	**Gly***	Arg	Arg	Arg	Arg	Arg	Arg	Arg	Arg	Antisense RNA protein
MDV090	182	Ile	Met	Met	Met	Met	Met	Met	Met	Ile	SORF3 kinase-like protein
MDV090	222	**Val**	Ala	Ala	Ala	Ala	Ala	Ala	Ala	Ala	SORF3 kinase-like protein

*Those with an asterisk differ significantly within their R groups.

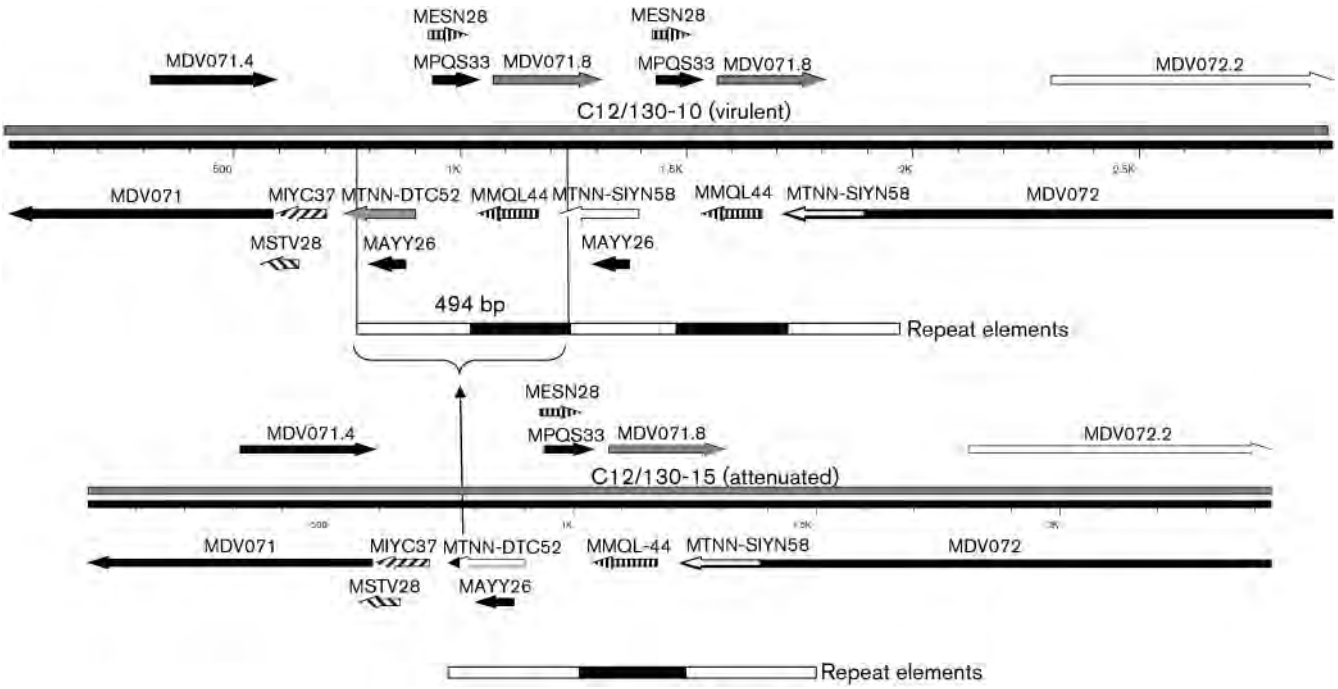

Fig. 3. Diagram of the region between genes MDV071 and MDV072 in the genomes of C12/130-10 and C12/130-15 showing a 494 bp insertion in the virulent strain C12/130-10. Repeat elements are denoted by alternating open and closed boxes. Small ORFs that are duplicated are named by their first and last four amino acids followed by the number of amino acids in the ORF. Duplicated ORF MTTN-SIYN58 originated using an in-frame alternative start codon within the larger gene MDV072.

(MDV050) in C12/130-15 and the Gly substitution (MDV083) in C12/130-10 are probably most significant since they are predicted to affect the structure of the tegument protein and antisense RNA proteins, respectively. Whether these SNPs have a role in pathogenicity is not known, but there is evidence in the literature that SNPs are involved in virulence with other herpesviruses (Quinlivan *et al.* 2005, 2007; Nugent *et al.* 2006; Goodman *et al.* 2007).

The insertion within the promoter region of LORF10 of virulent C12/130-10 is the only gross mutation identified in the comparison. None of the previously sequenced GaHV-2 genomes contain this insertion. In fact, three copies of the insertion were identified in the parental DNA by sequencing cloned PCR products. Since these insertions appear to be duplications, it is plausible that the duplicated repeat elements may affect the expression of MDV071 (LORF10). Seventy high scoring transcription factor-binding sites (e.g. CdXA homeobox, AP-1/jun, GATA-3, OCT-1, USF, HSF2, HSF1, NF-E1b and NF-E1C) have been found in this region by using the web-based TFsearch (Heinemeyer *et al.* 1998, 1999). This may be of significance since LORF10 is a homologue of myristoylated proteins found in other alphaherpesviruses including MeHV-1, EHV-1, -4, -9, BHV-1, -5 and VZV. The role of this protein in the life cycle of herpesviruses is not well characterized, but there is some evidence that the BHV-1 homologue may influence the host's immune response by downregulating MHC-II expression in bovine monocytes (Schwyzer *et al.* 2002). Recently, a polypeptide was demonstrated from an ORF (MDV072.2), which is antisense and overlapping to MDV072 encoding LORF11(Tian *et al.* 2010). It is plausible that the repeat element insertions in virulent C12/130-10 may affect the expression of this downstream 206 aa encoding gene.

In addition to mapping attenuating mutations, this paper provides additional evidence for the mixed-genotype nature of GaHV-2. Two BAC clones derived from a single viral DNA source of the very virulent strain C12/130 when reconstituted *in vitro* under minimal passages function differently in animal studies. Previously, we have used deep sequencing to identify mixed-genotype population in *in vitro* serial passage attenuation experiments (Spatz, 2010). Although it is tempting to suggest that this large DNA virus exists as a quasispecies, additional animal experiments are needed to quantify the number of mutations per kilobase that can occur in animals infected with reconstituted virus from defined BAC recombinants.

METHODS

Virus and cells. Primary or secondary CEFs were maintained in Medium 199 (Gibco-BRL) supplemented with 10 % newborn calf serum. A viral stock of C12/130 wild-type was generated from

splenoctyes extracted from chicken 6 days p.i. and passaged twice on CEFs. This was then used to generate the C12/130 BAC clones. The method for generating virus stocks in CEFs transfected with pC12/130-10 and pC12/130-15 is essentially that described by Petherbridge *et al.* (2004).

***In vitro* growth kinetics.** The rates of *in vitro* growth of the parental wild-type C12/130, vC12/130-10 and vC12/130-15 were studied by analysing the genome copy numbers at various time points p.i. For this, CEFs in 60 mm dishes were infected with 100 p.f.u. of virus stocks and incubated at 38.5 °C and 5 % CO_2. At various time intervals (0, 12, 24, 48, 72, 96 and 120 h) p.i., DNA was extracted from the infected cells using the DNeasy 96 Blood & Tissue kit (Qiagen) and then used for determining the *in vitro* growth kinetics of the viruses by real-time qPCR by using methods described previously (Baigent *et al.* 2005).

***In vivo* growth kinetics.** Growth of the reconstituted viruses were examined in 2-week-old specific-pathogen-free Rhode Island Red chickens maintained at the Poultry Production Unit of the Institute for Animal Health. All experiments were carried out in separate rooms according to UK Home Office guidelines. Randomly divided groups of chicks were infected intra-abdominally with 1000 p.f.u. of wild-type C12/130, vC12/130-10 or vC12/130-15 viruses. A further group inoculated with non-infected CEFs served as the negative control. Blood samples were taken into equal volumes of 3 % sodium citrate at 4, 7, 14, 21 and 28 days p.i. and PBLs were separated over Histopaque 1083 (Sigma). Feathers from the axillary tract were taken at the same time points, and DNA samples extracted from PBLs and feathers (DNeasy 96 Blood & Tissue kit; Qiagen) were used for determining the *in vivo* growth kinetics of the viruses by real-time qPCR using a meq-ovotransferrin duplex real-time qPCR test (Baigent *et al.* 2005).

DNA sequencing and analysis. Large-scale preparation of BAC DNA from *Escherichia coli* DH10B cells harbouring pC12/130-10 and pC12/130-15 was achieved by silica-based affinity chromatography by using commercially available kits (Qiagen). Sequencing of 5.0 μg pC12/130-10 and pC12/130-15 was carried out commercially on a pyrosequencing platform, the Genome Sequencer 20 (GS20) System (454 Life Sciences), using an eight lane gasket. The construction of random libraries of pC12/130-10 and pC12/130-15 DNA was done by using the methodology described previously (Margulies *et al.* 2005). DNA sequences of pC12/130-10 and pC12/130-15 were assembled from 54 248 and 16 253 reads, respectively, using GS *De novo* Assembler (454 Life Sciences) and Sequencher (Gene Codes). The average length of each read was 150 nt. The final sequences of pC12/130-10 and pC12/130-15 represent a 30-fold and ninefold coverage at each base pair, respectively. Ambiguities in the sequencing data of pC12/130-10 and pC12/130-15 were resolved by resequencing PCR products generated in reactions containing BAC DNA templates, high fidelity Platinum *Taq* DNA polymerase (Invitrogen) and custom primers using Sanger-based DNA sequencing methodology.

To investigate whether the mutations that differed among the two BAC clones were introduced during cloning manipulations, PCR products were generated in reactions that contained either pC12/130-10, pC12/130-15 or parental C2/130 DNA as templates with primers whose binding sites flanked the mutated regions. High fidelity Platinum *Taq* DNA polymerase (Invitrogen) was used in the amplification reactions and products were sequenced at the South Atlantic Area sequencing facility (Athens, GA) and Polymorphic DNA Technologies, Inc. (Alameda, CA) by using the BigDye terminator cycle Sanger sequencing protocol. These were analysed on a model ABI-3730 XL DNA Analyser (Applied Biosystems) by using dideoxy methodology. DNA sequences were maintained and analysed by using Lasergene (DNASTAR), NCBI Entrez and other web-based tools. Homology searches were conducted using the NCBI programs BLASTP and PSI-BLAST (Schäffer *et al.* 2001) with default settings. Published mRNA data (Maray *et al.* 1988; Peng *et al.* 1995; Peng & Shirazi 1996a, b) were compared to pC12/130-10 and pC12/130-15 genomes using PROT_Map (SoftBerry, Mount Kisco, NY). Transcription factor-binding sites were investigated by using the TFsearch program (Maray *et al.* 1988; Peng *et al.* 1995; Peng & Shirazi, 1996a, b; Heinemeyer *et al.* 1998, 1999). Multiple alignments of proteins and nucleotide sequences were generated using MAFFT, Multalign, MUSCLE and MEGA 4.1 (Corpet, 1988; Edgar, 2004; Kumar *et al.* 2004; Katoh *et al.* 2005). Nucleotide sequence data of pC12/130-10 and pC12/130-15 have been assigned the GenBank accession numbers FJ436096 and FJ436097, respectively.

ACKNOWLEDGEMENTS

We thank Jeremy Volkening for his excellent technical assistance and skills in bioinformatics and graphics. The authors would like to thank Dr Joel Schaley for critical evaluation of this report.

REFERENCES

Baigent, S. J., Petherbridge, L. J., Howes, K., Smith, L. P., Currie, R. J. & Nair, V. K. (2005). Absolute quantitation of Marek's disease virus genome copy number in chicken feather and lymphocyte samples using real-time PCR. *J Virol Methods* **123**, 53–64.

Barrow, A. & Venugopal, K. (1999). Molecular characteristics of very virulent European MDV isolates. *Acta Virol* **43**, 90–93.

Barrow, A. D., Burgess, S. C., Baigent, S. J., Howes, K. & Nair, V. K. (2003a). Infection of macrophages by a lymphotropic herpesvirus: a new tropism for Marek's disease virus. *J Gen Virol* **84**, 2635–2645.

Barrow, A. D., Burgess, S. C., Howes, K. & Nair, V. K. (2003b). Monocytosis is associated with the onset of leukocyte and viral infiltration of the brain in chickens infected with the very virulent Marek's disease virus strain C12/130. *Avian Pathol* **32**, 183–191.

Calnek, B. W. (2001). Pathogenesis of Marek's disease virus infection. *Curr Top Microbiol Immunol* **255**, 25–55.

Corpet, F. (1988). Multiple sequence alignment with hierarchical clustering. *Nucleic Acids Res* **16**, 10881–10890.

Edgar, R. C. (2004). MUSCLE: multiple sequence alignment with high accuracy and high throughput. *Nucleic Acids Res* **32**, 1792–1797.

Goodman, L. B., Loregian, A., Perkins, G. A., Nugent, J., Buckles, E. L., Mercorelli, B., Kydd, J. H., Palù, G., Smith, K. C. & other authors (2007). A point mutation in a herpesvirus polymerase determines neuropathogenicity. *PLoS Pathog* **3**, e160.

Heinemeyer, T., Wingender, E., Reuter, I., Hermjakob, H., Kel, A. E., Kel, O. V., Ignatieva, E. V., Ananko, E. A., Podkolodnaya, O. A. & other authors (1998). Databases on transcriptional regulation: TRANSFAC, TRRD and COMPEL. *Nucleic Acids Res* **26**, 362–367.

Heinemeyer, T., Chen, X., Karas, H., Kel, A. E., Kel, O. V., Liebich, I., Meinhardt, T., Reuter, I., Schacherer, F. & Wingender, E. (1999). Expanding the TRANSFAC database towards an expert system of regulatory molecular mechanisms. *Nucleic Acids Res* **27**, 318–322.

Isfort, R. J., Qian, Z., Jones, D., Silva, R. F., Witter, R. & Kung, H. J. (1994). Integration of multiple chicken retroviruses into multiple chicken herpesviruses: herpesviral gD as a common target of integration. *Virology* **203**, 125–133.

Jones, D., Isfort, R., Witter, R., Kost, R. & Kung, H. J. (1993). Retroviral insertions into a herpesvirus are clustered at the junctions of the short repeat and short unique sequences. *Proc Natl Acad Sci U S A* **90**, 3855–3859.

Katoh, K., Kuma, K., Toh, H. & Miyata, T. (2005). MAFFT version 5: improvement in accuracy of multiple sequence alignment. *Nucleic Acids Res* **33**, 511–518.

Kumar, S., Tamura, K. & Nei, M. (2004). MEGA3: Integrated software for Molecular Evolutionary Genetics Analysis and sequence alignment. *Brief Bioinform* **5**, 150–163.

Lee, L. F., Kieff, E. D., Bachenheimer, S. L., Roizman, B., Spear, P. G., Burmester, B. R. & Nazerian, K. (1971). Size and composition of Marek's disease virus deoxyribonucleic acid. *J Virol* **7**, 289–294.

Lee, L. F., Wu, P., Sui, D., Ren, D., Kamil, J., Kung, H. J. & Witter, R. L. (2000). The complete unique long sequence and the overall genomic organization of the GA strain of Marek's disease virus. *Proc Natl Acad Sci U S A* **97**, 6091–6096.

Maray, T., Malkinson, M. & Becker, Y. (1988). RNA transcripts of Marek's disease virus (MDV) serotype-1 in infected and transformed cells. *Virus Genes* **2**, 49–68.

Margulies, M., Egholm, M., Altman, W. E., Attiya, S., Bader, J. S., Bemben, L. A., Berka, J., Braverman, M. S., Chen, Y. J. & other authors (2005). Genome sequencing in microfabricated high-density picolitre reactors. *Nature* **437**, 376–380.

Niikura, M., Dodgson, J. & Cheng, H. (2006). Direct evidence of host genome acquisition by the alphaherpesvirus Marek's disease virus. *Arch Virol* **151**, 537–549.

Nugent, J., Birch-Machin, I., Smith, K. C., Mumford, J. A., Swann, Z., Newton, J. R., Bowden, R. J., Allen, G. P. & Davis-Poynter, N. (2006). Analysis of equid herpesvirus 1 strain variation reveals a point mutation of the DNA polymerase strongly associated with neuropathogenic versus nonneuropathogenic disease outbreaks. *J Virol* **80**, 4047–4060.

Osterrieder, K. & Vautherot, J.-F. (2004). *The Genome Content of Marek's Disease-Like Viruses. Marek's Disease:an Emerging Problem.* Oxford, UK: Elsevier.

Peng, Q. & Shirazi, Y. (1996a). Characterization of the protein product encoded by a splicing variant of the Marek's disease virus Eco-Q gene (Meq). *Virology* **226**, 77–82.

Peng, Q. & Shirazi, Y. (1996b). Isolation and characterization of Marek's disease virus (MDV) cDNAs from a MDV-transformed lymphoblastoid cell line: identification of an open reading frame antisense to the MDV Eco-Q protein (Meq). *Virology* **221**, 368–374.

Peng, Q., Zeng, M., Bhuiyan, Z. A., Ubukata, E., Tanaka, A., Nonoyama, M. & Shirazi, Y. (1995). Isolation and characterization of Marek's disease virus (MDV) cDNAs mapping to the BamHI-I2, BamHI-Q2, and BamHI-L fragments of the MDV genome from lymphoblastoid cells transformed and persistently infected with MDV. *Virology* **213**, 590–599.

Petherbridge, L., Brown, A. C., Baigent, S. J., Howes, K., Sacco, M. A., Osterrieder, N. & Nair, V. K. (2004). Oncogenicity of virulent Marek's disease virus cloned as bacterial artificial chromosomes. *J Virol* **78**, 13376–13380.

Quinlivan, M., Gershon, A. A., Steinberg, S. P. & Breuer, J. (2005). An evaluation of single nucleotide polymorphisms used to differentiate vaccine and wild type strains of varicella-zoster virus. *J Med Virol* **75**, 174–180.

Quinlivan, M., Gershon, A. A., Al Bassam, M. M., Steinberg, S. P., LaRussa, P., Nichols, R. A. & Breuer, J. (2007). Natural selection for rash-forming genotypes of the varicella-zoster vaccine virus detected within immunized human hosts. *Proc Natl Acad Sci U S A* **104**, 208–212.

Roizman, B., Carmichael, L. E., Deinhardt, F., de-The, G., Nahmias, A. J., Plowright, W., Rapp, F., Sheldrick, P., Takahashi, M. & Wolf, K. (1981). *Herpesviridae.* Definition, provisional nomenclature, and taxonomy. The Herpesvirus Study Group, the International Committee on Taxonomy of Viruses. *Intervirology* **16**, 201–217.

Schäffer, A. A., Aravind, L., Madden, T. L., Shavirin, S., Spouge, J. L., Wolf, Y. I., Koonin, E. V. & Altschul, S. F. (2001). Improving the accuracy of PSI-BLAST protein database searches with composition-based statistics and other refinements. *Nucleic Acids Res* **29**, 2994–3005.

Schwyzer, M., Fischer-Bracher, C., Fraefel, C., Bächi, T., Nuñez, R., Engels, M. & Ackermann, M. (2002). Transduction of Vero cells and bovine monocytes with a herpes simplex virus-1 based amplicon carrying the gene for the bovine herpesvirus-1 Circ protein. *Vet Microbiol* **86**, 165–174.

Smith, L. P., Petherbridge, L. J., Baigent, S. J., Simpson, J. & Nair, V. (2011). Pathogenicity of a very virulent strain of Marek's disease herpesvirus cloned as infectious bacterial artificial chromosomes. *J Biomed Biotechnol* **2011**, 412829.

Spatz, S. J. (2010). Accumulation of attenuating mutations in varying proportions within a high passage very virulent plus strain of Gallid herpesvirus type 2. *Virus Res* **149**, 135–142.

Spatz, S. J. & Rue, C. A. (2008). Sequence determination of a mildly virulent strain (CU-2) of Gallid herpesvirus type 2 using 454 pyrosequencing. *Virus Genes* **36**, 479–489.

Spatz, S. J. & Silva, R. F. (2007a). Polymorphisms in the repeat long regions of oncogenic and attenuated pathotypes of Marek's disease virus 1. *Virus Genes* **35**, 41–53.

Spatz, S. J. & Silva, R. F. (2007b). Sequence determination of variable regions within the genomes of gallid herpesvirus-2 pathotypes. *Arch Virol* **152**, 1665–1678.

Spatz, S. J., Petherbridge, L., Zhao, Y. & Nair, V. (2007). Comparative full-length sequence analysis of oncogenic and vaccine (Rispens) strains of Marek's disease virus. *J Gen Virol* **88**, 1080–1096.

Spatz, S. J., Rue, C., Schumacher, D. & Osterrieder, N. (2008). Clustering of mutations within the inverted repeat regions of a serially passaged attenuated gallid herpesvirus type 2 strain. *Virus Genes* **37**, 69–80.

Tian, M., Zhao, Y., Shi, M., Lin, Y., Zou, N., Liu, P., Wen, X., Cao, S. & Huang, Y. (2010). A novel protein-coding ORF72.2 gene was identified from Marek's disease virus strain CVI988. *Virol J* **7**, 371.

Tulman, E. R., Afonso, C. L., Lu, Z., Zsak, L., Rock, D. L. & Kutish, G. F. (2000). The genome of a very virulent Marek's disease virus. *J Virol* **74**, 7980–7988.

Volkening, J. D. & Spatz, S. J. (2009). Purification of DNA from the cell-associated herpesvirus Marek's disease virus for 454 pyrosequencing using micrococcal nuclease digestion and polyethylene glycol precipitation. *J Virol Methods* **157**, 55–61.

Witter, R. L. (1997). Increased virulence of Marek's disease virus field isolates. *Avian Dis* **41**, 149–163.

Witter, R. L. (2001a). Marek's disease virus vaccines-past, present and future (chicken vs. virus-a battle of the centuries). Current progression Marek's disease research. In *Proceedings of the 6th International Symposium on Marek's disease.* Edited by K. A. Schat, R. M. Morgan, M. S. Parcells and J. L. Spencer. Kennett Square, PA: American Association of Avian Pathologists.

Witter, R. L. (2001b). Protective efficacy of Marek's disease vaccines. *Curr Top Microbiol Immunol* **255**, 57–90.

Zhao, Y., Petherbridge, L., Smith, L. P., Baigent, S. & Nair, V. (2008). Self-excision of the BAC sequences from the recombinant Marek's disease virus genome increases replication and pathogenicity. *Virol J* **5**, 19.

Jiang et al. Virology Journal 2011, 8:447
http://www.virologyj.com/content/8/1/447

VIROLOGY JOURNAL

RESEARCH Open Access

Chicken interferon alpha pretreatment reduces virus replication of pandemic H1N1 and H5N9 avian influenza viruses in lung cell cultures from different avian species

Haijun Jiang[1,2], Hanchun Yang[1] and Darrell R Kapczynski[2*]

Abstract

Background: Type I interferons, including interferon alpha (IFN-α), represent one of the first lines of innate immune defense against influenza virus infection. Following natural infection of chickens with avian influenza virus (AIV), transcription of IFN-α is quickly up regulated along with multiple other immune-related genes. Chicken IFN-α up regulates a number of important anti-viral response genes and has been demonstrated to be an important cytokine to establish anti-viral immunity. However, the mechanisms by which interferon inhibit virus replication in avian species remains unknown as does the biological activity of chicken interferon in other avian species.

Methods: In these studies, we assessed the protective potential of exogenous chicken IFN-α applied to chicken, duck, and turkey primary lung cell cultures prior to infection with the pandemic H1N1 virus (A/turkey/Virginia/SEP-4/2009) and an established avian H5N9 virus (A/turkey/Wisconsin/1968). Growth kinetics and induction of select immune response genes, including IFN-α and myxovirus-resistance gene I (Mx), as well as proinflammatory cytokines (IL-1β and IL-6), were measured in response to chicken IFN-α and viral infection over time.

Results: Results demonstrate that pretreatment with chicken IFN-α before AIV infection significantly reduced virus replication in both chicken-and turkey-origin lung cells and to a lesser degree the duck-origin cells. Virus growth was reduced by approximately 200-fold in chicken and turkey cells and 30-fold in duck cells after 48 hours of incubation. Interferon treatment also significantly decreased the interferon and proinflammatory response during viral infection. In general, infection with the H1N1 virus resulted in an attenuated interferon and proinflammatory response in these cell lines, compared to the H5N9 virus.

Conclusions: Taken together, these studies show that chicken IFN-α reduces virus replication, lower host innate immune response following infection, and is biologically active in other avian species.

Keywords: avian influenza, interferon, chicken, duck, turkey

Background

Avian influenza (AI) is a viral disease of poultry that can occur in many different bird species, with wild aquatic birds, including ducks, considered the natural reservoir for the AI viruses in the environment [1]. Both high and low pathogenic avian influenza viruses are continually being isolated from wild and domestic species of birds, causing concern of outbreaks in the poultry industry. In addition, recent outbreaks of human infections caused by influenza viruses containing genes of avian lineage, including H1N1, H5N1, H7N2, H7N3, H7N7, and H9N2, demonstrates that AI viruses can be transmitted directly to humans from domestic poultry [2]. Thus, domestic poultry can act as intermediate hosts for the transmission of influenza viruses from wild aquatic birds to humans due to the inherent closeness of rearing.

* Correspondence: darrell.kapczynski@ars.usda.gov
[2]Exotic and Emerging Avian Disease Unit, Southeast Poultry Research Laboratory, Agricultural Research Service, USDA, 934 College Station Road, Athens, GA, 30605, USA
Full list of author information is available at the end of the article

BioMed Central

© 2011 Jiang et al; licensee BioMed Central Ltd. This is an Open Access article distributed under the terms of the Creative Commons Attribution License (http://creativecommons.org/licenses/by/2.0), which permits unrestricted use, distribution, and reproduction in any medium, provided the original work is properly cited.

Interferons (IFNs) are a group of polypeptides that are secreted from most all eukaryotic cells in response to external signals. They are classified into three groups, designated type I, type II and type III. Type I IFN (α and β), are expressed rapidly after viral infection, and represent a first line of defense initiated by the innate immune response. Chicken type I IFN (ChIFN) was the first IFN to be discovered over 50 years ago and was described as a virus-induced factor able to interfere with influenza virus replication in chorioallantoic membranes of chicken embryos [3]. IFNs generally have been considered to be host species specific, yet it is known that several IFN proteins show various degrees of cross-species activity. Turkey IFN-α shares 91% and 82% identity with chicken IFN-α at the nucleotide (nt) and amino acid (aa) sequence levels, respectively. Duck IFN (DuIFN) is 73% identical to the ChIFN at the nt level but only 50% identical at the aa level [4]. Bertram et al. reported functional homology in supernatants of PHA-stimulated chicken and duck lymphocytes using in vitro proliferation assays [5]. Chicken and turkey type I IFN have also been shown to be cross-reactive [6]. However, at least one report indicates that natural DuIFN has little or no cross-reactivity on chicken cells [7].

Immediately following infection of chickens with avian influenza virus (AIV) most cells begin to express proinflammatory cytokines, including IL-1β and IL-6, and Type I IFN genes, which results in a general antiviral response through the activation of a broad range of effector molecules, including Myxovirus resistance gene I (Mx), RNA-activated protein kinase (PKR) and 2',5'-oligoadenylate synthetases (OAS) [8-10]. Chickens have a single *Mx* gene (*Mx1*) that is induced by type I IFN [11]. The original evaluation of chicken Mx1 indicated the encoded protein lacked antiviral activity [12]. Ko et al., however, reported that the chicken *Mx1* gene is highly polymorphic, and cDNAs of some but not all *Mx1* alleles transfected into mouse 3T3 cells conferred protection against vesicular stomatitis virus (VSV) and highly pathogenic AI *in vitro* [13]. Recently, we demonstrated *in vivo* differences against AI in chickens with Mx1 variant alleles [14]. At least one report indicates duck Mx does not enhance resistance to influenza virus [15].

Beginning in April 2009, cases of acute respiratory disease were reported in humans and swine in Mexico caused by a novel H1N1 influenza A virus which was subsequently declared a pandemic [16]. Reports of the pH1N1 virus in turkeys was first observed in Chile, and later in North America on turkey breeder farms in Virginia and California, as well as Canada http://www.ars.usda.gov/2009h1n1/. The pH1N1 has also been detected in other species including dogs [17] and ferrets [18]. The pH1N1 is a triple reassortant virus containing genes from human (PB1), avian (PB2, PA), and swine (HA, NP, NA, M, NS) influenza viruses. The presence of avian and swine influenza virus genes in the pH1N1 raises the potential for infection in poultry following exposure to infected humans or swine. This is especially true for turkeys because of their known susceptibility to type A influenza viruses and the history of infection with triple reassortant viruses [19-22].

Our understanding of the immunological response to avian influenza by different avian species is largely unknown. In this study, we compared the growth kinetics of two avian influenza viruses containing both mammalian and avian origin genes (H1N1), or avian genes only (H5N9), in primary lung cell cultures from three common domestic poultry species (chicken, duck and turkey). The influence of chicken IFN-α on viral replication and host innate immune response genes following infection was also determined. Overall, chicken IFN-α reduced virus replication in all cell lines tested and decreased interferon and proinflammatory responses following AIV infection.

Results

Pretreatment with rChIFN-α inhibits AIV replication

To investigate the antiviral potential of chicken IFN-α against AIV *in vitro*, chicken, duck, and turkey primary lung cells were pretreated with 1000 U/ml rChIFN-α for18 hours prior to infection and viral growth was measured over 48 hours. As show in Figure (1A and 1C), at 2 hpi, reduced viral titers were first observed in chicken and turkey lung cell cultures pretreated with rChIFN-α. From 12 to 48 hpi, rChIFN-α significantly reduced virus replication compared to sham-treated cells ($P < 0.05$). At 24 and 48 hpi, virus growth was reduced by approximately 200-fold in both chicken and turkey lung cells. In duck lung cells, results demonstrate that pretreatment with rChIFN-α before AIV infection reduced virus replication, albeit to a lesser degree than observed with chicken or turkey cells (Figure 1B). At 2 hpi, no reduction in virus titer was observed. From 12 to 48 hpi, a reduction of virus titer was observed by approximately 30-fold in duck cells. Although no statistical difference was observed, a biological difference is apparent. These data demonstrate that rChIFN-α can reduce virus replication and is biologically active in other avian species.

Pretreatment with rChIFN-α inhibits H1N1 and H5N9 virus NP expression

To further demonstrate rChIFN-α pretreatment inhibits the replication of AIV, immunofluorescence assays to detect viral nuclear protein were performed. Figure 2 demonstrates decreased levels of viral NP expression at 24 hpi in the rChIFN-α treated chicken lung cells than untreated-infected cells with both H1N1 and H5N9 AIV. Similar staining patterns were observed for both duck

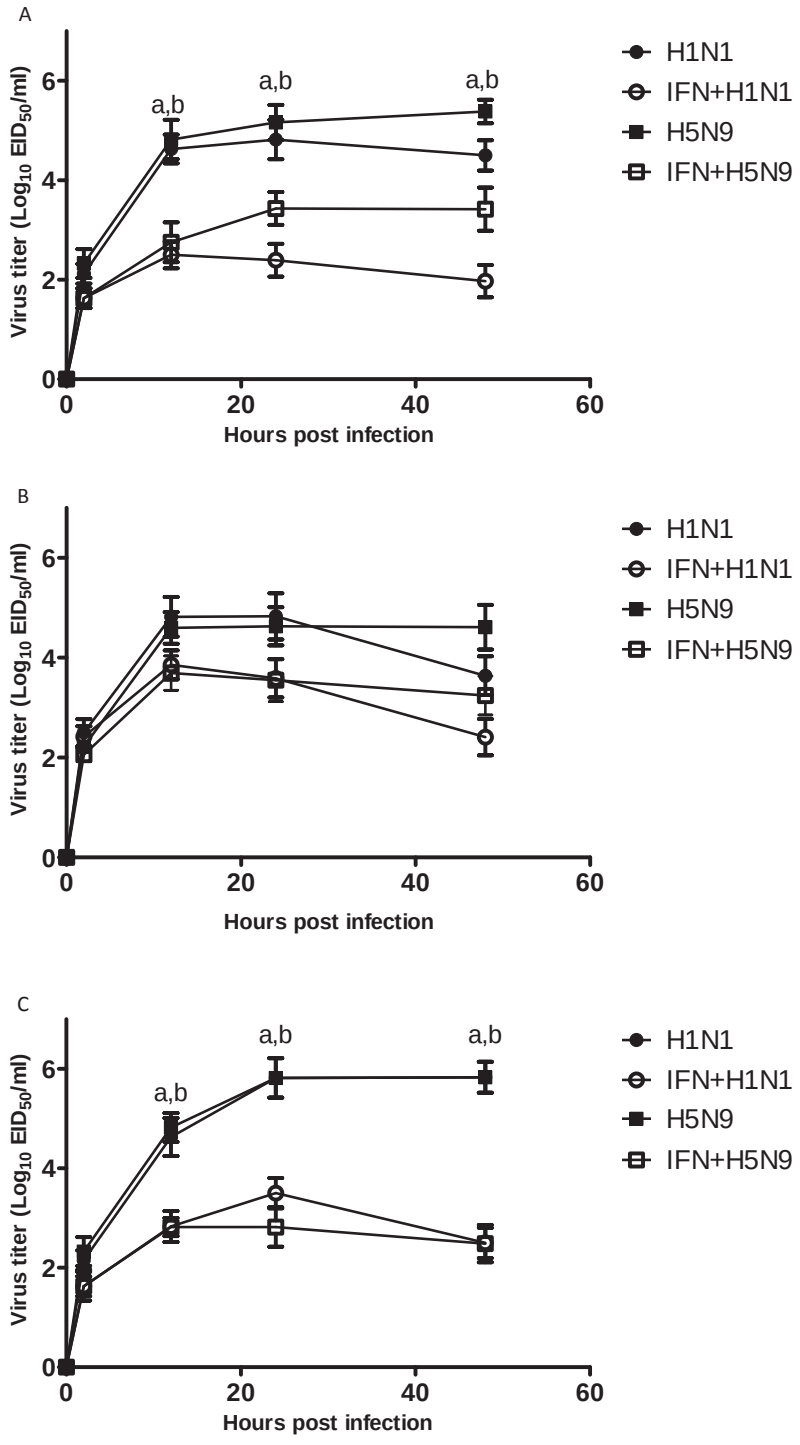

Figure 1 Recombinant ChIFN-α reduces avian influenza virus replication. Inhibition of avian influenza virus (H1N1 and H5N9) replication in primary lung cell cultures derived from chicken (A), duck (B), and turkey (C) after rChIFN-α (1000 U/ml) pretreatment in vitro. Cells were infected with A/turkey/Virginia/2009 H1N1 or A/turkey/Wisconsin/68 H5N9 at MOI 0.1. Supernatants were harvested at the times indicated and viral titers were determined following injection into SPF embryos. The mean (and standard deviations) of three independent experiments are shown. Different lowercase letters denote significance in titer following rChIFN-α treatment groups (within columns) ($P < 0.05$) as determined by one-way ANOVA. Statistical differences ($P < 0.05$) following treatment between virus groups are shown by lowercase letter.

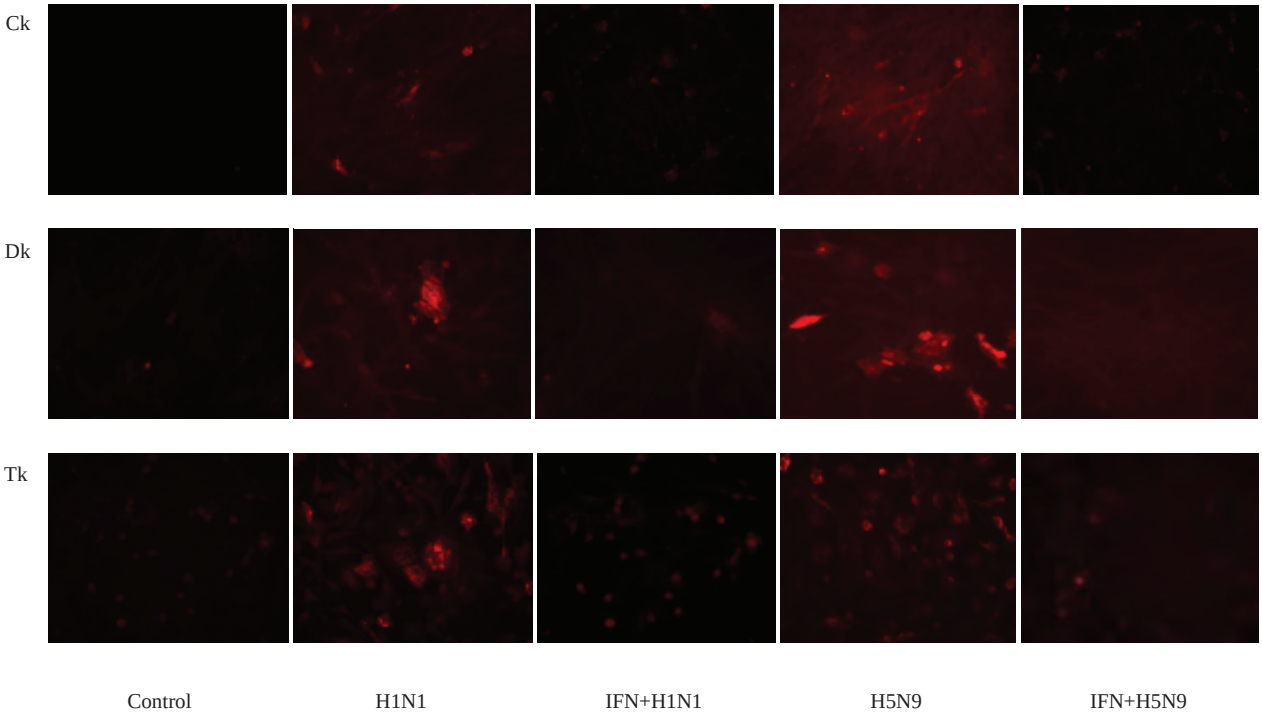

Figure 2 Recombinant ChIFN-α inhibits pH1N1 and H5N9 virus nuclear protein expression. Primary chicken, turkey, and duck lung cells were pretreated with or without rChIFN-α (1000 U/ml) for 18 h. Monolayers were infected with either H1N1 or H5N9 avian influenza virus (MOI = 0.1) for 1 h, and replaced with fresh media. After 24 hours, cells were fixed and viral antigens were reacted with mouse-derived monoclonal antibody (P13C11) specific for type A influenza virus nucleoprotein followed by detection with Texas Red-labeled goat anti-mouse IgG antibody. Magnification 400×.

and turkey lung cell cultures (data not shown). No staining was observed in any uninfected control cells. These results indicated that the pretreatment of cells with rChIFN-α strongly inhibits viral NP production.

Reduced CPE following rChIFN-α pretreatment following AIV infection

The protective effect of rChIFN-α against CPE was determined in pretreated and virus-infected lung cell cultures. In uninfected-control chicken lung cells with or without IFN-α treatment, epithelial-like cell cultures were observed with clearly defined nucleus and cytoplasm in individual cells (Figure 3A and 3B). Morphologically, no CPE was observed for lung cells pretreated with rChIFN-α alone (Figure 3B). Additionally, chicken IFN-α was noncytotoxic based on cell viability after 48 hours exposure on all species tested (data not shown). Strong CPE was observed in both the H1N1 (Figure 3C) and H5N9 (Figure 3E) infected cells at 24 hpi, including decreased cell numbers and holes in monolayer with decreased direct cell-to-cell contact. However, pretreatment of monolayers with rChIFN-α abrogated the CPE observed in the virus infected cultures (Figure 3D and 3F). These results demonstrate that pretreatment of cells with rChIFN-α protected cells against virus induced CPE.

Interferon-treatment attenuate the cytokine gene expression

We next investigated the effects of rChIFN-α on the innate immune response of avian lung cells to AIV using quantitative real-time RT-PCR. AIV infected and rChIFN-α pretreated cells were compared for induction of IFN-α, Mx, IL-1β and IL-6 mRNA at 12, 24 and 48 hpi. In all cell types tested, IFN-α pretreatment did not increase expression of the pro-inflammatory cytokines or IFN-α, but did up regulate Mx gene expression 2-5 fold (data not shown). In chicken lung cells, both H1N1 and H5N9 viruses induced an increased IFN-α response compared to sham-infected cells after infection that peaked early and declined over time (Figure 4). In contrast, rChIFN-α pretreatment resulted in a significant decrease of IFN-α expression after viral infection. Expression of the Mx gene was markedly higher in chicken lung cells after viral infection, especially in the H5N9 group which increased expression approximately 120-fold over the sham-infected cells. However, rChIFN-α pretreatment significantly reduced expression at all time points taken. Both viruses tested up regulated the proinflammatory cytokine genes, IL-1β and IL-6, after infection. Pretreatment with rChIFN-α significantly reduced expression compared to virus-infected cells. In general the H5N9

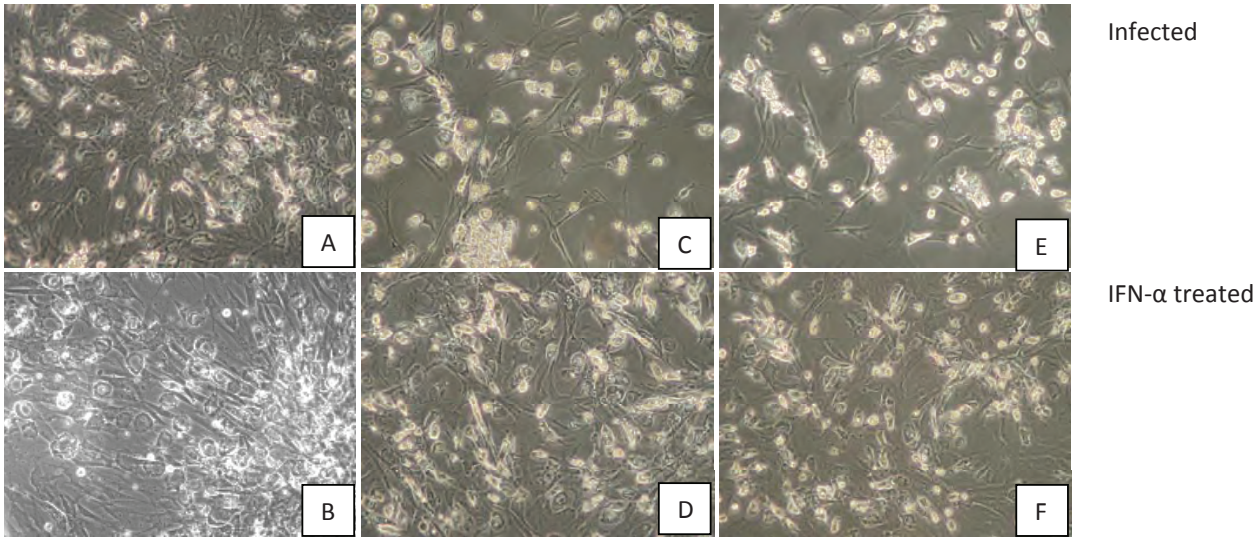

Figure 3 Reduced cytopathic effect following rChIFN-α pretreatment following AIV infection. Primary chicken lung cell monolayers were pretreated with 1000 U/ml of rChIFN-α and infected with either H1N1 of H5N9 at 0.1 MOI. Negative control cells include no treatment/no virus (A), and IFN-α only (B). Protection from cytopathic effect was observed in cells infected with virus only, H1N1 (C) and H5N9 (E), compared with IFN-α treated cells that were then infected with H1N1 (D) or H5N9 (F). At 24 hpi the monolayers were digitally photographed using an inverted microscope at 200× magnification (Olympus America Inc., Melville, NY).

virus stimulated a higher innate immune response in chicken cells with the four genes examined than the H1N1 virus.

In duck lung cells, neither H1N1 nor H5N9 viruses induced an increased IFN-α response compared to sham-infected cells (Figure 5). However, an increase in Mx expression was observed after H5N9, but not H1N1, infection that peaked with a 12-fold increase at 48 hpi. Pretreatment of cells with rChIFN-α significantly reduced Mx expression at all times tested. IL-6 gene expression was only up regulated following H5N9 infection, whereas the H1N1 virus did not induce up regulation of either IL-6 or IL-1β.

In turkey lung cells, both H1N1 and H5N9 viruses induced an increased IFN-α response compared to sham-infected cells that also peaked early after infection and declined over time (Figure 6). rChIFN-α pretreatment significantly decreased the magnitude of IFN-α expression following H1N1 and H5N9 infection. Following virus infection, expression of the Mx gene was markedly high with both viruses inducing approximately 270-fold increase. Interestingly, pretreatment with rChIFN-α reduced Mx expression after virus infection, but not to the levels observed in either the chicken or duck cells, which were reduced to < 2 fold increase. Both viruses up regulated the IL-1β and IL-6, after infection in turkey cells, although the H5N9 stimulated a more robust response. Pretreatment with rChIFN-α significantly reduced the proinflammatory responses compared to virus-infected cells.

Discussion

Avian influenza viruses present a permanent concern to the poultry industry and the recent emergence of pandemic H1N1 and highly pathogenic avian influenza H5/H7 subtypes serves as a reminder that influenza remains a severe threat throughout the world. Beside vaccination, there is an urgent need for new antiviral strategies to protect and treat against influenza. A significant portion of that strategy is to determine the influence of host-derived immune proteins on virus replication. Because AIV initially replicates on mucosal surfaces of avian species, including the respiratory tract, we chose to compare the immunological effect on replication in cells from this tissue. We report here that pretreatment with rChIFN-α before AIV infection reduced virus replication in chicken, duck and turkey lung cells.

Our study demonstrates that rChIFN-α reduces virus infection by limiting AIV replication, determined by decreased viral titers and decreased production of viral NP. The NP is important for maintaining the structure of the ribonucleoprotin complex, as well as genome replication by interacting with viral RNA [23-25]. Thus a reduction of viral protein synthesis appears to be at least on mechanism of anti-viral effect following rCHIFN-α treatment. Previously, three mechanisms of antiviral effects

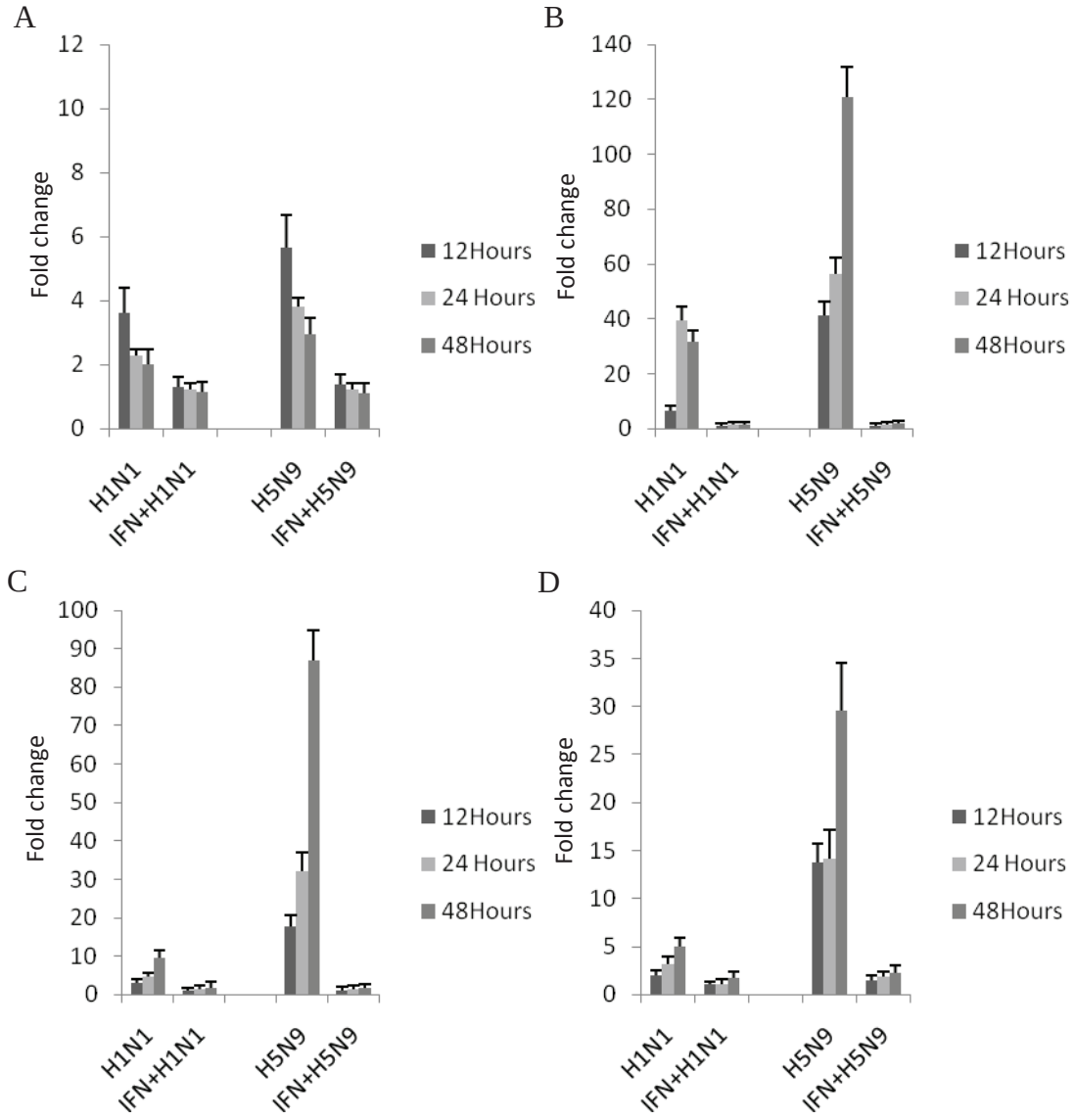

Figure 4 Relative expression of select immune response genes following pretreatment of primary chicken lung cells with 1000 U/ml rChIFN-α, and infection with H1N1 or H5N9, compared to control (untreated/uninfected) cells. The relative expression of IFN-α (A), Mx (B), IL-6 (C), and IL-1β (D) was measured following mock treatment at various time points post infection in three independent experiments. RNA from lung cells was normalized using the 28S house-keeping gene. Data are expressed as fold change in mRNA levels between interferon treated and infected cells compared with those from untreated and uninfected (negative control) cells.

induced by IFN-α have been described in mice and humans, including activation of PKR, OAS, and Mx. Both PKR and OAS are important effector molecules that mediate a cellular response to foreign RNA structures [26,27]. Although neither PKR nor OAS induction was measure in this study, we show here that rChIFN-α pretreatment does up regulate Mx in chicken, turkey and duck cells, and positively correlated with decreasing virus replication. Further studies to determine the nature of viral inhibition with Mx proteins derived from different avian species are ongoing.

Previous studies have shown that chicken IFN-α administered to chicken by oral ingestion or intravenous injection can inhibit avian viruses including H9N2 AIV, Newcastle disease virus, infectious bursal disease virus, infectious bronchitis virus, Rous sarcoma virus, and Marek's disease virus [28,29]. In our studies, the presence of rChIFN-α significant limited the ability of these viruses to replicate, especially in the chicken and turkey lung cell cultures. Previous research indicates that chicken and turkey type I IFNs have been shown to be cross-reactive, such that some level of cross protection

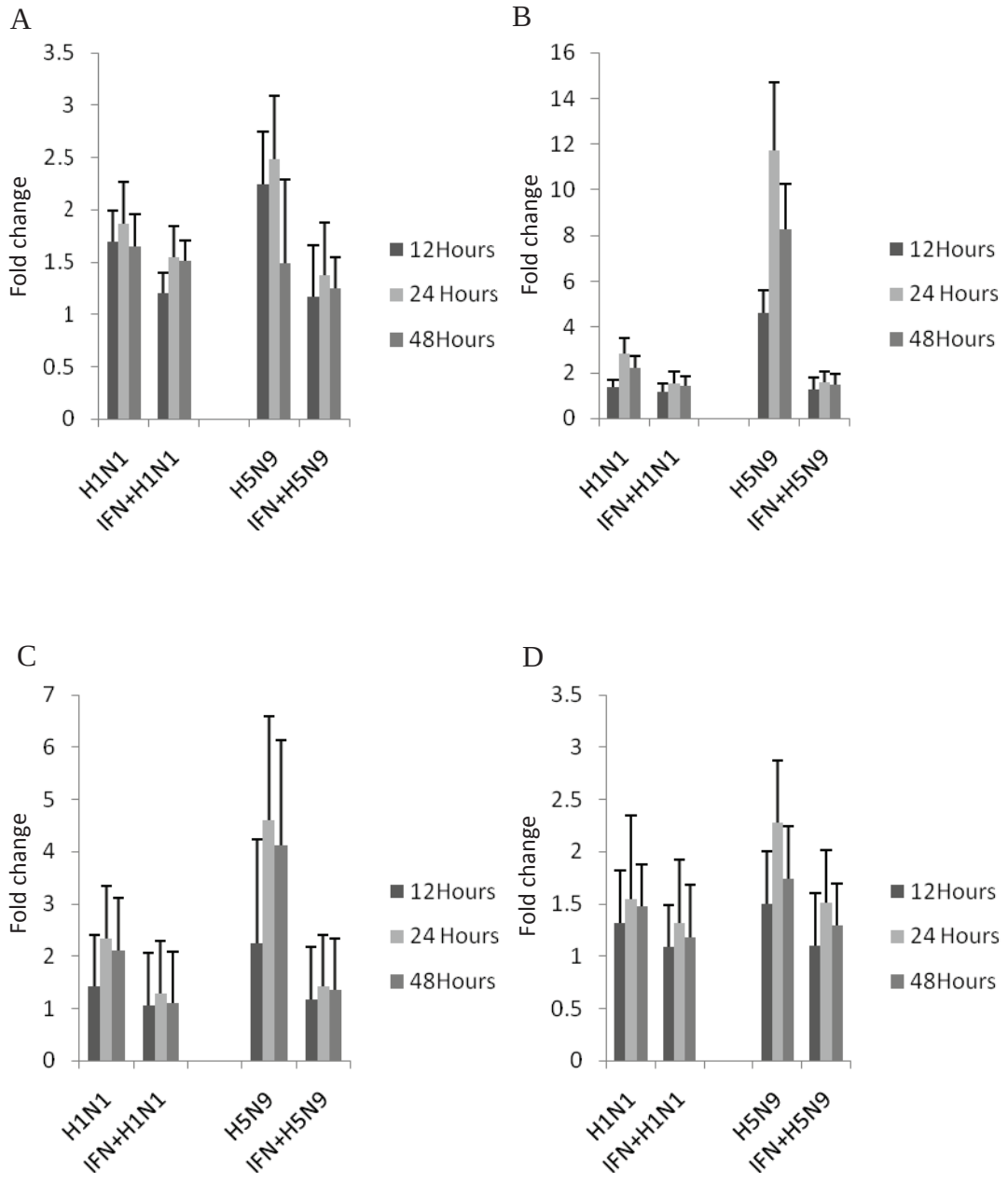

Figure 5 Relative expression of select immune response genes following pretreatment of primary duck lung cells with 1000 U/ml rChIFN-α, and infection with H1N1 or H5N9, compared to control (untreated/uninfected) cells. The relative expression of IFN-α (A), Mx (B), IL-6 (C), and IL-1β (D) was measured following mock treatment at various time points post infection in three independent experiments. RNA from lung cells was normalized using the GADPH house-keeping gene. Data are expressed as fold change in mRNA levels between interferon treated and infected cells compared with those from untreated and uninfected (negative control) cells.

was not unexpected in the turkey lung cells. The rChIFN-α did not reduce titers on duck cells to the level observed in the chicken or turkey lung cells. However, a moderate biological effect (> 1 $\log_{10}$ reduction) was evident in the absence of statistical differences. Because of the amino acid differences between chicken and duck IFN, it seems likely that rChIFN-α is not as efficient at inducing an antiviral effect in this species. Whether this effect is due to decreased IFN-α receptor affinity or downstream transcription factor activation for cytokine expression remains to be determined.

When virus replication was compared between the three kinds of primary lung cells, we observed that both viruses replicate to the highest titers on the turkey lung cells, followed by chicken lung cells and duck lung cells. This data suggest that turkey may be more susceptible

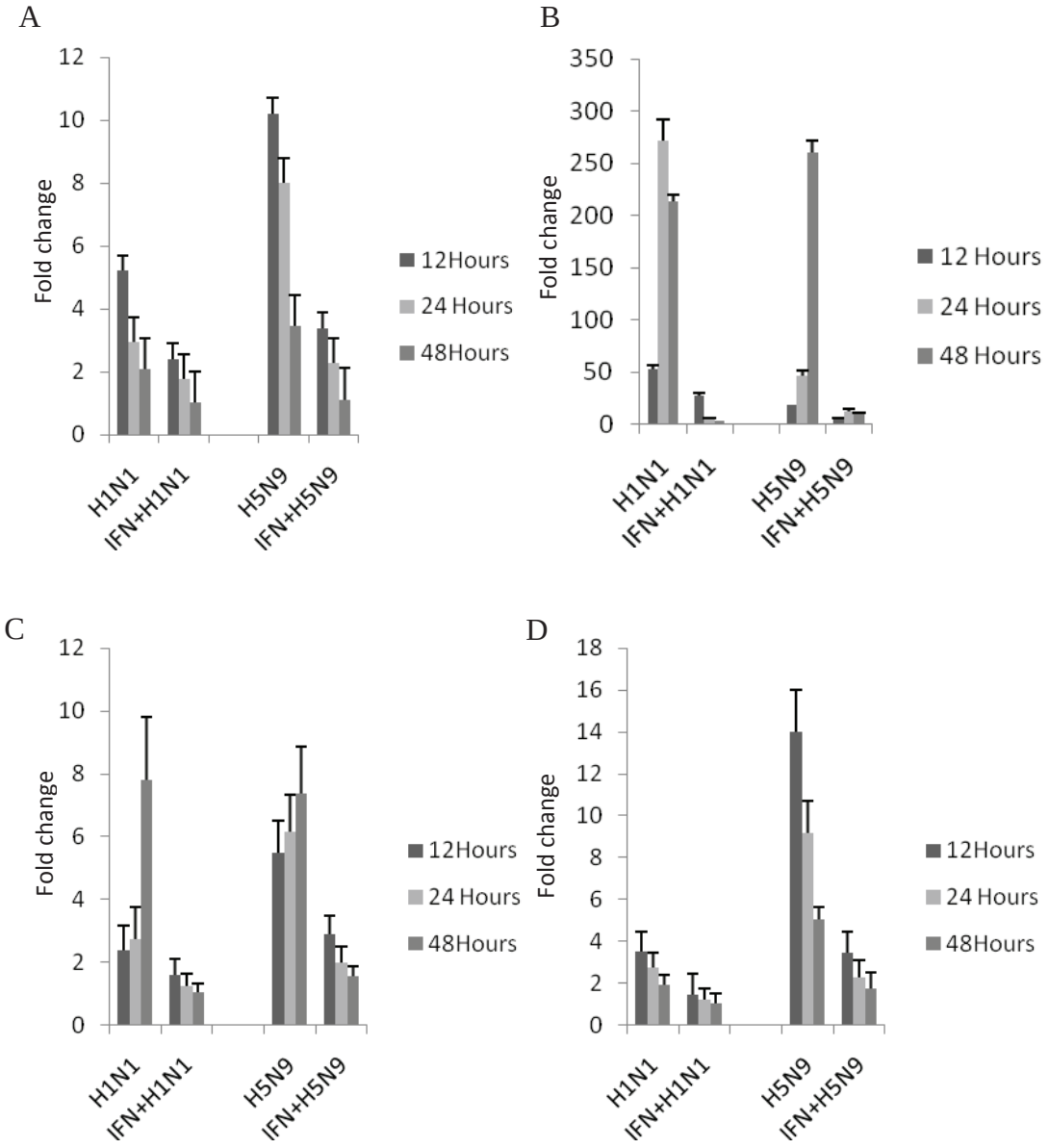

Figure 6 Relative expression of select immune response genes following pretreatment of primary turkey lung cells with 1000 U/ml rChIFN-α, and infection with H1N1 or H5N9, compared to control (untreated/uninfected) cells. The relative expression of IFN-α (A), Mx (B), IL-6 (C), and IL-1β (D) was measured following mock treatment at various time points post infection in three independent experiments. RNA from lung cells was normalized using the 28S house-keeping gene. Data are expressed as fold change in mRNA levels between interferon treated and infected cells compared with those from untreated and uninfected (negative control) cells.

to H1N1 and H5N9 virus than white leghorn chickens and Pekin ducks. This result may not be unexpected since both viruses are of turkey origin and maybe be better adapted for this species. These results also highlight the role of turkeys as intermediate host in the transmission of influenza viruses from domestic poultry to humans. The detection of α2,3 (avian type) and α2,6 (mammalian type) sialic-acid-linked receptors in the turkeys further indicate that this species can replicate both avian and mammalian viruses [19,30,31]. This is consistent with some reports that turkeys were more susceptible to disease from LPAI virus than chickens and ducks [32-34].

Interestingly, interferon treatment significantly decreased the interferon and proinflammatory response after viral infection. The decreased proinflammatory response positively correlated with decreased virus replication, and may explain the reason for this observation. In addition, infection with the H1N1 virus produced a decreased expression of the innate immune genes tested,

including Mx, IL-1β and IL-6 than observed with the H5N9 virus. This result is consistent with some recent reports that indicate pandemic H1N1 isolates induce weaker cytokines responses in human cells [35,36]. In general, a robust cytokine response is associated with highly pathogenic influenza viruses, including H5N1 viruses, and it is thought that this cytokine dysregulation may contribute to disease severity [37]. Our results with low pathogenic AI suggests that a suboptimal cytokine response maybe in part explain how H1N1 could escape the innate immune defense by impeding cytokine response. This phenomenon maybe characteristic of low pathogenic AI viruses as well since they also have demonstrated the ability to limit the host's antiviral Mx response in chickens in vivo [38]. Data presented here will contribute to a better understanding of the avian host response to the low pathogenic AI viruses, and our model of testing primary avian lung cell cultures will be useful for monitoring new AIV isolates for changes in innate immune modulation.

Conclusions

The present study demonstrates that pretreatment with rChIFN-α prior to infection with the pandemic H1N1 and H5N9 avian influenza viruses not only significantly reduced virus replication in both chicken-and turkey-origin lung cells, and to a lesser degree the duck-origin lung cells, but also significantly decreased the interferon and proinflammatory response after viral infection. Thus, under the scenario of avian influenza, rChIFN-α might provide an additional option in the prevention and therapy against low pathogenic AIV infection. Similar conclusions were recently described following oral administration of rChIFN-α and H9N2 AIV infection [28]. Further investigation into the molecular mechanisms of protection induced by chicken IFN-α are underway and will add more information on its anti-viral role.

Methods

Virus and cell culture infection

The low pathogenic AI viruses H1N1 A/turkey/Virginia/SEP-4/2009 (H1N1) and H5N9 A/turkey/Wisconsin/68 (H5N9) were propagated in the allantoic cavities of 11 day of embryonating specific pathogen free (SPF) turkey eggs. Viral titers were determined as previously described [39]. All experiments using infectious virus were conducted in a biosafety level 2 (BSL-2) facilities at the Southeast Poultry Research Laboratory (SEPRL), Agricultural Research Service, United States Department of Agriculture (USDA) in Athens, Georgia.

Cells isolation and culture

Avian lung primary cells were isolated as described previously with minor modifications [40]. Briefly, lungs from four-week-old specific pathogen-free (SPF) white leghorn chickens, six-week-old SPF Beltsville White turkeys and eight-week-old commercial Pekin ducks were aseptically collected and trypsinized before culturing in 12-well tissue culture plate coated with 0.01% (w/v) calf skin collagen (Sigma Chemical Co., St. Louis, Mo.). Cells were cultured at 1×10^6 lung cells per ml of Dulbecco's modified Eagle's medium (DMEM) supplemented with 1% L-glutamine, 1% sodium pyruvate, 1% MEM nonessential amino acids, 1% antibiotic-antimycotic solution (Sigma), and 10% chicken serum in a humidified incubator at 37°C. All animals used in these studies were housed and handled in compliance with our Institutional Animal Care and Use Committee guidelines and procedures.

rChIFN-α treatment and virus infection

Lung cells were grown overnight in 12-well plates (Fisher Scientific, Atlanta, Ga). Immediately before IFN treatment, the cells were washed with warm PBS and subsequently treated with 1000 U/ml of recombinant chicken IFN-α (rChIFN-α, AbD Serotec Co., Oxford, UK) for 18 hours in MEM containing 0.2% bovine albumin (BA) and antibiotics. After treatment, rChIFN-α was aspirated and cells were washed with PBS. Thereafter, cells were inoculated with H1N1 or H5N9 at a multiplicity of infection (MOI) of 0.1 diluted in DMEM containing antibiotics for one hour at 37°C with gentle agitation every 10 minutes. After one hour of incubation, unabsorbed virus was removed and cells were washed with PBS. Fresh media supplemented with 0.01 μg/ml TPCK trypsin (Sigma) were added per well and the plate were incubated at 37°C and 5% CO2. At 0, 2, 12, 24 and 48 hours post infection (hpi), supernatants were collected and stored at -80°C until used for titrations. Lung cells were harvested for RNA extraction at 12, 24, 48 hpi. Virus titers was determined using the method of Reed and Muench and expressed as log10 50% embryo infectious dose (EID_{50}) [41]. Controls included one plate without virus and another one plate without either rChIFN-α or virus. The plate was then incubated under the same conditions as above.

Immunofluorescence assays for virus nuclear protein (NP)

To analyze antiviral effect of rChIFN-α on virus replication, primary avian lung cells were cultured on glass cover slips in 24-well plate. After rChIFN-α treatment and virus infection for 24 hours (as described above), cells were washed with PBS twice, fixed and permeabilized with ice-cold methanol. Viral antigens were detected with mouse-derived monoclonal antibody specific for a type A influenza virus nucleoprotein (developed at Southeast Poultry Research Laboratory, USDA) [42]. Cells were then stained with TRITC-conjugated anti-mouse IgG antibody (Sigma). The stained cells

were visualized with immunofluorescence microscopy (Olympus America Inc., Melville, NY) under 400× magnification.

Cytopathic effect (CPE) of rChIFN-α pretreatment on virus infection

To visually compare virus inhibition following rChIFN-α treatment, primary avian lung cells were seeded as above on glass cover slips in 24-well plate. Following rChIFN-α treatment, cells were virally infected as described above. After 24 hours, the cells were fixed with ice-cold acetone and CPE was visualized by inverted microscopy (Olympus).

Isolation of RNA and analysis of cytokine expression by real-time RT-PCR (RRT-PCR)

RNA was extracted using the RNeasy mini kit (Qiagen) in accordance with the manufacturer's instructions. Relative cytokine expression in lung cells was examined by RRT-PCR. IL-1β, IL-6, IFN-α, and Mx expression were determined as previously described [14,43]. Briefly, quantitative RRT-PCR was performed for each sample in triplicate in a total volume of 25 μl, consisting of 12.5 μl iQ Sybrgreen supermix (Bio-Rad Laboratories, Los Angeles, CA, USA) with 1 μl of each primer at concentration of 10 pmol/μl, 5.5 μl RNase/DNase-free water, and 5 μl diluted RNA. PCR conditions were the same for each targeted gene and are as follows: 10 min at 50°C, 95°C for 5 min, followed by 45 cycles of 95°C for 10 s and 56°C for 30 s. Primers for chicken 28 s, IFN-α, IL-1β [14]; turkey 28 s, IL-1β, IL-6 [44]; duck GAPDH, IL-1β, IL-6, IFN-α [45] have been previously described. The other primers were designed using the Primer Express software program (Applied Biosystems, Foster City, California, USA) and sequences used in this study for individual avian species are presented in Table 1. The specificity for each primer set was tested by both subjecting the PCR products to 1.5% agarose gel electrophoresis (data not shown) and analyzing the melting curve in the iCycler iQ real-time PCR detection system (Bio-Rad) after each real-time PCR reaction.

RNA from individual lung cell sample was normalized using the 28S for chicken and turkey and GAPDH for duck. For each gene, amplification was verified using four 10-fold serial dilutions of standard spleen cell RNA in the same PCR run. Expression was determined by the standard curve method [46]. Data are expressed as fold change in cytokine messenger RNA (mRNA) levels in infected groups compared with those from uninfected, untreated groups.

Statistical analyses

Data are expressed as the mean ± standard error. Statistical differences were analyzed with Tukey one-way ANOVA using Prism 5 (GraphPad Co., San Diego, CA). All statistical tests were performed using $P \leq 0.05$.

Table 1 Real-time quantitative RT-PCR primers used in this study[1]

RNA target	Primer Sequence (5'-3')	Species
28S	F: GGCGAAGCCAGAGGAAACT	C, T
	R: GACGACCGATTTGCACGTC	
GADPH	F: ATGTTCGTGATGGGTGTGAA	D
	R: CTGTCTTCGTGTGTGGCTGT	
IFN-α	F: GACAGCCAACGCCAAAGC	C, T
	R: GTCGCTGCTGTCCAAGCATT	
IFN-α	F: TCCTCCAACACCTCTTCGAC	D
	R: GGGCTGTAGGTGTGGTTCTG	
Mx	F: CAGGACATCAACGACAATCT	C, T
	R: TTGCCAGATGAGGGATAGTA	
Mx	F: TCAATCACTTTCCTCACCAG	D
	R: CCTTCTGCTTGTGTTGAGAC	
IL-6	F: GCGAGAACAGCATGGAGATG	C
	R: GTAGGTCTGAAAGGCGAACAG	
IL-6	F: GCTCGCCGGCTTCGA	T
	R: GGTAGGTCTGAAAGGCGAACAG	
IL-6	F: TTCGACGAGGAGAAATGCTT	D
	R: CCTTATCGTCGTTGCCAGAT	
IL-1β	F: ACATGTCGTGTGTGATGAG	C
	R: CAG CCGGTAGAAGATGAAGC	
IL-1β	F: GCTCTACATGTCGTGTGTGATGAG	T
	R: TGTCGATGTCCCGCATGA	
IL-1β	F: TCGACATCAACCAGAAGTGC	D
	R: GAGCTTGTAGCCCTTGATGC	

[1] F, forward primer; R, reverse primer; C, chicken; T, turkey; D, duck.

Acknowledgements
The authors wish to thank Cam Greene and Aniko Zsak for expert technical help. This research was supported by USDA, ARS, CRIS project 6612-32000-053.

Author details
[1]Key Laboratory of Zoonosis of Ministry of Agriculture, College of Veterinary Medicine and State Key Laboratory of Agrobiotechnology, China Agricultural University, Beijing, People's Republic of China. [2]Exotic and Emerging Avian Disease Unit, Southeast Poultry Research Laboratory, Agricultural Research Service, USDA, 934 College Station Road, Athens, GA, 30605, USA.

Authors' contributions
HJ and DRK carried out virus growth on cell culture as well as RRT-PCR for avian cytokines. HJ performed immunohistochemistry and cytology of primary avian lung cultures. HY participated in study design and coordination. HJ and DRK wrote the manuscript. All authors approved the final manuscript.

Competing interests
The authors declare that they have no competing interests.

Received: 27 April 2011 Accepted: 22 September 2011
Published: 22 September 2011

References

1. Webby RJ, Webster RG: Are we ready for pandemic influenza? *Science* 2003, **302**:1519-1522.

2. Akey BL: **Low-pathogenicity H7N2 avian influenza outbreak in Virgnia during 2002.** *Avian Dis* 2003, **47**:1099-1103.
3. Isaacs A, Lindenmann J: **Virus interference. I. The interferon.** *Proc R Soc Lond B Biol Sci* 1957, **147**:258-267.
4. Schultz U, Kock J, Schlicht HJ, Staeheli P: **Recombinant duck interferon: a new reagent for studying the mode of interferon action against hepatitis B virus.** *Virology* 1995, **212**:641-649.
5. Bertram EM, Jilbert AR, Kotlarski I: **An homologous in vitro assay to detect lymphokines released by PHA-activated duck peripheral blood lymphocytes and spleen cells.** *Vet Immunol Immunopathol* 1997, **56**:163-174.
6. Suresh M, Karaca K, Foster D, Sharma JM: **Molecular and functional characterization of turkey interferon.** *J Virol* 1995, **69**:8159-8163.
7. Ziegler RE, Joklik WK: **Effect of interferon on multiplication of avian sarcoma virus B77 in duck embryo fibroblasts.** *J Interferon Res* 1981, **1**:521-538.
8. Garcia-Sastre A: **Inhibition of interferon-mediated antiviral responses by influenza A viruses and other negative-strand RNA viruses.** *Virology* 2001, **279**:375-384.
9. Sarmento L, Pantin-Jackwood M, Kapczynski DR, Swayne DE, Afonso CL: **Immediate early responses of avian tracheal epithelial cells to infection with highly pathogenic avian influenza virus.** *Dev Biol (Basel)* 2008, **132**:175-183.
10. Daviet S, Van Borm S, Habyarimana A, Ahanda ML, Morin V, Oudin A, Van Den Berg T, Zoorob R: **Induction of Mx and PKR failed to protect chickens from H5N1 infection.** *Viral Immunol* 2009, **22**:467-472.
11. Schumacher B, Bernasconi D, Schultz U, Staeheli P: **The chicken Mx promoter contains an ISRE motif and confers interferon inducibility to a reporter gene in chick and monkey cells.** *Virology* 1994, **203**:144-148.
12. Bernasconi D, Schultz U, Staeheli P: **The interferon-induced Mx protein of chickens lacks antiviral activity.** *J Interferon Cytokine Res* 1995, **15**:47-53.
13. Ko JH, Jin HK, Asano A, Takada A, Ninomiya A, Kida H, Hokiyama H, Ohara M, Tsuzuki M, Nishibori M, *et al*: **Polymorphisms and the differential antiviral activity of the chicken Mx gene.** *Genome Res* 2002, **12**:595-601.
14. Ewald SJ, Kapczynski DR, Livant EJ, Suarez DL, Ralph J, McLeod S, Miller C: **Association of Mx1 Asn631 variant alleles with reductions in morbidity, early mortality, viral shedding, and cytokine responses in chickens infected with a highly pathogenic avian influenza virus.** *Immunogenetics* 2011, 363-375.
15. Bazzigher L, Schwarz A, Staeheli P: **No enhanced influenza virus resistance of murine and avian cells expressing cloned duck Mx protein.** *Virology* 1993, **195**:100-112.
16. Dawood FS, Jain S, Finelli L, Shaw MW, Lindstrom S, Garten RJ, Gubareva LV, Xu X, Bridges CB, Uyeki TM: **Emergence of a novel swine-origin influenza A (H1N1) virus in humans.** *N Engl J Med* 2009, **360**:2605-2615.
17. Dundon WG, De Benedictis P, Viale E, Capua I: **Serologic evidence of pandemic (H1N1) 2009 infection in dogs, Italy.** *Emerg Infect Dis* 2010, **16**:2019-2021.
18. Munster VJ, de Wit E, van den Brand JM, Herfst S, Schrauwen EJ, Bestebroer TM, van de Vijver D, Boucher CA, Koopmans M, Rimmelzwaan GF, *et al*: **Pathogenesis and transmission of swine-origin 2009 A(H1N1) influenza virus in ferrets.** *Science* 2009, **325**:481-483.
19. Kapczynski DR, Gonder E, Liljebjelke K, Lippert R, Petkov D, Tilley B: **Vaccine-induced protection from egg production losses in commercial turkey breeder hens following experimental challenge with a triple-reassortant H3N2 avian influenza virus.** *Avian Dis* 2009, **53**:7-15.
20. Choi YK, Lee JH, Erickson G, Goyal SM, Joo HS, Webster RG, Webby RJ: **H3N2 influenza virus transmission from swine to turkeys, United States.** *Emerg Infect Dis* 2004, **10**:2156-2160.
21. Tang Y, Lee CW, Zhang Y, Senne DA, Dearth R, Byrum B, Perez DR, Suarez DL, Saif YM: **Isolation and characterization of H3N2 influenza A virus from turkeys.** *Avian Dis* 2005, **49**:207-213.
22. Yassine HM, Al-Natour MQ, Lee CW, Saif YM: **Interspecies and intraspecies transmission of triple reassortant H3N2 influenza A viruses.** *Virol J* 2007, **4**:129.
23. Honda A, Mizumoto K, Ishihama A: **Minimum molecular architectures for transcription and replication of the influenza virus.** *Proc Natl Acad Sci USA* 2002, **99**:13166-13171.
24. Yamanaka K, Ishihama A, Nagata K: **Reconstitution of influenza virus RNA-nucleoprotein complexes structurally resembling native viral ribonucleoprotein cores.** *J Biol Chem* 1990, **265**:11151-11155.
25. Baudin F, Bach C, Cusack S, Ruigrok RW: **Structure of influenza virus RNP. I. Influenza virus nucleoprotein melts secondary structure in panhandle RNA and exposes the bases to the solvent.** *Embo J* 1994, **13**:3158-3165.
26. Garcia MA, Gil J, Ventoso I, Guerra S, Domingo E, Rivas C, Esteban M: **Impact of protein kinase PKR in cell biology: from antiviral to antiproliferative action.** *Microbiol Mol Biol Rev* 2006, **70**:1032-1060.
27. Ronni T, Matikainen S, Sareneva T, Melen K, Pirhonen J, Keskinen P, Julkunen I: **Regulation of IFN-alpha/beta, MxA, 2',5'-oligoadenylate synthetase, and HLA gene expression in influenza A-infected human lung epithelial cells.** *J Immunol* 1997, **158**:2363-2374.
28. Meng S, Yang L, Xu C, Qin Z, Xu H, Wang Y, Sun L, Liu W: **Recombinant Chicken Interferon-alpha Inhibits H9N2 Avian Influenza Virus Replication In Vivo by Oral Administration.** *J Interferon Cytokine Res* 2011.
29. Plachy J, Weining KC, Kremmer E, Puehler F, Hala K, Kaspers B, Staeheli P: **Protective effects of type I and type II interferons toward Rous sarcoma virus-induced tumors in chickens.** *Virology* 1999, **256**:85-91.
30. Kimble B, Nieto GR, Perez DR: **Characterization of influenza virus sialic acid receptors in minor poultry species.** *Virol J* 2010, **7**:365.
31. Pillai SP, Lee CW: **Species and age related differences in the type and distribution of influenza virus receptors in different tissues of chickens, ducks and turkeys.** *Virol J* 2010, **7**:5.
32. Tumpey TM, Kapczynski DR, Swayne DE: **Comparative susceptibility of chickens and turkeys to avian influenza A H7N2 virus infection and protective efficacy of a commercial avian influenza H7N2 virus vaccine.** *Avian Dis* 2004, **48**:167-176.
33. Spackman E, Gelb J, Preskenis LA, Ladman BS, Pope CR, Pantin-Jackwood MJ, McKinley ET: **The pathogenesis of low pathogenicity H7 avian influenza viruses in chickens, ducks and turkeys.** *Virol J* 2010, **7**:331.
34. Pillai SP, Pantin-Jackwood M, Yassine HM, Saif YM, Lee CW: **The high susceptibility of turkeys to influenza viruses of different origins implies their importance as potential intermediate hosts.** *Avian Dis* 2010, **54**:522-526.
35. Zeng H, Pappas C, Katz JM, Tumpey TM: **The 2009 pandemic H1N1 and triple-reassortant swine H1N1 influenza viruses replicate efficiently but elicit an attenuated inflammatory response in polarized human bronchial epithelial cells.** *J Virol* 2011, **85**:686-696.
36. Osterlund P, Pirhonen J, Ikonen N, Ronkko E, Strengell M, Makela SM, Broman M, Hamming OJ, Hartmann R, Ziegler T, Julkunen I: **Pandemic H1N1 2009 influenza A virus induces weak cytokine responses in human macrophages and dendritic cells and is highly sensitive to the antiviral actions of interferons.** *J Virol* 2010, **84**:1414-1422.
37. de Jong MD, Simmons CP, Thanh TT, Hien VM, Smith GJ, Chau TN, Hoang DM, Chau NV, Khanh TH, Dong VC, *et al*: **Fatal outcome of human influenza A (H5N1) is associated with high viral load and hypercytokinemia.** *Nat Med* 2006, **12**:1203-1207.
38. Degen WG, Smith J, Simmelink B, Glass EJ, Burt DW, Schijns VE: **Molecular immunophenotyping of lungs and spleens in naive and vaccinated chickens early after pulmonary avian influenza A (H9N2) virus infection.** *Vaccine* 2006, **24**:6096-6109.
39. Lavrentieva IN, Medvedeva TE, Golubev DB: **Characterization of the reproduction of influenza A epidemic viruses in cell cultures.** *Acta Virol* 1986, **30**:137-142.
40. Seo SH, Webster RG: **Cross-reactive, cell-mediated immunity and protection of chickens from lethal H5N1 influenza virus infection in Hong Kong poultry markets.** *J Virol* 2001, **75**:2516-2525.
41. Reed LJ, Muench H: **A simple method for estimating fifty percent endpoints.** *American Journal of Hygiene* 1938, **27**:493-497.
42. Wasilenko JL, Lee CW, Sarmento L, Spackman E, Kapczynski DR, Suarez DL, Pantin-Jackwood MJ: **NP, PB1, and PB2 viral genes contribute to altered replication of H5N1 avian influenza viruses in chickens.** *J Virol* 2008, **82**:4544-4553.
43. Kapczynski DR, Kogut MH: **Measurement of avian cytokines with real-time RT-PCR following infection with the avian influenza virus.** *Methods Mol Biol* 2008, **436**:127-134.
44. Mayne RK, Powell F, Else RW, Kaiser P, Hocking PM: **Foot pad dermatitis in growing turkeys is associated with cytokine and cellular changes indicative of an inflammatory immune response.** *Avian Pathol* 2007, **36**:453-459.
45. Adams SC, Xing Z, Li J, Cardona CJ: **Immune-related gene expression in response to H11N9 low pathogenic avian influenza virus infection in**

chicken and Pekin duck peripheral blood mononuclear cells. *Mol Immunol* 2009, **46**:1744-1749.

46. Morrison TB, Weis JJ, Wittwer CT: **Quantification of low-copy transcripts by continuous SYBR Green I monitoring during amplification.** *Biotechniques* 1998, **24**:954-958, 960, 962.

doi:10.1186/1743-422X-8-447
Cite this article as: Jiang *et al.*: Chicken interferon alpha pretreatment reduces virus replication of pandemic H1N1 and H5N9 avian influenza viruses in lung cell cultures from different avian species. *Virology Journal* 2011 **8**:447.

Submit your next manuscript to BioMed Central and take full advantage of:

- **Convenient online submission**
- **Thorough peer review**
- **No space constraints or color figure charges**
- **Immediate publication on acceptance**
- **Inclusion in PubMed, CAS, Scopus and Google Scholar**
- **Research which is freely available for redistribution**

Submit your manuscript at
www.biomedcentral.com/submit

BioMed Central

Kapczynski et al. BMC Proceedings 2011, 5(Suppl 4):S13
http://www.biomedcentral.com/1753-6561/5/S4/S13

BMC Proceedings

PROCEEDINGS Open Access

Cross reactive cellular immune responses in chickens previously exposed to low pathogenic avian influenza

Darrell R Kapczynski[1*], Karen Liljebjelke[1], Gururaj Kulkarni[2], Henry Hunt[2], Hai Jun Jiang[1], Daniel Petkov[1]

From International Symposium on Animal Genomics for Animal Health (AGAH 2010)
Paris, France. 31 May – 2 June 2010

Abstract

Background: Avian influenza (AI) infection in poultry can result in high morbidity and mortality, and negatively affect international trade. Because most AI vaccines used for poultry are inactivated, our knowledge of immunity against AI is based largely on humoral immune responses. In fact, little is known about cellular immunity following a primary AI infection in poultry, especially regarding cytotoxic T lymphocytes (CTL's).

Methods: In these studies, major histocompatibility complex (MHC)-defined (B^2/B^2) chickens were infected with low pathogenic AI (LPAI) H9N2 and clinical signs of disease were monitored over a two weeks period. Splenic lymphocytes from infected and naïve birds were examined for cross reactivity against homologous and heterologous (H7N2) LPAI by ex vivo stimulation. Cellular immunity was determined by cytotoxic lysis of B^2/B^2 infected lung target cells and proliferation of T cells following exposure to LPAI.

Results: Infection with H9N2 resulted in statistically significant weight loss compared to sham-infected birds. Splenic lymphocytes derived from H9N2-infected birds displayed lysis of both homologous (H9N2) and heterologous (H7N2) infected target cells, whereas lymphocytes obtained from sham-infected birds did not. T cell proliferation was determined to be highest when exposed to the homologous virus.

Conclusions: Taken together these data extend the findings that cellular immunity, including CTL's, is cross reactive against heterologous isolates of AI and contribute to protection following infection.

Background

Cell-mediated immunity (CMI) is antigen specific immunity mediated by T lymphocytes and has been suggested to be an important factor to the development of protection in chickens vaccinated against viral diseases [1]. The subsets of T lymphocytes: CD4+ helper cells and CD8+ cytotoxic cells constitute the principal cells of the CMI response. For influenza, CD8+ CTL's play a crucial role in controlling infectious virus from the lungs of mice [2][3]. A number of recent studies have provided evidence that CMI directed against viral epitopes conserved among influenza A viruses, such as those within the nucleoprotein (NP) and hemagglutinin (HA), may contribute to protection against influenza [4][5]. In fact, influenza virus NP-specific CTL's generated through vaccination or introduced by adoptive transfer enhance viral clearance and lead to recovery of the host and protection from death [6]. The objectives of this study were to determine the level of cross reactive CMI against homologous and heterologous isolates of LPAI.

Methods

Birds

Two-day-of age chickens were received from the USDA-ARS-Avian Disease Oncology Laboratory (East Lansing, Michigan) containing the B^2/B^2 defined MHC allele

* Correspondence: darrell.kapczynski@ars.usda.gov
[1]Southeast Poultry Research Laboratory, Agricultural Research Service, USA, Department of Agriculture, 934 College Station Road, Athens, GA 30605, USA
Full list of author information is available at the end of the article

BioMed Central
© 2011 Kapczynski et al; licensee BioMed Central Ltd. This is an open access article distributed under the terms of the Creative Commons Attribution License (http://creativecommons.org/licenses/by/2.0), which permits unrestricted use, distribution, and reproduction in any medium, provided the original work is properly cited.

(Line 15.6-2). Birds were placed in Horsfall units in BSL3E facilities (USDA-ARS, Athens, Georgia, USA) and provided feed and water *ad libitum*.

Viruses

Low pathogenic AI viruses of H9N2 (A/Chicken/NJ/12220/97) and H7N2 (A/Turkey/Virginia/4259/02) subtypes were propagated in the allantoic cavities of 9-11 day of embryonation SPF chicken eggs. Viral titers were determined as previously described [7].

H9N2 infection

Two-week-old chickens (6 per group) were inoculated via the intranasal route with 10^7 EID_{50} of H9N2 AI virus or sham inoculum in 0.2 ml volume (1/2 each nare) at 2 weeks of age. Chicken were monitored daily for clinical signs of disease and weight loss monitored at 2, 4 and 7 days post inoculation (p.i.) following H9N2 primary infection. Mean weight was compared by ANOVA using the Tukey Test (SigmaStat).

CTL lysis of target cells

Splenic lymphocytes were harvested from B^2/B^2 infected and control chickens, three each, at 10 days post- infection as previously described [8]. MHC-matched lung cells were obtained as previously described and used as target cells for CTL assay [9]. Lung cells were infected with either H9N2 or H7N2 AI at an MOI of 2 for 16 hours prior to testing. CTL activity was monitored using the CytoTox96 nonradioactive assay (Promega) with the % cells lysed determined by detection of cytosolic lactate dehydrogenase in supernatants from control and infected target cells.

Proliferation

Lymphocyte proliferation as a measure of cellular memory was performed with almarBlue™ (Invitrogen) as previously described, using BPL-inactivated H9N2 (5 μg/ml) or H7N2 (5 μg/ml) [8]. The T cell mitogen, concanavalin A (5 μg/ml), was used as a positive control.

Results

Weight loss following H9N2 infection

Infection with A\Chicken\NJ\97 (H9N2) following a natural route of exposure (intranasal) significantly decreased weight gains at day 2, 4 and 7 post-inoculation compared to control (uninfected) chickens (Fig 1). In general, H9N2 infected birds weighed approximately 10% less than the sham inoculated group at each time point. Apart from weight loss, overt signs of clinical disease or respiratory distress were not observed in the H9N2 challenged group throughout the course of the study.

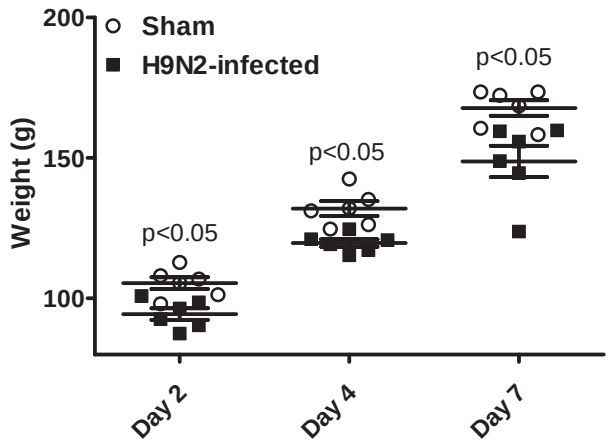

Figure 1 Effect of A/chicken/NJ/97 (H9N2) infection on weight gain in MHC-defined (B^2/B^2) chickens at 2, 4 and 7 days post infection. Two-week old birds received either PBS (Sham) or 10^7 EID_{50} H9N2 per bird via intranasal route. Bird weight was significantly reduced between the two groups on each day tested (p<0.05).

Lysis of homologous and heterologous infected B^2/B^2 lung cells

Splenic T cells from inbred chickens infected with H9N2 AI lysed target cells infected with either homologous or H7N2 AI at all effector:target (E:T) ratios tested (Fig 2). A dose response based on E:T ratios was observed. At E:T ratio of 40:1, 52 % of H9N2-infected B^2/B^2 lung target

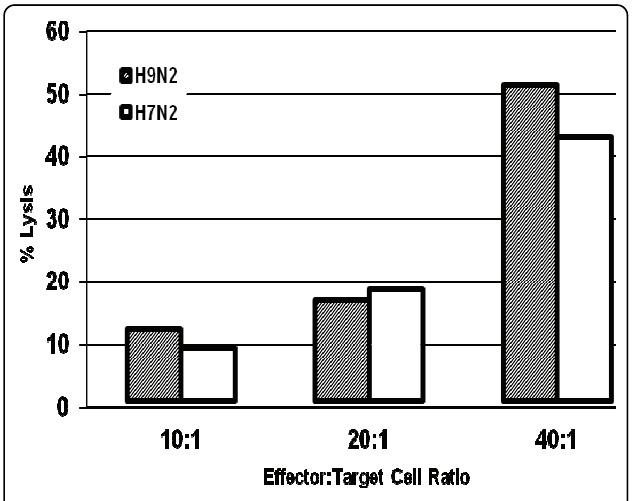

Figure 2 Recognition of homologous and heterologous LPAI ex vivo by splenocytes derived from H9N2-infected chickens. The cross-reactivity of lymphocytes was tested with MHC- matched B2/B2 lung cell cultures infected with H9N2 or H7N2 LPAI. Effector: target (E:T) ratios were 10, 20 and 40 for all subjects. Standard deviation of the means was <10%. Spontaneous lysis from splenocytes derived from naive birds were <7 % against either virus (data not shown).

cells were lysed, while 43 % of H7N2-infected target cells were lysed. At lower E:T ratios, approximately 18 % (20:1) and 10 % (10:1) of infected target cells were lysed in either H9N2 or H7N2-infected lung cells. The splenic T cells from H9N2 infected birds did not lyse uninfected target cells, although spontaneous lysis was approximately 7 % (data not shown). In addition, lymphocytes obtained from sham-infected birds did not lyse infected or control lung cell cultures (data not shown).

Proliferation

Splenocytes from H9N2 infected birds were tested for CMI memory response against homologous and heterologous AI via lymphocyte proliferative. The results (Fig. 3) indicate an increased proliferation response, as determined as an increase in the percent of alamaBlue™ reduced by the lymphocytes, against both the H9N2 and H7N2 virus. The highest proliferative response was against the homologous virus (42%), which was less than the response to the T-cell mitogen, concanavalin A (ConA). The T cell proliferative response to the heterologous virus was approximately half (25%) of that observed against the homologous virus.

Discussion

The main objective of the present research was to examine CMI following infection with low pathogenic AI, and to identify cross reactive T cell immunity in chickens.

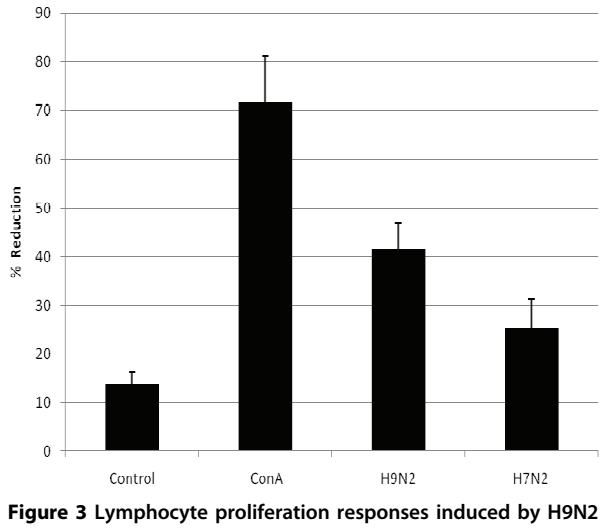

Figure 3 Lymphocyte proliferation responses induced by H9N2 infection in MHC-defined chickens against homologous and heterologous AI. Groups of chickens received either sham or H9N2 infection. Spleens of individual birds were removed, and lymphocyte proliferation was evaluated using the alamarBlue™ method. Samples were read at 48 hours and the percent alamarBlue™ reduced, as an indicator of proliferation, presented per group. Proliferation by lymphocytes from sham birds against either AI virus was <12 % (data not shown).

Using birds with a genetically defined MHC haplotype (B^2/B^2), we found CTL's isolated from H9N2 infected birds were active against homologous and heterologous isolates of AI based on lysis of MHC-matched target cells and T cell proliferation. In addition, memory T cells demonstrated proliferation in the presence of either isolate tested. These data suggest that antigenic peptides found in both isolates are presented by MHC-class I and II molecules that lead to production of memory CTL's and stimulated proliferation of T cells, respectively. The proteins containing these peptides remain to be determined, although at least one report has identified a T cell epitope on the HA protein which could activate both chicken $CD4^+$ and $CD8^+$ cells [4].

For this study birds infected with a LPAI H9N2 isolate were the source of lymphocytes and examining cross reactivity against a heterologous H7N2 isolate. We provide evidence that the H9N2 AI virus can induce cross reactive CMI against the H7N2 AI isolate. Because the majority of vaccines used across the world to protect poultry from AI are inactivated, they must be matched to the field subtype. While these vaccines induce protective antibodies against homologous subtypes based on HA, little to no protective cross reactivity is afforded against heterologous isolates [10]. In contrast, Seo et al. was able to adaptively transfer $CD8^+$ lymphocytes from H9N2-infected chickens and demonstrate protection from H5N1 lethal challenge [9]. Whether the cross reactive CMI demonstrated here could protect against a H7N2 challenge in vivo, remains to be determined.

Conclusions

Taken together these data extend the findings that CMI, including production of CTL's, is cross reactive against heterologous isolates of AI infection, and contribute to protection following infection.

Acknowledgements

The authors acknowledge the expert technical assistance of Aniko Zsak and Cam Greene. In addition we recognize Roger Brock and James Doster for assistance with animal care. This research was supported by USDA, ARS CRIS project 6612-32000-053-00D.

This article has been published as part of *BMC Proceedings* Volume 5 Supplement 4, 2011: Proceedings of the International Symposium on Animal Genomics for Animal Health (AGAH 2010). The full contents of the supplement are available online at http://www.biomedcentral.com/1753-6561/5?issue=S4.

Author details

[1]Southeast Poultry Research Laboratory, Agricultural Research Service, USA, Department of Agriculture, 934 College Station Road, Athens, GA 30605, USA. [2]Avian Disease and Oncology Laboratory, Agricultural Research Service, USA, Department of Agriculture, 3606 East Mount Hope Road, East Lansing, Michigan, 48823, USA.

Authors' contributions

DRK designed the experiments, carried out the analysis, and drafted the manuscript. KL and DP performed the animal experiments in BSL3E, and

together with HJ helped perform the ex vivo experiments. HH and GK developed the model and provided expertise with the MHC birds. All authors approved the final manuscript.

Competing interests

The authors declare that they have no competing interests.

Published: 3 June 2011

References

1. Sharma JM: **Introduction to poultry vaccines and immunity.** *Adv Vet Med* 1999, **41**:481-94.
2. Brincks EL, *et al*: **CD8 T cells utilize TRAIL to control influenza virus infection.** *J Immunol* 2008, **181(7)**:4918-25.
3. Topham DJ, Tripp RA, Doherty PC: **CD8+ T cells clear influenza virus by perforin or Fas-dependent processes.** *J Immunol* 1997, **159(11)**:5197-200.
4. Haghighi HR, *et al*: **Identification of a dual-specific T cell epitope of the hemagglutinin antigen of an h5 avian influenza virus in chickens.** *PLoS One* 2009, **4(11)**:e7772.
5. Singh S, *et al*: **Avian influenza viral nucleocapsid and hemagglutinin proteins induce chicken CD8+ memory T lymphocytes.** *Virology* 2010, **399(2)**:231-8.
6. Ada GL, Jones PD: **The immune response to influenza infection.** *Curr Top Microbiol Immunol* 1986, **128**:1-54.
7. Swayne DE, Senne DA, Beard CW: **Avian Influenza.** In *A laboratroy manual for the isolation and identification of avian pathogens.* Kennett Square: American Association of Avian Pathologists;Swayne DE 1996:150-5.
8. Kapczynski DR: **Evaluating the cell-mediated immune response of avian species to avian influenza viruses.** *Methods Mol Biol* 2008, **436**:113-26.
9. Seo SH, Webster RG: **Cross-reactive, cell-mediated immunity and protection of chickens from lethal H5N1 influenza virus infection in Hong Kong poultry markets.** *J Virol* 2001, **75(6)**:2516-25.
10. Swayne DE, Kapczynski DR: **Strategies and challenges for eliciting immunity against avian influenza virus in birds.** *Immunol Rev* 2008, **225**:314-31.

doi:10.1186/1753-6561-5-S4-S13
Cite this article as: Kapczynski *et al.*: Cross reactive cellular immune responses in chickens previously exposed to low pathogenic avian influenza. *BMC Proceedings* 2011 **5**(Suppl 4):S13.

Submit your next manuscript to BioMed Central and take full advantage of:

- **Convenient online submission**
- **Thorough peer review**
- **No space constraints or color figure charges**
- **Immediate publication on acceptance**
- **Inclusion in PubMed, CAS, Scopus and Google Scholar**
- **Research which is freely available for redistribution**

Submit your manuscript at
www.biomedcentral.com/submit

BioMed Central

AVIAN DISEASES 55:633–641, 2011

Pandemic H1N1 Influenza Virus in Chilean Commercial Turkeys with Genetic and Serologic Comparisons to U.S. H1N1 Avian Influenza Vaccine Isolates

Darrell R. Kapczynski,[AF] Eric Gonder,[B] Becky Tilley,[B] Andres Hernandez,[C] Jorge Hodgson,[C] Helen Wojcinski,[D] Haijun Jiang,[E] and David L. Suarez[A]

[A]Southeast Poultry Research Laboratory, Agricultural Research Service, United States Department of Agriculture, 934 College Station Road, Athens, GA 30605
[B]Goldsboro Milling Company, Goldsboro, NC 27534
[C]Sopraval S.A., La Calera, Chile
[D]Hybrid Turkeys, Ann Arbor, MI 48103
[E]Laboratory of Zoonosis of Ministry of Agriculture, College of Veterinary Medicine and State Key Laboratory of Agrobiotechnology, China Agricultural University, Beijing, People's Republic of China

Received 21 April 2011; Accepted and published ahead of print 24 July 2011

SUMMARY. Beginning in April 2009, a novel H1N1 influenza virus caused acute respiratory disease in humans, first in Mexico and then around the world. The resulting pandemic influenza A H1N1 2009 (pH1N1) virus was isolated in swine in Canada in June 2009 and later in breeder turkeys in Chile, Canada, and the United States. The pH1N1 virus consists of gene segments of avian, human, and swine influenza origin and has the potential for infection in poultry following exposure to infected humans or swine. We examined the clinical events following the initial outbreak of pH1N1 in turkeys and determined the relatedness of the hemagglutinin (HA) gene segments from the pH1N1 to two H1N1 avian influenza (AI) isolates used in commercial turkey inactivated vaccines. Overall, infection of turkey breeder hens with pH1N1 resulted in ≥50% reduction of egg production over 3–4 weeks. Genetic analysis indicated one H1N1 AI vaccine isolate (A/turkey/North Carolina/17026/1988) contained approximately 92% nucleotide sequence similarity to the pH1N1 virus (A/Mexico/4109/2009); whereas, a more recent AI vaccine isolate (A/swine/North Carolina/00573/2005) contained 75.9% similarity. Comparison of amino acids found at antigenic sites of the HA protein indicated conserved epitopes at the Sa site; however, major differences were found at the Ca2 site between pH1N1 and A/turkey/North Carolina/127026/1988. Hemagglutinin-inhibition (HI) tests were conducted with sera produced in vaccinated turkeys in North Carolina to determine if protection would be conferred using U.S. AI vaccine isolates. HI results indicate positive reactivity (HI titer ≥ 5 $\log_2$) against the vaccine viruses over the course of study. However, limited cross-reactivity to the 2009 pH1N1 virus was observed, with positive titers in a limited number of birds (6 out of 20) beginning only after a third vaccination. Taken together, these results demonstrate that turkeys treated with these vaccines would likely not be protected against pH1N1 and current vaccines used in breeder turkeys in the United States against circulating H1N1 viruses should be updated to ensure adequate protection against field exposure.

RESUMEN. Virus de la influenza H1N1 pandémico en pavos comerciales de Chile y comparaciones genéticas y serológicas con aislamientos vacunales de los Estados Unidos del virus de la influenza aviar H1N1.

A partir de abril del 2009, un virus nuevo de influenza H1N1 causó una enfermedad respiratoria aguda en seres humanos, inicialmente en México y luego alrededor del mundo. El virus de influenza pandémica A H1N1 2009 (pH1N1) fue aislado de cerdos en Canadá en junio del 2009 y más tarde en pavos reproductores de Chile, en Canadá y en los Estados Unidos. El virus pH1N1 se compone de segmentos genéticos de cepas de origen aviar, humano y porcino del virus de la influenza y cuenta con el potencial de infección en aves comerciales después de la exposición con personas o con cerdos infectados. Se examinaron los eventos clínicos que siguieron después del brote inicial de pH1N1 en pavos y se determinó la relación de los segmentos genéticos de la hemaglutinina (HA) entre el virus pH1N1 con los aislamientos de influenza aviar H1N1 usados como vacunas inactivadas en pavos comerciales. En general, la infección en pavos reproductores con el virus pH1N1 resultó en una reducción ≥ 50% de la producción de huevos durante 3–4 semanas. El análisis genético indicó que el aislamiento H1N1 usado como vacuna contra el virus (A/pavo/Carolina del Norte/17026/1988) mostró aproximadamente un 92% de similitud en las secuencias de nucleótidos con los virus pH1N1 (A/Mexico/4109/2009), mientras que un virus vacunal más reciente de influenza aviar (A/porcino/Carolina del Norte/00573/2005) contenía 75.9% de similitud. La comparación de las secuencias de aminoácidos de los sitios antigénicos de la proteína HA indica la presencia de epítopes conservados en el sitio Sa, sin embargo, se encontraron diferencias importantes en el sitio Ca2 entre el virus pandémico pH1N1 y el virus A/pavo /Carolina del Norte/127026/1988. Las pruebas de inhibición de la hemaglutinación (HI) se llevaron a cabo con sueros producidos en pavos vacunados en Carolina del Norte para determinar si se confirió protección por los aislamientos usados como vacunas de los Estados Unidos. Los resultados de la pruebas de inhibición de la hemoaglutinación indicaron reactividad positiva (título HI ≥ 5 $\log_2$) contra los virus utilizados como vacuna a lo largo del estudio. Sin embargo, se observó reactividad cruzada limitada al virus pH1N1 2009, con títulos positivos en un número limitado de aves (6 de 20) que se empezaron a observar sólo después de una tercera vacunación. En conjunto, estos resultados demuestran que los pavos tratados con estas vacunas probablemente no están protegidos contra las cepas pH1N1 y las vacunas utilizadas en pavos reproductores en los Estados Unidos contra los virus H1N1 que están circulando deben ser actualizadas para garantizar una protección adecuada contra la exposición en el campo.

Key words: avian influenza virus, pandemic H1N1, vaccines, turkeys, hemagglutinin, immunology

Abbreviations: AI = avian influenza; gal = galactose; GMT = geometric mean hemagglutinin inhibition titer; HA = hemagglutinin; HI = hemagglutinin inhibition; IAV = influenza A virus; pH1N1 = pandemic H1N1; SA = sialic acid

[F]Corresponding author. E-mail: darrell.kapczynski@ars.usda.gov

Influenza A viruses (IAVs) belong to the *Orthomyxoviridae* family and have been shown to infect many different animal species, including birds and mammals. In April 2009, pandemic H1N1 influenza virus (pH1N1) was first reported in humans from Mexico and eventually declared a pandemic event by the World Health Organization in June 2009. The genetic makeup of this virus was determined to contain gene segments of human, swine, and avian origin creating a triple-reassortant that had never before been isolated (4,5). Detailed genetic analysis of this virus indicates the hemagglutinin (HA), nucleoprotein, and nonstructural genes were of North American swine lineage; the neuraminidase and matrix genes were derived from Eurasian swine lineage; and the polymerase genes, PA and PB2, originated from avian origin, while the PB1 gene was from human lineage (8).

Unlike other bird species, turkeys are susceptible to a wide spectrum of IAVs, including avian and mammalian origin, and are commonly infected with swine IAV (27,41). Clinical signs of IAV infection in turkeys range from asymptomatic to severe and include increased mortality, decreased egg production and hatchability, abnormal egg shell quality, and respiratory disease with decreased feed conversion (6,27,33). Interspecies infection by IAVs is one mechanism for genetic and antigenic drift or shift, which may result in viruses with enhanced virulence and host range in populations without preexisting immunity (3,15,20,24,25,28). The molecular mechanisms for crossing species is multifactoral, with the viral HA origin and receptor expression of the host being major contributors to these events (12). The HA of avian origin IAVs preferentially bind to sialic acid (SA) residues on host cells containing SAα2,3 linked to galactose (gal), found in many bird species (10,19,38). In contrast, mammalian influenza viruses have been described to preferably bind to SAα2,6gal (19,22). Swine possess receptors for both avian (SAα2,3gal) and mammalian (SAα2,6gal) influenza viruses and are thought to be an example of a host in which genetically reassorted influenza viruses can originate (3,11,20). We recently demonstrated that turkey oviduct tissue contain both SAα2,3gal and SAα2,6gal residues, which provides a molecular platform for infection with mammalian influenza viruses in this tissue (13). Because turkey breeder hens are artificially inseminated through oviduct application of turkey semen on a weekly basis, the close proximity of human contact is proposed to be a primary mode of transmission of the pH1N1 virus from human into turkeys (30).

In the United States, commercial production of turkeys and swine as a source of animal protein commonly occurs on the same farm or in close proximity in separate housing. Thus during an IAV outbreak, isolates with similar genetic and antigenic characteristics are typically recovered from both species on a particular farms, especially of H1 and H3 subtype (13,44,45). These influenza isolates are routinely utilized as autogenous inactivated vaccines and may be applied to both species (E. Gonder, personal observations). In fact, the United States has successfully used killed vaccines in poultry, primarily in turkeys in the states of Minnesota and North Carolina, since the 1980s as part of a controlled marketing program (23). Vaccination of turkeys against IAVs is the primary measure to protect against clinical disease, namely the significant drops in egg production (6,14,33). In the United States, turkey hens typically receive multiple vaccinations against influenza just prior to and when egg production begins (typically at 26 wk of age) to protect hens from egg production losses.

Immunity to influenza is largely based on antibodies produced against the HA protein, and vaccines with greater genetic similarity to the field virus provide superior immunity than less-matched isolates (28). Because of the recent outbreaks of pH1N1 in commercial turkey hens, we sought to compare the antigenic and genetic relatedness of H1N1 avian influenza (AI) isolates used in autogenous vaccine

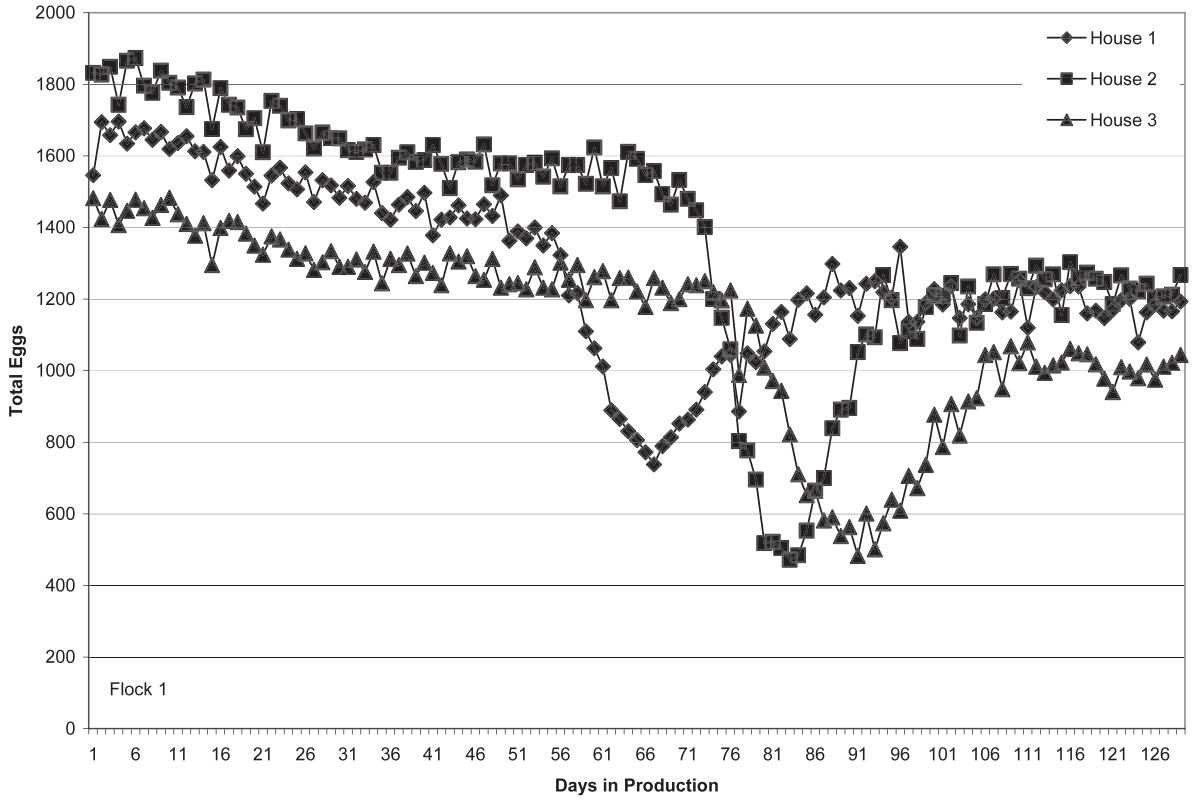

Fig. 1. Index case of pH1N1 field infection in flocks of laying turkey hens in Chile. Birds from three different turkey flocks (1, 2, and 3) became infected with the pH1N1 influenza virus. Birds in different houses within a flock displayed clinical signs of pH1N1 infection, particularly decreased egg production. Eggs were collected daily and drops in egg production following infection were reported in each house of the infected flocks.

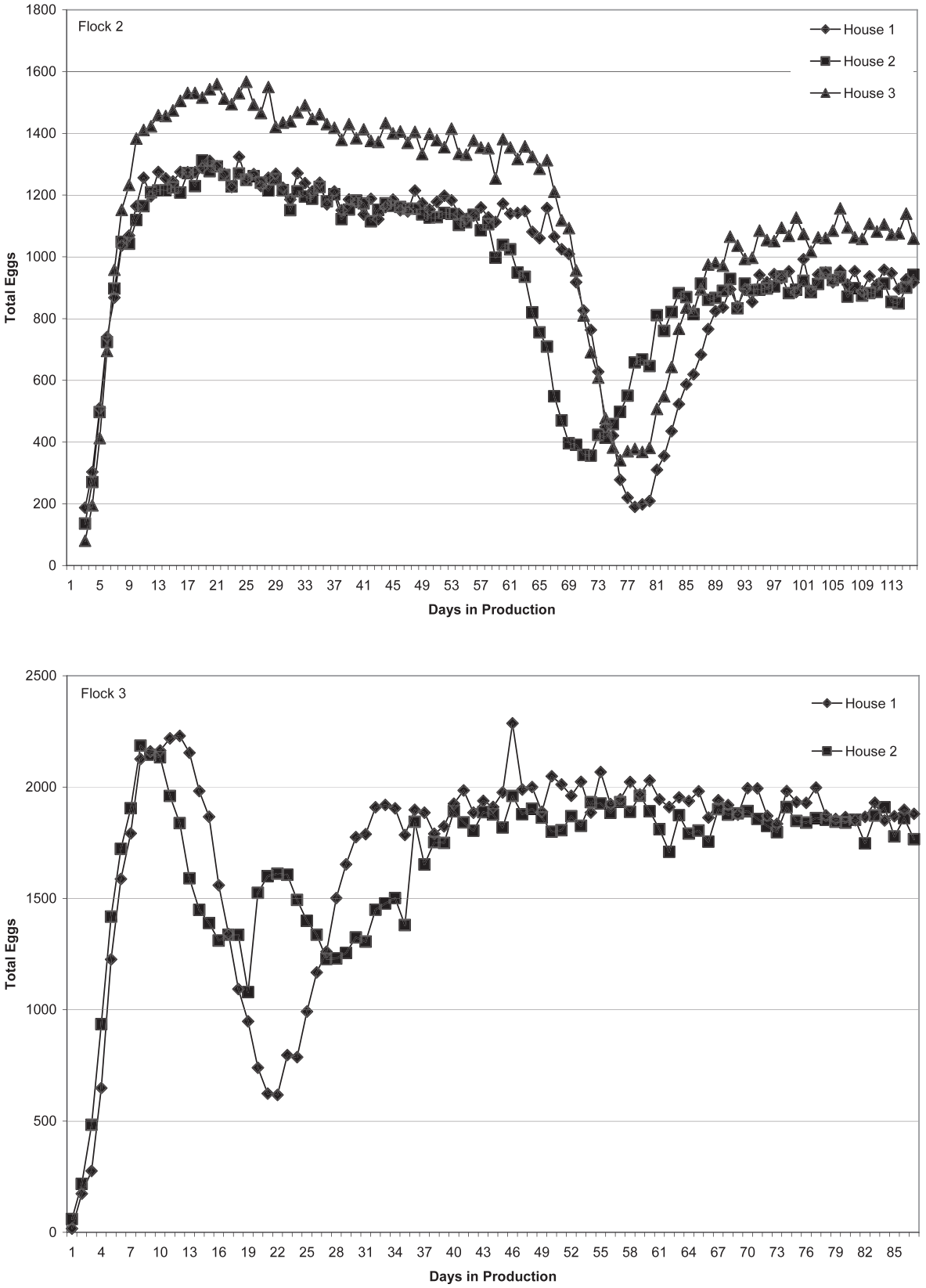

Fig. 1. Continued.

preparations to the pH1N1 virus to determine the relatedness and protection potential. Serologic cross-reactivity of sera taken from two flocks of commercial laying hens undergoing field vaccination were evaluated by hemagglutination inhibition assay against homologous and pH1N1 viruses. We report here that although a high level of genetic relatedness exists between the H1N1 isolates, cross-reactive HI titers to the pH1N1 vaccines failed to induce protective levels of HI antibody in most hens necessary to prevent disease in the event of a field outbreak.

A

B

	A/Tk/Chile/28317/09	A/Tk/NC/17026/88	A/Sw/NC/00573/05	A/Tk/NC/16108/03 (H3N2)
A/Mexico/4108/09	99.9	91.9	75.9	52.6
A/Tk/NC/17026/88	91.7	----	77.9	52.6

Fig. 2. (A) Genetic comparison of H1N1 viruses used in these studies. Phylogenetic analysis of HA nucleotide gene segments of the different H1N1 avian vaccine viruses to the pH1N1 influenza viruses. Viruses with similar H1 gene segments were isolated in human, swine, and turkey species. The H1N1 isolates used in these studies are shown in bold. The tree was generated by the Maximum Likelihood method with 1000 bootstrap replicates in a heuristic search with MEGA5 software. (B) Percent nucleotide similarity between avian H1N1 influenza viruses and pH1N1 influenza viruses. Similarity was determined using MegAlign-DNASTAR program with pair-wise analysis.

MATERIALS AND METHODS

Egg production during index pH1N1 infection in Chile. Egg production was monitored following initial decrease in numbers of eggs and shell quality. Total numbers of eggs collected daily from three individual flocks of turkeys. The birds were maintained in multiple houses during the production cycle.

Viruses. Four different influenza viruses were used in these studies. The three H1N1 isolates were A/swine/North Carolina/00573/2005 (A/Sw/NC/05), A/turkey/North Carolina/170268/1988 (A/Tk/NC/88), and the pandemic virus, A/Mexico/4108/2009 (A/Mex/09). In addition, an H3N2 turkey isolate, A/turkey/North Carolina/16108/2003 (A/Tk/NC/03), was used in the vaccine preparation for turkeys on the North Carolina farm. The isolates were propagated in specific-pathogen-free chicken embryos as previously described (13). Work with the 2009 pH1N1 virus was performed under biosafety level 3 conditions. The turkey vaccine viruses were inactivated and formulated into a trivalent oil-emulsion autogenous vaccine containing equal concentrations of each virus. The H3N2 virus used in these studies was a recently described triple-reassortant containing gene segments of avian, human, and swine origin (3,13,33).

Turkeys and vaccination. Two groups of turkey breeder hens (Nicholas 300, Nicholas Turkeys, Lewisburg, WV) were field vaccinated onsite at 18, 26, and 30 wk of age with the autogenous trivalent oil emulsion vaccine administered via subcutaneous route. Blood was collected from 20 turkeys (10 per group) via wing vein at 17.4, 20.3, 23.4, 26.4, 28.5, 30.6, 33.6, 36.5, 39.5, and 42.5 wk of age. Serum was individually harvested and stored at −20 C until tested.

Serology. The hemagglutination inhibition (HI) test was performed using beta-propiolactone-inactivated homologous H1N1 (A/Tk/NC/88) and H3N2 (A/Tk/NC/03) AI virus, and the pH1N1 (A/Mex/09) influenza virus, with serum as previously described (35). Titers greater than 4 $\log_2$ were considered protective.

Sequence analysis. Nucleotide sequence analysis and multiple alignments of the H1 HA gene were performed using CLUSTAL W (Lasergene, v. 7.0, DNASTAR, Madison, WI). Nucleotide sequences of

the HA genes of influenza viruses isolated from avian, swine, and human sources that have been previously published were obtained from NCBI-Influenza Virus Resource (http://www.ncbi.nlm.nih.gov/genomes/FLU/FLU.html). The nucleotide sequences were aligned and compared, and an evolutionary tree was inferred by using the Maximum Likelihood method based on the Tamura-Nei model (31) with 1000 bootstrap replicates in a heuristic search using MEGA5 (32). Comparison of conserved amino acid differences at the major antigenic sites of the HA molecule were determined as previously described, using H3 numbering (1,17).

RESULTS

Pandemic H1N1 infection in turkeys. This original outbreak of pH1N1 in turkey breeder hens in Chile in 2009 was determined using serology (commercial ELISA) followed by subsequent virus isolation and typing. AI vaccines are not permitted for use in turkeys in Chile so none of the infected flocks had been previously vaccinated against IAVs. The infected birds displayed dramatic drops in egg production (Fig. 1). In all flocks, serum samples were tested 2–3 days after drops in egg production became apparent.

In three separate turkey breeder flocks, representing eight different houses, egg production fell by at least 50% (Flock 3, house 2) and up to approximately 80% (Flock 2, house 1). Flocks 1 and 2 were separated by approximately 2 miles and had separate entrances into the facilities. However, these two flocks did share the same turkey insemination crews. In contrast, Flock 3 was located approximately 30 miles from the other two flocks and had a separate turkey insemination crew. The duration of decreased egg production following pH1N1 infection typically lasted about 25 days, although production levels never fully returned to pre-infection levels following recovery. Recovery from disease typically occurred in approximately 25 days after the onset of clinical disease. Feed samples taken during the outbreak were negative for IAVs (data not shown).

Phylogenetic analysis of the HA_1 gene of the H1 subtype influenza viruses used in these studies. We constructed a phylogenetic tree using maximum-likelihood, in which avian, swine, and human, HA_1 sequences available from public databases were compared. The tree with the highest log likelihood (−9526.6275) is shown. The percentage of trees in which the associated taxa clustered together is shown next to the branches. The tree is drawn to scale, with branch lengths measured in the number of substitutions per site. Sequence analysis demonstrated that the pH1N1 isolates were highly similar, regardless of species or country of origin, and contained >99% sequence similarity. The pH1N1 viruses exhibited approximately 94% similarity to swine isolates of U.S. origin (Swine/OH/891/2001) and 86% similarity to swine isolates from England (Swine/England/283902/93). The turkey isolate A/Tk/NC/88 was determined to be the most closely related AI vaccine isolate to the pH1N1 influenza viruses isolated from humans in Mexico, California, and Chile, and turkeys in Chile (Fig. 2A). Approximately 92% sequence similarity was observed between this isolate and the pH1N1 viruses (Fig. 2B). The A/Tk/NC/88 isolate also shared 94%–99.6% similarity to the U.S. swine influenza viruses isolated between 1976 (Swine/NJ/11/76) and 2003 (Swine/NC/9675/2003) as well as 93% similarity to swine isolates from England (Swine/England/117316/86 and Swine/England/283902/93). Interestingly, the HA gene from this virus also shares 96% similarity with isolates from chickens, CK/PA/35154/91 and CK/NY/21665-73/98. These results demonstrate the stability of these viruses in both avian and swine species. In contrast, HA sequence from the second H1N1 AI isolate used in the vaccine formulation (A/Sw/NC/05) shared only 77.9% similarity to the A/Tk/NC/88 isolate and 72%–76% similarity to pH1N1 isolates. As expected, the avian H1N1 viruses tested in these studies contained little HA gene sequence similarity to the H3N2 virus used in the vaccine formulation, which contained only 52.6% similarity.

Mapping of antigenic epitopes in HA protein. Amino acid alignment of the HA1 protein from two pH1N1 isolates, A/Ca/04/09 and A/Mex/09, the more related vaccine isolate A/Tk/NC/88, and a phylogenetically related swine H1N1 isolate (A/Sw/WI/98) are shown in Fig. 3. Major amino acid changes were observed at the antigenic site Ca1 between the pH1N1 isolates and the vaccine isolate, including positions, 182 (I→V), 184 (D→N), 186 (G→E), 221 (R→K), and 255 (K→T). Additional changes at the Ca2 site included positions 154 (H→Y), 158 (K→N), 238 (D→G), and 240 (E→A). Only one change, position 171 (G→E), was observed at the Sa site between these viruses. Few amino acid differences were observed between the turkey vaccine isolate and swine isolate in the antigenic sites, most notably at the Ca1 site, positions 182 (I→V) and 186 (G→E). A number of amino acid differences were found outside of these antigenic domains between pH1N1 and turkey vaccine, including positions 143(D→E), 144 (S→T), 146 (K→R), 274 (E→K), 276 (N→G), and 277 (A→S).

Homologous and heterologous cross-reactive HI titers. Serum from 10 birds in each of two flocks was obtained from hens field-vaccinated with a trivalent autogenous AI vaccine containing two H1N1 isolates and a H3N2 isolate over a 21-wk period. Antibody cross-reactivity was tested against homologous and pH1N1 viruses with the HI assay. The prevaccination geometric mean HI titer (GMT, $\log_2$) obtained at 17 wk of age ranged from 2.9 for the H3N2 vaccinated group to 2.0 for both the avian and pandemic H1N1 isolates (Fig. 4). Following primary vaccination at 18 wk of age, the GMTs against the homologous influenza viruses increased to 3.2 and 9.1 at 23.4 weeks of age against the H1N1 and H3N2 viruses. No change in cross-reactivity was observed against the pH1N1 virus following primary vaccination.

After secondary vaccination at 26 wk of age, HI titers against both vaccine viruses was approximately 7.6, while titers against the pH1N1 virus were 2.5, with one serum sample at 4. After tertiary vaccination at 30 wk of age, titers against the H3N2 virus remained >8.5 throughout the course of study. Titers against the avian H1N1 remained >6 until the last three sampling days when they were approximately 4 on each day tested. Interestingly, titers against the pH1N1 virus increased to a GMT of 3.8 at week 33.6, with 6 of 20 sera ≥4. At weeks 36.5 and 42.5, 4 of 20 sera displayed GMT of ≥5 against the pH1N1 virus.

DISCUSSION

This is the first comparison of genetic and antigenic relatedness of pH1N1 viruses from human and swine origin to H1-based vaccine viruses used in commercial U.S. turkeys. The recent outbreaks of pH1N1 in South and North American commercial turkey flocks caused us to investigate if currently available vaccines would protect these birds from future outbreaks.

The source of the index case report of pH1N1 infection of breeder turkeys in Chile remains unknown, but genetic data suggest it was originally derived from human or swine sources. The mode of human transmission to turkeys is supported by at least one worker testing positive for pH1N1 during the time of clinical disease, although it is unknown if this individual had direct contact with the birds. Swine contact did not occur on the index farm, making human introduction the likely source. The pH1N1 infection in turkeys resulted in significant drops in egg production in flocks of hens not vaccinated for AI (18). However, transmission between

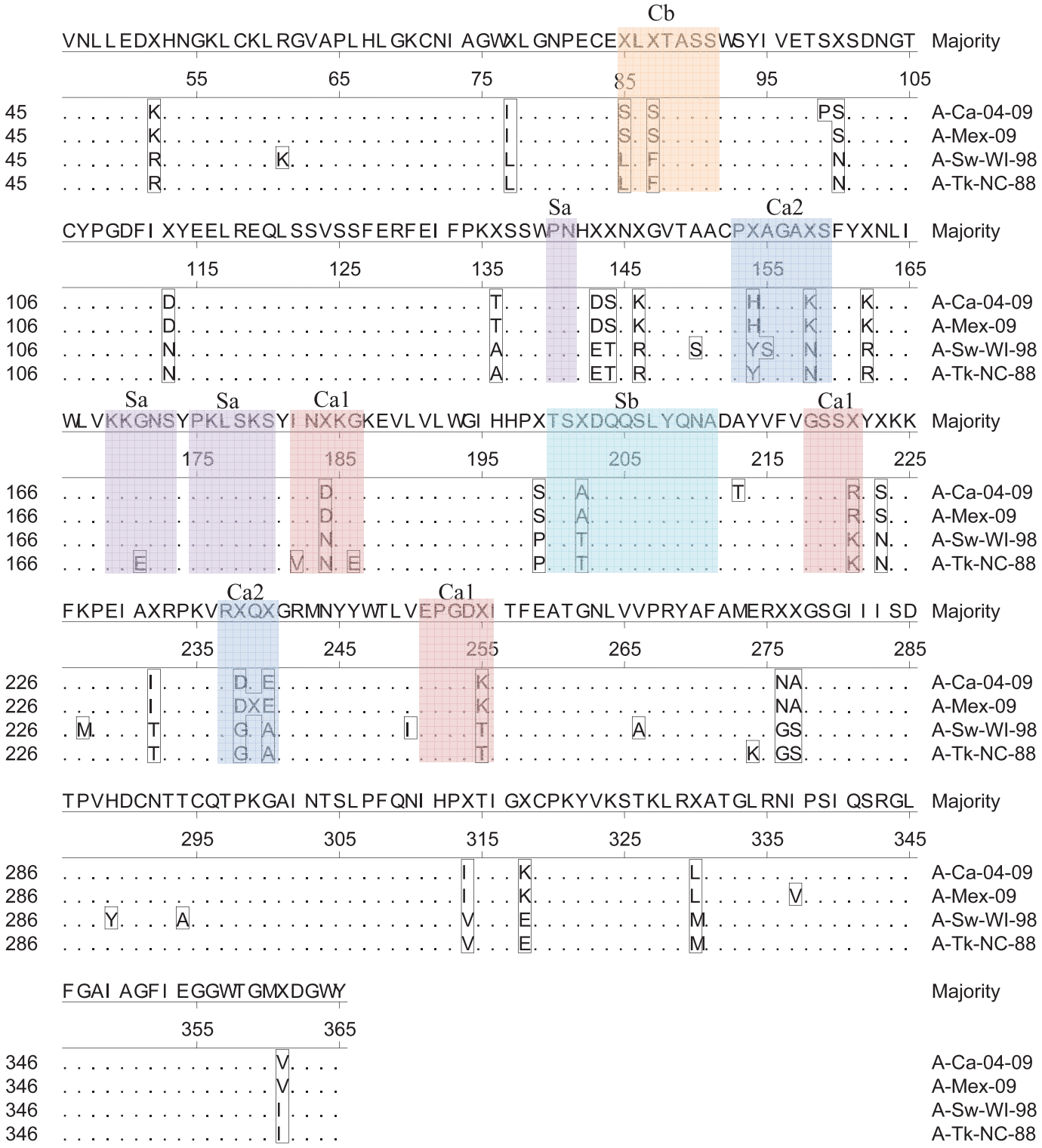

Fig. 3. Comparison of amino acids found at various antigenic sites in HA from various H1N1 isolates. Alignment of human HA sequences from the 2009 H1N1 pandemic, A-Ca-04-09 and A-Mex-09, to phylogenetically similar swine (A-Sw-WI-98) and turkey autogenous vaccine isolate (A-Tk-NC-88). The antigenic sites Cb (85–91), Sa (140–141, 169–173, 175–180), Sb (200–211), Ca1 (182–186, 218–221, 251–256), and Ca2 (153–159, 237–240) are indicated in color shaded boxes, based on H1 antigenic regions previously described by Manicassamy *et al.* (17).

birds through direct contact through the fecal-oral or respiratory route may have contributed to the spread of disease within houses. The clinical disease associated with this virus (mild with reproductive symptoms) in turkeys is similar to previous field reports and experimental studies with IAVs that demonstrate egg production losses in breeder hens infected with isolates containing HA gene segments of either mammalian or swine origin (13,25,27,30,42). Of significant note is the timing of the drops in egg production in each flock. The onset of disease begins in each of the flocks, but not simultaneously in each house, suggesting separate introductions of the virus in each house on different days. In some cases the time between individual house introductions was a matter of days and in

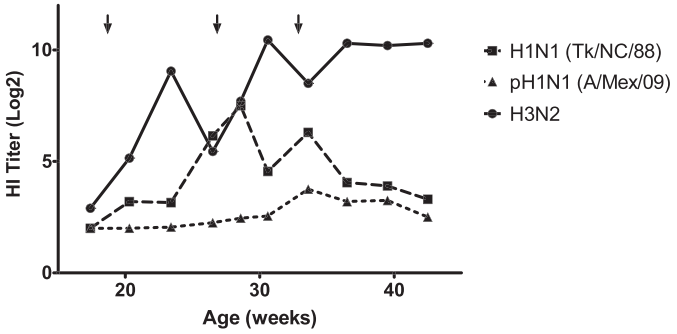

Fig. 4. Serologic cross-reactivity of turkeys vaccinated with inactivated trivalent AI vaccine to homologous H1N1 and a pH1N1 influenza isolate. Serum ($n = 20$) from two flocks of vaccinated turkeys was followed over the course of 48 wk from grow-out to egg production. Birds received vaccinations at 18, 26, and 32 wk of age (black arrows) with a trivalent inactivated AI vaccine containing two H1N1 isolates and an H3N2 isolate. Sera were tested with against homologous H1N1 (A/Tk/NC/88) and H3N2 (A/Tk/NC/03) AI vaccine viruses, as well as the pH1N1 influenza virus (A/Mex/09). Mean HI titers ($\log_2$) are shown.

others a matter of weeks. For example, hens in Flock 1, house 1, began to show a decrease in egg production at approximately 53 days of production, while egg drops were not observed in hens from house 3 until day 79 (Fig. 1A). In contrast, hens of Flock 2, houses 1 and 3 appeared to show drops in egg production within a day or two. The impact on egg production lasted approximately 3 wk before natural recovery, after which birds laid eggs at increased levels that did not return to pre-infection levels.

Previous research indicates turkey breeders, but not meat-type birds, are susceptible to infection with pH1N1 virus (21,30,34). In a commercial setting, laying turkey hens are handled on a weekly basis during the production period. During this handling time, hens are artificially inseminated with turkey semen. Due to the close associated with the mucosal surfaces of the reproductive tract, it is hypothesized that this breeding practice may constitute a significant risk for infection from humans to birds or birds to humans. The presence of receptors for both avian and mammalian influenza viruses in turkey reproductive tissue also implicates this species as a potential mixing vessel for generation of novel recombinant IAVs (13).

Comparisons of nucleotide relatedness of current AI vaccines to the pH1N1 virus were done to predict if vaccinated laying turkey breeder hens would be protected against challenge with the pH1N1. Results from these studies demonstrated a high degree of relatedness following alignment of the HA gene from the pH1N1 with a current AI vaccine isolate (Tk/NC/88). The HA gene from the second H1N1 vaccine isolate, A/Sw/NC/05, was determined to be less related to the pH1N1 viruses. This virus was also detected in turkeys in North Carolina during the time of isolation (E. Gonder, personal communications). Interestingly, avian origin H1N1 viruses containing human HA gene segments have only recently been characterized (37). Further analysis into the origins and genetic makeup of this virus are ongoing.

The HA of influenza is a trimeric protein that mediates attachment to host cells through a globular-head domain containing a sialic acid receptor binding site (7). Using monoclonal antibody analysis, Gerhard *et al.* (9) identified a number of antigenic epitopes on the influenza HA protein, Ca, Cb, Sa, and Sb, important for anti-hemagglutination activity, which were later mapped to specific amino acid locations (2,9,36,39). Mapping these epitopes onto the three-dimensional structure showed the antigenic sites comprise residues from discontinuous primary amino acid sequence. In particular, the Ca sites connect adjacent monomers of HA and may be involved with HA trimerization during formation (43). Amino acid comparison and alignment of HA_1 was examined and compared at the major antigenic sites regions important in anti-influenza antibody response to determine if these residues were conserved between pH1N1 and Tk/NC/88 vaccine virus (36,42). In spite of a high degree of similarity, almost half of the amino acid differences were observed in the major antigenic sites. In particular, the Ca1 region with five amino acid differences and the Ca2 region with four amino acid changes contained the most differences from the pH1N1 viruses and meet the proposed requirement for influenza variants of epidemiological importance (40). Overall 14 amino acids changes at the different major antigenic sites of the HA genes were observed between the pH1N1 and avian H1N1 vaccine isolates. It should be noted that several amino acid differences were observed immediately outside of the major antigenic sites and likely influence the antigenic structure of the HA protein. Taken together, these antigenic differences provide a explanation for the lack of cross-reactive HI antibodies induced in turkeys vaccinated with U.S. avian H1 vaccine isolates to the pH1N1 virus.

Because antibodies against the HA protein induce virus-neutralizing antibodies, selection of vaccine isolates needs to closely match those found in the field. Previous research has demonstrated the greater the genetic similarity between HA of vaccine and field virus, the greater the reduction in challenge virus replication and shedding from the respiratory tract (26,28). Serum HI antibody titers are commonly used surrogates of protection against IAVs, but antigenic relatedness as it pertains to vaccine protection and nucleotide relatedness is not clearly defined (16,29,35). Based on the >92% similarity between the pH1N1 and Tk/NC/88 vaccine isolate, some degree of serologic cross-reactivity between these viruses was expected. However, the impact of the differences at the major antigenic sites on inducing cross-reactive antibodies was unknown. Interestingly, positive HI antibody titers (>4) were not produced against the pH1N1 virus until after the third vaccination and only in a limited number of birds. It is possible the increase in cross-reactive HI titers after the third vaccination represented antigen processing of conserved epitopes in the major antigenic regions of the HA between the vaccine and pH1N1 isolates. Another explanation for the decreased reactivity observed here may be the combined trivalent vaccine formulation. It is possible that the other vaccine viruses contained more dominant epitopes because protective titers were observed after the first vaccination against both the homologous Tk/NC/88 and H3N2 viruses. However, vaccine-challenge studies are needed to determine if these birds would be protected against pH1N1 challenge.

In conclusion, the recent outbreak of pH1N1 in breeder turkeys appears to have come from human introduction. Because turkeys contain receptors to support replication of both mammalian and avian origin viruses, like swine, they represent a vessel from which future pandemic viruses may emerge. While a fair degree of HA nucleotide sequence similarity was observed between the pH1N1 viruses and the vaccine viruses, the major differences in antigenic relatedness determined here correlated with decreased cross-reactive HI antibodies. It is apparent from these studies that currently used H1-based IAV vaccines used in turkey breeder hens would not protect against production losses in the event of pH1N1 introduction. While these viruses have to date only rarely been isolated from turkey hens, the testing and production of efficacious vaccines against them is critical to control future outbreaks in susceptible species.

REFERENCES

1. Brownlee, G. G., and E. Fodor. The predicted antigenicity of the haemagglutinin of the 1918 Spanish influenza pandemic suggests an avian origin. Philos. Trans. R. Soc. Lond. B Biol. Sci. 356:1871–1876. 2001.

2. Caton, A. J., G. G. Brownlee, J. W. Yewdell, and W. Gerhard. The antigenic structure of the influenza virus A/PR/8/34 hemagglutinin (H1 subtype). Cell 31:417–427. 1982.

3. Choi, Y. K., J. H. Lee, G. Erickson, S. M. Goyal, H. S. Joo, R. G. Webster, and R. J. Webby. H3N2 influenza virus transmission from swine to turkeys, United States. Emerg. Infect. Dis. 10:2156–2160. 2004.

4. Cohen, J. Pandemic influenza. Straight from the pig's mouth: swine research with swine influenzas. Science 325:140–141. 2009.

5. Dawood, F. S., S. Jain, L. Finelli, M. W. Shaw, S. Lindstrom, R. J. Garten, L. V. Gubareva, X. Xu, C. B. Bridges, and T. M. Uyeki. Emergence of a novel swine-origin influenza A (H1N1) virus in humans. N. Engl. J. Med. 360:2605–2615. 2009.

6. Elbers, A. R., G. Koch, and A. Bouma. Performance of clinical signs in poultry for the detection of outbreaks during the avian influenza A (H7N7) epidemic in The Netherlands in 2003. Avian Pathol. 34:181–187. 2005.

7. Gamblin, S. J., L. F. Haire, R. J. Russell, D. J. Stevens, B. Xiao, Y. Ha, N. Vasisht, D. A. Steinhauer, R. S. Daniels, A. Elliot, D. C. Wiley, and J. J. Skehel. The structure and receptor binding properties of the 1918 influenza hemagglutinin. Science 303:1838–1842. 2004.

8. Garten, R. J., C. T. Davis, C. A. Russell, B. Shu, S. Lindstrom, A. Balish, W. M. Sessions, X. Xu, E. Skepner, V. Deyde, M. Okomo-Adhiambo, L. Gubareva, J. Barnes, C. B. Smith, S. L. Emery, M. J. Hillman, P. Rivailler, J. Smagala, M. de Graaf, D. F. Burke, R. A. Fouchier, C. Pappas, C. M. Alpuche-Aranda, H. Lopez-Gatell, H. Olivera, I. Lopez, C. A. Myers, D. Faix, P. J. Blair, C. Yu, K. M. Keene, P. D. Dotson Jr, D. Boxrud, A. R. Sambol, S. H. Abid, K. St George, T. Bannerman, A. L. Moore, D. J. Stringer, P. Blevins, G. J. Demmler-Harrison, M. Ginsberg, P. Kriner, S. Waterman, S. Smole, H. F. Guevara, E. A. Belongia, P. A. Clark, S. T. Beatrice, R. Donis, J. Katz, L. Finelli, C. B. Bridges, M. Shaw, D. B. Jernigan, T. M. Uyeki, D. J. Smith, A. I. Klimov, and N. J. Cox. Antigenic and genetic characteristics of swine-origin 2009 A(H1N1) influenza viruses circulating in humans. Science 325:197–201. 2009.

9. Gerhard, W., J. Yewdell, M. E. Frankel, and R. Webster. Antigenic structure of influenza virus haemagglutinin defined by hybridoma antibodies. Nature 290:713–717. 1981.

10. Ito, T. Interspecies transmission and receptor recognition of influenza A viruses. Microbiol. Immunol. 44:423–430. 2000.

11. Ito, T., J. N. Couceiro, S. Kelm, L. G. Baum, S. Krauss, M. R. Castrucci, I. Donatelli, H. Kida, J. C. Paulson, R. G. Webster, and Y. Kawaoka. Molecular basis for the generation in pigs of influenza A viruses with pandemic potential. J. Virol. 72:7367–7373. 1998.

12. Ito, T., and Y. Kawaoka. Host-range barrier of influenza A viruses. Vet. Microbiol. 74:71–75. 2000.

13. Kapczynski, D. R., E. Gonder, K. Liljebjelke, R. Lippert, D. Petkov, and B. Tilley. Vaccine-induced protection from egg production losses in commercial turkey breeder hens following experimental challenge with a triple-reassortant H3N2 avian influenza virus. Avian Dis. 53:7–15. 2009.

14. Kapczynski, D. R., and D. E. Swayne. Influenza vaccines for avian species. Curr. Top. Microbiol. Immunol. 333:133–152. 2009.

15. Kuiken, T., E. C. Holmes, J. McCauley, G. F. Rimmelzwaan, C. S. Williams, and B. T. Grenfell. Host species barriers to influenza virus infections. Science 312:394–397. 2006.

16. Liljebjelke, K. A., D. I. Petkov, and D. R. Kapczynski. Mucosal vaccination with a codon-optimized hemagglutinin gene expressed by attenuated Salmonella elicits a protective immune response in chickens against highly pathogenic avian influenza. Vaccine 28:4430–4437. 2010.

17. Manicassamy, B., R. A. Medina, R. Hai, T. Tsibane, S. Stertz, E. Nistal-Villan, P. Palese, C. F. Basler, and A. Garcia-Sastre. Protection of mice against lethal challenge with 2009 H1N1 influenza A virus by 1918-like and classical swine H1N1 based vaccines. PLoS Pathog. 6:e1000745. 2010.

18. Mathieu, C., V. Moreno, P. Retamal, A. Gonzalez, A. Rivera, J. Fuller, C. Jara, C. Lecocq, M. Rojas, A. Garcia, M. Vasquez, M. Agredo, C. Gutierrez, H. Escobar, R. Fasce, J. Mora, J. Garcia, J. Fernandez, C. Ternicier, and P. Avalos. Pandemic (H1N1) 2009 in breeding turkeys, Valparaiso, Chile. Emerg. Infect. Dis. 16:709–711. 2010.

19. Matrosovich, M., A. Tuzikov, N. Bovin, A. Gambaryan, A. Klimov, M. R. Castrucci, I. Donatelli, and Y. Kawaoka. Early alterations of the receptor-binding properties of H1, H2, and H3 avian influenza virus hemagglutinins after their introduction into mammals. J. Virol. 74:8502–8512. 2000.

20. Olsen, C. W., S. Carey, L. Hinshaw, and A. I. Karasin. Virologic and serologic surveillance for human, swine and avian influenza virus infections among pigs in the north-central United States. Arch. Virol. 145:1399–1419. 2000.

21. Pantin-Jackwood, M., J. L. Wasilenko, E. Spackman, D. L. Suarez, and D. E. Swayne. Susceptibility of turkeys to pandemic-H1N1 virus by reproductive tract insemination. Virol. J. 7:27. 2010.

22. Rogers, G. N., J. C. Paulson, R. S. Daniels, J. J. Skehel, I. A. Wilson, and D. C. Wiley. Single amino acid substitutions in influenza haemagglutinin change receptor binding specificity. Nature 304:76–78. 1983.

23. Suarez, D. L., C. W. Lee, and D. E. Swayne. Avian influenza vaccination in North America: strategies and difficulties. Dev. Biol. (Basel) 124:117–124. 2006.

24. Suarez, D. L., E. Spackman, and D. A. Senne. Update on molecular epidemiology of H1, H5, and H7 influenza virus infections in poultry in North America. Avian Dis. 47:888–897. 2003.

25. Suarez, D. L., P. R. Woolcock, A. J. Bermudez, and D. A. Senne. Isolation from turkey breeder hens of a reassortant H1N2 influenza virus with swine, human, and avian lineage genes. Avian Dis. 46:111–121. 2002.

26. Swayne, D. E., M. Garcia, J. R. Beck, N. Kinney, and D. L. Suarez. Protection against diverse highly pathogenic H5 avian influenza viruses in chickens immunized with a recombinant fowlpox vaccine containing an H5 avian influenza hemagglutinin gene insert. Vaccine 18:1088–1095. 2000.

27. Swayne, D. E., and D. A. Halverson. Influenza. In: Diseases of poultry, 11th ed. Y. M. Saif, J. R. Glisson, H. J. Barnes, A. M. Fadly, L. McDougald, and D. E. Swayne, eds. Iowa State University Press, Ames, IA. pp. 135–160. 2003.

28. Swayne, D. E., and D. Kapczynski. Strategies and challenges for eliciting immunity against avian influenza virus in birds. Immunol. Rev. 225:314–331. 2008.

29. Swayne, D. E., C. W. Lee, and E. Spackman. Inactivated North American and European H5N2 avian influenza virus vaccines protect chickens from Asian H5N1 high pathogenicity avian influenza virus. Avian Pathol. 35:141–146. 2006.

30. Swayne, D. E., M. Pantin-Jackwood, D. Kapczynski, E. Spackman, and D. L. Suarez. Susceptibility of poultry to pandemic (H1N1) 2009 virus. Emerg. Infect. Dis. 15:2061–2063. 2009.

31. Tamura, K., and M. Nei. Estimation of the number of nucleotide substitutions in the control region of mitochondrial DNA in humans and chimpanzees. Mol. Biol. Evol. 10:512–526. 1993.

32. Tamura, K., D. Peterson, N. Peterson, G. Stecher, M. Nei, and S. Kumar. MEGA5: Molecular evolutionary genetics analysis using maximum likelihood, evolutionary distance, and maximum parsimony methods. Mol. Biol. Evol. 2011 Aug 18 [epub ahead of print].

33. Tang, Y., C. W. Lee, Y. Zhang, D. A. Senne, R. Dearth, B. Byrum, D. R. Perez, D. L. Suarez, and Y. M. Saif. Isolation and characterization of H3N2 influenza A virus from turkeys. Avian Dis. 49:207–213. 2005.

34. Terregino, C., R. De Nardi, R. Nisi, F. Cilloni, A. Salviato, M. Fasolato, and I. Capua. Resistance of turkeys to experimental infection with an early 2009 Italian human influenza A(H1N1)v virus isolate. Euro. Surveill. 14:19360. 2009.

35. Tumpey, T. M., D. R. Kapczynski, and D. E. Swayne. Comparative susceptibility of chickens and turkeys to avian influenza A H7N2 virus infection and protective efficacy of a commercial avian influenza H7N2 virus vaccine. Avian Dis. 48:167–176. 2004.

36. Underwood, P. A. Mapping of antigenic changes in the haemagglutinin of Hong Kong influenza (H3N2) strains using a large panel of monoclonal antibodies. J. Gen. Virol. 62(Pt 1):153–169. 1982.

37. Vincent, A. L., W. Ma, K. M. Lager, M. R. Gramer, J. A. Richt, and B. H. Janke. Characterization of a newly emerged genetic cluster of H1N1 and H1N2 swine influenza virus in the United States. Virus Genes 39:176–185. 2009.

38. Wan, H., and D. R. Perez. Quail carry sialic acid receptors compatible with binding of avian and human influenza viruses. Virology 346:278–286. 2006.

39. Wiley, D. C., I. A. Wilson, and J. J. Skehel. Structural identification of the antibody-binding sites of Hong Kong influenza haemagglutinin and their involvement in antigenic variation. Nature 289:373–378. 1981.

40. Wilson, I. A., and N. J. Cox. Structural basis of immune recognition of influenza virus hemagglutinin. Annu. Rev. Immunol. 8:737–771. 1990.

41. Yassine, H. M., M. Q. Al-Natour, C. W. Lee, and Y. M. Saif. Interspecies and intraspecies transmission of triple reassortant H3N2 influenza A viruses. Virol. J. 4:129. 2007.

42. Yassine, H. M., C. W. Lee, D. L. Suarez, and Y. M. Saif. Genetic and antigenic relatedness of H3 subtype influenza A viruses isolated from avian and mammalian species. Vaccine 26:966–977. 2008.

43. Yewdell, J. W. Monoclonal antibodies specific for discontinuous epitopes direct refolding of influenza A virus hemagglutinin. Mol. Immunol. 47:1132–1136. 2010.

44. Zhou, N. N., D. A. Senne, J. S. Landgraf, S. L. Swenson, G. Erickson, K. Rossow, L. Liu, K. Yoon, S. Krauss, and R. G. Webster. Genetic reassortment of avian, swine, and human influenza A viruses in American pigs. J. Virol. 73:8851–8856. 1999.

45. Zhou, N. N., D. A. Senne, J. S. Landgraf, S. L. Swenson, G. Erickson, K. Rossow, L. Liu, K. J. Yoon, S. Krauss, and R. G. Webster. Emergence of H3N2 reassortant influenza A viruses in North American pigs. Vet. Microbiol. 74:47–58. 2000.

ACKNOWLEDGMENTS

We wish to thank Joan Beck, Aniko Zsak, and Cam Greene for expert technical help. This research was supported by USDA, ARS CRIS project 6612-32000-053.

Viruses **2012**, *4*, 28-61; doi:10.3390/v4010028

OPEN ACCESS

viruses

ISSN 1999-4915

www.mdpi.com/journal/viruses

Article

Analysis of the Genome of the Sexually Transmitted Insect Virus *Helicoverpa zea* Nudivius 2

John P. Burand [1,†,*], Woojin Kim [1,†], Claudio L. Afonso [2], Edan R. Tulman [2], Gerald F. Kutish [2], Zhiqiang Lu [2] and Daniel L. Rock [2]

[1] Department of Plant, Soil and Insect Sciences, University of Massachusetts Amherst, Amherst, MA 01003, USA; E-Mail: wjkim@psis.umass.edu

[2] Plum Island Animal Disease Center, Agricultural Research Service, U.S. Department of Agriculture, Greenport, NY 11944, USA; E-Mails: claudio.afonso@ars.usda.gov (C.L.A.); edan.tulman@uconn.edu (E.R.T.); gkutish@netzero.net (G.F.K.); zhiqiang.lu@dhs.gov (Z.L.); dlrock@illinois.edu (D.L.R.)

† The authors contributed equally to this work.

* Author to whom correspondence should be addressed; E-Mail: jburand@microbio.umass.edu; Tel.: +1-413-545-3629; Fax: +1-413-545-2115.

Received: 29 November 2011; in revised form: 30 December 2011 / Accepted: 31 December 2011 / Published: 6 January 2012

Abstract: The sexually transmitted insect virus *Helicoverpa zea* nudivirus 2 (HzNV-2) was determined to have a circular double-stranded DNA genome of 231,621 bp coding for an estimated 113 open reading frames (ORFs). HzNV-2 is most closely related to the nudiviruses, a sister group of the insect baculoviruses. Several putative ORFs that share homology with the baculovirus core genes were identified in the viral genome. However, HzNV-2 lacks several key genetic features of baculoviruses including the late transcriptional regulation factor, LEF-1 and the palindromic *hrs*, which serve as origins of replication. The HzNV-2 genome was found to code for three ORFs that had significant sequence homology to cellular genes which are not generally found in viral genomes. These included a presumed juvenile hormone esterase gene, a gene coding for a putative zinc-dependent matrix metalloprotease, and a major facilitator superfamily protein gene; all of which are believed to play a role in the cellular proliferation and the tissue hypertrophy observed in the malformation of reproductive organs observed in HzNV-2 infected corn earworm moths, *Helicoverpa zea*.

Keywords: nudivirus; sterile insects; baculovirus; sexually transmitted virus; virus genome; juvenile hormone esterase; HzNV-2; HzNV-1; corn earworm; *Helicoverpa zea*

1. Introduction

Helicoverpa zea nudivirus 2 (HzNV-2) was originally identified as being responsible for the sterility of infected corn earworm moths (*H. zea*) in a colony of this insect established and maintained at Stoneville MS (USA). HzNV-2 [a.k.a. gonad specific virus (GSV), Hz-2V] is an enveloped, rod-shaped, double stranded DNA (dsDNA) virus which is a member of the newly described *Nudivirus* genus [1]. Other members of this group include: the *Oryctes rhinoceros* nudivirus (OrNV), *Gryllus bimaculatus* nudivirus (GbNV) and the nudivirus (HzNV-1), initially identified in a cell line established from ovarian tissues of *H. zea* moths. Although the nudiviruses (NV) are considered a loosely associated group of non-occluded insect pathogenic dsDNA viruses, the recent analysis of OrNV genome has provided a foundation for common elements of some of the disparate members of this group [2,3]. In addition, this work describes possible evolutionary linkages between these viruses and other large dsDNA viruses of arthropods including the baculoviruses, the hytrosaviruses and the nimaviruses. Significant homology has also been found between several nudivirus genes and genes coding for both nucleocapsid proteins of bracoviruses and genes involved in the replication of these polydnaviruses. These findings have led to the suggestion that polydnavirus originated from the integration of a nudivirus ancestor into the genome of a braconid wasp [4].

Our initial characterization of the HzNV-2 genome revealed that this virus shared a 93% sequence identity with HzNV-1 [1]. This was an interesting finding in view of the fact that, while both viruses can replicate in tissue culture cells, only HzNV-2 has the ability to replicate in an insect host. In as much as the replication of either of these two viruses in cell culture can lead to establishment of persistently infected cell lines, persistent replication of HzNV-2 in the insect host, results in fertile *H. zea* moths, which are asymptomatic carriers of the virus. Productive replication of HzNV-2 on the other hand appears to be limited to the reproductive tissues of the infected moth resulting in the malformation of these tissues and sterility of the infected host. These infected moths then serve to transmit the virus to other moths during mating attempts making HzNV-2 the causative agent of the only known sexually transmitted viral diseases of insects.

HzNV-2 infected female moths lack some reproductive structures including, ovaries, bursa copulatrix, accessory glands and spermatheca, and have grossly deformed, enlarged common and lateral oviducts, which appear as a large “Y-shaped” structure. This is a condition which has been referred as being agonadal [5,6]. In both pupae and adult females, the branches of the “Y-shaped” structure are much larger than the corresponding normal, lateral oviducts. EM observations of the branch structure in 7-day-old, infected pupae shows a high level of virus replication in cells within this structure. Viral replication in these structures results in hypertrophy of the oviducts and proliferation of cells that make up these tissues [6]. In female reproductive tissues, virus replication culminates in the formation of a “viral plug” which serves to protract the mating behavior of these females, as well as serve as a source of contaminating virus for males attempting to mate [7]. In addition, infected females

produce five to seven times more sex pheromone than uninfected females and attract twice as many male mates [8].

The ability of HzNV-2 to manipulate molecular processes of the host, particularly the massive cellular and tissue transformations observed in oviducts of infected females, suggests this virus is able to direct the alteration of the physiology and gene expression in infected host tissues. In order to better understand the evolutionary relationship between HzNV-1 and HzNV-2, and to begin to identify viral genes responsible for the pathology and unique biology of this insect pathogenic virus, we undertook the sequencing of the genome of HzNV-2.

2. Results and Discussion

2.1. Genome Features

The genome of HzNV-2 was found to be a circular dsDNA molecule of 231,621 bp. This is in good agreement with the previous restriction endonuclease size estimate of 225 to 235 kb [9], making it the largest of the insect viruses with dsDNA genomes.

The HzNV-2 genome has a G+C content of 41.9% and contains 376 ORFs coding more than 60 aa, of which 113 ORFs are likely to encode proteins. Of these putative genes, 66 ORFs are found on the forward strand and 47 on the reverse, all arranged evenly, producing 29 clusters of 1 to 6 ORFs in the viral genome. With sizes ranging from 5.7 kb to 189 bp, the average identified ORF was 1.4 kb in length. The gene density was one gene per 2.05 kb, and the coding density was 68%. The location, size, and direction of these ORFs is shown in Table 1 and Figure 1. For descriptive purposes, the HzNV-2 genome map is presented in linear form, and gene homologues of HzNV-1 are excluded (from Table 1, with the exception of HzNV-1 p34 and p51 late proteins which were the best blast matches) because of their high sequence homologies, which were over 90% in most cases. HzNV-1 and other nudivirus homologues are also listed in Table 1.

Unlike the baculoviruses, which have clusters of repeated, imperfect palindromic sequences, the so-called homologous regions (*hrs*) [10], no *hrs* were found in HzNV-2 genome. No *hrs* have been found thus far in any of the other NV, including HzNV-1 [11], and GbNV [12]. The *hrs* found in baculoviruses serve as origins of viral DNA replication [13], and all of the members of *Baculoviridae* family sequenced to date have *hrs* as a common feature of their genome. Although no *hrs* were identified in the HzNV-2 genome, abundant direct tandem repeated sequences were present. Six of the most significant direct repeats (*drs*) regions of 24 to 81 bp, which repeat 7 to 25 times (Table 2), were found by EMBOSS Etandem software. Five of the six *drs* in the HzNV-2 genome form a cluster at the 174.2–180 kb region.

In a search of GenBank database release 166, only 38 of the 113 putative HzNV-2 genes demonstrated clear homologies to genes in the current database other than putative HzNV-1 genes. These include six putative genes involved in DNA replication, four in transcription, five in nucleic acid metabolism, three structural proteins, and 14 with other functions. Hz2V058 and Hz2V073 had high homologies to the two HzNV-1 late genes, p34 and p51, respectively. The other 75 of 113 ORFs had poor or no homology to any known genes.

Figure 1. Genome map of HzNV-2. For descriptive purpose, circular genomic DNA is presented in linear form. The position of the first nucleotide was arbitrarily chosen. ORFs are numbered from left to right based on the position of the methionine initiation codon. ORFs transcribed to the right are located above the horizontal line; ORFs transcribed to the left are below.

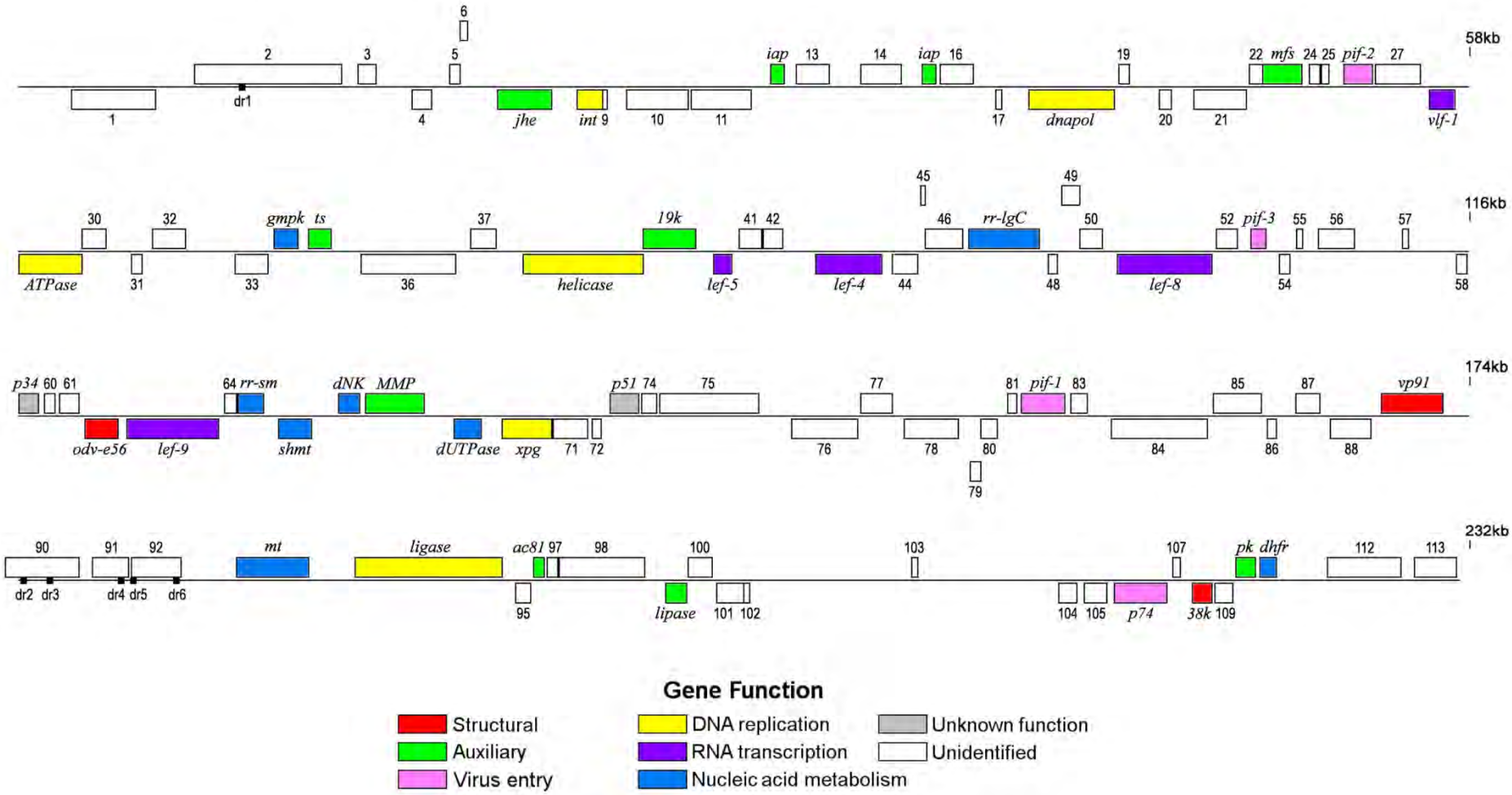

Table 1. HzNV-2 putative ORFs.

ORF	Strand [a]	Position		Length		Best Blast match			Signature [b]	HzNV-1 [c]
		start	end	(nt)	(aa)	Predicted function	Species/Viruses	E-value		
Hz2V001	R	5630	2298	3333	1111				TAF, H3	1
Hz2V002	F	7183	13047	5865	1955					154
Hz2V003	F	13677	14378	702	234					151
Hz2V004	R	16594	15830	765	255					150
Hz2V005	F	17366	17803	438	146					148
Hz2V006	F	17779	18063	285	95					
Hz2V007	R	21403	19241	2163	721	Carboxylesterase	*Drosophila pseudoobscura*	3×10^{-21}	Coesterase	145
Hz2V008	R	23425	22421	1005	335	Integrase	Monodon baculovirus	1×10^{-29}	INT_REC_C	144
Hz2V009	R	23621	23430	192	64					143
Hz2V010	R	26839	24425	2415	805					141
Hz2V011	R	29383	26969	2415	805					140
Hz2V012	F	30140	30700	561	187	Inhibitor of apoptosis protein	*Trichoplusia ni SNPV*	7×10^{-25}	BIR	138
Hz2V013	F	31151	32494	1344	448					137
Hz2V014	F	33735	35312	1578	526					
Hz2V015	F	36168	36713	546	182	Inhibitor of apoptosis protein	*Adoxophyes orana* GV	120	BIR	135
Hz2V016	F	36879	38201	1323	441					134
Hz2V017	R	39326	39138	189	63					133
Hz2V018	R	43848	40441	3408	1136	DNA polymerase	*Oryctes rhinoceros NV*	1×10^{-25}	POLBc	131
Hz2V019	F	44032	44442	411	137					130
Hz2V020	R	46083	45655	429	143					129
Hz2V021	R	49108	47033	2076	692					128
Hz2V022	F	49210	49731	522	174					
Hz2V023	F	49772	51307	1536	512	Membrane transporter	*Ades aegyptii*	1×10^{-135}	MFS_1	126
Hz2V024	F	51575	52000	426	142					125

Table 1. *Cont.*

ORF	Strand [a]	Position		Length		Best Blast match			Signature [b]	HzNV-1 [c]
		start	end	(nt)	(aa)	Predicted function	Species/Viruses	E-value		
Hz2V025	F	52066	52392	327	109					124
Hz2V026	F	52998	54137	1140	380	Per-os infectivity factor 2	*Gryllus bimaculatus* NV	5×10^{-37}	Baculo_44	123
Hz2V027	F	54224	56023	1800	600					122
Hz2V028	R	57374	56376	999	333	Very late expression factor 1	Monodon baculovirus	1×10^{-8}		121
Hz2V029	R	60667	58199	2469	823	DNA repair related ATPase	*Gryllus bimaculatus* NV	3×10^{-4}	SbcC	119
Hz2V030	F	60709	61674	966	322					118
Hz2V031	R	63063	62671	393	131					117
Hz2V032	F	63532	64803	1272	424					115
Hz2V033	R	68086	66803	1284	428					112
Hz2V034	F	68319	69323	1005	335	Guanosine monophosphate kinase	Monodon baculovirus	4×10^{-5}	GMPK	111
Hz2V035	F	69749	70621	873	291	Thymidylate synthase	*Bombyx mori*	4×10^{-131}	Thymidylat_synt	109
Hz2V036	R	75567	71800	3768	1256					107
Hz2V037	F	76171	77190	1020	340					106
Hz2V038	R	83046	78304	4743	1581	Helicase	*Culex nigripalpus* NPV	2.8	Pox_D5	104
Hz2V039	F	83048	85156	2109	703	19kDa protein	*Gryllus bimaculatus* NV	9×10^{-9}	Baculo_19	103
Hz2V040	R	86584	85862	723	241	Late expression factor 5	*Spodoptera exigua* NPV	6×10^{-3}	Baculo_LEF5	101
Hz2V041	F	86863	87756	894	298					100
Hz2V042	F	87845	88594	750	250					99
Hz2V043	R	92546	89928	2619	873	Late expression factor 4	*Gryllus bimaculatus* NV	3×10^{-18}		98
Hz2V044	R	94003	92963	1041	347					97
Hz2V045	F	94110	94313	204	68					
Hz2V046	F	94306	95775	1470	490					96
Hz2V047	F	96009	98822	2814	938	Ribonuclease reductase	*Spodoptera litura* NPV	0	Ribonuc_red_lgC	95
Hz2V048	R	99573	99214	360	120					94

Table 1. *Cont.*

ORF	Strand [a]	Position		Length		Best Blast match			Signature [b]	HzNV-1 [c]
		start	end	(nt)	(aa)	Predicted function	Species/Viruses	E-value		
Hz2V049	F	99730	100473	744	248					93
Hz2V050	F	100458	101336	879	293					
Hz2V051	R	105733	101939	3795	1265	Late expression factor 8	*Gryllus bimaculatus* NV	1×10^{-12}	RNA_pol_Rpb2_6	90
Hz2V052	F	105870	106712	843	281					89
Hz2V053	F	107253	107894	642	214	Per-os infectivity factor 3	*Gryllus bimaculatus* NV	2×10^{-10}		88
Hz2V054	R	108853	108413	441	147					87
Hz2V055	F	109110	109391	282	94					85
Hz2V056	F	109953	111365	1413	471					83
Hz2V057	F	113318	113530	213	71					
Hz2V058	R	115909	115496	414	138					81
Hz2V059	F	116202	116963	762	254	p34 late protein	*Helicoverpa zea* NV-1 [d]	8×10^{-147}		79
Hz2V060	F	117224	117595	372	124					78
Hz2V061	F	117803	118570	768	256					77
Hz2V062	R	120105	118786	1320	440	Odv-e56 structural protein	*Gryllus bimaculatus* NV	2×10^{-9}		76
Hz2V063	R	124121	120513	3609	1203	Late expression factor 9	Monodon baculovirus	1×10^{-60}		75
Hz2V064	F	124357	124818	462	154					74
Hz2V065	F	124932	125930	999	333	Ribonuclease reductase	*Xenopus tropicalis*	5×10^{-128}	Ribonuc_red_sm	73
Hz2V066	R	127832	126510	1323	441	Serine hydroxymethyltransferase	*Bombyx mori*	0	SHMT	72
Hz2V067	F	128939	129760	822	274	Deoxynucleotide kinase	*Drosophila melanogaster*	1×10^{-38}	dNK	71
Hz2V068	F	129972	132338	2367	789	Matrix metalloprotease	*Acyrthosiphon pisum*	3×10^{-69}	ZnMc_MMP, HX	70
Hz2V069	R	134585	133536	1050	350	dUTPase	*Culex quinquefasciatus*	2×10^{-38}	dUTPase	69
Hz2V070	R	137400	135430	1971	657	DNA excision repair enzyme	*Musca domestica* SGHV	2×10^{-7}	XPG	68
Hz2V071	R	138863	137478	1386	462					67
Hz2V072	R	139354	139019	336	112					66

Table 1. *Cont.*

ORF	Strand [a]	Position		Length		Best Blast match			Signature [b]	HzNV-1 [c]
		start	end	(nt)	(aa)	Predicted function	Species/Viruses	E-value		
Hz2V073	F	139721	140869	1149	383	p51 late protein	*Helicoverpa zea* NV-1 [d]	0		64
Hz2V074	F	141013	141564	552	184					63
Hz2V075	F	141693	145637	3945	1315					62
Hz2V076	R	149608	146981	2628	876					60
Hz2V077	F	149749	150978	1230	410					59
Hz2V078	R	153629	151443	2187	729					58
Hz2V079	R	154524	154090	435	145					
Hz2V080	R	155191	154481	711	237					
Hz2V081	F	155556	155936	381	127					56
Hz2V082	F	156150	157853	1704	568	Per-os infectivity factor 1	*Gryllus bimaculatus* NV	6×10^{-23}	DUF686	55
Hz2V083	F	158080	158742	663	221					54
Hz2V084	R	163557	159694	3864	1288					52
Hz2V085	F	163804	165702	1899	633					51
Hz2V086	R	166298	165954	345	115					
Hz2V087	F	167038	168003	966	322					49
Hz2V088	R	170084	168429	1656	552					47
Hz2V089	F	170456	172948	2493	831	vp91 capsid protein	*Gryllus bimaculatus* NV	4×10^{-14}		46
Hz2V090	F	173649	176570	2922	974					
Hz2V091	F	177136	178524	1389	463					
Hz2V092	F	178677	180614	1938	646					
Hz2V093	F	182846	185689	2844	948	Methyltransferase	*Helicoverpa zea* NPV	8×10^{-28}	FtsJ	37
Hz2V094	F	187572	193430	5859	1953	DNA ligase	*Apis mellifera*	4×10^{-86}	DNA_ligase_A_M	36
Hz2V095	R	194548	193964	585	195					34
Hz2V096	F	194663	195130	468	156	Ac81	*Gryllus bimaculatus* NV	6×10^{-12}	DUF845	33
Hz2V097	F	195232	195630	399	133					32

Table 1. *Cont.*

ORF	Strand [a]	Position		Length		Best Blast match			Signature [b]	HzNV-1 [c]
		start	end	(nt)	(aa)	Predicted function	Species/Viruses	E-value		
Hz2V098	F	195699	199133	3435	1145					31
Hz2V099	R	200794	199931	864	288	Esterase/lipase	*Psychromonas ingrahamii*	0.16	Aes	30
Hz2V100	F	200858	201796	939	313					29
Hz2V101	R	203059	201992	1068	356					28
Hz2V102	R	203298	203092	207	69					
Hz2V103	F	209783	209980	198	66					
Hz2V104	R	216330	215599	732	244					13
Hz2V105	R	217543	216668	876	292					12
Hz2V106	R	219936	217846	2091	697	p74 envelope protein	*Gryllius bimaculus* NV	5×10^{-57}	Baculo_p74	11
Hz2V107	F	220177	220464	288	96					
Hz2V108	R	221727	220951	777	259	38kDa protein	Monodon baculovirus	3×10^{-15}	DUF705	10
Hz2V109	R	222547	221819	729	243					9
Hz2V110	F	222677	223438	762	254	Protein kinase	*Trichomonas vaginalis*	5×10^{-18}	S_TKc	8
Hz2V111	F	223656	224297	642	214	Dihydrofolate reductase	*Heliothis virescens*	1×10^{-45}	DHFR	7
Hz2V112	F	226341	229232	2892	964					4
Hz2V113	F	229783	231468	1686	562					3

[a] The direction of the transcripts are indicated by F (forward) and R (reverse); [b] Functional motif found in Pfam and CDD database; [c] HzNV-1 ORFs corresponding to that of HzNV-2; [d] HzNV-1 ORFs which are the best match to that of HzNV-2.

Table 2. HzNV-2 direct repeat (*drs*) sequences.

	start	end	score	size	Count	%id	consensus
dr1	11711	12310	134	24	25	63.2	atgaagctgaggatgaatctgaac
dr2	174285	174572	132	36	8	79.2	gaaactcctaaatcaaaggatgaa cctaaagcaaag
dr3	175417	175656	124	60	4	88.3	atgaaaaagcaaaggctgaggcga aggctaaagccgatgctgctgcaa aagccaaagctg
dr4	178103	178390	182	24	12	85.8	ttataccagagagcaagccagaaa
dr5	178517	178921	104	81	5	72.8	acctaaagttgaatctaaagtagt ggaaccacctaaagcggaatctaa aacagtggaagctcctactaaaac agttgaagt
dr6	180236	180445	156	30	7	94.3	agctgccgctaaacgcaaagccg aggctga

Direct repeat sequences were found by using EMBOSS Etandem software with a cutoff score of 100.

Figure 2. Comparison of HzNV-1 and HzNV-2 genome sequence. The 228089 bp of the HzNV-1 genome sequence was subjected to rVISTA software to compare with 231621 bp of the HzNV-2 genome sequence. HzNV-2 is the base sequence, the sequence identity is plotted in 0~100% scale, and a region with 95% or higher identity is presented in red. The sequence window size is 100 bp.

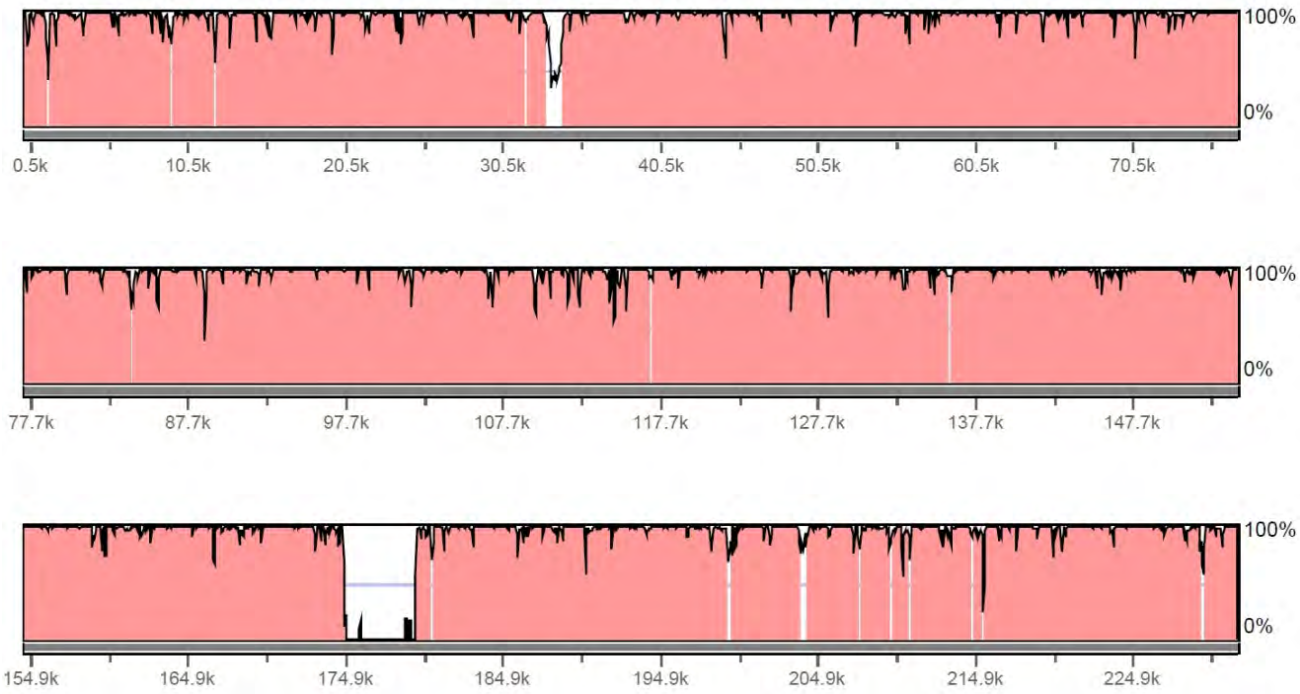

2.2. Evaluation of ORFs

Within the HzNV-2 genome sequence, a total of 376 virtual ORFs were identified that were longer than 60 aa and started with a methionine initiation codon. Minor ORFs, which were completely included within larger ORFs, were excluded. A total of 163 ORFs with a Glimmer score greater than 90 points were found among the 376 putative ORFs and were subjected to further evaluation. Hexamer scores were used to exclude ORFs with a low coding potential, and to eliminate ORFs which had a significant overlap with a portion of adjacent ORFs on either the same or complimentary strand. A

total of 113 ORFs among the 163 ORFs that passed the GLIMMER cutoff were selected for database search and physical characterization to identify possible functions of the putative genes.

In the initial analysis of the viral genome, it became clear that HzNV-2 was very closely related to the insect virus HzNV-1. Gene parity plot results demonstrated that 97 out of 113 putative HzNV-2 ORFs were found in the HzNV-1 genome without any overlap or inversion (Table 1). The global DNA sequence alignment between HzNV-1 and HzNV-2 by EMBOSS Matcher and rVISTA software showed 93.5% sequence identity with a 5.1 kb area at 174.7–179.8 kb region of HzNV-2 that showed significant gaps in the corresponding region of HzNV-1 genome (Figure 2). There were 3 ORF found in region: Hz2V090, Hz2V091, and Hz2V092. There were a total of 14 ORFs identified in the HzNV-2 genome that were not found in the HzNV-1 genome. None of these ORFs were determined to share sequence homology with any genes of know function.

The Genbank accession number of the Hz-2V genome sequence is JN418988.

2.3. Enzymes Related to DNA Replication and Repair

Five putative genes, Hz2V008 (integrase), Hz2V018 (dnapol), Hz2V029 (ATPase), Hz2V038 (helicase), Hz2V070 (excision\repair), and Hz2V094 (ligase) were orthologues of genes likely involved in DNA replication and repair. The C-terminal region of Hz2V008 had homology to the catalytic domain for integrase/recombinase, which has DNA breaking-rejoining activity. This region of Hz2V008 had relatively good similarity ($E = 2 \times 10^{-9}$) to the INT_REC_C conserved domain, which is related to phage integrase and bacterial and yeast recombinase. It contained well-conserved functional motif cores for DNA binding sites, catalytic residues, the active sites, and topoisomerase. The integrases from monodon baculovirus (MBV) and GbNV showed the best similarity ($E = 1 \times 10^{-29}$ and 2×10^{-11}, respectively) to Hz2V008 suggesting a possible common ancestral origin for these viral genes. Hz2V008 did not show homology with any baculovirus genes.

Hz2V018 had homology to DNA polymerase. The C-terminal region of Hz2V018 had ($E = 7 \times 10^{-10}$) similarity to the DNA dependent DNA polymerase type-B family (POLBc) conserved domain, which has DNA binding, polymerase, and 3'-5' exonuclease activity [14]. In this region, the well-conserved nucleotide binding motif, K(3x)NS(x)YG(2x)G, and the polymerase catalytic motif, YxDTD, were found at position 842–853 aa, and 892–897 aa, respectively. Hz2V018 also showed homology to the OrNV DNA polymerase.

Hz2V029 is an 823 aa long protein, with 256 aa at the N-terminal region which showed similarity ($E = 2 \times 10^{-3}$) to the C-terminal region of the SbcC conserved domain. The SbcC gene is a prokaryotic ortholog of the rad50 gene of humans that has ATPase activity and plays an important role in DNA double-strand break repair [15,16]. The SbcC gene is known to play a similar role during DNA replication in prokaryotes [17]. The highest similarities were detected for GbNV putitive desmoplakin ($E = 3 \times 10^{-4}$) and *Spodoptera frugiperda* ascovirus 1a SbcC/ATPase domain ($E = 4 \times 10^{-4}$).

Hz2V038 had homology to DNA helicase and was identified by the presence of a poxvirus D5 protein-like domain (Pox_D5) at its C-terminal region), [18]. Helicase is an essential gene for virus replication, and all baculoviruses contain a conserved helicase domain. 57.9% of residues of the conserved helicase domain aligned to over 186 aa of the Hz2V038 C-terminal region at position 1138–1323 aa, however, this similarity was relatively low ($E = 4 \times 10^{-3}$). *Culex nigripalpus*

helicase-1 was detected by a BLASTP search with Hz2V038, but with a poor score (E = 2.3). Hence PSI-BLAST was used to detect homologous genes. In the second iteration of PSI-BLAST, homologies to helicase genes of various baculoviruses were detected near the region of Pox_D5 domain. The *Ectoropis oblique* nucleopolyhedrovirus (NPV) helicase showed highest homology.

Hz2V070 had homology to xeroderma pigmentosum G (XPG) enzyme, which is related to other enzymes involved in nucleotide-excision repair and transcription-coupled repair of oxidative DNA damage. XPG has been shown to function by making a nick at the 3' side of the DNA strand damaged by UV radiation, which is then mended via the DNA excision repair system [19,20]. XPG is functionally and structurally related to flap endonuclease (FEN-1) enzyme [21], which functions in a manner analogous to the base excision DNA repair mechanism [22]. The homology between Hz2V070 and XPG was detected in the N-terminal region at position 28–256 aa, and CD-Search detected that the XPG domain had 245 of 319 residues aligned to the N-terminal region of Hz2V070 with relatively low similarity ($E = 6 \times 10^{-3}$). Because of the subtle homology of Hz2V070 to the XPG domain, BLASTP was able to detect only three homologues, found in genomes of the insect pathogenic, DNA viruses GbNV, OrNV and the salivary gland hypertrophy of *Musca domestica*, (MdSHGV), when the search was limited to the database subset of virus sequences.

Hz2V094 codes for a large putative protein composed of 1953 aa. This putative gene product had a highly conserved ($E = 3 \times 10^{-46}$) ATP-depentent DNA ligase domain of 201 aa in length that had high similarity to the DNA_Ligase_A_M conserved domain. The best match was to *Apis melifera* DNA ligase III ($E = 5 \times 10^{-84}$). The DNA ligase catalytic domain was located at the end of C-terminal region of Hz2V094. It also showed homology to other ligases at positions 480–714 aa and 1541–1929 aa regions. There was a more than 800 aa insertion between these two regions that did not show homology to any other genes.

2.4. Proteins Involved in RNA Transcription

There are five putative genes, Hz2V028 (*vlf-1*), Hz2V040 (*lef-5*), Hz2V043 (*lef-4*), Hz2V051 (*lef-8*), and Hz2V063 (*lef-9*), identified in the HzNV-2 genome that shared homology with baculovirus genes known to be involved in transcription. This is a very interesting result since these genes are all conserved baculovirus core genes that function in transcription and expression of late and very late genes. Baculoviruses share six common genes related to transcription, *p47*, *lef-4*, *lef-5*, *lef-8*, *lef-9*, and *vlf-1* [23]. The recent analysis of the OrNV genome sequence identified all six of these core genes in the genome of this virus, as well as in the genome of HzNV-1, and GbNV [2]. Our analysis identified all of these genes as well, except for *p47*.

These five common genes can be categorized into two groups. Both *lef-5* and *vlf-1* are transcription initiation factors, while *lef-4*, *lef-8* and *lef-9* along with *p47* encode subunits of RNA polymerase [24]. Hz2V028 showed homology to baculovirus very late expression factor 1 (vlf-1), which is essential for burst expression of the very late baculovirus genes, *polyhedrin* and *p10* [25]. *Vlf-1* is a transcription initiation factor that recognizes and binds to the promoter motif, DTAAG, of baculovirus very late genes [26] and is also involved in capsid assembly and DNA packaging [27]. Transient expression studies with the baculovirus very late promoter motif and HzNV-1 RNA polymerase demonstrated however, that HzNV-1 does not recognize the DTAAG motif [28]. This result indicates that HzNV-2

vlf-1, which has a 93% aa sequence similarity with the HzNV-1 *vlf-1* homologue, possibly recognizes a different late or very late promoter motif than does the baculovirus *vlf-1*. This is not surprising since the similarity of Hz2V028 to baculovirus *vlf-1* was relatively low ($E = 2 \times 10^{-2}$).

Hz2V040 had homology to late expression factor 5 (*lef-5*). LEF-5 has a characteristic zinc ribbon motif for DNA binding, which is often found in eukaryotic transcription elongation factors. However, LEF-5 along with baculovirus RNA polymerase, has transcriptional initiation activity at the late gene promoter [29]. Hz2V040 showed relatively low similarity to the C-terminal region of the Baculo_LEF-5 conserved domain ($E = 6 \times 10^{-3}$) at position 165–193 aa. This region also showed homology to the zinc finger motif (ZnF_C2C2) which is well conserved, especially at the positions of cysteine residues. Hence, Hz2V040 probably has a secondary structure similar to the DNA binding motif of baculovirus LEF-5 and therefore, DNA binding activity. Hz2V040 showed the best homology to *Spodoptera furugiperda* NPV *lef*-5 ($E = 6 \times 10^{-3}$). Interestingly, *lef*-5 homologues were also found in the other NV, GbNV and OrNV, however, these homologues were not detected by BLASTP because of their subtle similarities. None the less, these nudivirus homologues were detected by PSI-BLAST at their zinc ribbon domain.

The best match of Hz2V043 was to late expression factor 4 (*lef*-4) of GbNV ($E = 3 \times 10^{-18}$). LEF-4 has guanyltransferase and RNA triphosphatase activity and is thought to play a role in mRNA capping, which is essential for baculovirus replication [24,30,31]. Hz2V043 (873 aa) was almost twice as long as the homologue of *Autographa californica* NPV (AcMNPV) (464 aa), and the C-terminal region of this ORF showed homology to the *lef*-4 gene of GbNV and OrNV. Two KxDG motifs, characteristic of RNA capping enzymes capable of forming a stable enzyme-nucleotide monophosphate complex for guanylation [32], were found at positions 641 aa and 764 aa. This result supports the possibility of Hz2V043 having mRNA 5'-capping activity, despite its low similarity to baculovirus *lef-4* genes.

Hz2V051 showed homology to late expression factor 8 (*lef-8*). *Lef-8*, in conjunction with *lef-9*, encodes one of the main catalytic subunits of the baculovirus RNA polymerase. Hz2V051 showed the best similarity to GbNV *lef-8* ($E = 1 \times 10^{-12}$); however, the similarity to other baculovirus *lef-8* genes was relatively low. Hz2V051 was 1265 aa long, and the region at position 650–1112 aa was detected as an RNA_pol_Rpb2_6 conserved domain. This C-terminal region of Hz2V051 contains a conserved sequence motif GxKx4HGQ/NKG at 858–869 aa, which is found in both prokaryotic and eukaryotic RNA polymerases as well as those of the insect baculoviruses [33].

Hz2V063 had homology to the N-terminal region of the NV and baculovirus late expression factor 9 (LEF-9). OrNV LEF-9 showed good similarity ($E = 2 \times 10^{-8}$) at this region, however, the similarity of baculovirus LEF-9 detected by PSI-BLAST at this region was low. Hz2V063 contained an HADQDGD motif at position 286–292 aa, which is similar to the structure of the NTDCDGD motif of AcMNPV LEF-9 [34] and the NADFDGD motif of the vaccinia virus RNA polymerase large subunit [35]. LEF-9, in association with LEF 8, comprises the baculovirus RNA polymerase [36]. The exact function of LEF-9 in the polymerase, however, is not clear.

2.5. Genes Involved in Virus Entry

Baculoviruses also have common core genes encoding structural proteins related to their *per os* infectivity. HzNV-2 was found to have four genes, Hz2V026, Hz2V053, Hz2V082, and Hz2V106, which are homologues to these baculovirus *per os* infectivity factors (PIF). These *pif* genes are also well conserved in other NVs [1,2]. The identification of putative HzNV-2 *pif* genes is a very interesting result since, in contrast to the baculoviruses and other NVs, HzNV-2 is not highly infectious *per os* [5]. The presence of *pif* gene homologues in the HzNV-2 genome suggests a common mode of entry into cells which has been evolutionarily conserved among these different viruses.

Hz2V026 showed best similarity to GbNV *pif-2* gene ($E = 5 \times 10^{-37}$) and showed good similarity to AcMNPV *pif-2* ($E = 7 \times 10^{-11}$). The *pif-2* gene product which in addition to playing a role in oral infection by baculoviruses, is also a structural component of the occlusion-derived virus envelope [37]. Interestingly, the positions of cysteine residues were well conserved between Hz2V026 and the other *pif-2* genes. This result indicates that the HzNV-2 PIF-2 homologue might form disulfide bonds in the same manner and therefore have a very similar secondary structure to the *pif-2* gene products of these other viruses.

Hz2V053 was found to be a homologue of the baculovirus *pif-3* gene and showed good similarity to GbNV *pif-3* gene ($E = 2 \times 10^{-10}$). Similarity to other baculovirus *pif-3* genes was low, but as with PIF-2, the positions of cysteine residues were well conserved between Hz2V053, the PIF-3 of GbNV and those of other baculoviruses [38]. Despite the low similarity to baculovirus *pif-3*, Hz2V053 does contain an N-terminal transmembrane domain at position 3-19 aa, characteristic of other PIF-3s.

Hz2V082 is a homologue of the baculovirus *pif-1* gene. This gene showed the best similarity to the GbNV *pif-1* gene ($E = 6 \times 10^{-23}$) and homology with other baculovirus *pif-1* genes at the region of 70–350 aa. PIF-1 is a viral structural protein which, along with PIF-2, is responsible for oral infectivity by mediating the direct binding of the virus particle to host cells [39]. As with the other PIFs, the position of cysteine residues in PIF-1 and Hz2V08 are well conserved. When Hz2V082 was subjected to ANTHEPROT, three transmembrane domains and a putative N-terminal signal peptide cleavage site were found. This result suggests that the localization of Hz2V082 gene product in the virus membrane is similar to that of the *Spodoptera Littoralis* NPV (SlNPV) PIF-1. However, the topology of the HzNV-2 protein in the membrane might be slightly different, since the SlNPV PIF-1, and the PIF-1 other baculovirus have an additional fourth putative transmembrane domain [40].

Hz2V106 showed homology with the bacuolvirus *p74* gene, which codes for a critical oral infection factor of baculoviruses. P74 is a highly conserved envelope protein of baculoviruses that mediates specific binding of the virus particle to host cells [41]. The best similarity found for Hz2V106 was with the GbNV *p74* gene ($E = 5 \times 10^{-57}$). The proposed secondary structure of the *p74* gene product of *Choristoneura fumiferana* granulovirus (GV) illustrates that it has a characteristic positioning of cysteine residues that allows for the formation of disulfide bonds within its C-terminal transmembrane membrane anchoring domain [42]. Hz2V106 has six cysteine residues at positions 99, 104, 138, 169, 217, and 231 with three C-terminal transmembrane domains at 494–516 aa, 639–661 aa, and 665–687 aa, which are in a very similar context to those in the highly conserved baculovirus P74 protein.

2.6. Enzymes Involved in Nucleic Acid Metabolism

Seven putative HzNV-2 ORFs, Hz2V035, Hz2V047, Hz2V065, Hz2V066, Hz2V067, Hz2V069, and Hz2V093, showed homology to previously identified genes from eukaryotes, prokaryotes, and viruses that coded for proteins having activity related to nucleic acid metabolism.

Hz2V035 was a homologue of thymidylate synthase (TS). It contained the highly conserved TS functional domain and showed over 80% sequence identity to other TS genes. The HzNV-2 TS gene showed the best similarity to that of *Bombyx mori* TS ($E = 4 \times 10^{-131}$) and also showed high similarity to the TS genes of herpesvirus, NV, iridovirus, and other viruses. So far, no baculovirus TS genes have been found. TS is well conserved across species and is involved in the synthesis of dTMP precursors from dUTP [43,44]. Interestingly, all identified viral TS genes are thought to be acquired from their hosts in independent incidents rather than originating from a common ancestor [45,46].

Hz2V047 and Hz2V065 were homologues to ribonucleotide reductase large (RR1) and small subunit (RR2), respectively. These genes also showed homology to a variety of RR genes with over 70% amino acid similarities. The best match was to SlNPV RR1 ($E = 0$). RR1 and RR2 are involved in reducing ribonucleotides into deoxyribonucleotides to produce precursors of DNA [47] and are commonly found in viruses as well as prokaryotes and eukaryotes.

Hz2V066 showed homology to the serine hydroxymethyltransferase (SHMT) conserved domain ($E = 7 \times 10^{-171}$). SHMT catalyzes the reversible interconversion of serine and glycine with tetrahydrofolate [48]. This is the major source of one-carbon groups used in the biosynthesis of compounds containing methyl groups and purine rings, as well as in thymidylate biosynthesis [49]. Hz2V066 showed the greatest similarity to the *Bombyx mori* SHMT gene ($E = 0$). SHMT is a cellular gene, and to date has not been found in any other eukaryotic viruses.

Hz2V067 was homologous to deoxynucleotide kinase (dNK), with the best match to dNK of *Drosophila melanogaster* ($E = 1 \times 10^{-38}$) having 57% similarity. dNK catalyzes the phosphorylation of deoxyribonucleosides to yield corresponding monophosphates and is a key enzyme involved in the salvage of deoxyribonucleosides [50].

Hz2V069 is a 350 aa long ORF, of which over 150 aa of the N-terminal region showed homology with the dUTP phosphatase (dUTPase) domain ($E = 1 \times 10^{-31}$). The best match was *Culex quinquefasciatus* dUTPase ($E = 2 \times 10^{-38}$), however, this gene product is also often found as a protein component of animal viruses [51]. dUTPase provides a substrate for TS and maintains low dUTP:dTTP ratio to minimize the misincorporation of uracil into virus DNA during replication [52]. dUTPase also plays an important role during virus replication in terminally-differentiated or non-dividing cells that have a low level of cellular dUTPase expression [53]. Hence, dUTPase might be a key enzyme related to HzNV-2 replication and latency in asymptomatic carriers.

Hz2V093 encoded a 948 aa long protein that showed homology to methyltransferase (MT) at the N-terminal region of this protein. The best match was *H. zea* NPV ORF65 ($E = 8 \times 10^{-28}$). MT is often found in NPVs, but other than HzNV-1, it has not been found in NVs. Baculovirus methyltransferase along with LEF-4 is believed to be involved in RNA capping of late and very late gene transcripts, however, it is not essential for virus replication [54].

Hz2V111 was a homologue of dihydrofolate reductase (DHFR). The best match was *Heliothis virescens* DHFR (1×10^{-45}), with good homology to herpesvirus DHFR. DHFR reduces dihydrofolate

to tetrahydrofolate, which is required to regenerate methylenetetrahydrofolate by thymidylate synthase, an essential step in the biosynthesis of deoxythymine phosphate for DNA synthesis [55]. DHFR was also found in MdSGHV, however, it has not yet been found in any baculoviruses.

2.7. Structural Proteins

Hz2V062 was a homologue of the baculovirus *odv-e56* gene, which encodes an occlusion-derived virus envelope protein. It showed the best match to GbNV *odv-e56*, while the similarity to other baculovirus *odv-e56* was very low. Odv-e56 is one of the baculovirus late genes which utilize a TAAG promoter motif for its expression [56]. A TAAG motif, however, was not found within the 500 bp region upstream of Hz2V062. This observation is also indicative of the possibility that the late or very late gene regulation mechanism of HzNV-1 and HzNV-2 has evolved differently from that of baculoviruses.

Hz2V089 was a homologue of baculovirus *vp91*. The VP91 in baculoviruses is localized near the nuclear membrane of the infected cell and is associated with the virion capsid [57]. The C-terminal region of Hz2V089 showed homology to the GbNV *vp91* gene ($E = 4 \times 10^{-14}$) and also other baculovirus *vp91* genes as well.

Hz2V108 was a homologue of baculovirus 38K protein gene which codes a structural protein associated with the virus nucleocapsid [58]. The 38K protein plays an important role in nucleocapsid assembly, interacting with the other nucleocapsid proteins, VP1054, VP39, VP80, and 38K itself [58]. The best match was MBV baculovirus (3×10^{-15}).

2.8. Auxiliary and Undefined Genes

Hz2V007 codes for a putative protein composed of 721 aa. This putative gene product showed highest similarity to the *Bombyx mori* carboxylesterase (COE) ($E = 4 \times 10^{-21}$) and also had a high similarity to *Anopheles gambiae* juvenile hormone esterase (JHE) ($E = 2 \times 10^{-19}$). Hz2V007 had a COE domain at position 25–202 aa that had significant similarity to other highly conserved COE domains ($E = 6 \times 10^{-31}$). Almost the entire peptide sequence of Hz2V007 at position 1–632 aa lined up with the COE domain with relatively high similarity ($E = 5 \times 10^{-11}$).

Juvenile hormone (JH) is produced in the corpora allata, of insects, and acts as a transcriptional regulator, controlling the expression of a variety of genes involved in physiological, developmental, and reproductive processes in insects. One pathway for the control of JH titer in insects is by degradation via JHE [59]. The high similarity between Hz2V007 and insect JHEs is a very interesting result since it suggests that HzNV-2 can control the physiology of the infected host insects by regulating JH levels and ultimately the level of gene expression in various tissues during their development, at specific times during the replication cycle of the virus.

To compare Hz2V007 with other insect JHEs, nine JHEs peptide sequences from four different insect orders were selected from Genbank including *D.mel* COE-6, one hymenopteran (*Apis melifera*), one coleopteran (*Tenebrio molitor*), three dipterans (*Drosophila melanogaster*, *Aedes aegypti*, and *Anopheles gambiae*), and three lepidopterans (*Heliothis virecens*, *Manduca sexta*, and *Bombyx mori*). Sequence alignments of the entire coding region of each JHE with Hz2V007 were performed by EMBOSS Water software. Hz2V007 showed highest peptide sequence identity and similarity within

the catalytic domain of *A. gambiae* JHE (30.1% and 43.9% respectively), and the lowest with *H. virescens* JHE (20.4% and 34.6%). This level of similarity was relatively low compared with the range of sequence identities and similarities found among the nine insects JHEs, which had identities ranged between ~28.6 and 61.2% and similarities between ~61.2 and 77.1%.

To investigate the phylogenetic positioning of Hz2V007 among these insect JHEs, molecular phylogenetic analysis using neighbor-joining in MUSCLE and ClustalX was performed. The results demonstrated that Hz2V007 grouped with the JHEs from lepidopteron insects, rather than to dipteran JHEs to which it had the highest sequence similarity (Figure 3). This result may reflect the closer relationship between HzNV-2 and lepidopteran insects, from which the virus was most likely to have obtained the ancestral form of Hz2V007.

Figure 3. Phylogenetic analysis of JHEs and Hz2V007. Phylogenetic analysis of selected JHEs and Hz2V007. Multiple sequences were aligned using MUSCLE, and the tree was inferred using neighbor-joining in ClustalX. *D. melanogaster* corboxylesterase-6 gene was used as the outgroup. The robustness of the tree was tested using bootstrap analysis (1000 replicates). The percent values are presented at the nodes.

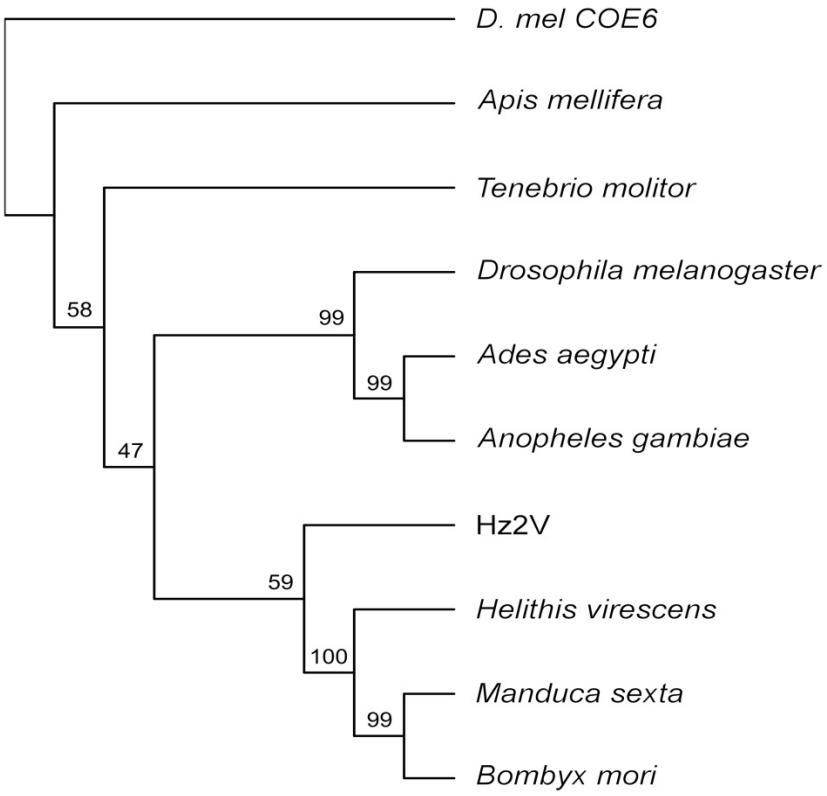

Another characteristic feature that Hz2V007 shares with other JHEs was a signal peptide. A possible cleavable signal peptide was found at position 1–20 aa, flanked by a putative cleavage site between 20 and 21 aa. The signal peptide sequences, which are responsible for secretion of insect JHE, were found in all nine JHEs.

The signal peptide sequence prediction and phylogenetic analysis results alone are not sufficient to predict the JHE activity of Hz2V007. To further assess its possible JHE activity, Hz2V007 and four JHEs from each order were chosen, and multiple sequence alignment was performed to compare

functional motifs within the catalytic domain of the JHEs with corresponding regions of Hz2V007. Most of the JHEs have five conserved catalytic motifs, RF, DQ, GxSxG, E, and GxxHxxD/E [60]. In Hz2V007, an intact RF motif was found at position 53 aa and partially conserved DQ, GxSxG and GxxHxxD motifs were found at 165 aa, 191 aa, and 544 aa, respectively. An E motif was not identified (Figure 4).

The average polypeptide length of the nine JHEs is 573 aa, and the entire polypeptide sequence of JHE corresponded to the region at 1–632 aa of Hz2V007. This means that Hz2V007 has 89 aa of C-terminal flanking sequence beyond the JHE sequence. This region showed no significant homology to any known sequences in the database. Interestingly, the SMART program predicted a transmembrane domain in this C-terminal region of Hz2V007 at position 686–719 aa, while it predicted an N-terminal signal peptide sequence for secretion. This result suggests a unique localization of the Hz2V007 gene product. TMHMM analysis results predicted that the N-terminal JHE-like region would reside outside of the cell, anchored on the cell membrane by the C-terminal transmembrane domain. From these results, it can be inferred that HzNV-2 captured the JHE gene from its lepidopteran host and evolved to alter its catalytic characteristics and specifically localize the Hz2V007 product at the surface of cells in infected tissue. When one considers the role of JH and JHE in controlling development and reproduction of insects, Hz2V007 might be a key gene responsible for the malformation of reproductive tissue functioning to regulate JH titers and gene expression in these tissues of the infected hosts.

Hz2V012 and Hz2V015 encoded inhibitor of apoptosis (IAP) homologues. The IAP gene was first found in baculoviruses suppressing apoptosis of virus infected host cells [61]. The baculovirus IAPs have 1~3 baculovirus IAP repeat (BIR) conserved domains, and inhibit apoptosis by acting as inhibitors of the caspase family of protease enzymes. Baculovirus IAPs also contain a RING-finger motif and a zinc-binding site in their C-terminal region. The RING-finger motif is not required for anti-apoptotic activity [62,63]; however, it is important for regulation of IAPs by ubiquitin ligase [64,65]. Hz2V012 and Hz2V015 (termed IAP 1 and IAP 2) were 187aa and 182aa long peptides, respectively. These were both much shorter than other cellular or baculovirus IAPs. The best match of IAP 1 was the *Trichplusia ni* (cabbage looper) NPV IAP gene ($E = 7 \times 10^{-25}$), and the best match of IAP 2 was *Adoxophyes orana* GV IAP 3 ($E = 1 \times 10^{-26}$). IAP-1 had two BIR domains without a RING-finger motif, while IAP 2 had one BIR domain with a C-terminal RING-finger motif. These are interesting results because most of the baculovirus IAPs have two BIR domains with one RING-finger motif at the C-terminal region. The exact role of the IAP genes of HzNV-2 still needs to be confirmed experimentally.

Figure 4. A schematic presentation of functional domains and motifs in Hz2V007. The functional domains identified by CDD and pfam database searches are presented in orange and blue, respectively. The transmembrane domains are presented in red. Multiple JHE sequence alignments are presented using ClustalX, and the locations of conserved residues in the active sites of JHE are indicated with triangles. T. mol (*T. molitor*), A.mol (*A. melifera*), D.mel (*D. melanogaster*), H.vir (*H. virecens*).

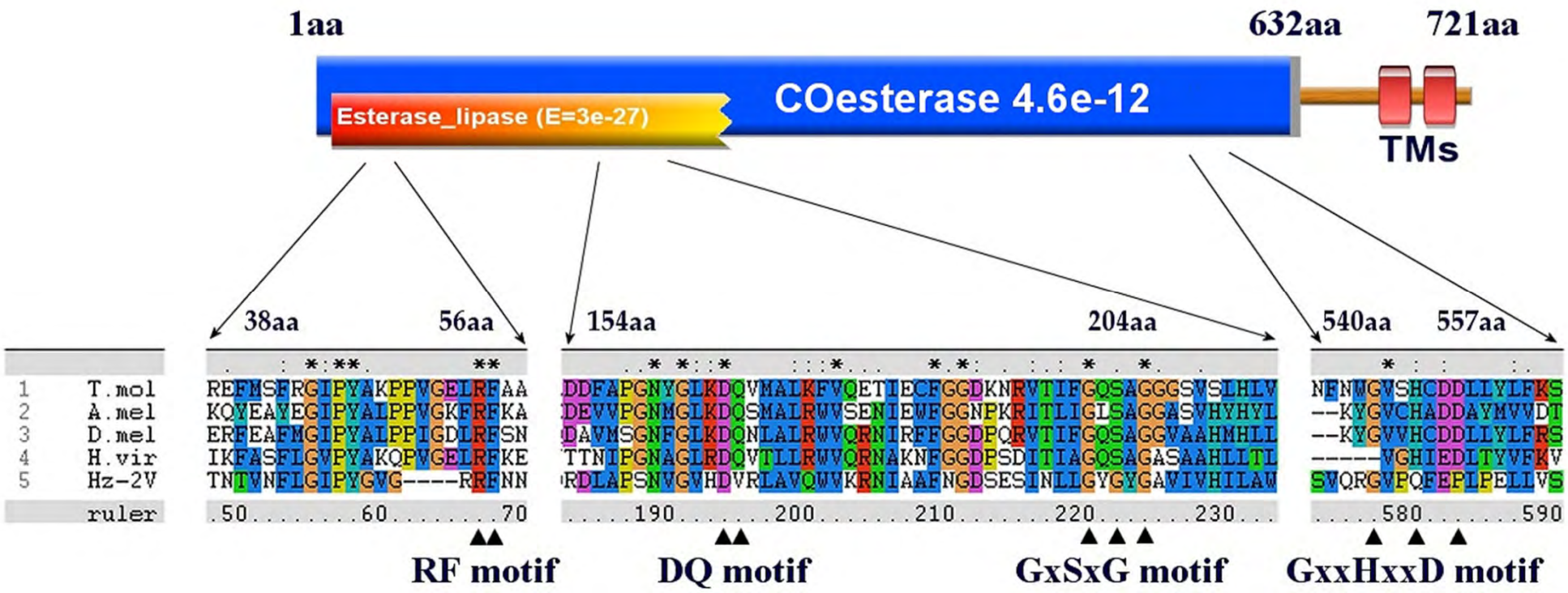

Hz2V023 had total of 12 characteristic transmembrane domains and showed homology to the major facilitator superfamily (MFS) conserved domain ($E = 5 \times 10^{-10}$). MFS is a family of transporter genes found ubiquitously in living organisms, which code for single-polypeptide carrier proteins involved in the uptake or efflux of small molecules. The primary functions of the MFS is uptake of sugar, and drug efflux [66]. Hz2V023 showed the best match to *A. aegypti* adenylate cyclase ($E = 1 \times 10^{-135}$).

Hz2V034 had homology to the guanosine monophosphate kinase (GMPK) motif at position 57–96 aa. The similarity was relatively low ($E = 1 \times 10^{-3}$), but the conserved catalytic motif of GMPK, G-X2-G-X-G-K was found at position 61–67 aa as G-M-S-C-S-G-K with one aa mismatch at position 64 aa. GMPK catalyzes the reversible transfer of the terminal phosphoryl group of ATP and GMP to yield ADP and GDP [67]. This is an important step in the biosynthesis of GTP. GMPK also plays an important role in the recycling of the secondary messenger cGMP [68]. Hz2V034 showed best similarity to the hypothetical protein of MBV ($E = 4 \times 10^{-5}$).

Hz2V039 had homology to the baculovirus 19K protein gene (AcMNPV ORF96) which codes for a protein of unknown function. The 19K gene homologues are commonly found in baculoviruses, and Hz2V039 showed best similarity to GbNV ORF87 ($E = 9 \times 10^{-9}$). Hz2V059 and Hz2V073 encoded HzNV-1 *p34* and *p51* late gene homologues, respectively. Originally, *p34* and *p51* genes, which were detected from 8 to 24 hr post infection, were found in a cDNA library of HzNV-1 infected Tn-368 culture cells [28,69].

Hz2V068 encoded a zinc-dependent matrix metalloprotease (ZnMc_MMP) conserved domain ($E = 2 \times 10^{-38}$) and hemopexin-like repeat (HX) domains ($E = 6 \times 10^{-26}$) at the C-terminal flanking region. MMPs are zinc and calcium dependent enzymes, which are synthesized as proenzymes in connective tissues [70]. MMPs play an important role in cellular differentiation and morphogenesis being responsible for pericellular proteolysis of the extracellular matrix and other cell surface molecules. The activities of MMPs are regulated by a tissue inhibitor of metalloprotease (TIMP). [71]. The HX domain is often found in MMPs and their TIMPs. The signature of the MMP active site, HEXXHXUGUXH (U = bulky hydrophobic aa), was found at position 412–122 aa of Hz2V068, and putative TIMP-binding sites were found at the position 346–434 aa region. A possible cleavable signal peptide for secretion was also found at position 1–18 aa. Hz2V068 showed best similarity to *Acyrthosiphon pisum* (aphid) MMP ($E = 3 \times 10^{-69}$). Baculoviruses also have a metalloprotease, known as enhancin. Enhancin is incorporated in the occlusion body derived virus (ODV) and is thought to aid in the infection pathway via the degradation of intestinal mucin, a major protein component of the insect peritrophic membrane [72]. Hz2V068, however, shares a greater homology with cellular MMPs than with the baculoviral enhancins, which lack the hemopexin domain and a signal peptide.

Hz2V096 showed homology to AcMNPV ORF81 (*ac81*). The *ac81* homologue is found in all baculoviruses, and is hence considered a baculovirus core gene [73]. A recent study of BmNPV ORF67, another homologue of Ac81, revealed that although its exact function is not known, it is a non-structural, late protein, detected in the cytoplasm of infected cells interacting with the cellular protein actin A3 [74]. Hz2V096 showed the best match to GbNV ORF14 ($E = 6 \times 10^{-14}$) and relatively low similarity to other baculovirus *ac81* homologues; however, the C-terminal transmembrane domain and the positions of cysteine residues common to Ac81s were conserved. Hence Ac81 homologues and Hz2V096 probably share similar secondary structure and perform similar functions during virus replication.

Hz2V099 showed homology to a prokaryotic acetylesterase (Aes) homologue. Aes is a member of esterase/lipase superfamily, and the Aes conserved domain was detected in Hz2V099 with relatively low similarity ($E = 9 \times 10^{-4}$). The Aes gene was first found in *Escherichia coli* and showed homology to lipase and esterase. Functional studies of the Aes protein demonstrated it had acetylesterase activity [75] and functioned in the control of a transcriptional activator [76].

Hz2V110 showed homology to the serine/threonine protein kinase (S_TKc) conserved domain ($E = 1 \times 10^{-28}$). Serine/threonine protein kinase catalyzes phosphorylation of serine and threonine residues, a major process in regulating cellular functions, especially protein phosphorylation in signal transduction [77].

2.9. Comparison of HzNV-2 and Baculovirus Genome Contents

A total of 13 complete baculovirus genome sequences have been compared, and 30 conserved core genes were found to be present in all baculoviruses [73]. These genes were organized into six categories based on their functions; replication, transcription, virus entry, structural proteins, auxiliary, and unknown. A total of 16 HzNV-2 genes found to share homology with the some of these baculovirus conserved core genes (Table 3). A total of 20 HzNV-1 genes have been reported to share homologies with baculovirus core genes (2). The HzNV-2 was found to contain homologues of all of these HzNV-1 genes however, no ORFs having homology with the 4 baculovirus core genes p47, ac68, vp39 and p33 were found in the HzNV-2 genome.

Among the DNA replication related baculovirus core genes, the most essential ones, DNA polymerase and helicase, were found in HzNV-2. However, LEF 1, DNA primase [78], and LEF 2, the LEF 1 associated protein [79], were not found in HzNV-2. Also *hrs*, the characteristic palindromic structures in baculovirus genomic DNA that function as transcriptional enhancers [80] and/or as origins of replication, were not found in HzNV-2. The absence of *lef-1*, *lef-2*, and *hrs* demonstrate that HzNV-2 possibly has a different viral DNA replication initiation mechanism than that of baculoviruses.

Five of the six conserved baculovirus core genes involved in transcription were found in HzNV-2. These five genes were *lef-4*, *lef-8*, and *lef-9*, which are the subunits of the baculovirus RNA polymerase, and LEF-5 and VLF-1, which are the late gene transcriptional factors of the baculovirus. The only conserved baculovirus gene involved in transcription that was not found in HzNV-2 was *p47*, one of the RNA polymerase subunits with unknown function [30]. It is interesting that HzNV-2 has baculovirus RNA polymerase and transcription factor homologues because having an alpha-amanitin resistant RNA polymerase is the one of the most distinctive features of the baculovirus compared with other DNA viruses [81]. Therefore, the presence of conserved homologues in HzNV-2 related to the transcription mechanism of baculoviruses supports the hypothesis that HzNV-2 and baculoviruses possibly evolved from a common ancestor.

Another group of conserved baculovirus core genes are the genes related to virus entry. The *p74*, *pif-1*, *pif-2*, and *pif-3* genes which are the *per os* infectivity factors, belong to this group. In the HzNV-2 genome, all four of the *per os* infectivity related genes were found, while the fusion protein gene *p47* was not. This is a very interesting result since the primary route of transmission of HzNV-2 is not *per os* but rather by mating or through transovarial transmission. The similarity of *p74* and the

pif genes to the HzNV-2 homologues were very low, so it is possible that these genes evolved in HzNV-2 to target reproductive tissue cells instead of the midgut cells.

The baculovirus fusion protein, P47 is thought to play a role in systemic viral infections [82], The hymenopteran baculoviruses, *Neodiprion sertifer* NPV [83], and *Neodiprion lecontei* NPV [84], which also lack a fusion protein, replicate only in the midgut cells and do not exhibit systemic infection. This localized pathology compares with that of HzNV-2 in terms of non-systematic and tissue-specific infection. Hence, it is possible that the progeny virus of HzNV-2 in the target tissue could spread by cell surface specific binding of virus utilizing P74 and PIFs and not systemically via the fusion protein as do baculoviruses.

HzNV-2 shares three of the eight baculovirus conserved genes coding for structural proteins, *odv-e56*, *vp91*, and *38K*, a capsid protein gene. ODV-e56 and VP91 are the virus structural proteins, while 38K is related to nucleocapsid assembly. The other five baculovirus conserved genes, *odv-e27*, *gp41*, *p6.9*, *vp39*, and *vp1054*, were not found in HzNV-2. GP41, P6.9, and VP39 are structural proteins which compose the nucleocapsid. VP1054 is responsible for nucleocapsid assembly and directly interacts with VP39 and 38K [84]. Only the 38K homologue was found in HzNV-2. The ODV-E27 is a structural protein and is considered a viral cyclin. It arrests host cells at the G_2/M phase of the cell cycle with continuing viral DNA replication [85]. The absence of an *odv-e27* homologue in HzNV-2 might be expected since the pathogenesis of this virus in infected reproductive tissue is thought to occur with the development of reproductive tissue during the late larval and early adult stages of host insects.

Baculovirus alkaline exonuclease (alk-exo) while categorized as an auxiliary gene, has both 5'-3' exonuclease and endonuclease activity, as well as the ability to form complexes with the single strand binding protein and LEF 3. Alk-exo enzyme participates in dsDNA repair and is possibly responsible for the maturation of virus DNA in addition to maintenance of virus genome integrity [86,87]. An alk-exo homologue was not found in HzNV-2, perhaps due to HzNV-2's use of different DNA replication and repair mechanisms. Of the six baculovirus conserved genes, *ac68*, *ac81*, *ac92*, *ac96*, *ac109* and *ac142*, with unknown function, only *ac81* and *ac96* were found in HzNV-2.

Table 3. Comparison of conserved baculovirus core genes and HzNV-2.

Gene Function	Genes present in HzNV-2	Genes absent in HzNV-2
Replication	*dnapol* (*ac65*), *helicase* (*ac95*)	*lef-1* (*ac14*), *lef-2* (*ac6*)
Transcription	*lef-4* (*ac90*), *lef-5* (*ac99*), *lef-8* (*ac50*), *lef-9* (*ac62*), *vlf-1* (*ac77*)	*p47* (*ac40*)
Virus entry	*p74* (*ac138*), *pif-1* (*ac119*), *pif-2* (*ac22*), *pif-3* (*ac115*)	*ld130* (*ac23*)
Structural	*p91* (*ac83*), *38K* (*ac98*), *odv-e56* (*ac148*)	*odv-e27* (*ac144*), *gp41* (*ac80*), *p6.9* (*ac100*), *vp39* (*ac89*), *vp1054* (*ac54*)
Auxiliary		*alk-exo* (*ac133*)
Unknown	*ac81*, *19K* (*ac96*)	*ac68*, *ac92*, *ac109*, *ac142*

Another characteristic of baculovirus conserved genes is a core gene cluster, which is a set of four genes (*helicase*, *ac96*, *38K*, and *lef-5*) found in the same relative position and direction in all known baculovirus genomes. This conserved gene cluster is very distinctive since extensive genome rearrangements are believed to have occurred in the evolution of baculoviruses [73]. HzNV-2 has a baculovirus core gene cluster-like region; however, it was observed to be different from that found in baculoviruses. The location and orientation of *helicase* and *ac96* were the same as in the baculovirus gene cluster, however *lef-5* was on the opposite strand, and orientation compare to its position in the baculovirus core cluster. The most distinctive difference was the location of *38k* gene. In baculoviruses, *38k* is located between the *ac96* and *lef-5* gene on the opposite DNA strand. The HzNV-2 *38k* homologue, however, is located 91 kb downstream of the *helicase* gene (Figure 5). This result may again reflect the divergence of HzNV-2 and baculoviruses during evolution from a common ancestor.

Figure 5. Comparison of the conserved core cluster of a baculovirus and corresponding region in HzNV-2. (**A**) Gene arrangement in the conserved core cluster of baculovirus; (**B**) Gene arrangement around HzNV-2 gene. The relative positions and orientations of *helicase* and *ac96* are the same in both baculovirus and HzNV-2, however, HzNV-2 has *lef-5* on the opposite DNA strand and *38 K* at 136 kb downstream (also 91 kb upstream) of the *helicase* gene.

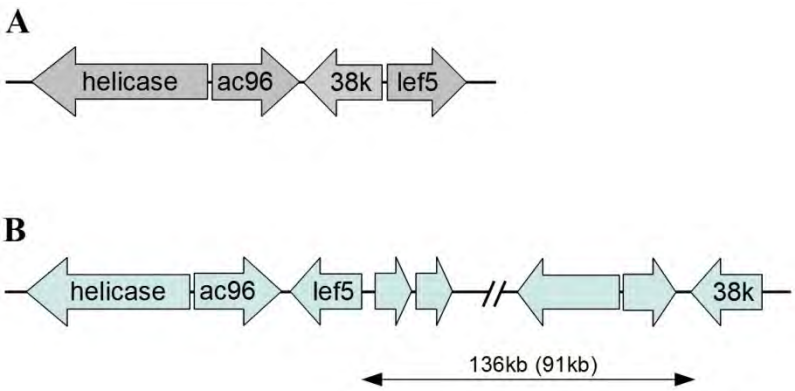

2.11. Phylogenetic Analysis

DNA polymerase is one of key phylogenetic characteristics of virus taxonomy, therefore, a phylogenetic analysis was performed using this gene to assess the relationship of HzNV-2 to other insect DNA viruses. For this analysis, eleven DNA polymerase sequences were chosen from NPVs, GVs, entomopoxviruses, and NVs. A multiple sequence alignment was performed by MUSCLE, and a phylogenetic tree was built by neighbor-joining using MEGA4. The result demonstrated that Hz2V018 (the HzNV-2 DNA polymerase) grouped with GbNV, OrNV, and HzNV-1 DNA polymerase, while the baculovirus and entomopoxvirus DNA polymerases have monophyletic lineages (Figure 6A). This result showed that as expected, HzNV-2 DNA polymerase is more closely related to other NV DNA polymerases than to those of other insect viruses.

A similar approach was applied to the virus entry related protein genes. Although the similarities between these viruses are relatively low, *p74* and the *pif* genes are well-conserved genes in

baculoviruses and NV. A possible explanation might be a diverging evolution of the *p74* and *pif* genes from an ancestral virus during host range expansion. The attachment and entry of viruses into cells is a key process in replication and is obligatory for horizontal transmission between susceptible hosts. The conservation of genes involved in this process across these different dsDNA viruses of insects (2), suggests that they share features of this process which have been maintained during their evolution. A total of 14 sets of *p74*, *pif-1*, *pif-2*, and *pif-3* genes chosen from baculoviruses and NV were combined for phylogenetic analysis. As with the DNA polymerase tree result, HzNV-2 grouped with other NV while the baculoviruses had a monophyletic lineage. This result demonstrated that the *p74* and *pif* genes of HzNV-2 are more closely related to those of NV and more distantly related to those of baculoviruses (Figure 6B). This result suggest that while there are some common elements in the process used by these viruses to enter host cells, and that NVs may share an aspect of this pathway which is different from that used by baculoviruses. Similar phylogenic analysis was performed in the genome analysis of the MdSGHV with results similar to those presented here (Figures 6A,B) [46].

Figure 6. Phylogenetic analysis of selected insect DNA viruses and HzNV-2. (**A**) DNA polymerase; (**B**) combined sequence analysis *of p74*, *pif-1*, *pif-2* and *pif-3*; Multiple sequence alignments were performed by MUSCLE, and then the tree was inferred using neighbor-joining in MEGA4. The robustness of the tree was tested using bootstrap analysis (1000 replicates). The percent values are presented at the nodes. Organisms included in this analysis, with abbreviated names: *Autographa californica* NPV (AcNPV), *adoxophyes honmai* NPV (AdhoNPV), *Amsacta moorei* entomopoxvirus (AmEntPox), *Bombyx mori* NPV (BmNPV), *Culex nigripalpus* NPV (CuniNPV), *Cydia pomonella* granulovirus (CpGV), *Euproctis pseudoconspersa* NPV (EpNPV), *Gryllus bimaculatus* nudivirus (GbNV), *Lymantria dispar* MNPV (LdMNPV), *Melanoplus sanguinipes* entomopoxvirus (MsEPV), *Neodiprion lecontei* NPV (NeleNPV), *Neodiprion sertifer* NPV (NeseNPV), *Orgyia pseudotsugata* NPV (OpNPV), *Oryctes rhinoceros nudivirus* (OrNV), *Plutella xylostella* GV (PxGV).

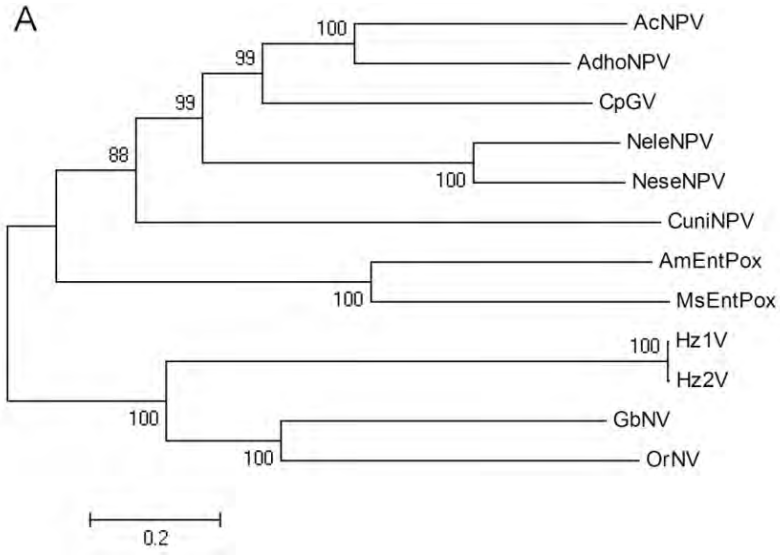

Figure 6. *Cont.*

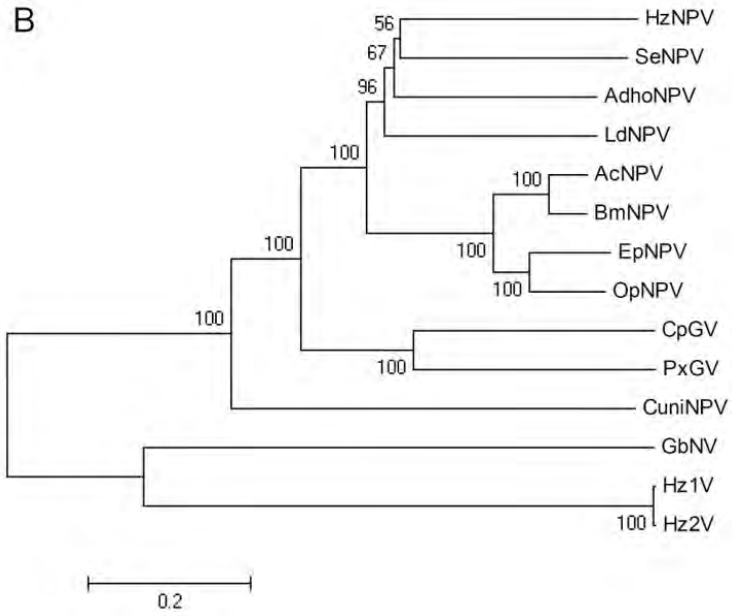

3. Experimental Section

3.1. Source of Viruses

HzNV-2 viral particles were injected into newly emerged female moths from a laboratory colony of healthy *H. zea*, as outlined by Rallis and Burand [6]. After mating with healthy male moths, eggs laid by the injected female moths were collected from the mating chambers, then transferred into hatching chambers. Newly hatched larvae were reared on an artificial diet in environmental chambers under a light:dark cycle of 16:8 hours at 26 °C and upon emergence, progeny individuals were examined for signs of HzNV-2 infection, as described by Raina and Adams [88] and Hamm *et al*. [5]. Infected female moths with a visible, viral plug were collected as the source of viruses. The virus in the plugs were suspended in phosphate buffered saline (PBS) (136 mM NaCl, 1.4 mM KH2PO4, 8 mM Na2HPO4, 2.6 mM KCl, pH7.3), and used for virus particle preparation.

3.2. Virus Purification and DNA Extraction

The crude virus preparation in PBS, collected from the plugs, was layered on a sucrose gradient (25–55%), and centrifuged at 22,000 rpm at 4 °C for 1 h using a Beckman SW28 rotor. The purified virus band in the sucrose gradient was collected, diluted in TE buffer (10 mM Tris-HCl, 1mM EDTA, pH 8.0) or PBS, and centrifuged to pellet the purified virus particles. The purified virus particles were then suspended in TE or PBS and stored at −20 °C for DNA extraction.

The purified virus particles were incubated at 37 °C for 1 h with protease K at 1 mg/mL and sodium dodecyl sulfate (SDS) at 1% to solublize the virus envelope and structural proteins. The viral DNA was extracted twice with phenol, chloroform, and isoamylalcohol (25:24:1), followed by DNA precipitation with 0.3 M sodium acetate and 100% ethanol at −80°C for 1 hour. The extracted viral DNA was centrifuged at 12,000 rpm for 15 min at 4 °C, washed three times with 70% ethanol, air-dried, resuspended in TE and stored at −20°C.

3.3. DNA Sequencing

Random DNA fragments of 1.5 to 6.5 kbp were obtained by partial enzymatic digestion with *Tsp*509I (New England Biolabs). The DNA fragments were cloned into the *Eco*RI site of pUC19 plasmid, and grown in *Escherichia coli* DH10B cells. Plasmids containing virus DNA fragments were purified by an alkaline lysis method. The fragments were sequenced from both ends of the cloning site with M13 forward and reverse primers using the dideoxy chain termination method [89] on a PRISM 3700 automated DNA sequencer (PE Biosystems). Chromatogram traces were base-called with PHRED and assembled with PHRAP [90,91]. Confirmatory assemblies were performed with the TIGR [92] and CAP3 [93] sequence assembly computer programs. The HzNV-2 virus DNA was sequenced to an average of 13-fold coverage at each base position.

3.4. Sequence Analysis

Open reading frames (ORFs) longer than 60 amino acids (aa) with a methionine start codon were evaluated for coding potential using the Hexamer [94] and Glimmer [95,96] computer programs. Protein homology searches were performed using the BLAST, PSI-BLAST [97], FASTA [98], and HMMER [99] computer programs with the databases: PROSITE, Pfam, Prodom, and GenBank [100]. Global sequence alignment was performed using rVISTA [101]. Conserved domain searches were performed using the SMART [102] and CD-Search [103] computer programs with Swiss-Prot and CDD [104] databases. CGC [105], EMBOSS [106], Psort [107], TMHMM [108,109], SignalP 3.0 [110], and ANTHEPROT [111] computer programs were used for general analysis, signal peptide prediction, transmembrane domain prediction, and physical characterization of proteins. Phylogenetic analysis was performed by using ClustalX [112], MUSCLE [113], and MEGA4 [114].

4. Summary and Conclusions

We report here the complete nucleotide sequence and the annotation of the genome of the NV HzNV-2. This analysis showed HzNV-2 and HzNV-1 to have 93% sequence identity. Based on the high degree of sequence identity between these two NVs, it now appears that the IMC-Hz-1 ovarian cell line, from which HzNV-1 was originally isolated [115,116], was established from the ovaries of *H. zea* moths persistently infected with a NV which resembled HzNV-2. If this were the case, it is highly unlikely that females with grossly malformed reproductive tissues, characteristic of HzNV-2 infected insects, would have been selected for use in establishing an ovarian cell line. This possibility along with the absence of any observed pathology in HzNV-1 infected insects, suggest that genes responsible for the pathology caused by HzNV-2 may be missing in the HzNV-1 genome [11]. In this study, a total of 16 ORFs were identified in the HzNV-2 genome, that were not previously found in HzNV-1. Unfortunately, none of these 16 ORFs were determined to share sequence homology with any genes of know function, and therefore could not be directly associated with the pathology observed in HzNV-2 infected insects. Nonetheless, the genetic similarity between HzNV-1 and HzNV-2 indicates that these two viruses are very closely related, having a very recent, common ancestor.

In a recent study, 20 HzNV-1 genes were found to share homologies with baculovirus core genes (2). Homologues of all of these HzNV-1 genes were found in the HzNV-2 genome however, there

were no ORFs in HzNV-2 found to have homology with the 4 baculovirus core genes *p47*, *ac68*, *vp39* and *p33*. Interestingly, Hz1V075, which was found to be homologues to the OrNV *p47* was also reported to be homologous to OrNV *lef-9* (2). In our analysis, Hz2V063 was found to be homologous to Hz1V075 and MBV *lef-9*, but not to any *p47* ORFs. If Hz2V063 and Hz1V075 both have activity found associated with the two separate ORFs encoded by baculoviruses and other NVs, then this would suggest an important point of divergence of HzNVs from other N*Vs*.

An interesting feature of the HzNV-2 genome is the presence of a large number of cellular gene homologues. The HzNV-2 genome contains 12 genes which have homology to cellular genes. The majority of the cellular gene homologues in HzNV-2 are related to nucleic acid metabolism and DNA replication; 9 of the 12 cellular genes found in HzNV-2 are TS, dUTPase, DHFR, RR1, RR2, dNK, SHMT and ligase. The three other HzNV-2 genes found to more closely resemble host genes than viral genes (Hz2V023, Hz2068 and Hz2V007) are thought to code for proteins which could be involved in the regulation of molecular processes in the infected host leading to cell proliferation and tissue malformation observed in the reproductive structures of infected insects.

It was interesting to find that HzNV-2 coded for a major facilitator superfamily (MFS) protein gene (Hz2V023). MFS genes are found ubiquitously in living cells [66] and have never before been identified in a viral genome. These transmembrane proteins are involved in the movement of small molecules, in and out of cells and could act to facilitate the enhanced metabolism required for the cell proliferation observed in HzNV-2 infected reproductive tissues.

Hz2V068 which encodes both an MMP domain and an HX domain could also play an important role in altering the pattern of cell differentiation and morphogenesis. It is possible that this viral gene product could function in the proteolysis of the extracellular matrix and cell surface molecules, altering cell differentiation during HzNV-2 replication, resulting in the malformation of reproductive tissues during their development in infected insects.

It was very surprising to find that HzNV-2 contains, Carboxylesterase (Hz2V007) which shares significant homology with *A. gambiae* JHE, suggesting that Hz2V007 codes for a protein that may have JHE activity. In holometabolous insects such as *H. zea* and *Drosophila*, the developmental process of molting is controlled by two hormones, the steroid, 20-hydroxyecdysone (ecdysone) and the sesquiterpenoid, juvenile hormone (JH). These two hormones work in concert to regulate gene expression during molting, directing insect growth and tissue development [117]. The predicted JHE activity of Hz2V007, coupled with increased cellular metabolic functions resulting from Hz2V023, MFS activity and tissue remodeling by Hz2V068, coded MMP could all contribute to malformation of virus infected tissues and the unique pathology observed in HzNV-2 infected moths. It has not yet been determined how each of these novel virus genes function, but we believe that it is the expression of these genes, along with several of the other cellular gene homologues identified in the HzNV-2 genome, which are responsible for the pathology and unique biology of this insect pathogenic virus.

Acknowledgments

This material is based upon work supported by USDA NRICGP Grant #2001-35302-10885, the Cooperative State Research Extension, Education Service, U.S. Department of Agriculture, the

Massachusetts Agricultural Experiment Station and the Department of Plant Soil and Insect Science, under Projects No. MAS00909 and MAS00972.

Conflict of Interest

The authors declare no conflict of interest.

References and Notes

1. Wang, Y.-J.; Burand, J.P.; Jehle, J.A. Nudivirus genomics: Diversity and classification. *Virol. Sin.* **2007**, *22*, 128–136.
2. Wang, Y.; Bininda-Emonds, O.R.P.; van Oers, M.M.; Vlak, J.M.; Jehle, J.A. The genome of oryctes rhinoceros nudivirus provides novel insight into the evolution of nuclear arthropod-specific large circular double-stranded DNA viruses. *Virus Genes* **2011**, *42*, 444–456.
3. Wang, Y.; Jehle, J.A. Nudiviruses and other large, double-stranded circular DNA viruses of invertebrates: New insights on an old topic RID C-2243-2009. *J. Invertebr. Pathol.* **2009**, *101*, 187–193.
4. Bezier, A.; Annaheim, M.; Herbiniere, J.; Wetterwald, C.; Gyapay, G.; Bernard-Samain, S.; Wincker, P.; Roditi, I.; Heller, M.; Belghazi, M.; *et al.* Polydnaviruses of braconid wasps derive from an ancestral nudivirus. *Science* **2009**, *323*, 926–930.
5. Hamm, J.J.; Carpenter, J.E.; Styer, E.L. Oviposition day effect on incidence of agonadal progeny of Helicoverpa zea (Lepidoptera: Noctuidae) infected with a virus. *Ann. Entomol. Soc. Am.* **1996**, *89*, 266–275.
6. Rallis, C.P.; Burand, J.P. Pathology and ultrastructure of Hz-2V infection in the agonadal female corn earworm, Helicoverpa zea. *J. Invertebr. Pathol.* **2002**, *81*, 33–44.
7. Burand, J.P.; Rallis, C.P. *In vivo* dose-response of insects to Hz-2V infection. *Virol. J.* **2004**, *1*, 15.
8. Burand, J.P.; Tan, W.; Kim, W.; Nojima, S.; Roelofs, W. Infection with the insect virus Hz-2v alters mating behavior and pheromone production in female Helicoverpa zea moths. *J. Insect Sci.* **2005**, *5*, 6.
9. Lu, H. Characterization of a novel baculovirus, gonad-specific virus, GSV. Ph.D. dissertation, University of Massachusetts, Amherst, MA, USA, 1997.
10. Cochran, M.A.; Faulkner, P. Location of homologous DNA sequences interspersed at five regions in the baculovirus AcMNPV genome. *J. Virol.* **1983**, *45*, 961–970.
11. Cheng, C.H.; Liu, S.M.; Chow, T.Y.; Hsiao, Y.Y.; Wang, D.P.; Huang, J.J.; Chen, H.H. Analysis of the complete genome sequence of the Hz-1 virus suggests that it is related to members of the Baculoviridae. *J. Virol.* **2002**, *76*, 9024–9034.
12. Wang, Y.; Kleespies, R.G.; Huger, A.M.; Jehle, J.A. The genome of Gryllus bimaculatus nudivirus indicates an ancient diversification of baculovirus-related nonoccluded nudiviruses of insects. *J. Virol.* **2007**, *81*, 5395–5406.
13. Pearson, M.N.; Rohrmann, G.F. Lymantria dispar nuclear polyhedrosis virus homologous regions: characterization of their ability to function as replication origins. *J. Virol.* **1995**, *69*, 213–221.

14. Shamoo, Y.; Steitz, T.A. Building a replisome from interacting pieces: Sliding clamp complexed to a peptide from DNA polymerase and a polymerase editing complex. *Cell* **1999**, *99*, 155–166.
15. Bressan, D.A.; Baxter, B.K.; Petrini, J.H. The Mre11-Rad50-Xrs2 protein complex facilitates homologous recombination-based double-strand break repair in Saccharomyces cerevisiae. *Mol. Cell Biol.* **1999**, *19*, 7681–7687.
16. Hopfner, K.P.; Karcher, A.; Shin, D.S.; Craig, L.; Arthur, L.M.; Carney, J.P.; Tainer, J.A. Structural biology of Rad50 ATPase: ATP-driven conformational control in DNA double-strand break repair and the ABC-ATPase superfamily. *Cell* **2000**, *101*, 789–800.
17. Mascarenhas, J.; Sanchez, H.; Tadesse, S.; Kidane, D.; Krisnamurthy, M.; Alonso, J.C.; Graumann, P.L. Bacillus subtilis SbcC protein plays an important role in DNA inter-strand cross-link repair. *BMC Mol. Biol.* **2006**, *7*, 20.
18. Evans, E.; Klemperer, N.; Ghosh, R.; Traktman, P. The vaccinia virus D5 protein, which is required for DNA replication, is a nucleic acid-independent nucleoside triphosphatase. *J. Virol.* **1995**, *69*, 5353–5361.
19. O'Donovan, A.; Davies, A.A.; Moggs, J.G.; West, S.C.; Wood, R.D. XPG endonuclease makes the 3' incision in human DNA nucleotide excision repair. *Nature* **1994**, *371*, 432–435.
20. Cooper, P.K.; Nouspikel, T.; Clarkson, S.G.; Leadon, S.A. Defective transcription-coupled repair of oxidative base damage in Cockayne syndrome patients from XP group G. *Science* **1997**, *275*, 990–993.
21. Hosfield, D.J.; Mol, C.D.; Shen, B.; Tainer, J.A. Structure of the DNA repair and replication endonuclease and exonuclease FEN-1: Coupling DNA and PCNA binding to FEN-1 activity. *Cell* **1998**, *95*, 135–146.
22. Kim, K.; Biade, S.; Matsumoto, Y. Involvement of flap endonuclease 1 in base excision DNA repair. *J. Biol. Chem.* **1998**, *273*, 8842–8848.
23. Jehle, J.A.; Blissard, G.W.; Bonning, B.C.; Cory, J.S.; Herniou, E.A.; Rohrmann, G.F.; Theilmann, D.A.; Thiem, S.M.; Vlak, J.M. On the classification and nomenclature of baculoviruses: A proposal for revision. *Arch. Virol.* **2006**, *151*, 1257–1266.
24. Guarino, L.A.; Xu, B.; Jin, J.; Dong, W. A virus-encoded RNA polymerase purified from baculovirus-infected cells. *J. Virol.* **1998**, *72*, 7985–7991.
25. Mclachlin, J.R.; Miller, L.K. Identification and characterization of Vlf-1, a baculovirus gene involved in very late gene-expression. *J. Virol.* **1994**, *68*, 7746–7756.
26. Yang, S.; Miller, L.K. Activation of baculovirus very late promoters by interaction with very late factor 1. *J. Virol.* **1999**, *73*, 3404–3409.
27. Vanarsdall, A.L.; Okano, K.; Rohrmann, G.F. Characterization of the role of very late expression factor 1 in baculovirus capsid structure and DNA processing. *J. Virol.* **2006**, *80*, 1724–1733.
28. Guttieri, M.C.; Burand, J.P. Nucleotide sequence, temporal expression, and transcriptional mapping of the p34 late gene of the Hz-1 insect virus. *Virology* **1996**, *223*, 370–375.
29. Guarino, L.A.; Dong, W.; Jin, J. *In vitro* activity of the baculovirus late expression factor LEF-5. *J. Virol.* **2002**, *76*, 12663–12675.
30. Jin, J.; Dong, W.; Guarino, L.A. The LEF-4 subunit of baculovirus RNA polymerase has RNA 5'-triphosphatase and ATPase activities. *J. Virol.* **1998**, *72*, 10011–10019.

31. Knebel-Morsdorf, D.; Quadt, I.; Li, Y.; Montier, L.; Guarino, L.A. Expression of baculovirus late and very late genes depends on LEF-4, a component of the viral RNA polymerase whose guanyltransferase function is essential. *J. Virol.* **2006**, *80*, 4168–4173.
32. Shuman, S.; Liu, Y.; Schwer, B. Covalent catalysis in nucleotidyl transfer reactions: essential motifs in Saccharomyces cerevisiae RNA capping enzyme are conserved in Schizosaccharomyces pombe and viral capping enzymes and among polynucleotide ligases. *Proc. Natl. Acad. Sci. U. S. A.* **1994**, *91*, 12046–12050.
33. Passarelli, A.L.; Todd, J.W.; Miller, L.K. A baculovirus gene involved in late gene expression predicts a large polypeptide with a conserved motif of RNA polymerases. *J. Virol.* **1994**, *68*, 4673–4678.
34. Lu, A.; Miller, L.K. Identification of three late expression factor genes within the 33.8- to 43.4-map-unit region of Autographa californica nuclear polyhedrosis virus. *J. Virol.* **1994**, *68*, 6710–6718.
35. Broyles, S.S.; Moss, B. Homology between RNA polymerases of poxviruses, prokaryotes, and eukaryotes: Nucleotide sequence and transcriptional analysis of vaccinia virus genes encoding 147-kDa and 22-kDa subunits. *Proc. Natl. Acad. Sci. U. S. A.* **1986**, *83*, 3141–3145.
36. Acharya, A.; Gopinathan, K.P. Characterization of late gene expression factors lef-9 and lef-8 from Bombyx mori nucleopolyhedrovirus. *J. Gen. Virol.* **2002**, *83*, 2015–2023.
37. Pijlman, G.P.; Pruijssers, A.J.; Vlak, J.M. Identification of pif-2, a third conserved baculovirus gene required for per os infection of insects. *J. Gen. Virol.* **2003**, *84*, 2041–2049.
38. Li, X.; Song, J.; Jiang, T.; Liang, C.; Chen, X. The N-terminal hydrophobic sequence of Autographa californica nucleopolyhedrovirus PIF-3 is essential for oral infection. *Arch. Virol.* **2007**, *152*, 1851–1858.
39. Ohkawa, T.; Washburn, J.O.; Sitapara, R.; Sid, E.; Volkman, L.E. Specific binding of Autographa californica M nucleopolyhedrovirus occlusion-derived virus to midgut cells of Heliothis virescens larvae is mediated by products of pif genes Ac119 and Ac022 but not by Ac115. *J. Virol.* **2005**, *79*, 15258–15264.
40. Kikhno, I.; Gutierrez, S.; Croizier, L.; Croizier, G.; Ferber, M.L. Characterization of pif, a gene required for the per os infectivity of Spodoptera littoralis nucleopolyhedrovirus. *J. Gen. Virol.* **2002**, *83*, 3013–3022.
41. Haas-Stapleton, E.J.; Washburn, J.O.; Volkman, L.E. P74 mediates specific binding of Autographa californica M nucleopolyhedrovirus occlusion-derived virus to primary cellular targets in the midgut epithelia of Heliothis virescens larvae. *J. Virol.* **2004**, *78*, 6786–6791.
42. Rashidan, K.K.; Nassoury, N.; Tazi, S.; Giannopoulos, P.N.; Guertin, C. Choristoneura fumiferana Granulovirus p74 protein, a highly conserved baculoviral envelope protein. *J. Biochem. Mol. Biol.* **2003**, *36*, 475–487.
43. Carreras, C.W.; Santi, D.V. The catalytic mechanism and structure of thymidylate synthase. *Annu. Rev. Biochem.* **1995**, *64*, 721–762.
44. Perryman, S.M.; Rossana, C.; Deng, T.L.; Vanin, E.F.; Johnson, L.F. Sequence of a cDNA for mouse thymidylate synthase reveals striking similarity with the prokaryotic enzyme. *Mol. Biol. Evol.* **1986**, *3*, 313–321.

45. Chen, H.H.; Tso, D.J.; Yeh, W.B.; Cheng, H.J.; Wu, T.F. The thymidylate synthase gene of Hz-1 virus: A gene captured from its lepidopteran host. *Insect Mol. Biol.* **2001**, *10*, 495–503.
46. Garcia-Maruniak, A.; Maruniak, J.E.; Farmerie, W.; Boucias, D.G. Sequence analysis of a non-classified, non-occluded DNA virus that causes salivary gland hypertrophy of Musca domestica, MdSGHV. *Virology* **2008**, *377*, 184–196.
47. Jordan, A.; Reichard, P. Ribonucleotide reductases. *Annu. Rev. Biochem.* **1998**, *67*, 71–98.
48. Blakley, R.L. The interconversion of serine and glycine: Participation of pyridoxal phosphate. *Biochem. J.* **1955**, *61*, 315–323.
49. Blakley, R.L. *The Biochemistry of Folic Acid and Related Pteridines*; North-Holland Pub. Co.: Amsterdam, The Netherlands, 1969; pp. xxi, 570.
50. Ives, D.H.; Ikeda, S. Life on the salvage path: The deoxynucleoside kinase of Lactobacillus acidophilus R-26. *Progr. Nucleic Acid Res. Mol. Biol.* **1998**, *59*, 205–255.
51. Elder, J.H.; Lerner, D.L.; Hasselkus-Light, C.S.; Fontenot, D.J.; Hunter, E.; Luciw, P.A.; Montelaro, R.C.; Phillips, T.R. Distinct subsets of retroviruses encode dUTPase. *J. Virol.* **1992**, *66*, 1791–1794.
52. Chen, R.; Wang, H.; Mansky, L.M. Roles of uracil-DNA glycosylase and dUTPase in virus replication. *J. Gen. Virol.* **2002**, *83*, 2339–2345.
53. Miller, R.J.; Cairns, J.S.; Bridges, S.; Sarver, N. Human immunodeficiency virus and AIDS: Insights from animal lentiviruses. *J. Virol.* **2000**, *74*, 7187–7195.
54. Wu, X.; Guarino, L.A. Autographa californica nucleopolyhedrovirus orf69 encodes an RNA cap (nucleoside-2'-O)-methyltransferase. *J. Virol.* **2003**, *77*, 3430–3440.
55. Schnell, J.R.; Dyson, H.J.; Wright, P.E. Structure, dynamics, and catalytic function of dihydrofolate reductase. *Annu. Rev. Biophys. Biomol. Struct.* **2004**, *33*, 119–140.
56. Braunagel, S.C.; Elton, D.M.; Ma, H.; Summers, M.D. Identification and analysis of an Autographa californica nuclear polyhedrosis virus structural protein of the occlusion-derived virus envelope: ODV-E56. *Virology* **1996**, *217*, 97–110.
57. Russell, R.L.; Rohrmann, G.F. Characterization of P91, a protein associated with virions of an Orgyia pseudotsugata baculovirus. *Virology* **1997**, *233*, 210–223.
58. Wu, W.; Liang, H.; Kan, J.; Liu, C.; Yuan, M.; Liang, C.; Yang, K.; Pang, Y. Autographa californica multiple nucleopolyhedrovirus 38K is a novel nucleocapsid protein that interacts with VP1054, VP39, VP80, and itself. *J. Virol.* **2008**, *82*, 12356–12364.
59. Gilbert, L.I.; Granger, N.A.; Roe, R.M. The juvenile hormones: Historical facts and speculations on future research directions. *Insect Biochem. Mol. Biol.* **2000**, *30*, 617–644.
60. Ward, V.K.; Bonning, B.C.; Huang, T.; Shiotsuki, T.; Griffeth, V.N.; Hammock, B.D. Analysis of the catalytic mechanism of juvenile-hormone esterase by site-directed mutagenesis. *Int. J. Biochem.* **1992**, *24*, 1933–1941.
61. Crook, N.E.; Clem, R.J.; Miller, L.K. An apoptosis-inhibiting baculovirus gene with a zinc finger-like motif. *J. Virol.* **1993**, *67*, 2168–2174.
62. Uren, A.G.; Coulson, E.J.; Vaux, D.L. Conservation of baculovirus inhibitor of apoptosis repeat proteins (BIRPs) in viruses, nematodes, vertebrates and yeasts. *Trends Biochem. Sci.* **1998**, *23*, 159–162.

63. Miller, L.K. An exegesis of IAPs: Salvation and surprises from BIR motifs. *Trends Cell Biol.* **1999**, *9*, 323–328.
64. Joazeiro, C.A.; Weissman, A.M. RING finger proteins: Mediators of ubiquitin ligase activity. *Cell* **2000**, *102*, 549–552.
65. Wilson, R.; Goyal, L.; Ditzel, M.; Zachariou, A.; Baker, D.A.; Agapite, J.; Steller, H.; Meier, P. The DIAP1 RING finger mediates ubiquitination of Dronc and is indispensable for regulating apoptosis. *Nat. Cell Biol.* **2002**, *4*, 445–450.
66. Pao, S.S.; Paulsen, I.T.; Saier, M.H., Jr. Major facilitator superfamily. *Microbiol. Mol. Biol. Rev.* **1998**, *62*, 1–34.
67. Konrad, M. Cloning and expression of the essential gene for guanylate kinase from yeast. *J. Biol. Chem.* **1992**, *267*, 25652–25655.
68. Hall, S.W.; Kuhn, H. Purification and properties of guanylate kinase from bovine retinas and rod outer segments. *Eur. J. Biochem.* **1986**, *161*, 551–556.
69. Guttieri, M.C.; Burand, J.P. Location, nucleotide sequence, and regulation of the p51 late gene of the Hz-1 insect virus: Identification of a putative late regulatory element. *Virus Genes* **2001**, *23*, 17–25.
70. Murphy, G.J.; Murphy, G.; Reynolds, J.J. The origin of matrix metalloproteinases and their familial relationships. *FEBS Lett.* **1991**, *289*, 4–7.
71. Nagase, H.; Woessner, J.F., Jr. Matrix metalloproteinases. *J. Biol. Chem.* **1999**, *274*, 21491–21494.
72. Wang, P.; Granados, R.R. An intestinal mucin is the target substrate for a baculovirus enhancin. *Proc. Natl. Acad. Sci. U. S. A.* **1997**, *94*, 6977–6982.
73. Herniou, E.A.; Olszewski, J.A.; Cory, J.S.; O'Reilly, D.R. The genome sequence and evolution of baculoviruses. *Annu. Rev. Entomol.* **2003**, *48*, 211–234.
74. Chen, H.Q.; Chen, K.P.; Yao, Q.; Guo, Z.J.; Wang, L.L. Characterization of a late gene, ORF67 from Bombyx mori nucleopolyhedrovirus. *FEBS Lett.* **2007**, *581*, 5836–5842.
75. Peist, R.; Koch, A.; Bolek, P.; Sewitz, S.; Kolbus, T.; Boos, W. Characterization of the aes gene of Escherichia coli encoding an enzyme with esterase activity. *J. Bacteriol.* **1997**, *179*, 7679–7686.
76. Joly, N.; Danot, O.; Schlegel, A.; Boos, W.; Richet, E. The Aes protein directly controls the activity of MalT, the central transcriptional activator of the Escherichia coli maltose regulon. *J. Biol. Chem.* **2002**, *277*, 16606–16613.
77. Edelman, A.M.; Blumenthal, D.K.; Krebs, E.G. Protein serine/threonine kinases. *Annu. Rev. Biochem.* **1987**, *56*, 567–613.
78. Mikhailov, V.S.; Rohrmann, G.F. Baculovirus replication factor LEF-1 is a DNA primase. *J. Virol.* **2002**, *76*, 2287–2297.
79. Evans, J.T.; Leisy, D.J.; Rohrmann, G.F. Characterization of the interaction between the baculovirus replication factors LEF-1 and LEF-2. *J. Virol.* **1997**, *71*, 3114–3119.
80. Guarino, L.A.; Summers, M.D. Interspersed homologous DNA of autographa californica nuclear polyhedrosis virus enhances delayed-early gene expression. *J. Virol.* **1986**, *60*, 215–223.
81. Grula, M.A.; Buller, P.L.; Weaver, R.F. alpha-Amanitin-Resistant viral RNA synthesis in nuclei isolated from nuclear polyhedrosis virus-infected Heliothis zea Larvae and Spodoptera frugiperda cells. *J. Virol.* **1981**, *38*, 916–921.

82. Pearson, M.N.; Groten, C.; Rohrmann, G.F. Identification of the lymantria dispar nucleopolyhedrovirus envelope fusion protein provides evidence for a phylogenetic division of the Baculoviridae. *J. Virol.* **2000**, *74*, 6126–6131.
83. Garcia-Maruniak, A.; Maruniak, J.E.; Zanotto, P.M.; Doumbouya, A.E.; Liu, J.C.; Merritt, T.M.; Lanoie, J.S. Sequence analysis of the genome of the Neodiprion sertifer nucleopolyhedrovirus. *J. Virol.* **2004**, *78*, 7036–7051.
84. Lauzon, H.A.; Lucarotti, C.J.; Krell, P.J.; Feng, Q.; Retnakaran, A.; Arif, B.M. Sequence and organization of the Neodiprion lecontei nucleopolyhedrovirus genome. *J. Virol.* **2004**, *78*, 7023–7035.
85. Belyavskyi, M.; Braunagel, S.C.; Summers, M.D. The structural protein ODV-EC27 of Autographa californica nucleopolyhedrovirus is a multifunctional viral cyclin. *Proc. Natl. Acad. Sci. U. S. A.* **1998**, *95*, 11205–11210.
86. Mikhailov, V.S.; Okano, K.; Rohrmann, G.F. Baculovirus alkaline nuclease possesses a 5'-->3' exonuclease activity and associates with the DNA-binding protein LEF-3. *J. Virol.* **2003**, *77*, 2436–2444.
87. Li, L.; Rohrmann, G.F. Characterization of a baculovirus alkaline nuclease. *J. Virol.* **2000**, *74*, 6401–6407.
88. Raina, A.K.; Adams, J.R. Gonad-specific virus of corn-earworm. *Nature* **1995**, *374*, 770–770.
89. Sanger, F.; Air, G.M.; Barrell, B.G.; Brown, N.L.; Coulson, A.R.; Fiddes, J.C.; Hutchison, C.A.; Slocombe, P.M.; Smith, M. Nucleotide-sequence of bacteriophage Phichi174 DNA. *Nature* **1977**, *265*, 687–695.
90. Ewing, B.; Hillier, L.; Wendl, M.C.; Green, P. Base-calling of automated sequencer traces using phred. I. Accuracy assessment. *Genome Res.* **1998**, *8*, 175–185.
91. Ewing, W.R.; Choi, Y.M.; Becker, M.; Manetta, V.; Green, D.; Davis, R.; Mason, H.; Ly, C.; Cha, D.; McGarry, D.; *et al.* Sulfonamidopyrrolidinones: Design, SAR and parenteral activity of a novel class of factor Xa inhibitors. *Abstr. Paper. Am. Chem. Soc.* **1998**, *215*, U920–U920.
92. Sutton, G.G.; White, O.; Adams, M.D.; Kerlavage, A.R. TIGR assembler: A new tool for assembling large shotgun sequencing projects. *Genome Sci. Technol.* **1995**, *1*, 9–19.
93. Huang, X.; Madan, A. CAP3: A DNA sequence assembly program. *Genome Res.* **1999**, *9*, 868–877.
94. *Hexamer*. Available online: ftp://ftp.sanger.ac.uk/pub/rd/ (accessed on 1 January 2012).
95. Salzberg, S.L.; Delcher, A.L.; Kasif, S.; White, O. Microbial gene identification using interpolated Markov models. *Nucleic Acids Res.* **1998**, *26*, 544–548.
96. Delcher, A.L.; Harmon, D.; Kasif, S.; White, O.; Salzberg, S.L. Improved microbial gene identification with GLIMMER. *Nucleic Acids Res.* **1999**, *27*, 4636–4641.
97. Altschul, S.F.; Madden, T.L.; Schaffer, A.A.; Zhang, J.; Zhang, Z.; Miller, W.; Lipman, D.J. Gapped BLAST and PSI-BLAST: A new generation of protein database search programs. *Nucleic Acids Res* **1997**, *25*, 3389–3402.
98. Pearson, W.R. Rapid and sensitive sequence comparison with FASTP and FASTA. *Meth. Enzymol.* **1990**, *183*, 63–98.
99. Eddy, S.R.; Mitchison, G.; Durbin, R. Maximum discrimination hidden Markov models of sequence consensus. *J. Comput. Biol.* **1995**, *2*, 9–23.
100. Burks, C. Molecular biology database list. *Nucleic Acids Res.* **1999**, *27*, 1–9.

101. Loots, G.; Ovcharenko, I. VISTA 2.0: Evolutionary analysis of transcription factor binding sites. *Nucleic Acids Res.* **2004**, *32*, W217–W221.
102. Schultz, J.; Milpetz, F.; Bork, P.; Ponting, C.P. SMART, a simple modular architecture research tool: identification of signaling domains. *Proc. Natl. Acad. Sci. U. S. A.* **1998**, *95*, 5857–5864.
103. Marchler-Bauer, A.; Bryant, S.H. CD-Search: Protein domain annotations on the fly. *Nucleic Acids Res.* **2004**, *32*, W327–331.
104. Marchler-Bauer, A.; Anderson, J.B.; DeWeese-Scott, C.; Fedorova, N.D.; Geer, L.Y.; He, S.; Hurwitz, D.I.; Jackson, J.D.; Jacobs, A.R.; Lanczycki, C.J.; *et al.* CDD: A curated Entrez database of conserved domain alignments. *Nucleic Acids Res.* **2003**, *31*, 383–387.
105. Devereux, J.; Haeberli, P.; Smithies, O. A comprehensive set of sequence analysis programs for the VAX. *Nucleic Acids Res.* **1984**, *12*, 387–395.
106. Rice, P.; Longden, I.; Bleasby, A. EMBOSS: The european molecular biology open software suite. *Trends Genet.* **2000**, *16*, 276–277.
107. Nakai, K.; Horton, P. PSORT: A program for detecting sorting signals in proteins and predicting their subcellular localization. *Trends Biochem. Sci.* **1999**, *24*, 34–36.
108. Sonnhammer, E.L.; von Heijne, G.; Krogh, A. A hidden Markov model for predicting transmembrane helices in protein sequences. *Proc. Int. Conf. Intell. Syst. Mol. Biol.* **1998**, *6*, 175–182.
109. Krogh, A.; Larsson, B.; von Heijne, G.; Sonnhammer, E.L. Predicting transmembrane protein topology with a hidden Markov model: Application to complete genomes. *J. Mol. Biol.* **2001**, *305*, 567–580.
110. Bendtsen, J.D.; Nielsen, H.; von Heijne, G.; Brunak, S. Improved prediction of signal peptides: SignalP 3.0. *J. Mol. Biol.* **2004**, *340*, 783–795.
111. Deleage, G.; Combet, C.; Blanchet, C.; Geourjon, C. ANTHEPROT: An integrated protein sequence analysis software with client/server capabilities. *Comput. Biol. Med.* **2001**, *31*, 259–267.
112. Thompson, J.D.; Gibson, T.J.; Plewniak, F.; Jeanmougin, F.; Higgins, D.G. The CLUSTAL_X windows interface: Flexible strategies for multiple sequence alignment aided by quality analysis tools. *Nucleic Acids Res.* **1997**, *25*, 4876–4882.
113. Edgar, R.C. MUSCLE: Multiple sequence alignment with high accuracy and high throughput. *Nucleic Acids Res.* **2004**, *32*, 1792–1797.
114. Tamura, K.; Dudley, J.; Nei, M.; Kumar, S. MEGA4: Molecular Evolutionary Genetics Analysis (MEGA) software version 4.0. *Mol. Biol. Evol.* **2007**, *24*, 1596–1599.
115. Granados, R.R.; Nguyen, T.; Cato, B. An insect cell line persistently infected with a baculovirus-like particle. *Intervirology* **1978**, *10*, 309–317.
116. Hink, W.F.; Ignoffo, C.M. Establishment of a new cell line (IMC-HZ-1) from ovaries of cotton bollworm moths, Heliothis zea (boddie). *Exp. Cell Res.* **1970**, *60*, 307–309.
117. Dubrovsky, E.B. Hormonal cross talk in insect development. *Trends Endocrinol. Metab.* **2005**, *16*, 6–11.

© 2012 by the authors; licensee MDPI, Basel, Switzerland. This article is an open access article distributed under the terms and conditions of the Creative Commons Attribution license (http://creativecommons.org/licenses/by/3.0/).

AVIAN DISEASES 56:000–000, 2012

Characterization of Live LaSota Vaccine Strain–Induced Protection in Chickens upon Early Challenge with a Virulent Newcastle Disease Virus of Heterologous Genotype

Ingrid Cornax, Patti J. Miller, and Claudio L. Afonso[A]

Southeast Poultry Research Laboratory, Agricultural Research Service, U.S. Department of Agriculture, Athens, GA 30605

Received 27 December 2011; Accepted 26 February 2012; Published ahead of print 27 February 2012

1

SUMMARY. Newcastle disease (ND) is a major threat to the international poultry industry, causing bird mortality, reduction in growth and egg production, and trade restrictions. The primary strategy available to the poultry industry to control virulent Newcastle disease virus (NDV), the causative agent of ND, is vaccination. LaSota and other commonly used live-virus NDV vaccine strains were developed in the 1950s and 1960s and show a great degree of genetic divergence from currently circulating NDV strains. In order to characterize protective immunity induced by LaSota against a heterologous NDV strain, we vaccinated groups of specific-pathogen-free (SPF) chickens with LaSota (virus titers ranging from 10^2 to 10^8 egg infective dose 50 [EID_{50}] in 10-fold increments) and challenged the birds 14 days later with ZJ1 strain, an NDV strain that was isolated in the year 2000 from geese in China. We monitored multiple parameters of immunity, including serum antibody titers, antigen-specific lymphocyte proliferation, and splenic cytokine expression and determined that SPF birds vaccinated with an adequate titer of LaSota strain live vaccine are fully protected from morbidity and mortality due to challenge with ZJ1 strain NDV, and we concluded that in the absence of interfering maternal antibody, protection due to vaccination increases with vaccine titer until a threshold titer is reached, beyond which, little or no further benefit can be elucidated.

RESUMEN. Caracterización de la protección inducida por la cepa vacunal viva LaSota en pollos durante un desafío temprano con un virus virulento de la enfermedad de Newcastle de genotipo heterólogo.

La enfermedad de Newcastle es una gran amenaza para la industria avícola internacional, ya que causa mortalidad de aves, reducción en el crecimiento y en la producción de huevos y restricciones comerciales. La estrategia primaria disponible para la industria avícola para controlar el virus virulento de la enfermedad de Newcastle, que es el agente causante de la enfermedad de Newcastle, es la vacunación. La cepa LaSota y otras cepas vacunales del virus de Newcastle de uso común se desarrollaron en los años 1950 y 1960 y muestran un alto grado de divergencia genética con relación a las cepas circulantes del virus de Newcastle. A fin de caracterizar la inmunidad protectora inducida por la cepa LaSota en contra de una cepa heteróloga del virus de Newcastle, se vacunaron grupos de aves pollos libres de patógenos específicos con LaSota (con títulos virales que van desde 10^2 hasta 10^8 dosis infectantes en embrión de pollo [EID50] con incrementos de 10 veces) y las aves se desafiaron 14 días después la cepa ZJ1 cepa, una cepa de Newcastle que se aisló en el año 2000 de gansos en China. Se hizo un seguimiento de varios parámetros de la inmunidad, incluyendo los títulos de anticuerpos séricos, la proliferación de linfocitos específica de antígeno y la expresión de citoquinas por los esplenocitos. Se determinó que las aves libres de patógenos específicos vacunados con un título adecuado de la vacuna LaSota están totalmente protegidas contra la morbilidad y la mortalidad debidas al desafío con la cepa ZJ1 y se llegó a la conclusión de que en ausencia de anticuerpos maternos que puedan interferir, la protección inducida por la vacunación puede aumentar con el título de la vacuna hasta que se alcanza un título límite, más allá del cual, no se observa un beneficio adicional.

Key words: Newcastle disease virus, NDV, LaSota, live-virus vaccination, ZJ1

Abbreviations: Ct = cycle threshold; EID = egg infective dose; ND = Newcastle disease; NDV = Newcastle disease virus; NP = nucleoprotein; nvNDV, neurotropic velogenic Newcastle disease virus; P = phosphoprotein; M, matrix; F, fusion; HN, hemagglutinin-neuraminidase; SPF = specific pathogen free; vvNDV = viscerotropic velogenic Newcastle disease virus

Newcastle disease (ND) is a continuing threat and challenge to the international poultry industry. ND causes major losses acutely by causing high levels of bird mortality, decreased growth, and reduced egg production, and chronically by restricting trade and by forcing producers to implement expensive measures to prevent disease spread. Since there is no effective treatment for ND, the poultry industry relies primarily on vaccination and biosecurity to control the disease (3,19,22). The causative agent of ND, virulent Newcastle disease virus (NDV), also known as avian paramyxovirus type 1, belongs to the *Avulavirus* genus within the *Paramyxoviridae* family. Virions have a single-stranded, negative-sense, nonsegmented RNA genome that codes for six structural proteins: nucleoprotein (NP), phosphoprotein (P), matrix (M), fusion (F), hemagglutinin-neuraminidase (HN), and RNA polymerase (L) (3). The HN and F glycoproteins allow NDV to attach and fuse to the host cell membranes, thereby initiating infection. Antibodies against HN and F neutralize the virus and are a primary component of vaccine-induced protection versus NDV (21).

Newcastle disease virus strains have been categorized into different pathotypes based on the disease they produce in chickens. The most commonly used vaccine strains: LaSota, B1, and Ulster, are lentogenic strains that produce no or only mild clinical signs in adult birds. Lentogenic-strain live-virus vaccines have been used for more than 50 yr to provide protection from disease caused by mesogenic and velogenic strains (3,11,13). Mesogenic strains cause neurologic and respiratory disease but very little mortality. Viscerotropic velogenic strains (vvNDV) are characterized by acutely fatal disease, usually with hemorrhagic lesions in the digestive tract of infected birds; neurotropic velogenic strains (nvNDV) cause high mortality after severe respiratory and neurologic disease, generally in the absence of gut lesions (13). Both mesogenic and velogenic isolates are defined by the World Organization for Animal Health as being virulent for the purposes of trade (15).

[A]Corresponding author. E-mail: Claudio.Afonso@ars.usda.gov

Table 1. Primer sequences for quantitative reverse transcription PCR; previously published (7).

Gene	Primer sequences (5′-3′)	Product size (bp)
IFN γ	Forward: gtgaagaaggtgaaagatatcatgga Reverse: gctttgcgctggattctca	71
IL-6	Forward: gctcgccggcttcga Reverse: ggtaggtctgaaaggcgaacag	71
IL-2	Forward: ttggaaaatatcaagaacaagattcatc Reverse: tcccaggtaacactgcagagttt	93
IFN β	Forward: gcccacacactccaaaacactg Reverse: ttgatgctgaggtgagcgttg	150
B-actin	Forward: agaggctcccctgaaccccaaagc Reverse: ctggatggctacatacatggctgg	94

Based on whole genome sequence analysis, NDV shows two major class divisions (class I and II), and class II, the major class of interest to the poultry industry, is further divided into at least 10 genotypes (I–X) (13). The most widely used NDV vaccine strain, LaSota, belongs to genotype II, while the majority of circulating velogenic viruses in the world belong to genotypes V–VII (5,13). Although all NDV strains belong to the same serotype, the protection provided by genotype II vaccines against heterologous challenge has been subject to some controversy. Yu *et al.* (23) and Qin *et al.* (17) reported the presence of genotype VII antigenic variants that could produce disease in birds vaccinated with LaSota. Unfortunately, these cross-protection experiments lacked corroborating data about the immune status of the birds prior to and after challenge. Two other groups, Jeon *et al.* (8) and Liu *et al.* (12), demonstrated that commercial genotype II vaccine strains could provide complete protection against morbidity and mortality and reduce shedding of heterologous challenge virus strains (genotypes III, VIg, VIb, VIId, and IX). In order to characterize the immune response induced by LaSota vaccination and to examine how LaSota strain can protect against heterologous challenge, we vaccinated groups of specific-pathogen-free (SPF) chickens with different titers of LaSota strain virus and challenged them with ZJ1 (Goose/China/ZJ1/2000) strain NDV, a genotype VII strain of vvNDV isolated from geese in China (12). We monitored morbidity and mortality, measured NDV specific cell-mediated and humoral immune responses due to LaSota vaccination, and measured relative changes in splenic cytokine expression in response to challenge.

MATERIALS AND METHODS

Chickens. Mixed-sex, specific-pathogen-free (SPF) white Leghorn chickens were acquired from the Southeast Poultry Research Laboratory flocks. Prevaccination sera samples were taken from 10% of the birds prior to group randomization. Birds were housed, vaccinated, and challenged in BSL 3 Enhanced (E) facilities. All birds were housed in Horsfall isolation units with feed and water *ad libitum*.

Viruses. LaSota NDV strain Chicken/New Jersey (LaSota)/1946, of low virulence and commonly used as a vaccine, and the recombinant virulent NDV constructed in 2007 (rZJ1/2007) of the wild type NDV ZJ1 strain, originally isolated in 2000 (Goose/China/ZJ1/2000), were propagated and titrated in 9–11-day-old SPF chicken embryos via the chorioallantoic sac route.

Experimental design. Four-week-old SPF white Leghorn chickens were arbitrarily divided into nine treatment groups: 1) brain heart infusion–NC; 2) brain heart infusion–ZJ1; 3) 10^2 LaSota; 4) 10^3 LaSota; 5) 10^4 LaSota; 6) 10^5 LaSota; 7) 10^6 LaSota; 8) 10^7 LaSota; and 9) 10^8 LaSota. Groups 1 and 2 contained 10 birds each, and groups 3–9 had 20 birds each. Birds were vaccinated 3 days after group randomization. Groups 1 and 2 received 100 µl of brain heart infusion (BHI) via intranasal (50 µl IN) and eye drop (50 µl ED) routes. Birds in groups 3–9 received live LaSota virus suspended in BHI (50 µl IN and 50 µl ED), with group 3 receiving a target titer of 10^2 egg-infectious dose 50 (EID_{50}) per bird, and each group thereafter receiving a 10-fold higher dose. Birds were monitored daily for clinical signs of vaccine reaction (conjunctivitis, lethargy, and snicking). Four days after vaccination, oropharyngeal swabs were taken for virus isolation. Seven days after vaccination, whole blood was collected via wing-vein into EDTA-containing syringes from four birds per group for lymphocyte proliferation assay.

At day 14 postvaccination, blood was collected via wing-vein for serology, and the birds in groups 2–9 were challenged with live ZJ1 strain NDV suspended in BHI with a target titer of $10^{6.5}$ EID_{50} per bird split evenly between oral and eye-drop routes. Birds in group 1 were given BHI without ZJ1 strain NDV (BHI NC) in the same amount and via the same route. Birds were monitored daily for overt clinical signs of ND (conjunctivitis, depression, edema, muscle tremors, torticollis, paralysis of wings and legs) and mortality. Birds displaying severe signs of disease, unable to eat and drink, were euthanized by cervical dislocation. Oropharyngeal swabs were taken on days 2 and 4 postchallenge, and cloacal swabs were taken on day 4 postchallenge for virus isolation. On day 3 postchallenge, two birds each from groups 1 and 2 and four birds each from groups 3–9 were euthanized by cervical dislocation, and their spleens were collected for RNA isolation. These birds were randomly chosen before challenge to prevent interference with morbidity/mortality and virus isolation data analysis. On day 14 postchallenge, all surviving birds were anesthetized with ketamine/xylazine solution, and blood was collected for serology via cardiac puncture just prior to euthanasia by cervical dislocation.

NDV enzyme-linked immunosorbent assay (ELISA). Serum was tested for antibodies against NDV with a commercial ELISA test (Flockcheck™ IDEXX Laboratories Inc., Westbrook, ME). Chicken serum samples were diluted 1:500 and incubated in kit-provided 96-well microtiter plates coated with NDV-antigen. The ELISA was performed according to manufacturer's instructions.

Virus isolation. Swabs were collected into 2 ml of BHI broth containing antibiotics (1000 units/ml penicillin G, 200 µg/ml gentamicin sulfate, and 4 µg/ml amphotericin B; Sigma-Aldrich, St. Louis, MO) and stored at −80 C. Virus isolation was performed in SPF embryonated chicken eggs following standard procedures (2).

Splenic cytokine expression. Changes in the splenic expression of interferon γ (IFNγ), interleukin 6 (IL-6), interleukin 2 (IL-2), and interferon β (IFNβ) were determined by quantitative reverse transcription PCR (qRT-PCR). Genes were chosen based on previous research showing these genes to be the major cytokines involved in the host immune response to NDV (7,20).

RNA isolation. Spleen cell suspensions were generated by pushing freshly isolated tissue through a 70-mM-pore-size mesh cup, immediately into Trizol (Invitrogen, Carlsbad, CA), and then samples were stored at −80 C after collection of all samples for that day. Samples were later thawed at room temperature, and chloroform was added according to the manufacturer's protocol. Samples were incubated for 10 min on ice. Following centrifugation at 2400 × *g* for 15 min, the aqueous phase was removed, mixed with an equal volume of 70% ethanol, and applied to Qiagen RNeasy Midi Prep columns (Qiagen, Valencia, CA). RNA quantity was assessed using a Nanodrop spectrophotometer on the RNA-40 setting, and quality was assessed using a nanochip on a Bioanalyser (Agilent Technologies). All RNA samples had an RNA integrity number greater than 8.6, with a mean of 9.4.

Quantitative RT-PCR. Relative changes in splenic RNA expression of IFNγ, IL-6, IL-2, IFNβ, and β-actin were measured as changes in SYBR green fluorescence after amplification with specific primer sets, as in Ecco *et al.* (7) (Table 1). Reactions were done in triplicate on 20-µl reaction mixtures containing 60 ng of total RNA, 500 nM of each primer, 10 µl of 2X master mix SYBR, and 0.16 µl of enzyme mix (125X) (PowerSYBR® Green RNA-to-CT™ 1-Step Kit; Applied Biosystems, CA). Amplification and detection of specific products were performed using the Applied Biosystems 7500 Fast Real-Time PCR System with the following cycle profile: one cycle at 48 C for 30 min and 95 C for 15 min, followed by 40 cycles at 95 C for 15 sec and at

Table 2. Vaccine and challenge-virus back-titrations (EID_{50}/100 µl).

Target titer	Actual titer
Vaccine	
BHI[A]	0
10^2 LaSota	$10^{2.3}$
10^3 LaSota	$10^{3.1}$
10^4 LaSota	$10^{4.1}$
10^5 LaSota	$10^{5.5}$
10^6 LaSota	$10^{6.5}$
10^7 LaSota	$10^{7.1}$
10^8 LaSota	$10^{8.5}$
Challenge	
BHI	0
$10^{6.5}$ ZJ1	$10^{6.75}$

[A]BHI = brain heart infusion.

58 C for 32 sec. A dissociation curve was added to the end of all reactions, and the melting curve was analyzed.

Quantification of changes in relative cytokine RNA expression. Relative changes in gene expression were calculated according to the Pflaffl method (16) using LinReg version 12 (18) to calculate individual primer efficiency by linear regression. All cycle threshold fluorescence (Ct) values were corrected to BHI-NC for each gene of interest and the endogenous control (β-actin).

Lymphocyte proliferation assay. Lymphocyte proliferation in response to ultraviolet (UV)-inactivated ZJ1 strain NDV, measured by AlamarBlue reduction, was used as an indicator of cell-mediated immunity.

Lymphocyte preparation. Whole blood samples (5 ml of blood anticoagulated with EDTA) were gently layered onto 5 ml of 63% Percoll gradient (3.15 ml of Percoll [Sigma-Aldrich]; 0.5 ml of 1.5 M NaCl solution, and 1.35 sterile distilled water) in a 15-ml conical tube. The conical tubes were centrifuged at 1250 × g for 20 min. The cells at the interface were collected and suspended in 5 ml of RPMI 1640 (Invitrogen) supplemented with 8% fetal bovine serum (Invitrogen), 2% chicken serum (Sigma-Aldrich), and 1% PenStrep (Invitrogen). The cell suspension was centrifuged at 400 × *g* for 4 min, and the supernatant was removed. The cells were resuspended at 1×10^6 cells/ml, seeded into six-well cell culture plates and incubated for 60 min at 41 C in a 5% CO_2 incubator. Nonadherent cells were removed, resuspended at 1×10^6/ml (viability by Trypan blue exclusion was 90–95%), aliquoted into 96-well cell culture plates (100 µl per well in nine wells), and incubated overnight.

Proliferation assay. After 24 hr, 100-µl aliquots of proliferation media, including either Concanavalin A (ConA, 12.5 µg/ml; Sigma-Aldrich) as a positive control, media as a negative control, or UV-inactivated ZJ1 strain NDV (titer prior to inactivation = $10^{6.5}$ EID_{50}/100 µl), were added in triplicate wells. Twenty-two microliters of AlamarBlue (Biosource International, Inc., Camarillo, CA) were added to all wells and three blank wells containing 200 µl of media alone. AlamarBlue reduction was measured after 48 hr of incubation as described (10).

Statistical analysis. All data analysis was performed using JMP version 9 software (SAS Institute, Raleigh, NC). Frequencies of virus isolation for treatment groups were compared by contingency analysis of means for proportions. One-way analysis of variance with the Tukey-Kramer method of means comparisons was used to compare group serum NDV antibody ELISA titers, relative changes in splenic cytokine expression, and AlamarBlue reduction. Differences in prechallenge and postchallenge serum ELISA titers were analyzed by Student *t*-test. Bivariate fit analysis was used to determine the correlation between relative changes in splenic cytokine expression and group serum NDV antibody ELISA titer. All tests were performed with a 5% level of significance.

RESULTS

To determine the titer of LaSota that prevents mortality and NDV shedding after early challenge with a heterogenic NDV strain,

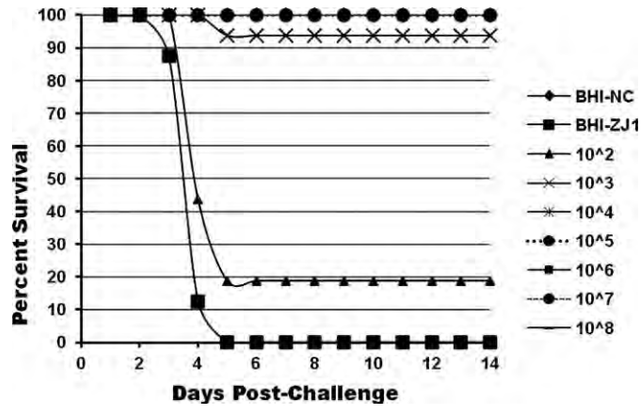

Fig. 1. Survival post-ZJ1 challenge. Chickens in each vaccine group were challenged at day 14 postvaccination with $10^{6.5}$ EID_{50} ZJ1 strain NDV or sham-challenged with brain heart infusion. Mortality was monitored for 14 days after challenge. BHI-NC indicates brain heart infusion sham-vaccinated, and sham-challenged (n = 8); BHI-ZJ1 indicates brain heart infusion, sham-vaccinated, and ZJ1 challenged (n = 8); all other groups were vaccinated with LaSota at indicated titer (EID_{50}) and challenged with ZJ1 (n = 16).

groups of 4-wk-old SPF white Leghorn chickens were inoculated with increasing doses of live LaSota NDV (virus titers ranging from 10^2 to 10^8 EID_{50}/100 µl) or BHI-control and challenged at day 14 postinoculation with $10^{6.5}$ EID_{50}/100 µl of wild-type ZJ1 (Table 2).

Morbidity and mortality. Birds were observed throughout the trial period for clinical signs of ND. No clinical signs of ND were observed in any birds prior to vaccination or challenge; however, one bird in group 3 died prior to vaccination. There were no clinical signs of vaccine reaction in any group (data not shown). After challenge, all birds in the ZJ1-challenged BHI-control (BHI-ZJ1) group displayed moderate to severe conjunctivitis and severe depression 2–4 days after ZJ1-inoculation, and 100% mortality was seen at day 5 postchallenge (Fig. 1). In the 10^2 LaSota group, all birds displayed moderate to severe conjunctivitis and severe depression at days 2–4 postchallenge, and 81.75% mortality was seen at day 5 postchallenge. Birds vaccinated with 10^3 LaSota virus displayed mild to moderate conjunctivitis and mild depression at days 3–4 postchallenge. At day 4 postchallenge, one bird in the 10^3 group was moderately depressed and recumbent and died on day 5 postchallenge. Birds in all other groups showed no clinical signs of ND after challenge.

Serum NDV antibody titers. Blood was collected for measurement of serum NDV antibody titer at day 14 postvaccination (prechallenge) and day 14 postchallenge (Table 3). Prechallenge, all birds inoculated with a LaSota titer of 10^3 EID_{50}/100 µl or less had negative serum NDV antibody ELISA titers (less than 300). Birds in all other groups had titers of 1500 or greater, with increases in prechallenge titer occurring in conjunction with increased vaccine virus titer. After challenge, birds in the 10^2, 10^3, and 10^4 LaSota groups seroconverted with statistically significant increases in serum titer ($p \leq 0.01$) of 7863 ± 450 (mean ± standard error of the mean), 5882 ± 1013, and 1732 ± 609, respectively. Birds in the remaining groups showed no significant increase in serum ELISA titer after challenge and had significantly lower postchallenge titers than birds in the 10^2 and 10^3 LaSota groups (all p-values < 0.05).

Virus shedding. Oral swabs were taken from all birds at day 4 postinoculation with LaSota and days 2 and 4 post–ZJ1-challenge (Table 4). Cloacal swabs were taken from all birds at day 4 postchallenge. All birds vaccinated with a LaSota titer of 10^4 EID_{50}/

Table 3. Serum NDV antibody ELISA titer.

Treatment group	*N* pre/postchallenge	Prechallenge[A]	Postchallenge
BHI-no challenge	8/8	29.49 ± 12.52[E]	25.94 ± 8.08[D]
BHI-ZJ1 challenge	8/0	30.04 ± 10.10[E]	NS
10^2 LaSota	16/4	82.72 ± 38.76[E]	8069.44 ± 536.17[B]
10^3 LaSota	16/15	233.08 ± 62.76[E]	6492.83 ± 873.86[B]
10^4 LaSota	16/16	1713.55 ± 265.22[DE]	3446.22 ± 548.71[C]
10^5 LaSota	16/16	1528.63 ± 162.50[D]	2477.17 ± 428.05[C]
10^6 LaSota	16/16	3074.76 ± 531.19[C]	3188.83 ± 317.64[C]
10^7 LaSota	16/16	3031.59 ± 381.63[C]	4248.60 ± 604.77[BC]
10^8 LaSota	16/16	4167.05 ± 625.93[B]	3977.67 ± 571.37[C]

[A]Results are expressed as group mean serum ELISA titer ± standard error of the mean. Titers of 300 or greater are considered positive. Means within the same column with different superscripts (B–E) are significantly different by Tukey-Kramer ($p \leq 0.05$). BHI = brain heart infusion. NS = no survivors at time of blood collection.

100 µl or greater were shedding virus at day 4 postvaccination. Thirteen of 15 birds in the 10^3 LaSota and 1 of 16 birds in the 10^2 LaSota group were shedding virus at day 4 postvaccination. At day 2 postchallenge, all BHI-ZJ1 birds and 10^2 LaSota group birds were shedding virus. Significant numbers of 10^3 LaSota birds (13/15) were also shedding virus postchallenge. Large numbers of birds in groups vaccinated with a LaSota titer of 10^4 EID_{50}/100 µl or greater were shedding virus (range 3/16 to 8/16 birds); however, this was a statistically significantly lower incidence of shedding than was seen in the BHI-ZJ1, 10^2, and 10^3 LaSota birds. As on day 2 postchallenge, at day 4 postchallenge, significantly more birds in the BHI-ZJ1, 10^2, and 10^3 groups were shedding virus orally and cloacally than birds in groups vaccinated with 10^4 EID_{50}/100 µl LaSota or greater.

Splenic cytokine expression. At day 3 postchallenge, 4 birds per treatment group were euthanized, and their spleens were collected to measure changes in mRNA expression of IFNγ, IL-6, IL-2, and IFNβ (Table 5). The quality of RNA of spleens collected from birds vaccinated with 10^5 LaSota virus was too low to allow for analysis by qRT-PCR. IFNγ expression in the spleen was significantly up-regulated in the BHI-ZJ1 and the 10^2 LaSota groups (23.09- to 32.61-fold). IL-6 expression was also up-regulated in the BHI-ZJ1 and 10^2 LaSota groups, but to lesser extent than that seen with IFNγ (6.47- to 8.15-fold). There were significant inverse correlations between IFNγ expression and prechallenge serum NDV antibody titer ($R^2 = 0.652$, $p < 0.001$) and also between IL-6 expression and prechallenge ELISA titers ($R^2 = 0.596$, $p < 0.001$) (Fig. 2). Birds displaying low serum NDV antibody titers expressed higher levels of IFNγ and IL-6 mRNA in the spleen. There were mild increases (2.93- and 2.58-fold, respectively) in IL-2 expression in the 10^2 and the 10^3 LaSota groups postchallenge. IFNβ expression appeared to be up-regulated in all challenged groups. The 10^3 and 10^7 LaSota groups showed significant increases over BHI-NC (8.19- and 7.95-fold, respectively); the other groups showed very similar up-regulation (ranging from 3.87- to 7.23-fold), which was not statistically significant.

NDV-antigen-specific lymphocyte proliferation. To measure the cell-mediated immune response to vaccination, blood lymphocytes were isolated from four birds per treatment at day 7 postvaccination. Lymphocyte proliferation in response to ConA or UV-inactivated ZJ1 virus was measured by AlamarBlue reduction. Lymphocytes from all groups reduced AlamarBlue in response to ConA stimulation (range 4–6%, data not shown). There were no statistically significant differences in AlamarBlue reduced between groups; however, lymphocytes from birds that had been vaccinated with 10^4 EID_{50}/100 µl or greater tended to reduce less AlamarBlue in response to UV-inactivated ZJ1 than lymphocytes from birds vaccinated with less than 10^5 EID_{50}/100 µl (Fig. 3).

DISCUSSION

The major strategy employed by the poultry industry to control ND, along with stringent biosecurity, is vaccination. However, creating an effective vaccine strategy poses many challenges. For example, although all strains of NDV belong to the same serogroup, they display a great amount of genetic variability. Commercially available vaccine strains, such as LaSota, were derived from genotypes that were actively circulating during the 1940s and 1960s and are not closely related to the virulent NDV strains that are now in existence and currently in global circulation. Due to this large gap in amino acid homology between vaccine strain and

Table 4. Virus isolation in SPF embryonated chicken eggs.

Treatment group	4 days after vaccination, oral swabs (positive/total)	2 days after ZJ1 challenge, oral swabs (positive/total)	4 days after ZJ1 challenge, oral swabs (positive/total)	4 days after ZJ1 challenge, cloacal swabs (positive/total)
BHI-no challenge	0/8[AB]	0/8[B]	0/8[B]	0/8[B]
BHI-ZJ1 challenge	0/8[B]	8/8[C]	8/8[C]	7/8[C]
10^2 LaSota	1/16[B]	16/16[C]	16/16[C]	16/16[C]
10^3 LaSota	13/15[C]	13/15[C]	9/15[C]	9/15[C]
10^4 LaSota	16/16[C]	5/16[B]	3/16[B]	2/16[B]
10^5 LaSota	16/16[C]	5/16[B]	1/16[B]	0/16[B]
10^6 LaSota	16/16[C]	8/16[B]	0/16[B]	1/16[B]
10^7 LaSota	16/16[C]	3/16[B]	0/16[B]	0/16[B]
10^8 LaSota	16/16[C]	4/16[B]	0/16[B]	0/16[B]

[A]Proportions within the same column with different superscripts (B–C) are significantly different by analysis of means for proportions (chi-square, $p \leq 0.05$)). BHI = brain heart infusion.

Table 5. Splenic cytokine expression 3 days after ZJ1 challenge.

Group	Fold-change splenic mRNA Expression			
	IFNγ[A]	IL-6	IL-2	IFNβ
BHI-ZJ1	32.61 ± 2.94[B]	8.15 ± 0.45[B]	2.38 ± 0.10[BCD]	6.61 ± 0.37[BC]
10^2 LaSota	23.09 ± 1.04[B]	6.47 ± 0.17[B]	2.93 ± 0.42[B]	5.37 ± 0.28[BC]
10^3 LaSota	11.28 ± 4.47[C]	3.05 ± 1.24[C]	2.58 ± 0.42[BC]	8.19 ± 1.34[B]
10^4 LaSota	2.64 ± 0.69[C]	1.43 ± 0.43[C]	0.97 ± 0.21[D]	6.25 ± 2.48[BC]
10^6 LaSota	8.47 ± 2.24[C]	2.85 ± 0.86[C]	2.08 ± 0.18[BCD]	7.23 ± 1.43[BC]
10^7 LaSota	4.96 ± 0.24[C]	1.66 ± 0.12[C]	1.14 ± 0.29[D]	7.95 ± 0.78[B]
10^8 LaSota	3.14 ± 0.84[C]	1.42 ± 0.06[C]	1.49 ± 0.08[CD]	3.87 ± 0.39[C]

[A]Data are presented as mean fold-change ± standard error of the mean. Fold-change was calculated relative to unchallenged BHI control using the Pflaffl method (16). Means within the same column with different superscripts (B–D) are significantly different by Tukey-Kramer ($p \leq 0.05$). BHI-ZJ1 = brain heart infusion control challenged with ZJ1 strain of NDV.

circulating virulent strains (12% to 20%), there are valid concerns about the ability of vaccine strains to provide adequate protection against challenge with novel variants of NDV.

In order to identify potential differences against heterologous challenge in protective immunity induced by LaSota, a commonly used NDV vaccine strain from genotype II, we vaccinated groups of SPF chickens with LaSota (virus titers ranging from 10^2 to 10^8 EID_{50} in 10-fold increments) and challenged the birds 14 days later with the genotype VII strain ZJ1. As was seen in a previous study (12), we determined that SPF birds properly vaccinated in a laboratory setting with an adequate titer of LaSota strain live-vaccine were fully protected from morbidity and mortality due to challenge with ZJ1 strain NDV, and we posit that in the absence of interfering maternal antibody, protection due to vaccination increases with vaccine titer until a threshold is reached, beyond which, little or no further benefit can be elucidated.

Birds vaccinated with titers higher than 10^4 EID_{50} LaSota were fully protected from morbidity and mortality, had a significantly lower incidence of virus shedding postchallenge, and had significantly higher prechallenge serum NDV antibody ELISA titers than unvaccinated birds and birds vaccinated with lower LaSota titers. Vaccine doses below 10^4 EID_{50} showed partial protection against ZJ1-challenge, with most birds in the 10^2 LaSota group and one of the birds in the 10^3 LaSota group dying postchallenge, and all birds in both groups displaying overt clinical signs of ND. Serum NDV antibody ELISA titers were also significantly lower in the 10^2 and 10^3 LaSota groups. ZJ1-specific cell-mediated immunity, as measured by antigen-specific *in vitro* lymphocyte proliferation, visibly increased in groups vaccinated with 10^5 EID_{50} LaSota or greater as compared to the birds in the 10^2, 10^3, and 10^4 LaSota groups. This disparity between humoral and cell-mediated immune data may indicate that humoral immunity due to neutralizing antibody is more important in the development of ND immunity, or it could be a function of differences in assay sensitivity (19). Surprisingly, hemagglutination-inhibition assays are typically performed to analyze antibody production after NDV infection or vaccination, even though they are only able to detect antibodies to the hemagglutinin-neuraminidase protein (3). We chose to use an ELISA system able to detect antibodies to the entire virus to evaluate the immune response, as they have a high degree of correlation with the HI results (4,6). Another method occasionally employed by researchers to measure humoral immunity is the serum neutralization assay. We were unable to perform a serum neutralization assay within the scope of this paper; however, the strong correlation between serum ELISA antibody titer and protection from challenge

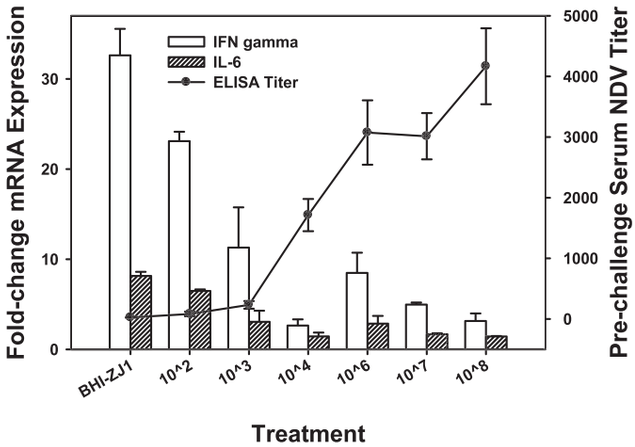

Fig. 2. Splenic interferon gamma (IFNγ) and interleukin 6 (IL-6) expression *vs.* serum NDV antibody ELISA titer. Relative changes in splenic cytokine expression (bars) were measured by quantitative reverse transcription PCR at day 3 post-ZJ1 challenge, and group serum NDV antibody titers (line) were measured by ELISA at day of challenge. Data are represented as group means ± standard error of the mean ($n = 4$).

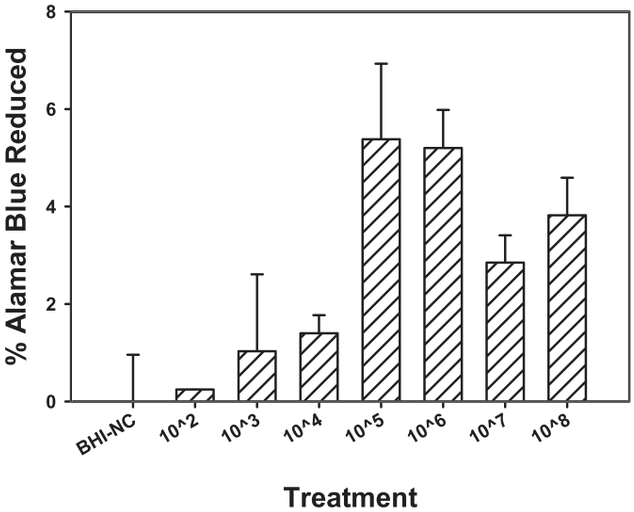

Fig. 3. Antigen-specific lymphocyte AlamarBlue reduction. Lymphocytes were isolated from EDTA-coagulated whole blood at day 7 postvaccination and stimulated to proliferate *in vitro* with UV-inactivated ZJ1-strain NDV (pre-inactivation titer = $10^{6.5}$ EID_{50}/100 μl). Proliferation data are represented as group mean percent AlamarBlue reduced ± standard error of the mean ($n = 4$).

suggests that serum from well-vaccinated chickens was able to neutralize invading virions.

Cytokines are produced by immune cells in order to coordinate the appropriate immune response to a pathogen. Traditionally, cytokines are separated into multiple categories: pro-inflammatory/innate cytokines (IFNα, IFNβ, IL-1β, and IL-6), T-helper-cell type 1 cytokines (IFNγ and IL-2), and T-helper-cell type 2 cytokines (IL-4 and IL-10). Pro-inflammatory cytokines, such as IL-1β and IL-6, are a major part of the innate immune response and are known to induce sickness behavior: anorexia, lethargy, and fever. IFNα and IFNβ are type I interferons and are the major mediators of the innate antiviral response within the host. The antiviral response occurs as a nonspecific reaction to virus infection and is characterized by decreased cell proliferation and increased display of intracellular antigens by all host cells in order to decrease virus spread and increase antiviral surveillance by the immune system. IL-2 is responsible for inducing the cell-mediated arm of the adaptive immune system, which aims to eliminate intracellular pathogens via the proliferation and activation of cytotoxic T cells. IFNγ also aids in cell-mediated immunity by activating macrophages and stimulating the innate antiviral response and by serving as a bridge between the innate and adaptive immune systems. T-helper-cell type 2 cytokines are responsible inducing a humoral immune response by inducing antigen-specific B cells to proliferate and secrete antibody (1,9).

Groups displaying overt clinical signs postchallenge (BHI-ZJ1-challenge control, 10^2, and 10^3) had up-regulated splenic expression of IFNγ and IL-6, while birds that were well-protected from challenge expressed relatively lower levels of IL-6 and IFNγ mRNA in the spleen. Furthermore, there was a significant negative correlation between serum NDV antibody ELISA titer and IFNγ/IL-6 expression, with a nearly linear decline in relative IL-6/IFNγ expression relating to a nearly linear increase in NDV antibody titers with increasing LaSota vaccine titers. This relationship between protection and IL-6/IFNγ expression is especially interesting since IL-6 and IFNγ have been implicated as key mediators of tissue damage, sickness behavior, and mortality due to ''inflammatory cytokine storm'' induction (7). Decreased expression in protected birds could indicate that the challenge virus could not penetrate the mucosa in a high enough amount to cause a systemic immune response. In other words, the local mucosal immune system has been sufficiently primed by live LaSota vaccine titers of at least 10^4 EID_{50} to allow for efficient clearance of the heterologous challenge virus and prevention of systemic disease. As opposed to IL-6/IFNγ, splenic expression of IL-2 and IFNβ did not show any clear pattern related to vaccine titer. However, the mild changes in splenic IL-2 expression tended to be in the less vaccinated groups. These results are similar to those seen in previous studies measuring splenic cytokine expression at 3 days postchallenge with virulent strains of NDV (7,20). It is possible that at a different postchallenge time point or in a different organ, such as the Harderian gland, a clearer pattern of IL-2 and IFNβ expression would be evident.

By using a range of LaSota virus titers to vaccinate SPF chickens against NDV challenge, we were able to elucidate a clear pattern of protection that related directly to the ability of the vaccine virus to proliferate at the site of infection. At titers below 10^4 EID_{50}, less than 100% of the vaccinated birds shed virus at the oral mucosa; this lower incidence of shedding was directly related to decreased protection from disease in these vaccinated groups, with 10^3 EID_{50} LaSota vaccinated birds having a higher incidence of shedding and a higher level of protection than the 10^2 EID_{50} LaSota group. As vaccine titer increased from 10^2 EID_{50} to 10^4 EID_{50}, there was a clear increase in vaccine-induced protection that is evident as a nearly linear increase in serum NDV antibody ELISA titers, a nearly linear decrease in splenic IL-6 and IFNγ expression, and an increase in antigen-specific lymphocyte proliferation.

At vaccine titers beyond 10^5 EID_{50}, serum antibody titers continued to rise; however, there was no change in the incidence of virus shedding, the lymphocyte proliferative response, or splenic cytokine expression. These data could suggest that serum antibody titer is the most sensitive method for measuring protection against NDV challenge, or they could suggest that beyond a certain serum antibody titer, no additional protection can be elucidated. This is in agreement with earlier studies that found neutralizing antibody principally functions in the prevention of infection during virus challenge, whereas cell-mediated immunity functions in the clearance of active infection (19,22). This may indicate that beyond a certain serum antibody titer, the mucosal surfaces become saturated and can no longer bind extra antibodies to prevent infection. If this is truly the case, then finding this ''threshold'' serum antibody titer that identifies protection would be of great value in the field, since unnecessarily high vaccine titers have been associated with high costs due to vaccine reaction (drop in growth and egg production) and vaccine costs. In this study, with SPF birds under experimental conditions, once an antibody titer of about 1500 was reached, the birds were completely protected from morbidity and mortality and exhibited little systemic immune response to challenge. Unfortunately, this pattern will not be as clear in the field, where problems due to vaccine mass-application techniques, comorbidity, and maternal antibody reduce the uniformity of a group immune response. It is also possible that changing the challenge dose could alter this minimum ''threshold.'' A lower challenge dose could be more easily neutralized with fewer antibodies, and at a sufficiently high dose, no amount of antibody can truly prevent infection. Ideally, future experiments should test these interactions by using birds with different levels of maternal antibody crossed by different levels of live vaccine and challenge virus titer crossed by different methods of application.

As was found in previous studies, LaSota can protect against heterologous challenge (8,12). However, this study only examined LaSota-induced protection against one genetically divergent strain, and the possibility that new strains have evolved or will evolve antigenic divergence allowing for vaccine escape cannot be ignored. Nevertheless, disease due to the vast majority of NDV strains can be prevented by effective delivery of live LaSota vaccine; therefore, in addition to developing new strain-matched NDV vaccines to provide better protection and prevent shedding of challenge viruses (14), great effort should be focused on improving vaccine delivery, determining ideal levels of maternal and postvaccinal serum antibody titer, and determining causes of vaccine failure not related to genetic divergence in the field.

REFERENCES

1. Abbas, A. K., and A. H. Lichtman. Introduction to immunology. In: Cellular and molecular immunology, 5th ed. Elsevier Saunders, Philadelphia. pp. 1–40. 2005. 7

2. Alexander, D. Newcastle disease virus and other avian paramyxoviruses. In: Isolation and identification of avian pathogens. D. Swayne, J. Glisson, M. Jackwood, J. Pearson, and W. Reed, eds. American Association of Avian Pathologists, Kennett Square. pp. 156–163. 1998. 8

3. Alexander, D. J., and Senne, D. A., Newcastle disease, other avian paramyxoviruses, and pneumovirus infections. In: Diseases of poultry, 12th ed. Y. M. Saif, ed. Blackwell, Ames, IA. pp. 75–115. 2008.

4. Brown, J., R. Resurreccion, and T. Dickson. The relationship between the hemagglutination-inhibition test and the enzyme-linked

9 immunosorbent assay for the detection of antibody to Newcastle disease. Avian Dis. 34. 1990.

5. Chong, Y. L., A. Padhi, P. J. Hudson, and M. Poss. The effect of vaccination on the evolution and population dynamics of avian paramyxovirus-1. PLoS Pathog. 6:e1000872. 2010.

6. Cvelic-Cabrilo, V., H. Mazija, Z. Bidin, and W. Ragland. Correlation of hemagglutination inhibition and enzyme-linked immunosorbent assays for antibodies to Newcastle disease virus. Avian Pathol. 21:509–512. 1992.

7. Ecco, R., C. Brown, L. Susta, C. Cagle, I. Cornax, M. Pantin-Jackwood, P. J. Miller, and C. L. Afonso. *In vivo* transcriptional cytokine responses and association with clinical and pathological outcomes in chickens infected with different Newcastle disease virus isolates using formalin-fixed paraffin-embedded samples. Vet. Immunol. Immunopathol. 141:221–229. 2011.

8. Jeon, W.-J., E.-K. Lee, Y.-J. Lee, O.-M. Jeong, Y.-J. Kim, J.-H. Kwon, and K.-S. Choi. Protective efficacy of commercial inactivated Newcastle disease virus vaccines in chickens against a recent Korean epizootic strain. J. Vet. Sci. 9:295–300. 2008.

9. Kaiser, P., L. Rothwell, E. E. Galyov, P. A. Barrow, J. Burnside, and P. Wigley. Differential cytokine expression in avian cells in response to invasion by *Salmonella typhimurium*, *Salmonella enteritidis* and *Salmonella gallinarum*. Microbiology 146:3217–3226. 2000.

10. Kapczynski, D. R. Evaluating the cell-mediated immune response of avian species to avian influenza viruses. Meth. Mol. Biol. 436:113–126. 2008.

11. Kapczynski, D. R., and D. J. King. Protection of chickens against overt clinical disease and determination of viral shedding following vaccination with commercially available Newcastle disease virus vaccines upon challenge with highly virulent virus from the California 2002 exotic Newcastle disease outbreak. Vaccine 23:3424–3433. 2005.

12. Liu, X. F., H. Q. Wan, X. X. Ni, Y. T. Wu, and W. B. Liu. Pathotypical and genotypical characterization of strains of Newcastle disease virus isolated from outbreaks in chicken and goose flocks in some regions of China during 1985–2001. Arch. Virol. 148:1387–1403. 2003.

13. Miller, P. J., E. L. Decanini, and C. L. Afonso. Newcastle disease: evolution of genotypes and the related diagnostic challenges. Infect. Gen. Evol. 10:26–35. 2010.

14. Miller, P. J., C. Estevez, Q. Yu, D. L. Suarez, and D. J. King. Comparison of viral shedding following vaccination with inactivated and live Newcastle disease vaccines formulated with wild-type and recombinant viruses. Avian Dis. 53:39–49. 2009.

15. [OIE] World Organization for Animal Health. Manual of diagnostic tests and vaccines for terrestrial animals: mammals, birds and bees. In: Biological Standards Commission. World Organization for Animal Health, Paris. pp. 576–589. 2009.

16. Pflaffl, M. A new mathematical model for relative quantification in real-time PCR. Nucl. Acids Res. 29:2002–2007. 2001.

17. Qin, Z.-M., L.-T. Tan, H.-Y. Xu, B.-C. Ma, Y.-L. Wang, X.-Y. Yuan, and W.-J. Liu. Pathotypical characterization and molecular epidemiology of Newcastle disease virus isolates from different hosts in China from 1996 to 2005. J. Clin. Microbiol. 46:601–611. 2008.

18. Ramakers, C., J. M. Ruijter, R. H. L. Deprez, and A. F. M. Moorman. Assumption-free analysis of quantitative real-time polymerase chain reaction (PCR) data. Neurosci. Lett. 339:62–66. 2003.

19. Reynolds, D., and A. Maraqa. Protective immunity against Newcastle disease: the role of cell-mediated immunity. Avian Dis. 44:145–154. 2000. 10

20. Rue, C. A., L. Susta, I. Cornax, C. C. Brown, D. R. Kapczynski, D. L. Suarez, D. J. King, P. J. Miller, and C. L. Afonso. Virulent Newcastle disease virus elicits a strong innate immune response in chickens. J. Gen. Virol. 92:931–939. 2011.

21. Seal, B. S., D. J. King, and H. S. Sellers. The avian response to Newcastle disease virus. Develop. Comp. Immunol. 24:257–268. 2000.

22. Young, D., R. Randall, J. Hoyle, and B. Souberbielle. Clearance of persistent paramyxovirus infection is mediated by cellular immune responses but not serum neutralizing antibody. J. Virol. 64:5403–5411. 1990.

23. Yu, L., Z. Wang, Y. Jiang, L. Chang, and J. Kwang. Characterization of newly emerging Newcastle disease virus isolates from the People's Republic of China and Taiwan. J. Clin. Microbiol. 39:3512–3519. 2001.

ACKNOWLEDGMENTS

We wish to thank Timothy Olivier and Dawn Williams-Coplin for their excellent technical assistance and Roger Brock for his animal care assistance. This study was funded by USDA ARS CRIS number 6612-32000-049.

AVIAN DISEASES 56:128–133, 2012

Characterization of Newcastle Disease Viruses Isolated from Cormorant and Gull Species in the United States in 2010

Diego G. Diel,[A] Patti J. Miller,[A] Paul C. Wolf,[B] Randall M. Mickley,[C] Anthony R. Musante,[D] Daniel C. Emanueli,[E] Kirk J. Shively,[F] Kerri Pedersen,[G] and Claudio L. Afonso[AH]

[A]United States, Department of Agriculture (USDA), Agricultural Research Service, Southeast Poultry Research Laboratory, 934 College Station Road, Athens, GA 30605
[B]USDA, Animal and Plant Health Inspection Service (APHIS), Wildlife Services, 644 Bayfield Street, Suite 215, St. Paul, MN 55107
[C]USDA, APHIS, Wildlife Services 9 Main Street, Suite 1M, Sutton, MA 01590
[D]USDA, APHIS, Wildlife Services, 59 Chenell Drive, Suite 7, Concord, NH 03301
[E]USDA, APHIS, Wildlife Services, 1568 Whitehall Road, Annapolis, MD 21409
[F]USDA, APHIS, Wildlife Services, 79 Leighton Road, Suite 12, Augusta, ME 04330
[G]USDA, APHIS, Wildlife Services, 4101 LaPorte Avenue, Fort Collins, CO 80521

Received 23 August 2011; Accepted and published ahead of print 6 October 2011

SUMMARY. Newcastle disease virus (NDV), a member of the genus *Avulavirus* of the family *Paramyxoviridae*, is the causative agent of Newcastle disease (ND), a highly contagious disease that affects many species of birds and which frequently causes significant economic losses to the poultry industry worldwide. Virulent NDV (vNDV) is exotic in poultry in the United States; however, the virus has been frequently associated with outbreaks of ND in cormorants, which poses a significant threat to poultry species. Here, we present the characterization of 13 NDV isolates obtained from outbreaks of ND affecting cormorants and gulls in the states of Minnesota, Massachusetts, Maine, New Hampshire, and Maryland in 2010. All 2010 isolates are closely related to the viruses that caused the ND outbreaks in Minnesota in 2008, following the new evolutionary trend observed in cormorant NDV isolates since 2005. Similar to the results obtained with the 2008 isolates, the standard United States Department of Agriculture F-gene real-time reverse-transcription PCR (RRT-PCR) assay failed to detect the 2010 cormorant viruses, whereas all viruses were detected by a cormorant-specific F-gene RRT-PCR assay. Notably, NDV-positive gulls were captured on the eastern shore of Maryland, which represents a significant geographic expansion of the virus since its emergence in North America. This is the first report of vNDV originating from cormorants isolated from wild birds in Maryland and, notably, the first time that genotype V vNDV has been isolated from multiple wild bird species in the United States. These findings highlight the need for constant epidemiologic surveillance for NDV in wild bird populations and for consistent biosecurity measures to prevent the introduction of the agent into domestic poultry flocks.

RESUMEN. Caracterización de los virus de la Enfermedad de Newcastle aislados de Cormoranes y de gaviotas en los Estados Unidos en el 2010.

La enfermedad de Newcastle virus (NDV), un miembro del género *Avulavirus* de la familia *Paramyxoviridae*, es el agente causal de la enfermedad de Newcastle (ND), una enfermedad altamente contagiosa que afecta a muchas especies aviares y que con frecuencia causa importantes pérdidas económicas para la industria avícola en todo el mundo. La enfermedad de Newcastle virulenta (vNDV) es exótica para las aves comerciales en los Estados Unidos, sin embargo, el virus ha sido asociado con frecuencia a los brotes de enfermedad de Newcastle en cormoranes, lo que representa una amenaza significativa para las aves comerciales. En este trabajo se presenta la caracterización de 13 cepas del virus de Newcastle obtenidas de los brotes de la enfermedad de Newcastle que afectaron a los cormoranes y gaviotas en los estados de Minnesota, Massachusetts, Maine, New Hampshire, y Maryland en el año 2010. Todos los aislamientos del 2010 están estrechamente relacionados con el virus que causó los brotes de Newcastle en Minnesota en el año 2008, siguiendo la nueva tendencia de evolución observada en los aislamientos de Newcastle de cormoranes desde el 2005. De manera similar con los resultados obtenidos de los aislamientos del 2008, la técnica estándar de transcripción reversa y reacción en cadena de la polimerasa en tiempo real (RRT-PCR) para el gene de la proteína F, desarrollada por el Departamento de Agricultura de los Estados Unidos, no pudo detectar los virus de cormoranes del año 2010, mientras que todos los virus fueron detectados por un ensayo RRT-PCR para la proteína F específica de los virus de cormoranes. De manera sobresaliente, gaviotas positivas al virus de Newcastle fueron capturadas en la costa oriental de Maryland, lo que representa una expansión geográfica significativa del virus desde su aparición en América del Norte. Este es el primer reporte del aislamiento del virus de Newcastle de aves silvestres en Maryland y, sobre todo, es la primera vez que el genotipo V del virus de Newcastle ha sido aislado de varias especies de aves silvestres en los Estados Unidos. Estos resultados destacan la necesidad de una constante vigilancia epidemiológica para la enfermedad de Newcastle en las aves silvestres y de las medidas de bioseguridad constantes para prevenir la introducción del agente en las parvadas de aves comerciales.

Key words: Newcastle disease virus, NDV, Newcastle disease, cormorants, gulls, outbreak

Abbreviations: bp = base pairs; F = fusion protein; HI = hemagglutination-inhibition; ICPI = intracerebral pathogenicity index; L = large polymerase; M = matrix protein; ND = Newcastle disease; NDV = Newcastle disease virus; NP = nucleoprotein; OIE = World Organization for Animal Health; P = phosphoprotein; RRT-PCR = real-time reverse-transcription PCR; SEPRL = Southeast Poultry Research Laboratory; SPF = specific pathogen free; USDA = United States Department of Agriculture; V = V protein; vNDV = virulent Newcastle disease virus

Newcastle disease (ND) is a highly contagious disease that affects many species of birds and which frequently causes significant economic losses to the poultry industry worldwide (3). The causative agent of ND is Newcastle disease virus (NDV) or avian paramyxovirus type 1, a member of the genus *Avulavirus* of the family *Paramyxoviridae* (14). The NDV genome consists of a single-stranded, negative-sense RNA molecule of approximately 15.2 kb that contains six genes encoding

[H]Corresponding author. E-mail: claudio.afonso@ars.usda.gov

seven proteins (nucleoprotein [N]; phosphoprotein [P]; V protein [V]; matrix protein [M]; fusion protein [F]; and large polymerase [L]) (14,20).

Newcastle disease is characterized by a wide range of clinical signs depending on the virulence of the virus strain and species of bird affected (15). Historically, NDV strains have been classified as velogenic (highly virulent), mesogenic (moderately virulent), and lentogenic (mildly virulent), based on the pathogenicity in chickens and chicken embryos (2,20). Velogenic strains are further divided into neurotropic and viscerotropic, with neurotropic strains causing respiratory and neurologic signs and viscerotropic strains causing hemorrhagic intestinal lesions (2,20). Virulent NDV (vNDV) outbreaks must be reported to the World Organisation for Animal Health (OIE). The OIE defines ND as an infection caused by an avian paramyxovirus type 1 that has an intracerebral pathogenicity index (ICPI) in 1-day-old chickens of 0.7 or greater, has multiple basic amino acid residues (at least three residues) at the C-terminus of the fusion (F) protein cleavage site (residues 113–116) and a phenylalanine residue at position 117 (17). All velogenic and some mesogenic strains of NDV are considered virulent for chickens.

NDV is known for its ability to infect many species of birds with more than 250 species in 27 orders being susceptible (3). NDV infections in wild birds represent a constant threat to the poultry industry and pose significant difficulties to disease control strategies (3). Although infections of wild birds are usually subclinical with most NDV isolates being lentogenic, outbreaks of velogenic NDV have been frequently reported in cormorants in several regions of the world including Canada and northern states of the United States (7,9,13,18). In this species, the disease is characterized mainly by neurologic signs including head tremors, ataxia, and paralysis of the legs and wings, circling, and in some cases blindness (12,13). High mortality rates (up to 92%) are observed in juvenile birds with adult birds being more resistant to the disease, although paresis and other neurologic signs have been reported (7,11).

NDV has been associated with cormorants and gulls since 1949, when hemagglutination-inhibition (HI) antibodies were detected in birds captured in Scotland (5). In North America, the first outbreak of NDV in cormorants and gulls was reported in 1975 in Canada (8) and then in 1990 in the provinces of Alberta, Saskatchewan, and Manitoba (26). In 1992, the disease was observed for the first time in cormorants in the United States, resulting in the death of approximately 20,000 double-crested cormorants (*Phalacrocorax auritus*) in seven northern states and in one province of Canada (7). Since then, vNDV has been repeatedly reported in cormorants in United States and Canada (7,9,12,13,18), indicating that it became established in this species (3,7). Notably, in the United States, pigeons and cormorants represent the only known natural reservoirs of vNDV in wild bird populations (3,16); therefore, it is important to continually evaluate the evolution and pathogenicity of NDV isolates obtained from these species.

Here, we present the characterization of 13 NDV isolates obtained from outbreaks of ND that occurred in 2010 in the states of Minnesota, Massachusetts, Maine, New Hampshire, and Maryland. NDV isolates were obtained from double-crested cormorants, great cormorants (*Phalacrocorax carbo*), herring gulls (*Larus argentatus*), and great black-backed gulls (*Larus marinus*). Detection of NDV in herring and great black-backed gulls in Maryland represents a significant geographic and host range expansion for the virus in wildlife (22). This is the first report of vNDV originating from cormorants isolated from wild birds in Maryland and, notably, the first time that genotype V vNDV has been isolated from multiple wild bird species in the United States. These observations highlight the need for constant epidemiologic surveillance for NDV in wild bird populations and for consistent biosecurity measures to prevent the introduction of the agent into domestic poultry flocks.

MATERIALS AND METHODS

Viruses and virus isolation. Thirteen NDV isolates were obtained from the United States Department of Agriculture (USDA) Southeast Poultry Research Laboratory (SEPRL) repository. The viruses were isolated from oral and/or cloacal swabs samples collected during outbreaks of ND affecting cormorants (double-crested and great cormorants) and gulls (herring and black-backed gulls) in the states of Minnesota, Massachusetts, Maine, New Hampshire, and Maryland in 2010. Viruses were isolated from swab samples by standard virus isolation in specific-pathogen-free (SPF) embryonated chicken eggs (2).

ICPI test. The pathogenicity of nine cormorant–gull NDV isolates was assessed by using the ICPI test (2). One-day-old SPF chickens were inoculated intracerebrally with 0.1 ml of a 1:10 dilution of infective allantoic fluid. Chicks were monitored during an 8-day observation period and scored as normal (score = 0), sick or paralyzed (score = 1), and dead (score = 2). Total scores were determined and the mean daily scores were calculated to obtain the ICPI (2).

RNA extraction and real-time RT-PCR (RRT-PCR). All NDV isolates ($n = 13$) were propagated in SPF embryonated chicken eggs. Total RNA was extracted from allantoic fluid using TRIzol® LS (Invitrogen, Carlsbad, CA) following the manufacturer's protocol. All isolates were tested using the USDA standard F-gene RRT-PCR assay (25) and a cormorant-specific F-gene RRT-PCR assay (18).

Sequencing of the fusion gene. The complete F-gene coding sequences or a 374-base pair (bp) region of the F-gene (1) were amplified from the genome of all NDV isolates by using the Superscript™ III One-step RT-PCR kit (Invitrogen) and F-gene-specific primers (1,25). PCR reactions were subjected to electrophoresis in 1% agarose gels and the DNA bands were excised from the gel and purified by using the QIAquick Gel Extraction Kit (Qiagen, Valencia, CA).

All sequencing reactions were performed with fluorescent dideoxynucleotide terminators in the ABI 3700 automated sequencer (Applied Biosystems Inc., Foster City, CA). Sequence editing and assembly was performed with LaserGene sequence analysis software package (LaserGene, version 5.07; DNAStar, Inc., Madison, WI).

Phylogenetic analysis. A 373-bp region of the F-gene (1) was used to construct the phylogenetic trees and to localize the 2010 cormorant–gull NDV isolates ($n = 13$) among other class II genotype reference sequences ($n = 67$). Phylogenetic analysis was performed by using MEGA4 software (MEGA, version 4) (23). The evolutionary distances were inferred by using the neighbor-joining method (19) with 100 bootstrap replicates and included the first, second, and third coding and noncoding positions.

Accession numbers. The sequences of the F-gene of the NDV isolates characterized in the present study are available on GenBank under the accession numbers JN255784, JN255773, JN255774, JN255775, JN255776, JN255777, JN255778, JN255779, JN255780, JN255781, JN255782, JN255783, JN255784, JN255785.

RESULTS

During the 2010 cormorant–gull NDV outbreaks in Minnesota, Massachusetts, Maine, New Hampshire, and Maryland, the USDA SEPRL received 62 samples (oral and/or cloacal swabs) collected from various avian species including double-crested cormorants (*Phalacrocorax auritus*; $n = 31$), great cormorants (*Phalacrocorax carbo*; $n = 2$), great black-backed gulls (*Larus marinus*; $n = 15$), herring gulls (*Larus argentatus*; $n = 2$), and mallards (*Anas platyrhynchos*; $n = 1$). NDV was isolated or detected by RRT-PCR in 32 (62.7%) of these samples, including samples from double-crested and great cormorants and from great black-backed and herring gulls. Thirteen of these isolates were characterized in the present study. All isolates were subjected to

Table 1. Virulent Newcastle disease viruses isolated from cormorants and gulls in the United States in 2010.

SEPRL no.	GenBank Accession no.	Date collected	Species	Location	Fusion protein RRT-PCR: USDA F-test	Fusion protein RRT-PCR: Cormorant F-test	Sequencing	Fusion protein cleavage site aa sequence[A]	ICPI
648	JN255784	08/26/2010	DCCO[B]	Leech Lake, MN	−	+	Full fusion	^{110}R-G-K-R-Q-K-R-F^{117}	1.43
649	JN255773	08/26/2010	DCCO	Leech Lake, MN	−	+	374 region	^{110}R-G-K-R-Q-K-R-F^{117}	ND[C]
650	JN255774	09/11/2010	DCCO	Barnstable County, MA	−	+	Full fusion	^{110}R-G-K-R-Q-K-R-F^{117}	1.55
651	JN255775	06/13/2010	DCCO	Salisbury, MA	−	+	Full fusion	^{110}R-G-K-R-Q-K-R-F^{117}	1.51
652	JN255785	09/17/2010	DCCO	Portsmouth, NH	−	+	Full fusion	^{110}R-G-K-R-Q-K-R-F^{117}	1.39
653	JN255776	09/15/2010	DCCO	Barnstable County, MA	−	+	374 region	^{110}R-G-K-R-Q-K-R-F^{117}	ND
654	JN255777	09/17/2010	GRCO[D]	Seabrook, NH	−	+	Full fusion	^{110}R-G-K-R-Q-K-R-F^{117}	ND
655	JN255778	09/2010	GBBG[E]	Poplar Island, MD	−	+	Full fusion	^{110}R-G-K-R-Q-K-R-F^{117}	1.38
656	JN255779	09/2010	HERG[F]	Poplar Island, MD	−	+	Full fusion	^{110}R-G-K-R-Q-K-R-F^{117}	1.39
657	JN255780	09/2010	GBBG	Poplar Island, MD	−	+	374 region	^{110}R-G-K-R-Q-K-R-F^{117}	ND
658	JN255781	10/02/2010	DCCO	Portland, ME	−	+	Full fusion	^{110}R-G-K-R-Q-K-R-F^{117}	1.45
659	JN255782	10/11/2010	DCCO	Kennebunk, ME	−	+	Full fusion	^{110}R-G-K-R-Q-K-R-F^{117}	1.53
660	JN255783	09/18/2010	DCCO	Lewiston, ME	−	+	Full fusion	^{110}R-G-K-R-Q-K-R-F^{117}	ND

[A]Fusion protein cleavage site amino acid residues 110 to 117.
[B]DCCO = double-crested cormorant (*Phalacrocorax auritus*).
[C]ND = not determined.
[D]GRCO = great cormorant (*Phalacrocorax carbo*).
[E]GBBG = great black-backed gull (*Larus argentatus*).
[F]HERG = herring gull (*Larus marinus*).

phylogenetic analysis to determine the evolutionary distances to other NDV strains and eight isolates were further characterized for their pathogenicity in 1-day-old chickens by standard ICPI tests.

Clinical signs observed in birds affected by ND during the 2010 outbreaks included torticollis, paralysis of the legs and wings, tremors, and lack of muscular coordination. Approximately 1100 birds died during these outbreaks and among the affected species were double-crested cormorants, great cormorants, black-backed gulls, and herring gulls. Other avian species such as ring-billed gulls, mallards, egrets, terns, and American white pelicans were found dead (22); however, no evidence of NDV infection was detected in these species (data not shown). A summary with the information about the NDV isolates characterized here is presented in Table 1.

To assess the pathogenicity of the 2010 cormorant NDV isolates, eight viruses were subjected to the ICPI test in 1-day-old chickens. All viruses presented ICPI values between 1.38 and 1.55 (Table 1), which is typical for viruses isolated from cormorants (18), and characterize them as vNDV based on the OIE standards. Additionally, all viruses presented a virulent fusion protein cleavage site with three basic amino acids at the C-terminus of the protein (positions 113–116) and a phenylalanine residue at position 117 (Table 1) (17).

All isolates were tested by the USDA-validated RRT-PCR F-gene assay (25) and by the cormorant RRT-PCR assay (18). Similar to the results obtained with the 2008 cormorant isolates (18), the USDA-validated F-gene assay failed to detect all 2010 isolates, whereas all isolates were detected by the cormorant F-gene RRT-PCR assay (Table 1).

The evolutionary distances between the 2010 cormorant isolates and other NDV strains were assessed by phylogenetic analysis. A 373-bp region of the F-gene (1) was used for the phylogenetic analysis of 13 isolates from 2010 and other reference strains (n = 67). All 2010 cormorant isolates clustered with the 2008 cormorant isolates within the class II genotype V group (Fig. 1). The nearest ancestors of the 2010 viruses are the viruses G/2008/US/MN/284019481, G/2008/US/MN/284019485, and G/2008/US/MN/284019495 obtained in the 2008 cormorant ND outbreak in Minnesota. Both 2008 and 2010 viruses are closely related to a virus isolate obtained during an outbreak in Nevada in 2005 (cormorant/2005/US/NV/19529-04), suggesting a common ancestor for these viruses (Fig. 1). Phylogenetic analysis of the complete coding sequences of the F-gene revealed a similar distribution of the viruses in the phylogenetic tree, with the 2010 isolates clustering with the 2008 viruses within the class II genotype V group (data not shown).

→

Fig. 1. Phylogenetic analysis of the 2010 cormorant NDV isolates and other reference strains on GenBank. A 373-bp region of the F-gene was used to construct the phylogenetic tree and to localize the 2010 isolates among other NDV strains. The evolutionary history was inferred using the neighbor-joining method (19). The optimal tree with the sum of branch length = 2.27030740 is shown. The percentage of replicate trees in which the associated taxa

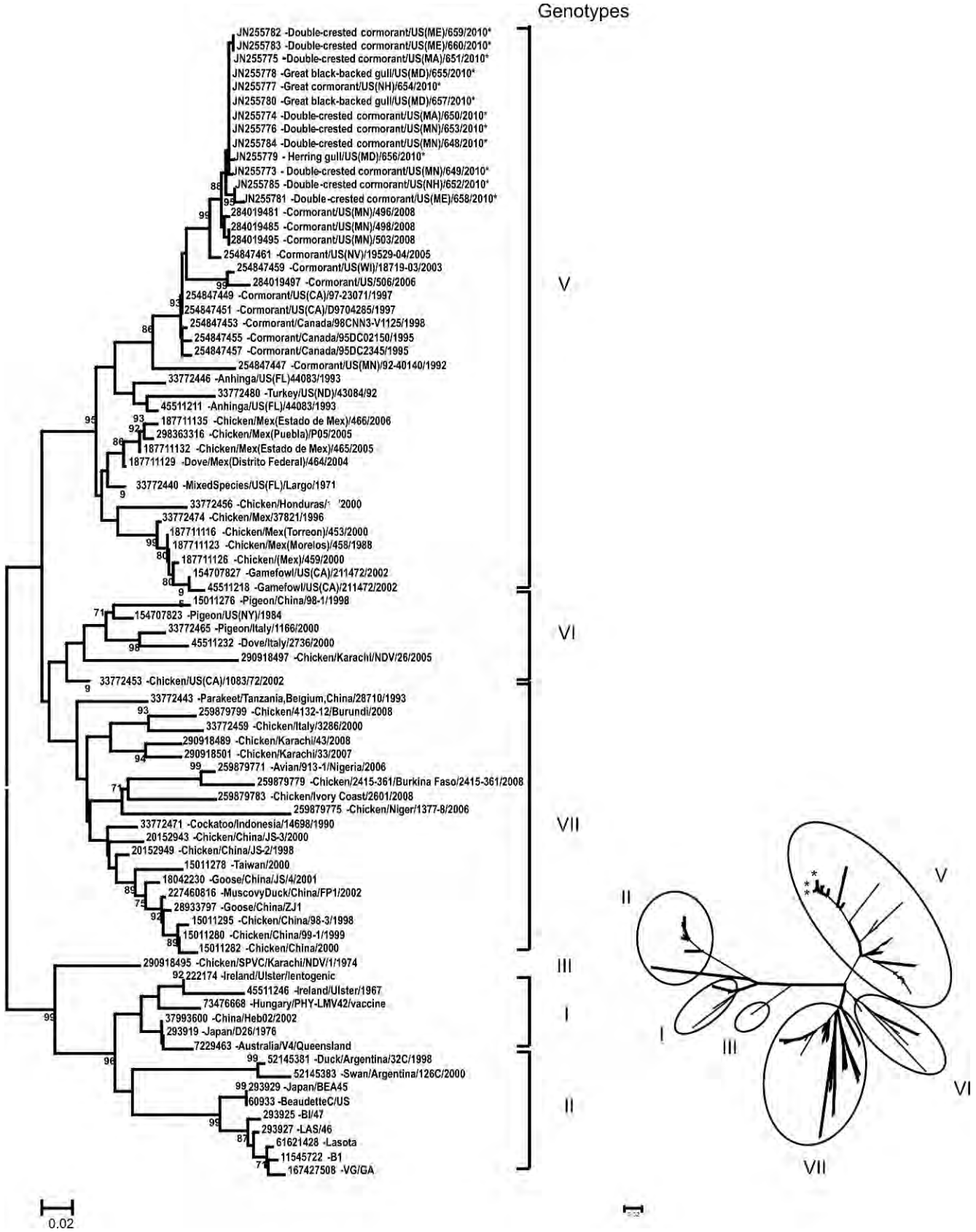

clustered together in the bootstrap test (100 replicates) is shown next to the branches (6). The tree is drawn to scale, with branch lengths in the same units as those of the evolutionary distances used to infer the phylogenetic tree. The evolutionary distances were computed using the maximum composite likelihood method (24) and are in the units of the number of base substitutions per site. Codon positions included were 1st+2nd+3rd+Noncoding. All positions containing gaps and missing data were eliminated from the dataset (complete deletion option). There were a total of 14,903 positions in the final dataset. Phylogenetic analysis was conducted in MEGA4 (23). * = NDV isolates obtained during the 2010 outbreak.

DISCUSSION

In this study we present the characterization of 13 NDV isolates obtained during outbreaks of ND that affected cormorants and gulls in the states of Minnesota, Massachusetts, Maine, New Hampshire, and Maryland in 2010. Notably, NDV-positive gulls were captured on the eastern shore of Maryland, 60 mi away from commercial poultry houses that are part of the Delmarva Poultry Industry. This represents the first report of NDV isolation from wild birds in Maryland, indicating a significant eastward expansion of the virus since its emergence in North America (22).

NDV emerged in cormorants in North America in 1990 (26), and the first occurrence of the disease in cormorants in the United States was in 1992 (7). Since then, vNDV has been frequently associated with outbreaks of ND in cormorants, leading to variable mortality rates (<1 to 92%) in juvenile birds (7,9,12,13,18). The periodic occurrence of ND in cormorants indicates that vNDV became established in this species (7). Indeed, pigeons and cormorants are the only known natural reservoirs of vNDV in the wild in the United States (3,16), highlighting the importance of constant epidemiologic surveillance and proactive characterization of NDV isolates circulating in these species.

The pathogenicity of cormorant NDV isolates has not changed since its emergence in this species in 1949 (5), with all characterized isolates being classified as mesogenic or velogenic neurotropic viruses (7,9,12,13,18). The isolates characterized here presented ICPI values ranging from 1.38 to 1.55, which is consistent with vNDV strains (3,17). The clinical signs (torticollis, paralysis of the legs and wings, tremors, and lack of muscular coordination) observed in affected birds during the 2010 outbreaks (22) are consistent with the involvement of the central nervous system and further suggest that these viruses belong to the neurotropic NDV pathotype. However, the possibility that some of these isolates belong to the viscerotropic pathotype cannot be formally excluded.

Virulent NDV is exotic in poultry in the United States (3), but the frequent association of the virus with outbreaks in cormorants poses a significant threat to the poultry industry. Here, vNDV was isolated from wild birds (gulls) collected in close proximity (~60 miles) to the Delmarva poultry industry in Maryland, which is of great concern given the high concentration of poultry in this area. Isolation of vNDV from gulls represents an additional risk to poultry flocks, given that these birds are often found in poultry farms (10) and, therefore, could potentially introduce the virus into poultry flocks. Although of rare occurrence, there is strong evidence indicating that vNDV has been transmitted from cormorants to a turkey flock in North Dakota in 1992 (9,21), which highlights the importance of consistent biosecurity measures to prevent the introduction of vNDV, circulating in wild bird populations, into commercial poultry flocks.

Phylogenetic analysis revealed that the 2010 cormorant NDV isolates are closely related to the NDV strains that caused the outbreak in Minnesota in 2008 (18) with all 2010 isolates clustering with the 2008 viruses in the class II genotype V group (Fig. 1). Notably, since the emergence of ND in cormorants in North America, all viruses have been classified in the same genetic lineage of genotype V, suggesting co-evolution of the virus with this particular host species. Analysis of the nucleotide sequences of the F-gene cleavage site revealed that the evolutionary changes observed in the 2008 viruses, which led to failure of the USDA F-gene RRT-PCR assay in detecting the cormorant viruses (18), are also present in the 2010 viruses. Indeed, the USDA-validated F-gene RRT-PCR assay failed to detect the 2010 isolates, whereas all viruses were detected by the cormorant F-gene RRT-PCR assay (18). These findings suggest that the 2010 isolates may have originated from the 2008 viruses or that the two outbreaks may have been caused by the same epizootic virus.

Although vNDV has been frequently associated with outbreaks of ND in cormorants, the epidemiology of NDV infection in this species is still not completely understood. It has been hypothesized that adult birds may play a critical role in maintaining NDV in cormorant populations (4). Adult and older juvenile birds, which are resistant to clinical ND, may carry NDV subclinically, thus spreading the virus to birds from distinct geographic areas during wintering (4). Birds subclinically infected in wintering grounds reinitiate the disease cycle in the nesting sites after spring migration (4). This dynamic cycle of NDV in cormorants may partially explain the eastward expansion of the virus during the 2010 outbreaks when compared to the 2008 outbreaks. It is possible that adult birds subclinically infected during the 2008 outbreaks in Minnesota have spread the virus, during wintering, to birds from eastern nesting sites, thereby leading to the 2010 outbreaks in Massachusetts, Maine, New Hampshire, and Maryland. However, a complete epidemiologic–surveillance study is needed to draw definitive conclusions about the source of the 2010 outbreaks.

In summary, the 2010 cormorant NDV isolates are closely related to the 2008 viruses, following the new evolutionary trend observed in cormorant NDV isolates since 2005. Although such evolutionary changes had no apparent effect on virus virulence, they are responsible for the failure of the USDA-validated F-gene RRT-PCR assay to detect the cormorant and gull viruses, making necessary the use of a cormorant-specific F-gene RRT-PCR assay (18) for the diagnosis of NDV in these species. Isolation of virulent NDV from multiple wild bird species (cormorants and gulls) and in close proximity with the Delmarva poultry industry in Maryland poses a significant threat to poultry species and highlights the need for constant epidemiologic surveillance for NDV in wild bird populations and for consistent biosecurity measures to prevent the introduction of the agent into commercial poultry flocks.

REFERENCES

1. Aldous, E. W., J. K. Mynn, J. Banks, and D. J. Alexander. A molecular epidemiological study of avian paramyxovirus type 1 (Newcastle disease virus) isolates by phylogenetic analysis of a partial nucleotide sequence of the fusion protein gene. Avian Pathol. 32:239–256. 2003.

2. Alexander, D. J. Newcastle disease and other avian paramyxoviruses. In: A laboratory manual for the isolation and identification of avian pathogens, 4th ed. D. E. Swayne, J. R. Glisson, M. W. Jackwood, J. E. Pearson, and W. M. Reed, eds. International Book Distributing Co., Tallahassee, FL. pp. 156–163. 2006.

3. Alexander, D. J., and D. A. Senne. Newcastle disease, other avian paramyxoviruses, and pneumovirus infections. In: Diseases of poultry, 12th ed. Y. M. Saif, A. M. Fadly, J. R. Glisson, L. R. McDougald, L. K. Nolan, and D. E. Swayne, eds. Blackwell Publishing, Ames, IA. pp. 75–98. 2008.

4. Allison, A. B., N. L. Gottdenker, and D. E. Stallknecht. Wintering of neurotropic velogenic Newcastle disease virus and West Nile virus in double-crested cormorants (Phalacrocorax auritus) from the Florida Keys. Avian Dis. 49:292–297. 2005.

5. Blaxland, J. D. Newcastle disease in shags and cormorants and its significance as a factor in the spread of the disease among domestic poultry. Vet. Rec. 63:731–733. 1951.

6. Felsenstein, J. Confidence limits on phylogenesis: an approach using the bootstrap. Evolution 39:783–791. 1985.

7. Glaser, L. C., I. K. Barker, D. V. Weseloh, J. Ludwig, R. M. Windingstad, D. W. Key, and T. K. Bollinger. The 1992 epizootic of Newcastle disease in double-crested cormorants in North America. J. Wildl. Dis. 35:319–330. 1999.

8. Heckert, R. A. Ontario. Newcastle disease in cormorants. Can. Vet. J. 34:184. 1993.

9. Heckert, R. A., M. S. Collins, R. J. Manvell, I. Strong, J. E. Pearson, and D. J. Alexander. Comparison of Newcastle disease viruses isolated from

cormorants in Canada and the USA in 1975, 1990 and 1992. Can. J. Vet. Res. 60:50–54. 1996.

10. Kuiken, T. Review of Newcastle disease in cormorants. J. Waterbirds Soc.; Waterbirds 22:333–347. 1999.

11. Kuiken, T., D. Frandsen, and A. Clavijo. Newcastle disease in cormorants. Can. Vet. J. 39:299. 1998.

12. Kuiken, T., F. A. Leighton, G. Wobeser, K. L. Danesik, J. Riva, and R. A. Heckert. An epidemic of Newcastle disease in double-crested cormorants from Saskatchewan. J. Wildl. Dis. 34:457–471. 1998.

13. Kuiken, T., G. Wobeser, F. A. Leighton, D. M. Haines, B. Chelack, J. Bogdan, L. Hassard, R. A. Heckert, and J. Riva. Pathology of Newcastle disease in double-crested cormorants from Saskatchewan, with comparison of diagnostic methods. J. Wildl. Dis. 35:8–23. 1999.

14. Lamb, R. A., and G. D. Parks. Paramyxoviridae: the viruses and their replication. In: Field's virology, 5th ed. D. M. Knipe, P. M. Howley, D. E. Griffin, R. A. Lamb, M. A. Martin, B. Roizman, and S. E. Straus, eds. Lippincott Williams & Wilkins, Philadelphia. pp. 1449–1496. 2007.

15. McLachland, N. J., and E. J. Dubovi. Paramyxoviridae. In: Fenner's veterinary virology, 4th ed. N. J. McLachland, and E. J. Dubovi, eds. Academic Press, London. pp. 299–325. 2011.

16. Miller, P. J., and C. L. Afonso. Newcastle disease virus. In: Encyclopedia of life sciences. John Wiley and Sons, Ltd., Chichester, U.K. pp. 1–9. 2011.

17. [OIE] World Organisation for Animal Health. Newcastle Disease. In: Manual of diagnostic tests for terrestrial animals: mammals, birds and bees, 7th ed. OIE, Paris, France. pp. 576–589. 2009.

18. Rue, C. A., L. Susta, C. C. Brown, J. M. Pasick, S. R. Swafford, P. C. Wolf, M. L. Killian, J. C. Pedersen, P. J. Miller, and C. L. Afonso. Evolutionary changes affecting rapid identification of 2008 Newcastle disease viruses isolated from double-crested cormorants. J. Clin. Microbiol. 48:2440–2448. 2010.

19. Saitou, N., and M. Nei. The neighbor-joining method: a new method for reconstructing phylogenetic trees. Mol. Biol. Evol. 4:406–425. 1987.

20. Samal, S. K. Paramyxoviruses of animals. In: Encyclopedia of virology, 3rd ed. Lippincott Williams and Wilkins, Philadelphia. pp. 40–47. 2008.

21. Seal, B. S. Analysis of matrix protein gene nucleotide sequence diversity among Newcastle disease virus isolates demonstrates that recent disease outbreaks are caused by viruses of psittacine origin. Virus Genes 11:217–224. 1995.

22. Sleeman, J. Summary of 2010 Newcastle disease virus outbreaks in wild birds in upper Midwest and the Northeast. Wildl. Health Bull. 2010:1–3. 2010.

23. Tamura, K., J. Dudley, M. Nei, and S. Kumar. MEGA4: Molecular evolutionary genetics analysis (MEGA) software version 4.0. Mol. Biol. Evol. 24:1596–1599. 2007.

24. Tamura, K., M. Nei, and S. Kumar. Prospects for inferring very large phylogenies by using the neighbor-joining method. Proc. Natl. Acad. Sci. U. S. A. 101:11030–11035. 2004.

25. Wise, M. G., D. L. Suarez, B. S. Seal, J. C. Pedersen, D. A. Senne, D. J. King, D. R. Kapczynski, and E. Spackman. Development of a real-time reverse-transcription PCR for detection of Newcastle disease virus RNA in clinical samples. J. Clin. Microbiol. 42:329–338. 2004.

26. Wobeser, G., F. A. Leighton, R. Norman, D. J. Myers, D. Onderka, M. J. Pybus, J. L. Neufeld, G. A. Fox, and D. J. Alexander. Newcastle disease in wild water birds in western Canada, 1990. Can. Vet. J. 34:353–359. 1993.

ACKNOWLEDGMENTS

We thank Dawn Williams-Coplin and Tim Olivier for technical assistance and the SEPRL sequencing facility personnel for nucleotide sequencing.

JCM Journals.ASM.org

Complete Genome and Clinicopathological Characterization of a Virulent Newcastle Disease Virus Isolate from South America

Diego G. Diel,[a] Leonardo Susta,[b] Stivalis Cardenas Garcia,[a,c] Mary L. Killian,[d] Corrie C. Brown,[b] Patti J. Miller,[a] and Claudio L. Afonso[a]

USDA, ARS, Southeast Poultry Research Laboratory, Athens, Georgia, USA[a]; Department of Pathology, College of Veterinary Medicine, The University of Georgia, Athens, Georgia, USA[b]; Investigación Aplicada S.A. (IASA), Tehuacán, Puebla, Mexico[c]; and USDA, National Veterinary Services Laboratories, Ames, Iowa, USA[d]

Newcastle disease (ND) is one of the most important diseases of poultry, negatively affecting poultry production worldwide. The disease is caused by Newcastle disease virus (NDV) or avian paramyxovirus type 1 (APMV-1), a negative-sense single-stranded RNA virus of the genus *Avulavirus*, family *Paramyxoviridae*. Although all NDV isolates characterized to date belong to a single serotype of APMV-1, significant genetic diversity has been described between different NDV isolates. Here we present the complete genome sequence and the clinicopathological characterization of a virulent Newcastle disease virus isolate (NDV-Peru/08) obtained from poultry during an outbreak of ND in Peru in 2008. Phylogenetic reconstruction and analysis of the evolutionary distances between NDV-Peru/08 and other isolates representing established NDV genotypes revealed the existence of large genomic and amino differences that clearly distinguish this isolate from viruses of typical NDV genotypes. Although NDV-Peru/08 is a genetically distinct virus, pathogenesis studies conducted with chickens revealed that NDV-Peru/08 infection results in clinical signs characteristic of velogenic viscerotropic NDV strains. Additionally, vaccination studies have shown that an inactivated NDV-LaSota/46 vaccine conferred full protection from NDV-Peru/08-induced clinical disease and mortality. This represents the first complete characterization of a virulent NDV isolate from South America.

Newcastle disease (ND), is one the most important diseases of poultry, negatively affecting poultry production worldwide (2). ND is caused by Newcastle disease virus (NDV) or avian paramyxovirus type 1 (APMV-1), a negative-sense single-stranded RNA virus of the genus *Avulavirus*, family *Paramyxoviridae* (2). The NDV genome is ~15.2 kb in length and contains six genes encoding at least seven proteins named nucleoprotein (NP), phosphoprotein (P), matrix protein (M), fusion protein (F), hemagglutinin-neuraminidase (HN), RNA-dependent RNA polymerase (L), and V protein, which is produced through editing of the phosphoprotein mRNA (2). ND is characterized by a wide range of clinical manifestations, which vary in severity from subclinical respiratory or enteric infections to fatal neurological or enteric hemorrhagic disease (17).

Although all NDV isolates characterized to date belong to a single serotype, the avian paramyxovirus serotype 1 (APMV-1), significant genetic diversity has been recognized among different NDV isolates (16). Historically, NDV isolates have been classified into two major groups (class I and II), based on their genome lengths and the nucleotide sequences of their genomes (1, 4, 14, 15, 32). Class I viruses are distributed worldwide and have been isolated mainly from waterfowl and shorebirds (7, 8). Class II viruses have been divided into 11 genotypes (I to XI) (4, 14), with genotypes V, VI, VII, and VIII being the predominant genotypes circulating worldwide (14, 15). Among these, genotype VII viruses are particularly important given that they have been associated with many of the most recent outbreaks in Asia, Africa, and the Middle East (12, 14, 15, 32, 34). Additionally, a recent outbreak of ND in South America (Venezuela) has been attributed to a genotype VII virus, suggesting that viruses of this genotype are spreading worldwide (20). Notably, recent phylogenetic studies have shown that NDV is continuously evolving, with viruses of different genotypes undergoing simultaneous changes at different geographic locations, which eventually leads to diagnostic failures (14, 21, 23).

Virulent NDV (vNDV) occurs in at least six of the seven continents of the world and is enzootic in several countries, posing a constant threat to the poultry industry (14). In 2010, infection by vNDV was confirmed in 80 countries, including infections in wild birds in Israel, Kenya, Mongolia, Germany, Italy, Canada, and the United States and infections in domestic poultry in countries of North and South America, Europe, Africa, and Asia (18). In South America, vNDV infection is endemic in some of the northern countries, such as Venezuela, Colombia, and Suriname, while in southern countries, including Chile, Argentina, Uruguay, and Brazil, the disease is only occasionally reported (19). Although vNDV circulates and frequently causes outbreaks in South America, very little information is available on the epidemiology and evolutionary trends of the isolates circulating in that continent. Virulent NDV is exotic in poultry in the United States (31), and migration and/or illegal importation of birds from areas where vNDV is endemic represents a constant threat to the U.S. poultry industry (9, 10, 30). The last outbreak of ND in poultry in the U.S., for example, occurred in California during 2002 and 2003, likely as a result of illegal importation of birds and led to depopulation of more than 3 million birds and containment costs of more than U.S. $160 million (31). These observations highlight the importance of constant epidemiological surveillance for NDV and the need

Received 6 October 2011 Returned for modification 31 October 2011
Accepted 21 November 2011
Published ahead of print 30 November 2011
Address correspondence to P. J. Miller, patti.miller@ars.usda.gov.
Copyright © 2012, American Society for Microbiology. All Rights Reserved.
doi:10.1128/JCM.06018-11

for a proactive characterization of the isolates circulating worldwide. Here we present the complete genome and the clinicopathological characterization of a genetically distinct NDV isolate (poultry/Peru/1918-03/2008 [NDV-Peru/08]) obtained during an outbreak of ND reported by the Official Veterinary Services (SENASA) in Peru in 2008.

MATERIALS AND METHODS

Viruses. The NDV isolate poultry/Peru/1918-03/2008 (NDV-Peru/08) was obtained from the USDA National Veterinary Services Laboratories (NVSL) repository (after authorization by the Official Veterinary Services of Peru [SENASA]). The virus was isolated from swab samples during an outbreak of ND affecting domestic poultry flocks in the region of Pachacutec, Arequipa, Peru, in 2008. Egg passage 2 (EP2) virus stocks were used for RNA extraction and in all pathogenesis experiments in the present study. The NDV strain LaSota/46 was obtained from the SEPRL repository and grown in 9- to 10-day-old specific-pathogen-free (SPF) embryonated chicken eggs (ECE). Allantoic fluid collected from NDV-LaSota/46-inoculated eggs was used for the production of an inactivated vaccine as described below.

Eggs and chickens. Embryonated chicken eggs and chickens were obtained from the SEPRL SPF white Leghorn flock. Birds were housed in negative pressure isolators under biosafety level 3 (BSL-3) enhanced containment and received food and water *ad libitum*.

ICPI test. Pathogenicity of NDV-Peru/08 was assessed by using the standard intracerebral pathogenicity index (ICPI) test (3). Day-old chicks were inoculated intracerebrally with 0.1 ml of a 1:10 dilution of infective allantoic fluid. Chicks were monitored during an 8-day observation period and scored as follows: normal, 0; sick or paralyzed, 1; or dead, 2. Total scores were determined, and the mean daily score was calculated to obtain the ICPI (3).

RNA isolation and sequencing. The NDV-Peru/08 isolate was propagated in SPF embryonated chicken eggs. Total RNA was extracted from allantoic fluids using TRIzol LS (Invitrogen, Carlsbad, CA) following the manufacturer's instructions. The F gene sequence was determined by PCR amplification of the complete gene (primers available upon request), followed by sequencing of the amplicon with fluorescent dideoxynucleotide terminators in an ABI 3700 automated sequencer (Applied Biosystems, Inc., Foster City, CA).

The complete genome sequence of NDV-Peru/08 was determined by using a shotgun reverse transcription (RT)-PCR/sequencing approach. Amplification reactions were performed with the one-step RT-PCR kit (Qiagen, Valencia, CA) and the following set of degenerated primers: beg2 (5′-CGCGTCGACTACTACGGGTAGA-3′) and end-r (5′-GTACCCGG GGATCCTTTTTTCTAA-3′) and FR26RV-N (5′-GCCGGAGCTCTGC AGATATC-3′) and FR20RV (5′-GCCGGAGCTCTGCAGATATC-3′). The PCR amplicons were subjected to electrophoresis in 1% agarose gels, and DNA bands with lengths of 500 to 1,000 bp and those longer than 1,001 bp were excised from the gels and purified by using the QuickClean DNA gel extraction kit (Qiagen, Valencia, CA). The purified PCR products were cloned in the TOPO TA vector (Invitrogen, Carlsbad, CA) according to the manufacturer's instructions and subjected to DNA sequencing as described above. Sequence editing and assembly were performed with the LaserGene sequence analysis software package (LaserGene, version 5.07; DNAStar, Inc., Madison, WI).

Phylogenetic analysis. The complete F and the complete genome sequences were used to construct the phylogenetic trees and to localize NDV-Peru/08 among other class II reference strains. Phylogenetic analysis was performed by using the MEGA5 software (MEGA, version 5) (28). The evolutionary distances were inferred using MEGA 5 (27) and were expressed based on the number of nucleotide substitutions per site. The codon positions included in the analysis were the 1st, 2nd, 3rd, and noncoding. All positions containing gaps and missing data were eliminated from the data set (the "complete deletion" option). Analysis of recombination was performed using RDP3 (13). The numbers used in the phylogenetic trees represent the GenInfo Identifier (GI) sequence identification number in GenBank.

Sequence alignment. Alignment and comparison of the nucleotide and amino acid sequences between NDV-Peru/08 and selected strains representing established NDV genotypes were performed by using the software ClustalW (29).

Animal inoculations. The clinicopathological features of NDV-Peru/08 infection were assessed in chickens. Forty 4-week-old SPF white Leghorn chickens were randomly allocated to four experimental groups, consisting of two NDV-Peru/08-infected groups (group 1, $n = 10$; and group 2, $n = 10$) and two mock-infected (control) groups ($n = 10$). Birds were inoculated with a virus suspension (0.1 ml) containing 10^5 50% embryo infectious doses (EID_{50})/0.1 ml. Half of the inoculum (0.05 ml) was applied to the conjunctival sac, and half (0.05 ml) to the choanal cleft (26). Mock-infected control birds were inoculated as described above with 0.1 ml of phosphate-buffered saline (PBS). Birds were monitored daily for characteristic clinical signs of Newcastle disease. Two birds of groups 1 (NDV-Peru/08) and 2 (PBS control) were euthanized and necropsied at 2 and 5 days postinoculation (dpi), and all birds *in extremis* (presenting a severe clinical condition) were euthanized regardless of the sampling schedule. Tissue samples consisting of eyelid, spleen, bursa of Fabricius, thymus, Harderian gland, proventriculus, small intestine, cecal tonsils, large intestine, air sacs, trachea, lung, heart, esophagus, pharynx, crop, brain, liver, pancreas, kidney, comb, head of the femur, and nasal turbinate were collected and fixed in 10% neutral buffered formalin for 52 h. All sampled tissues were processed for histological examination and/or immunohistochemistry (IHC) using standard procedures (26). Oral and cloacal swabs were collected on days 2, 3 and 4 postinoculation (p.i.) and processed for virus isolation as described below. Birds of groups 2 (NDV-Peru/08) and 4 (PBS control) were monitored daily for characteristic clinical signs of Newcastle disease, and the time of death was recorded and used to plot the survival curves and to calculate the mean death time.

Virus isolation and quantitation. Virus shedding was assessed in oral and cloacal secretions from all inoculated birds. Swab samples were cleared by centrifugation at $1,000 \times g$ for 20 min, and the supernatant was subjected to virus isolation in 9- to 10-day-old embryonated chicken eggs as previously described (26). Positive samples were tested by hemagglutination (HA) and hemagglutination inhibition (HI) to determine the presence of NDV. Additionally, positive samples were subjected to virus quantitation in embryonated chicken eggs. Serial 10-fold dilutions (10^{-5} to 10^{-10}) were inoculated in 9- to 10-day-old embryonated chicken eggs, and viral titers were determined as EID_{50}/0.1 ml according to the method of Reed and Muench.

IHC. Expression and distribution of the viral nucleoprotein (NP) were assessed by immunohistochemistry (IHC). Tissue sections (4 μm) were subjected to deparaffinization followed by antigen retrieval (Vector antigen unmasking solution; Vector Laboratories, Burlingame, CA) and blocking of nonspecific antigens (universal blocking reagent; Biogenex, San Ramon, CA) according to the manufacturer's instructions. Samples were incubated overnight with the anti-NP antibody at 4°C (26), washed, incubated with an alkaline phosphatase-labeled polymer anti-rabbit Fc (LabVision polymer; LabVision, Fremont, CA), and developed by using the chromogen Vector Red substrate (Vector Laboratories, Burlingame, CA) (26). Sections were counterstained with hematoxylin, mounted, and examined under a light microscope.

Vaccine production. Allantoic fluid collected from ECE inoculated with NDV-LaSota/46 or mock inoculated (sham) was clarified by centrifugation at $1,000 \times g$ for 15 min. The virus titer was determined as EID_{50}/0.1 ml, as described above, and a water-in-oil emulsion inactivated vaccine was prepared as previously described (16).

Vaccination studies. The efficacy of a traditional inactivated vaccine in conferring protection against NDV-Peru/08 challenge was assessed in chickens. Four-week-old SPF white Leghorn chickens were randomly allocated into two experimental groups consisting of an NDV-LaSota/46-

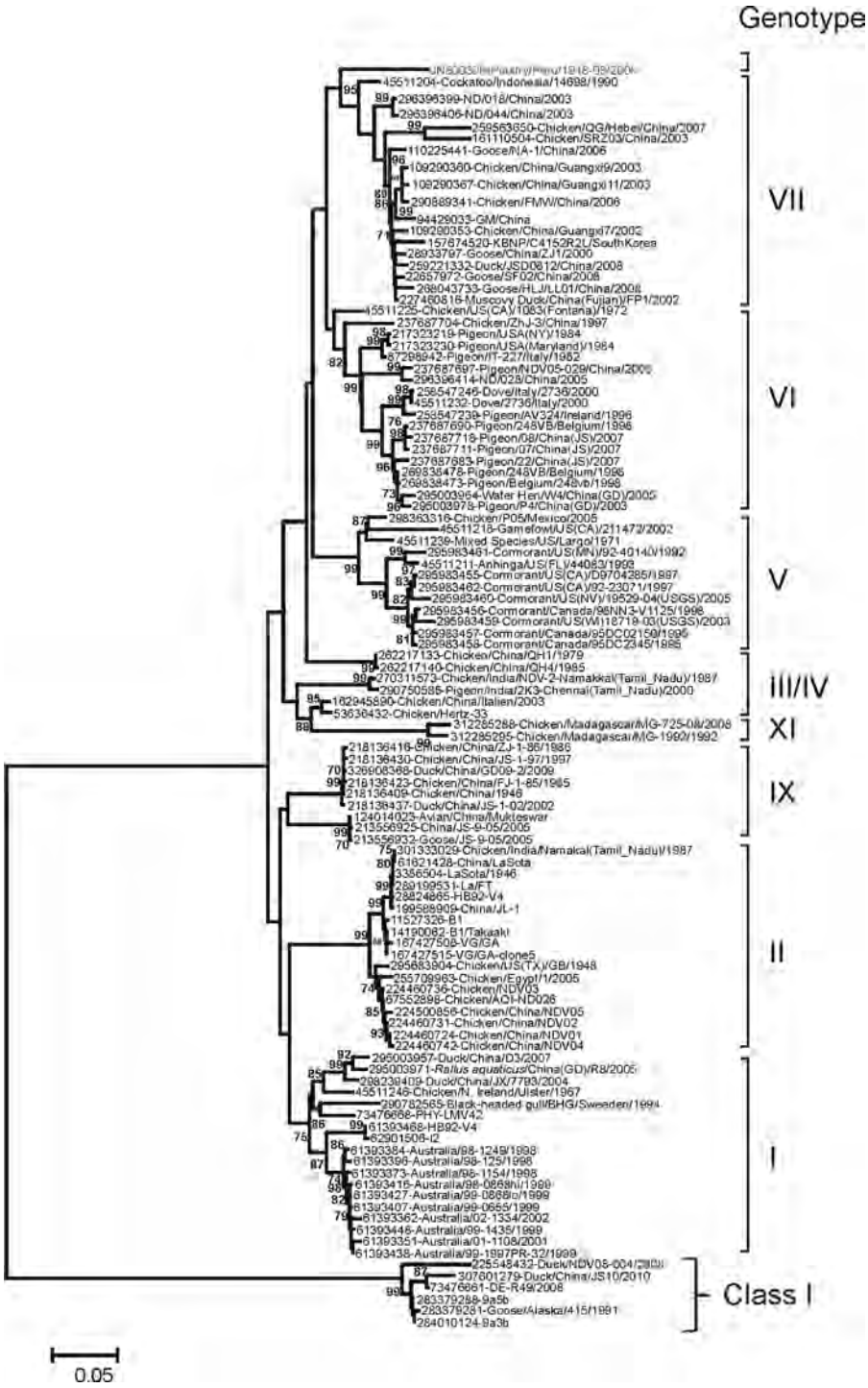

FIG 1 Phylogenetic analysis based on the complete fusion (F) gene sequence of 104 taxa available in GenBank. The evolutionary history was inferred using the neighbor-joining method (24). The optimal tree with the sum of branch lengths of 2.35304957 is shown. The percentage of replicate trees in which the associated taxa clustered together in the bootstrap test (100 replicates) is shown next to the branches (6). The tree is drawn to scale, with branch lengths in the same units as those of the evolutionary distances used to infer the phylogenetic tree. The evolutionary distances were computed using the maximum composite likelihood method (27) and are in units representing the number of base substitutions per site. The rate variation among sites was modeled with a gamma distribution (shape parameter = 1). The differences in the composition bias among sequences were considered in evolutionary comparisons. All positions containing gaps and missing data were eliminated from the data set ("complete deletion" option). There were a total of 1,661 positions in the final data set. Phylogenetic analyses were conducted in MEGA5 (28).

vaccinated group ($n = 10$) and a control sham-vaccinated group ($n = 10$). Birds were vaccinated subcutaneously with 0.5 ml of the oil emulsion vaccines. Three weeks after vaccination, all birds were challenged with NDV-Peru/08 as described above and monitored for clinical signs of ND during a 14-day observation period. Serum samples were collected at days 0 and 21 postvaccination and day 14 postchallenge and tested for the presence of NDV antibodies by the hemagglutination inhibition assay.

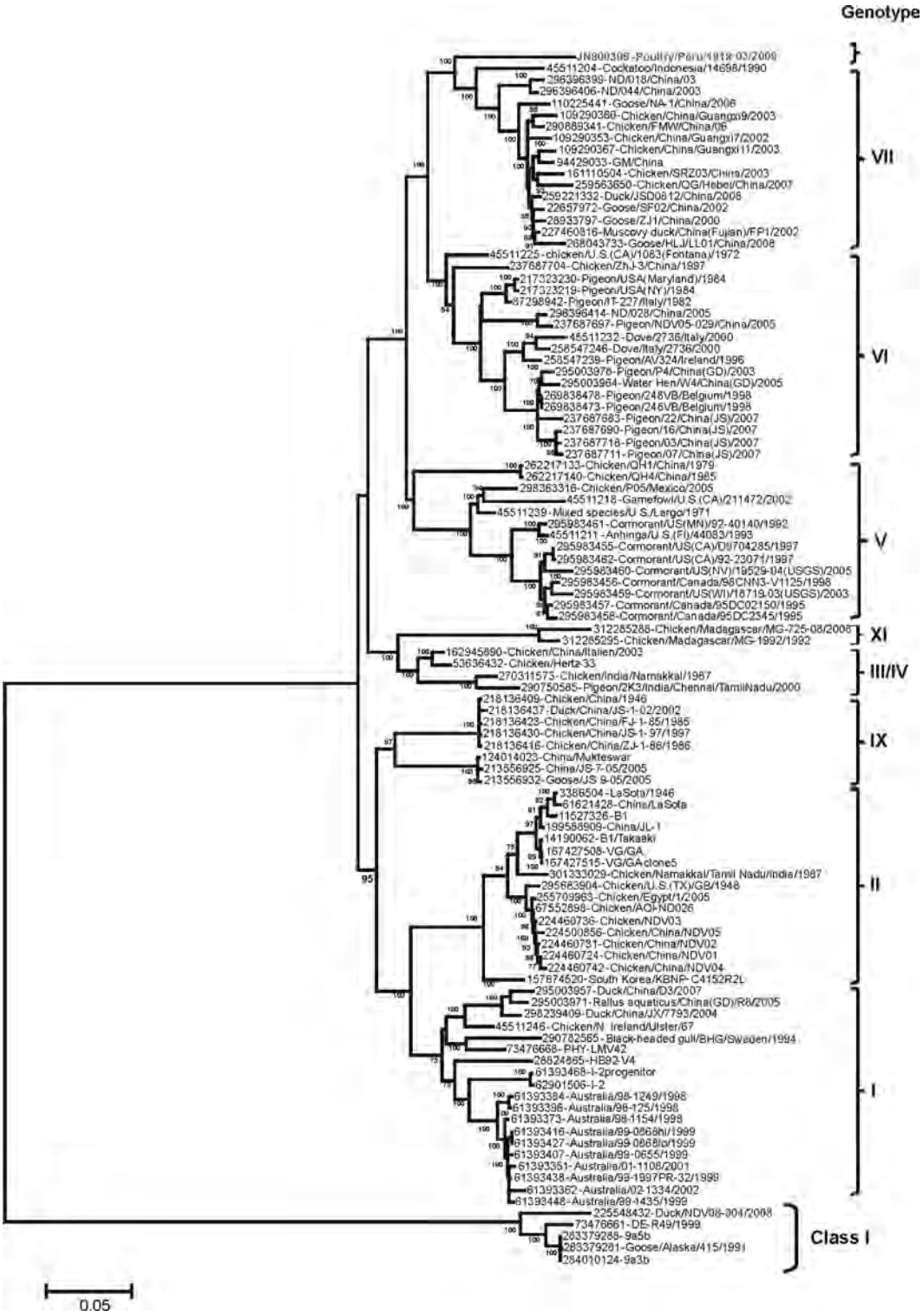

FIG 2 Phylogenetic analysis based on the complete genome sequence of 104 taxa available in GenBank. The evolutionary history was inferred using the neighbor-joining method (24). The optimal tree with the sum of branch lengths of 2.50688796 is shown. The percentage of replicate trees in which the associated taxa clustered together in the bootstrap test (100 replicates) is shown next to the branches (6). The tree is drawn to scale, with branch lengths in the same units as those of the evolutionary distances used to infer the phylogenetic tree. The evolutionary distances were computed using the maximum composite likelihood method (27) and are in units representing the number of base substitutions per site. The rate variation among sites was modeled with a gamma distribution (shape parameter = 1). The differences in the composition bias among sequences were considered in evolutionary comparisons. All positions containing gaps and missing data were eliminated from the data set ("complete deletion" option). There were a total of 15,034 positions in the final data set. Phylogenetic analyses were conducted in MEGA5 (28).

TABLE 1 Estimates of evolutionary distances between NDV-Peru/08 and viruses representing other established NDV genotypes

Genotype	No. of base substitutions/site in genotype[a]:							
	I	II	III/IV	V	VI	VII	IX	NDV-Peru/08
I		(0.0037)	(0.0036)	(0.0043)	(0.0047)	(0.0048)	(0.0030)	(0.0056)
II	0.1423		(0.0047)	(0.0051)	(0.0051)	(0.0053)	(0.0041)	(0.0071)
III/IV	0.1464	0.1696		(0.0041)	(0.0036)	(0.0051)	(0.0030)	(0.0059)
V	0.2038	0.2289	0.1641		(0.0028)	(0.0035)	(0.0039)	(0.0041)
VI	0.1924	0.2226	0.1604	0.1576		(0.0033)	(0.0036)	(0.0041)
VII	0.2042	0.2262	0.1715	0.1655	0.1371		(0.0043)	(0.0036)
IX	0.1357	0.1576	0.1183	0.1772	0.1753	0.1864		(0.0053)
NDV-Peru/08	0.218	0.2432	0.1893	0.1804	0.1491	0.1255	0.2011	

[a] The number of base substitutions per site is shown for NDV-Peru/08 and genotypes of class II viruses. All results are based on the pairwise analysis of 98 sequences. The numbers of sequences analyzed per group were as follows: I, $n = 16$; II, $n = 18$; III/IV, $n = 6$; V, $n = 12$; VI, $n = 18$; VII, $n = 16$; IX, $n = 8$; and poultry/Peru/08 (NDV-Peru/08), $n = 1$. Analyses were conducted using the maximum composite likelihood method in MEGA5. The codon positions included were the 1st + 2nd + 3rd + noncoding. All positions containing gaps, and missing data were eliminated from the data set ("complete deletion" option). There were a total of 15,034 positions in the final data set. Values in parentheses are standard errors, obtained by a bootstrap procedure (500 replicates).

Nucleotide sequence accession number. The complete genome sequence of the NDV isolate poultry/Peru/1918-03/2008 is available in GenBank under accession no. JN800306.

RESULTS

NDV-Peru/08 belongs to the velogenic NDV pathotype. The pathogenicity of NDV-Peru/08 was initially assessed by sequencing of the fusion (F) protein cleavage site and by the standard ICPI test. Sequencing of the F protein cleavage site revealed the presence of three basic amino acid residues at positions 113, 115, and 116 and a phenylalanine at position 117 (^{112}R-R-Q-K-R-F^{117}). Intracerebral inoculation of NDV-Peru/08 in day-old chicks resulted in an ICPI of 1.78, which is typical of velogenic NDV strains (15, 31, 32).

Phylogenetic analysis of the complete F gene and the complete genome sequences demonstrate that NDV-Peru/08 is genetically distinct from other established NDV genotypes. Phylogenetic analysis based on the F gene revealed that NDV-Peru/08 is clearly distinct from viruses representing other known NDV genotypes (Fig. 1). To confirm the results obtained by the analysis of the F gene, we performed a phylogenetic analysis based on the complete genome sequence of NDV-Peru/08 and other reference NDV strains ($n = 104$). Similar to the results obtained in the analysis of the F gene, the compete genome phylogenetic reconstruction resulted in NDV-Peru/08 forming an isolated branch separate from the viruses of other known class II genotypes (Fig. 2). The viruses that appear most closely related to NDV-Peru/08 are the strains cockatoo/Indonesia/14698/90 (GI 45511204), ND/03/044 (GI 286396406), and ND/03/018 (GI 286396399), which were isolated in Asia and belong to genotype VII and subgenotypes VIIa (cockatoo/Indonesia/14698/90) and VIId (ND/03/044 and ND/03/018). Phylogenetic analysis performed with individual genes of the data set of 104 complete genomes (coding for F, NP, P, M, HN, and L) revealed a similar phylogenetic topology (data not shown). No recombination events were observed in the NDV-Peru/08 genome (data not shown).

The evolutionary distances between the complete genome of NDV-Peru/08 and those of strains of other class II genotypes (I, II, III/IV, V, VI, and VII) revealed that NDV-Peru/08 is significantly distant from viruses of all other NDV genotypes (Table 1). The distance between NDV-Peru/08 and the viruses of genotype VII, for example, is 0.1255, which is in the range of the distances observed between other genotypes (Table 1) and is markedly larger than the mean distance within genotype VII viruses (0.0406; standard error, 0.0009) (data not shown). Notably, the distances observed between NDV-Peru/08 and viruses of genotypes I and II (vaccine-like viruses) were 0.218 and 0.2432, respectively, and are the largest distances observed among all NDV genotypes (Table 1). Similar results were obtained when the F gene sequences were used to calculate the evolutionary distances (data not shown).

TABLE 2 Nucleotide and amino acid comparison between the Newcastle disease virus isolate NDV-Peru/08 and viruses representing other genotypes within class II[a]

Protein	% identity for virus by genotype[b]:															
	I, Ulster/67		II, LaSota		III, JS/7/05/Ch		IV, Italien		V, Anhinga/93		VI, Fontana/72		VII, ZJ1/2000		IX, FJ/1/85/Ch	
	nt	aa	nt	aa	nt	aa	nt	aa	nt	aa	nt	aa	nt	aa	nt	aa
NP	85	93	84	91	87	93	90	95	88	93	88	93	91	96	87	94
P	82	81	81	80	84	82	84	85	84	80	85	80	87	85	85	81
M	85	89	84	88	86	89	88	93	85	92	85	92	91	95	86	91
F	84	90	82	88	84	90	87	92	86	91	86	91	89	93	84	91
HN	85	89	83	86	84	87	86	89	85	89	86	89	90	93	84	88
L	87	94	85	92	87	94	88	95	88	95	88	95	91	96	87	94
Complete genome	84.8		82.5		85		86.8		85.9		89.9		89.6		84.8	

[a] Alignment was performed by using ClustalW.
[b] Accession numbers: I, AY562891; II, AF077761; III, FJ430159; IV, EU283914; V, AY562886; VI, AY562888; VII, AF431744; IX, FJ436304.

TABLE 3 Genomic features of Newcastle disease virus isolate NDV-Peru/08

Protein	Gene start positions (nt)	3′ UTR (length nt)[a]	Coding sequence positions (nt)	5′ UTR (nt length)	Gene end positions (nt)	Length of: Intergenic region (nt)	Gene (nt)	Protein (aa)
NP	56–65	66	122–1591	217	1798–1808	1	1,469	489
P	1810–1819	73	1883–3080	180	3250–3260	1	1,197	395
M	3262–3271	34	3286–4390	112	4493–4502	1	1,073	364
F	4504–4513	46	4550–6211	84	6285–6285	31	1,661	553
HN	6327–6336	91	6418–8133	195	8318–8328	47	1,715	571
L	8376–8387	11	8387–15001	77	15069–15078		6,614	2,204

[a] UTR, untranscribed region.

A comparison of the nucleotide and amino acid sequences between NDV-Peru/08 and selected class II reference strains representing genotypes I, II, III, IV, V, VI, VII, and IX is presented in Table 2. Alignment of the complete genome sequences revealed that NDV-Peru/08 shares 89.9% and 89.6% nucleotide identity with NDV strains Fontana/72 (genotype VI) and ZJ1/2000 (genotype VII), respectively. Notably, the lowest nucleotide identity was observed between NDV-Peru/08 and the vaccine strains Ulster/67 (84.4%; genotype I) and LaSota/46 (82.5%; genotype II). Similar to the complete genome nucleotide sequence analysis, comparison of the nucleotide and amino acid sequences of each gene confirmed that NDV-Peru/08 shares the highest nucleotide and amino acid identity with the strains of genotypes VI and VII, while the lowest degree of identity was observed between NDV-Peru/08 and the vaccine-like strains of genotypes I and II (Table 2).

Genomic features of NDV-Peru/08. The genome of NDV-Peru/08 is 15,192 nucleotides (nt) in length, it contains a 6-nt insertion in the 5′ noncoding region of the NP gene between positions 1738 and 1743 and a G+C content of 46.2%. A summary of the genomic features of NDV-Peru/08, including the gene start, gene end, and intergenic and coding regions is presented in Table 3.

Infection of chickens with NDV-Peru/08 results in characteristic velogenic viscerotropic Newcastle disease. The clinicopathological characteristics and the virulence of NDV-Peru/08 were assessed in chickens. All NDV-Peru/08-inoculated birds presented severe prostration, had mucous diarrhea, and died or were euthanized by day 5 postinoculation (mean death time, 4.7 days) (Fig. 3). Gross lesions were initially observed by day 2 p.i. and consisted of conjunctivitis, multifocal necrosis, and hemorrhages in the intestine and cecal tonsils, as well as mottling and multifocal necrosis in the spleen. Additionally, atrophy of the thymus was observed by day 3 p.i. and was characterized by a marked reduction in size and by the presence of gelatinous edema and perithymic hemorrhages. Multifocal hemorrhages were also observed in the pharynx by day 4 p.i. Control group birds did not exhibit any clinical signs or pathological changes.

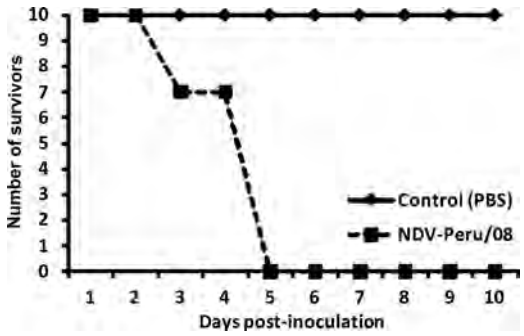

FIG 3 Survival curve. Three birds of the NDV-Peru/08-inoculated group (group 2) died on day 3 postinoculation, and the remaining birds died on day 5 p.i. (mean death time, 4.7 days).

Typical histological changes associated with velogenic viscerotropic NDV infection, including lymphoid depletion and necrosis, accumulation of macrophages, necrotic debris, and scattered heterophils, were observed in multiple organs of NDV-Peru/08-inoculated birds (Fig. 4A, panels b and d; Table 4). Lesions were more severe as the disease progressed and peaked at day 4 p.i. A summary of the severity and distribution of the lesions is presented in Table 4. Control group birds did not present histological changes.

Immunohistochemical staining for NDV nucleoprotein (NP) revealed a widespread distribution of the virus (Table 4), with antigen load and distribution peaking at 4 dpi. The strongest staining intensity was observed in the eyelids, lymphoid organs, and mucosa-associated-lymphoid tissue (MALT) aggregates of various organs (Table 4; Fig. 4B, panels a and b), with positive cells consisting mainly of lymphocytes and macrophages.

All birds inoculated with NDV-Peru/08 shed the virus in oral and cloacal swabs. The virus was isolated from samples collected on days 2, 3, and 5 p.i., with virus titers ranging from $10^{3.7}$ to $10^{5.9}$ EID_{50}/0.1 ml and from $10^{2.9}$ to $10^{5.4}$ EID_{50}/0.1 ml in oral and cloacal secretions, respectively.

Inactivated NDV-LaSota/46 vaccine confers protection against NDV-Peru/08-induced disease and mortality. The efficacy of an inactivated NDV-LaSota/46 vaccine in conferring protection against NDV-Peru/08 challenge was assessed in chickens. All NDV-LaSota/46-vaccinated birds seroconverted (HI titers between 64 and 128, geometric mean titer [GMT] of 105.95) and were fully protected from clinical disease and mortality induced by NDV-Peru/08 infection, whereas all birds from the sham-vaccine group presented typical clinical signs of velogenic viscerotropic NDV strains, including severe prostration and diarrhea, and died by day 5 p.i.

DISCUSSION

Virulent Newcastle disease virus (vNDV) is endemic in many countries of North, Central, and South America, and outbreaks of ND are frequently reported to the World Organization for Animal Health (OIE). In June and July of 2008, simultaneous outbreaks of ND were confirmed in domestic poultry in Peru (provinces of Arequipa and Cusco). The high morbidity and

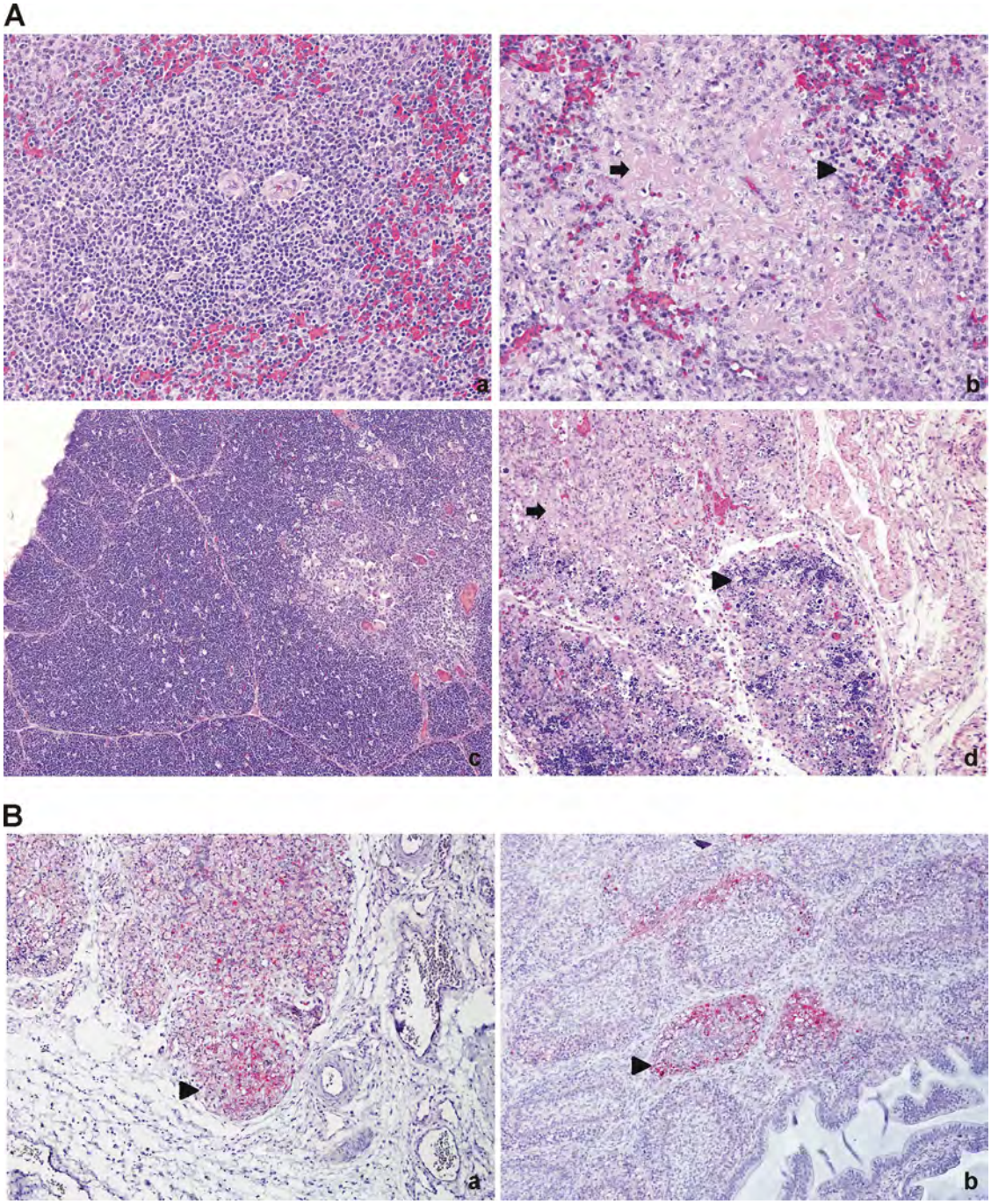

FIG 4 Histological changes and distribution of Newcastle disease virus nucleoprotein in NDV-Peru/08-infected tissues. (A) Histological changes (panels b and d) consisted of lymphoid depletion and necrosis (arrows), accumulation of macrophages (arrowheads), and scattered heterophils. Panel a, spleen, PBS control, 40×; panel b, spleen, NDV-Peru/08, 40×; panel c, thymus, PBS control, 20×; panel d, thymus, NDV-Peru/08, hematoxylin and eosin staining. (B) Immunohistochemical staining for Newcastle disease virus nucleoprotein. Shown is positive staining in the thymus (panel a, 20×) and bursa of Fabricius (panel b, 20×). Positive cells consisted mainly of lymphocytes and macrophages (arrowheads).

mortality rates (75.6%) of the 2008 outbreak and the clinicopathological characteristics of NDV-Peru/08 resemble the clinical presentation described for the highly virulent viruses of genotypes V and VII that circulate in Central America, Africa, Asia, and the Middle East (26). Although the source of the 2008 outbreak in Peru is still unknown, field epidemiological investigations reported to the OIE suggest that the virus was likely introduced through live birds that were added to the affected flocks (19). However, a complete epidemiological investigation, including sampling of domestic and wild bird species, is needed to define the actual source of the outbreak and origin of the virus.

TABLE 4 Distribution and severity of lesions and distribution and intensity of viral antigen staining in tissues of NDV-Peru/08-inoculated birds

Tissue[a]	Result on postinoculation day[b]:		
	2	3	4
Eyelid			
HE	++	++	++
IHC	++	+++	+++
Spleen			
HE	++	+++	+++
IHC	++	++	+++
Thymus			
HE	+	++	+++
IHC	−	++	++++
Bursa			
HE	+	+	+++
IHC	+	++	++
Harderian gland			
HE	−	+	−
IHC	−	+	+++
Proventriculus			
HE	+	++	−
IHC	−	++++	+++
Pancreas			
HE	+	−	++
IHC	−	−	++
Small intestine			
HE	−	−	+
IHC	+	−	++
Mekel's diverticulum			
HE	+	−	++
IHC	−	−	++
Cecal tonsils			
HE	+	++	+++
IHC	+++	+++	++++
Large intestine			
HE	−	+	+
IHC	−	++	++
Air sacs			
HE	−	−	−
IHC	−	−	+
Trachea			
HE	−	−	−
IHC	−	+	−
Lung			
HE	−	−	+ (BALT)
IHC	−	+ (BALT)	++ (BALT)
Pharynx			
HE	+	++	++
IHC	−		+
Brain			
HE	−	−	−
IHC	−	−	+ (cerebellum)
Liver			
HE	−	−	+ (MALT)
IHC	−	−	−
Kidney			
HE	−	−	−
IHC	−	−	+
Comb			
HE	−	−	−
IHC	−	−	++
Femur			
HE	−	−	+
IHC	−	−	+

[a] HE, hematoxylin and eosin staining; IHC, immunohistochemistry staining for NDV nucleoprotein.

[b] BALT, bronchus-associated lymphoid tissue; MALT, mucosa-associated lymphoid tissue. For HE, the results are scored by tissue as follows: (i) spleen, +, moderate hyperplasia, ++, lymphocytic depletion, +++, moderate (<50%) lymphocyte depletion, histiocytic accumulation, and multifocal necrosis, and ++++, severe (>50%) lymphocytic depletion, histiocytosis, and necrosis; (ii) thymus, cecal tonsil, gut-associated lymphoid tissue (GALT), and bursa, +, mild lymphocytic depletion, ++, moderate (<50%) lymphocytic depletion with necrosis and histiocytosis, and +++, severe (>50%) lymphocytic depletion, necrosis, and histiocytosis; (iii) bone marrow, +, mild (<20%) bone marrow necrosis, ++, moderate (20 to 50%) bone marrow necrosis, and +++, severe (>50%) bone marrow necrosis; (iv) pancreas, +, mild (<3 areas) vacuolation and degeneration, and ++, moderate (>3 areas) vacuolation and degeneration; and (v) brain, +, vascular reactivity, ++, vascular reactivity and perivascular cuffing, and +++, vascular reactivity, perivascular cuffing, and gliosis. For IHC staining, the results are scored as follows: −, no IHC signal detected; +, rare cells in the section are positive on IHC; ++, positive cells seen in <50% of all high-magnification fields (HMF); +++, positive signal seen in 50 to 75% of HMF; and ++++, abundant positive signal in more than 75% of HMF.

Recent phylogenetic studies have shown that NDV is continuously evolving, with viruses of different genotypes undergoing simultaneous changes in distinct geographic locations (4, 5, 11, 22, 25, 33, 34). The results presented here indicate that NDV-Peru/08 has evolved and significantly diverged from viruses representing all known NDV genotypes. Classification of NDV-Peru/08 into one of the existing NDV genotypes or into a new genotype, however, is still uncertain, and isolation of additional viruses with similar genetic and phylogenetic properties is needed in order to classify this isolate.

Historically, NDV isolates have been classified as lentogenic, mesogenic, or velogenic based on to the clinicopathological outcome of the infection in chickens (3). Clinicopathological characterization of NDV-Peru/08 revealed that this virus behaves as a typical velogenic viscerotropic strain. The mortality rate (100%) and mean death time (4.7 days) observed in NDV-Peru/08-inoculated birds are characteristic of highly virulent strains of genotypes V, VI, and VII (21, 26, 31). Histological examination and immunohistochemical staining of tissue samples collected from multiple organs confirmed the tropism of NDV-Peru/08 for lymphoid tissues associated with the gastrointestinal tract and, to a

lesser extent, with the respiratory system. A similar tropism is seen in infections with the highly virulent genotype VII viruses (26).

The data presented here provide evidence that a genetically distinct virus, most closely related to but different from isolates of genotypes VI and VII caused the outbreak of ND in Peru. Notably, the evolutionary distances between NDV-Peru/08 and vaccine-like viruses of genotypes I and II are the largest distances observed between all genotypes. Given the genetic differences observed between NDV-Peru/08 and vaccine-like viruses (Table 1 and 2), vaccination studies were performed with chickens. Results of these experiments demonstrated that, under biosafety level 3 conditions and using SPF birds, a traditional inactivated NDV vaccine strain from genotype II (NDV-LaSota/46) fully protected chickens from NDV-Peru/08-induced clinical disease and mortality. These observations suggest that the genetic diversity of NDV-Peru/08 is not reflected in antigenic changes that significantly affect the immune response elicited by the inactivated NDV-LaSota/46 vaccine. However, whether these findings will be observed under field conditions and with vaccine strains from other NDV genotypes remains to be determined.

In summary, complete genome- and protein-level analysis of the evolutionary distances between NDV-Peru/08 and strains of established NDV genotypes demonstrated that this isolate is distinct from viruses of typical NDV genotypes. Given the lack of epidemiological data from the 2008 outbreak and from other NDV isolates circulating in South America, it is unclear whether similar viruses are still circulating in that continent, or whether that outbreak was a unique episode caused by this isolate. Continuous characterization of novel NDV isolates that occasionally emerge and cause outbreaks or of those that frequently circulate worldwide are important to improve the current understanding of NDV epidemiology and evolution and for the development of improved control and diagnostic strategies.

ACKNOWLEDGMENTS

We thank Dawn Williams-Coplin and Tim Olivier for technical assistance, Roger Brock for help with animal experiments, and the SEPRL sequencing facility personnel for nucleotide sequencing. We also acknowledge the generous support of CEVA Biomune for the vaccination studies and the National Direction of Animal Health of Peru (SENASA) for invaluable collaboration and for sharing information on the outbreak.

This work was supported by USDA funding CRIS 6612-32000-049.

REFERENCES

1. **Aldous EW, Mynn JK, Banks J, Alexander DJ.** 2003. A molecular epidemiological study of avian paramyxovirus type 1 (Newcastle disease virus) isolates by phylogenetic analysis of a partial nucleotide sequence of the fusion protein gene. Avian Pathol. **32**:239–256.
2. **Alexander DJ, Senne DA.** 2008. Newcastle disease, other avian paramyxoviruses, and pneumovirus infections, p 75–98. *In* Saif M, et al (ed), Diseases of poultry, 12th ed. Blackwell Publishing, Ames, IA.
3. **Alexander DJ, Swayne DE.** 1998. Newcastle disease virus and other avian paramyxoviruses, p 156–163. *In* Swayne DE, Glisson JR, Jackwood MW, Pearson JE, Reed WM (ed), A laboratory manual for the isolation and identification of avian pathogens, vol 4. American Association of Avian Pathologists, Kennett Square, PA.
4. **Czegledi A, et al.** 2006. Third genome size category of avian paramyxovirus serotype 1 (Newcastle disease virus) and evolutionary implications. Virus Res. **120**:36–48.
5. **Ding Z, et al.** 2010. Genetic analysis of avian paramyxovirus-1 (Newcastle disease virus) isolates obtained from swine populations in China related to commonly utilized commercial vaccine strains. Virus Genes **41**:369–376.
6. **Felsenstein J.** 1992. Estimating effective population size from samples of sequences: a bootstrap Monte Carlo integration method. Genet. Res. **60**: 209–220.
7. **Kim LM, King DJ, Suarez DL, Wong CW, Afonso CL.** 2007. Characterization of class I Newcastle disease virus isolates from Hong Kong live bird markets and detection using real-time reverse transcription-PCR. J. Clin. Microbiol. **45**:1310–1314.
8. **Kim LM, Suarez DL, Afonso CL.** 2008. Detection of a broad range of class I and II Newcastle disease viruses using multiplex real-time reverse transcription polymerase chain reaction assay. J. Vet. Diagn. Invest. **20**:414–425.
9. **Kinde H, et al.** 2005. The isolation of exotic Newcastle disease (END) virus from nonpoultry avian species associated with the epidemic of END in chickens in southern California: 2002–2003. Avian Dis. **49**:195–198.
10. **Lancaster JE, Alexander DJ.** 1975. Newcastle Disease virus and spread, p 1–79.Canada Department of Agriculture, monograph no. 11. Canada Department of Agriculture, Ottawa, Canada.
11. **Linde AM, et al.** 2010. Complete genome characterisation of a Newcastle disease virus isolated during an outbreak in Sweden in 1997. Virus Genes **41**:165–173.
12. **Liu XF, Wan HQ, Ni XX, Wu YT, Liu WB.** 2003. Pathotypical and genotypical characterization of strains of Newcastle disease virus isolated from outbreaks in chicken and goose flocks in some regions of China during 1985–2001. Arch. Virol. **148**:1387–1403.
13. **Martin DP.** 2009. Recombination detection and analysis using RDP3. Methods Mol. Biol. **537**:185–205.
14. **Miller PJ, Decanini EL, Afonso CL.** 2010. Newcastle disease: evolution of genotypes and the related diagnostic challenges. Infect. Genet. Evol. **10**: 26–35.
15. **Miller PJ, Kim LM, Ip HS, Afonso CL.** 2009. Evolutionary dynamics of Newcastle disease virus. Virology **391**:64–72.
16. **Miller PJ, King DJ, Afonso CL, Suarez DL.** 2007. Antigenic differences among Newcastle disease virus strains of different genotypes used in vaccine formulation affect viral shedding after a virulent challenge. Vaccine **25**:7238–7246.
17. **OIE.** 2009. Manual of diagnostic tests and vaccines for terrestrial animals: mammals, birds and bees, 5th ed, vol 1, part 2, chapter 2.3.14, p 576–589. Biological Standards Commission, World Organization for Animal Health, Paris, France.
18. **OIE.** 2011. World Animal Health Information Database (WAHID) Interface. http://web.oie.int/wahis/public.php?page=home&WAHIDPHPSESSID=4d95e8777ff8b8a615b31617ac4c7835.
19. **OIE.** 2008. World Animal Health Information Database (WAHID) Interface. Event summary: Newcastle disease, Peru. World Organization for Animal Health, Paris, France. http://web.oie.int/wahis/public.php?page=event_summary&reportid=7326.
20. **Perozo F, Afonso RMCL, Fernandez R, Rojo F.** 2011. Genotype VII velogenic viscerotropic Venezuelan Newcastle disease virus isolate: live (AvinewR) and killed (Gallimune NDR) vaccination, abstr 169P, p 49. Abstr. 2011 Int. Poultry Scientific Forum, Atlanta, GA, 24 to 25 January 2011.
21. **Perozo F, Merino R, Afonso CL, Villegas P, Calderon N.** 2008. Biological and phylogenetic characterization of virulent Newcastle disease virus circulating in Mexico. Avian Dis. **52**:472–479.
22. **Qiu X, et al.** 2011. Entire genome sequence analysis of genotype IX Newcastle disease viruses reveals their early-genotype phylogenetic position and recent-genotype genome size. Virol. J. **8**:117.
23. **Rue CA, et al.** 2010. Evolutionary changes affecting rapid identification of 2008 Newcastle disease viruses isolated from double-crested cormorants. J. Clin. Microbiol. **48**:2440–2448.
24. **Saitou N, Nei M.** 1987. The neighbor-joining method: a new method for reconstructing phylogenetic trees. Mol. Biol. Evol. **4**:406–425.
25. **Seal BS.** 2004. Nucleotide and predicted amino acid sequence analysis of the fusion protein and hemagglutinin-neuraminidase protein genes among Newcastle disease virus isolates. Phylogenetic relationships among the Paramyxovirinae based on attachment glycoprotein sequences. Funct. Integr. Genomics **4**:246–257.
26. **Susta L, Miller PJ, Afonso CL, Brown CC.** 2010. Clinicopathological characterization in poultry of three strains of Newcastle disease virus isolated from recent outbreaks. Vet. Pathol. **48**:349–360.
27. **Tamura K, Nei M, Kumar S.** 2004. Prospects for inferring very large phylogenies by using the neighbor-joining method. Proc. Natl. Acad. Sci. U. S. A. **101**:11030–11035.
28. **Tamura, K., et al.** MEGA5: molecular evolutionary genetics analysis using

maximum likelihood, evolutionary distance, and maximum parsimony methods Mol. Biol. Evol. **28**:2731–2739.
29. **Thompson JD, Higgins DG, Gibson TJ.** 1994. CLUSTAL W: improving the sensitivity of progressive multiple sequence alignment through sequence weighting, position-specific gap penalties and weight matrix choice. Nucleic Acids Res. **22**:4673–4680.
30. **Utterback WW, Schwartz JH.** 1973. Epizootiology of velogenic viscerotropic Newcastle disease in southern California, 1971–1973. J. Am. Vet. Med. Assoc. **163**:1080–1088.
31. **Wakamatsu N, King DJ, Kapczynski DR, Seal BS, Brown CC.** 2006. Experimental pathogenesis for chickens, turkeys, and pigeons of exotic Newcastle disease virus from an outbreak in California during 2002–2003. Vet. Pathol. **43**:925–933.
32. **Wang Z, et al.** 2006. Genotyping of Newcastle disease viruses isolated from 2002 to 2004 in China. Ann. N. Y. Acad. Sci. **1081**:228–239.
33. **Wu S, et al. 9 November** 2010, posting date. Genetic diversity of Newcastle disease viruses isolated from domestic poultry species in Eastern China during 2005–2008. Arch. Virol. [Epub ahead of print.] doi:10.1007/s00705-010-0851-5.
34. **Yu L, Wang Z, Jiang Y, Chang L, Kwang J.** 2001. Characterization of newly emerging Newcastle disease virus isolates from the People's Republic of China and Taiwan. J. Clin. Microbiol. **39**:3512–3519.

10TH EDITION

DISEASES OF SWINE

EDITED BY

Jeffrey J. Zimmerman
Locke A. Karriker
Alejandro Ramirez
Kent J. Schwartz
Gregory W. Stevenson

WILEY-BLACKWELL
A John Wiley & Sons, Inc., Publication

AMERICAN ASSOCIATION SWINE VETERINARIANS

30 Swinepox Virus

Gustavo Delhon, Edan R. Tulman, Claudio L. Afonso, and Daniel L. Rock

RELEVANCE

Swinepox (SWP) is a mild, acute disease of swine characterized by typical poxviral lesions of the skin. SWP is distributed worldwide and is usually associated with poor sanitation. Morbidity may be high in individual herds where young pigs are most severely affected, but mortality is usually negligible. Clinical signs and epidemiology are usually sufficient for SWP diagnosis.

ETIOLOGY

SWP virus (SWPV) is the sole member of the genus *Suipoxvirus* in the family *Poxviridae* (Moyer et al. 2000). The SWPV virion is morphologically similar to vaccinia virus, exhibiting a brick-like structure approximately 320 × 240 nm in horizontal section (Figure 30.1) (Blakemore and Abdussalam 1956; Cheville 1966a; Teppema and De Boer 1975). The virion is composed of a central biconcave core or nucleoid bordered by two ellipsoid lateral bodies and at least two lipid membranes (Blakemore and Abdussalam 1956; Cheville 1966a; Conroy and Meyer 1971; Kim and Luong 1975; Smid et al. 1973; Teppema and De Boer 1975). SWPV is ether-sensitive.

The SWPV genome is a double-stranded DNA molecule of 146 kilobase pairs predicted to contain 150 genes. It shares features common with other members of the *Poxviridae*, including a conserved central genomic region containing genes necessary for intracytoplasmic replication and virion structure (Afonso et al. 2002). Although genetically related to viruses of other poxviral genera (*Capripoxvirus*, *Leporipoxvirus*, *Yatapoxvirus*), SWPV represents a distinct poxvirus genus and contains in terminal genomic regions a unique complement of genes predicted to affect virus/host interaction and aspects of SWPV virulence and host range (Afonso et al. 2002; Massung et al. 1993).

Despite reports of limited antigenic cross-reactivity, SWPV is antigenically distinct, as evidenced by the failure of SWPV antibodies to cross-protect, cross-neutralize, or efficiently immunoprecipitate viral proteins of other poxviruses (De Boer 1975; Massung and Moyer 1991; Meyer and Conroy 1972; Ouchi et al. 1992; Shope 1940).

Although some isolates have been reported to induce first-passage cytopathic effect (CPE) on swine cells (Afonso et al. 2002; Paton et al. 1990), SWPV generally replicates poorly on initial isolation in swine cell cultures. It requires multiple passages before inducing CPE, but maintains pathogenicity for swine (Garg and Meyer 1972; Kasza and Griesemer 1962; Kasza et al. 1960; Meyer and Conroy 1972). CPE, characterized by cytoplasmic vacuoles and inclusion bodies, nuclear "vacuoles," and cell rounding and clumping (Borst et al. 1990; De Boer 1975; Kasza et al. 1960; Meyer and Conroy 1972), is seen 3–5 days postinoculation (PI), and isolated plaques remain relatively small in size (<1.5 mm) (Kasza et al. 1960; Massung and Moyer 1991; Meyer and Conroy 1972). Infection of cell cultures results in detectable expression of early and late SWPV mRNA by 4 and 8 hours PI, respectively, and viral protein synthesis by 4 hours PI (Massung and Moyer 1991).

Most attempts to grow or adapt SWPV for growth in nonswine cell cultures or on chicken chorioallantoic membranes have failed (Garg and Meyer 1972; Kasza et al. 1960; Meyer and Conroy 1972), indicating a host-range restriction for replication at the cellular level. Culture-adapted SWPV has been shown to replicate,

Diseases of Swine, Tenth Edition. Edited by Jeffrey J. Zimmerman, Locke A. Karriker, Alejandro Ramirez, Kent J. Schwartz, Gregory W. Stevenson.
This chapter is public domain. Published 2012 by John Wiley & Sons, Inc.

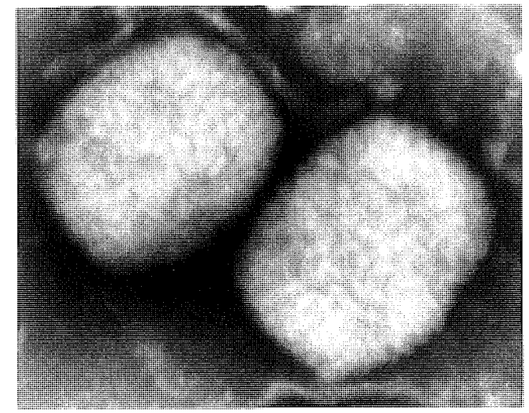

30.1. *Negative stain of swinepox virus particles with characteristic brick shape and complex woven pattern of surface filaments (courtesy of D. A. Gregg).*

albeit to lower titers, in nonswine cell lines (Barcena and Blasco 1998; Hahn et al. 2001).

Due to its restricted host range, SWPV has been proposed as a vaccine expression vector (Foley et al. 1991; Tripathy 1999). Genetically engineered SWPV vectors expressing pseudorabies (Aujeszky's disease) virus and classical swine fever virus antigens have been constructed and, in the case of pseudorabies, shown to induce immune responses in pigs (Hahn et al. 2001; van der Leek et al. 1994). In addition, SWPV is able to express antigens and nonchemical adjuvants in nonswine cells and may represent a safe, host-range restricted, vaccine vector for nonswine species (Barcena and Blasco 1998; Winslow et al. 2003, 2005). Availability of the complete genome sequence and identification of SWPV virulence and host-range genes should enable engineering of live-attenuated, host-range restricted, SWPV vaccine vectors with enhanced efficacy and greater versatility (Afonso et al. 2002).

ROLE IN PUBLIC HEALTH

There is no evidence that SWPV is infectious for humans or plays a role in public health.

EPIDEMIOLOGY

The pig is the only known host of SWPV. Unlike vaccinia virus, SWPV failed to experimentally infect or adapt to several mammalian and avian species (Schwarte and Biester 1941; Shope 1940), with only a single report of nonproductive SWPV infection following intradermal inoculation of rabbits (Datt 1964). This restricted host range suggests that swine represent the reservoir of SWPV in nature.

SWP is present worldwide. Limited serological survey data from Europe indicated that 8–19% of swine serum samples contained anti-SWPV antibodies (De Boer 1975; Paton et al. 1990). Young swine are most often affected, as adult swine rarely present with clinical disease (Kasza et al. 1960; McNutt et al. 1929). Morbidity rates can be high (up to 100%), but mortality is generally negligible (less than 5%) (De Boer 1975). Overall, SWP is of little economic consequence.

Natural transmission of SWP is not well understood, but is often associated with poor sanitation. SWP has been associated with louse (*Haematopinus suis*) infestation. Lice are able to mechanically transmit SWPV and are thought to affect the extent and distribution of cutaneous lesions, which often occur in less keratinized abdominal and inguinal regions (Kasza et al. 1960; Manninger et al. 1940; Shope 1940). However, SWP without evidence of louse involvement has been described, suggesting a role for other insect vectors or the possibility of horizontal transmission (De Boer 1975; Jubb et al. 1992; Paton et al. 1990; Schwarte and Biester 1941). Vertical SWPV transmission is indicated by sporadic cases of congenital infection resulting in stillborn fetuses with generalized lesions (Afonso et al. 2002; Borst et al. 1990; Paton et al. 1990).

PATHOGENESIS

SWPV may enter the host through preexisting skin abrasions and preferentially replicates in epidermal keratinocytes of the stratum spinosum (Meyer and Conroy 1972). Although mature viral particles have been observed in epidermal basal cells (Teppema and De Boer 1975) and viral antigen has been detected in dermal macrophages (Cheville 1966b), there is no indication that these cell types support virus replication. With the exception of moderate changes in superficial lymph nodes, tissues other than the skin are rarely affected. Infectious virus can be readily isolated from the skin of infected animals as early as 3 days post-intradermal inoculation (Kasza and Griesemer 1962) and from regional lymph nodes only if skin lesions are severe (Kasza and Griesemer 1962). A viremic stage has been suggested to account for virus spread from the primary to secondary sites of replication in the skin and for congenital infection, however, virus has not been isolated from the blood of infected animals (Borst et al. 1990; Kasza and Griesemer 1962; Paton et al. 1990; Shope 1940).

Functional studies on SWPV pathogenesis are lacking. The complement of virus genes with putative roles in virulence and host range suggests that modulation of host immune responses and inhibition of apoptosis may play a role in the course of the disease (Afonso

et al. 2002; Kawagishi-Kobayashi et al. 2000; Massung et al. 1993). SWPV contains genes with sequence similarity to cellular and viral genes encoding CD47, and proteins that bind interferon (IFN)-α/β, IFN-γ, tumor necrosis factor (TNF)-α, interleukin-18 (IL-18), and CC chemokines. Products of these genes potentially modulate host immune responses, including natural killer (NK) and T-cell responses, and may facilitate SWPV replication and dissemination. SWPV TNF-binding protein has been shown to interact with high affinity with porcine TNF but not with TNF from other species (Rahman et al. 2006). SWPV encodes proteins similar to host major histocompatibility complex (MHC)-I, NFκB activators, Bcl-2 family proteins, serine proteases, and PKR, some of which in other poxviruses are known to interfere with or delay inflammatory responses at the site of virus replication.

CLINICAL SIGNS

SWPV causes eruptive dermatitis in pigs. Animals up to 3 months of age are the most susceptible, with adults usually developing a mild, self-limiting form of the disease. Multiple cutaneous lesions are commonly found on the flanks, belly, inner side of the legs, ears, and less frequently, on the face of affected animals (De Boer 1975; Jubb et al. 1992; Kim and Luong 1975; McNutt et al. 1929; Olufemi et al. 1981; Schwarte and Biester 1941). Lesions can also be found in the teats of sows and on the face, lips, and tongue of suckling pigs (Olufemi et al. 1981). In congenital infections, lesions are observed over the entire body and in the oral cavity (Borst et al. 1990; Paton et al. 1990). When virus transmission is associated with mechanical vectors, the distribution of lesions tends to reflect the vector's preferred feeding areas.

The incubation period is thought to be 4–14 days under field conditions (De Boer 1975; McNutt et al. 1929) and 3–5 days after intradermal or intravenous virus inoculation (Kasza and Griesemer 1962; Schwarte and Biester 1941), although longer periods have been described (Shope 1940).

Initial lesions are flat, pale, rounded areas 3–5 mm in diameter (maculae). Over the course of 2 days, these progress to papulae 1–2 mm in height, 1–2 cm in diameter, and occasionally confluent (Figure 30.2). The appearance of papulae may be accompanied by a slight and transient increase in body temperature and loss of appetite (Kasza and Griesemer 1962; Kasza et al. 1960). A true vesicle stage is absent or transient (Borst et al. 1990; Datt 1964; Kasza and Griesemer 1962; Meyer and Conroy 1972). The lesions usually become umbilicated and shrink about a week after appearing. They are replaced by crusts, which are eventually shed, leaving discolored spots (Kasza and Griesemer 1962). Complete recovery is observed 15–30 days postexposure, but it may be delayed if secondary bacterial infection occurs

30.2. Swinepox lesions on the skin of a naturally infected pig (courtesy of B. Brodersen).

(De Boer 1975; McNutt et al. 1929; Miller and Olson 1980; Schwarte and Biester 1941).

LESIONS

The most conspicuous histological change caused by SWPV infection is hydropic degeneration of stratum spinosum keratinocytes (Figure 30.3A,B) (Borst et al. 1990; Cheville 1966a; Kasza and Griesemer 1962; McNutt et al. 1929; Meyer and Conroy 1972; Olufemi et al. 1981; Paton et al. 1990; Schwarte and Biester 1941; Teppema and De Boer 1975). Hyperplasia of epidermal cells is not as marked as in poxviral infections of other mammals, an observation that might be related to the lack of an SWPV-encoded homolog of the poxviral epidermal growth factor-like gene (Afonso et al. 2002; McNutt et al. 1929; Schwarte and Biester 1941). The cytoplasm of affected cells is brightened and enlarged, contains eosinophilic inclusion bodies resembling poxviral type B inclusion bodies (Teppema and De Boer 1975) (Figure 30.3B), and reacts strongly with antibodies against viral antigens (Cheville 1966b). Hydropic degeneration and inclusion bodies are also observed in the outer root sheaths of the hair follicles (Kasza and Griesemer 1962; Meyer and Conroy 1972). The nucleus of affected cells exhibits margination of chromatin and a large, central "vacuole" resembling the nuclear clearing observed in sheeppox virus-infected keratinocytes (Figure 30.3B) (Cheville 1966a; Kasza and Griesemer 1962; McNutt et al. 1929; Meyer and Conroy 1972; Plowright and Ferris 1958; Teppema and De Boer 1975). No significant fluid accumulation is observed between keratinocytes. Apical keratinocytes undergo necrosis at later stages of infection. Leukocyte

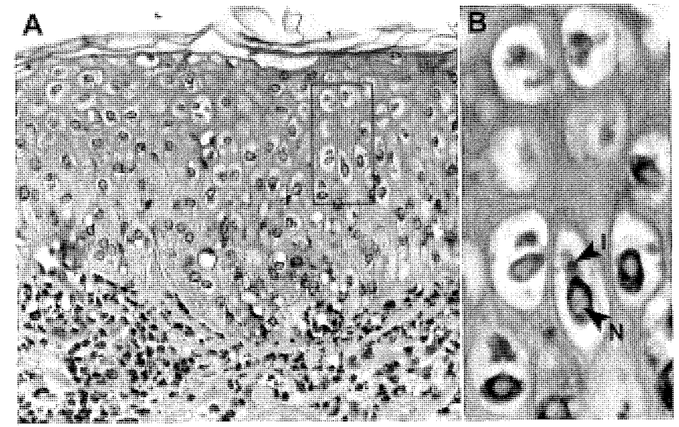

30.3. Histopathological changes caused by swinepox virus. (A) Skin section showing hydropic degeneration in the stratum spinosum of the epidermis and inflammatory cells in the dermis. (B) Magnification of the boxed area in A showing ballooned keratinocytes containing cytoplasmic inclusion bodies (I) and central nuclear clearing (N). Hematoxylin and eosin (courtesy of D. A. Gregg).

infiltration is observed in the underlying dermis and, to a lesser degree, the affected epidermis (Figure 30.3A), with few viral antigen-containing dermal macrophages (Cheville 1966b). When involved, the inguinal lymph nodes present edema, hyperemia, hyperplasia, and few virus antigen-containing cells (Cheville 1966a; Kasza and Griesemer 1962).

Ultrastructurally, infected cells exhibit a marked decrease in keratin precursors (tonofilaments) and loss of intercellular interdigitations characteristic of the stratum spinosum (Cheville 1966a; Teppema and De Boer 1975). Individual inclusion bodies consist of electrodense central cores surrounded by lamellar bodies and maturing viral particles (viroplasm) (Cheville 1966a; Conroy and Meyer 1971; Kim and Luong 1975; Smid et al. 1973; Teppema and De Boer 1975). The large, well-defined nuclear "vacuole" can be more accurately described as a region of low electron density, which lacks a surrounding membrane and contains cross-striated fibrils similar to those observed in the cytoplasm.

DIAGNOSIS

Presumptive SWP diagnosis is based on the observation of pox lesions on the skin of affected animals. Differential diagnosis includes vesicular diseases, allergic skin reactions, sunburn, bacterial dermatitis, ringworm, and skin parasitosis (*Acarus* (*Tyroglyphus*) spp., sarcoptic mange) (Blood and Radostits 1989; Yager and Scott 1985). SWPV involvement can be confirmed by electron microscopy and histopathology and includes pathognomonic epidermal changes: ballooned stratum spinosum keratinocytes containing cytoplasmic eosinophilic inclusion bodies and a "vacuolated" nucleus. SWPV involvement may be definitively confirmed using SWPV-specific antibodies to neutralize virus isolated on swine cell cultures (primary swine kidney cells, PK-15 cell line) (Borst et al. 1990; Meyer and Conroy 1972; Paton et al. 1990) or by performing immunocytochemistry on tissue samples or infected cell cultures (Garg and Meyer 1973; Mohanty et al. 1989; Paton et al. 1990). Papular/pustular exudate or crusted materials are clinical samples of choice for virus isolation. At least seven blind passages should be attempted before considering the sample negative (De Boer 1975).

Virus neutralization and precipitating antibody tests to detect SWPV-specific antibodies in convalescent serum have been described (De Boer 1975; Shope 1940). Since swine do not reliably develop high levels of neutralizing antibodies (Kasza et al. 1960; Shope 1940), negative test results should be interpreted with caution.

The availability of the SWPV genome sequence and the identification of unique SWPV gene sequences will permit the development of rapid, sensitive, and specific polymerase chain reaction-based detection and diagnostic assays (Afonso et al. 2002).

Although differential diagnosis of SWP from a vaccinia virus infection in pigs was important when human smallpox vaccination was practiced, this no longer represents a diagnostic concern (Shope 1940).

IMMUNITY

Convalescent swine are resistant to SWPV challenge, indicating that infection induces protective immunity (De Boer 1975; Garg and Meyer 1972; Kasza et al. 1960; Schwarte and Biester 1941; Shope 1940). However, the

immune mechanisms associated with protection are not known. SWPV neutralizing activity is present in swine sera as early as 7 days PI. However, low neutralizing titers, delayed kinetics of antibody response, and lack of neutralizing antibodies at 50 days PI have been reported (Kasza et al. 1960; Meyer and Conroy 1972; Shope 1940; Williams et al. 1989). Suckling pigs may also be protected by maternal antibody (Manninger et al. 1940), although high neonatal mortality rates have been observed (Olufemi et al. 1981). Decreased mitogen and SWPV-induced proliferative responses have been observed in peripheral blood mononuclear cells from experimentally infected swine (Williams et al. 1989).

PREVENTION AND CONTROL

No specific treatment for SWPV exists. Antibiotic regimens are recommended for the treatment of secondary bacterial infection. Given that SWP is of relatively low economic impact, no vaccine has been developed. Good animal husbandry, including ectoparasite control, should be practiced.

REFERENCES

Afonso CL, Tulman ER, Lu Z, et al. 2002. J Virol 76:783–790.
Barcena J, Blasco R. 1998. Virology 243:396–405.
Blakemore F, Abdussalam M. 1956. J Comp Pathol 66:373–377.
Blood DC, Radostits OM. 1989. Veterinary Medicine: A Textbook of the Diseases of Cattle, Sheep, Pigs, Goats and Horses, 7th ed. London: Bailliere Tindall, pp. 571–958.
Borst GH, Kimman TG, Gielkens AL, van der Kamp JS. 1990. Vet Rec 127:61–63.
Cheville NF. 1966a. Am J Pathol 49:339–352.
——. 1966b. Pathol Vet 3:556–564.
Conroy JD, Meyer RC. 1971. Am J Vet Res 32:2021–2032.
Datt NS. 1964. J Comp Pathol 74:62–69.
De Boer GF. 1975. Arch Virol 49:141–150.
Foley PL, Paul PS, Levings RL, et al. 1991. Ann N Y Acad Sci 646:220–222.
Garg SK, Meyer RC. 1972. Appl Microbiol 23:180–182.
——. 1973. Res Vet Sci 14:216–219.
Hahn J, Park S-H, Song J-Y, et al. 2001. J Virol Methods 93:49–56.
Jubb TF, Ellis TM, Peet RL, Parkinson J. 1992. Aust Vet J 69:99.
Kasza L, Bohl EH, Jones DO. 1960. Am J Vet Res 21:269–273.
Kasza L, Griesemer RA. 1962. Am J Vet Res 23:443–450.
Kawagishi-Kobayashi M, Cao C, Lu J, et al. 2000. Virology 276: 424–434.
Kim JCS, Luong LC. 1975. Vet Med Small Anim Clin 70: 1043–1045.
Manninger R, Csontos J, Salyi J. 1940. Uber die atiologie des pockenartigen ausschlages der ferkel. Archiv fur Tierheilkunde 75:159–179.
Massung RF, Jayarama V, Moyer RW. 1993. Virology 197: 511–528.
Massung RF, Moyer RW. 1991. Virology 180:355–364.
McNutt SH, Murray C, Purwin P. 1929. Am Vet Med Assoc 74: 752–761.
Meyer RC, Conroy JD. 1972. Res Vet Sci 13:334–338.
Miller RC, Olson LD. 1980. Am J Vet Res 41:341–347.
Mohanty PK, Verma PC, Rat A. 1989. Acta Virol 33:290–296.
Moyer RW, Arif B, Black DN, Boyle DB, et al. 2000. Family *Poxviridae*. In MHV van Regenmortel, CM Fauquet, DHL Bishop, EB Carstens, MH Estes, SM Lemon, J Maniloff, MA Mayo, DJ McGeoch, CR Pringle, RB Wickner, eds. Virus Taxonomy: Classification and Nomenclature of Viruses. The Seventh Report of the International Committee on Taxonomy of Viruses. San Diego, CA: Academic Press, pp. 137–157.
Olufemi BE, Ayoade GO, Ikede BO, et al. 1981. Vet Rec 109: 278–280.
Ouchi M, Fujiwara M, Hatano Y, et al. 1992. J Vet Med Sci 54: 731–737.
Paton DJ, Brown IH, Fitton J, Wrathall AE. 1990. Vet Rec 127:204.
Plowright W, Ferris RD. 1958. Br J Exp Pathol 39:424–435.
Rahman MM, Barrett JW, Brouckaert P, McFadden G. 2006. J Biol Chem 281:22517–22526.
Schwarte LH, Biester HE. 1941. Pox in swine. Am J Vet Res 2: 136–140.
Shope RE. 1940. Swine pox. Arch Gesamte Virusforsch 1: 457–467.
Smid B, Valicek L, Mensik J. 1973. Zentralbl Veterinarmed B 20: 603–612.
Teppema JS, De Boer GF. 1975. Arch Virol 49:151–163.
Tripathy DN. 1999. Adv Vet Med 41:463–480.
van der Leek ML, Feller JA, Sorensen G, et al. 1994. Vet Rec 134: 13–18.
Williams PP, Hall MR, McFarland MD. 1989. Vet Immunol Immunopathol 23:149–159.
Winslow BJ, Cochran MD, Holzenburg A, et al. 2003. Virus Res 98:1–15.
Winslow BJ, Kalabat DY, Brown SM, et al. 2005. Vet Microbiol 111:1–13.
Yager JA, Scott DW. 1985. The skin and appendages. In KVF Jubb, JA Yager, DW Scott, eds. Pathology of Domestic Animals, Vol. 1, 3rd ed. Orlando, FL: Academic Press, pp. 407–549.

J. Comp. Path. 2011, Vol. ■, 1–9

Available online at www.sciencedirect.com

ScienceDirect

ELSEVIER
www.elsevier.com/locate/jcpa

Early Occurrence of Apoptosis in Lymphoid Tissues from Chickens Infected with Strains of Newcastle Disease Virus of Varying Virulence

L. Harrison*, C. Brown*, C. Afonso†, J. Zhang* and L. Susta*

** Department of Veterinary Pathology, College of Veterinary Medicine, University of Georgia and † Southeast Poultry Research Laboratory, Agricultural Research Service, United States Department of Agriculture, Athens, GA 30605, USA*

Summary

Newcastle disease virus (NDV), the causative agent of Newcastle disease, is a prevalent problem in the poultry industry and often the cause of severe economic loss. There are many strains of the virus and these have varying virulence. The most virulent strains cause systemic lesions of lymphoid tissues, with necrosis and severe lymphoid depletion. Less virulent strains do not cause as much necrosis, but may predispose to secondary infection with other pathogens. Apoptosis or programmed cell death, has been demonstrated to play a role in the pathogenesis of other paramyxovirus infections, notably those caused by measles and canine distemper viruses. To investigate the role of apoptosis in lymphoid organs during NDV infection, immunohistochemistry for determination of expression of caspase-3, a marker of imminent apoptosis, was performed on formalin-fixed paraffin wax-embedded tissues (spleen, thymus, caecal tonsils and bursa of Fabricius) from 4-week-old chickens infected with NDV strains of varying virulence 2 days previously. The amount of apoptosis was proportional to the severity of the clinical disease elicited by the strains.

© 2011 Elsevier Ltd. All rights reserved.

Keywords: apoptosis; chicken; lymphoid tissue; Newcastle disease virus

Introduction

Newcastle disease virus (NDV) is a concern of the poultry industry worldwide as it causes significant morbidity and mortality as well as economically damaging trade restrictions (OIE, 2008). Newcastle disease is caused by viruses belonging to the avian paramyxovirus-1 (APMV-1) group, part of the genus *Avulavirus*, family Paramyxoviridae (Alexander, 1998, 2001, 2003).

Among NDV strains, virulence and capacity to induce disease vary greatly, and historically the viruses have been classified into three pathotypes: low virulence (lentogens), moderate virulence (mesogens) or high virulence (velogens) (Alexander, 2003). The internationally accepted standard for strain classification is the intracerebral pathogenicity index (ICPI), which involves inoculation of day-old chicks and scoring illness and death over a 10-day period (OIE, 2008). Conventionally, lentogens have an ICPI < 0.7, mesogens between 0.7 and 1.5, and velogens > 1.5 (Alexander, 1998). However, these virulence groups (lentogen, mesogen and velogen) are very broad categories, and degree of clinical disease does not always segregate with ICPI. There are cases, for example, in which a strain is considered 'virulent' by ICPI, but does not cause much in the way of clinical disease (Susta *et al.*, 2011; Wakamatsu *et al.*, 2006b, c). This is also complicated by the fact that velogens can be further divided into viscerotropic and neurotropic based on their tropism for nervous tissue and ability to cause neurologic signs, thus causing the category of the 'velogens' to span over various manifestations of severe disease.

Apoptosis is a multistep, multipathway process that leads to cell death. It is important both in physiological and pathological conditions, and relies on the activation of a number of proteolytic enzymes, called caspases, that ultimately lead to denaturation of the cytoplasm, fragmentation of the nucleus and cell destruction without induction of inflammation

Correspondence to: L. Susta (e-mail: lsusta@uga.edu).

0021-9975/$ - see front matter
doi:10.1016/j.jcpa.2011.03.005

© 2011 Elsevier Ltd. All rights reserved.

Please cite this article in press as: Harrison L, et al., Early Occurrence of Apoptosis in Lymphoid Tissues from Chickens Infected with Strains of Newcastle Disease Virus of Varying Virulence, Journal of Comparative Pathology (2011), doi:10.1016/j.jcpa.2011.03.005

ARTICLE IN PRESS

(Robbins and Cotran, 2009). Apoptosis is associated with many viral infections and can function to either enhance or decrease viral survival, depending on the circumstances. Caspase-3 is an effector caspase, which is activated as a pre-terminal event in the caspase cascade and so can be considered as a marker of impending apoptosis (Robbins and Cotran 2009).

Numerous in-vitro experiments have shown that NDV triggers the apoptotic process (Ravindra *et al.*, 2008a, b; 2009a, b). Few in-vivo apoptosis studies are available, but it appears that with the most virulent NDV strains, apoptosis in lymphoid tissue increases (Kommers *et al.*, 2002).

The more virulent NDV strains cause severe acute systemic clinical disease and death (Brown *et al.*, 1999b; Kommers *et al.*, 2002; 2003a, b; Wakamatsu *et al.*, 2006a). The microscopical lesions associated with these strains consist of massive damage to the lymphoid system, including severe splenic disruption, ulceration of intestinal epithelium overlying the lymphoid aggregates, and rapid depletion of the bursa of Fabricius (Brown *et al.*, 1999b; Kommers *et al.*, 2001; 2002; 2003a, b; Wakamatsu *et al.*, 2006a, c).

Similar targeting of the lymphoid tissues has been observed with other viruses in the Paramyxoviridae family, such as measles (Vidalain *et al.*, 2001), rinderpest (Stolte *et al.*, 2002), canine distemper (all belonging to *Morbillivirus* genus) (McCullough *et al.*, 1974; Schobesberger *et al.*, 2005), and porcine Rubulavirus (PoRV, *Rubulavirus* genus) (Rodriguez-Ropon *et al.*, 2003). With these viruses, lymphocyte apoptosis, lymphoid tissue atrophy and subsequent immune-depression are determinants of disease expression, leaving hosts that survive the acute infection very susceptible to secondary infections. However, the extent to which damage to the lymphoid tissues in NDV infection is due to direct viral effects leading to necrosis and how much is related to apoptosis is largely unknown.

The aims of the present study were to characterize the presence and extent of apoptosis in the lymphoid organs during early NDV infection and to investigate the nature of NDV-induced lymphocytic depletion.

Materials and Methods

Tissues

Tissues for this study included archived formalin-fixed, paraffin wax-embedded spleen, thymus, bursa of Fabricius and caecal tonsils (intestinal lymphoid aggregates) harvested in identical manner from several different experiments examining the pathogenesis of NDV infection. For this experiment, archived blocks from a total of 20 birds were used: eight of the birds were infected with four high-virulence viruses, six with three viruses of intermediate virulence, four with two low-virulence viruses and there were two control specific pathogen-free uninfected birds.

In all cases, tissues were taken from two birds infected with each strain, at 2 days post infection (dpi) after administration of approximately 10^5 EID_{50} units of virus via eyedrop instillation. In those studies, birds were killed by intravenous injection of pentobarbital and tissues were collected into 10% neutral buffered formalin immediately *post mortem*. After 52 h in formalin, tissues were processed routinely and embedded in paraffin wax. Archived wax blocks were stored at room temperature. All studies involved 4-week-old white leghorn chickens from the same source flock kept at the Southeast Poultry Research Laboratory (SEPRL).

Viruses

Nine strains of NDV were examined in this study. Table 1 lists the viruses, their origin, the ICPI, severity of clinical disease, time to death and the respective literature references. Based on the clinical signs and time to death, birds were grouped into three general categories. Category 1 contained all viruses where birds

Table 1
Details of NDV strains used in this study

Virus	*Clinical disease*	*Time to death*	*ICPI*	*References*
Long Bien 78	Severe, acute	3 days	1.88	Susta *et al.*, 2011
Chicken CA/S0212676	Severe, acute	3–5 days	1.76	Wakamatsu *et al.*, 2006a
rZJ1	Severe, acute	4 days	1.86	Animal experiment conducted in our laboratory, data not published
93-28710	Severe, acute	5 days	1.88	Seal *et al.*, 1998; Brown *et al.*, 1999b
Nevada Cormorant	Nervous	9 days	1.53	Susta *et al.*, 2011
Roakin	Mild to moderate	No death recorded	1.60	Seal *et al.*, 1998; Brown *et al.*, 1999b
Anhinga	Minimal	No death recorded	1.31	Brown *et al.*, 1999b; Kommers *et al.*, 2003b
B1	None	NA	0.13	Seal *et al.*, 1998; Brown *et al.*, 1999b
QV4	None	NA	0.39	Seal *et al.*, 1998; Brown *et al.*, 1999b

Please cite this article in press as: Harrison L, et al., Early Occurrence of Apoptosis in Lymphoid Tissues from Chickens Infected with Strains of Newcastle Disease Virus of Varying Virulence, Journal of Comparative Pathology (2011), doi:10.1016/j.jcpa.2011.03.005

Table 2
Apoptotic cell counts by category and organ

Category	*Sample size (n)*	*Organs*							
		Spleen		*Thymus*		*Bursa*		*Gut*	
		*Mean ± SD**	*SS†*	*Mean ± SD*	*SS*	*Mean ± SD*	*SS*	*Mean ± SD*	*SS*
Category 1 (velogens)	80	22.43 ± 2.5	Yes for all $P < 0.0001$	17.5 ± 2.9	Yes for all $P < 0.0001$	15.9 ± 2	Yes for all $P < 0.0001$	21.6 ± 2	Yes for all $P < 0.0001$
Category 2 (mesogens)	60	4.6 ± 2.58	Yes to negative $P = 0.02$	5.65 ± 2.5	Yes to negative $P = 0.0049$	8.9 ± 2.5	Yes to negative and lentogens $P < 0.0001$	8.0 ± 2.5	Yes to negative and lentogens $P = 0.0001$
Category 3 (lentogens)	40	2.01 ± 2.7	NO $P = 0.308$	3.46 ± 2.7	NO $P = 0.101$	2.25 ± 2.7	NO $P = 0.225$	2.72 ± 2.7	NO $P = 0.155$
PBS	20	0.12 ± 3	$P = 0.38$	0.1 ± 2.2	$P = 0.101$	0.18 ± 1.9	$P = 0.225$	0.15 ± 3	$P = 0.155$

*Mean ± SD positive cells/×40 field. There are four strains in category 1, three strains in category 2 and two strains in category 3; each strain represents data from two birds, each bird's organ counts are derived from ten ×40 fields.
†SS, statistical significance. For the fields that are statistically significant, the highest *P* value (out of three) is provided. For the fields that are not statistically significant, the lowest (out of three) value is provided.

became severely clinically ill, had severe lesions and died within 5 days of inoculation. Category 3 consisted of those viruses historically classified as 'lentogens' which in our study caused no clinical disease, lesions or mortality. Category 2 consisted of all strains that fell between categories 1 and 2 and caused birds to become clinically ill only after 8 days of infection, and in which lesions and mortality were inconsistent.

There were four strains that met the criteria of Category 1: 93-28710, isolated from a Chinese parakeet at an American quarantine station (ICPI 1.88) (Seal *et al.*, 1998; Brown *et al.*, 1999b); Chicken CA/S0212676, from a 2002 outbreak in California (ICPI 1.76) (Wakamatsu *et al.*, 2006a); rZJ1, a plasmid-rescued virus from a 2000 isolate from an outbreak in geese in China (ICPI 1.86) (Liu *et al.*, 2007); Long Bien 78, a 2002 isolate from a duck at the Long Bien market in Vietnam (ICPI 1.88) (Susta *et al.*, 2011). Category 2 consisted of three strains: Roakin, initially isolated from birds in New Jersey in 1946 (ICPI 1.60); Anhinga, originally isolated from a captive population in a water park in Florida in 1993 (ICPI 1.31) (Brown *et al.*, 1999b; Kommers *et al.*, 2003b); NV Cormorant, a 2005 isolate from a double crested cormorant in NV, USA (ICPI 1.53) (Susta *et al.*, 2011). Category 3 consisted of: B1, a low-virulence strain used in many vaccines and first isolated in New Jersey in 1947 (ICPI 0.13); QV4, isolated in 1966 in Australia (ICPI 0.39) (Seal *et al.*, 1998; Brown *et al.*, 1999b; Alexander, 2003). In addition, two non-infected birds (inoculated with phosphate buffered saline [PBS]) were used as controls. ICPI values were determined at the time of the original bird experiment using the same standard technique and using chickens from the same source flock at SEPRL (OIE, 2008).

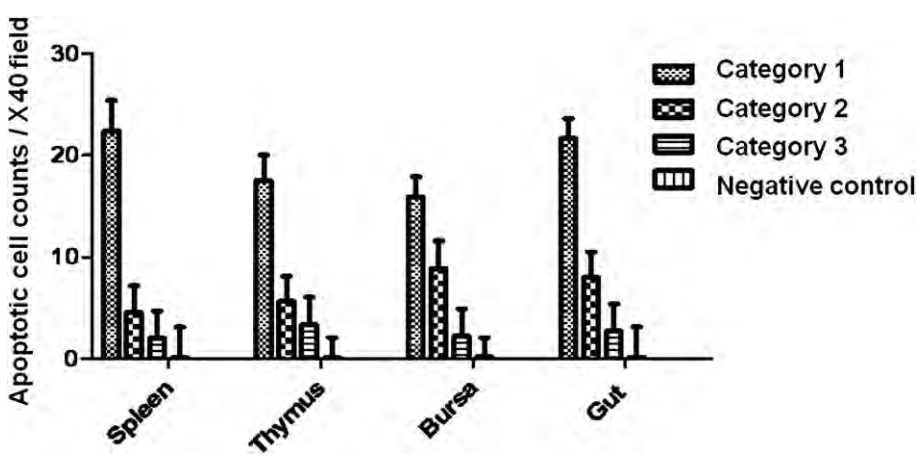

Fig. 1. Graphic representation of apoptotic cell counts, by category and lymphoid organ.

Please cite this article in press as: Harrison L, et al., Early Occurrence of Apoptosis in Lymphoid Tissues from Chickens Infected with Strains of Newcastle Disease Virus of Varying Virulence, Journal of Comparative Pathology (2011), doi:10.1016/j.jcpa.2011.03.005

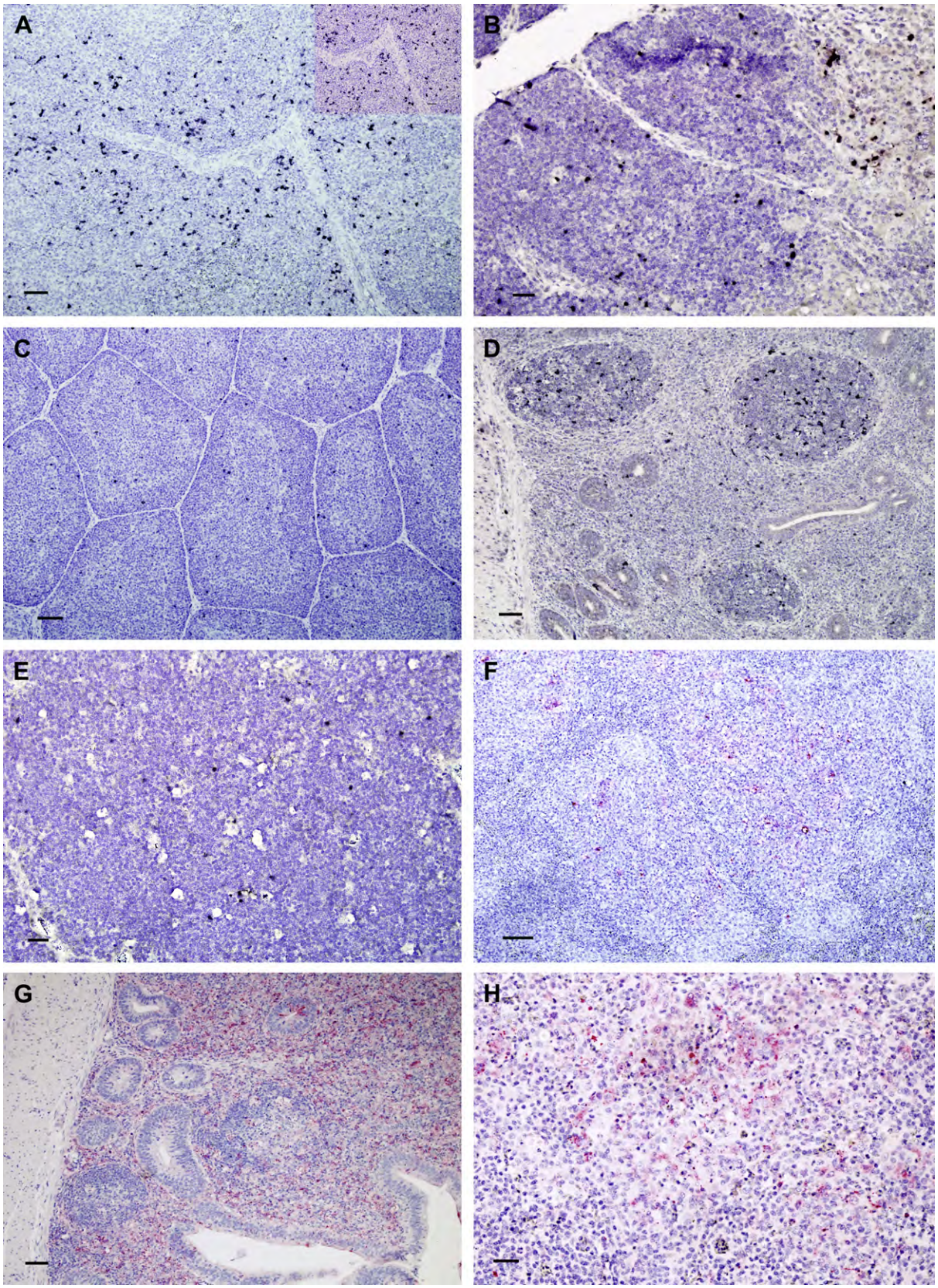

Please cite this article in press as: Harrison L, et al., Early Occurrence of Apoptosis in Lymphoid Tissues from Chickens Infected with Strains of Newcastle Disease Virus of Varying Virulence, Journal of Comparative Pathology (2011), doi:10.1016/j.jcpa.2011.03.005

ARTICLE IN PRESS

Immunohistochemistry

Sections (4 μm) were cut onto positively charged slides and dewaxed immediately prior to immunohistochemistry (IHC). For caspase-3 IHC, sections were subject to antigen retrieval by steaming for 15 min in citrate buffer (Biogenex, San Ramon, CA, USA). Following antigen retrieval, blocking was performed with universal blocking reagent (Biogenex). Primary rabbit anti-active caspase-3 (Anti-ACTIVE® Caspase-3 polyclonal antibody; Promega, Madison, WI, USA) was diluted at 1 in 2,000 in antibody diluent (DAKO, Carpinteria, CA, USA). Sections were incubated with primary antibody for 1 h at room temperature. An isotype control was performed with normal rabbit serum (diluted 1 in 300) in place of the primary antibody.

Sections used for detection of NDV nucleoprotein (NP) were subject to antigen retrieval using a citrate buffer solution (Vector Laboratories, Burlingame, CA, USA) and microwaved at lowest power for 15 min. The primary antibody was raised in rabbit against a synthetic peptide of the NDV NP (amino acid sequence: TAYETADESETRRIC). Primary antibody was applied to the sections at a dilution of 1 in 8,000 in antibody diluent (Zymed® Laboratories Inc., San Francisco, CA, USA) at 37°C for 1 h or at 4°C overnight.

After incubation with primary antibodies, the slides were washed and incubated with an alkaline phosphatase-linked polymer system (Labvision Corp., Fremont, CA, USA) directed against the Fc fragment of the rabbit immunoglobulin. The reaction was 'visualized' by means of naphthol-based Vector Red (Vector Laboratories) or tetrazolium-based (NBT-BCIP) chromogens. Slides were lightly counterstained with Mayer's haematoxylin and coverslipped using Permount (Fisher Scientific, Fair Lawn, NJ, USA). Serial sections immunolabelled for expression of active caspase-3 and NDV NP were compared in order to assess expression of the two antigens in the same areas of tissue.

Statistical Analysis

Cells positive for active caspase-3 expression were counted at ×400 magnification (field of view = 0.45 mm), in 10 randomly chosen fields within each organ. The same microscope (Olympus, model CH2) was used for all counts. The results were expressed as the arithmetic mean ± standard deviation (SD) of positively labelled cells by organ in each virulence category. The means were compared using analysis of variance (ANOVA) and Dunnett's multiple comparison test for matched group. $P < 0.05$ was considered statistically significant.

Results

Active Caspase-3

Results for expression of active caspase-3 are presented in Table 2 and Fig. 1. When cells were positive, the signal was always confined to the cytoplasm, with a fine granular pattern equally distributed throughout the cytoplasmic space. Signal within the spleen was strongest in the periarteriolar lymphoid sheaths in cells morphologically consistent with macrophages (large amount of pale cytoplasm and a vesicular and often indented nucleus) (Fig. 2A). In the thymus (Fig. 2B) and bursa of Fabricius (Fig. 2C), signal appeared in both cortical and medullary regions and was predominantly in cells morphologically consistent with lymphocytes. Areas of positive active caspase-3 labelling were also found in intestinal lymphoid tissue, where signal was present in both macrophage-like cells and lymphocytes (Fig. 2D).

Numerical scores were highest with the NDV strains in Category 1, with significantly more apoptosis in all lymphoid organs than with any other strain categories and also negative controls. For strains in Category 2, apoptosis within the bursa of Fabricius and the intestinal tissue was significantly greater than in organs from birds infected with lentogens or negative controls; whereas splenic and thymic rates of apoptosis were significantly higher compared only with controls, but not with birds in Category 3. Although the numerical values for Category 3 and the control birds were different, there was not a significant difference between these two groups (Fig. 2E).

Fig. 2. (A) Spleen from a chicken infected with Long Bien (Category 1) strain, 2 dpi. There is intense immunolabelling for active caspase-3 around the penicillary arteries in cells compatible with macrophages. IHC. Bar, 100 μm (inset 50 μm). (B) Thymus from a chicken infected with California 2002 (Category 1) strain, 2 dpi. There is intense immunolabelling for active caspase-3 both in the cortex and medulla. IHC. Bar, 50 μm. (C) Bursa of Fabricius from a chicken infected with Nevada Cormorant (Category 2) strain, 2 dpi. There is immunolabelling for active caspase-3 of cells morphologically compatible with lymphocytes both in the cortex and medulla. IHC. Bar, 100 μm. (D) Caecal tonsils from a chicken infected with rZJ1 (Category 1) strain, 2 dpi. There is immunolabelling for active caspase-3 in numerous cells within the lymphoid aggregate in the lamina propria. IHC. Bar, 50 μm. (E) Thymus from a chicken infected with B1 (Category 3) strain, 2 dpi. Scattered cells express active caspase-3. IHC. Bar, 50 μm. (F) Spleen from a chicken infected with 93-2871 (Category 1) strain, 2 dpi. Numerous cells are immunolabelled for NDV NP, mainly around the penicillary arteries. IHC. Bar, 100 μm. (G) Caecal tonsils from a chicken infected with California 2002 (Category 1) strain, 2 dpi. Numerous cells within the lamina propria express NDV NP. IHC. Bar, 50 μm. (H) Thymus from a chicken infected with rZJ1 (Category 1) strain, 2 dpi. There is immunolabelling of scattered cells within the medulla for NDV NP. IHC. Bar, 50 μm.

Please cite this article in press as: Harrison L, et al., Early Occurrence of Apoptosis in Lymphoid Tissues from Chickens Infected with Strains of Newcastle Disease Virus of Varying Virulence, Journal of Comparative Pathology (2011), doi:10.1016/j.jcpa.2011.03.005

ARTICLE IN PRESS

Table 3
Presence of NDV as detected by IHC

Strain	*Spleen*	*Thymus*	*Bursa*	*Intestinal lymphoid tissue*
Category 1				
Long Bien 78	+ + +	+ +	+	+ +
Chicken CA/S0212676	+ +	+ +	+ +	+ + +
rZJ1	+ +	+ +	–	+ +
93-2871-	+ +	+ +	–	+ +
Category 2				
Nevada Cormorant	–	–	–	–
Roakin	–	–	–	–
Anhinga	–	–	–	–
Category 3				
B1	–	–	–	–
QV4	–	–	–	–
Negative control	–	–	–	–

–, no positive signal in any part of the organ; +, rare scattered positive cells in few high-power fields; + +, labelling in several high-power fields; + + +, labelling in every high-power field.

NDV Nucleoprotein

Results for expression of NDV NP are presented in Table 3. Positive signal was detected only in tissues harvested from birds infected with viruses in Category 1, and was present in spleen, caecal tonsils, thymus and bursa. In the spleen, NP was detected mainly in large cells surrounding the penicillary arterioles. These cells were morphologically compatible with macrophages (Fig. 2F). In intestinal lymphoid tissue (caecal tonsil), virus was mainly confined to large macrophages with vacuolated cytoplasm (Fig. 2G). In the bursa, there was labelling of both cortical and medullary regions, often involving entire scattered follicles. The thymus showed multifocal labelling of both cortical and medullary regions (Fig. 2H). Immunolabelling for NDV was cytoplasmic and had a fine to coarse granular pattern. There was no labelling in any organs of birds infected with viruses from categories 2 or 3. Similarly, tissues from non-infected control birds were negative for the presence of NDV NP.

Discussion

The present study has measured the amount of apoptosis in lymphoid tissues 2 days after birds were infected in a uniform manner with NDV strains of varying virulence. Some apoptosis was present in all lymphoid organs from infected birds, although there were notable differences according to virulence of strains. Because of the difficulties in matching the standard pathogenicity indices with the clinical behaviour of the virus, the different strains were categorized on the basis of clinical data. With this classification, the Roakin and Nevada Cormorant strains fell into Category 2, while by standard pathogenicity criteria they are considered to be velogens (Alexander, 1998). The viscerotropic velogenic strains 93-28710, Chicken CA/S0212676, rZJ1 and Long Bien 78 fell into category 1; the lentogenic strains QV4 and B1 into category 3. By standard pathogenicity indices, these viruses are velogens and lentogens, respectively. Overall, the apoptotic rates coincided with the classification scheme adopted, with viruses included in Category 1 having the highest apoptotic count, those in Category 3 having the lowest apoptotic count and viral strains in Category 2 a mid-range apoptotic rate. As our categories correspond roughly to severity of the clinicopathological disease, apoptosis behaves correspondingly.

Our findings agree with a previous study conducted in our laboratory, in which 4-week-old chickens infected with three different virulent strains had an increased apoptotic rate in the spleen, thymus and bursa of Fabricius, as shown by the terminal deoxynucleotidyl transferase-mediated dUTP nick-end labelling (TUNEL) method and IHC for expression of active caspase-3. However, in the previous study, apoptosis was not investigated with avirulent strains and statistical analysis was not attempted (Kommers *et al.*, 2002).

Caspase-3 is an effector caspase (Porter and Janicke, 1999; Stadelmann and Lassmann, 2000) and is one of the last to be activated at the end of the apoptotic cascade. Therefore, its activation takes place immediately before the morphological alteration of apoptosis and reactivity for active caspase-3 can be considered as a snapshot of the impending process. Apoptosis in tissues from birds infected with the viral strains that had the most severe clinical disease (Category 1) was statistically greater than the amount of apoptosis seen in tissues from birds infected with strains in Categories 2 and 3. The average number of apoptotic cells in the spleen, thymus and intestinal lymphoid tissue was three to four times greater than the average number of apoptotic cells in the same organs affected by the strains in Category 2 and an even greater difference was seen with the strains in Category 3. These Category 1 viruses were also the strains for which the highest amount of viral protein was observed within the affected tissues. This suggests that greater virus replication is important for induction of apoptosis. However, because increased apoptosis was observed also in organs in which NP was not detected, a possible role of indirect viral effects in triggering apoptosis should be considered. This has been observed also in infections with other paramyxoviruses, such as those caused by measles and distemper viruses, in which apoptosis is initiated

Please cite this article in press as: Harrison L, et al., Early Occurrence of Apoptosis in Lymphoid Tissues from Chickens Infected with Strains of Newcastle Disease Virus of Varying Virulence, Journal of Comparative Pathology (2011), doi:10.1016/j.jcpa.2011.03.005

ARTICLE IN PRESS

by immune modulation rather than by direct viral damage (Schneider-Schaulies *et al*., 2003; Moss *et al*., 2004; Schobesberger *et al*., 2005).

Although NDV infection has been shown to induce apoptosis by activation of both intrinsic and extrinsic pathways in cell cultures (Ravindra *et al*., 2009a), the exact mechanism by which NDV infection triggers apoptosis *in vivo* has not been entirely determined. NDV is a well known inducer of type I interferons (IFNs) *in vitro* (Park *et al*., 2003), which, in turn, have been demonstrated to induce apoptosis by the up-regulation of numerous proteins that also have an anti-viral effect, such as protein kinase R (PKR), adenosine deaminase acting on RNA (ADAR) and 2′-5′ oligoadenylate synthetase (OAS) (Samuel, 2001). Therefore, an increased production of IFNs might increase apoptosis. In addition, in-vitro experiments have shown that NDV viruses defective for the production of V protein, which blocks the downstream pathway of type I IFNs through STAT1 ubiquitination, have an increased rate of apoptosis, suggesting that the IFN pathway is a major determinant of apoptosis in NDV infection (Thyrell *et al*., 2002; Platanias, 2005; Elmore, 2007). Increased apoptosis also could be the effect of production of IFN-γ, which has been shown to be increased by in-situ hybridization in the spleen of birds infected with velogenic NDV strains (Brown *et al*., 1999a). Also, other acute-phase cytokines, such as tumour necrosis factor (TNF)-α, might play a role in the induction of apoptosis. The latter would act through the activation of the family of TNFα-receptors, which in turn are able to convert procaspase-8 into active caspase-8 (Robbins and Cotran, 2009).

The reports that describe the pathological characteristic of the Category I viruses used in this study showed that at time points later than 2 dpi, there is severe necrosis of the lymphoid tissues with accumulation of large numbers of macrophages associated with extensive immunolabelling for NDV NP or reactivity for NDV matrix mRNA as detected by in-situ hybridization (Brown *et al*., 1999b; Kommers *et al*., 2002; Wakamatsu *et al*., 2006a). This suggests that an apoptotic wave precedes severe necrosis, which is associated with marked viral replication. Therefore, with velogenic strains, the exact role of apoptosis in lymphoid organs is not entirely clear, since it takes place immediately before such an intense necrotic event. It is probable that apoptosis in lymphoid organs might play a more important role in the pathogenesis of Category 2 strains (mostly mesogens), in which the delayed course of the disease might reflect a transient immune depression that could promote or worsen secondary infections.

In some organs, such as the spleen and caecal tonsils, NDV expression was observed mainly in cells morphologically consistent with macrophages, whereas caspase-3 immunolabelling was observed in cells morphologically consistent with both lymphocytes and macrophages. This possibly indicates that infected macrophages play a role in inducing the apoptosis of non-infected cells, through immune signalling. This appears to be the case for measles virus infection, in which indirect immune suppression and lymphopenia have been associated with the immune suppressive properties of dendritic cells infected with the virus (Schneider-Schaulies *et al*., 2003).

For the viruses in Category 2, no NDV antigen was detected in the lymphoid organs, which is in accordance with findings of previous studies (Brown *et al*., 1999b). However, active caspase-3 expression in caecal tonsils and the bursa was statistically higher with category 3 infections and in controls, and higher than controls only in the spleen and thymus. Therefore, even if these strains have the ability to cause only mild to moderate disease in SPF chickens (Alexander, 1998, 2003; Brown *et al*., 1999b), the increased apoptosis in the lymphoid tissue might reflect some degree of immune depression that under field conditions might be likely to lead to other infections.

Viruses in category 3 had a higher count than controls; however, this was not statistically significant. This is reflected by the lack of disease associated with these strains and could be a consequence of a minimal systemic spread of the virus.

In summary, the results of the present study have shown that NDV induces early apoptosis in the lymphoid tissues of infected chickens and that the increased apoptotic rate is statistically correlated with the severity of disease caused by each strain. Apoptosis does not seem only to be the immediate result of viral replication within the cell and it is most likely the consequence of both direct viral replication and indirect effects. While with very virulent strains the apoptosis seems to directly contribute to lymphoid depletion and to the demise of the animals, the increased apoptotic rate in lymphoid organs with viruses of moderate virulence probably assumes more importance in field conditions, where possible immune depression can facilitate secondary infections and complicate the clinical picture.

Conflict of Interest

None of the authors of this paper has a financial or personal relationship with other people or organizations that could inappropriately influence or bias the content of the paper.

Please cite this article in press as: Harrison L, et al., Early Occurrence of Apoptosis in Lymphoid Tissues from Chickens Infected with Strains of Newcastle Disease Virus of Varying Virulence, Journal of Comparative Pathology (2011), doi:10.1016/j.jcpa.2011.03.005

ARTICLE IN PRESS

References

Alexander DJ (1998) Newcastle disease and other paramyxoviruses. In: *A Laboratory Manual For The Isolation, Identification and Characterization of Avian Pathogens*, 4th Edit., DE Swayne, JR Glisson, MW Jackwood, JE Pearson, WM Reed, Eds., American Association of Avian Pathologists, Kennett Square, pp. 156–163.

Alexander DJ (2001) Gordon memorial lecture. Newcastle disease. *British Poultry Science*, **42**, 5–22.

Alexander DJ (2003) Newcastle disease, other avian paramyxoviruses, and pneumovirus infection. In: *Diseases of Poultry*, 11th Edit., YM Shaif, HJ Barnes, JR Glisson, AM Fadly, JR McDouglad *et al.*, Eds., Iowa State University Press, Ames, pp. 64–83.

Brown C, King DJ, Seal BS (1999a) Detection of a macrophage-specific antigen and the production of interferon gamma in chickens infected with Newcastle disease virus. *Avian Diseases*, **43**, 696–703.

Brown C, King DJ, Seal BS (1999b) Pathogenesis of Newcastle disease in chickens experimentally infected with viruses of different virulence. *Veterinary Pathology*, **36**, 125–132.

Elmore S (2007) Apoptosis: a review of programmed cell death. *Toxicologic Pathology*, **35**, 495–516.

Kommers GD, King DJ, Seal BS, Brown CC (2001) Virulence of pigeon-origin Newcastle disease virus isolates for domestic chickens. *Avian Diseases*, **45**, 906–921.

Kommers GD, King DJ, Seal BS, Brown CC (2003a) Pathogenesis of chicken-passaged Newcastle disease viruses isolated from chickens and wild and exotic birds. *Avian Diseases*, **47**, 319–329.

Kommers GD, King DJ, Seal BS, Brown CC (2003b) Virulence of six heterogeneous-origin Newcastle disease virus isolates before and after sequential passages in domestic chickens. *Avian Pathology*, **32**, 81–93.

Kommers GD, King DJ, Seal BS, Carmichael KP, Brown CC (2002) Pathogenesis of six pigeon-origin isolates of Newcastle disease virus for domestic chickens. *Veterinary Pathology*, **39**, 353–362.

Liu YL, Hu SL, Zhang YM, Sun SJ, Romer-Oberdorfer A *et al.* (2007) Generation of a velogenic Newcastle disease virus from cDNA and expression of the green fluorescent protein. *Archives of Virology*, **152**, 1241–1249.

McCullough B, Krakowka S, Koestner A (1974) Experimental canine distemper virus-induced lymphoid depletion. *American Journal of Pathology*, **74**, 155–170.

Moss WJ, Ota MO, Griffin DE (2004) Measles: immune suppression and immune responses. *International Journal of Biochemistry and Cell Biology*, **36**, 1380–1385.

OIE (World Organization for Animal Health) (2008) *Manual of Diagnostic Tests and Vaccines for Terrestrial Animals*, Vol. 1, OIE, Paris, pp. 576–589.

Park MS, Garcia-Sastre A, Cros JF, Basler CF, Palese P (2003) Newcastle disease virus V protein is a determinant of host range restriction. *Journal of Virology*, **77**, 9522–9532.

Platanias LC (2005) Mechanisms of type-I- and type-II-interferon-mediated signalling. *Nature Reviews Immunology*, **5**, 375–386.

Porter AG, Janicke RU (1999) Emerging roles of caspase-3 in apoptosis. *Cell Death and Differentiation*, **6**, 99–104.

Ravindra PV, Tiwari AK, Ratta B, Bais MV, Chaturvedi U *et al.* (2009a) Time course of Newcastle disease virus-induced apoptotic pathways. *Virus Research*, **144**, 350–354.

Ravindra PV, Tiwari AK, Ratta B, Chaturvedi U, Palia SK *et al.* (2009b) Newcastle disease virus-induced cytopathic effect in infected cells is caused by apoptosis. *Virus Research*, **141**, 13–20.

Ravindra PV, Tiwari AK, Ratta B, Chaturvedi U, Palia SK *et al.* (2008a) Induction of apoptosis in Vero cells by Newcastle disease virus requires viral replication, de-novo protein synthesis and caspase activation. *Virus Research*, **133**, 285–290.

Ravindra PV, Tiwari AK, Sharma B, Rajawat YS, Ratta B *et al.* (2008b) HN protein of Newcastle disease virus causes apoptosis in chicken embryo fibroblast cells. *Archives of Virology*, **153**, 749–754.

Robbins SL, Cotran RS (2009) Cellular adaptations, cell injury and cell death. In: *Pathologic Basis of Disease*, V Kumar, AK Abbas, N Fausto, Eds., Saunders-Elsevier, Philadelphia, pp. 26–32.

Rodriguez-Ropon A, Hernandez-Jauregui P, Sanchez-Torres L, Favila-Castillo L, Estrada-Parra S *et al.* (2003) Apoptosis in lymph nodes and changes in lymphocyte subpopulations in peripheral blood of pigs infected with porcine rubulavirus. *Journal of Comparative Pathology*, **128**, 1–8.

Samuel CE (2001) Antiviral actions of interferons. *Clinical Microbiology Reviews*, **14**, 778–809.

Seal BS, King DJ, Locke DP, Senne DA, Jackwood MW (1998) Phylogenetic relationships among highly virulent Newcastle disease virus isolates obtained from exotic birds and poultry from 1989 to 1996. *Journal of Clinical Microbiology*, **4**, 1141–1145.

Schneider-Schaulies S, Klagge IM, Ter Meulen V (2003) Dendritic cells and measles virus infection. *Dendritic Cells and Virus Infection*, **276**, 77–101.

Schobesberger M, Summerfield A, Doherr MG, Zurbriggen A, Griot C (2005) Canine distemper virus-induced depletion of uninfected lymphocytes is associated with apoptosis. *Veterinary Immunology and Immunopathology*, **104**, 33–44.

Stadelmann C, Lassmann H (2000) Detection of apoptosis in tissue sections. *Cell and Tissue Research*, **301**, 19–31.

Stolte M, Haas L, Wamwayi HM, Barrett T, Wohlsein P (2002) Induction of apoptotic cellular death in lymphatic tissues of cattle experimentally infected with different strains of rinderpest virus. *Journal of Comparative Pathology*, **127**, 14–21.

Susta L, Miller PJ, Afonso C, Brown C (2011) Clinicopathological characterization in poultry of three strains of Newcastle disease virus isolated from recent outbreaks. *Veterinary Pathology*, **48**, 349–360.

Thyrell L, Erickson S, Zhivotovsky B, Pokrovskaja K, Sangfelt O *et al.* (2002) Mechanisms of interferon-alpha induced apoptosis in malignant cells. *Oncogene*, **21**, 1251–1262.

Please cite this article in press as: Harrison L, et al., Early Occurrence of Apoptosis in Lymphoid Tissues from Chickens Infected with Strains of Newcastle Disease Virus of Varying Virulence, Journal of Comparative Pathology (2011), doi:10.1016/j.jcpa.2011.03.005

ARTICLE IN PRESS

Vidalain PO, Azocar O, Rabourdin-Combe C, Servet-Delprat C (2001) Measle virus-infected dendritic cells develop immunosuppressive and cytotoxic activities. *Immunobiology*, **204**, 629–638.

Wakamatsu N, King DJ, Kapczynski DR, Seal BS, Brown CC (2006a) Experimental pathogenesis for chickens, turkeys, and pigeons of exotic Newcastle disease virus from an outbreak in California during 2002–2003. *Veterinary Pathology*, **43**, 925–933.

Wakamatsu N, King DJ, Seal BS, Peeters BP, Brown CC (2006b) The effect on pathogenesis of Newcastle disease virus LaSota strain from a mutation of the fusion cleavage site to a virulent sequence. *Avian Diseases*, **50**, 483–488.

Wakamatsu N, King DJ, Seal BS, Samal SK, Brown CC (2006c) The pathogenesis of Newcastle disease: a comparison of selected Newcastle disease virus wild-type strains and their infectious clones. *Virology*, **353**, 333–343.

[*Received, November 25th, 2010*
Accepted, March 2nd, 2011]

Please cite this article in press as: Harrison L, et al., Early Occurrence of Apoptosis in Lymphoid Tissues from Chickens Infected with Strains of Newcastle Disease Virus of Varying Virulence, Journal of Comparative Pathology (2011), doi:10.1016/j.jcpa.2011.03.005

Journal of General Virology (2011), **92**, 544–551 DOI 10.1099/vir.0.027540-0

A single amino acid substitution in the haemagglutinin–neuraminidase protein of Newcastle disease virus results in increased fusion promotion and decreased neuraminidase activities without changes in virus pathotype

Carlos Estevez,[1]† Daniel J. King,[1] Ming Luo[2] and Qingzhong Yu[1]

[1]Southeast Poultry Research Laboratory, Agricultural Research Service, United States Department of Agriculture, 934 College Station Road, Athens, GA 30605, USA

[2]Department of Microbiology, University of Alabama at Birmingham, Birmingham, AL 35294, USA

Correspondence
Qingzhong Yu
qingzhong.yu@ars.usda.gov

Received 24 September 2010
Accepted 24 November 2010

Attachment of Newcastle disease virus (NDV) to the host cell is mediated by the haemagglutinin–neuraminidase (HN), a multifunctional protein that has receptor recognition, neuraminidase (NA) and fusion promotion activities. The process that connects receptor binding and fusion triggering is poorly understood and amino acid residues important for the functions of the protein remain to be fully determined. During the process of generating an infectious clone of the Anhinga strain of NDV, we were able to rescue a NDV with highly increased fusogenic activity *in vitro* and decreased haemagglutinating activity, as compared with the wild-type parental strain. Sequencing of this recombinant virus showed a single mutation at amino acid position 192 of the HN protein (Ile→Met). In the present study, we characterized that single amino acid substitution (I192M) in three strains of NDV by assessing the NA activity and fusogenic potential of the mutated versus wild-type proteins in cell cultures. The original recombinant NDV harbouring the mutation in the HN gene was also used to characterize the phenotype of the virus in cell cultures, embryonated chicken eggs and day-old chickens. Mutation I192M results in low NA activity and highly increased cell fusion *in vitro*, without changes in the viral pathotype of recombinant viruses harbouring the mutation *in vivo*. The results obtained suggest that multiple regions of the HN-protein globular head are important for fusion promotion, and that wild-type levels of NA activity are not absolutely required for viral infection.

INTRODUCTION

Paramyxoviruses are important respiratory pathogens in humans and animals. Human parainfluenza, mumps, Newcastle disease, canine distemper and Sendai viruses are some of the pathogens included in this family (Lamb & Parks, 2007). Paramyxovirus infections are initiated by receptor recognition and binding of the virion to sialyl glycoconjugates on the host cell surface, followed by fusion of the virus lipid envelope with the membrane of the host cell (Connaris *et al.*, 2002; Lamb & Parks, 2007). In Newcastle disease virus (NDV) infections, this process is mediated by the interaction of two viral surface glycoproteins, the haemagglutinin–neuraminidase (HN) and fusion (F) proteins.

The HN of NDV is a class II integral membrane protein, found as a tetramer in the virion, which mediates receptor recognition of sialic acid at the end of host-cell-surface proteins and possesses neuraminidase (NA) activity, necessary to prevent virus progeny self-aggregation during budding (Lamb & Parks, 2007). A third function of the protein is fusion promotion, which is thought to be mediated by interactions of the HN with the F protein (Palermo *et al.*, 2007; Porotto *et al.*, 2005). The F protein is a class I membrane protein present as a trimer in the virion, which is closely associated with HN in the viral membrane. Interactions of the HN tetramer with its receptor are believed to generate conformational changes in this protein, which, in turn, promote changes in the tertiary structure of the F protein, allowing the latter to go from its native structural form (a metastable state), to a pre-hairpin state (in which the fusion peptide is released and interacts with the host cell membrane), to a post-fusion form that allows the viral envelope to approximate to the host cell membrane through the formation of a hairpin structure (referred to as a six-helix bundle) of the protein trimer that results in fusion of these lipid bilayers

†Present address: Texas Veterinary Medical Diagnostic Laboratory, 1 Sippel Road, TAMUS 4471, College Station, TX 77843, USA.

(Lamb *et al.*, 2006). Although the described interaction between the HN and F proteins is generally agreed upon, the relationships between receptor recognition, HN structure, the HN–F interaction and fusion are still poorly understood (Lamb & Parks, 2007; Lamb *et al.*, 2006; Li *et al.*, 2004; Morrison, 2003).

The crystal structure of the HN and F proteins of NDV have been elucidated (Chen *et al.*, 2001; Crennell *et al.*, 2000), and a lot of information has been obtained regarding their three-dimensional structure. The HN displays the six-bladed β-propeller folding typical of other known NAs (Connaris *et al.*, 2002). The receptor recognition/binding and catalytic site for the NA activities have been located to a single large cavity at the top of the globular head of the protein (Lamb *et al.*, 2006). A second receptor binding site (lacking NA activity) has been described for NDV and other paramyxoviruses. It is located at the interface of the monomers of the dimeric units of the HN protein that form the protein tetramers, and is believed to participate in fusion promotion (Palermo *et al.*, 2007; Zaitsev *et al.*, 2004). Crystallographic studies, in which the HN crystals are soaked in solutions of the inhibitor 2-deoxy-2,3-dehydro-*N*-acetyl-neuraminic acid (Neu5Ac2en), revealed that the receptor site presents features that are common to other NAs (Connaris *et al.*, 2002). These include a highly conserved arginine triad at positions 174, 416 and 498, which is very sensitive to mutations and is essential for receptor recognition. Mutations at these residues decrease NA, fusion promotion and haemagglutination (HA) activities to different extents (Connaris *et al.*, 2002). Unique to HN of paramyxoviruses is a large cavity found around the O^4 position of the receptor sialic acid molecule (when HN is bound to its receptor), which is thought to be required to effect the conformational changes associated with fusion promotion. This conserved cavity is lined with several hydrophobic amino acids, including Arg174, Ile175, Ile192 and Asp198 (Ryan *et al.*, 2006). Previous research work has shown that mutations at positions Asp198 and Arg174 decrease receptor recognition and fusion promotion (Connaris *et al.*, 2002; Li *et al.*, 2004), while mutations at Ile175 can induce an increased or decreased fusogenic phenotype, depending on the strain of NDV from which the HN gene has been obtained for the *in vitro* work (Li *et al.*, 2004). Receptor recognition requires the concerted interaction of some of these conserved residues with different parts of the sialic acid molecule that serves as a receptor for the virus. The major anchor points for the receptor molecule are the triad of arginine residues R174, R416 and R498, which interacts with the sialic acid carboxyl group; residues E258 and Y317, which interact with the glycerol moiety of the molecule; and residue Y299 which interacts with the methyl group of the acetamido moiety of the receptor (Connaris *et al.*, 2002). Upon binding to the sialic acid receptor, a series of amino acid movements have been observed in crystallographic studies of the HN protein. For instance, residue R174 moves from its normal position to the large acidic cavity that is found around the O^4 atom of the receptor molecule (Ryan *et al.*, 2006). Movement of residue Arg174 leads to further shifts in other amino acids positions, such as Tyr526 and Lys236, which are thought to be important for the catalytic activity of the protein (Connaris *et al.*, 2002; Crennell *et al.*, 2000; Ryan *et al.*, 2006). Also important for fusion promotion are structural changes that propagate through the surface of the protein upon receptor binding and that result in activation of the second binding site located in the HN-dimer interface (Zaitsev *et al.*, 2004). After cleavage of the sialic acid receptor, a loop containing residue Asp198 moves from its original position; this leads to movement of the loops that form the second binding site including one involving residue 169, another involving residues 516, 517 and 519, and a third loop involving residues 552 and 553 (Zaitsev *et al.*, 2004). Binding of sialic acid to this second binding site drives the F protein to its fusogenic state, thus ensuring fusion.

In our laboratory, the mesogenic NDV strain Anhinga/US(FL)/44083/93 (Anh) was previously used to generate an infectious clone and for reverse genetics studies using this viral strain (Estevez *et al.*, 2007). During rescue, one of the recombinant viruses obtained showed a marked increase in fusogenic activity *in vitro* and low haemagglutinating activity as compared with the parental strain. Sequence analysis of the genome of this virus showed a single amino acid substitution at position 192 (Ile→Met) of the HN gene. This Ile amino acid at position 192 turned out to be highly conserved in the HN protein of most analysed NDV strains.

To date, no work has been performed characterizing HN proteins with mutations at position Ile192, despite its being a conserved residue in all NDV strains and despite it being part of a highly conserved structural element of the NDV HN protein. In the present study, we characterized an amino acid mutation of Ile to Met at position 192 in HN proteins from three different strains of NDV *in vitro*, and *in vivo* for a recombinant virus harbouring this mutation.

RESULTS

Mutation I192M in expressed NDV HN proteins decreases NA activity and haemadsorption, and increases fusion promotion

To determine if the mutation I192M in the HN of NDV affects its functionality, the transiently expressed mutant or wild-type HN proteins from the plasmids were assessed for NA activity, haemadsorption (HAd) and fusion promotion activity. As summarized in Table 1, Vero cell-expressed mutant HN proteins harbouring the I192M amino acid substitution showed a significantly decreased ($P<0.05$) NA activity in comparison with the wild-type protein in the viral strains assessed (ranging from 8.7 to 16.22 % of that of the Anh-wt HN protein), as shown by the results of the fluorimetric NA test. This diminished activity was not due

Table 1. NA, cell expression of HN and HAd activities of wild-type and mutant HN proteins

The biological activities of the wild-type and mutated HN proteins are shown. All values are indicated as a percentage of the activity of the wild-type Anh HN protein in each test. NA and haemadsorption (HAd) activities are corrected for the level of protein expression. Strains: Anh, Anhinga/US(FL)/44083/93; TkND, Turkey/US(ND)/43084/92; CA02, Game fowl/US(CA)/211472/02.

Protein	NA	HAd	Cell expression
Anh HN wt	100.0	100.0	100.0
Anh HN I192M	8.7*	23.5*	106.9
TkND HN wt	106.1	101.9	106.6
TkND HN I192M	8.7*	8.4*	91.8
CA02 HN wt	106.2	62.3	99.3
CA02 HN I192M	16.2*	8.9*	109.3

*Statistically significant differences, $P<0.05$.

to differences in expression levels of the proteins from the plasmid constructs since all the proteins were expressed to similar levels, as demonstrated by the ELISA test performed on transfected monolayers. Similarly, haemadsorption was diminished in the mutated forms of the protein when compared with wild-type (8.4–23.5 % of the levels found in the Anh-wt HN protein) regardless of the NDV strain used to obtain the HN genes, as observed in the HAd test performed (Table 1). Despite diminished HAd and NA activity, the mutant proteins showed a significant increase ($P<0.05$) in fusion promotion in the strains tested in this study, as evidenced by a two- to fourfold increase in the average number of nuclei in 20 fusion foci induced by the expressed mutant HN proteins, compared with that induced by the wild-type forms of these HN proteins (Table 2).

Recombinant viruses harbouring mutation I192M in the HN protein are viable and can be rescued by reverse genetics

Our laboratory has previously developed a reverse genetics system for pathogenesis studies using an infectious clone of the Anhinga strain of NDV. Taking advantage of this system, we rescued recombinant NDV of the Anhinga strain harbouring mutation HN I192M, named rAnh-I192M. The growth kinetics of rAnh-I192M were compared with those of the rescued wild-type Anhinga strain, rAnh-wt, in cell culture and in embryonated chicken eggs. Mutated rAnh-I192M virus grew to titres similar to those of the wild-type recombinant virus in embryonated chicken eggs ($\log_{10}$ 9.4 and 9.1 $TCID_{50}$ ml^{-1}, respectively), while exhibiting an accelerated growth pattern in Vero-cell monolayers in comparison with wild-type virus, as demonstrated by the virus growth curve assay performed (Fig. 1).

Table 2. Fusion promotion

The nuclei counts of fused cells are presented (mean of 20 fusion events).

Protein	Nuclei count (mean)
Anh HN wt	5.35
Anh HN I192M	12.50*
TkND HN wt	5.85
TkND HN I192M	27.60*
CA02 HN wt	4.80
CA02 HN I192M	10.40*

*The number of nuclei in fused cells was significantly different ($P<0.05$) when mutated and wild-type HN proteins of the same virus strain were compared.

The mutant virus rAnh-I192M shows an increased fusogenic phenotype and diminished HA and NA activities

When comparing the phenotypes of the rescued viruses in cell culture, it was found that Vero-cell monolayers infected with the same m.o.i. as wild-type or mutated virus showed marked differences in their fusion activities by 24 h post-inoculation. The rAnh-I192M virus induces larger fusion foci than wild-type virus (Fig. 2), which increased markedly by the second day post-inoculation (not shown). The microplate HA test performed with these viruses showed that mutated virus has a lower HA titre when compared with the wild-type strain (32 and 512, respectively). The NA activity of virus rAnh-I192M was

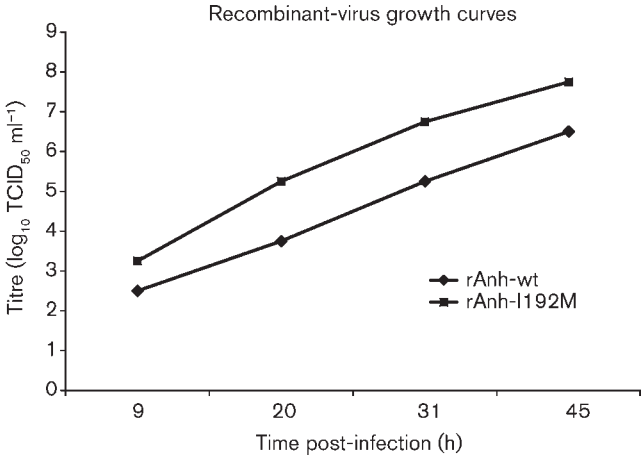

Fig. 1. Virus growth curves of mutated and wild-type Anhinga viruses. Vero-cell monolayers were infected with rAnh-wt or rAnh-I192M at an m.o.i. of 10, and samples of cell culture supernatants were collected at the time points indicated. Virus titres of the collected samples were assessed in Vero cells in triplicate and are presented as mean $\log_{10}$ $TCID_{50}$ ml^{-1}.

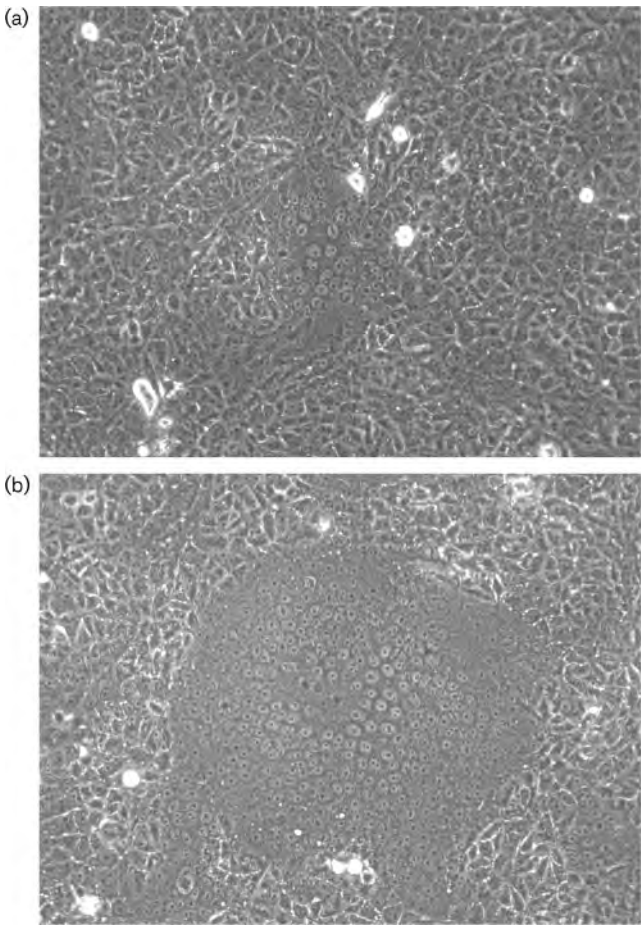

Fig. 2. Fusion promotion of rescued rAnh-wt and rAnh-I192M viruses in Vero cells. Vero-cell monolayers were infected at an m.o.i. of 0.5 with rAnh-wt (a) or rAnh-I192M (b). At 24 h post-inoculation, the monolayers were digitally photographed using an inverted microscope at ×100 magnification (CK40; Olympus). An increased fusogenic phenotype is observed in cells infected with the rAnh-I192M virus.

also diminished in comparison with virus rAnh-wt, mutated virus having roughly 24 % of the NA activity of the rescued wild-type strain. These results are detailed in Table 3.

Table 3. Biological activities and pathotyping tests of recombinant viruses

HA, Haemagglutination titre in microplate format; MDT, mean death time (h) in embryonated chicken eggs; ICPI, intracerebral pathogenicity index; NA, neuraminidase activity of mutated virus expressed as a percentage of the wild-type value.

Virus	HA	NA	MDT (h)	ICPI
rAnh-wt	512	100 %	89	0.91
rAnh-I192M	32	23.9 %	85	1.10

Presence of mutation I192M in the HN of the rAnh-I192M virus did not affect the virus pathotype

The NDV Anhinga strain has been previously characterized as a mesogenic virus by standard pathotyping tests (King & Seal, 1998). The pathotype of rAnh-wt and rAnh-I192M viruses was assessed by the mean death time (MDT) and intracerebral pathogenicity index (ICPI) tests. As shown in Table 3, the MDT in embryonated chicken eggs was 89 h for rAnh-wt, and 85 h for rAhn-I192M virus, while the ICPI values were 0.91 and 1.10, respectively. These results indicate that these viruses can be classified as mesogens, according to the classification used by Alexander (1998). Despite diminished HA and NA activities, the I192M mutation in the recombinant virus did not result in a pathotype change.

DISCUSSION

In this study we have characterized the effects of a mutation at position 192 (Ile→Met) of HN proteins derived from selected NDV strains, as well as characterizing a recombinant virus harbouring this mutation, using *in vitro* and *in vivo* tests. This I192M mutation resulted in decreased HAd and NA activities and increased fusion promotion activity, but no pathotype change.

The HN protein of paramyxoviruses is highly important for the biology of this family of viruses. It determines tropism, mediates virus penetration by its interaction with the F protein and prevents virus aggregation during budding. Receptor recognition and the NA activity of the protein are topographically located to a cavity in the globular head of HN, which is lined with highly conserved amino acid residues, not only in paramyxoviruses but also in other known NAs (Connaris *et al.*, 2002; Ryan *et al.*, 2006). In our experiment, we have found a substitution for one of these conserved amino acids (I192M) that results in changes in the activity of the HN protein. This substitution of isoleucine with methionine, which is a non-polar amino acid, preserves the hydrophobic character of the conserved cavity. Our computer modelling shows that Ile192 is at the base of the loop that contains residue Asp198, a residue that is thought to be important for the catalytic activity of site I and whose movement is necessary for activation of the second binding site (Fig. 3a) (Zaitsev *et al.*, 2004). The side chain of the isoleucine is also part of the large conserved cavity unique to paramyxoviruses. The effects observed with the mutation I192M may result from several different mechanisms. The presence of the larger side chain of the methionine residue in the lining of the cavity in site I of the protein might prevent normal coupling of the sialic acid molecule in the binding site by steric hindrance or disruption of the native conformation of the binding site. This may account for the diminished HAd activity shown by the cell culture-expressed mutant HN protein, as well as for the low HA titre of the rescued virus harbouring the mutation.

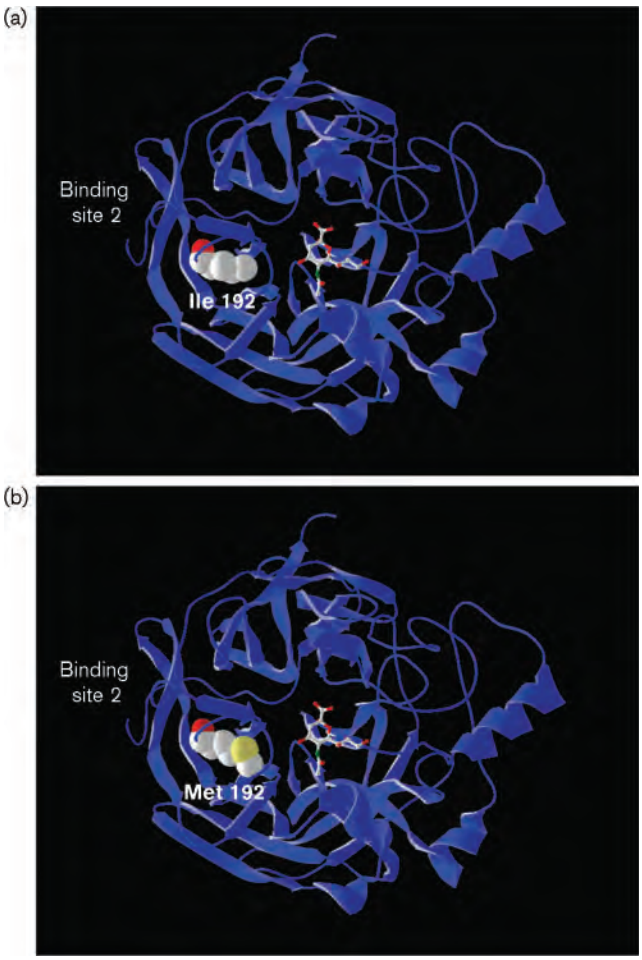

Fig. 3. Molecular model of wild-type and mutated forms of NDV HN proteins of the Anhinga strain. Molecular models of HN proteins show the wild-type isoleucine (in space filling form) at position 192 (a). The mutated protein showing the bulkier methionine residue is depicted in (b). The receptor sialic acid is shown inserted in the cavity atop the globular head (ball and stick form).

The effect of the mutation on the activity of NA is interesting, as it may be related to the highly fusogenic phenotype of the mutant protein. As described previously, Met192 is located in the loop that contains residue Asp198 which is important for NA activity. Upon receptor binding this loop is located above the sugar ring of the substrate, where Asp198 is thought to participate in the hydrolysis of the molecule (Zaitsev *et al.*, 2004). After hydrolysis, the loop moves away from the substrate, and this movement seems to propagate through the protein, resulting in activation of the second binding site and triggering of fusion by the F protein. It is conceivable that the mutation shifts this loop away from the active site, which may result in diminished contact of Asp198 with the substrate (thus diminishing NA activity), and causing movements in the protein that can trigger fusion promotion more effectively. The effects of the mutation on the activation of the second binding site remain to be determined.

Previous studies have shown that the HN protein forms a tetramer in the viral surface, and that the stalk region is also implicated in the activation of the fusion activity of the F protein (Yuan *et al.*, 2005). Met192 is located away from the stalk region, so it seems unlikely that the fusogenic phenotype of the mutant protein is the result of influences of the mutation on the stalk region.

As shown by the rescue of virus harbouring the mutated HN protein, mutation I192M is not disruptive for the biology of the virus. The rescued virus was infective in *in vitro* systems as well as *in vivo*. Interestingly, the rescued virus showed a growth advantage in Vero cell cultures. It is possible that, although the virus has a lower receptor affinity and diminished NA activity, the increased fusion promotion compensates for these phenotypes, resulting in increased virus titres in infected monolayers. This mutation did not result in attenuation of the virus, as shown by the pathotyping tests performed. This is interesting because it seems to indicate that the HA and NA activity levels are not correlated with pathogenicity in NDV. Moreover, these results indicate that there is some flexibility in these HN-protein functions, and also that wild-type levels of these activities are not absolutely required for virus infectivity.

In summary, we have shown that residue Ile192 can affect NA activity, fusion promotion and receptor recognition in NDV, regardless of viral strain. It is likely that the observed fusogenic phenotype is the result of changes in the dynamics of fusion triggering by sialic acid binding. It was also shown that mutation I192M is compatible with the biology of this virus and that it does not induce changes in the viral pathotype.

METHODS

Cell cultures. Vero-cell monolayers (CCL-81; ATCC) were used for plasmid expression of wild-type and mutated forms of HN proteins derived from the viruses used in this study. Rescue of recombinant viruses was performed using HEp-2 cell monolayers (CCL-23; ATCC). Propagation of rescued viruses was performed on 9-day-old embryonated chicken eggs (obtained from the specific pathogen free white leghorn flock maintained by Southeast Poultry Research Laboratory). All cell monolayers were grown in high-glucose Dulbecco's modified Eagle's medium (DMEM) supplemented with 100 U ml^{-1} penicillin, 100 μg ml^{-1} streptomycin, 0.25 μg ml^{-1} amphotericin B (Thermo Scientific) and 10 % FBS (Invitrogen) and kept at 37 °C under a 5 % CO_2 atmosphere unless otherwise indicated.

Viruses and viral RNA extraction. The mesogenic NDV strain Anhinga/US(FL)/44083/93 (Anh) and the velogenic strains Turkey/US(ND)/43084/92 (TkND) and Game fowl/US(CA)/211472/02 (CA02), obtained from a repository bank at the Southeast Poultry Research Laboratory (USDA–ARS), were propagated in 9-day-old embryonated specific-pathogen-free (SPF) chicken eggs as a stock. Viral RNA was extracted from the virus stock using Trizol-LS reagent (Invitrogen) according to the manufacturer's instructions. The modified vaccinia virus Ankara/T7 recombinant (MVA/T7, a gift

of Dr Bernard Moss, Laboratory of Viral Diseases, National Institute of Allergy and Infections Diseases, National Institutes of Health) was used during viral rescue and plasmid-derived HN expression *in vitro* to provide the T7 bacteriophage polymerase (Wyatt *et al.*, 1995).

Construction of HN- and F-protein expression plasmids. The entire coding regions of the HN and F genes of NDV strains Anh, TkND and CA02 were amplified from viral RNA by RT-PCR and ligated into protein-expression plasmid pTM1 (kindly provided by Dr B. Moss) (Moss *et al.*, 1990). The plasmids obtained were named pAnh–HNwt, pTkND–HNwt, pCA02–HNwt, pAnh–F, pTkND–F and pCA02–F and encoded within them are the HN and F protein genes derived from the parental strains described. Transcription from these plasmids is driven by the bacteriophage T7 RNA polymerase. Primers used to amplify the HN and F coding regions are available upon request.

Construction of an infectious clone and supporting protein expression plasmids of the Anhinga strain of NDV. A reverse-genetics system for the generation of recombinant viruses of the NDV Anhinga strain was developed in our laboratory previously (Estevez *et al.*, 2007). cDNAs encoding the complete complement of the genome of the NDV Anhinga strain, and the nucleoprotein (N), phosphoprotein (P) and polymerase (L) protein genes were generated by RT-PCR and ligated into a modified pBluescript-based vector (complement of the virus genome) (Stratagene) or the pTM protein expression plasmid (N, P, L protein genes), as described elsewhere (Estevez *et al.*, 2007). Transcription from the modified pBluescript-based vector is also driven by the T7 RNA polymerase. The final construct containing the whole virus genome was named pFLC–Anhwt. Protein expression plasmids were named pTM–N, pTM–P and pTM–L.

Site-directed mutagenesis of HN proteins. Plasmids pAnh–HNwt, pTkND–HNwt, pCA02–HNwt and pFLC–Anhwt were modified to contain a single nucleotide mutation (T→A) at position 576 of the coding region of the HN protein. This mutation changes the highly conserved isoleucine residue at position 192 to methionine. The exchange was performed by site-directed mutagenesis using a QuikChange Multi Site-Directed Mutagenesis kit (Stratagene) following the manufacturer's recommendations. Primers used for the mutagenesis reactions are available upon request. Plasmids harbouring the mutation were named pAnh–HNI192M, pTkND–HNI192M, pCA02–HNI192M and pFLC–AnhI192M.

Cell surface expression of wild-type and mutated HN proteins. Vero-cell monolayers in 96-well plate format were grown to 95 % confluency overnight in DMEM containing 10 % FBS without antibiotics. These monolayers were transfected with 0.1 μg of protein expression plasmid pAnh–HNwt, pTkND–HNwt, pCA02–HNwt, pAnh–HNI192M, pTkND–HNI192M or pCA02–HNI192M, using 24 wells per plasmid construct. Transfection was performed with the aid of Lipofectamine 2000 transfection reagent (Invitrogen), at an inclusion rate of 0.2 μl per well. Recombinant MVA/T7 was added at an m.o.i. of 3. Transfected cell monolayers were incubated for 5 h at 37 °C and then the supernatant was discarded and replaced with DMEM containing 100 U ml^{-1} penicillin, 100 μg ml^{-1} streptomycin, 0.25 μg ml^{-1} amphoteraction B and 10 % FBS. After 19 h of incubation, the cell surface expression of the HN protein was detected using a cell ELISA system as described by Bousse *et al.* (1995), with some modifications. Briefly, the cell monolayers were washed once with PBS and fixed, using a 4 % paraformaldehyde solution, for 8 min at room temperature. The cells were washed with PBS, overlaid with 100 μl of a 1 : 250 dilution of an anti-NDV chicken polyclonal serum stock in PBS and incubated at 4 °C for 45 min. The cell monolayers were washed again and incubated with a 1 : 5000 dilution of a secondary rabbit anti-chicken antibody conjugated with HRP (Fitzgerald Industries) for 30 min at room temperature. After a final set of washes, the cells were reacted with 200 μl of a 1 × solution of Sigma Fast OPD reagent (Sigma-Aldrich). After 30 min of incubation, the A_{450} of the reaction was read in a Biotek Synergy HT Microplate Reader (Biotek Instruments).

Neuraminidase activity. NA activity was determined by a fluorimetric procedure as described by Potier *et al.* (1979), with some modifications. Vero-cell monolayers in 96-well-plate formats were transfected using 0.1 μg of protein expression plasmid encoding the wild-type HN proteins (pAnh–HNwt, pTkND–HNwt, pCA02–HNwt) or the mutated proteins (pAnh–HNI192M, pTkND–HNI192M or pCA02–HNI192M), and 0.2 μl of Lipofectamine 2000 and MVA/T7 (m.o.i. of 3), as described previously. After 18 h of incubation at 37 °C the transfected cells were washed with PBS and overlaid with 30 μl of 0.1 M sodium acetate buffer containing 1 mM of the substrate 2′-(4-methylumbelliferyl)-α-D-*N*-acetylneuraminic acid (MU-Neu5Ac; Sigma-Aldrich). Cells were incubated for 1 h at 37 °C. The reaction was stopped by the addition of 0.25 M glycine buffer (0.25 M glycine in ethanol). The fluorescence of the 4-methylumbelliferone released in the supernatant after cleavage by the HN proteins present in the monolayers was determined using a fluorometer at wavelengths of 365 nm for excitation and 450 nm for emission.

HAd test. HA activity was assayed as described previously (Li *et al.*, 2004) with modifications. Briefly, Vero cells in 24-well-formats were transfected with the same expression plasmids and procedures utilized in the NA activity assay. The transfected monolayers were washed with PBS, before adding a 3 % (v/v) chicken red blood cell (CRBC) suspension in PBS, followed by incubation at 4 °C for 30 min. After removal of unbound CRBC by repeated washings with ice-cold PBS, bound cells were lysed using a red blood cell lysis buffer (50 mM Tris, pH 7.4, 5 mM EDTA, 150 mM NaCl, and 0.5 % NP-40). A_{530} was measured.

Fusion promotion. To assess the differences in the fusion promotion capability of wild-type versus mutated HN proteins, Vero-cell monolayers in six-well formats were transfected with 0.2 μg of pAnh–HNwt, pTkND–HNwt, pCA02–HNwt, pAnh–HNI192M, pTkND–HNI192M or pCA02–HNI192M, and 0.2 μg of the homotypic F protein of each of the NDV strains used. Differences in fusion promotion were assessed by counting the mean number of nuclei present in twenty fusion foci per HN protein type at 24 h post-transfection.

Viral rescue from infectious clones. Recombinant viruses encoding wild-type and mutated forms of the HN protein of the NDV Anhinga strain were generated by transfection of HEp-2-cell monolayers as described (Estevez *et al.*, 2007). HEp-2-cell monolayers were grown to 90 % confluency and co-transfected with plasmid pFLC–Anhwt or pFLC–AnhI192M, plus supporting plasmids pTM–N, –P and –L, with the addition of Lipofectamine 2000 (3 μl per well) and MVA/T7 (m.o.i. of 3). After 3 days of incubation, 400 μl of the cell supernatants were injected into the allantoic cavity of 9-day-old embryonated SPF chicken eggs to amplify the rescued viruses. These viral stocks were further amplified in eggs and their titres determined by infecting Vero-cell monolayers with 50 μl of serial tenfold dilutions of the original stock. Titres were calculated by the Reed & Muench (1938) method and are expressed as $TCID_{50}$.

Recombinant virus growth curves. Single-step growth curves were determined for the rescued Anhinga viruses encoding the wild-type and I192M mutant forms of the HN protein. Briefly, Vero-cell monolayers in six-well plate formats were infected at an m.o.i. of 10. Six hundred microlitre samples of cell supernatant were collected at 9, 20, 31 and 45 h post-infection, which were frozen at −80 °C until used. Virus titres of the collected samples were assessed by inoculation of Vero-cell monolayers (96-well formats) with 50 μl of serial tenfold dilutions (three replicates per dilution) of each of the time-point samples collected. Calculation of titres was performed using the Reed &

Muench (1938) method, taking as an end point the highest dilution in which the cytopathic effect of the virus was observed.

Pathotyping of wild-type and mutated viruses. Recombinant virus pathotypes were assessed using MDT in embryonated chicken eggs and ICPI tests as described by Alexander (1998). The MDT was performed with samples of viruses in allentoic fluid by inoculating 9-day-old SPF chicken eggs with 100 µl of a serial tenfold dilution in PBS, of the viruses encoding the wild-type or I192M mutant HN gene (five eggs per dilution). Embryo mortality was recorded daily by candling the inoculated eggs twice a day. The ICPI was assessed by inoculating day-old SPF chicks intracerebrally with a 1 : 10 dilution of infective allantoic fluid of the wild-type and mutant viruses. The birds were observed daily for 8 days and scored normal, sick or dead. Calculations of the MDT and ICPI were performed as described (Alexander, 1998).

Fusion phenotype, HA and NA activities of rescued viruses. The fusion phenotype of the rescued viruses was assessed by inoculating Vero-cell monolayers with the wild-type and recombinant viruses at an m.o.i. of 0.5. Fusion foci were photographed at 24 h post-inoculation. HA titres of the viruses were obtained by using the microplate HA test. Fifty microlitres of a 1×10^7 $TCID_{50}$ ml^{-1} stock sample of each virus was used in triplicate to perform twofold serial dilutions in PBS, which were followed by the addition of 50 µl of a 0.5 % CRBC solution (0.51 % (v/v) in PBS). The HA titre was defined as the reciprocal of the last dilution in which HA of the chicken RBC was observed. The NA activity of the viral stocks was determined using the fluorometric assay as described previously, with modifications. Twenty microlitres of a 1×10^7 $TCID_{50}$ ml^{-1} stock sample of each virus was diluted in 30 µl of 0.1 M sodium acetate buffer containing 1 mM of MU-Neu5Ac. The reaction was incubated at 37 °C for 1 h, and stopped by adding 150 µl of the 0.25 M glycine buffer. The fluorescence of the 4-methylumbelliferone released during the reaction was determined using a fluorometer at wavelengths of 365 nm for excitation and 450 nm for emission.

Sequencing and molecular modelling. All sequences were confirmed by dideoxy chain-termination sequencing, using an Applied Biosystems-PRISM fluorescent big dye sequencing kit and an ABI 3730 DNA sequencer (ABI). Nucleotide sequence editing, assembling and analysis were performed using the DNASTAR program (DNASTAR). The three-dimensional structures of the wild-type and I192M mutant HN proteins were generated with the aid of the Swiss-PdbViewer program (Guex & Peitsch, 1997), which is freely available at http://www.expasy.org/spdbv/. The structure of mutant I192M was modelled using the coordinates of the Newcastle HN crystal structure (PDB code 1E8U) and the program MODELLER (Marti-Renom *et al.*, 2000).

Statistical analysis. Statistical significance of the differences found was analysed using a single factor ANOVA test followed by Tukey's test, performed with the aid of the data analysis package included in the Excel program (Microsoft).

ACKNOWLEDGEMENTS

The authors wish to thank Timothy Olivier and Xiuqin Xia for outstanding technical assistance, Joyce Bennett and Melissa Scott for automatic nucleotide sequencing and Bernard Moss for the gifts of TM1 expression plasmid and MVA/T7 recombinant virus. This work was supported by the USDA-ARS CRIS project 6612-32000-049-00D.

REFERENCES

Alexander, J. A. (1998). Newcastle disease virus and other avian paramyxoviruses. In *A Laboratory Manual for the Isolation and Identification of Avian Pathogens*, 4th edn. Edited by D. Swayne, J. R. Glisson, M. W. Jackwood, J. E. Pearson & W. M. Reed. Kennett Square, PA: American Association of Avian Pathologists.

Bousse, T., Takimoto, T. & Portner, A. (1995). A single amino acid change enhances the fusion promotion activity of human parainfluenza virus type 1 hemagglutinin-neuraminidase glycoprotein. *Virology* **209**, 654–657.

Chen, L., Gorman, J. J., McKimm-Breschkin, J., Lawrence, L. J., Tulloch, P. A., Smith, B. J., Colman, P. M. & Lawrence, M. C. (2001). The structure of the fusion glycoprotein of Newcastle disease virus suggests a novel paradigm for the molecular mechanism of membrane fusion. *Structure* **9**, 255–266.

Connaris, H., Takimoto, T., Russell, R., Crennell, S., Moustafa, I., Portner, A. & Taylor, G. (2002). Probing the sialic acid binding site of the hemagglutinin-neuraminidase of Newcastle disease virus: identification of key amino acids involved in cell binding, catalysis, and fusion. *J Virol* **76**, 1816–1824.

Crennell, S., Takimoto, T., Portner, A. & Taylor, G. (2000). Crystal structure of the multifunctional paramyxovirus hemagglutinin-neuraminidase. *Nat Struct Biol* **7**, 1068–1074.

Estevez, C., King, D., Seal, B. & Yu, Q. (2007). Evaluation of Newcastle disease virus chimeras expressing the haemagglutinin-neuraminidase protein of velogenic strains in the context of a mesogenic recombinant virus backbone. *Virus Res* **129**, 182–190.

Guex, N. & Peitsch, M. C. (1997). SWISS-MODEL and the Swiss-PdbViewer: an environment for comparative protein modeling. *Electrophoresis* **18**, 2714–2723.

King, D. J. & Seal, B. S. (1998). Biological and molecular characterization of Newcastle disease virus (NDV) field isolates with comparisons to reference NDV strains. *Avian Dis* **42**, 507–516.

Lamb, R. A. & Parks, G. D. (2007). *Paramyxoviridae*: the viruses and their replication. In *Field's Virology*, 5th edn, pp. 1449–1498. Edited by D. M. Knipe & P. M. Howley. Philadelphia, PA: Lippincott Williams & Wilkins.

Lamb, R. A., Paterson, R. G. & Jardetzky, T. S. (2006). Paramyxovirus membrane fusion: lessons from the F and HN atomic structures. *Virology* **344**, 30–37.

Li, J., Quinlan, E., Mirza, A. & Iorio, R. M. (2004). Mutated form of the Newcastle disease virus hemagglutinin-neuraminidase interacts with the homologous fusion protein despite deficiencies in both receptor recognition and fusion promotion. *J Virol* **78**, 5299–5310.

Marti-Renom, M. A., Stuart, A. C., Fiser, A., Sanchez, R., Melo, F. & Sali, A. (2000). Comparative protein structure modeling of genes and genomes. *Annu Rev Biophys Biomol Struct* **29**, 291–325.

Morrison, T. G. (2003). Structure and function of a paramyxovirus fusion protein. *Biochim Biophys Acta* **1614**, 73–84.

Moss, B., Elroy-Stein, O., Mizukami, T., Alexander, W. A. & Fuerst, T. R. (1990). Product review. New mammalian expression vectors. *Nature* **348**, 91–92.

Palermo, L. M., Porotto, M., Greengard, O. & Moscona, A. (2007). Fusion promotion by a paramyxovirus hemagglutinin-neuraminidase protein: pH modulation of receptor avidity of binding sites I and II. *J Virol* **81**, 9152–9161.

Porotto, M., Murrell, M., Greengard, O., Doctor, L. & Moscona, A. (2005). Influence of the human parainfluenza virus 3 attachment protein's neuraminidase activity on its capacity to activate the fusion protein. *J Virol* **79**, 2383–2392.

Potier, M., Mameli, L., Belisle, M., Dallaire, L. & Melancon, S. B. (1979). Fluorometric assay of neuraminidase with a sodium

(4-methylumbelliferyl-α-D-*N*-acetylneuraminate) substrate. *Anal Biochem* **94**, 287–296.

Reed, L. J. & Muench, H. (1938). A simple method of estimating fifty percent endpoints. *Am J Hyg* **27**, 493–497.

Ryan, C., Zaitsev, V., Tindal, D. J., Dyason, J. C., Thomson, R. J., Alymova, I., Portner, A., von Itzstein, M. & Taylor, G. (2006). Structural analysis of a designed inhibitor complexed with the hemagglutinin-neuraminidase of Newcastle disease virus. *Glycoconj J* **23**, 135–141.

Wyatt, L. S., Moss, B. & Rozenblatt, S. (1995). Replication-deficient vaccinia virus encoding bacteriophage T7 RNA polymerase for transient gene expression in mammalian cells. *Virology* **210**, 202–205.

Yuan, P., Thompson, T. B., Wurzburg, B. A., Paterson, R. G., Lamb, R. A. & Jardetzky, T. S. (2005). Structural studies of the parainfluenza virus 5 hemagglutinin-neuraminidase tetramer in complex with its receptor, sialyllactose. *Structure* **13**, 803–815.

Zaitsev, V., von Itzstein, M., Groves, D., Kiefel, M., Takimoto, T., Portner, A. & Taylor, G. (2004). Second sialic acid binding site in Newcastle disease virus hemagglutinin-neuraminidase: implications for fusion. *J Virol* **78**, 3733–3741.

Journal of General Virology (2011), **92**, 000–000 DOI 10.1099/vir.0.029306-0

The cellular endosomal sorting complex required for transport pathway is not involved in avian metapneumovirus budding in a virus-like-particle expression system

Yuejin Weng,[1,2,3] Wuxun Lu,[1,3] Aaron Harmon,[1,2,3] Xiaoxiao Xiang,[1,3] Qiji Deng,[2,3] Minxun Song,[4] Dan Wang,[1,3] Qingzhong Yu[5] and Feng Li[1,2,3]

Correspondence
Feng Li
feng.li@sdstate.edu

[1]Department of Biology and Microbiology, South Dakota State University, Brookings, SD 57007, USA

[2]Department of Veterinary and Biomedical Sciences, South Dakota State University, Brookings, SD 57007, USA

[3]Center for Infectious Disease Research and Vaccinology, South Dakota State University, Brookings, SD 57007, USA

[4]Institute of Poultry Science, Shandong Academy of Agricultural Sciences, Jinan 250023, PR China

[5]Southeast Poultry Research Laboratory, Agricultural Research Services, U. S. Department of Agriculture, Athens, GA 30605, USA

Received 5 December 2010
Accepted 18 January 2011

Avian metapneumovirus (AMPV) is a paramyxovirus that principally causes respiratory disease and egg production drops in turkeys and chickens. Together with its closely related human metapneumovirus (HMPV), they comprise the genus *Metapneumovirus* in the family *Paramyxoviridae*. Little is currently known about the mechanisms involved in the budding of metapneumovirus. By using AMPV as a model system, we showed that the matrix (M) protein by itself was insufficient to form virus-like-particles (VLPs). The incorporation of M into VLPs was shown to occur only when both the viral nucleoprotein (N) and the fusion (F) proteins were co-expressed. Furthermore, we provided evidence indicating that two YSKL and YAGL segments encoded within the M protein were not a functional late domain, and the endosomal sorting complex required for transport (ESCRT) machinery was not involved in metapneumovirus budding, consistent with a recent observation that human respiratory syncytial virus, closely related to HMPV, uses an ESCRT-independent budding mechanism. Taken together, these results suggest that metapneumovirus budding is independent of the ESCRT pathway and the minimal budding machinery described here will aid our future understanding of metapneumovirus assembly and egress.

INTRODUCTION

Avian metapneumovirus (AMPV) is a paramyxovirus that causes acute respiratory disease in turkeys. In recent years this virus has emerged as a major economic problem for the turkey industry worldwide (Catelli *et al.*, 2006, 2010; Easton *et al.*, 2004; Govindarajan & Samal, 2004; Naylor *et al.*, 2004, 2007; Njenga *et al.*, 2003; Toquin *et al.*, 2003, 2006; Velayudhan *et al.*, 2005, 2008). AMPV infection can also result in variable degrees of clinical illness in other avian species including chickens (Easton *et al.*, 2004; Njenga *et al.*, 2003). For AMPV, there are four subgroups, namely, A, B, C and D (Easton *et al.*, 2004). Interestingly, sequence analysis has discovered that the AMPV subgroup C is more closely related to human metapneumovirus (HMPV) than to any other AMPV subgroup (Govindarajan & Samal, 2005; Toquin *et al.*, 2003; van den Hoogen *et al.*, 2001, 2002).

Metapneumovirus is a negative ssRNA virus that codes for nucleoprotein (N), phosphoprotein (P), matrix (M) protein, fusion protein (F), M2-1 and M2-2, small hydrophobic protein (SH), attachment protein (G) and the large polymerase protein (L) with the gene order 3′-leader-N-P-M-F-M2-SH-G-L-trailer-5′ (Easton *et al.*, 2004). AMPV-C and HMPV share 80 % amino acid identity, with N and M being the most conserved proteins and SH and G proteins the most variable (Govindarajan & Samal, 2005; Toquin *et al.*, 2003; van den Hoogen *et al.*, 2002). Although it is not clear that any cross-species transmission by these two closely related viruses can occur, a recent study has suggested that HMPV can experimentally infect turkeys

and cause respiratory symptoms (Velayudhan *et al.*, 2006). In addition, a recent evolutionary study of HMPV and AMPV led to a hypothesis that the human virus may have evolved from its avian counterpart and at some point was transmitted to humans (de Graaf *et al.*, 2008). These findings clearly demonstrate the necessity of a comparative study of these two viruses for the better understanding of molecular biology and pathogenesis of the metapneumovirus subgroup. In the paramyxovirus family, metapneumovirus is closely related to respiratory syncytial virus that infects both human and animals (Easton *et al.*, 2004). Both groups of viruses are assigned to the subfamily *Pneumovirinae* of the family *Paramyxoviridae*.

The M protein of paramyxoviruses is the most abundant structural protein in the virion and the unique topological location of the M protein has helped create an assumption that M might be the primary driving force for paramyxovirus budding (Takimoto & Portner, 2004). Paramyxoviruses such as Sendai virus (SeV) and human parainfluenza virus type 1 are able to release virus-like-particles (VLPs) with the expression of M alone (Ciancanelli & Basler, 2006; Coronel *et al.*, 1999; Irie *et al.*, 2007; Pantua *et al.*, 2006; Patch *et al.*, 2007), while other paramyxoviruses including mumps and simian virus 5 (SV5) can only produce VLPs when M proteins are expressed in combination with other viral proteins (Li *et al.*, 2009; Schmitt *et al.*, 2002). Recent studies of influenza A viral budding have also demonstrated that the M protein alone is insufficient to form VLPs (Chen *et al.*, 2007; Wang *et al.*, 2010a).

M proteins of some already studied paramyxoviruses also encode a domain with late budding function, termed L-domain, which is required for the efficient release of budding virions from the plasma membrane of infected cells (Chen & Lamb, 2008). The L-domain is firstly identified in retroviral Gag proteins with three core motifs (PPxY, PT/SAP and YPXL, where x can be any amino acid), and it has been shown that interactions of L-domains with the endosomal sorting complex required for transport (ESCRT) machinery are critical to the completion of retroviral particle release and spread of infections (Demirov & Freed, 2004; Freed, 2002). Study examining the budding requirements of SV5, the prototype of paramyxovirus, has identified a novel L-domain consisting of FPIV core sequence in the SV5 M protein necessary for viral budding (Schmitt *et al.*, 2005). Despite the L-domain peptide sequence being variable from that of retroviruses, SV5 utilizes ESCRT machinery to assist in viral budding (Schmitt *et al.*, 2005). Characterization of the budding requirements for other paramyxoviruses has yielded conflicting data. For example, early SeV VLP studies suggested that Alix [apoptosis-linked gene 2 (ALG-2)-interacting protein], a host protein involved in apoptosis and endosomal membrane trafficking, was required to promote VLPs release by interacting with either an YLDL L-domain in the M protein or the C protein (Irie *et al.*, 2007). However, a recent study provided the evidence suggesting that SeV budding, at least in the course of virus infection, was not sensitive to inhibition of the ESCRT pathway (Gosselin-Grenet *et al.*, 2007). In an effort to identify the L-domain in Nipah virus (NiV), one group reported on the identification of the YMYL sequence in the M protein as a functional L-domain (Ciancanelli & Basler, 2006), whereas another study suggested that the YPLGVG segment in NiV M protein has a late budding function (Patch *et al.*, 2008). Compared to the well-studied retrovirus, little is known about the molecular mechanism and cellular machinery involved in paramyxovirus budding; however, there is growing evidence that some members of paramyxovirus bud through an ESCRT-independent pathway and such viruses include NiV and human respiratory syncytial virus (HRSV) (Patch *et al.*, 2008; Utley *et al.*, 2008; Wang *et al.*, 2010b).

To understand the mechanism of metapneumovirus assembly and release, we have in this study characterized the requirements for metapneumovirus budding by using the AMPV-C model system. Specifically, we addressed the following questions. What are the functional requirements for metapneumovirus budding? Does the M protein of metapneumovirus, like Ms in many enveloped viruses, play an important role in budding? Are two YSKL and YAGL sequences encoded within the M protein functional in inducing virus budding? Is the ESCRT pathway involved in metapneumovirus budding? The results of these studies identified the minimal budding machinery for metapneumovirus and revealed new fundamental information about the potential mechanism involved in metapneumovirus assembly and egress.

RESULTS

The M protein alone of AMPV-C is not sufficient to bud and form extracellular VLPs

Initially, we asked whether the AMPV-C M protein alone can form VLPs. For this study, the pCAGGS vector containing a chicken β-actin promoter was used due to its capability of viral protein expression in a wide variety of systems (Chen *et al.*, 2007; Irie *et al.*, 2007; Li *et al.*, 2009; Niwa *et al.*, 1991; Schmitt *et al.*, 2002). A standardized viral budding assay was used in this study (Garrus *et al.*, 2001; Jin *et al.*, 2007; Li *et al.*, 2002). All cDNA expression clones encoding AMPV-C proteins were developed by regular RT-PCR and cloning cDNA procedures (Yu *et al.*, 2010) (Fig. 1a).

Transfection of 293T cells with increasing amounts of pM expression vector resulted in a dose-dependent expression of intracellular M proteins; however, none of the transfected cells produced VLPs (Fig. 1b). In contrast, transfected 293T cells with as little as 0.5 μg of human immunodeficiency virus (HIV)-1 Gag plasmid gave rise to Gag particles. These results suggest that the AMPV-C M protein by itself is insufficient to bud into VLPs.

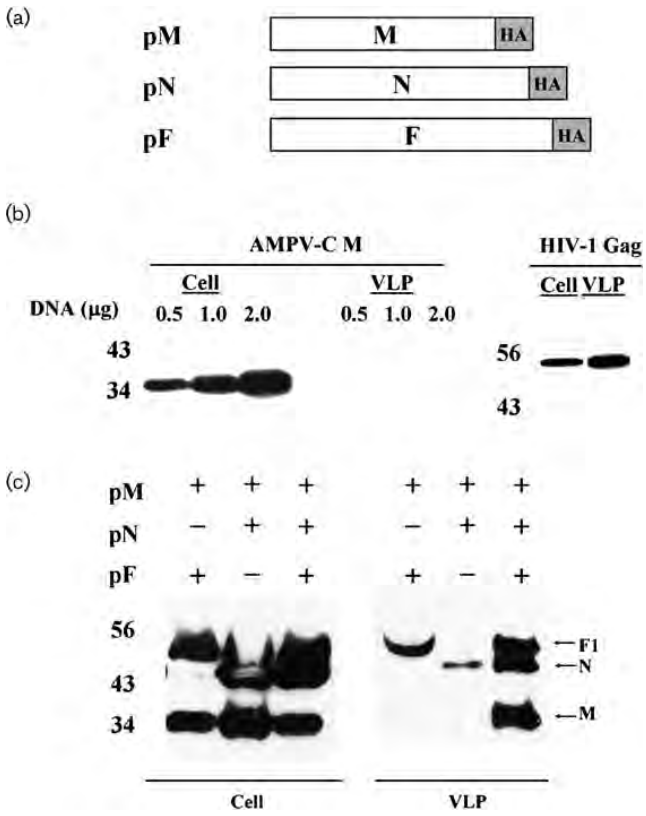

Fig. 1. Requirements of viral N and F proteins for the incorporation of the M protein into extracellular VLPs. (a) Viral protein expression constructs used in viral budding assay are schematically shown. An HA epitope tag (YPYDVPDYA) was appended in-frame to the C terminus of M, N and F proteins of AMPV-C, resulting in pCAG-M, pCAG-N and pCAG-F, respectively. (b) M alone is insufficient to form extracellular VLPs. VLPs production by 293T cells transfected with increasing amounts of pCAG-M expression plasmid (0.5, 1.0 and 2.0 μg). VLPs and cell lysates were analysed by Western blot with anti-HA mAb (left panel). Also shown is VLPs production by 293T cells transfected with pHIV-1 Gag plasmid (0. 5μg) (right panel). Note that the HIV-1 Gag and AMPV-C M data were obtained from different experiments under similar experimental conditions, and lanes corresponding to HIV-1 Gag cellular lysates and extracellular VLPs have been placed together arbitrarily according to their migration positions in the gel. Protein molecular mass markers (in kDa) are indicated on the left of gel. (c) Expression of viral N and F proteins is needed for the incorporation of the M protein into extracellular VLPs. VLPs production was derived from 293T cells transfected with pCAG-M plasmid, either with pCAG-N or pCAG-F or both in combination. At 48 h post-transfection, VLPs and cell lysates were analysed in Western blot with an anti-HA epitope tag mAb. Note that the F protein is probably a cleaved form responding to an F1 subunit (based on the molecular mass calculation). The results presented are a representative of five independent experiments and numbers on the left here and elsewhere indicate the migration positions of molecular mass markers (in kDa).

Requirements of viral N and F proteins for the incorporation of M into extracellular VLPs

The failure of AMPV-C M in forming extracellular VLPs is somewhat reminiscent of a VLP production defect previously reported for the M protein of SV5 (Schmitt *et al.*, 2002). The results of this study coupled with the fact that two viral envelope proteins (G and SH) can be deleted without substantially affecting growth kinetics of metapneumovirus *in vitro* (Biacchesi *et al.*, 2004, 2005) directed our focus to the potential involvement of viral F and N proteins. We asked whether co-expression of these two proteins was capable of instigating the competence of M protein budding into extracellular VLPs. To address this question, we generated AMPV-C N and F protein expression constructs (pN and pF) containing an inserted haemagglutinin (HA) epitope tag at the C terminus of either protein using the strategy described previously (Fig. 1a).

Co-expression of both N and F proteins with the M protein efficiently generates extracellular M-containing VLPs (Fig. 1c). Notably, M VLP production defect cannot be efficiently overcome by the presence of just one protein (N or F specifically), indicating that a co-operative action provided by N and F is needed to incorporate M into budding particles. The F protein (Fig. 1c) is probably a cleaved form responding to an F1 subunit (based on the molecular mass calculation). Also we found that N and F, when expressed alone or in combination, were able to release to the culture medium independently of the expression of the M protein (data not shown). Secretion of the F protein has been reported previously in NiV when F was expressed alone (Patch *et al.*, 2007). The observation of M's inability in inducing VLP production in multiple experiments, coupled with the fact that VLP production by N and F are constantly demonstrated, suggests a primary role of these two proteins in driving AMPV-C virus particle production. This hypothesis clearly warrants future investigation.

To validate VLPs produced by co-expression of M/N/F proteins, we performed a density gradient analysis of VLPs made from this system (Patch *et al.*, 2007). The results showed that three proteins predominantly co-migrated in the no. 3 gradient fraction, indicating that they are packaged in the same particle (Fig. 2a). Absence of the F protein in the no. 2 fraction or little M protein was detected in both no. 2 and no. 4 fractions may reflect variable expression levels of the respective proteins. Importantly, analysis of infectious virus particles produced by Vero cells under the same experimental condition followed by probing with an anti-AMPV-C N protein mAb (Yu *et al.*, 2006) revealed a similar pattern in which the majority of virus particles was associated with the no. 3 gradient fraction and less so with no. 2 fraction and little with no. 4 fraction (Fig. 2b). The data further supported that VLPs generated by our co-expression system resembles

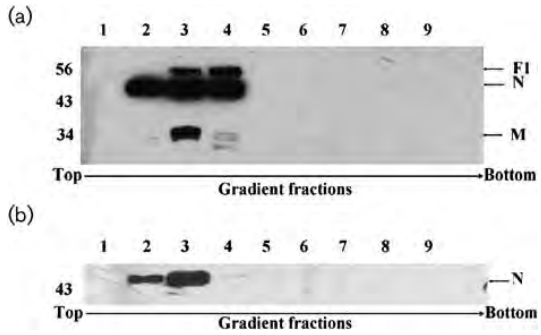

Fig. 2. Density gradient analysis of VLPs and infectious virus particles of AMPV-C. Pellets corresponding to each of the sucrose fractions (1.0 ml) collected from the top of the sucrose gradient as described in the above method were obtained and VLP-derived proteins were analysed with an anti-HA mAb (Sigma-Aldrich) (a) or proteins derived from infectious virus particles of AMPV-C were analysed with an anti-N mAb (b), respectively.

authentic virus particles of AMPV-C in terms of particle density.

Involvement of putative L domains and the ESCRT pathway in AMPV-C budding

The M protein of AMPV-C encodes two putative L domains, YSKL and YAGL, which have been suggested previously for a role in directing viral budding (Munir & Kapur, 2003). Bioinformatic analysis of N and F protein sequences did not enable us to identify any of the previously described L-domain motifs in these two proteins. YPXL-like domain with the late budding function is identified in a variety of viruses, including retroviruses and paramyxoviruses (Chen & Lamb, 2008; Demirov & Freed, 2004). With the minimal budding machinery we identified from the above experiments, we next asked whether these two putative L-domains are functional in AMPV-C budding. We were also interested in examining whether the ESCRT pathway, the well-defined budding mechanism for retrovirus and other enveloped RNA viruses (Chen & Lamb, 2008; Demirov & Freed, 2004), plays a role in AMPV-C budding.

To this end, three M mutants were generated in the pCAGEN vector. Two mutants termed $M^{\Delta L1}$ and $M^{\Delta L2}$, contained an AAAA segment in substitution of YSKL and YAGL sequences in the native locations, respectively. The other mutant, termed $M^{\Delta L1/L2}$, was created in which two putative L-domains, YSKL and YAGL, were changed to AAAA segments (Fig. 3a). As demonstrated in Fig. 3(b), similar levels of intracellular M protein expression were observed among cells transfected with the parental M and its derivatives, indicating that the substitutions did not substantially alter overall intracellular expression of the M proteins. Interestingly, none of these mutations disrupted M1 budding as similar amounts of VLPs were produced among wild-type (WT) M and its three mutants (Fig. 3b). 1
The results demonstrated that two putative L-domains are not functional in providing late budding function for AMPV-C budding at least in our experimental conditions.

In a virus budding assay, extracellular VLPs are normally pelleted from transfected cells after 48 h, which may not allow for accurate measurement within a kinetic range. To potentially overcome this shortcoming, we modified our assay by collecting and pelleting extracellular VLPs at 24 and 36 h following transfection, and examined the budding efficiency of the double mutant $M^{\Delta L1/L2}$ in the presence of F and N proteins. Only at 36 h post-transfection (Fig. 3c) were both WT M and $M^{\Delta L1/L2}$ mutant incorporated into VLPs with an indistinguishable efficiency, further confirming that putative L-domains are dispensable in AMPV-C budding, particularly M incorporation to VLPs. Interestingly, we noticed that at 24 h post-transfection the N protein was the only protein budding out. This observation suggests that N may play an early role in the nucleating budding process, which clearly warrants further investigation.

We next determined whether the ESCRT pathway is involved in AMPV-C budding by taking advantage of a set of well-studied dominant-negative inhibitors that block retroviral Gag particle release by disrupting the ESCRT pathway by different mechanisms. These inhibitors include: (i) TSG-5′, the N-terminal fragment of the tumour susceptibility gene 101 (Tsg101), which suppresses L-domain PTAP-dependent HIV-1 Gag particle release by binding 2
PTAP L-domain and blocking its function (Demirov *et al.*, 2002; Goila-Gaur *et al.*, 2003; Luttge *et al.*, 2008; Shehu-Xhilaga *et al.*, 2004); (ii) TSG-3′, the C-terminal fragment of Tsg101, which inhibits HIV-1 Gag budding mediated by either L-domain PTAP or PPXY by globally disrupting the class E VPS pathway (Demirov *et al.*, 2002; Goila-Gaur *et al.*, 2003; Luttge *et al.*, 2008; Shehu-Xhilaga *et al.*, 2004); (iii) a fragment of Alix, composed of residues 364–716 (Alix 364–716), which blocks L-domain YPXL/LXXLF-dependent HIV-1 Gag particle production by inhibiting the recruitment of ALIX protein (Lee *et al.*, 2007; Luttge *et al.*, 2008; Munshi *et al.*, 2007); (iv) an ATPase-deficient mutant of Vps4A (E228Q) that broadly blocks the pinch-off of many enveloped viruses that exclusively depend on the ESCRT pathway (Garrus *et al.*, 2001). TSG-5′, TSG-3′ and the Alix fragment were kindly provided by Eric Freed at National Cancer Institute, while Vps4A (E228Q) was a gift of W. Sundquist, University of Utah.

To examine the sensitivity of AMPV-C VLPs release to overexpression of these dominant-negative budding inhibitors, we transfected 293T cells expressing triple plasmids (M, N and F) with plasmids expressing TSG-5′, TSG-3′, Alix 364–716 or Vps4A (E228Q). Their effects on VLP production were determined by a virus budding assay (Fig. 4). As a positive control, inhibition of HIV-1 Gag particle release by TSG-3′ or Vps4A (E228Q) expression was also tested. For quantification of specific protein levels, protein

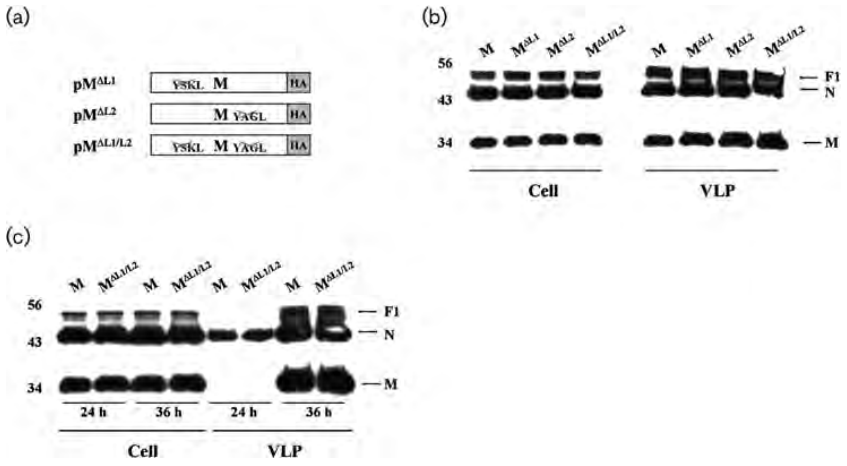

Fig. 3. Two putative L-domains are not functional in providing late budding function. (a) Schematic diagram of M mutants used in the viral budding assay. Three M-derived mutants, pCAG-M$^{\Delta L1}$, pCAG-M$^{\Delta L2}$ and pCAG-M$^{\Delta L1/L2}$ were constructed. pCAG-M$^{\Delta L1}$ and pCAG-M$^{\Delta L2}$ contained an AAAA segment in substitution of YSKL and YAGL sequences in the native locations, respectively. pCAG-M$^{\Delta L1/L2}$ was created in which both YSKL and YAGL were changed to an AAAA segment. (b) VLPs production by 293T cells transfected with pCAG-N and pCAG-F plasmids (1.0 μg each), either with WT M or mutant M plasmids (2.0 μg) as indicated. At 48 h post-transfection, VLPs and cell lysates were analysed in Western blot with anti-HA mAb. The results presented are representative of four independent experiments. (c) VLPs production by 293T cells transfected with pCAG-N and pCAG-F plasmids (1.0 μg each), either with WT M or mutant M$^{\Delta L1/L2}$ plasmids (2.0 μg). At 24 and 36 h post-transfection, VLPs and cell lysates were prepared and analysed in Western blot with anti-HA mAb (Sigma-Aldrich). The results presented are a representative of three independent experiments.

bands that were visualized in Western blots were scanned into a computer and analysed by using IMAGEQUANT software (NIH). The relative virus release efficiency was calculated as the ratio of VLP-associated viral proteins to total viral proteins (cell plus VLP).

As reported previously (Demirov *et al.*, 2002; Garrus *et al.*, 2001; Goila-Gaur *et al.*, 2003; Luttge *et al.*, 2008), expression of both TSG-3′ and Vps4A (E228Q) greatly inhibited HIV-1 Gag release, confirming that our assay conditions can effectively measure virus budding requiring the ESCRT pathway (Fig. 4a). For example, overexpression of these inhibitors significantly reduced HIV-1 Gag particle release and the inhibition rate ranged from 50 to 70 % compared with untreated controls. In contrast, AMPV-C VLPs release was not inhibited under the assay conditions as amounts of VLPs were basically identical between treated and untreated samples (Fig. 4b). The data collectively suggests that the ESCRT pathway is not involved in AMPV-C VLP release.

DISCUSSION

In the present study, we have characterized the budding machinery of AMPV-C. Our result on the inability of AMPV-C M protein in forming extracellular VLPs clearly places AMPV-C, likely metapenumoviruses, into a specialized group of paramyxoviruses (also containing mumps virus and SV5) whose viral M proteins alone are insufficient to form VLPs (Li *et al.*, 2009; Schmitt *et al.*, 2002). Also similar to this group of viruses, the M protein of AMPV-C can be efficiently incorporated into extracellular VLPs by co-expression of its N and F proteins.

During the course of our work, we noticed that two putative L-domains within the AMPV-C M protein are not authentic L-domains in the promotion of VLP release. This discovery is further substantiated by evidence showing that AMPV-C VLP budding is insensitive to inhibition by specific dominant-negative inhibitors that block L-domain functions and the ESCRT protein network. It should be noted that all dominant-negative inhibitor proteins used in this study are derived from human cells, while AMPV-C is a virus that infects poultry. Due to host specificity and speciation of certain proteins (both cellular and viral) within any system, the potential for poor interaction between the two aforementioned proteins remains. The human protein-derived inhibitors we used however have been successfully shown to suppress the budding function of L-domains from viruses that infect chicken, equine and feline (Luttge *et al.*, 2008; Medina *et al.*, 2005; Shehu-Xhilaga *et al.*, 2004). This evidence, when coupled with the fact that these proteins are involved in ECSRT machinery and are remarkably conserved amongst different species (Chen & Lamb, 2008; Morita & Sundquist, 2004), allow us to postulate that the protein inhibitors from humans are likely to be effective in blocking non-human viruses that employ the ESCRT pathway for their particle budding and egress. Thus, we conclude based on our data that AMPV-C may utilize a budding mechanism different from that of

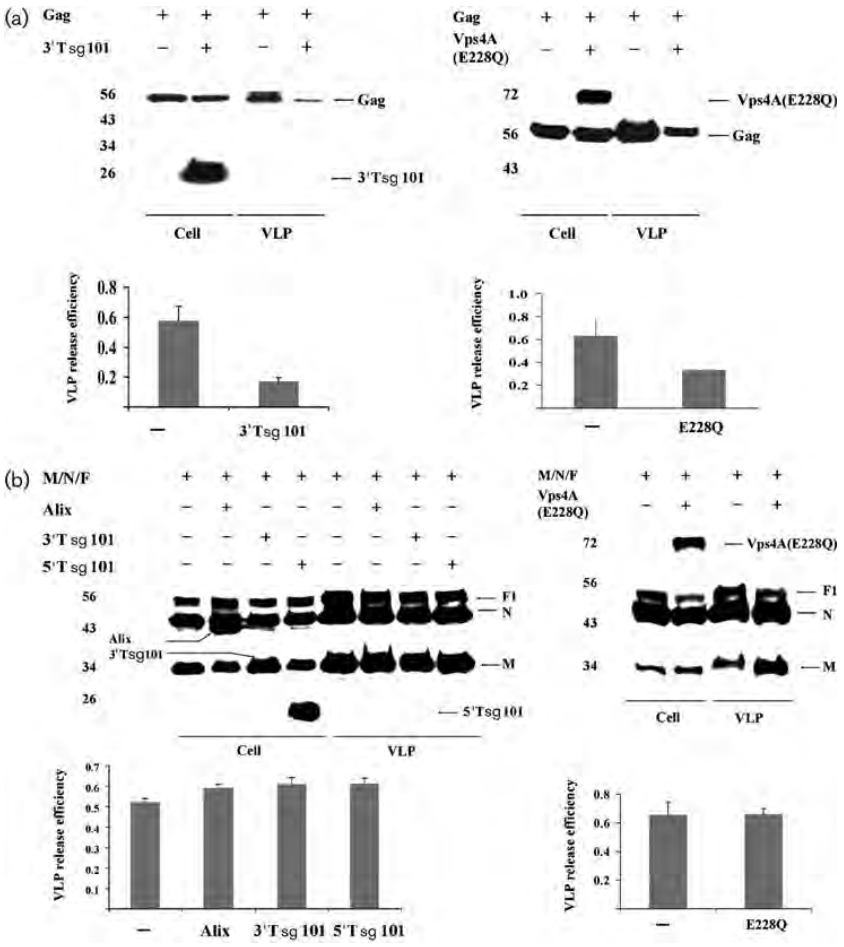

Fig. 4. The ESCRT pathway is not involved in AMPV-C budding. VLPs production by HIV-1 Gag expression vector in the absence and presence of 3′ Tsg101 or Vps4A (E228Q) protein served as a control to validate viral budding assay (a). Western blotting procedure as described in Methods was used to analyse Gag protein expression and Gag VLPs production probed by HIV-Ig (NIH AIDS Research and Reference Program). AMPV-C VLPs production was derived from 293T cells transfected with three expression plasmids (M, N and F), either with or without each of the dominant-negative inhibitors as indicated (b). At 36 h post-transfection, VLPs and cell lysates were analysed in Western blot with anti-HA mAb. Viral protein levels were quantified by ImageJ software (http://rsbweb.nih.gov/ij/), and the VLP release efficiency for AMPV-C or HIV-1 Gag was calculated as the ratio of VLP-associated proteins to total viral proteins (cells plus VLP), and the results represent means from at least three independent experiments. Error bars indicate SD. Note that the Vps4A (E228Q) and HIV-1 Gag or AMPV-C M/N/F VLP data were obtained from different experiments under similar experimental conditions, and have been placed together arbitrarily according to their migration positions in the gel.

retroviruses and many RNA-enveloped viruses, depending on which L-domains are in concert with the ESCRT pathway (Chen & Lamb, 2008; Morita & Sundquist, 2004).

The family *Paramyxoviridae* contains viruses with different genetic background that induce a wide range of distinct clinical illnesses in humans and animals (Knipe *et al.*, 2001). This divergence is also reflected in the L-domains and associated cellular pathways that paramyxoviruses utilize for their budding. Several studies have shown that several paramyxoviruses including SV5, SeV and NiV possess L-domains (Ciancanelli & Basler, 2006; Irie *et al.*, 2007; Patch *et al.*, 2008; Schmitt *et al.*, 2002). Despite sequence variations, these L-domains interact with various components of the ESCRT machinery to promote virus budding. However, in contrast to these paramyxoviruses, a recent study has provided direct evidence that HRSV does not encode an L-domain, and this virus utilizes a Rab11 pathway for virus budding instead of ESCRT machinery (Utley *et al.*, 2008). It is worthwhile mentioning that in addition to HRSV, influenza A virus and alphavirus budding are also insensitive to inhibition by dominant-negative Vps4 inhibitors (Bruce *et al.*, 2010; Chen *et al.*, 2007; Taylor *et al.*, 2007). Involvement of the Rab11 pathway has been established in a recent paper (Bruce *et al.*, 2010) for influenza A virus budding and filament formation. Considering a close genetic relatedness between metapneumovirus and RSV, it will be interesting to examine whether the Rab11 pathway is involved in AMPV-C virus budding. Regardless of the mechanism concerning how AMPV-C buds, the results presented in this study highlights the many diversified strategies viruses employ for their budding that have been previously unappreciated. This study represents the first step in defining viral proteins and host cell machinery required for metapenmovirus assembly and budding.

METHODS

Plasmids. PCR and cloning were performed with proof-reading Vent DNA polymerase (New England Biolabs) under standard reaction conditions and the integrity of all PCR-derived DNA fragments were verified by sequencing. All primers and sequences are available from the authors upon request. For the expression of AMPV-C viral proteins that were used in viral budding assay, cDNA sequences encoding N, P and M of AMPV-C were individually amplified from a pLF-2.1 plasmid (containing AMPV-C genome except for L-trailer-5′ sequence) (Yu *et al.*, 2010) by PCR, and subcloned into the eukaryotic expression vector pCAGEN (Addgene plasmid 11160; Addgene) to generate pCAG-N, pCAG-P and pCAG-M, respectively. To facilitate

the detection of protein expression, an HA epitope tag was placed at the C terminus of viral proteins. To study the functions of the two putative L-domains within the M protein in AMPV-C budding, we replaced the YSKL or YAGL sequence with a sequence of AAAA residues and these two substitution constructs were named pCAG-$M^{\Delta L1}$ and pCAG-$M^{\Delta L2}$, respectively. An additional M mutant, designated pCAG-$M^{\Delta L1/\Delta L1}$, was generated in which both YSKL and YAGL motifs were simultaneously mutated to the AAAA segment. A pHIV-1 Gag plasmid that expresses HIV-1 Gag precursor with HA tag at the C terminus was used as a control in viral budding assay.

Plasmids encoding GFP-tagged ATP hydrolysis-deficient Vps4A E228Q mutant (Vps4Awt and Vps4AEQ) were kindly provided by W. Sundquist (University of Utah, USA). HA-tagged derivatives of Tsg101, TSG-5′ and TSG-3′ in the pcGNM2 expression vector, were gifts of Z. Sun (Stanford University, USA) through Eric Freed (National Cancer Institute at Frederick, Frederick, MD, USA). Expression vector for the V-domain of hAlix (residues 364–716) was kindly provided by Eric Freed (National Cancer Institute at Frederick, Frederick, MD, USA).

Cells and antibodies. 293T, HeLa, COS-1 and Vero cells were cultured in Dulbecco's minimal essential medium supplemented with 10 % FBS. mAb against the HA epitope was purchased from Sigma-Aldrich. Polyclonal rabbit anti-GFP was obtained from Santa Cruz Biotechnology. Secondary antibodies such as donkey anti-rabbit IgG-HRP, goat anti-mouse IgG-HRP and goat anti-human IgG-HRP were purchased from Abcam. Human immunoglobulin from HIV-1-infected patients (HIV-Ig) was obtained through the NIH AIDS Research and Reference Reagent Program, Division of AIDS, NIAID. Mouse anti-AMPV N protein mAb was described in our previous publication (Yu *et al.*, 2006).

Viral budding assay. 293T cells or other cells grown in 60 nm plates were transfected with the following amounts of plasmid DNA: 2.0 μg pCAG-M, alone or with 1 μg pCAG-N or pCAG-F, or with a combination of pCAG-N and pCAG-F (1 μg each plasmid). The total amount of transfected DNA in each sample was held constant using an empty vector lacking a coding region to compensate for any variations. Transfection was performed by using TransIT-LT1 (Mirus) following the procedure outlined by the manufacturer. For the preparation of VLPs, at 48 h after transfection, the culture medium was harvested and pelleted by centrifugation at 2000 ***g*** for 10 min. The clarified supernatants were firstly passed through 0.22 μm filter before layered onto a 20 % sucrose cushion (PBS) and centrifuged at 100 000 ***g*** for 2 h at 4 °C in a Beckman Ti rotor (Beckman Coulter). The resuspension of pellet followed by low-speed centrifugation were subject to further analysis as VLPs. For the preparation of cell lysates, at 48 h post-transfection, cells were harvested and lysed in the lysis buffer (25 mM Tris/HCl, pH 8.0, 150 mM NaCl, 1 % deoxycholic acid, 1 % Triton X-100) in the presence of 1× protease inhibitor cocktail (Pierce). The cell lysates were prepared by the removal of nuclei by centrifugation at 2000 ***g*** at 4 °C for 10 min. VLPs and cell lysates were separated on a 12 % SDS-PAGE and transferred to a nitrocellulose membrane (Pierce) followed by blocking in PBS buffer containing 0.5 % Tween-20 and 5 % dry milk powder. Viral proteins were detected by standard Western blotting procedure coupled with the ECL system (Pierce) with appropriate primary and secondary antibodies as described above. The same procedure was also performed to analyse VLPs production by HIV-1 Gag and to characterize the effects of dominant-negative inhibitors targeting ESCRT pathway on the budding of AMPV-C and HIV-1 Gag, respectively.

Density gradient analysis of VLPs and infectious virus particles. 293T cells were transfected with expression plasmids (M, N and F) as described above. At 72 h post-transfection, culture medium was collected, clarified and filtered, and then centrifuged through 20 % sucrose cushion (w/v) in PBS at 100 000 ***g*** for 2 h at 4 °C. Density gradient analysis of VLPs upon co-expression of M, N and F proteins was performed according to a protocol developed by Patch *et al.* (2007). Briefly, the resulting pellet collected from the above centrifugation of 20 % sucrose cushion was resuspended in PBS and clarified supernatants were then loaded directly onto the top of a continuous sucrose gradient of 5–50 % sucrose. The gradient was centrifuged in a SW41 rotor at 100 000 ***g*** for 16 h at 4 °C. Fractions (1.0 ml) were collected from the top and each fraction was then pelleted through 20 % sucrose cushion (w/v) in PBS at 100 000 ***g*** for 2 h at 4 °C. Resuspended pellets corresponding to each fraction were analysed in SDS-PAGE/Western blotting assay as described above. The same density gradient analysis protocol was used to characterize infectious virus particles generated by Vero cells infected with AMPV-C and Western blotting assay was probed with mouse anti-N mAb.

ACKNOWLEDGEMENTS

We thank Xiuqin Xia for outstanding technical assistance, and Elizabeth Kolb for editing the manuscript. We thank Eric Freed (NCI) for providing the TSG-5′, TSG-3′ and Alix fragment plasmids, and W. Sundquist (University of Utah) for providing the Vps4A (E228Q) plasmid. We acknowledge use of the SDSU-FGCF Core. This work was supported by SDSU AES 3AH-203 to F. L., and USDA, ARS CRIS project 6612-32000-056-00D (to Q. Y.).

REFERENCES

Biacchesi, S., Skiadopoulos, M. H., Yang, L., Lamirande, E. W., Tran, K. C., Murphy, B. R., Collins, P. L. & Buchholz, U. J. (2004). Recombinant human metapneumovirus lacking the small hydrophobic SH and/or attachment G glycoprotein: deletion of G yields a promising vaccine candidate. *J Virol* **78**, 12877–12887. doi:10.1128/JVI.78.23.12877-12887.2004.

Biacchesi, S., Pham, Q. N., Skiadopoulos, M. H., Murphy, B. R., Collins, P. L. & Buchholz, U. J. (2005). Infection of nonhuman primates with recombinant human metapneumovirus lacking the SH, G, or M2-2 protein categorizes each as a nonessential accessory protein and identifies vaccine candidates. *J Virol* **79**, 12608–12613. doi:10.1128/JVI.79.19.12608-12613.2005.

Bruce, E. A., Digard, P. & Stuart, A. D. (2010). The Rab11 pathway is required for influenza A virus budding and filament formation. *J Virol* **84**, 5848–5859. doi:10.1128/JVI.00307-10.

Catelli, E., Cecchinato, M., Savage, C. E., Jones, R. C. & Naylor, C. J. (2006). Demonstration of loss of attenuation and extended field persistence of a live avian metapneumovirus vaccine. *Vaccine* **24**, 6476–6482. doi:10.1016/j.vaccine.2006.06.076.

Catelli, E., Lupini, C., Cecchinato, M., Ricchizzi, E., Brown, P. & Naylor, C. J. (2010). Field avian metapneumovirus evolution avoiding vaccine induced immunity. *Vaccine* **28**, 916–921. doi:10.1016/j.vaccine.2009.10.149.

Chen, B. J. & Lamb, R. A. (2008). Mechanisms for enveloped virus budding: can some viruses do without an ESCRT? *Virology* **372**, 221–232. doi:10.1016/j.virol.2007.11.008.

Chen, B. J., Leser, G. P., Morita, E. & Lamb, R. A. (2007). Influenza virus hemagglutinin and neuraminidase, but not the matrix protein, are required for assembly and budding of plasmid-derived virus-like particles. *J Virol* **81**, 7111–7123. doi:10.1128/JVI.00361-07.

Ciancanelli, M. J. & Basler, C. F. (2006). Mutation of YMYL in the Nipah virus matrix protein abrogates budding and alters subcellular localization. *J Virol* **80**, 12070–12078. doi:10.1128/JVI.01743-06.

Coronel, E. C., Murti, K. G., Takimoto, T. & Portner, A. (1999). Human parainfluenza virus type 1 matrix and nucleoprotein genes transiently expressed in mammalian cells induce the release of virus-like particles containing nucleocapsid-like structures. *J Virol* **73**, 7035–7038.

de Graaf, M., Osterhaus, A. D., Fouchier, R. A. & Holmes, E. C. (2008). Evolutionary dynamics of human and avian metapneumoviruses. *J Gen Virol* **89**, 2933–2942. doi:10.1099/vir.0.2008/006957-0.

Demirov, D. G. & Freed, E. O. (2004). Retrovirus budding. *Virus Res* **106**, 87–102. doi:10.1016/j.virusres.2004.08.007.

Demirov, D. G., Ono, A., Orenstein, J. M. & Freed, E. O. (2002). Overexpression of the N-terminal domain of TSG101 inhibits HIV-1 budding by blocking late domain function. *Proc Natl Acad Sci U S A* **99**, 955–960. doi:10.1073/pnas.032511899.

Easton, A. J., Domachowske, J. B. & Rosenberg, H. F. (2004). Animal pneumoviruses: molecular genetics and pathogenesis. *Clin Microbiol Rev* **17**, 390–412. doi:10.1128/CMR.17.2.390-412.2004.

Freed, E. O. (2002). Viral late domains. *J Virol* **76**, 4679–4687. doi:10.1128/JVI.76.10.4679-4687.2002.

Garrus, J. E., von Schwedler, U. K., Pornillos, O. W., Morham, S. G., Zavitz, K. H., Wang, H. E., Wettstein, D. A., Stray, K. M., Côté, M. & Rich, R. L. (2001). Tsg101 and the vacuolar protein sorting pathway are essential for HIV-1 budding. *Cell* **107**, 55–65. doi:10.1016/S0092-8674(01)00506-2.

Goila-Gaur, R., Demirov, D. G., Orenstein, J. M., Ono, A. & Freed, E. O. (2003). Defects in human immunodeficiency virus budding and endosomal sorting induced by TSG101 overexpression. *J Virol* **77**, 6507–6519. doi:10.1128/JVI.77.11.6507-6519.2003.

Gosselin-Grenet, A. S., Marq, J. B., Abrami, L., Garcin, D. & Roux, L. (2007). Sendai virus budding in the course of an infection does not require Alix and VPS4A host factors. *Virology* **365**, 101–112. doi:10.1016/j.virol.2007.03.039.

Govindarajan, D. & Samal, S. K. (2004). Sequence analysis of the large polymerase (L) protein of the US strain of avian metapneumovirus indicates a close resemblance to that of the human metapneumovirus. *Virus Res* **105**, 59–66. doi:10.1016/j.virusres.2004.04.014.

Govindarajan, D. & Samal, S. K. (2005). Analysis of the complete genome sequence of avian metapneumovirus subgroup C indicates that it possesses the longest genome among metapneumoviruses. *Virus Genes* **30**, 331–333. doi:10.1007/s11262-005-6775-6.

Irie, T., Shimazu, Y., Yoshida, T. & Sakaguchi, T. (2007). The YLDL sequence within Sendai virus M protein is critical for budding of virus-like particles and interacts with Alix/AIP1 independently of C protein. *J Virol* **81**, 2263–2273. doi:10.1128/JVI.02218-06.

Jin, J., Sturgeon, T., Chen, C., Watkins, S. C., Weisz, O. A. & Montelaro, R. C. (2007). Distinct intracellular trafficking of equine infectious anemia virus and human immunodeficiency virus type 1 Gag during viral assembly and budding revealed by bimolecular fluorescence complementation assays. *J Virol* **81**, 11226–11235. doi:10.1128/JVI.00431-07.

Knipe, D. M. , Howley, P. M., Griffin, D. E., Lamb, R. A., Martin, M. A., Roizman. B. & Straus, S. E. (editors) (2001). *Fields Virology*. Philadelphia, PA: Lippincott Williams & Wilkins.

Lee, S., Joshi, A., Nagashima, K., Freed, E. O. & Hurley, J. H. (2007). Structural basis for viral late-domain binding to Alix. *Nat Struct Mol Biol* **14**, 194–199. doi:10.1038/nsmb1203.

Li, F., Chen, C., Puffer, B. A. & Montelaro, R. C. (2002). Functional replacement and positional dependence of homologous and heterologous L domains in equine infectious anemia virus replication. *J Virol* **76**, 1569–1577. doi:10.1128/JVI.76.4.1569-1577.2002.

Li, M., Schmitt, P. T., Li, Z., McCrory, T. S., He, B. & Schmitt, A. P. (2009). Mumps virus matrix, fusion, and nucleocapsid proteins cooperate for efficient production of virus-like particles. *J Virol* **83**, 7261–7272. doi:10.1128/JVI.00421-09.

Luttge, B. G., Shehu-Xhilaga, M., Demirov, D. G., Adamson, C. S., Soheilian, F., Nagashima, K., Stephen, A. G., Fisher, R. J. & Freed, E. O. (2008). Molecular characterization of feline immunodeficiency virus budding. *J Virol* **82**, 2106–2119. doi:10.1128/JVI.02337-07.

Medina, G., Zhang, Y., Tang, Y., Gottwein, E., Vana, M. L., Bouamr, F., Leis, J. & Carter, C. A. (2005). The functionally exchangeable L domains in RSV and HIV-1 Gag direct particle release through pathways linked by Tsg101. *Traffic* **6**, 880–894. doi:10.1111/j.1600-0854.2005.00323.x.

Morita, E. & Sundquist, W. I. (2004). Retrovirus budding. *Annu Rev Cell Dev Biol* **20**, 395–425. doi:10.1146/annurev.cellbio.20.010403.102350.

Munir, S. & Kapur, V. (2003). Regulation of host cell transcriptional physiology by the avian pneumovirus provides key insights into host-pathogen interactions. *J Virol* **77**, 4899–4910. doi:10.1128/JVI.77.8.4899-4910.2003.

Munshi, U. M., Kim, J., Nagashima, K., Hurley, J. H. & Freed, E. O. (2007). An Alix fragment potently inhibits HIV-1 budding: characterization of binding to retroviral YPXL late domains. *J Biol Chem* **282**, 3847–3855. doi:10.1074/jbc.M607489200.

Naylor, C. J., Brown, P. A., Edworthy, N., Ling, R., Jones, R. C., Savage, C. E. & Easton, A. J. (2004). Development of a reverse-genetics system for avian pneumovirus demonstrates that the small hydrophobic (SH) and attachment (G) genes are not essential for virus viability. *J Gen Virol* **85**, 3219–3227. doi:10.1099/vir.0.80229-0.

Naylor, C. J., Ling, R., Edworthy, N., Savage, C. E. & Easton, A. J. (2007). Avian metapneumovirus SH gene end and G protein mutations influence the level of protection of live-vaccine candidates. *J Gen Virol* **88**, 1767–1775. doi:10.1099/vir.0.82755-0.

Niwa, H., Yamamura, K. & Miyazaki, J. (1991). Efficient selection for high-expression transfectants with a novel eukaryotic vector. *Gene* **108**, 193–199. doi:10.1016/0378-1119(91)90434-D.

Njenga, M. K., Lwamba, H. M. & Seal, B. S. (2003). Metapneumoviruses in birds and humans. *Virus Res* **91**, 163–169. doi:10.1016/S0168-1702(02)00256-3.

Pantua, H. D., McGinnes, L. W., Peeples, M. E. & Morrison, T. G. (2006). Requirements for the assembly and release of Newcastle disease virus-like particles. *J Virol* **80**, 11062–11073. doi:10.1128/JVI.00726-06.

Patch, J. R., Crameri, G., Wang, L. F., Eaton, B. T. & Broder, C. C. (2007). Quantitative analysis of Nipah virus proteins released as virus-like particles reveals central role for the matrix protein. *Virol J* **4**, 1. doi:10.1186/1743-422X-4-1.

Patch, J. R., Han, Z., McCarthy, S. E., Yan, L., Wang, L. F., Harty, R. N. & Broder, C. C. (2008). The YPLGVG sequence of the Nipah virus matrix protein is required for budding. *Virol J* **5**, 137. doi:10.1186/1743-422X-5-137.

Schmitt, A. P., Leser, G. P., Waning, D. L. & Lamb, R. A. (2002). Requirements for budding of paramyxovirus simian virus 5 virus-like particles. *J Virol* **76**, 3952–3964. doi:10.1128/JVI.76.8.3952-3964.2002.

Schmitt, A. P., Leser, G. P., Morita, E., Sundquist, W. I. & Lamb, R. A. (2005). Evidence for a new viral late-domain core sequence, FPIV, necessary for budding of a paramyxovirus. *J Virol* **79**, 2988–2997. doi:10.1128/JVI.79.5.2988-2997.2005.

Shehu-Xhilaga, M., Ablan, S., Demirov, D. G., Chen, C., Montelaro, R. C. & Freed, E. O. (2004). Late domain-dependent inhibition of equine infectious anemia virus budding. *J Virol* **78**, 724–732. doi:10.1128/JVI.78.2.724-732.2004.

Takimoto, T. & Portner, A. (2004). Molecular mechanism of paramyxovirus budding. *Virus Res* **106**, 133–145. doi:10.1016/j.virusres.2004.08.010.

Taylor, G. M., Hanson, P. I. & Kielian, M. (2007). Ubiquitin depletion and dominant-negative VPS4 inhibit rhabdovirus budding without affecting alphavirus budding. *J Virol* **81**, 13631–13639. doi:10.1128/JVI.01688-07.

Toquin, D., de Boisseson, C., Beven, V., Senne, D. A. & Eterradossi, N. (2003). Subgroup C avian metapneumovirus (MPV) and the recently isolated human MPV exhibit a common organization but have extensive sequence divergence in their putative SH and G genes. *J Gen Virol* **84**, 2169–2178. doi:10.1099/vir.0.19043-0.

Toquin, D., Guionie, O., Jestin, V., Zwingelstein, F., Allee, C. & Eterradossi, N. (2006). European and American subgroup C isolates of avian metapneumovirus belong to different genetic lineages. *Virus Genes* **32**, 97–103. doi:10.1007/s11262-005-5850-3.

Utley, T. J., Ducharme, N. A., Varthakavi, V., Shepherd, B. E., Santangelo, P. J., Lindquist, M. E., Goldenring, J. R. & Crowe, J. E., Jr (2008). Respiratory syncytial virus uses a Vps4-independent budding mechanism controlled by Rab11-FIP2. *Proc Natl Acad Sci U S A* **105**, 10209–10214. doi:10.1073/pnas.0712144105.

van den Hoogen, B. G., de Jong, J. C., Groen, J., Kuiken, T., de Groot, R., Fouchier, R. A. & Osterhaus, A. D. (2001). A newly discovered human pneumovirus isolated from young children with respiratory tract disease. *Nat Med* **7**, 719–724. doi:10.1038/89098.

van den Hoogen, B. G., Bestebroer, T. M., Osterhaus, A. D. & Fouchier, R. A. (2002). Analysis of the genomic sequence of a human metapneumovirus. *Virology* **295**, 119–132. doi:10.1006/viro.2001.1355.

Velayudhan, B. T., McComb, B., Bennett, R. S., Lopes, V. C., Shaw, D., Halvorson, D. A. & Nagaraja, K. V. (2005). Emergence of a virulent type C avian metapneumovirus in turkeys in Minnesota. *Avian Dis* **49**, 520–526. doi:10.1637/7388-052805R.1.

Velayudhan, B. T., Nagaraja, K. V., Thachil, A. J., Shaw, D. P., Gray, G. C. & Halvorson, D. A. (2006). Human metapneumovirus in turkey poults. *Emerg Infect Dis* **12**, 1853–1859.

Velayudhan, B. T., Noll, S. L., Thachil, A. J., Halvorson, D. A., Shaw, D. P., Goyal, S. M. & Nagaraja, K. V. (2008). Comparative pathogenicity of early and recent isolates of avian metapneumovirus subtype C in turkeys. *Can J Vet Res* **72**, 371–375.

Wang, D., Harmon, A., Jin, J., Francis, D. H., Christopher-Hennings, J., Nelson, E., Montelaro, R. C. & Li, F. (2010a). The lack of an inherent membrane targeting signal is responsible for the failure of the matrix (M1) protein of influenza A virus to bud into virus-like particles. *J Virol* **84**, 4673–4681. doi:10.1128/JVI.02306-09.

Wang, Y. E., Park, A., Lake, M., Pentecost, M., Torres, B., Yun, T. E., Wolf, M. C., Holbrook, M. R., Freiberg, A. N. & Lee, B. (2010b). Ubiquitin-regulated nuclear-cytoplasmic trafficking of the Nipah virus matrix protein is important for viral budding. *PLoS Pathog* **6**, e1001186. doi:10.1371/journal.ppat.1001186.

Yu, Q., Estevez, C. N. & Kapczynski, D. R. (2006). Production and characterization of monoclonal antibodies that react to the nucleocapsid protein of avian metapneumovirus subtype C. *Avian Dis* **50**, 419–424. doi:10.1637/7513-020606R.1.

Yu, Q., Estevez, C., Song, M., Kapczynski, D. & Zsak, L. (2010). Generation and biological assessment of recombinant avian metapneumovirus subgroup C (AMPV-C) viruses containing different length of the G gene. *Virus Res* **147**, 182–188. doi:10.1016/j.virusres.2009.10.021.

Virus Research 160 (2011) 102–107

Contents lists available at ScienceDirect

Virus Research

journal homepage: www.elsevier.com/locate/virusres

Topology and cellular localization of the small hydrophobic protein of avian metapneumovirus

Qiji Deng[a,1], Yuejin Weng[a,b,c,1], Wuxun Lu[b,c], Andrew Demers[b,c], Minxun Song[d], Dan Wang[b,c], Qingzhong Yu[e], Feng Li[a,b,c,*]

[a] Department of Veterinary and Biomedical Sciences, South Dakota State University, Brookings, SD 57007, United States
[b] Department of Biology and Microbiology, South Dakota State University, Brookings, SD 57007, United States
[c] Center for Infectious Disease Research and Vaccinology, South Dakota State University, Brookings, SD 57007, United States
[d] Institute of Poultry Science, Shandong Academy of Agricultural Sciences, Jinan 250023, China
[e] Southeast Poultry Research Laboratory, Agricultural Research Services, U.S. Department of Agriculture, Athens, GA 30605, United States

ARTICLE INFO

Article history:
Received 13 March 2011
Received in revised form 24 May 2011
Accepted 25 May 2011
Available online 6 June 2011

Keywords:
Avian metapneumovirus
Topology
Subcellular localization
Transport

ABSTRACT

The small hydrophobic protein (SH) is a type II integral membrane protein that is packaged into virions and is only present in certain paramyxoviruses including metapneumovirus. In addition to a highly divergent primary sequence, SH proteins vary significantly in size amongst the different viruses. Human respiratory syncytial virus (HRSV) encodes the smallest SH protein consisting of only 64 amino acids, while metapneumoviruses have the longest SH protein ranging from 174 to 179 amino acids in length. Little is currently known about the cellular localization and topology of the metapneumovirus SH protein. Here we characterize for the first time metapneumovirus SH protein with respect to topology, subcellular localization, and transport using avian metapneumovirus subgroup C (AMPV-C) as a model system. We show that AMPV-C SH is an integral membrane protein with $N_{in}C_{out}$ orientation located in both the plasma membrane as well as within intracellular compartments, which is similar to what has been described previously for SH proteins of other paramyxoviruses. Furthermore, we demonstrate that AMPV-C SH protein localizes in the endoplasmic reticulum (ER), Golgi, and cell surface, and is transported through ER–Golgi secretory pathway.

© 2011 Elsevier B.V. All rights reserved.

1. Introduction

Avian metapneumovirus (AMPV), previously known as turkey rhinotracheitis virus or avian pneumovirus, causes acute respiratory disease in turkeys and has recently emerged as a major economic problem for the turkey industry (Branigan et al., 2006; Catelli et al., 2010; Easton et al., 2004; Govindarajan et al., 2006; Naylor et al., 2007; Njenga et al., 2003; Toquin et al., 2006; Velayudhan et al., 2005). AMPV also infects chickens and causes "swollen head syndrome" (Njenga et al., 2003). AMPV is a paramyxovirus with a negative single-stranded RNA genome, which codes for nucleoprotein (N), phosphoprotein (P), matrix protein (M), fusion protein (F), M2-1 and M2-2 proteins, small hydrophobic protein (SH), attachment glycoprotein (G), and the large polymerase protein (L) (Collins and Crowe, 2007; Easton et al., 2004). Based on its genome and biological characteristics, AMPV and its human counterpart human metapneumovirus (HMPV) are assigned to the genus Metapneumovirus within the subfamily Pneumovirinae. However, HRSV and AMPV/HMPC are different because the former have NS1 and NS2 proteins, while the latter does not encode such proteins (Collins and Crowe, 2007; Easton et al., 2004).

For AMPV, there exist four subgroups, namely, A, B, C, and D (Easton et al., 2004; Velayudhan et al., 2008). Interestingly, sequence analysis has revealed that AMPV subgroup C is more closely related to HMPV than to any of the other AMPV subgroups (Govindarajan and Samal, 2005; Toquin et al., 2003; van den Hoogen et al., 2001, 2002). For example, AMPV-C and HMPV share a total of 80% amino acid identity, with N and M being the most conserved proteins and SH and G proteins the most variable. Like HRSV, both AMPV and HMPV encode three surface glycoproteins: F, G, and SH (Collins and Crowe, 2007). Studies of HMPV biology show that F protein is involved with virus–cell fusion as well as cell–cell fusion during viral replication (de Graaf et al., 2009; Herfst et al., 2008; Schowalter et al., 2006, 2009). HMPV G protein plays a role in the promotion of viral attachment and fusion (Biacchesi et al., 2004a,b, 2005). A recent study has described HMPV G as an important virulence factor that inhibits the host's innate immunity by targeting

* Corresponding author at: Department of Veterinary and Biomedical Sciences, South Dakota State University, Brookings, SD 57007, United States.
Tel.: +1 605 688 6036; fax: +1 605 688 6003.
E-mail address: feng.li@sdstate.edu (F. Li).
[1] These authors are equally contributed.

0168-1702/$ – see front matter © 2011 Elsevier B.V. All rights reserved.
doi:10.1016/j.virusres.2011.05.020

RIG-I, a major intracellular viral RNA sensor (Bao et al., 2008b). Little is known about the biology of the SH protein for both AMPV and HMPV. HMPV SH appears to be involved in the regulation of various host immune responses but is not essential for HMPV replication both *in vitro* and *in vivo* (Bao et al., 2008a; Biacchesi et al., 2004b, 2005; Fuentes et al., 2007; Naylor et al., 2004), although mutant viruses with the deletion of SH have slightly delayed replication kinetics (Biacchesi et al., 2004a,b, 2005). In contrast to HMPV replication, a recent study of AMPV subgroup A and B viruses shows that the SH protein is required for efficient virus replication both in cell culture and in infected turkeys, and suggests that SH may play a role in mediating the cell–cell fusion process in these viruses (Ling et al., 2008).

The SH protein is only present in certain paramyxoviruses, which include mumps, PIV5 (also known as simian virus 5, SV5), human and animal RSV, and metapneumovirus (Collins and Crowe, 2007; Collins and Graham, 2008; Easton et al., 2004; He et al., 2001). The SH protein itself varies considerably in size: HRSV encodes the smallest SH protein containing 64 amino acids, whereas HMPV has the longest SH protein with 179 amino acids (Biacchesi et al., 2003; van den Hoogen et al., 2002). AMPV closely resembles its human counterpart encoding an SH protein with 174–175 amino acids in length (Biacchesi et al., 2003; van den Hoogen et al., 2002). Early studies of HRSV and PIV5 have demonstrated that SH is a type II transmembrane protein adopting a $N_{in}C_{out}$ orientation in the membrane, and is not absolutely essential for virus attachment, assembly, or infectivity at least *in vitro* (Collins and Mottet, 1993; Collins et al., 1990; Hiebert et al., 1988; Olmsted and Collins, 1989). In the present work, we characterized SH protein of metapneumovirus with respect to topology, subcellular localization, and trafficking using AMPV-C as a model system. We demonstrated that the SH protein of AMPV-C is: (i) an integral membrane protein with $N_{in}C_{out}$ orientation, (ii) presented both in the plasma membrane and within intracellular compartments, and (iii) transported to the cell surface through the conventional ER–Golgi secretory pathway.

2. Materials and methods

2.1. Plasmids

PCR and cloning was performed with proof-reading Vent DNA polymerase (New England Biolabs) under standard reaction conditions. The integrity of all PCR-derived DNA fragments was verified by sequencing. All primers and sequences are available from the authors upon request. For the expression of viral SH proteins that were used in this study, cDNA sequence encoding SH was amplified from a pLF-2.1 plasmid (containing a large portion of the genome derived from AMPV subgroup C virus, Colorado strain) by PCR, and subcloned into the eukaryotic expression vector pCAGGS (Addgene plasmid 11160, Addgene) to generate a pSH. Our protocol for the generation of the pLF-2.1 plasmid has been described previously (Yu et al., 2010). To facilitate the detection of SH protein expression and study the topology of the SH protein, an HA epitope tag was placed at the N-terminus or the C-terminus of SH, resulting in two constructs designated $p^{HA}SH$ and pSH^{HA}, respectively.

To study SH protein localization in the endoplasmic reticulum (ER) region, bimolecular fluorescence complementation (BiFC) assay for visualization of SH protein was developed. For the construction of BiFC plasmids (Hemerka et al., 2009; Wang et al., 2010), sequences encoding the amino (residues 1–173, VN) or carboxyl (residues 155–238, VC) fragments of the venus fluorescence protein were fused to the N terminus of SH protein producing two specific BiFC plasmids: pVN-SH and pVC-SH.

All plasmids were verified by DNA sequencing and further confirmed in Western-blot assay for protein expression.

2.2. Cells and antibodies

COS-1 cells were cultured in Dulbecco's minimal essential medium (DMEM) supplemented with 10% fetal bovine serum. Monoclonal antibody against the HA epitope and a Cy3-conjugated rabbit anti-ERGIC-53 antibody were purchased from Sigma–Aldrich. Polyclonal rabbit anti-GFP was obtained from Santa Cruz Biotechnology. Rabbit anti-giantin (an integral Golgi protein) was obtained from Covance. Alexa Fluor® 594 goat anti-rabbit IgG (H + L) and ER-Tracker dye (red) were purchased from Invitrogen. Rabbit anti-calnexin (ER Molecular Chaperone) was purchased from Cell Signaling Technology. Secondary antibodies such as donkey anti-rabbit IgG-HRP and goat anti-mouse IgG-HRP were purchased from Abcam.

2.3. Selective membrane permeabilization and immunocytochemistry

COS-1 cells grown on coverslips were transfected with SH expression plasmids (pSH^{HA} and $p^{HA}SH$, 0.5 μg DNA each). Twenty-four hours after transfection, cells were washed and fixed with 4% (w/v) paraformaldehyde (Electron Microscopy Sciences). Cells were then selectively permeabilized at 4 °C with either 0.5% (v/v) Triton X-100 (Sigma–Aldrich) or 5 μg/ml Digitonin (Fluka) prior to incubation with the appropriate primary antibody directly conjugated with FITC or with secondary antibody conjugated to FITC. Transfected cells with no permealization were used as control. Cells were finally washed briefly in PBS before being mounted on a slide with Vectashield mounting medium (Vector Laboratories). DAPI (Invitrogen) was used for staining the nuclei of cells. Fluorescent imaging of fixed cells was conducted using a FluoView FV300 confocal system (Olympus America Inc., Melville, N.Y.) equipped with an IX81 Microscope. Digital images were processed with Adobe Photoshop (version 6). All images were taken under similar experimental conditions (i.e., exposure time, magnification, and intensification), and processing was standardized for all images shown in this study.

For protein colocalization, cells expressing SH^{HA} protein were fixed and permeabilized with either Digitonin or Triton X-100 prior to incubation with combinations of primary antibodies and Alexa Fluor® 594-conjugated goat secondary antibodies. DAPI was used to stain the nucleus. For the SH protein transport inhibition experiment, 5 μg/ml Brefeldin A (BFA) (Sigma–Aldrich) was added to COS-1 cells at 6 h posttransfection. BFA was maintained in cell culture throughout experiments that lasted 24 h on average. A similar procedure as described above was used to visualize SH protein or cellular markers (Calnexin, ERGIC-53, and Giantin). Calnexin is a chaperon protein present in the endoplasmic reticulum (ER), and is used as a maker for visualizing ER compartment. ERGIC-53 is a cellular maker for ER–Golgi intermediate compartment whereas Giantin is specifically to mark Golgi compartment.

2.4. Bimolecular fluorescence complementation and confocal microscopy

Bimolecular fluorescence complementation (BiFC) coupled with confocal microscopy was used to characterize protein–protein interactions in living cells. COS-1 cells, grown on 12-well plates containing glass coverslips, were transfected either with previously selected or various combinations of BIFC plasmids or individual BiFC plasmid (1.0 μg each plasmid). At 24 h posttransfection, cell monolayers were fixed and stained with DAPI (Invitrogen). Image collection and processing was performed as described above. ER-Tracker dye (red) coupled with BiFC detection of SH proteins were used to characterize SH protein localization in ER according to manufacture's instruction (Invitrogen).

Table 1
Topology prediction of aMPV-C SH protein.[a]

Software tool	Cytoplasmic (inside)	Transmembrane	Extracellular (outside)	Source
Phobius	1–28	29–52	53–175	http://phobius.sbc.su.se/
SPOCTOPUS	1–29	30–50	51–175	http://octopus.cbr.su.se/
SCAMPI	1–28	29–49	50–175	http://scampi.cbr.su.se/
TOPCONS	1–28	29–49	50–175	http://topcons.net/
TopPred	1–28	29–49	50–175	http://mobyle.pasteur.fr/
HMMTOP	1–28	29–48	49–175	http://www.enzim.hu/
TMpred	1–28	29–49	50–175	www.ch.embnet.org
TMHMM	53–175	30–52	1–29	http://www.cbs.dtu.dk/

[a] SH protein sequence used for analysis is derived from Gene bank No: AY590688.

3. Results and discussion

3.1. Topology of the AMPV-C SH protein

To gain insight into the topology of the AMPV-C SH protein, various on-line tools were combined for the prediction of SH topology. As summarized in Table 1, seven of the eight computer programs examined predicted that AMPV-C SH protein is a single-pass type II integral-membrane protein with $N_{in}C_{out}$ orientation. The predicted consensus working model is that the SH protein possesses a 28-residue N-terminal cytoplasmic tail, a 21-residue transmembrane domain, and a 126-residue C-terminal ectodomain, although the exact length, particularly of the residues spanning the membrane, still needs to be evaluated experimentally. It should be noted that the SH topology presented here is consistent with the current working model proposed previously for the SH protein of paraxomoviruses, including HMPV and AMPV (Collins and Mottet, 1993; Collins et al., 1990; Hiebert et al., 1988; Olmsted and Collins, 1989; Toquin et al., 2003).

To experimentally evaluate the accuracy of the predicted model, and to gain more information on the topology of AMPV-C SH protein, we chose to apply an immunocytochemical method coupled with use of detergents (digitonin and Triton X-100) to selectively permeabilize cells. This method has been successfully used for determination of the topology of various viral envelope proteins (Agnihothram et al., 2007; Carrere-Kremer et al., 2002; Cocquerel et al., 2002; Dultz et al., 2008; Froeschke et al., 2003; Griffin et al., 2005; Holden et al., 2005; Schrempf et al., 2007). We inserted an HA epitope tag at either the N or C terminus of SH and the resultant constructs were termed $p^{HA}SH$ and pSH^{HA}, respectively. COS-1 cells were transfected with either $p^{HA}SH$ or pSH^{HA}. At 24 h posttransfection, cells were fixed with 4% formaldehyde. After fixation, cells were treated with either 0.5% Triton X-100 or 5 μg/ml digitonin. Control cells were incubated in PBS. An anti-HA monoclonal antibody coupled with anti-mouse IgG-FITC was used to stain the detergent-treated and untreated cells. Nuclei of COS-1 cells were stained with DAPI. The SH localization patterns amongst these cells were then examined by confocal microscopy.

The SH fusion protein containing an HA tag at its C-terminus, SH^{HA} was readily detected by anti-HA antibody on the surface of intact cells without any detergent treatment (Fig. 1B). In contrast, anti-HA antibody was unable to detect an HA tag inserted at the N-terminus of the SH protein (^{HA}SH) on the cell surface, as indicated by the lack of green fluorescence (Fig. 1A). With complete solubilization of the cell membranes using 0.5% Triton X-100, both SH fusion constructs were visualized intracellularly with anti-HA antibody, exhibiting a characteristic ER reticular staining with a more pronounced pattern in the SH^{HA} protein. These results indicate that SH has its C terminus oriented toward the extracellular environment while maintaining its N-terminus in the cytosol, which is in good agreement with the predicted model of SH topology by computer programs (Table 1).

Digitonin is able to permeabilize the plasma membrane while leaving intracellular membranes intact (Agnihothram et al., 2007; Carrere-Kremer et al., 2002; Griffin et al., 2005; Holden et al., 2005; Lundin et al., 2003). Permeabilization of the plasma membrane, not other limiting membranes inside the cell, is due to the higher concentration of cholesterol present in the plasma membrane (Agnihothram et al., 2007; Carrere-Kremer et al., 2002; Griffin et al., 2005; Holden et al., 2005; Lundin et al., 2003). Protein epitopes in the cytosol are accessible in digitonin-treated cells, while intra-luminal targets remain protected. As expected, in digitonin-treated cells, ^{HA}SH protein with its HA tag epitope being oriented toward the cytosolic side of the membrane displayed predominant staining of intracellular vesicles with less profound staining observed at the cell surface (Fig. 1A). In contrast, the SH^{HA} protein with the HA tag epitope being oriented toward the cell surface or lumen of intracellular compartments exhibited the majority of staining at the cell surface (Fig. 1B). To validate our staining protocol, we performed immunostaining experiments using an antibody specific for calnexin that is a chaperon protein present in the endoplasmic reticulum (ER). Immunofluorescence staining showed that calnexin was detected and located in ER region in cells treated with Triton X-100 (Fig. 1C, left panel). In contrast, in cells treated with digitonin no immunofluorescence signal for calnexin was observed (Fig. 1C, right panel), confirming that the digitonin treatment used in our experiment selectively disrupts the plasma membrane. Taken together, these results confirm the suggestion that the SH protein is an integral membrane protein and adopts a $N_{in}C_{out}$ orientation typical of type II transmembrane proteins.

3.2. Cellular localization and intracellular trafficking of the SH protein

The results presented in Fig. 1 indicate that the SH protein likely resides in the ER–Golgi region and is transported to the plasma membrane, which is similar to studies of the SH proteins of other paramyxoviruses (Hiebert et al., 1988; Olmsted and Collins, 1989; Rixon et al., 2004). To determine the cellular localization of AMPV-C SH protein, a protein colocalization experiment was performed. Three well-characterized markers for labeling ER and Glogi compartments; ER-Tracker red dye (ER), ERGIC-53 (ER–Golgi intermediate compartment), and Giantin (Golgi), were used in our study. Because ER-Tracker red dye can be bleached in the presence of detergents, visualization of ER-associated SH protein by bimolecular fluorescent complementation assay (BiFC) was used to examine SH localization in the ER region together with staining cells by ER-Tracker red dye. As demonstrated in the upper panel of Fig. 2A, fluorescent signals of SH protein through BiFC were seen both internally as well as on the cell surface, which was reminiscent of the subcellular localization pattern displayed by the SH fusion protein in detergents-treated cells (Fig. 1). SH protein colocalized with the ER/Golgi markers (Fig. 2A), indicating that AMPV-C SH protein is present in both the ER and the Golgi. Similar results were also obtained with the ^{HA}SH fusion protein alone (data not shown).

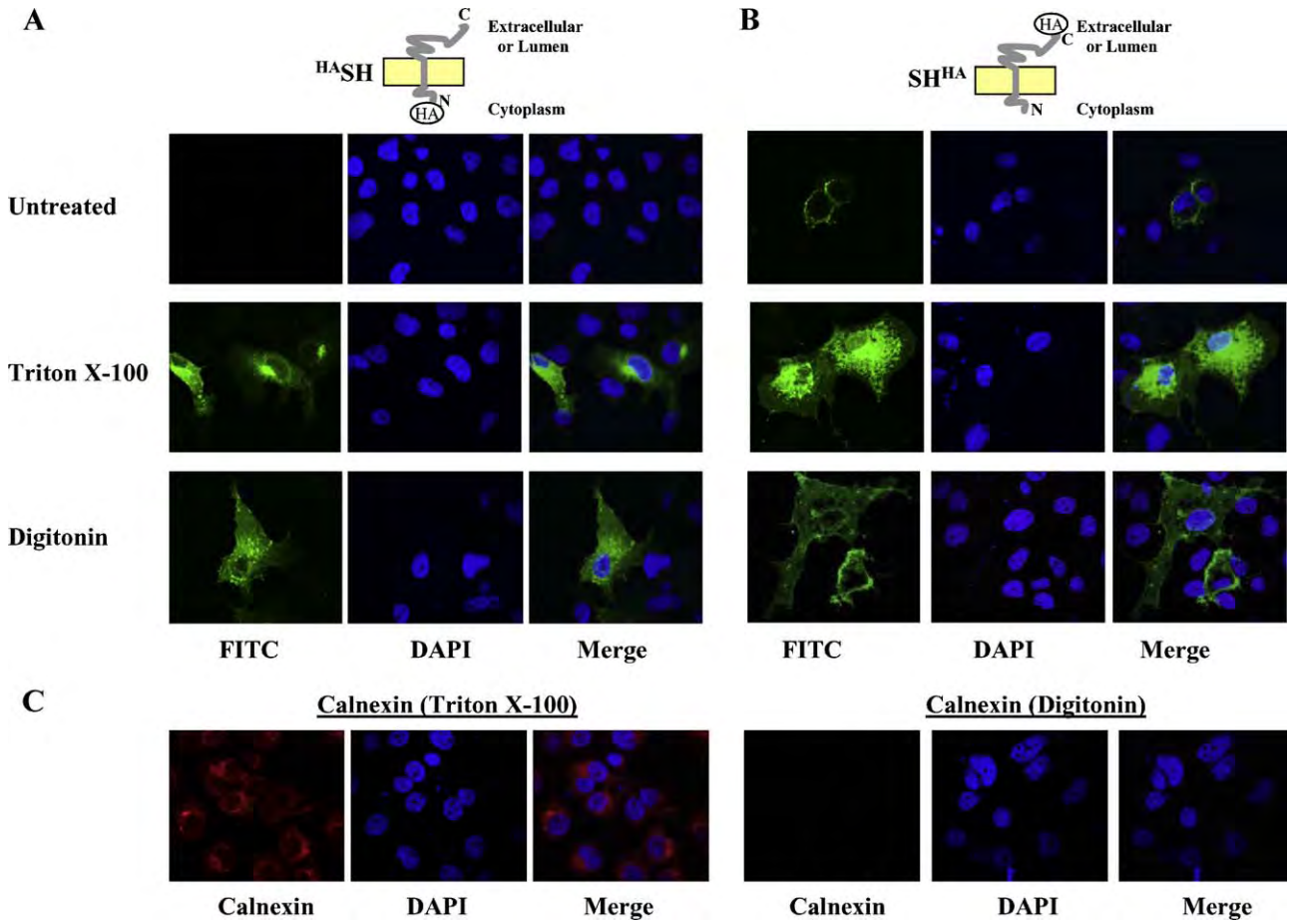

Fig. 1. Determination of the topology of AMPV-SH protein by epitope tagging. COS-1 cells were transfected with $p^{HA}SH$ (A) or pSH^{HA} (B) plasmid and analyzed by indirect immunofluorescence. Cells were fixed with paraformaldehyde at 24 h post transfection, and either permeabilized with Triton X-100, digitonin, or left unpermeabilized and immunostained with the anti-HA monoclonal antibody. A schematic representation of the topology of the different SH proteins tagged with a HA epitope is presented at the top of the figure. (C) COS-1 cells were treated with either Triton X-100 or digitonin and then labeled for the ER with rabbit anti-Calnexin antibody followed by secondary anti-rabbit-Cy3 antibody.

To strengthen the above observation of protein localization and determine precisely if the AMPV-C SH protein is transported to the plasma membrane through the ER–Golgi secretory pathway, we incubated cells expressing SH^{HA} protein in the presence or absence of 5 μg/ml of Brefeldin A (BFA) and examined protein localization by immunocytochemical staining (Fig. 2B). BFA is known to block protein transport through the ER–Golgi to the plasma membrane by disrupting anterograde protein transport from the ER to the Golgi apparatus (Fujiwara et al., 1988). In untreated cells, SH^{HA} proteins were either diffusely distributed throughout the cytoplasm or accumulated in the plasma membrane (Fig. 2B, left panels). Cells permeabilized with Triton X-100 exhibited more perinuclear staining of SH^{HA} proteins. In contrast, in BFA-treated cells permeabilized with digitonin or Triton X-100 SH^{HA} proteins were primarily located in intracellular compartments, not the plasma membrane (Fig. 2B, right panels). Disruption of the SH^{HA} protein localization to the plasma membrane by BFA treatment suggests that AMPV-C SH protein utilizes the ER–Golgi secretory pathway to reach the cell surface. It should be noted that some background fluorescence present in intracellular compartments in digitonin-treated cells expressing SH^{HA} was observed (Fig. 2B) in several repeated experiments. We attributed the observed background staining to some unknown factors that are likely caused by SH protein expression. For example, we suspect that SH protein may interact with some structures in limiting membranes of intracellular compartments and this interaction could enable digitonin selectively disrupting such membranes and exposing SH^{HA} protein residing in the lumen of intracellular compartments. Future study is required to address this hypothesis.

3.3. Conclusion and discussion

In summary, our study has demonstrated that AMPV-C SH protein is an integral membrane protein with classical type II $N_{in}C_{out}$ orientation that is transported through the ER–Golgi complex to the cell surface. The combined use of several computer-based programs that predict protein sorting signals including TargetP and SignalP failed to reveal a signal peptide in the SH protein of AMPV-C (data not shown) (Emanuelsson et al., 2007). It is probable that AMPV-C SH utilizes a signal peptide anchor sequence that induces protein translocation to the ER–Golgi region as proposed previously for HRSV SH protein (Collins and Mottet, 1993; Collins et al., 1990; Olmsted and Collins, 1989). Our data confirmed that AMPV-C SH proteins are initially localized in the ER and then transported to the cell surface through the ER–Golgi secretory pathway. The abundant expression of AMPV-C SH protein in the ER–Golgi network may have a biological implication in specific anti-host responses. Studies of other small integral membrane proteins in several viruses including picornavirus and influenza A virus revealed that these proteins are involved in the alteration of MHC class I transport, disrupt antigen presentation, and trigger cellular inflammasomes (Ichinohe et al., 2010; Moffat et al., 2007). It will be interesting to see

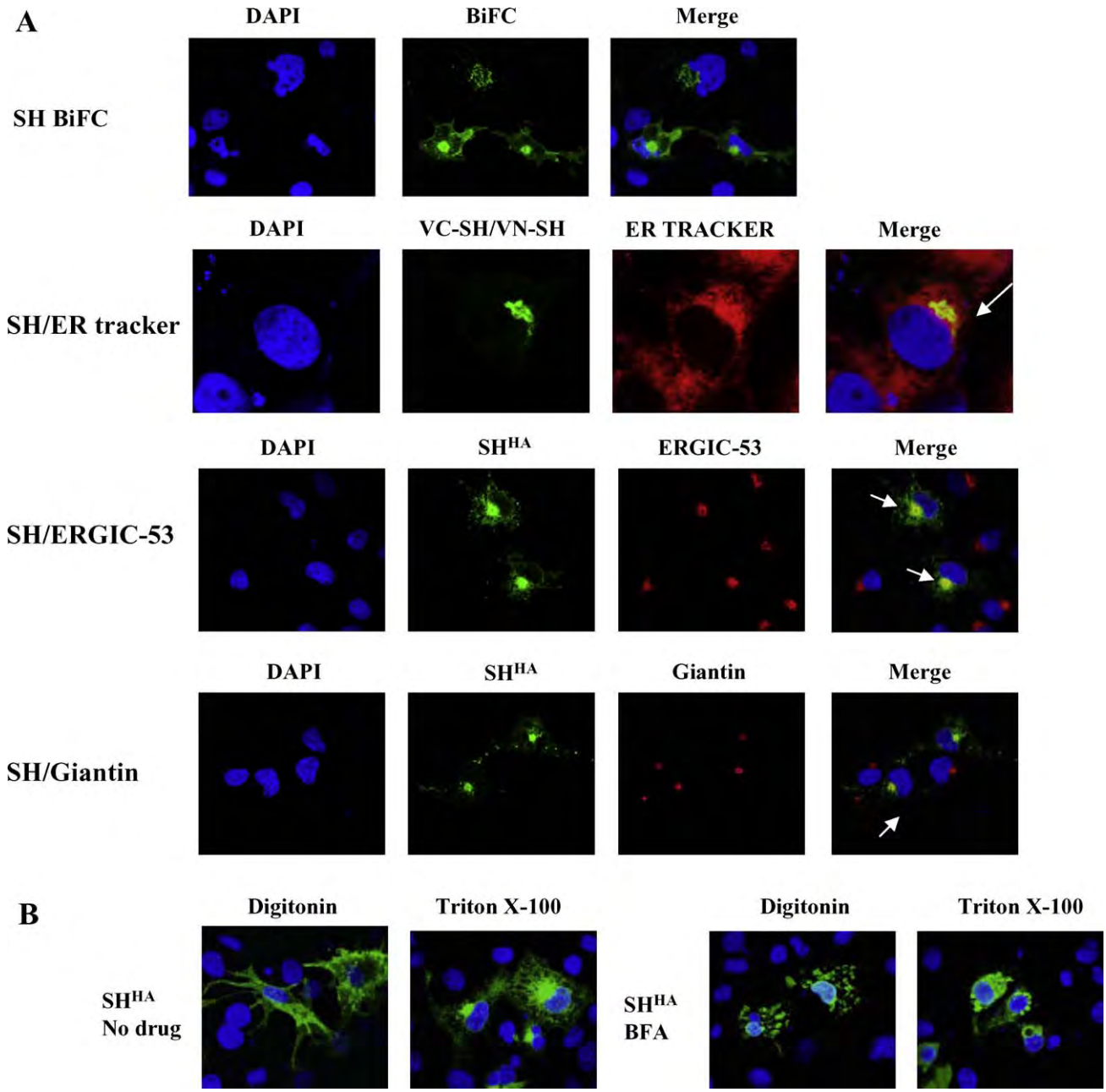

Fig. 2. Cellular localization and intracellular trafficking of AMPV-C SH protein. (A) Cellular localization of AMPV-C SH protein. COS-1 cells transiently transfected with pSH^{HA} were fixed, permeabilized with Triton X-100, and stained with DAPI (blue), an anti-HA monoclonal antibody (green), and antibodies against Giantin (red) or ERGIC-53 (red). For SH BiFC, At 24 h post transfection, cells expressing VN-SH and VC-SH were fixed, stained with DAPI, and imaged with a confocal microscope at a 60× magnification. For SH ER colocalization, cells were transiently co-transfected with SH BiFC constructs VN-SH and VC-SH (Green). Cells were then stained with ER Tracker dye (red). Merged profiles were shown in the very right panels and white arrows indicate colocalization. Sixty× magnification confocal microscope was used for both SH/ERGIC-53 and SH/Giantin colocalization, while 120× magnification was employed for SH/ER colocalization. (B) Characterization of the inhibitory effect on SH protein transport by BFA. COS-1 cells grown on glass coverslips were transfected with pSH^{HA} plasmid in the presence or absence of inhibitor BFA (5 μg/ml). Cells were fixed with formaldehyde at 24 h post transfection, permeabilized with digitonin or Triton X-100, and immunostained with the anti-HA monoclonal antibody. (For interpretation of the references to color in this figure legend, the reader is referred to the web version of the article.)

if AMPV-C SH has any of these effects. If this proves to be the case for AMPV-C SH, the results may help to explain why metapenumovirus infections in animal models often result in persistent infection after recovery from an acute phase of viral infection (Alvarez et al., 2004; Liu et al., 2009).

Acknowledgments

We thank Elizabeth Kolb for editing the manuscript and Xiuqin Xia for outstanding technical assistance. This work was supported by the SD AES Fund (3AH-203) to FL, and USDA, ARS CRIS project 6612-32000-056-00D (to QY).

References

Agnihothram, S.S., York, J., Trahey, M., Nunberg, J.H., 2007. Bitopic membrane topology of the stable signal peptide in the tripartite Junin virus GP-C envelope glycoprotein complex. J. Virol. 81 (8), 4331–4337.

Alvarez, R., Harrod, K.S., Shieh, W.J., Zaki, S., Tripp, R.A., 2004. Human metapneumovirus persists in BALB/c mice despite the presence of neutralizing antibodies. J. Virol. 78 (24), 14003–14011.

Bao, X., Kolli, D., Liu, T., Shan, Y., Garofalo, R.P., Casola, A., 2008a. Human metapneumovirus small hydrophobic protein inhibits NF-kappaB transcriptional activity. J. Virol. 82 (16), 8224–8229.
Bao, X., Liu, T., Shan, Y., Li, K., Garofalo, R.P., Casola, A., 2008b. Human metapneumovirus glycoprotein G inhibits innate immune responses. PLoS Pathog. 4 (5), e1000077.
Biacchesi, S., Pham, Q.N., Skiadopoulos, M.H., Murphy, B.R., Collins, P.L., Buchholz, U.J., 2005. Infection of nonhuman primates with recombinant human metapneumovirus lacking the SH, G, or M2-2 protein categorizes each as a nonessential accessory protein and identifies vaccine candidates. J. Virol. 79 (19), 12608–12613.
Biacchesi, S., Skiadopoulos, M.H., Boivin, G., Hanson, C.T., Murphy, B.R., Collins, P.L., Buchholz, U.J., 2003. Genetic diversity between human metapneumovirus subgroups. Virology 315 (1), 1–9.
Biacchesi, S., Skiadopoulos, M.H., Tran, K.C., Murphy, B.R., Collins, P.L., Buchholz, U.J., 2004a. Recovery of human metapneumovirus from cDNA: optimization of growth in vitro and expression of additional genes. Virology 321 (2), 247–259.
Biacchesi, S., Skiadopoulos, M.H., Yang, L., Lamirande, E.W., Tran, K.C., Murphy, B.R., Collins, P.L., Buchholz, U.J., 2004b. Recombinant human Metapneumovirus lacking the small hydrophobic SH and/or attachment G glycoprotein: deletion of G yields a promising vaccine candidate. J. Virol. 78 (23), 12877–12887.
Branigan, P.J., Day, N.D., Liu, C., Gutshall, L.L., Melero, J.A., Sarisky, R.T., Del Vecchio, A.M., 2006. The cytoplasmic domain of the F protein of Human respiratory syncytial virus is not required for cell fusion. J. Gen. Virol. 87 (Pt 2), 395–398.
Carrere-Kremer, S., Montpellier-Pala, C., Cocquerel, L., Wychowski, C., Penin, F., Dubuisson, J., 2002. Subcellular localization and topology of the p7 polypeptide of hepatitis C virus. J. Virol. 76 (8), 3720–3730.
Catelli, E., Lupini, C., Cecchinato, M., Ricchizzi, E., Brown, P., Naylor, C.J., 2010. Field avian metapneumovirus evolution avoiding vaccine induced immunity. Vaccine 28 (4), 916–921.
Cocquerel, L., Op de Beeck, A., Lambot, M., Roussel, J., Delgrange, D., Pillez, A., Wychowski, C., Penin, F., Dubuisson, J., 2002. Topological changes in the transmembrane domains of hepatitis C virus envelope glycoproteins. EMBO J. 21 (12), 2893–2902.
Collins, P.L., Crowe, J.E.J., 2007. Respiratory syncytial virus and metapneumovirus. In: Knipe, D.M., Howley, P.M., Griffin, D.E., Lamb, R.A., Martin, M.A., Roizman, B., Straus, S.E. (Eds.), Field Virology. , 5th ed. Lippincott Williams & Wilkins, Philadelphia, PA, pp. 1601–1646.
Collins, P.L., Graham, B.S., 2008. Viral and host factors in human respiratory syncytial virus pathogenesis. J. Virol. 82 (5), 2040–2055.
Collins, P.L., Mottet, G., 1993. Membrane orientation and oligomerization of the small hydrophobic protein of human respiratory syncytial virus. J. Gen. Virol. 74 (Pt 7), 1445–1450.
Collins, P.L., Olmsted, R.A., Johnson, P.R., 1990. The small hydrophobic protein of human respiratory syncytial virus: comparison between antigenic subgroups A and B. J. Gen. Virol. 71 (Pt 7), 1571–1576.
de Graaf, M., Schrauwen, E.J., Herfst, S., van Amerongen, G., Osterhaus, A.D., Fouchier, R.A., 2009. Fusion protein is the main determinant of metapneumovirus host tropism. J. Gen. Virol..
Dultz, E., Hildenbeutel, M., Martoglio, B., Hochman, J., Dobberstein, B., Kapp, K., 2008. The signal peptide of the mouse mammary tumor virus Rem protein is released from the endoplasmic reticulum membrane and accumulates in nucleoli. J. Biol. Chem. 283 (15), 9966–9976.
Easton, A.J., Domachowske, J.B., Rosenberg, H.F., 2004. Animal pneumoviruses: molecular genetics and pathogenesis. Clin. Microbiol. Rev. 17 (2), 390–412.
Emanuelsson, O., Brunak, S., von Heijne, G., Nielsen, H., 2007. Locating proteins in the cell using TargetP, SignalP and related tools. Nat. Protoc. 2 (4), 953–971.
Froeschke, M., Basler, M., Groettrup, M., Dobberstein, B., 2003. Long-lived signal peptide of lymphocytic choriomeningitis virus glycoprotein pGP-C. J. Biol. Chem. 278 (43), 41914–41920.
Fuentes, S., Tran, K.C., Luthra, P., Teng, M.N., He, B., 2007. Function of the respiratory syncytial virus small hydrophobic protein. J. Virol. 81 (15), 8361–8366.
Fujiwara, T., Oda, K., Yokota, S., Takatsuki, A., Ikehara, Y., 1988. Brefeldin A causes disassembly of the Golgi complex and accumulation of secretory proteins in the endoplasmic reticulum. J. Biol. Chem. 263 (34), 18545–18552.
Govindarajan, D., Buchholz, U.J., Samal, S.K., 2006. Recovery of avian metapneumovirus subgroup C from cDNA: cross-recognition of avian and human metapneumovirus support proteins. J. Virol. 80 (12), 5790–5797.
Govindarajan, D., Samal, S.K., 2005. Analysis of the complete genome sequence of avian metapneumovirus subgroup C indicates that it possesses the longest genome among metapneumoviruses. Virus Genes 30 (3), 331–333.
Griffin, S., Clarke, D., McCormick, C., Rowlands, D., Harris, M., 2005. Signal peptide cleavage and internal targeting signals direct the hepatitis C virus p7 protein to distinct intracellular membranes. J. Virol. 79 (24), 15525–15536.
He, B., Lin, G.Y., Durbin, J.E., Durbin, R.K., Lamb, R.A., 2001. The SH integral membrane protein of the paramyxovirus simian virus 5 is required to block apoptosis in MDBK cells. J. Virol. 75 (9), 4068–4079.
Hemerka, J.N., Wang, D., Weng, Y., Lu, W., Kaushik, R.S., Jin, J., Harmon, A.F., Li, F., 2009. Detection and characterization of influenza A virus PA-PB2 interaction through a bimolecular fluorescence complementation assay. J. Virol. 83 (8), 3944–3955.
Herfst, S., Mas, V., Ver, L.S., Wierda, R.J., Osterhaus, A.D., Fouchier, R.A., Melero, J.A., 2008. Low-pH-induced membrane fusion mediated by human metapneumovirus F protein is a rare, strain-dependent phenomenon. J. Virol. 82 (17), 8891–8895.
Hiebert, S.W., Richardson, C.D., Lamb, R.A., 1988. Cell surface expression and orientation in membranes of the 44-amino-acid SH protein of simian virus 5. J. Virol. 62 (7), 2347–2357.
Holden, P., Keene, D.R., Lunstrum, G.P., Bachinger, H.P., Horton, W.A., 2005. Secretion of cartilage oligomeric matrix protein is affected by the signal peptide. J. Biol. Chem. 280 (17), 17172–17179.
Ichinohe, T., Pang, I.K., Iwasaki, A., 2010. Influenza virus activates inflammasomes via its intracellular M2 ion channel. Nat. Immunol. 11 (5), 404–410.
Ling, R., Sinkovic, S., Toquin, D., Guionie, O., Eterradossi, N., Easton, A.J., 2008. Deletion of the SH gene from avian metapneumovirus has a greater impact on virus production and immunogenicity in turkeys than deletion of the G gene or M2-2 open reading frame. J. Gen. Virol. 89 (Pt 2), 525–533.
Liu, Y., Haas, D.L., Poore, S., Isakovic, S., Gahan, M., Mahalingam, S., Fu, Z.F., Tripp, R.A., 2009. Human metapneumovirus establishes persistent infection in the lungs of mice and is reactivated by glucocorticoid treatment. J. Virol. 83 (13), 6837–6848.
Lundin, M., Monne, M., Widell, A., Von Heijne, G., Persson, M.A., 2003. Topology of the membrane-associated hepatitis C virus protein NS4B. J. Virol. 77 (9), 5428–5438.
Moffat, K., Knox, C., Howell, G., Clark, S.J., Yang, H., Belsham, G.J., Ryan, M., Wileman, T., 2007. Inhibition of the secretory pathway by foot-and-mouth disease virus 2BC protein is reproduced by coexpression of 2B with 2C, and the site of inhibition is determined by the subcellular location of 2C. J. Virol. 81 (3), 1129–1139.
Naylor, C.J., Brown, P.A., Edworthy, N., Ling, R., Jones, R.C., Savage, C.E., Easton, A.J., 2004. Development of a reverse-genetics system for Avian pneumovirus demonstrates that the small hydrophobic (SH) and attachment (G) genes are not essential for virus viability. J. Gen. Virol. 85 (Pt 11), 3219–3227.
Naylor, C.J., Ling, R., Edworthy, N., Savage, C.E., Easton, A.J., 2007. Avian metapneumovirus SH gene end and G protein mutations influence the level of protection of live-vaccine candidates. J. Gen. Virol. 88 (Pt 6), 1767–1775.
Njenga, M.K., Lwamba, H.M., Seal, B.S., 2003. Metapneumoviruses in birds and humans. Virus Res. 91 (2), 163–169.
Olmsted, R.A., Collins, P.L., 1989. The 1A protein of respiratory syncytial virus is an integral membrane protein present as multiple, structurally distinct species. J. Virol. 63 (5), 2019–2029.
Rixon, H.W., Brown, G., Aitken, J., McDonald, T., Graham, S., Sugrue, R.J., 2004. The small hydrophobic (SH) protein accumulates within lipid-raft structures of the Golgi complex during respiratory syncytial virus infection. J. Gen. Virol. 85 (Pt 5), 1153–1165.
Schowalter, R.M., Chang, A., Robach, J.G., Buchholz, U.J., Dutch, R.E., 2009. Low-pH triggering of human metapneumovirus fusion: essential residues and importance in entry. J. Virol. 83 (3), 1511–1522.
Schowalter, R.M., Smith, S.E., Dutch, R.E., 2006. Characterization of human metapneumovirus F protein-promoted membrane fusion: critical roles for proteolytic processing and low pH. J. Virol. 80 (22), 10931–10941.
Schrempf, S., Froeschke, M., Giroglou, T., von Laer, D., Dobberstein, B., 2007. Signal peptide requirements for lymphocytic choriomeningitis virus glycoprotein C maturation and virus infectivity. J. Virol. 81 (22), 12515–12524.
Toquin, D., de Boisseson, C., Beven, V., Senne, D.A., Eterradossi, N., 2003. Subgroup C avian metapneumovirus (MPV) and the recently isolated human MPV exhibit a common organization but have extensive sequence divergence in their putative SH and G genes. J. Gen. Virol. 84 (Pt 8), 2169–2178.
Toquin, D., Guionie, O., Jestin, V., Zwingelstein, F., Allee, C., Eterradossi, N., 2006. European and American subgroup C isolates of avian metapneumovirus belong to different genetic lineages. Virus Genes 32 (1), 97–103.
van den Hoogen, B.G., Bestebroer, T.M., Osterhaus, A.D., Fouchier, R.A., 2002. Analysis of the genomic sequence of a human metapneumovirus. Virology 295 (1), 119–132.
van den Hoogen, B.G., de Jong, J.C., Groen, J., Kuiken, T., de Groot, R., Fouchier, R.A., Osterhaus, A.D., 2001. A newly discovered human pneumovirus isolated from young children with respiratory tract disease. Nat. Med. 7 (6), 719–724.
Velayudhan, B.T., McComb, B., Bennett, R.S., Lopes, V.C., Shaw, D., Halvorson, D.A., Nagaraja, K.V., 2005. Emergence of a virulent type C avian metapneumovirus in turkeys in Minnesota. Avian Dis. 49 (4), 520–526.
Velayudhan, B.T., Noll, S.L., Thachil, A.J., Halvorson, D.A., Shaw, D.P., Goyal, S.M., Nagaraja, K.V., 2008. Comparative pathogenicity of early and recent isolates of avian metapneumovirus subtype C in turkeys. Can. J. Vet. Res. 72 (4), 371–375.
Wang, D., Harmon, A., Jin, J., Francis, D.H., Christopher-Hennings, J., Nelson, E., Montelaro, R.C., Li, F., 2010. The lack of an inherent membrane targeting signal is responsible for the failure of the matrix (M1) protein of influenza A virus to bud into virus-like-particles. J. Virol..
Yu, Q., Estevez, C., Song, M., Kapczynski, D., Zsak, L., 2010. Generation and biological assessment of recombinant avian metapneumovirus subgroup C (aMPV-C) viruses containing different length of the G gene. Virus Res. 147 (2), 182–188.

Veterinary Pathology
48(2) 349-360
© The American College of
Veterinary Pathologists 2011
Reprints and permission:
sagepub.com/journalsPermissions.nav
DOI: 10.1177/0300985810375806
http://vet.sagepub.com

Clinicopathological Characterization in Poultry of Three Strains of Newcastle Disease Virus Isolated From Recent Outbreaks

L. Susta[1], P. J. Miller[2], C. L. Afonso[2], and C. C. Brown[1]

Abstract

Newcastle disease is a severe threat to the poultry industry and is caused by Newcastle disease virus, a member of the genus *Avulavirus*, family Paramyxoviridae. The virus is rapidly evolving, and several new genotypes have been discovered in the past few years. Characterization of these strains is important to evaluate field changes, anticipate new outbreaks, and develop adequate control measures. Three Newcastle disease isolates (APMV-1/duck/Vietnam, Long Bien/78/2002, APMV-1/chicken/Australia/9809-19-1107/1998, and APMV-1/double-crested cormorant/USA, Nevada/19529-04/2005) from recent outbreaks were investigated via clinicopathological assessment, immunohistochemistry (IHC), in situ hybridization, virus isolation, and serology in experimentally infected 4-week-old chickens. Phylogenetic studies showed that Australia isolate belongs to class II genotype I, Long Bien to class II genotype VIId, and Nevada cormorant to class II genotype V. Even though all 3 viruses had a virulent fusion protein cleavage site and ICPI values greater than 1.5, they all differed in their ability to cause clinical signs, in their lesions, and in their viral distribution in body tissues. The Long Bien isolate showed the most severe clinicopathological picture and the most widespread viral distribution. The Australia and Nevada cormorant isolates had a milder pathological phenotype, with viral replication restricted to only a few organs. The variability in clinicopathological characteristics despite the similarity in ICPI suggests that full clinicopathological assessment is necessary to fully characterize new isolates and that there are differences in pathogenesis among viruses of different genotypes.

Keywords

avian paramyxovirus 1, Newcastle disease virus, chickens, pathogenesis, immunohistochemistry, in situ hybridization

Newcastle disease virus (NDV), synonymous with avian paramyxovirus-1 (APMV-1), is the causative agent of Newcastle disease (ND), an infection that threatens poultry worldwide.[1-3] The poultry industry loses millions of dollars annually from morbidity, mortality, and trade losses due to ND.[3] NDV belongs to the Mononegavirales order, Paramyxoviridae family, Paramyxovirinae subfamily, and *Avulavirus* genus. The genome is negative sense RNA of approximately 15,200 bases, and it contains 6 genes that encode an equal number of structural proteins, which are from 3′ to 5′: nucleoprotein (NP), phosphoprotein (P), matrix (M), fusion (F), hemagglutinin–neuraminidase (HN), and polymerase (L). Although all ND viruses belong to a single serotype, APMV-1 serotype, isolates differ in virulence in poultry, which translates into a wide range of clinical signs, often making it challenging to recognize NDV as the cause of the clinical problem in the field.[1] Historically, strains were classified according to the time to death after inoculation of embryonating eggs, with those strains that caused death the fastest (and therefore more virulent) termed *velogens* and those in which the embryos survived for much longer periods of time termed *lentogens*. Those strains falling in between were called *mesogens*.[1,31] Today, classification of the different strains is carried out by 2 internationally recognized methods. The intracerebral pathogenicity index (ICPI) involves inoculating 1-day-old chicks intracerebrally and scoring birds as normal, sick, or dead over a period of 8 days, to result in a score from 0.0 to 2.0. Those strains scoring greater than 0.7 are considered "notifiable" to the international community through the World Organization for Animal Health, and any strain with a score greater than 1.5 is considered a velogen.[2,31] The second internationally recognized test is to sequence the F protein cleavage site to evaluate the presence of multiple basic amino acids and

[1] Department of Veterinary Pathology, College of Veterinary Medicine, University of Georgia, Athens, Georgia, USA
[2] Southeast Poultry Research Laboratory, Agricultural Research Service, United States Department of Agriculture, Athens, Georgia, USA

Corresponding Author:
Corrie Brown, Department of Veterinary Pathology, CVM, UGA, Athens, GA 30602-7388
Email: corbrown@uga.edu

Downloaded from vet.sagepub.com at UNIV OF GEORGIA LIBRARY on March 10, 2011

phenylalanine, which is considered an indication of virulence and therefore notifiable.[11,29]

Outbreaks of ND are reported frequently from many parts of the world, with the most severe disease being caused by virulent strains. The USA is considered free of virulent NDV strains, but occasionally pathogenic strains enter through wild birds or informal (illegal) trade. The last outbreak of ND occurred in California in 2002–2003 and resulted in depopulation of more than 3 million birds and containment costs exceeding US$160 million.[37]

There is some correlation between viral virulence and phylogenetic analysis of virus evolution. According to phylogenetic distances, often carried out on the sequence of the F gene, NDV isolates are divided in 2 classes (I and II), and class II is further divided into 9 genotypes.[26,27] Comparison of phylogenetic analysis with biological characteristics of the NDV isolates demonstrates that viruses of class I are mainly composed of avirulent strains, usually circulating among wild birds, whereas viruses of class II are more frequently virulent[8,26] and mainly isolated from poultry. Within class II, most outbreaks worldwide are caused by viruses of genotypes V, VI, and VII, even though occasional outbreaks caused by viruses from other genotypes do occur. Particularly important are viruses of genotype VIId, which lately have caused several outbreaks in China, Vietnam, Indonesia, Pakistan, and Africa.[17,27,28]

NDV is a continuously evolving virus with evidence of accelerated evolution of the virulent strains,[26] and there are reports of increased pathogenicity, outbreaks in vaccinated animals, and increased host range.[15,25,26,28,30,38] Therefore, it is important to conduct clinicopathological characterization of new strains that are isolated during the course of outbreaks worldwide to determine how the viruses are changing. Full characterization of the clinical disease and pathogenesis in poultry could also affect the diagnostic aspects of the disease and implementation of control measures. Characterization of the genomic sequences, genotyping of the new isolates, and identification of their nearest ancestors could help identify the source of new outbreaks.

In this study, 3 different strains of NDV from recent outbreaks were characterized through sequencing, phylogenetic analysis, ICPI, and clinicopathological assessment. The latter was performed by inoculating 4-week-old chickens via a natural route (eye drop instillation). The resulting disease was characterized through virus isolation (VI), serology, and clinicopathological observations, including histology, immunohistochemistry (IHC), and in situ hybridization in multiple body tissues.

The first virus, APMV-1/duck/Vietnam, Long Bien/78/2002, in this article referred as *Long Bien*, was initially isolated from ducks in a Vietnam market during 2002. The second virus, APMV-1/chicken/Australia/9809-19-1107/1998, here referred to as *Australia*, was isolated during a large outbreak in Australia that occurred from 1998 to 2000. This virus and other isolates from this same outbreak were unusual in that they are the only known virulent representatives of class II, genotype I. There is evidence[12,17,39] that the origin of these viruses can be traced back to low-virulence NDV circulating in waterfowl just prior to the outbreak. The third virus, APMV-1/double-crested cormorant/USA, Nevada/19529-04/2005, and here referred as *Nevada cormorant*, is an isolate responsible for significant morbidity and mortality in cormorants in the state of Nevada in 2005 and in other US states in 2008.[36]

Methods

Viruses

APMV-1/duck/Vietnam, Long Bien /78/2002 (Long Bien), APMV-1/chicken/Australia/9809-19-1107/1998 (Australia), and APMV-1/double-crested cormorant/USA, Nevada/19529-04/2005 (Nevada cormorant) were obtained from the Southeast Poultry Research Laboratory (SEPRL) NDV repository. Each virus was propagated by 1 passage in 9- to 10-day-old embryonated chicken eggs inoculated by the chorioallantoic route.

Eggs and Chickens

The source of embryonating chicken eggs and chickens was the SEPRL SPF White Leghorn flock. Birds were housed in negative pressure isolators under biosafety level-3–enhanced conditions at SEPRL and were provided food and water ad libitum.

Intracerebral Pathogenicity Index Test

To characterize the viruses, ICPI was performed using standard protocols.[2] Briefly, chickens were inoculated at 1 day of age with 0.1 ml of a 1:10 dilution of infective allantoic fluid. Chicks were monitored daily and scored as normal, sick or paralyzed, and dead to compile a score for the 8-day observation period.[2]

Clinicopathological Assessment in Chickens

Three groups of ten 4-week-old SPF White Leghorn chickens were inoculated bilaterally in the conjunctival sac with 0.1 ml of viral inoculum. Phosphate-buffered saline was used for the noninfected control birds. The target dose of inoculum was $10^{5.0}$ 50% embryo infectious doses (EID_{50}). The actual infectious doses as determined by back titration in embryonating chicken eggs were $10^{5.5}$ EID_{50} for Long Bien, $10^{4.5}$ EID_{50} for Australia, and $10^{5.3}$ EID_{50} for Nevada cormorant. The birds were monitored clinically every day, and 2 birds of each group were euthanatized after taking oropharyngeal and cloacal swabs at 2, 5, 10, and 14 days post inoculation (dpi). Birds whose condition became critical were euthanatized regardless of the scheduled sampling day.

Blood samples for serology were collected at 10 and 14 dpi. Tissues (eyelid, spleen, bursa of Fabricius, thymus, Harderian gland, proventriculus, small intestine, cecal tonsils, large intestine, air sac, trachea, lung, heart, esophagus, pharynx, crop, brain, liver, pancreas, kidney, comb, head of left femur including bone marrow, and nasal turbinate) were collected and fixed by immersion in 10% neutral buffered formalin for

Downloaded from vet.sagepub.com at UNIV OF GEORGIA LIBRARY on March 10, 2011

approximately 52 hours. The sections of femur and turbinate were decalcified in 5% formic acid for 3–4 hours. All sampled tissues were routinely processed into paraffin, and 3-μm sections were cut for hematoxylin and eosin staining, IHC, and in situ hybridization (ISH).

Immunohistochemistry

All sampled tissues were examined by IHC to detect viral nucleoprotein. Briefly, after deparaffinization, tissue sections were subjected to antigen retrieval by microwaving for 20 minutes at minimum power in Vector antigen unmasking solution (Vector Laboratories, Burlingame, CA) followed by application of universal blocking reagent (Biogenex, San Ramon, CA) as recommended by the manufacturer. The primary antibody, made in rabbit, was raised against a synthetic nucleoprotein peptide (TAYETADESETRRIC) and used at 1:8000 dilution. The detection system was an alkaline phosphatase–labeled polymer specific for the Fc portion of rabbit immunoglobulin (LabVision, Fremont, CA). Chromogen was a naphthol-based dye (Fast Red, Dako, Carpinteria, CA). Sections were counterstained lightly with hematoxylin and cover-slipped with Permount for a permanent record.

In Situ Hybridization

Selected tissue sections from the NDV-infected birds were probed with a negative-sense digoxigenin-labeled 850 base riboprobe representing the 5′ end of the matrix gene of the NDV Fontana (CA1083) as previously described.[7] The matrix gene from the Fontana strain was cloned into pCRII transcription vector (Invitrogen, Carlsbad, CA), and anti-sense riboprobes were generated using RNA polymerase in the presence of labeled nucleotides. This probe was used for hybridization with all the 3 strains in this study, because sequence information indicated a very high grade of identity (Long Bien 92%; Nevada cormorant 89%; Australia 88%) with the probed strains (NCBI accession no. AY562988).

For hybridization, sections from selected blocks were deparaffinized, rehydrated, digested with 100 μg/ml proteinase K for 15 minutes, and hybridized overnight at 42°C with approximately 20 ng of probe in standard sodium citrate, 50% formamide, 5% blocking reagent (Boehringer Mannheim, Indianapolis, IN), 1% *N*-lauroylsarcosine, and 0.02% sodium dodecyl sulfate. Following stringent washes, bound probes were visualized by the addition of anti-digoxigenin alkaline phosphatase and the chromogen/substrate nitroblue tetrazolium and 5-bromo-4-chloro-3-indolylphosphate.

Virus Isolation and Titration of Swabs

For those birds used in the clinicopathological assessment experiment, oral and cloacal swabs were obtained from each bird immediately prior to euthanasia and placed in separate tubes containing 1.5 ml of brain–heart infusion broth (BHI) with antibiotics (2000 U of penicillin G/ml, 200 μg of gentamicin sulfate/ml, and 4 μg of amphotericin B/ml; Sigma Chemical Co., St. Louis, MO). Swab sample tubes were centrifuged at 1000 × *g* for 20 minutes, and the supernatant was removed for virus isolation and titration. Virus infectivity titers were calculated from the result of inoculation of 9- to 10-day old SPF embryonating chicken eggs with serial 10-fold dilutions in BHI containing antibiotics (100 U of penicillin G/ml and 50 μg of gentamicin sulfate/ml). NDV in infected dead or surviving embryos was identified by hemagglutination (HA) activity in amnio-allantoic fluid harvested from chilled eggs. NDV was confirmed in HA-positive samples by hemagglutination inhibition (HI) test with NDV-specific antiserum.

Serology

The HA and HI tests were conducted by conventional microtiter methods with serum separated from the blood samples taken at day 10 and 14 dpi. Four HA units per 25 μ1 of β-propiolactone-inactivated NDV LaSota was used as test antigen in completing the HI test.

RNA Isolation, Polymerase Chain Reaction Amplification, and Sequencing

RNA was extracted from allantoic fluids using Trizol LS (Invitrogen, Carlsbad, CA) according to manufacturer's instructions. Briefly, 750 μl of Trizol LS reagent was added to 250 μl of allantoic fluid, vortexed, and incubated at room temperature for 7 minutes. The RNA was separated into the aqueous phase with the addition of 200 μl of chloroform, precipitated with isopropanol, and then centrifuged to pellet the RNA. After 1 wash with 70% ethanol, RNA was dried and resuspended in RNase-free water. Polymerase chain reaction (PCR) amplification of the RNA was performed using the Qiagen One Step reverse transcription (RT)–PCR kit (Qiagen, Valencia, CA). Amplified products were separated on a 1% agarose gel, the bands excised and eluted using the QIAquick Gel extraction kit (Qiagen), and the samples quantified using a standard spectrophotometer. All sequencing reactions were performed with fluorescent dideoxynucleotide terminators in an automated sequencer (ABI 3700 automated sequencer; Applied Biosystems Inc., Foster City, CA). Nucleotide sequence editing and analyses were conducted with the LaserGene sequence analysis software package (LaserGene, version 5.07; DNAStar, Inc., Madison, WI) using the full-length genome positions from the NDV LaSota vaccine strain complete genome. The regions sequenced were a 374 base pair partial F gene (positions 4554–4917), and the complete coding region for the F gene (positions 4544–6205), as previously described.[18] All RNA and DNA procedures were performed in biological safety cabinets, and standard anticontamination protocols were followed and RNase-free reagents used at all times to minimize contamination.

Sequence Alignment and Tree Construction

The coding sequence of 51 NDV full fusion genes were aligned using ClustalW as implemented in the BioEdit Sequence

Downloaded from vet.sagepub.com at UNIV OF GEORGIA LIBRARY on March 10, 2011

Alignment Editor (http://www.mbio.ncsu.edu/BioEdit/bioedit.html) and edited manually based on the amino acid sequence. Maximum likelihood (ML) phylogenetic analysis with bootstrap values for n = 100 replicates was performed using PHYML 2.4.4 software and using the general time reversible 7 model of nucleotide substitutions, ML estimates of base frequencies, estimated transition/transversion ratio, proportions of invariable sites with 4 categories of substitution rates estimated γ-shape parameter 1.136, and estimated proportion of invariant sites 0.292.[13]

Results

Pathogenicity Index—ICPI

The ICPI values were 1.88 for Long Bien, 1.88 for Australia, and 1.53 for Nevada cormorant. Therefore, all the viruses could be considered velogens according to OIE standards and notifiable to the international community.[2,31]

Clinical Disease, Virus Isolation, and Serology

Results for observed clinical signs are presented in Table 1. Results for virus isolation are presented in Table 2. For all 3 strains, all infected birds with the 3 strains developed clinical disease, and virus was successfully isolated from at least 1 oral and cloacal sample from all 3 groups of animals. Birds inoculated with the Long Bien isolate had severe illness, characterized by marked depression, reluctance to move, and high mortality, with all of the birds dying or being euthanatized by 3 dpi. Two birds inoculated with the Australia isolate showed depression and open-mouth breathing between days 3 and 5. Mild neurological signs, such as head tremors and twitch, were noted in this group between 4 and 9 dpi, but all became clinically normal by 10 dpi. Birds inoculated with the Nevada cormorant isolate had marked neurological signs by 4 dpi consisting of head tremors, twitching, recumbency, and paralysis; by 10 dpi all these animals were euthanatized with severe neurologic signs.

NDV was isolated from all the birds inoculated with Long Bien and Australia isolates starting from 2 dpi. In the group inoculated with Nevada cormorant virus, at 2 dpi NDV was isolated only from 1 bird, whereas all the sampled birds were positive by 5 dpi. By day 10, virus isolation was positive (Australia and Nevada cormorant isolates only, because all Long Bien birds were dead by this time) but at very low titers and only for the cloacal swabs. Seroconversion ($\geq$:128) occurred in birds infected with Australia and Nevada cormorant isolates at 10 dpi (data not shown). Serology was not performed on animals infected with Long Bien because they were all euthanatized by day 3.

Pathology

Gross findings are presented in Table 1. The most striking findings were in birds inoculated with the Long Bien isolate. By 2 dpi, the birds had severe edema and petechial hemorrhages of the eyelid and mottled spleens. On day 3, the spleens were uniformly enlarged and had multifocal to coalescing white stippling (necrosis), both on the surface and in cut section (Fig. 1). Other lesions were thymic hemorrhages, proventricular hemorrhages, multiple foci of necrosis in the small intestine (Fig. 2), and edema, necrosis, and hemorrhage of the cecal tonsils.

The birds infected with the Australia isolate had minimal to moderate petechiation of eyelids and moderately enlarged spleens by days 2 and 3. At days 5 and 6, the spleens were enlarged, and proventricular hemorrhages were present in 2 birds.

The birds infected with the Nevada cormorant isolate had minimal gross lesions. There was mild conjunctivitis by 2 dpi, moderately congested and mottled spleen at 5 dpi, and moderate thymic atrophy in 1 bird at day 9. There were no abnormal gross findings in the noninfected control birds.

Histology

Histological as well as IHC findings are presented in Table 3. The most severe lesions were observed in birds infected with the Long Bien isolate, starting at day 2 and culminating at day 3. These lesions were mainly confined to the site of inoculation (eyelid), the lymphoid organs (spleen, thymus, bursa), or the lymphoid aggregates of the intestines (cecal tonsils and other gut-associated lymphoid tissue). In the eyelid, the lesions were characterized by severe edema, hemorrhage, multifocal areas of necrosis associated with fibrin exudation, and pleomorphic inflammatory infiltrate, mainly composed of heterophiles and macrophages. In the lymphoid organs (thymus, bursa, spleen, and intestinal lymphoid patches, especially cecal tonsils), lesions consisted of severe necrosis, marked lymphocyte depletion, infiltration of numerous macrophages, and moderate heterophilic infiltrate. In the intestines, the severe necrosis of the lymphoid-dependent areas was associated with focal to locally extensive ulceration of the epithelium and accumulation of necrotic material within the intestinal lumen. Multifocal areas of necrosis were observed within the pancreas. By 3 dpi, at the level of the physis and metaphysis, especially in the areas beneath the articular cartilage, there were multifocal areas of bone marrow necrosis.

In birds infected with the Australia strain, similar lesions were observed within the eyelid and lymphoid organs, but these were much less intense than those with Long Bien and reached their peak at 4 dpi. The most severe lesions were in the bursa and cecal tonsils and consisted mainly of necrosis, lymphocyte depletion, and accumulation of macrophages. The heart, at 5 and 6 dpi, had multifocal myonecrosis with accumulation of macrophages. At day 10, there was moderate nonsuppurative encephalitis, consisting of multifocal areas of lymphoplasmacytic perivascular cuffing.

Birds infected with the Nevada cormorant isolate had minimal lesions within the lymphoid tissues but showed severe nonsuppurative encephalitis and moderate myocarditis. The encephalitis was confined between day 5 and 10 and was

Downloaded from vet.sagepub.com at UNIV OF GEORGIA LIBRARY on March 10, 2011

Table 1. Clinical and Pathological Findings of Chickens Infected With Newcastle Disease Virus Strains

Strain inoculated	2 dpi		3 dpi		4 dpi		5 dpi		6 dpi		10 dpi	
	Clinical	Pathological	Clinical	Pathological	Clinical	Pathological	Clinical	Pathological	Clinical	Pathological	Clinical	Pathological
PBS	Normal	Normal	Normal	Normal	Normal	Normal	Normal	Normal	Normal	Normal	Normal	Normal
Long Bien	Depression, severe conjunctivitis	Eyelids, Ed (2/2)[a]; spleen, Nec (2/2); cecal tonsils, Ed (1/2)	Severe depression; conjunctivitis; 1 spontaneously dead bird	Eyelid, Ed+Hem; spleen, Nec proventriculus, Hem; intestine, Hem+Nec (4/4)	All birds dead	—	—	—	—	—	—	—
Australia	Normal	Conjunctivitis (2/2)	Slight depression; 1 bird open-mouth breathing	Eyelid, Hem (1/2); spleen, Mot (1/2); cecal tonsils, Hem (1/2)	Depression; 1 bird very sick	Eyelid, Hem; intestine, Hem; kidney, Hem (1/1)	1 bird very sick with open-mouth breathing; another bird slightly depressed	Proventriculus and intestine, Hem (1/2); enlarged spleen (1/2)	1 bird severe depression; 2 with slight depression	Proventriculus and Intestine, Hem (1/1)	Recovered	No gross lesions
Nevada cormorant	Normal	Thymus, Hem (2/2); spleen, Mot (1/2)	Depression; slight conjunctivitis	Slight conjunctivitis	Depression; nervous signs; comb hemorrhages	No necropsy at this time	Depression; nervous signs	Spleen, Mot (4/4); eyelid, Hem (1/4)	2 depressed; 2 paralyzed	Cecal tonsils, Ed (1/2); spleen, Mot (1/2)	Paresis, recumbency, and depression; 1 head twitch	Thin and easily pliable femurs (2/2); thymic atrophy (1/2)

dpi, days post infection; Ed, edema; Hem, hemorrhage; Mot, mottled; Nec, necrosis; PBS, phosphate buffered saline.
[a] Numbers of birds showing lesions out of the total number of birds per group necropsied on that day.

Downloaded from vet.sagepub.com at UNIV OF GEORGIA LIBRARY on March 10, 2011

Table 2. Virus Isolation and Titration of Oral (O) and Cloacal (C) Swab Samples

	PBS		Nevada Cormorant(5.3)[a]		Australia(4.5)		Long Bien(5.5)	
dpi	O	C	O	C	O	C	O	C
2	–[b]	–[c]	$<10^{0.5}$(1/2)[d]	– (0/2)	$10^{0.7}$(1/2)	$10^{0.7}$(1/2)	$>10^{3.5}$(2/2)	$>10^{3.5}$(1/2); $10^{3.1}$(1/2)
3	nc	nc	nc	nc	$>10^{3.5}$(2/4)	$10^{0.9}$(1/2); $10^{1.7}$(1/2)	$>10^{3.5}$(4/4)	$>10^{3.5}$(4/4)
4	nc	nc	nc	nc	$>10^{3.5}$(1/1)	$>10^{3.5}$(1/1)	nc	nc
5	–	–	$10^{3.3}$(1/4)[e]; $10^{3.5}$(3/4)	$10^{1.9}$(1/4); $10^{3.1}$(1/4); $10^{1.5}$(1/4); $>10^{3.5}$(1/4)	$>10^{3.5}$(2/2)	$10^{2.9}$(1/2); $10^{2.7}$(1/2)	nc	nc
6	nc	nc	$10^{2.9}$(1/2); $10^{3.5}$(1/2)	$10^{1.5}$(1/2); $10^{0.5}$(1/2)	$10^{2.5}$(1/1)	$10^{1.7}$(1/1)	nc	nc
10	–	–	– (0/2)	$<10^{0.5}$(1/4)	– (0/2)	$10^{1.5}$(1/2)	nc	nc

dpi, days post inoculation; nc, not collected; PBS, phosphate buffered saline.
[a] Number in parentheses is the viral titer of inoculum per 0.1 ml.
[b] No virus recovered from undiluted swab fluids inoculated into 3 eggs, 0.2 ml per egg.
[c] Viral titer of swab sample per 0.1 ml.
[d] Low titer but positive.
[e] Number of birds displaying that value/total number of animals sampled.

characterized by perivascular accumulations of lymphocytes, macrophages, rare plasma cells, and hypertrophy of the endothelial cells (Fig. 3). The myocarditis was characterized by multifocal necrosis associated with moderate macrophage infiltration. One bird infected with Nevada cormorant at day 5 had severe laryngitis, with necrosis of the epithelial layer (ulceration), accumulation of fibrin, and infiltration with heterophiles and macrophages.

Immunohistochemistry

In the infected cells, the immunolabeling for NDV was intracytoplasmic and finely to coarsely granular. Long Bien–infected birds had the broadest viral distribution (23/25 different tissues were positive) and the most intense signal, starting from day 2 and culminating at day 3. The organs with the strongest signal were the eyelids, the lymphoid organs, and the mucosa-associated lymphoid aggregates in multiple organs (Fig. 4). In these tissues, the positive cells consisted mainly of lymphocytes and macrophages. In the spleen, the immunoreactivity was confined to the fixed-macrophage–dependent areas around the penicillary arteries, whereas the lymphocyte-dependent areas were devoid of signal. In the respiratory system, the positive signal was confined to the nasal and tracheal mucosa, scattered lymphoid aggregates closely associated with the secondary and tertiary bronchi (bronchus-associated lymphoid tissue), and the squamous epithelium of the atria, air capillaries, and air sacs. In the digestive tract, intense positivity for NDV was observed only within the submucosal lymphoid aggregates, and no staining was observed associated with the epithelial lining. Scattered Kupffer cells in the liver and several epithelial cells in the distal tubules of the kidneys had positive signal for NDV. In the bone marrow, numerous osteoclasts and mononuclear cells just beneath the growth plate or surrounding areas of necrosis showed intense immunolabeling (Fig. 5). In the heart, the staining was limited to the epicardium. Birds infected with the Australia isolate had a more limited viral distribution (15/25 positive tissues) and lesser amounts of signal even in the positive tissues when compared with Long Bien, but the pattern of staining and the type of infected cells was the same as described above. The viral distribution was mainly limited to the lymphoid organs and lymphoid aggregates and reached its peak at 5 dpi. In the intestines of these animals, immunolabeling was also present within the submucosal and myenteric plexuses in cells (Fig. 6) consistent with neurons and glial cells. Tissues from birds infected with the Nevada cormorant isolate had minimal signal for NDV, which was primarily confined to the portal of entry (eyelid), with the exception of moderate immunolabeling of scattered neurons within the brains of birds at day 6 and 10 dpi (Fig. 7).

In Situ Hybridization

In selected sections, the negative sense riboprobe for NDV matrix gene labeled the same structures and cells immunolabeled with IHC. The type of staining was cytoplasmic and evenly distributed (Figs. 8 and 9).

Sequencing and Phylogeny

Results of sequencing and phylogenetic trees are presented in Fig. 10. (Detailed correspondence between names used in the tree and NCBI accession numbers are available in the online supplement. To view the online supplement, please go to http://www.vet.sagepub.com/supplement.)

The Genome sequences of the viruses were submitted to Gene Bank under the following names:

APMV-1/duck/Vietnam, Long Bien/78/2002: **GU332646**
APMV-1/chicken/Australia/9809-19-1107/1998: **GU332645**
APMV-1/double-crested cormorant/USA, Nevada/19529-04/2005: **253317813**

Phylogenetic analysis with full fusion sequences for the 3 selected strains revealed that the Nevada cormorant isolate

Downloaded from vet.sagepub.com at UNIV OF GEORGIA LIBRARY on March 10, 2011

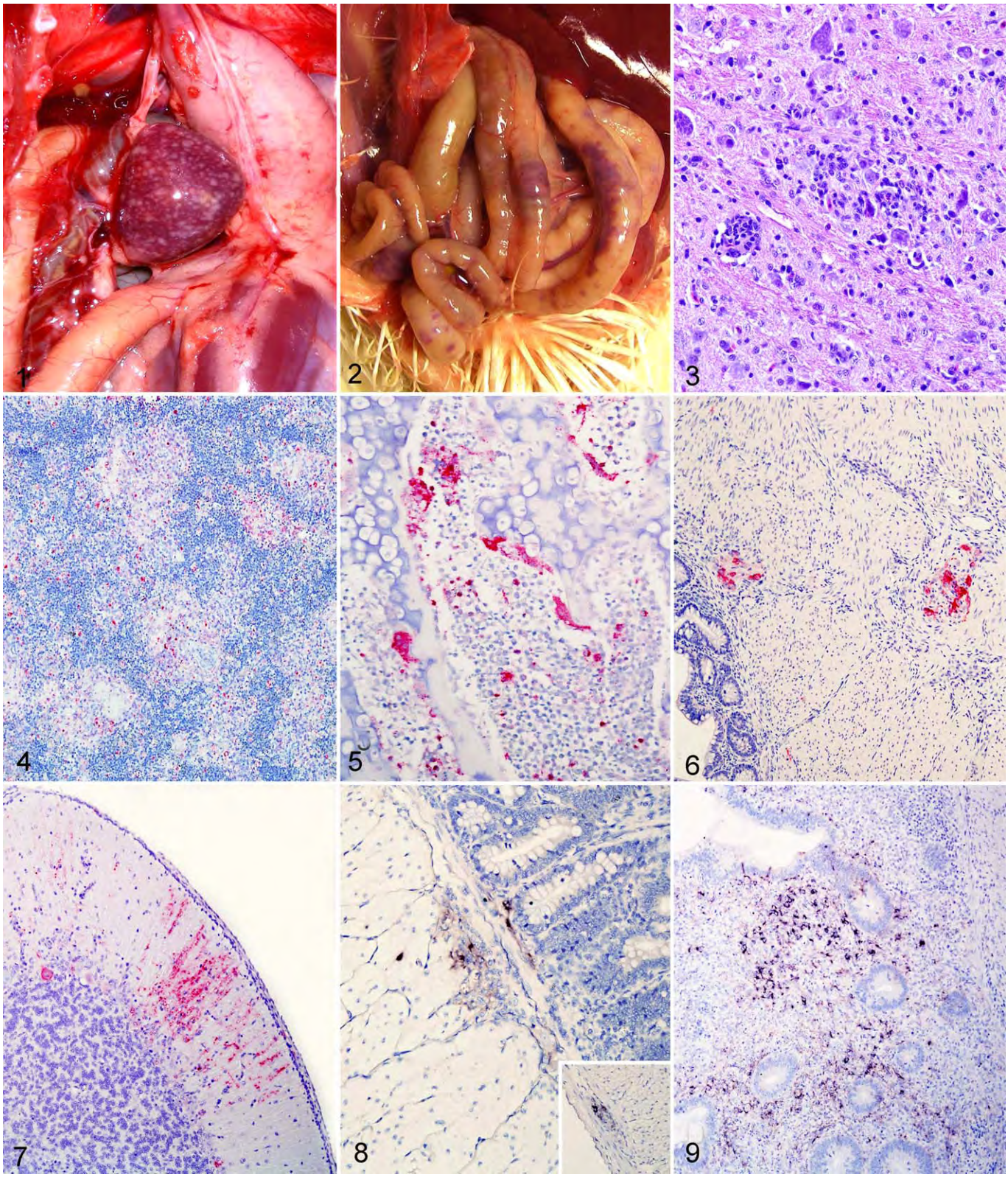

Figure 1. Spleen; chicken infected with Long Bien strain, 2 dpi. Enlarged and diffusely mottled spleen indicating necrosis. **Figure 2.** Small intestine; chicken infected with Long Bien strain, 3 dpi. Areas of hemorrhages and necrosis in the small intestine. **Figure 3.** Brain; chicken infected with Nevada cormorant strain, 5 dpi. Perivascular cuffs in the white matter, and focal area of gliosis. Hematoxylin and eosin. **Figure 4.** Spleen; chicken infected with Long Bien strain, 3 dpi. Extensive presence of viral antigen (red) within the histiocytes surrounding the penicillary arteries. Immunohistochemistry for Newcastle disease virus (NDV) antigen, alkaline phosphatase method, hematoxylin counterstain. **Figure 5.** Femur, physis; chicken infected with Long Bien strain, 3 dpi. Numerous osteoclasts and fewer mononuclear cells are strongly positive

Downloaded from vet.sagepub.com at UNIV OF GEORGIA LIBRARY on March 10, 2011

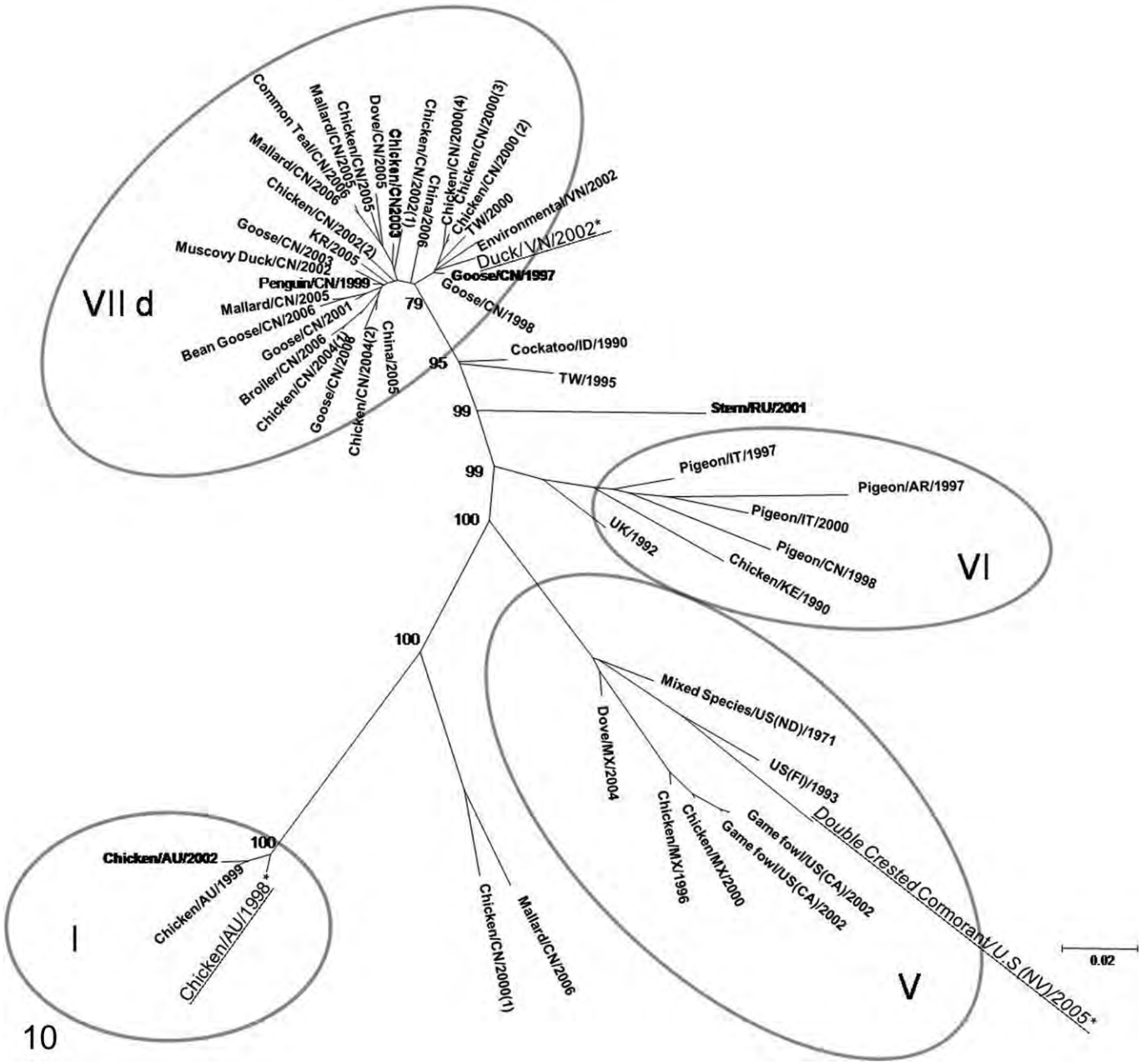

Figure 10. Evolutionary relationships of 3 selected NDV isolates in comparison to reference genotypes. The evolutionary history was inferred using the maximum likelihood method. The optimal tree with the sum of branch length is shown, and bootstrap values greater than 70 are included in the nodes. The tree is drawn to scale, with branch lengths in the same units as those of the evolutionary distances used to infer the phylogenetic tree. Correspondence between tree names and GenBank accession numbers are presented in Table 4 as online supplement. The name of the viruses described in the article are followed by an asterisk and underlined. Roman numbers within circles indicate the genotype.

Figure 5 continued. for NDV nucleoprotein. Immunohistochemistry for NDV, alkaline phosphatase method, hematoxylin counterstain. **Figure 6.** Intestine; chicken infected with Australia strain, 4 dpi. Immunohistochemistry (red) demonstrates viral protein within neurons in submucosal and myenteric plexuses. Immunohistochemistry for NDV, alkaline phosphatase method, hematoxylin counterstain. **Figure 7.** Cerebellum; chicken infected with Nevada cormorant strain, 6 dpi. NDV nucleoprotein (red) is present within the axons and the glial cells of the molecular layer and in few Purkinje cells. Immunohistochemistry, alkaline phosphatase method, hematoxylin counterstain. **Figure 8.** Intestine; chicken infected with Australia strain, 4 dpi. Riboprobe in situ hybridization (ISH) (brown) shows that the viral messenger RNA is present (therefore virus is replicating) in the submucosal and myenteric (inset) plexuses. 5-Bromo-4-chloro-3-indolylphosphate (NBT-BCIP), hematoxylin counterstain. **Figure 9.** Intestine; chicken infected with Australia strain, 5 dpi. ISH (brown) demonstrates intracytoplasmic presence of viral messenger RNA in macrophages of the cecal tonsils. NBT-BCIP, hematoxylin counterstain.

Downloaded from vet.sagepub.com at UNIV OF GEORGIA LIBRARY on March 10, 2011

Table 3. Distribution and Intensity of the Lesions[a] and Immunohistochemical[b] Staining for Newcastle Disease Virus Nucleoprotein

		Vietnam		Nevada Cormorant			Australia		
Organs		2 dpi	3 dpi	2 dpi	5–6 dpi[c]	9 dpi	2–3 dpi	4–6 dpi	10 dpi
Eyelid	HE	++	+++	+	+	+	+	++	–
	IHC	+++	+++++	–	+	–	+	++	–
Spleen	HE	++	++++	+	+	+	+	+	+
	IHC	+++	++++	–	–	–	+/–	++	–
Thymus	HE	++	+++	–	–	–	–	–	–
	IHC	+++	+++++	–	–	–	+	++	–
Bursa	HE	++	+++	–	–	–	–	++	–
	IHC	++	++++	–	–	–	–	+	–
Cecal tonsils	HE	++	+++	–	+	+	–	++	–
	IHC	++++	++++	–	–	–	+	++	–
Pancreas	HE	–	++	–	–	–	–	–	–
	IHC	–	++	–	–	–	–	–	–
Lung	HE	–	–	–	–	–	–	–	–
	IHC	+	++	–	–	–	–	+/–	–
Heart	HE	–	–	–	+	+	+	++	–
	IHC	–	++	–	–	–	–	+/–	–
Brain	HE	–	–	–	+++	+++	–	–	++
	IHC	–	–	–	+	+	–	–	–
Bone marrow	HE	–	+++	–	–	–	–	–	–
	IHC	+	+++	–	+/–	–	–	+	–

dpi, days post infection; HE, hematoxylin and eosin; IHC, immunohistochemisty.

[a] Spleen: +moderate hyperplasia of lymphocytes; ++ mild lymphocytic depletion; +++moderate (<50%) lymphocyte depletion, histiocytic accumulation and multifocal necrosis; ++++ (>50%) severe lymphocytic depletion, histiocytosis and necrosis. Thymus, cecal tonsil, GALT, bursa, and thymus: +mild lymphocytic depletion, ++ (<50%) moderate lymphocytic depletion with necrosis and histiocytosis, +++ (>50%) severe lymphocytic depletion, necrosis and histiocytosis. Bone marrow: mild + (<20%) bone marrow necrosis; ++ mild (20–50%) bone marrow necrosis; +++ severe (>50%) bone marrow necrosis. Pancreas: + mild (<3 areas) vacuolation and degeneration; ++ moderate (>3 areas) vacuolation and degeneration. Brain: + vascular reactivity; ++ vascular reactivity and perivascular cuffing; +++vascular reactivity, perivascular cuffing, gliosis.

[b] – = no IHC signal present. + = rare cells in the section are positive on IHC. ++ = positive cells seen, <50% of all high-power fields (HPF). +++ = positive signal seen in 50 to 75% of HPF. ++++ = abundant positive signal in >75% of HPF.

[c] Results shown from days on which tissues had most intense staining.

belongs to a new branch of genotype V that is clearly separated from other viruses that caused outbreaks in cormorant in 2008.[35] The Australia isolate belongs to genotype I viruses and groups with other contemporary Australian viruses. The Long Bien isolate falls within genotype VIId and is most closely related to isolates from China in 2000 from chickens and geese (Fig. 10). All 3 viruses, Australia, Long Bien, and Nevada cormorant, have a virulent fusion cleavage site motif.[31] The –R R K K R F– motif was present in Long Bien, –R R Q R R F– in the Australia isolate, and –R R Q K R F– in the Nevada cormorant virus.

Discussion

Although all 3 viruses were considered virulent, by both ICPI and fusion protein amino acid sequence, these strains showed differing clinicopathological pictures, both in severity and in distribution of the virus through various tissues of the body.

The Long Bien isolate belongs to genotype VIId, and to the authors' knowledge this is the first full clinicopathological characterization of an isolate belonging to this genotype. Clinicopathologically, the phenotype of Long Bien was similar to other previously described virulent NDV strains belonging to genotypes II, V, VI, and VIIa.[7,19-21,37] Long Bien strain caused severe disease, with birds succumbing rapidly after infection. By IHC, the viral tropism was mainly for lymphoid tissues, but viral protein was also very evident in the respiratory epithelium of trachea, lung, and air sacs and in the renal epithelium. Within the lymphoid tissues, and particularly in the spleen, the majority of the immunolabeled cells were morphologically compatible with macrophages, specifically those surrounding the penicillary arteries in the spleen. This tropism for cells belonging to the monocytes–macrophage series was supported by visualization of positive osteoclasts within the bone marrow, as these cells are derived from a subset of circulating monocytes.[6,40]

The Australia isolate, another velogen, had a less severe clinicopathological presentation. Lesions were milder, and viral distribution, as detected by IHC, was more limited. Lymphoid tissue appeared to be the primary target, but damage in these areas and associated IHC signal were much less than those seen with Long Bien. An unexpected finding was the presence of abundant viral nucleoprotein and ISH staining within the myenteric plexuses of the intestines, which was most notable at 5 dpi and was not associated with any inflammatory changes. The positive ISH signal using a negative riboprobe

Downloaded from vet.sagepub.com at UNIV OF GEORGIA LIBRARY on March 10, 2011

indicates that the virus is actively replicating in these cells, as the probe will bind only to positive sense RNA, which would be the replicative intermediate of the virus (which is negative sense) or the viral messenger RNA. Although some NDV strains are known for their ability to invade nervous tissue, it is usually the central nervous system that is affected, making this tropism for the peripheral nervous system unusual. Only 1 report in the literature, concerning an outbreak in Japan in vaccinated flocks, describes immunohistochemical staining of the intestinal nerves, but the genotype of the investigated virus was type VII, whereas the Australia virus is genotype I.[30]

The marked differences in the clinicopathological assessment between the 2 velogenic strains with the highest ICPI, Australia and Long Bien, is also mirrored by the phylogenetic distances. Genotype VIId (Long Bien) encompasses numerous markedly virulent strains that are currently circulating in southeast Asia, Africa, and the Middle East and have also been reported to have increased host range.[15,16,26,27,38] On the other hand, the Australia isolate belongs to genotype I, a clade that contains mainly nonvirulent strains that often circulate in wild birds and waterfowl. It has been known that on rare occasions these strains can mutate and become virulent. This has been demonstrated for the 1998–2000 NDV outbreaks in Australia (of which our strain is an isolate) and the 1997 outbreaks in Ireland. In these cases, the virulent isolate viruses have been traced back to previously circulating nonpathogenic strains that acquired virulence by mutation of the F protein cleavage site.[4,8,12] Even though both Australia and Long Bien strains had the same ICPI value (1.88) and a virulent F gene cleavage site, they displayed strikingly different clinicopathological syndromes when inoculated into 4-week-old birds. Long Bien behaved as a full-fledged VVND (Velogenic Viscerotropic Newcastle Disease), acting very similarly to other virulent strains even if genetically distant, whereas Australia had a much milder pathotype. The reason for this is unknown, but it might be linked to the fact that class I viruses are usually adapted to waterfowl and not usually to chickens.[12] In addition, it should be considered that the F gene is not the only determinant of virulence but that other genes may also be involved in the disease-inducing ability of NDV strains. For example, the HN protein has been shown to influence tissue tropism and to trigger apoptosis in vitro,[14,33] the P gene has been demonstrated to inhibit the interferon pathway through the production of the V protein,[32] and the L gene has been associated with virulence through RNA processing ability.[34] The work presented here confirms that neither ICPI nor fusion protein cleavage is sufficient to fully predict the outcome of virus infection in poultry.[9]

Phylogenetic analysis revealed that our third strain (Nevada cormorant) belongs to a distinct subgroup of genotype V recently isolated from cormorants.[35] Although the ICPI of this virus was 1.53, which makes this virus technically a velogen (>1.5),[2] and its fusion protein has a virulent cleavage sequence, Nevada cormorant isolate behaved similarly to many previously described mesogens of genotype V,[7] although the degree of neurologic involvement was more marked than what has been described.[7] Mesogens do not usually produce severe clinical signs in SPF chickens but can occasionally cause neurological signs.[1] The virus was detected by IHC only at the inoculation site (eyelid) and in the brain (only 4 birds). The presence of viral nucleoprotein and RNA, as revealed by IHC and in situ hybridization, was mainly in neurons of the cerebral cortex, the nuclei of the brainstem, and the cerebellum, thus accounting for the neurological signs. The involvement of the respiratory system was minimal. As described for the cormorants infected with NDV,[5,10,22-24] clinicopathological findings in the chickens involved mainly the nervous system, suggesting that the tropism and the behavior of the virus were similar in different hosts. The development of clinical disease in chickens inoculated with a strain rescued from wild birds (cormorant) underlines the important role that wild birds could have in the natural or accidental transmission of virulent strain to commercial flocks.

This article is the first to fully characterize through sequencing and clinicopathological observation the recently isolated strains Australia, Nevada cormorant, and Long Bien. The constant characterization of newly isolated strains that circulate within and outside the United States will allow for assessment of eventual variation in their pathogenicity for poultry species. Such information will be helpful in devising appropriate prevention and control measures. This study reinforces the concept that standard indices and sequence analysis of NDV isolates may not fully predict their pathogenicity in susceptible animals, therefore making animal experiments important tools for a complete characterization of new isolates.

Declaration of Conflicting Interests

The authors declared that they had no conflicts of interest with respect to their authorship or the publication of this article.

Financial Disclosure/Funding

The authors declared that they received no financial support for their research and/or authorship of this article.

References

1. Alexander DJ: Newcastle disease, other avian paramyxovirus, and pneumovirus infections. *In*: Diseases of Poultry, eds. Saif YM, Barnes HJ, Glisson JR, Fadly AM, McDougald LR, Swayne DE, 11th ed., pp. 541–569. Iowa State University Press, Ames, IA, 2003.
2. Alexander DJ: Newcastle disease. *In*: A Laboratory Manual for the Isolation and Identification of Avian Pathogens, eds. Swayne DE, Jackwood MW, Pearson JE, Reed WM, 4th ed., pp. 156–163. American Association of Avian Pathologists, Kennett Square, PA, 1998.
3. Alexander DJ: Gordon memorial lecture: Newcastle disease. Br Poult Sci **42:**5–22, 2001.
4. Alexander DJ, Banks J, Collins MS, Manvell RJ, Frost KM, Speidel EC, Aldous EW: Antigenic and genetic characterisation of Newcastle disease viruses isolated from outbreaks in domestic fowl and turkeys in Great Britain during 1997. Vet Rec **145:**417–421, 1999.

Downloaded from vet.sagepub.com at UNIV OF GEORGIA LIBRARY on March 10, 2011

5. Allison AB, Gottdenker NL, Stallknecht DE: Wintering of neurotropic velogenic Newcastle disease virus and West Nile virus in double-crested cormorants (Phalacrocorax auritus) from the Florida Keys. Avian Dis **49:**292–297, 2005.
6. Banks WJ: Musculoskeletal system. *In*: Applied Veterinary Histology, 3rd ed., pp. 113–114, St. Louis, MO: CV Mosby; 1993.
7. Brown C, King DJ, Seal BS: Pathogenesis of Newcastle disease in chickens experimentally infected with viruses of different virulence. Vet Pathol **36:**125–132, 1999.
8. Czegledi A, Ujvari D, Somogyi E, Wehmann E, Werner O, Lomniczi B: Third genome size category of avian paramyxovirus serotype 1 (Newcastle disease virus) and evolutionary implications. Virus Res **120:**36–48, 2006.
9. de Leeuw OS, Koch G, Hartog L, Ravenshorst N, Peeters BP: Virulence of Newcastle disease virus is determined by the cleavage site of the fusion protein and by both the stem region and globular head of the haemagglutinin-neuraminidase protein. J Gen Virol **86:**1759–1769, 2005.
10. Glaser LC, Barker IK, Weseloh DV, Ludwig J, Windingstad RM, Key DW, Bollinger TK: The 1992 epizootic of Newcastle disease in double-crested cormorants in North America. J Wildl Dis **35:**319–330, 1999.
11. Glickman RL, Syddall RJ, Iorio RM, Sheehan JP, Bratt MA: Quantitative basic residue requirements in the cleavage-activation site of the fusion glycoprotein as a determinant of virulence for Newcastle disease virus. J Virol **62:**354–356, 1988.
12. Gould AR, Kattenbelt JA, Selleck P, Hansson E, Della-Porta A, Westbury HA: Virulent Newcastle disease in Australia: molecular epidemiological analysis of viruses isolated prior to and during the outbreaks of 1998-2000. Virus Res **77:**51–60, 2001.
13. Guindon S, Gascuel O: A simple, fast, and accurate algorithm to estimate large phylogenies by maximum likelihood. Syst Biol **52:**696–704, 2003.
14. Huang Z, Panda A, Elankumaran S, Govindarajan D, Rockemann DD, Samal SK: The hemagglutinin-neuraminidase protein of Newcastle disease virus determines tropism and virulence. J Virol **78:**4176–4184, 2004.
15. Huang Y, Wan HQ, Liu HQ, Wu YT, Liu XF: Genomic sequence of an isolate of Newcastle disease virus isolated from an outbreak in geese: a novel six nucleotide insertion in the non-coding region of the nucleoprotein gene: brief report. Arch Virol **149:**1445–1457, 2004.
16. Jinding C, Ming L, Tao R, Chaoan X: A goose-sourced paramyxovirus isolated from southern China. Avian Dis **49:**170–173, 2005.
17. Kattenbelt JA, Stevens MP, Gould AR: Sequence variation in the Newcastle disease virus genome. Virus Res **116:**168–184, 2006.
18. Kim LM, King DJ, Curry PE, Suarez DL, Swayne DE, Stallknecht DE, Slemons RD, Pedersen JC, Senne DA, Winker K, Afonso CL: Phylogenetic diversity among low-virulence newcastle disease viruses from waterfowl and shorebirds and comparison of genotype distributions to those of poultry-origin isolates. J Virol **81:**12641–12653, 2007.
19. Kommers GD, King DJ, Seal BS, Brown CC: Pathogenesis of chicken-passaged Newcastle disease viruses isolated from chickens and wild and exotic birds. Avian Dis **47:**319–329, 2003.
20. Kommers GD, King DJ, Seal BS, Brown CC: Virulence of six heterogeneous-origin Newcastle disease virus isolates before and after sequential passages in domestic chickens. Avian Pathol **32:**81–93, 2003.
21. Kommers GD, King DJ, Seal BS, Carmichael KP, Brown CC: Pathogenesis of six pigeon-origin isolates of Newcastle disease virus for domestic chickens. Vet Pathol **39:**353–362, 2002.
22. Kuiken T, Heckert RA, Riva J, Leighton FA, Wobeser G: Excretion of pathogenic Newcastle disease virus by double-crested cormorants (Phalacrocorax auritus) in absence of mortality or clinical signs of disease. Avian Pathol **27:**541–546, 1998.
23. Kuiken T, Leighton FA, Wobeser G, Danesik KL, Riva J, Heckert RA: An epidemic of Newcastle disease in double-crested cormorants from Saskatchewan. J Wildl Dis **34:**457–471, 1998.
24. Kuiken T, Wobeser G, Leighton FA, Haines DM, Chelack B, Bogdan J, Hassard L, Heckert RA, Riva J: Pathology of Newcastle disease in double-crested cormorants from Saskatchewan, with comparison of diagnostic methods. J Wildl Dis **35:**8–23, 1999.
25. Liu H, Wang Z, Wang Y, Sun C, Zheng D, Wu Y: Characterization of Newcastle disease virus isolated from waterfowl in China. Avian Dis **52:**150–155, 2008.
26. Miller PJ, Decanini EL, Afonso CL: Newcastle disease: Evolution of genotypes and the related diagnostic challenges [published online ahead of print September 30, 2009]. Infect Genet Evol **10:**26–35, 2009.
27. Miller PJ, Kim LM, Ip HS, Afonso CL: Evolutionary dynamics of Newcastle disease virus. Virology **391:**64–72, 2009.
28. Miller PJ, King DJ, Afonso CL, Suarez DL: Antigenic differences among Newcastle disease virus strains of different genotypes used in vaccine formulation affect viral shedding after a virulent challenge. Vaccine **25:**7238–7246, 2007.
29. Nagai Y, Klenk HD, Rott R: Proteolytic cleavage of the viral glycoproteins and its significance for the virulence of Newcastle disease virus. Virology **72:**494–508, 1976.
30. Nakamura K, Ohtsu N, Nakamura T, Yamamoto Y, Yamada M, Mase M, Imai K: Pathologic and immunohistochemical studies of Newcastle disease (ND) in broiler chickens vaccinated with ND: severe nonpurulent encephalitis and necrotizing pancreatitis. Vet Pathol **45:**928–933, 2008.
31. OIE World Organization for Animal Health: Manual of Diagnostic Tests and Vaccines for Terrestrial Animals, 6th ed., pp. 576–589. OIE, Paris, France, 2008.
32. Park MS, Shaw ML, Munoz-Jordan J, Cros JF, Nakaya T, Bouvier N, Palese P, Garcia-Sastre A, Basler CF: Newcastle disease virus (NDV)-based assay demonstrates interferon-antagonist activity for the NDV V protein and the Nipah virus V, W, and C proteins. J Virol **77:**1501–1511, 2003.
33. Ravindra PV, Tiwari AK, Sharma B, Rajawat YS, Ratta B, Palia S, Sundaresan NR, Chaturvedi U, Kumar GB, Chindera K, Saxena M, Subudhi PK, Rai A, Chauhan RS: HN protein of Newcastle disease virus causes apoptosis in chicken embryo fibroblast cells. Arch Virol **153:**749–754, 2008.
34. Rout SN, Samal SK: The large polymerase protein is associated with the virulence of Newcastle disease virus. J Virol **82:**7828–7836, 2008.

Downloaded from vet.sagepub.com at UNIV OF GEORGIA LIBRARY on March 10, 2011

35. Rue C, Susta L, Brown CC, Pasick JM, Swafford SR, Wolf PC, Killian ML, Pedersen JC, Miller PJ, Afonso CL: Evolutionary changes affecting rapid diagnostic of 2008 Newcastle disease viruses isolated from double-crested Cormorants [published online ahead of print January 27, 2010]. J Clin Microbiol.
36. USGS National Wildlife Health Center QWMR, July 2005 to September 2005. http://www.nwhc.usgs.gov/publications/quarterly_reports/2005_qtr_3.jsp. Accessed: 2005.
37. Wakamatsu N, King DJ, Kapczynski DR, Seal BS, Brown CC: Experimental pathogenesis for chickens, turkeys, and pigeons of exotic Newcastle disease virus from an outbreak in California during 2002–2003. Vet Pathol **43:**925–933, 2006.
38. Wan H, Chen L, Wu L, Liu X: Newcastle disease in geese: natural occurrence and experimental infection. Avian Pathol **33:**216–221, 2004.
39. Westbury H: Newcastle disease virus: an evolving pathogen? Avian Pathol **30:**5–11, 2001.
40. Yavropoulou MP, Yovos JG: Osteoclastogenesis—current knowledge and future perspectives. J Musculoskelet Neuronal Interact **8:**204–216, 2008.

Downloaded from vet.sagepub.com at UNIV OF GEORGIA LIBRARY on March 10, 2011

Avian Pathology (April 2011) **40(2),** 145–152

Taylor & Francis
Taylor & Francis Group

Neurological lesions in chickens experimentally infected with virulent Newcastle disease virus isolates

Roselene Ecco[1], Leonardo Susta[1], Claudio L. Afonso[2], Patti J. Miller[2] and Corrie Brown[1]*

[1]*Department of Pathology, College of Veterinary Medicine, The University of Georgia, 501 D. W. Brooks Drive, Athens, GA 30602-7388, USA, and* [2]*Southeast Poultry Research Laboratory, ARS-USDA, SAA, 934 College Station Road, Athens, GA 30605, USA*

Distribution, character, and severity of lesions were evaluated in tissues from the central nervous system of chickens inoculated with 10 different Newcastle disease virus (NDV) isolates: CA 1083, Korea 97-147, Australia (all velogenic viscerotropic), Texas GB and Turkey North Dakota (both velogenic neurotropic), Nevada cormorant, Anhinga and Roakin (all mesogenic), and B1 and QV4 (lentogenic). Tissues for the present study included archived formalin-fixed, paraffin-embedded brain (all strains) plus spinal cord (two strains). Encephalitis was observed in all velogenic viscerotropic and velogenic neurotropic strains, and in some mesogenic strains. In general, the encephalitic lesions began at 5 days post infection, with more severe lesions occurring around 10 days post infection. At this time point, especially in the grey matter of the brain, cerebellum and spinal cord, there were neuronal necrosis, neuronal phagocytosis, and clusters of cells with microglial morphology. Axonal degeneration and demyelination was also observed. Immunohistochemistry (IHC) for viral nucleoprotein confirmed the presence of virus. In the areas of encephalomyelitis, IHC for CD3 revealed that many of the inflammatory cells were T lymphocytes. IHC using an antibody for glial fibrillar acid protein showed reactive astrogliosis, which was most pronounced at the later time points.

Downloaded by [National Agricultural Library] at 09:01 24 August 2012

Introduction

Newcastle disease (ND) causes considerable impact on the poultry industry worldwide, with significant morbidity and mortality, and high economic losses. Occurrence of the disease requires reporting to the World Organization for Animal Health (Office International des Epizooties) and subsequent trade restrictions (Alexander & Senne, 2008). ND is caused by different strains of avian paramyxovirus-1 (APMV-1), *Avulavirus* genus, *Paramyxoviridae* family. Newcastle disease virus (NDV) has a negative-sense, single-stranded, filamentous RNA genome and a glycoprotein/lipid membrane (Phillips *et al.*, 1998; Wise *et al.*, 2004).

Classification of ND strains has been implemented through the use of pathogenicity indices, mainly the mean death time in embryonated eggs and the intracerebral pathogenicity index (ICPI). The mean death time consists of inoculation via the chorioallantoic route of 10-day-old embryonated chicken eggs, and subsequent scoring of the time to embryo death (Alexander & Senne, 2008; Office International des Epizooties, 2008). The ICPI involves intracerebral inoculation of 1-day-old chicks, followed by numerical scoring of the clinical signs over an 8-day period. The ICPI is the internationally recognized method for the classification of the different NDV isolates, and strains that score >0.7 are considered reportable to the international community. Another internationally recognized method for classification is the amino acid sequence of the fusion protein cleavage site. Strains with at least three arginine or lysine residues between positions 113 and 116 and a phenylalanine residue at position 117 are considered virulent and are therefore notifiable (Alexander & Senne, 2008).

The virulence of NDV varies greatly among the different isolates. The clinical signs, lesions and severity depend on the virulence of the virus (Bhaiyat *et al.* 1995; Alexander & Senne, 2008), species, immune status, age and concurrent diseases (Alexander & Senne, 2008; Farkas *et al.*, 2009). Because of the wide span of virulence, NDV isolates have been divided into three major groups, from the most to the least virulent: velogenic, mesogenic and lentogenic. The velogens have been further divided into viscerotropic (VVND) and neurotropic (VNND) based on behaviour in adult chickens subsequent to cloacal inoculation. Velogenic viscerotropic NDV strains inoculated in this manner produce a high mortality rate (approaching 100%) and haemorrhagic intestinal lesions centred over lymphoid areas; neurotropic velogenic NDV have a lower mortality rate (50%) and cause mainly nervous signs. The mesogenic viruses in general are associated with a low mortality rate, and cause mild respiratory or nervous signs; lentogenic viruses cause minimal or subclinical infection (Alexander & Senne, 2008).

In the present study, we describe and compare the lesions and the reaction of the neuropil and glial cells in the central nervous system (CNS) in chickens inoculated with 10 different NDV isolates. Also, 12 regions of the brain using the new anatomical nomenclature (Reiner

*To whom correspondence should be addressed. E-mail: corbrown@uga.edu
Received 26 October 2010
ISSN 0307-9457 (print)/ISSN 1465-3338 (online)/11/020145-08 © 2011 Houghton Trust Ltd
DOI: 10.1080/03079457.2010.544289

et al., 2004) were analysed, considering the intensity and spatial distribution of the lesions. Using an antibody directed against the viral nucleoprotein, the distribution and relative amounts of the virus were determined. In addition, the character of the inflammation and glial reaction was partially assessed through immunohistochemical identification of lymphocytes and astrocytes.

Materials and Methods

Tissue samples. Tissues for the present study included archived formalin-fixed, paraffin-embedded brain without (eight cases) or with (two strains; Turkey ND and Anhinga) spinal cord from experimentally infected male and female 4-week-old White Leghorn specific pathogen free chickens. All of the tissues had been harvested in an identical manner from several different pathogenesis experiments (Brown *et al.*, 1999; Susta *et al.*, 2011). Every experiment was approved by the Institutional Animal Care and Use Committee. In all cases, birds were infected with approximately 10^5 $TCID_{50}$ units of virus via eye-drop instillation. Birds were sampled at 2, 5, and 10 days post infection (d.p.i.) or if severely ill. For each time period and strain, two chickens were euthanized and tissues harvested. Birds were euthanized with intravenous injection of pentobarbital and tissues collected into 10% neutral buffered formalin immediately post mortem. After 52 to 54 h in formalin, tissues were processed for histology. Archived paraffin blocks were stored at room temperature. All chickens for all these studies were from the same source flock kept at the Southeast Poultry Research Laboratory. All the tissues in this study were from these experiments. A list of the viruses used, their pathotype and the initial publication for each study is presented in Table 1.

Histopathology. For the present study, brain tissues were examined histologically *de novo.* All the brains consisted of sagittal sections (taken from the median plane). These sections allowed analysis of the telencephalon (cerebrum), cerebellum, thalamus, midbrain and hindbrain (medulla oblongata). Figure 1 illustrates the location of these brain regions. For those strains having spinal cord available (two strains: Turkey ND and Anhinga), sections were longitudinal (cervical, thoracic and lumbar) from two strains. A list of all lesions seen by light microscopy in these sections was prepared. The lesions observed in the brains and spinal cords were graded according to the lesion severity and character. Specific lesions included: inflammatory cell infiltration, endothelial hypertrophy, vasculitis, increase of the cellularity of the neuropil (microgliosis and astrogliosis), chromatolysis, neuronal necrosis and neuronophagy, axonal degeneration and demyelinization. Each anatomic region of the brain was examined for the presence of these lesions.

Table 1. *Viruses in archived tissue used in the present study.*

Strain designation	Full name of strain	Classification of pathotype	Reference
CA 1083	Chicken/US/CA 1083 (Fontana)/72	VVND	Brown *et al.* (1999)
Korea 97-147	Korea 97-147	VVND	Lee *et al.* (2004)
Australia	Chicken /Australia/ 9809-19-1107/1998	VVND	Susta *et al.* (2011)
Texas GB	Chicken/US/Texas GB/48	VNND	Brown *et al.* (1999)
Turkey ND	Chicken/US/Turkey ND/43084/92	VNND	Brown *et al.* (1999)
Nevada cormorant	Double crested cormorant/US/ Nevada/19529-04/ 2005	Mesogen	Susta *et al.* (2011)
Anhinga	Chicken/US[FL]/ Anhinga/93 44083/ 93	Mesogen	Brown *et al.* (1999)
Roakin	Chicken/US/ Roakin/48	Mesogen	Brown *et al.* (1999)
B1	Chicken/US/B1/48	Lentogen	Brown *et al.* (1999)
QV4	Chicken /Australia / Queensland (QV4)/ 31	Lentogen	Brown *et al.* (1999)

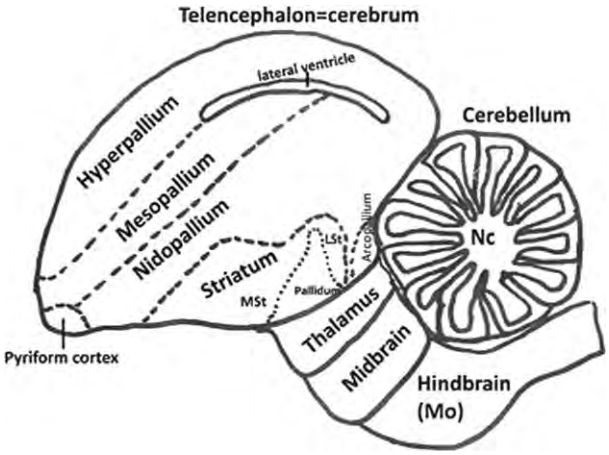

Figure 1. *Schematic diagram showing view of the avian brain according to the actual names. Diagram adapted from Reiner* et al. *(2004). LSt, lateral striatum; MSt, medial striatum; Nc, nuclei cerebelaris; Mo, medulla oblongata.*

Immunohistochemistry. *For Newcastle disease virus.* Brains from all of the birds—and in addition, for two of the strains, spinal cords—were available, and were processed via immunohistochemistry (IHC) to detect viral nucleoprotein. Unstained sections were subjected to heat-mediated antigen retrieval by microwaving for 20 min at minimum power (approximately 600 W) in unmasking solution (Vector Laboratories, Burlingame, California, USA). Following antigen retrieval, blocking was done with universal blocking reagent (Biogenex, San Ramon, California, USA) as recommended by the manufacturer. The primary antibody, made in rabbits, was an antipeptide, against the nucleoprotein, used at 1:8000 dilution. The slides were incubated with biotinylated goat anti-rabbit antibody and then with avidin–biotin alkaline phosphatase (Vector Laboratories) at room temperature. The reaction was revealed using a naphthol-based dye (Fast Red; DAKO, Carpinteria, California, USA). Negative controls consisted of the brains of age-matched, non-infected chickens.

For T lymphocytes and astrocytes. Selected sections of nervous system showing inflammation were processed via IHC with polyclonal rabbit anti-human CD3 (A 0452-DAKO) and monoclonal mouse anti-glial fibrillar acid protein (GFAP) (MU020-UC; Biogenex).

For CD3, unstained sections were subjected to antigen retrieval by microwaving for 20 min at minimum power in unmasking solution (Vector Laboratories). Following antigen retrieval, blocking was done with universal blocking reagent (Biogenex) and then incubated with the primary anti-CD3 antibody (polyclonal rabbit) at a 1:100 dilution, at 4°C overnight. After incubation, the slides were washed and incubated with an alkaline phosphatase-linked polymer system (Labvision Corporation, Fremont, California, USA) for 30 min at room temperature. As a positive control, the spleen of a specific pathogen free chicken was used. The reaction was revealed using Vector Red (Vector Laboratories).

Selected sections of the brain that had inflammation and increased cellularity in the neuropil were examined by IHC for the presence of GFAP using an automated method (DAKO autostainer). Slides were subjected to antigen retrieval using citrate buffer with pH 6.0 (HK086-9K; Biogenex) followed by heat. Endogenous peroxidase was blocked using 3% hydrogen peroxide (H312-500; Fischer Scientific, Fair Lawn, New Jersey, USA). The slides were incubated with the primary antibody (monoclonal mouse anti-GFAP, MU020-UC; Biogenex) for 60 min at a 1:600 dilution. The secondary antibody used was a biotinylated horse anti-mouse IgG (BA-2001; Vector Laboratories). The detection system

Downloaded by [National Agricultural Library] at 09:01 24 August 2012

used was the labelled streptavidin–biotin streptavidin–horseradish peroxidase (K1016; DAKO). The reaction was revealed by 3,3'-diaminobenzidine tetrahydrochloride (K3466; DAKO) chromogen to yield a brown staining. The cerebellum of a non-infected specific pathogen free chicken was used as a negative control.

In all procedures, tissue sections were counterstained with Gills II haematoxylin, dehydrated through graded alcohol, cleared in xylene, and cover slipped with Permount.

Results

Clinical disease. The clinical findings have been reported in previous publications for each strain. For purposes of clarity, some are repeated here. As described in previous publications, birds infected with a viscerotropic velogenic strain (CA 1083) were severely depressed at 2 d.p.i. and died or were euthanized when moribund between 4 and 5 d.p.i. (Brown *et al.*, 1999). With another viscerotropic velogen, Korea 97-147, birds died between 4 and 5 d.p.i. with mild neurologic signs consisting of head twitch and severe depression (data not published). Birds infected with a third viscerotropic velogenic strain (Australia) demonstrated depression between 3 and 4 d.p.i., and mild neurologic signs including depression and head tremors between 4 and 9 d.p.i. but at 10 d.p.i., they were clinically normal and were euthanized (Susta *et al.*, 2011). With the Texas GB strain (neurotropic velogen), birds were bright and alert at 2 d.p.i. but were in lateral recumbency and unable to right themselves by 5 d.p.i. Chickens inoculated with the second velogenic neurotropic strain, Turkey ND, were clinically normal at 5 d.p.i. but by 10 d.p.i. were depressed, with unilateral leg paresis. Birds inoculated with mesogenic (Roakin and Anhinga) and lentogenic (B1 and QV4) isolates demonstrated no signs of clinical disease (Brown *et al.*, 1999). However, birds inoculated with another mesogenic strain (Nevada cormorant) had severe neurologic signs (recumbency and paralysis) between 4 and 10 d.p.i. (Susta *et al.*, 2011).

Histopathology. Histologic changes were seen in the brains from birds in all strains associated with neurologic signs, which includes the VVND strains (CA 1083, Korea 97-147, Australia) the VNND strains (Turkey ND, Texas GB), and the Nevada cormorant strain (mesogenic). In addition, histologic changes were seen in the brains of birds infected with Anhinga virus (mesogenic strain), even though no overt neurologic signs were recorded for these birds. The brains of birds from chickens infected with Roakin (mesogen) and the two lentogens (B1, QV4) were histologically unremarkable.

For those strains that produced encephalitis and for which there was more than one sampling period in which the encephalitis was present, inevitably the lesion severity was more severe at the later time point. The degree of pathologic changes in the various regions of the brain from the one or two time periods available for each of the strains is presented in Table 2. In general, when multiple brain sections were available from one strain at a certain time point, there was good similarity of lesion distribution and severity.

In all cases where lesions were observed, it was possible to observe some degree of encephalitis (or encephalomyelitis) and microgliosis. Microglial cells occurred predominantly around vessels or surrounding necrotic neurons. Additional alterations such as vasculitis, vascular proliferation, axonal degeneration, demyelination and astrogliosis were present in some strains. Findings for each strain are described in more detail below.

For the VVND strains (Korea 97-147 and Australia), the inflammatory lesions consisted of one to two layers of lymphocytes in and around vascular walls. Encephalitis was observed in the nuclei cerebellaris, mesopallium, nidopallium, hyperpallium and meninges corresponding to these regions. In these areas there was mild microgliosis. The inflammatory lesions had moderate intensity and multifocal distribution. Chromatolysis and some necrotic neurons were also observed. In birds infected with VVND CA 1083 strain, in the midbrain, nuclei cerebellaris and medulla oblongata there was mild encephalitis, moderate multifocal haemorrhage and oedema around vessels.

For the VNND strains (Turkey ND and Texas GB), inflammatory lesions were initially observed at 5 d.p.i. Inflammatory lesions in general were more pronounced, especially with Turkey ND, and in addition to the perivascular cuffs of lymphocytes there was widespread chromatolysis, axonal degeneration and necrotic neurons. In birds infected with the Texas GB strain, moderate microgliosis was also observed at 10 d.p.i. At this time point, all these changes were most prominent in the striatum and medulla oblongata. In the birds infected with Turkey ND, lesions became progressively more severe at around 10 d.p.i. and were distributed extensively throughout all regions of brain, including telencephalon. The inflammation was characterized as three to four layers of lymphocytes and fewer plasma cells in the walls and around vessels (Figure 2). In some venules, numerous endothelial cells were hypertrophic, and had large nuclei with vesiculated chromatin protruding into the vascular lumen. Multifocal vascular proliferation was observed in the molecular layer of the cerebellum and medulla oblongata. Multifocal and mild to moderate inflammation was observed in the subarachnoid spaces in the midbrain and cerebellum, and occasionally in the cerebrum. Neuronal necrosis associated with neuronophagia and microgliosis (Figure 3), occasional mitosis, vacuolization of neuropil and astrocytosis were observed in the grey matter. Axonal degeneration (Figure 4) was present in the white matter and grey matter of the medulla oblongata and spinal cord. In the cerebellar folia (junction between granular and molecular layers) there was multifocal loss of Purkinje cells associated with areas of inflammation and vascular proliferation (Figure 5). All the lesions had a multifocal to coalescing distribution.

In birds infected with one of the mesogenic strains, Nevada cormorant, less severe lesions were observed at 5 d.p.i., becoming progressively more severe at 6 and 9 d.p.i. The lesions were similar to those described for Turkey ND strain. However, the intensity was less in the cerebrum and there was slightly less neuronal necrosis. The regions affected most intensely were the medulla oblongata, midbrain, thalamus and molecular layer of cerebellum. In these areas, axonal spheroids were present.

For another mesogenic strain (Anhinga) evaluated at 10 d.p.i., the inflammatory lesions were moderate and multifocal, and distributed in the striatum, midbrain, medulla oblongata, molecular layer of cerebellum, nuclei

Downloaded by [National Agricultural Library] at 09:01 24 August 2012

Downloaded by [National Agricultural Library] at 09:01 24 August 2012

Table 2. *Distribution and intensity of histological lesions and stain for virus in different areas of the nervous system[a] in chickens experimentally infected with different NDV isolates.*

Strain	Pathotype	d.p.i.	Stain	Me	H	M	N	Hp	St	Th	Mb	Cc	Nc	Mo	Sc
CA 1083 (Fontana)	VVND	5	HE	−	−	−	−	−	−	−	−	−	+	+	NE
			IHC	−	−	+	+ +	−	−	−	−	+	−	+	NE
Korea 97-147	VVND	5	HE	−	+	+ +	+ +	+ +	−	−	+ +	+	+ +	+ +	NE
			IHC	−	+ +	+ + +	+	+	+	−	+ + +	+ +	+	+	NE
Australia	VVND	10	HE	−	−	+ +	+ +	−	+ +	+ +	−	+	−	+ +	NE
			IHC	−	−	−	−	−	−	−	−	−	−	−	NE
Texas GB	VNND	5	HE	−	−	−	+	−	−	−	+ +	−	+ +	+ +	NE
			IHC	−	−	−	−	−	−	−	+	+ +	−	+ +	NE
Texas GB	VNND	10	HE	+	+	−	+	−	+ + +	+	+	−	+ +	+ +	NE
			IHC	−	+	−	−	−	+	−	−	−	−	−	NE
Turkey ND	VNND	5	HE	−	−	−	−	−	−	−	+ +	+ +	+ +	+ +	+ +
			IHC	−	+ + +	+	+	−	+ +	+ +	+ + +	+ +	+	+ +	+
Turkey ND	VNND	10	HE	+ +	+ + +	+ + +	+ + +	+ + +	+ +	+ +	+ +	+ + +	+ + +	+ + +	+ + +
			IHC	−	+ +	+ +	+ +	+	+ +	+ +	+	−	−	−	+ +
Nevada cormorant	Mesogen	6	HE	+	+	+	+	+	+	+	+ +	−	+ +	+ +	NE
			IHC	−	+ +	+	+ +	+	+ +	+	+	+ +	+	+ +	NE
Nevada cormorant	Mesogen	9	HE	+	+	+ +	+ +	+	+ +	+ + +	+ + +	+ + +	+ + +	+ + +	NE
			IHC	−	+ +	+	+	−	−	+ +	+	+	−	+	NE
Anhinga	Mesogen	10	HE	−	+	−	+	+	+ +	+	+	+	+ +	+ +	+ + +
			IHC	−	−	−	−	−	−	−	−	+	−	+	−
Roakin	Mesogen	5;10	HE	−	−	−	−	−	−	−	−	−	−	−	NE
			IHC	−	−	−	−	−	−	−	−	−	−	−	NE
B1	Lentogen	10	HE	−	−	−	−	−	−	−	−	−	−	−	NE
			IHC	−	−	−	−	−	−	−	−	−	−	−	NE
QV4	Lentogen	10	HE	−	−	−	−	−	−	−	−	−	−	−	NE
			IHC	−	−	−	−	−	−	−	−	−	−	−	NE

−, no lesions/no virus signal; +, mild lesions/virus signal; + +, moderate lesions/virus signal; + + +, marked lesions/virus signal; NE, not evaluated; HE, haematoxylin and eosin; Me, meninges; H, hyperpallium; M, mesopallium; N, nidopallium; Hp, hippocampus; St, striatum; Th, thalamus; Mb, midbrain; Cc, cerebellar cortex; Nc, nuclei cerebelaris; Mo, medulla oblongata; Sc, spinal cord. [a]The nomenclature of the avian brain, and abbreviations, was described according to Reiner *et al.* (2004) and www.avianbrain.org.

Downloaded by [National Agricultural Library] at 09:01 24 August 2012

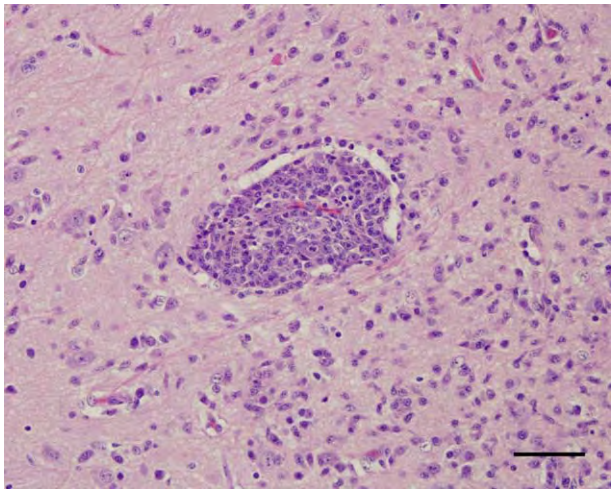

Figure 2. *Cerebrum (mesopallium), 4-week-old chicken, experimentally infected with Turkey ND strain. 10 d.p.i. Marked infiltration of lymphocytes and plasma cells in and around the vascular wall. Haematoxylin and eosin. Bar = 50 μm.*

cerebellaris, and grey matter of the spinal cord. The lesions were most intense in the spinal cord. The inflammatory lesions were characterized by one to three layers of lymphocytes and some plasma cells in and around vascular walls. These lesions were associated with mild to moderate microgliosis, axonal degeneration and mild demyelinization (particularly in the medulla oblongata and spinal cord). Lesions were not observed in the brain and spinal cord of the birds at 5 d.p.i.

In chickens infected with the Roakin (mesogen) strain and the two lentogenic strains (B1 and QV4), all of the brains at 2, 5, and 10 d.p.i were examined. There was never any inflammation detected in the nervous tissue.

Immunohistochemistry. *For Newcastle disease virus.* Results are presented in Table 2. In general, immunohistochemical signals were seen in multiple regions of the brain. They were always present as multiple granules identifiable in the cytoplasm of neurons, some glial cells and rarely endothelial cells. In general, the viral nucleoprotein signal was more intense and distributed in

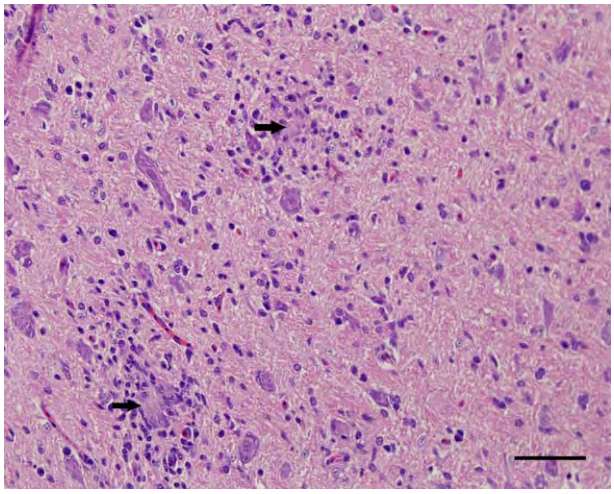

Figure 3. *Medulla oblongata, 4-week-old chicken, experimentally infected with Nevada cormorant strain. 9 d.p.i. Necrotic neurons undergoing phagocytosis (arrow) by many microglial cells. Haematoxylin and eosin. Bar = 50 μm.*

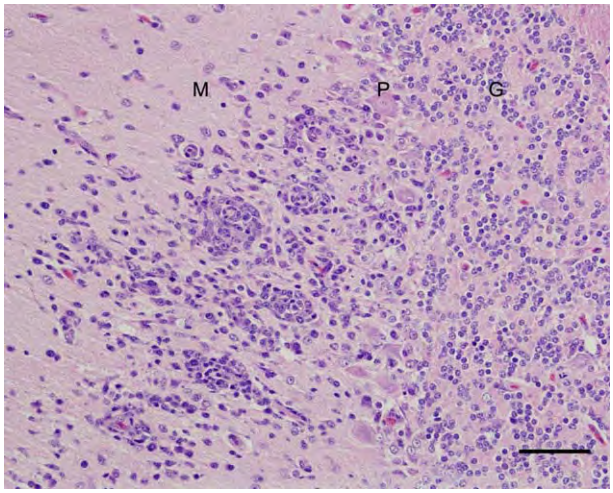

Figure 4. *Cerebellum, 4-week-old chicken, experimentally infected with Turkey ND strain. 10 d.p.i. The molecular layer (M) has focal encephalitis and vascular proliferation. Some Purkinje cells in the subjacent Purkinje cell layer (P) are missing. In the granular layer (G), there are no changes. Haematoxylin and eosin. Bar = 50 μm.*

multifocal areas at 5 d.p.i. In those birds with lesions evaluated around 10 d.p.i, virus was identifiable by IHC in lesser amounts in the brain, often associated with lesions. However, in many cases, there would be no association between degree or location of inflammation and presence of moderate IHC signal (Figure 6). Viral nucleoprotein was not detected in the brains of chickens infected with the Australia strain (VVND virus). Similarly, virus was not detected in any of the birds infected with strains without encephalitis (Roakin, a mesogen, and B1, QV4, lentogens).

For T lymphocytes and astrocytes. Results are presented in Table 3. Many inflammatory cells in the wall and around vessels were positive by IHC-CD3 (T lymphocytes) in the brains of all chickens that presented encephalitis. In the brains with marked inflammation examined at 10 d.p.i. (Turkey ND) and 9 d.p.i. (Nevada cormorant), some CD3-positive cells were also present in

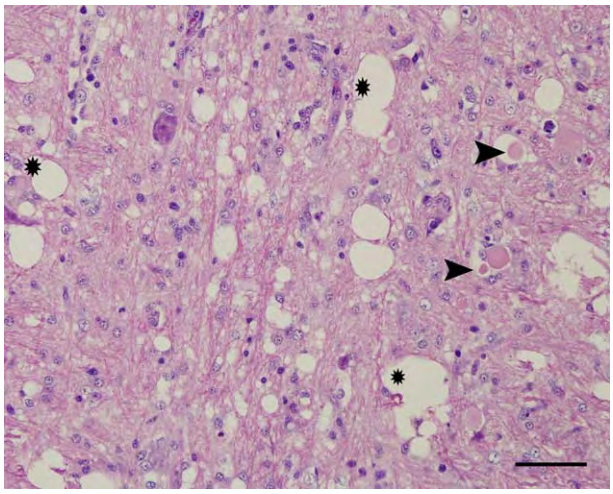

Figure 5. *Medulla oblongata, 4-week-old chicken, experimentally infected with Turkey ND strain. Spongy changes (*), axonal spheroids (arrow head) and hypertrophy of the nuclei of astrocytes. Haematoxylin and eosin. Bar = 50 μm.*

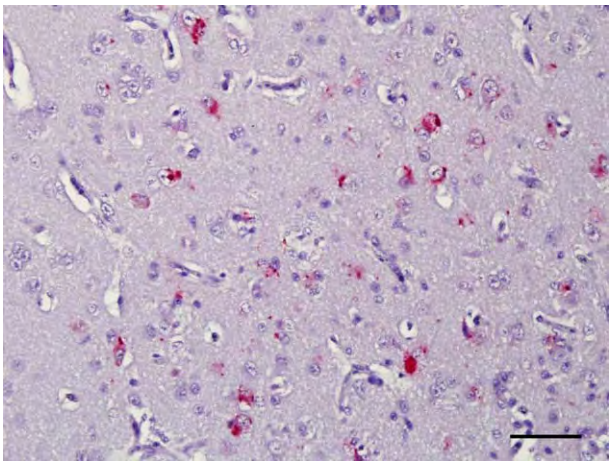

Figure 6. *Hyperpallium, 4-week-old chicken, experimentally infected with Korea 97-147 strain. 5 d.p.i. Immunohistochemistry for viral nucleoprotein (NDV). Multiple granules are identifiable in the cytoplasm of neurons. Bar = 50 μm.*

the neuropil around vessels. For GFAP, the signal revealed an increased number of astrocytes, as well as increased thickness of the astrocyte processes (astrogliosis), in the parenchyma of the CNS in chickens with encephalitis that survived to 9 or 10 d.p.i. An exception was the chickens infected with the Australia strain (VVND) in which birds were sampled until 10 d.p.i., but still there was no increase in GFAP noted. In chickens infected with Anhinga strain (mesogen), the reaction was minimal. Astrogliosis was strongest in those chickens infected with Turkey ND and Nevada cormorant, and was especially prominent in the medulla oblongata, hyperpallium (Figure 7) and molecular layer of cerebellum. These are also the two strains for which spinal cord was also available, and it was apparent that this reaction extended into this region as well (Figure 8). The astrocytic reaction was more prominent surrounding areas of intense perivascular cuffs.

Discussion

The present study showed the distribution and extent of neurologic lesions in chickens infected with different strains of NDV. With the lentogens, there was never any evidence of encephalitis or presence of viral nucleoprotein in the brain as detected by IHC. Similarly, with one of the mesogens, Roakin, encephalitis was not a feature and there was no virus present in the brain. For all of the other strains, distinct encephalitic lesions in birds infected with Texas GB, Turkey ND and Nevada cormorant strains became increasingly severe over time. In all these brains, the predominance of lesions was observed especially in the grey matter. The inflammatory lesions were similar in character but differed somewhat in severity in all strains that had encephalitis.

For those two strains that caused death by 5 d.p.i. (CA 1083 and Korea 97-147, both VVND viruses), the inflammation in the brain was mild or moderate, respectively, and multifocal. The amount of virus seen in the brain, as determined by IHC, was mild and multifocal for CA 1083, suggesting that the virus had not replicated extensively in the nervous tissue. For the Korea strain, a moderate to marked amount of viral protein IHC signal indicated a more extensive presence

Table 3. *Greatest histologic severity lesions, degree of inflammation, signal for CD3 and intensity of signal for GFAP.*

Strain	Pathotype	d.p.i.	Severity	CD3	GFAP
CA 1083 (Fontana)	VVND	5	+	Positive	Negative
Korea 97-147	VVND	5	+ +	Positive	Negative
Australia	VVND	10	+ +	Positive	Negative
Texas GB	VNND	10	+ +	Positive	1
Turkey ND	VNND	5	+ +	Positive	Negative
Turkey ND	VNND	10	+ + +	Positive	3
Nevada cormorant	Mesogen	6	+ +	Positive	Negative
Nevada cormorant	Mesogen	9	+ + +	Positive	2
Anhinga	Mesogen	10	+ +	Positive	1

+, mild lesions; + +, moderate lesions; + + +, marked lesions; 1, mild; 2, moderate; 3, marked.

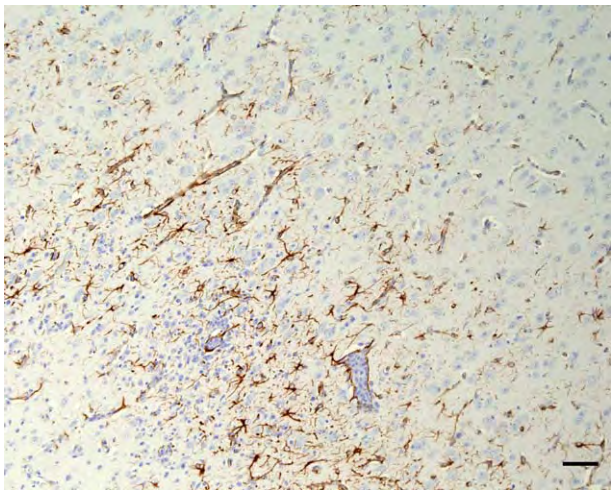

Figure 7. *Cerebrum (hyperpallium), 4-week-old chicken, experimentally infected with Turkey ND strain. 10 d.p.i. Immunohistochemistry for GFAP. Many GFAP-positive astrocytes can be observed in the areas of inflammation. Bar = 50 μm.*

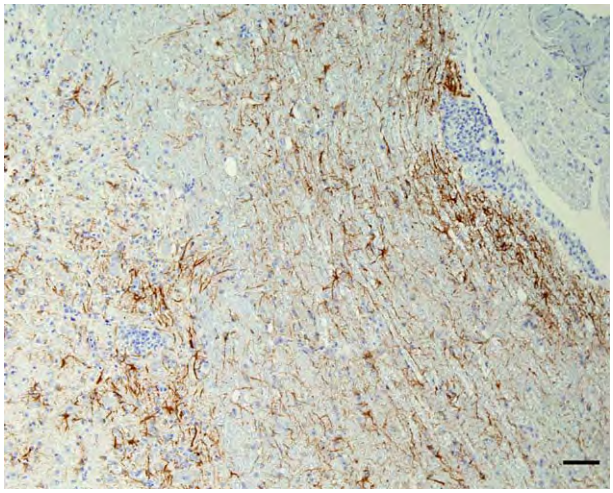

Figure 8. *Spinal cord, 4-week-old chicken, experimentally infected with Turkey ND strain. 10 d.p.i. Immunohistochemistry for GFAP. Grey matter and a focal area under meninges with inflammatory changes and a moderate increase of GFAP expression around. Bar = 50 μm.*

Downloaded by [National Agricultural Library] at 09:01 24 August 2012

Downloaded by [National Agricultural Library] at 09:01 24 August 2012

of virus in the brain. Disease progression with VVND virus is rapidly fatal, with birds often succumbing within 4 to 5 d.p.i. (Kommers *et al.*, 2002; Alexander & Senne, 2008). The other VVND strain, Australia, behaved in a very different manner, in that birds survived until 10 d.p.i., which is unusual for a strain in this category. Although these birds had encephalitic lesions similar to the other groups, there was no evidence of viral protein as detected by IHC. The inability to detect virus in the brains of birds infected with the Australia virus could indicate a resolution of the lesions, with disappearance of the antigen, as has been reported previously using fluorescent antibody techniques (Wilczynski, 1977). Alternatively, a small amount of virus below the limits of the detection could be generating inflammatory lesions.

For VNND virus (Turkey ND and Texas GB) and a mesogen Nevada cormorant, the amount of virus present in brain was minimal, but lesions were in general more severe. The neurotropic velogenic form is more usually characterized as slower in onset, with birds in general remaining bright and alert but later becoming depressed to variable degrees, with paresis or paralysis most prominent at 5 days or later (Brown *et al.*, 1999).

In general, mesogens are not thought to be so virulent, but some strains behave more like the neurotropic strains than the more classical mesogens such as Roakin. In our study, Nevada cormorant and Anhinga, both mesogens, created encephalitis and especially with Nevada cormorant strain, all lesions were remarkably similar to those seen with the VNND strains. There was involvement of all regions of the brain. Mild malacia, axonal degeneration and demyelinization were observed especially in chickens infected with Turkey ND and Nevada cormorant strains. These lesions were found particularly in the medulla oblongata, molecular layer of cerebellum and spinal cord (the latter only available for Turkey ND) and were also observed in other studies. Kuiken *et al.* (1999) observed axonal degeneration, characterized by swelling and fragmentation of axons in the brachial and lumbosacral plexus of double-crested cormorants (infected naturally with APMV-1/cormorant/Saskatchewan-Canada/2035/95). Nakamura *et al.* (2008) detected NDV by immunohistochemistry in the peripheral nerves in chickens infected experimentally with VVND virus (APMV1/chicken/Japan/Fukuoka-11/2004).

The main inciting factor for neurologic problems appears to be viral infection of neurons with associated neuronal necrosis. Other investigators have reported on neuronal damage by NDV (Stevens *et al.*, 1976; Wilczyinski *et al.* 1977). In the present study we detected viral nucleoprotein within neuronal cytoplasm immunohistochemically, as have other authors (Kuiken *et al.*, 1999; Kommers *et al.*, 2001; Nakamura *et al.*, 2008), suggesting association between virus and neuronal damage. However, viral replication might not be the only mechanism of neuroparenchymal damage. Lesions characterized by endothelial hypertrophy, and mild to moderate proliferative vasculitis, were observed in chickens evaluated at 9 and 10 d.p.i. in our study, especially in the molecular layer of cerebellum. It may be that some of the damage is due to vascular compromise, in addition to the direct neuronal necrosis caused by the virus.

The principal protagonists of CNS inflammation are microglia, blood-borne macrophages and astrocytes (Leme & Chadi, 2001). Astrocytes become activated, undergoing remarkable changes in cell shape and functionality in response to diverse CNS injuries such as trauma, infectious diseases or chemical insults (Stichel & Müller, 1998; Leme & Chadi, 2001; Pozner *et al.* 2008). These cells proliferate and increase in size, and also produce a dense network of interdigitated processes (astrogliosis) that surround the lesion, and fill the space vacated by the dead or dying cells (Stichel & Müller, 1998; Leme & Chadi, 2001). Response of microglial cells occurs within the CNS parenchyma associated with injured neurons. These neurons produce chemokines that attract the microglial cells to the site of the lesion (Streit, 2000).

Microglial infiltration and astrocyte activation characterized the reaction observed in many areas of the parenchyma (especially grey matter) of the brain and spinal cord in this study. In those birds that died or were euthanized at the later time points (10 d.p.i.), numerous GFAP-positive astrocytes and processes were detected, especially around vessels with inflammatory changes. Reactive astrogliosis is a feature of many viral encephalitides in which viral infection of astrocytes is probably the prime stimulus. This reaction is expected in axonal degeneration and neuronal necrosis. After injury, proliferation of both cells and processes occurs. Astrocytes are the cells primarily responsible for repair and scar formation in the brain (Maxie & Youssef, 2007). Astrogliosis was also observed in the molecular layer of the cerebellum (Bergmann-glia). Ajtai & Kálmán (1998) reported marked immunopositivity for GFAP around the lesion site 1 week after traumatic injury to the cerebellum of chickens. Our results indicated that avian Bergmann-glia also express GFAP in viral injury.

In summary, although the strains typically classified as "neurotropic" ND are known to cause neurologic impairment and damage in the CNS, it seems that all but the least virulent strains of NDV are capable of invading the CNS and causing pathologic impairment. The underlying mechanism in all cases seems to be infection of neurons leading to neuronal necrosis, and subsequent inflammatory response. The primary component of the inflammatory reaction is T lymphocytes, and astrogliosis increases with the time of the lesion. In addition, there may be some vascular compromise that can enhance the lesion extent.

Acknowledgements

R.E. was supported by the Brazilian government sponsoring agency Conselho Nacional de Desenvolvimento Científico e Tecnológico (CNPq) and Universidade Federal de Minas Gerais (UFMG). The present work was funded by USDA CRIS project number 6612-32000-049-00D. Mention of trade names or commercial products in this manuscript is solely for the purpose of providing specific information and does not imply recommendation or endorsement by the US Department of Agriculture.

References

Ajtai, B.M. & Kálmán, M. (1998). Glial fibrillary acidic protein expression but no glial demarcation follows the lesion in the molecular layer of cerebellum. *Brain Research*, *802*, 285–288.

Alexander, D.J. & Senne, D.A. (2008). Newcastle disease. In Y.M. Saif, A.M. Fadly, J.R. Glisson, L.R. McDougald, L.K. Nolan & D.E. Swayne, (Eds.). *Diseases of Poultry* 12th edn (pp. 75–115). Ames, Iowa: Blackwell Publishing.

Bhaiyat, M.I., Kobayashi, Y., Itakura, C., Islam, M.A. & Kida, H. (1995). Brain lesions in chickens experimentally infected with a neuroadapted strain of mesogenic Newcastle disease virus. *Journal of Veterinary Medical Science*, *57*, 237–244.

Brown, C., King, D.J. & Seal, B.S. (1999). Pathogenesis of Newcastle disease in chickens experimentally infected with viruses of different virulence. *Veterinary Pathology*, *36*, 125–132.

Farkas, T., Székely, É., Belák, S. & Kiss, I. (2009). Real-time PCR-based pathotyping of Newcastle disease virus by use of TaqMan minor groove binder probes. *Journal Clinical Microbiology*, *47*, 2114–2123.

Kommers, G.D., King, D.J., Seal, B.S. & Brown, C.C. (2001). Virulence of pigeon-origin Newcastle disease virus isolates for domestic chickens. *Avian Diseases*, *45*, 906–921.

Kommers, G.D., King, D.J., Seal, B.S., Carmichael, K.P. & Brown, C.C. (2002). Pathogenesis of six pigeon-origin of Newcastle disease virus for domestic chickens. *Veterinary Pathology*, *39*, 353–362.

Kuiken, T., Wobeser, G., Leighton, F.A., Haines, D.M., Chelack, B., Bogdan, J., *et al.* (1999). Pathology of Newcastle disease in double-crested cormorants from Saskatchewan, with comparison of diagnostic methods. *Journal Wildlife Diseases*, *35*, 8–23.

Lee, Y.J., Sung, H.W., Choi, J.G., Kim, J.H. & Song, C.S. (2004). Molecular epidemiology of Newcastle disease viruses isolated in South Korea using sequencing of the fusion protein cleavage site region and phylogenetic relationships. *Avian Pathology*, *33*, 482–491.

Leme, R.J. & Chadi, G. (2001). Distant microglial and astroglial activation secondary to experimental spinal cord lesion. *Arquivos de Neuro-psiquiatria*, *59*, 483–492.

Maxie, M.G. & Youssef, S. (2007). Nervous system. In M.G. Maxie, (Ed.). *Jubb, Kennedy, and Palmer's Pathology of Domestic Animals* Vol. 1, 5th edn (pp. 281–457). Toronto: Elsevier.

Nakamura, K., Ohtsu, N., Nakamura, T., Yamamoto, Y., Yamada, M., Mase, M. & Imai, K. (2008). Pathologic and immunohistochemical studies of Newcastle disease (ND) in broiler chickens vaccinated with ND: severe nonpurulent encephalitis and necrotizing pancreatitis. *Veterinary Pathology*, *45*, 928–933.

Office International des Epizootes. (2008). *Manual of Diagnostic Tests and Vaccines for Terrestrial Animals*. Paris: World Organization for Animal Health.

Phillips, R.J., Samson, A.C.R. & Emmerson, P.T. (1998). Nucleotide sequence of the 5′-terminus of Newcastle disease virus and assembly of the complete genomic sequence: agreement with the "rule of six". *Archives of Virology Journal*, *143*, 1993–2002.

Pozner, R.G., Collado, S., de Giusti, C.J., Ure, A.E., Biedma, M.E., Romanowski, V., *et al.* (2008). Astrocyte response to Junin virus infection. *Neuroscience Letters*, *445*, 31–35.

Reiner, A., Perkel, D.J., Mello, C.V. & Jarvis, E.D. (2004). Songbirds and the revised avian brain nomenclature. *Annals of the New York Academy of Sciences*, *1016*, 77–108.

Stevens, J.G., Nakamura, R.M., Cook, M.L. & Wilczynski, S.P. (1976). Newcastle disease as a model for paramyxovirus-induced neurological syndromes: pathogenesis of the respiratory disease and preliminary characterization of the ensuing encephalitis. *Infection and Immunity*, *13*, 590–599.

Stichel, C.C. & Müller, H.W. (1998). The CNS lesion scar: new vistas on an old regeneration barrier. *Cell and Tissue Research*, *294*, 1–9.

Streit, W.J. (2000). Microglial response to brain injury: a brief synopsis. *Toxicologic Pathology*, *28*, 28–30.

Susta, L., Miller, P.J., Afonso, C.L., Brown, C.C. (2011). Clinicopathological characterization in poultry of three strains of Newcastle disease virus isolated from recent outbreaks. *Veterinary Pathology*, *48*.

Wilczynski, S.P., Cook, M.L. & Stevens, J.G. (1977). Newcastle disease as a model for paramyxovirus-induced neurologic syndromes. II. Detailed characterization of the encephalitis. *American Journal of Pathology*, *89*, 649–666.

Wise, M.G., Sellers, H.S., Alvarez, R. & Seal, B.S. (2004). RNA-dependent RNA polymerase gene analysis of worldwide Newcastle disease virus isolates representing different virulence types and their phylogenetic relationship with other members of the paramyxoviridae. *Virus Research*, *104*, 71–80.

Downloaded by [National Agricultural Library] at 09:01 24 August 2012

Newcastle Disease Virus

Patti J Miller, *Southeast Poultry Research Laboratory, Athens, Georgia, USA*

Claudio L Afonso, *Southeast Poultry Research Laboratory, Athens, Georgia, USA*

Based in part on the previous version of this Encyclopedia of Life Sciences (ELS) article, Newcastle Disease Virus by Bruce S Seal and Daniel J King.

Advanced article

Article Contents

- Introduction
- Classification
- Structure
- Replication
- Virulence
- Epidemiology
- Clinical Features
- Control

Online posting date: 15th July 2011

Newcastle disease virus (NDV), a member of the *Avulavirus* genus in the *Paramyxoviridae* family, has a ribonucleic acid (RNA) genome that is negative sense, nonsegmented and single-stranded. The genome codes for six structural proteins: nucleocapsid, phosphoprotein (P), matrix, fusion, hemagglutinin–neuraminidase and the RNA-directed RNA polymerase, in addition to the nonstructural V protein that is produced by a frame shift in the P coding region. Virulent forms of NDV (vNDV) contain multiple basic amino acids in the fusion cleavage site along with a phenylalanine (F) at position 117, are found worldwide and are endemic in some countries. Infections of poultry species with vNDV lead to trade restrictions. Although all NDV strains are of one serotype, their genomes evolve over time, becoming more diverse. Strains of NDV have been used as viral vectors to formulate vaccines for other infectious diseases and experimentally to treat human cancers. The virus causes conjunctivitis in humans.

Introduction

Newcastle disease virus (NDV), also known as *avian paramyxovirus 1* (APMV-1), is a member of the order *Mononegavirales* because it has a single-strand, negative-sense ribonucleic acid (RNA) genome. Although previously classified in the genus *Rubulavirus*, NDV is now categorised as an *Avulavirus* in the subfamily *Paramyxovirinae* of the family *Paramyxoviridae* (Lamb *et al*., 2005). Out of the 10 *avian paramyxovirus* serotypes 3, APMV-1, APMV-2 and APMV-3, are responsible for significant disease in poultry (Alexander and Senne, 2008; Miller *et al*., 2010a). The remaining serotypes are either rarely found in poultry or cause less severe disease. APMV1 is certainly the most economically important of the *avian paramyxovirus* serotypes. The APMV serotypes have been defined using serological tests, mainly the hemagglutination inhibition assay. Previously, NDV isolates were named after investigators or geographic areas, following initial isolation. Now it is acceptable to identify NDV isolates similar to the system used to designate influenza viruses. Consequently, NDV isolates should be listed by host of origin/geographic location/number assigned to the isolate if one exists/year of isolation, as given in **Table 1**. **See also**: Avian Influenza Viruses; Measles Virus; Mumps Virus; Viral Classification and Nomenclature

From a practical perspective, NDV isolates were originally classified as one of the three main pathotypes, based upon the clinical forms of disease they caused in chickens. Lentogens are viruses of low virulence (loNDV) and cause mild respiratory or enteric infections. Virus isolates of intermediate virulence that manifest themselves clinically as primarily respiratory pathogens, but do not cause high mortality, are termed mesogens. Highly virulent NDV (vNDV) isolates that cause mortality are designated velogens. Both mesogens and velogens are both defined as virulent (vNDV). Velogenic forms are further classified as neurotropic or viscerotropic, based on clinical manifestation following infection of chickens (Alexander and Senne, 2008). However, these pathotypes did not consistently predict disease in poultry infected with isolates from wild birds and pigeons. A more useful system, from the point of view of regulating trade, defines NDV as being virulent (vNDV) or of low virulence (loNDV). All vNDV isolates are considered 'listed' and as defined in the International Animal Health Code by the Office International des Epizooties (OIE), any event with infections of epidemiological significance must be reported to the OIE (OIE, 2010). Participating nations are required to report Newcastle disease (ND) outbreaks within 24 h by telex, telegram or fax via their representative veterinary administration. Infections with NDV isolates that have an intracerebral pathogenicity index (ICPI) in day-old chickens (*Gallus gallus*) of equal to or greater than 0.7 or that have three or more basic amino acids (lysine or arginine) demonstrated (either directly or deducted) in the fusion

eLS subject area: Virology

How to cite:
Miller, Patti J; and Afonso, Claudio L (July 2011) Newcastle Disease Virus. In: eLS. John Wiley & Sons, Ltd: Chichester.
DOI: 10.1002/9780470015902.a0001077.pub3

This is a US Government work and is in the public domain in the United States of America.

Table 1 Representative NDV isolates with fusion protein cleavage site sequence, virulence and genotype information

Virus[a]	F sequence[b]	ICPI[c]	Genotype[d]
Chicken/US (NY) 13828/1995	GGERQERL	0.00	Class I, genotype 1
Duck/US (OH)/ 04612/2004	GGERQERL	0.01	Class I, genotype 2
Mixed Poultry/HK/1967.5/2003	GGERQERL	ND	Class I, genotype 3
Mallard/US (MD)/ 02-336/2002	GGERQERL	0.00	Class I, genotype 4
Mallard/US (MD)/ 01-523/2000	GGERQERL	0.00	Class I, genotype 5
Mallard/US (MD)/ 04-211/2004	GGERQERL	0.00	Class I, genotype 7
Dunlin/US (DE)/ A100-2093/2000	GGERQERL	0.00	Class I, genotype 8
Blue-winged Teal/US (TX)/ 02-4/2002	GGERQERL	0.09	Class I, genotype 9
Chicken/US (NY)/13828/1995	GGERQERL	0.00	Class II, genotype I
Ruddy Turnstone/US (DE)/1675/2002	GGERQERL	0.00	Class II, genotype Ia
Chicken/Australia/QV4/1966	GGGKQGRL	0.21	Class II, genotype I
Chicken/US (NJ)/LaSota/1946	GGGRQGRL	0.19	Class II, genotype II
Ruddy Turnstone/US (DE)/492/2002	GGGKQGRL	0.00	Class II, genotype IIa
Chicken/US (TX)/GB/1948	GGRRQKRF	1.80	Class II, genotype II
Anhinga/US (FL)/44083/1993	RGRRQKRF	1.45	Class II, genotype V
Turkey/US (ND)/43084/1992	RGRRQKRF	1.63	Class II, genotype V
Psittacine/US/Largo/1971	GGRRQKRF	1.76	Class II, genotype V
Pigeon/US (NY)/1984	GGRRQKRF	1.54	Class II, genotype VIb
Chicken/US (CA)/1083/Fontana/1972	GGRRQKRF	1.76	Class II, genotype VIc
Chicken/Pakistan/07-5/2007	GGRRQKRF	1.88	Class II, genotype VII
Chicken/Pakistan/08-15/2006	GGRRQKRF	1.64	Class II, genotype VII
Chicken/US (CA) 24225/1998	GGRRQKRF	1.88	Class II, genotype VIII

[a]Isolate name: species identified/country (location)/isolate name or number/year isolated.
[b]Amino acids represent the cleavage site from residues 110 to 117 of the fusion protein. The F2 portion is on the *N*-terminal side with the F1 on the *C*-terminal portion of the space representing cleavage.
[c]Intracerebral pathogenicity index as determined in day-old chicks as an indication of virulence with a maximum value of 2.
[d]Class and genotype is listed.

cleavage site (positions 113–116) with a phenylalanine (F) at position 117, must be reported (OIE, 2010). The significance of the fusion cleavage site in virulence is explained in the section 'Virulence'. In the United States, vNDV are classified as Select Agents and their possession are subject to additional regulations (USDA, 2008).

Classification

Isolates of NDV are classified into two large groups, class I and class II, with each of these being further divided into 6 and 10 genotypes, respectively (Ballagi-Pordany *et al.*, 1996; Czegledi *et al.*, 2006; Kim *et al.*, 2007a). Some of these genotypes are depicted in **Figure 1**. The various genotypes circulate simultaneously in different parts of the world (Miller *et al.*, 2010b). For instance, in the United States up until the 1970s class II genotype II viruses, both virulent and viruses of low virulence, circulated in the poultry population. After the 1970s, virulent genotype V isolates replaced the virulent genotype II viruses and led to sporadic outbreaks in poultry in the United States. Presently, viruses of low virulence of class I and class II genotypes I and II circulate in the poultry populations and virulent class II genotypes V and VI circulate in pigeons and double-crested cormorants, respectively. Class II genotype VII isolates produce severe lesions in infected chickens and circulate throughout Africa and Asia. Recently, class II genotype VII isolates have also been isolated in Venezuela (Perozo *et al.*, 2011). Although both loNDV and vNDV evolve as they pass through birds over time, it is believed that the vNDV isolates have an increased opportunity to evolve since they are able to replicate in target cells in organs other than the those of the gastrointestinal and respiratory systems (Miller *et al.*, 2009b).

Structure

NDV is an enveloped virus that contains a negative-sense, single-strand RNA genome of 15 186, 15 192 or 15 198 nucleotides (Czegledi *et al.*, 2006). From a 3′–5′ direction, the viral genome codes for a nucleoprotein (NP), phosphoprotein (P), matrix protein (M), fusion protein (F), haemagglutinin–neuraminidase (HN) protein and an RNA-directed RNA large polymerase protein (L), as depicted in **Figure 2**. Short non-coding regions occur between each gene; these are important for transcriptional regulation. The RNA genome is also flanked by 3′ and 5′ nontranslated regions designated the leader and trailer sequences, respectively. The genomic and antigenomic promoter regions require two discontinuous regions for

This is a US Government work and is in the public domain in the United States of America.

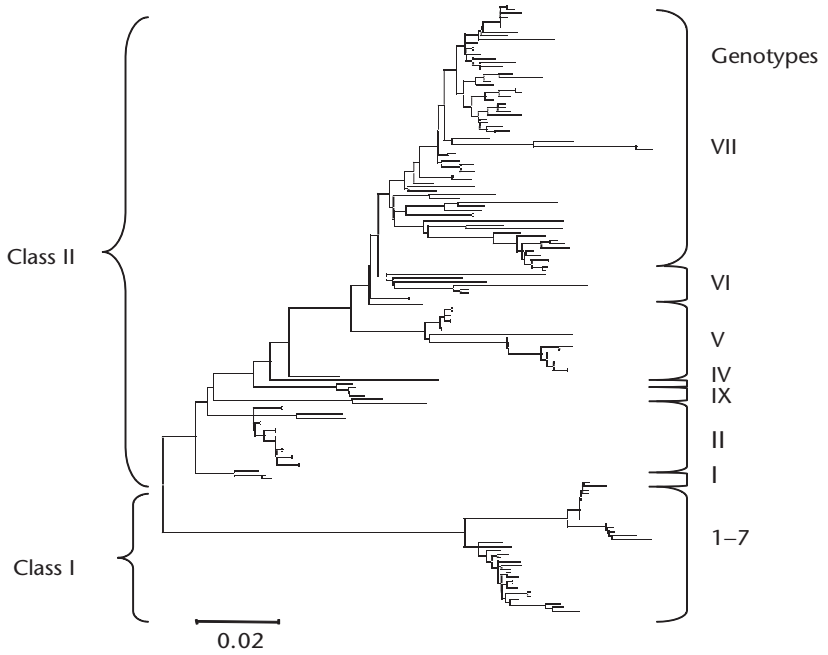

Figure 1 Phylogenetic tree of 161 APMV1 isolates containing an amino acid analysis of the full fusion protein using the neighbour-joining method/JTT matrix-based with gamma distribution. Class I with 7 of 10 genotypes and class II with 7 of 10 genotypes are represented.

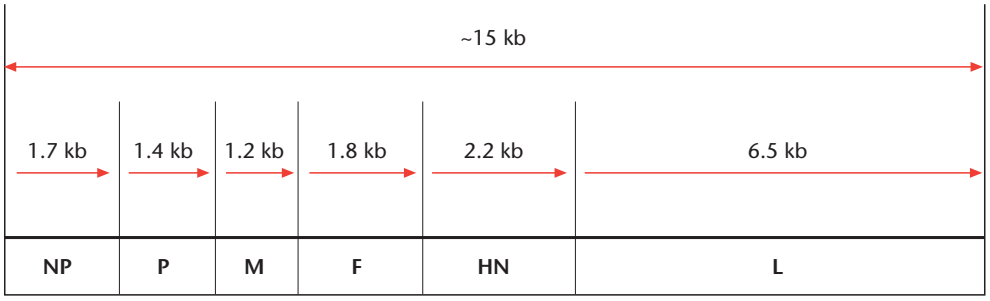

Figure 2 *Newcastle disease virus* genome. NP, nucleoprotein; P, phosphoprotein; M, matrix protein; F, fusion protein; HN, haemagglutinin–neuraminidase protein; L, RNA-directed RNA polymerase.

efficient RNA promoter activity (Marcos *et al*., 2005). **See also**: RNA Virus Genomes; Virus Structure; Viruses: Genomes and Genomics

Genome replication can be reconstituted in *cell culture* by co-expressing the entire genomic RNA in the presence of the NP, P and L proteins together, forming the minimal transcription unit. The NP is the major constituent of the NDV nucleocapsid. The relatively conserved *N*-terminal portion of the protein probably mediates RNA binding as well as the NP–NP interaction required for nucleocapsid formation. The polycistronic P gene encodes a protein of 395 amino acids. A smaller protein, designated V, is also encoded by the P gene due to transcriptional modification of P gene messenger RNA (mRNA) (Samson *et al*., 1991). This occurs by polymerase addition of an extra G at the editing site sequence during transcription. A smaller nonstructural protein, the W protein, exists through the addition of two extra G nucleotides (Steward *et al*., 1993) and has inconsistent lengths even among related isolates (Ujvari, 2006). The *N*-terminal portion of P binds to NP, whereas the *C*-terminal portion of P is required for transcriptional activity, and therefore may be a binding site for the L protein. The L protein, also known as the large polymerase, is an RNA-dependent RNA polymerase that is about 2000 amino acids in length. The L protein has been found to be involved with the virulence of an isolate individually (Rout and Samal, 2008), but also when associated with the NP and P proteins (Dortmans *et al*., 2010). **See also**: Replication of Viruses Infecting Eukaryotes; RNA Plant and Animal Virus Replication

The M protein has 364 amino acids and is responsible for coordinating viral assembly at the plasma membrane of an infected cell. The M protein interacts with the *C*-terminus of NP and facilitates assembly of the ribonucleoprotein

This is a US Government work and is in the public domain in the United States of America.

(RNP) core and glycoproteins of the virion. The F and HN proteins are glycoproteins located in the virion membrane. The F protein is a type-I membrane protein, with an *N*-terminal signal sequence and a *C*-terminal hydrophobic transmembrane region spanning the viral membrane and acting as a membrane anchor. It has 553 amino acids, and the biologically active F protein is generated by cleavage of a 68 000 F0 precursor molecule into a 56 000 *C*-terminal F1 fragment and a 12 000 *N*-terminal F2 fragment. These two fragments remain tightly associated after cleavage by disulfide bonds. This proteolytic cleavage of the F0 precursor is required for fusion activity and virion infectivity. The HN is a type-II integral membrane protein of approximately 570 amino acids with a calculated molecular weight of 62 000 and is the major antigenic determinant of NDV. The HN protein sizes vary among isolates, and larger HN proteins of low virulence NDV isolates (HN0) with alternative stop codons in the HN gene also require cleavage for infectivity (Millar *et al*., 1986). The HN has two primary functions. One is recognition of sialic acid-containing receptors on the target cell. The other function is cleavage of the same carbohydrate moiety from cell surface molecules, preventing aggregation of virions at the cell surface. The HN is required for functional cell fusion during infection, and therefore interacts with F and plays a role in virulence (Panda *et al*., 2004; Yan *et al*., 2009). **See also**: Membrane Proteins; Virus Host Cell Receptors

By electron microscopy, NDV is viewed as a relatively spherical, but can also be a pleomorphic particle with a diameter of approximately 100–500 nm, with filamentous forms also present. A lipid-bilayer membrane obtained from the host cell during budding of the virus encases the virion. The NDV membrane has 8 nm surface projections that represent the F and HN proteins. An 18 nm helical nucleocapsid structure composed of the NP, P and L proteins in association with genomic RNA is usually observed as a free structure or escaping from disrupted virions. This RNP structure is typical of viruses with negative-strand RNA genomes. The M protein is involved structurally in contact with both the cytoplasmic tails of the F and HN proteins and the RNP. **See also**: Electron Microscopy; Viral Capsids and Envelopes: Structure and Function

Replication

Viral replication is initiated by virion adsorption to a host cell receptor that presumably contains sialic acid (Villar and Barroso, 2006). Attachment is mediated by the HN protein of NDV, while fusion of the viral envelope with the cell membrane, is caused by the F protein. However, the HN protein of NDV also participates in and enhances the fusion process. Following fusion the nucleocapsid is released into the cytoplasm of the infected cell, where intracellular replication occurs. However, the M protein contains a nuclear localisation signal and may be found in the nucleus during infection (Coleman and Peeples, 1993). **See also**: Replication of Viruses Infecting Eukaryotes

The purified NDV genome, like other members of the *Mononegavirales*, is not infectious, like many positive-strand RNA viruses. The viral L protein present in the virion RNP catalyses initial transcription of the viral genome, producing positive-strand mRNA early during replication. Once viral proteins are synthesised, viral genomic RNA replication is initiated with transcription of a plus-sense antigenome. The antigenome serves as a template for the negative-sense genome synthesis. The final step in replication involves ordered assembly of viral proteins in the membrane of the infected cell and the subsequent release of the infectious virus particle. Nucleocapsids bind to viral M proteins lining modified cellular membranes, and virions bud into the extracellular environment through infected cell membranes containing F and HN proteins. The correct assembly and release of ND virions from infected host cells are dependent on the presence of lipid rafts found on the plasma membrane.

Virulence

ICPI and real-time reverse transcription-polymerase chain reaction (rRT-PCR) with sequencing of the F cleavage site are most commonly used to determine the virulence of an NDV isolate. Initially, pathotype prediction involves the inoculation of NDV into specific pathogen-free, embryonated chicken eggs to determine mean death time (MDT). Further testing entails inoculation of chickens to determine the ICPI and the intravenous pathogenicity index (IVPI). In general, vNDV display a MDT of 90 to less than 60 h, an ICPI of 0.7–2.0 and an IVPI of 0.5–3.0. Additionally, vNDV can be differentiated by its ability to replicate for multiple cycles in most avian and mammalian cell types without the addition of a protease (King, 1993). Although all NDV isolates will replicate in chicken embryo kidney cells, loNDV require the addition of trypsin for replication in avian fibroblasts or most continuous cell types of mammalian origin.

For many laboratories the primary molecular basis for determining NDV virulence is through the use of rRT-PCR, first with a primer and probe set to diagnose the virus as a NDV and then with a second primer and probe set to define the virus as virulent (Wise *et al*., 2004). In addition to different genotypes circulating in different parts of the world, the viruses collect mutations that require the assays to be updated and/or different assays to be used in different areas (Kim *et al*., 2007b; Fuller *et al*., 2010; Khan *et al*., 2010; Miller *et al*., 2010b; Rue *et al*., 2010). Subsequently, the amino acid sequence of the F cleavage site (**Table 1**) and the ability of specific cellular proteases to cleave the F (Nagai *et al*., 1976) may be used to further categorise the isolate. This is similar to the role of the cleavage site for the haemagglutinin protein (HA) of avian influenza A viruses for virulence in chickens.

Before sequencing was widely used, the clinical signs produced in chickens or eggs after infection distinguished NDV strains. However, it is now possible to quite accurately predict virulence based on the sequence of the

This is a US Government work and is in the public domain in the United States of America.

F cleavage site. vNDV with dibasic amino acids (R = arginine, K = lysine) surround glutamine (Q) at residue 114 of the F cleavage site recognition sequence of mesogenic or velogenic NDV (RRQRR, RRQKR or RRKKR). Fewer basic amino acids are present in the F cleavage site of lentogenic NDV isolates (GRQGR or GKQGR) than either mesogenic or velogenic strains. The presence of dibasic amino acids in the F allows for systemic spread of vNDV, whereas loNDV replication is limited to mucosal surfaces of avian tissues, primarily respiratory or intestinal epithelium. However, there are pigeon strains of NDV known as pigeon paramyxovirus type 1 (PPMV-1) that have basic amino acids at the fusion cleavage site and are virulent for pigeons, but not for chickens (Meulemans *et al*., 2002; Dortmans *et al*., 2009). In lentogenic NDV strains, the HN protein is also produced as a precursor form that is cleaved, expelling a 90 amino acid *C*-terminal polypeptide chain. The molecular basis for this HN cleavage has not been explored as extensively as that of the F protein cleavage mechanism (Millar *et al*., 1988). The V protein of NDV has been shown to inhibit $\propto$ interferon through the carboxy-terminus, contributing to the virulence of the virus (Huang *et al*., 2003; Park *et al*., 2003). The large polymerase protein (L) has also been found to affect virulence both with the involvement of the NP and P (Dortmans *et al*., 2010) and by itself (Rout and Samal, 2008).

Several subtilisin-like, Golgi-membrane associated endoproteinases have been identified that are ubiquitously expressed in most eukaryotic tissue cell types and in cultured eukaryotic cells. These include furin or 'paired basic amino acid-cleaving enzymes', which are expressed by the constitutive secretory pathway and recognise the dibasic amino acid motif of many cellular and viral proproteins. Proteinases identified in neuroendocrine cells, the proprotein convertases (PC1/PC3), are localised to secretory vesicles responsible for processing in the regulated secretory pathway, but do not process the vNDV F (Gotoh *et al*., 1992a).

Blood-clotting factor Xa has been identified as a virus-activating proteinase (VAP) capable of processing NDV Fs containing only a single arginine at the cleavage site found in loNDV. Originally believed to be synthesised only in the liver, factor Xa was subsequently isolated from amniotic and allantoic cells of chick embryos (Gotoh *et al*., 1992b). The spread of loNDV is restricted to tissue surfaces, like the respiratory or gastrointestinal tracts, containing factor Xa or another VAP capable of cleaving the Fs of loNDV. **See also**: Endoplasmic Reticulum to Golgi Transport: Methods

Epidemiology

Outbreaks of ND were first reported in poultry from Java, Indonesia and Newcastle upon Tyne, England in 1926. The disease currently has a worldwide distribution. The virus has a wide host range, with most, if not all, species of birds being susceptible to infection by NDV. Three ND panzootics are considered to have occurred since it was first described during the 1920s. This first panzootic was thought to have originated in Asia, and over the next 30 years spread throughout the world. A second panzootic apparently emerged in the Middle East during the late 1960s, and outbreaks of severe disease occurred in several countries by the early 1970s. Rapid spread of NDV during the second panzootic is attributed to increased international commercial poultry trade and importation of NDV-infected psittacine pet birds. During the 1980s, a third panzootic apparently originated in the Middle East; it involved pigeons and doves, and rapidly spread to other parts of the world, resulting in disease outbreaks among pigeons in several countries. Feed contaminated by infected pigeons resulted in ND outbreaks among commercial poultry in England.

Viscerotropic velogenic vNDV has entered the United States via illegal importation of psittacines, and were the causal agent of the major outbreak in southern California during the early 1970s. Outbreaks of ND in cormorants since the early 1990s through 2010 in the north-central United States and southern Canada have been attributed to neurotropic mesogenic vNDV isolates that are phylogenetically similar to viruses isolated during the 1970s. A ND outbreak in range-reared turkeys in the US state of North Dakota during 1992 was attributed to virus transmitted from infected cormorants. In 2010, a similar vNDV was isolated for the first time in double-crested cormorants in Maryland, which is outside previously known geographic range of ND outbreaks in cormorants (Sleeman, 2010). Sporadic epizootic outbreaks of ND occurred in Western Europe from 1992 to 1996, and during 1998 viscerotropic vNDV caused major disease problems among commercial poultry farms in Venezuela. In Australia during 1998–2000, vNDV was detected among poultry that evolved from a loNDV progenitor rather than from the introduction of a vNDV (Gould *et al*., 2001). During the autumn of 2002 into the spring of 2003, an ND outbreak caused by introduction of vNDV in smuggled fighting chickens occurred in southern California of the United States and resulted in moratoriums on export of California poultry. The source of worldwide ND outbreaks has not always been determined, but certainly multiple sources of vNDV including free-living birds do exist. Any source of vNDV is a threat to commercial poultry with the potential of impacting international trade. From 2005 through 2010 at least 112 countries reported outbreaks of NDV to the World Organization for Animal Health (http://www.oie.int). The vNDV isolates on the African and Asian continents are particularly troublesome with the presence of new vNDV genotypes (Cattoli *et al*., 2010) and genotypes that are increasing virulence for species once felt somewhat resistant (Liu *et al*., 2008).

Clinical Features

Infection by NDV can range from subclinical to a highly fulminant disease, depending on the viral pathotype and

This is a US Government work and is in the public domain in the United States of America.

host species. In general, gallinaceous birds, such as chickens or turkeys, are highly susceptible to disease from vNDV infections, whereas ducks and geese may not display symptoms upon infection. However, reports from Asia of ducks and geese with high mortality rates from vNDV suggest that these species may be more affected by strains of NDV adapted to these species (Wan *et al*., 2004). Many types of psittacine birds and pigeons may carry vNDV without symptoms, and as mentioned previously, outbreaks of neurotropic vNDV have caused die-offs among nesting cormorants in North America. Certainly other factors, such as host immune state, infection with other agents, stress and vaccination status, are important in affecting the severity of disease caused by vNDV.

Usually, loNDV do not cause severe disease in adult birds; however, these loNDV can produce mild respiratory disease that may lead to air sacculitis and, if complicated by secondary infections, may produce mortality. Viral replication of loNDV is primarily limited to mucosal surfaces and to the respiratory and gastrointestinal epithelial surfaces, but also has been detected in myocardial tissue by *in situ* hybridisation. vNDV of intermediate virulence will cause respiratory disease and decreased egg production and occasionally may cause nervous disorders and mortality. In these cases vNDV replication can be detected in air sac epithelium and myocardium during infection of chickens, with splenic lymphoid hyperplasia and myocardial inflammation common.

The most virulent vNDV may manifest itself in two different forms resulting in high morbidity and mortality. Neurotropic vNDV causes severe respiratory distress initially, followed by paresis and paralysis. The symptoms referred to as torticollis are characterised by twisting of the neck, and may be accompanied by lowering of a wing to the same side or unilateral leg paresis. Typically, mortality may be lower than with viscerotropic vNDV, but it may well be greater than 50% with morbidity of 70–90%. Diarrhoea is not common during this form of the disease. The spleen may be congested or enlarged and the air sacs may be affected. Perivascular cuffing and neuronal degeneration confined to the central nervous system are results of neurotropic vNDV infection of chickens. Viral nucleic acid can be detected in the air sac epithelium and in macrophage-type cells within the myocardium. Interestingly, vNDV nucleic acid detection is infrequent in the central nervous system of chickens infected with neurotropic vNDV isolates, suggesting that inflammation may be the cause of the neurological symptoms or that the virus is located in peripheral nervous tissue.

Viscerotropic vNDV can cause acute systemic illness and death of chickens within 5 days or less. In unvaccinated chicken flocks, mortality may approach 100%. These virus types may cause initial respiratory symptoms followed by muscular tremors, torticollis, paralysis of the extremities and diarrhoea resulting in high mortality. Haemorrhagic lesions are prominent in the proventriculus, caeca and small intestine. Splenic necrosis occurs, and the spleen will become devoid of mononuclear cells, with extensive fibrin deposits. Intestinal lymphoid tissues are destroyed, most prominently in the caecal tonsil. Lymphoid depletion also occurs in the bursa and thymus of infected chickens. Disruption of the myocardial tissue results, with accumulation of macrophage-type cells in the heart. Viral nucleic acid may be detected extensively as early as 2 days post-infection in the spleen, caecal lymphoid tissue and lungs, with multiple foci in the myocardium and neurons of the central nervous system.

Humans are also susceptible to NDV infections. These manifest primarily as a conjunctivitis from aerosolised virus or rubbing the eyes with virus-contaminated hands. These infections can occur in research or diagnostic laboratories as a result of poor biosecurity, or in chicken houses during vaccination procedures. **See also**: Animal Viruses Pathogenic for Humans

Control

The occurrence of ND, an infection of birds with vNDV, requires reporting of that occurrence to the OIE within 24 h of an outbreak (OIE, 2010). The OIE was established to minimise trans-border spread of serious animal diseases and make available information necessary to achieve this goal worldwide. The classification of isolates as vNDV is based on procedures approved by the OIE. Individual countries have strict import regulations with established quarantine procedures. Many countries have legislated eradication policies that may include compulsory slaughter of infected birds and any avian species in contact with diseased birds. In several countries a 'test and slaughter' policy exists, whereas others routinely vaccinate to prevent ND outbreaks. Whatever the policy, outbreaks of ND result in international trade restrictions whenever disease occurs.

The diagnosis of NDV involves the identification of virus through virus isolation of swab fluids or infected tissues or by confirming the presence of RNA using rRT-PCR. This is followed by direct nucleotide sequencing of amplified products to characterise NDV isolates. Differences can be detected in the F cleavage sequence that correlate genotypically with virulence among various pathotypes, and genomic sequences can be used for NDV molecular epidemiology, as shown in **Table 1**. Many molecular assays using real-time PCR and rRT-PCR are available to diagnose NDV quickly. However, these assays need to be reevaluated over time to ensure that the conserved sequences they were based on are still relevant to the NDV circulating in the field and it is possible that different assays will be needed for different areas of the world to ensure the best results (Fuller *et al*., 2010). Panels of monoclonal antibodies may be employed to group NDV isolates according to antigenic differences (Alexander *et al*., 1984). In addition, NDV antibodies from seroconversion can be identified by a haemagglutination inhibition assay or an enzyme-linked immunosorbent assay. In addition, novel viruses that circulate in wild bird species must be identified

This is a US Government work and is in the public domain in the United States of America.

and evaluated for their potential to affect poultry species (Miller *et al*., 2010a). Sequencing of viral genomes using random priming methods is a useful method that does not rely on previously known sequence data and can be used if real-time PCR fails to identify NDV. **See also**: Enzyme-linked Immunosorbent Assay; Monoclonal Antibodies: Diagnostic Uses; Next Generation Sequencing Technologies and Their Applications; Polymerase Chain Reaction (PCR)

Rapid dissemination of the disease in the 1960s and 1970s led to development of both inactivated and live virus vaccines for control of ND in poultry. Vaccination with loNDV has been the most common method employed for disease prevention in commercial poultry because of its cost-effectiveness. Inactivated oil-emulsion vaccines are usually produced from infective allantoic fluid, and require injection of birds individually. Recombinant ND vaccines containing the F and HN protein genes have been constructed using various vectors such as fowlpox or turkey herpesvirus (HVT) that must also be administered to individual birds. In contrast, infectious live vaccine virus may be ingested or inhaled, after mass application of live virus vaccines in food or drinking water or by large droplet aerosol. In addition, the live vaccine virus can be transmitted from vaccinated birds to other birds in the flock that may not have received the vaccine. The Queensland V4, B1, LaSota and VG/GA strains of NDV are currently the most widely used live virus vaccines for disease prevention and are marketed globally. In countries that have high ambient temperatures or have difficulties maintaining a cold chain, thermostable live vaccines, such as I2, may be used. The I2 strain was specifically selected for use in countries that do not have access to continual refrigeration because this virus is able to survive in higher ambient temperatures for a longer time before becoming inactivated compared to other commercial ND vaccine strains. **See also**: Vaccination; Vaccination of Animals

NDVs identical to wild-type isolates of NDV can be produced from cloned complementary deoxyribonucleic acid (cDNA) by a viral rescue system (Peeters *et al*., 1999; Romer-Oberdorfer *et al*., 1999). These infectious clones have been used to study viral replication and the importance of more subtle molecular determinants to pathogenesis. Also, this may allow for construction of unique vaccine strains to control both ND and potentially other important diseases of poultry and possibly humans (Huang *et al*., 2004; Bukreyev *et al*., 2005; Veits *et al*., 2006; Ge *et al*., 2007; Miller *et al*., 2009a; Elankumaran *et al*., 2010).

Strains of NDV used as vaccines have been administered for more than 50 years and have been studied extensively. In addition, they are applied world wide to help control outbreaks of ND. For these two reasons, it is now common to use the genomes of vaccine strains of NDV as a system to deliver genes of other avian diseases to birds while they are already being vaccinated for ND. Some of the avian applications, such as the insertion of influenza genes into the NDV genome can also be applied to human vaccines since humans are susceptible to some avian and swine influenza strains. Furthermore, some NDV strains have been used as experimental oncolytic agents in humans due to their potential to replicate better in tumour cells than they do in normal human cells.

References

Alexander DJ, Russell PH and Collins MS (1984) Paramyxovirus type 1 infections of racing pigeons: 1 characterisation of isolated viruses. *Veterinary Record* **114**(18): 444–446.

Alexander DJ and Senne DA (2008) Newcastle disease, other avian paramyxoviruses, and pneumovirus infections. In: Saif Y M, Fadly A M and Glisson J R *et al*. (eds) *Diseases of Poultry*, pp. 75–116. Ames: Iowa State University Press.

Ballagi-Pordany A, Wehmann E, Herczeg J, Belak S and Lomniczi B (1996) Identification and grouping of Newcastle disease virus strains by restriction site analysis of a region from the F gene. *Archives of Virology* **141**(2): 243–261.

Bukreyev A, Huang Z, Yang L *et al*. (2005) Recombinant Newcastle disease virus expressing a foreign viral antigen is attenuated and highly immunogenic in primates. *Journal of Virology* **79**(21): 13275–13284.

Cattoli G, Fusaro A, Monne I *et al*. (2010) Emergence of a new genetic lineage of Newcastle disease virus in West and Central Africa – implications for diagnosis and control. *Veterinary Microbiology* **142**(3–4): 168–176.

Coleman NA and Peeples ME (1993) The matrix protein of Newcastle disease virus localizes to the nucleus via a bipartite nuclear localization signal. *Virology* **195**(2): 596–607.

Czegledi A, Ujvari D, Somogyi E *et al*. (2006) Third genome size category of avian paramyxovirus serotype 1 (Newcastle disease virus) and evolutionary implications. *Virus Research* **120**(1–2): 36–48.

Dortmans JC, Koch G, Rottier PJ *et al*. (2009) Virulence of pigeon paramyxovirus type 1 does not always correlate with the cleavability of its fusion protein. *Journal of General Virology* **90**(part 11): 2746–2750.

Dortmans JC, Rottier PJ, Koch G *et al*. (2010) The viral replication complex is associated with virulence of Newcastle disease virus (NDV). *Journal of Virology* **84**(19): 10113–10120.

Elankumaran S, Chavan V, Qiao D *et al*. (2010) Type I interferon sensitive recombinant Newcastle disease dirus for oncolytic virotherapy. *Journal of Virology* **84**(8): 3835–3844.

Fuller CM, Brodd L, Irvine RM *et al*. (2010) Development of an L gene real-time reverse-transcription PCR assay for the detection of avian paramyxovirus type 1 RNA in clinical samples. *Archives of Virology* **155**(6): 817–823.

Ge J, Deng G, Wen Z *et al*. (2007) Newcastle disease virus-based live attenuated vaccine completely protects chickens and mice from lethal challenge of homologous and heterologous H5N1 avian influenza viruses. *Journal of Virology* **81**(1): 150–158.

Gotoh B, Ohnishi Y, Inocencio NM *et al*. (1992a) Mammalian subtilisin-related proteinases in cleavage activation of the paramyxovirus fusion glycoprotein: superiority of furin/PACE to PC2 or PC1/PC3. *Journal of Virology* **66**(11): 6391–6397.

Gotoh B, Yamauchi F, Ogasawara T *et al*. (1992b) Isolation of factor Xa from chick embryo as the amniotic endoprotease responsible for paramyxovirus activation. *Federation of European Biochemical Societies Letters* **296**(3): 274–278.

This is a US Government work and is in the public domain in the United States of America.

Gould AR, Kattenbelt JA, Selleck P *et al*. (2001) Virulent Newcastle disease in Australia: molecular epidemiological analysis of viruses isolated prior to and during the outbreaks of 1998–2000. *Virus Research* **77**(1): 51–60.

Huang Z, Elankumaran S, Yunus AS *et al*. (2004) A recombinant Newcastle disease virus (NDV) expressing VP2 protein of infectious bursal disease virus (IBDV) protects against NDV and IBDV. *Journal of Virology* **78**(18): 10054–10063.

Huang Z, Krishnamurthy S, Panda A *et al*. (2003) Newcastle disease virus V protein is associated with viral pathogenesis and functions as an alpha interferon antagonist. *Journal of Virology* **77**(16): 8676–8685.

Khan TA, Rue CA, Rehmani SF *et al*. (2010) Phylogenetic and biological characterization of Newcastle disease virus isolates from Pakistan. *Journal of Clinical Microbiology* **48**(5): 1892–1894.

Kim LM, King DJ, Curry PE *et al*. (2007a) Phylogenetic diversity among low virulence Newcastle disease viruses from waterfowl and shorebirds and comparison of genotype distributions to poultry-origin isolates. *Journal of Virology* **81**(22): 12641–12653.

Kim LM, King DJ, Suarez DL *et al*. (2007b) Characterization of class I Newcastle disease virus isolates from Hong Kong live bird markets and detection using real-time reverse transcription-PCR. *Journal of Clinical Microbiology* **45**(4): 1310–1314.

King DJ (1993) Newcastle disease virus passage in MDBK cells as an aid in detection of a virulent subpopulation. *Avian Diseases* **37**(4): 961–969.

Lamb RA, Collins PL, Kolakofsky D *et al*. (2005) Family Paramyxoviridae. In: Fauquet CM, Mayo MA and Maniloff J *et al*. (eds) *Virus Taxonomy, Eighth Report of the International Committee on Taxonomy of Viruses*, pp. 655–668. San Diego: Elsevier Academic Press.

Liu H, Wang Z, Wang Y *et al*. (2008) Characterization of Newcastle disease virus isolated from waterfowl in China. *Avian Diseases* **52**(1): 150–155.

Marcos F, Ferreira L, Cros J *et al*. (2005) Mapping of the RNA promoter of Newcastle disease virus. *Virology* **331**(2): 396–406.

Meulemans G, van den Berg TP, Decaesstecker M *et al*. (2002) Evolution of pigeon Newcastle disease virus strains. *Avian Pathology* **31**(5): 515–519.

Millar NS, Chambers P and Emmerson PT (1986) Nucleotide sequence analysis of the haemagglutinin–neuraminidase gene of Newcastle disease virus. *Journal of General Virology* **67** (part 9): 1917–1927.

Millar NS, Chambers P and Emmerson PT (1988) Nucleotide sequence of the fusion and haemagglutinin–neuraminidase glycoprotein genes of Newcastle disease virus, strain Ulster: molecular basis for variations in pathogenicity between strains. *Journal of General Virology* **69**(part 3): 613–620.

Miller PJ, Afonso CL, Spackman E *et al*. (2010a) Evidence for a new avian paramyxovirus serotype-10 detected in rockhopper penguins from the Falkland islands. *Journal of Viroloy* **84**(21): 11496–11504.

Miller PJ, Decanini EL and Afonso CL (2010b) Newcastle disease: evolution of genotypes and the related diagnostic challenges. *Infection, Genetics and Evolution* **10**(1): 26–35.

Miller PJ, Estevez C, Yu Q *et al*. (2009a) Comparison of viral shedding using inactivated and live Newcastle disease vaccines formulated with wild-type and recombinant viruses. *Avian Diseases* **53**(2): 39–49.

Miller PJ, Kim LM, Ip HS *et al*. (2009b) Evolutionary dynamics of Newcastle disease virus. *Virology* **391**(1): 64–72.

Nagai Y, Klenk HD and Rott R (1976) Proteolytic cleavage of the viral glycoproteins and its significance for the virulence of Newcastle disease virus. *Virology* **72**(2): 494–508.

OIE (2010) Terrestrial animal health code. *Newcastle Disease*, vol. 2, Section 10, article 10.13.1. OIE, Paris. http://web.oie.int/eng/normes/mcode/en_chapitre_1.10.13.htm#rubrique_maladie_de_newcastle_inactivation

Panda A, Elankumaran S, Krishnamurthy S *et al*. (2004) Loss of N-linked glycosylation from the hemagglutinin–neuraminidase protein alters virulence of Newcastle disease virus. *Journal of Virology* **78**(10): 4965–4975.

Park MS, Shaw ML, Munoz-Jordan J *et al*. (2003) Newcastle disease virus (NDV)-based assay demonstrates interferon-antagonist activity for the NDV V protein and the Nipah virus V, W, and C proteins. *Journal of Virology* **77**(2): 1501–1511.

Peeters BP, de Leeuw OS, Koch G *et al*. (1999) Rescue of Newcastle disease virus from cloned cDNA: evidence that cleavability of the fusion protein is a major determinant for virulence. *Journal of Virology* **73**(6): 5001–5009.

Perozo F, Marcano R, Afonso Cl *et al*. (2011) *Genotype VII Velogenic Viscerotropic Venezuelan Newcastle Disease Virus Isolate: Live (Avinew®) and Killed (Gallimune ND®) Vaccination. Southern Conference Avian Diseases*. Atlanta, GA, USA: SCAD.

Romer-Oberdorfer A, Mundt E, Mebatsion T *et al*. (1999) Generation of recombinant lentogenic Newcastle disease virus from cDNA. *Journal of General Virology* **80**(part 11): 2987–2995.

Rout SN and Samal SK (2008) The large polymerase protein is associated with the virulence of Newcastle disease virus. *Journal of Virology* **82**(16): 7828–7836.

Rue CA, Susta L, Brown CC *et al*. (2010) Evolutionary changes affecting rapid diagnostic of 2008 Newcastle disease viruses isolated from double-crested cormorants. *Journal of Clinical Microbiology* **48**(7): 2440–2448.

Samson AC, Levesley I and Russell PH (1991) The 36K polypeptide synthesized in Newcastle disease virus-infected cells possesses properties predicted for the hypothesized 'V' protein. *Journal of General Virology* **72**(part 7): 1709–1713.

Sleeman J (2010) Summary of 2010 Newcastle disease virus outbreaks in wild birds in upper Midwest and Northeast. *Wildlife Health Bulletin* #2010-07. U.N. Wildlife. http://www.nwhc.usgs.gov/publications/wildlife_health_bulletins/WHB_2010_07_Newcastle_Summary.pdf

Steward M, Vipond IB, Millar NS *et al*. (1993) RNA editing in Newcastle disease virus. *Journal of General Virology* **74**(part 12): 2539–2547.

Ujvari D (2006) Complete nucleotide sequence of IT-227/82, an avian paramyxovirus type-1 strain of pigeons (*Columba livia*). *Virus Research* **32**(1): 49–57.

USDA (2008) *Animals and Plant Products. Possession, Use and Transfer of Select Agents and Toxins*. Animal and Plant Health Inspection Service, United States Department of Agriculture, Washington, DC. 9CFR, part 121, section 3b, 818.

Veits J, Wiesner D, Fuchs W *et al*. (2006) Newcastle disease virus expressing H5 hemagglutinin gene protects chickens

This is a US Government work and is in the public domain in the United States of America.

against Newcastle disease and avian influenza. *Proceedings of the National Academy of Science of the USA* **103**(21): 8197–8202.

Villar E and Barroso IM (2006) Role of sialic acid-containing molecules in paramyxovirus entry into the host cell: a minireview. *Glycoconjugate Journal* **23**(1–2): 5–17.

Wan HQ, Chen LG, Wu LL *et al*. (2004) Newcastle disease in geese: natural occurrence and experimental infection. *Avian Pathology* **33**(2): 216–221.

Wise MG, Suarez DL, Seal BS *et al*. (2004) Development of a real-time reverse transcription PCR for detection of newcastle disease virus RNA in clinical samples. *Journal of Clinical Microbiology* **42**(1): 329–338.

Yan Y, Rout SN, Kim SH *et al*. (2009) Role of untranslated regions of the hemagglutinin–neuraminidase gene in replication and pathogenicity of newcastle disease virus. *Journal of Virology* **83**(11): 5943–5946.

Further Reading

Alexander DJ (2001) Gordon memorial lecture. Newcastle disease. *British Poultry Science* **42**(1): 5–22.

Alexander DJ, Cross GM, Higgins DA *et al*. (1988) *Developments in Veterinary Virology: Newcastle Disease*, pp. 1–365. Boston: Kluwer Academic Publishers.

Lamb RA and Parks GD (2009) Paramyxoviridae: the viruses and their replication. In: Fields BN, Knipe DM and Howley PM (eds) *Field's Virology*, 5th edn, pp. 1449–1496. Philadelphia: Lippincott, Williams and Wilkins.

This is a US Government work and is in the public domain in the United States of America.

JOURNAL OF VIROLOGY, July 2011, p. 6832–6843 Vol. 85, No. 14
0022-538X/11/$12.00 doi:10.1128/JVI.00609-11
Copyright © 2011, American Society for Microbiology. All Rights Reserved.

A Reassortment-Incompetent Live Attenuated Influenza Virus Vaccine for Protection against Pandemic Virus Strains▽

Rong Hai,[1] Adolfo García-Sastre,[1,2,3] David E. Swayne,[4] and Peter Palese[1,3]*

Department of Microbiology,[1] Institute of Global Health and Emerging Pathogens,[2] and Department of Medicine, Division of Infectious Diseases,[3] Mount Sinai School of Medicine, New York, New York, and USDA-ARS, Southeast Poultry Research Laboratory, Exotic and Emerging Avian Viral Diseases Research Unit, Athens, Georgia 30605-2195[4]

Received 27 March 2011/Accepted 26 April 2011

Although live-attenuated influenza vaccines (LAIV) are safe for use in protection against seasonal influenza strains, concerns regarding their potential to reassort with wild-type virus strains have been voiced. LAIVs have been demonstrated to induce enhanced mucosal and cell-mediated immunity better than inactivated vaccines while also requiring a smaller dose to achieve a protective immune response. To address the need for a reassortment-incompetent live influenza A virus vaccine, we have designed a chimeric virus that takes advantage of the fact that influenza A and B viruses do not reassort. Our novel vaccine prototype uses an attenuated influenza B virus that has been manipulated to express the ectodomain of the influenza A hemagglutinin protein, the major target for eliciting neutralizing antibodies. The hemagglutinin RNA segment is modified such that it contains influenza B packaging signals, and therefore it cannot be incorporated into a wild-type influenza A virus. We have applied our strategy to different influenza A virus subtypes and generated chimeric B/PR8 HA (H1), HK68 (H3), and VN (H5) viruses. All recombinant viruses were attenuated both *in vitro* and *in vivo*, and immunization with these recombinant viruses protected mice against lethal influenza A virus infection. Overall, our data indicate that the chimeric live-attenuated influenza B viruses expressing the modified influenza A hemagglutinin are effective LAIVs.

Influenza A viruses (IAV), members of the *Orthomyxoviridae* family of negative-strand RNA viruses, are formidable pathogens, causing significant morbidity and mortality worldwide (18). Seasonal epidemics caused by slight permutations in the antigenic regions of the viral surface proteins kill thousands of people each year in the United States (18). Pandemic-scale influenza A virus disease occurs when the reassortment of genomic segments between different virus subtypes results in a virus that is virulent in humans and that is antigenically novel in the human population (18). During the last 100 years, there have been four global pandemics: the 1918 Spanish pandemic (H1N1 subtype), the 1957 Asian pandemic (H2N2 subtype), the 1968 Hong Kong pandemic (H3N2subtype), and the 2009 swine-origin flu (H1N1 subtype). Among those, the most devastating outbreak was the 1918 pandemic, which claimed the lives of an estimated 100 million people worldwide (1). Sixteen different influenza A virus hemagglutinin (HA) subtypes have been identified (7, 29); however, most modern humans have been exposed to only two to three of those subtypes (H1, H2, and H3); this limited immune exposure is concerning, since a virus from any of the other 13 to 14 subtypes that gained the ability to transmit and cause disease in humans would not be controlled by existing human immunity (11). The severe disease in humans caused by sporadic primary transmission events of H5 highly pathogenic influenza A viruses (HPAI) highlights the threat that novel subtypes pose to the human population (3, 23).

Vaccination is still the best means of protection from influenza virus infections (17, 19). There are presently two types of FDA-approved influenza vaccines: an inactivated vaccine and a cold-adapted live-attenuated vaccine. Although the inactivated form has long been the mainstay weapon in the fight against influenza, the live-attenuated influenza vaccine (LAIV) does have several advantages over the inactivated vaccine. The intranasal delivery of the LAIV can induce a broader immunologic response, engaging both enhanced mucosal and cellular immunity. While providing effective and possibly enhanced immunity against influenza disease, serious concerns exist regarding the administration of LAIVs in prepandemic circumstances. Although the risk is low, one cannot exclude the possibility that an attenuated vaccine strain, containing a novel hemagglutinin gene, will recombine with a wild-type virus to generate a fully virulent virus expressing the hemagglutinin from the vaccine strain. Consequently, even though multiple LAIV candidates have been generated and demonstrated to have protective efficacy (4, 13, 15, 22, 24, 28), these live vaccines are not likely to be used in prepandemic situations.

To address this safety concern, we have designed a system for generating reassortment-incapable virus strains that could be used as LAIVs in prepandemic circumstances. Our system is based on a chimeric influenza B/A approach in which a recombinant and attenuated influenza B virus (rIBV) is rescued that expresses a modified ectodomain of the influenza A hemagglutinin (see Fig. 1A and 6A). Previous studies have demonstrated the feasibility of generating recombinant influenza A viruses expressing the hemagglutinin of a B virus (5, 10); there is no known reassortment capability between influenza A and B viruses (8, 12, 14, 26). We have generated three reassortment-incapable viruses using this influenza A/B chi-

* Corresponding author. Mailing address: Department of Microbiology, Mount Sinai School of Medicine, One Gustave Levy Place, New York, NY 10029-6574. Phone: (212) 241-7318. Fax: (212) 722-3634. E-mail: peter.palese@mssm.edu.
▽ Published ahead of print on 4 May 2011.

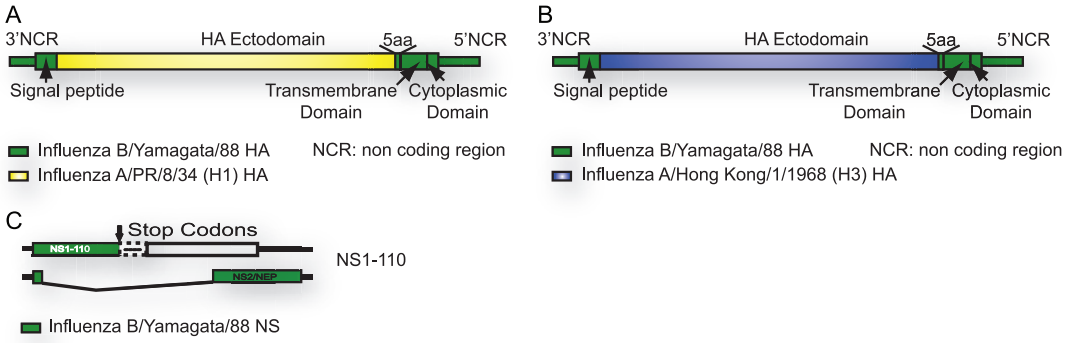

FIG. 1. Schematic design of HA and nonstructural gene (NS) segments used to generate chimeric recombinant influenza B/Ya88 viruses (rIBVs). Diagram of the rIBV expressing the A/PR/8/34 (H1) HA ectodomain (A) and the A/Hong Kong/1/1968 (H3) HA ectodomain (B). The majority of the HA ectodomain was from the influenza A virus, whereas the rest of the HA protein was from the influenza B virus. (C) The truncated form of NS1-110 was generated by the introduction of two stop codons (indicated by the arrow) after the codons corresponding to amino acid 80 or 110 and a deletion of 100 nucleotides (indicated by a dotted box). NCR, noncoding region.

mera strategy in an attenuated influenza B virus background. Our influenza B-based vaccine strains express the hemagglutinin from either the H1 or H3 hemagglutinin or the hemagglutinin from a prototypic H5 subtype influenza A virus.

The recombinant viruses generated demonstrate attenuated growth *in vitro* and are not pathogenic in mice. Further, the immunization of mice with the chimeric A/B viruses provided protective immunity against disease caused by the homologous influenza A virus. We suggest that a robust human vaccine against H5 or other potential pandemic subtypes (16) can be generated using this novel replication-incompetent live-attenuated vaccine system.

MATERIALS AND METHODS

Cells and viruses. 293T and Madin-Darby canine kidney (MDCK) cells were obtained from the American Type Culture Collection (ATCC; Manassas, VA) and maintained in Dulbecco's modified Eagle's medium (DMEM) and minimal essential medium (both from Gibco, Carlsbad, CA), respectively, supplemented with 10% fetal calf serum (HyClone, Logan, UT) and 1% penicillin-streptomycin (Gibco). The MDCK cell line, expressing both green fluorescent protein-chloramphenicol acetyltransferase (GFP-CAT) and firefly luciferase under the control of the beta interferon (IFN-β) promoter (MDCK pIFNβ), was maintained in the medium containing 1 mg of hygromycin B/ml and 2 mg of Geneticin/ml (9).

All recombinant influenza B viruses used in these experiments were propagated in 8-day-old embryonated chicken eggs for 3 days at 33°C (9). All recombinant influenza A viruses were propagated in 8-day-old embryonated chicken eggs for 2 days at 37°C.

Construction of plasmids. The reverse-genetic plasmids used for generating influenza B viruses were constructed in our previous study (9). The plasmids encoding the chimeric A/B HAs were derivatives of the corresponding wild-type (WT) A/HA segment. Briefly, the chimeric pDZ-B/VN HA was constructed by swapping the A/VN/1203 hemagglutinin (without a polybasic cleavage site) into the B/HA sequence using QuikChange XL site-directed mutagenesis (see Fig. 6A). A similar strategy was applied to construct the plasmids for pDZ-B/PR8 HA and pDZ-B/HK68 HA (Fig. 1A and B).

Rescue of recombinant chimeric IBVs. Rescue of influenza B viruses from plasmid DNA was performed as previously described (6, 9). Briefly, for the generation of recombinant B viruses, 293T-MDCK cell cocultures were cotransfected with 1 μg of each of the eight plasmids using Lipofectamine 2000 (Invitrogen, Carlsbad, CA). At 12 h posttransfection, the medium was replaced with Dulbecco's modified essential medium (DMEM) containing 0.3% bovine serum albumin (BSA), 10 mM HEPES, and 1.5 μg/ml TPCK (L-1-tosylamide-2-phenylethyl chloromethyl ketone)-treated trypsin. At 3 days posttransfection, virus-containing supernatant was inoculated into 8-day-old embryonated chicken eggs. Allantoic fluid was harvested after 3 days of incubation at 33°C and assayed for the presence of virus by the hemagglutination of chicken red blood cells and by plaque formation in MDCK cells.

Growth kinetics of recombinant viruses in MDCK cells. To analyze viral replication, confluent IFN-competent MDCK cells were infected at a multiplicity of infection (MOI) of 0.05 and incubated at 33°C in minimal essential medium containing 0.3% BSA and 1.5-μg/ml TPCK-treated trypsin. Viral titers in supernatants were determined by plaque assay on MDCK cells.

Western blotting and indirect immunofluorescence analysis. One well of a six-well dish of confluent MDCK cells was infected (MOI of 2) with the indicated recombinant influenza viruses or mock infected with phosphate-buffered saline (PBS) for 1 h at 33°C. At 15 h postinfection (hpi), cells were lysed in 1× protein loading buffer as described previously (9). The reduced cell lysates were subjected to Western blot analysis by using monoclonal antibody against A/PR8/HA (PY102), A/HK68/HA (12D1), A/VN04/HA (M08), and B/NP (B017), as well as polyclonal antibody against NS1 or monoclonal anti-actin (Sigma, St. Louis, MO). The final Western blotting bands were visualized using an enhanced chemiluminescence protein detection system (PerkinElmer Life Sciences, Boston, MA).

For immunofluorescence analysis, confluent monolayers of MDCK cells on 15-mm coverslips were infected with recombinant viruses at an MOI of 2. At 15 hpi, cells were fixed and permeabilized by treatment with methanol-acetone (ratio, 1:1) at −20°C for 20 min. After being blocked with 1% bovine serum albumin in PBS containing 0.1% Tween 20, cells were incubated for 1 h with a monoclonal antibody directed against A/PR8/HA (PY102), A/HK68/HA (12D1), and A/VN04/HA (M08) as mentioned above. After three washes with PBS containing 0.1% Tween 20, cells were incubated for 1 h with Alexa Fluor 594-conjugated anti-mouse immunoglobulin G (IgG; Invitrogen, Carlsbad, CA). After one additional wash, cells were counterstained with 4′,6′-diamidino-2-phenylindole (DAPI; Invitrogen, Carlsbad, CA). Following the final two washes, infected cells were analyzed by fluorescence microscopy with an Olympus IX70 microscope.

Bioassay to measure IFN production. We used the MDCK pIFNβ cell line to evaluate the levels of IFN produced in cells infected with influenza B viruses. The experimental procedure was adapted from our former study (9). Briefly, six-well dishes of confluent MDCK pIFNβ cells were infected at an MOI of 2 with different recombinant B viruses for 12 h, with PBS as the mock infection control. The expression of GFP was visualized by fluorescence microscopy with an Olympus IX70 microscope. Cell lysates were prepared for luciferase assay.

Mouse immunization and challenge. Eight-week-old female BALB/c mice (Jackson Laboratory, Bar Harbor, ME) were anesthetized with a mixture of ketamine and xylazine administered intraperitoneally and infected intranasally with 10-fold serial dilutions of different rIBVs (in 50-μl volumes) as indicated below. To determine lung virus titers, mice were euthanized at day 3 or 6 postinfection. Lungs were homogenized and resuspended in 1 ml sterile PBS containing 0.3% BSA, and the titers were evaluated on MDCK cells.

Three weeks after immunization, mice were challenged by intranasal infection with the influenza A/PR8 H1N1 virus at 1×10^3 PFU (pathology) or 1×10^2 PFU (virus lung replication), the influenza A/PR8 HK68:HA/NA H3N2 virus at

1×10^6 PFU (pathology) or 5×10^4 PFU (virus lung replication), or the influenza A/PR8 VN:HA/NA H5N1 virus at 5×10^3 PFU (pathology) or 1×10^3 PFU (virus lung titer).

Eight-week-old female C57BL/6 PKR$^{-/-}$ mice were anesthetized and infected intranasally with 10-fold serial dilutions of the recombinant B/VN HA NS1-110 chimeric viruses. Three weeks postimmunization, mice were challenged by intranasal infection with influenza B/Ya88 virus at 1×10^6 PFU.

All animal procedures performed in this study were in accordance with Institutional Animal Care and Use Committee (IACUC) guidelines and have been approved by the IACUC of the Mount Sinai School of Medicine.

Passive immunization and challenge. Eight-week-old BALB/c mice were passively immunized with 200 μl of polyclonal sera from mice previously vaccinated with different recombinant viruses and then lethally challenged with influenza A viruses 24 h later. Survival and body weight loss were monitored for 14 days postchallenge.

Assessment of pathogenicity and infectivity for chickens. The ability of the recombinant wild-type (rWT) B/Ya88 and rIBV-VN04HA to infect or cause disease in chickens was assessed by intranasal and intravenous inoculation studies, respectively, in 4-week-old specific-pathogen-free White Plymouth Rock chickens as previously described (24).

ELISAs and enzyme-linked immunospot (ELISpot) assays. To assess the levels of virus-specific antibodies present in immunized mice, enzyme-linked immunosorbent assays (ELISAs) were performed on diluted serum samples and nasal and lung washes, as described earlier (9). In brief, serum was obtained from mice right before viral challenge and stored at −80°C. We coated 96-well ELISA plates (Immulon4; Dynex, Chantilly, VA) with 50 μl (10 μg/ml) of the appropriate influenza A viruses. After being washed with PBS, coated wells were blocked with PBS containing 1% BSA and then incubated with diluted serum. After 1 h of incubation at room temperature, wells were rinsed with PBS and incubated with a secondary anti-mouse IgG conjugated to peroxidase (Invitrogen, Carlsbad, CA). Rinsed wells were incubated with colorimetric substrate (4-nitrophenyl phosphate; Invitrogen, Carlsbad, CA) for 30 min and read with a plate reader that measured the optical density at 405 nm (OD_{405}; DTX880 multimode detector; Beckman Coulter).

To detect antigen-specific cytotoxic T lymphocytes, we used the ELISpot assay to measure the number of IFN-γ-producing spleen cells in response to stimulation with influenza B/Ya88 viral peptide presented on major histocompatibility complex (MHC) class I, as described previously (25). The assay was performed using an ELISpot kit (R&D Systems). Pooled splenocytes of immunized mice were counted and incubated with anti-CD8 beads (Miltenyi Biotec) in buffer (PBS, pH 7.2, 0.5% BSA, and 2 mM EDTA; degassed for 15 min). CD8$^+$ T cells were purified by adherence and elution from LS MACS columns (Miltenyi Biotec) and then counted. Splenocytes from naïve mice (including antigen-presenting cells) were infected with the rWT at an MOI of 5 for 2 h in a volume of 100 μl, treated with 6 μl of 0.5-mg/ml mitomycin C (Sigma) to stop cell growth, and used to stimulate CD8$^+$ T cells from vaccinated mice. Infected splenocytes (2×10^5) from naïve mice were added to each well. Purified CD8$^+$ T cells (1×10^6, 5×10^5, and 2.5×10^5) from vaccinated mice were added to wells in triplicate. The plate was read using an ELISpot plate reader (Cellular Technology, Ltd.).

RESULTS

Generation of an attenuated recombinant influenza B virus expressing either the PR8 or HK68 hemagglutinin. The truncation of the NS1 protein in both influenza A and B viruses has been shown to significantly attenuate virus growth; NS1-truncated influenza viruses have been developed as candidate live-attenuated influenza vaccines (9, 21, 22). The recombinant influenza B virus with a truncated NS1 protein with a 110-amino-acid final length is currently a promising influenza B vaccine candidate, since it can grow to high titers *in vitro* and has proven safe and protective (9). Using this recombinant influenza B virus possessing a truncated NS1 (rIBV-NS110), we constructed two novel vaccine strains comprising the rIBV-NS110 virus expressing the hemagglutinin ectodomain of two influenza A viruses, A/Puerto Rico/8/34 (rIBV-NS110-PR8HA, H1) and A/Hong Kong/68 (rIBV-NS110-HK68HA, H3).

The segments coding for hemagglutinin in these chimeric viruses retain the signal peptide sequence and the transmembrane and cytoplasmic domains of B/Yamagata/16/88. Of note, we also replaced the last five amino acids of the A virus hemagglutinin ectodomain with those of the sequence from the B virus hemagglutinin. The resulting recombinant viruses are composed of seven genomic segments from B/Yamagata/88 (with a truncated NS1) plus a chimeric eighth segment coding for the influenza A hemagglutinin while retaining regions of the influenza B hemagglutinin segment required for packaging (Fig. 1).

Recombinant influenza B viruses express both truncated NS1 and influenza A hemagglutinin. To determine whether the recombinant viruses express the corresponding influenza A hemagglutinin and the truncated NS1-110 protein, we infected MDCK cells with rIBV-NS110-PR8HA or rIBV-NS110-HK68HA. Mock-infected cells were used as a negative control. At 15 hpi, cells were lysed, the lysates were resolved on an SDS-PAGE gel, and viral proteins were detected by Western blot analysis (Fig. 2A and B). As shown in Fig. 2A, both rIBV-NS110 viruses express the truncated NS1 protein at the expected molecular weight using a polyclonal antibody against the aminoterminal portion of NS1, whereas the rWT B virus expresses the full-length NS1. In addition, both recombinant chimeric viruses express their corresponding influenza A hemagglutinin, with rIBV-NS110-PR8 and rIBV-NS110-HK68 expressing the PR8 hemagglutinin and the HK68 hemagglutinin, respectively. The expression of PR8 hemagglutinin and HK68 hemagglutinin in infected MDCK cells also was analyzed and detected by indirect immunofluorescence, further indicating that the influenza A HAs are indeed expressed in rIBV-NS110-AHA-infected cells (Fig. 2C).

The efficient induction of interferons (IFNs) during viral replication is a hallmark of NS1 truncation mutant viruses of both influenza A and B origins (9, 21). To characterize the IFN induction by rIBV-NS110-AHA viruses, we used the MDCK pIFNβ cell line. MDCK pIFNβ cells were infected with rWT B virus or the two rIBV-NS110-AHA viruses at an MOI of 2, and PBS was used as a negative control. At 15 hpi, we observed significantly higher GFP signals in rIBV-NS110-AHA-infected cells than in either the rWT B virus- or mock-infected cells (data not shown). In addition, rIBV-NS110-AHA infection induced 5-log-higher levels of luciferase activity than those induced by the wild-type B virus and mock infection (Fig. 2D).

rIBV-NS110-AHA viruses are attenuated *in vitro* and *in vivo*. Safety is the primary concern in determining whether chimeric rIBV-NS110 viruses can be used as live-attenuated vaccines. To address this, we first investigated the multistep replication kinetics of rIBV-NS110-AHA in MDCK cells. MDCK cells were infected at an MOI of 0.05, and the virus present in supernatants from infected cells was measured at different time points postinfection by plaque assay on MDCK cells. The growth characteristics of the rIBV-NS110-AHA viruses were different from those of the rWT B virus (Fig. 2E). The peak titer of the rIBV-NS110-PR8HA virus was close to 2 logs lower than that of the rWT B virus, while the peak titer of the rIBV-NS110-HK68HA virus was even lower (Fig. 2E). These observations are consistent with those in our previous study of the influenza B NS1-110 mutant virus (9). In addition, the plaque sizes of the two rIBV-NS110-AHA viruses also were

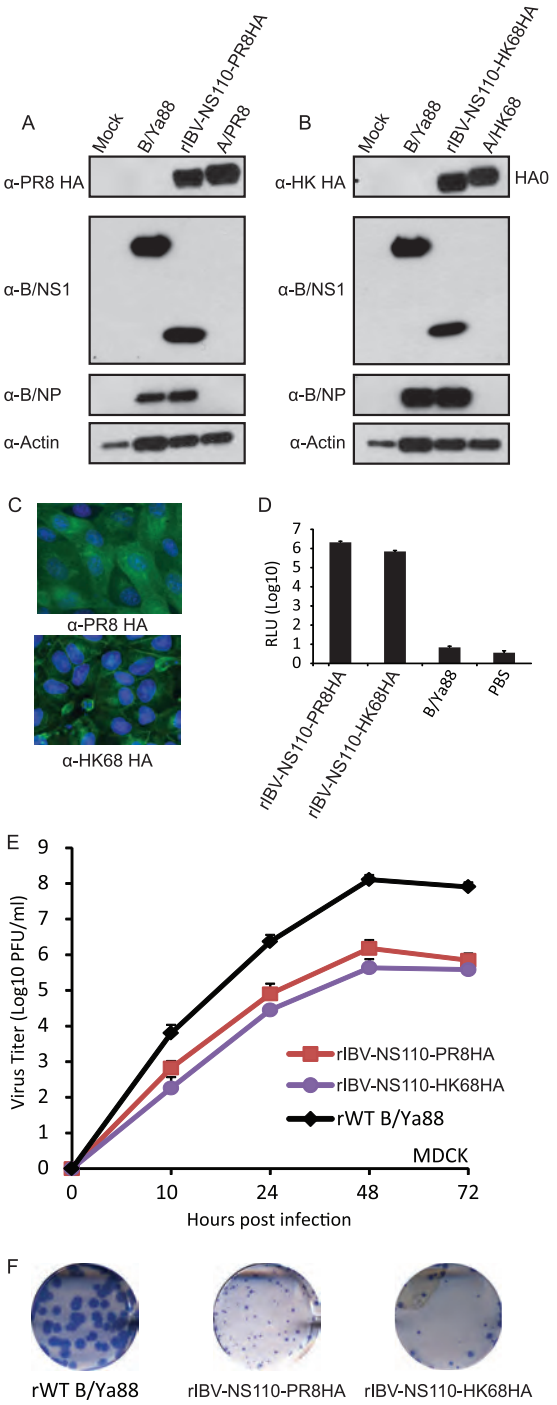

FIG. 2. Characterization of recombinant chimeric influenza B/Yamagata/88 viruses. Western blot analysis of the rIBV-NS110-PR8HA (A) and rIBV-NS110-HK68HA (B). Extracts from MDCK cells mock infected or infected with the indicated viruses (15 hpi) were probed with specific antibodies against PR8 HA (PY102) (α-PR8 HA), HK68 HA (12D1) (α-HK68 HA), B/NS1 (polyclonal antibody) (α-B/NS1), and B/NP (B017) (α-B/NP) to monitor viral infection, and β-actin (α-Actin) was used as an internal loading control. (C) The stable expression of the chimeric hemagglutinin during infection was further assessed by immunofluorescence analysis using either a PR8 HA-specific or an HK68 HA-specific monoclonal antibody. Nuclei were stained with DAPI. IFN-α/β induction by B viruses was evaluated using the MDCK pIFNβ cell line, which expresses the firefly luciferase (FF-Lucif) gene under the control of the IFN-β promoter (9). (D) The cells were infected with the recombinant influenza B viruses. Fifteen hours postinfection, the activation of the IFN-β promoter was determined by assessing firefly luciferase activity. (E) Multicycle growth curves of the recombinant viruses in MDCK cells infected at an MOI of 0.05 and titrated by plaque assay on MDCK cells. (F) Plaque size phenotypes of the chimeric B NS1-110 viruses in MDCK cells at 3 days p.i.

smaller than that of the rWT B virus (Fig. 2F). These results demonstrate that the two recombinant viruses are attenuated *in vitro*.

We next investigated the attenuation of rIBV-NS110-AHA *in vivo* by measuring viral replication in lungs, along with weight loss and survival rates in mice. To evaluate pulmonary viral replication, BALB/c mice were infected with 1×10^5 PFU of recombinant B viruses. As shown in Fig. 3, rIBV-NS110-AHA virus replication in the lungs was 2 to 3 logs lower than that of the rWT B virus at 3 days postinfection. In addition, rIBV-NS110-AHA viruses were cleared more rapidly and were undetectable in the lungs 6 days postinfection. Weight loss is an important index for evaluating influenza virus pathogenicity *in vivo*. We infected BALB/c mice ($n = 4$) intranasally with 10-fold serial dilutions of each recombinant virus (1×10^5 to 1×10^2 PFU) and measured body weight daily for 14 days postinfection. Only mice infected with 1×10^5 PFU of rIBV-NS110-PR8HA lost about 15% of their initial weight at 7 days postinfection, but they eventually regained the weight. The weight loss likely is due to the specific mouse-adapted character of the PR8 hemagglutinin. In summary, both rIBV-NS110-AHAs have an attenuated phenotype *in vitro* and *in vivo*.

Vaccination with rIBV-NS110-AHA elicits an antibody response in BALB/c mice. Antibodies that target the influenza virus hemagglutinin protein are the main protective mechanism against influenza infection and therefore are a critical component of a successful vaccine. To analyze the efficiency of rIBV-NS110-AHAs in inducing a protective humoral response, we evaluated the antibody response following vaccination. Mice were immunized with rIBV-NS110-PR8HA, rIBV-NS110-HK68HA, or rWT B virus, and antibodies in the sera were analyzed by ELISA 21 days postvaccination (Fig. 4). Immunization with rIBV-NS110-PR8HA or rIBV-NS110-HK68HA induced virus HA-specific IgG antibodies in the sera of vaccinated mice (Fig. 4A and B). To further evaluate whether the antibodies could confer protection *in vivo*, we immunized mice with sera from previously vaccinated animals and found that sera from the three highest vaccine dose groups conferred full protection upon challenge with the same dose (1×10^3 PFU) of PR8 virus (Fig. 4C). Sera from the lowest vaccine dose (1×10^2 PFU) could not protect mice from death but did prolong their survival by 3 days compared to that of the control polyclonal sera treatment groups (Fig. 4C).

rIBV-NS110-AHA protects against lethal influenza A virus challenge in BALB/c mice. To determine whether robust antibody response to two influenza A subtypes, H1 and H3, correlated with *in vivo* protection, mice were immunized with rIBV-NS110-PR8HA or rIBV-NS110-HK68HA and challenged with rPR8 or X31 (rPR8 expressing the HA and neuraminidase [NA] of HK68), and lungs were harvested at 3 and

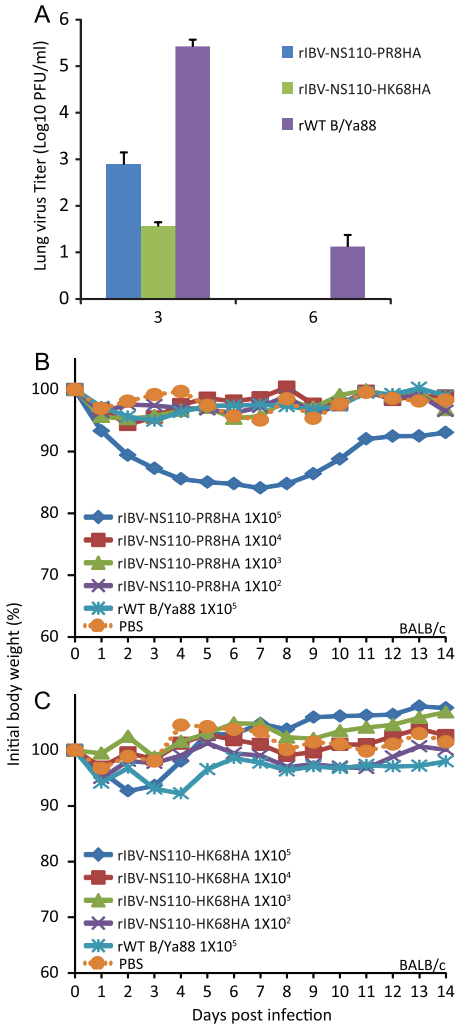

FIG. 3. Pathogenicity of chimeric rIBV-NS110-PR8HA or rIBV-NS110-HK68HA in BALB/c mice. (A) Pulmonary replication of chimeric virus in mice. Average lung titers ± standard deviations are depicted. The limit of detection was 5 PFU. Also shown is the percent change in weight following intranasal (i.n.) infection with 10-fold serial dilutions of rIBV-NS110-PR8HA (B) or rIBV-NS110-HK68HA (C), from 1×10^5 PFU to 1×10^2 PFU. Control mice were intranasally infected with 1×10^5 PFU of rWT B/Ya88 virus or mock treated with PBS.

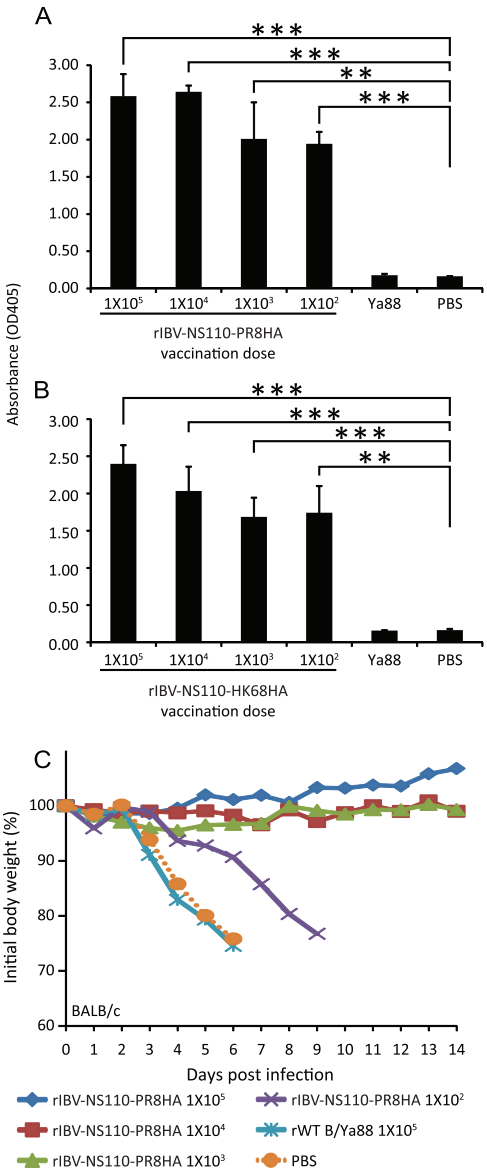

FIG. 4. Mice immunized with chimeric viruses generate influenza A virus-specific antibodies. Eight-week-old female BALB/c mice (n = 3) were immunized with the indicated viruses or with rIBV and PBS as negative controls. Serum samples were collected 21 days postvaccination. Specific IgG antibodies against A/PR8 virus (A) or A/X31 virus (B) were detected by ELISA as described in Materials and Methods. Eight-week-old female BALB/c mice (n = 4) were passively immunized with a total 200 μl of the indicated polyclonal sera (intraperitoneal route) 24 h prior to viral challenge. After antibody administration, the mice were challenged with 1,000 PFU PR8 virus. (C) Body weight of passively immunized mice challenged with PR8 virus. *, $P < 0.05$; **, $P < 0.01$; and ***, $P < 0.001$ versus PBS control).

6 days postchallenge to determine viral burden. Mice immunized with rIBV-NS110-PR8HA and challenged with rPR8 had no detectable virus in the lungs at both 3 and 6 days postinfection (Fig. 5A), whereas control mice (rWT B virus infected or mock treated with PBS) had significant amounts of virus in their lungs. Similarly, mice immunized with rIBV-NS110-HK68HA and challenged with X31 (Fig. 5B) had significantly smaller amounts of virus at day 3 postinfection than control groups and had no detectable virus at 6 days postinfection. These observations indicated that immunization with recombinant chimeric B viruses conferred protection against PR8 and X31 lung infection.

To further evaluate whether the vaccination could deliver full protection to animals against lethal viral infection, mice then were challenged with a lethal dose of either rPR8 or X31. Mice immunized with either rIBV-NS110-PR8HA (Fig. 5C) or rIBV-NS110-HK68HA (Fig. 5D) survived lethal viral challenge without exhibiting any symptoms during the course of 14 days postinfection. In contrast, both the rWT B virus-immunized and mock-immunized mice showed significant weight loss, and all animals succumbed to infection by day 5. Of note, mice immunized with 1×10^2 and 1×10^3 PFU rIBV-NS110-HK68HA lost about 15% of their initial weight in the first 3

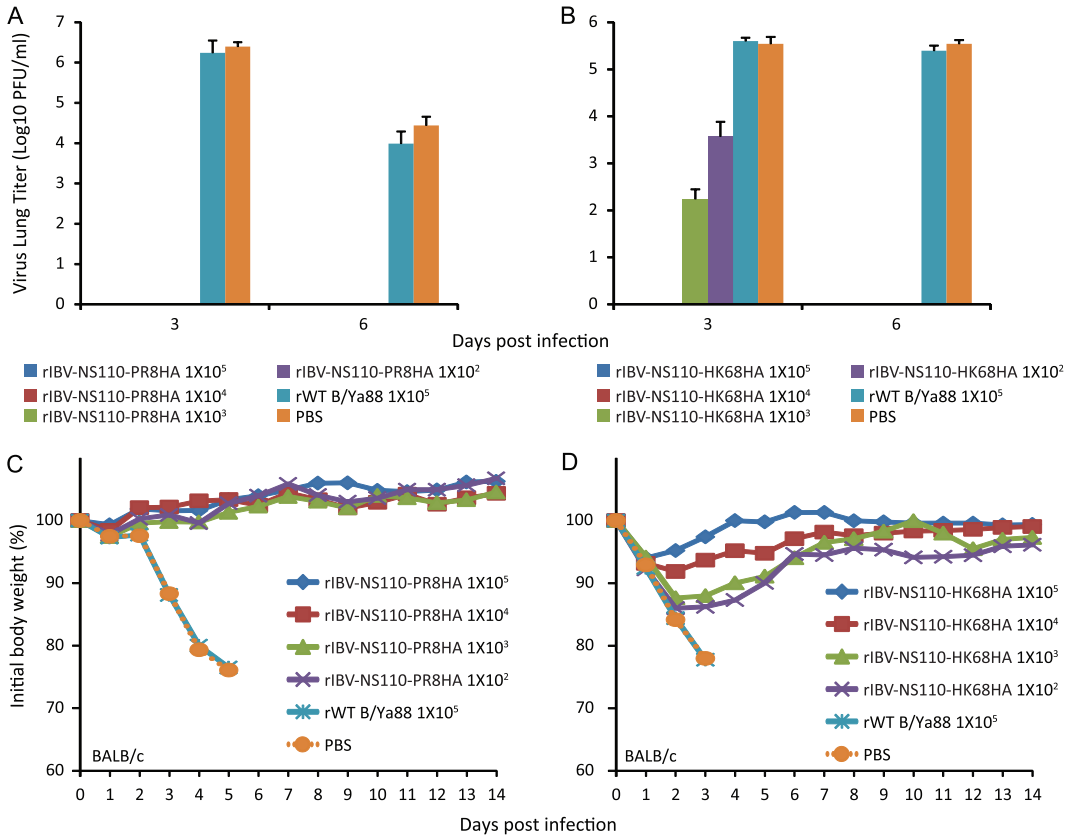

FIG. 5. Vaccination with the chimeric rIBV-NS110-AHA protects BALB/c mice against lethal infection with influenza A virus. Eight-week-old female BALB/c mice ($n = 10$) were vaccinated with 10-fold serial dilutions of rIBV-NS110-PR8HA (A and C) or rIBV-NS110-HK68HA (B and D) (from 1×10^5 PFU to 1×10^2 PFU). Control groups were immunized with 1×10^5 PFU rWT B/Ya88 virus or mock treated with PBS. Three weeks postvaccination, for viral lung replication study the mice were infected with either 1×10^2 PFU of A/PR8 virus ($n = 6$) or 5×10^4 PFU of A/X31 virus ($n = 6$). For stringent viral survival studies, mice were infected with a higher dose of 1×10^3 PFU of A/PR8 virus ($n = 4$) or 1×10^6 PFU of A/X31 virus ($n = 4$). (A and B) The pulmonary replication of influenza A viruses in vaccinated mice on days 3 and 6 p.i. Average lung titers ± standard deviations are depicted. The limit of detection was 5 PFU. (C and D) Animals were monitored for body weight changes and survival for a total of 14 days postchallenge.

days postchallenge but quickly regained their weight after day 4 postinfection. Ultimately, all vaccinated mice survived lethal challenge, whereas all control mice succumbed to lethal challenge with PR8 or X31 around 3 days postinfection.

Generation of rIBV-NS110 expressing the HA of VN04 (H5). Thus far, we have demonstrated the feasibility of using the recombinant influenza B virus possessing a truncated NS1 and an influenza A hemagglutinin as candidate vaccines against two representative influenza A virus subtypes, namely, H1 and H3, which currently are cocirculating in the human population. As shown above, both rIBV-NS110-AHAs are attenuated in growth *in vitro* and apathogenic in mice, and more importantly, they induced an immune response that protects against lethal influenza A virus (H1 and H3) challenge. Because the influenza A virus of the H5 subtype has the potential to cause the next pandemic, we used a similar approach to construct an rIBV-NS110 expressing the ectodomain of A/Vietnam/1203/04 (rIBV-NS110-VN04HA), which is of the H5 subtype (Fig. 6A). We then carried out similar experiments to evaluate rIBV-NS110-VN04HA as a candidate for a prepandemic LAIV.

We first examined the proper expression of the chimeric VN04 hemagglutinin in rIBV-NS110-VN04HA-infected cells. As expected, the VN04 hemagglutinin protein was detected in rIBV-NS110-VN04HA-infected MDCK cells by Western blot analysis and immunostaining assays (Fig. 6B and C), indicating that the recombinant virus properly expresses VN04 hemagglutinin protein. We next examined the ability of rIBV-NS110-VN04HA to induce an IFN response. We observed an increase in GFP expression and an enhancement of firefly luciferase activity in MDCK pIFNβ cells after rIBV-NS110-VN04HA infection compared to those of the controls at 15 hpi (Fig. 6D and E). Thus, our data demonstrate that rIBV-NS110-VN04HA induces an appropriate IFN-β response which is known to be associated with attenuation *in vivo* of NS1-truncated influenza viruses (9, 21, 22).

Growth characteristics of rIBV-NS110-VN04HA virus in cell culture, mice, and chickens. Comparably to the H1 and H3 chimeric viruses, rIBV-NS110-VN04HA grew to a level of about 2 logs less than that of the rWT B virus (Fig. 7A), which translated to smaller plaque sizes (Fig. 7B). We next investigated rIBV-NS110-VN04HA replication characteristics in both BALB/c and C57BL/6 PKR$^{-/-}$ mice. C57BL/6 PKR$^{-/-}$ mice have compromised immunity due to a deficiency in protein kinase R (PKR) and previously have been shown to be an

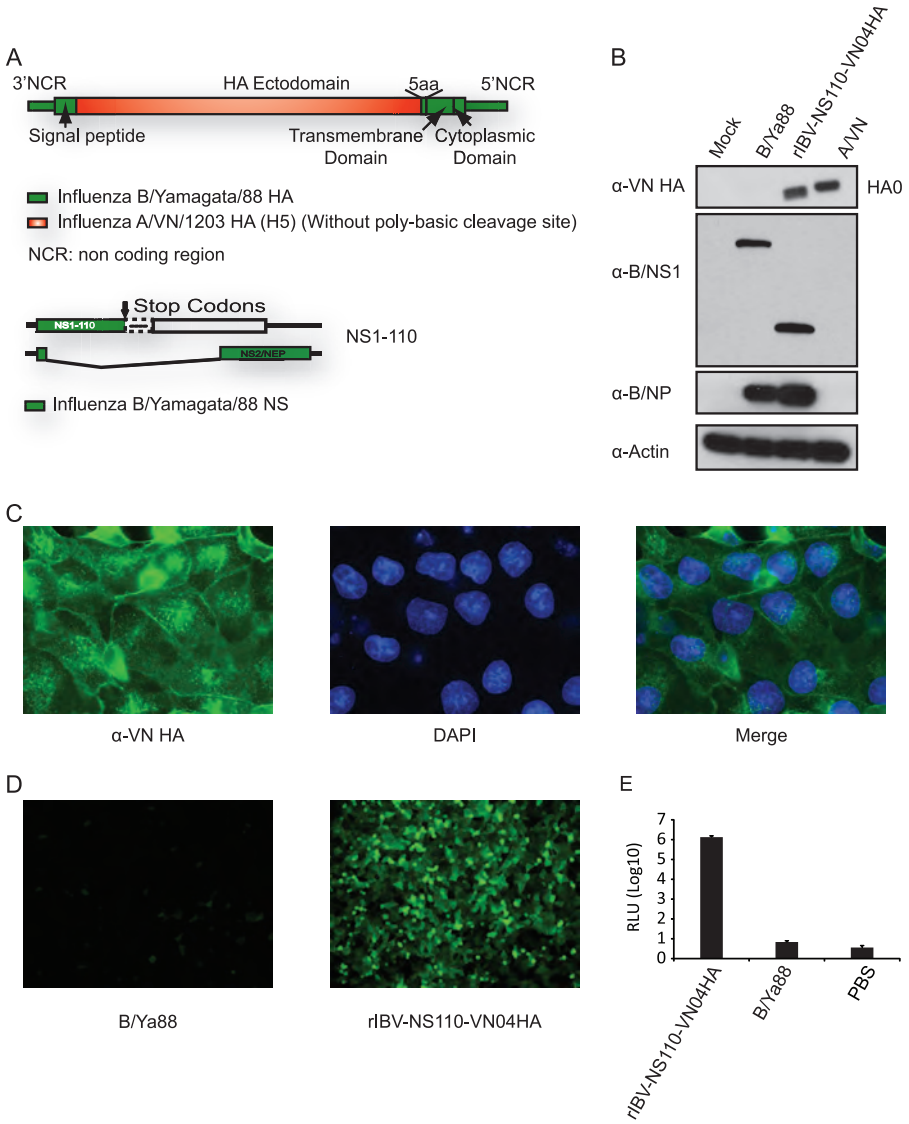

FIG. 6. Characterization of recombinant influenza B/Yamagata/88 viruses expressing VN H5 HA ectodomain (rIBV-NS110-VN04HA). (A) Schematic design of HA and NS segments used to generate rIBV-NS110-VN04HA. The stable expression of chimeric hemagglutinin during infection was monitored by Western blotting (B) and immunofluorescence analysis (C). Extracts from MDCK cells mock infected or infected with the indicated viruses (15 hpi) were probed with specific antibodies against VN HA (M08) (α-VN HA), B/NS1 (polyclonal antibody) (α-B/NS1), and B/NP (B017) (α-B/NP) to monitor viral infection, and β-actin (α-Actin) was used as an internal loading control. (C) Immunofluorescence analysis was performed using a VN HA-specific monoclonal antibody. Nuclei were stained with DAPI. MDCK pIFNβ cells were infected with the recombinant B viruses or mock-treated with PBS to evaluate IFN-α/β induction by rIBV-NS110-VN04HA. Fifteen hours postinfection, the activation of the IFN-β promoter was determined by assessing the GFP expression level (D) and firefly luciferase activity (E).

alternative animal model for studying the pathogenesis and growth kinetics of non-mouse-adapted B virus strains (9). Only about 100 PFU per ml of rIBV-NS110-VN04HA was detected in lung tissues of BALB/c mice 3 days postinfection, which was 3 logs lower than that in rWT B virus-infected mice (Fig. 7C). Only the infection of BALB/c mice with the highest dose (5×10^5 PFU) of rIBV-NS110-VN04HA led to a 10% weight loss in the first 5 days postinfection (Fig. 7E). Similar observations were obtained with C57BL/6 $PKR^{-/-}$ mice. rIBV-NS110-VN04HA viruses replicated at low levels early in the infection and caused no weight loss after 14 days postinfection. In summary, both mouse strains showed no mortality or morbidity after infection with rIBV-NS110-VN04HA, which indicates that this virus is attenuated in mice.

As this is the first time that a hemagglutinin of avian origin is expressed on the B virus background, we tested whether such genetic manipulation of the B virus enabled it to infect chickens. To abolish the potential negative interference from the attenuation brought about by the truncated NS1 protein, we generated an rIBV-VN04HA virus with the wild-type NS1 gene. As shown in Table 1, no morbidity or mortality was observed in chickens infected with either the rWT B virus or the rIBV-VN04HA virus. No viruses were recovered from any intranasally inoculated chicken. Of note, we did detect seroconversion in the chickens

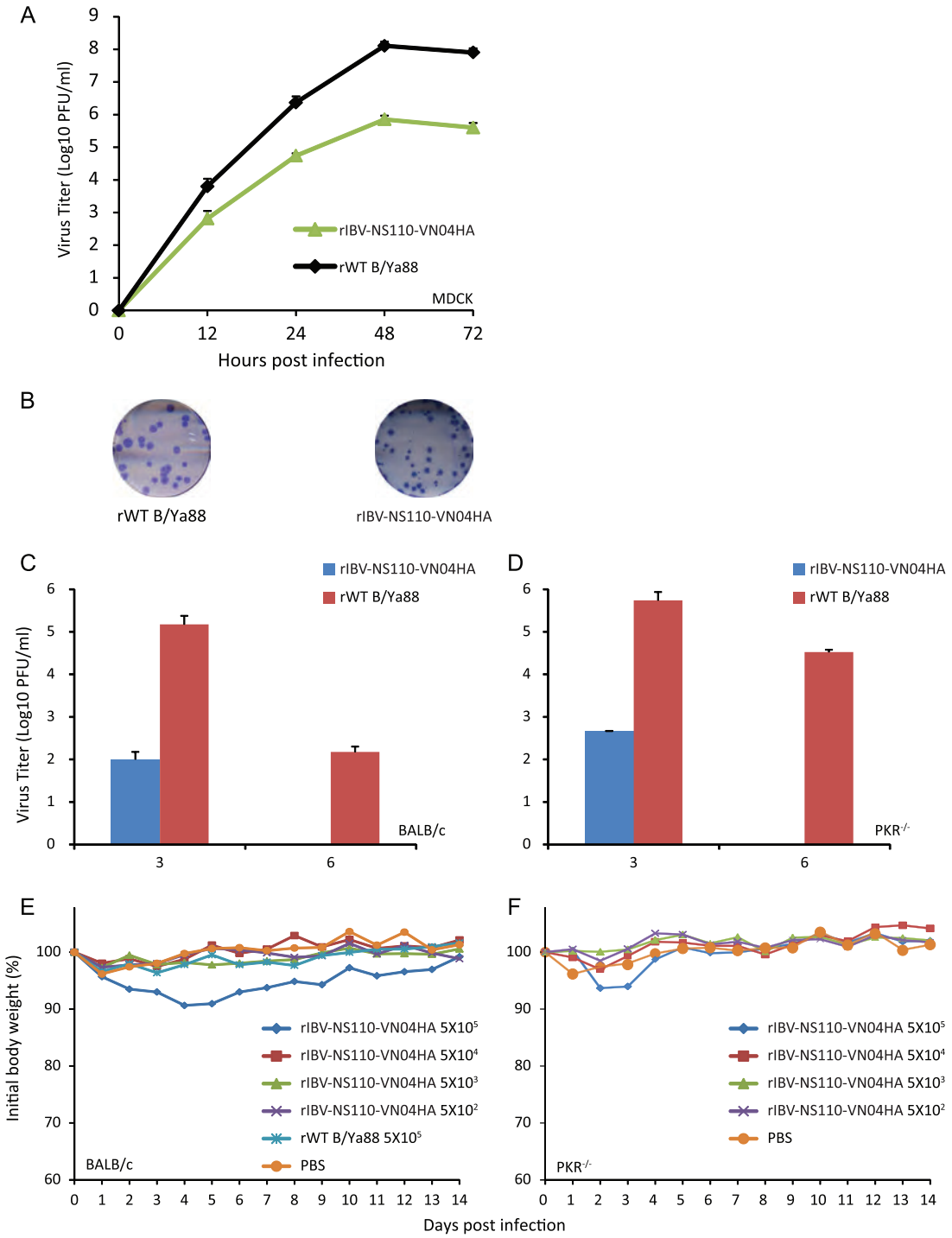

FIG. 7. Chimeric rIBV-NS110-VN04HA is attenuated both *in vitro* and *in vivo*. (A) Multicycle growth curves of the recombinant viruses in MDCK cells infected at an MOI of 0.05 and titrated by plaque assay on MDCK cells. (B) Plaque size phenotypes of the rIBVs in MDCK cells at 3 days p.i. Eight-week-old BALB/c (C) and C57BL/6 PKR$^{-/-}$ (D) mice ($n = 6$) were infected intranasally with 1×10^5 PFU of the indicated viruses. Average lung titers ± standard deviations are depicted. The limit of detection was 5 PFU. Following viral infection, BALB/c (E) and C57BL/6 PKR$^{-/-}$ (F) mice were weighed daily, and the average body weights of surviving animals in each group up to day 14 p.i. are indicated as percentages of the original body weights.

intravenously inoculated with the chimeric B virus (Table 1). Seroconversion also was observed in animals receiving the rWT B virus (Table 1). Thus, we conclude that the rIBV-VN04HA virus is unlikely to cross the species barrier to infect chickens.

Vaccination with rIBV-NS110-VN04HA elicits antibody responses in BALB/c mice. We next wished to evaluate the production of VN HA-specific IgGs in the sera of BALB/c mice immunized with rIBV-NS110-VN04HA. As shown in Fig. 8A,

TABLE 1. Direct assessment of infection of recombinant B viruses in chickens[a]

Virus strain	No. of birds	Route	Morbidity	Mortality	HI serology (GMT)
rWT B/Ya88	5	i.n.	0/5	0/5	1/5 (<8)
rIBV-VN04HA	5	i.n.	0/5	0/5	0/5 (<8)
rWT B/Ya88	10	i.v.	0/10	0/10	10/10 119
rIBV-VN04HA	10	i.v.	0/10	0/10	3/10 (<8)

[a] HI, hemagglutination inhibition assay; GMT, geometric mean titer; i.n., intranasal (i.n. dose, $10^{5.7}$ 50% egg infective doses [EID_{50}]); i.v., intravenous. (i.v. dose, $10^{6.9}$ EID_{50}).

vaccination elicited a significant increase in levels of antibodies against VN hemagglutinin, and antibody titers increased in a dose-dependent manner with the amount of rIBV-NS110-VN04HA administered.

Immunization with rIBV-NS110-VN04HA protects against lethal H5 challenge in BALB/c mice. To evaluate whether vaccination with rIBV-NS110-VN04HA can protect against infection with a potentially pandemic H5 virus, we challenged rIBV-NS110-VN04HA-vaccinated mice with 5×10^3 PFU of an A virus expressing the HA (without the polybasic cleavage site) and NA of VN04 on a PR8 backbone (rPR8-VN04HANA; 50% lethal dose, 316 PFU), which previously has been used in our laboratory as a substitute challenge virus for WT HPAI H5 virus (27).

BALB/c mice were immunized with different doses of rIBV-NS110-VN04HA, rWT B virus, or PBS. At days 3 and 6 postchallenge, three mice per group were euthanized, and their lungs were harvested for the analysis of viral burden. We detected around 10^4 PFU viruses in animals receiving the lowest vaccine dose (5×10^2 PFU) at day 3 postchallenge, which still was 1 log lower than the level in control animals receiving the rWT B virus or PBS (Fig. 8B). At day 6 postchallenge, we did not detect any residual virus from any of the rIBV-NS110-VN04HA-vaccinated animals, whereas 10^5 PFU viruses were detected in the lungs of the two control groups. These results indicate that vaccination with rIBV-NS110-VN04HA can significantly decrease viral burden after challenge with rPR8-VN04HANA. To further evaluate the protection of animals from disease or death, we challenged the vaccinated animals with 5×10^3 PFU of rPR8-VN04HANA. We observed a 5% weight loss in mice immunized with 5×10^3 PFU rIBV-NS110-VN04HA (Fig. 8C). In contrast, all control mice immunized with either rWT B virus or PBS succumbed to viral challenge (Fig. 8C).

Vaccination with rIBV-NS110-VN04HA elicits antibody responses and increases influenza-specific IFN-γ-secreting CD8$^+$ T cells in PKR$^{-/-}$ mice. We measured the humoral response against the rWT B virus in rIBV-NS110-VN04HA-immunized C57BL/6 PKR$^{-/-}$ mice. Similarly to what we observed regarding the humoral response against influenza A viruses in BALB/c mice, the vaccination of C57BL/6 PKR$^{-/-}$ mice induced a potent increase in anti-B virus-specific antibodies (Fig. 9A). In addition, to determine whether rIBV-NS110-VN04HA vaccination induced a CD8$^+$ T-cell response, we also examined the production of IBV-specific CD8$^+$ T cells in immunized C57BL/6 PKR$^{-/-}$ mice. Purified CD8$^+$ T cells were pooled from vaccinated mice ($n = 3$) at 21 days postvaccination and stimulated with splenocytes from naïve mice that were infected *in vitro* with rWT B virus for 2 h (Fig. 9B). We quantified the number of IBV-specific CD8$^+$ T cells using an ELISpot reader and found that the vaccination of C57BL/6 PKR$^{-/-}$ mice with

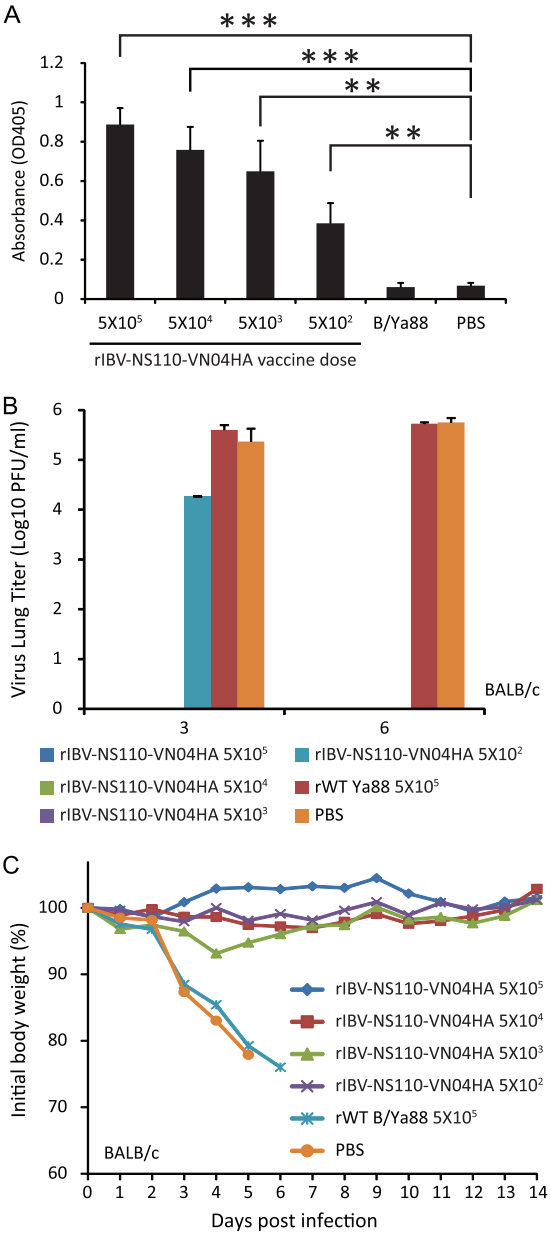

FIG. 8. Vaccination with chimeric A/B viruses protects BALB/c mice from lethal infection with influenza A virus. Eight-week-old female BALB/c mice ($n = 13$) were immunized with the indicated viruses or rWT B/Ya88 virus, and PBS was used as a negative control. Serum samples were collected 21 days postvaccination ($n = 3$). A/PR8 VN HA/NA virus-specific antibodies (A) were detected by ELISA as described in Materials and Methods. The rest of the immunized mice were infected with either 1×10^3 PFU of rPR8-VN04HANA virus for viral lung replication study ($n = 6$) or 5×10^3 PFU of rPR8-VN04HANA virus for pathology study ($n = 4$). (B) Pulmonary viral replication in vaccinated BALB/c mice on days 3 and 6 p.i. Average lung titers ± standard deviations are depicted. The limit of detection was 5 PFU. (C) After viral challenge, animals ($n = 4$) were monitored for body weight changes and survival for a total of 14 days postchallenge. *, $P < 0.05$; **, $P < 0.01$; and ***, $P < 0.001$ versus PBS control.

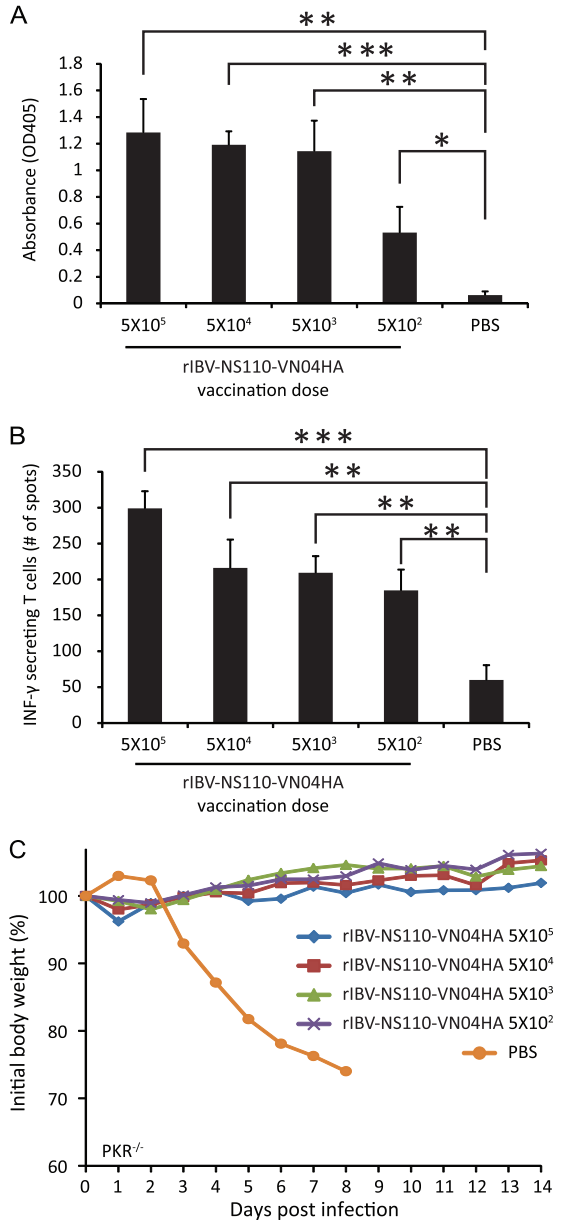

FIG. 9. Vaccination with chimeric A/B viruses protects C57BL/6 PKR$^{-/-}$ mice from lethal infection with the parental influenza B/Ya88 virus. Eight-week-old female C57BL/6 PKR$^{-/-}$ mice (n = 10) were immunized with 10-fold serial dilutions of rIBV-NS110-VN04HA, from 1×10^5 PFU to 1×10^2 PFU, and PBS was used as a negative control. At 21 days postvaccination, serum samples were collected (n = 3). (A) B/Ya88 virus-specific antibodies were detected by ELISA as described in Materials and Methods. CD8$^+$ T cells were isolated from splenocytes (n = 3). (B) Splenocytes from naïve mice were infected with rWT B/Ya88 viruses and used as antigen-presenting cells in an ELISpot assay with CD8$^+$ T cells from vaccinated mice. The experiment was performed in triplicate, and the average number of spots per well ± standard deviations is graphed. In each group, the other four immunized mice per group were infected with 1×10^6 PFU of rWT B virus for pathology study (n = 4). (C) After viral challenge, C57BL/6 PKR$^{-/-}$ mice were monitored for body weight changes and survival for a total of 14 days postchallenge. *, $P < 0.05$; **, $P < 0.01$; and ***, $P < 0.001$ versus PBS control.

rIBV-NS110-VN04HA enhanced the number of CD8$^+$ T cells that recognized B virus peptides (Fig. 9B).

Immunization with rIBV-NS110-VN04HA protects against lethal B virus challenge in PKR$^{-/-}$ mice. Given that influenza B viruses contribute to a large number of influenza cases annually, it would be of practical benefit to have a vaccine that protects against both A and B viruses. To this end, we wished to determine whether our recombinant B virus-based vaccine expressing the ectodomain of an A virus hemagglutinin would have protective efficacy against lethal challenge with IBV. We immunized C57BL/6 PKR$^{-/-}$ mice with different doses of rIBV-NS110-VN04HA and then challenged the mice with 1×10^6 PFU rWT B/Ya88. No weight loss was observed in mice immunized with rIBV-NS110-VN04HA in the 14 days postchallenge, whereas all control animals immunized with PBS succumbed to virus infection before day 8 postinfection (Fig. 9C).

In conclusion, we have shown that mice immunized once with a recombinant B virus expressing an A virus hemagglutinin is able to induce a robust immune response and protect against both influenza A and B virus challenge in mice.

DISCUSSION

Preexposure immunization, either through the use of inactivated vaccines or LAIVs, has been proven to be the most cost-effective method to prevent influenza virus infection (2). With regard to LAIVs, however, the possibility that the hemagglutinin segment from a vaccine strain could reassort with a wild-type circulating IAV would prevent the use of live vaccines in prepandemic scenarios. To address this issue, we propose a different approach in vaccine design by using a recombinant B virus-based LAIV expressing the hemagglutinin of an A virus, which is reassortment incompetent with circulating A viruses. Our vaccine model takes advantage of the fact that there is no known reassortment between influenza A and B viruses; we have incorporated the portion of the influenza A hemagglutinin that is required for the induction of protective immunity into an influenza B virus, and in doing so we have removed the influenza A packaging signals that would enable the incorporation of the gene segment into a wild-type influenza A virus. We show that our design strategy could be applied to multiple influenza A virus subtypes, including two seasonal subtypes (H1 and H3) and one potential pandemic virus subtype (H5).

In light of what has been described, the generation of this recombinant B virus-based LAIV against A viruses has several innovations over the previous generation of LAIVs. The chimeric influenza A/B virus that initially was rescued by Flandorfer at al. grew poorly *in vitro* (5). However, after several passages, it grew to titers comparable to those of wild-type IAV strains. Flandorfer at al. identified one mutation, the most C-terminal amino acid of the IBV HA ectodomain, which was mutated from an IBV-specific histidine back to an IAV-specific tyrosine; that single change appeared to be responsible for the observed enhancement in replication (5). Based on their observations, we designed our chimeric HA segment to include the last five amino acids of the IBV HA ectodomain (Fig. 1 and 6A).

When the chimeric HA segment was inserted into a WT B

virus background, the recombinant influenza B virus containing the chimeric hemagglutinin segment replicated as well as the rWT B virus (data not shown). Although we are not sure why those membrane-proximal amino acids are required for the enhanced replication, there are two possible explanations for this observation: (i) the membrane-proximal amino acids are important for maintaining the stability of the chimeric protein, or (ii) the membrane-proximal amino acids are important for the efficient incorporation of the protein into the viral membrane. Of note, we also attempted to rescue a virus that maintained the membrane-proximal 10 amino acids of the B virus sequence. However, we were not able to rescue that virus. This indicated that the extra five amino acids from the B virus are genetically incompatible with the A hemagglutinin ectodomain. The interaction between these hemagglutinin elements may play a vital role in the expression or stability of the hemagglutinin protein.

The present recombinant viruses are unable to donate their A virus hemagglutinins to influenza A viruses because of the restrictions imposed by the packaging sequences. However, these viruses could accept influenza B virus hemagglutinin genes from circulating wild-type strains. Such reassortant viruses would be comparable to the wild-type strains in circulation.

Even though vaccination with different chimeric B viruses at different doses protected A virus-infected mice from death (Fig. 5 and 8), the data indicated that there were differences in the immunogenicity of the different chimeric B virus vaccines. Immunization with PR8 HA chimeric B virus induced higher IgG antibody responses (Fig. 4A and B) and lower viral replication of the challenge virus in the lung (Fig. 5A and B) than vaccination with HK68 HA chimeric B virus. The difference likely is due to the higher replication capacity of the PR8 HA chimeric virus compared to that of the HK68 HA chimeric virus (Fig. 2E and 3A).

It is interesting that recombinant B viruses expressing an H5 hemagglutinin do not infect chickens productively, indicating that the expression of a single surface protein of an avian A virus on an otherwise B virus backbone does not yield a recombinant virus that has the means to transmit to avian species. This observation underscores the importance of other B virus factors which block a successful infection of species other than humans.

Our serologic and cellular studies indicate that both humoral and cellular immune responses specific for non-hemagglutinin viral proteins, such as the neuraminidase and nucleoprotein, were sufficient to protect mice from lethal rWT B virus infection. A similar observation has been made in an earlier study of influenza A virus (20). It is not clear if this phenomenon would translate to human immunity, since people typically need to be immunized regularly with novel circulating influenza B viruses despite the high conservation of internal genes between seasonal B strains.

In summary, we have designed a live-attenuated vaccine model that might be safely used during prepandemic disease scenarios. Importantly, we also have demonstrated that our reassortment-incapable live vaccine strains can elicit a protective immune response in mice against a potential pandemic influenza virus subtype.

ACKNOWLEDGMENTS

We are grateful to Janice Chen, Gene S. Tan, and Taia T. Wang for helpful discussions and critical reviews. We also thank Lily Ngai for excellent technical assistance. We express our appreciation to John Steel for supplying the construct containing the VN04 hemagglutinin gene without a polybasic cleavage site.

This work was supported by CRIP (Center for Research on Influenza Pathogenesis; NIAID contract HHSN266200700010C) and by the following grants from the NIH: UO1 AI070469, 1RC1 AI086061, P01 AI 058113, and U54 AI057158.

REFERENCES

1. **Basler, C. F., et al.** 2001. Sequence of the 1918 pandemic influenza virus nonstructural gene (NS) segment and characterization of recombinant viruses bearing the 1918 NS genes. Proc. Natl. Acad. Sci. U. S. A. **98:**2746–2751.
2. **Beyer, W. E., A. M. Palache, J. C. de Jong, and A. D. Osterhaus.** 2002. Cold-adapted live influenza vaccine versus inactivated vaccine: systemic vaccine reactions, local and systemic antibody response, and vaccine efficacy. A meta-analysis. Vaccine **20:**1340–1353.
3. **Claas, E. C., et al.** 1998. Human influenza A H5N1 virus related to a highly pathogenic avian influenza virus. Lancet **351:**472–477.
4. **Fan, S., et al.** 2009. Immunogenicity and protective efficacy of a live attenuated H5N1 vaccine in nonhuman primates. PLoS Pathog. **5:**e1000409.
5. **Flandorfer, A., A. Garcia-Sastre, C. F. Basler, and P. Palese.** 2003. Chimeric influenza A viruses with a functional influenza B virus neuraminidase or hemagglutinin. J. Virol. **77:**9116–9123.
6. **Fodor, E., et al.** 1999. Rescue of influenza A virus from recombinant DNA. J. Virol. **73:**9679–9682.
7. **Fouchier, R. A., et al.** 2004. Avian influenza A virus (H7N7) associated with human conjunctivitis and a fatal case of acute respiratory distress syndrome. Proc. Natl. Acad. Sci. U. S. A. **101:**1356–1361.
8. **Ghate, A. A., and G. M. Air.** 1999. Influenza type B neuraminidase can replace the function of type A neuraminidase. Virology **264:**265–277.
9. **Hai, R., et al.** 2008. Influenza B virus NS1-truncated mutants: live-attenuated vaccine approach. J. Virol. **82:**10580–10590.
10. **Horimoto, T., et al.** 2003. Generation of influenza A viruses with chimeric (type A/B) hemagglutinins. J. Virol. **77:**8031–8038.
11. **Johnson, N. P., and J. Mueller.** 2002. Updating the accounts: global mortality of the 1918-1920 "Spanish" influenza pandemic. Bull. Hist. Med. **76:** 105–115.
12. **Kaverin, N. V., et al.** 1983. Studies on heterotypic interference between influenza A and B viruses: a differential inhibition of the synthesis of viral proteins and RNAs. J. Gen. Virol. **64:**2139–2146.
13. **Li, S., et al.** 1999. Recombinant influenza A virus vaccines for the pathogenic human A/Hong Kong/97 (H5N1) viruses. J. Infect. Dis. **179:**1132–1138.
14. **Mikheeva, A., and Y. Z. Ghendon.** 1982. Intrinsic interference between influenza A and B viruses. Arch. Virol. **73:**287–294.
15. **Min, J. Y., et al.** 2010. A live attenuated H7N7 candidate vaccine virus induces neutralizing antibody that confers protection from challenge in mice, ferrets, and monkeys. J. Virol. **84:**11950–11960.
16. **Nabel, G. J., C. J. Wei, and J. E. Ledgerwood.** 2011. Vaccinate for the next H2N2 pandemic now. Nature **471:**157–158.
17. **Palese, P.** 2006. Making better influenza virus vaccines? Emerg. Infect. Dis. **12:**61–65.
18. **Palese, P., and M. L. Shaw.** 2007. Orthomyxoviridae: the viruses and their replication, p. 1647–1689. *In* D. M. Knipe, P. M. Howley, D. E. Griffin, R. A. Lamb, M. A. Martin, B. Roizman, and S. E. Straus (ed.), Fields virology, 5th ed. Lippincott Williams & Wilkins, Philadelphia, PA.
19. **Palese, P., and A. Garcia-Sastre.** 2002. Influenza vaccines: present and future. J. Clin. Investig. **110:**9–13.
20. **Rangel-Moreno, J., et al.** 2008. B cells promote resistance to heterosubtypic strains of influenza via multiple mechanisms. J. Immunol. **180:**454–463.
21. **Solórzano, A., et al.** 2005. Mutations in the NS1 protein of swine influenza virus impair anti-interferon activity and confer attenuation in pigs. J. Virol. **79:**7535–7543.
22. **Steel, J., et al.** 2009. Live attenuated influenza viruses containing NS1 truncations as vaccine candidates against H5N1 highly pathogenic avian influenza. J. Virol. **83:**1742–1753.
23. **Subbarao, K., et al.** 1998. Characterization of an avian influenza A (H5N1) virus isolated from a child with a fatal respiratory illness. Science **279:**393–396.
24. **Suguitan, A. L., Jr., et al.** 2006. Live, attenuated influenza A H5N1 candidate vaccines provide broad cross-protection in mice and ferrets. PLoS Med. **3:**e360.
25. **Talon, J., et al.** 2000. Influenza A and B viruses expressing altered NS1 proteins: a vaccine approach. Proc. Natl. Acad. Sci. U. S. A. **97:**4309–4314.

26. **Tanaka, T., M. Urabe, H. Goto, and K. Tobita.** 1984. Isolation and preliminary characterization of a highly cytolytic influenza B virus variant with an aberrant NS gene. Virology **135:**515–523.
27. **Wang, T. T., et al.** 2010. Vaccination with a synthetic peptide from the influenza virus hemagglutinin provides protection against distinct viral subtypes. Proc. Natl. Acad. Sci. U. S. A. **107:**18979–18984.
28. **Watanabe, T., S. Watanabe, J. H. Kim, M. Hatta, and Y. Kawaoka.** 2007. Novel approach to the development of effective H5N1 influenza A virus vaccines: use of M2 cytoplasmic tail mutants. J. Virol. **82:**2486–2492.
29. **Webster, R. G., W. J. Bean, O. T. Gorman, T. M. Chambers, and Y. Kawaoka.** 1992. Evolution and ecology of influenza A viruses. Microbiol. Rev. **56:**152–179.

Rev. sci. tech. Off. int. Epiz., 2011, **30** (3), 839-870

Assessment of national strategies for control of high-pathogenicity avian influenza and low-pathogenicity notifiable avian influenza in poultry, with emphasis on vaccines and vaccination

D.E. Swayne [1, 2]*, G. Pavade [1], K. Hamilton [1], B. Vallat [1] & K. Miyagishima [1]

(1) World Organisation for Animal Health (OIE), 12 rue de Prony, Paris 75017, France
(2) World Organisation for Animal Health (OIE) Collaborating Centre for Research on Emerging Avian Diseases, Exotic and Emerging Avian Viral Diseases Research Unit, Southeast Poultry Research Laboratory, Agricultural Research Service, United States Department of Agriculture, 934 College Station Road, Athens, Georgia 30605, United States of America
*Corresponding author

Special thanks to OFFLU, the joint OIE and Food and Agriculture Organization of the United Nations (FAO) animal influenza network of experts and FAO staff for assistance during this research study

Submitted for publication: 29 September 2011
Accepted for publication: 21 October 2011

Summary

Twenty-nine distinct epizootics of high-pathogenicity avian influenza (HPAI) have occurred since 1959. The H5N1 HPAI panzootic affecting Asia, Africa and Eastern Europe has been the largest among these, affecting poultry and/or wild birds in 63 countries. A stamping-out programme achieved eradication in 24 of these epizootics (and is close to achieving eradication in the current H5N2 epizootic in South African ostriches), but vaccination was added to the control programmes in four epizootics when stamping out alone was not effective. During the 2002 to 2010 period, more than 113 billion doses of avian influenza (AI) vaccine were used in at-risk national poultry populations of over 131 billion birds. At two to three doses per bird for the 15 vaccinating countries, the average national vaccination coverage rate was 41.9% and the global AI vaccine coverage rate was 10.9% for all poultry. The highest national coverage rate was nearly 100% for poultry in Hong Kong and the lowest national coverage was less than 0.01% for poultry in Israel and the Netherlands. Inactivated AI vaccines accounted for 95.5% and live recombinant virus vaccines for 4.5% of the vaccines used. Most of these vaccines were used in the H5N1 HPAI panzootic, with more than 99% employed in the People's Republic of China, Egypt, Indonesia and Vietnam. Implementation of vaccination in these four countries occurred after H5N1 HPAI became enzootic in domestic poultry and vaccination did not result in the enzootic infections. Vaccine usage prevented clinical disease and mortality in chickens, and maintained rural livelihoods and food security during HPAI outbreaks. Low-pathogenicity notifiable avian influenza (LPNAI) became reportable to the World Organisation for Animal Health in 2006 because some H5 and H7 low-pathogenicity avian influenza (LPAI) viruses have the potential to mutate to HPAI viruses. Fewer outbreaks of LPNAI have been reported than of HPAI and only six countries used vaccine in control programmes, accounting for 8.1% of the total H5/H7 AI vaccine usage, as compared to 91.9% of the vaccine used against HPAI. Of the six countries that have used vaccine to control LPNAI, Mexico, Guatemala, El Salvador and Italy have been the biggest users. In countries with enzootic HPAI and LPNAI, development and implementation of exit strategies has been difficult.

Keywords

Animal disease – Avian disease – Avian influenza – Avian influenza virus – High-pathogenicity avian influenza – Immunity – Low-pathogenicity avian influenza – Low-pathogenicity notifiable avian influenza – Poultry – Vaccination – Vaccine – Vaccine bank.

Introduction

High-pathogenicity avian influenza (HPAI) and low-pathogenicity notifiable avian influenza (LPNAI) in poultry are reportable to the World Organisation for Animal Health (OIE) by its 178 Member Countries (56). The causal agents of LPNAI are limited to the H5 and H7 haemagglutinin subtypes of low-pathogenicity avian influenza (LPAI) viruses. Reporting HPAI and LPNAI outbreaks is necessary for animal health transparency (to minimise the risk of international disease spread), for fair trade and for the enhancement of our knowledge of the worldwide avian influenza (AI) outbreak situation in animals, which enables the development of effective, common control strategies. Traditionally, HPAI control strategies have used various components, including rapid diagnostics and accurate surveillance, elimination of infected flocks, enhanced biosecurity, and education/training of poultry workers (50). Such combinations of components have been effective in eradicating most outbreaks when implemented to a high level, especially within stamping-out or culling programmes.

Since 1959, there have been 29 HPAI epizootics (45, 59). Twenty-four have been handled with stamping-out strategies without vaccination, which has resulted in eradication. However, the largest HPAI epizootic or, more appropriately, panzootic of the last 50 years has been the H5N1 HPAI that emerged in the People's Republic of China (hereafter referred to as China), first reported in 1996, and has since spread to poultry and wild birds in 63 countries or regions (16, 60). In many of these countries, the H5N1 HPAI poultry outbreaks have been eradicated through traditional stamping-out programmes but, in some countries, stamping out alone has not achieved infection control or eradication. Thus, vaccination has been added as an additional control component to maintain rural livelihoods and reduce the number of clinical outbreaks.

The number of H5/H7 LPNAI outbreaks since 1959 remains unknown because LPNAI was not an OIE-listed disease before 2006. Low-pathogenicity notifiable AI became reportable because of the unpredictable ability of H5 and H7 LPAI viruses to mutate and become HPAI viruses, as occurred in the United States of America (USA) in 1983 (H5N2), Mexico in 1994 (H5N2), Italy in 1999 (H7N1), Chile in 2002 (H7N3) and Canada in 2004 and 2007 (H7N3) (47). Thus, H5 and H7 LPAI viruses were unique and needed special status for surveillance, control and eradication in poultry, as compared to non-H5/H7 LPAI viruses, hence their reclassification as LPNAI viruses.

Vaccination has been used as a tool to control and eradicate multiple subtypes of LPAI in poultry since the late 1970s, with the licensing and use of oil-emulsified inactivated AI vaccines (48). Most recently, vaccines have been used against H5 and H7 LPNAI in the USA, Italy, Mexico, Guatemala and El Salvador, with and without controlled slaughter (3, 48, 53). The latter three countries have used both oil-emulsified inactivated AI vaccines and recombinant fowl poxvirus-vectored vaccine with an H5 AI gene insert. For HPAI, the first field uses of poultry vaccination were in Mexico against H5N2 HPAI (1995) (53) and Pakistan against H7N3 (1995) (35). Vaccination for H5N1 HPAI was first implemented during 2002 in Hong Kong and soon thereafter in Indonesia and China (2004) (48). Poultry vaccination programmes against H5N1 HPAI have been reported in Russia, Egypt, the Netherlands, France, Vietnam and Pakistan (48). The current study examines the control components used in HPAI and LPNAI outbreaks from 2002 to 2010 and in current emergency plans, primarily focusing on vaccines and vaccination as a single tool in a comprehensive AI control strategy.

Materials and methods

Questionnaire on avian influenza vaccines and vaccination

A questionnaire survey was conducted, using the official channel of communication between the OIE and its Delegates, in the 80 countries that had reported HPAI and/or LPNAI outbreaks in poultry or wild birds between 2002 and 2010. The objective was to determine what lessons countries have learned from their past experiences in AI control and how they have modified ongoing AI control strategies to improve control and eradication.

The questionnaire was in two formats. A shorter format of 20 questions was sent to 42 countries, focusing principally on overall AI control strategies, with a few questions on AI vaccines and vaccination. A longer format, consisting of the initial 20 questions, plus an additional 17 that focused on how AI vaccines had been used, was sent to 38 countries that had or potentially had used H5 and/or H7 AI vaccines, based on information contained in the OIE World Animal Health Information Database (WAHID), published reports or field intelligence information. This longer-format questionnaire covered various topics, namely: general AI vaccine use policy, AI vaccine bank questions, vaccine usage, vaccination strategy, including exit strategy, and vaccine licensing. The questionnaire was available in English and French versions. The latter was sent to Francophone countries in Europe and Africa. The English version of the questionnaire is available as an appendix at the end of this paper. The responses for each question were grouped and compiled in a database (Access, Microsoft, Seattle, Washington, USA) and for numerical data analysis (Excel, Microsoft, Seattle, Washington, USA). The responses were analysed and interpreted.

Other data sets

The national poultry population data were obtained from one of three sources, in order of preference:

i) the OIE WAHID Interface, Animal Population (59)

ii) staff of the Veterinary Services of individual countries

iii) the statistical database of the Food and Agriculture Organization of the United Nations (FAOSTAT) (15).

From FAOSTAT, national poultry production was calculated by summing the figures of poultry slaughtered for meat (chickens, ducks, geese, guinea fowl, turkeys and others) and poultry for egg production (chickens and others). National poultry density was based on information about stocks of poultry and agricultural land, as obtained from FAO (http://kids.fao.org/glipha/). Poultry data were collected from the WAHID database for HPAI and LPNAI outbreaks and the species of birds affected (59).

Avian influenza vaccine coverage (%) was calculated for selected poultry species in selected countries, based on the data available on doses of vaccine administered (from the current survey), vaccination protocol and poultry production data, generated as above (15). The percentage of coverage was calculated using an estimated average of two doses of vaccine per bird per year if poultry species were not specified or the country did not specify the vaccination programme. If vaccination was conducted only in layers or breeders, three doses were used for annual use calculations.

For selected countries with vaccine usage, Chief Veterinary Officers and their staff, and field veterinarians were interviewed and secondary information was collected to supplement the original questionnaire.

Results and discussion

All countries (short and long questionnaires)

General avian influenza control strategies and components

A total of 69 out of 80 (86%) countries completed and returned the questionnaire. Responses were received from countries on all six inhabited continents:
– Asia (24 countries)
– Africa (10 countries)
– North America (5 countries)
– South America (1 country)
– Europe (28 countries)
– Australia and Oceania (1 country).

Of these 69 countries, 27 (39%) had experienced HPAI outbreaks in poultry only, 11 (16%) experienced HPAI outbreaks in wild birds only and 26 (38%) had HPAI outbreaks in both poultry and wild birds. Five (7%) countries had LPNAI outbreaks only while 14 (20%) had both HPAI and LPNAI outbreaks in poultry. Not all of the 69 responding countries completed every question in the survey.

For all countries, a national AI control programme was in place. The most frequently mentioned components in the plans included:
– quarantine and additional movement restrictions or controls
– tracing poultry in the outbreak area
– enhanced biosecurity measures
– farmer and public education and awareness about the disease
– active and passive surveillance of poultry and wild birds
– monitoring
– rapid diagnostics
– culling (stamping out) of positive cases
– disinfection of facilities and equipment
– decontamination and disposal of infectious materials
– compensation.

Some countries also listed a crisis management framework, high-throughput rapid diagnostic testing, early processing of at-risk non-infected poultry, emergency vaccination and, occasionally, pen-side testing as a screening tool. The criteria for deciding which group of poultry should be culled varied greatly between individual countries (59). For some countries, culling was only practised on infected premises, while other countries also culled dangerous contacts, epidemiologically linked farms or all poultry in a village. Some used a zone approach to culling, covering 0.5, 1 or 3 km in radius. Risk zones were also implemented in some countries, which incorporated varying levels of movement restriction and surveillance.

For HPAI, culling poultry in flocks, farms and villages was consistently used as a method for eliminating infected poultry or those suspected to be infected. For LPNAI, culling and disposal were most frequently used, but some alternatives were practised, including:

– slaughter of unknown/undiagnosed infected commercial poultry without recall of products; time-delayed marketing or controlled slaughter of commercial infected poultry to allow recovery from acute LPNAI virus infections

– quarantine of recovered layer farms with marketing of washed eggs

– release of quarantined egg layer flocks if demonstration of LPNAI virus was negative (59) (data from current survey).

Two developing countries allowed slaughter of clinically normal village poultry and/or commercial poultry that were infected with LPNAI (data from current survey) (59). Seropositive flocks without recovery of the virus or detection of the viral genome have a low risk of disseminating the virus if specific management and biosecurity procedures are used (25). Payment for destruction of such flocks by national governments through compensation programmes is fair to the farmer and causes the lowest risk to animal health, but requires a large outlay of financial and physical resources. However, if compensation is not available, marketing virus-negative flocks that have recovered from LPNAI is of low risk for disease spread to other flocks and to public health, if adequate biosecurity processes are used.

Compensation programmes were present in 48 of 69 (70%) countries and were linked to stamping out of infected flocks. The funding was provided by the government in 41 countries (85%) and via a government/industry partnership in six countries (13%). One country (2%) did not specify a funding source.

Vaccines and vaccination were included as an option for 58% and 39% of the countries in their HPAI and H5/H7 LPNAI control strategies, respectively, with 58% of the countries having written plans with specific criteria for vaccine usage. However, only 14% had actually completed AI vaccine and vaccination simulation exercises or worked out the logistics of implementing a vaccination programme. Table-top exercises were conducted twice yearly in the USA, annually in Australia, and every two years or at unspecified time periods in most other countries. In 2010, Chinese Taipei conducted three table-top exercises. Only 21 countries have used AI vaccine to control HPAI or LPNAI in poultry, eight countries have used vaccine in preventive programmes, 14 in emergency programmes and eight in routine vaccination programmes. Eight countries have used AI vaccines in more than one type of vaccination programme. For example, China initiated an emergency vaccination programme in 2004, vaccinating poultry in buffer zone or outbreak areas, but in late 2005 this was changed to a routine (mass) vaccination programme for all poultry in the country (10).

However, the specific control components were only listed qualitatively as traits, and no assessment was included of the quantitative implementation and practice of each component in the comment section of the questionnaire. In the WAHID database on H5N1 HPAI outbreaks (59), the components listed in control measures were very similar between different countries, but the outcomes varied dramatically: some countries declared the disease to have been eradicated three months after the last flock had been stamped out and the premises disinfected (with the lack of infection attested by proper surveillance [55]), but other countries reported that enzootic infection had become established. Such outcome variations suggest that qualitative implementation of specific components, along with epidemiological, environmental and geographical factors, varied with individual countries, resulting in inconsistency in stopping the spread of the AI virus. This had a severe impact upon the total number of cases and outbreaks and, ultimately, the time it took to control and eradicate the disease.

A companion study indicated that the strength of the country's Veterinary Services, as measured by the scores achieved in an OIE Evaluation of Performance of Veterinary Services (PVS), had an impact on HPAI control; i.e. higher PVS scores were associated with a decreased AI eradication time, mortality rate, culling rate and occurrence of outbreaks (39). In addition, countries that were Members of the Organisation for Economic Co-operation and Development (OECD) had fewer HPAI outbreaks, shorter outbreaks, earlier eradication times, lower poultry mortality rates and higher poultry culling rates than non-OECD countries (39). This indicates that countries that are transparent, and provide adequate funding for the development and maintenance of efficiently performing Veterinary Services, have better control of HPAI.

Avian influenza vaccine and vaccination from 2002 to 2010

Field trials had been conducted with H5 vaccines in 25% and H7 vaccines in 7% of the countries before the implementation of field vaccination programmes or their inclusion in emergency response plans. In field implementation of vaccination, 30% of countries had used vaccines for HPAI control: 16% in poultry, 10% in zoological and other collections of birds and 4% in both categories. By contrast, 12% had used vaccines to control H5/H7 LPNAI and 17% to control non-H5/H7 LPAI but, in both of these virus categories, the vaccine was only used in poultry. For non-H5/H7 LPAI, H9N2 was the most common subtype for which vaccine was used as a control tool, and was reported by ten countries. Vaccine was also used, although to a lesser extent and in a restricted/targeted population or geographic region, against other LPAI subtypes in poultry. They included subtypes causing swine influenza in Canada (H3) and the USA (H1 and H3) in breeder turkeys; H6 in Germany, South Africa (ostrich breeders only) and the USA; and H2, H4 and H10 in the USA. In the USA, the vaccines were mostly used in turkeys, especially turkey breeder hens.

Avian influenza vaccine bank

Vaccination against AI can be used as a preventive, emergency or routine practice in control programmes for HPAI and LPNAI (30). Vaccine banks are a necessary part of any emergency vaccination plan when other disease control measures alone are insufficient to contain the

outbreak. In addition, implementation of an effective emergency vaccination programme also requires fully developed application plans and an understanding of the logistics of a vaccination campaign in the field. Preventive vaccination programmes may take a slightly longer time to implement than emergency vaccination programmes but are most effective when kept small in size and targeted to high-value or high-risk populations, such as genetic stocks of commercial poultry, zoo birds, rare birds or endangered species. Preventive vaccination programmes require less planning in advance than emergency vaccination programmes, but a vaccine bank and some logistical infrastructure may be necessary for rapid implementation, should an outbreak occur in the border area of a neighbouring country. If the HPAI or LPNAI becomes widespread and enzootic, routine vaccination may assist in reducing disease incidence and allow the continuation of poultry production in rural settings, to maintain the livelihoods and food security of the rural poor. A routine vaccination programme requires a steady, direct supply of commercial vaccine and cannot rely upon an emergency AI vaccine bank.

With the spread of H5N1 HPAI from south-east and eastern Asia across central Asia to Eastern Europe, the Middle East and Africa during 2005 to 2006, many countries began to develop emergency vaccination plans and vaccine banks. This development, alongside targeted preventive plans, accelerated with the appearance of dead wild birds infected with H5N1 HPAI virus in Europe during the winter of 2006 (26).

In the survey, 13 countries (19%) reported development of an H5 and/or H7 national AI vaccine bank containing frozen virus (4 of 13), processed antigen (1 of 13) and/or final oil-emulsified product (10 of 13). The vaccines or pre-vaccine products were held by governments (8 of 13), private companies (2 of 13) or both (3 of 13). The seed strains used in the inactivated oil-emulsified vaccines included:

– H5 and H7 LPNAI viruses from previous outbreaks in poultry (H5N2, H5N7, H5N9, H7N2 and H7N3)

– an H5N1 HPAI virus

– an H5N1 classic reassortant LPAI virus with the haemagglutinin gene from an H5 wild waterfowl virus

– reverse-genetic-generated LPAI viruses (two H5N1 viruses and an H5N3 virus).

Ten countries had only H5 in the vaccine bank while three countries had both H5 and H7 vaccines in the bank. The quantity of vaccine ranged from 0.5 to 55 million doses per subtype, but most countries had ≤3.5 million doses of each subtype. Such modest quantities would limit emergency vaccination programmes to zoo birds, endangered bird species and valuable genetic collections of poultry, or targeted vaccination to high-risk poultry groups within a small geographic region. Such a small number of doses would not support a massive or routine vaccination campaign. Many of the first doses in the banks were acquired in 2006 (n = 4), when the risk of introducing the H5N1 HPAI virus from infected migratory wild birds was perceived as high in Europe and western Asia (42). Some countries acquired vaccines for their banks during 2007 (n = 1), 2008 (n = 1), 2009 (n =1) and 2010 (n = 3). The vaccines' expiration dates ranged from one to four years. A few countries indicated that future vaccines would be purchased as rotating stocks from commercial vaccine manufacturers, but most countries did not have plans to purchase replacement vaccines for their bank. Some countries have opted out of vaccine banks, perceiving the cost of replacing and maintaining a vaccine bank to be unsustainable when the perceived risks of introduction from migratory birds have declined and significant improvements have been made in biosecurity for poultry production systems, as well as in rapid diagnostics and surveillance programmes.

The cost of vaccines and vaccination is mainly covered by federal and/or state or provincial governments but, in some countries, the commercial sector has responsibility for vaccine and vaccination costs within private companies. For emergency vaccination in the European Union (EU), 50% of the cost of vaccination is covered by the EU and 100% of the vaccine cost.

In 2006, the OIE set up a regional vaccine bank for AI vaccines in Africa, funded under the EU Pan-African Programme for the Control of Epizootics, and in 2007 it also established a global vaccine bank for AI vaccines

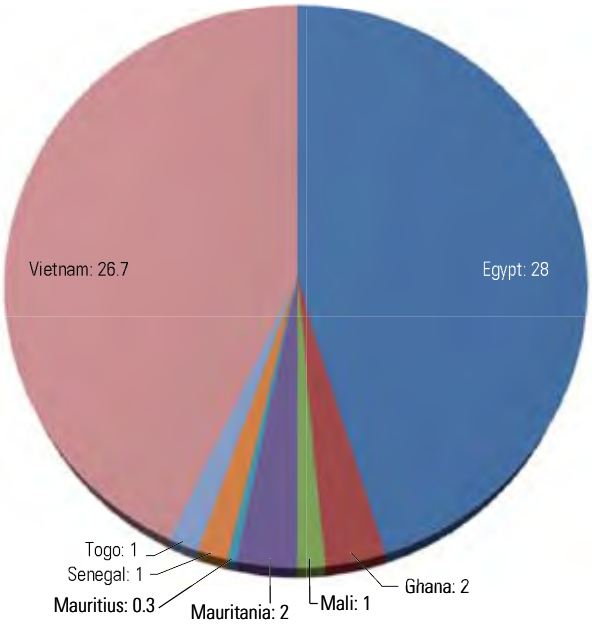

Fig. 1
Countries that used the World Organisation for Animal Health H5N2 avian influenza vaccine bank and number of doses employed

funded by the Canadian International Development Agency (Fig. 1) (58). Only 39 (57%) respondents indicated that they were aware of the OIE H5 vaccine bank. Eight countries obtained vaccine doses from the OIE vaccine bank, totalling 62 million H5N2 doses. The vaccines were provided to Egypt, Ghana, Mali, Mauritania, Mauritius, Senegal, Togo and Vietnam, but Egypt and Vietnam accounted for the majority of the doses: 28 million and 26.7 million doses, respectively (Fig. 1). In Egypt and Vietnam, these AI vaccine doses were used in the field, but the doses provided to the other six countries (7.3 million) have not been used. The OIE AI regional and global vaccine banks are virtual entities.

Thirty-two countries listed several circumstances for potentially using the vaccine bank or AI vaccines in general, including:

– a rapid eradication in poultry not achieved using other measures, including stamping out (28%)

– risk assessments indicating significant and immediate threat of spread, either from a neighbouring country or within the country (19%)

– the presence of enzootic AI in poultry (13%)

– the occurrence of an HPAI outbreak (6%)

– the presence of virus strains with a high risk for zoonotic infection (3%)

– the difficulty of rapidly destroying infected poultry (3%)

– infections in endangered or rare species of birds (3%)

– changes in the international spread pattern of the AI virus (3%)

– structural changes in a country's poultry industries (3%)

– changes in the clinical presentation of the disease (3%).

Factors associated with use or non-use of avian influenza vaccines in control programmes

Fifty-eight countries reported on why they had not used or would not use AI vaccines. The most consistent responses focused on a few common themes:

– traditional control measures, including stamping out, to control and eradicate HPAI and LPNAI in sporadic to widespread outbreaks had proved successful

– there were negative aspects to AI vaccines and vaccination, such as:

i) the potential for silent infections and subclinical shedding of the AI virus

ii) difficulty in identifying infections in a vaccinated population

iii) the high cost of vaccines and their labour-intensive administration, especially when individually injecting birds using inactivated vaccines

iv) the delay in protection for seven to 14 days after administration

v) trade restrictions imposed by importing countries (Table I).

Table I
Responses of 58 countries concerning why they had not or would not use avian influenza vaccines to control high-pathogenicity avian influenza or low-pathogenicity notifiable avian influenza

Reasons for not using vaccines in avian influenza control	Responses
Eradication is possible or has been successful using stamping out and other control measures	24%
Vaccination does not prevent infection and creates clinically silent shedders	22%
Difficulty of differentiating the non-infected from infected birds in vaccinated populations (i.e. DIVA)	17%
High cost of vaccines and vaccination	16%
Vaccination would result in trade restrictions	14%
Presence of small or sporadic outbreaks, or low risk of spread of outbreak	10%
Lack of vaccination plan or policy	9%
No outbreaks or freedom from outbreaks	5%
Seven to 14 days are needed to induce an adequate level of immunological protection in a large poultry population	5%
Vaccination would mask detection of other avian influenza infections	3%
Vaccination in rural sector is difficult due to inability to trace movements of live poultry	3%
Lack of adequate human resources for vaccination	3%
Vaccines have to be injected individually to each bird and some require two doses	2%
Lack of public acceptance	2%
Vaccination promotes enzootic disease	2%
Vaccination results in increased laxity in biosecurity	2%
Vaccination is less efficient than depopulation	2%
Avian influenza outbreak only in low-density poultry production area	2%

By contrast, 45 countries would consider using AI vaccines in the future or had used AI vaccines in the past. Their most consistent reasons for doing so included:

– the inability to control or eradicate an HPAI or LPNAI outbreak using stamping out and other control measures

– a large outbreak with a high risk of spread

– positive aspects of the vaccine, such as:

i) decreasing the susceptibility of poultry to infection

ii) decreasing virus shedding

iii) preventing clinical disease and mortality in birds (Table II).

Long questionnaire only

General vaccine usage

The survey indicated that countries have used H5/H7 AI vaccines in the past eight years (2002–2010) in emergency, preventive and routine vaccination programmes (Tables III to VII). The majority of the countries used AI vaccines in an emergency programme after an outbreak of AI had occurred within the country (80%). Less frequently, some countries used vaccine in a preventive programme before AI had entered their borders (42%), or as routine vaccination after AI became enzootic in their country's poultry population (36%). Countries have vaccinated and/or were vaccinating different types of birds to control or eradicate AI. Most frequently, it was chickens (meat chickens, broiler breeders, egg chickens and layer breeders), ducks (meat ducks and breeder ducks) and turkeys (meat turkeys and turkey breeders) that were vaccinated. However, other poultry species, including meat geese, breeder geese, quail, guinea fowl, pheasants, peacocks, grouse and ostriches, have all been vaccinated. In addition, zoo, hunting, companion, conservation and endangered birds received a minimal quantity of AI vaccine (Table V). The doses used per year, vaccination coverage rates, national poultry populations, and national poultry densities are summarised in Tables III, IV and V for HPAI and in Tables VI and VII for LPNAI.

When it is stated that a country has a vaccination programme for poultry, the general public and public health officials may incorrectly assume that 100% of the poultry within the country have been vaccinated. However, the availability of vaccine and logistics of vaccination dictate how close a country can come to 100% coverage. In addition, many countries do not need mass vaccination campaigns and can target only high-risk poultry for vaccination. The FAO has classified poultry production into four systems, often called sectors. For this study, the authors used the FAO classification system:

– sector 1: high biosecurity, industrial, vertically integrated production

– sector 2: moderate-to-high biosecurity, commercial poultry, non-vertically integrated production, using both slaughterhouses and live markets

Table II
Responses of 45 countries concerning the conditions under which they would consider using or had already used avian influenza vaccines to control high-pathogenicity avian influenza or low-pathogenicity notifiable avian influenza

Reasons for using vaccines in avian influenza control	Responses
Stamping out and other measures not adequate for control	29%
Widespread outbreaks	24%
High risk of spread	13%
To protect valuable birds, such as poultry breeders or endangered bird species	9%
To decrease animal susceptibility through improved immunity	7%
Enzootic disease	7%
To reduce virus shedding and infection pressure	4%
To decrease clinical infections and mortality	4%
In high-risk areas because of neighbouring infections	4%
As low-level support for stamping out by industry or citizens	4%
To control localised infection	2%
Persistence of avian influenza in a population of one species	2%
To prevent low-pathogenicity avian influenza virus from mutating into a high-pathogenicity avian influenza virus	2%
To decrease economic losses	2%
For a geographic 'immunity ring' to prevent spread	2%
Presence of adequate resources for vaccination programme	2%
Animal welfare concerns	2%
Against high-risk zoonotic avian influenza viruses	2%

Table III
Number of doses of H5 or H7 avian influenza vaccine used in poultry against high-pathogenicity avian influenza and the coverage rate for 15 countries from 2002 to 2010

Country	Year	Species	National poultry population (1,000s)[a]	Dose (1,000s)[b]	Subtype	Vaccine coverage (%)	Poultry density (birds/km² of agricultural land)[c]	Global usage (%)
China	2004	Poultry	**e** 14,862,137	5,266,885[d]	H5	17.4	933	
	2005	Poultry	15,203,486	12,889,931[d]	H5	41.6	n/a	
	2006	Poultry	15,544,835	18,905,901[d]	H5	59.6	971	
	2007	Poultry	14,597,919	20,361,127[d]	H5	68.4	985	
	2008	Poultry	15,503,531	22,603,952[d]	H5	71.5	n/a	
	2009	Poultry	**e** 15,971,298	23,687,824[d]	H5	72.8	n/a	
	2010	Not available	**e** 16,439,065	n/a	H5	n/a	n/a	
	Subtotal		**108,122,271**	**103,715,621**		**47.1**	**963**	90.99
Côte d'Ivoire	2006	Broiler & layer breeders & other Galliformes[e]	31,995	8,000	H5	12.5	158	<0.01
Egypt	2006	Poultry	534,060	496,000	H5	43.0	3,633	
	2007	Poultry	598,807	1,235,000	H5	65.2	3,667	
	2008	Poultry	551,154	1,300,000	H5	83.3	n/a	
	2009	Poultry	548,100	1,350,000	H5	75.8	n/a	
	2010	Poultry	**e** 545,046	917,926	H5	82.0	n/a	
	Subtotal		**2,777,167**	**5,298,926**		**69.9**	**3,650**	4.65
France	2006	Meat & breeder ducks & breeder geese	832,049	816	H5	0.05	778	<0.01
Hong Kong	2002	Meat chickens	8,406	1,400	H5	11.1	n/a	
	2003	Meat chickens	10,154	10,400	H5	68.3	124,714	
	2004	Meat chickens	7,821	12,600	H5	107.4	125,000	
	2005	Meat chickens	11,676	18,600	H5	106.2	n/a	
	2006	Meat chickens	9,155	13,700	H5	99.8	148,333	
	2007	Meat chickens	7,273	10,500	H5	96.2	149,167	
	2008	Meat chickens	4,662	6,348	H5	90.8	n/a	
	2009	Meat chickens	3,510	5,793	H5	110.0	n/a	
	2010	Meat chickens	**e** 4,000	6,233	H5	103.9	n/a	
	Subtotal		**66,657**	**85,573**		**86.2**	**136,804**	0.08
Indonesia	2004		**e** 1,266,124	398,000	H5	15.7	2,370	
	2005		1,283,702	443,400	H5	17.3	n/a	
	2006		**e** 1,301,280	402,900	H5	15.5	2,518	
	2007		1,318,858	398,500	H5	15.1	2,703	
	2008		1,526,819	370,000	H5	12.1	n/a	
	2009		1,350,858	300,000	H5	11.1	n/a	
	2010		**e** 1,382,858	330,000	H5	11.9	n/a	
	Subtotal		**9,430,499**	**2,642,800**		**14.0**	**2,530**	2.32
Israel	2006	Ostriches	379,644	6[f]	H5	<0.01	8,470	<0.01
Kazakhstan	2006	Village poultry	58,823	7,000	H5	6.0	12.6	
	2007	Village poultry	67,678	7,000	H5	5.6	n/a	
	2008	Village poultry	62,061	7,000	H5	5.6	n/a	
	2009	Village poultry	73,402	7,000	H5	4.8	n/a	
	2010	Village poultry	78,262	7,000	H5	4.5	n/a	
	Subtotal		**335,226**	**35,000**		**5.2**	**12.6**	0.03

e: estimate based on surrounding years
DPR Korea: Democratic People's Republic of Korea
n/a: not available
a) Population data source: China, Indonesia, and the Netherlands (WAHID, Animal populations); Hong Kong, Mongolia and Russia (Chief Veterinary Officer staff); Côte d'Ivoire, Egypt, France, Israel, Kazakhstan, DPR Korea, Pakistan, Sudan and Vietnam (FAOSTAT); national poultry populations: low <25 million, moderate <250 million, high <2.5 billion, very high ≥2.5 billion
b) Data sourced from current survey questionnaire
c) National poultry density was based on information on poultry/agricultural land (km^2) available from FAO (kids.fao.org/glipha/). National poultry density: low <75, moderate <750, high <7,500, very high ≥7,500 birds/km^2

Table III (cont.)
Number of doses of H5 or H7 avian influenza vaccine used in poultry against high-pathogenicity avian influenza and the coverage rate for 15 countries from 2002 to 2010

Country	Year	Species	National poultry population (1,000s)[(a)]	Dose (1,000s)[(b)]	Subtype	Vaccine coverage (%)	Poultry density (birds/km² of agricultural land)[(c)]	Global usage (%)
DPR Korea[(g)]	2005	Chickens	55,550	2,202	H7	1.98	819	<0.01
Mongolia	2005	Chickens	142	357	H5	83.8	n/a	
	2006	Chickens	212	377	H5	59.3	0.1	
	2007	Chickens	295	475	H5	53.7	0.2	
	2008	Chickens	360	517	H5	47.9	n/a	
	2009	Chickens	399	661	H5	55.2	n/a	
	2010	Chickens	426	412	H5	32.2	n/a	
	Subtotal		**1,834**	**2,799**		**50.9**	**0.2**	<0.01
Netherlands	2006	Hobby poultry and free-range layers	92,584	32	H5	0.02	4,807	
	2007	Hobby poultry and free-range layers	92,763	21	H5	0.01	4,951	
	2008	Hobby poultry and free-range layers	95,129	15	H5	0.01	n/a	
	Subtotal		**280,476**	**68**		**0.01[(h)]**	**4,879**	<0.01
Pakistan	2004	Layers, broiler & layer breeders	434,940	12,100	H7	0.7	701	
	2005	Layers, broiler & layer breeders	443,383	14,100	H7	0.8	n/a	
	2006	Layers, broiler & layer breeders	534,603	21,400	H5/H7	1.0	871	
	2007	Layers, broiler & layer breeders	575,688	21,400	H5/H7	0.9	932	
	2008	Layers, broiler & layer breeders	618,809	21,400	H5/H7	0.9	n/a	
	2009	Layers, broiler & layer breeders	667,662	18,400	H5/H7	0.7	n/a	
	2010	Layers, broiler & layer breeders	**e** 716,515	23,400	H5/H7	0.8	n/a	
	Subtotal		**3,991,600**	**108,800**		**0.8**	**835**	0.12
Russia	2006	Poultry	**e** 372,581	107,000	H5	14.4	164	
	2007	Poultry	**e** 409,429	97,900	H5	12.0	171	
	2008	Poultry	**e** 449,922	82,000	H5	9.1	n/a	
	2009	Poultry	**e** 494,420	79,000	H5	8.0	n/a	
	2010	Poultry	543,319	59,427	H5	5.5	n/a	
	Subtotal		**2,269,671**	**425,327**		**9.4**	**168**	0.37
Sudan	2006	Broilers, layers & broiler & layer breeders	34,576	3,177	H5	4.6	27	
	2007	Broilers, layers, & broiler & layer breeders	36,150	3,149	H5	4.4	26	
	Subtotal		**70,726**	**6,326**		**4.5**	**27**	<0.01
Vietnam	2005	Chickens & ducks	322,590	244,500	H5	63.7	n/a	
	2006	Chickens & ducks	343,696	274,630	H5	67.9	2,129	
	2007	Chickens, ducks & geese	358,000	353,930	H5	75.2	2,243	
	2008	Chickens & ducks	419,100	268,000	H5	49.4	n/a	
	2009	Chickens & ducks	476,700	272,570	H5	42.2	n/a	
	2010	Chickens & ducks	**e** 534,300	212,880	H5	31.1	n/a	
	Subtotal		**2,454,386**	**1,626,510**		**52.3**	**2,186**	1.43
	Total		**131,099,262[(i)]**	**113,982,174[(i)]**		**41.9**		100.00

d) Reported in ml for inactivated avian influenza vaccine and by dose for recombinant vaccines; one dose was 0.5 ml for chickens and 1 ml for ducks and geese. Calculations for coverage rate were based on population distribution of ducks, geese and meat chickens (80%) and egg-type chickens (20%), with two doses for ducks, geese and meat chickens and three doses for egg-type chickens. One exception was Hong Kong where the native breed chicks are smaller than commercial chicks and received 0.25 ml as a first dose (half the manufacturer's recommended dose) and 0.5 ml as the second dose

e) Other Galliformes: quail, guinea fowl, pheasants, peacocks, grouse, etc.

f) 6,020 ostriches on one commercial farm were vaccinated with one dose per bird, 1 ml vaccine per dose

g) Autogenous avian influenza vaccine was used in chickens in DPR Korea against H7N7 high-pathogenicity avian influenza during 2005. Vaccine doses were estimated at two doses per bird and 1,101,000 birds were vaccinated (59). The poultry density was not available for 2005 and was estimated based on the average for the years 2004 and 2006

h) In 2006, 2007 and 2008, 0.27%, 0.14% and 0.07% of the 3 million national hobby poultry population were vaccinated, respectively, compared to <0.01% of the 90–92 million national commercial poultry population over the same period

i) World poultry production 2002–2010 = 520,030,922,000 birds; at-risk population = 25.2% of world poultry production; vaccinated proportion of world's poultry population = 10.9%. Of total vaccines used, 95.5% were inactivated H5 and/or H7 vaccines and 4.5% were live recombinant vaccines

Table IV
Number of doses of H5 and/or H7 vaccine used and vaccine coverage rates for specific poultry categories in Egypt, Pakistan and Vietnam based on available data (2004 to 2009)

Country	Years	Species	Poultry population (1,000s)[(a)]	Dose (1,000s)[(b)]	Vaccine coverage (%)
Egypt	2006–2009	Meat & breeder chickens	1,860,552	1,469,162	78.2
		Meat & breeder ducks	60,000	27,007	15.0
		Meat & breeder geese	40,000	1,686	1.4
		Meat & breeder turkeys	8,105	1,686	10.4
		Other meat poultry & breeders[(c)]	172,000	1,359	0.5
		Layers & layer breeders	91,464	86,715	31.6
		Subtotal	**2,232,121**	**1,587,615**	**67.0**
Pakistan	2004–2009	Broiler & layer breeders	54,000	55,800	25.8
		Layers	474,000	53,000	2.8
		Broilers	2,707,600	0	0.0
		Subtotal	**3,235,600**	**108,800**	**0.8**
Vietnam	2005–2009	Broilers	1,327,890	826,250	51.7
		Meat ducks	322,000	580,380	90.1
		Subtotal	**1,649,890**	**1,406,630**	**58.1**

a) Population data source: Egypt (FAOSTAT, Production, Livestock Primary); Pakistan (FAOSTAT, Production, Livestock Primary); Vietnam – data from current survey for broiler and layer breeders
b) Data sourced from current survey questionnaire
c) Other Galliformes: quail, guinea fowl, pheasants, peacocks, grouse, etc.

– sector 3: minimal-to-low biosecurity, smallholder, commercial, including waterfowl, and sold mainly through live markets

– sector 4: low-to-minimal biosecurity, mainly village and backyard production.

The ease with which a national poultry population can be vaccinated depends on the number of premises and the size of the population. The survey indicated that the more poultry in sectors 1 and 2, the higher the coverage rate, because there are fewer farms to organise for vaccination and, since all aspects of production are integrated, cooperation between management and the farmer is easier. By comparison, if there are more poultry within sectors 3 and 4, which have more premises and independent management systems, there tends to be a lower coverage rate. With both LPNAI and HPAI, most of the world's AI vaccine use occurs in developing and transition countries.

High-pathogenicity avian influenza vaccine use

Chickens, ducks, geese, turkeys and other poultry

Vaccination was first used against HPAI in Mexico during 1995, when 383 million doses of inactivated oil-emulsified vaccine, made from a 1994 precursor H5N2 LPNAI virus, were used (53). The combined use of the vaccine and other control measures were associated with the eradication of the H5N2 HPAI virus by mid-1995 and Mexico's declaration of freedom from HPAI in December 1995 (53). However, the predecessor H5N2 LPNAI virus has continued to circulate in central Mexico, resulting in the continued use of vaccines in the H5N2 LPNAI control programme (Table VI).

The second use of vaccine for HPAI control began in Pakistan in 1995, against H7N3 HPAI (35). This programme used a homologous inactivated HPAI virus in an aqueous vaccine, principally in broiler breeders. However, the greatest use of vaccine for HPAI control has been against the H5N1 HPAI panzootic that began with a first report in domestic geese from Guangdong, China, in 1996, was first detected outside China in 2001 in the live poultry markets of northern Vietnam, and caused large outbreaks in poultry in Indonesia and the Republic of Korea in 2003 (28, 36, 43, 60). After 2003, the H5N1 HPAI virus spread to infect poultry and wild birds in 63 countries on the Asian, African and European continents (16).

From 2002 to 2010, over 113 billion doses of AI vaccine were used in the at-risk poultry population of more than 131 billion birds to protect against H5 or H7 HPAI in 15 countries (Table III). Programmes initiating AI vaccination against the H5N1 panzootic began in 2002 in Hong Kong, 2004 in Indonesia and China, 2005 in the Democratic People's Republic of Korea (DPR Korea), Vietnam and Mongolia, and in 2006 in the nine remaining countries/regions (Table III). The years 2002 to 2005 were growth years for vaccine use, as AI vaccine-manufacturing capacity and inventories increased to meet demand, and vaccination logistics were developed to implement programmes in the field, especially in China (Table III) (Fig. 2). The yearly use of vaccine was at its highest from 2006 to 2009, at over 26 billion doses per year, when all 15 countries had fully implemented vaccine programmes (Fig. 2). The top four users of AI vaccine were China (90.99%), Egypt (4.65%), Indonesia (2.32%) and Vietnam

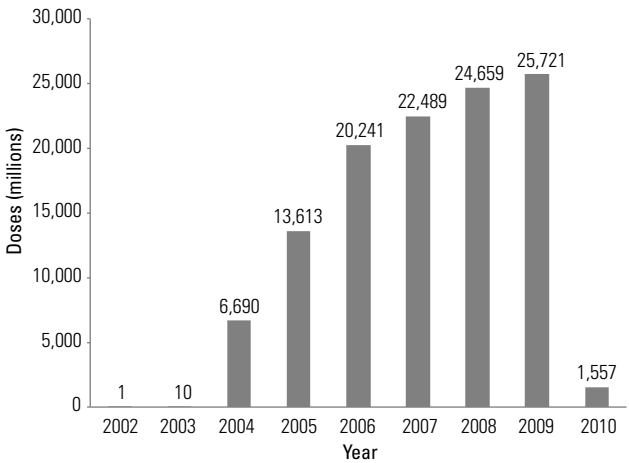

Fig. 2
Number of doses of avian influenza vaccine used between 2002 and 2010 against high-pathogenicity avian influenza
Data for China in 2010 were not available.

(1.43%), all of which had enzootic H5N1 HPAI infections in poultry. The remaining 11 countries had minor usage, accounting for less than 0.7% in total, as follows:
– Russia (0.37%)
– Pakistan (0.12%)
– Hong Kong (0.08%)
– Kazakhstan (0.03%)
– Côte d'Ivoire (<0.01%)
– DPR Korea (<0.01%)
– France (<0.01%)
– Israel (<0.01%)
– Mongolia (<0.01%)
– the Netherlands (<0.01%)
– Sudan (<0.01%).

The majority of vaccine (>99.5%) was used in the ten countries with a high (≥750 birds/km^2) to very high (≥7,500 birds/km^2) national poultry density, while less than 0.5% was used in the five countries with a moderate (<750 birds/km^2) to low (<75 birds/km^2) national poultry density.

Five countries/regions had routine AI vaccination programmes: China, Egypt, Hong Kong, Indonesia and Vietnam (Table III). These countries had high to very high national poultry densities (963; 3,650; 136,804; 2,530 and 2,186 birds/km^2, respectively) and low to very high national poultry populations (14.6–16.4 billion, 534–599 million, 3.5–11.7 million, 1.3–1.4 billion and 323–534 million birds, respectively).

Hong Kong had the highest vaccination coverage rate at more than 90.8%, after full implementation of its vaccination programme in 2004, but the numbers of poultry involved were quite small: 3.5 to 11.7 million per year, when compared to the production figures of other countries in Table III, excluding Mongolia. The calculated coverage rate exceeded 100% for four years because of variations in chick placements, the number of chicks sold on multi-age farms for long rearing periods with normal chick mortality and culling during grow-out, and wastage of vaccine in large dose bottles. Poultry in Hong Kong were raised by the small commercial systems of sector 3. Currently, only 30 registered farms are allowed to produce chickens for the live poultry market, with tight government control of the process. Hong Kong lacks the big commercial poultry systems of sectors 1 and 2, as well as the village or household poultry of sector 4. It is the only country/region whose mass vaccination policy approached 100% implementation in the field. In addition to vaccinated locally grown birds, vaccinated commercial live poultry were imported daily into Hong Kong from mainland China through a single wholesale market.

In the four countries that accounted for over 99% of vaccination use (China, Egypt, Indonesia and Vietnam) the peak vaccination coverage rate was 83.3% (Egypt in 2008) and the lowest rate was 11.1% (Indonesia in 2009) (Table III). Most of the production in all four of these countries takes place in sector 3 (small commercial farms) and sector 4 (village or backyard poultry), and both sectors have inherent logistical problems in applying any type of vaccine to such a large number of premises/households with low numbers of birds per premises. For example, surveys of vaccination coverage rates, based on H5 haemagglutination inhibition (HI) antibodies, showed vaccination rates of between 20% and 40% in sector 4 in Indonesia (33), and less than 20% in sector 4 in Egypt (21). By contrast, sectors 1 and 2 have a much higher vaccination compliance rate because fewer farms are involved, the owners are better educated on animal health issues and these sectors have the funds to implement economically oriented vaccination programmes, including hiring professional vaccination crews.

Interestingly, estimates of poultry production in developing countries vary significantly, especially for poultry produced on small farms (sector 3) and in the village/backyard (sector 4). For example, in Egypt, the vaccine coverage rates were based on a conservative 550 million poultry per year from FAOSTAT (15), but one domestic source (21) estimated poultry production of between 800 million and 1.4 billion birds per year, which suggests the average coverage rate would be much lower than the authors calculated; i.e. between 27.8% and 48.6%, instead of the 69.9% reported in Table III. In China, the annual H5 AI vaccine usage was the highest of all countries, with between 18.9 and 23.7 billion doses used per year from 2006 to 2009. This number was slightly below the semi-quantitative number of 25 billion doses produced for domestic use yearly (34), but double the previously published range of 11.5 to 13.2 billion doses per year (10).

From the survey, all the vaccines used have been inactivated AI vaccines, except in China, where 4.5% (5.1 billion) have been live recombinant fowl poxvirus (rFPV) vaccine with H5 and N1 AI gene inserts (rFPV-AIV-H5N1: 613 million doses) and recombinant Newcastle disease virus (rNDV) with H5 AI haemagglutinin gene inserts (rNDV-AIV-H5: 4.4 billion doses). A previous report listed recombinant vaccine usage in China between 2004 and 2008 at 5.7 billion doses (rFPV-AIV-H5N1 = 613 million; rNDV-AIV-H5 = 5.1 billion doses) (10). The reason for such discrepancies is not clear, but the numbers used in this study were based on the questionnaire from the OIE Delegate in China and were reported in ml for inactivated vaccine, which had to be converted into doses, based on the volume for a dose in each species, and the percentage of the species in the poultry population.

Some countries used a targeted AI vaccination approach in their emergency control programmes; Pakistan, for example, which has a high national poultry population (435 to 717 million/year) and a high national poultry density (835 birds/km^2), conducted ring vaccination around outbreaks, resulting in vaccination of 0.7% to 1.0% of poultry per year. Similarly, Russia, with a high national poultry population (373 to 543 million/year) and a moderate national poultry density (168 birds/km^2), targeted its vaccination at village (sector 4) and small commercial flocks (sector 3), primarily in Siberia and eastern Russia, resulting in vaccination coverage rates of between 5.5% and 14.4% of poultry per year (Table III). Pakistan has had cases of both H5 and H7 HPAI in poultry and, since 2006, has used a bivalent H5/H7 vaccine (58).

France and the Netherlands, which have high and moderate national poultry populations (832 million and 93–95 million birds/year, respectively) and high national poultry densities (778 and 4,879 birds/km^2, respectively), used a targeted preventive vaccination approach for poultry that could not be brought indoors during a high-risk period, i.e. when migratory waterfowl were dying of H5N1 HPAI in 2006. France vaccinated flocks of geese and ducks (816,000 doses, covering 0.05% of the national poultry population) during 2006 (Table III). The Netherlands vaccinated hobby poultry (26,000 doses) and free-range commercial layers (42,000 doses on eight farms) between 2006 and 2008 (Table III). The Netherlands programme resulted in vaccination of 0.01% to 0.02% of the national poultry population. However, the proportion of vaccinated birds from the national hobby population (0.27%, 0.14% and 0.07% of three million birds for 2006, 2007 and 2008, respectively) was slightly greater than the proportion of vaccinated birds from the national commercial poultry population (<0.01% of 90–92 million) (Table III). The use of vaccine was discontinued as the risk and interest decreased in France and the Netherlands. Israel vaccinated 6,020 ostriches on a commercial farm after outbreaks in galliform poultry during 2006, but no vaccination was conducted in chickens, turkeys, ducks or other poultry species (Table III) (59). The vaccinated ostriches were used for breeding or destroyed; none were slaughtered for food.

Côte d'Ivoire, Kazakhstan, Mongolia and Sudan were exceptions to the generalisation that AI vaccine was used mainly by countries with high national poultry populations (≥250 million) and/or high poultry densities (>750 birds/km^2) (Table III). Mongolia had a very small national poultry population (142,000 to 426,000 poultry/year) and low poultry density (0.1 to 0.2 birds/km^2), but chose to conduct a preventive vaccination programme in small commercial layer flocks and backyard poultry around three human population centres because of perceived transmission risks from the presence of H5N1 HPAI virus infections and deaths in migratory waterfowl. Mongolia has a very low population of village poultry: only 8% of rural households keep poultry. To date, Mongolia has not experienced H5N1 HPAI viral infections in poultry. Kazakhstan also conducted preventive vaccination in village poultry, beginning in two geographic regions in 2006, in response to deaths in wild birds caused by H5N1 HPAI virus, but has not experienced outbreaks in poultry. Côte d'Ivoire, DPR Korea and Sudan have moderate poultry populations (32, 55.6 and 35–36 million, respectively) and low-to-high poultry densities (158, 819 and 27 birds/km^2, respectively), but chose to conduct targeted emergency vaccination programmes following outbreaks of H7N7 HPAI during 2005 (DPR Korea) and H5N1 HPAI during 2006 (Côte d'Ivoire and Sudan). Côte d'Ivoire vaccinated sector 2 commercial and sector 4 village poultry while Sudan vaccinated 90% of sector 1 and 80% of sector 2 commercial farms, respectively. The Côte d'Ivoire programme ended in 2006. The Sudanese programme ended in December 2007, after vaccinating poultry on 99 farms and no additional HPAI cases in poultry for 15 months. The Democratic People's Republic of Korea had an outbreak of H7N7 in layers during 2005 and implemented an H7N7 AI vaccination programme, using an autogenous vaccine, with 1.1 million chickens being vaccinated (59).

Most countries did not provide a detailed breakdown of the types of birds in their poultry population, so it was not always possible to accurately determine what percentage of the various poultry species had been vaccinated. However, semi-quantitative data were available for some countries and these provided evidence of vaccination programmes being targeted towards particular types of poultry within a country. In Egypt, outbreaks have occurred in both commercial and village poultry, affecting mainly meat and egg-producing chickens (1). Using available estimates of poultry populations and their types between 2006 and 2009 (Table IV), the highest AI vaccine coverage rate was achieved in meat (78.2%) and layer (31.6%) chickens,

Table V
Number of doses of H5 or H7 avian influenza vaccine used in zoo, hunting, companion, conservation or endangered birds to protect against high-pathogenicity avian influenza viruses

Country	Year	Number of premises	Vaccine doses (number of birds vaccinated)	Subtype	References
Austria	2005–2006	2	596[a] (298)	H5	(13)
Belgium	2003	NR	NR	H7	(13)
	2005–2006	10	2,350[a] (1,175)	H5	Survey (13)
	2007	NR	900	H5	Survey
	2008	NR	300	H5	Survey
Denmark	2005–2006	12	2,170[a] (1,085)	H5	(13)
Egypt	2006	NR	30,000	H5	Survey
	2007	NR	30,000	H5	Survey
	2008	NR	31,000	H5	Survey
	2009	NR	31,000	H5	Survey
	2010	NR	31,000	H5	Survey
Estonia	2005–2006	1	520[a] (260)	H5	(13)
France	2005–2006	138	54,000[a] (27,000)	H5	(13, 27)
	2007–2009	NR	NR	H5	Survey
Germany	2003	NR	NR	H7	(13)
	2005–2006	32	NR	H5	(13)
	2007	10	NR	H5	Survey
	2008	4	NR	H5	Survey
	2009	5	NR	H5	Survey
Hong Kong		2	NR	H5	Survey
Hungary	2005–2006	8	2,782[a] (1,391)	H5	(13)
Ireland	2005–2006	2	426[a] (213)	H5	(13)
Israel	2006	NR	11,681 (11,681)	H5	Survey
Italy	2005–2006	4	1,850[a] (925)	H5	(13)
	2007	NR	6,000	H5	Survey
	2008	NR	1,000	H5	Survey
Kuwait	2007	NR	NR	H5	Survey
Netherlands	2003	NR	400	H7	Survey
	2004	NR	4,000	H7	Survey
	2005–2006	23	8,000 (6,444)	H7+H5	Survey
	2007	NR	4,000	H5+H7	Survey
	2008	NR	3,000	H5+H7	Survey
	2009	NR	2,000	H5+H7	Survey
Portugal	2005–2006	2	400 (197)	H5	Survey (13)
	2006	NR	200		Survey
Singapore	2005	1	179 (118)	H5	(38)
Spain	2005–2006	21	9,680[a] (4,840)	H5	(13)
Sweden	2005–2006	9	1,284[a] (642)	H5	(13)
Switzerland	2005–2006	4	730[a] (365)	H5	(19)
United Arab Emirates	2006–2007	2	242[a] (121)	H5	(37)
Total		**292**	**271,690**		

NR: not reported
a) Estimate based on two doses per bird reported

while meat ducks had 15%, turkeys 10.4% and other poultry had less than 1.4% coverage rates (Table IV). By contrast, Pakistan has mainly focused its vaccination programme on long-lived poultry, i.e. breeders and layers (35). The highest AI vaccine coverage rate was in broiler and layer breeders (25.8%). There was low coverage (2.8%) among layers and no AI vaccine use at all among broilers (Table IV). Finally, Vietnam had higher AI vaccine

Table VI
Number of doses of H5 or H7 avian influenza vaccine used in poultry against low-pathogenicity notifiable avian influenza and coverage rate for individual countries from 2002 to 2010

Country	Year	Species	National poultry population (1,000s)[a]	Dose (1,000s)[b]	Subtype	Vaccine coverage (%)	Poultry density (birds/km² of agricultural land)[c]	Global use (%)
El Salvador	2002	Chickens	53,700	64,865	H5	60.4	n/a	
	2003	Chickens	53,068	68,680	H5	64.7	812	
	2004	Chickens	62,980	66,278	H5	52.6	789	
	2005	Chickens	77,495	70,297	H5	45.4	n/a	
	2006	Chickens	79,606	81,710	H5	51.3	888	
	2007	Chickens	83,655	81,106	H5	48.5	948	
	2008	Chickens	75,600	64,150	H5	42.4	n/a	
	2009	Chickens	76,566	68,238	H5	44.6	n/a	
	2010	Chickens	**e** 77,532	73,890	H5	47.7	n/a	
	Subtotal		**640,202**	**639,214**		**49.9**	**859**	1.95
Guatemala[d]	2002	Chickens	92,500	**e** 47,327	H5	25.6	n/a	
	2003	Chickens	88,310	**e** 57,327	H5	32.5	644	
	2004	Chickens	88,792	**e** 109,902	H5	61.9	681	
	2005	Chickens	88,955	120,795	H5	67.9	n/a	
	2006	Chickens	100,256	**e** 122,587	H5	61.1	859	
	2007	Chickens	89,360	123,729	H5	69.2	704	
	2008	Chickens	88,500	111,933	H5	63.2	n/a	
	2009	Chickens	88,503	131,798	H5	74.5	n/a	
	2010	Chickens	**e** 88,506	**e** 120,267	H5	67.9	n/a	
	Subtotal		**813,682**	**898,338**		**55.2**	**722**	6.33
Italy	2002	Poultry	574,279	7,849	H7	0.7	n/a	
	2003	Poultry	499,919	75,434	H7	7.5	839	
	2004	Poultry	512,340	51,047	H7 & H5/H7	5.0	839	
	2005	Poultry	505,725	36,162	H5/H7	3.6	n/a	
	2006	Poultry	462,720	12,313	H5/H7	1.3	845	
	2007	Poultry	529,891	10,625	H7 & H5/H7	1.0	900	
	2008	Poultry	**e** 562,455	3,905	H7 & H5/H7	0.4	n/a	
	Subtotal		**3,647,329**	**197,335**		**2.7**	**856**	9.36
Mexico[e]	2002	Chickens	1,389,182	**e** 938,492	H5	33.8	n/a	
	2003	Chickens	1,406,663	**e** 933,027	H5	33.2	397	
	2004	Chickens	1,492,904	**e** 927,594	H5	31.1	414	
	2005	Chickens	1,579,522	874,080	H5	27.7	n/a	
	2006	Chickens	1,631,009	837,854	H5	25.7	463	
	2007	Chickens	1,676,140	1,121,265	H5	33.5	477	
	2008	Chickens	1,715,640	820,335	H5	23.9	n/a	
	2009	Chickens	1,747,220	1,106,793	H5	31.7	n/a	
	2010	Chickens	**e** 1,778,800	755,792	H5	21.2	n/a	
	Subtotal		**14,417,080**	**8,315,232**		**28.8**	**438**	82.28

e = estimated
a) Population data source: FAOSTAT
b) Data sourced from current survey questionnaire
c) National poultry density was based on information about stocks of poultry/agricultural land (km^2) obtained from FAO (available at: kids.fao.org/glipha/)
d) Estimates of inactivated vaccine doses for 2002, 2003, 2004, 2006 and 2010 were based on the average for 2005 and 2007–2009; and combined with recombinant vaccine data
e) 2002–2004 vaccine doses were estimated from exponential regression analysis based on data from 2005 to 2010
f) Breeder mallards whose offspring are used for hunting release; national poultry population for 2007
g) National poultry density (2007)
h) 5.76 billion doses of inactivated vaccine (57%), and 4.35 billion doses of recombinant fowl poxvirus containing an H5 haemagglutinin gene insert from A/turkey/Ireland/1983 (43%)

Table VI (cont.)
Number of doses of H5 or H7 avian influenza vaccine used in poultry against low-pathogenicity notifiable avian influenza and coverage rate for individual countries from 2002 to 2010

Country	Year	Species	National poultry population (1,000s)[a]	Dose (1,000s)[b]	Subtype	Vaccine coverage (%)	Poultry density (birds/km² of agricultural land)[c]	Global use (%)
Portugal	2008	Mallard breeders[f]	205,444	9	H5	<0.01	n/a	
	2009	Mallard breeders	207,386	9	H5	<0.01	n/a	
	2010	Mallard breeders	**e** 209,328	9	H5	<0.01	n/a	
	Subtotal		**622,158**	**27**		**<0.01**	**1,273**[g]	<0.01
United States	2003	Layers	9,315,812	4,200	H7	0.02	527	
	2004	Layers	9,518,525	4,200	H7	0.02	544	
	Subtotal		**18,834,337**	**8,400**		**0.02**	**536**	0.08
	Total		**34,593,539**	**10,058,546**				

coverage rates in meat ducks (>90%) than in meat chickens (51.7%) (Table IV). With domestic ducks playing an important role as an asymptomatic reservoir of H5N1 HPAI virus in Vietnam (20), a higher vaccination rate in domestic ducks would assist in reducing environmental contamination with the H5N1 virus, resulting in a lower exposure and outbreak rate in galliform poultry.

Zoo, hunting, companion, conservation and endangered birds

No AI vaccines have been specifically licensed for zoo, hunting, companion, conservation or endangered species of birds, but H5 and H7 AI vaccines licensed for chickens are available and have been used in AI preventive vaccination programmes for non-poultry species. Such poultry AI vaccines were safe, producing only minor swellings at the injection sites of a few birds (41). However, the stress of catching and handling the birds for vaccination and blood sampling resulted in low mortality rates in some species (13).

From 2002 to 2010, a total of 20 countries used 271,690 doses of H5 or H7 AI vaccine in zoo, hunting, companion, conservation and endangered species of birds on over 292 premises (Table V), representing 0.000003% of the total number of AI vaccine doses used in birds (Table III). The largest vaccination programme of zoo and bird collections occurred in the EU. Seventeen countries were approved by the European Commission for preventive vaccination programmes against H5N1 HPAI among birds held in zoos and by other approved bodies, institutes and centres of Member States (13, 14). From 2005 to 2006, the programme was implemented in 13 Member States, with the use of five different H5N2 (A/duck/Potsdam/1402/86 and A/chicken/Mexico/232/94/CPA) or H5N9 (A/turkey/Wisconsin/68 and A/chicken/Italy/221/1998 [n = 2]) oil-emulsified inactivated vaccines, developed and licensed for chickens and turkeys (13). In these 13 countries, 44,721 birds were vaccinated between 2005 and 2006, representing 374 species and 19 taxonomic orders (13). Fifty percent of the birds seroconverted after a single vaccination and 82% after the second vaccination, as determined by HI titres ≥16 (13). Sero conversion rates varied with the species, family and order of birds, as well as the individual study country, but, in general, a booster vaccination significantly increased the serological titres, based on the HI test. Although challenge testing was not undertaken, the HI titres suggested protection rates of 71% (27), 80% (40), 82% (41), 84% (2, 38), 94% (37) and 96% to 100% (19) after a two-dose regime, depending on the species and assuming an HI protective titre of ≥16, ≥32 or ≥40. Birds from the orders Anseriformes, Ciconiformes, Falconiformes, Galliformes, Phoenicopteriformes and Psittaciformes had seroconversion rates of ≥82% after one immunisation (13). However, typically six months after vaccination, titres began to decrease, suggesting the need for an annual booster (13, 19). In addition to the EU programme, vaccination of zoo or captive-held non-poultry birds was conducted in Egypt and Israel (data from current survey), Hong Kong (current survey), Kuwait (current survey), Singapore (38), Switzerland ([19], current survey), and the United Arab Emirates (37). Furthermore, H7 vaccination programmes were used in zoos in Belgium, Germany and the Netherlands, after the 2003 H7N7 HPAI outbreaks in poultry (13).

In most zoos, an AI vaccination programme against H5N1 was not implemented as the principal method of protection from HPAI. The first line of defence was based on biosecurity measures (such as indoor housing, sanitation and hygiene programmes, the addition of netting to separate bird collections housed outdoors from wild birds, and isolation and quarantine facilities), veterinary care to ensure early detection of disease and screening birds before their entry into the collections (13).

Vaccination is not the cause of enzootic high-pathogenicity avian influenza virus infections

The authors would be cautious about suggesting that AI vaccine usage has resulted in enzootic infections. Multiple factors are associated with enzootic HPAI virus infections. Eleven countries/regions have used AI vaccine in poultry without the HPAI virus becoming enzootic:

– Côte d'Ivoire
– France
– Hong Kong
– Israel
– Kazakhstan
– Mongolia
– the Netherlands
– DPR Korea
– Pakistan
– Russia
– Sudan.

Côte d'Ivoire and Sudan used emergency AI vaccination in poultry, along with other measures in their comprehensive AI control programmes, after the H5N1 HPAI outbreaks occurred. This combination of control measures resulted in elimination of the virus and the discontinuation of vaccination after three months (for Côte d'Ivoire) and 16 months (for Sudan) (59) (data from current survey). The Netherlands and France conducted preventive targeted vaccination for outdoor-reared poultry that could not be brought indoors after cases of H5N1 occurred among wild birds in Europe in 2006. France had a single case of H5N1 HPAI in a turkey flock before the vaccination programme began. Neither France nor the Netherlands recorded cases of H5N1 HPAI in poultry during the vaccination programme. The programme was discontinued in France after 2006 and in the Netherlands after 2008 (Table III).

Kazakhstan and Mongolia conducted preventive vaccination programmes in poultry in response to H5N1 infections and deaths in wild birds in both countries. Mongolia's AI vaccination programme was implemented in 2005 and is scheduled to be discontinued in 2011, while Kazakhstan used vaccine throughout 2011 (Table III) (data from current survey). No cases of H5N1 HPAI have been reported in poultry, either from Kazakhstan or Mongolia (59). Israel only vaccinated a single ostrich flock in 2006 and H5N1 outbreaks were eradicated, based on a stamping-out programme in poultry. The eradication was confirmed by surveillance data.

Hong Kong implemented a routine national AI vaccination programme beginning in 2002, with full implementation by late 2003 (data from current survey). Extensive surveillance identified the H5N1 HPAI virus in dead wild birds from 2002 to 2010, but only one infected vaccinated poultry flock was identified during that period (2008) (59). The Democratic People's Republic of Korea had a single disease event on three farms in 2005 and eradication was achieved (59). Vaccine was used only during 2005, with no recurrence in 2006 or later years (59). Russia had 117 outbreaks in 2005, 93 in 2006, 23 in 2007 and one in 2008. It began a vaccination programme in 2006, and no poultry cases were reported between 2009 and 2011 (59). Pakistan had outbreaks of H7N3 HPAI during 2003 and 2004, and H5N1 in 2006 (14 outbreaks), 2007 (32 outbreaks) and 2008 (seven outbreaks), but no cases between 2009 and 2011 (59). Pakistan vaccinated poultry against H7N3 in 2004 and 2005, and against both H5N1 and H7N3 from 2005 to 2010 (data from current survey).

At present, there are four countries with enzootic H5N1 HPAI clinical disease in poultry (Bangladesh, Egypt, Vietnam and Indonesia). Two countries (China and eastern India) have recurring reports of H5N1 infections, especially in domestic ducks and poultry in the live poultry markets of China (9, 12, 22, 23, 29, 54, 59). Bangladesh had its first outbreak of H5N1 HPAI on 5 February 2007. It has not used vaccine in its control programme but has focused on targeted stamping out and other measures for individual outbreaks (59). Outbreaks of H5N1 HPAI were first reported in Egypt on 17 February 2006 and 343 outbreaks occurred all over the country before a nationwide vaccination programme was begun, one month after the first official report of the outbreaks. However, the full vaccination programme was not immediately implemented because of lack of vaccine-manufacturing facilities within Egypt and logistics delays in importing sufficient vaccine doses (18). Over 573 outbreaks occurred within the first five weeks after the first official reported outbreak. During those weeks, less than 1% of the poultry population had been vaccinated (7, 18). In Indonesia, the first cases occurred in July 2003, but the government AI vaccination programme was not established until June 2004 (43). By June, over 312 outbreaks had occurred, with over 10.9 million poultry deaths (57). Vietnam had its first three outbreaks in poultry during December 2003, followed by 1,747 outbreaks in 2004 (57). By the end of 2004, 24% of communes and 60% of towns had reported cases of HPAI in poultry and 17% of the poultry population had died as a result of infection or culling. The vaccination programme was implemented in Vietnam during October 2005 (44). In China, the first outbreak occurred on a small goose farm in Guangdong during 1996 (60). Infections were identified in domestic ducks from five eastern provinces between 1999 and 2002 (11). In the first two months of 2004, there were 48 H5N1 outbreaks across 16 provinces, extending from the eastern province of Zhejiang to the remote western province of Xinjiang; from the southern provinces of Guangxi and Guangdong to the northern province of Jilin (57). These geographically widespread outbreaks occurred during the eight years preceding the implementation of a vaccination programme in mid-2004. These data support the idea that enzootic H5N1 HPAI

virus infections became established among poultry in China, Egypt, Indonesia and Vietnam before the implementation of official vaccination programmes.

Low-pathogenicity avian influenza vaccine usage

Between 2002 and 2010, the total number of vaccine doses used in poultry against H5 and H7 LPNAI was much smaller (10.1 billion, 8.1%) than that used for HPAI (>113 billion, 91.9%) (Tables III & VI). Vaccine was used in six countries with average national poultry densities ranging from 536 to 1,273 birds/km^2 (Table VI). The majority of vaccines used were oil-emulsified inactivated vaccines (5.76 billion doses, 57%), but a large amount of rFPV with an H5 haemagglutinin gene insert was also used (4.35 billion doses, 43%).

The top user was Mexico (82.28%), which has continued H5N2 vaccine use in broilers, broiler breeders, layers and layer breeders to control H5N1 LPNAI after eliminating H5N2 HPAI in 1995 (Table VI). In addition, H5N2 vaccine was used in El Salvador and Guatemala after H5N2 LPNAI outbreaks began there in 2001 and 2000, respectively, making them the third- (1.95%) and second- (6.33%) highest users of vaccine against LPNAI, respectively (45). All three countries used inactivated H5N2 vaccine, made from a 1994 H5N2 LPNAI field virus from an early Mexican H5N1 LPNAI outbreak. Since 1998, Mexico has used an rFPV vaccine with a haemagglutinin gene insert from A/turkey/Ireland/83 (H5N8).

The fourth-highest user of vaccine against LPNAI was Italy, which has a high national poultry density (856 birds/km^2) (Table VI). The Po Valley of north-eastern Italy, where the outbreaks occurred, raises 70% of Italy's meat turkeys (8). The regions of Veneto and Lombardy have 45 million poultry on 4,760 km^2 of land, making a densely populated poultry area of 9,500 birds/km^2 (31). Multiple incursions of H5 and H7 LPNAI have occurred, from 2002 to 2003 (H7N3), from 2004 to 2005 (H5N2 and H7N3), and from 2006 to 2011 (H7N3) (4, 8, 31) (data from current survey). Italy reported the use of 197 million doses of inactivated H7 or bivalent H5/H7 between 2002 and 2008 in northern Italy (Table VI). The vaccination programmes were targeted in two ways:

– geographically, at northern Italy

– at the most susceptible poultry species, primarily meat turkeys and some layers, along with vaccination of minimal numbers of cockerels and capons (32).

Previous studies have demonstrated that turkeys are more susceptible than chickens to the H7N2 LPNAI virus, which caused outbreaks in Virginia, West Virginia and North Carolina during 2002 (51). In addition, turkeys were more susceptible than chickens to infection by wild-bird LPAI viruses (49). Vaccinating turkeys increases their resistance to LPNAI virus infection: a vaccinated turkey requires at least 2log$_{10}$ greater exposure to the virus than a non-vaccinated turkey (5). According to the survey, on a national poultry population basis, only 2.71% of the poultry in Italy were vaccinated. However, when examining specific types of poultry, peak vaccine usage was in 2003, when meat turkeys had a coverage rate of 84%, layers 23% and meat chickens 0.23% (Table VII). The vaccine was used only in sectors 1 and 2 poultry, where the infections were focused, although, in the later outbreaks of 2006 to 2008, asymptomatic infections in village poultry were identified but AI vaccine was not used (4). The questionnaire indicated that vaccination ended in 2008 because of improvements in poultry management between 2000 and 2008, including:

– better biosecurity

– all-in, all-out rearing of turkeys in 'micro-areas'

– separate rearing of male and female turkeys, to eliminate partial load-out marketing of female turkeys at 19 weeks, while leaving males until 24 weeks.

As various other control measures were implemented, the need for vaccination decreased, as shown by the yearly decline in vaccine use between 2003 and 2008, and its complete cessation in mid-2008 (Table VII). Italy also developed and implemented a heterologous neuraminidase AI vaccine to allow differentiation of infected poultry in the vaccinated population, i.e. 'differentiation of infected from vaccinated animals' (DIVA) (6).

Since 1978, the USA has used targeted vaccination in Minnesota turkeys against various subtypes of LPAI viruses, including some H5 and H7 LPNAI epizootics (25). From 1979 to 2000, 22.7 million doses of LPAI vaccine were used to control 108 epizootics, of which 20 were due to H5 or H7 subtypes (24). Over time, as the industry learned the limitations of vaccination and as rearing moved from outdoors to indoors by 1998, AI vaccine use declined to minimal then to no use (25). By contrast, from 2004 to 2010, 13.4 million doses of bivalent H1N1 and H3N4 vaccines were used in turkey breeders as targeted vaccination to control the drops in egg production induced by swine influenza virus (D. Lauer, personal communication, 2011). In this present survey for LPNAI, the USA reported using H7 AI vaccine in only a single commercial enterprise, producing layers, in a low-density poultry state (261 birds/km^2) in 2003 and 2004. This, along with enhanced biosecurity measures and marketing changes, resulted in the eradication of the virus. Vaccine coverage was low, based on the national poultry population (i.e. 0.02% for all poultry and 0.62% for the national layer/pullet population) (Table VII). However, since the vaccination was targeted at a single, large, layer company in Connecticut, the coverage rate was actually 56% of the state's chicken inventory. Based on global usage,

Table VII
Variation in vaccination of different poultry types within a country against low-pathogenicity notifiable avian influenza during 2002 to 2010

Country	Year	Species	National poultry population (1,000s)[(a)]	Vaccine dose (1,000s)[(b)]	Vaccine coverage rate (%)
Italy	2003	Meat chickens	1,061	1,061	0.23
	2004		1,261	1,261	0.31
	2002	Layers	5,831	5,831	4.92
	2003		26,830	26,830	22.85
	2004		13,263	13,263	11.33
	2005		7,577	7,577	6.55
	2006		3,959	3,959	3.57
	2007		6,194	6,194	5.34
	2008		1,070	1,070	0.89
	2002	Meat turkeys	2,018	2,018	2.24
	2003		47,242	47,242	84.05
	2004		36,171	36,171	64.35
	2005		28,318	28,318	47.80
	2006		8,202	8,202	15.30
	2007		4,425	4,425	7.98
	2008		2,835	2,835	4.73
United States	2003	Layers	339,300	4,200	0.62[(c)]
	2004		342,500	4,200	0.61[(c)]

a) Population data source: FAOSTAT
b) Data sourced from current survey questionnaire
c) 56% vaccination coverage rate based on Connecticut state chicken inventory (available at: www.nass.usda.gov/Publications/Ag_Statistics/2005/05_ch8.PDF, Table 8-44. 3,745,000 chickens for 2003)

this was 0.08% of the vaccine used for LPNAI between 2002 and 2010. The programme used two different DIVA strategies:

– virological testing of mortality cases from non-vaccinated sentinel and vaccinated layers
– serology in non-vaccinated sentinel birds (52).

A similar targeted vaccination programme was used in 1995 in a single turkey production company in the Moroni Valley, Utah (17). The programme used two million doses of inactivated H7N3 vaccine over a four-month period.

Portugal experienced an outbreak of H5N2 LPNAI in a single game-bird holding of mallard ducks (*Anas platyrhynchus*) during September 2007, controlling it through depopulation of infected, outdoor-reared ducks. The unique genetics of the mallard strain were preserved through vaccinating the indoor-reared breeder ducks and monitoring for infection in non-vaccinated sentinel ducks. The progeny were not vaccinated, and were used for restocking wild game populations.

H5 and H7 AI vaccines have not been used in zoological or other collections of non-poultry birds to protect against LPNAI viruses. The lack of morbidity and mortality from infections by LPNAI viruses in non-poultry species makes the benefit of any vaccination questionable.

Vaccination protocols

Fourteen countries provided the vaccination protocols used in their campaigns. For the most part, two vaccinations were used across all poultry types, including meat ducks and geese, but three vaccinations were typical for chicken and duck layers and breeders, with semi-annual or yearly boosters. One country used four vaccinations in chicken layers and breeders before 20 weeks of age. Some countries vaccinated broilers with their first vaccination at seven to ten days and a booster at three to four weeks. However, two countries used only a single vaccination in broilers. One country used three vaccinations in ducks, turkeys, guinea fowl and larger poultry.

Post-vaccination strategies

Thirteen countries conducted post-vaccination surveillance, by serological assay, to assess field protection. The most common test was the HI test, using a minimum protective titre of 1:16 (in five countries), 1:32 (in one country), 1:64 (in one country) and 1:128 (in two countries). Two countries used the enzyme-linked immunosorbent assay to determine immunity status.

Identification of infected birds in vaccinated populations

Thirty countries responded to the question about identifying infected birds within a vaccinated population. Sixteen of these countries (53%) had a strategy to distinguish infected birds from vaccinated birds (i.e. a DIVA strategy). Fourteen of these 16 countries (88%) used non-vaccinated sentinels and clinical observation (14%), virological testing (50%) and/or serological testing (79%), ranging from every two weeks to four times per year. Seven (50%) countries employed heterologous neuraminidase vaccines and serological testing for anti-neuraminidase antibodies against the field virus in vaccinated birds, using a neuraminidase inhibition test or immunological detection of anti-neuraminidase antibody. Thirteen (93%) conducted examinations for the field virus in vaccinated birds by virus isolation (33%) and/or detection of the H5 or H7 genome (67%), through real-time reverse transcription polymerase chain reaction assay.

Vaccine licensing and registration

Twenty of 69 (29%) countries have licensed AI vaccines. Eight (12%) countries manufactured their vaccines, 12 (17%) countries imported them and two (3%) countries did both. All 20 countries required a challenge test for licensure or registration. The vaccine licence was most frequently valid for either five years (n = 8; 40%) or one year (n = 7; 35%), but three (15%) countries had no expiration date, one had a three-year licence (5%) and one did not respond (5%). A process was in place to allow the updating of vaccine seed strains in 14 (70%) countries. Most countries released each vaccine batch based on sterility, safety, stability and immunogenicity potency tests, but one country required a challenge test to release each vaccine batch. Eighteen countries have a regulatory method to license or register live recombinant (vectored) vaccines for AI, but only six have licensed such vaccines (Canada, China, France, Mexico, the USA and Vietnam).

Exit strategy

Twenty-eight countries replied to the question on exit strategies, 18 of which (64%) responded that they had an exit strategy from vaccine use. The exit strategy varied: some countries have a specific predetermined date for the cessation of vaccination (Pakistan: 2011; Mexico: 2013; Vietnam: 2015), while others carry out surveillance and wait until risk assessment data indicates that infection is absent, e.g. no infections in the previous six to three months. However, exit strategies in HPAI-enzootic countries have proved difficult to implement.

Conclusions

Between 1959 and 2010, 24 of 29 HPAI disease events were eradicated, primarily by comprehensive control programmes that included stamping out of infected and suspected to be infected poultry. In four of the 29 HPAI disease events, countries used vaccine as a component of their control programme to maintain poultry production by preventing poultry morbidity and mortality, reducing infection and virus shedding, buying time to re-organise their poultry production and maintaining rural livelihoods.

A survey of the OIE Delegates of 69 countries that had experienced HPAI and/or LPNAI outbreaks between 2002 and 2010, demonstrated that each country had a national AI control programme with common components, such as: rapid diagnostics/early detection, active and passive surveillance of poultry and wild birds, quarantine and movement restrictions, tracing of poultry in outbreak areas, enhanced biosecurity measures, farmer and public education on AI, monitoring, eliminating positive poultry, disinfection of facilities and equipment, decontamination and disposal of infectious materials, and compensation. Although the components were similar between countries, the variability in the number of outbreaks and time until eradication suggest that individual countries varied significantly in the quantitative implementation and practice of each component.

The first vaccine usage for HPAI control occurred during 1995 in Mexico (H5N2) and Pakistan (H7N3), but widespread use was not seen until 2004, with the H5N1 HPAI panzootic of Asia, Europe and Africa. Major conclusions from the survey covering 2002 to 2010 included the following.

– The majority of countries had an option for AI vaccination in their HPAI control plans, but fewer countries had an AI vaccination option in their H5 and H7 LPNAI control plans.

– Over half of the countries had written vaccination plans, but only a small number had completed simulation exercises or worked out the logistics of implementing a vaccination programme and/or an exit strategy.

– One-third of the countries had used vaccines for HPAI control, while only one-sixth had used vaccines to control H5 and H7 LPNAI or non-H5/H7 LPAI (mainly H9N2 LPAI).

– To provide vaccine for emergency use, only 13 countries had developed H5 and/or H7 national AI vaccine banks, with eight countries receiving help from donors through international and national donor organisations.

– The most common reasons for not using AI vaccines included:

i) traditional control measures, including stamping out, were effective in eradication campaigns

ii) AI vaccines and vaccination were perceived to have certain negative consequences, such as the potential for silent infections and subclinical shedding of AI virus, and the imposition of trade restrictions on poultry products by importing countries.

– The most common reasons for using AI vaccines included:

i) traditional control methods failed to control or eradicate the infection

ii) the outbreaks were large with a high risk of spread

iii) AI vaccination was perceived to have certain positive consequences, such as a decrease in susceptibility to infection, a decrease in virus shedding and the prevention of clinical disease and mortality.

– The majority of countries used AI vaccine as an emergency measure, with half of these using AI vaccine as preventive or routine measure.

– More than 113 billion doses of AI vaccine were used in the at-risk poultry population of >131 billion birds in 15 countries, to protect against HPAI, from 2002 to 2010.

– Most countries did not achieve a 100% AI vaccine coverage rate in their poultry population because of the limited availability of the vaccine and the complex logistics of vaccination, especially in countries with large poultry populations in the village/household and small farm sectors. This suggests that a more targeted vaccination approach would be more realistic and successful.

– The majority of AI vaccine was used in four countries with enzootic H5N1 HPAI virus infections and mass vaccination programmes: China (90.99%), Egypt (4.65%), Indonesia (2.32%) and Vietnam (1.43%). The remaining 11 countries used a more targeted vaccination approach with minimal usage; i.e. accounting for less than 1% of the total AI vaccine use.

– More countries used AI vaccine in non-poultry birds in zoos and other collections than in poultry species, but the overall number of doses used in non-poultry species was very low, representing less than 0.000003% of the total.

– Employing the AI vaccine did not lead to enzootic HPAI virus infections, since:

i) three countries used H5 or H7 AI vaccine and did not have HPAI in their poultry

ii) eight countries used AI vaccines and eradicated HPAI virus infections

iii) China, Egypt, Indonesia and Vietnam had enzootic or recurring H5N1 HPAI before vaccination commenced

iv) Bangladesh and eastern India have not used AI vaccine and have enzootic or recurring H5N1 HPAI.

– The total vaccine use against H5/H7 LPNAI was low: 8.1% of total vaccine usage (compared to more than 91.9% against HPAI). Most of the vaccine against LPNAI was used in Central America and Italy. Vaccine usage in Italy against LPNAI has been eliminated as improvements have been made in managing and rearing poultry.

– The most consistent vaccination protocols used two vaccinations for meat birds and three to four vaccinations for breeder and layer birds. The use of a single vaccination for short-lived broilers and meat ducks did not provide consistent immunity and protection, especially in the presence of maternal antibodies.

– The HI test was most commonly used for field assessment of post-vaccination immunity, with the minimum protective titre being 1:16 to 1:128.

– Infected birds in the vaccinated population were identified using a variety of test methods, including:

i) clinical, serological and virological assessment of non-vaccinated sentinels (88%)

ii) heterologous neuraminidase vaccines and serological testing for anti-neuraminidase antibodies against the field virus in vaccinated birds (50%)

iii) examination of vaccinated birds for the field virus (80%).

– Twenty countries have licensed AI vaccines, including six countries which have licensed live recombinant vaccines. In all 20 countries a challenge test is required to demonstrate efficacy. Some licences were issued for as little as one year and others had no expiration date. The manufacturing base for AI vaccines was small with only eight countries manufacturing vaccines, while the other countries relied on importation.

– Most countries had an exit strategy for ending the use of AI vaccine. Some countries have a projected cessation date, such as 2011 (Pakistan), 2013 (Mexico) or 2015 (Vietnam); other countries use risk assessment data and only stop vaccinating when surveillance indicates that infection has been absent for a certain period, e.g. three to six months. In countries with enzootic HPAI and LPNAI, developing and implementing exit strategies has proved difficult.

– Problems in vaccine and vaccination control strategies have involved both vaccine efficacy and vaccination effectiveness. Vaccine quality and efficacy have improved tremendously over the past seven years. There is evidence of antigenic drift of H5N1 HPAI viruses in the field, and some evidence of failure to protect by classic H5 vaccines, but recent designer, reverse genetic vaccines have provided optimal protection against emerging variant field strains. Most field vaccination failures have been the result of improper or suboptimal application of vaccines.

Recommendations

Several recommendations for more effective HPAI and LPNAI control programmes can be made:

– Stamping-out programmes are preferred for HPAI and LPNAI control and eradication.

– Vaccination can be an effective adjunct component under defined conditions:

i) as a preventive measure when there is a high risk of the introduction of HPAI and/or LPNAI into a country

ii) as an emergency measure following the introduction of HPAI or LPNAI, when stamping-out programmes are not effective in getting ahead of the spread

iii) as a routine measure when enzootic infection exists.

– Emergency AI vaccination programmes need advanced planning, plans and logistics should be practised in the field, and vaccine banks should be developed and used effectively.

– Preventive AI vaccination can be improved with advanced planning, but is not as time-sensitive as emergency AI vaccination programmes.

– Routine AI vaccination programmes can be used to maintain rural livelihoods and food security, and to reduce human exposure and infections, but they are logistically difficult to implement, unlikely to successfully vaccinate all poultry, and expensive to sustain, with low potential for effective HPAI elimination.

– AI vaccines can be used in preventive or emergency programmes to protect zoo birds, endangered species and other valuable, non-poultry species to maintain biodiversity, and such vaccine use should not prevent trade in poultry and poultry products.

– All vaccination programmes should include statistically valid, post-vaccination immunity studies at the flock and within-flock levels to assess the success of the programme.

– As the AI outbreak matures, and epidemiological data become available, routine vaccination programmes should be updated to become risk-based, with resources being focused on the populations and reservoirs at highest risk.

– An exit strategy is crucial in any country using AI vaccination and should be developed based on specific field conditions, while resources should be redirected to high-risk conditions/populations, with a risk-based, phase-out strategy.

– There is no one AI control solution for all countries; each AI strategy must be specific to the country and production sectors concerned.

Acknowledgements

This study was conducted as part of an OFFLU research secondment/sabbatical by the corresponding author (D.E. Swayne) from the United States Department of Agriculture (USDA) to OFFLU. OFFLU is the joint OIE/FAO network of expertise on animal influenzas. Financial support for the research staff (K. Hamilton, G. Pavade and D.E. Swayne) was provided by the Agricultural Research Service, USDA (CRIS #6612-32000-048-00D), and by the OIE World Fund for Animal Health and Welfare from contributions from the following donors: the Canadian International Development Agency (CIDA) and the Department for International Development (DFID) in the United Kingdom.

Special thanks go to the following:

– OIE Delegates and their staff in the 69 countries/regions who completed and returned the questionnaire: Afghanistan, Albania, Australia, Austria, Azerbaijan, Bangladesh, Belgium, Benin, Bhutan, Bosnia, Bulgaria, Cambodia, Cameroon, Canada, Chile, the People's Republic of China, Chinese Taipei, Côte d'Ivoire, Croatia, the Czech Republic, Denmark, the Dominican Republic, Egypt, France, Georgia, Germany, Ghana, Greece, Haiti, Hong Kong (Special Administrative Region), Hungary, India, Iraq, Israel, Italy, Japan, Jordan, Kazakhstan, Kuwait, the Lao People's Democratic Republic, Malaysia, Mexico, Mongolia, Myanmar, Nepal, the Netherlands, Nigeria, Pakistan, Poland, Portugal, the Republic of Korea, Romania, Russia, Saudi Arabia, Slovakia, Slovenia, South Africa, Spain, Sudan, Sweden, Switzerland, Thailand, Togo, Turkey, Ukraine, the United Kingdom, the USA, Vietnam and Zimbabwe

– OIE Delegates and their staff for interviews and secondary questionnaire information from China, Egypt, Indonesia, the Netherlands, Portugal and Vietnam

– FAO staff in Rome and Regional Offices for documents, interviews and conference presentations

– OIE staff in Headquarters and Regional and Sub-Regional Representations for technical, logistic and other support.

References

1. Aly M.M., Arafa A. & Hassan M.K. (2008). – Epidemiological findings of outbreaks of disease caused by highly pathogenic H5N1 avian influenza virus in poultry in Egypt during 2006. *Avian Dis.*, **52** (2), 269–277.

2. Bertelsen M.F., Klausen J., Holm E., Grondahl C. & Jorgensen P.H. (2007). – Serological response to vaccination against avian influenza in zoo-birds using an inactivated H5N9 vaccine. *Vaccine*, **25** (22), 4345–4349.

3. Capua I., Marangon S., Dalla P. & Santucci U. (2000). – Vaccination for avian influenza in Italy. *Vet. Rec.*, **147** (26), 751.

4. Capua I., Schmitz A., Jestin V., Koch G. & Marangon S. (2009). – Vaccination as a tool to combat introductions of notifiable avian influenza viruses in Europe, 2000 to 2006. *In* Avian influenza (T. Mettenleiter, ed.). *Rev. sci. tech. Off. int. Epiz.*, **28** (1), 245–259.

5. Capua I., Terregino C., Cattoli G. & Toffan A. (2004). – Increased resistance of vaccinated turkeys to experimental infection with an H7N3 low-pathogenicity avian influenza virus. *Avian Pathol.*, **33** (2), 158–163.

6. Capua I., Terregino C., Cattoli G., Mutinelli F. & Rodriguez J.F. (2003). – Development of a DIVA (differentiating infected from vaccinated animals) strategy using a vaccine containing a heterologous neuraminidase for the control of avian influenza. *Avian Pathol.*, **32** (1), 47–55.

7. Castellan D. (2006). – FAO Mission in support of avian influenza prevention and control in Egypt. Food and Agriculture Organization of the United Nations (FAO), Cairo, Egypt, 1–30.

8. Cecchinato M., Comin A., Bonfanti L., Terregino C., Monne I., Lorenzetto M. & Marangon S. (2011). – Epidemiology and control of low pathogenicity avian influenza infections in rural poultry in Italy. *Avian Dis.*, **55** (1), 13–20.

9. Chen H. (2004). – H5N1 avian influenza in China. *Science in China (Series C)*, **52** (5), 419–427.

10. Chen H. (2009). – Avian influenza vaccination: the experience in China. *In* Avian influenza (T. Mettenleiter, ed.). *Rev. sci. tech. Off. int. Epiz.*, **28** (1), 267–274.

11. Chen H., Deng G., Li Z., Tian G., Li Y., Jiao P., Zhang L., Liu Z., Webster R.G. & Yu K. (2004). – The evolution of H5N1 influenza viruses in ducks in southern China. *Proc. natl Acad. Sci. USA*, **101** (28), 10452–10457.

12. Chen J., Fang F., Yang Z., Liu X., Zhang H., Zhang Z., Zhang X. & Chen Z. (2009). – Characterization of highly pathogenic H5N1 avian influenza viruses isolated from poultry markets in central China. *Virus Res.*, **146** (1–2), 19–28.

13. European Food Safety Authority (EFSA) (2007). – Opinion of the Scientific Panel on Animal Health and Welfare (AHAW) on a request from the Commission related with the vaccination against avian influenza of H5 and H7 subtypes as a preventive measure carried out in Member States in birds kept in zoos under Community approved programmes. Available at: www.efsa.europa.eu/en/efsajournal/pub/450.htm (accessed on 19 July 2011).

14. European Union Commission (2011). – Avian influenza – vaccination. Vaccination in zoos. Available at: ec.europa.eu/food/animal/diseases/controlmeasures/avian/eu_resp_vaccination_en.htm (accessed on 19 May 2011).

15. Food and Agriculture Organization of the United Nations (FAO) (2011). – FAOSTAT. Available at: faostat.fao.org/site/339/default.aspx (accessed on 19 June 2011).

16. Food and Agriculture Organization of the United Nations (FAO) (2011). – Highly pathogenic avian influenza. *Transboundary Anim. Dis. Bull.*, **37**, 21–29.

17. Frame D.D., McCluskey B.J., Buckner R.E. & Halls F.D. (1996). – Results of an H7N3 avian influenza vaccination program in commercial meat turkeys. *In* Proc. 46th Western Poultry Disease Conference, University of California, Davis, California, 32.

18. Freiji M. (2006). – Lessons learnt from avian influenza H5N1 epidemic in Egypt. *In* Proc. Conference on Co-ordinated Response Strategy to Avian Influenza, 29 May 2006, International Financial Corporation, World Bank Group, Cairo, Egypt.

19. Furger M., Hoop R., Steinmetz H., Eulenberger U. & Hatt J. (2008). – Humoral immune response to avian influenza vaccination over a six-month period in different species of captive wild birds. *Avian Dis.*, **52** (2), 222–228.

20. Gilbert M., Xiao X., Pfeiffer D.U., Epprecht M., Boles S., Czarnecki C., Chaitaweesub P., Kalpravidh W., Minh P.Q., Otte M.J., Martin V. & Slingenbergh J. (2008). – Mapping H5N1 highly pathogenic avian influenza risk in Southeast Asia. *Proc. natl Acad. Sci. USA*, **105** (12), 4769–4774.

21. Government of Egypt (2010). – Integrated National Plan for avian and human influenza. Animal health and livelihood sustainability strategy. Ministry of Agriculture and Land Reclamation, Cairo, Egypt, 1–27.

22. Guan Y., Peiris M., Kong K.F., Dyrting K.C., Ellis T.M., Sit T., Zhang L.J. & Shortridge K.F. (2002). – H5N1 influenza viruses isolated from geese in southeastern China: evidence for genetic reassortment and interspecies transmission to ducks. *Virology*, **292** (1), 16–23.

23. Guan Y., Smith G.J.D., Webby R. & Webster R.G. (2009). – Molecular epidemiology of H5N1 avian influenza. *In* Avian influenza (T. Mettenleiter, ed.). *Rev. sci. tech. Off. int. Epiz.*, **28** (1), 39–47.

24. Halvorson D.A. (2002). – Twenty-five years of avian influenza in Minnesota. *In* Proc. 53rd North Central Avian Disease Conference, 6–8 October, Minneapolis, Minnesota, 65–69.

25. Halvorson D.A. (2008). – Control of low pathogenicity avian influenza. *In* Avian influenza (D.E. Swayne, ed.). Blackwell, Ames, Iowa, 513–536.

26. Hesterberg U., Harris K., Stroud D., Guberti V., Busani L., Pittman M., Piazza V., Cook A. & Brown I. (2009). – Avian influenza surveillance in wild birds in the European Union in 2006. *Influenza & Other Respir. Viruses*, **3** (1), 1–14.

27. Lécu A., De Langhe C., Petit T., Bernard F. & Swam H. (2009). – Serologic response and safety to vaccination against avian influenza using inactivated H5N2 vaccine in zoo birds. *J. Zoo Wildl. Med.*, **40** (4), 731–743.

28. Lee C., Suarez D.L., Tumpey T.M., Sung H., Kwon Y., Lee Y., Choi J., Joh S., Kim M., Lee E., Park J., Lu X., Katz J.M., Spackman E., Swayne D.E. & Kim J. (2005). – Characterization of highly pathogenic H5N1 avian influenza A viruses isolated from South Korea. *J. Virol.*, **79** (6), 3692–3702.

29. Li K.S., Guan Y., Wang J., Smith G.J.D., Xu K.M., Duan L., Rahardjo A.P., Puthavathana P., Buranathai C., Nguyen T.D., Estoepangestie A.T.S., Chaisingh A., Auewarakul P., Long H.T., Hanh N.T.H., Webby R.J., Poon L.L.M., Chen H., Shortridge K.F., Yuen K.Y., Webster R.G. & Peiris J.S.M. (2004). – Genesis of a highly pathogenic and potentially pandemic H5N1 influenza virus in eastern Asia. *Nature*, **430** (6996), 209–213.

30. Marangon S., Busani L. & Capua I. (2007). – Practicalities of the implementation of a vaccination campaign for avian influenza. *Avian Dis.*, **51**, 297–303.

31. Marangon S., Capua I., Pozza G. & Santucci U. (2004). – Field experiences in the control of avian influenza outbreaks in densely populated poultry areas. *Dev. Biol. (Basel)*, **119**, 155–164.

32. Marangon S., Cristalli A. & Busani L. (2007). – Planning and executing a vaccination campaign against avian influenza. *Dev. Biol. (Basel)*, **130**, 99–108.

33. Mariner J. (2011). – Final report: operational research in Indonesia for more effective control of highly pathogenic avian influenza. International Livestock Research Institute, Nairobi, Kenya, 1–154.

34. Ministry of Agriculture of China (2011). – Feasibility of production of human AI vaccine in AI vaccine manufacturers in China. Available at: https://docs.google.com/viewer?a=v&q=cache:uUO0-Lh8buwJ:www.who.int/entity/csr/disease/influenza/MoA_China.pdf+doses+H5N1+vaccine+China+poultry&hl=en&gl=uk&pid=bl&srcid=ADGEEShIePfcLg60zi-mBdj3ydbTzvlP1XUUGXlnX372bXmhdIAeYu310LwdVVoGMuXjdnFBIPXb_WyIs0tSloGI_IroLS1bWIDF5PTuWtJK11t6WWcYr3Bj6b2h5zdLqJXUoOyFe3mi&sig=AHIEtbTECX3XNlHTbeKs9aSVOclhVA0MHw (accessed on 20 September 2011).

35. Naeem K. & Siddique N. (2006). – Use of strategic vaccination for the control of avian influenza in Pakistan. *Dev. Biol. (Basel)*, **124**, 145–150.

36. Nguyen D.C., Uyeki T.M., Jadhao S., Maines T., Shaw M., Matsuoka Y., Smith C., Rowe T., Lu X., Hall H., Xu X., Balish A., Klimov A., Tumpey T.M., Swayne D.E., Huynh Lien P.T., Nghiem H.K., Nguyen Hanh H.T., Hoang L.T., Cox N.J. & Katz J.M. (2005). – Isolation and characterization of avian influenza viruses, including highly pathogenic H5N1, from poultry in live bird markets in Hanoi, Vietnam, in 2001. *J. Virol.*, **79** (7), 4201–4212.

37. Obon E., Bailey T.A., O'Donovan D., McKeown S., Kent J., Joseph S. & Wernery U. (2007). – Humoral response to H5N2 vaccination in exotic birds in the United Arab Emirates. *Vet. Rec.*, **161** (25), 860–861.

38. Oh S., Martelli P., Hock O.S., Luz S., Furley C., Chiek E.J., Wee L.C. & Keun N.M. (2005). – Field study on the use of inactivated H5N2 vaccine in avian species. *Vet. Rec.*, **157** (10), 299–300.

39. Pavade G., Awada L., Hamilton K. & Swayne D.E. (2011). – The influence of economic indicators, poultry density and the performance of Veterinary Services on the control of high pathogenicity avian influenza in poultry. *Rev. sci. tech. Off. int. Epiz.*, **30** (3), 661-671.

40. Philippa J., Baas C., Beyer W., Bestebroer T., Fouchier R., Smith D., Schaftenaar W. & Osterhaus A. (2007). – Vaccination against highly pathogenic avian influenza H5N1 virus in zoos using an adjuvanted inactivated H5N2 vaccine. *Vaccine*, **25** (19), 3800–3808.

41. Philippa J.D., Munster V.J., Bolhuis H., Bestebroer T.M., Schaftenaar W., Beyer W.E., Fouchier R.A., Kuiken T. & Osterhaus A.D. (2005). – Highly pathogenic avian influenza (H7N7): vaccination of zoo birds and transmission to non-poultry species. *Vaccine*, **23** (50), 5743–5750.

42. Pittman M. & Laddomada A. (2008). – Legislation for the control of avian influenza in the European Union. *Zoonoses public Hlth*, **55** (1), 29–36.

43. Sawitri S.E., Darminto, Weaver J. & Bouma A. (2007). – The vaccination programme in Indonesia. *Dev. Biol. (Basel)*, **130**, 151–158.

44. Sims L.D. & Brown I.H. (2008). – Multi-continental epidemic of H5N1 high pathogenicity avian influenza (1996–2007). *In* Avian influenza (D.E. Swayne, ed.). Blackwell, Ames, Iowa, 251–286.

45. Suarez D.L., Spackman E. & Senne D.A. (2003). – Update on molecular epidemiology of H1, H5, and H7 influenza virus infections in poultry in North America. *Avian Dis.*, **47** (3 Suppl.), 888–897.

46. Swayne D.E. (2008). – The global nature of avian influenza. *In* Avian influenza (D.E. Swayne, ed.). Blackwell, Ames, Iowa, 123–143.

47. Swayne D.E. & Halvorson D.A. (2008). – Influenza. *In* Diseases of poultry (Y.M. Saif, J.R. Glisson, A.M. Fadly, L.R. McDougald & L. Nolan, eds). Blackwell, Ames, Iowa, 153–184.

48. Swayne D.E. & Kapczynski D.R. (2008). – Vaccines, vaccination and immunology for avian influenza viruses in poultry. *In* Avian influenza (D.E. Swayne, ed.). Blackwell, Ames, Iowa, 407–451.

49. Swayne D.E. & Slemons R.D. (2008). – Using mean infectious dose of high- and low-pathogenicity avian influenza viruses originating from wild duck and poultry as one measure of infectivity and adaptation to poultry. *Avian Dis.*, **52** (3), 455–460.

50. Swayne D.E. & Suarez D.L. (2000). – Highly pathogenic avian influenza. *In* Diseases of poultry: world trade and public health implications (C.W. Beard & M.S. McNulty, eds). *Rev. sci. tech. Off. int. Epiz.*, **19** (2), 463–482.

51. Tumpey T.M., Kapczynski D.R. & Swayne D.E. (2004). – Comparative susceptibility of chickens and turkeys to avian influenza A H7N2 virus infection and protective efficacy of a commercial avian influenza H7N2 virus vaccine. *Avian Dis.*, **48** (1), 167–176.

52. Turner J., Clothier H.J. & Kaye M. (2005). – Influenza surveillance in Victoria, 2004. *Commun. Dis. Intell.*, **29** (1), 71–76.

53. Villarreal C. (2007). – Experience in control of avian influenza in the Americas. *Dev. Biol. (Basel)*, **130**, 53–60.

54. Webster R.G., Guan Y., Peiris M., Walker D., Krauss S., Zhou N.N., Govorkova E.A., Ellis T.M., Dyrting K.C., Sit T., Perez D.R. & Shortridge K.F. (2002). – Characterization of H5N1 influenza viruses that continue to circulate in geese in southeastern China. *J. Virol.*, **76** (1), 118–126.

55. World Organisation for Animal Health (OIE) (2010). – Chapter 10.4. Avian influenza. *In* Terrestrial Animal Health Code. OIE, Paris. Available at: www.oie.int/index.php?id=169&L=0&htmfile=chapitre_1.10.4.htm (accessed on 19 June 2011).

56. World Organisation for Animal Health (OIE) (2010). – Terrestrial Animal Health Code. OIE, Paris. Available at: www.oie.int/en/international-standard-setting/terrestrial-code/access-online/ (accessed on 19 May 2011).

57. World Organisation for Animal Health (OIE) (2011). – Animal health data (prior to 2005). *In* Handistatus II. OIE, Paris. Available at: web.oie.int/wahis/public.php?page=home (accessed on 27 July 2011).

58. World Organisation for Animal Health (OIE) (2011). – Vaccine bank. OIE, Paris. Available at: www.oie.int/en/support-to-oie-members/vaccine-bank/ (accessed on 19 June 2011).

59. World Organisation for Animal Health (OIE) (2011). – World Animal Health Information System. OIE, Paris. Available at: web.oie.int/wahis/public.php?page=home (accessed on 19 May 2011).

60. Xu X., Subbarao K., Cox N.J. & Guo Y. (1999). – Genetic characterization of the pathogenic influenza A/goose/Guangdong/1/96 (H5N1) virus: similarity of its hemagglutinin gene to those of H5N1 viruses from the 1997 outbreaks in Hong Kong. *Virology*, **261** (1), 15–19.

ANNUAL REVIEWS Further
Click here for quick links to Annual Reviews content online, including:
• Other articles in this volume
• Top cited articles
• Top downloaded articles
• Our comprehensive search

Avian Influenza: Public Health and Food Safety Concerns*

Revis Chmielewski and David E. Swayne

Southeast Poultry Research Laboratory, Agricultural Research Service, U.S. Department of Agriculture, Athens, Georgia 30605; email: David.Swayne@ars.usda.gov

Annu. Rev. Food Sci. Technol. 2011.2:37-57. Downloaded from www.annualreviews.org
by U.S. Department of Agriculture on 03/01/11. For personal use only.

Annu. Rev. Food Sci. Technol. 2011. 2:37–57

First published online as a Review in Advance on September 14, 2010

The *Annual Review of Food Science and Technology* is online at food.annualreviews.org

This article's doi:
10.1146/annurev-food-022510-133710

Copyright © 2011 by Annual Reviews.
All rights reserved

1941-1413/11/0410-0037$20.00

*This is a work of the U.S. Government and is not subject to copyright protection in the United States.

Keywords

bird flu, high pathogenicity avian influenza (HPAI), low pathogenicity avian influenza (LPAI), H5N1, H7N7

Abstract

Avian influenza (AI) is a disease or asymptomatic infection caused by *Influenzavirus* A. AI viruses are species specific and rarely cross the species barrier. However, subtypes H5, H7, and H9 have caused sporadic infections in humans, mostly as a result of direct contact with infected birds. H5N1 high pathogenicity avian influenza (HPAI) virus causes a rapid onset of severe viral pneumonia and is highly fatal (60% mortality). Outbreaks of AI could have a severe economic and social impact on the poultry industry, trade, and public health. Surveillance data revealed that H5N1 HPAI has been detected in imported frozen duck meat from Asia, and on the surface and in contaminated eggs. However, there is no direct evidence that AI viruses can be transmitted to humans via the consumption of contaminated poultry products. Implementing management practices that incorporate biosecurity principles, personal hygiene, and cleaning and disinfection protocols, as well as cooking and processing standards, are effective means of controlling the spread of the AI viruses.

Annu. Rev. Food Sci. Technol. 2011.2:37-57. Downloaded from www.annualreviews.org
by U.S. Department of Agriculture on 03/01/11. For personal use only.

INTRODUCTION

What is the Bird Flu?

Avian influenza (AI) is a disease or asymptomatic infection caused by viruses in the family *Orthomyxoviridae*, genus *Influenzavirus* A, which contains a genome composed of eight segments of single-stranded negative-sense RNA (Swayne & Halvorson 2008). The virus surface contains spikes of hemagglutinin and neuraminidase glycoproteins. The segmented RNA allows for the easy reassortment of the viral genome. The viral genome encodes for ten proteins: one nucleocapsid (NP), three transcriptase proteins (PB-1, PB-2, and PA), the hemagglutinin and neuraminidase surface glycoproteins (HA and NA), two matrix proteins (M1 and M2), and two nonstructural proteins (NS1 and NS2) (Alexander 2000, Lee & Saif 2009). Nucleocapsid and the three transcriptases (PB-1, PB-2, and PA) form the ribonucleoprotein complex that is responsible for mRNA transcription. AI viruses are characterized by their subtypes, pathotypes, genetic lineages, and clades. AI viruses are subtyped by their surface HA and NA glycoproteins, which are major determinants of the pathogenicity, transmission, and adaptation of the AI virus to other species, but these three traits plus infectivity are multigenic. However, the major determinant of pathogenicity is the HA. The HA is important for attachment and entrance into cells to replicate, whereas the function of neuraminidase is to release newly formed viruses (Swayne & Halvorson 2008). There are 16 different hemagglutinin (H1–16) and nine different neuraminidase (N1–9) subtypes. Such viruses have been detected in more than 100 species of wild birds, mostly from the orders *Anseriformes* (ducks, geese, and swans) and *Charadriiormes* (gulls, terns, and shorebirds), but usually without causing clinical signs and are thus of low pathogenicity (LP) (Stallknecht & Brown 2007). Mammals such as humans, pigs, horses, seals, whales, and cats have been sporadically infected with AI viruses (Swayne & Halvorson 2008). In the cases involving carnivores, infection occurred mainly through the consumption of H5N1 HPAI virus–infected birds or their products. Only H5 and H7 have been seen in nature in the high pathogenicity (HP) form, but most H5 and H7 AI viruses are of LP. Most commercially reared poultry in developed countries are free of AI viruses and such infections are rare (Swayne 2008b). When AI is present, it is usually as low pathogenicity avian influenza (LPAI) virus, but if infected by high pathogenicity avian influenza (HPAI) virus, the outcome can be devastating with near 100% mortality in chickens and turkeys. Commonly used vernacular for Eurasian H5N1 HPAI is bird flu, but technically, any AI virus could be termed bird flu.

Human Infection

AI viruses are considered species specific and rarely cross the species barrier (Cox & Uyeki 2008). However, since 1959, some AI virus isolates of subtypes H5, H7, and H9 have caused sporadic infections in humans (INFOSAN IFSAN- 2004). H5N1 HPAI virus was isolated from a domestic goose in Guangdong, China in 1996, and the following year was isolated from an outbreak in the live bird markets in Hong Kong. During the live bird market outbreaks of 1997, the first human case of H5N1 occurred in May, and by the end of 1997, there were 18 hospitalized cases with six fatalities. Other incidences of human infections associated with H5N1 HPAI outbreaks in poultry were reported in China in 2003 and throughout Southeast Asia from 2004 to the present. Human infections were mostly due to direct contact with infected birds (CDC 2006, WHO 2006). Unlike the human H1N1 and H3N2 seasonal flu as upper respiratory infection and low mortality, the H5N1 HPAI virus causes a rapid onset of severe viral pneumonia and has a high fatality rate (60% mortality). There are many cultural practices that increase the risk of exposure of human to HPAI virus. In many Southeast Asian and Middle Eastern countries, poultry flocks are reared in the backyard, rooftops, or in close proximity to human dwellings with close interaction with humans.

Annu. Rev. Food Sci. Technol. 2011.2:37-57. Downloaded from www.annualreviews.org
by U.S. Department of Agriculture on 03/01/11. For personal use only.

The close proximity of birds to humans increases the risk of transmission to humans via aerosol or large airborne droplets, fecal contamination with dispersion via fomites, and direct contact with infected birds. Also, sick birds may be slaughtered for consumption in the developing world, leading to increased risk of exposure (WHO 2005a). H5N1 HPAI virus has expanded its host range, as it has infected dogs and other mammals through the consumption of uncooked infected poultry, wild birds, or their products (Thanawongnuwech et al. 2005, CDC 2007, WHO 2007). This has raised concern that dogs and other pets have the potential to be intermediate carriers that can transfer the H5N1 influenza virus to humans. Although rare, evidence of direct human-to-human transmission of H5N1 associated with a poultry outbreak occurred in Southeast Asia. Sustained human-to-human transmissibility of H5N1 HPAI would require genetic adaption of AI PB2 internal protein (Hatta et al. 2001, WHO 2008, Gao et al. 2009). In addition, because the human population lacks immunity to H5, H7, and H9 viruses, emergence of a pandemic virus that is adapted to humans could be devastating. To date, there have been 493 human infections with 293 fatalities due to H5N1, 114 infections due to H7N7 HPAI with one death, and four infections of young children from H9N2 LPAI viruses (Cox & Uyeki 2008, WHO 2010). Currently, these AI viruses are not adapted to humans and a pandemic has not developed.

Economic Consequence to Poultry Producers

The Food and Agriculture Organization (FAO) estimated the global poultry production in 2007 at 83.7 million metric tons with 8.1 million metric tons in global trade (FAO 2007). The United States, China, the European Union (EU), and Brazil were the largest producers of poultry, with Brazil, the United States, and the EU being the largest exporters. The United States exported 2.3 million metric tons of poultry meat in 2005. Outbreaks of AI since the 1990s have had severe economic and social effects on the poultry industry, international agricultural trade, and public health (Burns et al. 2008). Reductions in consumer sales both domestically and internationally owing to fear and loss of confidence, additional costs for implementing control and prevention measures such as culling, block eradication, and compensation to producers, and other costs (restocking costs, biosecurity, surveillance, vaccinations) are some of the economic consequences of an outbreak (Yalcin 2006). There is also the loss in the export market due to international embargoes and the loss of market share due to competition from other poultry-producing nations. Importing nations also bear the economic impact of increased cost for importing product because of a lack of international competition (Lokuge 2005, McLeod et al. 2005). In regions of the world where there have been HPAI outbreaks, changes in the consumption pattern have been evident, with temporary decreases in poultry consumption. For example, the domestic impact in Turkey in 2006, where 2.5 million birds were culled due to an outbreak of H5N1 HPAI, had a cost of $226 million. In the capital city, Ankara, there was a 54% decrease in sales of poultry products, with a 32% decrease in poultry meat prices, and prices of eggs and other poultry products also decreased (WHO 2005a, Oner et al. 2006, Yalcin 2006).

At least 62 countries reported outbreaks of H5N1 HPAI in either domesticated or wild birds between 1996 and 2010 (OIE 2009). The HPAI virus has caused devastating economic losses to poultry growers and rural households in Asia, Europe, and Africa (McLeod et al. 2005, Otte et al. 2008, FAO 2010). In developing countries, most poultry production occurs in small backyard flocks in rural and periurban areas, so outbreaks economically impacted these small farmers more than commercial industries. Between 1996 and 2003, there were 1,645 H5N1 HPAI outbreaks worldwide that resulted in 43 million birds dead or destroyed, and between 2004 and 2007 more than 250 million birds died or were destroyed (McLeod et al. 2005). The economic consequence of HPAI outbreaks in Southeast Asia for 2003–2005 was between 0.5% and 2% of the area's GDP,

Annu. Rev. Food Sci. Technol. 2011.2:37-57. Downloaded from www.annualreviews.org
by U.S. Department of Agriculture on 03/01/11. For personal use only.

or about $10 billion. More than 50% of the Southeast Asian population derived its income from poultry. For example, in Indonesia 20% of the commercial farm workers lost their jobs as a result of the outbreak. In Vietnam, 44 million birds, or 17% of the bird population, were culled at a cost of $120 million (World Bank 2010). HPAI outbreaks have had a major impact on the livelihood of small and large farmers and have negatively impacted the nutritional stature of millions of people in the developing world.

Effect on International Trade

AI is a notifiable disease and is defined by the World Organization for Animal Health [Office Internationale des Epizooties (OIE)] Terrestrial Animal Health Codes as a poultry disease caused by influenza A viruses of subtypes H5 and H7 or AI virus with an intravenous pathogenicity index of 1.2 or higher. The worldwide monitoring of notifiable diseases is the responsibility of the OIE. Although H5N1 HPAI is primarily an animal health issue, the increasing frequency of human infection has raised concerns about its pandemic potential. The world human and animal health organizations [FAO, OIE, and World Health Organization (WHO)] are collaborating with and aiding countries in the development of risk management strategies to reduce the circulation of AI viruses in the poultry population, to assess the risk of human exposure from production-to-consumption, and to implement mitigation measures. The OIE is responsible for the phytosanitary safety standards (SPS) for the international trade of terrestrial animals and animal products, including poultry. These standards are implemented by national veterinary agencies of the importing and exporting countries. The World Trade Organization enforces the standards in an effort to prevent disease transmission and to ascertain fair trade (OIE 2009). The individual countries may implement trade embargoes on countries that have reported notifiable diseases, such as AI and virulent Newcastle disease, as nontariff trade barriers, but such embargoes must be science based and not political in scope.

International trade implications following an outbreak with HPAI could be economically severe. Gaining the confidence of importing nations require improvements in biosecurity systems, surveillance, vaccination, and other preventative measures (Lokuge 2005, McLeod et al. 2005) At least ten Southeast Asian countries have been impacted by H5N1 HPAI since 2003, although the countries most severely impacted have been China, Cambodia, Indonesia, Laos, and Thailand. Southeast Asian countries account for a quarter of the world's poultry production, and one third to one half of the population derives income from poultry, hence the consequence of HPAI outbreaks with the limitation of trade within and between countries has been devastating to their economies and worsened food security for rural communities. In 2004, Thailand was the fourth largest exporter of poultry and poultry products in the world. The country exported 40% of its poultry production, primarily to Europe and Japan, but following the HPAI outbreak and the ban on international trade of poultry, its poultry industry was economically devastated by losing 50% of its export market (Lokuge 2005). The Netherlands experienced a similar reduction in exports (30%) following its H7N7 HPAI outbreak in 2003. Exporting countries that did not have concurrent outbreaks of HPAI had the advantage of gaining export market share when such outbreaks occurred in Asia. Trade embargoes or bans imposed on a country due to animal disease outbreaks affect all poultry producers as well as importing countries.

Concerns Related to Food-Borne Transmission

Surveillance data revealed that H5N1 HPAI virus was detected in imported frozen duck meat and on the surface and in internal contents of contaminated eggs (Tumpey et al. 2002, Beato et al.

2009, Harder et al. 2009). Experimentally, HPAI virus was detected in breast and thigh meat, and blood and bones, as well as in eggs of HPAI virus–infected chickens (Swayne 2006). Although there is no direct evidence that AI has been transmitted to humans via the consumption of contaminated poultry products, there is anecdotal and experimental evidence that the consumption of uncooked poultry blood or meat has transmitted the H5N1 HPAI virus to carnivorous animals, including tigers, leopards, domestic cats, domestic dogs, and a stone martin (WHO 2005a, CDC 2007, Writ. Comm. Second WHO Consult. Clin. Aspects Hum. Infect. Avian Influenza A Virus 2008).

VIRUS ECOLOGY AND EPIDEMIOLOGY

Natural Reservoirs

Wild waterfowl and shorebirds are natural reservoirs for LPAI viruses, whose replication is primarily limited to the epithelial cells of the intestinal tract (Ito et al. 2000, Webster et al. 2007), and infected birds remain asymptomatic but shed the virus into the environment via feces, and less frequently saliva and nasal secretions (Hinshaw 1985). One of the primary routes of transmission is via the fecal-oral route. LPAI viruses can survive up to 20 days in chicken manure (−4°C) (CDC 2006), in water for at least 10 days (Guan et al. 2002a, Domanska-Blicharz et al. 2010), and on fomites for up to three weeks (Lu et al. 2003), and can replicate in feather follicles and survive on feathers for at least six days (Tiwari et al. 2006, Yamamoto et al. 2008). However, survival is highly temperature and moisture content dependent, i.e., survival is shortened by high environmental temperatures and dry conditions. LPAI viruses with antigenic subtypes H3 and H6, as well as N2, N6, and N8, were the most frequently isolated viruses from wild ducks, whereas H9, H11, and H13 were predominant HA subtypes in shorebirds and gulls (Suarez 2008, Swayne & Halvorson 2008). By contrast, HPAI viruses have not been maintained in wild bird reservoirs but have been derived from H5 and H7 LPAI viruses after circulation in poultry populations (Horimoto et al. 1995). The insertion of multiple basic amino acids, insertion of large amounts of extraneous RNA coding for additional amino acids, substitution of nonbasic with basic amino acids, or loss of shielding glycosylation sites in the cleavage site of HA motif can enable a H5 or H7 LP virus to become HP (Perdue et al. 1996, Suarez 2008).

H5 in Poultry

Many neuraminidase subtypes have been linked with H5 subtypes associated with poultry in both HP (N1–3 and N8–9) and LP (N1–9) forms. The largest outbreak of HPAI in the past 50 years has been the H5N1 HPAI epizootic in Asia, Africa, and Europe (1996–present). This epizootic has affected at least 62 countries and has been isolated from infected poultry flocks in Asia, the Middle East, Africa, and Europe, as well as, but less frequently, from waterfowl, shorebirds, passerine birds, pigeons, and falcons (Stallknecht & Brown 2007). H5N1 HPAI virus was first reported in 1996 in China (HPAI virus type strain A/goose/Guangdong/1/1996) followed by reports of outbreaks in live poultry markets (LPM) of Hong Kong and in humans in 1997, and spread in 2003–2004 through eastern and southeastern Asia, affecting poultry, captive birds, and the human population. Genetic characterization of the Hong Kong viruses revealed that these H5 viruses had the H5 HA gene from A/goose/Guangdong/1/96, NA gene from H6N1 LPAI virus related to A/teal/HK/W312/97, and the internal genes of H9N2 LPAI virus associated with Japanese quail or H6N1 viruses (Xu et al. 1999, Guan et al. 2002a, Kim et al. 2009). Surveillance and phylogenetic analysis revealed that in Hong Kong between 1999 and 2002 there was transmission of H5N1 HPAI virus from domestic poultry to domestic ducks. In general, the ducks were less susceptible

Annu. Rev. Food Sci. Technol. 2011.2:37-57. Downloaded from www.annualreviews.org by U.S. Department of Agriculture on 03/01/11. For personal use only.

Annu. Rev. Food Sci. Technol. 2011.2:37-57. Downloaded from www.annualreviews.org
by U.S. Department of Agriculture on 03/01/11. For personal use only.

to AI virus infection than chickens and remain asymptomatic when infected. However, in 2002 a H5N1 HPAI virus appeared in Hong Kong that infected and killed captive-reared ducks in a wildlife park.

LPAI viruses usually replicate in the intestines of the ducks. However, the H5N1 HPAI virus in ducks produces primary infection with higher titers in the respiratory tract than in the intestinal tract. Recent studies revealed that some species of ducks have high susceptibility to the H5N1 virus. Experimental evidence with wild-type mallard and Muscovy ducks indicates that mallards may be more resistant to the H5N1 virus than Muscovy ducks (Hulse-Post et al. 2005; Kim et al. 2009; C Cagle, J Wasilenko, E Spackman E, TL To, T Nguyen, M Pantin-Jackwood, unpublished results). However, when mallards become immunocompromised due to another infection, the birds have increased susceptibility to H5N1 infection (Ramirez-Nieto et al. 2010). Since appearing in 1996, the H5N1 HPAI virus has changed genetically, by drifting, to have 10 distinguishable clades (clade 0–9) with at least six subclades. A few of these subclades (2.1, 2.2, 2.3, 2.5) have been responsible for the human H5N1 infections and deaths, with clade 2.2 being the most frequently reported in humans in Asia, Europe, the Middle East, and Africa (CDC 2007, Webster et al. 2007). Other aspects of concern are the transmission of H5N1 from domestic birds to migratory aquatic birds, as occurred in Qinghai Lake, China in 2005 (Chen et al. 2006). Today, the H5N1 HPAI viruses have predominantly replicated in the respiratory tract and less so in the intestinal tract. Some wild waterfowls are more susceptible to H5N1 virus infection than others (Webster et al. 2007, WHO 2007).

The persistence of H5N2 LPAI virus in the poultry population of Mexico for over a year eventually led to critical mutations that resulted in the 1994 outbreak of H5N2 HPAI. Phylogenetic analysis indicated the H5N2 LPAI virus that circulated in the poultry population in Mexico in 1993 was derived from a North American lineage circulating in migratory aquatic birds, which was mutated by adding an insert of two basic amino acids and substitution of a nonbasic with basic amino acid in the HA cleavage site, and consequently caused an outbreak of HPAI in 1994–1995 (Horimoto et al. 1995, Perdue et al. 1996). Mexico initiated a vaccination program in January 1995, and the last HPAI virus was isolated in June 1995. However, H5N2 LPAI virus has continued to circulate.

H7 in Poultry

Several NA combinations with H7 HA subtypes have been reported for LPAI (N1–4, N7, and N9) and HPAI (N1, N3, N4, and N7) viruses in birds and/or humans. Since 1995, infection of poultry with H7 AI viruses has greatly increased, as well as its geographic spread. Outbreaks of H7N1 LPAI occurred in Italy (1999–2001) and in Canada (2000). H7N2 LPAI outbreaks occurred in the Unites States (1996–98, 2002, 2003, 2004) and the United Kingdom (2007). H7N3 LPAI outbreaks occurred in Italy (2002–2003), Chile (2002), Canada (2004), the United Kingdom (2006), and Pakistan (2001–2004), whereas H7N7 LPAI outbreaks occurred in Australia (1976, 1979), the United Kingdom (1996), Ireland (1995, 1998), and Germany (2001, 2003). Outbreaks of H7N1 HPAI have occurred in Italy (1999–2000), whereas outbreaks of H7N3 HPAI occurred in the United Kingdom (1963), Australia (1992 and 94), Pakistan (1995–2004), Chile (2002), and Canada (2004). In Australia, there were outbreaks of H7N4 HPAI (1997) and H7N7 HPAI (1976, 1985, and 1996), but the most severe outbreak of H7N7 HPAI occurred in The Netherlands (2003) (Capua & Alexander 2004, Belser et al. 2009). The H7N7 HPAI virus in the Netherlands resulted in the culling of 30 million birds. Since 1995, at least 75 million poultry (chicken/turkey) worldwide have been culled or depopulated because of H7 HPAI epizootics (Capua & Alexander 2004, Swayne 2008c, Belser et al. 2009). For LPAI viruses in the United States, the LPM system has various frequencies of poultry infected with various LPAI viruses. H7N2 LPAI viruses have

been circulating in LPM from 1994 to 2006, whereas H5N2 LPAI viruses have been sporadically isolated from LPM in the northeast United States since 1983 (Senne et al. 2003, Suarez et al. 2002, Senne 2010). Phylogenetic analysis of H7N2 LPAI isolates from commercial poultry outbreaks in Pennsylvania (1997–98, and 2001–2002); Virginia, West Virginia, and North Carolina (2002); and in Connecticut (2003) were linked to H7N2 LPAI viruses circulating in the LPM in the northeastern United States (Spackman et al. 2003, Akey 2009). The fact that H5 and H7 LPAI viruses can mutate to HPAI viruses after circulating in the poultry population (Horimoto et al. 1995, Dusek et al. 2009) has prompted surveillance studies to track the genetic changes of the H5 and H7 subtypes circulating in LPM in the United States over a seven-year period (Horimoto et al. 1995, Spackman et al. 2003). These researchers noted specific substitution changes at the hemagglutinin cleavage site of H7 with the addition of basic amino acids.

Annu. Rev. Food Sci. Technol. 2011.2:37-57. Downloaded from www.annualreviews.org
by U.S. Department of Agriculture on 03/01/11. For personal use only.

Public Health Concerns

Outbreaks of HPAI viruses in wild and domestic birds are rare, but once infection occurs it can be serious from veterinary, medical, and public health perspectives. Since the outbreaks of H5N1 HPAI in poultry and humans in Hong Kong in 1997 and H7N7 HPAI in the Netherlands in 2003, there have been concerns that AI viruses could persist in some poultry populations and emerge as a pandemic virus for humans through multiple mutations or reassortment. For an AI virus to cause a pandemic requires the virus to develop the ability to be transmitted from human-to-human and cause high morbidity or mortality rates. During the twentieth century, the emerged viruses had been new hemagglutinin subtypes for which the human population has no exposure and thus no immunity (CDC 2007). The 2009 pandemic H1N1 was the result of a reintroduction of H1N1, which over time had mutated and reassorted influenza A genes from various avian, human, and swine influenza viruses (Dunham et al. 2009, Liu et al. 2009, Sinha et al. 2009). Today, AI viruses of concern as potential pandemic strains are some H5, H7, and H9 subtypes that have crossed the human species barrier multiple times to produce sporadic infections. This will be discussed in following sections (Li et al. 2003, WHO 2005, CDC 2007, Webster et al. 2007, Pappas et al. 2007).

H5 in Humans

Although very rare, subtype H5 AI viruses have crossed the species barrier to produce sporadic infections of humans (Gilsdorf et al. 2006, Cox & Uyeki 2008, Writ. Comm. Second WHO Consult. Clin. Aspects Hum. Infect. Avian Influenza A Virus 2008). The first case of transmission of H5 HPAI virus from birds to humans occurred in association with the LPM of Hong Kong in 1997, which caused 18 hospitalized cases and six fatalities. To date, 493 human cases of H5N1 illness have been reported, of which 292 died, for a case fatality rate of 60% (WHO 2005a, 2010; Kim et al. 2009). The vast majority of human infections occurred as a result of direct exposure to live or dead infected poultry, with one instance through the consumption of raw duck blood, and another in which individuals in Azerbaijan (2006) became infected while defeathering dead wild swans (Gilsdorf et al. 2006, WHO 2007, Writ. Comm. Second WHO Consult. Clin. Aspects Hum. Infect. Avian Influenza A Virus 2008). Although human-to-human transmission of AI virus is limited, reports of this type of transmission have occurred in Thailand (2004), Vietnam (2004), Azerbaijan (2006), Indonesia (2006), Pakistan (2007), and Egypt (2007), usually as a result of one of the family members having direct contact with infected poultry prior to infecting members of the household or one family member or health care worker becoming infected from an infected patient (CDC 2006, WHO 2008). These transmissions were mainly among family members and

Annu. Rev. Food Sci. Technol. 2011.2:37-57. Downloaded from www.annualreviews.org
by U.S. Department of Agriculture on 03/01/11. For personal use only.

not communal. H5N1 HPAI viruses continued to evolve, although transmission from the avian to human host is relatively low. However, with increased exposure to a human host, the chance of the virus adapting for efficient human infectivity increases or reassorting with a human-adapted influenza virus may occur.

The symptoms of H5N1 HPAI virus infection in humans include fever, severe respiratory disease, dyspnea, multi-organ failure, and death, with an incubation period between five and ten days (Tam 2002, Ungchusak et al. 2005, Gilsdorf et al. 2006). The case fatality rate has been approximately 60%. In 2004, patients in Thailand infected with HPAI virus exhibited drastically different clinical symptoms than seasonal flu. Within two to eight days following exposure, patients symptoms progressed from flu-like to vomiting, diarrhea, and abdominal pain (Yuen et al. 1998, Ungchusak et al. 2005, WHO 2005a).

H7 in Humans

Humans have rarely been infected with H7 AI viruses, but when infected they usually had symptoms of mild respiratory disease and conjunctivitis. The North American H7 LPAI and HPAI viruses caused milder, self-limiting infection with no human-to-human transmission, as compared with the Eurasian 2003 H7N7 HPAI virus in which limited human-to-human transmission occurred. There have been sporadic reports of individual cases of mild respiratory disease due to H7N2, H7N3, and H7N7 virus infections. In the United Kingdom in 1996, a patient was infected with H7N7 LPAI virus after an eye abrasion, leading to conjunctivitis. In the United States (Virginia, 2002; New York, 2003) and the United Kingdom (2007), patients infected with H7N2 LPAI viruses developed mild respiratory symptoms. These infections were phylogenetically linked with the H7N2 circulating in the live bird market (Spackman et al. 2003, Suarez et al. 2009). Similarly, other sporadic cases of H7N3 LPAI and HPAI virus infections occurred in Canada (2004), resulting in two cases of conjunctivitis and mild respiratory symptoms. In Wales in 2007, an infection with H7N2 LPAI virus was associated with poultry obtained from a live bird market (Nguyen-Van-Tam et al. 2006, Editorial team 2007). The patients had symptoms of conjunctivitis, flu-like symptoms, and neurological and gastrointestinal symptoms (Capua & Alexander 2004, Editorial team 2007). However, the greatest numbers of H7 human cases were associated with the H7N7 HPAI epizootic in the Netherlands in 2003, which also spread to neighboring commercial farms in Belgium and Germany. Eighty-nine farm workers became infected; 78 with conjunctivitis, five with conjunctivitis and flu-like symptoms, two with flu-like symptoms, four with other symptoms, and one death from severe respiratory disease. Three of the cases were as a result of human-to-human transmission from a farm worker to his family (Fouchier et al. 2004, Koopmans et al. 2004). Phylogenetic analysis revealed the H7N7 virus from a patient and viruses from infected chickens were identical, indicating that the HA had nearest homology with A/mallard/Netherland/12/00 (H7N3) and the NA had nearest homology with A/mallard/NL/2/00 (H10N7) viruses isolated from mallards. All the internal genes (NP, PA, PB1 and 2, NS, MA) of the outbreak isolate were of the Eurasian lineage. The genomic analysis from the fatal case (A/NL/219/03) had a 26-nucleotide substitution, of which four were in the HA gene and eight in the PB2 gene (Fouchier et al. 2004). The Eurasian lineage of H7N7 HPAI virus maintained tropism toward α2-3 sialic acid cell membrane receptor, which preferentially binds to cells in avian species. HA of the North American H7N2 LPAI virus (A/turkey/Virginia/4529/02 and A/chicken /Connecticut/260413-2/03), and the H7N3 HPAI virus (A/chicken/Canada/504/04) had adapted to recognize and have increased affinity for α2-6 sialic acid cell receptors, which preferentially bind to some human cells, but neither virus changed sufficiently to be pandemic viruses. Nevertheless, the Eurasian lineage of the H7N7 HPAI virus (2003) caused one fatality, indicating greater

virulence for humans and that other factors such as mutation in the PB2 (E627K) internal protein may have contributed to the human pathogenicity of the Eurasian lineage (Belser et al. 2009).

Other AI Subtypes: H9

There have been sporadic cases of humans infected with H9N2 LPAI viruses. Outbreaks of H9N2 have occurred throughout the world beginning in the 1990s in poultry flocks in China, Pakistan, and the Middle East. There were reported outbreaks in Europe, such as in domestic ducks, chickens, and turkeys in Germany (1995–1998), in ostriches in South Africa, and in turkeys in the United States, the Middle East, and Korea (Capua & Alexander 2004). However, these H9N2 viruses were not associated with human infections. By comparison, rare H9N2 human infections occurred in China in 1999 and again in 2003, producing self-limiting mild respiratory disease. These infections occurred in young children (Capua & Alexander 2004).

Annu. Rev. Food Sci. Technol. 2011.2:37-57. Downloaded from www.annualreviews.org
by U.S. Department of Agriculture on 03/01/11. For personal use only.

EVOLUTION AND PATHOGENICITY

Genetic Changes in the Virus: Antigenic Drift and Antigenic Shift

AI viruses are genetically unstable and are constantly evolving. The antigenic variation for some HA subtypes is large, with conserved regions being as little as 30% of the genome (Lee & Saif 2009). Genetic changes occur either by antigenic drift or by antigenic shift.

Antigenic Drift

AI viruses lack a proofreading and error correction mechanism during replication, therefore small, constant genetic changes occur due to point mutation, deletion, or substitution, which can result in new mutants (CDC 2005, Escorcia et al. 2008). The insertion of multiple basic amino acids in the cleavage site of the HA motif can enable an H5 or H7 LPAI virus to become an HPAI virus. An example of such a mutational event occurred with the H5N2 LPAI virus that appeared in Mexico in 1993, circulated in poultry for more than one year, and mutated into an HPAI virus in November 1994. By 1995, phylogenetic analysis revealed that the virus had acquired an insertion of two additional basic amino acids and a basic for nonbasic substitution at the hemagglutinin proteolytic cleavage site, which was responsible for the acquired HP phenotype. Genetic analysis also revealed the poultry LPAI virus originated from the LPAI virus of migrating waterfowls prior to introduction into the poultry population (Horimoto et al. 1995, Perdue et al. 1996). Since 1995, the H5N2 LPAI virus has continued to circulate among poultry in Mexico with continued antigenic drift in the protective epitopes of the HA protein as compared to the 1994 vaccine seed strain. Outbreaks as a result of the mutation of H5 and H7 LPAI to the HPAI viruses have also occurred in Pennsylvania (1983) and Italy (2000), respectively (Kawaoka et al. 1984, Donatelli et al. 2001, Spackman et al. 2003, Suarez et al. 2009)

Antigenic Shift

Reassortment of gene segments has occurred due to coinfection of a host with more than one subtype of influenza A virus. Such a mechanism was responsible for development of the human pandemic H1N1 (1918), H2N2 (1957), and H3N2 (1968) viruses that arose in the human population. This shift in gene segments has also occurred in birds, with H5N1 HPAI virus appearing in Hong Kong in 1997, following the reassortment of the H5 gene from H5N1 of Guangdong

Annu. Rev. Food Sci. Technol. 2011.2:37-57. Downloaded from www.annualreviews.org
by U.S. Department of Agriculture on 03/01/11. For personal use only.

lineage virus, NA from an H6N1 virus, and internal genes (NS, PB2, M, and PA) from the H9N2 virus (Xu et al. 1999, Guan et al. 2002a). This suggests that poultry were infected with a reassortant virus of wild waterfowl origin that circulated in the poultry and adapted by optimizing AI virus gene segments through mutations and reassortment.

Host Restriction

The ability of the virus to infect a host depends on its affinity to bind with the host cell receptor and initiate the replication process. In general, receptor binding contributes to the infectivity of AI viruses. The virus HA binds to the host α-sialic acid cell receptors, so the receptor cell motif restricts the ability of viruses to bind and invade the host cell. The HA of most AI viruses has the affinity for α2-3 sialic acid receptors that are predominant on avian cells, whereas human influenza A viruses have the affinity for α2-6 sialic acid receptors that are predominant on human cells. Although α2-3 sialic acid is predominant in avian species, including chickens, turkeys, and ducks, some investigators have found that reduced numbers of α2-6 sialic acid receptors may be expressed in the epithelial tissue of many organs in various poultry species (Ito et al. 2000, Gambaryan et al. 2002, Matrosovich et al. 2004, Kuchipudi et al. 2009). Influenza viruses have found other means of circumventing host restrictions. For example, virus adaptation to its host after passage in that species can result in changes in viral molecular structure. Adaptation of virus from wild duck-to-chicken produces common adaptive changes such as the shortening of the NA stalk by deletion of 19 amino acids. Pathogenicity studies revealed that a deletion in the stalk of the NA of AI viruses resulted in increased viral replication and an increase in pathogenicity in chickens (Webster et al. 1992, Matrosovich et al. 2004, Munier et al. 2010, Ramirez-Nieto et al. 2010). Genetic adaptations are evident in H9N2 LPAI viruses in Asia that have acquired human virus-like specificity for binding to α2-6 sialic acid receptors and in H5N1 HPAI viruses that have selective tropism for α2-3 sialic acid receptors that are present in the alveoli of the lower human lungs (Matrosovich et al. 2004, Wan et al. 2008).

Adaptive Mutation to Infect Humans

Viral adaptation is an important factor in enabling human cell receptor binding and virus transmission. Influenza viruses alter the receptor-binding properties of HA to increase infectivity and transmission. The HA proteins in H5N1 HPAI viruses have low affinity for α2-6 sialic acid receptors (human), therefore adaptations are needed to efficiently infect and transmit between humans. Studies of the HA binding of AI viruses to sialic acid receptors of host cells revealed that mutation of amino acid residues 226leu and 228ser at the HA binding site increased the binding affinity for the human α2-6 sialic acid receptors. Mutation of the PB2 internal protein at amino acid residues 627K and 701N was also correlated with increased virus replication efficiency and host range, but did not increase virus transmission. These studies indicated that multiple genes may regulate virus replication and transmission. Genetic studies of the H5N1 HPAI virus clade 2.2 revealed changes both in the HA receptor site and PB2 genes. These changes imply that H5N1 (clade 2.2) is evolving its efficiency for transmission to humans, but additional undefined changes are necessary for the virus to become a pandemic virus (Gao et al. 2009).

Pathogenicity in Birds

AI viruses are also classified by pathotypes, i.e., LPAI and HPAI viruses. Birds infected with LPAI virus can exhibit mild signs such as ruffled feathers, a decrease in egg production, and mild

Annu. Rev. Food Sci. Technol. 2011.2:37-57. Downloaded from www.annualreviews.org
by U.S. Department of Agriculture on 03/01/11. For personal use only.

respiratory disease that lasts for approximately 10 days. Birds infected with HPAI viruses exhibit severe respiratory and neurological signs, multiple organ failure, and death within 48–96 h. The peak mortality rate is between 90% and 100%. The H5 and H7 AI viruses have been introduced into the poultry population as LPAI viruses (WHO 2005a) and, with adaptation and sustained replication, this has led to the emergence of HPAI viruses. In addition to tissue tropism and adaptive mutation, protease activity of the host on the HA cleavage site of the virus is one of the major determinants for pathogenicity. The ability of the host proteases to cleave the HA is important for infectivity and viral spread (Hatta et al. 2001, Lee & Saif 2009), hence the conversion of LPAI to HPAI viruses is dependent on changing the cleavability of HA from trypsin-like enzymes to the host's furin-like proteases (Hatta et al. 2001, Lee & Saif 2009). LPAI viruses can replicate in localized tissues (respiratory and digestive) in which trypsin-like proteases are present, whereas HPAI viruses replicate systemically in most organs and cell types by using ubiquitous furin-like proteases or trypsin-like proteases. In LPAI viruses, there are two basic amino acids at the HA cleavage site motif (Walker & Kawaoka 1993). This restricts the cleavage of this site to extracellular trypsin-like enzymes present primarily in the respiratory and digestive tracts. In HPAI viruses, the multiple basic amino acids at the HA cleavage sites can be cleaved by a larger range of intracellular enzymes (furin and subtilisin) commonly found in many organs and tissues allowing the virus to infect and grow systemically, i.e., pantropic (Hulse-Post et al. 2005).

TRANSMISSION/DISTRIBUTION

The transmissibility of AI viruses to poultry or humans is dependent on the virus strain, environmental factors, and host species susceptibility.

Bird Transmission and Exposure

As the natural reservoir for AI, infected waterfowl are believed to pass the AI virus to domestic poultry by the fecal-oral route through contaminated water sources, feed, and housing facilities/shared environment, where infectious virus can be excreted by birds for up to 10 days. The virus can survive at 4°C in feces for at least 35 days (Brown et al. 2007, Stallknecht & Brown 2007). Transmission is possible via aerosols or airborne droplets, as well as by wind dispersion of fomites including contaminated dust. Indirect exposures occur through surface contamination of equipment, clothing, and shoes from dust, feces, secretions, and contaminated feathers (CDC 2006, Gilsdorf et al. 2006, Yamamoto et al. 2009).

In developing countries such as Vietnam, Indonesia, and Egypt, it is estimated that 80%–85% of poultry are reared in small flocks outdoors or on rooftops as village poultry (Branckaert & Guye 1997, Biswas et al. 2009). These flocks are a vital source for the LPM and are valuable commodities to these subsistence growers, whose cultural preference is to consume freshly slaughtered meat. The close living proximity of these small backyard or rooftop flocks to humans increases the chance for AI virus transmission through contact with contaminated feces or airborne virus. There are also exposures due to bird respiratory secretions, contaminated dust, and contaminated bodies of water such as ponds. Surveillance studies in the United States have traced H7N2 LPAI virus from the LPM system to poultry on commercial farms (turkeys; layer, breeder, and meat chickens) in the northeastern United States, resulting in millions of infected birds. Historically, the LPM system in Hong Kong also contributed to the interaction of domestic quail and domestic chickens, giving rise to the reassortant H5N1 HPAI viruses (Spackman et al. 2003, Duan et al. 2007, Suarez et al. 2009, WHO 2005a). However, interspecies transmissions of AI viruses have occurred in other species as well. H1N1 and H3N2 commonly circulate in swine in Europe and the United States, and have

Annu. Rev. Food Sci. Technol. 2011.2:37-57. Downloaded from www.annualreviews.org
by U.S. Department of Agriculture on 03/01/11. For personal use only.

crossed species to infect turkeys, particularly breeder hens, which require a lower exposure dose of virus to produce a productive infection in turkeys than is needed to infect chickens (Pillai et al. 2010). H1N2 swine influenza virus has also infected turkeys. Recently, several flocks of breeder turkey hens in Canada, Chile, and the United States were infected with 2009 pandemic H1N1 virus, and the field syndrome was experimentally reproduced by reproductive tract insemination (Suarez et al. 2009, Pantin-Jackwood et al. 2010). Epidemiologic evidence in the Canadian case suggested that a poultry worker with respiratory illness may have transmitted the virus to the turkey flock (OIE 2009).

Human Transmission

Most reports indicate that human infection with H5N1 HPAI virus was the result of direct contact with live or dead infected birds. An exposure survey in Hong Kong in 1997 determined that 3%–10% of the poultry workers involved in the culling of birds in the live bird market were seropositive for H5N1 when surveyed after working in the depopulation program (Bridges et al. 2000, Katz et al. 2008). People at greatest risk for AI virus exposure and infection include farm workers, live bird market workers, butchers and home processors of poultry, hunters that slaughter, eviscerate, and defeather infected wild birds, and those preparing to cook contaminated meat getting viruses on their hands and transferring them by touching mucus membranes (WHO 2005b, 2007). Veterinarians are also at high risk when working with infected flocks. Other sources of exposure are due to cultural practices of slaughtering sick birds and close living conditions between human and infected birds (INFOSAN IFSAN- 2004). Direct human-to-human transmission mostly occurs in clusters as a result of family or health-care worker exposure (WHO 2004, 2008). There appears to be an undefined human genetic factor that is responsible for the familial association.

Food Transmission: Meat

In some countries, the cultural preference for the consumption of freshly slaughtered poultry meat supports village production systems and LPM, which increases the risk of transmission of AI virus (Katz et al. 2008). AI virus has survived in imported raw infected meat, such as frozen infected duck carcasses, in Korea (2001), Japan (2003), and Germany (2007), and was isolated from chicken thigh and breast meat from experimental studies with HPAI viruses (Tumpey et al. 2002, Swayne & Beck 2004, Mase et al. 2005, Beato et al. 2009, Harder et al. 2009). The titers of H5N1 HPAI virus recovered from experimentally infected chicken thigh meat were as high as 10^7 EID_{50} (median egg infectious dose) g^{-1} (Swayne & Beck 2004, Swayne 2006, Thomas & Swayne 2007). In Southeast Asia, one of the cultural practices is to slaughter sick poultry instead of accepting an economic loss. Butchering or home slaughtering of sick birds increases the risk of AI virus exposure through cross contamination from live and dead birds to human handlers or airborne virus generation during slaughter. Improper cooking, handling, and preparation may allow AI virus survival and increases the potential for productive exposure, therefore the consumption of raw or undercooked food is not advisable. Although there is no evidence of human infection due to food consumption, there is one anecdotal incident of infection through the consumption of raw duck blood, and natural and experimental infection in mammals occurred when infected meat was consumed by tigers, leopards, house cats, dogs, ferrets, and other mammals (Beato et al. 2009). Experimental studies in simulated LPM slaughter of H5N1 HPAI virus–infected chickens produced airborne viruses that were transmitted to chickens and ferrets, resulting in fatal infections (Swayne 2005, 2008a; D.E. Swayne, unpublished data). In commercially produced poultry, HPAI virus–infected poultry are destroyed and not used for human food consumption.

Annu. Rev. Food Sci. Technol. 2011.2:37-57. Downloaded from www.annualreviews.org
by U.S. Department of Agriculture on 03/01/11. For personal use only.

Eggs

HPAI virus has been found on egg shells and internally in albumen and yolk from eggs produced by experimentally infected chicken, but with LPAI viruses, only egg shells have been determined to be contaminated and not the internal contents (Cappucci et al. 1985, Promkuntod et al. 2006). When experimentally added to products, H5N2 LPAI virus survived in egg yolk and albumen for at least 17 days when held at 4°C–20°C (de Wit et al. 2004), but LPAI viruses have not been shown to contaminate eggs from the field (de Wit et al. 2004). Most birds infected with HPAI virus stop laying eggs, but the last few eggs produced may be infected. No human cases from consumption of infected eggs have been reported, but pigs were infected from consuming raw eggs with shell from H7N7 HPAI virus–infected flocks in the Netherlands (WHO 2007). In many developed countries, markets have developed for deshelled, liquid eggs because of a drop in demand for shelled eggs (Lokuge 2005). Early HPAI virus infection of a flock before clinical signs provides the possibility of AI virus–contaminated eggs being included in the liquid egg product. However, the egg pasteurization process inactivates HPAI and LPAI viruses (Swayne & Beck 2004).

Water

Fecal-contaminated water can be a source of infectious AI virus. AI virus can survive in water for at least 10 days and for up to a year (Brown et al. 2007, Domanska-Blicharz et al. 2010). The survival and infectivity of AI is influenced by temperature, pH, and salinity of the water. Survival increases as temperature decreases (Guan et al. 2002b, Brown et al. 2007, Domanska-Blicharz et al. 2010). Open bodies of water such as ponds and lakes may be a haven for AI virus–infected migratory ducks and birds, which may become AI virus contaminated and used as a water source for domesticated birds. When ducks were experimentally infected with AI virus, they shed as much as $10^{7.8}$EID g^{-1} in their feces, which in turn can contaminate the water source (Brown et al. 2007, Stallknecht & Brown 2007, Stallknecht et al. 2010). This reinforces the need for growers to implement proper biosecurity measures to ensure that potable water does not become contaminated with AI virus from wild bird sources.

Fomites

Equipment, surfaces, shoes, and clothes can be sources of contamination, as AI viruses can survive up to three weeks on some fomites (Lu et al. 2003, Tiwari et al. 2006).

PREVENTION/CONTROL

Farm to Table Risk Management

The control of AI in poultry, from village to commercial sectors, requires farm-to-table risk management. Some of the basic needs include implementation of good agricultural practices such as training of workers in good management and biosecurity practices, in particular poultry cullers, establishing a biosecure environment to isolate poultry from potential AI virus carriers, supplying a source of potable water, providing a feed supply that is secure and free of contaminants, disinfection and decontamination of the premises and equipment prior to the introduction of a new flock or after culling of poultry flocks, establishing routine composting of litter and carcasses for all flocks, and safe disposal of carcasses from known infected farms (Brglez & Hahn 2008, Swayne 2008b, Guan et al. 2009). Good risk communication with workers, veterinarians, and suppliers is

Annu. Rev. Food Sci. Technol. 2011.2:37-57. Downloaded from www.annualreviews.org
by U.S. Department of Agriculture on 03/01/11. For personal use only.

essential to manage risk. Following an outbreak, disease surveillance and inspection, controlled depopulation, rapid culling, and potentially a vaccination program must be implemented. Although the vaccination program may be country specific, a delay in this control measure when rapid depopulation is not a viable option could result in enormous economic cost, whereas rapid intervention could dramatically reduce costs and the spread of infection. From a national level, effective risk communication with growers and producers is essential as affected countries must address improvements in biosecurity as a cost-effective investment (Koopmans & Duizer 2004, Lokuge 2005). In developed countries, commercially produced HPAI virus infected poultry and their products are prohibited from going into the food chain. In addition, LPAI and HPAI viruses are rare in commercial and noncommercial poultry in developed countries.

In developing countries with H5N1 HPAI virus infections, on a local level safe food handling such as keeping raw meat separate from cooked foods, cleaning of all work surfaces, cooking meat to the proper temperature (70°C), and maintaining proper storage temperatures must be practiced. It is essential to inform food preparers that AI can survive refrigeration and freezing. Low temperature increases its stability (INFOSAN IFSAN- 2004), so refrigeration is not a means of control. Therefore practicing good hygiene is essential to prevent cross contamination (INFOSAN IFSAN- 2004). Effective vaccination prevents systemic infection of poultry and mitigates the risk of H5N1 HPAI virus from being in meat and other poultry products (Swayne & Suarez 2007).

In 2004, WHO began contemplating whether H5N1 HPAI virus–infected poultry products (refrigerated or frozen carcass) or eggs may pose some risk to human health in developing countries. Deshelled liquid eggs are typically pasteurized to inactivate bacteria such as *Salmonella*. The pasteurization processes have been validated with established critical limits in the HACCP

Table 1 Thermal death times (D_T) for low pathogenicity avian influenza A/Ck/NY/13142-5/1994 and high pathogenicity avian influenza A/Ck/PA/1370/1983 in egg products (imitation egg, whole homogenized egg, liquid egg white, 10% salted egg, dried egg white) heated at 55°C to 63°C

Temp °C	Imitation egg product (IEP)		Whole homogenized eggs (WHE)		Liquid egg white (LEW)		10% salted egg (SEW)	
	D_T							
	[1]LPAI-NY	[2]HPAI-PA	[1]LPAI-NY	[2]HPAI-PA	[1]LPAI-NY	[2]HPAI-PA	[1]LPAI-NY	[2]HPAI-PA
55	2.9 min	18.6 min	6.7 min	11 min	6.6 min	4.3 min	41 s	20.3 s
56.7	1.4 min	8.5 min	20 min	4.5 min	52 s	33 s	36 s	<20 s
57	0.8 min	3.8 min	1.6 min	3.2 min	21 s	23 s	22 s	<20 s
58	0.7 min	2.6 min	22 s	22 s	<19 s	<19 s	<20 s	<20 s
59	0.7 min	2 min	<20 s	<19 s	<19 s	<19 s	<20 s	<20 s
61	0.5 min	0.8 min	<20 s	<19 s	<19 s	<19 s	<20 s	<20 s
63	<0.1	<0.5	<20 s	<19 s	<19 s	<19 s	<20 s	<20 s

[1]low pathogenicity avian influenza A/Ck/NY/13142-5/1994.
[2] high pathogenicity avian influenza A/Ck/PA/1370/1983.
LPAI-IEP: Log $_{10}$D-value = $0.0239(\text{Temp})^2 - 2.8927(\text{Temp})x + 87.30$.
HPAI-IEP: Log $_{10}$D-value = $-0.3565(\text{Temp}) + 1.6407$.
LPAI-HWE: Log $_{10}$D -value = $0.0305(\text{Temp})^2 - 3.7702(\text{Temp}) + 116$.
HPAI-HWE: Log $_{10}$D -value = $0.0324(\text{Temp})^2 - 4.0265(\text{Temp}) + 124.75$.
LPAI-LEW: Log $_{10}$D value = $0.0467(\text{Temp})^2 - 5.6432(\text{Temp}) + 169.77$.
HPAI-LEW: Log $_{10}$D -value = $0.057(\text{Temp})^2 - 6.8432(\text{Temp}) + 204.5$.
LPAI-SEW: Log $_{10}$D -value = $0.0115(\text{Temp})^2 - 1.3848(\text{Temp}) + 41.32$.
HPAI-SEW: Log $_{10}$D-value = Undetectable after 20 s of heat exposure regardless to temperature.

Annu. Rev. Food Sci. Technol. 2011.2:37-57. Downloaded from www.annualreviews.org
by U.S. Department of Agriculture on 03/01/11. For personal use only.

Table 2 FSIS pasteurization standards for egg products with thermal death times (D_T) based on the thermal inactivation of *Salmonella*

FSIS Standards		
	Temp °C	**Inactivation time for 7 log10 of *Salmonella***
Whole egg	60	3.5 min
Whole blend	60	6.2 min
Whole blend	61.1	3.5 min
Liquid egg white	55.6	6.2 min
Liquid egg white	56.7	3.5 min
10% salted yolk	62.2	6.2 min
10% salted yolk	63.3	3.5 min
Imitation egg product	56.7	4.6 min
Dried egg white (pan dried)	51.7	5 d
Dried egg white (spray dried)	54.4	7 d

(Hazard Analysis Critical Control Point) process control and risk management scheme (Whiting & Buchanan 1997). Thermal inactivation data have been obtained to validate the United States pasteurization standards for egg products. AI viruses, HP and LP, were artificially inoculated in whole homogenized eggs, liquid egg whites, 10% salted egg, dried egg whites, and imitation egg products. The inoculated egg products were heat treated at various time and temperature combinations to obtain pasteurization inactivation curves. Heat inactivation data were generated for poultry eggs products (**Table 1**) showing the time required to inactivate AI viruses by one log at a specific temperature (D_T-value). The heat inactivation data for AI virus inoculated in the egg products (whole homogenized eggs, liquid egg whites, 10% salted egg, and dried egg whites) revealed that the USDA pasteurization standards were adequate to inactivate HPAI (A/Ck/PA/1370/1983) virus (**Tables 1** and **2**) and that a standard cooking temperature of 70°C for poultry meat would adequately inactivate HPAI viruses in chicken meat at levels produced in experimental studies (**Table 3**) (Swayne & Beck 2004, Thomas & Swayne 2007, Thomas et al. 2008, Chmielewski & Swayne 2010).

Table 3 Thermal death times (D_T) for highly pathogenic avian influenza A/Ck/PA/1370/1983 in chicken meat heated at 57.8°C to 73.9°C and the FSIS pasteurization standard for cooking meat

	[1]HPAI-PA/83	[1]HPAI- PA/83	FSIS standards based on 1% fat level
Temp °C	[2]**D-value**	**log10 (EID50) reduction of HPAI virus titer using FSIS time to inactivate 7log10 *Salmonella***	**Time to inactivate 7log10 *Salmonella***
57.8	4 min	15.8	63.3 min
58.9	2.2 min	18	39.7 min
60	1.2 min	21	25.2 min
61.1	37.6 s	25.6	16.1 min
70	0.24 s	91.3	21.9 s
73.9	0.03 s	33/s	<10 s

[1]high pathogenicity avian influenza A/Ck/PA/1370/1983.
[2]Log $_{10}$D-value = [(-0.2157)(temperature) + 14.677].

Annu. Rev. Food Sci. Technol. 2011.2:37-57. Downloaded from www.annualreviews.org
by U.S. Department of Agriculture on 03/01/11. For personal use only.

CONCLUSIONS

AI outbreaks have caused severe economic losses and agricultural trade restrictions. Migratory aquatic birds cannot be controlled, but biosecurity measures can be established to prevent interaction of wild birds and domestic poultry, thereby reducing the risk of AI virus introduction into domestic poultry. The LPM system may be a reservoir for some AI viruses, so risk management strategies have to be implemented, including AI testing and restriction of infected birds from sale, implementing appropriate cleaning, disinfection, and hygiene practices, and enforcing movement restrictions and one-directional movement of poultry from farm to market. H5N1 HPAI viruses have caused sporadic infection of humans, primarily from direct contact with infected birds, producing a high case fatality rate (60%) for human infections, but with limited human-to-human spread and rare transmission through raw food products. AI viruses are a minor food safety issue, as cooking and pasteurization are effective in inactivating the virus, and poultry meat is seldom consumed without undergoing heat treatment or cooking sufficient to inactivate the virus.

SUMMARY POINTS

1. AI is caused by type A influenza viruses, and infections in humans can range from asymptomatic to mild respiratory disease, and in chickens symptoms range from decreased egg production to fatal systemic disease. On the rare occasions when humans were infected with H5N1 HPAI virus, the disease was serious and had a high case fatality rate of 60%. Most other human infections with AI viruses have been mild and self limiting.
2. Wild ducks and other aquatic birds are the natural host of LPAI viruses and exhibit no signs of illness when infected.
3. Transmission of AI viruses among wild birds and poultry usually results from exposure to contaminated feces, respiratory secretions, and feathers, and occasionally from cannibalization of carcasses. Between farms, spread is through airborne viruses, viruses adherent to dust, and contaminated equipment, shoes, and clothing. Poultry in LPM systems and village flocks are a high risk for being infected and spreading AI viruses.
4. The economic consequence of HPAI outbreaks is severe due to the cost of culling and bird replacement, loss of customer confidence, local and international trade losses, the cost of biosecurity, and the cost for veterinary and infrastructure improvement. All segments of the poultry industry within a country lose as a result of international trade embargoes.
5. There is concern for public health from the H5N1 HPAI viruses because of human infections and fatalities.
   a. Most infections have resulted from direct exposure to live or dead infected poultry.
   b. There is limited evidence of human-to-human transmission.
   c. There are rare cases of human AI virus infections obtained through consumption of raw or undercooked contaminated poultry products.
6. Various components are needed for successful control and mitigation strategies.
   a. Most countries prohibit HPAI virus–infected poultry from entering the food chain, but in developing countries, asymptomatic or sick HPAI virus–infected village poultry may enter the food chain.

b. Management practices that incorporate biosecurity principles are the key to preventing infection of poultry flocks by AI viruses.

c. Essential components for control include quarantine of infected flocks with depopulation and environmentally sound disposal, cleaning and disinfection of facilities, and composting of manure.

d. Education and risk communication are essential for all persons involved in poultry production to know how they can prevent the spread of the virus.

e. Standard cooking and pasteurization processes are effective at inactivating both LPAI and HPAI viruses in food products.

Annu. Rev. Food Sci. Technol. 2011.2:37-57. Downloaded from www.annualreviews.org
by U.S. Department of Agriculture on 03/01/11. For personal use only.

DISCLOSURE STATEMENT

Funding for avian influenza virus inactivation research reported in this paper was provided by Current Research Information System Project 6612-32000-048-00D, Foreign Agricultural Service of United States Department of Agriculture, and the American Egg Board.

LITERATURE CITED

Akey ŠBL. 2009. Low-pathogenicity H7N2 avian influenza outbreak in Virginia during 2002. *Avian Dis.* 47:1099–103

Alexander DJ. 2000. A review of avian influenza in different bird species. *Vet. Microbiol.* 74:3–13

Beato MS, Capua I, Alexander DJ. 2009. Avian influenza viruses in poultry products: a review. *Avian Pathol.* 38:193–200

Belser JA, Bridges CB, Katz JM, Tumpey TM. 2009. Past, present, and possible future human infection with influenza virus A subtype H7. *Emerg. Infect. Dis.* 15:860–65

Biswas PK, Christensen JP, Ahmed SSU, Das A, Rahman MH, et al. 2009. Risk for infection with highly pathogenic avian influenza virus (H5N1) in backyard chickens, Bangladesh. *Emerg. Infect. Dis.* 15:1931–36

Branckaert RDS, Guèye EF. 1997. Poultry as a tool in poverty eradication and promotion of gender equality. In *FAO's Programme for Support to Family Poultry Production*, *Proc. Workshop*, pp. 1–9. Rome: FAO

Brglez B, Hahn J. 2008. Methods for disposal of poultry carcasses. See Swayne 2008a, pp. 333–52

Bridges CB, Katz JM, Seto WH, Chan PKS, Tsang D, et al. 2000. Risk of influenza A (H5N1) infection among health care workers exposed to patients with influenza A (H5N1), Hong Kong. *J. Infect. Dis.* 181:344–48

Brown JD, Swayne DE, Cooper RJ, Burns RE, Stallknecht DE. 2007. Persistence of H5 and H7 avian influenza viruses in water. *Avian Dis.* 51:285–89

Burns A, van der Mensbrugghe D, Timmer H. 2008. Evaluating the economic consequences of avian influenza. In *Global Development Finance*, pp. 1–6. **http://siteresources.worldbank.org/EXTAVIANFLU/Resources/EvaluatingAHIeconomics_2008.pdf**

Cappucci DT, Johnson DC, Brugh M, Smith TM, Jackson CF, et al. 1985. Isolation of avian influenza virus (subtype H5N2) from chicken eggs during a natural outbreak. *Avian Dis.* 29:1195–2000

Capua I, Alexander DJ. 2004. Avian influenza: recent developments. *Avian Pathol.* 33:393–404

CDC. 2005. Avian influenza (bird flu). In *Influenza Viruses*, pp. 1–3. **http://www.cdc.gov/flu/avian/gen-info/pdf/flu_viruses.pdf**

CDC. 2006. Avian influenza (flu). In *Avian Influenza A Virus Infections of Humans*, pp. 1–3. **http://www.cdc.gov/flu/avian/gen-info/avian-flu-humans.htm**

CDC. 2007. Avian influenza: current H5N1 situation. In *Avian Influenza* (*Bird Flu*), pp. 1–4. **http://www.cdc.gov/flu/avian/outbreaks/current.htm**

Chen H, Smith GJD, Li KS, Wang J, Fan XH, et al. 2006. Establishment of multiple sublineages of H5N1 influenza virus in Asia: implications for pandemic control. *Proc. Natl. Acad. Sci. USA* 103:2845–50

Annu. Rev. Food Sci. Technol. 2011.2:37-57. Downloaded from www.annualreviews.org
by U.S. Department of Agriculture on 03/01/11. For personal use only.

Chmielewski R, Swayne DE. 2010. Thermal inactivation of Newcastle virus in imitation egg product. *Res. Prog. Rep. Am. Egg Board.* 3 June 2010:1–9

Cox N, Uyeki TM. 2008. Public health implications of avian influenza viruses. See Swayne 2008a, pp. 453–84

de Wit JJ, Fabri THF, Hoogkamer A. 2004. *Survival of Avian Influenza Virus on Eggs*, Gezondheidsdienst voor Dieren, Res. Dev. Poult. Health, Deventer, the Netherlands

Domanska-Blicharz K, Minta Z, Smietanka K, March S, van den Berg T. 2010. H5N1 high pathogenicity avian influenza virus survival in different types of water. *Avian Dis.* 54:734–37

Donatelli I, Campitelli L, Trani LD, Puzelli S, Selli L, et al. 2001. Characterization of H5N2 influenza viruses from Italian poultry. *J. Gen. Virol.* 82:623–30

Duan L, Campitelli L, Fan XH, Leung YH, Vijaykrishna D, et al. 2007. Characterization of low-pathogenic H5 subtype influenza viruses from Eurasia: implications for the origin of highly pathogenic H5N1 viruses. *J. Virol.* 81:7529–39

Dunham EJ, Dugan VG, Kaser EK, Perkins SE, Brown IH, et al. 2009. Different evolutionary trajectories of European avian-like and classical swine H1N1 influenza A viruses. *J. Virol.* 83:5485–94

Dusek RJ, Bortnerb JB, DeLibertoc TJ, Hoskinsb J, Fransona JC, et al. 2009. Surveillance for high pathogenicity avian influenza virus in wild birds in the pacific flyway of the United States, 2006–2007. *Avian Dis.* 53:222–30

Influenza team (ECDC). 2007. Low Pathogenicity Avian Influenzas and human health. *Euro. Surveill.* 12(5):E070531.3. **http://www.eurosurveillance.org/ew/2007/070531.asp#3**

Escorcia M, Vázquez L, Méndez ST, Rodríguez-Ropón A, Lucio E, Nava GM. 2008. Avian influenza: genetic evolution under vaccination pressure. *Virology* 5:1–5

FAO. 2007. Food Outlook Global Market Analysis. In *Meat and Meat Product Prices*, pp. 30–31. Rome: FAO. **http://www.fao.org/giews/english/fo/index.htm#2007**

FAO. 2010. Despite many successes, avian influenza still threatens: FAO calls for sustained action on H5N1 and emerging infections. In *FAO Media Centre*, Rome. **http://www.fao.org/news/story/en/item/41276(icode/FAO)**

Fouchier RAM, Schneeberger PM, Rozendaal FW, Broekman JM, Kemin SAG, et al. 2004. Avian influenza A virus (H7N7) associated with human conjunctivitis and a fatal case of acute respiratory distress syndrome. *Proc. Natl. Acad. Sci. USA* 101:1356–61

Gambaryan A, Webster R, Matrosovich M. 2002. Differences between influenza virus receptors on target cells of duck and chicken. *Arch. Virol.* 147:1197–208

Gao Y, Zhang Y, Shinya K, Deng G, Jiang Y, et al. 2009. Identification of amino acids in HA and PB2 critical for the transmission of H5N1 avian influenza viruses in a mammalian host. *PLoS Pathog.* 5:e1000709

Gilsdorf A, Boxall N, Gasimov V, Agayev I, Mammadzade F, et al. 2006. Two clusters of human infection with influenza A/H5N1 virus in the Republic of Azerbaijan, February–March. *Eurosurveillance* 11:122–26

Guan J, Chan M, Grenier C, Wilkie DC, Brooks BW, Spencer JL. 2009. Survival of avian influenza and Newcastle disease viruses in compost and at ambient temperatures based on virus isolation and real-time reverse transcriptase PCR. *Avian Dis.* 53:26–33

Guan Y, Peiris JSM, Lipatov AS, Ellis TM, Dyrting KC, et al. 2002a. Emergence of multiple genotypes of H5N1 avian influenza viruses in Hong Kong SAR. *Proc. Natl. Acad. Sci. USA* 99:8950–55

Guan Y, Peiris M, Kong KF, Dyrting KC, Ellis TM, et al. 2002b. H5N1 influenza viruses isolated from geese in Southeastern China: evidence for genetic reassortment and interspecies transmission to ducks. *Virology* 292:16–23

Harder TC, Teuffert J, Starick E, Gethmann J, Grund C, et al. 2009. Highly pathogenic avian influenza virus (H5N1) in frozen duck carcasses, Germany, 2007. *Emerg. Infect. Dis.* 15:1–8

Hatta M, Gao P, Halfmann P, Kawaoka Y. 2001. Molecular basis for high virulence of Hong Kong H5N1 influenza A viruses. *Science* 293:1840–42

Hinshaw VS. 1985. The nature of avian influenza in migratory waterfowl, including interspecies transmission. In *1986 Proc. 2nd Int. Symp. Avian Influenza*, pp. 133–41. Athens, GA: Am. Assoc. Avian Pathol.

Horimoto T, Rivera E, Pearson J, Senne D, Krauss S, et al. 1995. Origin and molecular changes associated with emergence of a highly pathogenic H5N2 influenza virus in Mexico. *Virology* 213:223–30

Annu. Rev. Food Sci. Technol. 2011.2:37-57. Downloaded from www.annualreviews.org
by U.S. Department of Agriculture on 03/01/11. For personal use only.

Hulse-Post DJ, Sturm-Ramirez KM, Humberd J, Seiler P, Govorkova EA, et al. 2005. Role of domestic ducks in the propagation and biological evolution of highly pathogenic H5N1 influenza viruses in Asia. *Proc. Natl. Acad. Sci. USA* 102:10682–87

INFOSAN IFSAN-. 2004. Avian influenza. In *INFOSAN Inf. Note No. 2/04*. 3 pp.

Ito T, Suzuki Y, Suzuki T, Takada A, Horimoto T, et al. 2000. Recognition of N-glycolylneuraminic acid linked to galactose by the alpha 2,3 linkage is associated with intestinal replication of influenza A virus in ducks. *J. Virol.* 74:9300–5

Katz JM, Veguilla V, Belser JA, Maines TR, Hoeven NV, et al. 2008. The public health impact of avian influenza viruses. *Poult. Sci.* 88:872–79

Kawaoka Y, Naeve CW, Webster RG. 1984. Is virulence of H5N2 influenza viruses in chickens associated with loss of carbohydrate from the hemagglutinin? *Virology* 139:303–16

Kim J-K, Negovetich NJ, Forrest HL, Webster RG. 2009. Ducks: the "Trojan horses" of H5N1 influenza. *Influenza Respir. Viruses* 3:121–28

Koopmans M, Duizer E. 2004. Foodborne viruses: an emerging problem. *Int. J. Food Microbiol.* 90:23–41

Koopmans M, Wilbrink B, Conyn M, Natrop G, van der Nat H, et al. 2004. Transmission of H7N7 avian influenza A virus to human beings during a large outbreak in commercial poultry farms in the Netherlands. *Lancet* 363:587–93

Kuchipudi SV, Nelli R, White GA, Bain M, Chang KC, Dunham S. 2009. Differences in influenza virus receptors in chickens and ducks: Implications for interspecies transmission. *J. Mol. Genet. Med.* 3:143–51

Lee C-W, Saif YM. 2009. Avian influenza virus. *Comp. Immunol. Microbiol. Infect. Dis.* 32:301–10

Li KS, Xu KM, Peiris JSM, Poon LLM, Yu KZ, et al. 2003. Characterization of H9 subtype influenza viruses from the ducks of Southern China: a candidate for the next influenza pandemic in humans? *J. Virol.* 77:6988–94

Liu J, Bi Y, Qin K, Fu G, Yang J, et al. 2009. Emergence of European avian influenza virus-like H1N1 swine influenza A viruses in China. *J. Clin. Microbiol.* 48:2643–46

Lokuge B. 2005. *Avian influenza, world food trade and WTO rules: The economics of transboundary disease control. Rep*. Work. Pap. Jan., The Aust. Natl. Univ., Canberra

Lu H, Castro AE, Pennick K, Liu J, Yang Q, et al. 2003. Survival of avian influenza virus H7N2 in SPF chickens and their environment. *Avian Dis.* 47:1015–21

Mase M, Eto M, Tanimura N, Imai K, Tsukamoto K, et al. 2005. Isolation of a genotypically unique H5N1 influenza virus from duck meat imported into Japan from China. *Virology* 339:101–9

Matrosovich MN, Matrosovich TY, Gray T, Roberts NA, Klenk H-D. 2004. Human and avian influenza viruses target different cell types in cultures of human airway epithelium. *Proc. Natl. Acad. Sci. USA* 101:4620–24

McLeod A, Morgan N, Prakash A, Hinrichs J. 2005. *Economic and Social Impact of Avian Influenza*. Rome: FAO Emerg. Cent. Transbound. Anim. Dis. Oper. (ECTAD)

Munier S, Larcher T, Cormier-Aline F, Soubieux D, Su B, et al. 2010. A genetically engineered waterfowl influenza virus with a deletion in the stalk of the neuraminidase has increased virulence for chickens. *J. Virol.* 84:940–52

Nguyen-Van-Tam JSN, Nair P, Acheson P, Baker A, Barker M, et al. 2006. Outbreak of low pathogenicity H7N3 avian influenza in UK, including associated case of human conjunctivitis. *Eurosurveillance* 11:1–2

OIE. 2009. OIE Terr. Anim. Health Code: Avian influenza, Article 10.4.1. In *Health Standards*. Paris, Fr.: OIE. **http://www.oie.int/eng/normes/mcode/en_chapitre_1.10.4.htm**

Oner AF, Bay A, Arslan S, Akdeniz H, Sahin HA, et al. 2006. Avian influenza A (H5N1) infection in eastern Turkey in 2006. *N. Engl. J. Med.* 355:2179–85

Otte J, Hinrichs J, Rushton J, Roland-Holst D, Zilberman D. 2008. Impacts of avian influenza virus on animal production in developing countries. *CAB Rev.: Perspect. Agric. Vet. Sci. Nutr. Nat. Resour.* 3:1–18

Pantin-Jackwood M, Wasilenko JL, Spackman E, Suarez DL, Swayne DE. 2010. Susceptibility of turkeys to pandemic-H1N1 virus by reproductive tract insemination. *Virol. J.* 7:27

Pappas C, Matsuoka Y, Swayne DE, Donis RO. 2007. Development and evaluation of an influenza virus subtype H7N2 vaccine candidate for pandemic preparedness. *Clin. Vaccine Immunol.* 14:1425–32

Perdue ML, Garcia M, Beck J, Brugh M, Swayne DE. 1996. An Arg-Lys insertion at the hemagglutinin cleavage site of an H5N2 avian influenza isolate. *Virus Genes* 12:77–84

Annu. Rev. Food Sci. Technol. 2011.2:37-57. Downloaded from www.annualreviews.org
by U.S. Department of Agriculture on 03/01/11. For personal use only.

Pillai SPS, Pantin-Jackwood M, Yassine HM, Saif YM, Lee CW. 2010. The high susceptibility of turkeys to influenza viruses of different origins implies their importance as potential intermediate hosts. *Avian Dis.* 54:522–26

Promkuntod N, Antarasena C, Prommuang P, Prommuang P. 2006. Isolation of avian influenza virus A subtype H5N1 from internal contents (albumen and allantoic fluid) of Japanese quail (*Coturnix coturnix japonica*) eggs and oviduct during a natural outbreak. *Ann. NY Acad. Sci.* 1081:171–73

Ramirez-Nieto G, Shivaprasad HL, Kim C-H, Lillehoj HS, Song H, et al. 2010. Adaptation of a mallard H5N2 low pathogenicity influenza virus in chickens with prior history of infection with infectious bursal disease virus. *Avian Dis.* 54:513–21

Senne DA. 2010. Avian influenza in North and South America, the Caribbean, and Australia, 2006–2008. *Avian Dis.* 54:179–86

Senne DA, Suarez DL, Pedersen JC, Panigrahy B. 2003. Molecular and biological characteristics of H5 and H7 avian influenza viruses found in live-bird markets of northeastern United States during 1994–2001. *Avian Dis.* 47:898–904

Sinha NK, Roy A, Das B, Das S, Basak S. 2009. Evolutionary complexities of swine flu H1N1 gene sequences of 2009. *Biochem. Biophys. Res. Commun.* 390:349–51

Spackman E, Senne DA, Davison S, Suarez DL. 2003. Sequence analysis of recent H7 avian influenza viruses associated with three different outbreaks in commercial poultry in the United States. *J. Virol.* 77:13399–402

Stallknecht DE, Brown JD. 2007. Wild birds and the epidemiology of avian influenza. *J. Wildl. Dis.* 43:S15–20

Stallknecht DE, Goekjian VH, Wilcox BR, Poulson RL, Brown JD. 2010. Avian influenza virus in aquatic habitats: What do we need to learn? *Avian Dis.* 54:461–65

Suarez D. 2008. Influenza A virus. See Swayne 2008a, pp. 3–22

Suarez DL, Spackman E, Senne DA. 2009. Update on molecular epidemiology of H1, H5, and H7 influenza virus infections in poultry in North America. *Avian Dis.* 47:888–97

Suarez DL, Woolcock PR, Bermudez AJ, Senne DA. 2002. Isolation from turkey breeder hens of a reassortant H1N2 influenza virus with swine, human, and avian lineage genes. *Avian Dis.* 46:111–21

Swayne DE. 2005. Occupational and consumer risks from avian influenza viruses. *Dev. Biol.* 124:85–90

Swayne DE. 2006. Microassay for measuring thermal inactivation of H5N1 high pathogenicity avian influenza virus in naturally infected chicken meat. *Int. J. Food Microbiol.* 108:268–71

Swayne DE, ed. 2008a. *Avian Influenza*. Ames, IA: Blackwell

Swayne DE. 2008b. Epidemiology of avian influenza in agricultural and other man-made systems. See Swayne 2008a, pp. 59–85

Swayne DE. 2008c. The global nature of avian influenza. See Swayne 2008a, pp. 123–43

Swayne DE, Beck JR. 2004. Heat inactivation of avian influenza and Newcastle disease viruses in egg products. *Avian Pathol.* 33:512–18

Swayne DE, Halvorson DA. 2008. Influenza. In *Diseases of Poultry*, ed. YM Saif, JR Glisson, AM Fadly, LR McDougald, L Nolan, pp. 153–84. Ames, IA: Blackwell

Swayne DE, Suarez DL. 2007. Current developments in avian influenza vaccines, including safety of vaccinated birds as food. *Dev. Biol.* 130:123–33

Tam JS. 2002. Influenza A (H5N1) in Hong Kong: an overview. *Vaccine* 20:S77–81

Thanawongnuwech R, Amonsin A, Tantilertcharoen R, Damrongwatanapokin S, Theamboonlers A, et al. 2005. Probable tiger-to-tiger transmission of avian influenza H5N1. *Emerg. Infect. Dis.* 11:699–701

Thomas C, King DJ, Swayne DE. 2008. Thermal inactivation of avian influenza and Newcastle disease viruses in chicken meat. *J. Food Prot.* 71:1214–22

Thomas C, Swayne DE. 2007. Thermal inactivation of H5N1 high pathogenicity avian influenza virus in naturally infected chicken meat. *J. Food Prot.* 70:674–80

Tiwari A, Patnayak DP, Chander Y, Parsad M, Goyal SM. 2006. Survival of two avian respiratory viruses on porous and nonporous surfaces. *Avian Dis.* 50:284–87

Tumpey TM, Suarez DL, Perkins LEL, Senne DA, Lee J-G, et al. 2002. Characterization of a highly pathogenic H5N1 avian influenza A virus isolated from duck meat. *J. Virol.* 76:6344–55

Ungchusak K, Auewarakul P, Dowell SF, Kitphati R, Auwanit W, et al. 2005. Probable person-to-person transmission of avian influenza A (H5N1). *N. Engl. J. Med.* 352:333–40

Annu. Rev. Food Sci. Technol. 2011.2:37-57. Downloaded from www.annualreviews.org
by U.S. Department of Agriculture on 03/01/11. For personal use only.

Walker JA, Kawaoka Y. 1993. Importance of conserved amino acids at the cleavage site of the haemagglutinin of a virulent avian influenza A virus. *J. Gen. Virol.* 74:311–14

Wan H, Sorrell EM, Song H, Hossain MJ, Ramirez-Nieto G, et al. 2008. Replication and transmission of H9N2 influenza viruses in ferrets: evaluation of pandemic potential. *PLoS ONE* 3:e2923

Webster RG, Bean WJ, Gorman OT, Chambers TM, Kawaoka Y. 1992. Evolution and ecology of influenza A viruses. *Microbiol. Rev.* 56:152–79

Webster RG, Krauss S, Hulse-Post D, Sturm-Ramirez K. 2007. Evolution of influenza A virus in wild birds. *J. Wildl. Dis.* 43:S1–6

Whiting RC, Buchanan RL. 1997. Development of a quantitative risk assessment model for *Salmonella enteritidis* in pasteurized liquid eggs. *Int. J. Food Microbiol.* 36:111–25

WHO. 2004. Avian influenza A(H5N1) in humans and in poultry in Asia: food safety considerations. In *Food Safety*, pp. 1–2. **http://www.who.int/foodsafety/micro/avian1/en/print.html**

WHO. 2005. Avian influenza frequently asked questions. In *Communicable Disease Surveillance and Response*, pp. 1–6. **http://www.who.int/csr/disease/avian_influenza/avian_faqs/en/print.html**

WHO. 2005a. Evolution of H5N1 avian influenza viruses in Asia. *Emerg. Infect. Dis.* 11:1515–21

WHO. 2005b. Highly pathogenic H5N1 avian influenza outbreaks in poultry and in humans: food safety implications. In *International Food Safety Authorities Network-Avian Influenza*, pp. 1–5. **www.who.int/foodsafety**

WHO. 2006. H5N1 avian influenza: timeline of major events. In *Global Alert and Response*, 10 pp. **http://www.who.int/csr/disease/avian_influenza/ai_timeline/en/index.html**

WHO. 2007. Questions and answers on avian influenza in relation to animal, food and water. In *Food Safety*, pp. 1–14. **http://www.who.int/foodsafety/micro/AI_QandA_Apr07_EN.pdf**

WHO. 2008. Update: WHO-confirmed human cases of avian influenza A(H5N1) infection, November 2003–May 2008. *Wkly Epidemiol. Rec.* 83:415–20

WHO. 2010. Avian influenza: cumulative number of confirmed human cases of avian influenza A/(H5N1) reported to WHO. In *Global Alert and Response*. **http://www.who.int/csr/disease/avian_influenza/country/cases_table_20WHO**

World Bank. 2010. Health, nutrition and population: economic impact of avian flu. In *Global Program for Avian Influenza and Human Pandemic*, pp. 1–4. Washington, DC: World Bank

Writ. Comm. Second WHO Consult. Clin. Aspects Hum. Infect. Avian Influenza A Virus. 2008. Update on avian influenza A (H5N1) virus infection in humans. *N. Engl. J. Med.* 358:261–73

Xu X, Subbarao K, Cox NJ, Guo Y. 1999. Genetic characterization of the pathogenic influenza A/Goose/Guangdong/1/96 (H5N1) virus: similarity of its hemagglutinin gene to those of H5N1 viruses from the 1997 outbreaks in Hong Kong. *Virology* 261:15–19

Yalcin C. 2006. Market impact of HPAI outbreaks: a rapid appraisal process-turkey. In *The Market and Trade Dimensions of Avian Influenza*, pp. 1–28. Rome: FAO

Yamamoto Y, Nakamura K, Okamatsu M, Yamada M, Mase M. 2008. Avian influenza virus (H5N1) replication in feathers of domestic waterfowl. *Emerg. Infect. Dis.* 14:149–51

Yamamoto Y, Nakamura K, Yamada M, Ito T. 2009. Zoonotic risk for influenza A (H5N1) infection in wild swan feathers. *J. Vet. Med. Sci.* 71:1549–51

Yuen KY, Chan PKS, Peiris M, Tsang DNC, Que TL, et al. 1998. Clinical features and rapid viral diagnosis of human disease associated with avian influenza A H5N1 virus. *Lancet* 351:467–71

Journal of Wildlife Diseases, 47(1), 2011, pp. 240–245
© Wildlife Disease Association 2011

Avian Influenza Viruses and Avian Paramyxoviruses in Wintering and Breeding Waterfowl Populations in North Carolina, USA

Virginia H. Goekjian,[1] Jennifer T. Smith,[1] Doug L. Howell,[2] Dennis A. Senne,[3] David E. Swayne,[4] and David E. Stallknecht[1,5] [1] Southeastern Cooperative Wildlife Disease Study, Department of Population Health, College of Veterinary Medicine, The University of Georgia, Athens, Georgia 30602, USA; [2] North Carolina Wildlife Resources Commission, Division of Wildlife Management, Surveys and Research Section, Edenton, North Carolina 27932, USA; [3] US Department of Agriculture, Animal and Plant Health Inspection Service, National Veterinary Services Laboratories, Ames, Iowa 50010, USA (retired); [4] Southeast Poultry Research Laboratory, Agricultural Research Service, US Department of Agriculture, Athens, Georgia 30605, USA; [5] Corresponding author (email: dstall@uga.edu)

ABSTRACT: Although wild ducks are recognized reservoirs for avian influenza viruses (AIVs) and avian paramyxoviruses (APMVs), information related to the prevalence of these viruses in breeding and migratory duck populations on North American wintering grounds is limited. Wintering (n=2,889) and resident breeding (n=524) ducks were sampled in North Carolina during winter 2004–2006 and summer 2005–2006, respectively. Overall prevalence of AIV was 0.8% and restricted to the winter sample; however, prevalence in species within the genus *Anas* was 1.3% and was highest in Black Ducks (7%; *Anas rubripes*) and Northern Shovelers (8%; *Anas clypeata*). Of the 24 AIVs, 16 subtypes were detected, representing nine hemagglutinin and seven neuraminidase subtypes. Avian paramyxoviruses detected in wintering birds included 18 APMV-1s, 15 APMV-4s, and one APMV-6. During summers 2005 and 2006, a high prevalence of APMV-1 infection was observed in resident breeding Wood Ducks (*Aix sponsa*) and Mallards (*Anas platyrhynchos*).

Key words: Avian influenza viruses, avian paramyxoviruses, ducks, North Carolina, wintering areas, wood ducks.

Ducks are reservoir hosts for a broad diversity of avian influenza viruses (AIVs) and avian paramyxoviruses (APMVs); APMVs isolated from free-living ducks include APMV-1, -2, -3, -4, -6, -7, -8 (Stallknecht et al., 1991), and -9 (Dundon et al., 2010). Avian influenza viruses, representing hemagglutinin (HA) subtypes 1–13, have been recovered from North American ducks (Stallknecht and Shane, 1988; Sharp et al., 1997). Currently, there is limited information on these viruses in ducks wintering in the southeastern United States, and no information related to the prevalence of AIVs or APMVs in naturally occurring or newly established breeding populations using this region. The objectives of this study were to 1) provide reliable prevalence estimates for a diversity of APMVs and AIVs in wintering waterfowl populations using southern wintering grounds of the Atlantic flyway and 2) provide novel information on the prevalence of APMVs and AIVs in resident breeding waterfowl populations.

Waterfowl were sampled by personnel of the North Carolina Wildlife Resources Commission (NCWRC) from 2004 to 2006. Samples collected from wintering waterfowl were obtained primarily from hunter-killed birds. Samples from 79 wintering Northern Pintails (*Anas acuta*) and all samples in summer were collected from ducks that were live-captured using rocket nets. During summer, only Mallards (*Anas platyrhnchos*) and Wood Ducks (*Aix sponsa*) were sampled at 10 sites within Camden, Gates, Pasquotank, Perquimans, Tyrrell, and Washington counties in North Carolina, USA (Fig. 1). Hunter-killed birds were sampled during October, November, December, and January from Beaufort, Bladen, Hyde, Martin, Onslow, Pamlico, Tyrrell, and Washington counties in eastern North Carolina (Fig. 1). Live-captured Northern Pintails were sampled during February after the

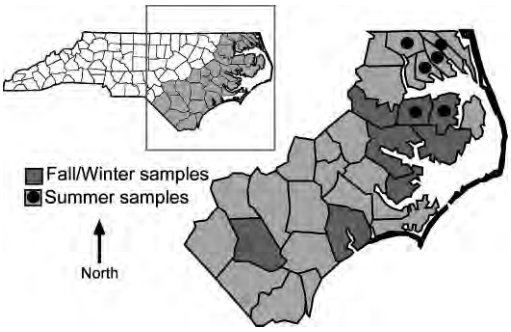

FIGURE 1. Counties where ducks were sampled during fall and winter 2004–2006 and summer 2005–2006.

conclusion of the 2005 waterfowl hunting season.

Cloacal swabs were collected from all birds by NCWRC personnel and placed in brain heart infusion broth as described previously (Hanson et al., 2008). Swabs were stored on cold packs or in a refrigerator (4 C) for no more than 3 days and were shipped overnight to the Southeastern Cooperative Wildlife Disease Study, University of Georgia, Athens, Georgia, USA, where they were stored at −80 C until testing. Virus isolation was attempted in specific-pathogen-free, 9-day-old embryonating chicken eggs (Hanson et al., 2008). Viral isolates were initially detected by hemagglutination assay as described previously (Stallknecht et al., 1990), and all positive AIV and APMV samples were identified and subtyped using hemagglutination inhibition and neuraminidase inhibition tests at the National Veterinary Services Laboratories, Ames, Iowa, USA. Subtypes were confirmed, or in the case of partial subtype identification, completed by reverse transcription-PCR using the methods of Lee et al. (2001), Tsukamoto et al. (2008, 2009), and Qiu et al. (2009).

During winters 2004–2006, 2,889 birds were tested, representing 23 species in the families Anatidae and Rallidae (Table 1). Most AIV isolations (21/24; 87.5%) came from species in the genus *Anas.* Overall AIV prevalence in *Anas* species was 1.3% (20/1,555) compared with 0.2% for all other species; annual AIV prevalence estimates for *Anas* species were 1.4% (3/206), 1.1% (6/557), and 1.4% (11/792) during 2004, 2005, and 2006, respectively. Recovered subtypes from *Anas* species included H1N1, H2N7, H3N2, H3N8, H4N1, H4N6, H5N1, H6N2, H7N3, H7N6, H10N3, H10N7, H11N3, and H11N9. One Black Duck (*Anas rubripes*) sampled during 2006 was dually infected with an H5N1 and an H4N1 AIV. An H6N1 was isolated from a Tundra Swan (*Cygnus columbianus*), and H6N1 and H4N8 were recovered from two Bufflheads (*Bucephala albeola*). Other isolates included APMV-1 ($n=18$), APMV-4 ($n=15$), and APMV-6 ($n=1$; Table 1).

Birds sampled from 8 June to 13 September 2005 included 46 Mallards and 256 Wood Ducks. From 5 July to 12 September 2006, 40 Mallards and 182 Wood Ducks were sampled. All samples tested negative for AIV; however, APMV-1 was recovered from 11% (5/46) and 25% (10/40) of sampled Mallards during 2005 and 2006, respectively. Peak APMV-1 prevalence in Mallards was observed on 27 July (4/14; 29%) during 2005 and 12 July (8/12; 67%) during 2006. For Wood Ducks, APMV-1 was isolated from 9% (22/256) and 13% (24/182) during 2005 and 2006, respectively. In Wood Ducks, a clear seasonal trend was observed both years (Fig. 2). In 2005, APMV-1 was detected in six of eight sampled areas located in five counties (Camden, Pasquotank, Perquimans, Tyrrell, and Washington), and during 2006, in two of four of the sampled areas (Gates and Perquimans counties).

The low prevalence of AIVs in wintering waterfowl in the southeastern United States is consistent with previous reports from wintering waterfowl in Arkansas (Webster et al., 1976); Louisiana (Stallknecht et al., 1990); Texas (Ferro et al., 2010); and Georgia, Alabama, and Florida (Dormitoriao et al., 2009), USA, as well as wintering waterfowl populations in Eu-

TABLE 1. Avian influenza viruses and avian paramyxoviruses isolated from wintering waterfowl in North Carolina, USA, 2004–2006.

Common name	Total tested	2004[a,b]	2005	2006
Anatidae				
Canada Goose (*Branta canadensis*)	9	0	0	9
Tundra Swan (*Cygnus columbianus*)	70	21	41 (H6N1)	8
Wood Duck (*Aix sponsa*)	348	76 (APMV1 [4])	137 (APMV4 [2])	135 (APMV1)
Gadwall (*Anas strepera*)	293	78	47 (H1N1)	168 (APMV1)
American Wigeon (*Anas americana*)	334	29	130 (APMV4)	175 (H3N8, H6N2)
American Black Duck (*Anas rubripes*)	60	11 (H3N2)	11 (H1N1)	38 (H5N1+H4N1[c], H11N9)
Mallard (*Anas platyrhynchos*)	69	36 (H10N7)	7	26 (H11N9, APMV4)
Blue-winged Teal (*Anas discors*)	71	4 (APMV1)	32 (H11N3, APMV4)	35 (APMV1 [2], APMV4)
Northern Shoveler (*Anas clypeata*)	80	4 (H1N1)	19 (H7N3 [2], H7N6)	57 (H10N3 [2], APMV1, APMV4 [2])
Northern Pintail (*Anas acuta*)	107	2	100	5
Green-winged Teal (*Anas crecca*)	541	42	211 (APMV1, APMV4)	288 (H2N7, H4N6, H10N7 [2], APMV1 [3], APMV4 [5], APMV6)
Redhead (*Aythya americana*)	13	2	9	2
Ring-necked Duck (*Aythya collaris*)	319	30	182 (APMV1 [2])	107 (APMV1)
Greater Scaup (*Aythya marila*)	8	0	6	2
Lesser Scaup (*Aythya affinis*)	87	11	56	20
Surf Scoter (*Melanitta perspicillata*)	13	0	0	13
Black Scoter (*Melanitta nigra*)	13	1	7	5
Bufflehead (*Bucephala albeola*)	129	4	104 (H6N1, H4N8)	21
Hooded Merganser (*Lophodytes cucullatus*)	117	30 (APMV1)	38	49
Common Merganser (*Mergus merganser*)	7	0	7	0
Red-breasted Merganser (*Mergus serrator*)	8	0	0	8
Ruddy Duck (*Oxyura jamaicensis*)	178	14	125	39 (APMV4)
Rallidae				
American Coot (*Fulica americana*)	15	9	6	0
Total	2,889	404	1,275	1,210

[a] Number tested (virus isolated [number of isolates]). If no number is given, one isolate was made.

[b] APMV1 = avian paramyxovirus-1, APMV2 = avian paramyxovirus-2, APMV4 = avian paramyxovirus-4; avian influenza viruses are identified by hemagglutinin (H) and neuraminidase (N) subtype.

[c] Dual avian influenza virus infection detected in a single bird. The dual infection was detected at the National Veterinary Services Laboratories, US Department of Agriculture (USDA), Ames, Iowa, USA, when an H4N1 virus was isolated from a sample that also tested positive to H5 by reverse transcription-PCR. The H5N1 subtype was subsequently isolated from this same sample at the Southeast Poultry Research Laboratory, Agricultural Research Service, USDA, Athens, Georgia, USA.

rope (Cattoli et al., 2007 [Italy]; Lebarbenchon et al., 2007 [France]; Busquets et al., 2010 [Spain]). Peak prevalence on wintering areas in the southeastern United States seems to be associated with early migrating duck populations, especially Blue-winged Teal (*Anas discors*; Stallknecht et al., 1990) and in ducks before prespring migration (Hanson et al., 2005). Similarly, on wintering areas in France, a

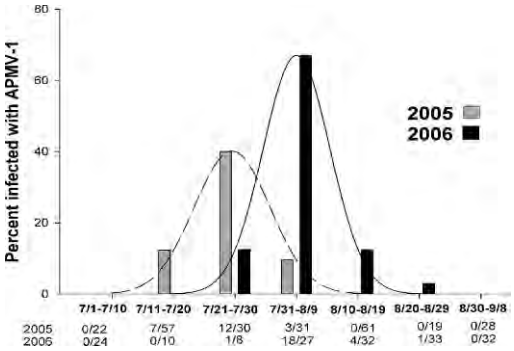

FIGURE 2. Prevalence of avian paramyxovirus 1 (APMV-1) in Wood Ducks sampled during summers 2005 and 2006. Number positive by virus isolation and the number sampled are presented below the x axis corresponding to the 10-day sample periods.

decline in AIV prevalence in ducks was observed from September to February (Lebarbenchon et al., 2010) and in northern Europe, a peak in AIV prevalence during spring migration was observed (Wallensten et al., 2007). The higher prevalence of AIV observed in *Anas* species also is consistent with the previous reports of AIV within Anseriformes (Olsen et al., 2006). Within this genus, AIV has been reported most often from Mallards, Blue-winged Teal, Northern Pintails, and American Black Ducks (Olsen et al., 2006). With the exception of the Northern Pintail, AIV was isolated from all of these species in the present study with the highest prevalence recorded from Black Ducks (7%) and Northern Shovelers (8%; *Anas clypeata*). Northern Shovelers are commonly infected with AIV on wintering grounds in North America (Hill et al., 2010) and Europe (Munster et al., 2007; Lebarbenchon et al., 2010), and they could potentially play an important role in AIV maintenance over the wintering period.

The subtype diversity observed in this study also mirrored previous findings from wintering duck populations in both North America and Europe. Although prevalence is generally low, the isolation of multiple subtypes is commonly reported (Stallknecht et al., 1990; Busquets et al., 2010). This may be related to the mixing of populations after AIV amplification during premigration staging, and transmission on the wintering grounds may be a critical overwintering mechanism. The failure to isolate AIV from ducks sampled during the summer may reflect the combined effects of species, and in Mallards, a limited population density. These negative results also could reflect reduced environmental persistence of these viruses in the aquatic habitats used by these ducks due to elevated summer water temperatures; based on experimental studies, AIV inactivation is increased with increased water temperature (Brown et al., 2009). Although AIV has been reported from Wood Ducks (Olsen et al., 2006), such isolations are uncommon. With Mallards, the summer sample was composed of a small number of birds, reflecting a limited resident population.

There is limited information on the epidemiology of APMV in wild duck populations, and information primarily relates to incidental virus isolations associated with AIV surveillance. The low prevalence of APMV-1 in wintering ducks in the present study is very similar to that reported in coastal Louisiana (Stallknecht et al., 1991). In that study, prevalence decreased from September through January but never exceeded 4%. The high prevalence of APMV-1 infections observed in Wood Ducks during 2005 and 2006 was not expected, and we are unaware of any similar reports from wild ducks, especially when sampled during the summer.

This study was funded by the North Carolina Wildlife Resources Commission and by Specific Cooperative Agreement 58-6612-2-0220 between the Southeast Poultry Research Laboratory and the Southeastern Cooperative wildlife Disease Study. We acknowledge the assistance of North Carolina Wildlife Resources Commission personnel, including Kimberly McCargo, Joseph Fuller, and wildlife technicians at the Edenton, New Bern,

and Suggs Mill Pond wildlife depots for assistance in collecting samples. Wendy Stanton, Wildlife Biologist, Pocosin Lakes National Wildlife Refuge, Columbia, North Carolina, captured and provided Mallards for sampling. Jerry Fringeli, Assistant Refuge Manager, helped coordinate collection of hunter-killed waterfowl on Mattamuskeet National Wildlife Refuge, Swan Quarter, North Carolina.

LITERATURE CITED

Brown, J. D., G. Goekjian, R. Poulson, S. Valeika, and D. E. Stallknecht. 2009. Avian influenza viruses in water: Infectivity is dependent on pH, salinity, and temperature. Veterinary Microbiology 136: 20–26.

Busquets, N., A. Alba, S. Napp, A. Sánchez, E. Serrano, R. Rivas, J. Núñez, and N. Majó. 2010. Influenza A virus subtypes in wild birds in northeastern Spain (Catalonia). Virus Research 149: 10–18.

Cattoli, G., C. Terregino, V. Guberti, R. De Nardi, A. Drago, A. Salviato, S. Fassina, and I. Capua. 2007. Influenza virus surveillance in wild birds in Italy: Results of laboratory investigations in 2003–2005. Avian Diseases 51 (Suppl): 414–416.

Dormitorio, T., J. Giambrone, K. Guo, and G. Hepp. 2009. Detection and characterization of avian influenza and other avian paramyxoviruses from wild waterfowl in parts of the southeastern United States. Poultry Science 88: 851–855.

Dundon, W. G., A. Heidari, R. De Nardi, C. Terreginio, I. Capua, and G. Cattoli. 2010. Genetic variation of Italian avian paramyxoviruses serotype 9. Virus Genes. doi 10.1007/s11262-010-0479-2.

Ferro, P. J., C. M. Budke, M. J. Peterson, D. Cox, E. Roltsch, T. Merendino, M. Nelson, and B. Lupiani. 2010. Multiyear surveillance for avian influenza virus in waterfowl from wintering grounds, Texas coast, USA. Emerging Infectious Diseases 16: 1224–1230.

Hanson, B. A., D. E. Swayne, D. A. Senne, D. S. Lobpries, J. Hurst, and D. E. Stallknecht. 2005. Avian influenza viruses and paramyxoviruses in wintering and resident ducks in Texas. Journal of Wildlife Diseases 41: 624–625.

———, M. P. Luttrell, V. H. Goekjian, L. Niles, D. E. Swayne, D. A. Senne, and D. E. Stallknecht. 2008. Is the occurrence of avian influenza virus in Chardriiformes species and location dependent? Journal of Wildlife Diseases 44: 351–361.

Hill, N. J., J. Y. Takekawa, C. J. Cardona, J. T. Ackerman, A. K. Schultz, K. A. Spragens, and W. M. Boyce. 2010. Waterfowl ecology and avian influenza in California: Do host traits inform us about viral occurrence? Avian Diseases 54: 426–432.

Lebarbenchon, C., S. van der Werf, F. Thomas, J.-T. Aubin, S. Saliha, F. Cuvelier, P. Jeannin, V. Roca, C.-M. Chang, Y. Kayser, B. Roche, J.-F. Guégan, F. Renaud, and M. Gauthier-Clerc. 2007. Absence of detection of highly pathogenic H5N1 in migratory waterfowl in southern France in 2005–2006. Infection, Genetics and Evolution 7: 604–608.

———, C.-M. Chang, V. Grandhomme, M. Dietrich, Y. Kayser, E. Elguero, F. Renaud, F. Thomas, S. van der Werf, and M. Gauthier-Clerc. 2010. Avian influenza circulation in the Carmargue (South of France) during the 2006–07 season. Avian Diseases, 54 (Suppl): 446–449.

Lee, M.-S., P.-C. Chang, J.-H. Shien, M.-C. Cheng, and H. K. Shieh. 2001. Identification and subtyping of avian influenza viruses by reverse transcription-PCR. Journal of Virological Methods 97: 13–22.

Munster, V. J., C. Baas, P. Lexmond, J. Waldenström, A. Wallensten, T. Fransson, G. F. Rimmelzwann, W. E. P. Beyer, M. Schetten, B. Olsen, A. D. M. E. Osterhaus, and R. M. Fouchier. 2007. Spatial, temporal, and species variation in prevalence of influenza A viruses in wild migratory birds. PLos Pathogens 3: e61. doi:10.1371/journal.ppat.0030061.st002.

Olsen, B., V. J. Munster, A. Wallensten, J. Waldenström, A. D. M. E. Osterhaus, and R. M. Fouchier. 2006. Global patterns of influenza A virus in wild birds. Science 312: 384–388.

Qiu, B.-F., W.-J. Liu, D.-X. Peng, S.-L. Hu, Y.-H. Tang, and X.-F. Liu. 2009. A reverse transcription-PCR for subtyping of the neuraminidase of avian influenza viruses. Journal of Virological Methods 155: 193–198.

Sharp, G. B., Y. Kawaoka, D. J. Jones, W. J. Bean, S. P. Pryor, V. Hinshaw, and R. G. Webster. 1997. Coinfection of wild ducks by influenza A viruses: Distribution patterns and biological significance. Journal of Virology 71: 6128–6135.

Stallknecht, D. E., and S. M. Shane. 1988. Host range of avian influenza virus in free-living birds. Veterinary Research Communications 12: 125–141.

———, ———, P. J. Zwank, and M. T. Kearney. 1990. Avian influenza viruses from migratory and resident ducks of coastal Louisiana. Avian Diseases 34: 398–405.

———, D. A. Senne, P. J. Zwank, S. M. Shane, and M. T. Kearney. 1991. Avian paramyxoviruses from migratory and wintering ducks in coastal Louisiana. Journal of Wildlife Diseases 27: 123–128.

Tsukamoto, K., H. Ashizawa, K. Nakanishi, N. Kaji, K. Suzuki, M. Okamatsu, S. Yamaguchi, and M. Mase. 2008. Subtyping of avian influenza viruses H1 to H15 on the basis of hemagglutinin genes by PCR assay and molecular determination of

pathogenic potential. Journal of Clinical Microbiology 46: 3048–3055.

———, ———, ———, ———, ———, M. Shishido, M. Okamatsu, and M. Mase. 2009. Use of reverse transcription PCR to subtype N1 to N9 neuraminidase genes of avian influenza viruses. Journal of Clinical Microbiology 47: 2301–2303.

Wallensten, A., V. J. Munster, N. Latorre-Margalef, M. Brytting, J. Elmberg, R. A. M. Fouchier, T. Frannsson, P. D. Haemig, M. Karlsson, Å. Lundkvist, A. D. N. E. Osterhaus, M. Stervander, J. Waldenström, and B. Olsen. 2007. Surveillance of influenza A virus in migratory waterfowl in northern Europe. Emerging Infectious Diseases 13: 404–411.

Webster, R. G., M. Morita, C. Pridgen, and B. Tumova. 1976. Ortho- and paramyxoviruses from migrating feral ducks: Characterization of a new group of influenza A viruses. Journal of General Virology 32: 217–225.

Submitted for publication 18 August 2010.
Accepted 24 September 2010.

Homo- and Heterosubtypic Low Pathogenic Avian Influenza Exposure on H5N1 Highly Pathogenic Avian Influenza Virus Infection in Wood Ducks (*Aix sponsa*)

Taiana P. Costa[1,2], Justin D. Brown[2], Elizabeth W. Howerth[1], David E. Stallknecht[2]*, David E. Swayne[3]

1 Department of Pathology, College of Veterinary Medicine, The University of Georgia, Athens, Georgia, United States of America, **2** Southeastern Cooperative Wildlife Disease Study, Department of Population Health, College of Veterinary Medicine, The University of Georgia, Athens, Georgia, United States of America, **3** Southeast Poultry Research Laboratory, United States Department of Agriculture, Agricultural Research Service, Athens, Georgia, United States of America

Abstract

Wild birds in the Orders Anseriformes and Charadriiformes are the natural reservoirs for avian influenza (AI) viruses. Although they are often infected with multiple AI viruses, the significance and extent of acquired immunity in these populations is not understood. Pre-existing immunity to AI virus has been shown to modulate the outcome of a highly pathogenic avian influenza (HPAI) virus infection in multiple domestic avian species, but few studies have addressed this effect in wild birds. In this study, the effect of pre-exposure to homosubtypic (homologous hemagglutinin) and heterosubtypic (heterologous hemagglutinin) low pathogenic avian influenza (LPAI) viruses on the outcome of a H5N1 HPAI virus infection in wood ducks (*Aix sponsa*) was evaluated. Pre-exposure of wood ducks to different LPAI viruses did not prevent infection with H5N1 HPAI virus, but did increase survival associated with H5N1 HPAI virus infection. The magnitude of this effect on the outcome of the H5N1 HPAI virus infection varied between different LPAI viruses, and was associated both with efficiency of LPAI viral replication in wood ducks and the development of a detectable humoral immune response. These observations suggest that in naturally occurring outbreaks of H5N1 HPAI, birds with pre-existing immunity to homologous hemagglutinin or neuraminidase subtypes of AI virus may either survive H5N1 HPAI virus infection or live longer than naïve birds and, consequently, could pose a greater risk for contributing to viral transmission and dissemination. The mechanisms responsible for this protection and/or the duration of this immunity remain unknown. The results of this study are important for surveillance efforts and help clarify epidemiological data from outbreaks of H5N1 HPAI virus in wild bird populations.

Citation: Costa TP, Brown JD, Howerth EW, Stallknecht DE, Swayne DE (2011) Homo- and Heterosubtypic Low Pathogenic Avian Influenza Exposure on H5N1 Highly Pathogenic Avian Influenza Virus Infection in Wood Ducks (*Aix sponsa*). PLoS ONE 6(1): e15987. doi:10.1371/journal.pone.0015987

Editor: Todd Davis, Centers for Disease Control and Prevention, United States of America

Received August 8, 2010; **Accepted** December 2, 2010; **Published** January 6, 2011

This is an open-access article distributed under the terms of the Creative Commons Public Domain declaration which stipulates that, once placed in the public domain, this work may be freely reproduced, distributed, transmitted, modified, built upon, or otherwise used by anyone for any lawful purpose.

Funding: Funding for this work was provided through specific Cooperative Agreement #58-6612-2-0220 between the Southeast Poultry Research Laboratory (http://www.ars.usda.gov/main/site_main.htm?modecode = 66-12-07-00) and the Southeastern Cooperative Wildlife Disease Study (SCWDS) (http://scwds.org/), through the continued sponsorship of SCWDS member state and federal agencies, and Current Research Information System project 6612-32000-048-00D. The funders had no role in the study design, data collection and analysis, decision to publish, or preparation of the manuscript.

Competing Interests: The authors have declared that no competing interests exist.

* E-mail: dstall@uga.edu

Introduction

Wild birds, especially those in the Orders Anseriformes and Charadriiformes, are the natural reservoirs for all known hemagglutinin (HA) (H1–H16) and neuraminidase (NA) (N1–N9) subtypes of avian influenza (AI) viruses [1,2,3,4,5]. It has been further suggested that wild birds might be involved in the geographic spread, transmission to humans, and maintenance of H5N1 highly pathogenic avian influenza (HPAI) virus in Eurasia and Africa [6,7,8].

Concurrent or successive infections with different low pathogenic avian influenza (LPAI) virus subtypes have been reported in both wild bird populations and poultry [9,10,11,12]. Existing experimental data suggest that AI virus infection in waterfowl is associated with a variable protective immune response. In Pekin ducks (*Anas platyrhynchos domesticus*) primary inoculation with a LPAI virus induced partial protection against repeated inoculation with the same virus [13]. Additionally, pre-exposure to LPAI viruses has been shown to induce partial protection against H5N1 HPAI virus infection in Canada geese (*Branta canadensis*) [14,15], mute swans (*Cygnus olor*) [16], mallards (*Anas platyrhynchos*) [17], and chickens [18,19,20] as evidenced by reduced morbidity, mortality, susceptibility, and/or viral shedding. Such protective immunity may be one possible explanation for unexpected field observations during natural outbreaks of H5N1 HPAI virus, including lower than anticipated morbidity in poultry in Hong Kong [21] and wild birds in Germany despite the presence of several hundred thousand susceptible birds in the affected area [22]. The mechanisms of this protective effect, however, are still poorly defined.

To better understand the epidemiology of H5N1 HPAI virus infections in wild bird populations, we experimentally investigated the effects that pre-exposure with homosubtypic (homologous HA) (H5N1 or H5N2) or heterosubtypic (heterologous HA) (H1N1) LPAI viruses had on the outcome of a Eurasian H5N1 HPAI virus challenge in wood ducks (*Aix sponsa*).

Materials and Methods

Ethics Statement

General animal care was provided under an Animal Use Protocol (A2007-10058-0) approved by the Institutional Animal

Care and Use Committee at The University of Georgia and the Southeast Poultry Research Laboratory (SEPRL), United States Department of Agriculture, Agricultural Research Service (Athens, Georgia, USA).

Animals

Twenty-five 4-month-old wood ducks were purchased from a waterfowl breeder. Both males and females were included in approximately equal numbers. Food and water were provided *ad libitum*. The wood duck was selected as the animal model due to the availability of data on the susceptibility, viral shedding patterns, and pathobiology associated with the H5N1 HPAI virus used in this study [23,24].

Viruses

Three North American and one Eurasian wild bird-origin LPAI viruses were selected for the pre-exposure portion of this study. The LPAI virus strains included: A/mallard/MN/355779/00 (H5N2) and A/blue-winged teal/LA/B228/86 (H1N1) (Southeastern Cooperative Wildlife Disease Study [SCWDS], Athens, Georgia, USA), A/mute swan/MI/451072-2/06 (H5N1) (SEPRL, Athens, Georgia, USA), and A/mallard/Netherlands/2/05 (H5N2) (Ron Fouchier, Erasmus University, Rotterdam, The Netherlands). The HPAI isolate A/whooper swan/Mongolia/244/05 (H5N1) (Mongolia/05) (SEPRL, Athens, Georgia, USA) was used as challenge virus. The Mongolia/05 virus is a clade 2.2 virus and is genetically representative of H5N1 HPAI viruses that have been reported in wild birds in Asia, Europe, and Africa [24]. The virus was originally isolated from a dead whooper swan during a large die-off of waterfowl, and it was chosen for use in this study because of its established lethality in wild waterfowl, particularly wood ducks [23,24,25].

Individual stocks of the LPAI and the HPAI viruses used in this study were produced by second passage in 9-day-old specific pathogen free (SPF) embryonating chicken eggs (ECE). Viral stocks were titrated in SPF ECE and median embryo infectious dose (EID_{50}) titers were calculated using previously described methods [26]. Viral stocks were diluted in sterile brain-heart-infusion (BHI) medium to yield a final titer of 10^6 EID_{50} per 0.1 mL for LPAI viruses and 10^4 per 0.1 mL for the H5N1 HPAI virus (single bird inoculum).

Experimental Design

Wood ducks were evenly divided into five groups. Each group was housed separately in biocontainment isolation units ventilated under negative pressure with a high efficiency particulate air filters on intake and exhaust. After four days of acclimation, four of the groups were inoculated via choanal cleft into the middle nasal cavity with 0.1 mL of one of the four LPAI viruses and designated accordingly: A/mallard/Netherlands/2/05 (H5N2) group; A/blue-winged teal/LA/B228/86 (H1N1) group; A/mute swan/MI/451072-2/06 (H5N1) group; and A/mallard/MN/355779/00 (H5N2) group. One group was not experimentally exposed to a LPAI virus and served as a negative control (naïve group). Blood was collected from all birds prior to LPAI virus inoculation and at 21 days post-LPAI virus exposure (LPAIV-dpe) to test for the presence of antibodies to AI virus. In addition, cloacal and oropharyngeal (OP) swabs were collected from each bird for virus isolation prior to the study and at 2, 4, 7, and 21 LPAIV-dpe. After LPAI virus inoculation, birds were observed daily for behavior changes and/or the development of any clinical signs. At 21 LPAIV-dpe, the four LPAI virus exposed groups and the naïve group were inoculated via choanal cleft with 0.1 mL of the Mongolia/05 virus. Cloacal and OP swabs were collected from all the birds at 0, 1, 2, 4, 8, and 10 days post-HPAI virus challenge (HPAIV-dpc), and from any birds that were found dead or were euthanized due the severity of their clinical condition. Blood samples were collected at 10 HPAIV-dpc to test for the presence of antibodies to AI virus. Birds were evaluated daily as described above. Wood ducks exhibiting severe clinical signs (paresis or paralysis and/or inability to eat or drink) were euthanized with intravenous administration of sodium pentobarbital (100 mg/kg), and a full necropsy was performed. The experiment was terminated at 10 HPAIV-dpc at which time all the remaining birds were euthanized, as described above, and full necropsies were performed. All experimental infections were performed in a Biosafety Level-3-Enhanced facility at the SEPRL.

Serology

All blood samples were collected from the right jugular vein. Serum samples were stored at $-20°C$ until tested for the presence of influenza A antibodies using two serologic assays. Samples were tested for antibodies directed against the conserved internal nucleoprotein of influenza A viruses using a blocking enzyme-linked immunosorbent assay (bELISA) (FlockChek Avian Influenza MultiS-Screen Antibody Test Kit, IDEXX Laboratories, Westbrook, Maine, USA) following the manufacturer's instructions. Additionally, all samples were further analyzed for presence of antibodies directed against specific HA subtypes using the hemagglutination inhibition (HI) test following procedures previously described [27]. The LPAI viruses used for the pre-exposure portion of the study and the Mongolia/05 challenge virus served as antigens for the HI test. Each treatment group was tested against the LPAI virus used for pre-exposure and all the groups were tested against the Mongolia/05. A 0.5% suspension of chicken erythrocytes in phosphate-buffered saline was used for the HI tests. Serum samples were pre-treated with chicken red blood cells prior to the HI test in order to neutralize any naturally occurring serum hemagglutinins. HI titers$\geq$8 were considered positive.

Virus Isolation

Cloacal and OP swabs were collected in sterile BHI medium with antimicrobial drugs (100 μg/mL gentamicin, 100 units/mL penicillin, and 5 μg/mL amphotericin B). Samples were stored at $-70°C$ until testing was performed. Isolation of virus was performed by inoculating the allantoic sac of four 9-day-old SPF ECE with the clarified BHI media containing the swab (0.25 mL per egg). Allantoic fluid was harvested from all inoculated SPF ECE after 4 days of incubation at 37°C and tested for the presence of hemagglutinating activity [28]. Any bird was considered positive in which one or more inoculated SPF ECE tested positive for the presence of virus on cloacal swabs at any time point after inoculation and/or on OP swabs at the second day post inoculation or later (to minimize the potential for identifying residual inoculum on oropharynx).

Histopathology and Immunohistochemistry

Samples of cerebrum, cerebellum, heart, lung, trachea, liver, spleen, esophagus, proventriculus, ventriculus, small intestine, large intestine, pancreas, adrenal, ovaries/testis, kidney, cloacal bursa, pectoral muscle, femur, nasal turbinates and sinus were collected from all the animals and fixed in 10% buffered formalin for histopathology and immunohistochemistry (IHC). After fixation, the tissues were processed and embedded in paraffin, and 5μm sections were stained with hematoxylin and eosin using standard histopathology protocols. Femur and nasal turbinates were decalcified with Kristensen's decalcifying solution before

being processed. Duplicate sections of all tissues were immunohistochemically stained by using a mouse-derived monoclonal antibody (P13C11) specific for type A influenza virus nucleoprotein antigen as the primary antibody (SEPRL, Athens, Georgia, USA). Procedures used to perform the immunohistochemical testing have been previously described [29]. Fast red was used as the substrate chromogen, and slides were counterstained with hematoxylin. Demonstration of viral antigen was based on chromogen deposition in the nucleus, with or without chromogen deposition in the cytoplasm.

Statistical Analysis

Fisher Exact Test with a level of significance (α) of 0.05 was used to evaluate the association between pre-exposure to each of the LPAI viruses and the survival following Mongolia/05 virus challenge. Chi-square (χ^2) distribution with α of 0.05 was employed to analyze the relation between survival following Mongolia/05 virus challenge and the serological status upon arrival.

Results

Pre-trial Status

Prior to the start of the study (0 LPAIV-dpe), 12 of the 25 wood ducks tested positive for influenza A virus nucleoprotein antibodies with the bELISA (Table 1). These 12 birds were distributed among the naïve and the four LPAI virus exposure groups. All 25 serum samples collected at 0 LPAIV-dpe were negative on HI tests, indicating the absence of pre-existing antibodies directed against the HA of the pre-exposure LPAI virus or the Mongolia/05 virus. Virus was not isolated from any cloacal or OP swabs collected at 0 LPAIV-dpe, indicating that no birds were actively infected at the start of the study.

LPAI Pre-exposure

All wood ducks in each of the five groups remained clinically and behaviorally normal, and had an average weight gain of 8.9% (2.0–15.3%) during the 21 days following the LPAI virus pre-exposure (data not shown).

Detection of viral shedding (Table 1) and seroconversion, based on the HI test (Tables 1 and 2), varied between LPAI-exposure groups. The A/mallard/Netherlands/2/05 (H5N2) virus did not replicate in any of the inoculated wood ducks, as demonstrated by lack of viral shedding and seroconversion (by both the bELISA and HI tests). The A/mute swan/MI/451072-2/06 (H5N1) virus was recovered from two of the five inoculated wood ducks; in both ducks virus was isolated from OP swabs collected at 2 LPAIV-dpe. Although both of these ducks were seronegative at 21 LPAIV-dpe on the H5 HI test (Table 2), antibodies were detected in one duck with the bELISA.

Viral shedding was detected in four of five wood ducks inoculated with the A/blue-winged teal/LA/B228/86 (H1N1) virus. Virus was reisolated from wood ducks in this group until 4 to 7 LPAIV-dpe (mean 4.75 days). Three out of the four ducks that excreted the A/blue-winged teal/LA/B228/86 (H1N1) virus seroconverted, as detected by H1 specific HI test; two of these

Table 1. Serological status before and after the experimental low pathogenicity avian influenza (LPAI) virus exposure, virus isolation data, and mortality of wood ducks (*Aix sponsa*) experimentally inoculated[a] with different subtypes of LPAI viruses and subsequently challenged with the highly pathogenic avian influenza (HPAI) virus A/whooper swan/Mongolia/244/05 (H5N1)[b].

		LPAI virus Pre-exposure		HPAI virus Challenge			
	Serological status upon arrival	Virus Isolation	Serology	Virus Isolation	Mortality		
GROUPS[c]	bELISA result (n)[e,f]	Prevalence[g], no. positive/total	HI[h] no. positive/total	Prevalence, no. positive/total	no. deaths/total (%)	% (n = 5)	MDT (d) (n = 5)
Naïve[d]	+ (1)	NA	NA	1/1	1/1 (100)	100	5
	− (4)	NA	NA	4/4	4/4 (100)		
A/mallard/Netherlands/2/05 (H5N2)	+ (2)	0/2	0/2	2/2	2/2 (100)	80	6
	− (3)	0/3	0/3	3/3	2/3 (66)		
A/blue-winged teal/LA/B228/86 (H1N1)	+ (2)	2/2	2/2	2/2	1/2 (50)	60	6
	− (3)	2/3	1/3	3/3	2/3 (66)		
A/mute swan/MI/451072-2/06 (H5N1)	+ (3)	0/3	0/3	3/3	1/3 (33)	20	8
	− (2)	2/2	0/2	2/2	0/2 (0)		
A/mallard/MN/355779/00 (H5N2)	+ (4)	4/4	3/4	4/4	0/4 (0)	0	NA
	− (1)	1/1	1/1	1/1	0/1 (0)		

[a]Birds were pre-exposed via choanal cleft with a dose of $10^6 EID_{50}$.
[b]Birds were challenged via choanal cleft with a dose of $10^4 EID_{50}$ 21 days after experimental pre-exposure to LPAI viruses.
[c]Groups of wood ducks (n = 5) experimentally pre-exposed to different LPAI viruses.
[d]The naïve group was not experimentally pre-exposed to LPAI virus.
[e]Abbreviations: bELISA = blocking ELISA; HI = hemagglutination inhibition; MDT = mean death time (days); + = positive; − = negative; NA = non applicable.
[f]bELISA result (number of birds). Twelve out of 25 birds had avian influenza nucleoprotein antibodies at the beginning of the trial, before experimental exposure to a LPAI virus.
[g]Number of birds that had at least one cloacal and/or oropharyngeal swab that tested positive on virus isolation after avian influenza virus exposure/total number of birds.
[h]HI using antigen against homosubtypic LPAI virus, either H5N2, H1N1, or H5N1. Serum samples were colleted 21 days after LPAI virus pre-exposure.
doi:10.1371/journal.pone.0015987.t001

three wood ducks also had detectable antibodies on bELISA at 21 LPAIV-dpe. The A/mallard/MN/355779/00 (H5N2) virus replicated efficiently in all the five inoculated wood ducks independently of the serological status at 0 LPAIV-dpe. Viral shedding in this group was detected until 2 to 4 LPAIV-dpe (mean 2.4 days). Seroconversion was detected in four of five wood ducks in this group with both the bELISA and H5 HI test.

A/whooper swan/Mongolia/244/05 (H5N1) Challenge

Serological Status. Serological status for each of the exposure groups, as determined by the HI test at 21 LPAIV-dpe (against the homosubtypic LPAI viruses used for pre-exposure) and at 10 HPAIV-dpc (against Mongolia/05 virus), is summarized in Table 2. Serological data for the naïve group were omitted from Table 2 because all the wood ducks in this group died after Mongolia/05 virus challenge. Data from the A/mallard/Netherlands/2/05 (H5N2) group were also omitted from Table 2 because none of these birds seroconverted after the LPAI virus pre-exposure, and four of five died after Mongolia/05 virus challenge. The only wood duck in this group that survived the Mongolia/05 virus challenge had an HI titer of 16 at 10 HPAIV-dpc.

Following the Mongolia/05 virus challenge (at 10 HPAIV-dpc), all of the surviving wood ducks in the A/mute swan/MI/451072-2/06 (H5N1) and A/mallard/MN/355779/00 (H5N2) groups had an increase in the HI titer against the LPAI virus used for pre-exposure. Three wood ducks that succumbed to Mongolia/05 virus infection (two birds in the A/blue-winged teal/LA/B228/86 (H1N1) group and one bird in the A/mute swan/MI/451072-2/06 (H5N1) group) had negative HI titers (<8) against the LPAI virus used for pre-exposure at 21 LPAIV-dpe (Table 2).

Morbidity and Mortality. Wood ducks that succumbed to the Mongolia/05 virus challenge (n = 13) progressively lost weight, while the ducks that survived (n = 12) experienced an initial weight loss during the first days after Mongolia/05 virus challenge, followed by a progressive weight gain throughout the remainder of the trial (data not shown). All wood ducks that succumbed to infection either exhibited premonitory neurologic signs or were found dead without overt clinical signs. The onset of morbidity or death ranged from 4 to 8 HPAIV-dpc. Clinical signs varied from mild to severe and included lethargy, incoordination, paresis, walking in circles, and head circling and tremors. One wood duck in the naïve group showed a unilateral cloudy blue eye one day before it was found dead at 5 HPAIV-dpc.

Mortality varied greatly among groups, ranging from 0 to 100% (Table 1). All five wood ducks in the naïve group died, with a mean death time (MDT) of 5 days (range 4–6 days). Among the LPAI

Table 2. Serological status, as determined by hemagglutination inhibition, of wood ducks (*Aix sponsa*) 21 days after experimental pre-exposure to low pathogenicity avian influenza (LPAI) viruses[a], and 10 days after challenge with the highly pathogenic avian influenza (HPAI) virus A/whooper swan/Mongolia/244/05 (H5N1)[b].

	Hemagglutination Inhibition Titer[c]		
	Homosubtypic LPAI virus antigen[d]		A/whooper swan/244/05 antigen[e]
Sera from exposed birds by group, bird ID	21 LPAIV-dpe[f]	10 HPAIV-dpc	10 HPAIV-dpc
A/blue-winged teal/LA/B228/86 (H1N1)			
11	<8	†	†
12	8	8	<8
13	8	†	†
14	16	16	<8
15	<8	†	†
A/mute swan/MI/451072-2/06 (H5N1)			
6	<8	128	16
7	<8	†	†
8	<8	256	128
9	<8	128	32
10	<8	256	512
A/mallard/MN/355779/00 (H5N2)			
16	8	128	8
17	<8	256	<8
18	16	64	<8
19	16	1024	32
20	8	32	<8

[a]Birds were inoculated via choanal cleft with a dose of $10^6 EID_{50}$ of different LPAI viruses. Serologic data of the naïve group were omitted due the 100% mortality observed in this group, and data of the A/mallard/Netherlands/2/05 (H5N2) group were omitted due to lack of seroconversion.
[b]Birds were challenged via choanal cleft with a dose of $10^4 EID_{50}$ of A/whooper swan/Mongolia/244/05 (H5N1), 21 days after experimental pre-exposure to different subtypes of LPAI viruses.
[c]Samples with HI titer≥8 were considered positive.
[d]HI using antigen against homosubtypic LPAI virus, either H1N1, H5N1, or H5N2.
[e]HI using antigen against A/whooper swan/Mongolia/244/05 (H5N1).
[f]Abbreviations: LPAIV-dpe = days after LPAI pre-exposure; HPAIV-dpc = days after H5N1 HPAI challenge; † = succumbed to HPAI H5N1 infection.
doi:10.1371/journal.pone.0015987.t002

virus pre-exposure groups, the observed mortality was 80% (4/5) in the A/mallard/Netherlands/2/05 (H5N2) group (MDT of 6 days; range 6 days); 60% (3/5) in the A/blue-winged teal/LA/B228/86 (H1N1) group (MDT of 6 days; range 5–7 days); and 20% (1/5) in the A/mute swan/MI/451072-2/06 (H5N1) group (MDT of 8 days). Neither morbidity nor mortality was observed in the group pre-exposed to the A/mallard/MN/355779/00 (H5N2). Based on the number of birds that survived the Mongolia/05 virus challenge, the level of protection induced by the exposure to the LPAI viruses was statistically significant in the A/mallard/MN/355779/00 (H5N2) ($P = 0.0079$) and A/mute swan/MI/451072-2/06 (H5N1) ($P = 0.0476$) groups. The groups pre-exposed to the other two LPAI viruses (the A/blue-winged teal/LA/B228/86 [H1N1] and the A/mallard/Netherlands/2/05 [H5N2] groups) did not have a statistically significant level of protection against the Mongolia/05 virus ($P > 0.05$).

The serological status of the wood ducks upon arrival had minimal if any effect on the outcome of Mongolia/05 virus infection, as demonstrated by similar mortality rates for birds within each group (Table 1). Statistical analyses revealed that the survival following Mongolia/05 virus challenge was not associated with the serological status upon arrival ($\chi^2 = 0.987$, $P > 0.05$).

Viral Shedding. After challenge, the Mongolia/05 virus was isolated from every wood duck in each of the five groups. In general, viral shedding via oropharynx was greater than via cloaca, as demonstrated by a higher number of isolations from OP than cloacal swabs (Table 3). Viral shedding via oropharynx was consistent in all wood ducks from 1 to 4 HPAIV-dpc and was intermittent in individual birds up to 10 HPAIV-dpc. Cloacal shedding was less consistent that oropharyngeal shedding. Positive cloacal swabs were detected every day after Mongolia/05 virus challenge, and the highest number of virus isolation from cloacal swabs was at 4 HPAIV-dpc. Furthermore, cloacal shedding was detected more frequently in birds that succumbed to Mongolia/05 virus infection than in birds that survived.

Necropsy Findings. Gross lesions were not detected in any of the wood ducks that survived the Mongolia/05 virus challenge and were necropsied at 10 HPAIV-dpc. All the wood ducks that succumbed to the Mongolia/05 virus infection had one or more of the following gross lesions: multifocal to coalescing areas (1- to 7-mm-diameter) of red mottling in the pancreas (10/13), congestion of meningeal vessels of the cerebrum and cerebellum (7/13), splenomegaly (5/13), multiple red foci in the adrenal glands (4/13), and a small tan spleen (2/13).

Histopathology and Immunohistochemistry. The histopathologic lesions observed in wood ducks that succumbed to Mongolia/05 virus infection and those that survived are described in Table 4 and illustrated on Figure 1. Among the 13 wood ducks that succumbed to infection, the most consistent microscopic lesions were observed in the central nervous system (CNS), pancreas, liver, and adrenal gland. Lesions of the CNS were characterized by moderate to severe, multifocal to coalescing, nonsuppurative encephalitis and neuronal necrosis. Moderate to severe choroiditis (Figure 1A), meningitis, gliosis, vacuolar degeneration (associated or not with lymphoplasmacytic infiltrate), and perivascular cuffing were also observed in the CNS. Pancreatic lesions were characterized by severe multifocal to coalescing necrosis of acinar cells (Figure 1C). Hepatic changes included multifocal hepatocellular necrosis and periportal/centrilobular hepatitis. Severe multifocal to coalescing necrosis of corticotrophic and chromaffin cells was seen in adrenal glands. Other variably detected microscopic lesions included: neuritis and necrosis of myenteric plexus of small intestine, shortening and fusion of intestinal villi, orchitis, oophoritis, pulmonary edema, tracheitis, sinusitis, necrosis of follicles in cloacal bursa, and degeneration of sheathed capillaries, lymphoid necrosis, and subcapsular hemorrhage in spleen (Table 4).

Positive IHC staining in association with histological lesions was consistently observed in nervous, digestive, and endocrine systems (Table 5, Figure 1) of the wood ducks that succumbed to Mongolia/05 virus infection, including: neurons and glial cells of cerebrum (Figure 1D), cerebellum, and brain stem, epithelial cells of choroid plexus (Figure 1B), neurons of myenteric and submucosal plexus of small and large intestines (Figure 1E), Kupffer cells and hepatocytes in the liver, acinar pancreatic cells, corticotrophic and chromaffin cells of adrenal gland, epithelial cells of trachea, epithelial cells of the seminiferous tubules, and granulosa cell layer of ovarian follicle. In wood ducks that succumbed to Mongolia/05 virus infection, positive immunohistochemical staining in the absence of microscopic lesions was routinely observed in cerebrum (4/13), cerebellum (3/13), brain stem (4/13), submucosal (8/13) and myenteric (5/13) plexus of small and large intestines, and sporadically in the meninges (1/13), salivary gland (1/13), cloacal bursa (1/13), testis (1/13), heart (2/13), nasal sinus (1/13), goblet cells of trachea (1/13), lung (1/13) and skin (2/13) (Table 5).

Among the 12 wood ducks that survived Mongolia/05 virus challenge and were necropsied at 10 HPAIV-dpc, the microscopic lesions included periportal/centrilobular lymphoplasmacytic hepatitis (10/12), splenic white pulp hyperplasia (4/12), severe nonsuppurative encephalitis (associated or not with meningitis) and marked perivascular cuffing (3/12) (Figure 1F), neuritis of myenteric plexus

Table 3. Clinical outcome and virus isolation data of wood ducks (*Aix sponsa*) challenged[a] with the highly pathogenic avian influenza virus A/whooper swan/Mongolia/244/05 (H5N1).

Clinical Outcome[b]	Virus isolation, HPAIV-dpc[c,d]													
	1		2		4		5[e]		6[e]		7		10	
	OP	CLO	OP	CLO	OP	CLO	OP	CLO	OP	CLO	OP	CLO	OP	CLO
Succumbed	12/13	1/13	13/13	4/13	13/13	11/13	4/12	4/12	4/8	4/8	0/2	0/2	NA	NA
Survived	10/12	0/12	10/12	2/12	9/12	1/12	*	*	*	*	1/12	0/12	1/12	3/12

[a]Birds were challenged via choanal cleft with a dose of $10^4 EID_{50}$ of A/whooper swan/Mongolia/244/05 (H5N1), 21 days after experimental pre-exposure to different subtypes of LPAI viruses.
[b]Five out of 13 birds that succumbed and six out of 12 birds that survived had pre-existing antibodies against avian influenza.
[c]Abbreviation: HPAIV-dpc = days post H5N1 HPAI challenge; OP = oropharyngeal swab; CLO = cloacal swab; NA = non applicable; * = not tested.
[d]no. of birds that shed the virus/total.
[e]Only birds that died were tested. Therefore, 4/12 birds were tested at 5 HPAIV-dpc, and 6/8 were tested at 6 HPAIV-dpc.
doi:10.1371/journal.pone.0015987.t003

Table 4. Histopathology lesions observed in wood ducks (*Aix sponsa*) that succumbed or survived after challenge with the highly pathogenic avian influenza virus A/whooper swan/Mongolia/244/05 (H5N1)[a].

System/Tissue	Lesion	Succumbed (n = 13)	Survived (n = 12)
Nervous			
Cerebrum	Neuronal degeneration, gliosis, perivascular cuffing, vacuolar degeneration	12	2
	Choroid plexus, necrosis, inflammation	7	0
Cerebellum	Purkinje cell necrosis, gliosis, perivascular cuffing, status spongiosus, gitter cells	10	0
	Meninges, inflammation, necrosis	2	1
Brain Stem	Vacuolation, gliosis, perivascular cuffing, central chromatolysis	10	1
Endocrine			
Pancreas	Acinar cells, necrosis	8	0
Adrenal Glands	Corticotrophic and chromaffin cells, necrosis	3	0
Digestive			
Liver	Necrosis, multifocal	10	0
	Periportal/centrilobular hepatitis	5	10
Small Intestine	Myenteric plexus, neuronal necrosis	2	0
	Myenteric plexus, neuritis	0	2
	Villi, shortening and fusion	1	0
Large Intestine	Villi, shortening and fusion	1	0
Reproductive			
Testis	Seminiferous tubules, necrosis	1	0
Ovary	Immature follicle, necrosis, inflammation	1	0
Respiratory			
Lung	Edema	4	2
Trachea	Tracheitis	1	0
Nasal Sinus	Sinusitis	1	1
Lymphoid			
Cloacal Bursa	Necrosis, follicle	1	0
Spleen	Sheathed capillaries, degeneration	1	0
	Lymphoid necrosis	1	0
	Subcapsular hemorrhage	1	1
	White pulp, hyperplasia	0	4
	Amyloidosis	0	1

[a]Wood ducks were challenged via choanal cleft with a dose of $10^4 EID_{50}$ of A/whooper swan/Mongolia/244/05 (H5N1) 21 days after experimental pre-exposure to different subtypes of low pathogenic avian influenza viruses.

doi:10.1371/journal.pone.0015987.t004

of small intestine (2/12), pulmonary edema (2/12), and splenic amyloidosis (1/12) and subcapsular hemorrhage (1/12) (Table 4).

Discussion

Wood ducks used in this study were acquired from a duck farm where several species of Anseriform and Galliform birds were raised outdoors and had direct contact with wild birds. Outdoor rearing of poultry is a major risk factor for exposure to AI virus [30], and could explain the 12 wood ducks that tested positive for influenza A group-specific antibodies prior to the start of the trial. Further testing revealed that all 25 wood ducks were seronegative on the HI test, indicating that none of the birds had pre-existing antibodies directed against the HA of the LPAI viruses used for pre-exposure or the Mongolia/05 challenge virus. Although unexpected, the presence of individual birds with pre-existing antibodies to influenza A nucleoprotein, which are non-neutralizing and non-protective [31,32], did not preclude us from acquiring useful data from this study. As shown on Table 1, within each of the LPAI virus-exposure groups, there was minimal differences in mortality (more or less than one bird) between wood ducks that had antibodies prior to the study and those that did not. This was further confirmed through statistical analyses, which revealed that the survival following Mongolia/05 challenge was not influenced by the serological status prior to the study.

The influence of pre-exposure to a LPAI virus on the outcome of a HPAI challenge varied from total protection (0% morbidity/mortality) to no protection (100% mortality) (Table 1). All the wood ducks in the naïve group died, confirming the high susceptibility of this species to Mongolia/05 virus observed in previous studies [23,24]. The North American A/mallard/MN/355779/00 (H5N2) and A/mute swan/MI/451072-2/06 (H5N1) viruses (both homosubtypic to Mongolia/05 challenge virus) induced a statistically significant level of protection, as evidenced by low mortality (0 and 20%, respectively) after H5N1HPAI virus challenge (Table 1). Alternatively, the Eurasian A/mallard/

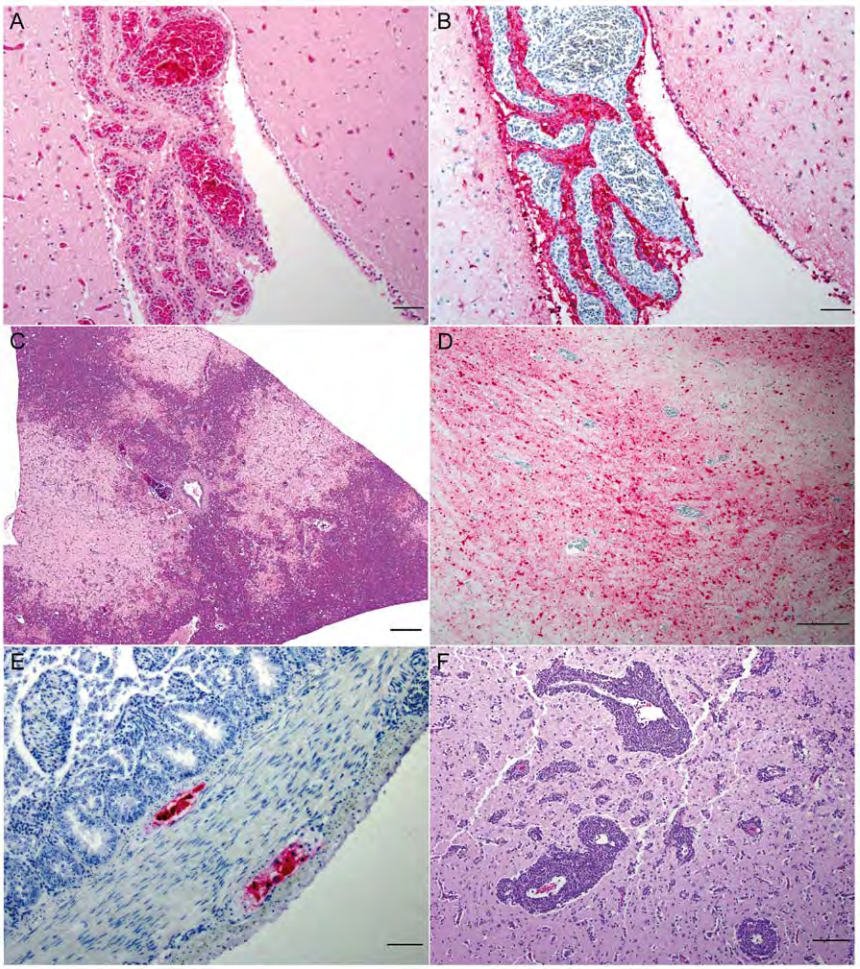

Figure 1. Histopathology and immunohistochemistry of different tissues from wood ducks (*Aix sponsa*) infected with A/whooper swan/Mongolia/244/05 (H5N1). (A) Brain, Choroid Plexus; wood duck that succumbed to Mongolia/05 virus infection. Severe choroiditis characterized by necrosis of epithelial cells of choroid plexus, vasculitis and heterophilic infiltrate. Hematoxylin-eosin staining. Bar 50μm. (B) Brain, Choroid Plexus; wood duck that succumbed to Mongolia/05 virus infection. Positive staining in epithelial cells of choroid plexus. Immunohistochemical staining: mouse-derived monoclonal antibody (P13C11), biotin-streptavidin alkaline-phosphatase detection method, Fast Red substrate-chromogen, hematoxylin counterstain. Bar 50μm. (C) Pancreas; wood duck that succumbed to Mongolia/05 virus infection. Severe multifocal to coalescing necrosis of acinar cells. Hematoxylin-eosin staining. Bar 200μm. (D) Brain, Cerebrum; wood duck that succumbed to Mongolia/05 virus infection. Intense positive immunohistochemical staining of neurons and glial cells. Immunohistochemical staining: mouse-derived monoclonal antibody (P13C11), biotin-streptavidin alkaline-phosphatase detection method, Fast Red substrate-chromogen, hematoxylin counterstain. Bar 200μm. (E) Small intestine; wood duck that succumbed to Mongolia/05 virus infection. Positive immunohistochemical staining in neurons of myenteric and submucosal plexus. Immunohistochemical staining: mouse-derived monoclonal antibody (P13C11), biotin-streptavidin alkaline-phosphatase detection method, Fast Red substrate-chromogen, hematoxylin counterstain. Bar 50μm. (F) Brain, Cerebrum; wood duck that survived the Mongolia/05 virus challenge. Severe nonsuppurative encephalitis characterized by marked perivascular cuffing. Hematoxylin-eosin staining. Bar 100μm.
doi:10.1371/journal.pone.0015987.g001

Netherlands/2/05 (H5N2) virus (also homosubtypic to Mongolia/05 challenge virus) did not replicate in the wood ducks and, consequently, provided no protective immunity. This was reflected by the high mortality (80%) in this group. The wood ducks pre-exposed to the A/blue-winged teal/LA/B228/86 (H1N1) virus (heterosubtypic to Mongolia/05 challenge virus) experienced moderate mortality (60%) relative to the other exposure groups; the level of protection observed in this group was not statistically significant. These observations suggest that humoral immunity against homosubtypic LPAI viruses play an important role in providing protection against H5N1 HPAI virus infection, as observed in previous studies [32,33,34]. These results also indicate that the development of a protective immune response is dependent on detectable replication of the LPAI virus.

An adequate humoral immune response to HA seems to be fundamental for the protection against challenge with H5N1 HPAI virus in multiple avian species [33]. In the current study, three wood ducks that succumbed to H5N1 HPAI virus infection (two birds in the A/blue-winged teal/LA/B228/86 [H1N1] group and one bird in the A/mute swan/MI/451072-2/06 [H5N1] group) had a negative HI titer against the homologous HA at 21 LPAIV-dpe when they were subsequently challenged with the Mongolia/05 virus (Table 2). Moreover, a higher HI titer against the homologous LPAI isolate was observed among surviving birds, particularly in wood ducks in the A/mute swan/MI/451072-2/06 (H5N1) and A/mallard/MN/355779/00 (H5N2) groups (Table 2). This increase in titer is not understood, but could either be an effect of the H5N1 HPAI virus challenge or related to the timing of

Table 5. Immunohistochemical analysis for nucleoprotein of avian influenza virus of wood ducks (*Aix sponsa*) that succumbed to infection (n = 13) with the highly pathogenic avian influenza virus A/whooper swan/Mongolia/244/05 (H5N1)[a].

System/Tissue	Cell Type	No. of wood ducks	No. of positive cells[b]
Nervous			
Cerebrum	Neuron	8*	+++
	Epithelial cell of choroid plexus	8	+++
	Glial cells	6*	+++
	Ependymal cells	3	+++
	Endothelium of blood vessels	2	+
	Meninges	1**	++
Cerebellum	Purkinje cells	8	+++
	Neurons	5*	++
	Glial cells	7*	+++
Brain Stem	Epithelial cell of choroid plexus	6	+++
	Neurons	6*	+++
	Glial cells	6*	+++
	Endothelium	1	+
Digestive			
Salivary Gland	Epithelium	1**	+
Esophagus	Endothelium of submucosa	1	+
Intestines	Myenteric plexus	8*	++
	Submucosal plexus	9*	++
Liver	Kupffer cells	8	++
	Hepatocytes	1	++
Endocrine			
Pancreas	Acinar cells	6	+++
Adrenal Glands	Corticotrophic and chromaffin cells	4	+++
Respiratory			
Nasal Sinus	Epithelial cells	1**	+
	Perivascular staining	1**	+
Trachea	Epithelial cells	1	+
	Globet cells	1**	+
Lung	Epithelial cells	1**	+
	Secondary bronchus, submucosa	1**	+
Integumentary			
Skin	Epidermis, basal layer	2**	+
	Endothelial cells	1**	+
Cardiovascular			
Heart	Myocytes	2**	+
Reproductive			
Ovary	Follicle, granulosa cell layer	1	+
Testis	Seminiferous tubules	1	+
	Fibrovascular stroma	1**	+
Lymphoid			
Cloacal Bursa	Follicle, epithelial tuft	2	+
	Follicle, medulla	1**	+

[a]Wood ducks were challenged via choanal cleft with a dose of $10^4 EID_{50}$ of A/whooper swan/Mongolia/244/05 (H5N1) 21 days after experimental pre-exposure to different subtypes of low pathogenic avian influenza viruses.
[b]Numbers of immunohistochemically positive cells: + = few; ++ = moderate; +++ = numerous.
*Positive immunohistochemical staining associated or not with microscopic lesions.
**Positive immunohistochemical staining not associated with microscopic lesions.
doi:10.1371/journal.pone.0015987.t005

the original immune response (31 LPAIV-dpe). It is currently not understood whether cell mediated immunity (CMI) is involved in the protective immune response against H5N1 HPAI virus. However, the wood duck in the A/mallard/Netherlands/2/05 (H5N2) group that survived the Mongolia/05 virus challenge did not develop HI detectable antibody against the homologous H5 used for pre-exposure (data not shown), suggesting that humoral immunity is not the only factor influencing the outcome of infection. Further investigations are needed to clarify the roles of humoral immunity against HA and NA and CMI in protection of birds against H5N1 HPAI virus challenge.

The Mongolia/05 virus replicated systemically in wood ducks and had a strong tropism for the CNS, pancreas, and adrenal gland. Failure and/or dysfunction of one or multiple of these organs were likely the cause of death. The cloudy eye observed in one wood duck in the naïve group has been frequently reported as a clinical sign of H5N1 HPAI virus infection in birds [17,23,35,36,37,38,39]. Although histopathologic examination was not performed on the eye of the wood duck in this study, the cloudiness may be caused by the deposition of fibrin or accumulation of white blood cells in the anterior chamber or corneal edema, both of which can be features of uveitis.

Consistent with other experimental studies, oropharyngeal shedding in all five wood duck groups was more pronounced than cloacal shedding (Table 3) [17,23,24,35,39]. In this study, viral shedding was not completely suppressed in any of the groups of wood ducks pre-exposed to a LPAI virus, contrary to what was observed in a previous experimental investigation with mallards [17]. Although wood ducks that succumbed to infection died between 4 and 8 HPAIV-dpc, the cloacal viral shedding observed in these birds was more prominent (based on number of birds shedding) than in birds that survived the HPAI virus challenge (Table 3). Presumably, this is the result of widespread viral replication in more severely affected wood ducks, which is supported by the presence of viral antigen in adrenal glands, pancreas, liver, myenteric and submucosal plexus of the intestines, and reproductive organs (ovaries and testicle) (Tables 4 and 5, Figure 1). Viral antigen in the pancreas and reproductive tissues is particularly relevant, as viral replication in these organs could contribute to fecal shedding. Viral titrations of cloacal and OP swabs were not performed in this study; therefore, the influence that pre-exposure to a LPAI virus has on the concentration of Mongolia/05 virus shedding in wood ducks is not known. A recent study observed that a previous exposure to a LPAI virus can reduce the concentration and duration of viral shedding via oropharynx and prevent cloacal shedding in mallards infected with H5N1 HPAI virus [17].

In summary, this study demonstrates that previous exposure to homosubtypic LPAI viruses in wood ducks may: prevent disease but not infection or viral shedding of H5N1 HPAI virus; decrease mortality associated with H5N1 HPAI virus infection; and increase MDT, thus prolonging the duration of H5N1 HPAI viral shedding. Furthermore, the degree of protection against the H5N1 HPAI virus varies in response to the LPAI virus subtype that the bird was previously infected with. The mechanisms responsible for this protection, as well as the extent (between different subtypes) and duration of this protective immunity still need to be elucidated in order to understand the epidemiology of AI viruses in waterfowl reservoirs and to better define the potential risks of unique AI viruses, such as H5N1 HPAI virus, to infect, move with, or become established in wild bird populations.

Acknowledgments

We thank the personnel of the Southeast Poultry Research Laboratory for their technical assistance, especially J. Beck, J. Doster, and K. Moresco. We deeply appreciate Dr. Fouchier for providing the A/whooper swan/Mongolia/244/05 (H5N1) virus.

Author Contributions

Conceived and designed the experiments: TPC JDB EWH D. E. Stallknecht D. E. Swayne. Performed the experiments: TPC JDB. Analyzed the data: TPC JDB EWH D. E. Stallknecht D. E. Swayne. Contributed reagents/materials/analysis tools: TPC JDB EWH D. E. Stallknecht D. E. Swayne. Wrote the paper: TPC JDB EWH D. E. Stallknecht D. E. Swayne.

References

1. Webster RG, Bean WJ, Gorman OT, Chambers TM, Kawaoka Y (1992) Evolution and ecology of influenza A viruses. Microbiol Rev 56: 152–179.
2. Stallknecht DE, Shane SM (1988) Host range of avian influenza virus in free-living birds. Vet Res Commun 12: 125–141.
3. Olsen B, Munster VJ, Wallensten A, Waldenstrom J, Osterhaus ADME, et al. (2006) Global patterns of influenza a virus in wild birds. Science 312: 384–388.
4. Süss J, Schäfer J, Sinnecker H, Webster RG (1994) Influenza virus subtypes in aquatic birds of eastern Germany. Arch Virol 135: 101–114.
5. Hinshaw VS, Webster RG, Turner B (1980) The perpetuation of orthomyxoviruses and paramyxoviruses in Canadian waterfowl. Can J Microbiol 26: 622–629.
6. Keawcharoen J, van Riel D, van Amerongen G, Bestebroer T, Beyer WE, et al. (2008) Wild ducks as long-distance vectors of highly pathogenic avian influenza virus (H5N1). Emerg Infect Dis 14: 600–607.
7. Gaidet N, Cattoli G, Hammoumi S, Newman SH, Hagemeijer W, et al. (2008) Evidence of infection by H5N2 highly pathogenic avian influenza viruses in healthy wild waterfowl. PLoS Pathog 4: e1000127.
8. Kilpatrick AM, Chmura AA, Gibbons DW, Fleischer RC, Marra PP, et al. (2006) Predicting the global spread of H5N1 avian influenza. Proc Natl Acad Sci U S A 103: 19368–19373.
9. Jonassen CM, Handeland K (2007) Avian influenza virus screening in wild waterfowl in Norway, 2005. Avian Dis 51: 425–428.
10. Sharp GB, Kawaoka Y, Jones DJ, Bean WJ, Pryor SP, et al. (1997) Coinfection of wild ducks by influenza A viruses: distribution patterns and biological significance. J Virol 71: 6128–6135.
11. Dugan VG, Chen R, Spiro DJ, Sengamalay N, Zaborsky J, et al. (2008) The evolutionary genetics and emergence of avian influenza viruses in wild birds. PLoS Pathog 4: e1000076.
12. Hinshaw VS, Bean WJ, Webster RG, Sriram G (1980) Genetic reassortment of influenza A viruses in the intestinal tract of ducks. Virology 102: 412–419.
13. Kida H, Yanagawa R, Matsuoka Y (1980) Duck influenza lacking evidence of disease signs and immune response. Infect Immun 30: 547–553.
14. Pasick J, Berhane Y, Embury-Hyatt C, Copps J, Kehler H, et al. (2007) Susceptibility of Canada geese (*Branta canadensis*) to highly pathogenic avian influenza virus (H5N1). Emerg Infect Dis 13: 1821–1827.
15. Berhane Y, Leith M, Embury-Hyatt C, Neufeld J, Babiuk S, et al. (2010) Studying possible cross-protection of Canada geese preexposed to North American low pathogenicity avian influenza virus strains (H3N8, H4N6, and H5N2) against an H5N1 highly pathogenic avian influenza challenge. Avian Dis 54: 548–554.
16. Kalthoff D, Breithaupt A, Teifke JP, Globig A, Harder T, et al. (2008) Highly pathogenic avian influenza virus (H5N1) in experimentally infected adult mute swans. Emerg Infect Dis 14: 1267–1270.
17. Fereidouni SR, Starick E, Beer M, Wilking H, Kalthoff D, et al. (2009) Highly pathogenic avian influenza virus infection of mallards with homo- and heterosubtypic immunity induced by low pathogenic avian influenza viruses. PLoS ONE 4: e6706.
18. Seo SH, Webster RG (2001) Cross-reactive, cell-mediated immunity and protection of chickens from lethal H5N1 influenza virus infection in Hong Kong poultry markets. J Virol 75: 2516–2525.
19. Seo SH, Peiris M, Webster RG (2002) Protective cross-reactive cellular immunity to lethal A/Goose/Guangdong/1/96-like H5N1 influenza virus is correlated with the proportion of pulmonary CD8(+) T cells expressing gamma interferon. J Virol 76: 4886–4890.
20. van der Goot JA, de Jong MC, Koch G, Van Boven M (2003) Comparison of the transmission characteristics of low and high pathogenicity avian influenza A virus (H5N2). Epidemiol Infect 131: 1003–1013.
21. Webster RG, Peiris M, Chen H, Guan Y (2006) H5N1 outbreaks and enzootic influenza. Emerg Infect Dis 12: 3–8.
22. Globig A, Staubach C, Beer M, Koppen U, Fiedler W, et al. (2009) Epidemiological and ornithological aspects of outbreaks of highly pathogenic avian influenza virus H5N1 of Asian lineage in wild birds in Germany, 2006 and 2007. Transbound Emerg Dis 56: 57–72.

23. Brown JD, Stallknecht DE, Valeika S, Swayne DE (2007) Susceptibility of wood ducks to H5N1 highly pathogenic avian influenza virus. J Wildl Dis 43: 660–667.
24. Brown JD, Stallknecht DE, Beck JR, Suarez DL, Swayne DE (2006) Susceptibility of North American ducks and gulls to H5N1 highly pathogenic avian influenza viruses. Emerg Infect Dis 12: 1663–1670.
25. Ellis TM, Bousfield RB, Bissett LA, Dyrting KC, Luk GS, et al. (2004) Investigation of outbreaks of highly pathogenic H5N1 avian influenza in waterfowl and wild birds in Hong Kong in late 2002. Avian Pathol 33: 492–505.
26. Reed LJ, Muench H (1938) A simple method of estimating fifty percent endpoint. Am J Epidemiol 27: 493–497.
27. Pedersen JC (2008) Hemagglutination-inhibition test for avian influenza virus subtype identification and the detection and quantitation of serum antibodies to the avian influenza virus. In: Spackman E, ed. Avian Influenza Virus. 1st ed. Totowa, NJ: Humana Press. pp 53–66.
28. Woolcock PR (2008) Avian influenza virus isolation and propagation in chicken eggs. In: Spackman E, ed. Avian Influenza Virus. 1st ed. Totowa, NJ: Humana Press. pp 35–46.
29. Pantin-Jackwood MJ () Immunohistochemical staining for the detection of the avian influenza virus in tissues. In: Spackman E, ed. Avian Influenza Virus. 1st ed. Humana Press 2008. pp 77–83.
30. Swayne DE (2008) Epidemiology of avian influenza in agricultural and other man-made systems. In: Swayne DE, ed. Avian Influenza. 1st ed. Ames, IA: Blackwell Publishing. pp 59–85.
31. Brown DW, Kawaoka Y, Webster RG, Robinson HL (1992) Assessment of retrovirus-expressed nucleoprotein as a vaccine against lethal influenza virus infections of chickens. Avian Dis 36: 515–520.
32. Webster RG, Kawaoka Y, Taylor J, Weinberg R, Paoletti E (1991) Efficacy of nucleoprotein and haemagglutinin antigens expressed in fowlpox virus as vaccine for influenza in chickens. Vaccine 9: 303–308.
33. Swayne DE, Kapczynski D (2008) Strategies and challenges for eliciting immunity against avian influenza virus in birds. Immunol Rev 225: 314–331.
34. Chambers TM, Kawaoka Y, Webster RG (1988) Protection of chickens from lethal influenza infection by vaccinia-expressed hemagglutinin. Virology 167: 414–421.
35. Brown JD, Stallknecht DE, Swayne DE (2008) Experimental infections of herring gulls (*Larus argentatus*) with H5N1 highly pathogenic avian influenza viruses by intranasal inoculation of virus and ingestion of virus-infected chicken meat. Avian Pathol 37: 393–397.
36. Brown JD, Stallknecht DE, Swayne DE (2008) Experimental infection of swans and geese with highly pathogenic avian influenza virus (H5N1) of Asian lineage. Emerg Infect Dis 14: 136–142.
37. Kim JK, Seiler P, Forrest HL, Khalenkov AM, Franks J, et al. (2008) Pathogenicity and vaccine efficacy of different clades of Asian H5N1 avian influenza A viruses in domestic ducks. J Virol 82: 11374–11382.
38. Sturm-Ramirez KM, Ellis T, Bousfield B, Bissett L, Dyrting K, et al. (2004) Reemerging H5N1 influenza viruses in Hong Kong in 2002 are highly pathogenic to ducks. J Virol 78: 4892–4901.
39. Sturm-Ramirez KM, Hulse-Post DJ, Govorkova EA, Humberd J, Seiler P, et al. (2005) Are ducks contributing to the endemicity of highly pathogenic H5N1 influenza virus in Asia? J Virol 79: 11269–11279.

Influenza-A Viruses in Ducks in Northwestern Minnesota: Fine Scale Spatial and Temporal Variation in Prevalence and Subtype Diversity

Benjamin R. Wilcox[1,2], Gregory A. Knutsen[3], James Berdeen[4], Virginia Goekjian[1], Rebecca Poulson[1], Sagar Goyal[5], Srinand Sreevatsan[5,6], Carol Cardona[6], Roy D. Berghaus[7], David E. Swayne[8], Michael J. Yabsley[1,2]*, David E. Stallknecht[1]

1 Southeastern Cooperative Wildlife Disease Study, Department of Population Health, College of Veterinary Medicine, The University of Georgia, Athens, Georgia, United States of America, **2** Daniel B. Warnell School of Forestry and Natural Resources, The University of Georgia, Athens, Georgia, United States of America, **3** Agassiz National Wildlife Refuge, U.S. Fish and Wildlife Service, Middle River, Minnesota, United States of America, **4** Minnesota Department of Natural Resources, Wetland Wildlife Populations and Research Group, Bemidji, Minnesota, United States of America, **5** Department of Veterinary Population Medicine, University of Minnesota, Saint Paul, Minnesota, United States of America, **6** Department of Veterinary Biomedical Sciences, University of Minnesota, Saint Paul, Minnesota, United States of America, **7** Department of Population Health, College of Veterinary Medicine, The University of Georgia, Athens, Georgia, United States of America, **8** Southeast Poultry Research Laboratory, Agricultural Research Service, U.S. Department of Agriculture, Athens, Georgia, United States of America

Abstract

Waterfowl from northwestern Minnesota were sampled by cloacal swabbing for Avian Influenza Virus (AIV) from July – October in 2007 and 2008. AIV was detected in 222 (9.1%) of 2,441 ducks in 2007 and in 438 (17.9%) of 2,452 ducks in 2008. Prevalence of AIV peaked in late summer. We detected 27 AIV subtypes during 2007 and 31 during 2008. Ten hemagglutinin (HA) subtypes were detected each year (i.e., H1, 3–8, and 10–12 during 2007; H1-8, 10 and 11 during 2008). All neuraminidase (NA) subtypes were detected during each year of the study. Subtype diversity varied between years and increased with prevalence into September. Predominant subtypes during 2007 (comprising ≥5% of subtype diversity) included H1N1, H3N6, H3N8, H4N6, H7N3, H10N7, and H11N9. Predominant subtypes during 2008 included H3N6, H3N8, H4N6, H4N8, H6N1, and H10N7. Additionally, within each HA subtype, the same predominant HA/NA subtype combinations were detected each year and included H1N1, H3N8, H4N6, H5N2, H6N1, H7N3, H8N4, H10N7, and H11N9. The H2N3 and H12N5 viruses also predominated within the H2 and H12 subtypes, respectively, but only were detected during a single year (H2 and H12 viruses were not detected during 2007 and 2008, respectively). Mallards were the predominant species sampled (63.7% of the total), and 531 AIV were isolated from this species (80.5% of the total isolates). Mallard data collected during both years adequately described the observed temporal and spatial prevalence from the total sample and also adequately represented subtype diversity. Juvenile mallards also were adequate in describing the temporal and spatial prevalence of AIV as well as subtype diversity.

Citation: Wilcox BR, Knutsen GA, Berdeen J, Goekjian V, Poulson R, et al. (2011) Influenza-A Viruses in Ducks in Northwestern Minnesota: Fine Scale Spatial and Temporal Variation in Prevalence and Subtype Diversity. PLoS ONE 6(9): e24010. doi:10.1371/journal.pone.0024010

Editor: Ron A. M. Fouchier, Erasmus Medical Center, Netherlands

Received January 25, 2011; **Accepted** August 2, 2011; **Published** September 13, 2011

This is an open-access article, free of all copyright, and may be freely reproduced, distributed, transmitted, modified, built upon, or otherwise used by anyone for any lawful purpose. The work is made available under the Creative Commons CC0 public domain dedication.

Funding: Funding was provided through Specific Cooperative Agreement 58-612-0220 between the Southeast Poultry Research Laboratory and SCWDS, and by the National Institutes of Health (NIH) and Department of Health and Human Services under Contract No. HHSN266200700007C. Contents are solely the responsibility of the authors and do not necessarily represent the official views of NIH. The funders had no role in study design, data collection and analysis, decision to publish, or preparation of the manuscript.

Competing Interests: The authors have declared that no competing interests exist.

* E-mail: myabsley@uga.edu

Introduction

Wild birds of the order Anseriformes (ducks, geese, and swans) are important reservoirs for avian influenza virus (AIV) [1,2]. Within these populations, transmission occurs through a fecal-oral route [3]. Prevalence of AIV in ducks varies by species, age, time, and location [2]. Most AIV isolations from North America and Europe have been reported from mallards (*Anas platyrhynchos*) and other species in the subfamily Anatinae, tribe Anatini (i.e., dabbling ducks) [2,4–6]. Juveniles tend to have greater infection rates than adults [1], probably because of the immunologically-naïve status of the former age cohort [4]. In North America, prevalence rates of AIV tend to peak during late summer, when waterfowl aggregate prior to fall migration [1]. Prevalence of infection at that time can be as high as 30% [1]. In contrast, prevalence of AIV infection in ducks on wintering grounds in the southern United States generally is ≤2% [7].

All 16 hemagglutinin (HA) and 9 neuraminidase (NA) subtypes of AIV exist in wild bird populations. However, the H1-12 subtypes predominate in wild duck populations in North America; other subtypes are either associated with gulls (H13, H16) or have not been reported from North America (H14, H15) [1,5,6,8,9]. Within Anseriform populations in both North America and Europe, the H3, H4, and H6 subtypes consistently account for most of the subtype diversity, and certain HA/NA combinations (e.g. H3N8, H4N6) appear to be over represented in these reported isolates [1,6,7,10,11].

There have been numerous studies related to the natural history of AIV in wild ducks [5]. Currently, there are global efforts to monitor AIV prevalence in such populations [6,12]. Although these efforts clearly have defined general spatial, temporal, and species-related epidemiologic patterns at a continental scale, few researchers have examined these relationships on a finer scale. Information related to short-term prevalence or subtype diversity related to fine-scale spatial and temporal variation in sampling efforts not only has application to understanding the epidemiology of these viruses in duck populations, but also the design and implementation of effective and cost-efficient surveillance programs.

In this study, we examined AIV in duck populations in Minnesota, USA from mid-summer to early fall during 2007–2008. The study period corresponds with the pre-migration congregation (hereafter, staging) and southward migration from this geographic area. To provide a historical perspective, we selected study sites at which avian influenza previously had been investigated. At Roseau River Wildlife Management Area (WMA), 7% of 60 mallards sampled during September 1973 were positive for AIV [13]. Similarly, 10.8% of 1,423 mallards and northern pintails (*Anas acuta*) sampled from Marshall and Roseau Counties, Minnesota during September 1998–2000 were positive for AIV [14]. The goals of the current study were to: 1) describe within-season (mid-July to October) variation of AIV prevalence over a small geographic area; 2) determine the spatial, temporal, host, and interacting factors that influence prevalence in our study area; 3) determine the effects of location, time, and host on the detection of subtype diversity; and 4) evaluate sampling efforts necessary to obtain reliable surveillance data from a localized study.

Methods

Ethics Statement

All procedures involving animals were approved by the University of Georgia Institutional Animal Care and Use Committee (A2010 6-101). Animals were collected under Minnesota Division of Fish and Wildlife permit 16282 and U.S. Fish and Wildlife Service, U.S. Department of the Interior permit MB779283-0.

Study Sites

All study sites were located in Northwestern Minnesota. The study sites were the Bemidji area (Beltrami County - 47°28′25.03″N, 94°52′49.00″W), Fosston area (Polk County - 47°34′36.31″N, 95°45′15.31″W), Thief Lake WMA (Marshall County - 48°29′12.85″N, 95°57′02.17″W), Roseau River WMA (Roseau County - 48°58′39.77″N, 96°00′32.08″W), and Agassiz National Wildlife Refuge (NWR; Marshall County - 48°18′02.90″N, 95°58′49.68″W; Fig. 1).

Sample Collection

Ducks were captured from July to October of 2007 and 2008 using 3 techniques that were dependent on the time of year: drive trapping, night lighting, and rocket-netting. We also sampled hunter-harvested birds during waterfowl hunting season. Birds were classified as juvenile or adult based on plumage characteristics [15], and AIV samples were collected as previously described [14]. Specifically, cloacal swabs were obtained using sterile cotton-tipped applicators (Puritan® Medical Products Company LLC, Guilford, ME) and placed in 2 ml of Brain Heart Infusion media (Becton Dickinson and Co., Sparks, MD) supplemented with penicillin G (1,000 units/ml), streptomycin (1 mg/ml), kanamycin (0.5 mg/ml), gentamicin (0.25 mg/ml), and amphotericin B (0.025 mg/ml) (Sigma Chemical Company, St. Louis, MO). Samples were stored at 4C (24–72 hrs), shipped overnight, and frozen at −80C until processed.

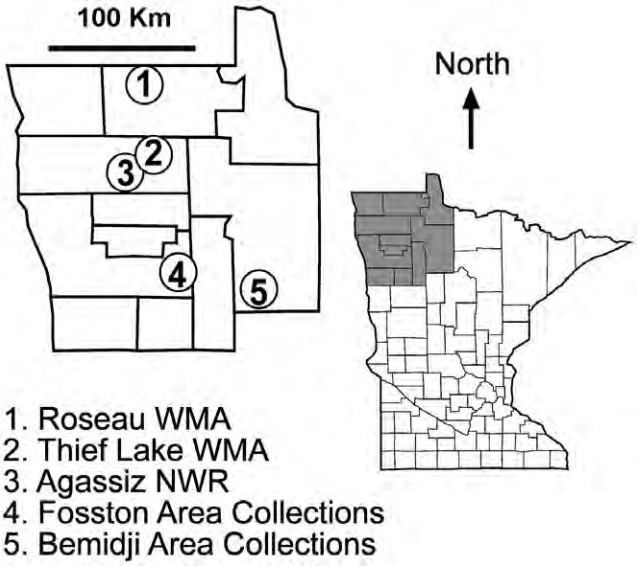

Figure 1. The location of sampled areas for avian influenza virus in northwestern Minnesota, USA, 2007 and 2008.
doi:10.1371/journal.pone.0024010.g001

Virus Isolation and Subtyping

To isolate viruses, samples were thawed, vortexed for 15 s, and centrifuged at 1,500× *g* for 15 min. The supernatant was inoculated (0.25 ml/egg) into four 9–11 day old specific-pathogen-free (SPF) embryonated chicken eggs via the allantoic route [7]. Eggs were incubated at 37C for 120 hr, after which amnio allantoic fluid was collected and tested by hemagglutination (HA) assay [16]. All HA-positive samples were tested by AIV matrix RT-PCR using primers from Fouchier (2000) [17]. Subtyping was done at the National Veterinary Services Laboratories (NVSL), Ames, Iowa using hemagglutination inhibition and neuraminidase inhibition tests [18] and via genotyping of the HA and NA genes at the University of Minnesota, St. Paul, Minnesota [19,20] and the University of California Davis [21] using standard Sanger sequencing for HA and NA segments. BLAST non-redundant database searching algorithm was applied to assign specific subtypes.

Data Analysis

Univariate associations between predictor variables and the results of virus isolation testing were evaluated using a chi-square test of independence. Multivariable analysis was performed using logistic regression with virus isolation as the dependent variable. Robust standard errors were used to account for the lack of independence between birds captured from the same site during a sampling season. Variables having a univariate association ($P<0.2$) with influenza prevalence were eligible for inclusion in the multivariable analysis. Variables were removed from the multivariable model in a stepwise fashion based on their level of significance until only those with $P<0.1$ remained. After reaching a preliminary main-effects model, all possible two-way interactions were evaluated. Date of sample collection was evaluated as both a categorical variable (i.e., month) and as a continuous variable (i.e., week and day), with Akaike's Information Criterion (AIC) being

used to determine its most appropriate functional form as a predictor. The fit of the final model was evaluated using the Hosmer-Lemeshow goodness of fit test. Residuals and influence statistics were used to screen for influential covariate patterns by plotting the delta deviance, delta chi-square, and delta beta values versus predicted probabilities. All analyses were performed using commercially available statistical software (Stata version 11.0, StataCorp LP, College Station, TX). Hypothesis tests assumed a two-sided alternative hypothesis and *P*-values <0.05 were considered statistically significant.

Results

During 2007 (July 11 – October 28) and 2008 (July 10 – October 15), 2,441 and 2,452 ducks were sampled in Minnesota, respectively (Table 1). Avian influenza viruses were isolated from 222 (9.1%) of sampled ducks during 2007 and from 438 (17.9%) of birds during 2008. Based on chi-square test of independence, the prevalence of AIV differed between mallards, other dabbling ducks (Tribe: Anatini), and the combined sample of divers (Tribes: Athyini, Mergini, Oxyurini) and wood ducks (*Aix sponsa*; S1 Table). Peak prevalence in mallards during 2007 and 2008 were approximately 20% and 35%, respectively.

During both 2007 and 2008 AIV prevalence peaked in late summer (late August or early September; Fig. 2). Based on chi-square testing of independence, prevalence significantly differed between years, month of sampling, age, and location (Table S1). Because the characteristics of sampled birds varied over time and location, a multivariable logistic regression analysis was performed to evaluate potential interactions and obtain adjusted effect estimates. The low prevalence of AIV in both the Fosston and Bemidji locations resulted in computational problems when interactions between location and the other variables were evaluated, and consequently observations from Fosston and Bemidji ($n = 330$) were excluded from the multivariable analysis. Because the preliminary analysis identified interactions between year, sampling date, and location; intermediate model selection steps were performed separately for each year. Ultimately, the same combination of predictors was identified as the best fitting model based on AIC comparisons for both 2007 and 2008. Both of these year-specific models (not reported) included an interaction between location and sampling date. The best fit of both models occurred when sampling date was included as the week of sample collection in its quadratic form (i.e., week and week^2). The sampling week variable was centered by subtracting the mean (week 36) from each observation to prevent collinearity with the squared week term. Because models for both years shared the same predictors, data from 2007 and 2008 were combined in the final multivariable model, which contained a significant three-way interaction between location, week of sample collection, and year. All interactions and main effects in the final model were also statistically significant, and results of the Hosmer-Lemeshow test indicated that the model fit the data well (H-L goodness-of-fit test, $P = 0.84$).

Results of the final multivariable model are reported in Table 2. Adjusted effect estimates for the age and species type variables in this model indicated that the odds of having a positive virus isolation result were 2.7 times higher for juvenile birds than for adults, and compared to mallards, odds ratios were 0.10 for divers and wood ducks, and 0.32 for the other dabblers. Overall, subtypes were determined for 607 of the 660 (93.5%) AIV isolated. During 2007, 27 subtypes were detected in 190 AIV isolates, and 31 subtypes were detected in 417 AIV isolates during 2008 (Fig. 3). Predominant subtypes during 2007 (representing at least 5% of subtype diversity) were H1N1, H3N6, H3N8, H4N6, H7N3, H10N7, and H11N9. Predominant subtypes during 2008 were H3N6, H3N8, H4N6, H4N8, H6N1, and H10N7. Overall, 10 HA subtypes were detected each year: H1, 3–8, and H10–12 during 2007 and H1–8, 10 and 11 during 2008. All NA subtypes were represented each year.

Although subtype diversity varied between years (Fig. 3), similar patterns were observed during each year. During both years, the

Table 1. The prevalence of AIV in waterfowl by species and year from northwestern Minnesota, USA.

Species[a]	2007		2008		Total	
	N	No. Pos (%)	N	No. Pos (%)	N	No. Pos (%)
Mallard (*Anas platyrhynchos*)	1691	185 (11.0%)	1426	346 (24.3%)	3117	532 (17.1%)
Other Dabblers						
Gadwall (*Anas strepera*)	12	1 (8.3%)	13	1 (7.7%)	25	2 (8.0%)
American Wigeon (*Anas americana*)	10	1 (10.0%)	52	3 (5.8%)	62	4 (6.5%)
American Black Duck(*Anas rubripes*)	8	1 (12.5%)	1	0 (0%)	9	1 (11.1%)
Blue-winged Teal (*Anas discors*)	193	21 (10.9%)	468	31 (6.6%)	661	52 (7.9%)
Northern Shoveler (*Anas clypeata*)	10	0 (0%)	61	26 (42.6%)	71	26 (36.6%)
Northern Pintail (*Anas acuta*)	31	2 (6.5%)	47	6 (12.8%)	78	8 (10.3%)
Green-winged Teal (*Anas crecca*)	116	5 (4.3%)	191	23 (12.0%)	307	28 (9.1%)
Wood Ducks and Divers						
Wood Duck (*Aix sponsa*)	186	0 (0%)	20	1 (5%)	206	1 (0.5%)
Redhead (*Aythya americana*)	3	1 (33.3%)	12	0 (0%)	15	1 (6.7%)
Ring-necked Duck (*Aythya collaris*)	83	4 (4.8%)	138	1 (0.7%)	221	5 (2.3%)

[a]Also includes Mallard/Gadwall Hybrid (n = 1, 2007, *Anas platyrhynchos/strepera*); Mallard/American Black Duck Hybrid (n = 5, 2007; 1, 2008, *Anas platyrhynchos/rubripes*); Canvasback (n = 18, 2007; 1, 2008, *Aythya valisineria*); Greater Scaup (n = 2, 2007, *Aythya marila*); Lesser Scaup (n = 23, 2007; 11, 2008, *Aythya affinis*); Bufflehead (n = 5, 2007; 3, 2008, *Bucephala albeola*), Common Goldeneye (n = 24, 2007; 6, 2008, *Bucephala clangula*); Hooded Merganser (n = 3, 2007, *Lophodytes cucullatus*); Common Merganser (n = 17, 2007, *Mergus merganser*); and Ruddy Duck (n = 1, 2008, *Oxyura jamaicensis*). AIV was not isolated from any of these species.

doi:10.1371/journal.pone.0024010.t001

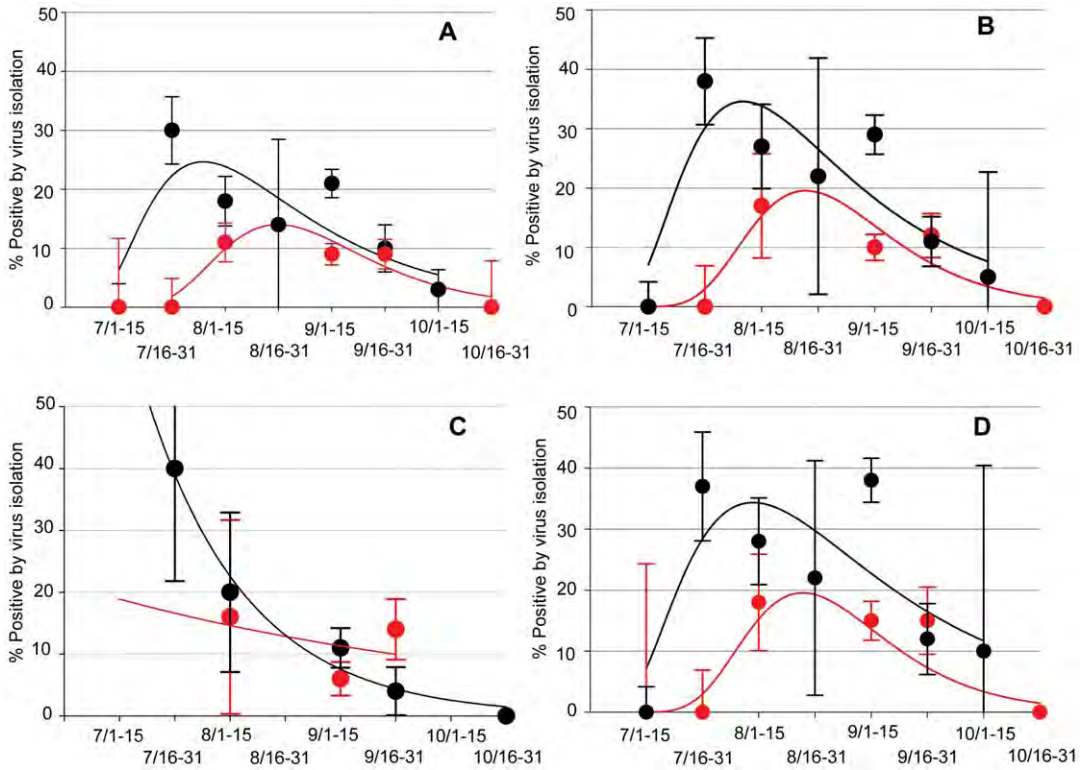

Figure 2. Epidemic curves showing the within-year temporal change in percent of ducks in northwestern Minnesota infected with avian influenza virus, 2007 (red lines) and 2008 (black lines; A = all species; B = Mallards; C = Adult Mallards; and D = Juvenile Mallards). Trend lines were calculated using SigmaPlot software (Systat Software Inc., Richmond California, USA) using a peak, log normal, 3 parameter function (A.B, and D) and exponential decay, single, 2 parameter functions (C).
doi:10.1371/journal.pone.0024010.g002

diversity of subtype combinations increased with the total number of isolates (Figure S1). During 2007, six subtypes were detected in viruses isolated during August; this increased to 23 subtype combinations isolated during early September and decreased to 11 subtypes detected during late September. During 2008, 13 subtypes were represented in July/August isolations, 27 subtypes in early September isolates, and 11 were detected during late September/early October. An overlap between predominant subtype combinations was observed between years with the H3N6, H3N8, H4N6, and H10N7 viruses, each comprising more than 5% of total isolates each year (Table 3). Additionally, within each HA subtype, the same predominant HA/NA subtype combinations were detected each year and included H1N1, H3N8, H4N6, H5N2, H6N1, H7N3, H8N4, H10N7, and H11N9. The H2N3 and H12N5 viruses also predominated within the H2 and H12 subtypes, respectively, but were only represented in a single year (H2 and H12 viruses were not detected during 2007 and 2008, respectively).

Subtype diversity detected at the three northwestern study sites (Thief Lake WMA, Roseau River WMA, and Agassiz NWR) is reported in Table 4. Only subtypes represented by more than one isolate during 2007 or 2008 are included and overall these included 13 and 20 subtypes during those years, respectively (Table 4). For the combined years, 25 of the 33 subtypes (76%) were detected at more than one of the study sites. The probability of detection of a specific subtype at multiple locations increased with the number of isolates of that subtype (Fig. 4).

Mallards were the predominant species sampled (63.7% of the total sample) and were the species with the greatest prevalence of AIV (80.5% of total detections). To determine whether surveillance of this species would adequately describe temporal variations of prevalence and subtype diversity at the northwestern Minnesota study sites, we compared annual data derived from mallards and from the total sample (i.e., all species). The mallard data in both years adequately described temporal prevalence (Fig. 2) and subtype diversity (Table S2). With regard to subtype diversity, only one subtype combination detected in the 2007 total sample and four 2008 subtype combinations were not represented in mallards during those years. These were an H6N6 detected in a northern pintail sampled during 2007 and an H3N9 from a green-winged teal (*Anas crecca*), H4N5 from a green-winged teal, H10N6 from a blue-winged teal (*Anas discors*), and H10N8 from an American wigeon (*Anas Americana*) that were isolated during 2008. Juvenile mallards comprised 39.6% of the total sample. Further, all but four detected subtypes (H1N4, H6N6, H7N8, and H8N4) were represented in juvenile mallards in 2007, and only five of the total subtypes (H3N9, H4N5, H10N6, H10N8 and H11N9) were not isolated from juvenile mallards detected from 2008 samples. Overall, the temporal pattern of AIV in juvenile mallards (Fig. 2D) was similar to that observed for the total duck sample (Fig. 2A) and the entire mallard sample (Fig. 2B) during both years.

Discussion

Our results indicate a seasonal trend in AIV prevalence within northwestern Minnesota that is consistent with previously described seasonal patterns in North America. This trend consists of a seasonal peak that starts in late July and peaks during August [2,4]. Locally, our observations also are consistent with a previous study in Minnesota from 1980–1983 that used a sentinel mallard

Table 2. Multivariable logistic regression model for the prediction of avian influenza virus isolation results in 4,563 waterfowl sampled in northwestern Minnesota, USA, 2007 and 2008.

Variable	Coefficient	†Robust SE	Odds Ratio (95% CI)	‡P
Year				
2007 (1)	Referent		NC*	<0.001
2008 (2)	1.658	0.079		
Location				
Thief Lake WMA (1)	Referent		NC	<0.001
Roseau River WMA (2)	−0.055	0.145		
Agassiz NWR (3)	−2.270	0.101		
Week (centered)	1.163	0.043	NC	<0.001
(Week)^2	−0.392	0.006	NC	<0.001
Age				
Adult	Referent			<0.001
Juvenile	0.996	0.181	2.7 (1.4, 3.9)	
Species type				
Mallard	Referent			<0.001
Other Dabblers	−1.147	0.142	0.32 (0.24, 0.42)	
Divers & Wood Ducks	−2.313	0.407	0.10 (0.04, 0.22)	
Location X Week				
2	−1.424	0.097	NC	<0.001
3	−0.362	0.101		
Location X (Week)^2				
2	0.376	0.009	NC	<0.001
3	0.402	0.011		
Year X Location				
2 2	−0.854	0.191	NC	<0.001
2 3	1.416	0.197		
Year X Week				
2	−2.892	0.055	NC	<0.001
Year X Location X Week				
2 2	3.078	0.102	NC	<0.001
2 3	1.810	0.126		
Constant	−2.674	0.160	---	<0.001

†Robust standard error (SE) adjusted for clustering within capture sites ($n = 24$).
‡P-value based on Wald chi-square statistics.
*NC – Not calculated because the odds ratio depends on the level of the interacting variables.
doi:10.1371/journal.pone.0024010.t002

system. Specifically, infected mallards in the earlier study first were detected during late July and early August during all four years of that study [22]. Prevalence and the specific timing of this peak varied slightly between years (Fig 2). Further, our predictive multivariable model suggests that temporal patterns may not be synchronized among study sites (Figure S1). Variations in seasonality were apparent in previous studies conducted in North America [23] and Europe [12]. In New York, prevalence peaked in late September [23], and in Europe, the peak appeared to extend from September until December [12]. These differences may be influenced by variations of migratory timing, population structure, or species abundance and diversity at different sites.

Consistent with previous studies [2,4,6], AIV prevalence was dependent on species and age. Mallards were much more likely to be infected than the combined samples of dabbling ducks or the diving ducks and wood ducks. Overall, prevalence in the dabbling duck species included in this study ranged from 7% in American wigeon to 37% in northern shoveler (*Anas clypeata*). These species-specific differences may be attributed to population density (mallards), behavior (dabbling ducks and wood ducks), feeding habits (surface feeding) [24], or possibly differences in susceptibility (diving ducks and wood ducks). Mallards have been suggested as the most important duck species related to AIV natural history, but the potential roles of other species in the maintenance and long-range movement of AIV should not be discounted. For example, a high prevalence of AIV infection in northern shoveler has been reported from birds sampled on waterfowl wintering grounds [2]. Likewise, both blue-winged teal and northern pintail have been suggested in the long-distance movement of these viruses [7,25].

Juveniles were almost three times more likely to be infected with AIV than adults (Table 2). This relationship has been previously

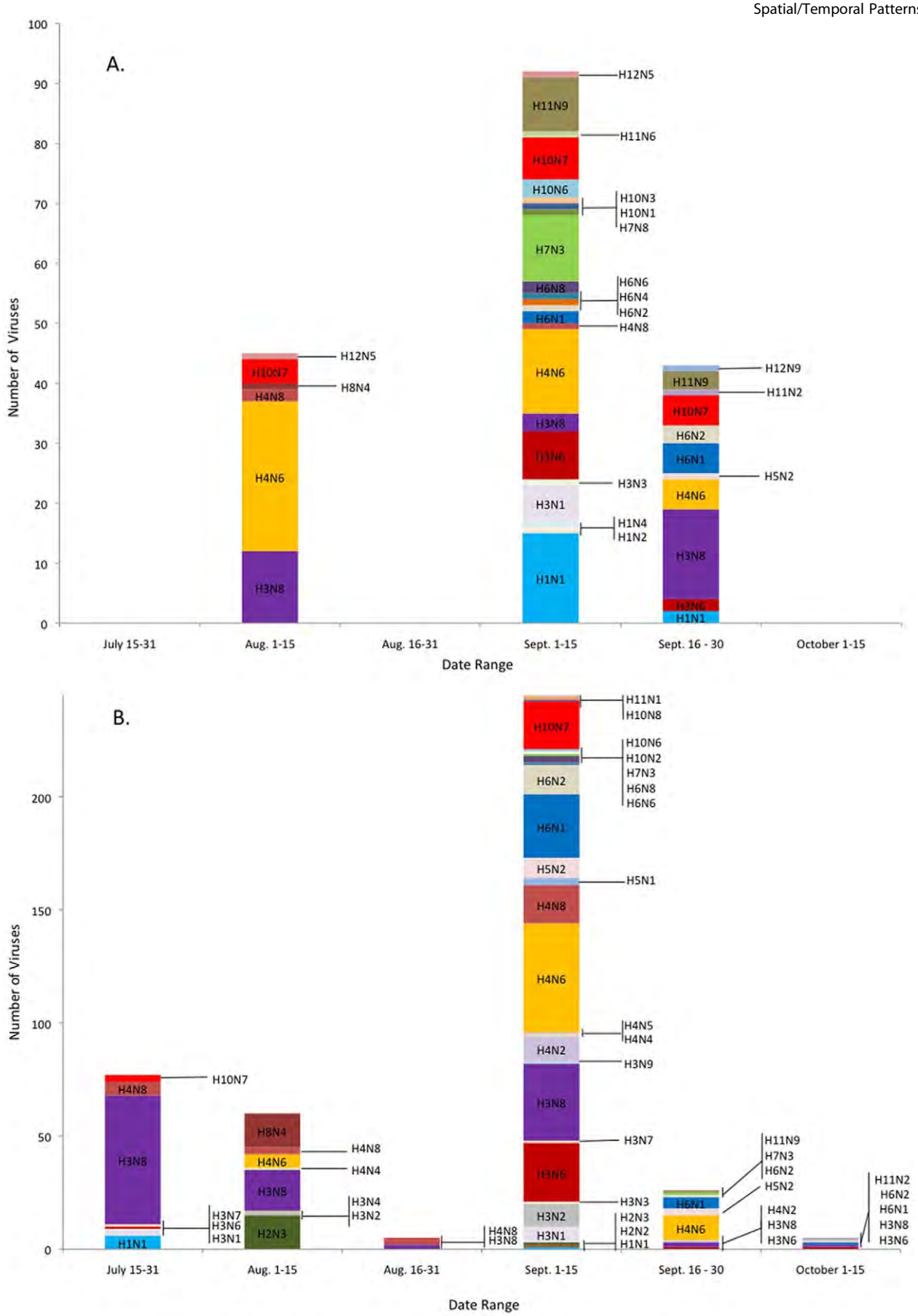

Figure 3. The temporal variation of subtype diversity of avian influenza viruses from ducks captured in northwestern Minnesota, USA (A = 2007; B = 2008). This graph demonstrates that the peak collection period to gather subtypes is early September.
doi:10.1371/journal.pone.0024010.g003

Table 3. Predominant hemagglutinin and neuraminidase subtype combinations detected in northwestern Minnesota, USA, 2007 and 2008, with a comparison to previous studies in North America and Europe.

Subtypes detected and percent (%)					
Alberta 1976–1990 (Sharp et al., 1997)	**Alberta 1976–2001 (Krauss et al., 2004)**	**Northern Europe 1998–2007 (Munster et al., 2007)**	**2007 Minnesota**	**2008 Minnesota**	**Total Minnesota**
H1N1 (2.6)	H1N1 (2.1)	H1N1 (6.0)	H1N1 (8.1)	H1N1 (1.6)	H1N1 (3.8)
H2N3 (0.7)	H2N3 (0.6)	H2N3 (4.2)	ND[†]	H2N3 (3.4)	H2N3 (2.3)
H3N8 (23.3)	H3N8 (22.8)	H3N8 (6.3)	H3N8 (15.3)	H3N8 (26.0)	H3N8 (22.4)
H4N6 (14.6)	H4N6 (12.5)	H4N6 (16.0)	H4N6 (20.7)	H4N6 (14.8)	H4N6 (16.8)
H5N2 (0.2)	H5N2 (0.2)	H5N2 (3.0)	H5N2 (0.5)	H5N2 (2.7)	H5N2 (2.0)
H6N2 (26.3)	H6N2 (20.8)	H6N2 (9.9)	H6N1 (3.2)	H6N1 (7.8)	H6N1 (6.2)
H7N3 (0.6)	H7N3 (0.7)	H7N7 (10.5)	H7N3 (5.4)	H7N3 (0.5)	H7N3 (2.1)
H8N4 (0.4)	H8N4 (0.3)	H8N4 (1.8)	H8N4 (0.5)	H8N4 (3.4)	H8N4 (2.4)
H9N1 (0.07)	H9N1 (0.1)	H9N2 (1.2)	ND	ND	ND
H10N7 (0.6)	H10N1, H10N6 (0.09)	H10N7 (1.2)	H10N7 (7.7)	H10N7 (5.5)	H10N7 (6.2)
H11N9 (0.6)	H11N9 (0.08)	H11N9 (4.8)	H11N9 (5.9)	H11N9 (0.2)	H11N9 (2.1)
H12N5 (0.3)	H12N5 (0.5)	H12N5 (1.2)	H12N5 (0.9)	ND	H12N5 (0.3)

[†]ND – Subtype not detected.

doi:10.1371/journal.pone.0024010.t003

Table 4. Spatial variation in AIV subtypes from sites sampled in northwestern Minnesota, USA, 2007 and 2008.

	2007				**2008**			
Subtypes	**Thief Lake WMA**	**Roseau River WMA**	**Agassiz NWR**	**n**	**Thief Lake WMA**	**Roseau River WMA**	**Agassiz NWR**	**n**
H1N1	15	2		17	4		3	7
H2N2				0		1	1	2
H2N3				0	1	14		15
H3N1	6			6	6		4	10
H3N2				0	6	3	2	11
H3N6	6		4	10	11	9	9	29
H3N7				0			2	2
H3N8	1	16	12	29	20	28	66	114
H4N2				0	3	3	6	12
H4N4					1	1		2
H4N6	13	28	3	44	27	18	19	64
H4N8		1		1	14	5	11	30
H5N1				0	1	2		3
H5N2		1		1	3	2	7	12
H6N1		7		7	4	18	12	34
H6N2		4		4	2	7	6	15
H6N8		2		2	1	1	1	3
H7N3	10		1	11			2	2
H8N4		1		1		15		15
H10N6	3			3	1			1
H10N7	6	6	4	16	3		21	24
H11N9	9	2	2	13			1	1
H12N5	1	1		2				
Total	70	71	26	167	108	127	173	408

doi:10.1371/journal.pone.0024010.t004

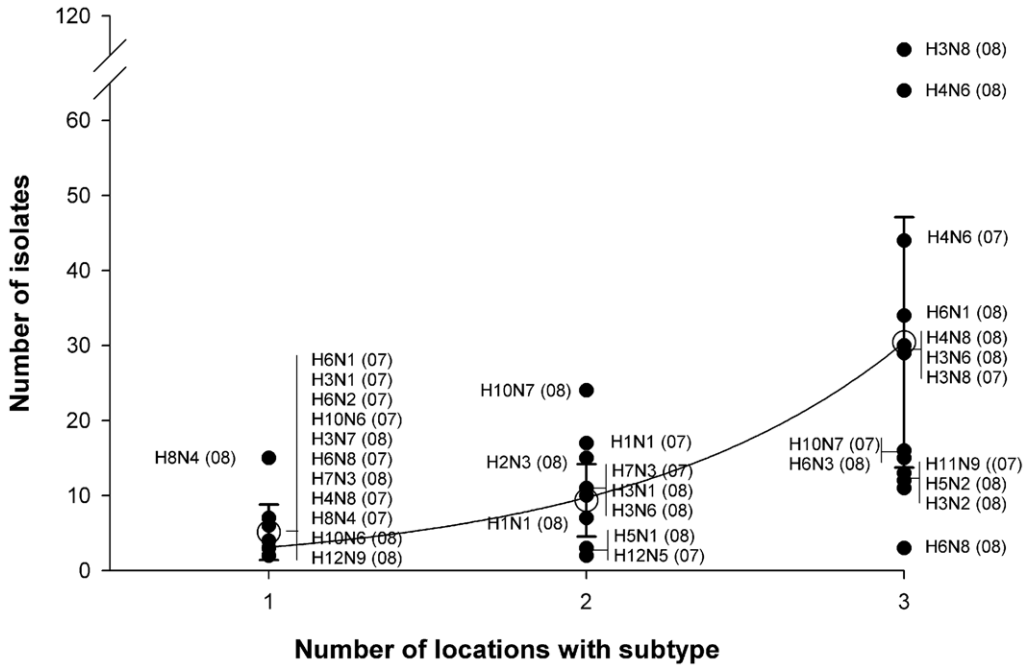

Figure 4. The number of subtype combinations of avian influenza virus that were detected in ducks captured at multiple sites in northwestern Minnesota, USA, 2007 and 2008.
doi:10.1371/journal.pone.0024010.g004

reported [4] and has been observed in numerous studies worldwide [5,6,12]. This may be related to pre-migration staging and the resultant concentration of immunologically naïve juveniles [4].

Because our sampling strategy identified interactive effects between location and time (2 week sampling periods) (Table 2), the marginal effects of location on AIV prevalence could not be independently evaluated. Because environmental and habitat-related characteristics of a wetland (e.g., water depth, water temperature and pH, or avian species composition utilizing the habitat) potentially could influence AIV transmission rates [26], additional work is needed to fully understand this potentially important variable.

Subtype diversity varied over the study period during both years, but most North American HA and NA subtypes were detected during both 2007 and 2008 (Fig. 3). Subtype diversity reflected the observed AIV prevalence (Fig. 2). Few virus subtypes were found early (early July) in either field season, but the number of subtypes increased from August into September and decreased in late September and October. The increased subtype diversity over time may reflect increased detectability related to peak prevalence, the introduction of new subtypes related to migration into the study sites, or reassortment events. In relation to detectability, subtype-specific prevalence (Table S2) often is very low. Specifically, the prevalence of an individual subtype (all species) ranged from 0.04–1.88% and 0.04–4.65% during 2007 and 2008, respectively. Two observations about migration were consistent between years. During both years, several predominant subtypes detected in July and August persisted to late September/early October (H3N8, H4N6, and H10N7 during 2007; H3N8 and H4N6 during 2008). Additionally, several subtypes (H7N3, H11N9, H1N1 during 2007 and H6N1 during 2008) were not detected until early September, when migrating birds probably began arriving in northwestern Minnesota.

The significance of reassortment to the natural history of AIV in wild bird populations is not well defined. The diversity observed within the H3 and H4 subtypes during 2007 and 2008 suggests that reassortment is common. During both years, H3N8 and H4N6 were the predominant subtypes. Numerous NA subtypes were associated with these HA types (H3N1, H3N3, H3N6, H4N8 during 2007; H3N1, H3N2, H3N3, H3N4, H3N6, H3N7, H3N9, H4N2, H4N4, H4N5, H4N8 during 2008). Similar diversity was associated with H6, H10, and H11 viruses during 2007 and H6 and H10 viruses during 2008 (Table S2). In contrast, only one subtype combination was observed with the H8 subtype (H8N4): this cannot be explained but is consistent with other studies (Table S2). Reassortment events are dependent on AIV coinfections, which have been reported in wild duck populations [10]. Because it is intuitive that the likelihood of coinfection is dependent on the prevalence of the potential parent viruses, the relationship between subtype diversity within an HA subtype and the number of isolates recovered is predictable (Fig. 4).

Although the subtypes detected varied annually, most HAs were detected each year. The dominant HA subtypes reported in North American waterfowl are H3, H4, and H6 viruses [2], which may cycle in these populations because of temporal changes in flock immunity [11]. Other HA subtypes have been reported as underrepresented (H2, H5, H7, H8, H9, and H13) or occur sporadically in ducks (H1, H10, H11, and H12) [11]. In our study, HA diversity was consistent with this pattern. The H4 viruses were most common during 2007, the H3 viruses were most common during 2008, and the H6 viruses were well represented during 2008. With the exception of H2, H9 and H12, all other HA subtypes were represented both years but prevalence often was very low (Table S2). The detection of most of these subtypes each year appears to reflect sampling intensity and the high number of isolates recovered. This observation implies that almost all of these HA subtypes are present at the northwestern Minnesota study sites annually.

During both 2007 and 2008, some subtype combinations were over represented. The predominant subtype combinations within

the HA types were H1N1, H2N3, H3N8, H4N6, H5N2, H6N1, H7N3, H8N4, H10N7, H11N9, and H12N5. This was consistent between years. Interestingly, with the exception of H6N1 and H7N3 (H7N7 in Europe) [6], these are the same subtype combinations that have been most reported from ducks in long-term studies in North America [2,4,23] and Europe [6,12] (Table 3). It is unknown why these predominant subtypes have been consistently detected in North America since 1976.

Our results suggest that AIV surveillance in northwestern Minnesota could be efficiently achieved by limiting testing to juvenile mallards (Fig. 2; Table S2). Prevalence and subtype diversity could be adequately described with a much reduced sample size based on juvenile mallards alone: in 2007, juvenile mallards represented 35.7% (871/2441) of the total sample and in 2008 juvenile mallards represented 47.3% (1,065/2252) of the total ducks sampled. These results likely were influenced by the large proportion of mallards (Table S1) in our total sample, but this approach should be considered when testing avian communities that are dominated by this species. Such an approach has application to efficiently recovering AIVs from the field and detecting annual variations in prevalence. This approach may not be applicable to situations in which the ecology of these viruses is less understood, where study questions relate the role of individual species in the natural history of these viruses, where mallards are not the predominant species, or in studies on the wintering grounds of North American waterfowl. Additionally, some subtypes such as the H9, H13, and H16 viruses are underrepresented or absent in ducks and may not be detected by this approach. Finally, although subtype diversity was captured, additional work is needed to determine if genetic diversity was adequately represented in the viruses recovered.

Supporting Information

Figure S1 The number of subtype combinations associated with each HA type and the number of those HA subtype detected during 2007 and 2008 (● = 2007 and ○ = 2008). The line is defined by the quadratic function $f = 9.4889 - 3.9055x + 2.9441x^2$ ($r^2 = 0.7607$, $P < 0.0001$).
(TIF)

Table S1 Summary of avian influenza virus isolation testing results for waterfowl sampled in northwestern Minnesota, USA, 2007 and 2008.
(DOCX)

Table S2 Subtype combination found in all sampled duck species, all mallards, and juvenile mallards and their associated rate of recovery from the total number of birds sampled in northwestern Minnesota, USA, 2007 and 2008.
(DOCX)

Acknowledgments

We thank the SCWDS staff that collected field samples and performed lab tests. We would also like to thank the staffs of the Minnesota Department of Natural Resources and Agassiz NWR for their assistance in the collection of samples, particularly Joel Huener, Margaret Anderson, John Braastad, and Gary Tischer.

Author Contributions

Conceived and designed the experiments: D. Stallknecht D. Swayne. Analyzed the data: BRW VG RP SG SS CC RDB. Wrote the paper: BRW MJY D. Stallknecht. Collection of field samples: BRW GAK JB.

References

1. Hinshaw VS, Webster RG, Turner B (1980) The perpetuation of orthomyxoviruses and paramyxoviruses in Canadian waterfowl. Can J Microbiol 26: 622–629.
2. Stallknecht DE, Shane SM (1988) Host range of avian influenza virus in free-living birds. Vet Res Commun 12: 125–141.
3. Hinshaw VS, Webster RG, Turner B (1979) Water-borne transmission of influenza A viruses. Intervirology 11: 66–69.
4. Hinshaw VS, Wood JM, Webster RG, Deibel R, Turner B (1985) Circulation of influenza viruses and paramyxoviruses in waterfowl originating from two different areas of North America. Bulletin of the World Health Organization 63: 711–719.
5. Olsen B, Munster VJ, Wallensten A, Waldenström J, Osterhaus ADME, et al. (2006) Global patterns of influenza A virus in wild birds. Science 312: 384–388.
6. Munster VJ, Baas C, Lexmond P, Waldenström J, Wallensten A, et al. (2007) Spatial, temporal, and species variation in prevalence of influenza A viruses in wild migratory birds. PLoS Pathog 3(5): e61. doi:10.1371/journal.ppat.0030061.
7. Stallknecht DE, Shane SM, Zwank PJ, Senne DA, Kearney MT (1990) Avian influenza viruses from migratory and resident ducks of coastal Louisiana. Avian Dis 34: 398–405.
8. Hinshaw VS, Webster RG (1982) The Natural History of Influenza A Viruses, In: Beare AS, ed. Basic and Applied Influenza Research. CRC Press: Boca Raton, FL, pp 79–104.
9. Süss J, Schäfer J, Sinnecker H, Webster RG (1994) Influenza virus subtypes in aquatic birds of eastern Germany. Arch of Virol 135: 101–114.
10. Sharp GB, Kawaoka Y, Jones DJ, Bean WJ, Pryor SP, et al. (1997) Coinfection of wild ducks by influenza A viruses: distribution patterns and biological significance. J Virol 71: 6128–6135.
11. Krauss SD, Walker D, Paul-Pryor S, Niles L, Chenghong L, et al. (2004) Influenza A virus in migrating aquatic birds in North America. Vector-borne and Zoonotic Diseases 4: 177–189.
12. Wallensten A, Munster VJ, Latorre-Margalef N, Brytting M, Elmberg J, et al. (2007) Surveillance of influenza A virus in migratory waterfowl in northern Europe. Emerg Infect Dis 13: 404–411.
13. Bahl AK, Pomeroy BS, Easterday BC, Mangundimedjo S (1975) Isolation of type A influenza viruses from the migratory waterfowl along the Mississippi flyway. J Wildl Dis 11: 360–363.
14. Hanson BA, Stallknecht DE, Swayne DE, Lewis LA, Senne DA (2003) Avian influenza viruses in Minnesota ducks during 1998-2000. Avian Dis 47: 867–871.
15. Carney SM (1992) Species, age and sex identification of ducks using wing plumage. U. S. Department of the Interior, U.S. Fish and Wildlife Service, Washington, D.C. 144 p.
16. Hirst G (1941) The agglutination of red cells by allantoic fluid of chick embryos infected with influenza virus. Science 94: 22–23.
17. Fouchier RAM, Bestebroer TM, Herfst S, Van Der Kemp L, Rimmelzwaan GF, et al. (2000) Detection of influenza A viruses from different species by PCR amplification of conserved sequences in the matrix gene. J Clin Microbiol 38: 4096–4101.
18. Spackman E (2008) Methods in Molecular Biology, Vol. 436: Avian Influenza Virus. Springer-Verlag, New York, LLC.
19. Hoffmann E, Stech J, Guan Y, Webster RG, Perez DR (2001) Universal primer set for the full-length amplification of all influenza A viruses. Archives of Virology 146: 2275–2289.
20. Chander Y, Jindal N, Stallknecht DE, Goyal SM (2010) Full length sequencing of all nine subtypes of the neuraminidase gene of influenza A viruses using subtype specific primer sets. J Virol Methods 165: 116–120.
21. Siembieda JL, Johnson CK, Cardona C, Anchell N, Dao N, et al. (2010) Influenza A viruses in wild birds of the Pacific flyway, 2005-2008. Vector Borne Zoonotic Dis 10: 793–800. Epub 2010 Jan 8.
22. Halvorson DA, Karunakaran D, Senne D, Kelleher C, Bailey C, et al. (1983) Simultaneous monitoring of sentinel ducks and turkeys in Minnesota. Avian Dis 27: 77–85.
23. Deibel R, Emord DE, Dukelow W, Hinshaw VS, Wood JM (1985) Influenza viruses and paramyxoviruses in ducks in the Atlantic flyway, 1977-1983, including an H5N2 isolate related to the virulent chicken virus. Avian Dis 29: 970–985.
24. Garamszegi LZ, Møller AP (2007) Prevalence of avian influenza and host ecology. Proceedings of the Royal Society B 274: 2003–2012.
25. Pearce JM, Ramey AM, Flint PL, Koehler AV, Fleskes JP, et al. (2009) Avian influenza at both ends of a migratory flyway: characterizing viral genomic diversity to optimize surveillance plans for North America. Evol Appl 2: 457–468. doi: 10.1111/j.1752-4571.2009.00071.x.
26. Brown JD, Swayne DE, Cooper RJ, Burns RE, Stallknecht DE (2007) Persistence of H5 and H7 Avian Influenza Viruses in Water. Avian Dis 51: 285–289.

Rev. sci. tech. Off. int. Epiz., 2011, **30** (3), 661-671

The influence of economic indicators, poultry density and the performance of Veterinary Services on the control of high-pathogenicity avian influenza in poultry

G. Pavade [(1)], L. Awada [(1)], K. Hamilton [(1)] & D.E. Swayne [(1, 2)*]

(1) World Organisation for Animal Health, 12 rue de Prony, 75017 Paris, France
(2) World Organisation for Animal Health Collaborating Centre for Research on Emerging Avian Diseases, Southeast Poultry Research Laboratory, Agricultural Research Service, United States Department of Agriculture, 934 College Station Road, Athens, GA 30605, United States of America
*Corresponding author: david.swayne@ars.usda.gov

Submitted for publication: 29 September 2011
Accepted for publication: 21 October 2011

Summary
High-pathogenicity avian influenza (HPAI) and low-pathogenicity notifiable avian influenza (LPNAI) in poultry are notifiable diseases that must be reported to the World Organisation for Animal Health (OIE). There are variations between countries' responses to avian influenza (AI) outbreak situations based on their economic status, diagnostic capacity and other factors. The objective of this study was to ascertain the significant association between HPAI control data and a country's poultry density, the performance of its Veterinary Services, and its economic indicators (gross domestic product, agricultural gross domestic product, gross national income, human development index and Organisation for Economic Co-operation and Development [OECD] status). Results indicate that as poultry density increases for least developed countries there is an increase in the number and duration of HPAI outbreaks and in the time it takes to eradicate the disease. There was no significant correlation between HPAI control and any of the economic indicators except membership of the OECD. Member Countries, i.e. those with high-income economies, transparency and good governance, had shorter and significantly fewer HPAI outbreaks, quicker eradication times, lower mortality rates and higher culling rates than non-OECD countries. Furthermore, countries that had effective and efficient Veterinary Services (as measured by the ratings they achieved when they were assessed using the OIE Tool for the Evaluation of Performance of Veterinary Services) had better HPAI control measures.

Keywords
Avian influenza – Control – Economic indicator – Eradication – OECD – OIE PVS tool – Veterinary Services.

Introduction

High-pathogenicity avian influenza (HPAI) and low-pathogenicity notifiable avian influenza (LPNAI) in poultry are notifiable diseases that must be reported to the World Organisation for Animal Health (OIE) (16). High-pathogenicity avian influenza is a highly infectious disease of poultry caused by H5 and H7 subtypes of type A influenza virus and it typically results in high mortality. Low-pathogenicity avian influenza is also caused by infections with influenza A viruses of H5 and H7 subtypes,

but it causes little or no mortality unless accompanied by secondary pathogens. The main risk from LPNAI viruses, and the reason for global efforts for their control, is that they have the capacity to change to HPAI viruses, and it is not possible to predict when this might happen. International reporting of HPAI and LPNAI outbreaks is necessary to prevent further spread through international trade, to increase global disease transparency, and to enhance knowledge of the worldwide avian influenza (AI) outbreak situation, thus allowing the development of effective, harmonised control strategies.

Local, national and regional level Veterinary Services play a key role in controlling AI by carrying out surveillance of animal diseases, including zoonoses, for early detection and rapid response (2). In order to effectively utilise financial and human resources to deal with AI control, it is important to understand the economic, social and governance factors that may affect the success and impact of control measures. Whilst following certain general principles, the control strategy for an individual country should be tailored to country-level factors such as the mixture of commercial, semi-commercial and village poultry production systems, and the availability of local financial and human resources (10).

There are variations in the ways in which countries respond to HPAI outbreaks and this paper examines some of the factors that explain these differences. More specifically, the authors analyse how a country's economic indicators, its poultry density, and the performance of its Veterinary Services influence its ability to prevent and control HPAI.

Materials and methods

Avian influenza control data

A total of 60 countries, territories or special administrative regions experienced outbreaks of HPAI in poultry between 2002 and 2010, and from data collected from Handistatus II (18) and the World Animal Health Information Database (WAHID) (19) the following parameters were calculated:

– outbreak duration in days: start date of the event until the last case has been diagnosed

– eradication time in days: start date of the event until three months after the last case has been stamped out and all affected establishments have been disinfected (in accordance with the OIE *Terrestrial Animal Health Code,* the absence of further outbreaks must be confirmed by surveillance during this three-month period [16])

– mortality rate:

$$\frac{\text{poultry deaths during an HPAI outbreak} \times 100{,}000}{\text{poultry population at a particular time in a year}}$$

– culling rate:

$$\frac{\text{total poultry culled during an HPAI outbreak} \times 100{,}000}{\text{poultry population at a particular time in a year.}}$$

Data on poultry population were obtained from the Statistical Database of the Food and Agriculture Organization of the United Nations (FAOSTAT) (7) and information on poultry density (head/km^2 of agriculture land) was obtained from the FAO Global Livestock Production and Health Atlas (6).

Economic indicators

Economic indicators allow analysis of the economic performance of a country. In this study the authors used the following economic indicators:

– gross domestic product (GDP) based on purchasing power parity

– agricultural gross domestic product (AGDP)

– percentage that AGDP contributes to total GDP (% AGDP)

– GDP per capita

– gross national income (GNI)

– human development index (HDI)

– membership of the Organisation for Economic Co-operation and Development (OECD) (3, 11, 13, 15).

Economic indicators were tested for correlation with AI control data sets.

A nation's GDP at purchasing power parity exchange rates is the sum value of all goods and services produced in the country valued at prices prevailing in the United States. This is the measure most economists prefer when looking at per-capita welfare and when comparing living conditions or use of resources across countries (3). Gross domestic product per capita is gross domestic product divided by mid-year population (15). Gross national income per capita at purchasing power parity rates is the sum of the value added by all resident producers plus any product taxes (less subsidies) not included in the valuation of output plus net receipts of primary income (compensation of employees and property income) from abroad in current international dollars (15). The HDI is a summary measure of human development. It measures the average achievements in a country in three basic areas: health, education and living standards (13).

Countries which experienced outbreaks of HPAI between 2002 and 2010 were analysed in order to establish if there was an association between their GDP, AGDP, % AGDP, GDP per capita, GNI and HDI and their HPAI control data sets. For the purpose of more detailed statistical analysis, the countries were classified into least developed countries,

developing/transition countries, and developed countries using the classifications of the United Nations Statistics Division (14), as follows:

a) least developed countries: Afghanistan, Bangladesh, Benin, Bhutan, Burkina Faso, Cambodia, Djibouti, the Lao People's Democratic Republic (LAO PDR), Myanmar, Niger, Sudan and Togo (12 countries)

b) developing/transition countries: Albania, Azerbaijan, Cameroon, Chile, the People's Republic of China (China), Côte d'Ivoire, Egypt, Ghana, Hong Kong Special Administrative Region, India, Indonesia, Iran, Iraq, Israel, Jordan, Kazakhstan, the Democratic Republic of Korea (DPR Korea), the Republic of Korea, Kuwait, Malaysia, Nepal, Nigeria, Pakistan, Palestinian territories, Russia, Saudi Arabia, Serbia, South Africa, Thailand, Turkey, Ukraine, Vietnam and Zimbabwe (33 countries)

c) developed countries: Belgium, Canada, the Czech Republic, Denmark, France, Germany, Hungary, Japan, the Netherlands, Poland, Romania, Spain, Sweden, the United Kingdom and the United States (15 countries).

Countries affected by HPAI outbreaks were also divided into OECD countries and non-OECD countries and their outbreak data were compared. Member Countries of the OECD are committed to market economies backed by democratic institutions and focused on the well-being of all citizens. These countries foster prosperity and fight poverty through economic growth and financial stability. The OECD countries included in this study were Belgium, Canada, Chile, the Czech Republic, Denmark, France, Germany, Hungary, Israel, Japan, the Republic of Korea, the Netherlands, Poland, Spain, Sweden, Turkey, the United Kingdom and the United States (18 countries) (11). The non-OECD countries included were Afghanistan, Albania, Azerbaijan, Bangladesh, Benin, Bhutan, Burkina Faso, Cambodia, Cameroon, China, Côte d'Ivoire, Djibouti, Egypt, Ghana, Hong Kong, India, Indonesia, Iran, Iraq, Jordan, Kazakhstan, DPR Korea, Kuwait, Lao PDR, Malaysia, Myanmar, Nepal, Niger, Nigeria, Pakistan, Palestinian territories, Romania, Russia, Saudi Arabia, Serbia, South Africa, Sudan, Thailand, Togo, Ukraine, Vietnam and Zimbabwe (42 countries).

Performance of Veterinary Services

The OIE has developed an assessment tool – the Tool for the Evaluation of Performance of Veterinary Services (PVS tool) – to assist Veterinary Services to establish their current level of performance, to identify gaps and weaknesses in their ability to comply with OIE international standards and to develop strategies to improve performance. The PVS tool defines effective Veterinary Services as those that have four fundamental components:

– the human, physical and financial resources to attract resources and retain professionals with technical and leadership skills

– the technical authority and capability to address current and new issues, including prevention and control of biological disasters, based on scientific principles

– sustained interaction with stakeholders in order to stay on course and carry out relevant joint programmes and services

– the ability to access markets through compliance with existing standards and the implementation of new disciplines such as the harmonisation of standards, equivalence and zoning (17).

Under each of these four fundamental components, six to twelve critical competencies have been elaborated to enable countries to establish the current level of performance of their Veterinary Services based on performance ratings ranging from level one (low performance) to level five (high performance). Twelve of the countries that experienced HPAI outbreaks during the period covered by this study had assessed their Veterinary Services immediately after the outbreak using the OIE PVS tool. The results of the evaluations of these 12 countries (country names withheld to maintain confidentiality – eight developing countries and four least developed countries) were analysed to ascertain the association between the success of AI control measures and 15 critical competencies (drawn from across the four fundamental components of the PVS tool [17]). The areas evaluated were:

– staffing (veterinarians)
– staffing (veterinary paraprofessionals)
– professional competencies of veterinarians and veterinary paraprofessionals
– continuing education
– stability of structures and sustainability of policies
– emergency funding
– capital investment
– veterinary laboratory diagnosis
– epidemiological surveillance
– early detection and emergency response
– disease prevention, control and eradication
– veterinary medicines and biologicals
– transparency
– compartmentalisation
– zoning.

More specifically, the study looked at the association between HPAI control data and the capacity of Veterinary Services to do the following:

a) ensure that Veterinary Services are staffed appropriately, i.e. define the needs of the service, draw up appropriate job descriptions and have procedures that ensure all veterinary positions are filled by professionals who have appropriate university-level qualifications

b) establish procedures for the appointment of veterinary paraprofessionals and ensure that technical positions are occupied by staff with the requisite technical knowledge

c) ensure that staff have the skills and knowledge to carry out their functions

d) maintain and improve the competence of the Veterinary Services personnel in terms of relevant information and understanding, measured in terms of the implementation of a training programme

e) implement and sustain policies over time

f) access extraordinary financial resources in order to respond to emergency situations or emerging issues

g) access funding for basic and additional investments (material and non-material) that lead to a sustained improvement in the Veterinary Services operational infrastructure

h) identify and record pathogenic agents, including those relevant for public health, that can adversely affect animals and animal products

i) determine, verify and report on the sanitary status of the animal populations under their mandate

j) detect and respond rapidly to a sanitary emergency such as a significant disease outbreak or food safety emergency

k) actively perform actions to prevent, control or eradicate OIE-listed diseases and/or to demonstrate that the country or a zone are free of relevant diseases

l) regulate veterinary medicines and veterinary biologicals, i.e. the authorisation, registration, import, production, labelling, distribution, sale and use of these products

m) notify the OIE of the sanitary status of their country and inform them of other relevant matters in accordance with established procedures

n) establish and maintain disease-free zones, as necessary and in accordance with the criteria established by the OIE

o) establish and maintain disease-free compartments as necessary and in accordance with the criteria established by the OIE.

Statistical data analysis

For each country, GDP, AGDP, % AGDP, GDP per capita, GNI, HDI, poultry density, and PVS evaluation scores were compared to HPAI control data to determine association by statistical analysis. The data were subjected to linear regression statistical analysis (Epi Info™ Version 3.5.3, Centers for Disease Control and Prevention, USA) to evaluate the *R* value (correlation coefficient) and R^2 value (coefficient of determination). All the *R* values were subjected to a test of significance to find out the significant *R* values at 5% level. *R* value denotes the strength of the correlation of the tested parameters with HPAI control data, while R^2 value indicates the fraction of variance that is shared between them.

High-pathogenicity avian influenza control data for OECD countries were compared with data from non-OECD countries. Student's *t* test was used to analyse data on the number of outbreaks, outbreak duration and eradication time, and the Chi-square test (Epi Info™ Version 3.5.3) was used to compare mortality and culling rates.

Results

Poultry density and economic indicators

Linear regression analysis of HPAI control data in poultry (2002 to 2010) with poultry density and economic indicators (GDP, AGDP, % AGDP, GDP per capita, GNI and HDI) are presented in Table I.

Poultry density of least developed countries showed significance ($p < 0.05$) for outbreak duration ($R = 0.92$), length of eradication time ($R = 0.92$) and number of cases ($R = 0.93$). This indicates a strong positive linkage, i.e. the higher the poultry density, the longer the duration of the disease, the longer the length of time to eradicate the disease, and the greater the number of cases. The R^2 values for these parameters were more than 0.85, indicating that more than 85% of the variability in outbreak duration, eradication time and number of outbreaks could be explained by the poultry density. Mortality and culling rates of least developed countries showed no correlation with poultry density.

The poultry density of developing/transition and developed countries showed insignificant *R* values for all HPAI control data, indicating that there was no correlation between them.

All *R* values for GDP, AGDP, % AGDP, GDP per capita, GNI and HDI were non-significant, indicating there was no significant correlation between HPAI control data and these economic indicators.

A comparison of the mean number of outbreaks, the mean mortality and culling rates, the mean outbreak duration and the mean eradication time in OECD countries and non-OECD countries is presented in Table II. There was

Table I
Linear regression comparison of high-pathogenicity avian influenza control data in poultry (2002 to 2010) with poultry density and economic indicators

Country classification	Variables	HPAI control data: Outbreak duration (days)		Eradication time (days)		Mortality rate (no./100,000 birds)		Culling rate (no./100,000 birds)		No. of outbreaks	
		R value	R^2 value	*R* value	R^2 value	*R* value	R^2 value	*R* value	R^2 value	*R* value	R^2 value
All countries	Poultry density	0.10	0.01	0	0	0.20	0.04	0.22	0.05	0.10	0.01
(*n* = 60)	GDP	– 0.28	0.08	0.20	0.04	– 0.10	0.01	0.17	0.03	– 0.20	0.04
	AGDP	0.14	0.02	0	0	0.10	0.01	0.24	0.06	0.17	0.03
	% AGDP	– 0.10	0.01	0.14	0.02	– 0.24	0.06	0.28	0.08	– 0.20	0.04
	GDP per capita	– 0.39	0.15	– 0.39	0.15	0	0	0.63	0.40	– 0.58	0.34
	GNI	0.20	0.04	0.20	0.04	– 0.10	0.01	0.22	0.05	– 0.24	0.06
	HDI	0.14	0.02	– 0.14	0.02	0	0	0	0	0	0
Least developed	Poultry density	0.92*	0.86	0.92*	0.85	0	0	0	0	0.93*	0.87
countries**	GDP	0	0	0	0	0.26	0.07	0	0	0	0
(*n* = 12)	AGDP	0	0	0	0	0.24	0.06	0.10	0.01	0	0
	% AGDP	– 0.26	0.07	– 0.30	0.09	– 0.10	0.01	– 0.17	0.03	– 0.24	0.06
	GDP per capita	– 0.10	0.01	– 0.10	0.01	0	0	0.10	0.01	– 0.20	0.04
	GNI	0.22	0.05	0	0	0.14	0.02	0	0	0.17	0.03
	HDI	0.17	0.03	0.22	0.05	0.10	0.01	0.10	0.01	0	0
Developing	Poultry density	– 0.14	0.02	– 0.14	0.02	– 0.14	0.02	0	0	– 0.10	0.01
countries***	GDP	0	0	0	0	0.10	0.01	0.14	0.02	0.10	0.01
(*n* = 33)	AGDP	0	0	0	0	0.10	0.01	0.14	0.02	0.10	0.01
	% AGDP	– 0.24	0.06	– 0.17	0.03	0	0	0.10	0.01	– 0.17	0.03
	GDP per capita	– 0.14	0.02	– 0.14	0.02	– 0.17	0.03	0.79	0.63	– 0.14	0.02
	GNI	0.14	0.02	0.10	0.01	– 0.24	0.06	– 0.28	0.08	0.14	0.02
	HDI	– 0.28	0.08	0	0	– 0.14	0.02	0	0	– 0.22	0.05
Developed	Poultry density	0.10	0.01	– 0.10	0.01	0	0	0.24	0.06	– 0.20	0.04
countries****	GDP	0	0	0	0	0.20	0.04	0.14	0.02	0.20	0.04
(*n* = 15)	AGDP	0.14	0.02	0.14	0.02	0.10	0.01	0.10	0.01	0	0
	% AGDP	– 0.10	0.01	– 0.10	0.01	0	0	– 0.10	0.01	0.10	0.01
	GDP per capita	– 0.26	0.07	– 0.26	0.07	0.14	0.02	0	0	– 0.17	0.03
	GNI	0.28	0.08	– 0.24	0.06	0.10	0.01	– 0.14	0.02	0.28	0.08
	HDI	– 0.14	0.02	0.22	0.05	– 0.10	0.01	0.28	0.08	– 0.24	0.06

% AGDP: percentage of agriculture contributed to GDP
AGDP: agricultural gross domestic product
GDP: gross domestic product
GNI: gross national income
HDI: human development index
HPAI: high-pathogenicity avian influenza
* Significant at $p < 0.05$

** Afghanistan, Bangladesh, Benin, Bhutan, Burkina Faso, Cambodia, Djibouti, Lao People's Democratic Republic, Myanmar, Niger, Sudan and Togo
*** Albania, Azerbaijan, Cameroon, Chile, People's Republic of China, Côte d'Ivoire, Egypt, Ghana, Hong Kong, India, Indonesia, Iran, Iraq, Israel, Jordan, Kazakhstan, Republic of Korea, Democratic People's Republic of Korea, Kuwait, Malaysia, Nigeria, Nepal, Pakistan, Palestinian territories, Russia, Saudi Arabia, Serbia, South Africa, Thailand, Turkey, Ukraine, Vietnam and Zimbabwe
**** Belgium, Canada, Czech Republic, Denmark, France, Germany, Hungary, Japan, Netherlands, Poland, Romania, Spain, Sweden, United Kingdom and United States

Table II
Comparison of the high-pathogenicity avian influenza control data of OECD countries (*n* = 18) with non-OECD countries (*n* = 42)

Group	Mean outbreak duration (days)	Mean eradication time (days)	Mean no. of outbreaks	Mean mortality rate (no./100,000 birds)	Mean culling rate (no./100,000 birds)
OECD countries***	86.97*	176.97*	19.31*	12.36**	924.04**
Non-OECD countries****	177.33*	267.82*	65.39*	27.70**	236.35**

OECD: Organisation for Economic Co-operation and Development
* Significant at $p < 0.05$ by Student's *t* test
** Significant at $p < 0.05$ by Chi-square test
***Belgium, Canada, Chile, Czech Republic, Denmark, France, Germany, Hungary, Israel, Japan, Republic of Korea, Netherlands, Poland, Spain, Sweden, Turkey, United Kingdom and United States
****Afghanistan, Albania, Azerbaijan, Bangladesh, Benin, Bhutan, Burkina Faso, Cambodia, Cameroon, People's Republic of China, Côte d'Ivoire, Djibouti, Egypt, Ghana, Hong Kong, India, Indonesia, Iran, Iraq, Jordan, Kazakhstan, Democratic Republic of Korea, Kuwait, Lao People's Democratic Republic, Malaysia, Myanmar, Nepal, Niger, Nigeria, Pakistan, Palestinian territories, Romania, Russia, Saudi Arabia, Serbia, South Africa, Sudan, Thailand, Togo, Ukraine, Vietnam and Zimbabwe

significant difference between the means, indicating that OECD countries had shorter outbreaks, shorter eradication times and fewer outbreaks than non-OECD countries. Also, OECD countries had lower mortality rates and higher culling rates than non-OECD countries.

Performance of Veterinary Services

Linear regression analysis of PVS tool critical competencies and HPAI control data is presented in Table III. The significant R values ($p < 0.05$) and R^2 values showed that there was significant correlation between HPAI data and certain critical competencies, as follows:

a) negative correlation of the staffing of Veterinary Services (veterinarians and other professionals) with HPAI eradication time, mortality rate, culling rate and number of outbreaks, i.e. as the appropriate staffing of the Veterinary Services by veterinarians increased, the time for eradication of AI, the mortality and culling rate associated with HPAI outbreaks and the occurrence of outbreaks decreased

b) negative correlation of the staffing of Veterinary Services (veterinary paraprofessionals) with mortality rate, i.e. when the number of technically qualified personnel increased, the mortality rate decreased

c) negative correlation of the professional competencies of veterinarians with mortality rate, i.e. as veterinary practices and attitudes improved and veterinary knowledge increased, the mortality rate due to the disease decreased

d) negative correlation of continuing education with mortality rate, i.e. as the competence of personnel in Veterinary Services increased through relevant training programmes, there was a decrease in the mortality rate

e) negative correlation of emergency funding with HPAI eradication time, i.e. when the financial resources of the Veterinary Services increased, there was a decrease in the eradication time of AI

f) negative correlation of veterinary laboratory diagnosis with HPAI eradication time and number of outbreaks, i.e. as the capacity to perform laboratory-based diagnosis of

Table III
Linear regression analysis of high-pathogenicity avian influenza control data with the critical competencies evaluated in the OIE Tool for the Evaluation of Performance of Veterinary Services

OIE PVS tool critical competencies	HPAI control data: HPAI eradication time (days)		Mortality rate (no./100,000 birds)		Culling rate (no./100,000 birds)		No. of HPAI outbreaks	
	R value	R^2 value	*R* value	R^2 value	*R* value	R^2 value	*R* value	R^2 value
Staffing (veterinarians and other professionals)	– 0.83*	0.70	– 0.57*	0.33	– 0.86*	0.74	– 0.83*	0.69
Staffing (veterinary paraprofessionals and other)	– 0.30	0.09	– 0.81*	0.67	– 0.24	0.06	– 0.28	0.08
Professional competencies of veterinarians	0	0	– 0.65*	0.43	0.10	0.01	– 0.22	0.05
Competencies of veterinary paraprofessionals	– 0.37	0.14	– 0.33	0.11	– 0.38	0.15	– 0.22	0.05
Continuing education	– 0.28	0.08	– 0.82*	0.68	– 0.43	0.19	– 0.20	0.04
Technical independence	– 0.20	0.04	– 0.10	0.01	– 0.34	0.12	– 0.31	0.10
Stability of structures and sustainability of policies	– 0.43	0.19	– 0.14	0.02	– 0.14	0.02	0	0
Coordination capability of Veterinary Services	– 0.26	0.07	– 0.10	0.01	– 0.28	0.08	– 0.28	0.08
Operational funding	0	0	– 0.14	0.02	– 0.17	0.03	– 0.17	0.03
Emergency funding	– 0.58*	0.34	– 0.10	0.01	– 0.26	0.07	– 0.40	0.16
Capital investment	– 0.31	0.10	0	0	– 0.34	0.12	– 0.47	0.23
Veterinary laboratory diagnosis	– 0.46	0.22	– 0.10	0.01	– 0.45	0.21	– 0.72*	0.53
Risk analysis	0	0	– 0.14	0.02	– 0.17	0.03	0.17	0.03
Quarantine and border security	0	0	0.10	0.01	0.14	0.02	0.10	0.01
Epidemiological surveillance	– 0.57*	0.32	– 0.26	0.07	– 0.48	0.24	– 0.45	0.21
Early detection and emergency response	0.20	0.04	0	0	– 0.24	0.06	– 0.38	0.15
Veterinary medicines and veterinary biologicals	0	0	– 0.40	0.16	– 0.64*	0.41	– 0.60*	0.37
Animal identification and movement control	– 0.20	0.04	– 0.31	0.10	– 0.14	0.02	0	0
Transparency	– 0.10	0.01	– 0.34	0.12	– 0.66*	0.44	– 0.59*	0.35
Zoning	0.24	0.06	– 0.26	0.07	– 0.20	0.04	0.38	0.15
Compartmentalisation	0.17	0.03	– 0.20	0.04	0	0	0.20	0.04
Disease prevention, control and eradication	– 0.80*	0.64	0.24	0.06	– 0.50*	0.25	– 0.86*	0.74

HPAI: high-pathogenicity avian influenza
PVS: Performance of Veterinary Services
*Significant at $p < 0.05$

pathogenic agents increased, there was a decrease in the eradication time and fewer outbreaks

g) negative correlation of epidemiological surveillance with HPAI eradication time, i.e. when there was more active and passive surveillance, there was a decrease in the time taken to eradicate HPAI

h) negative correlation of veterinary medicines and veterinary biologicals with culling rate and number of outbreaks, i.e. when the Veterinary Services had a greater capacity to regulate the registration, import, production, labelling, distribution, sale and use of veterinary medicines and biologicals, there was a reduction in the culling rate and number of outbreaks

i) negative correlation of transparency with culling rate and number of outbreaks, i.e. when the capacity of Veterinary Services to provide regular animal health status reports to the OIE increased, there was a decrease in the culling rate and number of outbreaks

j) negative correlation of disease prevention, control and eradication measures with HPAI eradication time, culling rate and number of outbreaks, i.e. as the Veterinary Services increased the number of prevention, control and eradication programmes for OIE-listed diseases, there was a decrease in HPAI outbreaks, eradication time and culling rate.

Discussion

Poultry density

High-density poultry farms located in least developed countries were associated with longer outbreaks, longer eradication times and an increased incidence of outbreaks. A high density of poultry facilitates the rapid transmission of the virus between birds and between farms, and could lead to environmental persistence of the virus for a longer period of time. This study corroborated earlier findings in some developing countries. In Vietnam, for example, medium poultry density was found to be a risk factor for HPAI outbreaks (8). Similarly, high poultry density was found to be associated with HPAI outbreaks in Thailand (12) and Hong Kong (9). The virus can move from bird to bird and farm to farm far more easily in a high poultry density zone than in a low density area, especially if between-farm biosecurity is poor. However, in developed and developing/transition countries, high poultry density was not associated with an increase in the number or duration of HPAI outbreaks or in eradication times. This suggests that in such countries other components of poultry management, such as better biosecurity and veterinary care, compensated for the increased poultry density and prevented increasing transmission and spread of HPAI viruses.

Economic development indicators

There was no significant correlation between GDP, AGDP, % AGDP, GDP per capita, GNI and HDI with HPAI control data. This suggests that several other factors, such as environment, ecology, poultry production systems and implementation of effective control programmes, may influence the occurrence and control/eradication of the disease in a country (5). Continuous or intermittent HPAI outbreaks have been reported in high-GDP countries such as China, Germany, India, Japan, the Republic of Korea, Malaysia and Russia, even though abundant resources are devoted to disease surveillance and biosecurity in these countries. In medium-GDP countries, such as Bangladesh, Egypt, Indonesia and Vietnam, the disease is prevalent and is endemic in nature. In contrast, Afghanistan, Benin and Bhutan, which are low-GDP countries, have only ever experienced occasional small outbreaks of HPAI. This indicates that the virus can cause disease in a country irrespective of its GDP and that control/eradication is complex and influenced by multiple factors. However, the OECD countries that have systems of economic development and governance which favour transparency, economic growth and financial stability had significantly fewer HPAI outbreaks, shorter outbreaks, shorter eradication times, lower mortality rates and higher culling rates than non-OECD countries.

Performance of Veterinary Services

If a country's Veterinary Services perform well it has a better chance of controlling and preventing HPAI outbreaks. Veterinary Services can only carry out their functions effectively if they have:

– appropriately qualified staff and a sufficient number of posts

– professionally competent staff who have regular access to continuous education and relevant training

– sound financial resources for continued operation of the Veterinary Services

– rapid laboratory-based diagnosis of pathogenic agents

– continuous epidemiological surveillance for various diseases and reporting of disease status to the OIE

– effective regulation of veterinary medicines and biologicals

– increased prevention, control and eradication measures for OIE-listed diseases.

Veterinary Services must perform optimally in all these areas if they are to implement effective control measures and prevent AI. If there is a decrease in the level of critical competencies, then there is the potential for outbreaks to become prolonged and difficult to eradicate.

The role of Veterinary Services is recognised as a 'global public good' by the World Bank. Veterinary Services are involved in the provision of animal health services, and this requires close working partnerships between veterinarians, veterinary assistants, and livestock and poultry farmers. When Veterinary Services fail in a single country, this creates a threat to the entire world. Animal disease outbreaks pose more of a problem when they occur in countries that have no effective surveillance and no preventive animal health network (1).

Veterinary Services at the national level play a key role in combating HPAI outbreaks and countries should evaluate their Veterinary Services using the OIE PVS tool or similar assessment tool to identify gaps and weaknesses in their ability to comply with OIE international standards on animal health. Once countries know how they are currently performing they can decide how best to reinforce their national preparedness plans for AI control in line with international standards and guidelines. They can also ensure that they strengthen their Veterinary Services in ways which will facilitate the early detection of HPAI outbreaks and the implementation of efficient control measures.

Although analysis of GDP, AGDP, % AGPD, GDP per capita, GNI and HDI did not indicate a direct economic link to HPAI control, the combined results of the OECD and PVS analyses suggest that countries which invested financial and human resources in their Veterinary Services had more effective disease control and preventive measures for HPAI. However, this is not solely a financial issue, but also involves multiple other factors connected to OECD membership, including transparency and good governance. Previously, a close relationship was demonstrated between GDP and public spending on National Prevention Systems for Animal Diseases and Zoonoses (NPS), and further linked livestock density, especially poultry density, and export of animal products in wealthier developing countries to increased levels of spending on NPS (4). Countries that produce and export meat have better veterinary governance and are associated with Veterinary Services that achieve high ratings when their critical competencies are evaluated (J. Commault, OIE unpublished data, 2011). In addition, the GDP per capita was positively linked to high-performing Veterinary Services. It should be noted, however, that a high GDP is not always sufficient for Veterinary Services to perform well in all areas: some high-GDP countries do not have high-performing Veterinary Services (J. Commault, OIE unpublished data, 2011). However, a country with a high GDP which is also transparent and well-governed is more likely to have good Veterinary Services and will therefore be better placed to control HPAI outbreaks.

Conclusions

A high poultry density in least developed countries was associated with increased duration of HPAI outbreaks, a longer time to eradicate the disease and a greater number of cases. Direct economic indicators such as GDP, AGDP, % AGDP, GDP per capita, GNI and HDI do not show a significant association with HPAI control data, but an indirect indicator of economic development (i.e. OECD membership) was positively linked to fewer HPAI outbreaks, shorter outbreak duration and eradication time, and a low mortality rate and high culling rate. Several of the core critical competencies that are evaluated by the OIE PVS tool have a significant association with improved HPAI control. For example, the disease is more effectively controlled when Veterinary Services are appropriately staffed, veterinarians have a high level of competence, and staff have regular opportunities to update their skills. Similarly, HPAI control is better in countries whose Veterinary Services have the capacity to access financial resources, carry out epidemiological surveillance, perform laboratory-based diagnosis, maintain transparency, and implement disease prevention and control measures. A country with a high level of competence in these areas can establish a good network of disease surveillance and implement control measures to tackle HPAI outbreaks. Such a network can be extended to LPNAI, Newcastle disease and other poultry diseases. Establishing the current level of performance of the Veterinary Services in a country and improving its level of advancement by addressing the deficiencies will help in implementing more effective measures against AI in control programmes. In total, the data imply that countries which are transparent, have good governance and provide adequate funding for the development and maintenance of efficiently performing Veterinary Services have better control of HPAI.

Acknowledgements

This study was conducted as part of an OFFLU research secondment/sabbatical by the corresponding author (D.E. Swayne) from the US Department of Agriculture. OFFLU is the joint OIE/FAO network of expertise on animal influenzas. Financial support for the research staff (K. Hamilton, G. Pavade & D.E. Swayne) was provided by the Agricultural Research Service, US Department of Agriculture (CRIS #6612-32000-048-00D) and by the OIE World Fund for Animal Health and Welfare from contributions from the following donors: the Canadian International Development Agency, and the Department for International Development in the United Kingdom. Special thanks to Francois Caya and the OIE staff in the Regional Activities Department for assistance with PVS data.

■

Journal of Food Protection, Vol. 74, No. 7, 2011, Pages 1161–1168
doi:10.4315/0362-028X.JFP-10-415

Thermal Inactivation of Avian Influenza Virus and Newcastle Disease Virus in a Fat-Free Egg Product

REVIS A. CHMIELEWSKI, JOAN R. BECK, AND DAVID E. SWAYNE*

U.S. Department of Agriculture, Agricultural Research Service, Southeast Poultry Research Laboratory, 934 College Station Road, Athens, Georgia 30605, USA

MS 10-415: Received 28 September 2010/Accepted 3 March 2011

ABSTRACT

High-pathogenicity avian influenza (HPAI) virus, low-pathogenicity avian influenza (LPAI) virus, virulent Newcastle disease virus (vNDV) and low-virulent Newcastle disease virus (lNDV) can be present on the eggshell surface, and HPAI viruses and vNDV can be present in the internal contents of chicken eggs laid by infected hens. With the increase in global trade, egg products could present potential biosecurity problems and affect international trade in liquid and dried egg products. Therefore, the generation of survival curves to determine decimal reduction times (D_T-values) and change in heat resistance of the viruses (z_D-value) within fat-free egg product could provide valuable information for development of risk reduction strategies. Thermal inactivation studies using A/chicken/Pennsylvania/1370/83 (H5N2) HPAI virus resulted in D_{55}-, D_{56}-, $D_{56.7}$-, D_{57}-, D_{58}-, and D_{59}-values of 18.6, 8.5, 3.6, 2.5, 0.4, and 0.4 min, respectively. The z_D-value was 4.4°C. LPAI virus A/chicken/New York/13142/94 (H7N2) had D_{55}-, $D_{56.7}$-, D_{57}-, D_{58}-, D_{59}-, and D_{60}-values of 2.9, 1.4, 0.8, 0.7, 0.7, and 0.5 min, respectively, and a z-value of 0.4°C. vNDV avian paramyxoviruses of serotype 1 (AMPV-1)/chicken/California/212676/2002 had D_{55}-, D_{56}-, $D_{56.7}$-, D_{57}-, D_{58}-, and D_{59}-values of 12.4, 9.3, 6.2, 5, 3.7, and 1.7 min, respectively. The z_D-value was 4.7°C. lNDV AMPV-1/chicken/United States/B1/1948 had D_{55}-, D_{57}-, D_{58}-, D_{59}-, D_{61}-, and D_{63}-values of 5.3, 2.2, 1.1, 0.55, 0.19, and 0.17 min, respectively, and a z_D-value of 1.0°C. Use of these data in developing egg pasteurization standards for AI and NDV-infected countries should allow safer trade in liquid egg products.

Avian health issues, principally Newcastle disease and high-pathogenicity avian influenza (HPAI), have limited global trade in poultry and poultry products. Newcastle disease is caused by avian paramyxoviruses of serotype 1 (APMV-1), of which some virulent forms of Newcastle disease virus (vNDV) infections can cause nearly 100% mortality in unvaccinated chickens, but other vNDV strains producing lower serious disease mortality rates have been used as non–tariff trade barriers. By comparison, low-virulent or lentogenic APMV-1 viruses (lNDV) can cause asymptomatic respiratory or intestinal infection, and on occasion, respiratory disease in poultry. vNDV strains have caused sporadic cases of human self-limiting conjunctivitis *(1)*.

Avian influenza (AI) is caused by infection of influenza virus A. Low-pathogenicity AI (LPAI) viruses typically cause asymptomatic infections, or at times, respiratory disease; drops in poultry egg production can be caused by any of the 16 hemagglutinin subtypes (H1 to H16). Conversely, HPAI viruses (limited to H5 and H7 subtypes) have caused severe disease in chickens and turkeys; the virus spreads to internal organs, resulting in a high fatality rates. In humans, H5, H7, and H9 AI viruses have caused sporadic infections after direct contact with infected birds, with high fatality rates for the H5N1 HPAI viruses (Guangdong lineage). vNDV and HPAI viruses result in severe economic losses to the poultry industries, disrupt trade in poultry and poultry products, and with some strains, have the potential to affect public health by causing mild to severe infections *(1, 12, 22, 31, 32)*.

HPAI viruses and vNDV pose some risk for dissemination in fresh and frozen raw poultry products, but the probability is remote. These viruses have been recovered from egg surfaces and internal egg contents, blood, and bones from infected chickens *(11, 29)*. More specifically, H5N1 HPAI viruses have been recovered from chicken thigh and breast meat, internal organs, and eggs produced by acutely infected chickens *(8, 27)*. In Korea, Japan, and Germany, H5N1 HPAI was recovered from frozen duck meat, but the contaminated products identified in Korea and Japan were imported from China *(18)*. In 1948, the importation of frozen chicken from Poland was implicated as the source of vNDV responsible for the Newcastle disease outbreak on poultry farms in England *(1)*. In contrast, LPAI viruses have not been detected in eggs or chicken meat, and the transmission of lNDV via eggs is unknown. AI virus and NDV survival in the environment and within materials is temperature and moisture dependent, wherein survival is shortened by high environmental temperatures and dry conditions *(10, 13, 16, 17, 21, 29, 33)*.

* Author for correspondence. Tel: 706-546-3433; Fax: 706-546-3161; E-mail: david.swayne@ars.usda.gov.

Egg products are traded globally for use in various food manufacturing processes. The U.S. Department of Agriculture (USDA) and Food and Drug Administration (FSIS) *(6)* mandates that commercial egg products must be pasteurized at specified time and temperature parameters to reduce pathogens below a zoonotic level. Pasteurization also extends the shelf life of commercial egg products. Although AI and AMPV-1 viruses are heat labile, the thermal inactivation of viruses is influenced by factors such as properties of the food product, the thermal stability of the strain or pathotype, and the process time–temperature. The FSIS pasteurization standards for egg products are based on a 5-log reduction of *Salmonella enterica* Enteritidis *(6)*. The pasteurization standard for plain whole egg is 60°C for 3.5 min, plain yolk is 60°C for 6.2 min, whole-egg blends is 61.1°C for 3.5 min, egg white with unadjusted pH is 57.7°C for 6.3 min, and egg white with adjusted pH is 4.3 min *(15)*. Other reformulated egg products such as imitation egg product (IEP), freeze-dried products, omelet mixes, eggnog mixes, noodles, and cake mixes are under the jurisdiction of the U.S. Food and Drug Administration (FDA), whose egg product inspection is voluntary *(4, 5, 7)*. These products are usually made from pasteurized egg products, and the law does not require repasteurization after reformulation. Despite this, manufacturers of egg products for direct consumption usually perform a second pasteurization process. In the United States, liquid egg white products constitute 24% of further-processed egg products *(22)*. Reformulated egg products such as IEP consist of at least 98% egg white and can contain up to 2% added ingredients *(3)*. The high percentage of egg white in IEP limits the temperature of pasteurization in order to maintain a desirable consistency and viscosity. The pasteurization recommended for IEP is 56.7°C for 4.6 min *(15)*.

The increased incidence of H5N1 HPAI poultry infections from some Asian, Eastern European, Middle Eastern, and African countries, along with the increase in global trade, raises concern that some poultry products could potentially pose biosecurity risks and affect (or have affected) trade. There is a need to develop standards for egg product pasteurization to inactivate AI viruses and NDV in various chicken egg products. The objective of this study was to develop predictive models for the inactivation of both AI viruses and NDV within a fat-free liquid egg product at various time and temperature heat processes. Linear and nonlinear regression models were used to determine thermal death times (*D*-values) and thermal resistance (z_D-values) of the viruses in fat-free egg product (FFEP). In addition, the experimental inactivation data of both AI viruses and NDV within a fat-free liquid egg product were validated against the FSIS pasteurization standard for *Salmonella* in IEP (56.7°C for 4.6 min), and the thermal process (*F* value) was calculated. The *F* value was also calculated with our predictive data at 57.7°C, along with the pasteurization standard for egg white without pH adjustment (57.7°C for 6.3 min) *(15)*. This study was based on one pasteurization cycle.

MATERIALS AND METHODS

Virus inoculum preparation. HPAI virus A/chicken/Pennsylvania/1370/83 (H5N2) (HPAI/PA/83), LPAI virus A/chicken/New York/13142-5/94 (H7N2) (LPAI/NY/94), vNDV APMV-1/chicken/California/212676/2002 (vNDV/CA/02), and lNDV APMV-1/chicken/United States/B1/1948 (lNDV/B1/48) were propagated by inoculation of 10-day-old, specific pathogen–free, embryonating white leghorn chicken eggs (Southeast Poultry Research Laboratory, Athens, GA) in chorioallantoic sacs. Titration of the virus stock was completed with standard tissue culture methods *(28)* and expressed as 50% tissue culture infectious doses (TID_{50}) *(25)*.

Sample preparation. Samples of FFEP (AllWhites Egg Whites, Crystal Farms, Lake Mills, WI) were artificially inoculated with a 1:10 dilution of virus, resulting in 10^6 to $10^{8.5}$ TID_{50}. Ninety-microliter aliquots of the artificially infected homogenized egg product were transferred into 200-μl, thin-walled thermocycler polypropylene tubes (Thermowell, Corning, Inc., Lowell, MA) and maintained at 4°C.

Heat inactivation. Samples were equilibrated at 25°C for 2 min and then heated to the desired temperature. On reaching the desired temperature, samples at time zero were removed, and the timing for pasteurization was commenced. The average come-up time to test temperature was 30 s. Samples were heated at 53, 55, 57, 58, 59, 61, and/or 63°C for 0, 1, 2, 3, 4, 6, 8, 12, and sometimes at 15 to 40 min in a PCR thermocycler heating block (GeneAmp 9700, PerkinElmer, Boston, MA), and were then cooled immediately to 4°C in a cooling block. For some sampling times, triplicate samples were pooled to obtain a final volume of 270 μl. The purpose of the pooling was to obtain sufficient volume to titer the undiluted sample (10^0) and to decrease the detection limit to 1 log. Samples were serially diluted (10^{-1} to 10^{-8}) in GIBCO Dulbecco's modified essential medium (Invitrogen, Carlsbad, CA) with 1 × antibiotic-antimycotic (HyClone, Thermo Scientific, Suwannee, GA) for inoculation into cell culture for determining infectious titer. Each experiment was replicated three times.

Tissue culture assay. Monolayers of chicken embryo fibroblast cells were used to titer AMPV-1 (NDV), and Madin-Darby canine kidney cells were used to titer AI viruses in 96-well microtiter plates. Monolayers were washed three times with phosphate-buffered saline, inoculated with 50 μl of virus inoculum, and incubated for 1 h. After incubation, 100 μl of medium supplemented with GIBCO trypsin-EDTA (0.05% trypsin, 0.53 mM EDTA; Invitrogen) was added to the inoculated monolayer and incubated at 37°C, with 5% CO_2, humidified atmosphere for 4 days. Titers of viruses were determined with a hemagglutination assay. In short, a 100-μl aliquot of supernatant from the inoculated tissue culture was transferred into a microtiter plate, 50 μl was serially diluted (1:2), and then overlaid with 0.5% chicken red blood cells. After 30 min of incubation, the presence or absence of agglutination was recorded. Virus titer was determined by calculation of the TID_{50} *(25)*.

Statistical data analysis. Inactivation curves were generated by plotting the log value of the TID_{50} as a function of the heating time at that temperature by using Excel 2003 (Microsoft Corp., Redmond, WA). The inactivation curves were examined to determine the best-fit statistical distribution. Linear, exponential, and polynomial curves were obtained. The *D*-values, or times (expressed in minutes) to inactivate the viral load by 90%, were calculated from the inverse value of the slope (1/–slope) of the linear regression plot. The *D*-values for the exponential plot were

TABLE 1. *Experimental* D_T*-values in FFEP for HPAI/PA/83*[a,b]

Temp (°C)	D_T-value (min)	SD[c]	Equation	R^{2d}
55	18.6	±0.01	$y = -0.0037x^2 + 0.0465x + 5.897$	0.96
56	8.5	±0.03	$y = -0.0149x^2 - 0.0876x + 5.884$	0.98
56.7	3.6	±0.02	$y = -0.0137x^2 - 0.251x + 6.0209$	0.99
57	2.5	±0.02	$y = -0.0124x^{2-} - 0.374x + 6.1291$	0.98
57.7	1.1[e]	NA[f]	NA	NA
58	0.4	±0.16	$y = -0.2286x^2 - 0.2057x + 5.6429$	0.91
59	0.4	±0.43	$y = -1.268x^2 - 0.0149x + 5.2577$	0.99

[a] D_T-values are the times required to reduce virus titer by 90% or 1 log TID_{50}.
[b] Experiments were replicated three times. The z_D-value was 4.3 ± 0.03°C, with its equation being $y = -0.3565x + 1.6407$, and its R^2 being 0.95.
[c] Standard deviations (SD) were generated from the thermal inactivation equation of HPAI-A/ck/PA/1370/83 (H5N2) infected with an initial titer of 6.25 log (TID_{50}/ml) in FFEP.
[d] The correlation coefficient (R^2) indicated the goodness of fit of the predictive equation.
[e] D_T predicted from plot of log D_T-values versus temperature.
[f] NA, not applicable.

based on inverse value of the exponential of the (slope); for polynomial distribution, the slopes were calculated by multiplying the exponent value by the coefficient and using the inverse value. The z_D-value is the change in temperature required to change the D_T-value by 1 log or 10-fold, and was determined with Excel 2003, by computing the regression of the mean log *D*-values versus heating temperatures. The z_D-value is the absolute value of the inverse slope.

The *F* value corresponds to the time–temperature combinations necessary to reduce the concentration of the target organism to an acceptable level; this value was expressed as a given number of *D*-values. For example, to obtain 5-log reduction of *Salmonella* in IEP required 4.6 min at 56.7°C; hence, to achieve a 1-log reduction at the same temperature would require 4.6/5, or 0.92 min. Therefore, if the D_T-value of the experimental data (56.7°C) was 2.3 min, then the *F* value for that process for the experiment would be 2.3 min. If the experimental organism was treated by the standard IEP process (4.6 min at 56.7°C), the resulting log reduction would be only 4.6/2.3, or 2 log.

RESULTS

Thermal inactivation of AI viruses and NDV. The thermal inactivation study generated survival curves, from which *D*-values for HPAI/PA/83, LPAI/NY/94, vNDV/CA/2002, and lNDV/B1/48 were calculated (Fig. 1). The thermal inactivation data for HPAI/PA/83 at 55 and 56°C had exponential declines in viral titers (Table 1). HPAI/PA/83 was resistant to heating at 55°C, requiring at least 93 min to inactivate viral population by 5 log, but by 56°C, the 5-log reduction required 43 min of heat exposure. Our inactivation data demonstrated that heating HPAI/PA/83 at 56.7°C required at least 18 min to inactivate 5 log of virus, whereas obtaining a similar reduction at 57 and 58°C would require 13 and 2 min, respectively. Using the FSIS pasteurization standard for IEP (56.7°C, with a minimum holding time of 4.6 min to obtain a 5-log reduction of *Salmonella*), an *F* value could be calculated. The pasteurization process of HPAI/PA/83 in FFEP would obtain a reduction of 1.3 log or a D_T-value of 1.3 when using the IEP standard (Table 2). Meanwhile, using the pasteurization standard for egg white with unadjusted pH (57.7°C with a minimum holding time of 6.3 min) would result in a D_T-value of 5.7 (Table 2).

The results of the *D*-values for LPAI/NY/94 (H7N2) are presented in Table 3. At 55°C, the inactivation rate was log linear; however, the inactivation curve plateau between 3 and 6 min suggests some thermal resistance at those times. Thermal inactivation of LPAI/NY/94 at 56.7°C required at least 5 min to inactivate 5 log of virus, whereas heating at 57°C required approximately 4 min for a similar log reduction. Viral inactivation between 58 and 59°C was complete in less than 2 min. Using the IEP pasteurization process for LPAI/NY/94 in FFEP would result in a D_T-value of 4.5, while the egg white pasteurization process would result in a D_T-value of 7.8 (Table 2).

The *D*-values for vNDV/CA/2002 are presented in Table 4. The thermal inactivation curves generated between 55 and 59°C demonstrated a constant log-linear rate of inactivation, indicating a similar degree of resistance in the viral population. Heating at 56.7°C required at least 31 min to inactivate 5 log of virus, while total inactivation (<7 log) occurred after 15 min of exposure at 59°C in FFEP. The pasteurization process of vNDV/CA/02 in FFEP resulted in a D_T-value of <1 by using the IEP standard (Table 2); when using the egg white pasteurization standard, the pasteurization process of vNDV/CA/02 in FFEP resulted in a D_T-value of 1.7 (Table 2).

The *D*-values for lNDV/B1/48 are presented in Table 5. lNDV/B1/48 demonstrated some thermal resistance between 55 and 58°C. Heating at 55°C required at least 26.5 min to inactivate 5 log of virus, while at 57°C, 11 min of heating was required to inactivate 5 log. At 59°C, there was total inactivation (>6-log reduction) within 4 min. The pasteurization (56.7°C, with holding time of 4.6 min) of lNDV/B1/48 in FFEP resulted in a D_T-value of 1.4, whereas using the pasteurization standards for egg white process resulted in a D_T-value of 3.3 (Table 2).

The estimated times (in minutes) to obtain a thermal process with a D_T-value of 5 (or a 5-log reduction) in FFEP at 56.7°C were 8 min for HPAI/PA/83, 5 min for LPAI/NY/94, 31 min for vNDV, and 19 min for lNDV/B1/48

TABLE 2. D-*value averages of HPAI/PA/83, LPAI/NY/94, vNDV/CA/2002, and lNDV/B1 in FFEP obtained from the prediction models, and the predicted number of log reductions achieved at standard pasteurization parameters*[a]

Virus	Temp (°C)	D_T-value[b]			Predicted no. of virus log reductions for virus in IEP or liquid egg white[c,d]
		1 min	2 min	3 min	
HPAI/PA/83	56.7	3.6	10.8	18	1.3
LPAI/NY/94	56.7	1.0	3.0	5	4.6
vNDV/CA/2002	56.7	6.2	18.6	31	<1
lNDV/B1	56.7	3.25	9.75	16.25	1.4
HPAI/PA/83	57.7	1.1	3.3	5.5	5.7
LPAI/NY/94	57.7	0.8	2.4	4.0	7.8
vNDV/CA/2002	57.7	3.7	11.1	18.5	1.7
lNDV/B1	57.7	1.9	5.7	9.5	3.3

[a] Parameters were 56.7°C for 4.6 min for IEP or 57.7°C for 6.3 min for egg whites, with unadjusted pH.
[b] D_T-value, time required to inactivate 1 log of virus at 56.7 or 57.7°C.
[c] Predicted number of viral log reductions (F value) achieved based on the USDA pasteurization standard of 56.7°C for 4.6 min in IEP.
[d] Predicted number of viral log reductions (F value) achieved based on the USDA pasteurization standard of 57.7°C for 6.3 min in egg white, without pH adjustment.

(Table 2). Those estimated times to obtain a thermal process with a D_T-value of 5 were higher than the 4.6 min required to inactivate a 5-log population of *Salmonella*. Meanwhile, the times to obtain a process with a D_T-value of 5 in FFEP at 57.7°C would be 5.5 min for HPAI/PA/83, 4 min for LPAI/NY/94, 18.5 min for vNDV, and 9.5 min for lNDV/B1/48 (Table 2). The proposed pasteurization standard for egg white (6.3 min at 57.7°C) should be considerably more effective in inactivating the viruses in FFEP than should the IEP pasteurization requirements (56.7°C). Nevertheless, the egg white pasteurization standard should be inadequate in inactivating a 5-log population for lNDV and vNDV, yet be effective in inactivating the 5-log population of both LPAI and HPAI within the required 6.3 min.

Modeling of thermal kinetics and determining the changes in thermal resistance. Our data for the inactivation of AI viruses and NDV were modeled with first-order kinetics or linear and nonlinear regression. Log-linear inactivation suggests a similar rate of inactivation within the viral population, but when the inactivation curves are up or down, as in an exponential or polynomial decline, the assumption is that there are variable degrees of resistance within the population. The change in thermal resistance of the virus for a temperature range (z_D-value) was calculated based on the plotting of the log D-values of the virus versus heating temperatures (in degrees Celsius) and using the absolute value of the inverse slope. Again, the z_D-value is defined as the change in temperature (in degrees Celsius) required to change the viral population by 1 log.

The z_D-values for HPAI/PA/83, LPAI/NY/94, vNDV/CA/2002, and lNDV/B1/48 are presented in Tables 1, 3, 4, and 5, respectively. The thermal death time curves for HPAI/PA/83 virus revealed an exponential rate of decline. The inactivation curve had a downward concave, suggesting that the remaining viral population became increasingly more susceptible to heat. However, the cumulative degree of thermal resistance between 55 and 59°C resulted in a z_D-value of 4.3°C, which indicates significant resistance of HPAI/PA/83 to differing temperatures (Table 1 and Fig. 1A). Comparatively, the z_D-value for LPAI/NY/94 with a change <0.5°C resulted in a 1-log decrease in the

TABLE 3. *Experimental* D_T-*values in FFEP for LPAI/NY/94*[a,b]

Temp (°C)	D_T-value (min)	SD[c]	Equation	R^{2d}
55	2.9	±0.03	$y = -0.348x + 5.435$	0.96
56.7	1.0	±0.06	$y = 0.13x^2 - 1.235x + 3.873$	0.99
57	0.8	±0.11	$y = 0.255\,x^2 - 1.763x + 3.872$	0.95
57.7	0.72[e]	NA[f]	NA	NA
58	0.6	±0.14	$y = 1.29x^2 - 3.489x + 3.4455$	0.99
59	0.5	±0.25	$y = -2x + 2.83$	0.92
61	0.4	±0.33	$y = -2.46x + 2.23$	0.99

[a] D_T-values are the times required to reduce virus titer by 90% or 1-log TID_{50}.
[b] Experiments were replicated three times. The z_D-value was 0.4 ± 0.03°C, with its equation being $y = 0.0275x^2 - 3.33x + 100.45$, and its R^2 being 0.99.
[c] Standard deviations (SD) were generated from the thermal inactivation equation of LPAI-A/ck/NY/13142/94 (H7N2) infected with an initial viral titer of 5.6 log (TID_{50}/ml) in FFEP.
[d] The correlation coefficient (R^2) indicated the goodness of fit of the predictive equation.
[e] D_T predicted from plot of log D_T-values versus temperature.
[f] NA, not applicable.

TABLE 4. *Experimental* D_T*-values in FFEP for vNDV/CA/2002*[a,b]

Temp (°C)	D_T-value (min)	SD[c]	Equation	R^{2d}
55	12.4	±0.005	$y = -0.081x + 8.630$	0.97
56	9.3	±0.007	$y = -0.1077x + 8.4224$	0.96
56.7	6.2	±0.02	$y = -0.162x + 8.431$	0.98
57	5.0	±0.05	$y = -0.198x + 8.392$	0.99
57.7	3.68[e]	NA[f]	NA	NA
58	3.7	±0.01	$y = -0.281x + 8.135$	0.98
59	1.7	±0.03	$y = -0.603x + 8.406$	0.98

[a] D_T-values are the times required to reduce virus titer by 90% or 1-log TID_{50}.
[b] Experiments were replicated three times. The z_D-value was 4.7 ± 0.02°C, with its equation being $y = -0.213x + 12.858$, and its R^2 being 0.97.
[c] Standard deviations (SD) were generated from the thermal inactivation equation for vNDV chicken/U.S.(CA)/212676/2002 artificially infected with an initial titer of 8.75 log (TID_{50}/ml) in FFEP.
[d] The correlation coefficient (R^2) indicated the goodness of fit of the predictive equation.
[e] D_T predicted from plot of log D_T-values versus temperature.
[f] NA, not applicable.

viral population (Table 3 and Fig. 1B), indicating that the LPAI virus is more sensitive to the changes in temperature than HPAI/PA/83. Similarly, for NDV, the highly virulent vNDV/CA/2002 was significantly more resistant to temperature changes than the lentogenic lNDV/B1/48 virus (Tables 4 and 5, and Fig. 1C and 1D).

DISCUSSION

The United States produces more than 200 million cases of shell eggs per year, of which 30.8% of them are processed as liquid egg product including liquid whole egg, liquid egg white, fortified whole eggs and yolk, sugared and salted whole eggs and yolks, and various blends of egg products *(3)*. The majority of liquid egg products is for commercial purposes and must be pasteurized before distribution for consumption, but not all egg products are required by law to be pasteurized *(30)*. Those exempt from the law include freeze-dried eggs, imitation eggs, and egg substitutes. These products are usually made from pasteurized eggs, but manufacturers are not mandated to repasteurize the formulated products. These egg products are under FDA jurisdiction *(30)*. IEP or egg substitute consists of mostly egg white (>98%), with some products being fat-free, while others might contain up to 2% added ingredients such as unsaturated fats and oils, vitamins, gums (xanthan, guar), and nonfat dry milk *(3)*. According to the USDA National Nutrient Database for Standard Reference, liquid or frozen fat-free egg substitute nutrient value consists of water, protein, total fat, carbohydrate, calcium, potassium, iron, sodium, vitamin A, and vitamin C (as reported in Table 6). These are similar to the content of the FFEP used in this study. By contrast, FFEP is >98% egg white and thus similar to liquid egg white product.

The FDA Federal Register Final Rule of 9 July 2009 *(7)* (''Prevention of *Salmonella enterica* Enteritidis in Shell Eggs during Production, Storage, and Transport'') and the Egg Product Inspection Act referenced the use of pasteurization of egg products in accordance with USDA requirements Title 9, Code of Federal Regulations (CFR) §590.570 *(6)*. The USDA Egg Product Inspection Act (Title 21, CFR §§118.3 and 118.6) *(5)* pasteurization guideline for IEP is 56.7°C, with a holding time of 4.6 min to obtain a 5-

TABLE 5. *Experimental* D_T*-values in FFEP for lNDV/B1/48*[a,b]

Temp (°C)	D_T-value (min)	SD[c]	Equation	R^{2d}
55	5.3	±0.02	$y = -0.1892x + 7.9566$	0.94
56.7	3.25	NA[e]	NA	
57	2.2	±0.07	$y = -0.0011x^4 + 0.0402x^3 - 0.4264x^2 + 0.8579x + 7.1828$	0.98
57.7	1.89[f]	NA	NA	NA
58	1.1	±0.13	$y = 0.0393x^3 - 0.4223x^2 + 0.04x + 7.5839$	0.99
59	0.55	±0.22	$y = 0.3083x^3 - 1.8089x^2 + 0.8649x + 6.7121$	0.99
61	0.19	±0.01	$y = -5.4x + 6.4$	1.0
63	0.17	±0.01	$y = -2.8x + 5.666$	0.75

[a] D_T-values are the times required to reduce virus titer by 90% or 1-log TID_{50}.
[b] Experiments were replicated three times. The z_D-value was 1.0 ± 0.15°C, with its equation being $y = -0.0047x^2 + 0.3038x - 1.6037$, and its R^2 being 0.99.
[c] Standard deviations (SD) were generated from the thermal inactivation equation for lNDV/B1/48 artificially infected with an initial titer of 6.75 log (TID_{50}/ml) in FFEP.
[d] The correlation coefficient (R^2) indicated the goodness of fit of the predictive equation.
[e] NA, not applicable.
[f] D_T predicted from plot of log D_T-values versus temperature.

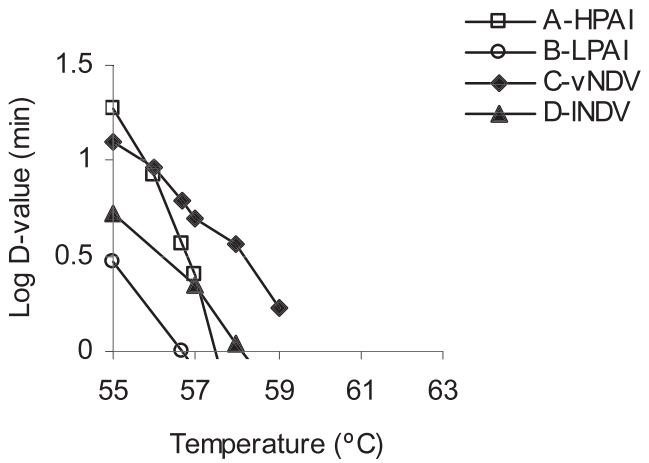

FIGURE 1. *Thermal death time curves for (A) HPAI-A/ck/PA/1370/83 (H7N2), (B) LPAI-A/ck/NY/13142/94 (H5N2), (C) vNDV chicken/U.S.(CA)/212676/2002), and (D) lNDV/B1 (chicken/U.S./B1/1948) in FFEP.*

log reduction (D_T-value of 5) of *Salmonella (3, 4).* In our study, we developed heat inactivation models for both LPAI and HPAI viruses, and lNDV and vNDV. The decimal reduction time (D_T) and thermal resistance due to changes in temperature (z_D) were obtained from the thermal inactivation models. The D_T-values at 56.7°C with holding time of 4.6 min in FFEP for both AI viruses and NDV were compared with the D_T-values of the USDA pasteurization for IEP to obtain a thermal process (F value) for FFEP. The thermal process was also calculated for FFEP, based on international egg pasteurization guidelines proposed by the United Egg Association and the American Egg Board for liquid egg white with unadjusted pH (57.7°C for 6.3 min) *(15).* The data produced were derived from one pasteurization cycle, although further-processed or reformulated egg product might be subjected to a second pasteurization process.

The thermal inactivation process in FFEP at 56.7°C, with a minimum holding time of 4.6 min showed that this pasteurization process did not achieve the 5-log population reduction as required in the pasteurization of egg products to eliminate *Salmonella.* If we used the liquid egg white standard, of which our FFEP is >98% liquid egg white, for *Salmonella* inactivation (unadjusted pH at 57.7°C for 6.3 min to inactivate 5 log) *(15),* the scenarios improved, with a better predictive model for virus inactivation. However, the quantity of virus titer reduction needed will be different for each of the four viruses. In a recent study, chicken hens infected with H5N2 HPAI virus produced eggs containing as high as 4.9 log 50% egg infectious dose (EID_{50})/ml virus on the surface of the shell, 1.2 to 4.8 log EID_{50}/ml in the yolk, and 1.5 to 6.1 log EID_{50}/ml in the egg albumen *(14).* Therefore, if we use this worst-case scenario and require IEP pasteurization standards of 6.1-log reductions for HPAI viruses, then the pasteurization temperature should be either higher than 56.7°C (the time parameter needs to be extended with longer holding time than 4.6 min) or a second pasteurization process is needed.

TABLE 6. *Nutritional content of FFEP in brand name egg product compared with the USDA national reference standard*

Nutrient	AllWhites Egg Whites (per 100 g)	USDA national database standard reference (per 100 g)
Protein	10 g	10 g
Total fat	0	0 g
Carbohydrate	1.8 g	2.0 g
Calcium	0	73 mg
Potassium	170 mg	213 mg
Iron	0	1.98 mg
Sodium	160 mg	199 mg

One limitation to this pasteurization process is that heating liquid egg white above 57°C can start the precipitation of the egg protein, resulting in coagulation at 73°C *(19)*; therefore, minimizing the holding time while increasing the processing temperature might be critical. With LPAI, virus has only been identified on the eggshell surface at 1.2 log EID_{50}/ml and not in the internal contents *(14).* This suggests that the IEP process (56.7°C, 4.6 min) would be more than adequate to inactivate completely any virus that could contaminate the albumen from the eggshell surface during the egg-cracking procedure. By contrast, there is a lack of data on the quantity of virus present on the eggshell surface and internal contents of eggs from vNDV- and lNDV-infected hens. However, because of similarities in pathogenesis of HPAI and LPAI viruses with vNDV and lNDV, respectively, the maximum vNDV quantity in albumen should be similar to the quantity for HPAI virus in egg albumen, while the lack of LPAI virus in internal contents of eggs should be expected for lNDV as well.

There are limited data available on the heat inactivation of AI viruses or NDV; therefore, some of the comparative data would be associated with *Salmonella,* the organism on which the pasteurization standard was based. Swayne and Beck *(27)* found that thermal inactivation of HPAI/PA/83 in fresh liquid egg white resulted in a $D_{56.7}$ of 33.1 s versus the 3.6 min observed with FFEP, and for vNDV/CA/02, the D_{57} was 21 s versus the 2.4 min in FFEP *(27).* The study by Swayne and Beck *(27)* demonstrated that a process resulting in a D_T-value of 5 would be achieved, thereby providing an adequate margin of safety, whereas our data of FFEP pasteurization were contrary to the fresh egg white data *(27).* The differences in D_T-values between the fresh liquid egg white study and our FFEP study could be attributed to the fact that filtering and heat processing might have reduced the functionality of inhibitory protein and enzymatic activity in FFEP, allowing the viruses an environment more suitable for survival. Fresh egg white also has higher protein content (12 to 15%) versus the FFEP protein content of 9 to 10%. The pH of both products was essentially the same; FFEP had a pH of 7.6, while fresh egg white's pH was 7.3. Similar variability in thermal inactivation data was observed in studies by Jin et al. *(20)* on the inactivation of *Salmonella* in liquid egg whites, wherein a $D_{56.6}$ of 0.37 min was recorded; Palumbo et al. *(24)* reported a $D_{56.6}$ of 1.44 min for a six-strain inoculum of *Salmonella* in egg

whites at pH 8.6. Meanwhile, Shuman and Sheldon *(26)* obtained a $D_{56.6}$ of 2.96 min for *Salmonella* in liquid egg white at pH 8.2, and a $D_{56.7}$ of 1.58 min for *Salmonella* at pH 9.1. Clearly, the thermal treatment of *Salmonella* in liquid egg white at various pH values did not achieve the thermal process with a D_T-value of 5, similar to the observation in our study. Many factors can influence the thermal stability of viruses, including strain types, heating medium, pH, microbial concentration, and experimental method *(20)*.

Previous research *(1, 27)* demonstrated that thermal stability or resistance of NDV and AI viruses might be dependent on the heating medium, for example, the change in thermal resistance value (z_D-value) for vNDV/CA/02 in whole, homogenized egg was 5.0°C, and for liquid egg whites was 4.4°C *(27)*. For HPAI/PA/03 in whole and liquid egg, the z_D-values were 3.6 and 1.9°C, respectively. In our study, the thermal resistance of the AI viruses and NDV in FFEP suggests that the HPAI and vNDV were more thermally resistant than were the low-virulent types, as a greater change in temperature was required to inactivate the viruses by 1 log. LPAI/NY/94 was the most sensitive to changes in temperature; lNDV/B1/48 was second most sensitive, whereas HPAI/PA/83 and vNDV/CA/2002 were the most resistant to changes in temperature.

In this study, the thermal inactivation models for AI viruses and NDV provide useful data, critical for quantitative risk assessments in determining the probability of viral exposure in egg products and the value of mitigation steps in consumer assurance. In previous research, HPAI/PA/83 (H5N2) was detected in egg and yolk samples in 57% of eggs laid by infected chickens during an outbreak in the northeastern United States. Unpublished work showed that eggs from HPAI virus–infected hens had an average titer of 2.6 log EID_{50}/ml, with titers as high as 6.1 log/ml for individual HPAI infected eggs, but no virus had been detected in internal contents of eggs from chickens infected with LPAI viruses. This emphasizes the importance to mitigate risk of viral transmission by setting thermal processing parameters that provide a margin of safety *(9)*. Our study showed that the virulent viruses tested were slightly more heat resistant than were the low-virulent pathotypes in FFEP, and that the thermal inactivation process at 56.7°C for 4.6 min might not adequately provide a margin of safety during pasteurization if the egg product is contaminated with >1 log of HPAI viruses or NDV. However, pasteurization at 57.7°C for 6.3 min might provide a moderate margin of safety for both HPAI and LPAI viruses, especially when considering that the come-up time to the temperature of interest inactivates at least 1 log of the virus population. Because most processed liquid egg products are pasteurized twice before reaching consumers, the possibility of egg products contamination with either AI viruses or NDV is miniscule. Moreover, there is no evidence of the spread of either lNDV or LPAI viruses by way of eggs, and the transmission of vNDV or HPAI viruses in eggs is rare. However, if such incidence were to occur, the viral titer would be considerably less than 5 log, due to the dilution effect from bulk production and the multiple sources of raw egg products. A scientific assumption more valid is to use the average titer, such as 2.6 log, for NDV- and AI virus-infected eggs rather than the maximum titer (6.1 log), because the cracked eggs are blended before the pasteurization process.

ACKNOWLEDGMENTS

The authors thank the American Egg Board for financial support and Hershell Ball of Michaels Foods for supplying products for this study.

REFERENCES

1. Alexander, D. J. 2001. Newcastle disease. *Br. Poult. Sci.* 42:5–22.
2. Alexander, D. J., and R. J. Manvel. 2004. Heat inactivation of Newcastle disease virus (strain Herts 33/56) in artificially infected chicken meat homogenate. *Avian Pathol.* 33:222–225.
3. American Egg Board. 2010. Shell egg distribution and consumption. Available at: www.aeb.org/egg-industry-facts/shell-egg-distribution-and-consumption. Accessed 15 August 2010.
4. Anonymous. 1993. Requirements for the specific standardized eggs and egg products. Title 21, Code of Federal Regulations, §2. Available at: http://www.access.gpo.gov/cgi-bin/cfrassemble.cgi?title=200521. Accessed 19 July 2010.
5. Anonymous. 2003. Egg product inspection act: prevention of *Salmonella Enteritidis* in shell eggs during production, storage and transportation. Title 21, Code of Federal Regulations, §16 and 118. Available at: www.accessdata.fda.gov/scripts/cdrh/cfdocs/cfCFR. Accessed 19 July 2010.
6. Anonymous. 2008. Pasteurization of liquid eggs. Title 9, Code of Federal Regulations, §590.570. Available at: http://www.access.gpo.gov/nara/cfr/waisidx_08/9cfr590_08.html. Accessed 4 September 2009.
7. Anonymous. 2009. Shell eggs. Title 21, Code of Federal Regulations, §115. Available at: www.accessdata.fda.gov/scripts/cdrh/cfdocs/cfCFR. Accessed 2 August 2010.
8. Beato, M. S., I. Capua, and D. J. Alexander. 2009. Avian influenza viruses in poultry products: a review. *Avian Pathol.* 38:193–200.
9. Cappucci, D. T., D. C. Johnson, M. Brugh, T. M. Smith, C. F. Jackson, J. E. Pearson, and D. A. Senne. 1985. Isolation of avian influenza virus (subtype H5N2) from chicken eggs during a natural outbreak. *Avian Dis.* 29:1195–2000.
10. Center for Food Security and Public Health. 2008. Newcastle disease: avian paramyxovirus-1 infection, goose paramyxovirus infection. Available at: http://www.cfsph.iastate.edu/Factsheets/pdfs/newcastle_disease.pdf. Accessed 30 March 2010.
11. Chen, J.-P., and C.-H. Wang. 2002. Clinical epidemiologic and experimental evidence for the transmission of Newcastle disease virus through eggs. *Avian Dis.* 46:461–465.
12. Cox, N., and T. M. Uyeki. 2008. Public health implications of avian influenza viruses, p. 453–484. *In* D. E. Swayne (ed.), Avian influenza. Blackwell Publishing, Ames, IA.
13. Domanska-Blicharz, K., Z. Minta, K. Smietanka, S. March, and T. van den Berg. 2010. H5N1 High-pathogenicity avian influenza virus survival in different types of water. *Avian Dis.* 54:734–737.
14. Eggert, D., and D. E. Swayne. 2011. Unpublished data.
15. Froning, G. W., D. Peters, P. Muriana, K. Eskridge, D. Travnicek, and S. Sumner. 2001. International egg pasteurization manual. United Egg Association and the American Egg Board, Parkview, IL.
16. Guan, Y., J. S. M. M. Peiris, K. F. Kong, K. C. Dyrting, T. M. Ellis, T. Sit, L. J. Zhang, and K. F. Shortridge. 2002. H5N1 influenza viruses isolated from geese in southeastern China: evidence for genetic re-assortment and interspecies transmission to ducks. *Virology* 292:16–23.
17. Guan, Y., J. S. M. Peiris, A. S. Lipatov, T. M. Ellis, K. C. Dyrting, S. Krauss, L. J. Zhang, R. G. Webster, and K. F. Shortridge. 2002. Emergence of multiple genotypes of H5N1 avian influenza viruses in Hong Kong SAR. *Proc. Natl. Acad. Sci. USA* 99:8950–8955.
18. Harder, T. C., J. Teuffert, E. Starick, J. Gethmann, C. Grund, S. Fereidouni, M. Durban, K.-H. Bogner, A. Neubauer-Juric, R. Repper, A. Hlinak, A. Engelhardt, A. Nöckler, K. Smietanka, Z. Minta, M.

Kramer, A. Globig, T. C. Mettenleiter, F. J. Conraths, and M. Beer. 2009. Highly pathogenic avian influenza virus (H5N1) in frozen duck carcasses, Germany, 2007. *Emerg. Infect. Dis.* 15:1–8.

19. Herald, T. J., F. A. Osorio, and D. M. Smith. 1989. Rheological properties of pasteurized liquid whole egg during frozen storage. *J. Food Sci.* 54:35–38.
20. Jin, T., H. Zhang, G. Boyd, and J. Tang. 2008. Thermal resistance of *Salmonella enteritidis* and *Escherichia coli* K12 in liquid egg determined by thermal death time disks. *J. Food Eng.* 84:608–614.
21. Lu, H., A. E. Castro, K. Pennick, J. Liu, Q. Yang, A. P. Dunn, D. Weinstock, and D. Henzler. 2003. Survival of avian influenza virus H7N2 in SPF chickens and their environment. *Avian Dis.* 47:1015–1021.
22. McLeod, A., N. Morgan, A. Prakash, and J. Hinrichs. 2005. Economic and social impact of avian influenza. Food and Agriculture Organization of the United Nations, Rome.
23. National Agricultural Statistics Services. 2010. Egg products: shell eggs broken. U.S. Department of Agriculture, Washington, DC.
24. Palumbo, M. S., S. M. Beers, S. Bhaduri, and S. A. Palumbo. 1996. Thermal resistance of *Listeria monocytogenes* and *Salmonella* spp. in liquid egg white. *J. Food Prot.* 59:1182–1186.
25. Reed, L. J., and H. Muench. 1938. A simple method of estimating fifty percent endpoints. *Am. J. Hyg.* 27:493–497.
26. Schuman, J. D., and B. W. Sheldon. 1997. Thermal resistance of *Salmonella* spp. and *Listeria monocytogenes* in liquid egg yolk and egg white. *J. Food Prot.* 60:634–638.
27. Swayne, D. E., and J. R. Beck. 2004. Heat inactivation of avian influenza and Newcastle disease viruses in egg products. *Avian Pathol.* 33:512–518.
28. Swayne, D. E., D. A. Senne, and C. W. Beard. 1998. Avian influenza, p. 150–155. *In* J. Glisson, M. Jackwood, and D. E. Swayne (ed.), A laboratory manual for the isolation and identification of avian pathogens, 4th ed. American Association of Avian Pathologists, University of Pennsylvania, Kennett Square.
29. Tiwari, A., D. P. Patnayak, Y. Chander, M. Parsad, and S. M. Goyal. 2006. Survival of two avian respiratory viruses on porous and nonporous surfaces. *Avian Dis.* 50:284–287.
30. U.S. Department of Agriculture, Food Safety and Inspection Service. 2010. Egg products and food safety, p. 1–4. Available at: http://origin-www.fsis.usda.gov/Fact_Sheets/Egg_Products_Preparation_Fact_Sheets/index.asp. Accessed 13 July 2010.
31. World Health Organization. 2004. Avian influenza A (H5N1) in humans and in poultry in Asia: food safety considerations, p. 1–2. Available at: http://www.who.int/foodsafety/micro/avian1/en/print.html. Accessed 19 March 2010.
32. Writing Committee of the Second World Health Organization Consultation on Clinical Aspects of Human Infection with Avian Influenza A (H5N1) Virus. 2008. Update on avian influenza A (H5N1) virus infection in humans. *N. Engl. J. Med.* 358:261–227.
33. Yamamoto, Y., K. Nakamura, M. Okamatsu, M. Yamada, and M. Mase. 2008. Avian influenza virus (H5N1) replication in feathers of domestic waterfowl. *Emerg. Infect. Dis.* 14:149–151.